The Investigation of “Impossible” Ring Sizes in the Macrocyclooligomerization of Depsipeptides and The Development and Mechanistic Exploration of RyR2 Selective Inhibitors

By

Abigail Nicole Smith

Dissertation

Submitted to the Faculty of the

Graduate School of Vanderbilt University

in partial fulfillment of the requirements

for the degree of

DOCTOR OF PHILOSOPHY

in

CHEMISTRY

January 31, 2022

Nashville, Tennessee

Approved:

Jeffrey N. Johnston, Ph.D.

Brian O. Bachmann, Ph.D.

Carmelo J. Rizzo, Ph.D.

Björn C. Knollmann, M.D., Ph.D.

To my family, who has never stopped believing in me and supporting me and

To my greatest inspiration, my niece Caroline

ACKNOWLEDGMENTS

I am forever grateful to the phenomenal support system I have had throughout graduate school, which without, this wouldn't have been possible. I have grown an incredible amount in graduate school, both as a scientist and as a person, thanks to my colleagues, mentors, family, and friends.

I first owe a great amount of gratitude to my professors I had at the University of Evansville. UE was a phenomenal undergraduate school that I had the privilege of attending, and during my time there, every single professor I studied under was exceptional. Particularly in the chemistry department, Dr. Kristy Miller saw my potential as a chemist and encouraged me to major in chemistry. Dr. Kaufman, Dr. Tod, Dr. Lynch, and Dr. Slade all reinforced this, encouraging me, challenging me, and providing endless opportunities to learn and develop. I owe a special thanks to Dr. Andy Lampkins, who was gracious enough to allow me to partake in summer research in his lab. A brilliant chemist and even better teacher, Dr. Lampkins taught me a great deal about organic chemistry. I learned many laboratory techniques that largely aided in my success throughout graduate school. Dr. Lampkins was also always willing to go above and beyond, helping me apply to internships, conferences, and scholarships. Without him, I would not be the chemist I am today.

I also want to acknowledge the wonderful mentors I gained through my summer internship at Eli Lilly and Company. I had the honor of working with Mark Rempala, who was one of the best mentors I have had, and I am lucky to be able to call him a friend today. He was incredibly patient with me, answering every question I had, taking the time to set-up new reactions with me, work through mechanisms, and listen to my presentations. I also met two other chemists who have become both mentors and friends, Mo Zia-Ebrahimi and Norm Hughes. During my time at Lilly, Mo was incredibly encouraging and always willing to help. Norm pushed me to really understand the reactions and mechanism of the chemistry I was pursuing and helped to develop my organic chemistry knowledge. Additionally, Mark, Mo, and Norm were and have continued to be phenomenal lunch buddies! I am grateful for all their help and advice throughout graduate school and during my transition to an industry career.

When I chose to come to Vanderbilt, I knew from the very start that I wanted to join Dr. Jeffrey Johnston's lab. At the time, this decision was largely based on my fascination with the chemistry his group was pursuing. Little did I know, this would become one of the best decisions I have

made. Working with Dr. Johnston has been an absolute blessing, and I cannot even begin to thank him for everything he has taught me. Dr. Johnston has an incredible work ethic and dedication to teaching his students in every single aspect of chemistry, even if that involves him repairing an instrument with you, or helping you set up a difficult reaction. He continuously helps with our professional development as well, providing funding for us to attend conferences, numerous opportunities to practice presenting our research, and advice for any career paths or questions we have. Thank you, Dr. Johnston, for being a great mentor and a big part of why I have enjoyed every minute of graduate school.

Another group I must thank for my experience in graduate school is all the past and present members of the Johnston lab. During my recruitment weekend, I remember going out to dinner with Thomas Struble and thinking that he was unbelievably intelligent, and I knew I wanted to learn from him. Turns out, my first impression was correct. He was a great mentor, leader, and teacher during my first year of graduate school. I also owe a big thanks to Matt Knowe, Jade Bing, Rashanique Quarrels, and Michael Crocker. These colleagues were incredibly kind (some of the kindest people I have ever met) and generous with their time. From my first day, I always felt comfortable approaching them with questions and boy did they get a lot of them from me. Thank you all for always being willing to talk with me, your constant feedback, advice, and many laughs. Without this group of older students to push me and help me grow, I would not be where I am today. I would also like to thank Mahesh Vishe and Suzanne Batiste for their guidance in reaction set-ups, NMR interpretations, and help with homework and problem sets. You each were always willing to talk through challenging problems with me, and for that I am incredibly grateful.

I want to give a special thanks to Jenna Payne and Jade Izaguirre, who joined Dr. Johnston's group the same year I did. These two have been my partners in crime throughout graduate school, from our "Union" meetings, to graduate classes and early mornings in lab. Jenna Payne has become one of my best friends throughout graduate school, and I am forever thankful that she (the extrovert) decided she was going to talk to me (the introvert) and become my friend. During our five years here, Jenna was always there to talk through our chemistry, go get food or coffee, bake me delicious desserts, run 5Ks, and so much more. Jenna is an incredibly talented chemist and a true team player, always offering to lend a hand to anyone that needs it. Thank you for constantly challenging me, sharing your love of chemistry with me, supporting me, and making me laugh.

Throughout my time in the Johnston lab, many new budding chemists joined the lab. Zihang Deng and Paige Thorpe were wonderful additions to the lab. Zihang is incredibly knowledgeable, and I have truly enjoyed our in-depth chemistry conversations and his kind and positive demeanor. He has already become a great mentor and leader in the lab. Paige Thorpe, in a similar manner to Jenna, decided that she wanted to be my friend and would talk to me every day until we were. During my last two years of graduate school, Paige has become one of my best friends. I have had the privilege of being able to mentor and work together with her on several different projects and while I may have been Paige's mentor, I have learned just as much from her as she has from me. Thank you for challenging me, listening to me, and providing endless entertainment. I will miss our goldfish and cake snack times, fieldtrips, our mutual obsession with *ent*-vert, and your jokes/insults (I am still not entirely sure which is which) and I can't wait to see what you will accomplish in the future.

I also want to give a special thanks to our newest additions to the Johnston lab – Preston, Scott, Kyle, and Melanie. Thank you all for your excitement and love of chemistry, French Toast Fridays, the memes, and constantly keeping me on my toes. Each one has added so much joy to my last year of graduate school, and I am excited to continue to watch all of you grow (and read all your future publications!).

Finally, I would like to thank my family. Every single member of my family has been incredibly supportive, not only throughout graduate school, but throughout my life. To my mom and dad, thank you for being the absolute best parents in the world. I can't even begin to describe how thankful I am for you both and how grateful I am for everything you have done for me. You guys have supported me in every endeavor I have pursued, provided constant encouragement, been there to comfort me when things don't work out, and celebrate when they do. Thank you for being my life-long role models, giving me a great sense of humor, teaching me the value of kindness and hard-work, and for being my best friends. To my brother Eli and my sister Alex – thank you for always putting up with me. I am so lucky to have two siblings who have both become my friends. Thank you for supporting me, always coming to visit me in Nashville so I didn't have to take as much time off work, and for all our hilarious jokes and laughs. I love you both and am so proud of the people you have grown into. Eli – thank you for finding Brice. She has been a wonderful addition to our family. Brice, thank you for supporting me, sharing my hatred for the patriarchy,

and constantly reminding me how strong all the women in our family are. Alex – thank you for giving me the greatest gift anyone has ever given me – my niece Caroline. Caroline brings so much joy to my life, inspires me every day, and motivates me to accomplish anything I set my mind too. I never knew how much this little person would affect my life, and I can't thank you enough. Caroline – thank you for teaching me patience, to love more than I ever thought possible, that hangry isn't a word, the phonics that I never learned, how to have the best sleepovers, and for continuing to push me to be the best role model that I can be. To my in-laws – I had no idea how lucky I was getting when I met David. Not only did I gain my lifelong partner, but also the best second family I could imagine. Thank you for supporting me and loving me like your own. Lastly, to David – I can't imagine my life without you. Thank you for your constant love and support. You have been a huge part of my graduate school career, from driving me to and from lab, encouraging and supporting all the crazy hours I needed to work, bringing me food and all the other things I forgot, helping me come up with titles for my publications, and taking such an interest in my education and my career. Thank you for always being the calm one, reassuring me when I doubt myself, and making me smile every single day. I can't wait for this next adventure together.

TABLE OF CONTENTS

Page

LIST OF FIGURES

LIST OF SCHEMES

LIST OF TABLES

Chapter I

I. RE-INVESTIGATION OF THE MACROCYCLOOLIGOMERIZATION REACTION: DISCOVERY OF THE FORMATION OF "IMPOSSIBLE" RING SIZE OLIGOMERS

1.1 Introduction to Cyclic Peptide and Depsipeptide Natural Product Therapeutics

Cyclic peptides and depsipeptides are a structurally privileged class of natural products, displaying a wide range of biological activity. These compounds have gained significant traction as potential therapeutics over the last few decades, largely due to their ability to reach traditionally difficult targets such as protein-protein interactions. Advances in molecular biology and the understanding of biological space has demonstrated that disease processes are often multifactorial and consist of complex networks of protein interactions, contributing to the failure of many new chemical entities (NCE) that function on single molecular targets. To inhibit proteins performing within their network as they drive disease mechanisms, molecules that can target larger protein surfaces are necessary.[1] The lack of distinct binding sites has limited small molecule drug discovery in many campaigns aimed at targeting protein-protein interactions, largely due to a lack of natural small molecule ligands that can serve as a starting point.[1] Success, however, has started to emerge with new classes of medium-sized molecules (500-1500 MW), in particular cyclic peptides and peptidomimetics, that are large enough to form interactions with larger, shallow surfaces among proteins. Over the last decade, the peptide drug market has grown by more than a factor of five, from $14 billion to over $70 billion.[1]

One of the challenges still associated with peptide therapeutics, however, is their inherently polar properties, which can be evident in their less than favorable pharmacokinetic and pharmacodynamic properties. However, there have been several key outliers, mainly cyclic peptides, that have been utilized by the chemistry community as models to study the behavior and increase the "drug-likeness" of these compounds. These include the immunosuppressant cyclosporine A, the anthelmintic emodepside, desmopressin, used for the treatment of hemophilia A, the immunosuppressant drug alisporivir, and linaclotide, used for the treatment of irritable bowel syndrome (Figure 1).[2] This class of compounds makes up a large cohort in the "Beyond Rule of Five" (Bro5) space, referring to Lipinski's Rule of Five.[3] Despite the growth in this field,

[1] Buckton, L. K.; Rahimi, M. N.; McAlpine, S. R. *Chem. Eur. J.* **2021**, *27*, 1487
[2] Santos, G. B.; Ganesan, A.; Emery, F. S. *ChemMedChem* **2016**, *11*, 2245
[3] Lipinski, C. A.; Lombardo, F.; Dominy, B. W.; Feeney, P. J. *Adv. Drug Delivery Rev.* **1997**, *23*, 3

substantial work remains to be done. While many cyclic peptides have been made orally bioavailable, in the last ten years, only one compound has been made that successfully binds to an intracellular target - romidepsin (Figure 1).[4] This potential, combined with the fact that most

Figure 1. Orally available cyclic peptides and peptidomimetics.

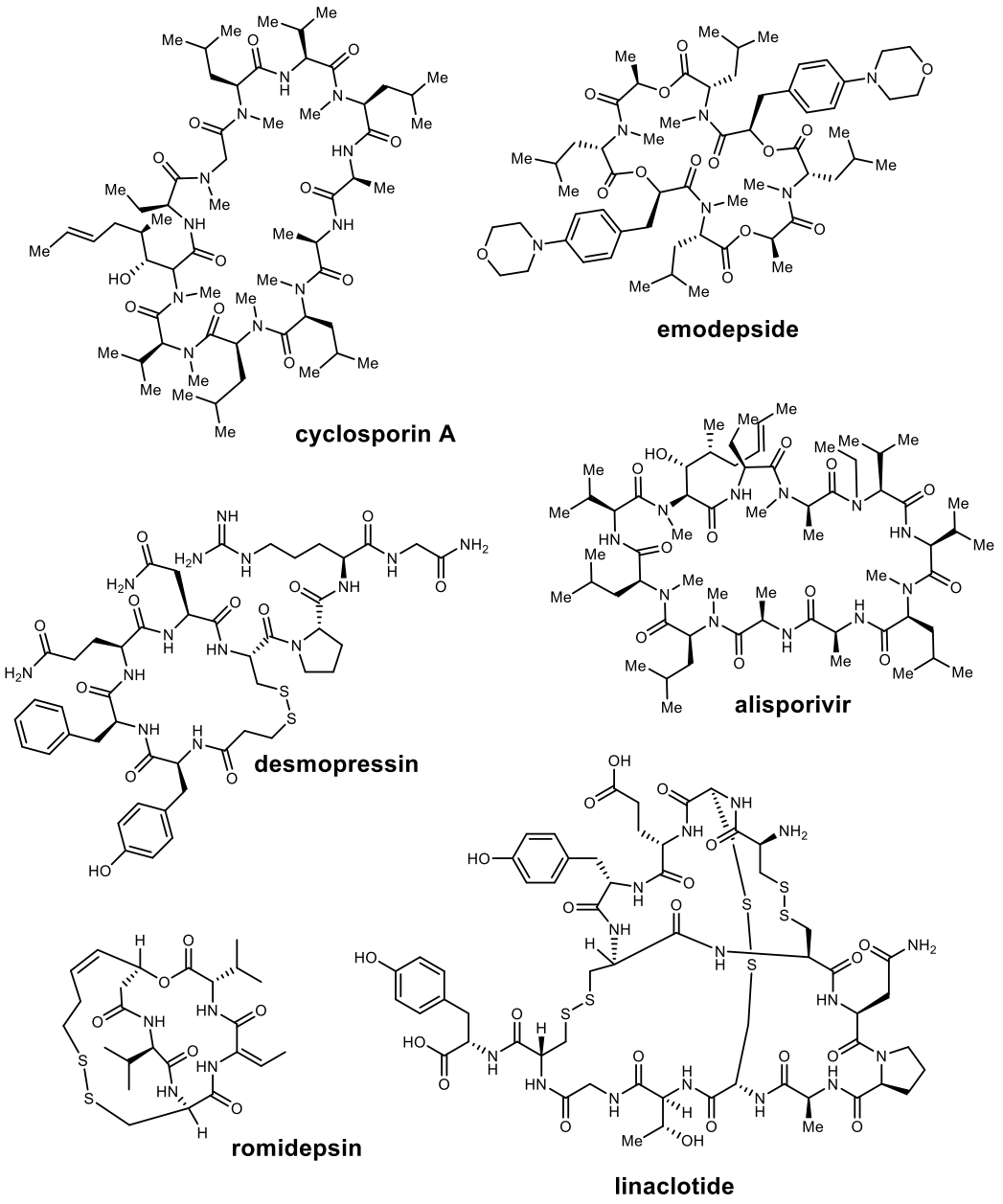

[4] https://www.accessdata.fda.gov/drugsatfda_docs/label/2009/ 022393lbl.pdf, 2009.

known drug targets are intracellular, highlights the need to explore this underdeveloped class of molecules.

Most cyclic peptides have less than 1% oral bioavailability, requiring IV delivery, and therefore lower patient compliance. To address this, many groups have developed and employed tactics to increase the "drug-likeness" of peptides, which has evolved a class of compounds commonly referred to as peptidomimetics. Recent innovators in the field, including Lokey[5], Kessler,[6] Yudin,[7] and Fairlie[8] have utilized a variety of chemical modifications inspired by nature such as amide *N*-permethylation,[9] replacement of amides with esters,[10] thioesters/thioamides,[11] or ketones,[12] incorporation of D-amino acids and non-proteinogenic amino acids,[13] side-chain modification, and the use of peptide stapling techniques.[14,15] Additionally, Lokey[16] and coworkers have uncovered extensive relationships between conformation of cyclic peptides and their passive permeability, often referred to as their chameleon ability,[17] and introduced a variety of techniques that can be incorporated to alter peptides conformation. However, while standardized methods to

[5] a) Representative examples include: Andrew, T. B.; Cayla, M. M.; Lokey, R. S. *Current Topics in Medicinal Chemistry* **2013**, *13*, 821 b)Naylor, M. R.; Bockus, A. T.; Blanco, M.-J.; Lokey, R. S. *Curr. Opin. Chem. Biol.* **2017**, *38*, 141

[6] Representative examples include: a) Beck, J. G.; Chatterjee, J.; Laufer, B.; Kiran, M. U.; Frank, A. O.; Neubauer, S.; Ovadia, O.; Greenberg, S.; Gilon, C.; Hoffman, A.; Kessler, H. *J. Am. Chem. Soc.* **2012**, *134*, 12125 b) Biron, E.; Chatterjee, J.; Ovadia, O.; Langenegger, D.; Brueggen, J.; Hoyer, D.; Schmid, H. A.; Jelinek, R.; Gilon, C.; Hoffman, A.; Kessler, H. *Angew. Chem. Int. Ed.* **2008**, *47*, 2595 c) Chatterjee, J.; Gilon, C.; Hoffman, A.; Kessler, H. *Acc. Chem. Res.* **2008**, *41*, 1331

[7] Representative examples include: a) White, C. J.; Yudin, A. K. *Nat. Chem.* **2011**, *3*, 509 b) Yudin, A. K. *Chem. Sci.* **2015**, *6*, 30 c) Zaretsky, S.; Scully, C. C. G.; Lough, A. J.; Yudin, A. K. *Chem. Eur. J.* **2013**, *19*, 17668

[8] Representative examples include: a) Craik, D. J.; Fairlie, D. P.; Liras, S.; Price, D. *Chem. Biol. Drug Des.* **2013**, *81*, 136 b) Nielsen, D. S.; Shepherd, N. E.; Xu, W.; Lucke, A. J.; Stoermer, M. J.; Fairlie, D. P. *Chem. Rev.* **2017**, *117*, 8094

[9] Chatterjee, J.; Rechenmacher, F.; Kessler, H. *Angew. Chem. Int. Ed.* **2013**, *52*, 254

[10] Choudhary, A.; Raines, R. T. *ChemBioChem* **2011**, *12*, 1801

[11] Zhang, W.; Li, J.; Liu, L.-W.; Wang, K.-R.; Song, J.-J.; Yan, J.-X.; Li, Z.-Y.; Zhang, B.-Z.; Wang, R. *Peptides* **2010**, *31*, 1832

[12] Torbeev, V. Y.; Mandal, K.; Terechko, V. A.; Kent, S. B. H. *Bioorg. Med. Chem. Lett.* **2008**, *18*, 6012

[13] Ding, Y.; Ting, J. P.; Liu, J.; Al-Azzam, S.; Pandya, P.; Afshar, S. *Amino Acids* **2020**, *52*, 1207

[14] Erak, M.; Bellmann-Sickert, K.; Els-Heindl, S.; Beck-Sickinger, A. G. *Bioorg. Med. Chem.* **2018**, *26*, 2759

[15] Andrew, T. B.; Cayla, M. M.; Lokey, R. S. *Current Topics in Medicinal Chemistry* **2013**, *13*, 821

[16] Representative examples include: a) Rezai, T.; Bock, J. E.; Zhou, M. V.; Kalyanaraman, C.; Lokey, R. S.; Jacobson, M. P. *J. Am. Chem. Soc.* **2006**, *128*, 14073 b) Bockus, A. T.; Lexa, K. W.; Pye, C. R.; Kalgutkar, A. S.; Gardner, J. W.; Hund, K. C. R.; Hewitt, W. M.; Schwochert, J. A.; Glassey, E.; Price, D. A.; Mathiowetz, A. M.; Liras, S.; Jacobson, M. P.; Lokey, R. S. *J. Med. Chem.* **2015**, *58*, 4581 c) Ahlbach, C. L.; Lexa, K. W.; Bockus, A. T.; Chen, V.; Crews, P.; Jacobson, M. P.; Lokey, R. S. *Future Medicinal Chemistry* **2015**, *7*, 2121

[17] Whitty, A.; Zhong, M.; Viarengo, L.; Beglov, D.; Hall, D. R.; Vajda, S. *Drug Discovery Today* **2016**, *21*, 712

synthesize cyclic peptides have been developed, many peptide derivatives, such as *N*-methyl peptides and depsipeptides, still present numerous synthetic challenges.

1.2 Leveraging Depsipeptides as Peptidomimetics

Peptides have long been considered "non-drug-like" compounds, largely due to their instability to proteases *in vivo*. However, the ability to modulate the structure and functions of peptides would be an incredibly useful tool towards developing novel therapeutics. This desire spurred the development of peptide-bond isosteres. A particularly interesting isostere is the ester bond (depsipeptide), in part an intriguing substitution because depsipeptides are so prevalent in nature. While there are many well-known peptide therapeutics, their depsipeptide counterpart is encountered far less often. Depsipeptides here, are defined as any peptide compound in which at least one amide bond has been replaced with an ester bond. The geometric parameters and resonance delocalization of an ester are comparable of those to an amide. Esters also have cis and trans conformations, in which the trans is more favorable. However, due to a weaker charge transfer from the bridging oxygen to the carbonyl group, esters have a lower rotational barrier between the two than amides (11 kcal/mol vs 20 kcal/mol).[18] An amide to ester substitution also results in a diminished capability to hydrogen bond by removing a hydrogen bond donor, which can have drastic effects on the stability and protein folding/secondary structure.[19] Esters also have increased torsional flexibility and weaker intramolecular associations, making them significantly

Figure 2. Bond lengths (Å) of amides compared to esters, and the *cis-trans* equilibrium of a peptide/peptide isostere bond.[a]

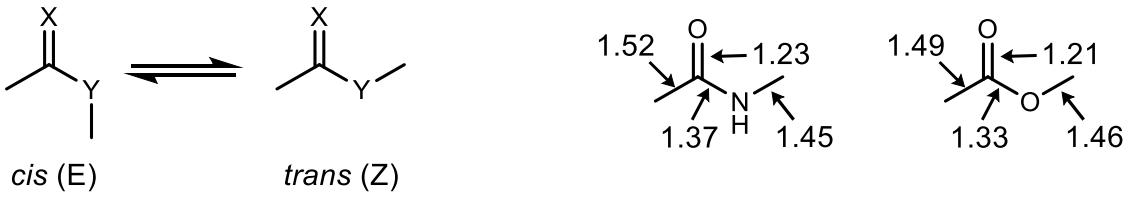

[a] These values were obtained from crystal structures and have also been calculated using density functional methods. See references cited above for more detail.

[18] Thakkar, B. S.; Svendsen, J. M.; Engh, R. A. *J. Phys. Chem. A* **2017**, *121*, 6830
[19] Thakkar, B. S.; Engh, R. A. *RSC Adv.* **2018**, *8*, 4445

less conformationally ridged (Figure 2).[20] While esters are more vulnerable to hydrolysis than amides, they are more resistant to amine and thiolate nucleophiles compared to other amide-bond isosteres, like thioamides.[10] Finally, ester substitutions of amide bonds have been shown to play a large role in increasing the cell permeability of peptides.[21]

Despite their prevalence in nature, non-natural product depsipeptide therapeutics are rare, due to difficulties encountered in isolation and purification of large amounts from natural sources, as well as significant challenges with the synthetic accessibility of these molecules. Solid phase peptide synthesis has now been the gold standard for several decades in traditional peptide synthesis, and these methods are now well established for peptides smaller than 60 units. There is no equivalent standard procedure for the solid phase synthesis of depsipeptides, and these syntheses often vary greatly on a case-to-case basis. Due to the chemical lability of the esters, many methods developed for peptide synthesis do not translate well to depsipeptide synthesis. New methodologies to synthesize depsipeptides, are therefore of incredible importance, and often a good place to start, is to examine how nature makes them.

1.2.1 Biosynthesis of Depsipeptides

Naturally occurring depsipeptides are biosynthesized by specialized multi-domain microbial enzymes known as nonribosomal peptide synthetases (NRPSs). NRPSs synthesize peptides using a modular synthetic scheme that resembles an assembly line. NRPS is made up of modules, which are a set of domains that together possess the activities required to add an acyl residue to the peptide chain.[22] A standard elongation model includes a condensation domain (C), an adenylation domain (A), and a peptidyl carrier protein domain (PCP). Non-ribosomal peptides (NRP) are small (2-20 residues), secondary metabolites, meaning they are not essential for organism survival, but provide advantages to the organism.[23] NRPs are unique in their structures, often branched or cyclic, and incorporate a variety of different monomers. These include L- and D- amino acids, hydroxy acids, keto acids, fatty acids, and aryl acids.[24] There are also many different modifying domains,

[20] Ramakrishnan, C.; Mitra, J. *Proceedings of the Indian Academy of Sciences - Section A, Chemical Sciences* **1978**, *87*, 13
[21] Schwochert, J.; Pye, C.; Ahlbach, C.; Abdollahian, Y.; Farley, K.; Khunte, B.; Limberakis, C.; Kalgutkar, A. S.; Eng, H.; Shapiro, M. J.; Mathiowetz, A. M.; Price, D. A.; Liras, S.; Lokey, R. S. *Org. Lett.* **2014**, *16*, 6088
[22] Marahiel, M. A.; Stachelhaus, T.; Mootz, H. D. *Chem. Rev.* **1997**, *97*, 2651
[23] O'Brien, J.; Wright, G. D. *Curr. Opin. Biotechnol.* **2011**, *22*, 552
[24] Caboche, S.; Leclère, V.; Pupin, M.; Kucherov, G.; Jacques, P. *J. Bacteriol.* **2010**, *192*, 5143

including methylation,[25] formylation,[26] epimerization,[27] residue cyclization,[28] oxidation,[29] reduction,[30] and hydroxylation.[31] Combined, all these modifications allow for functionally diverse natural products that display a wide range of biological activity. To date, all nonribosomal depsipeptide synthetases that have been characterized except for one (asperphenamate)[32] produce cyclic depsipeptides. While some linear products are occasionally observed, the cyclic products predominate in almost all systems. This is in stark contrast to nonribosomal peptide synthetases, in which many linear natural products are generated.

So far, over 1,300 naturally occurring cyclic depsipeptides have been characterized, and these compounds have been classified into a series of groups and curated in a database based off their chemical structures.[33] However, a separate characterization system has been established for the biosynthetic pathways (Figure 3).[34] In this classification, depsipeptides can be classified into three groups based on the stage at which an ester bond is introduced: elongation, termination, or elongation and termination. The stages at which the ester bond is introduced can be further broken down into classes that are catalyzed by a condensation domain (C_n) or a terminal domain (TE). This can be accomplished in an iterative or non-iterative pathway. The final classification depicts the origin of the hydroxyl nucleophile or the bridging ester oxygen. The next part of this chapter will detail some of these most common pathways in which depsipeptides are biosynthesized.

NRPS biosynthetic pathways in which the α-hydroxy acid residues are incorporated during elongation closely resemble typical NRPS that introduce amino acid residues. In the simplest sequence of events, the A domain of the elongation module recognizes a hydroxy acid, which is transferred to the PCP domain. The resulting substrate is used as the acceptor substrate in C domain catalyzed ester bond formation. For this pathway to occur, α-hydroxy acids must be readily available. However, α-hydroxy acids are not a common primary metabolism product, so the gene

[25] Mori, S.; Pang, A. H.; Lundy, T. A.; Garzan, A.; Tsodikov, O. V.; Garneau-Tsodikova, S. *Nat. Chem. Biol.* **2018**, *14*, 428
[26] Schoenafinger, G.; Schracke, N.; Linne, U.; Marahiel, M. A. *J. Am. Chem. Soc.* **2006**, *128*, 7406
[27] Stein, D. B.; Linne, U.; Hahn, M.; Marahiel, M. A. *ChemBioChem* **2006**, *7*, 1807
[28] Bloudoff, K.; Fage, C. D.; Marahiel, M. A.; Schmeing, T. M. *Proc. Natl. Acad. Sci. U. S. A.* **2017**, *114*, 95
[29] Schneider, T. L.; Shen, B.; Walsh, C. T. *Biochemistry* **2003**, *42*, 9722
[30] Alonzo, D. A.; Chiche-Lapierre, C.; Tarry, M. J.; Wang, J.; Schmeing, T. M. *Nat. Chem. Biol.* **2020**, *16*, 493
[31] van Wageningen, A. A.; Kirkpatrick, P. N.; Williams, D. H.; Harris, B. R.; Kershaw, J. K.; Lennard, N. J.; Jones, M.; Jones, S. J. M.; Solenberg, P. J. *Chem. Biol.* **1998**, *5*, 155
[32] Li, W.; Fan, A.; Wang, L.; Zhang, P.; Liu, Z.; An, Z.; Yin, W.-B. *Chem. Sci.* **2018**, *9*, 2589
[33] Taevernier, L.; Wynendaele, E.; Gevaert, B.; Spiegeleer, B. *Curr. Protein Pept. Sci.* **2017**, *18*, 425
[34] Alonzo, D. A.; Schmeing, T. M. *Protein Sci.* **2020**, *29*, 2316

Figure 3. Depsipeptide biosynthetic classification pathways.

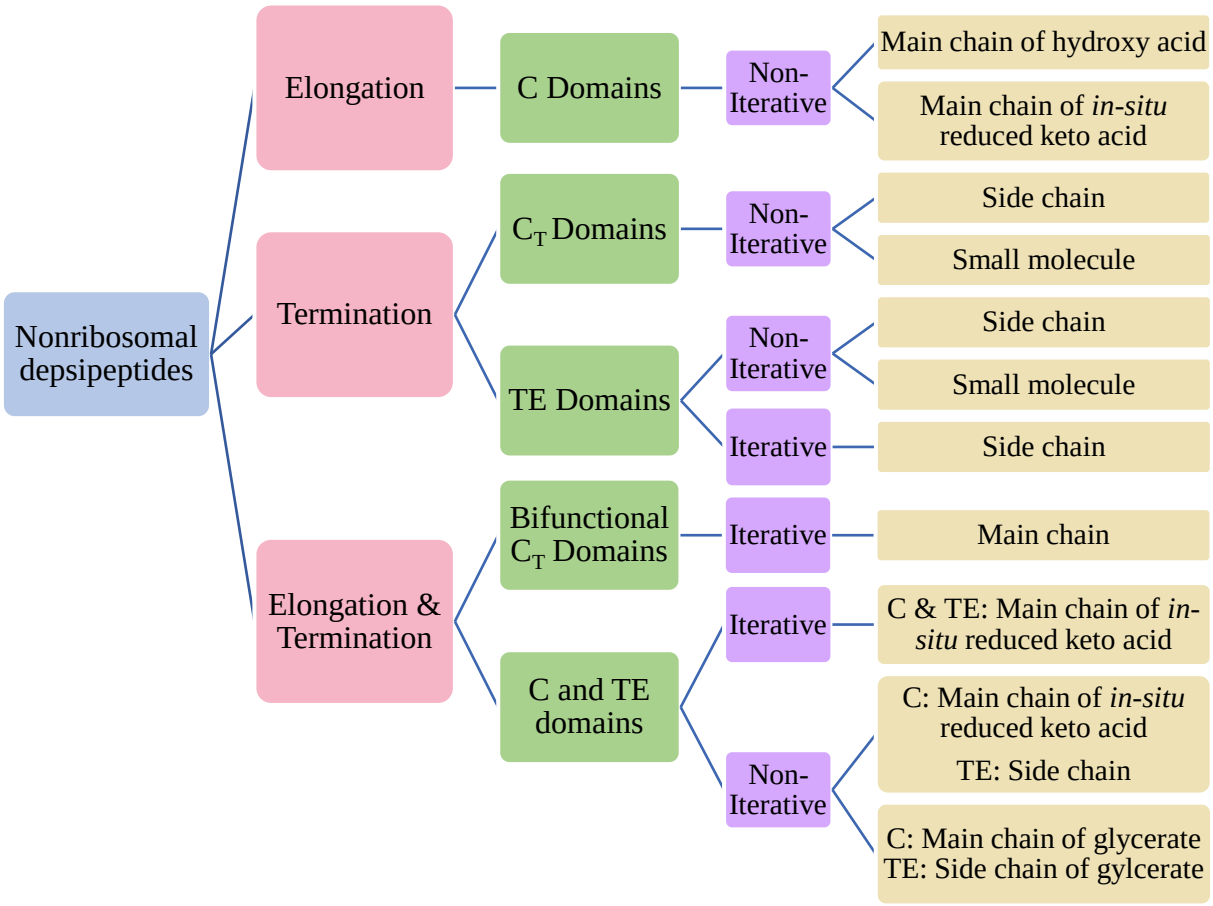

cluster must have free-standing ketoreductases that can convert α-keto acids into α-hydroxy acids.[35] Comparatively, α-keto acids are abundant in primary metabolism, often arising from glycolysis. An example of a biosynthetic pathway in which the ester bonds are formed during elongation is that of leualacin, a naturally occurring cyclic depsipeptide calcium channel blocker (Figure 4).[36] This simple biosynthetic pathway is predominantly seen in fungal species.[37] While bacterial depsipeptide synthetases can also form ester bonds during the elongation step, these gene

[35] Xu, Y.; Orozco, R.; Kithsiri Wijeratne, E. M.; Espinosa-Artiles, P.; Leslie Gunatilaka, A. A.; Patricia Stock, S.; Molnár, I. *Fungal Genet. Biol.* **2009**, *46*, 353
[36] Zhang, S.; Qiu, Y.; Kakule, T. B.; Lu, Z.; Xu, F.; Lamb, J. G.; Reilly, C. A.; Zheng, Y.; Sham, S. W. S.; Wang, W.; Xuan, L.; Schmidt, E. W.; Zhan, J. *J. Nat. Prod.* **2017**, *80*, 363
[37] Liuzzi, V. C.; Mirabelli, V.; Cimmarusti, M. T.; Haidukowski, M.; Leslie, J. F.; Logrieco, A. F.; Caliandro, R.; Fanelli, F.; Mulè, G. *Toxins* **2017**, *9*, 45

clusters typically have special modules known as ketoreductases (KR). These modules will select and reduce keto acids.[30]

Figure 4. Proposed biosynthetic pathway of depsipeptide, leualacin.

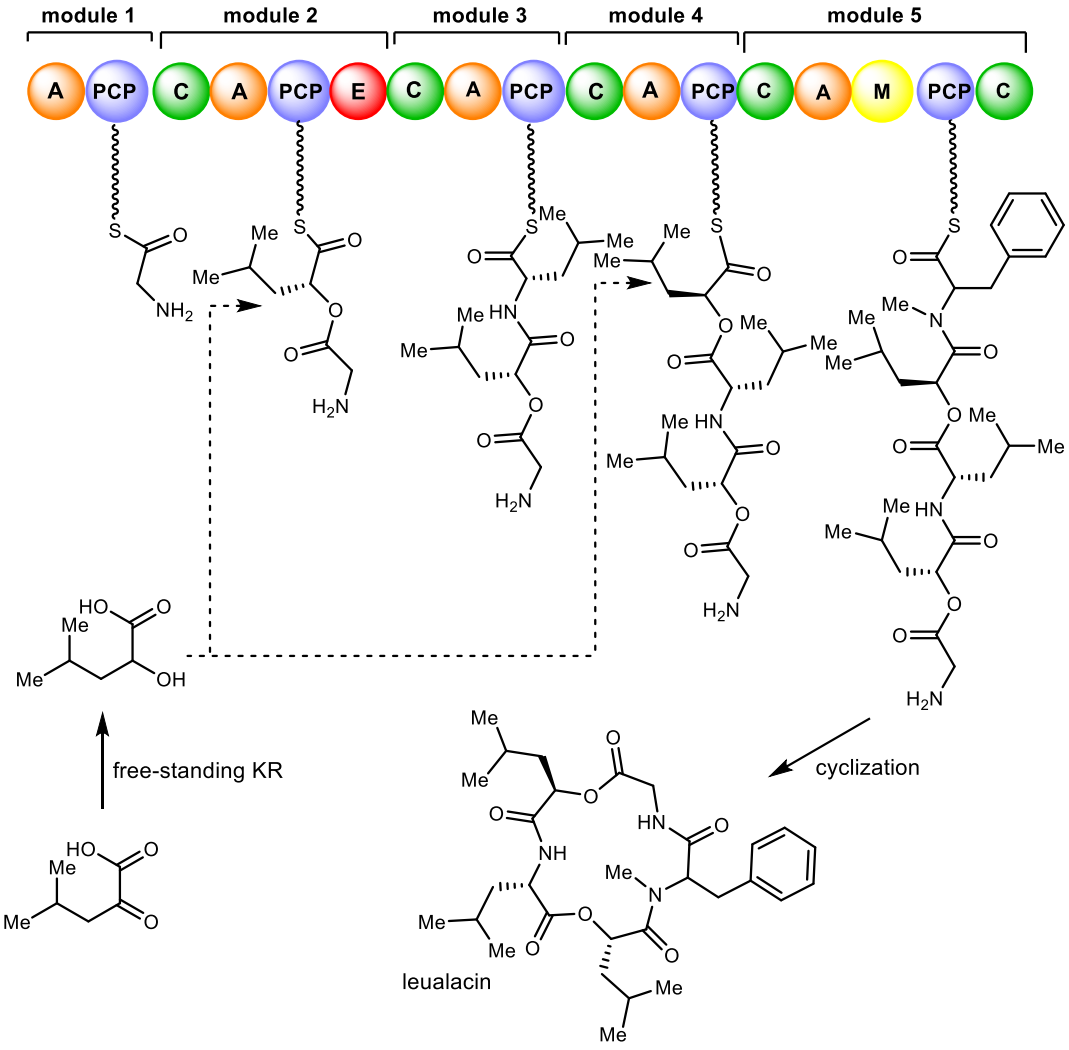

The next class of NRPSs incorporate the depsipeptide ester bonds during a termination step. In these examples, NPRSs contain a series of termination mechanisms, in which an ester bond is formed during the peptide release. This can be accomplished through a variety of different mechanisms, but a commonly employed domain is the C-terminal, or cyclizing c domains (C_T).[38] C_T domains catalyze the nucleophilic attack of an oxygen within the peptidyl intermediate onto

[38] Zhang, J.; Liu, N.; Cacho, R. A.; Gong, Z.; Liu, Z.; Qin, W.; Tang, C.; Tang, Y.; Zhou, J. *Nat. Chem. Biol.* **2016**, *12*, 1001

the terminal thioester carbonyl, resulting in cyclization and release of the depsipeptide (Figure **5**). The most well-known depsipeptide example that undergoes this type of biosynthetic pathway is cyclosporin A.[39] There are rare cases, such as that of asperphenamate, in which the release of the peptide results from nucleophilic attack intermolecularly by another small molecule.[32] This small molecule is usually suggested to be a product of another NRPS in which the terminal step is a reductive release to form a terminal alcohol. While this is a proposed biosynthetic pathway for a few depsipeptides, most of the gene clusters which may contain single α-hydroxy acyl residues have not yet been characterized.

Figure 5. Biosynthetic pathway in which C-terminal domain catalyzes cyclization and depsipeptide release.

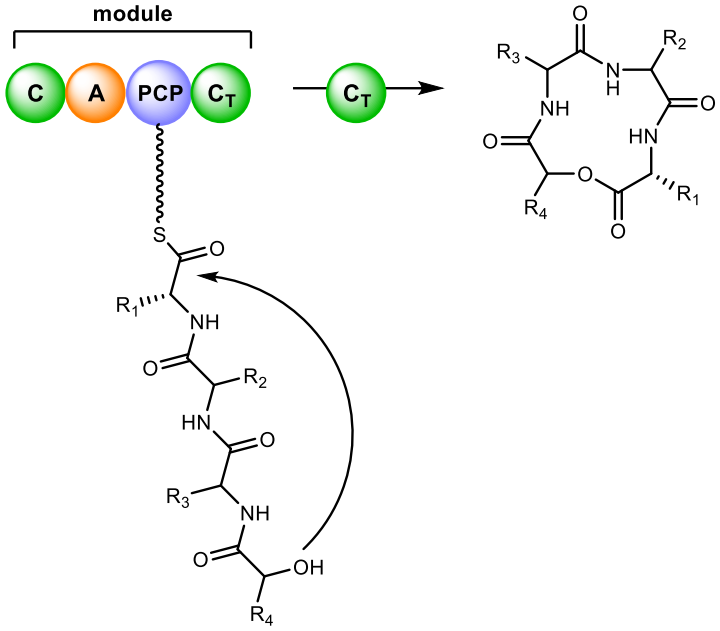

Another common biosynthetic pathway for the formation of the ester bond in depsipeptides is during the release step in the terminal thioester (TE) domains. Like the C_T domain cyclization, TE-mediated cyclization most often uses a side chain hydroxyl group on the peptide chain as the acceptor nucleophile. TE-mediated cyclizations occur by a two-step process, beginning with transfer of the peptide to the active serine site on the TE domain. In the second step, a nucleophile attacks the formed acyl intermediate to either cyclize the peptide if the attack is intramolecular, or

[39] Hoppert, M.; Gentzsch, C.; Schörgendorfer, K. *Arch. Microbiol.* **2001**, *176*, 285

to oligomerize or release a linear peptide if the nucleophilic attack is intermolecular (Figure 6).[40] The former is most common, generating cyclic depsipeptides. This pathway is a prevalent one, in which many well-known examples of naturally formed cyclic depsipeptides exist, including daptomycin,[41] fengycin,[42] lysobactin,[43] surfactin,[44] obafluorin,[45] polyoxypeptin A,[46] and spiruchostatins.[47] Finally, TE domains are also capable of serving a multi-functional purpose, first oligomerizing peptides and then catalyzing cyclization in an iterative fashion. This mode of action is seen with the biosynthesis of gramicidin S[48] and enterobactin.[49]

Figure 6. Biosynthetic pathway in which TE domain catalyzes ester bond formation.

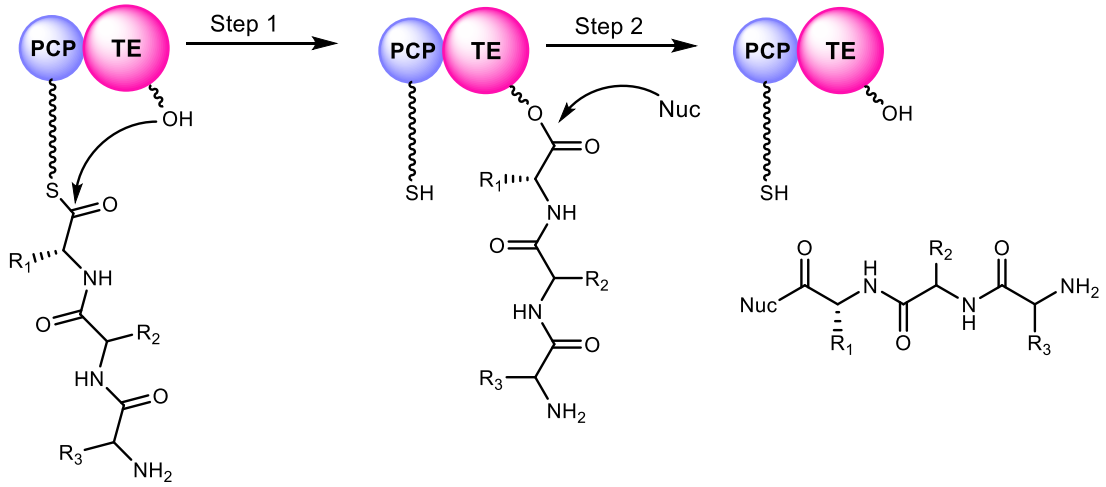

While biosynthetic gene clusters can introduce an ester in elongation or termination events, it is also known for these events to occur within the same biosynthetic cluster. This is most often seen in bacterial NRPS. This ester bond formation through elongation and termination can occur through one of two ways: bifunctional C_T domains, and C and T domains working in unison.

[40] Horsman, M. E.; Hari, T. P. A.; Boddy, C. N. *Nat. Prod. Rep.* **2016**, *33*, 183
[41] Richard, H. B. *Curr. Top. Med. Chem.* **2008**, *8*, 618
[42] Steller, S.; Vollenbroich, D.; Leenders, F.; Stein, T.; Conrad, B.; Hofemeister, J.; Jacques, P.; Thonart, P.; Vater, J. *Chem. Biol.* **1999**, *6*, 31
[43] Hou, J.; Robbel, L.; Marahiel, Mohamed A. *Chem. Biol.* **2011**, *18*, 655
[44] Koglin, A.; Löhr, F.; Bernhard, F.; Rogov, V. V.; Frueh, D. P.; Strieter, E. R.; Mofid, M. R.; Güntert, P.; Wagner, G.; Walsh, C. T.; Marahiel, M. A.; Dötsch, V. *Nature* **2008**, *454*, 907
[45] Kreitler, D. F.; Gemmell, E. M.; Schaffer, J. E.; Wencewicz, T. A.; Gulick, A. M. *Nat. Commun.* **2019**, *10*, 3432
[46] Du, Y.; Wang, Y.; Huang, T.; Tao, M.; Deng, Z.; Lin, S. *BMC Microbiology* **2014**, *14*, 30
[47] Potharla, V. Y.; Wang, C.; Cheng, Y.-Q. *J. Ind. Microbiol. Biotechnol.* **2014**, *41*, 1457
[48] Hoyer, K. M.; Mahlert, C.; Marahiel, M. A. *Chem. Biol.* **2007**, *14*, 13
[49] Gehring, A. M.; Mori, I.; Walsh, C. T. *Biochemistry* **1998**, *37*, 2648

Figure 7. Biosynthetic pathway of cyclic oligomeric depsipeptide class of enniatins, carried out by bifunctional iterative C_T domains.

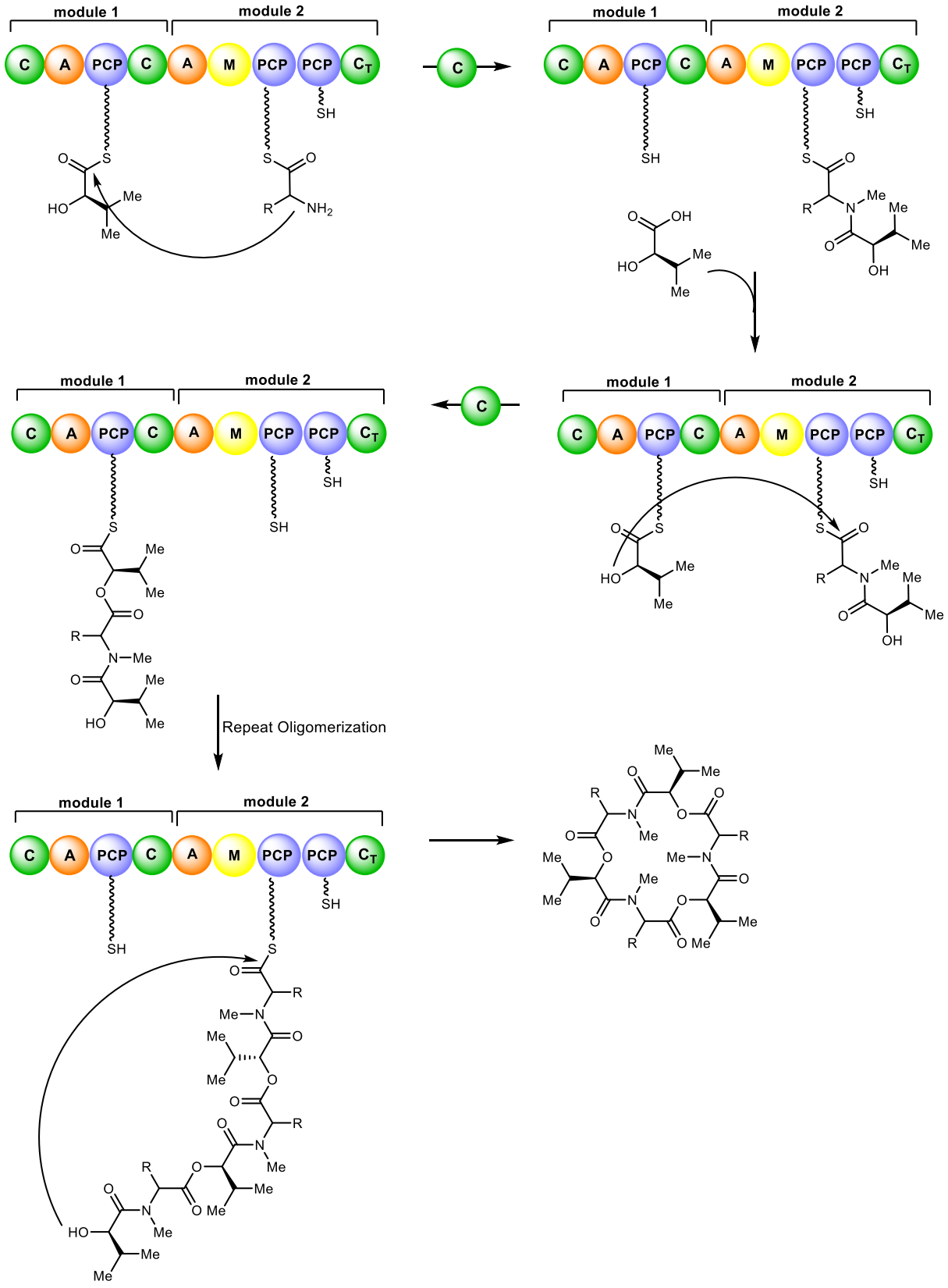

Many cyclic oligomeric depsipeptides are biosynthesized by the former pathway, including the enniatins, beauvericin,[37] and bassianolide,[50] all produced by bacterial NRPSs. The elongation cycle in these examples is unusual, in which two PCP domains alternate roles as acceptors and donors in condensation steps (Figure 7). In contrast to bacterial depsipeptides, the biosynthetic pathway in fungal depsipeptide synthetases is strikingly different for fungal cyclic oligomeric depsipeptides such as cereulide, valinomycin, and the antimycins, despite the chemical similarity between these compounds. In this synthetic pathway, ester bond formation is carried out through main chain hydroxyls originating from keto acid substrates.[34]

While there has been significant headway in the elucidation of biosynthetic pathways of depsipeptides, much remains to be discovered. Of note, are the unknown biosynthetic pathways for many fungal cyclic depsipeptides, including a compound of particular interest to the Johnston group: verticilide. The structural diversity of this class of natural products, as well as the increased interest in their pursuit as therapeutics will continue to drive the field to shed light on uncharacterized pathways. Continual knowledge gained from these biosynthetic pathways may also advance the chemical synthesis of many depsipeptides, as chemists find ways to replicate nature in their synthetic systems.

1.2.2 Chemical Synthesis of Depsipeptides

It has been said that the construction of ester bonds often constitutes the most challenging synthetic operation in efforts aimed at preparing complex natural products, and depsipeptides are no exception.[51] As ester bonds can be significantly prone to hydrolysis, synthetic methods often require their formation in a late-stage transformation. However, while nature does this well, final steps such as macrolactonization reactions are not a general synthetic solution in a chemist's hands. Furthermore, late-stage intermolecular ester couplings remain incredibly challenging in the steric and functionally rich environments that natural products provide, often requiring harsh conditions and elevated temperatures.[51] There are two major protocols that have been adopted for the chemical synthesis of depsipeptides: solid-phase synthesis and solution-phase synthesis. While solid-phase peptide synthesis is the current go-to method for the construction of many peptides, the solid-phase synthesis of depsipeptides is considerably more difficult. There are a variety of

[50] Xu, Y.; Orozco, R.; Kithsiri Wijeratne, E. M.; Espinosa-Artiles, P.; Leslie Gunatilaka, A. A.; Patricia Stock, S.; Molnár, I. *Fungal Genet. Biol.* **2009**, *46*, 353
[51] Tsakos, M.; Schaffert, E. S.; Clement, L. L.; Villadsen, N. L.; Poulsen, T. B. *Nat. Prod. Rep.* **2015**, *32*, 605

reasons surrounding this, a large one being the commercial availability of α-hydroxy acids. Many α-hydroxy acids are not naturally occurring and are either expensive or require multi-step syntheses to access, making solid phase synthesis in which a large excess of reagents is used unattractive. Additionally, there has been significantly less development of optimal protecting groups and coupling reagents for the formation of ester bonds compared to amide bonds. In many cases, removal of base-labile protecting groups has resulted in the epimerization of α-ester stereocenters, fragmentation through β-elimination, and the deprotection of acid-labile protecting groups has often resulted in hydrolysis of the ester bond.[52] With non-optimal coupling reagents, nucleophilic acyl substitution approaches are often unfeasible, due to the weak nucleophilicity of alcohols (Figure 8).

Figure 8. Nucleophilic acyl substitution approach to depsipeptide ester bond formation.

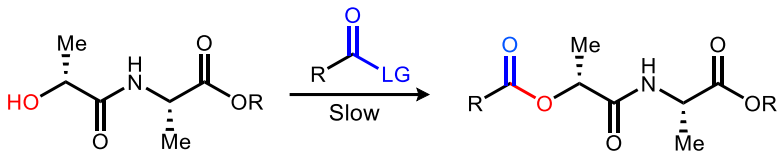

While this problem has been appreciated for decades, there is still not a single method of choice for solid phase depsipeptide synthesis. In fact, only a few examples exist in which all the ester bonds were formed on the resin, the most notable being Kuisle's synthesis of valinomycin.[53] More often than not, only the amide bonds of depsipeptides are formed on the resin, and the ester bond formation is carried out in solution. This approach has been used to access PF1022A, and emodepside.[54] These syntheses become even more complex when incorporating other variants, such as *N*-methyl amino acids, which generally lower yields and increase racemization. Due to a Thorpe-Ingold like effect, the incorporation of *N*-methyl peptides in depsipeptides can result in the decomposition to diketomorpholines, often resulting in cleavage from the resin (Figure 9). This has been observed in a variety of syntheses, including Lee's synthesis of PF1022A[55] and Bumpus's synthesis of angiotensin II.[56] Furthermore, in examples where ester bond formation on the resin

[52] Tulla-Puche, J.; Bayó-Puxan, N.; Moreno, J. A.; Francesch, A. M.; Cuevas, C.; Álvarez, M.; Albericio, F. *J. Am. Chem. Soc.* **2007**, *129*, 5322
[53] Kuisle, O.; Quiñoá, E.; Riguera, R. *J. Org. Chem.* **1999**, *64*, 8063
[54] Scherkenbeck, J.; Lüttenberg, S.; Ludwig, M.; Brücher, K.; Kotthaus, A. *Eur. J. Org. Chem.* **2012**, *2012*, 1546
[55] Lee, B. H. *Tetrahedron Lett.* **1997**, *38*, 757
[56] Khosla, M. C.; Smeby, R. R.; Bumpus, F. M. *J. Am. Chem. Soc.* **1972**, *94*, 4721

Figure 9. SPPS with N-methyl amino acids, often results in decomposition to diketomorpholines and cleavage from the resin

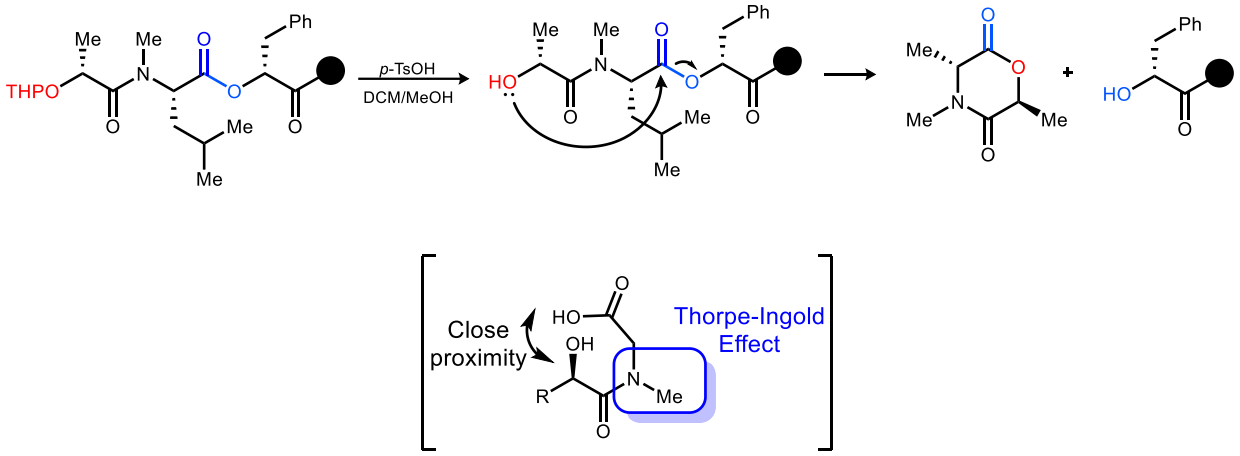

was accomplished, it is often only with 1-2 ester residues. Kuise and coworkers demonstrated this with their incorporation of 2 ester bonds into a peptide on a Wang Resin using DIC and DMAP.[53] Spengler and coworkers also devised a machine-assisted protocol to synthesize a family a depsipeptides, reaching up to 6 ester substitutions. It was at the expense of yield, however, accessing the final product in only 7% total yield.[57] It was only recently that a synthesis of a depsipeptide with regular alternating esters was accomplished via solid phase in moderate yields of 30-40% (Figure 10).[58] Even so, this work still only formed the amide bonds on resin and required solution phase couplings of each depsipeptide unit, an arduous task if incorporating different depsipeptide monomers. Furthermore, difficulties often encountered with Fmoc removal were still prevalent – a huge drawback considering the number of commercially available Fmoc-protected residues. In 2020, Puche and coworkers developed the first solid-phase synthesis route that circumvented common problems encountered with Fmoc protecting groups, by adding small percentages of organic acids to the Fmoc removal conditions (Figure 11). This methodology allowed for an exclusively solid-phase stepwise synthesis of a highly complex depsipeptide, all with Fmoc protected residues in an overall 22% yield.[59]

[57] Spengler, J.; Koksch, B.; Albericio, F. *Pept. Sci.* **2007**, *88*, 823
[58] Nguyen, M. M.; Ong, N.; Suggs, L. *Org. Biomol. Chem.* **2013**, *11*, 1167
[59] Lobo-Ruiz, A.; Tulla-Puche, J. *Eur. J. Org. Chem.* **2020**, *2020*, 183

Figure 10. SPPS method for the synthesis of depsipeptides.

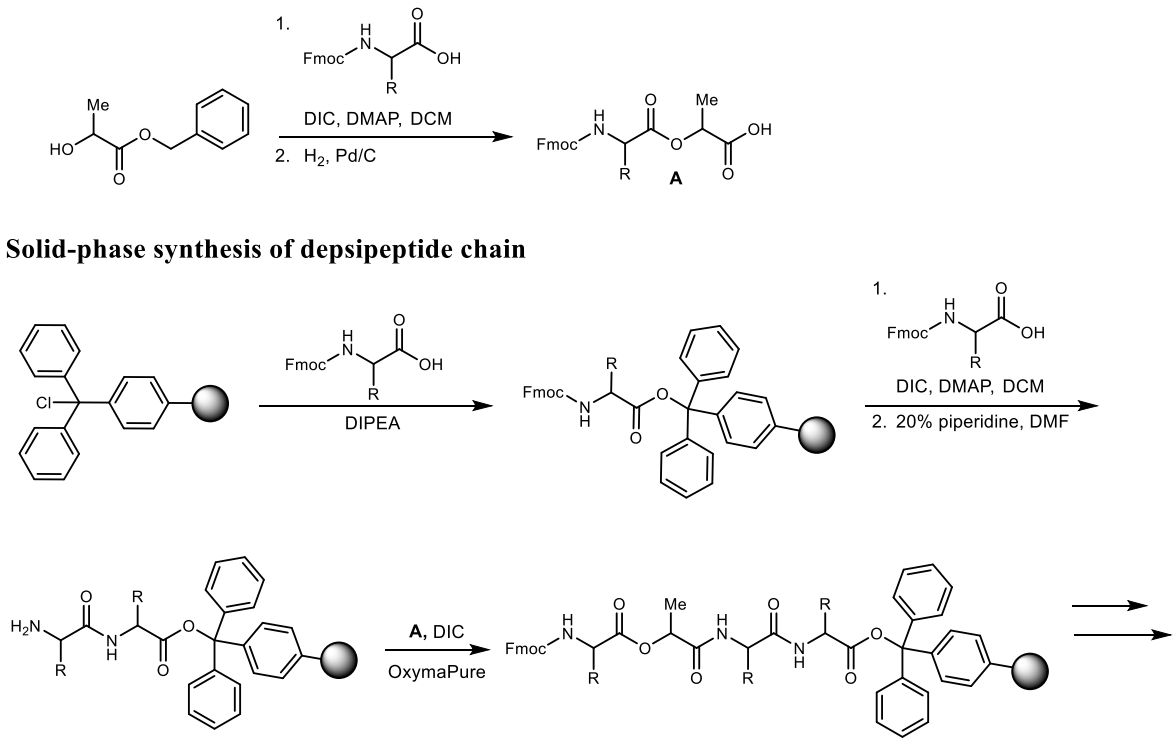

Figure 11. Complex depsipeptide synthesized exclusively in solid phase by Puche and coworkers

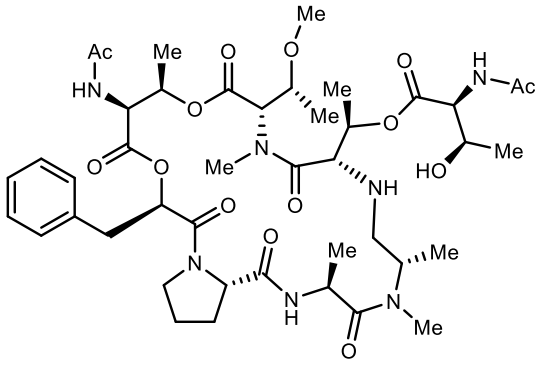

The difficulty of these synthesis of complex depsipeptides is perhaps best highlighted by YM-254890 (Figure 12). After discovering the potential biological activity of this naturally occurring depsipeptides, a contest was launched in 2005, offering a $100,000 reward to anyone who could synthesize at least 1 mg of the compound. However, out of the 228 participants, nobody succeeded.

It took until 2016 for the first total synthesis of YM-254890 to be achieved, using a combined approach of solid-phase and solution phase synthesis.[60] Today, combined strategies like this are considered the best alternative for the large-scale synthesis of peptide-based Active Pharmaceutical Ingredients (APIs) in the pharmaceutical industry.[61]

Figure 12. Naturally occurring cyclodepsipeptide YM-254890.

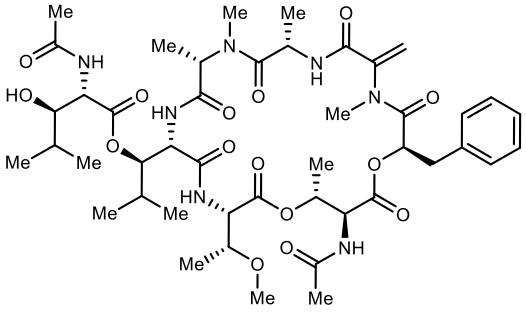

In solution phase synthesis, formation of the ester bond has been accomplished in a variety of different ways yet is almost always empirically determined on a case-by-case basis, as what works in some synthetic routes does not work in others. Generally, all the established chemical methods attempt to generate the ester bond through a dehydrative merger of a carboxylic acid and an alcohol. This is largely achieved through the activation of the carboxylate functionality, with few examples stemming from activation of the alcohol functionality. Classic modes of activation include acyl halides, carbodiimides, Yamaguchi anhydrides, Mitsunobu couplings, and occasionally ketene intermediates. Other methods such as ligation chemistry and a variety of traditional peptide coupling reagents have been utilized as well, though less frequently. It is also of note that there has been a significant amount of success with biomimetic strategies, such as those involving thioester intermediates, in macrolactonization chemistry.[62,63,64] This has not, however, been widely applied in intermolecular ester formation.

[60] Xiong, X.-F.; Zhang, H.; Underwood, C. R.; Harpsøe, K.; Gardella, T. J.; Wöldike, M. F.; Mannstadt, M.; Gloriam, D. E.; Bräuner-Osborne, H.; Strømgaard, K. *Nat. Chem.* **2016**, *8*, 1035
[61] Ferguson, J.R., et al. *Chem. Today* **2019**, 37, 48–52
[62] Corey, E. J.; Brunelle, D. J. *Tetrahedron Lett.* **1976**, *17*, 3409
[63] Corey, E. J.; Clark, D. A. *Tetrahedron Lett.* **1979**, *20*, 2875
[64] Corey, E. J.; Nicolaou, K. C. *J. Am. Chem. Soc.* **1974**, *96*, 5614

Acyl halide activation is largely accomplished by *in situ* formation of acyl fluorides (Figure 13). While acyl chlorides would be a preferred approach due to their ease to access, they are often incompatible with depsipeptide chemistry due to the formation of acidic byproducts when generated with reagents like thionyl chloride or phosphorous chloride.[65] Additionally, acid chlorides are prone to hydrolysis or racemization under basic conditions required for most

Figure 13. Fluorinating agents used for acyl halide synthesis.

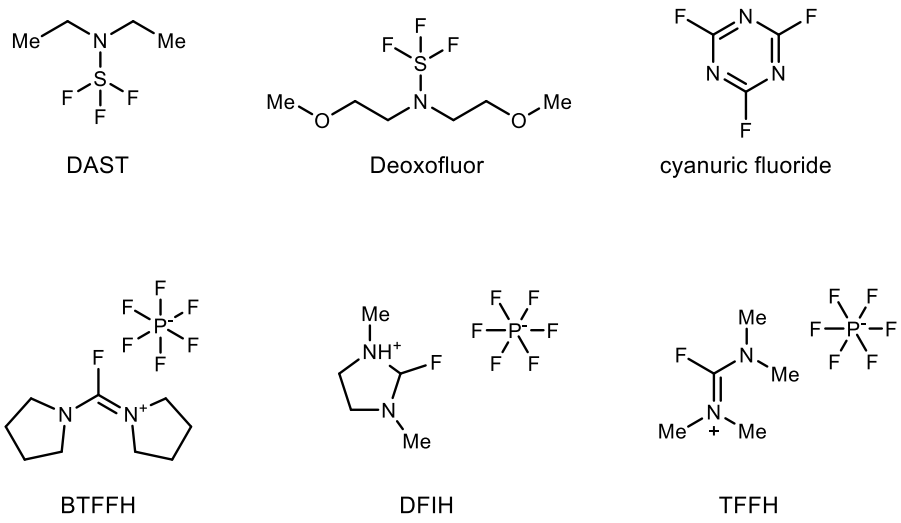

peptide couplings. Acyl fluoride species are less sensitive to moisture and are compatible with acid labile protecting groups. Due to their in-situ formation, acyl fluorides are also less prone to racemization problems.[66] With the emergence of new methods over the last few decades, acyl halide activation has seen less application, but can still be of use when other methods fail - a notable example of that being the synthesis of halipeptin A.[67]

Carbodiimide activation is one of the most employed activation methods for ester bond formation, first demonstrated by Steglich with the use of DCC and DMAP.[68] Since then, a variety of different carbodiimide reagents have been developed with more favorable properties, such as EDC, a water-soluble alternative that tremendously simplifies purification. DIC has also been employed frequently in solid phase depsipeptide synthesis due to its better solubility in organic

[65] M. F. Antell, in The Chemistry of Acyl Halides, ed. S. Patai, Interscience, London, 1972, pp. 35–68
[66] Jedrzejczak, M.; Motie, R. E.; Satchell, D. P. N.; Satchell, R. S.; Wassef, W. N. *Journal of the Chemical Society, Perkin Transactions 2* **1994**, 1471
[67] Yu, S.; Pan, X.; Lin, X.; Ma, D. *Angew. Chem. Int. Ed.* **2005**, *44*, 135
[68] Neises, B.; Steglich, W. *Angew. Chem. Int. Ed.* **1978**, *17*, 522

solvents. Carbodiimide activation occurs through an O-acylisourea, and one of the disadvantages of this mode of activation is the possibility of rearrangement to form an N-acylurea byproduct. Due to alcohols being weaker nucleophiles than amines, in esterification reactions, a significant amount of this by-product can be observed. There has been success in mitigating some of the N-acylurea byproduct with additives, such as DMAP, HOBt, and HOAt (Figure 14).[69,70] There have been several successful syntheses of depsipeptides that have incorporated carbodiimide activation, including the Boger synthesis of romoplanin,[71] the Pelay-Dimeno sythnesis of pipecolidepsin A,[72] the Nevado synthesis of iriomoteolide-3a.[73]

Figure 14. Carbodiimide intermediate and rearrangement product, alongside of common suppressing additives

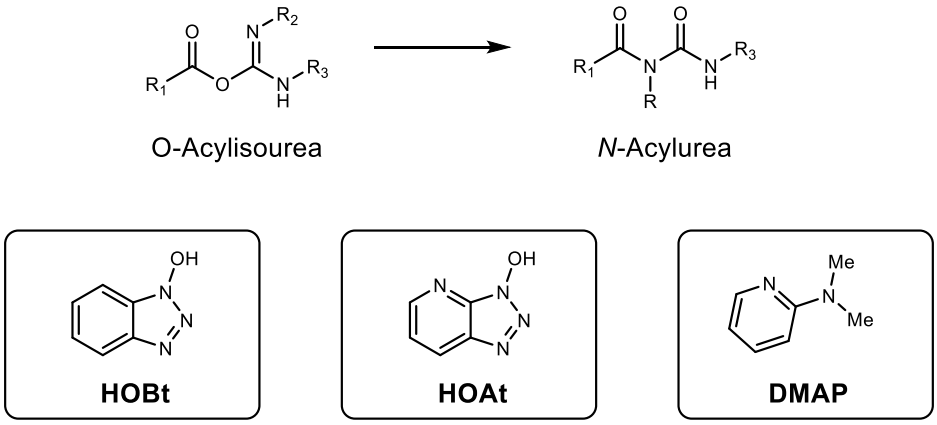

In 1979, Yamaguchi and coworkers developed the formation of an ester via alcoholysis of a mixed anhydride formed with 2,4,6-trichlorobenzoyl chloride (TCBC), now well-known as the Yamaguchi coupling reaction.[74] This mixed anhydride can be formed and isolated, or generated in-situ. This method of activation is reported to be applicable to primary, secondary, and tertiary alcohols, but has predominantly gained widespread application in macrolactonization

[69] Morales-Serna, J. A.; Vera, A.; Paleo, E.; García-Ríos, E.; Gaviño, R.; García de la Mora, G.; Cárdenas, J. *Synthesis* **2010**, *2010*, 4261
[70] Carpino, L. A. *J. Am. Chem. Soc.* **1993**, *115*, 4397
[71] Jiang, W.; Wanner, J.; Lee, R. J.; Bounaud, P.-Y.; Boger, D. L. *J. Am. Chem. Soc.* **2003**, *125*, 1877
[72] Pelay-Gimeno, M.; García-Ramos, Y.; Jesús Martin, M.; Spengler, J.; Molina-Guijarro, J. M.; Munt, S.; Francesch, A. M.; Cuevas, C.; Tulla-Puche, J.; Albericio, F. *Nat. Commun.* **2013**, *4*, 2352
[73] Cribiú, R.; Jäger, C.; Nevado, C. *Angew. Chem. Int. Ed.* **2009**, *48*, 8780
[74] Junji, I.; Kuniko, H.; Hiroko, S.; Tsutomu, K.; Masaru, Y. *Bull. Chem. Soc. Jpn.* **1979**, *52*, 1989

chemistry.[75] Since 1979, a variety of different Yamaguchi reagent modifications have been made to help improve chemoselectivity (MNBA), provide a less sterically hindered option (benzoyl chloride), and options that allow for mild reaction conditions (MNBA) as well as more controllable reactivity (TCE-DMAP) (Figure 15).[76,77,78]

Figure 15. Yamaguchi esterification reagents.

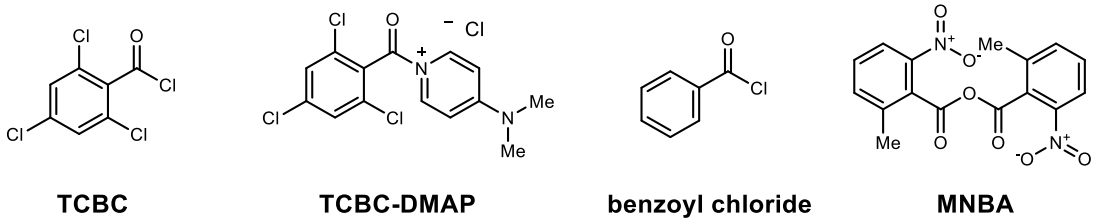

The Mitsunobu reaction is one of the examples in which the alcohol reactant is activated towards nucleophilic attack, in contrast to the carboxylic acid in most traditional activation methods. When chiral alcohols are utilized, the reaction normally proceeds with inversion of

Figure 16. Mitsunobu esterification azodicarboxylate reagents.

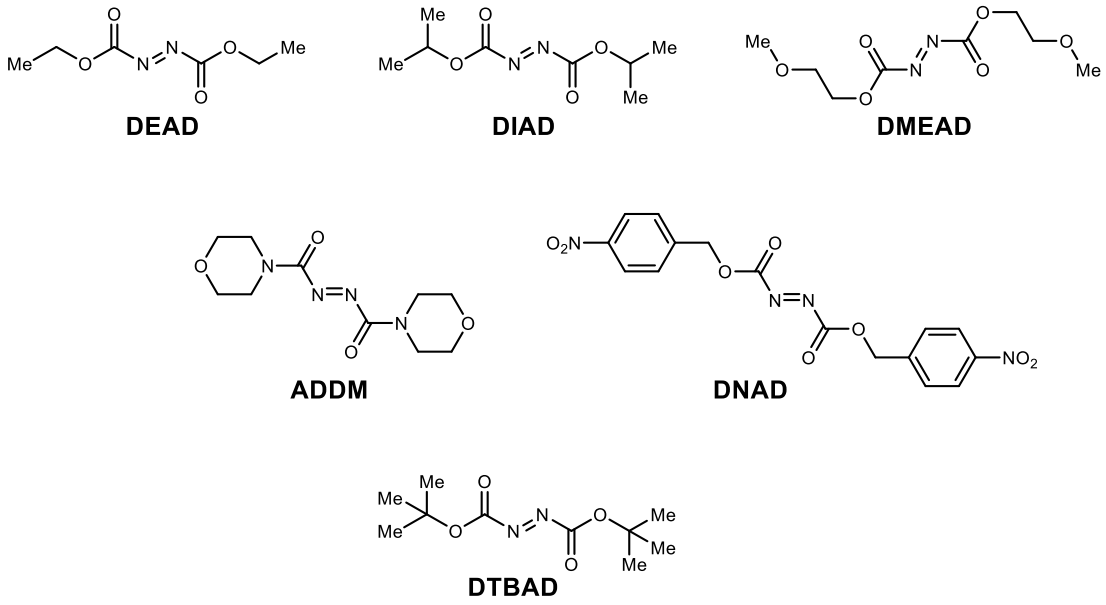

[75] Parenty, A.; Moreau, X.; Niel, G.; Campagne, J. M. *Chem. Rev.* **2013**, *113*, PR1
[76] Dhimitruka, I.; SantaLucia, J. *Org. Lett.* **2006**, *8*, 47
[77] El-Mekabaty, A. *Synth. Commun.* **2014**, *44*, 1
[78] Isamu, S.; Ryoutarou, I.; Mari, K. *Chem. Lett.* **2002**, *31*, 286

stereochemistry, with rare cases of retention with sterically hindered alcohols. While a useful approach, a significant downside of the reaction is difficulty with purification, largely due to the azodicarboxylates and their hydrazine by-products. To this end, several reports for alternative azodicarboxylates exist (Figure 16), in which the byproducts can be removed via an aqueous workup or filtration.[79,80,81,82] A Mitsunobu activation approach was taken with the Simon synthesis of depsipeptide FK228,[83] as well as the Johnston synthesis of the depsipeptide verticilide.[84]

1.2.3 Synthesis of α-Hydroxy Acids

A key component of the synthesis of depsipeptides involves the synthesis of their precursor components: amino acids and α-hydroxy acids. While a large body of work has been developed over the last decade towards the synthesis of enantioenriched unnatural amino acids, synthetic work with their counterparts, α-hydroxy acids has been less intense (Figure 17). Most often, chiral α-hydroxy acids are accessed via multi-step conversions of ester precursors. Two of the most frequently employed approaches are alpha oxidation, with stereo-control either from a chiral auxiliary such as Evan's oxazolidinones,[85,86,87,88] or the use of a chiral oxidant such as Davis's chiral oxaziridine.[89,90] Another well-known approach is diazotization chemistry, allowing access of α-hydroxy acids from α-amino acid precursors.[91] This methodology has been applied to access all of the hydroxy acid variants of naturally occurring amino acids but has been largely limited to amino acids that are commercially available. Asymmetric reduction of α-keto esters/acids is also prevalent, largely inspired by nature's synthesis of α-hydroxy acids and carried out mostly through enzymatic catalysis.[92,93] The direct asymmetric reduction of α-keto acids chemically is rare, with

[79] Hagiya, K.; Muramoto, N.; Misaki, T.; Sugimura, T. *Tetrahedron* **2009**, *65*, 6109
[80] Lanning, M. E.; Fletcher, S. *Tetrahedron Lett.* **2013**, *54*, 4624
[81] Yang, J.; Dai, L.; Wang, X.; Chen, Y. *Tetrahedron* **2011**, *67*, 1456
[82] Iranpoor, N.; Firouzabadi, H.; Khalili, D. *Org. Biomol. Chem.* **2010**, *8*, 4436
[83] Li, K. W.; Wu, J.; Xing, W.; Simon, J. A. *J. Am. Chem. Soc.* **1996**, *118*, 7237
[84] a) Original Manuscript: Batiste, S. M.; Johnston, J. N. *Proc. Natl. Acad. Sci. U. S. A.* **2016**, *113*, 14893 b) Correction Issued to Manuscript: *Proc. Natl. Acad. Sci. U. S. A.* **2021**, *118*, e2110836118
[85] Chang, J.-W.; Jang, D.-P.; Uang, B.-J.; Liao, F.-L.; Wang, S.-L. *Org. Lett.* **1999**, *1*, 2061
[86] Camps, P.; Pérez, F.; Soldevilla, N. *Tetrahedron: Asymmetry* **1997**, *8*, 1877
[87] Basavaiah, D.; Krishna, P. R. *Tetrahedron* **1995**, *51*, 12169
[88] Dubé, D.; Deschênes, D.; Tweddell, J.; Gagnon, H.; Carlini, R. *Tetrahedron Lett.* **1995**, *36*, 1827
[89] Vilaivan, T.; Bhanthumnavin, W. *Molecules* **2010**, *15*, 917
[90] Davis, F. A.; Sheppard, A. C.; Chen, B. C.; Haque, M. S. *J. Am. Chem. Soc.* **1990**, *112*, 6679
[91] Deechongkit, S.; You, S.-L.; Kelly, J. W. *Org. Lett.* **2004**, *6*, 497
[92] Lüttenberg, S.; Ta, T. D.; von der Heyden, J.; Scherkenbeck, J. *Eur. J. Org. Chem.* **2013**, *2013*, 1824
[93] Hoyos, P.; Sinisterra, J.-V.; Molinari, F.; Alcántara, A. R.; Domínguez de María, P. *Acc. Chem. Res.* **2010**, *43*, 288

only a few examples and limited substrate scopes.[94,95,96] The difficulty of this reaction stems from the ability of carboxylic acids to competitively bind to metal centers, often leading to deactivation. Additionally, the α-hydroxy acid product can serve as a ligand itself, making release from the catalyst difficult.[94] Other methods utilized to synthesis α-hydroxy acids include cyanohydrin formation followed by hydrolysis,[97,98,99] alkylation of glycolate

Figure 17. Traditional synthetic routes to access enantio-enriched α-hydroxy acids.

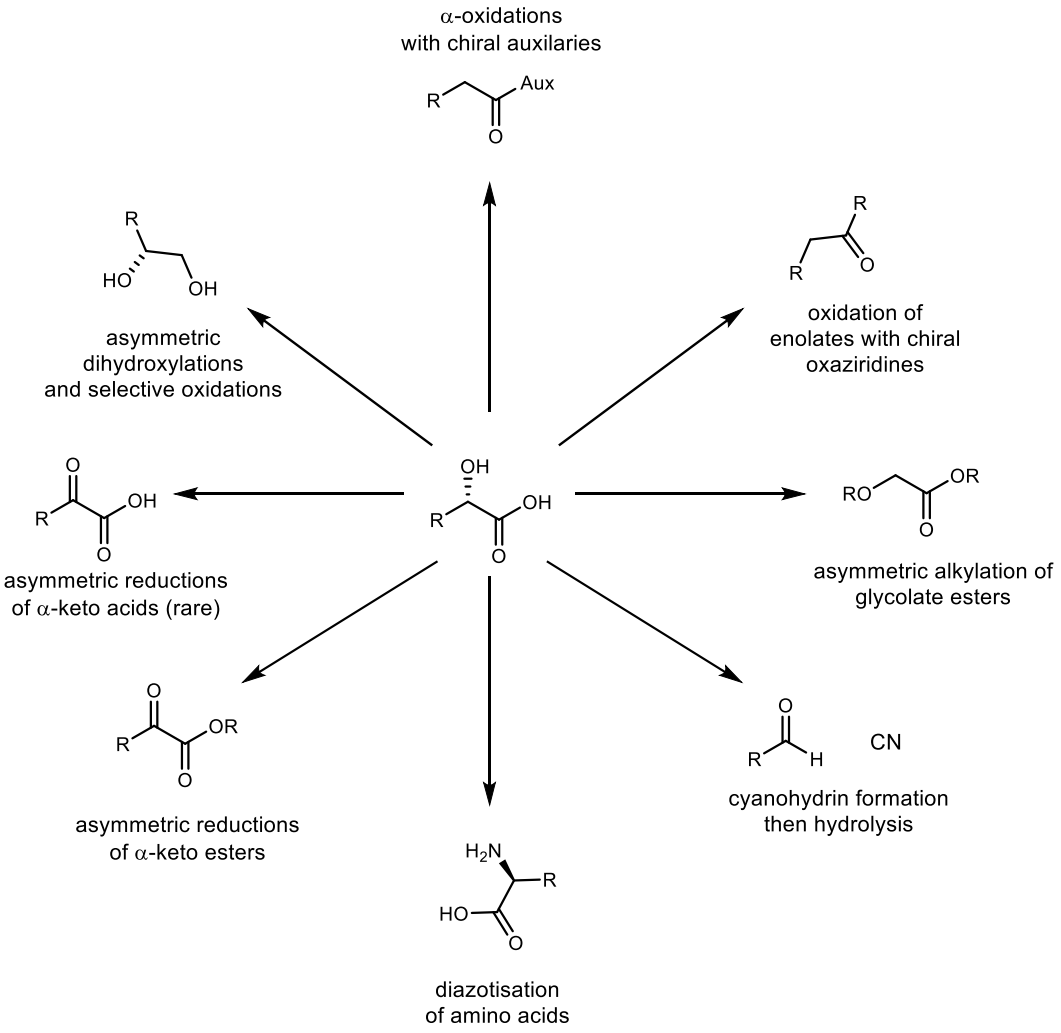

[94] Yan, P.-C.; Xie, J.-H.; Zhang, X.-D.; Chen, K.; Li, Y.-Q.; Zhou, Q.-L.; Che, D.-Q. *Chem. Commun.* **2014**, *50*, 15987
[95] Zhu, L.; Chen, H.; Meng, Q.; Fan, W.; Xie, X.; Zhang, Z. *Tetrahedron* **2011**, *67*, 6186
[96] Zhu, L.; Meng, Q.; Fan, W.; Xie, X.; Zhang, Z. *J. Org. Chem.* **2010**, *75*, 6027
[97] Hamashima, Y.; Sawada, D.; Kanai, M.; Shibasaki, M. *J. Am. Chem. Soc.* **1999**, *121*, 2641
[98] Kurono, N.; Arai, K.; Uemura, M.; Ohkuma, T. *Angew. Chem. Int. Ed.* **2008**, *47*, 6643
[99] Wang, W.; Liu, X.; Lin, L.; Feng, X. *Eur. J. Org. Chem.* **2010**, *2010*, 4751

esters,[100,101] and dihydroxylation of alkenes[102] followed by selective oxidation. Progress has been made in the asymmetric variants of these reactions, albeit with limited scope and applicability. Overall, ways to access α-hydroxy acids directly from their carboxylic acid counterparts is rare, and a survey of the current literature highlights the need and opportunity for continued development in this area.

1.3 Mitsunobu-Based Synthesis of Depsipeptides – A Total Synthesis of Verticilide

Keeping some of these synthetic challenges in mind, Batiste and Johnston developed a new streamlined synthesis of cyclic oligomeric depsipeptides, specifically en route to the synthesis of the natural product verticilide.[103] Batiste developed a 6-step synthesis to verticilide (Scheme 1), leveraging Umpolung Amide Synthesis (UmAS) and a macrocyclooligomerization (MCO) reaction.[84] The synthesis began with commercially available 5-hexynal (**1**), which is subjected to an enantioselective Henry reaction with bromonitromethane using the Blay ligand.[104] The formed secondary alcohol is then carried forward in crude form and protected as the methoxymethylene ether. Bromonitroalkane **2** is then subjected to UmAS reaction conditions to form a didepsipeptide

Scheme 1. Synthesis of the didepsipeptide monomer using an enantioselective Henry reaction.

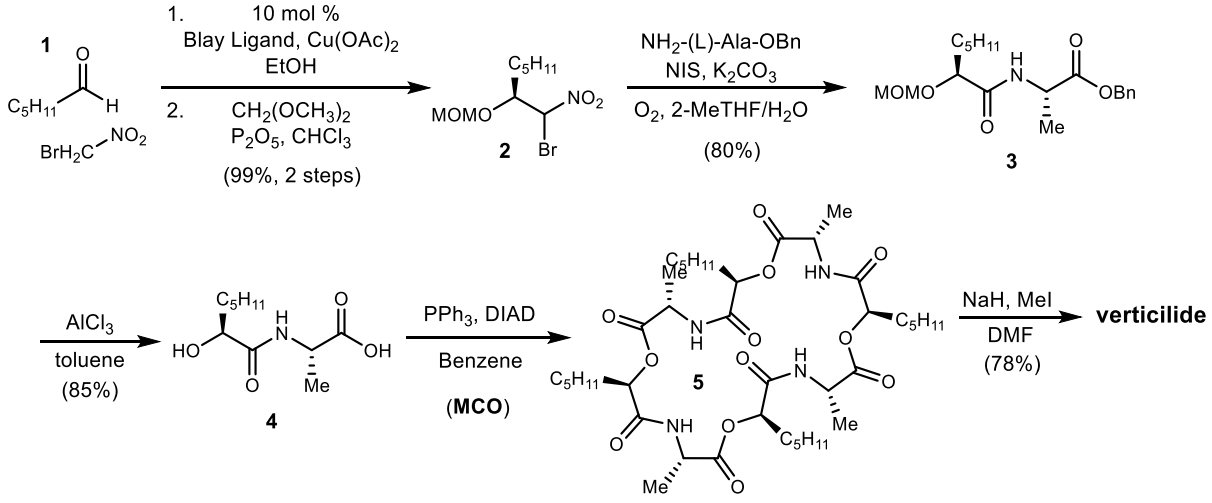

[100] Jung, J. E.; Ho, H.; Kim, H.-D. *Tetrahedron Lett.* **2000**, *41*, 1793
[101] Andrus, M. B.; Hicken, E. J.; Stephens, J. C.; Bedke, D. K. *J. Org. Chem.* **2005**, *70*, 9470
[102] Lohray, B. B.; Bhushan, V.; Krishna Kumar, R. *J. Org. Chem.* **1994**, *59*, 1375
[103] Monma, S.; Sunazuka, T.; Nagai, K.; Arai, T.; Shiomi, K.; Matsui, R.; Ōmura, S. *Org. Lett.* **2006**, *8*, 5601
[104] Blay, G.; Domingo, L. R.; Hernández-Olmos, V.; Pedro, J. R. *Chem. Eur. J.* **2008**, *14*, 4725

in just three steps. Following a global deprotection, depsipeptide **4** is subjected to an oligomerization/macrocyclization reaction. This reaction is carried out under Mitsunobu reaction conditions, where the depsipeptide oligomerizes and then cyclizes. Aside from the 24-membered ring (*N*-H precursor to verticilide), this oligomerization reaction produces other ring sizes in a single reaction, including 18-membered and 30-membered macrocycles. Once isolated, the 24-membered ring is then subjected to a final *N*-permethylation step to afford the natural product, verticilide in a 78% yield.

This developed methodology has several key advantages for the synthesis of depsipeptides. First, by utilizing Umpolung Amide Synthesis to form the amide bond, the possibility of epimerization of the alpha carbon is mechanistically avoided. This is accomplished by forgoing the use of an active ester intermediate. Compared to traditional amide bond synthesis, the polarity of Umpolung Amide Synthesis is reversed. In this case, the nitroalkane is acting as an acyl anion equivalent, and the nucleophilic component of the reaction. The same traditional amine feedstock is used but is now activated as the electrophile through a halonium ion. UmAS was developed in the Johnston lab in 2010,[105] and since then has been the topic of many studies within the group. Notably this includes extensive mechanistic work recently completely by Michael Crocker.[106] Mechanistically, UmAS starts with deprotonation of the nitroalkane to form the nitronate. The nitronate then attacks the haloamine to form the tetrahedral intermediate. Finally, the tetrahedral intermediate collapses to form the amide bond, through either an aerobic or anerobic pathway (Figure 18). The second advantage of this methodology was the development of the macrocyclization oligomerization reaction. Instead of employing a traditional approach of chain elongation through condensative couplings, the elongation steps and cyclization are accomplished all in one step. This allows for a drastically reduced step-count, and rapid access to analogues. Furthermore, the reaction produces numerous ring sizes in a single reaction, as well as allows for easy variation of the starting materials both structurally and stereochemically. Quick access to diversity and complex natural products makes this methodology attractive from a drug discovery point of view. Furthermore, Batiste reported the ability to shift the macrocycle size distribution by changing the starting monomer size, or by employing salts in the reaction for a templating effect,

[105] Shen, B.; Makley, D. M.; Johnston, J. N. *Nature* **2010**, *465*, 1027
[106] Crocker, M. S.; Foy, H.; Tokumaru, K.; Dudding, T.; Pink, M.; Johnston, J. N. *Chem* **2019**, *5*, 1248

allowing for an unusual amount of selectivity in an oligomerization reaction.[107] Finally, installing the *N*-methyl groups in the final step of the synthesis bypasses many of the difficulties encountered when working with *N*-methyl peptides.

Figure 18. Umpolung Amide Synthesis mechanism.

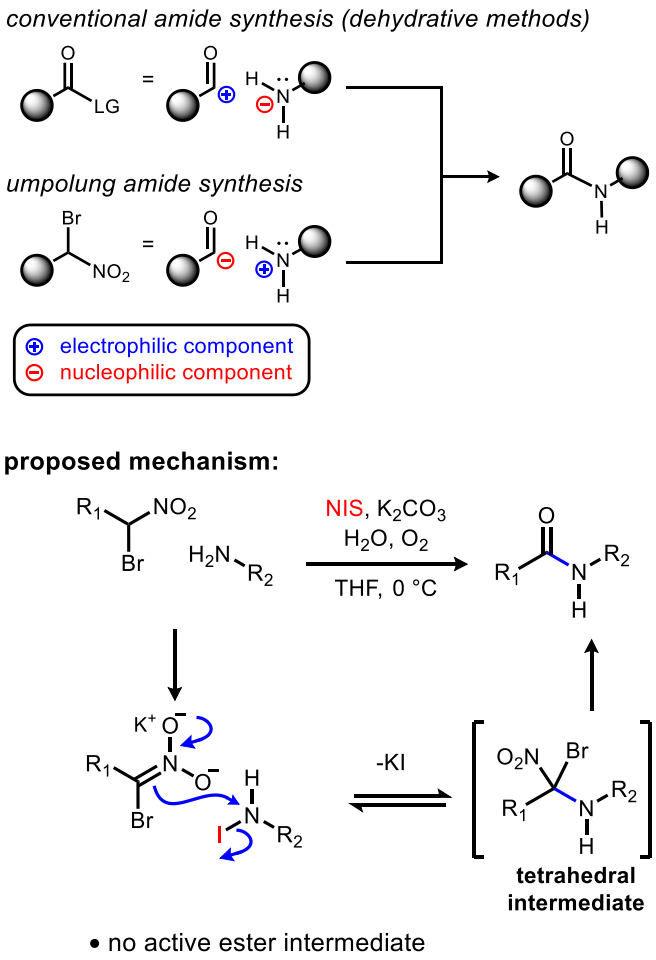

1.4 Oligomerization Reactions in Cyclic Peptide and Depsipeptide Synthesis

While the macrocyclooligomerization reaction was the first approach to provide rapid access to collections of natural product-like macrocycles, this work was inspired by other pioneers in the area. Esterification reactions of activated hydroxy acids have been used previously to access

[107] a) Original Manuscript: Batiste, S. M.; Johnston, J. N. *J. Am. Chem. Soc.* **2018**, *140*, 4560 b) Correction issued to original manuscript: Batiste, S. M.; Johnston, J. N. *J. Am. Chem. Soc.* **2021**, *143*, 6701

diolides, triolides, and oligolides.[108,109,110,111,112,113,114] Amidation reactions of activated polypeptides have also been commonly employed including Rothe and Kress's synthesis of valinomycin[115,116] (Figure 19) and Wipf and coworker's synthesis of westiellamide (Figure 20).[117,118] However, each of these syntheses presented challenges, including low yields, little selectivity, epimerization, and side reactions such as elimination, resulting from the slow reaction of a sterically hindered alcohol. A common feature of amidation oligomerizations is a five-membered heterocycle, such as a thiazole, oxazole, or furan incorporated into the peptide

Figure 19. Rothe and Kress's oligomerization approach to the synthesis of valinomycin.

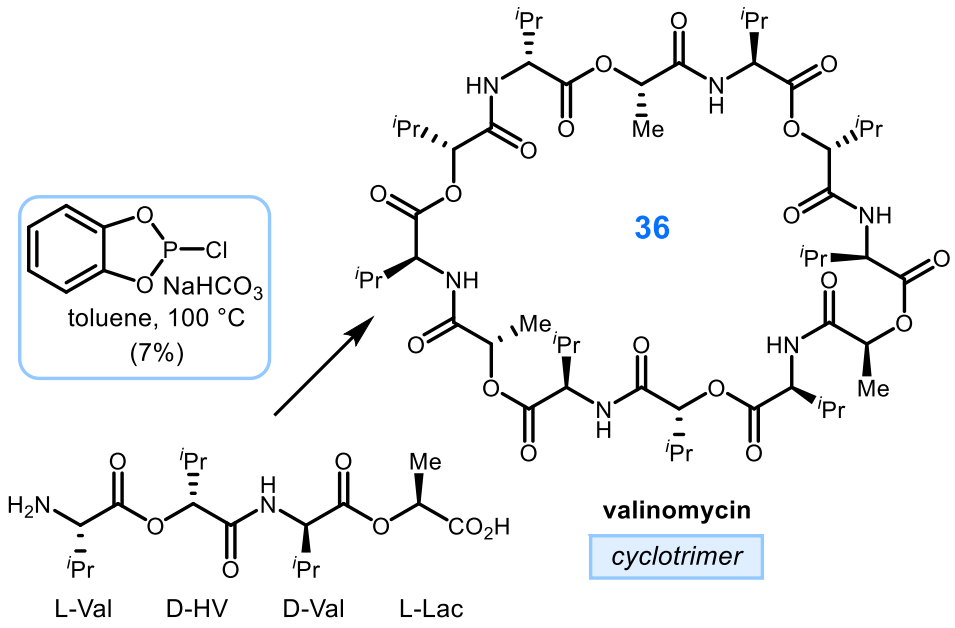

[108] Su, Q.; Beeler, A. B.; Lobkovsky, E.; Porco, J. A.; Panek, J. S. *Org. Lett.* **2003**, *5*, 2149
[109] Beeler, A. B.; Acquilano, D. E.; Su, Q.; Yan, F.; Roth, B. L.; Panek, J. S.; Porco, J. A. *J. Comb. Chem.* **2005**, *7*, 673
[110] Burke, S. D.; Heap, C. R.; Porter, W. J.; Song, Y. *Tetrahedron Lett.* **1996**, *37*, 343
[111] Burke, S. D.; McDermott, T. S.; O'Donnell, C. J. *J. Org. Chem.* **1998**, *63*, 2715
[112] Burke, S. D.; O'Donnell, C. J.; Porter, W. J.; Song, Y. *J. Am. Chem. Soc.* **1995**, *117*, 12649
[113] Barth, R.; Mulzer, J. *Angew. Chem. Int. Ed.* **2007**, *46*, 5791
[114] Mulzer, J.; Berger, M. *J. Org. Chem.* **2004**, *69*, 891
[115] Rothe, M.; Kreiss, W. *Angew. Chem. Int. Ed.* **1973**, *12*, 1012
[116] Rothe, M.; Kreiss, W. *Angew. Chem. Int. Ed.* **1977**, *16*, 113
[117] Wipf, P.; Miller, C. P.; Grant, C. M. *Tetrahedron* **2000**, *56*, 9143
[118] Wipf, P.; Miller, C. P. *J. Am. Chem. Soc.* **1992**, *114*, 10975

Figure 20. Wipf and co-worker's oligomerization approach to westiellamide.

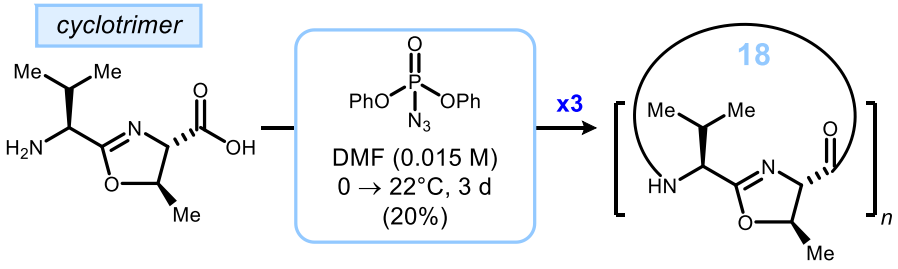

backbone (Figure 22).[119,120,121,122,123,124,125,126] This presumably enhances a conformation more favorable for cyclization. Additionally, these examples all required pre-activation of the acid and long reaction times. While most of this work has been carried out on primary amines, there are rare successful examples of oligomerization with a disubstituted amine (Figure 21).[127]

Figure 21. Example of amidation oligomerization with a disubstituted amine.

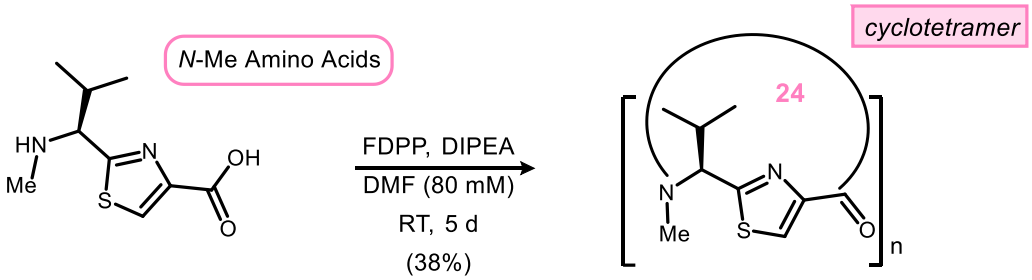

Wilson, C. *Tetrahedron,* **2005**, *61*, 1257

[119] Jayaprakash, S.; Pattenden, G.; Viljoen, M. S.; Wilson, C. *Tetrahedron* **2003**, *59*, 6637
[120] Bertram, A.; Blake, A. J.; Turiso, F. G.-L. d.; Hannam, J. S.; Jolliffe, K. A.; Pattenden, G.; Skae, M. *Tetrahedron* **2003**, *59*, 6979
[121] Bertram, A.; Pattenden, G. *Nat. Prod. Rep.* **2007**, *24*, 18
[122] Singh, Y.; Sokolenko, N.; Kelso, M. J.; Gahan, L. R.; Abbenante, G.; Fairlie, D. P. *J. Am. Chem. Soc.* **2001**, *123*, 333
[123] Sokolenko, N.; Abbenante, G.; Scanlon, M. J.; Jones, A.; Gahan, L. R.; Hanson, G. R.; Fairlie, D. P. *J. Am. Chem. Soc.* **1999**, *121*, 2603
[124] Bertram, A.; Hannam, J. S.; Jolliffe, K. A.; González-López de Turiso, F.; Pattenden, G. *Synlett* **1999**, *1999*, 1723
[125] Chakraborty, T. K.; Tapadar, S.; Raju, T. V.; Annapurna, J.; Singh, H. *Synlett* **2004**, *2004*, 2484
[126] Black, R. J. G.; Dungan, V. J.; Li, R. Y. T.; Young, P. G.; Jolliffe, K. A. *Synlett* **2010**, *2010*, 551
[127] Dudin, L.; Pattenden, G.; Viljoen, M. S.; Wilson, C. *Tetrahedron* **2005**, *61*, 1257

Figure 22. Representative examples of amidation cyclooligomerization reactions.

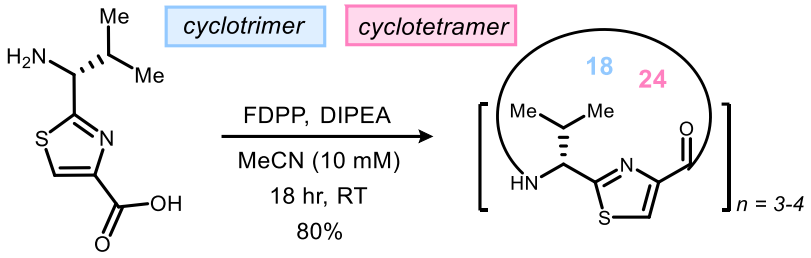

Pattenden, G. *Synlett* **1999**, *1999*, 1723.

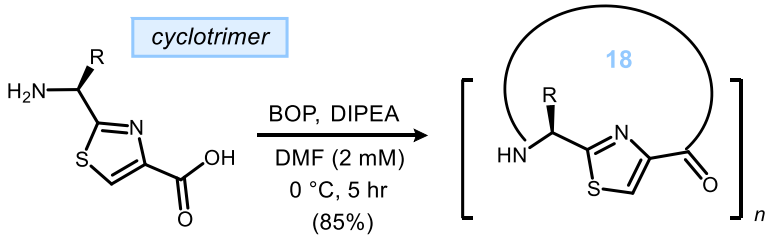

Fairlie, D. P. *J. Am. Chem. Soc*. **2001**, *123*, 333.

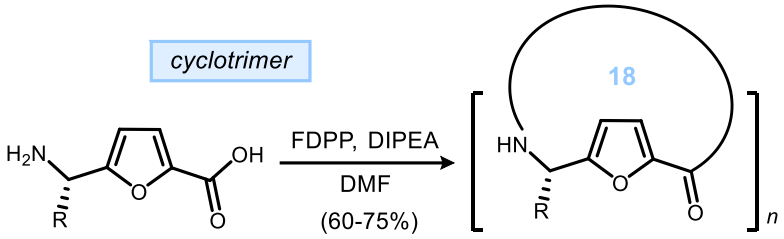

Singh, H. *Synlett* **2004**, *2004*, 2484

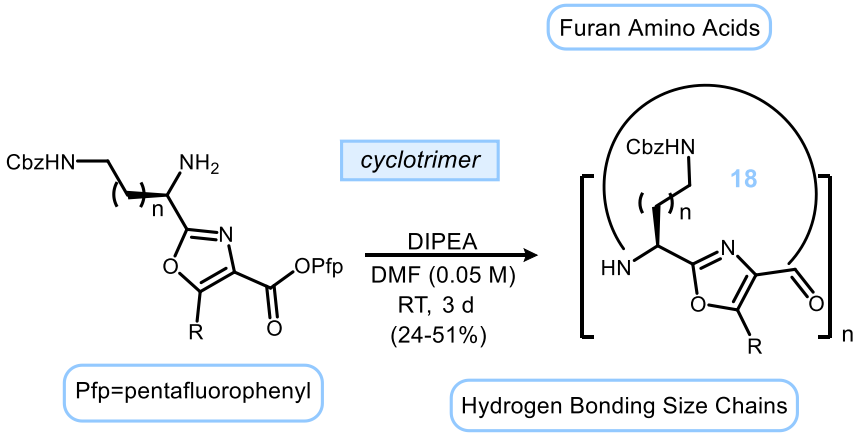

Jolliffe, K. A. *Synlett,* **2010**, *2010*, 551

1.5 Re-exploration of the Macrocyclooligomerization Reaction

We were initially interested in exploring ring size as a parameter to modulate biological activity. The MCO chemistry that was previously developed offered a unique platform to do so – specifically to access larger ring sizes, like a 36-membered ring, that are traditionally difficult to synthesize. I began by working to synthesize larger amounts of all the previously reported ring sizes (18-, 24-, 30-, and 36 – membered rings) to carry them through the final *N*-permethylation stage. When running these initial macrocyclization reactions with the didepsipeptide, only three ring sizes were observed instead of the four that were originally reported. These were initially determined to be 24-, 30-, and 36- membered rings based on previous characterization data. However, the 18- and 36-membered rings were reported to have the same retention time by HPLC, making it difficult to ascertain which one was forming. It is important to note, that the original assignments to these ring sizes were made based on fractionation in the workflow of purification, and the observation of the corresponding mass ions, albeit with relatively weak intensity. Due to these compounds being oligomeric by nature, symmetry is displayed in the ^{1}H and ^{13}C NMRs, making this data of little use in the characterization of which ring size has formed. This fractionation in the purification consisted of a silica plug run with varying amounts of methanol in dichloromethane (Table 1). The eluent was collected as three separate fractions, and it was reported that fraction 1 contained Mitsunobu by-products, fraction 2 contained the 18-, 24-, and 30-membered rings, and fraction 3 contained the 36-membered ring.

Table 1. Silica plug purification of crude MCO reaction mixtures (prior work).

Fraction	% MeOH	% DCM	Amount
1	0.5%	99.5%	50 mL
1	1%	99%	50 mL
2	2%	98%	50 mL
2	3%	97%	100 mL
3	20%	80%	100 mL

When re-examining the reaction conditions, it first appeared that several inconsistencies could be present. Each time a silica plug was run, the amount of silica was estimated. Along with using different columns, resulting in different band widths, the amount of MeOH measured is extremely

small. DCM is prone to evaporation, and if the solutions were made too far in advance, they could be different percentages than anticipated. Following this logic, if any of the "18- and 36-" membered ring would end up in another fraction, they would be indistinguishable in the HPLC purification, as they were reported to have the same retention time. Overall, this original procedure leaves little room for error.

At the time of re-investigation, the belief was that an 18-membered ring was the species not formed for three reasons. First, it was originally reported to form in very low yields and was completely suppressed when salts were incorporated as additives in the reactions. Secondly, the reactions were being run on a larger scale (20 mg vs 200 mg) than originally developed – we hypothesized that on a larger scale, for reasons not quite understood, we may not be seeing the 18-membered ring. Thirdly, we were running comparison reactions with the tetradepsipeptide, in which we were also seeing three ring sizes. Based on what was mechanistically possible for this reaction, it was presumed that each ring size must be a multiple of 12. Therefore, mechanistically, only a 36-membered ring should be possible, but not an 18-membered ring. This presumed 36-membered ring formed in the reaction with the tetradepsipeptide, had identical characterization

Figure 23. Overview (prior results and this work) of macrocyclizations with a depsipeptide and tetradepsipeptide monomer.

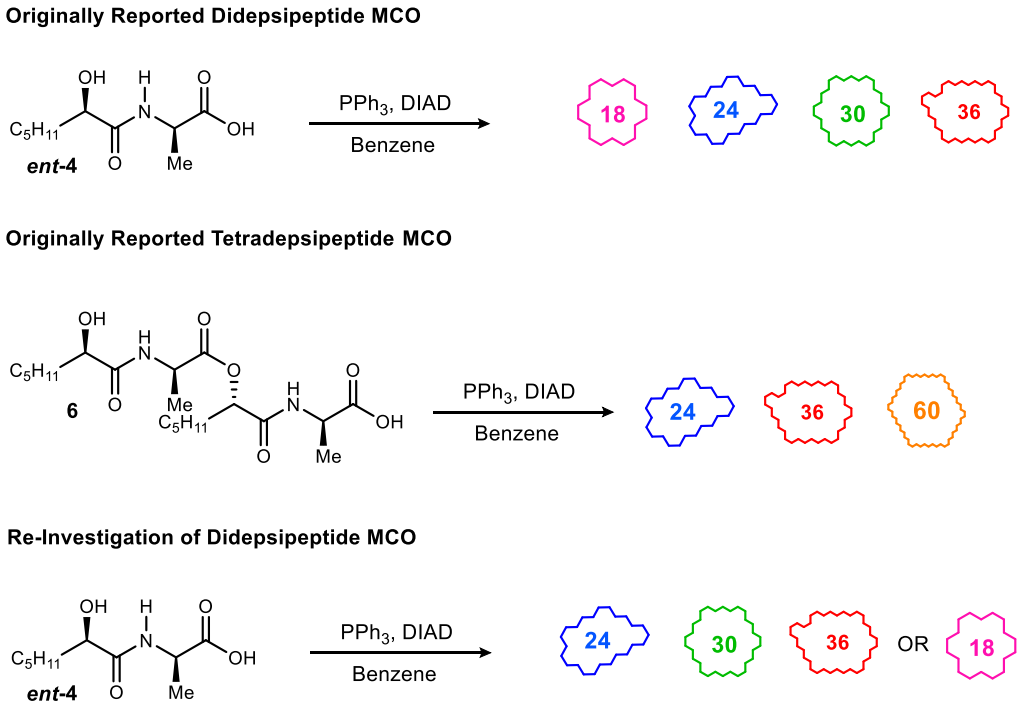

data to the macrocycle isolated from MCO reaction with the didepsipeptide monomer, thereby leading to the initial hypothesis that it was the 36-membered ring as well (Figure 23).

To gauge these hypotheses, numerous MCO reactions were carried out on the original scale (20 mg). Despite attempting many different conditions, varying the reagent equivalents, concentrations, solvents, and salt additives, the number of macrocycles formed from the reaction was unchanged – three products were consistently observed. Changes to the silica plug purification were incorporated, including varying the amount of silica used, the percentage of MeOH in DCM, and the column size. While some of this variation resulted in either 18- or 36-membered ring in both fraction 2 and fraction 3, following HPLC purification and combination, the compound that eluted in fraction 2 appeared to be identical to the compound eluting in fraction 3, therefore indicative that it was a single ring size. Overall, varying conditions for the cyclization or the purifications, never resulted in the isolation of an 18- or 36-membered ring that appeared different in any manner – they all presented the same proton and carbon NMR data, the same optical rotation, and identical R_f values. It was noted, however, that when trifluoroacetic acid (TFA) was present following HPLC purification, the NMR spectra could appear different, either through shifting or broadening of peaks. However, when removed with a base wash (confirmed by the absence of TFA by ^{19}F NMR), the NMR spectra would appear identical again. While still working to reproduce the original MCO conditions, we proceeded forward with the *N*-methylation step on the compounds synthesized thus far, hoping that the methylated products might provide some further clarification. The *N*-methylated variant of the 18-membered ring is the enantiomer of a natural product (verticilide B1) isolated by in 2012, so we anticipated having another opportunity for comparison of the methylated products to further aid in the characterization.[128]

1.5.1 Difficulties with N-methylation of Macrocycles

When attempting the *N*-methylation of the macrocycles, many difficulties were encountered. While the 24-membered ring could consistently be methylated, none of the other ring sizes appeared amendable to the methylation conditions. The conditions for *N*-methylation were largely vetted and optimized during former Johnston lab member Suzanne Batiste's synthesis of

[128] Ohshiro, T.; Matsuda, D.; Kazuhiro, T.; Uchida, R.; Nonaka, K.; Masuma, R.; Tomoda, H. *The Journal Of Antibiotics* **2012**, *65*, 255

verticilide.[129] The optimized conditions required the use of 10 eq of sodium hydride added in 3 aliquots, and 40 eq of methyl iodide in anhydrous DMF. These conditions, however, were incredibly sensitive to a variety of factors, including trace amounts of water, reaction time, and temperature. If even small amounts of water were present, *in-situ* sodium hydroxide formation could result in the cleavage of the ester linkages. The same decomposition as well as epimerization of stereocenters[130] was observed if the reaction was allowed to run longer than 30 minutes. Furthermore, if the reaction temperature rose above 0 °C, decomposition was often observed.

The methylation conditions for the various ring sizes were initially attempted on small amounts of macrocycles, anywhere between 3-10 mg. Initially, the reactions would be sporadically successful, and often, not proceed at all. After consistently isolated starting material, even when subjecting the usually reliable 24-membered ring, the question of the sodium hydride's quality came into play. It was hypothesized that there could be an outer coating on the sodium hydride powder, that was essentially encasing the active powder, preventing it from reacting. This effect would be amplified on small scale, as the amount of "reactive" sodium hydride would be lower. This effect was sometimes visually observed in the color of the sodium hydride, as over time, the light grey fluffy powder would become a darker grey color, and the lighter the grey sodium hydride used, the more often the reaction appeared to work. To test this hypothesis, we ran a series of experiments (Table 2). First, the quality of the methyl iodide was ensured by distillation prior to use. This led to no change in the reaction, and starting material was again isolated. We then increased the equivalents of both the methylating reagent and base, albeit with no successful results. Next, the reaction time and temperature were varied, in hopes that longer times or higher temperatures would allow for the decomposition of the "outer shell" and release of active sodium hydride. When the reaction was increased to room temperature and allowed to run for 25 min, starting material was again isolated. When the reaction was allowed to run for 24 hours at 0 °C, we obtained promising results: a 1:1 mixture of starting material to product. However, when

[129] Batiste, S. (2020). Rapid Synthesis by Rational Design: An Ion-Templated Macrocyclooligomerization-Based Approach to Prepare Collections of Natural Product-Like Cyclodepsipeptides, Leading to the Discovery of a New Antiarrhythmic Small Molecule [Doctoral dissertation, Vanderbilt University] Institutional Repository at Vanderbilt University. https://etd.library.vanderbilt.edu/etd-03252018-034947

[130] It is important to note that compounds with epimerized stereocenters are the suspected by-products of these reactions – this has not been confirmed by X-ray crystallography, or synthesis of diastereomers. Evidence to support this suspicion includes ^{1}H and ^{13}C NMR spectra consistent with a non-symmetrical macrocycle, as well as HRMS data that matches that of the desired product (if 18-membered ring was subjected, HRMS of this by-product would match the fully *N*-methylated 18-membered ring).

attempting to reproduce these results, we observed complete decomposition of the starting material after only 6 hours, again highlighting the sporadic behavior of these reactions. A series of solvents and additives were screened in hopes of changing the conformation of the macrocycle to favor methylation, but most were unfruitful. However, we found that adding 4 Å MS to the reaction did

Table 2. Investigation of cyclic depsipeptide methylation procedures.[a]

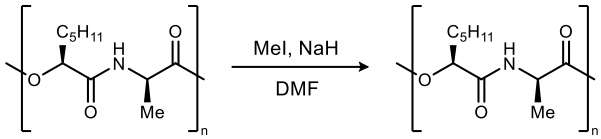

Entry	Ring Size	Methyl Source	Base	Solvent	Additive	Temp	Time	SM: product
1	36	MeI (40 eq)[b]	NaH (10 eq)	DMF	-	0 °C	25 min	100:0
2	36	MeI (60 eq)	NaH (16.5 eq)	DMF	-	0 °C	25 min	100:0
5	36	MeI (40 eq)	NaH (10 eq)	DMF	-	rt	25 min	100:0
8	24	MeI (40 eq)	NaH (10 eq)	DMF	-	0 °C	24 hrs	50:50
9	24	MeI (40 eq)	NaH (10 eq)	DMF	-	0 °C	6 hrs	decomp
4	36	MeOTf (40 eq)	NaH (10 eq)	DMF	-	0 °C	25 min	100:0
4	36	MeI (40 eq)	KH (10 eq)	DMF	-	0 °c	25 min	100:0
7	36	MeI (40 eq)	NaH (10 eq)	DMF:DCM (1:1)	-	0 °C	25 min	100:0
3	36	MeI (40 eq)	NaH (10 eq)	DMF	KBF_4	0 °C	25 min	100:0
6	36	MeI (40 eq)	NaH (10 eq)	DMF	$AgBF_4$	rt	1 hr	100:0
10	36	MeI (40 eq)	NaH (10 eq)	DMF	4 Å MS	0 °C	25 min	0:50
11	24[c]	MeI (40 eq)	NaH (10 eq)	DMF	-	0 °C	25 min	0:75

[a]Standard reaction conditions: 3-10 mg of macrocycle, 40 equiv of methylating agent, 10 equiv of base, DMF, 0 °C, 25 min reaction time. Note that at the time this chemistry was completed, it was believed to be on a 36-membered ring. We now know this ring was actually the 18-membered ring. All reactions were run in flame-dried vials and under argon. NaH was added as a suspension in DMF. DMF was dried over 4 Å molecular sieves. [b]Freshly distilled methyl iodide [c]Macrocycle scale: 20 mg

seem to improve the reaction conditions, yielding 50% of the desired product, accompanied by decomposition of the rest of the material.

After several months of experimentation, the final critical factor for these methylation conditions was uncovered. It was discovered that to obtain consistent results, it was necessary to run the reaction on larger than 15 mg scale. Considering that during the development of this reaction, it was always run on a larger scale, this difficulty in scale was not originally predicted. We hypothesize that this dependence on scale is directly correlated with the amount of active sodium hydride present. Overall, when we ensured a good commercial source of sodium hydride, completely anhydrous conditions, and a scale greater than 15 mg, the methylation conditions were reliable and reproducible.

These conditions were then applied to the believed 36-membered ring to give the methylated product. Once in hand, the characterization data for this ring size was compared to the data for the 18-membered natural product described in the literature. We found that the data between the two compounds was inconsistent, reaffirming the belief that this compound was a 36-membered ring. Verticilide B1 is reported as a symmetrical compound in deuterated chloroform. In our hands, the NMR spectra in $CDCl_3$ showed numerous conformations, stemming from cis/trans amide bond isomerization. We did, however, note a favored conformation in deuterated methanol. For a comparison, Table 3 shows the NMR chemical shifts of our macrocycle in MeOH with the listed data for verticilide B1 in $CDCl_3$. Another important note, is that in the original isolation paper of verticilide B1, the stereochemistry of the hydroxy heptanoic acid residues was not defined.[128] It is unclear from this data, if our 18-membered ring would be the enantiomer or a diastereomer. Proceeding forward, this was a key piece of data kept in mind.[131]

[131] We later received spectral data from the original Verticilide B1 publication[128], and their NMR spectrum were acquired in MeOD. Upon comparing our data, the compounds appear identical by NMR. Therefore, verticilide B1 can now have a stereochemical assignment as the enantiomer of our 18-membered ring.

Table 3. Comparison of ^{13}C and ^{1}H NMR Data from our 18-membered ring and verticilide B1 reported in the literature.

Verticilide B1 ^{13}C Chemical Shifts ($CDCl_3$)	**Unknown Ring Size ^{13}C Chemical Shifts (MeOD)**	**Differences in Chemical Shift Values**
172.2	172.9	0.7
167.5	172.4	4.9
72.4	72.8	0.4
53.5	53.7	0.4
32.5	32.5	0
31.8	31.9	0.1
31.5	31.3	0.2
26	26.2	0.2
23.5	23.6	0.1
14.5	14.5	0
14.3	14.3	0

Verticilide B1 ^{1}H Chemical Shifts ($CDCl_3$)	**Verticilide B1 Coupling Constant & Multiplicity ($CDCl_3$)**	**Unknown Ring Size ^{1}H Chemical Shifts (MeOD)**	**Unknown Ring Size Coupling Constant & Multiplicity ($CDCl_3$)**
5.36	dd (J = 7.6, 6.1 Hz, 1H)	5.35	dd (J = 8.8, 4.6 Hz, 1H)
5.06	q (J = 7.6 Hz, 1H)	5.00	q (J = 7.5 Hz, 1H)
3.08	s, 3H	3.09	s, 3H
1.78	m, 2H	1.84 - 1.76	m, 2H
1.42	d (J = 7.2 Hz, 3H)	1.45	d (J = 7.6 Hz, 3H)
1.50 - 1.34	m, 2H	1.39-1.29	m, 6H
1.34	m, 2H	-	-
1.34	m, 2H	-	-
0.92	t (J = 6.4 Hz, 3H)	0.93	t (J = 6.8 Hz, 3H)

1.5.2 Reassignment of the "36"-Membered Ring to an 18-Membered Ring

During the process of investigating the methylation conditions, a hypothesis was proposed that the larger macrocycles could be present in a variety of different conformations, some of which were unfavorable to methylation. Furthermore, from previous isothermal titration calorimetry (ITC) work in the group, it was considered that these macrocycles could be ionophores. We hypothesized that the macrocycles could be coordinating to Lewis acidic ions, which could also

affect conformation. To try to gain insight into potential conformations, crystals were grown for X-ray crystallography using dichloromethane. It was an exciting day in lab when first crystals were grown with the 24-membered ring! After acquisition of the structural data, a solid-state conformation of the 24-membered *N*-H macrocycle (Figure 24, **7**) was visualized. To compare different macrocycles, crystals were also grown for the suspected "36-membered ring". The suspected "36-membered ring" was actually an 18-membered ring (Figure 24, **8**). To confirm these surprising results, a large batch of "36-membered rings" samples were examined from a variety of different reactions conditions, both with the didepsipeptide MCO and the tetradepsipeptide MCO. All the crystal structure data returned the same results: an 18-membered ring. While this wasn't hard to imagine mechanistically with the didepsipeptide monomer in the MCO, this perplexing

Figure 24. Crystal structures of the 24- and 18-membered *N*-H macrocycles.

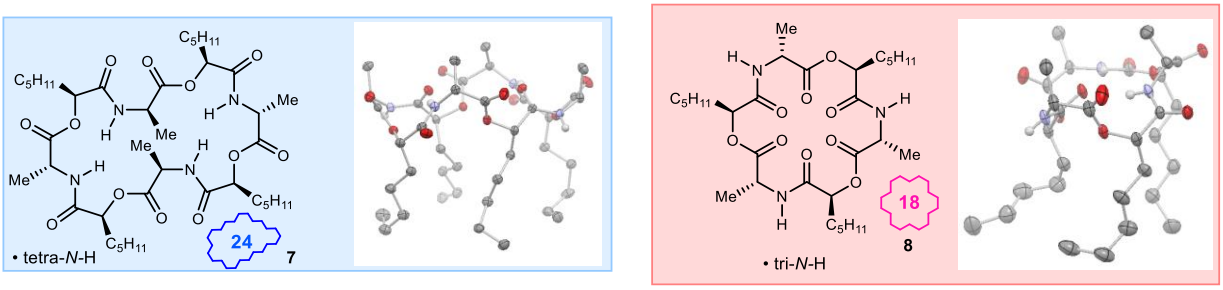

data challenged what was originally believed to be mechanistically possible in the MCO reaction with a tetradepsipeptide. Perhaps even more surprising, is that the stereochemistry was as expected from the MCO reaction (alternating D,L), which is distinct because each Mitsunobu reaction carried out inverts a stereocenter. This was a strong indication to us that the central ester bond was not simply undergoing hydrolysis to yield the two monomers, as that mixture would lead to diastereomers. Instead, something much more mechanistically unexpected, but still precise must be underway. This discovery led to a series of mechanistic studies working to understand this unusual behavior.

1.5.3 Synthesis of Authentic Samples of 36 and 18-Membered Rings[132]

At this point, it was hypothesized that a 36-membered ring had never been formed in the MCO conditions with any monomer size, and instead what was observed was the 18-membered ring.

[132] This section is taken in part from our publication: Smith, A. N.; Johnston, J. N. *J. Org. Chem.* **2021**, *86*, 7904

This hypothesis led to a series of questions: 1) if only the 18-membered ring was observed, why in some cases, does it look like a different macrocycle by NMR, ITC, and HRMS and 2) how is an 18-membered ring forming from an MCO reaction with a tetradepsipeptide in which only multiples of 12 should be mechanistically possible? To better understand the factors at play, synthetic routes to the 18- and 36-membered rings using a stepwise chain extension sequence and final macrolactonization were planned and executed to acquire authentic samples of each macrocycle.

Scheme 2. Enantioselective synthesis of differentially protected and unprotected didepsipeptide monomers.

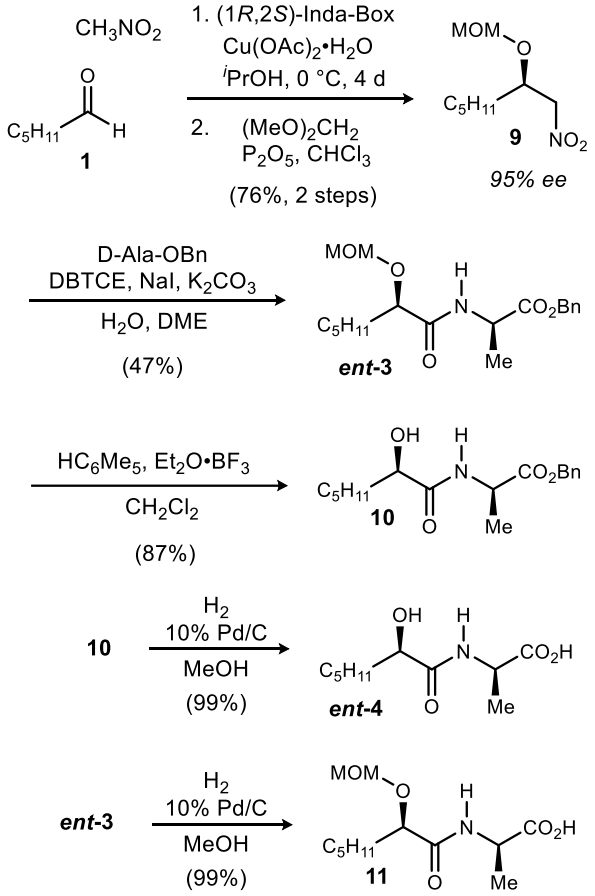

The synthetic approach relied on *O*-deprotected benzyl ester **10** and carboxylic acid **11** prepared using optimized procedures of those previously reported (Scheme 2).[84] These didepsipeptide units were coupled using a Mitsunobu protocol to form the tetradepsipeptide **12** (Scheme 3). This material was divided, with half that was *O*-deprotected to **14**, and half that was

hydrogenolyzed to **13** prior to segment coupling [4+4] using another Mitunobu reaction. The MOM-protecting group of the resulting octadepsipeptide **15** was removed, and the resulting alcohol was reacted with tetradepsipeptide carboxylic acid **13** using Mitsunobu conditions. This furnished the dodecadepsipeptide **16** in 60% yield. This material was deprotected at both termini, subjected to a Mitsunobu macrocyclization protocol (1 mM concentration), and then isolated as a 36-membered COD (**17**) (70% for 3-steps).

Scheme 3. Linear, stepwise synthesis of the 36-membered cyclic dodecadepsipeptide.

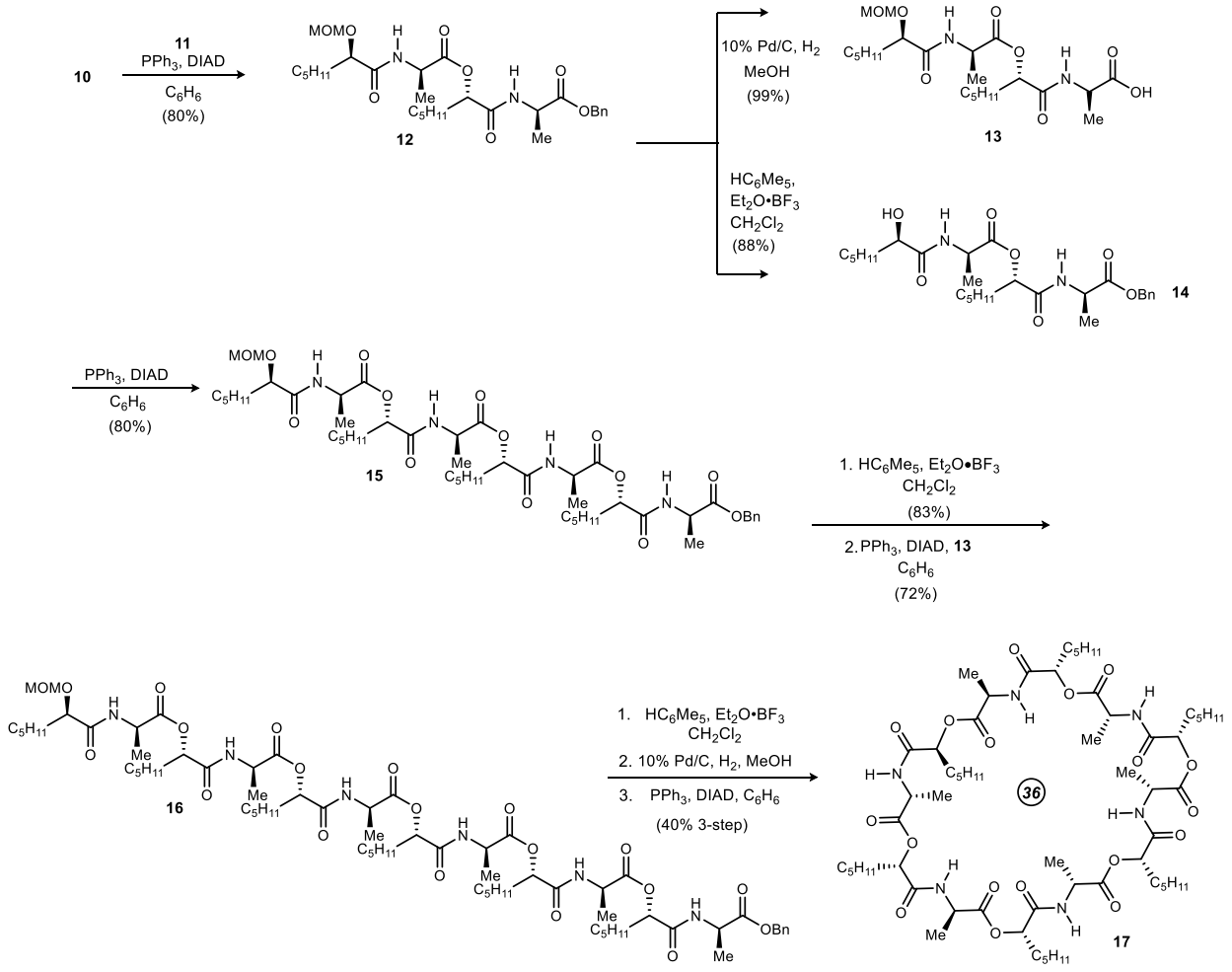

Analysis of **17** revealed a ^{1}H NMR spectrum with the characteristic number and type of peaks in this COD series, but it was distinct from the ^{1}H NMR spectrum of the material originally assigned to the 36-membered ring. More telling was the observation of an intense parent ion peak ($[M+Na]^{+}$ 1217.7146) by HRMS consistent with a 36-membered COD. This parent ion was far

Figure 25. Comparison of HRMS data from originally assigned '36' COD (**A**) formed by MCO, and authentic 36-membered COD (**B**)[a] formed through stepwise linear synthesis.

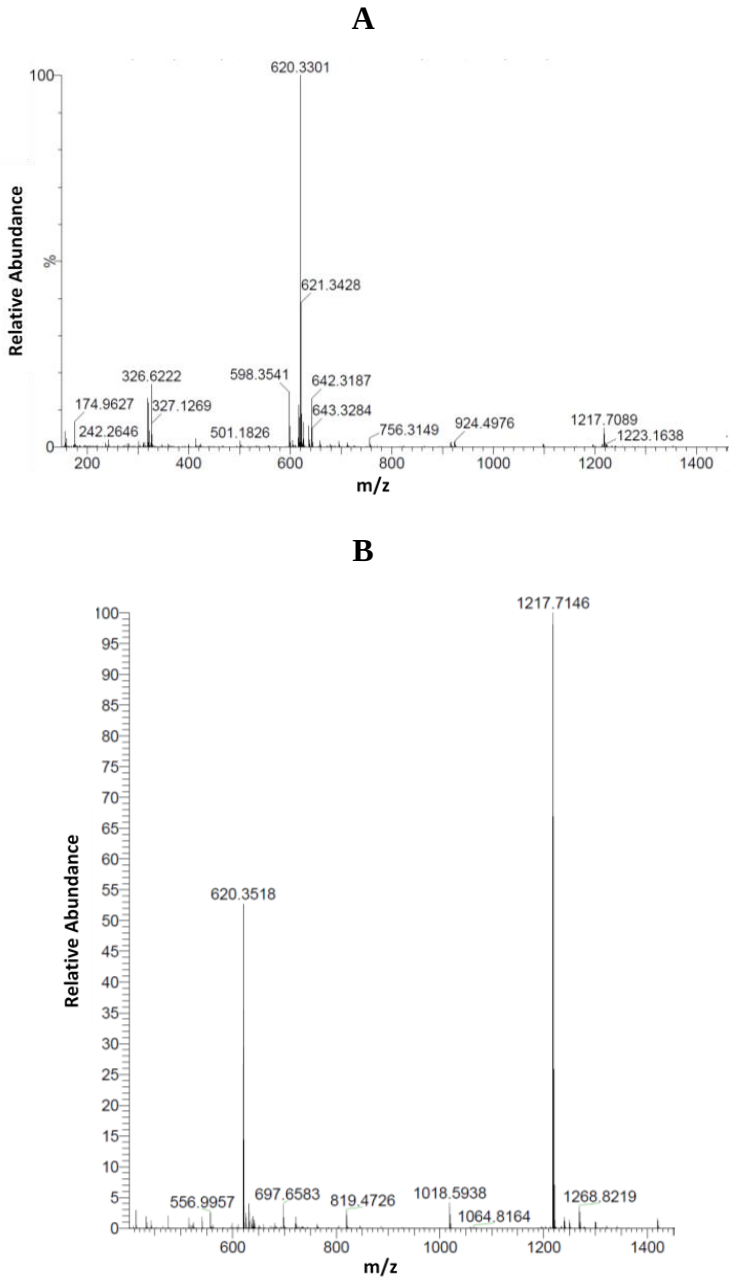

[a]Exact mass calculated for $[M^{36}+Na]^+$ = 1217.7148; $[M^{18}+Na]^+$ = 620.3523; $[M^{36}+2Na]^{2+}$ = 620.3523.

more intense than that observed in the original material (Figure 25). A second distinguishing feature in the HRMS spectrum for the authentic 36 membered ring is the absence of a singly-charged 620 Da ion $[M^{18}+Na]^+$. Instead, the ion peak at 620.3518 corresponds to $[M^{36}+2Na]^{2+}$.

The successful synthesis of **17** using a stepwise route provided compelling data to fingerprint the 36-membered COD **17**. Given that all other aspects of the spectroscopic data were consistent with a highly symmetrical oligomeric depsipeptide, the assignment of this material as the 36-membered ring was considered sound. The original material made in the MCO reactions was therefore assigned tentatively as the 18-membered ring, an 'impossible' product of the 12-mer oligomerization. Data consistent with this assignment included: a) a high degree of symmetry by ^{1}H NMR, indicating a product of the Mitsunobu reaction that produces homochiral α-oxy amide subunits, and b) intense adducts of the parent ions including $[M+H]^+$ at 598 and $[M+Na]^+$ at 620 consistent with an 18-membered COD (Figure 25).

Verification of this structure by independent synthesis was straightforward, leveraging a stepwise route analogous to the synthesis of the cyclododecadepsipeptide **17**. Hence, treatment of an *O*-deprotected tetradepsipeptide **14** with a benzyl deprotected didepsipeptide **11** under Mitsunobu conditions yielded the linear hexapeptide in 93% yield. A final MOM-deprotection, hydrogenolysis, and cyclization under dilute conditions gave the authentic 18-membered COD in a 75% yield over three steps (Scheme **4**). The ^{1}H NMR (**A**, Figure **26**) and HRMS (Figure 25) data mirrored the data associated with the compound originally assigned as the 36-membered ring (**D**, Figure **26**). However, an important factor noted at this time, was that broadening and slight shifting

Scheme 4. Linear, stepwise synthesis of the 18-membered cyclic hexadepsipeptide.

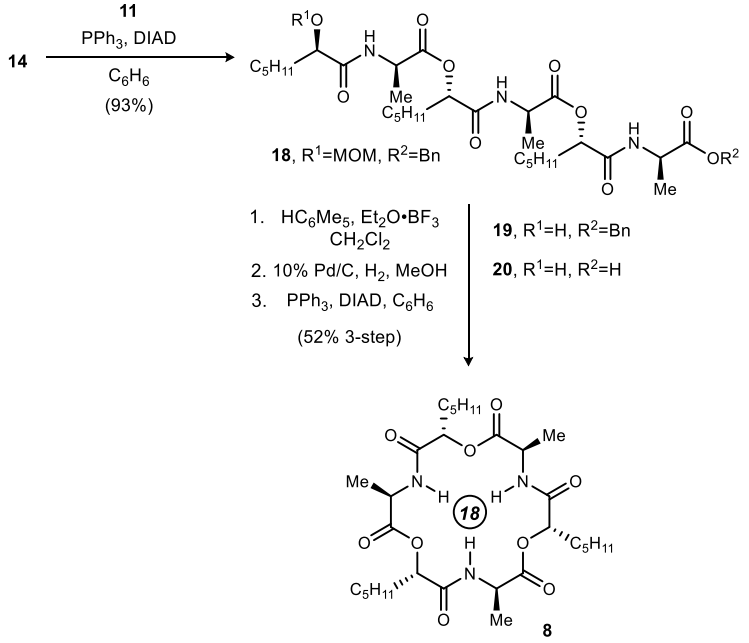

of α-oxy amide methine peaks in the proton NMR spectra is evident when any amount of trifluoroacetic acid (TFA) from HPLC purification is present. Even small amounts of TFA appear to affect chemical shift and coupling, as illustrated in Figure **26**, where the originally characterized 18-membered ring (spectrum C) appears reasonably distinct from the other samples (spectrum B and D). This difference contributed to the initial belief that two different compounds were forming in the MCO reactions. We have since confirmed that upon complete removal of TFA, by exhaustive base washes, the spectra overlap. From this data, we can conclude that the 18-membered COD is the major product when using didepsipeptide monomer. Although it is a minor COD formed from the tetradepsipeptide MCO, the 18-membered COD is clearly formed. The 36-membered COD is not formed in either MCO reaction, and attempts to change reaction conditions to favor its formation have been unsuccessful to-date (Scheme 5).

Figure 26. A) Full-scale ^{1}H NMR spectrum of the authentic 36-membered COD (**12**, Scheme 3), **B**) an authentic sample of the 18-membered COD, **C**) the originally assigned 18-membered ring formed in the MCO reaction, and **D**) the originally assigned 36-membered ring formed in the MCO reaction. Inset: expansion from 5.2-4.4 ppm.

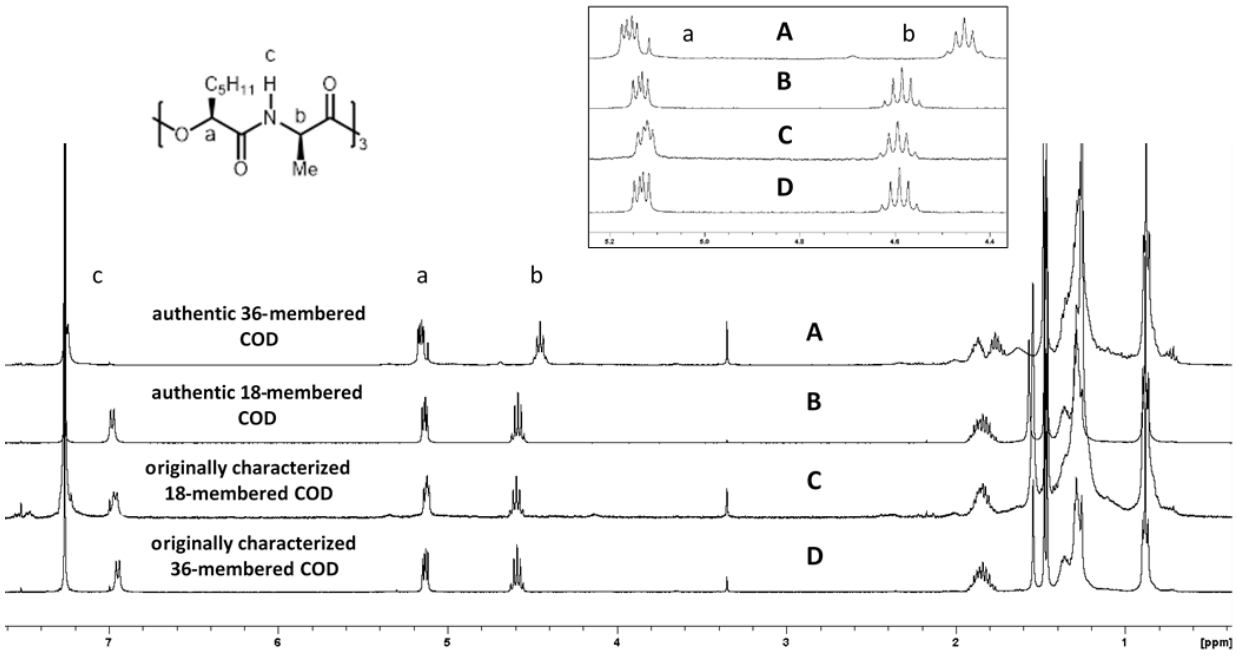

Figure 27. Full-scale ^{1}H NMR spectrum of authentic samples of all COD rings sizes.

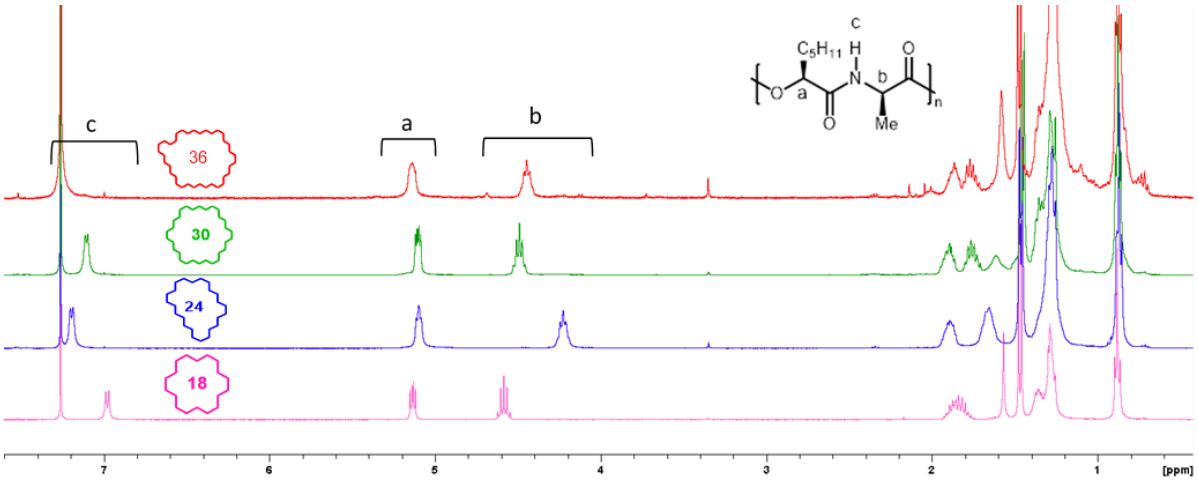

Scheme 5. Final revised MCO reaction profiles

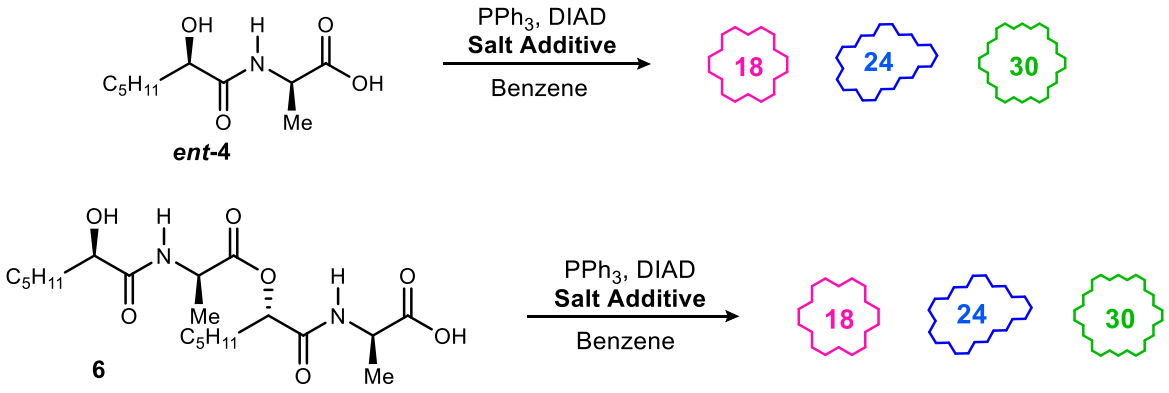

1.5.4 High Resolution Mass Spectrometry Studies[132]

At the time of the original investigation, the HRMS data supported the conclusions but required the perceived mechanistic limitations of a 12-atom monomer leading to lengths of only 24/36/48/60 to be decisive. In every spectrum of the 18-membered ring and "36"-membered ring formed in the MCO reactions, only singly charged ion peaks at both 620 Da and 1217 Da were observed. For an 18-membered ring, these ion peaks would correspond to $[M^{18}+Na]^+$ and $[2M^{18}+Na]^+$. For a 36 membered ring, these would correspond to $[1/2M^{36}+Na]^+$ and $[M^{36}+Na]^+$.

Figure 28. Comparison of the HRMS spectra and corresponding MS/MS spectrum of 620 and 1217 ion peaks in each sample of authentic 18-membered and 36-membered rings. (z = charge)

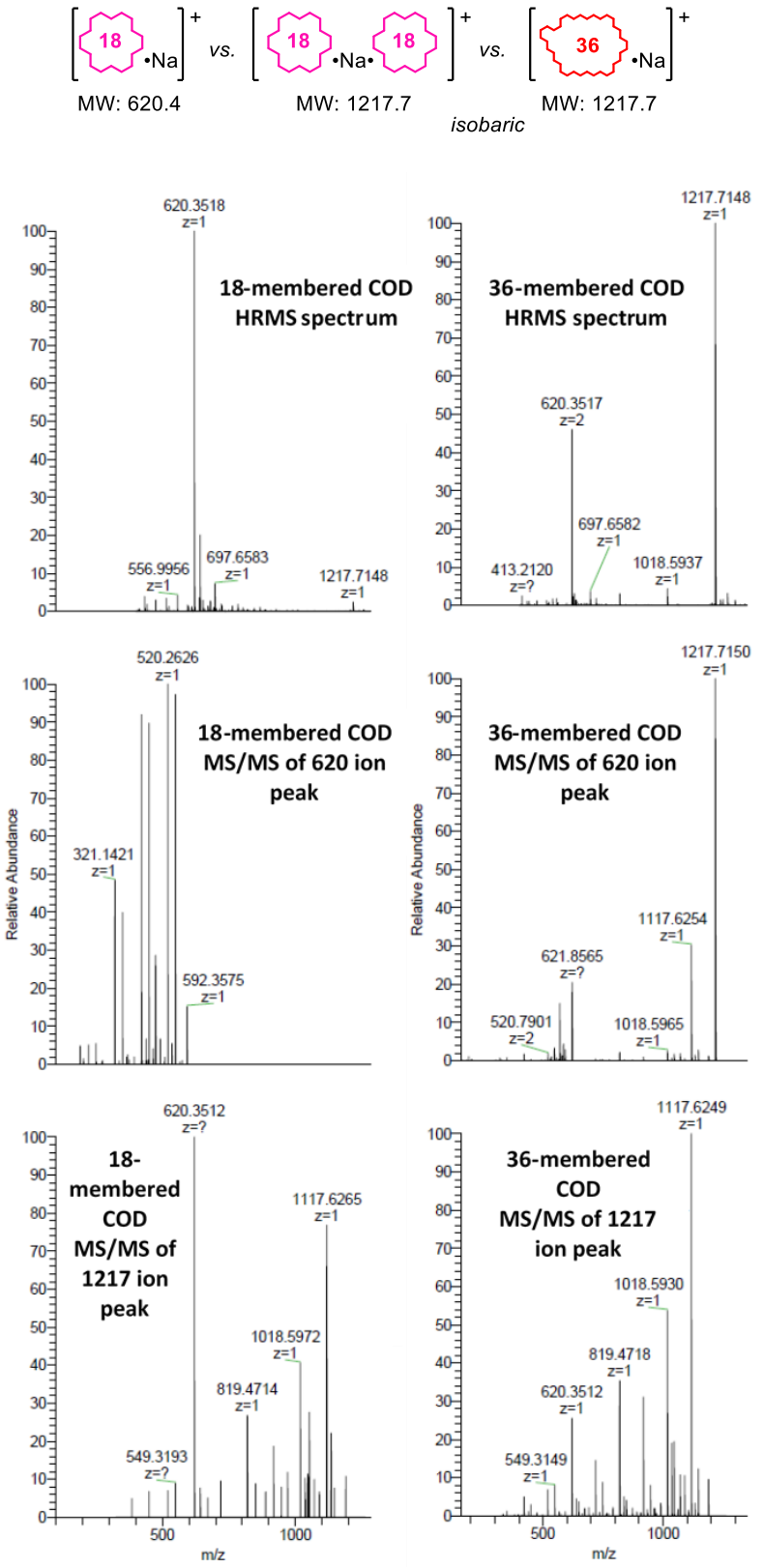

However, in all cases, the ion at 620 Da was more intense. It is important to distinguish that $[1/2M36+Na]^+$ is referring to a fragmented half of the 36 membered ring, not to be confused with $[M36+2Na]^{2+}/2$, which would indicate a doubly charged ion evident by isotopic peaks differing by only 0.5 mass units. Only after synthesis of the authentic samples of each ring size through a stepwise route was a clear difference apparent in the MS spectra (Figure 28). To further probe behaviors for these oligomers by HRMS, MS/MS experiments were applied to authentic samples of the 18- and 36-membered rings.

When the 620 Da ion is fragmented in each experiment, the results are remarkably different. From the 18-membered ring, the singly charged 620 Da ions gave no fragments above m/z of 620. However, when the doubly charged 620 Da ion for **17** $[M^{36}+Na]^{2+}$ was fragmented, an intense 1217 ion was observed, corresponding to $[M^{36}-Na]^+$. Additionally, there were a handful of fragments from the ring itself. When fragmenting the 1217 Da ion in each sample, again the MS2 patterns were distinct. The MS-MS of the 1217 ion from **8** showed the largest ion at 620 Da. This would correspond to the dissociation of the noncovalent dimer $[2M^{18}+Na]^+$ with loss of one macrocycle (M^{18}). Perhaps most intriguing, is the presence of fragments heavier than 620 Da. This would imply that the non-covalent interaction that forms the singly charged dimer ion is rather strong, as some of these dimers are experiencing fragmentation of the covalent bonds in the backbone of the macrocycle first.

1.5.5 Isothermal Titration Calorimetry and Templating Effects[132]

The reassignment of ring sizes forming in the MCO reactions demanded a reevaluation of the isothermal titration calorimetry (ITC) measurements from this series. We noted that our reported ion binding measurements for these macrocycles exhibited very different patterns for the 18-membered ring and putative 36-membered ring. With the knowledge that these compounds should be identical, we sought an understanding of the measurement difference with a prejudice toward possible contaminant(s). This careful analysis led to the finding that some of the original samples used for ITC contained (small) residual amounts of trifluoroacetic acid (TFA) from reverse-phase HPLC purification. Detection of this residual TFA was possible only via ^{19}F NMR, since the ^1H NMR of these samples can appear identical when there are only small amounts of TFA in the sample. Furthermore, this finding was unexpected since all these samples had been subjected to a standard base wash in a work-up after the HPLC purification. Hence, these macrocycles exhibit a

strong propensity to bind TFA. Armed with this knowledge, the original macrocycle samples were extensively base washed until TFA removal was confirmed by ^{19}F NMR, prior to repeating the ITC experiments. Truly TFA-free samples labeled 18 or "36"-membered ring from the MCO reactions then provided reproducible isotherms.

A complete series of TFA-free samples of 18, 24, 30, and 36-membered rings were next analyzed by ITC. This data is provided in Figure **29**, Figure 30, Figure 31, Figure 32, and Table 4. Overall, while the remeasured data still delineates cases of strong, selective binding, the binding data for this particular depsipeptide does not support a templating effect with sodium, potassium, or cesium. It is important to note that one explanation for the paradox involves disproportionation of the 'pre-24' chain. This complicates interpretation of the ion binding trends, as some (or all) of the paradoxical ring-formation may stem from a rate that involves templation. The benefit of adding cesium is clear, however, as the combined yield of three CODs is 86%, compared to 57% without cesium salt additive. This increase in yield results from the significant increase in production of the paradoxical 18-membered ring (46% vs. 29%).

As we noted originally, the ITC measurements could only be comprehensively obtained using methanol solvent. This contrasts the use of benzene for MCO reactions, although the salt additives are used at saturating concentrations in benzene. Attempts to prepare ITC runs in other organic solvents or solvent mixtures led to insufficient solubility of either the salts or the salt-macrocycle complexes. At the time of initial investigation with this series, we noted that solvent can have a strong effect on the magnitude of binding affinity, however, the goal was to observe possible trends in *relative* binding interactions. The trends observed in methanol, with the corrected ring sizes, still hold true. While it is disappointing that a correlation of affinity and MCO selectivity cannot be concluded for this particular MCO reaction, the potential ion binding abilities of this series of CODs remains unchanged. We have carefully reviewed other series of MCO reactions and have no reason to suspect TFA impurities in any other cases. First and foremost, there are no other series of macrocycles that display the same data that lead us to believe there was a mischaracterization. Each COD reported in other series have very distinct NMRs and significantly different HPLC retention times. For ITC data, one factor that indicated the presence of TFA in samples were isotherms that exhibited atypical S-shaped curves (Figure 33). While this can be a characteristic

of aggregate formation at the beginning of titration[133,134] and our initial suspicion, we now know that TFA impurity was responsible. No other series of COD isotherms appear to display this behavior. Additionally, some samples used in original experiments were still on hand and

Figure 29. Comparison of MCO reaction yields (di- and tetradepsipeptide monomers) and ITC data (corrected).[a]

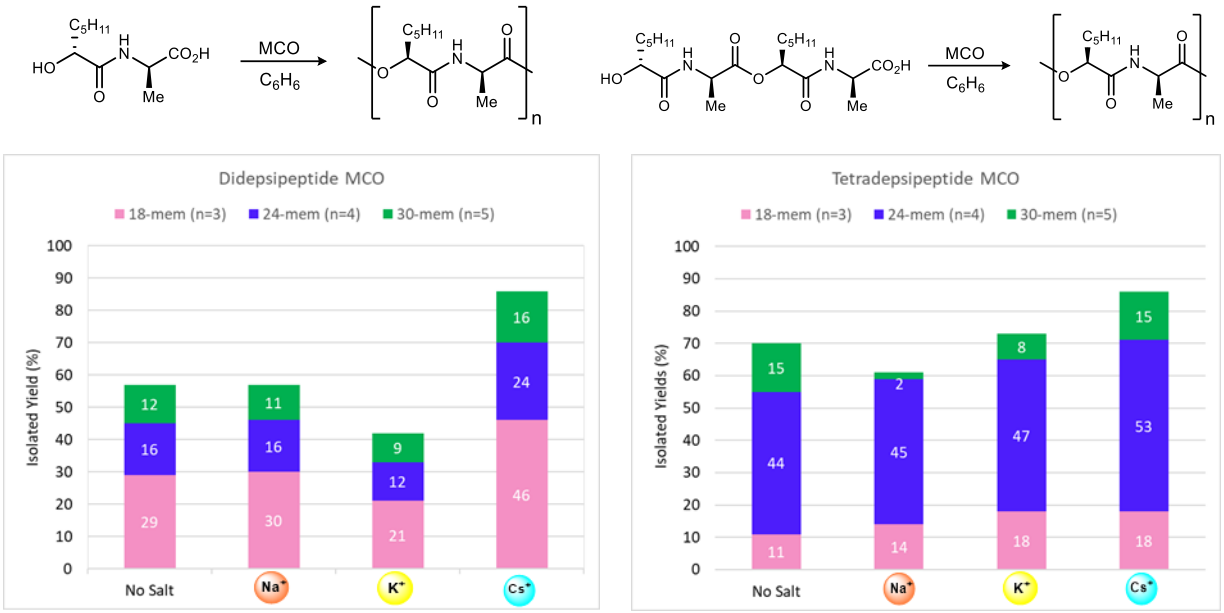

template	18-mem ring			24-mem ring			30-mem ring			36-mem ring		
	K_a (M^{-1})	ΔH	N	K_a (M^{-1})	ΔH	N	K_a (M^{-1})	ΔH	N	K_a (M^{-1})	ΔH	N
Na^+	$1.49x10^5$	-	2:1	$3.18x10^4$	-	1:1	$<1.00x10^3$	N/A	N/A	$<1.00x10^3$	N/A	N/A
K^+	$1.60x10^4$	-	1:1	$2.67x10^3$	-	1:1	$<1.00x10^3$	N/A	N/A	$2.72x10^4$	-	1:2
Cs^+	$<1.00x10^3$	N/A	N/A	$<1.00x10^3$	N/A	N/A	$1.98x10^4$	-	1:2	$<1.00x10^3$	N/A	N/A

[a]Association constant (K_a), binding stoichiometry (N), and enthalpy of binding (ΔH either positive (+) or negative (-)) determined by ITC using methanol solutions, whereas MCO is performed in benzene. See SI for complete details. K salt is KSCN for ITC measurements and KCl for MCO reaction conditions, Na is $NaPF_6$ for ITC measurements and $NaBF_4$ for MCO reaction conditions, and Cs salt is CsCl for both ITC data and MCO reaction conditions. $<1.00x10^3$ indicates no binding observed and therefore fields denoted with N/A (not applicable) were not measured. ITC data for the 36-membered ring prepared using the synthesis in Scheme 3, since this ring-size is not formed in MCO. Yields are averages of 3 or more replicates for each case, based on a theoretical yield of 18.3 mg (from didepsipeptide) and 19.1 mg (from tetradepsipeptide). The maximal observed yield variation was 12% (~2 mg) in the didepsipeptide series and 13.5% (2.6 mg) in the tetradepsipeptide series. ITC data for the 24-membered ring is the same as previously reported– these macrocycle samples contained no TFA and were replicated 10 times.

[133] Darby, S. J.; Platts, L.; Daniel, M. S.; Cowieson, A. J.; Falconer, R. J. *J. Therm. Anal. Calorim.* **2017**, *127*, 1201
[134] Clavería-Gimeno, R.; Velazquez-Campoy, A.; Pey, A. L. *Arch. Biochem. Biophys.* **2017**, *636*, 17

confirmed to be TFA-free by ^{19}F NMR. The potential application of ion binding in future chemistry remains promising, and this work highlights an important consideration for any depsipeptide MCO.

An important takeaway from this work, it that the ability of residual TFA, despite routine base wash of HPLC fractions, to adversely affect COD behavior is evident. While this was a problem specifically with depsipeptides here, routine ^{19}F-NMR analysis should be a consideration when using reversed phase HPLC purification buffered with TFA. Several patterns of behavior have been documented here, which could be essential when ^{19}F-NMR is not accessible.

Figure 30. ITC isotherms for the titration of (A) $NaPF_6$ (5.00 mM) and (B) KSCN (5.00 mM) into the 18-membered ring (300 µM) in MeOH at 25 °C

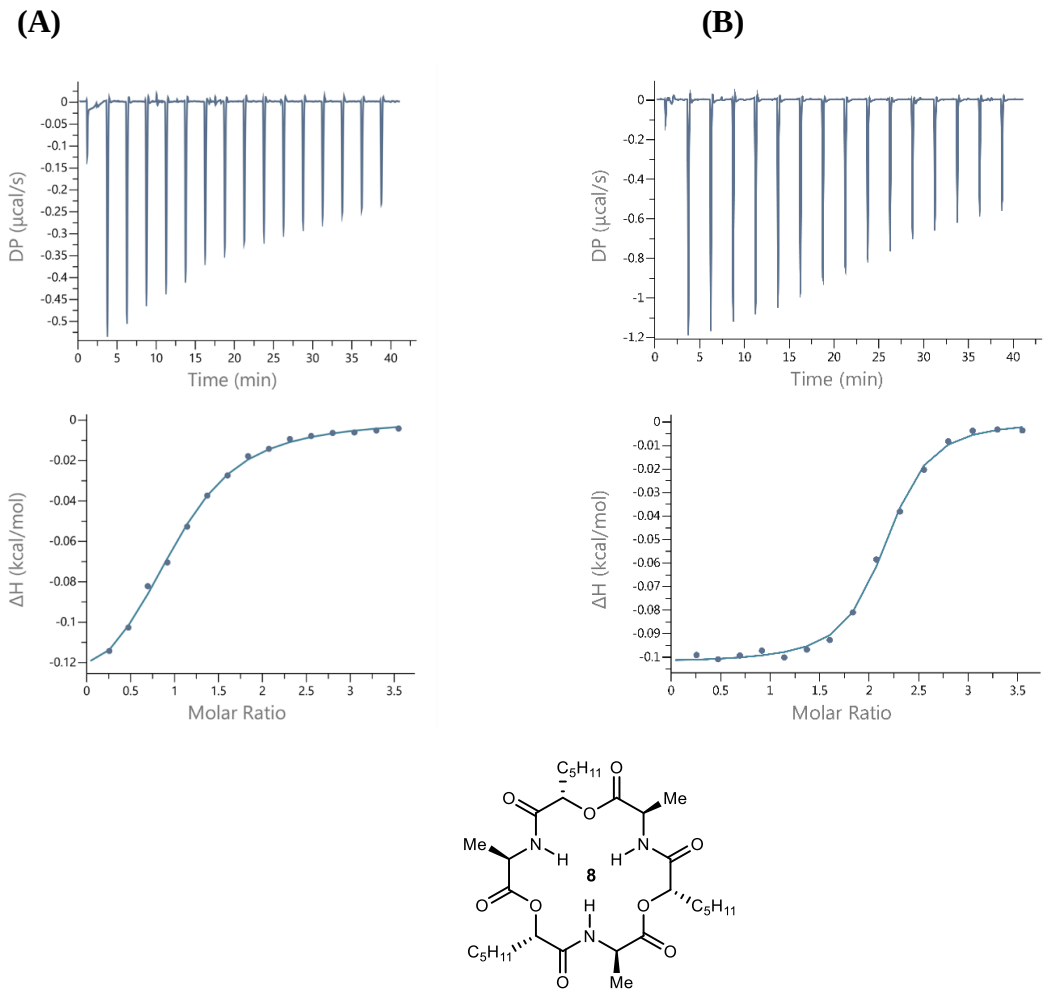

Figure 31. ITC isotherm for the titration of CsCl (5.00 mM) into the 30-membered ring (300 µM) in MeOH at 25 °C

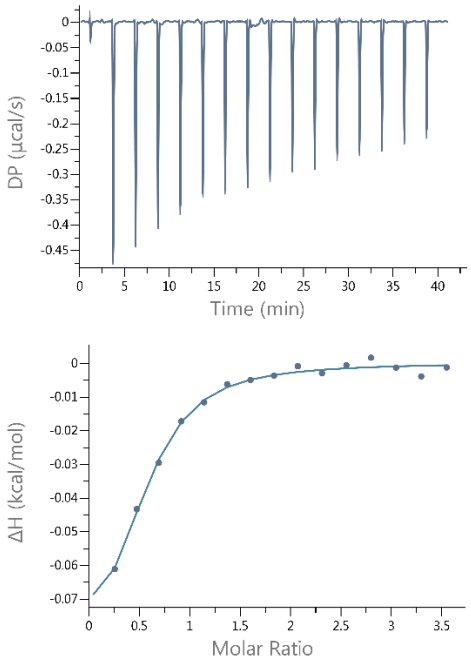

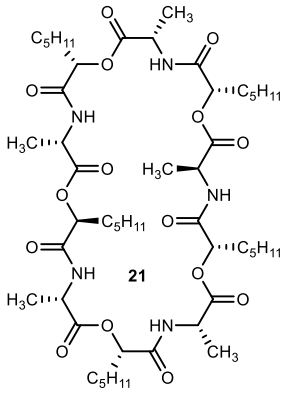

Figure 32. ITC isotherm for the titration of KSCN (5.00 mM) into the 36-membered ring (300 µM) in MeOH at 25 °C

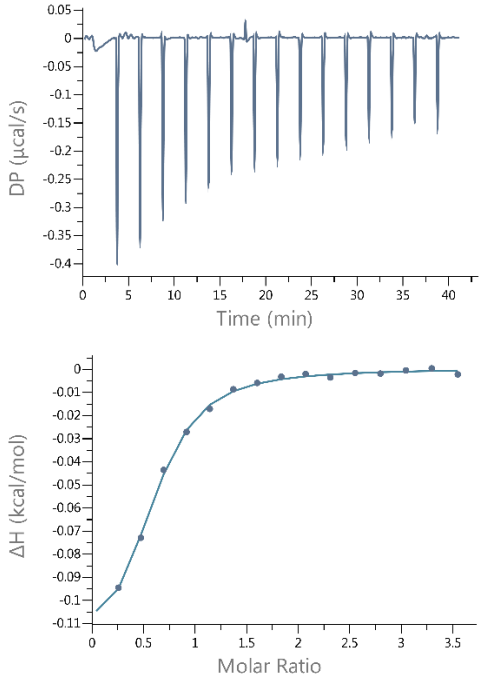

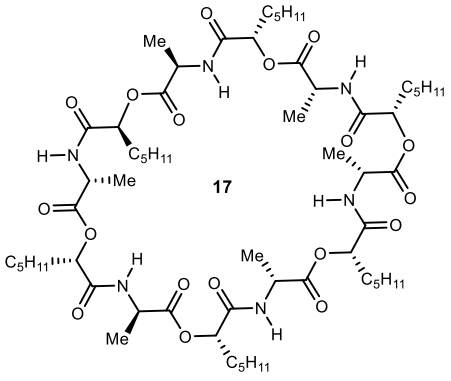

Table 4. Summary of experimentally determined thermodynamic values for binding

Macrocycle	Metal Ion	$K_a(M^{-1})$	N	ΔH (kcal mol^{-1})	ΔG (kcal mol^{-1})	-TΔS (kcal mol^{-1})
8	Na^+	(1.49±0.21) x 10^5	2.08	-0.103±0.002	-7.06	-6.96
8	K^+	(1.60±0.22) x 10^4	0.98	-0.146±0.007	-5.74	-5.59
21	Cs^+	(1.98±0.54) x 10^4	0.51	-0.093±0.012	-5.86	-5.77
17	K^+	(2.72±0.37) x 10^4	0.54	-0.130±0.007	-6.06	-5.93

Figure 33. Example of an S-shaped ITC curve compared to a normal sigmodal ITC curve; Isotherms shown are for the titration of $NaPF_6$ into the 18-membered ring in MeOH at 25 °C A) when TFA contaminate is present and B) when TFA has been removed

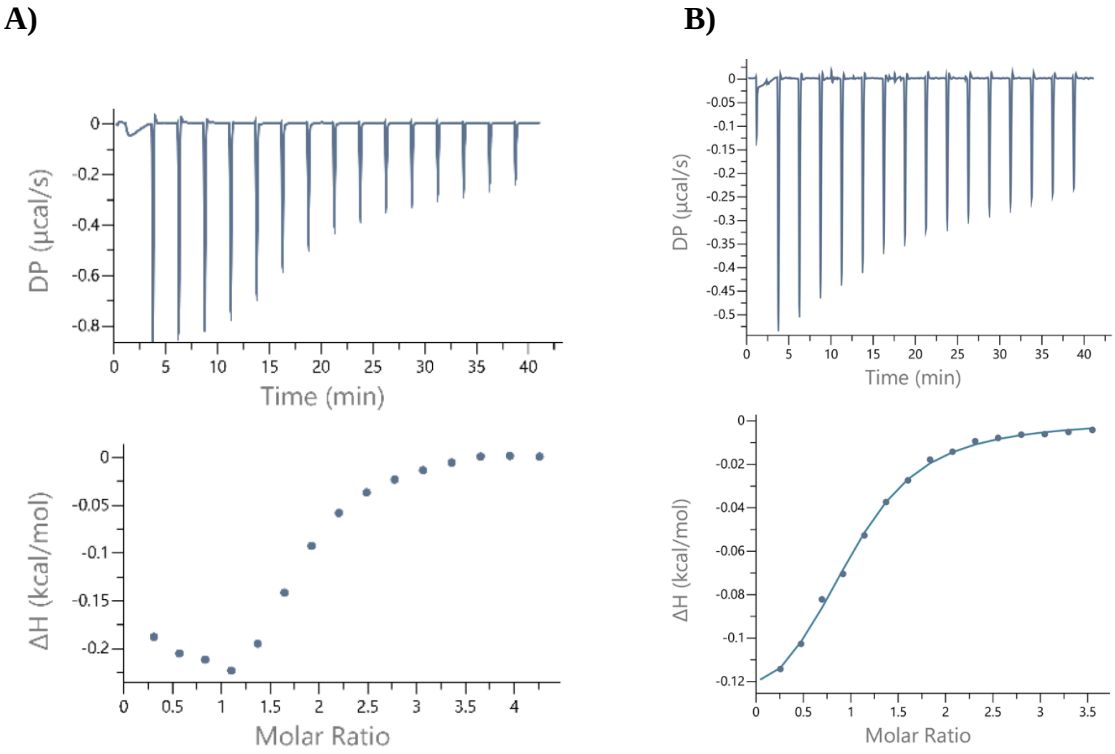

1.5.6 30-Membered Versus "60-Membered" Ring Data

A stepwise synthesis of the 60-membered ring was considered but not pursued. The original belief that a 60-membered ring existed was based on the same logic that was used for the 36-membered ring – from the MCO reaction with a tetradepsipeptide, a 30-membered ring should not be possible. Therefore, one that has similar characteristics could be a macrocycle twice its size (60-membered ring). Based on our discovery that the originally characterized "36-membered" ring is actually the 18-membered ring, we believe the originally characterized "60-membered" ring material is most likely another paradoxical product: the 30-membered COD. This reassignment is based on several components. First, when the original sample of what was assigned as the 60-membered ring was resubjected to HRMS analysis, the peak corresponding to a 60-membered ring was not observed. The HRMS data instead looked effectively identical to the 30-membered ring. We hypothesize that the HRMS peak for the 60-membered ring may have been an artifact. Furthermore, MS/MS on the 1018 ion (mass of the 30-membered ring) are identical between both samples from the MCO with the didepsipeptide and tetradepsipeptide

Figure 34. (A) Full scale HRMS of 30-membered ring (S3), (B) MS/MS of 1018 peak in a sample of 30-membered ring from MCO with the tetradepsipeptide, (C) MS/MS of 1018 peak in a sample of 30-membered ring from MCO with the didepsipeptide

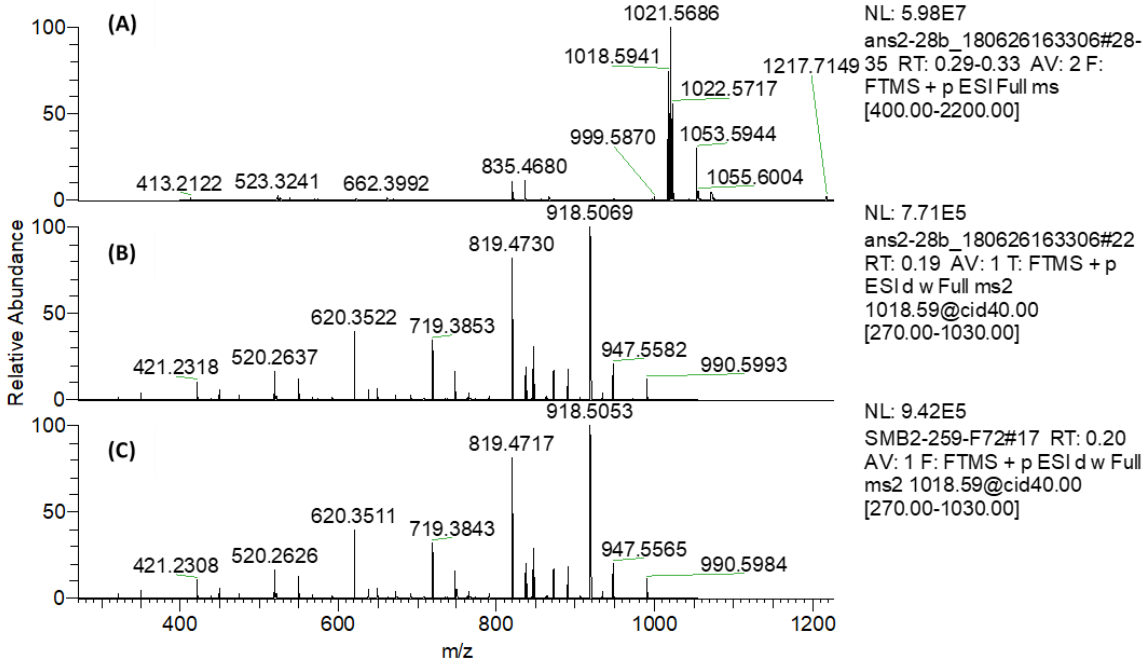

(Figure 34). Again, the slight differences in ^{1}H NMR are due to residual TFA, and once removed, the spectra overlap (Figure 35). The use of ^{1}H NMR analysis can clearly distinguish each COD, but the irregular movement of specific peak types undermines its utility as a predictor of ring-size. Due to the similarity between the cases, we did not find it necessary to make an authentic sample of a 60-membered COD.

Figure 35. (A)^{1}H NMR of 30-membered ring samples from MCO reaction with didepsipeptide and MCO reaction with tetradepsipeptide with no residual TFA present and (B) ^{1}H NMR of 30-membered ring samples from MCO reaction with didepsipeptide and MCO reaction with tetradepsipeptide with no residual TFA present.

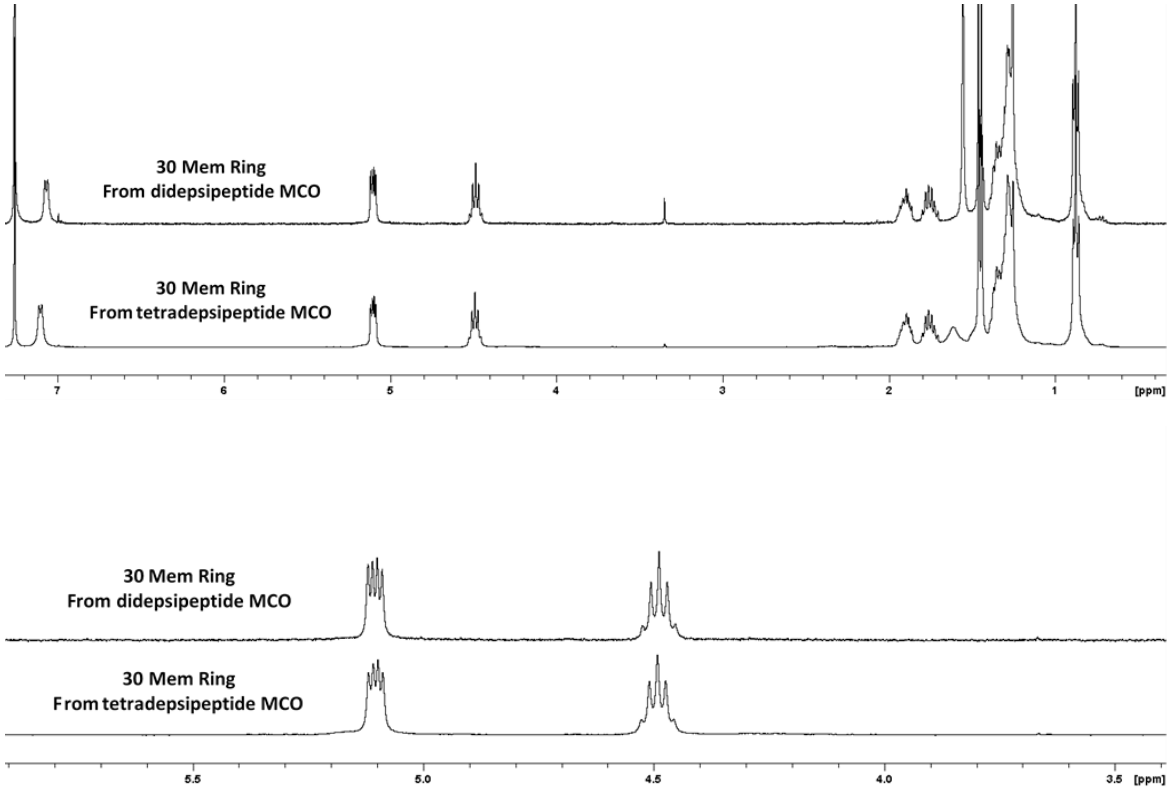

1.5.7 Initial Mechanistic Investigations

When postulating a possible mechanism, there are several plausible options to explore. The formation of an 18-membered COD from a 12-atom chain could result from 1) the presence of shorter monomers as impurities that co-oligomerize (e.g. 12+6) during MCO, 2) tetradepsipeptide monomer (12-atom chain) decomposition during reaction but pre-MCO, generating 6-atom chains, and 3) decomposition of oligomers to 6-atom monomers that then react with tetradepsipeptide monomer (e.g. 6+12). In the synthesis of these macrocyclic depsipeptides, the key oligomerization

step occurs through a Mitsunobu reaction in which the stereochemistry of the α-hydroxy amide is inverted. When probing the different mechanistic possibilities for simple tetradepsipeptide cleavage, almost all the options result in two linear peptides, heterochiral at the terminal α-hydroxy amide carbon. If this was occurring, the isolated macrocycles would be diastereomers heterochiral at one α-oxy amide, and the dissymmetry would likely be evident by ^{1}H NMR. Furthermore, these stereochemical analogues are separable by HPLC purification based on our previous work.[84] Throughout this reinvestigation, the combined yields of the three major MCOs were high, suggesting that any chain cleavage process was likely not random.

To rule out impure starting material as the source of adventitious didepsipeptide, the tetradepsipeptide was purified via reverse phase HPLC. There was no indication of didepsipeptide during this purification, and material purified in this manner produced the same array of products from MCO (Scheme 6, eq 1). HPLC-purified tetradepsipeptide was subjected to the same

Scheme 6. Summary of experiments probing the correlation of conditions to the formation of paradoxical ring-size CODs.

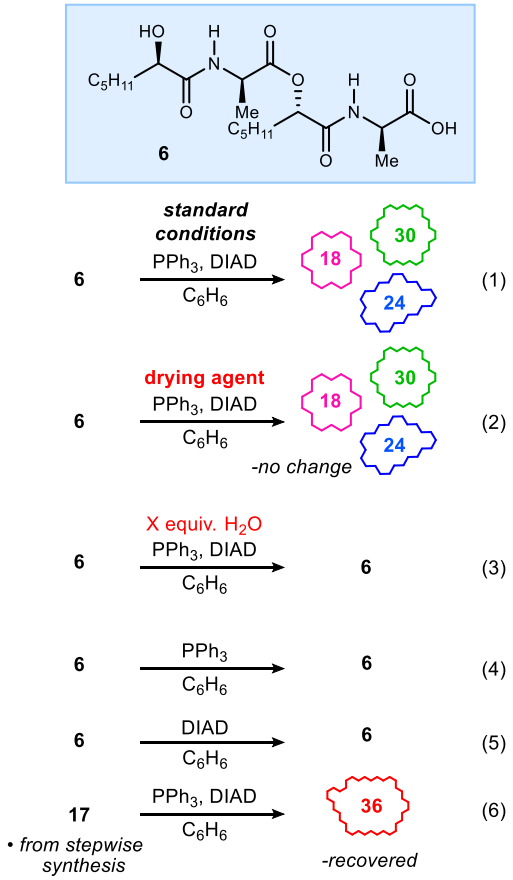

purification again, and no HPLC-induced decomposition was noted. We next tested the hypothesis that residual water in the reaction may cleave the central ester bond in the tetradepsipeptide in the MCO reaction or, separately, affect the level of possible anhydride species formed during the reaction. The formation of anhydrides in the Mitsunobu reaction has been studied,[135]and this pathway would be expected to form non-symmetrical CODs that we have yet to detect. Reactions with the tetradepsipeptide under dry conditions (Scheme 6, eq 2), or in the presence of a variety of drying agents did not decrease the amount of 18-membered ring or 30-membered ring formed in the reaction. Moreover, when varying amounts of water were added to the reaction (ranging from 0.25-5 equivalents) it yielded only starting material (no macrocycles) (Scheme 6, eq 3). To explore the possibility that DIAD or PPh_3 could cause cleavage of the tetradepsipeptide, we added each reagent to tetradepsipeptide in benzene for 12 hours. Both experiments returned only unreacted tetradepsipeptide with no sign of decomposition (Scheme 6, eq 4-5). Additionally, no decomposition was noted after stirring the starting material alone in benzene for several days. Hypothesizing that the rings could decompose after formation, and then recyclize to make smaller macrocycles, the authentic 36-membered ring was re-subjected to MCO reaction conditions (Scheme 6, eq 6). Again, no sign of decomposition was observed, and the starting material was recovered quantitatively. Finally, an experiment was investigated in which partially protected MOMO-tetradepsipeptide-CO_2H (**13**) was subjected to MCO reactions to determine if it was self-cleaving from the carboxylic acid terminus concomitant with the MCO reaction (Scheme 7).

Scheme 7. Evidence that MCO conditions can promote depsipeptide self-cleavage.

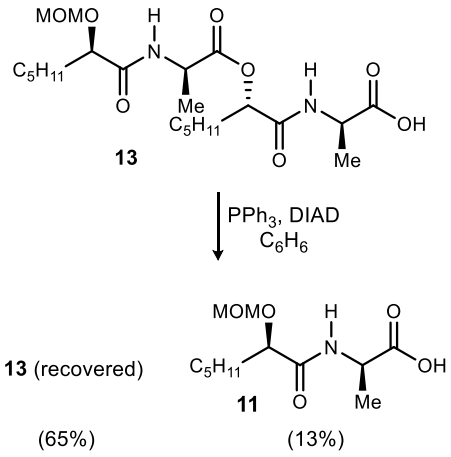

[135] Harvey, P. J.; von Itzstein, M.; Jenkins, I. D. *Tetrahedron* **1997**, *53*, 3933

While this experiment did result in mostly recovered starting material (65%), the protected didepsipeptide **11** was isolated by HPLC purification in 13% yield.

The observation of protected depsipeptide instability under the typical Mitsunobu reaction conditions employed in MCO provides a tangible basis on which to consider the 18-from-12 paradox. The formation of **11** from **13** does not readily explain the formation of the 18-membered ring (**8**) since an analogous cleavage of **6** would lead to *ent*-**4** and *epi*-**4**. While didepsipeptide *ent*-**4** would give the expected heterochiral CODs (L,D), didepsipeptide *epi*-**4** would lead to either homochiral CODs (D,D), or an epimer of **8** or **17**, both distinguishable by ^{1}H NMR. While it could be possible for the homochiral and heterochiral depsipeptides to only react with themselves, this would still generate a mixture of homochiral and heterochiral macrocyclic products (Scheme 8). The homochiral COD was synthesized and subjected to MCO conditions in prior work in the

Scheme 8. Simple ester hydrolysis would lead to a mixture of diastereomeric products.

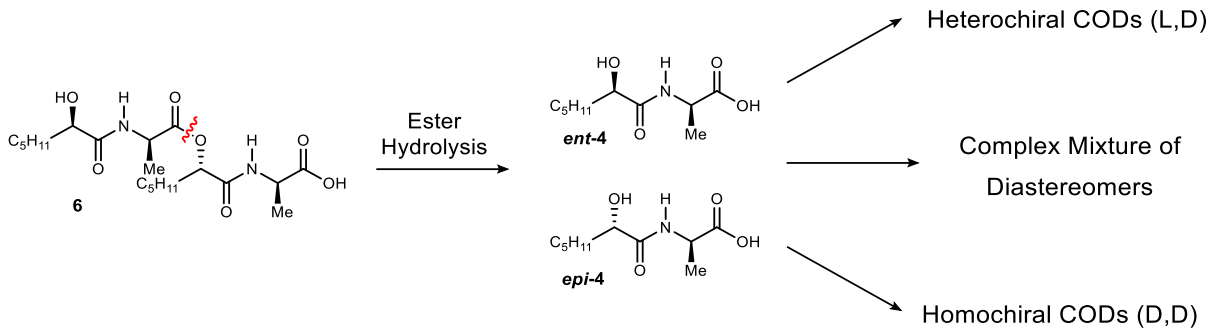

Johnston lab,[84] providing authentic samples to compare HPLC retention times. It was, therefore, a confident conclusion that this "self-reaction" was not the only mechanism occurring. To further ensure this was the case, an experiment was carried out in which *ent*-**4** and *epi*-**4**, the two didepsipeptides that would be the cleavage products of ester hydrolysis of the tetradepsipeptide, were subjected to the standard MCO conditions in the same reaction (Scheme 9). The resulting crude mixture was a complex mixture of diastereomeric compounds that was incredibly difficult to purify. Yet, these results provided important information. This reaction profile was strikingly different to the crude of MCO reactions, indicating that a simple ester cleavage into to depsipeptides was not a main mechanistic pathway. Furthermore, this experiment proved our assumption that these non-symmetrical analogues would have distinct NMS spectra

Scheme 9. Diastereomeric depsipeptides subjected to MCO conditions.

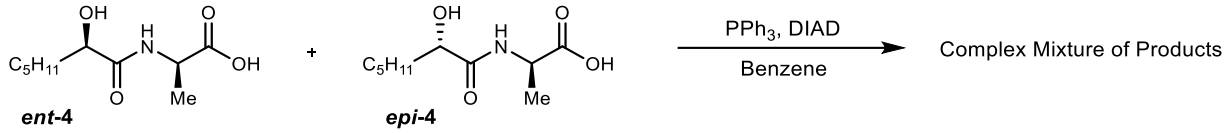

and HPLC retention times. Importantly, in our HPLC method, these diastereomers have overlapping retention times with the symmetrical analogues, making them difficult to separate, and therefore unlikely to miss. As a matter of current standard procedure, every fraction from the HPLC is examined when purifying these MCO reactions, and to date, there has been no evidence of any non-symmetrical analogues.

Our best rationale for the formation of **11** from **13** (Scheme 10) involves carboxylate addition to the central ester, collapse of this tetrahedral intermediate (a hemiorthoester)[136] to the anhydride isomer **23**, and then either anhydride hydrolysis, or similar transacylation to form an active ester. Despite our careful reexamination, this is our best evidence that small amounts of the linear depsipeptide chain are self-cleaving under the MCO reaction conditions. This occurrence, however, raises the question of why evidence of diastereomer formation is not observed. While the protected depsipeptide **11** is observed, didepsipeptide *epi*-**4,** where the α-hydroxy chiral center has already been inverted in a Mitsunobu reaction, should accompany it. The α-hydroxy amide configuration, therefore, is a label to determine the source of an MCO product; the expected heterochiral CODs (L,D) result from single-inversion Mitsunobu reactions. While the exact mechanism of cleavage is not certain, we outline a general pathway to explain this. These mechanistic proposals all stem from the formation of an anhydride (e.g. **18**). In one scenario, the pendant alcohol resulting from the anhydride formation could intramolecularly cleave the anhydride, resulting in diketomorpholine **24** and the dipeptide (*ent*-**4**) with the correct stereochemistry to participate in the MCO reaction to generate the heterochiral CODs (L,D)

[136] Literature studies of hemiorthoesters appear limited to five- and six-membered examples. Leading references: a) Austin, K.; Banwell, M.; Willis, A. *Arkivoc* **2006**, *xiii*, 1 b) McClelland, R. A.; Seaman, N. E.; Cramm, D. *J. Am. Chem. Soc.* **1984**, *106*, 4511 c) Capon, B.; Ghosh, A. K. *J. Am. Chem. Soc.* **1981**, *103*, 1765 d) Deslongchamps, P.; Chênevert, R.; Taillefer, R. J.; Moreau, C.; Saunders, J. K. *Can. J. Chem.* **1975**, *53*, 1601 e) Antonov, V. K.; Shkrob, A. M.; Shemyakin, M. M. *Tetrahedron Lett.* **1963**, *4*, 439 f) Lin, S.-Y.; Yu, H.-L.; Li, M.-J. *Polymer* **1999**, *40*, 3589 g) Chandrasekhar, S.; Kumar, H. V. *Tetrahedron Lett.* **2011**, *52*, 3561

Scheme 10. Mechanistic hypothesis for C-terminal didepsipeptide self-cleavage from the tetradepsipeptide prior to MCO.

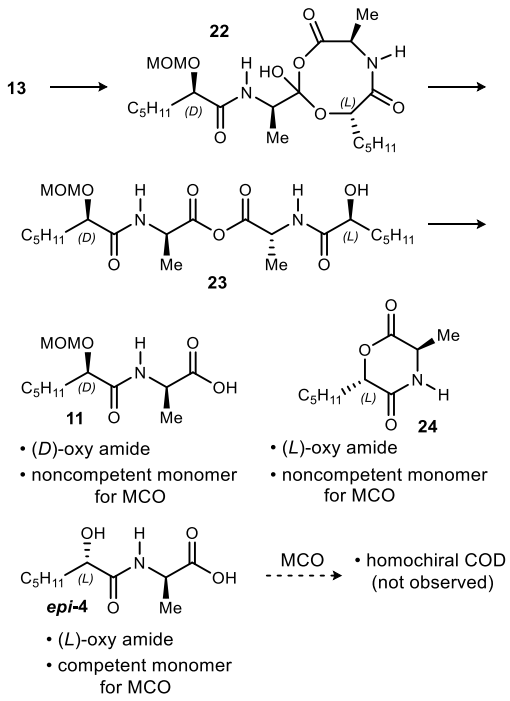

observed. The 18- and 30-membered ring formation support the presence of didepsipeptide *(ent-***4)**, which could react with the tetradepsipeptide and octadepsipeptide, respectively, to form the requisite COD linear precursors (pre-18, pre-30). Unfortunately, we have yet to isolate any diketomorpholine products from these reactions or see any indication of its presence in the crude reaction mixtures by ^{1}H NMR.[137] We speculate that this occurs with the tetradepsipeptide, but it is plausible that an analogous cleavage process could occur on a variety of linear depsipeptides.

Alternatively, a possible disproportionation mechanism is speculated. It is possible to imagine that a C-terminal didepsipeptide cleavage could occur on any linear oligomer (12,24,36, etc). If an anhydride were to form at the C-terminal end of an oligomer, one might imagine a disproportionation mechanism, in which a single didepsipeptide unit is transferred to another linear depsipeptide (Figure 36). For example, if an octadepsipeptide formed (pre-24), and then isomerized to an anhydride, it could be intercepted by another octadepsipeptide. This would lead

[137] A homochiral (D,D)-diketomorpholine is observed in the MCO of *epi*-**5** (ref.107) as the major product. While we would expect a heterochiral variant (L,D) in our case, if either were formed here, it should be detectable, owing to the remarkably distinct ^{1}H NMR peaks compared to other CODs.

to the pre-18 chain, as well as an anhydride variant of the pre-30 chain (*iso* pre-30), which upon isomerization, could form the pre-30 chain. This possibility provides an explanation why the diketomorpholine, homochiral macrocycles, and diastereomeric macrocycles are not observed under these reaction conditions. This type of mechanism could be related to a competitive transesterification process responsible for chain scission in the polymerization of hydroxy acids.[138,139]

Figure 36. A possible disproportionation mechanism to paradoxical ring sizes.

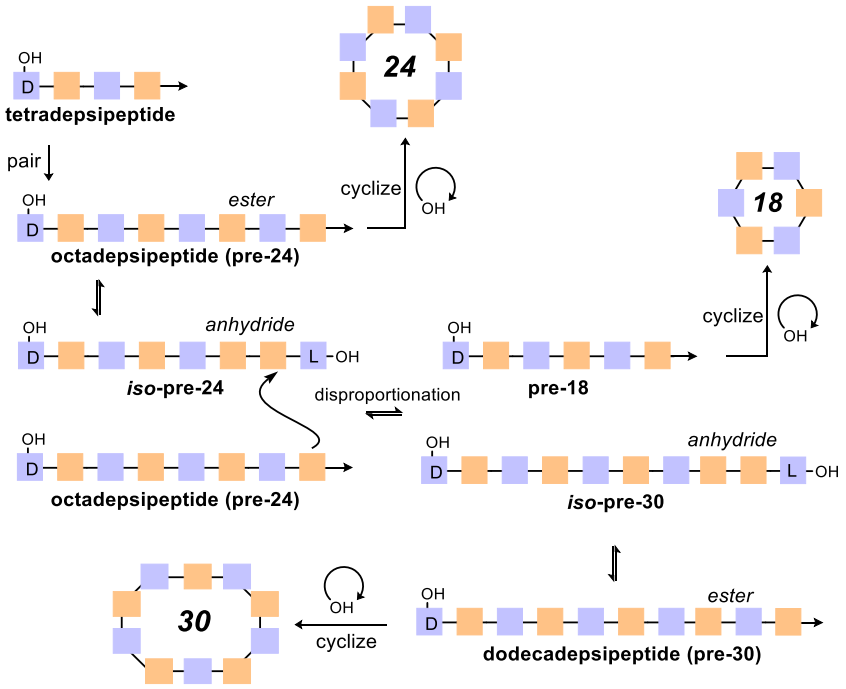

To work towards uncovering a possible mechanism, a series of labeling experiments were carried out. Deuterium was chosen as the isotopic label, as it presented the easiest route for introduction: commercially available labeled alanine-d_4. The experiments were carried out in the natural enantiomeric series, as the acquisition of the labeled natural amino acid L-alanine was more economically feasible than its labeled unnatural D counterpart. Initially, it was planned to synthesize the labeled octadepsipeptide and subject it to the MCO conditions, as this would be the

[138] Culkin, D. A.; Jeong, W.; Csihony, S.; Gomez, E. D.; Balsara, N. P.; Hedrick, J. L.; Waymouth, R. M. *Angew. Chem. Int. Ed.* **2007**, *46*, 2627
[139] Szymanski, R. *Macromol. Theory Simul.* **1998**, *7*, 27

key intermediate in our proposed disproportionation mechanism. The synthesis of the labeled octadepsipeptide was carried out using previously described methodology, substituting the alanine-d_4 for alanine-d_0. Once in hand, a series of MCO conditions varying the concentration were tested (0.02 – 0.005 M), all of which failed to produce any ring size other than the 24 membered ring. While disappointing, it is possible that the kinetics in this experiment are different than those in the MCO with the tetradepsipeptide monomer. Given the complexity of the reactions and the small scale, it was unfeasible to use *in-situ* reaction monitoring such as IR to monitor intermediates.

At this point, it was instead decided to attempt the labeling experiments with a tetradepsipeptide. The synthesis of labeled tetradepsipeptide 25 was carried out in the same manner as that of the labeled octadepsipeptide. Once synthesized, 10 mg of the labeled tetradepsipeptide was combined with 10 mg of the unlabeled tetradepsipeptide and subjected to standard tetradepsipeptide MCO conditions (Figure 37). The main goal of this experiment was to

Figure 37. First deuterium labeling study with a fully labeled tetradepsipeptide.

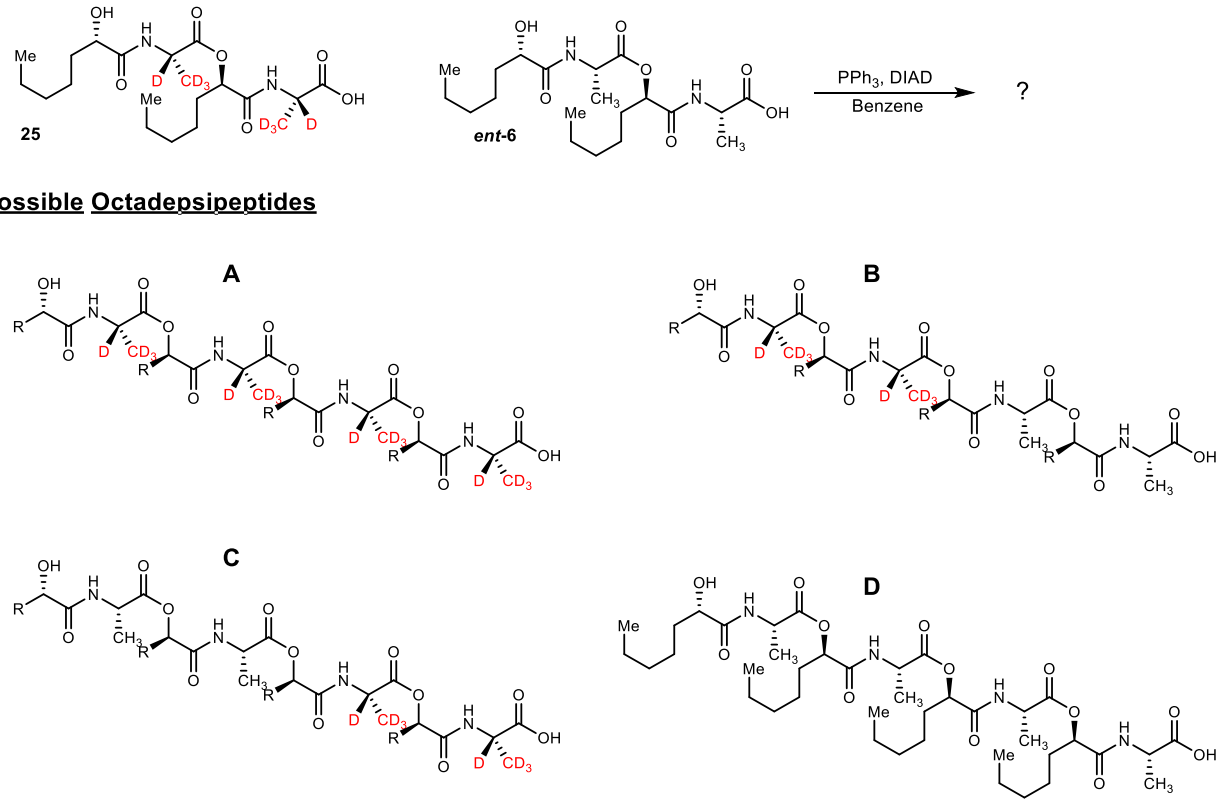

identify possible label cross-over, by unexpected label in products. For example, if no cross-over is present, it would indicate a mechanistic pathway that differed from the proposed disproportionation. However, if significant cross over is observed, it would be a piece of supporting evidence towards a more complex mechanistic pathway such as that depicted in Figure 36. Prior to carrying out the experiment, all possible 18- and 30-membered rings based on the hypothesized mechanism were mapped (Figure 38). The crude reaction mixtures were then analyzed using HRMS to determine the ring sizes present.

The results from the HRMS studies were striking – an extensive amount of cross-over was observed between the labeled and non-labeled tetradepsipeptide. With the 18- and 30-membered rings, every possible labeled product was observed, consistent with a possible disproportionation mechanism (Figure 39, Figure 41, and Figure 42). Furthermore, when looking at the ratio of which 30-membered rings should be most prevalent, one sees that there should be twice as much of D4 and D12 30-membered rings. If the assumption is made that all 30-membered rings ionized similarly, regardless of their extent of labeling, then this pattern holds true when looking at the intensity of each ion peak (Figure 41 and Figure 42). Further quantitative mass spectrometry studies would need to be carried out to further verify this possible pattern. With the 24-membered ring, the favored ring size in the tetradepsipeptide MCO, only the non-labeled, half-labeled, and fully labeled ring sizes were observed (Figure 40). The lack of a 1-residue or 3-residue labeled 24-membered ring argues against a mechanism in which a didepsipeptide is formed *in-situ* and polymerized. Instead, it supports a mechanism in which chain splicing occurs from longer chains to form the 18- and 30-membered ring (Figure 36). A comparison between the possible products and the observed products is shown in Table 5. A final important point to note here, is the possibility of diastereomers making up the different ring sizes – an aspect that wouldn't be evident using only HRMS analysis. However, based on acquired results from the tetradepsipeptide MCO experiments run thus far, where there has yet to be any evidence of diastereomers, almost certainly translates to this experiment as well.

Figure 38. Possible labeled 18- and 30-membered CODs from the respective octadepsipeptide anhydrides and their disproportionation with another octadepsipeptide.

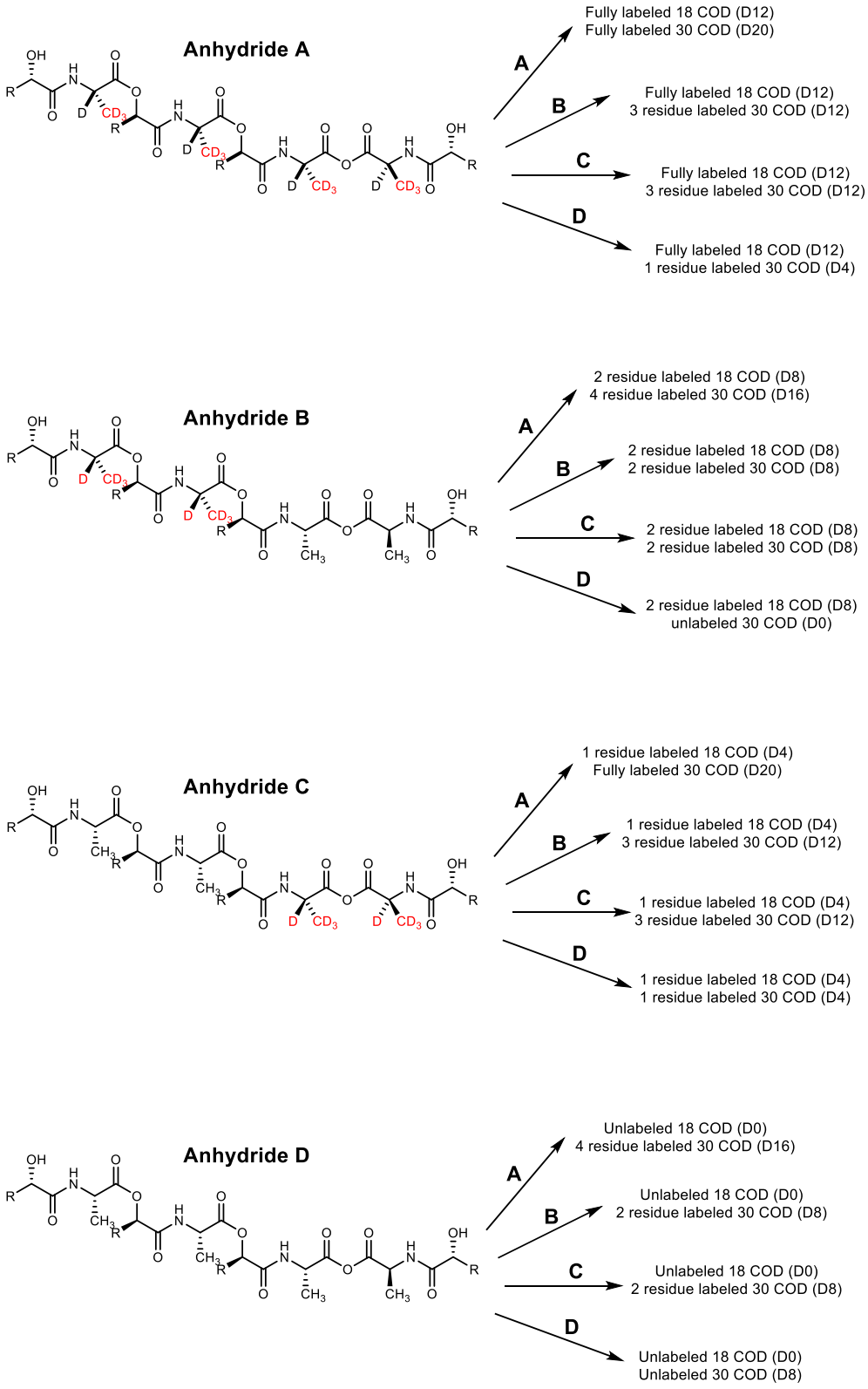

Figure 39. Observed masses for 18-membered ring from labeled tetradepsipeptide experiment.

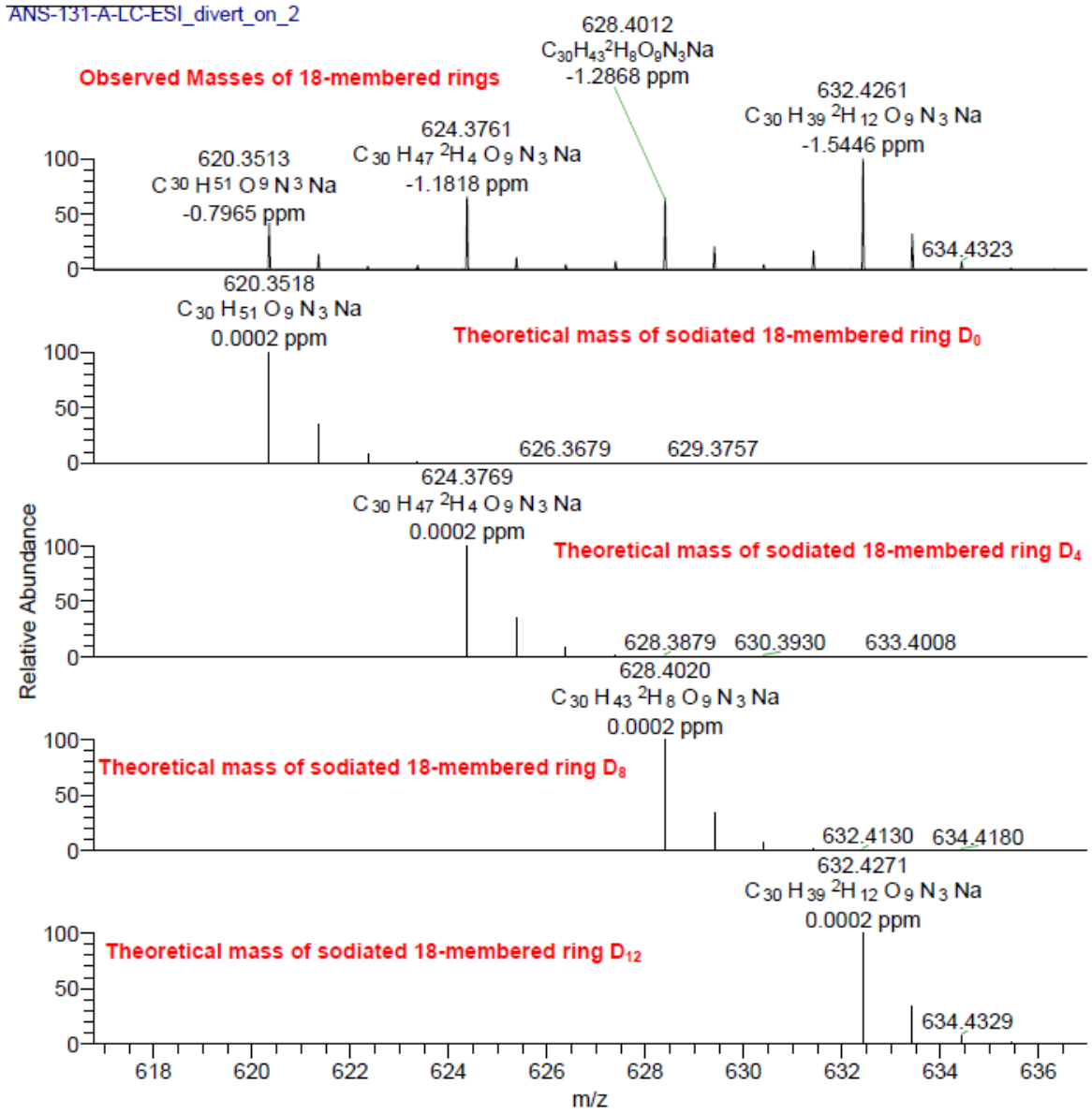

Figure 40. Observed masses for 24-membered ring from labeled tetradepsipeptide experiment.

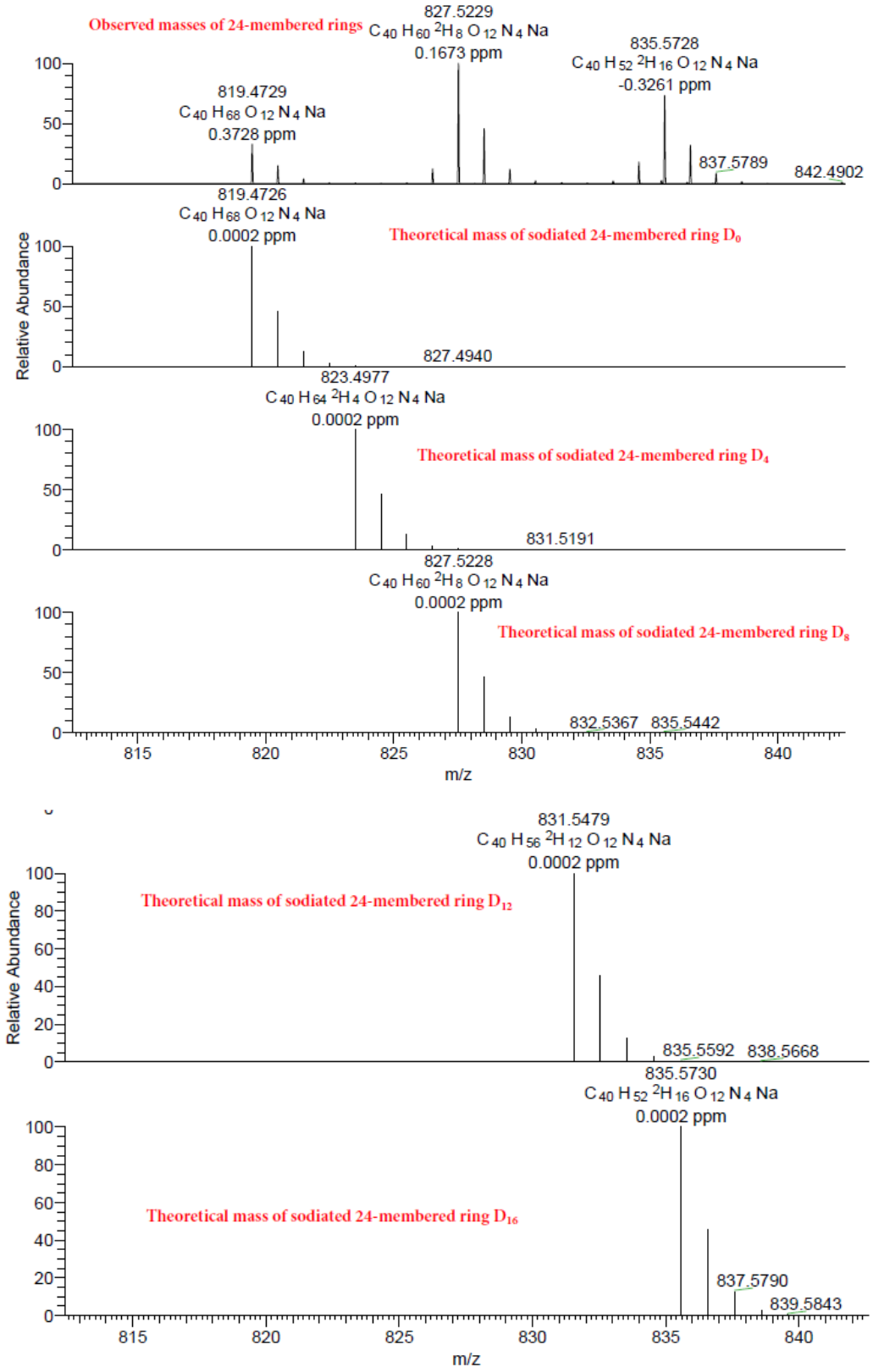

Figure 41. Observed higher masses for 30-membered ring from labeled tetradepsipeptide experiment.

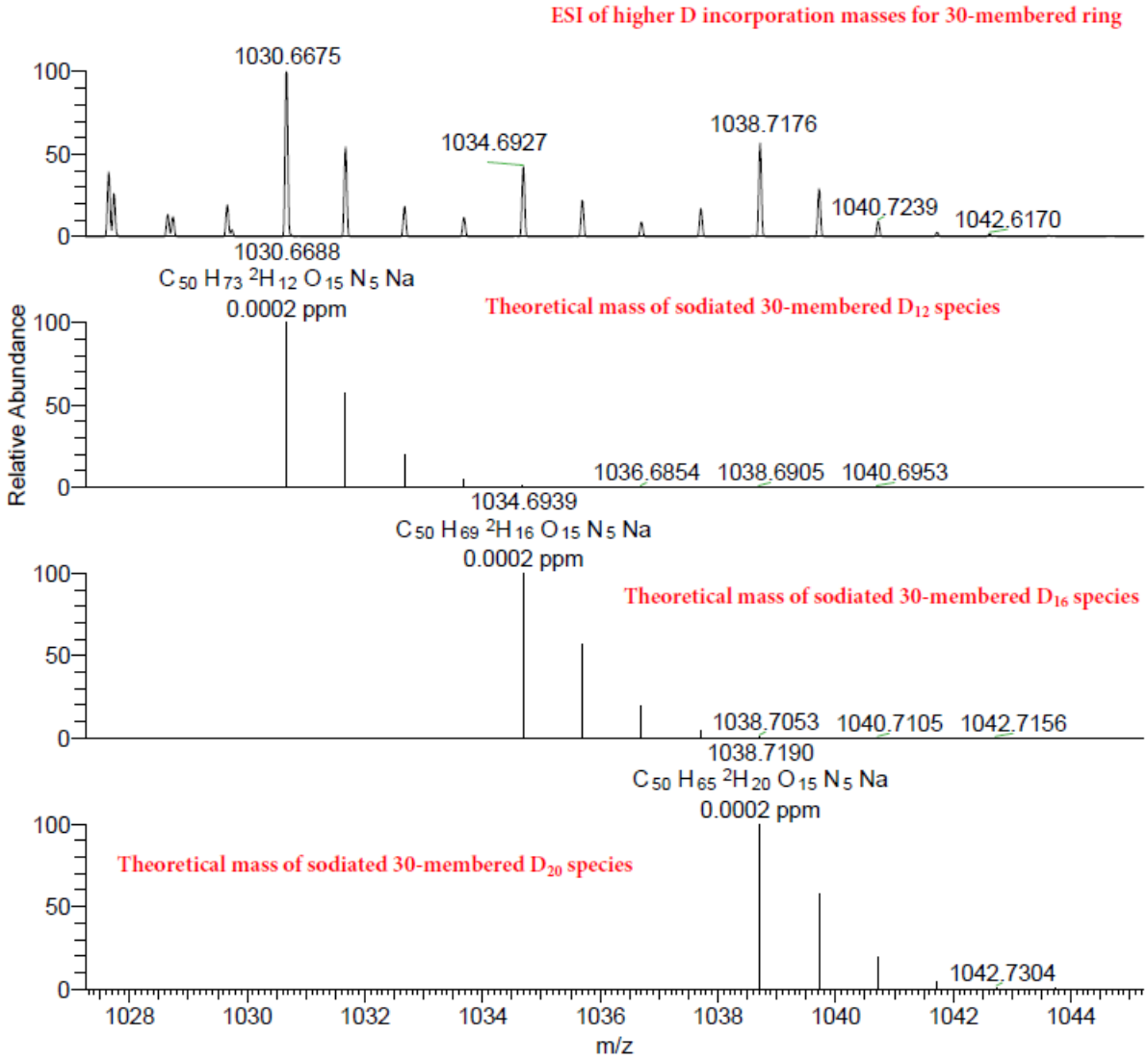

Figure 42. Observed lower masses for 30-membered ring from labeled tetradepsipeptide experiment.

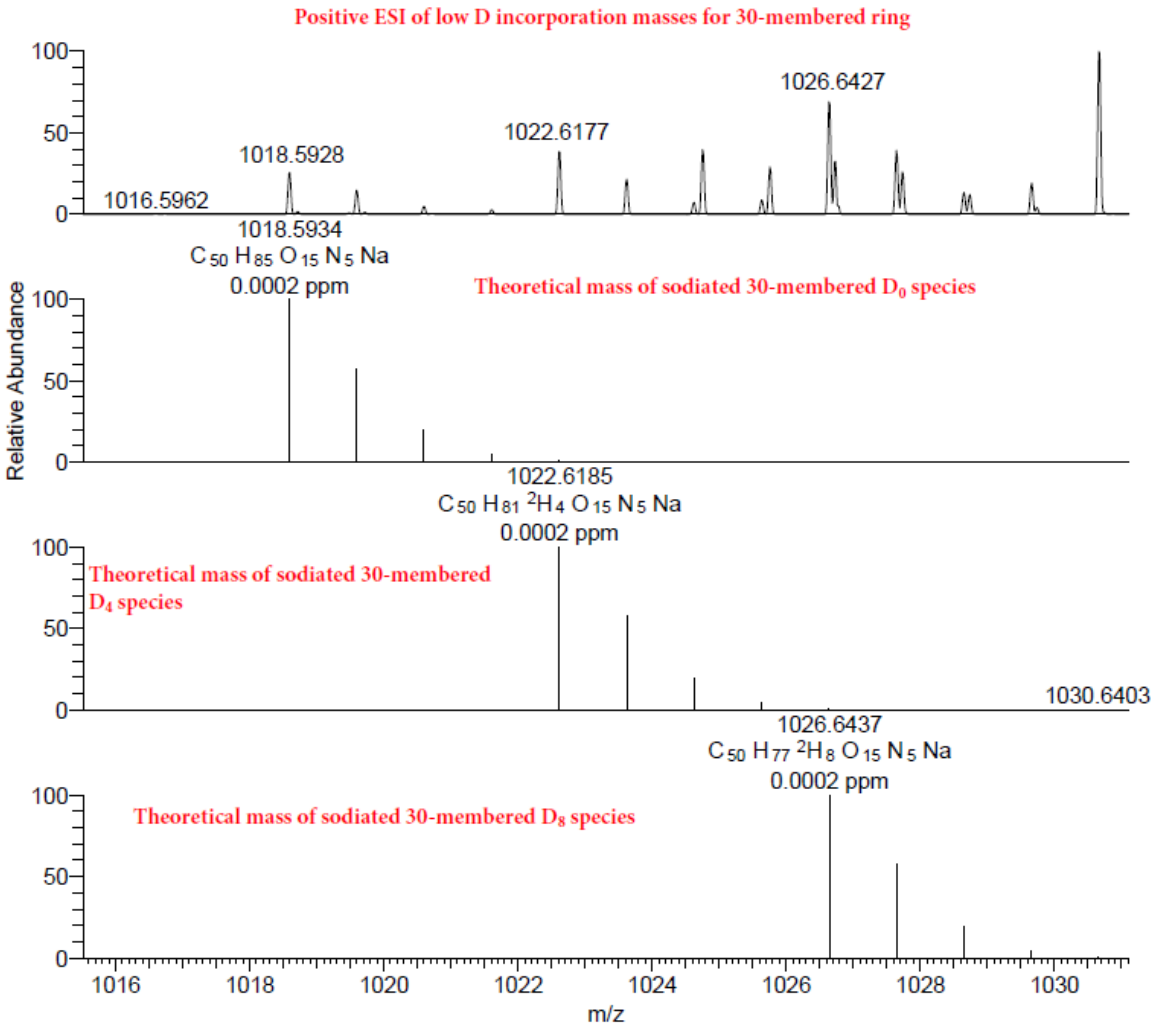

Table 5. Summary of observed HRMS masses and the corresponding ring size from labeling experiments.

Ring Size	Residues labeled	Total Deuterium Incorporation	Theoretical Mass	Observed Mass
18	0	D0	620.3518	620.3513
18	1	D4	624.3796	624.3761
18	2	D8	628.4020	628.4012
18	3	D12	632.4271	632.4261
24	0	D0	819.4726	819.4729
24	1	D4	823.4977	-
24	2	D8	827.5228	827.5299
24	3	D12	831.5479	-
24	4	D16	835.5730	835.5728
30	0	D0	1018.9534	1018.5928
30	1	D4	1022.6185	1022.6177
30	2	D8	1026.6437	1026.6427
30	3	D12	1030.6688	1030.6675
30	4	D16	1034.6939	1034.6927
30	5	D20	1038.7190	1038.7176

Following the first labeling study, another comparative experiment was carried out in which a partially deuterated tetradepsipeptide **26** was subjected to reaction conditions. In this case, only one of the two alanine residues incorporated deuterium (Figure 43). This label was strategically placed on the back-half of the tetradepsipeptide in which the α-amino ester stereocenter had already been inverted, with the goal of tracking the labeled depsipeptide in the products. In this simpler case, only one octadepsipeptide is formed. If the proposed disproportionation mechanism is predominating, there should only be an 18-membered ring with a single residue labeled (4D) and a 30-membered ring with 3 residues labeled (12D). In practice, the perplexing results of this experiment, however, brought up more unanswered questions. When analyzing the crude reaction mixture by LRMS, only a few products were observed: 1 residue labeled 18-membered ring, 2 residue labeled 24-membered ring, and 2 residue labeled 30-membered ring. While the 18- and 24-membered ring products were as expected, the 30-membered ring was not. The observation of a 2-residue labeled 30-membered ring is more in line with a mechanism in which the right terminal depsipeptide has been cleaved in a manner that renders it no longer reactive under the reaction

Figure 43. Possible labeled 18- and 30-membered CODs from the partially labeled tetradepsipeptide following a disproportionation mechanism.

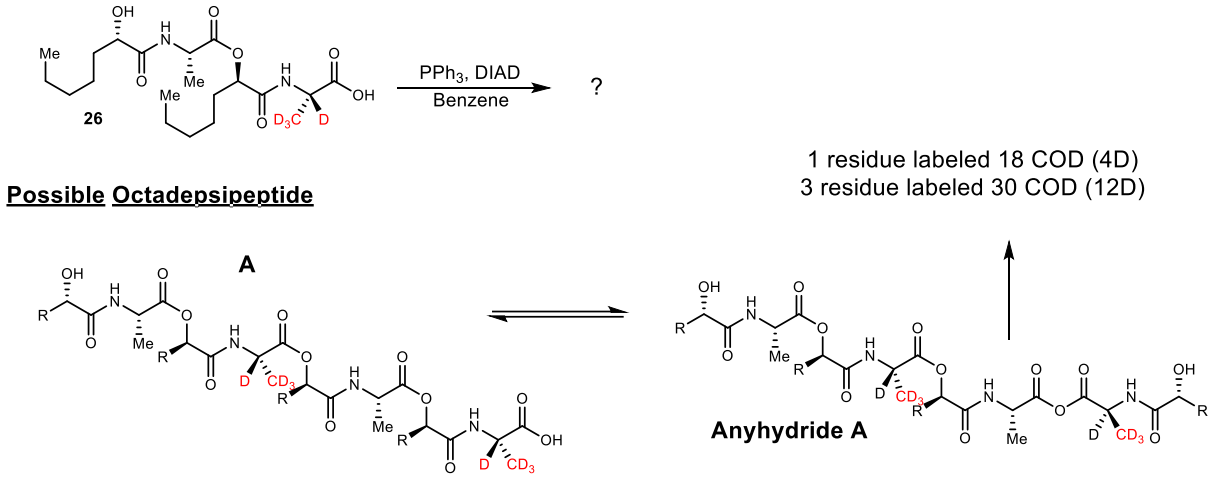

Figure 44. Mechanism that better aligns with results from the second deuterium labeling study.

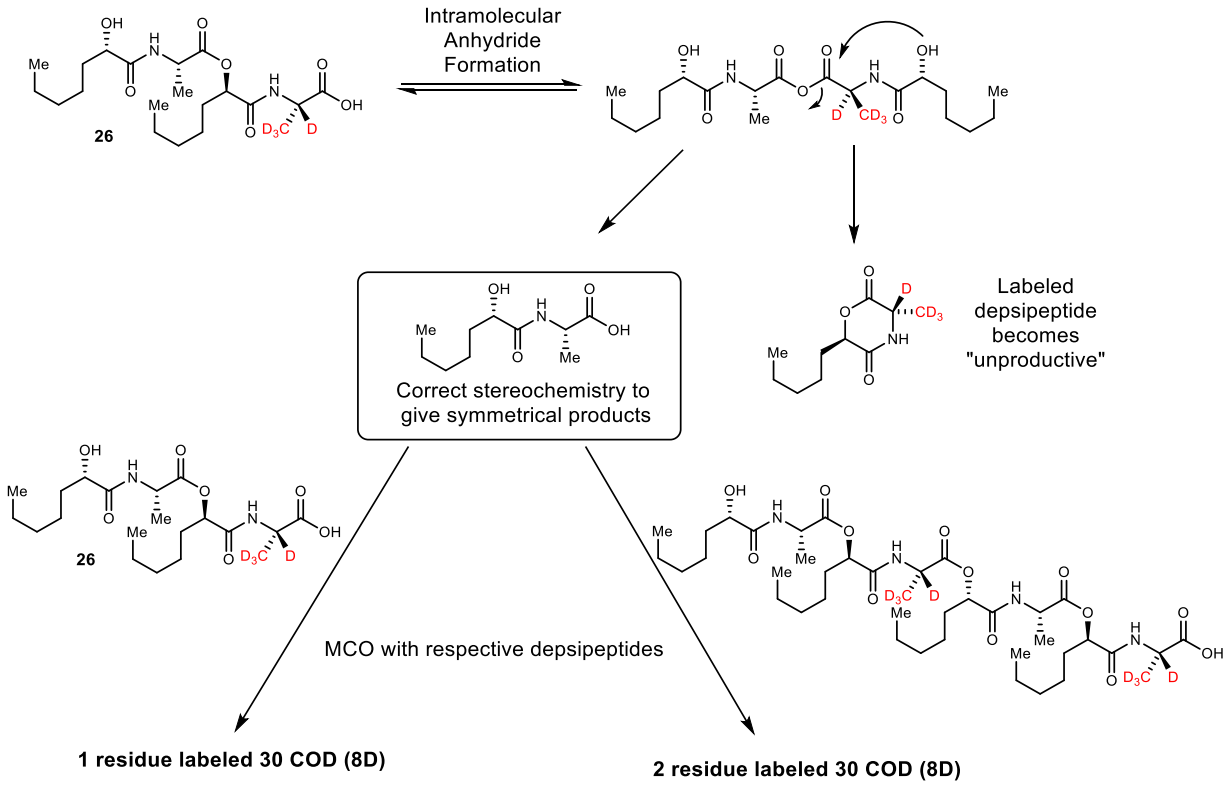

conditions. An example of this would be through formation of a diketomorpholine species, as demonstrated in Figure 44. This again, however raises the question of what happens to the labeled didepsipeptide? We see no indication of the 6-membered diketomorpholine species, either by NMR or by HRMS of the crude reaction mixture. Collectively, while each labeling study provided new insight into the reaction, at this point in time, neither point towards a single mechanism. Further mechanistic work is needed to help elucidate this complex behavior.

1.5.8 Other Series Mechanistic Perspective – MCO with Valinomycin

During our study of the MCO reaction, other series were explored to determine its applicability on a broader scale. One of these cyclic oligomeric depsipeptides targeted was valinomycin, a naturally occurring 36-membered COD with D and L valine, D-α-hydroxyisovaleric acid, and L-lactic acid residues (Figure 45). Unlike *ent*-verticilide, valinomycin is symmetrical at the tetradepsiptide unit instead of the didepsipeptide unit. When running the MCO reaction on the tetradepsipeptide of valinomycin, three products were consistently isolated: 1) a compound that appears to have similar characteristics to valinomycin but never quite matched by ^{1}H NMR, 2) montanastatin (**27**), the 24-membered ring variant of valinomycin that we confirmed by X-ray crystallography, and 3) an apparent "impossible" 18-membered ring (**29**) in 8-10% yield (Figure 46). Like *ent*-verticilide, in this case with the tetradepsipeptide as the starting material, an 18-membered ring should not be a possible product, as it is not a multiple of 12. However, all

Figure 45. Chemical structures of valinomycin and montanastatin.

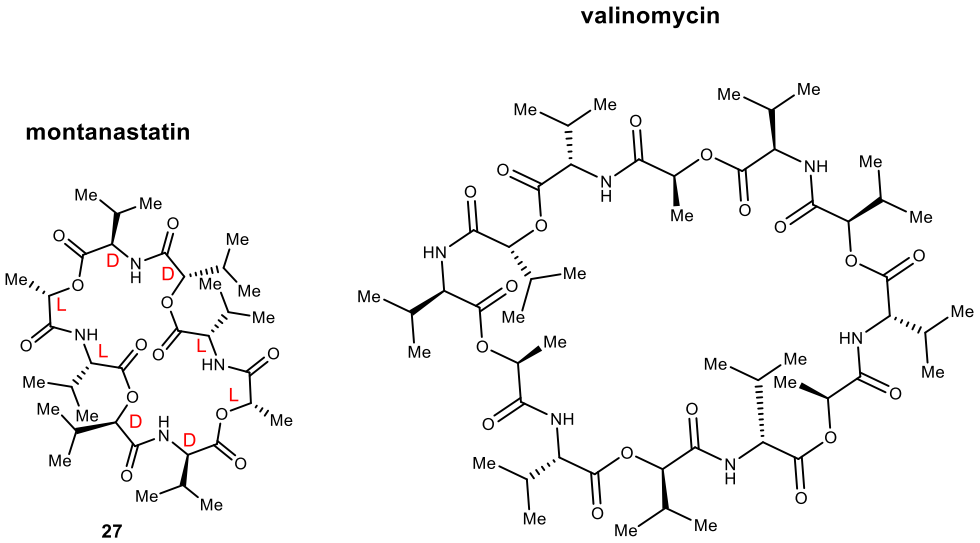

characterization data, including NMR and HRMS is consistent with an 18-membered ring. In this case, the symmetry of the molecule must be broken to form an 18-membered ring, making the NMR more distinct. Indeed, we see an NMR spectrum consistent with only one α-methyl group (a quartet at 5.25 ppm), three α-isopropyl groups adjacent to an *N*-H (doublet of doublets at 4.25, 4.55, and 4.81 ppm), and two α-isopropyl groups adjacent to an ester bond (doublets at 4.27 and 4.92 ppm). HRMS ion peaks within standard error are seen for salt adducts $[M+Na]^+$ and $[M+K]^+$. Furthermore, when looking at higher ion peaks, there are not any present that would correspond to a larger macrocycle as we see with the 18-membered ring in the verticilide case. Finally, we have seen in all our series to this point, the larger the macrocycle in the same series, the more lipophilic it becomes – this is evident in the elution from reverse phase prep HPLC. This 18-membered ring was the first macrocycle eluted, followed by the 24-membered ring, then the suspected 36-membered ring, consistent with behavior previously observed.

Figure 46. MCO reaction that produced an "impossible" 18-membered valinomycin analogue.

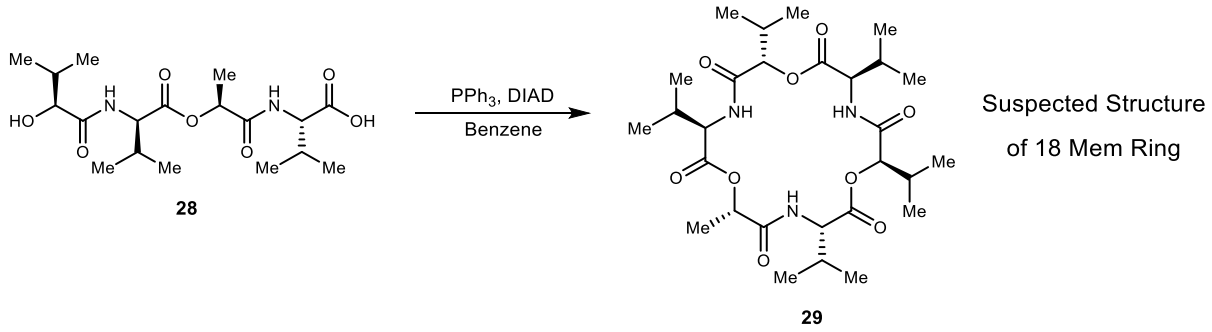

28 **29**

There are several mechanistic possibilities for the formation of this macrocycle. In this case, unlike with verticilide, we cannot confirm the stereochemistry. Due to valinomycin being an oligomer of the tetradepsipeptide instead of a didepsipeptide, any 18-membered ring would be unsymmetrical. However, it is reasonable to hypothesize that this cleavage is occurring in the same way as with the verticilide series, as it is the "front" didepsipeptide (**30**) of the tetradepsipeptide (**28**) that is responsible for the third residue in the observed 18-membered ring (**29**) (Figure 47). With the verticilide series, a possible mechanism in which intramolecular anhydride formation occurs, followed by intramolecular cleavage of the anhydride to give a didepsipeptide and diketomorpholine was proposed. This 18-membered ring formed in valinomycin would be

Figure 47. Precursors needed to form the observed 18-membered ring valinomycin analogue.

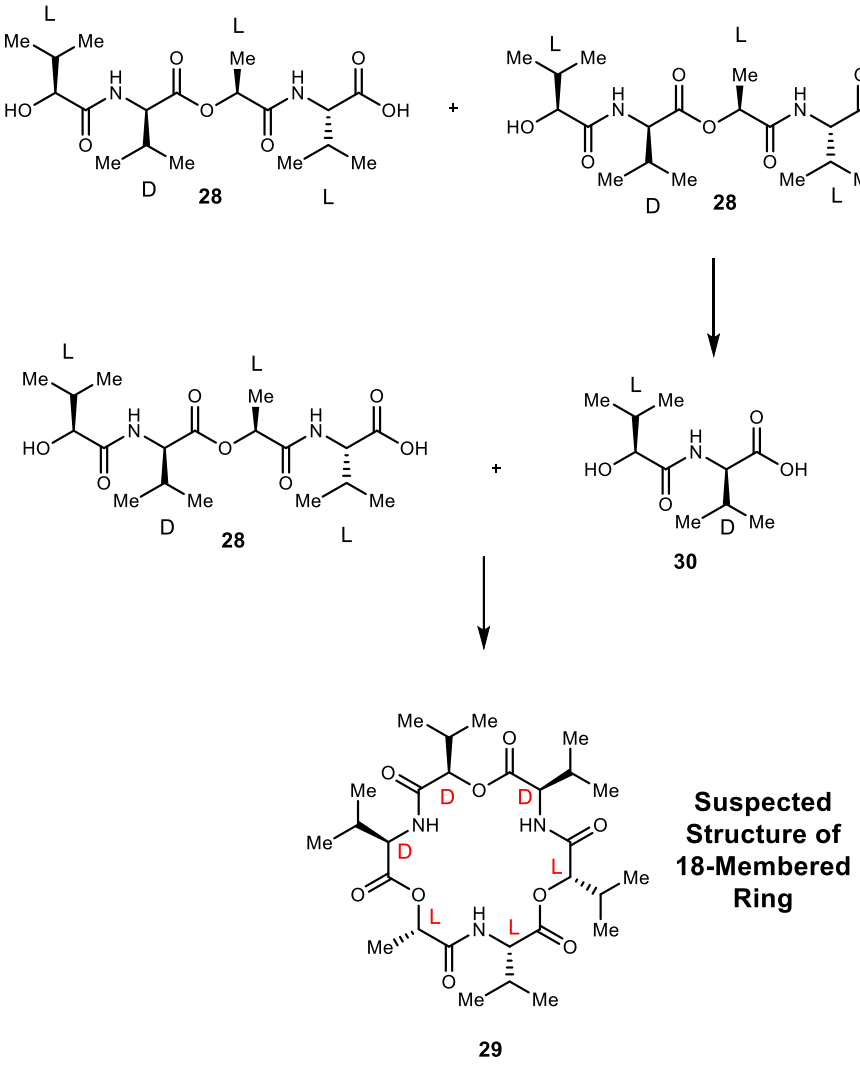

supportive of this type of mechanism (Figure 48). However, once again, no diketomorpholine species has been observed in crude ^{1}H NMR spectra or isolated. When assessing the previously proposed disproportionation mechanism in this series, inconsistencies are noted. In this case, only one “impossible” ring size was isolated and there is no evidence of a 30-membered macrocycle that would in theory be present as well (Figure 49). At this point, while it is evident that a similar cleavage mechanism is occurring, there is no conclusive evidence to point in the direction of either mechanism. Further mechanistic studies are needed to elucidate this complex behavior.

Figure 48. Possible mechanism for formation of the 18-membered valinomycin analogue.

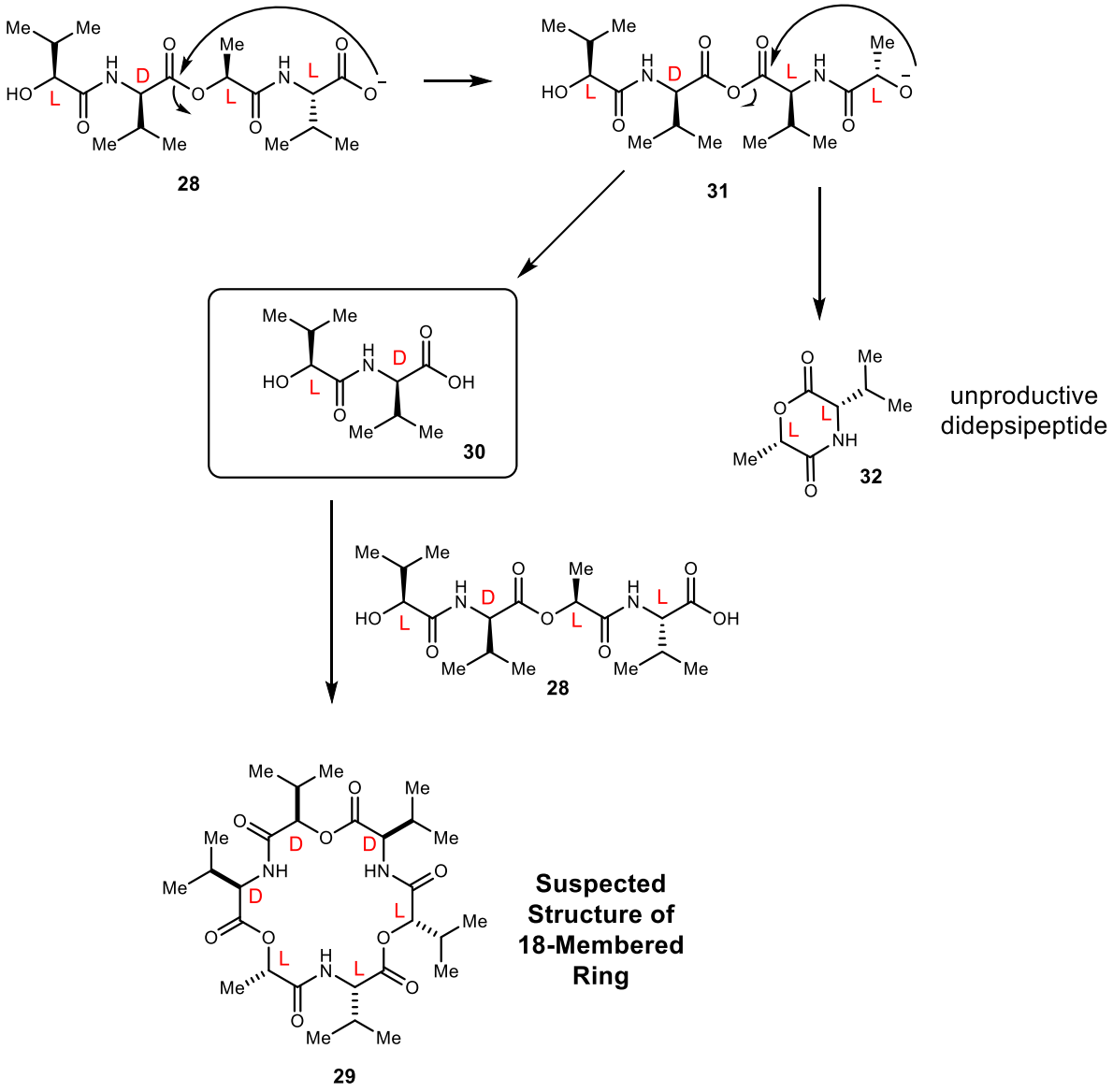

Figure 49. Disproportionation mechanism applied to valinomycin series.

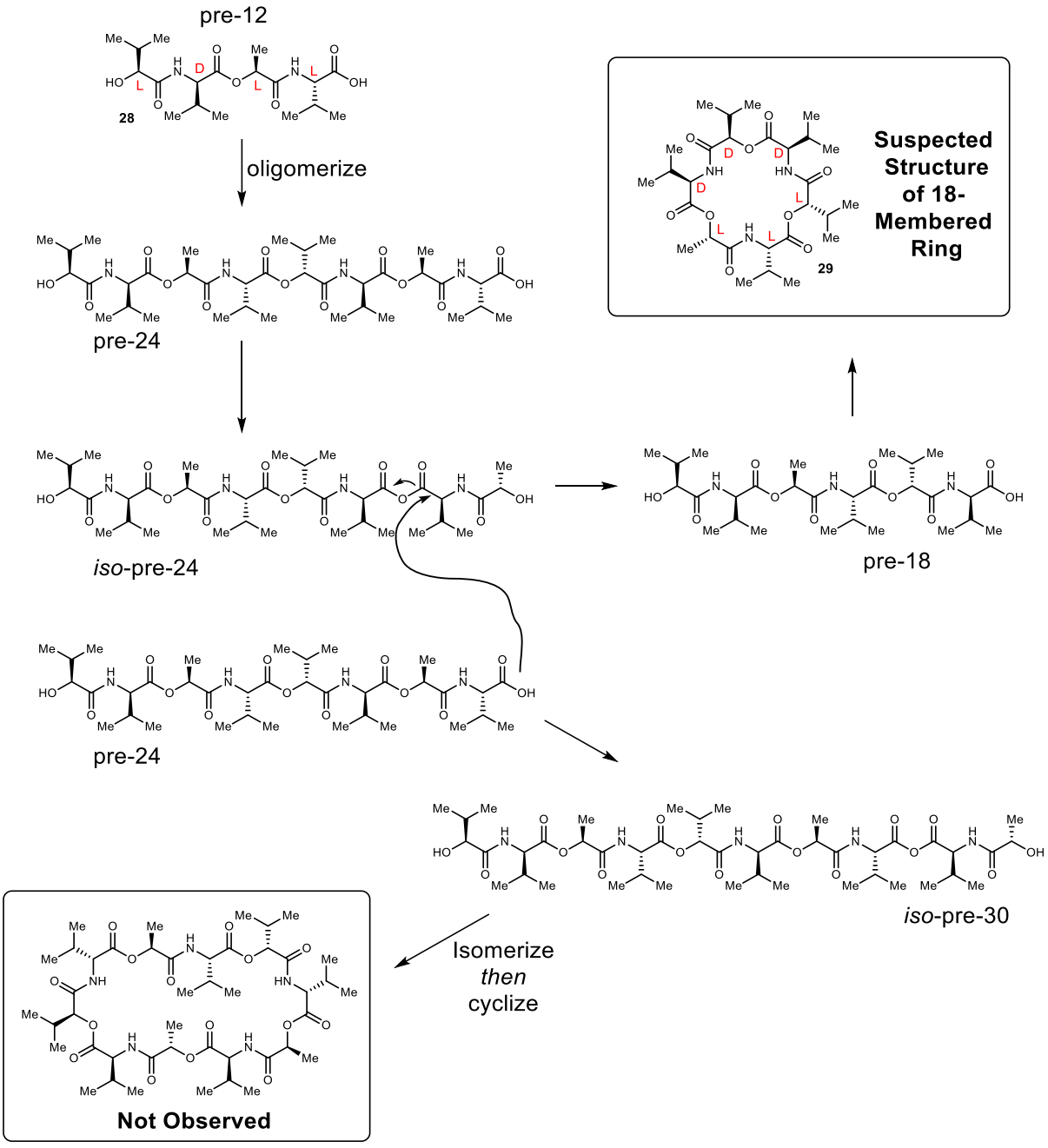

1.6 Conclusions and Outlook

In summary, we have re-examined a case in which we isolated a material from an MCO reaction, utilizing a tetradepsipeptide, with the original assignment as a 36-membered ring. Through synthesis of authentic 36-membered ring material using a stepwise route and analysis of its product, we have reassigned the 'original 36' material to be the 18-membered ring – a size not possible by direct oligomerization of a tetradepsipeptide (12 atom chain). While its relative stereochemistry confirms that it is formed during an MCO, its size is paradoxical since a hexadepsipeptide cannot form directly from a tetradepsipeptide. A protocol that allows for careful and accurate analysis of each MCO reaction has been developed, resituating these studies on sound analytical data. Our reanalysis of this case illuminates the paradox and explores several possible mechanisms, narrowing to an elongation that succumbs to an unusually competitive self-cleavage step. Importantly, the additive effects that have been shown to template certain MCO reactions are reevaluated, highlighting the possible insensitivity of this specific tetradepsipeptide conversion to added sodium or potassium salts. This work highlights the complex behavior at play when synthetically manipulating depsipeptides, and further mechanistic studies are warranted in the future to elucidate this behavior.

Chapter II

II. DEVELOPMENT OF ENT-VERTICILIDE AS AN RYR2 SELECTIVE PROBE

2.1 Background on RyR2 Dysfunction and RyR Channels as Drug Targets

Ryanodine receptors (RyR) are intracellular Ca^{2+} release channels in the sarcoplasmic reticulum (SR), named after the plant alkaloid ryanodine. Ryanodine has an incredibly high binding affinity for the open state of the channel and played a critical role in the purification and characterization of this class of ion channels.[140] At nanomolar concentration, ryanodine binds to lock the channel in an open subconductance state, and at micromolar concentration, it inhibits the channel, locking it into a fully closed state.[141] These are the largest known ion channels, with molecular masses greater than 2 megadaltons,[142] and play a critical role in many Ca^{2+} physiological processes, specifically controlling the release of calcium from the endoplasmic or sarcoplasmic reticulum. RyR channels are incredibly important in E-C (excitation-contraction) coupling in both skeletal and cardiac muscle.[141] Mammals have three isoforms of RyR: RyR1, located in skeletal muscle, RyR2, predominantly expressed in the cardiac muscle, and RyR3, which is localized mostly within the brain. RyR1 is the most extensively studied isoform, due to its high expression level and easier purification. The three mammalian isoforms share about 65% sequence homology, with three major regions of diversity, referred to as D1, D2, and D3. D1 is between residues 4210-4562 in the cardiac sequence (4254 and 4631 in the skeletal sequence), D2 is between residues 1353 and 1397 in the cardiac sequence (1342 and 1403 in the skeletal sequence), and D3 is between residues 1852 and 1890 in the cardiac sequence (1872 and 1923 in the skeletal sequence).[141]

Cryogenic electron microscopy (cryo-EM) has been the main tool utilized to gain insight into the structural complexities of RyR. There are numerous cryo-EM structures for segments of RyR channels, with resolution varying from 2.0 to 3.8 Å. It was only very recently that the full structures for RyR1 (rabbit)[143] and RyR2 (porcine)[144] were solved, in both closed and open states. Each RyR channel is a tetrameric structure, with a central ion-conducting pore, a cytoplasmic region with over 4500 residues, and a carboxyl terminal transmembrane domain. The transmembrane domains

[140] Sattelle, D. B.; Cordova, D.; Cheek, T. R. *Invertebrate Neuroscience* **2008**, *8*, 107
[141] Lanner, J. T.; Georgiou, D. K.; Joshi, A. D.; Hamilton, S. L. *Cold Spring Harbor perspectives in biology* **2010**, *2*, a003996
[142] Inui, M.; Saito, A.; Fleischer, S. *J. Biol. Chem.* **1987**, *262*, 15637
[143] Bai, X.-C.; Yan, Z.; Wu, J.; Li, Z.; Yan, N. *Cell Research* **2016**, *26*, 995
[144] Peng, W.; Shen, H.; Wu, J.; Guo, W.; Pan, X.; Wang, R.; Chen, S. R.; Yan, N. *Science* **2016**, *354*,

enclose the central pore, whereas the cytoplasmic regions serve as an area for interaction with protein modulators, such as calmodulin (CaM) and FKBP.[144] FKBP12 and FKBP12.6 play a significant role in the stabilization of the RyR complex, allowing the four subunits to open and close in a controlled manner.[145] CaM, is a calcium binding protein that functions as an intracellular calcium sensor, by binding to RyR in a calcium dependent manner. At submicromolar calcium concentrations, CaM inhibits RyR2, but activates RyR1 and RyR3. At micromolar calcium concentrations, CaM reduces the opening of the channel, inhibiting all isoforms of RyR.[145] While CaM and FKBP play significant roles in RyR regulation, a variety of other proteins also have influence on RyR regulation, including calsequestrin, junctin, and triadin.[146] Additionally, RyR channels can be directly or indirectly modulated by L-type Ca^{2+} channels.[147]

The large cytoplasmic domain of RyR channels is the site of most mutations that underlay many RyR related disease paths. Several malignant arrhythmia syndromes have been linked to mutations in cardiac RyR2 ion channels. RyR2 functions via a mechanism known as calcium-induced calcium release, and mutations in RyR2 can cause spontaneous Ca^{2+} release into the SR. This type of RyR2 dysfunction has been implicated in a variety of cardiovascular diseases that are characterized by ventricular arrhythmias, including catecholaminergic polymorphic ventricular tachycardia (CPVT) and arrhythmogenic right ventricular cardiomyopathy/dysplasia type 2 (ARVC/D2). These diseases both present as stress-or exercise induced ventricular tachycardia, with sudden cardiac death often being the first and only symptom. Accounting for 10-20% of adult deaths in the US, sudden cardiac death originating from ventricular arrythmias is a major public health concern. The Knollmann lab discovered that flecainide, a small molecule antiarrhythmic, could be administered to reduce VT episodes in CPVT patients.[148] While the mechanism of action of flecainide has been something of a controversy over the years, in a collaboration led by the Knollmann lab, we recently reported a study demonstrating that RyR2 channel inhibition is the principal mechanism of flecainide action in CPVT.[149] Based on strong evidence from preclinical and clinical studies, it is generally accepted that normalizing RyR2 function is a valid therapeutic

[145] Divet, A.; Paesante, S.; Bleunven, C.; Anderson, A.; Treves, S.; Zorzato, F. *J Muscle Res Cell Motil* **2005**, *26*, 7
[146] Handhle, A.; Ormonde, C. E.; Thomas, N. L.; Bralesford, C.; Williams, A. J.; Lai, F. A.; Zissimopoulos, S. *J. Cell Sci.* **2016**, *129*, 3983
[147] Tanabe, T.; Beam, K. G.; Adams, B. A.; Niidome, T.; Numa, S. *Nature* **1990**, *346*, 567
[148] Watanabe, H.; Chopra, N.; Laver, D.; Hwang, H. S.; Davies, S. S.; Roach, D. E.; Duff, H. J.; Roden, D. M.; Wilde, A. A. M.; Knollmann, B. C. *Nat. Med. (N. Y., NY, U. S.)* **2009**, *15*, 380
[149] Kryshtal, D. O.; Blackwell, D. J.; Egly, C. L.; Smith, A. N.; Batiste, S. M.; Johnston, J. N.; Laver, D. R.; Knollmann, B. C. *Circ. Res.* **2021**, *128*, 321

approach in CPVT, and RyR2 is considered a promising target for other disorders caused by hyperactive RyR2 channels.

While RyR2 is predominately expressed in cardiac muscle, small amounts RyR2 are also present in the brain. Mutations in neuronal RyR2 have been implicated in several diseases including Alzheimer's disease (AD), memory loss,[150] seizures,[151] and other neurodegeneration diseases. One study found that neuronal RyR2 channels in mice undergo post translational modifications by oxidation and PKA phosphorylation, causing spontaneous calcium leak from the ER.[152] This calcium leak activates other calcium dependent signaling pathways that ultimately contribute to AD pathogenesis. This finding supports the hypothesis that spontaneous intracellular Ca release could be an early factor in the development of AD, and treatment of mice with an RyR stabilizing drug could result in improved cognitive function. Additionally, dantrolene, a pan-RyR inhibitor has demonstrated some degree of neuroprotection in several disease mouse models, including Huntington's disease,[153] and cerebral ischemia.[154] While crossing the blood-brain-barrier presents a different set of challenges to therapeutic development, regulation of RyR2 dysfunction in the brain shows promise as a potential therapeutic target for neurodegenerative diseases.

2.2 Current RyR2 Inhibitors

There are several class Ic antiarrhythmic drugs that are marketed in the United States, including quinidine, procainamide, disopyramide, lidocaine, mexiletine, flecainide, and propafenone. Of these antiarrhythmics, only two have been found to have an effect on RyR2 channels: flecainide and propafenone (Figure 50).[155] Flecainide is currently the preferred drug therapy for CPVT, although propafenone has been proposed as an alternative to flecainide in patients that are symptomatic on β-blockers. Flecainide, however, has also been shown to act on sodium channels,

[150] Yuan, Q.; Deng, K. Y.; Sun, L.; Chi, S.; Yang, Z.; Wang, J.; Xin, H. B.; Wang, X.; Ji, G. *Sci Rep* **2016**, *6*, 21087
[151] Johnson, J. N.; Tester, D. J.; Bass, N. E.; Ackerman, M. J. *J Child Neurol* **2010**, *25*, 916
[152] Lacampagne, A.; Liu, X.; Reiken, S.; Bussiere, R.; Meli, A. C.; Lauritzen, I.; Teich, A. F.; Zalk, R.; Saint, N.; Arancio, O.; Bauer, C.; Duprat, F.; Briggs, C. A.; Chakroborty, S.; Stutzmann, G. E.; Shelanski, M. L.; Checler, F.; Chami, M.; Marks, A. R. *Acta Neuropathol* **2017**, *134*, 749
[153] Chen, X.; Wu, J.; Lvovskaya, S.; Herndon, E.; Supnet, C.; Bezprozvanny, I. *Molecular neurodegeneration* **2011**, *6*, 81
[154] Wei, H.; Perry, D. C. *J. Neurochem.* **1996**, *67*, 2390
[155] Hwang Hyun, S.; Hasdemir, C.; Laver, D.; Mehra, D.; Turhan, K.; Faggioni, M.; Yin, H.; Knollmann Björn, C. *Circulation: Arrhythmia and Electrophysiology* **2011**, *4*, 128

and this activity could be responsible for its pro-arrhythmic liability in some cases.[156,157] Several other therapeutics have been found to act on RyR2, including dantrolene[158] and tetracaine (Figure 50), but these are currently only experimental therapies for RyR2-related diseases. However, of all drugs known to act on RyR2, none are selective, either targeting other RyR channels or other ion channels (sodium channels). Only two compounds that are selective to RyR2 compounds have been preliminarily reported in the literature: *ent*-verticilide[159] and EL20.[160,161] To date, there are

Figure 50. Current small molecule RyR modulators and two reported RyR2 selective molecules.

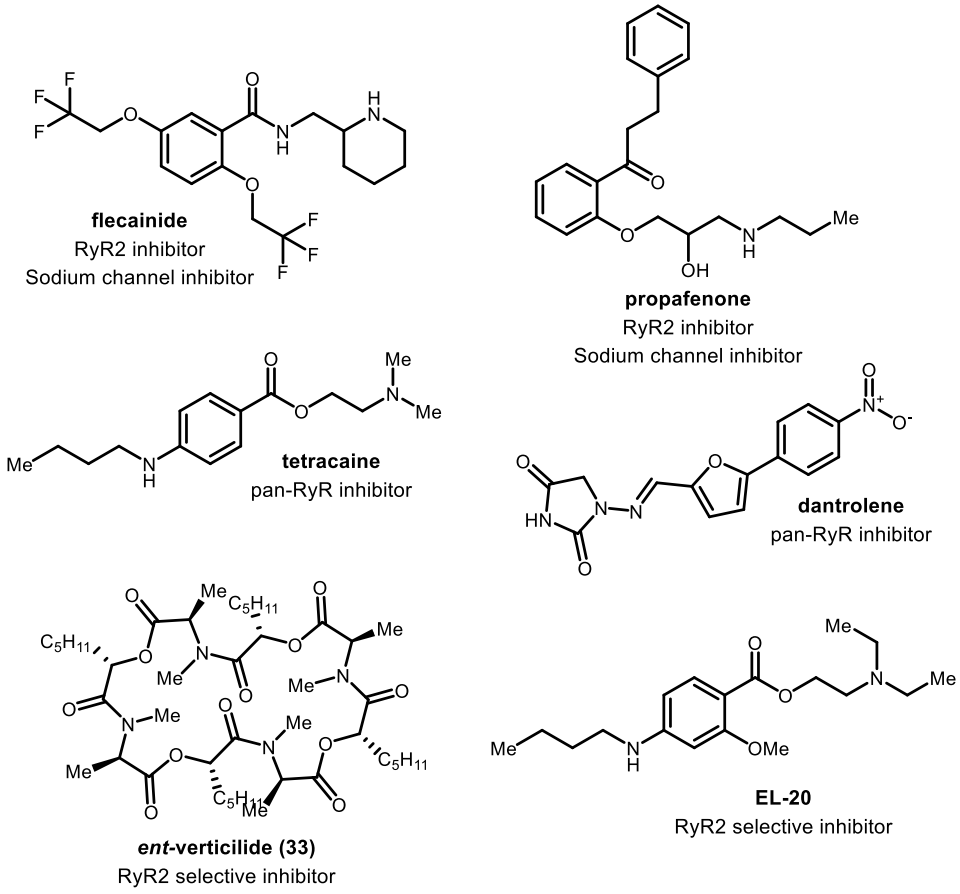

[156] Nathan, A. W.; Hellestrand, K. J.; Bexton, R. S.; Spurrell, R. A.; Camm, A. J. *Drugs* **1985**, *29 Suppl 4*, 45
[157] Echt, D. S.; Ruskin, J. N. *Am J Cardiol* **2020**, *125*, 1123
[158] Zhao, F.; Li, P.; Chen, S. R.; Louis, C. F.; Fruen, B. R. *J. Biol. Chem.* **2001**, *276*, 13810
[159] Batiste, S. M.; Blackwell, D. J.; Kim, K.; Kryshtal, D. O.; Gomez-Hurtado, N.; Rebbeck, R. T.; Cornea, R. L.; Johnston, J. N.; Knollmann, B. C. *Proc. Natl. Acad. Sci. U. S. A.* **2019**, *116*, 4810
[160] Klipp, R. C.; Li, N.; Wang, Q.; Word, T. A.; Sibrian-Vazquez, M.; Strongin, R. M.; Wehrens, X. H. T.; Abramson, J. J. *Heart Rhythm* **2018**, *15*, 578
[161] Word, T. A.; Quick, A. P.; Miyake, C. Y.; Shak, M. K.; Pan, X.; Kim, J. J.; Allen, H. D.; Sibrian-Vazquez, M.; Strongin, R. M.; Landstrom, A. P.; Wehrens, X. H. T. *J Cell Mol Med* **2021**, *25*, 6115

no clinically available RyR2-selective inhibitors. Hence, there is an urgent need for selective and potent RyR2 inhibitors, and an RyR2 selective probe would substantially enhance our understanding of RyR2 function and how to target these ion channels.

2.3 Background Summary of the Biological Activity of *Ent*-Verticilide

After completing the synthesis of verticilide, the Johnston lab had an interest in further exploring the biological activity. Verticilide was originally isolated by Omura's group in 2006 from the culture broth of *Verticilium* sp. FKI-10332 and was found to inhibit the binding of ryanodine to insect ryanodine receptors (cockroach), showing promise as a potential insecticidal agent.[103] It was therefore of interest to further explore the biological activity of verticilide against ryanodine receptors. The Knollmann lab here at Vanderbilt University Medical Center (VUMC), is a clinical pharmacology lab that studies RyR2 dysfunction and its implication in cardiac diseases like CPVT. In collaboration with the Knollmann lab, we investigated the natural product to determine its activity against mammalian RyR2, using a calcium spark assay.[162] In this assay, cardiomyocytes isolated from a CASQ2 gene knockout mouse, a validated model of severe CPVT in humans that exhibits pathologically increased RyR2 activity. Ventricular cardiomyocytes were isolated, permeabilized with saponin, and incubated with vehicle (DMSO) or 25 μM of compound. RyR2 activity was measured in the form of calcium sparks, which are elementary Ca^{2+} release events generated by spontaneous openings of intracellular RyR2 Ca^{2+} release channels. Importantly, saponin selectively permeabilizes the sarcolemmal membrane, leaving the SR membrane intact and ensuring equivalent access of the compound to the SR membrane where RyR2 resides. An example of a confocal line scan in shown in Figure 51.

Unfortunately, the natural product had no effect on the calcium sparks. However, the enantiomer of the natural product, *ent*-verticilide (**33**) had also been synthesized as a control to run in the spark assays. When testing *ent*-verticilide, it was discovered that this non-natural enantiomer significantly reduced RyR2-mediated spontaneous Ca^{2+} leak in cardiomyocytes. Furthermore, *ent*-verticilide selectively inhibited RyR2-mediated Ca^{2+} leak and exhibited higher potency (Figure 51)[163] and a distinct mechanism of action compared to the pan-RyR inhibitors tetracaine and

[162] Batiste, S. M.; Blackwell, D. J.; Kim, K.; Kryshtal, D. O.; Gomez-Hurtado, N.; Rebbeck, R. T.; Cornea, R. L.; Johnston, J. N.; Knollmann, B. C. *Proc. Natl. Acad. Sci. U. S. A.* **2019**, *116*, 4810

[163] The graphics in this figure were put together by Dan Blackwell and permission was requested and given to use these figures in this dissertation

dantrolene (not shown), and the antiarrhythmic drug flecainide. *ent*-(+)-Verticilide (**33**) prevented arrhythmogenic membrane depolarizations in cardiomyocytes without significant effects on the cardiac action potential and attenuated ventricular arrhythmia in catecholamine-challenged *Casq2*$^{-/-}$ mice (Figure 52). These findings established that *ent*-(+)-verticilide is a potent and selective

Figure 51. A) Representative confocal line scans of Ca^{2+} sparks in the absence (DMSO) or presence of 25 μM nat-verticilide or ent-verticilide in permeabilized Casq2$^{-/-}$ cardiomyocytes **B)** *ent*-Verticilide's selective inhibition of RyR2 vs. *nat*-Verticilide and pan-inhibitor tetracaine, and **C**) Percent change in spark frequency relative to vehicle (DMSO), obtained from wild-type myocytes.

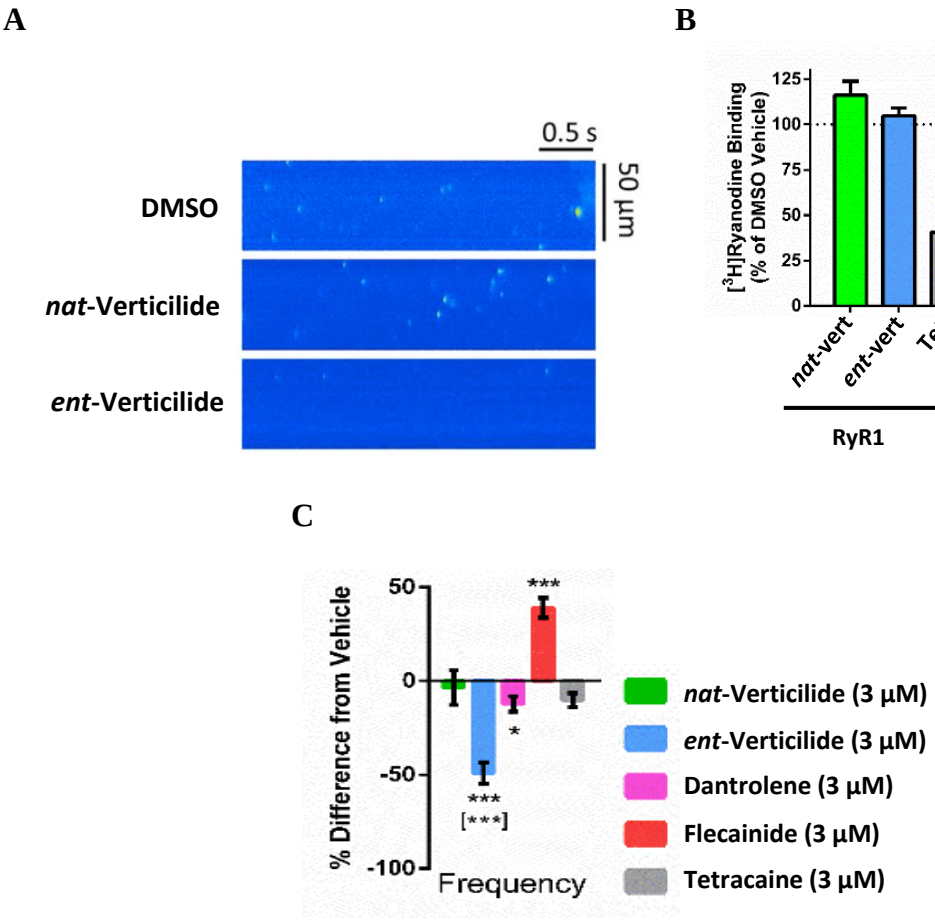

Figures were generated by Dan Blackwell. Data are presented as mean ± SEM. n ≥ 30 cells per group for A and C. n = 4 replicates for each concentration tested in B. *P < 0.05 vs. DMSO, **P < 0.01 vs. DMSO, ***P < 0.001 vs. DMSO by one-way ANOVA with t test. Bracketed asterisks indicate t test comparison between *ent*-verticilide and dantrolene.

inhibitor of RyR2-mediated diastolic Ca^{2+} leak, making it a new molecular tool to investigate the therapeutic potential of targeting RyR2 hyperactivity in heart and brain pathologies. This striking enantiomer-specific activity was a compelling launch point for the pharmacological studies of this

therapeutic lead, and from this discovery, we hoped to use *ent*-verticilide as a new scaffold for probe and therapeutic development.

Figure 52. A) Dose-response curve for *ent*-verticilide and tetracaine against RyR2 **B**) Quantification of catecholamine-induced ectopic beats by surface electrocardiogram in Casq2−/− mice injected intraperitoneally with 30 mg/kg (drug/body weight) *nat*-verticilide or *ent*-verticilide or DMSO of equivalent volume 30 min before recordings and **C)** Incidence of ventricular tachycardia (VT).

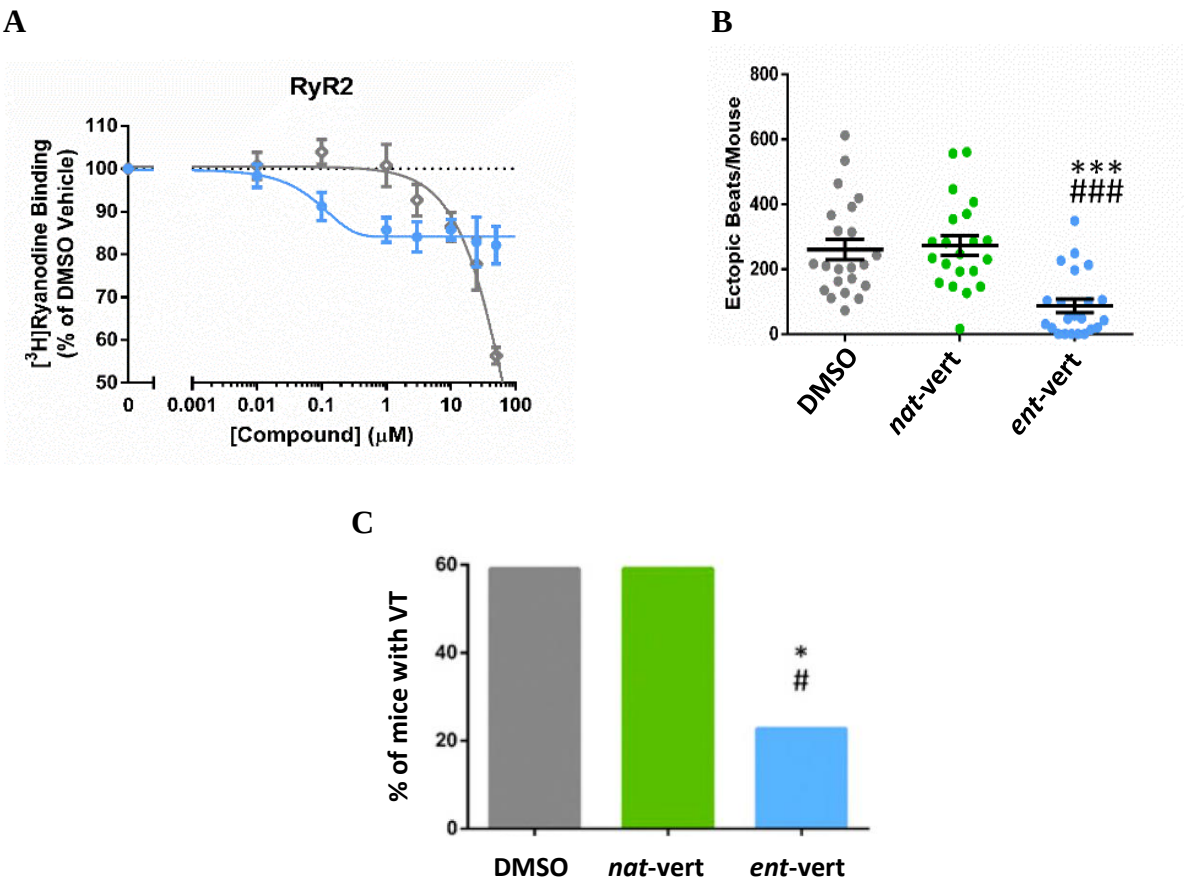

Figures were generated by Dan Blackwell. n = 4 replicates for each concentration tested in **A** and n = 22 mice per group for **B** and **C**. *P < 0.05 vs. DMSO, **P < 0.01 vs. DMSO, ***P < 0.001 vs. DMSO by t test for **A** or by Mann–Whitney U test for **B**. *P = 0.0305 for *ent*-verticilide vs. DMSO or # P = 0.0305 for *ent*-verticilide vs. *nat*-verticilide by Fisher's exact test for **C**. Data in **B** are presented as mean ± SEM.

2.4 *Ent*-Verticilide Structure-Activity-Relationship Campaign

2.4.1 Analogue Design and The Development of a New Synthetic Route

After the happenstance discovery of *ent*-verticilide as an RyR2 inhibitor, the next major consideration was how to move forward from that point. While a hit compound had been found,

very little was known about how this compound was interacting with RyR2. Furthermore, due to the little available structural data on RyR2 channels, gaining knowledge from a structural perspective would be a monumental undertaking, unlikely to succeed without any guidance towards a certain area of RyR2. When deciding how to move forward from this point, the vision was to simultaneously advance structure-activity relationship (SAR) studies to further delineate *ent*-verticilide-RyR2 interactions, and target engagement studies to better understand the mechanism of action of *ent*-verticilide.

The SAR studies began in a very directed manner, with the goal of finding an area of the molecule that was amendable to structural change, to identify a modification point for some of the mechanism of action analogues of interest. From this standpoint, *ent*-verticilide is a very structurally complex molecule in which many manipulations can be made (Figure 53). Specifically, *ent*-verticilide has:

- 8 stereocenters, alternating D and L,
- 4 α-amino esters, which could be altered through the side chain or the amide in the backbone,
- 4 α-oxy amides, which could again be altered through the side chain or the ester in the backbone
- 4 sites of *N*-methylation,
- and 4 repeating depsipeptide units, that could be altered in number (ring-size) or in the or in the depsipeptide structure, taking away the symmetry in the molecule.

The alpha-oxy alkyl side chains were identified early on as a potential site for modification. This was largely due to these being the least sterically hindered parts of the molecule, which would hopefully make them amendable to conjugation chemistry in the planned mechanism of action analogues. Additionally, these alkyl side chains were potentially the most accessible from a synthetic standpoint. To gauge this hypothesis, a small sampling of alkyl side chain modifications were made, first starting with increasing each alkyl side chain by a single carbon (**34**), as well as decreasing each side chain by a single carbon (**35**) (Figure 54). It was quickly discovered that these alkyl side chains were important to the activity of *ent*-verticilide, as the modification of all four, even slightly, completely ablated the activity. Even though all four side chains couldn’t be

Figure 53. Examination of *ent*-verticilide's unique structural features.

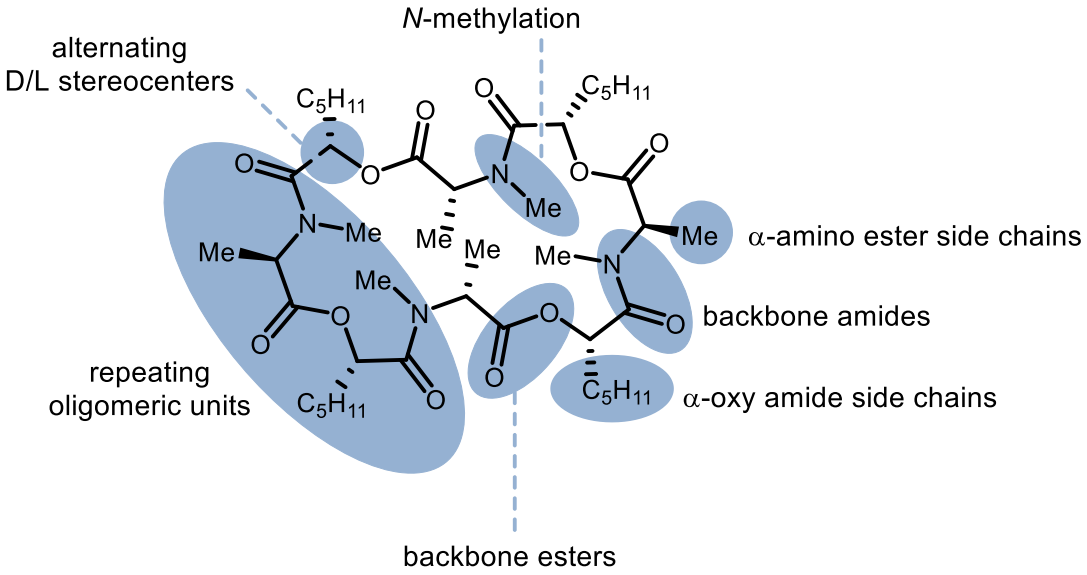

modified, it was still hypothesized that one or two of the side chains could be modified without loss of activity. However, to do so, a new synthetic route would need to be developed. The MCO chemistry was only applicable to compounds that were oligomeric in nature. Furthermore, it was not amenable to large-scale chemistry. In planning a new synthetic route, several key considerations were kept in mind. First, the chemistry needed to be applicable to a broad range of substrates. The goal was to be able to use the new methodology for most of the SAR analogues as well as the mechanism of action analogues. Second, the chemistry needed to be scalable. At the time, it was anticipated that soon, larger amounts of *ent*-verticilide would be necessary for the planned biological studies. Any target engagement work was also envisioned to require substantial amounts of compound. Therefore, a challenging analogue was designed as a test substrate to develop the new methodology: one that incorporated an alkyne into a single side chain (Figure 55, **36**).

While an MCO reaction could not be utilized to synthesize a non-symmetrical analogue, using sequential Mitsunobu reactions to access the linear octadepsipeptide variant, in a similar way to the stepwise synthesis of the 18- and 36-membered rings discussed in Chapter 1, was considered. However, post cyclization, the final *N*-permethylation step would require strongly basic conditions

Figure 54. First SAR analogues synthesized, modifying the alkyl side chains and activity results in calcium spark assays (collected by Dr. Dan Blackwell).

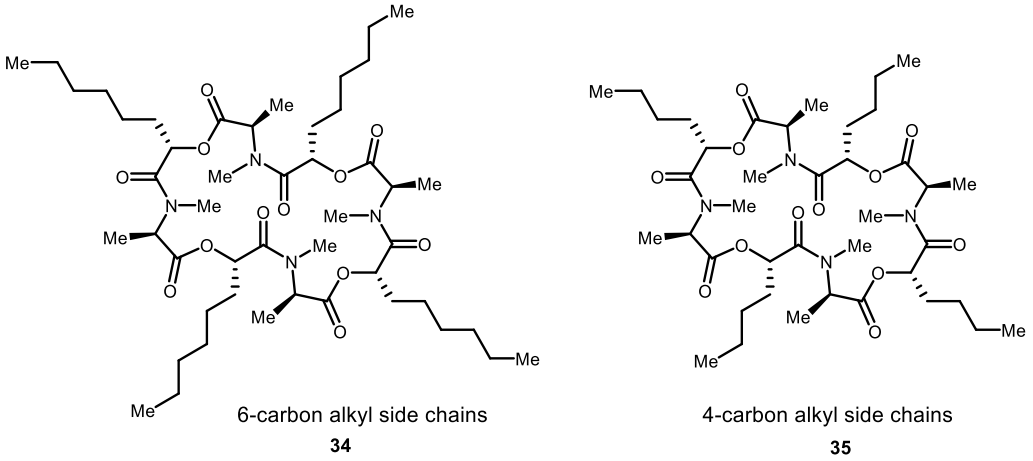

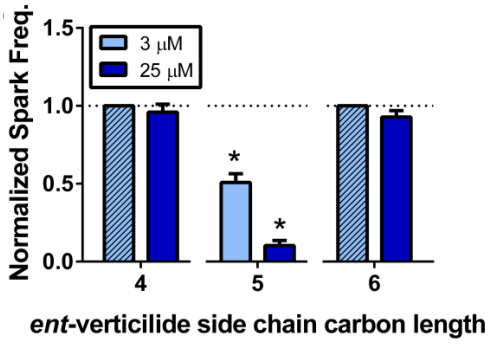

All data are normalized to vehicle (DMSO) treatment for the given day. Data presented as mean ± SEM from N > 18 cells per group (1 – 5 independent experiments). Hashed bars are placeholders and were not tested at that concentration. * $p < 0.01$ vs vehicle by Student's t-test.

and 10 equivalents of NaH, in which potential methylation of the alkyne was a concern. Furthermore, while feasible, the purification of the Mitsunobu byproducts after each coupling step would be far from trivial. Suzanne Batiste's substantial work with the development of methylation conditions, also provided guidance on the difficulty of working with *N*-methyl depsipeptides, and their propensity to cyclize to diketomorpholines. Keeping these challenges in mind, a new route was developed to access the targeted depsipeptide.

One of the key synthetic challenges in this new route, was the synthesis of the enantioenriched α-hydroxy acids. While many methods to access racemic α-hydroxy acids are known, asymmetric routes are much less developed, especially with alkyl substrates (see chapter 1 discussion). We aimed to develop a new method to access these alkyl α-hydroxy acid substrates using asymmetric

Figure 55. Targeted alkyne substrate for new synthetic route development.

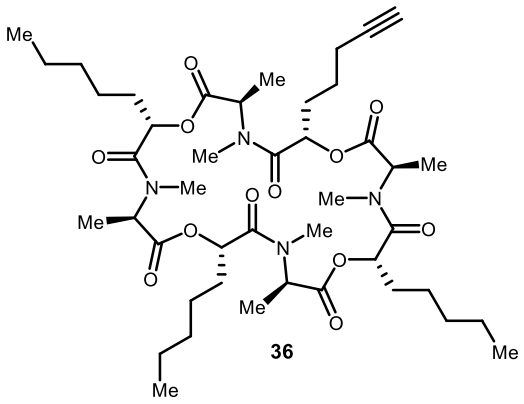

catalysis. Additionally, it would be ideal if we could use common intermediates to the MCO chemistry, allowing the utilization of starting materials for either route. To this end, we began the synthesis with commercially available 5-hexynal (**37**), which was oxidized to aldehyde **38** using IBX (Scheme 11). The formed aldehyde was then subjected to an enantioselective Henry reaction followed by a protection of the formed alcohol as the methoxymethylene ether. This nitroalkane (**39**), the same precursor used in the first synthesis of *ent*-verticilide, is then subjected to

Scheme 11. Optimized 4-step synthesis of α-hydroxy acids.

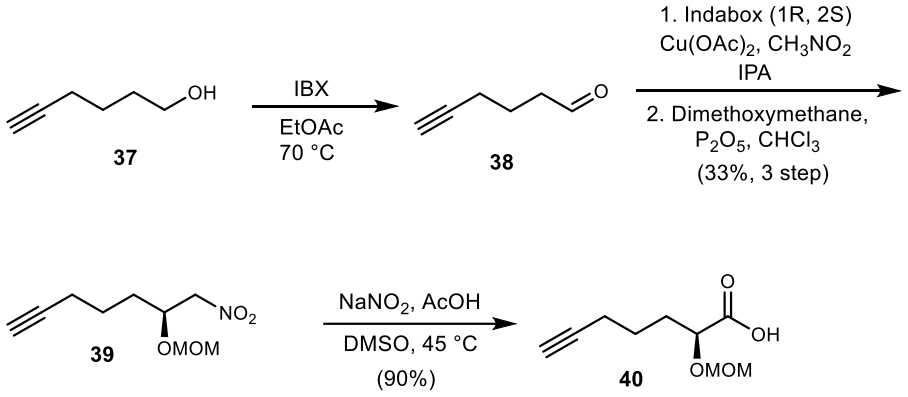

Mioskowski-Nef conditions[164] to form the protected α-hydroxy acid (**40**). During the development of this sequence, there were several stages that required extensive optimization. First, the oxidation step posed significant problems. While we had looked into starting with the commercially

[164] Matt, C.; Wagner, A.; Mioskowski, C. *J. Org. Chem.* **1997**, *62*, 234

available aldehyde and bypassing the oxidation all together, the high cost of the alkynal aldehyde ($1281 per gram) made it an impractical starting material. Initially, Swern oxidation conditions were attempted, which worked well to provide the desired aldehyde. However, the aldehyde proved incredibly difficult to purify, quickly decomposing on silica gel. Attempts to purify via cold silica column, distillation, or sodium bisulfite extraction[165] were also unsuccessful, often resulting in significant decomposition and low yields (Scheme 12, eq 1). However, when the aldehyde was carried forward into the Henry crude reaction mixture, no product formed. Instead, either starting material or complex decomposition was observed (Scheme 12, eq 2). Hypothesizing that some impurities from the reagents used under these oxidation conditions were responsible for the inactivity in the next step, different oxidation conditions were attempted. A series of conditions with chromium-based oxidants were attempted without success. Initial oxidation attempts with PCC resulted in gummy reactions mixtures, from which only small amounts of aldehyde could be extracted (Scheme 12, eq 3). Adding silica gel to the reaction[166] resulting in a much easier filtration and large amounts of aldehyde that appeared pure via ^{1}H NMR. However, when carried forward into the Henry, again the reaction continued to fail to produce any desired product (Scheme 12, eq 4). Cause was attributed to impurities that were not NMR active, stemming from the chromium reagents. We decided to use an oxidant system that would allow for easy filtration of both the left-over oxidant and any byproducts. This led us to attempt the oxidation with hypervalent iodine, starting with Dess–Martin periodinane (DMP) that was available on hand in the lab. While it was clear that the DMP oxidation was proceeding, it was incredibly slow, even when heated. After 21 days, only 30% had converted to product (Scheme 12, eq 5). While DMP is reported to be more soluble in DMSO, we wanted to avoid non-volatile solvents for work-up ease. Instead, we switched to using o-iodoxybenzoic acid (IBX)[167] as a different hypervalent iodine source, after reading reports of oxidations working well in solvents like EtOAc with only mild heating required.[168] Much to our delight, we found that after 3 hours of heating with IBX, full conversion to clean aldehyde was observed. Furthermore, a simple filtration led to very pure aldehyde, that was then subjected to the Henry conditions. It was an exciting day in the lab when the Henry reaction produced the desired nitroalkane that could be carried forward. Indeed, the crude nitroalkane was

[165] Au - Furigay, M. H.; Au - Boucher, M. M.; Au - Mizgier, N. A.; Au - Brindle, C. S. *JoVE* **2018**, e57639
[166] Luzzio, F. A.; Fitch, R. W.; Moore, W. J.; Mudd, K. J. *J. Chem. Educ.* **1999**, *76*, 974
[167] Frigerio, M.; Santagostino, M.; Sputore, S. *J. Org. Chem.* **1999**, *64*, 4537
[168] More, J. D.; Finney, N. S. *Org. Lett.* **2002**, *4*, 3001

Scheme 12. Attempted oxidation conditions.

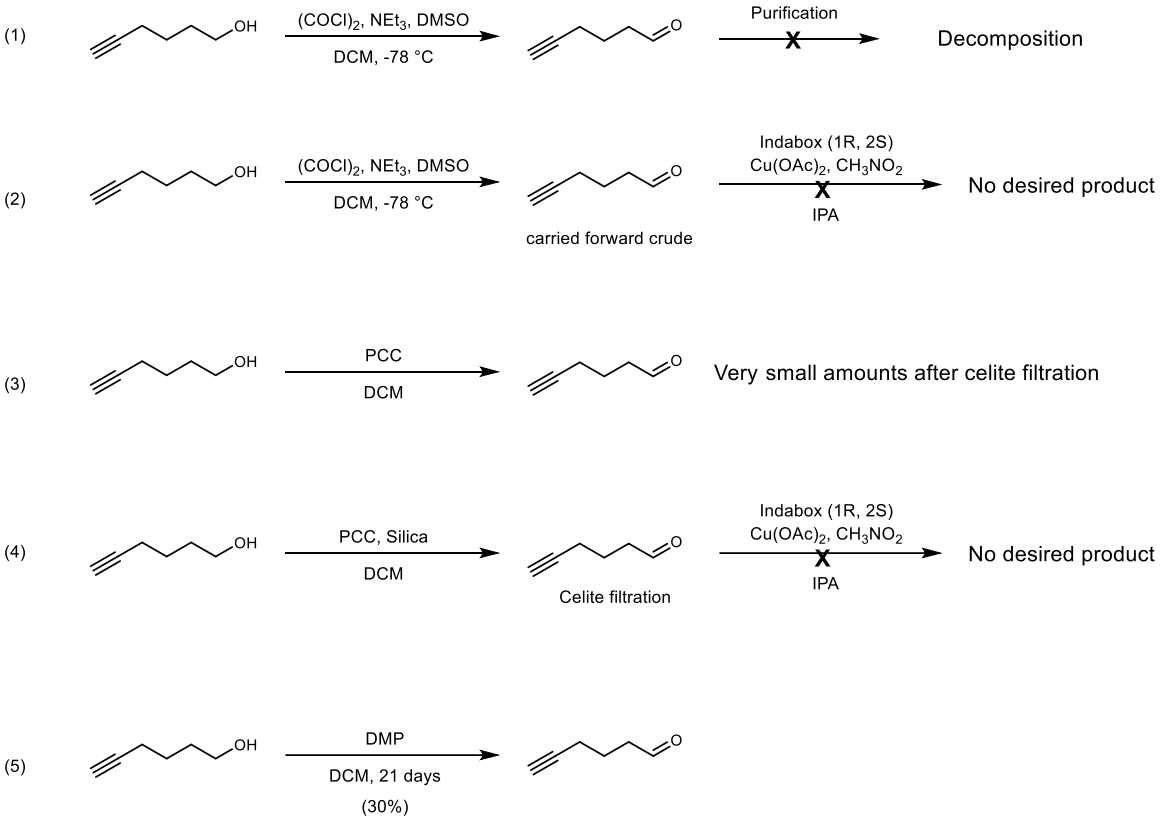

subjected to the MOM protection to afford protected α-hydroxy nitroalkane that was stable to silica purification. Overall, we were able to scale the 3-step reaction sequence to over a 25 gram-scale, in a 33% yield over 3-steps. The lower yield likely is a result of the volatility of this particular aldehyde, despite mild vacuum concentration to remove ethyl acetate after the oxidation.

The second key challenge in the synthetic development was the optimization of the Mioskowski-Nef reaction conditions. When initially carrying out the reaction, a significant amount of a byproduct was observed alongside the desired product. To identify and understand the formation of this byproduct, we looked in detail at the mechanism of the reaction.[164] Mioskowski proposed that under these reaction conditions, the combination of sodium nitrite and acetic acid produces nitrosonium in situ, which is the active electrophilic species. Upon deprotonation of the nitroalkane, the formed nitronate (**41**) can react with the nitrosonium ion to generate nitrolic acid

Scheme 13. Proposed Miowskowski-Nef reaction mechanism.

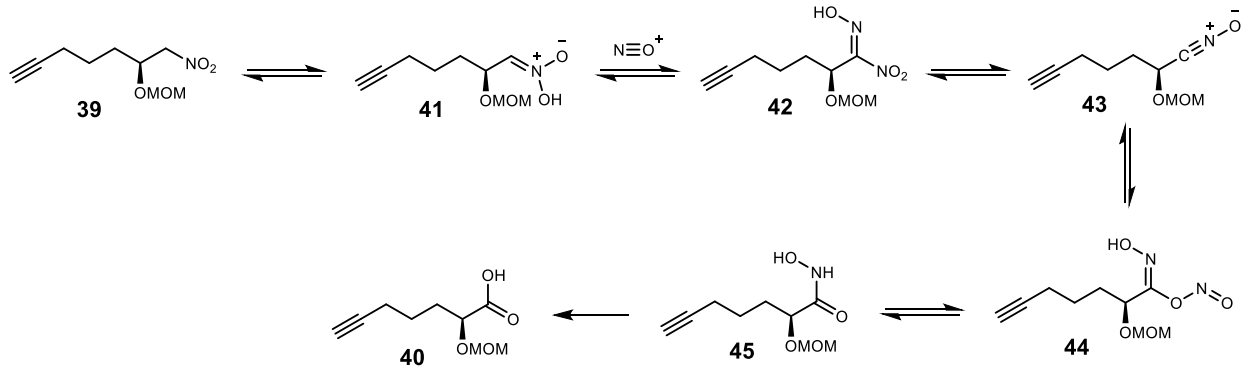

species **42**. It is then postulated the nitrolic acid is converted to species **44** through nitrile oxide intermediate **43**, followed by conversion to hydroxamic acid **45**, and final hydrolysis to give carboxylic acid **40**. From this, we hypothesized that if the reaction was proceeding through a nitrile oxide intermediate, we could be seeing intramolecular cyclization products with our alkyne species. With this in mind, it was indeed verified that the unknown byproduct was isoxazole

Scheme 14. Identification of by-product from Mioskowski-Nef reaction conditions and optimization to limit its formation.

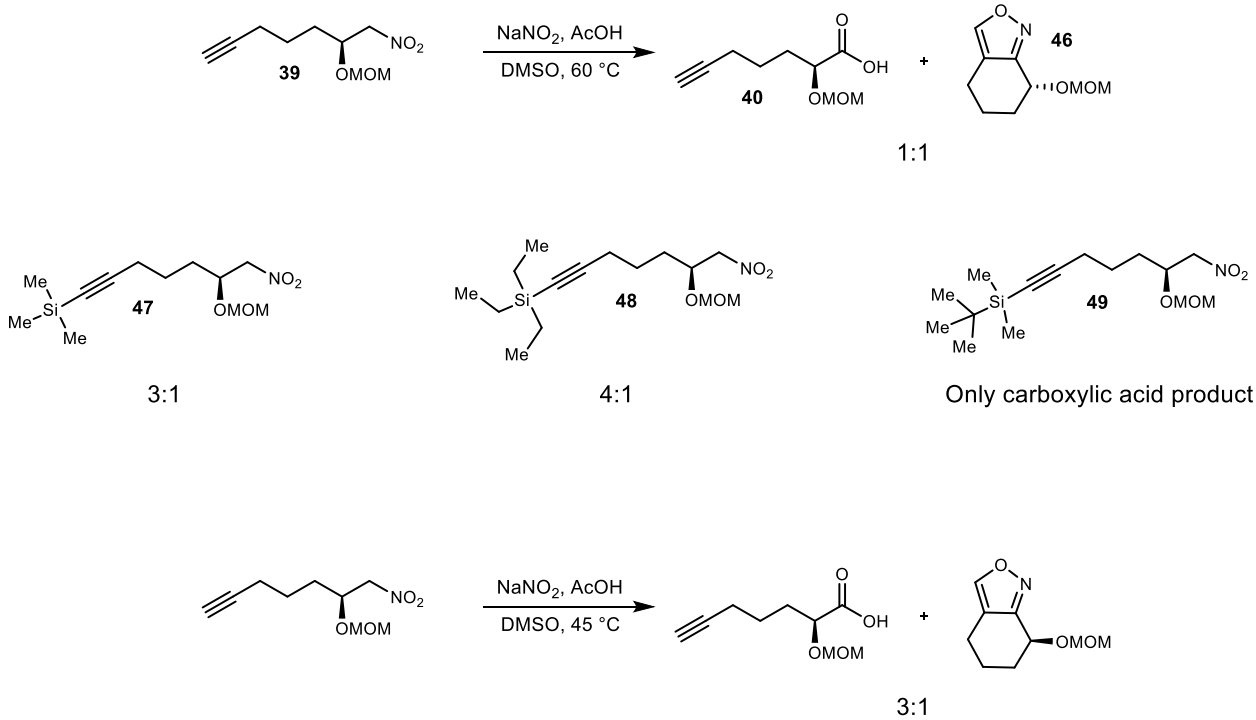

species **46**, formed from an intramolecular 2+3 cycloaddition reaction (Scheme 14). To prevent this undesired cyclization, it was hypothesized that increasing the steric bulk around the alkyne would favor the intermolecular reaction instead. A series of alkynal protecting groups were screened (Scheme 14). Our hypothesis proved to be correct, as we saw an increase in the ratio of our desired carboxylic acid to isoxazole (3:1). Furthermore, the larger the protecting group, the more desired product was favored, and adding a *tert*-butyldimethylsilyl (TBS) protecting group completely prevented the intramolecular cyclization. While exploring conditions for the Mioskowski-Nef reaction, however, we also discovered that varying the reaction temperature affected the ratio of desired product to the isoxazole. By decreasing the reaction temperature to 45 °C, we were able to favor the carboxylic acid in a 3:1 ratio. This surprising result alludes to potential deviations in the proposed reaction mechanism. The potential to reduce the amount of isoxazole species just by varying of reaction conditions suggests that intermediate **42** may proceed to intermediate **44** through a bifurcated pathway (Scheme 15), in which one of the pathways does not proceed through a nitrile oxide. Further mechanistic study is warranted here to make any definitive conclusions and would be a very interesting topic for further investigation.

Scheme 15. Revised input on possible Mioskowski-Nef.

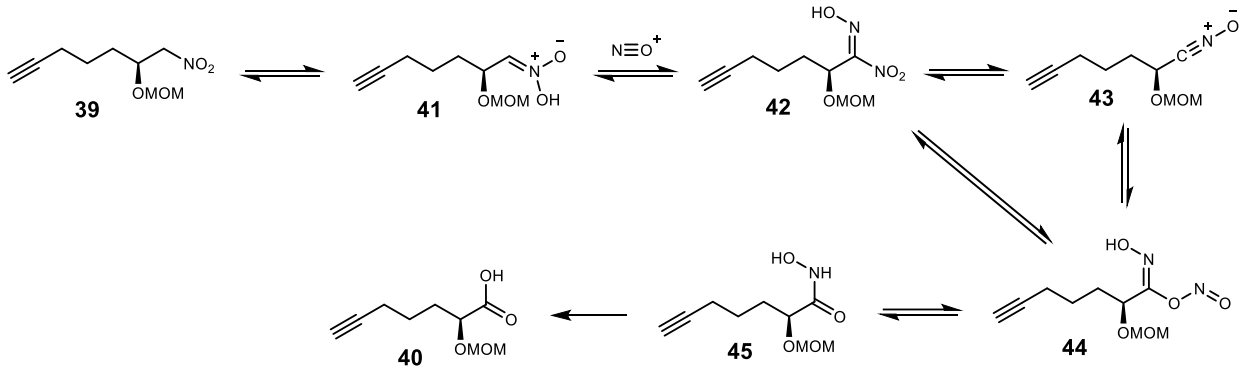

Once the α-hydroxy acid was formed, it was protected as the trichloroethyl ester (TCE). A deprotection afforded the free secondary alcohol, which was subjected to a Steglich esterification[68] with Boc-*N*-methyl alanine to form a didepsipeptide (Scheme 16). An important point to note, is the formation of the ester bond in the backbone instead of the amide. This allows us to incorporate the amino acid already methylated but avoids a scenario in which there would be a central methylated amide bond and a terminal unprotected alcohol that is incredibly prone to

diketomorpholine formation due to the Thorpe-Ingold effect (Figure 9). Omura and coworkers took a similar approach to depsipeptide formation in their synthesis of verticilide.[169] Additionally, the optimization of ester protecting groups was a key aspect of the synthesis. Many protecting groups were considered, but ultimately, TCE proved to be the best option in terms of its orthogonality to the alkyne, the acidic conditions needed to deprotect both the MOM and Boc groups, as well as the removal conditions being tolerant of the esters in the backbone of the depsipeptide. The depsipeptide **51** was then deprotected at the *N*-terminus and coupled to a hexadepsiepeptide unit (**53**) native to ent-verticilide (synthesized via the same methodology) with

Scheme 16. Synthesis of *ent*-verticilide alkyne analogue.

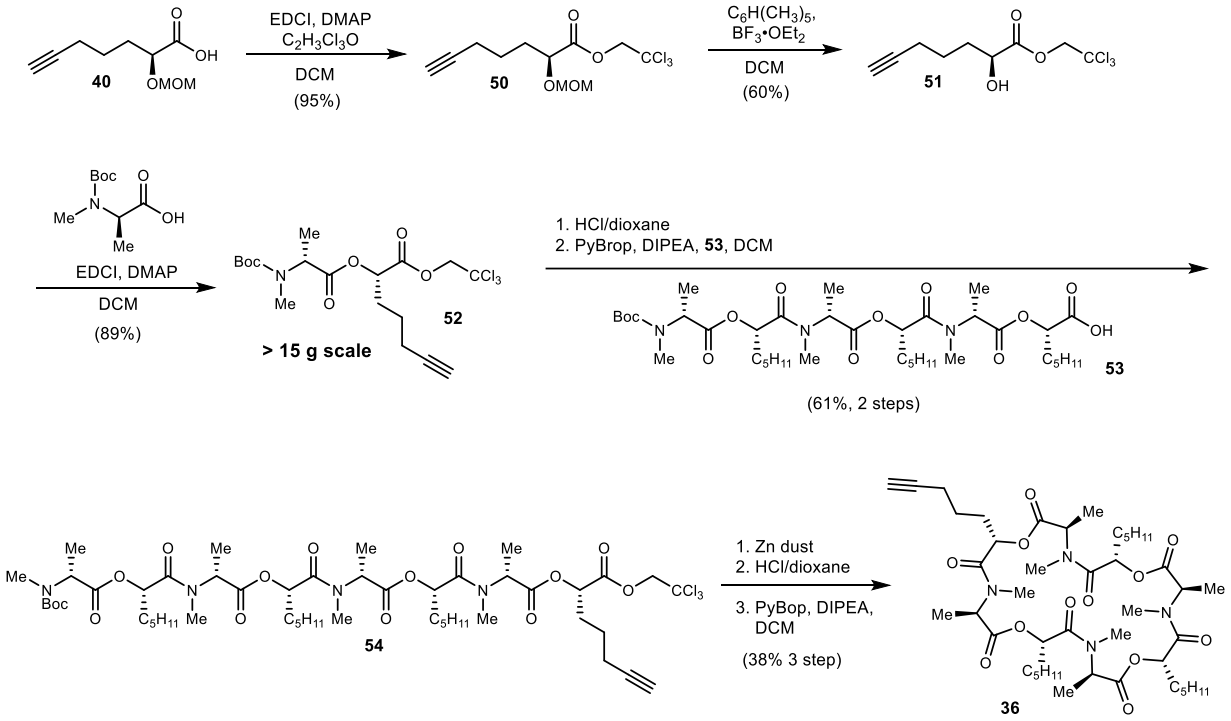

PyBrop as a coupling reagent. PyBrop was chosen due to its reported high efficiency particularly with secondary amines.[170] Once the linear octadepsipeptide was formed (**54**), deprotection at both termini followed by a final cyclization with PyBop[171] afforded the desired macrocycle (**36**) in a 38% yield over 3-steps. The key alkyne analogue was then tested in the calcium sparks assay,

[169] Monma, S.; Sunazuka, T.; Nagai, K.; Arai, T.; Shiomi, K.; Matsui, R.; Ōmura, S. *Org. Lett.* **2006**, *8*, 5601
[170] Frérot, E.; Coste, J.; Pantaloni, A.; Dufour, M.-N.; Jouin, P. *Tetrahedron* **1991**, *47*, 259
[171] Thakkar, A.; Trinh, T. B.; Pei, D. *ACS combinatorial science* **2013**, *15*, 120

which delivered the welcome result that it is a potent inhibitor of calcium sparks. This finding that one of the four alkyl side chains could be modified without a significant loss of activity was a promising starting point for mechanism of action work. Furthermore, the developed synthetic route was amendable to a broad range of substrates, allowing for the synthesis of over 50 SAR analogues, as well as the scale-up to gram amounts of final products.

2.4.2 Ring Size Variation

Considering cyclic depsipeptide natural products, nature appears to leverage ring-size to fine-tune biological activity, even if just by happenstance. Several prominent examples include valinomycin and montanastatin,[172] bassianolide and enniatin C,[173] beauvericin and bassiatin,[173] and the antimycins[174] (Figure 56). Although natural products are ripe with examples of diverse depsipeptides varying in ring size, few studies provide insight to the effect of a systematic variation of ring size and correlation of biological activity at a discrete target. Even then, ring-size is usually only explored as a parameter when the ring-size analogue is also a natural product. We speculated that the ability to vary only ring size while leaving functionality and other features unchanged might be realized with cyclic oligomeric depsipeptides (CODs).

Due to their oligomeric nature, CODs provide an effective platform to probe ring-size modified pharmacophores wherein size is manipulated while maintaining the functionality inherent to the biologically active molecule. Examples of the synthesis of non-natural analogues of cyclic depsipeptides include decabassianolide (analogue of bassianolide),[175] a 12-mer and 24-mer of beauvericin,[176] a tetradepsipeptide and cyclohexadepsipeptide analogue of valinomycin,[177] and a 12-mer of bassianolide.[176] More generally, there has been noteworthy work with the synthesis of ring-size analogues in the field of oligolides,[178,179] as well as cyclic peptides.[180,181,182] Yet, still

---

[172] Pettit, G. R.; Tan, R.; Melody, N.; Kielty, J. M.; Pettit, R. K.; Herald, D. L.; Tucker, B. E.; Mallavia, L. P.; Doubek, D. L.; Schmidt, J. M. *Bioorg. Med. Chem.* **1999**, *7*, 895
[173] Sivanathan, S.; Scherkenbeck, J. *Molecules* **2014**, *19*, 12368
[174] Liu, J.; Zhu, X.; Kim, S. J.; Zhang, W. *Nat. Prod. Rep.* **2016**, *33*, 1146
[175] Kanaoka, M.; Isogai, A.; Suzuki, A. *Agricultural and Biological Chemistry* **1979**, *43*, 1079
[176] Lücke, D.; Dalton, T.; Ley, S. V.; Wilson, Z. E. *Chem. Eur. J.* **2016**, *22*, 4206
[177] Rothe, M.; Kreiss, W. *Angew. Chem. Int. Ed.* **1973**, *12*, 1012
[178] Burke, S. D.; Heap, C. R.; Porter, W. J.; Song, Y. *Tetrahedron Lett.* **1996**, *37*, 343
[179] Seebach, D.; Hoffmann, T.; Kühnle, F. N. M.; Lengweiler, U. D. *Helv. Chim. Acta* **1994**, *77*, 2007
[180] Piekielna, J.; De Marco, R.; Gentilucci, L.; Cerlesi, M. C.; Calo, G.; Tömböly, C.; Artali, R.; Janecka, A. *Pept. Sci.* **2016**, *106*, 309
[181] Jelokhani-Niaraki, M.; Kondejewski, L. H.; Wheaton, L. C.; Hodges, R. S. *J. Med. Chem.* **2009**, *52*, 2090
[182] Kondejewski, L. H.; Farmer, S. W.; Wishart, D. S.; Kay, C. M.; Hancock, R. E. W.; Hodges, R. S. *J. Biol. Chem.* **1996**, *271*, 25261

Figure 56. Examples of naturally occurring COD varying by ring size.

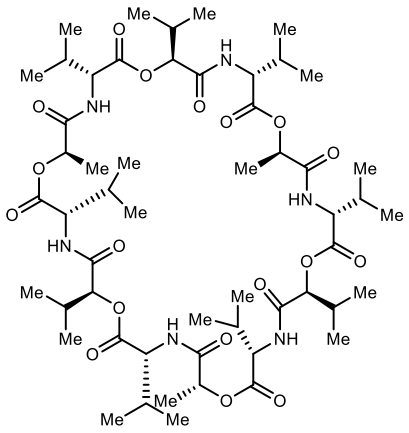

valinomycin (36-mem COD)

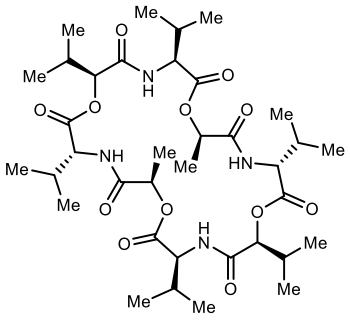

montanastatin (24-mem COD)

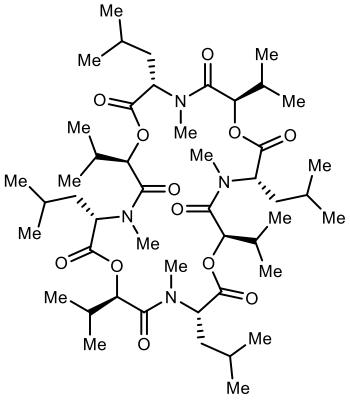

bassianolide (24-mem COD)

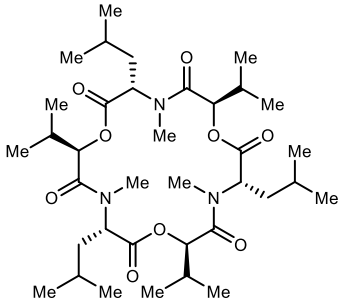

enniatin C (18-mem COD)

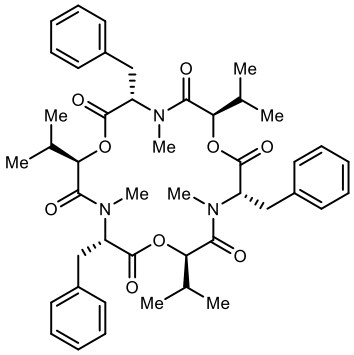

beauvericin (18-mem COD)

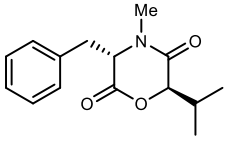

bassiatin (6-mem COD)

absent from most studies is a large range (>3) of ring sizes, other structural functionality left unchanged, or the evaluation of these compounds against a distinct biological target. Our discovery of *ent*-verticilide's activity against mammalian RyR2, paired with our MCO chemistry and synthetic ability to rapidly synthesize ring-size variants, positioned us to advance a structure-activity study to better understand ring-size and its effect on biological activity in the absence of any functional group change. This is particularly significant in cardiovascular disease, where macrocyclic compounds are rare in therapeutic development.[183]

To study this effect, we prepared 5 non-natural ring size congeners of *ent*-verticilide (24-membered COD), including 6-, 12-, 18-, 30-, and 36-membered CODs (Figure 57). Initially, the

Figure 57. *ent*-Verticilide and its ring-size analogues.

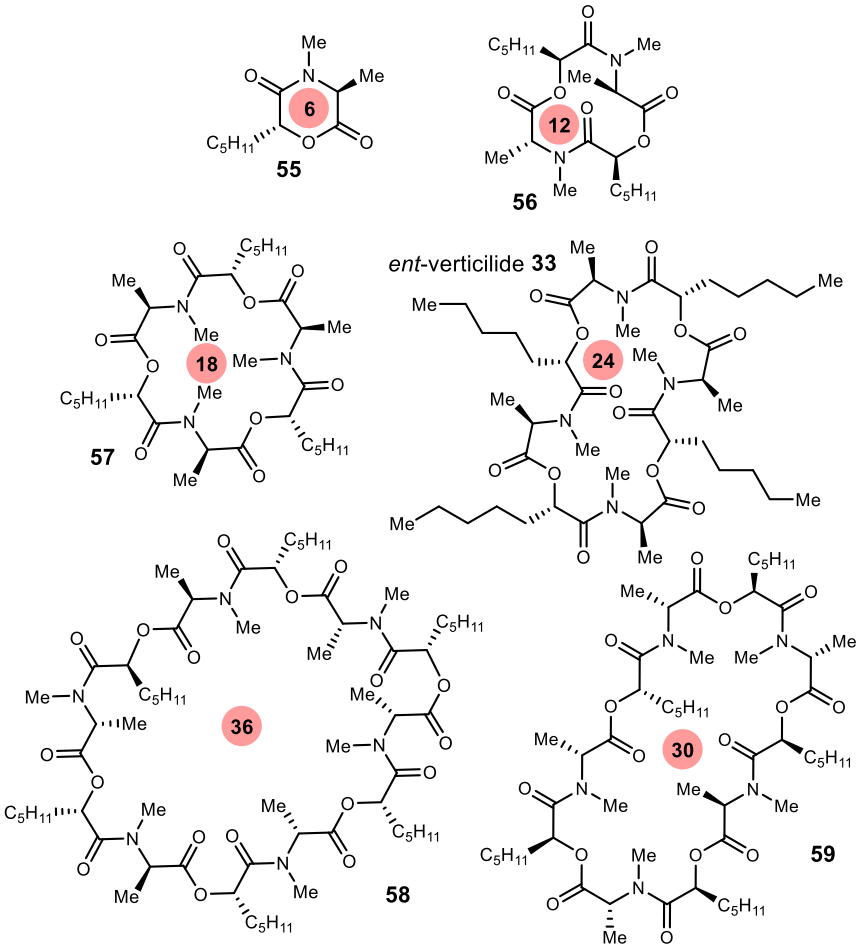

[183] Marsault, E.; Peterson, M. L. *J. Med. Chem.* **2011**, *54*, 1961

goal was to prepare the ring size analogues using the macrocyclooligomerization strategy. However, as discussed in Chapter 1, the larger ring sizes (30 and 36) were not amenable to the final *N*-permethylation conditions. Furthermore, ring sizes such as 6- and 12- were not accessible via the MCO reaction. We were able to access the 18- membered variant of ent-verticilide using the MCO chemistry, and the 6-, 12-, 30-, and 36-membered rings were synthesized via the route developed to synthesize the alkyne analogue of *ent*-verticilide (Scheme 11 and Scheme 16).

The activity of the ring size analogues was examined in cardiomyocytes isolated from a *CASQ2* gene knockout mouse, a validated model of severe catecholaminergic polymorphic ventricular tachycardia (CPVT) in humans that exhibits pathologically increased RyR2 activity. Ventricular cardiomyocytes were isolated, permeabilized with saponin, and incubated with vehicle (DMSO) or 25 μM of selected compound. RyR2 activity was measured in the form of calcium sparks, which are elementary Ca^{2+} release events generated by spontaneous openings of intracellular RyR2 Ca^{2+} release channels. Importantly, saponin selectively permeabilizes the sarcolemmal membrane, leaving the SR membrane intact and ensuring access of the compounds to the SR membrane where RyR2 resides.

The compounds were first screened by incubating cardiomyocytes for 10 minutes at 25 μM concentration and compared to vehicle (DMSO) conditions. The 18- and 24-membered rings significantly inhibited RyR2-mediated Ca^{2+} spark frequency, however the 6-, 12-, 30-, and 36-membered rings appeared to have no effect (Figure 58, A). To ensure there was no delayed binding effect with the inactive rings, longer incubation times for two of the macrocycles were investigated. Extending the incubation time to 60 minutes did not enable any measurable inhibition of spark frequency in either the 12- or 30-membered rings (Figure 58, B), suggesting that ring size is a necessary component for activity. Incubation with the 12- or 18-membered linear precursors also demonstrated no inhibition of spark activity – despite clear inhibition with the 18-membered ring – supporting the importance of a cyclic structure for activity (Figure 58C). To compare potency, concentration-response curves were generated for the 18- and 24-membered rings. Both compounds inhibited RyR2 with similar potency (Figure 58, D&E). The natural (D,L) versions of the 6-,18-, 24-, 30-, and 36- macrocycles were also prepared, but none of these were active in the assay.

Figure 58. Biological screen for cardiac ryanodine receptor (RyR2) activity. A) Calcium spark frequency in permeabilized murine cardiomyocytes was recorded as an index of RyR2 activity. Compounds were screened at 25 uM concentration after 10-minute incubation. *=p<0.001 by one-way ANOVA with Tukey's post-hoc test. B) Incubation time was extended to 60 minutes for the 12- and 30-membered rings. C) The seco-acid precursors to 12- and 18-membered ring synthesis were tested at 25 uM. D) Concentration response curve for the 18-membered ring and E) 24-membered ring. Cells were incubated for 30 minutes. * Figure was made by Dan Blackwell.

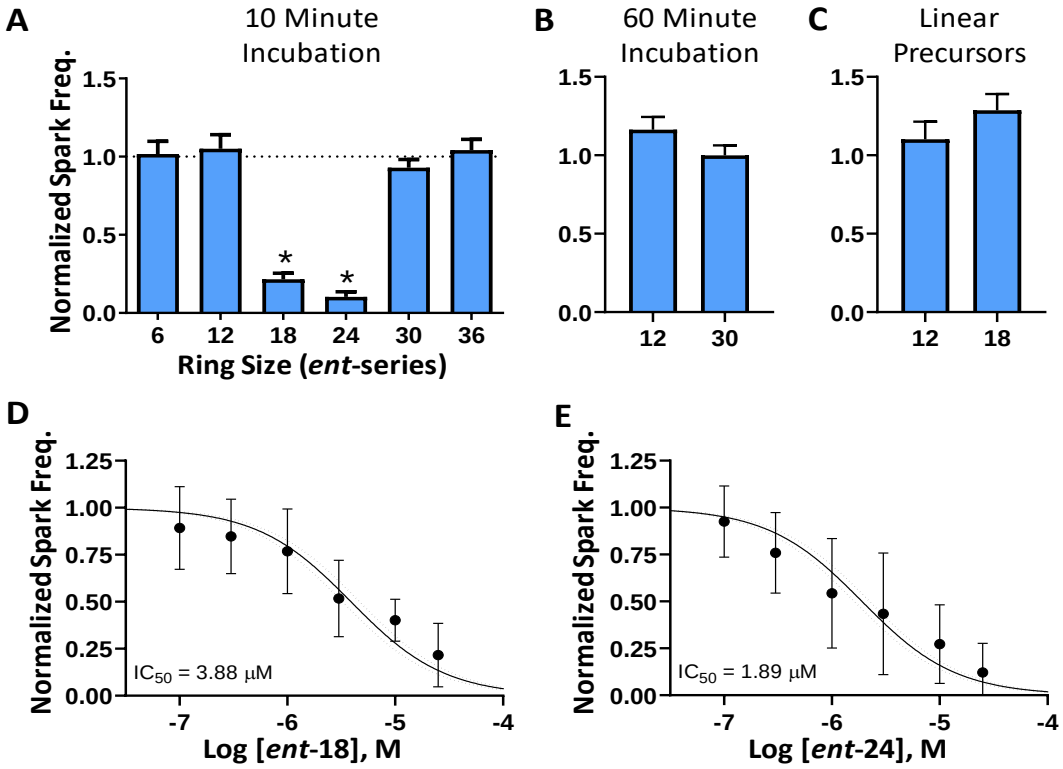

Of the five ring-size variants prepared, the 6-, 12-, 30-, and 36-membered ring did not alter calcium spark frequency. However, the 18-membered variant was a potent inhibitor (Figure 59). Several hypotheses were constructed by considering the impact of ring size on the conformation and degree of expected rigidity for this *ent*-verticilide series. The presentation of the methyl and pentyl side chains was expected to deviate significantly in the 6-membered ring variant, but as ring-size increases, the conformational mobility is predicted to increase. This is expected to reach a point of limited returns, however, if the COD flexibility begins to work against the tightest binding conformation. This could be the case with the 30- and 36-membered macrocycles. The 6- and 12-membered rings, on the other hand, mirror the difficulties that small molecules display in binding to large, complex targets. The lack of activity from these two ring sizes suggests that *ent*-

verticilide could be interacting with RyR2 over a large surface area, whereas the smallest two ring sizes cannot achieve a similar interaction.

Figure 59. Activity summary of ring size analogues.

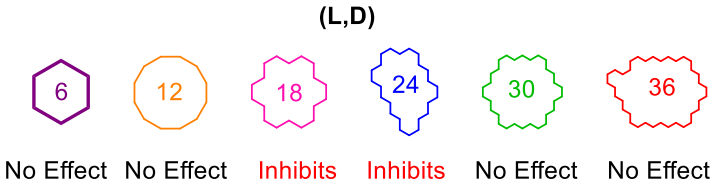

We also considered lipophilicity as a second factor. Larger molecular weight compounds can be more lipophilic than their small molecule counterparts. This increase in lipophilicity usually results in a corresponding decrease in aqueous solubility. However, a "chameleon-like" behavior has been attributed to certain macrocyclic compounds, describing their ability to adopt conformations that bury hydrophilic or hydrophobic functionality based on their environment.[17] This attribute of molecules well outside of the traditional realm of drug-likeness endows them with both the lipophilicity needed to cross cell membranes, as well as aqueous solubility. These two properties are crucial for activity with intracellular targets along with bioavailability. In this ring-size series, both the AlogP[184] values and the topical polar surface areas (TPSA)[185,186] were calculated to quantify the relative lipophilicity for each compound. These calculated values follow the expected trend - as the ring-size increases, lipophilicity increases (Table 6). In these initial studies, however, a corresponding decrease in solubility was not observed. Each ring-size was soluble in the aqueous buffer used in the calcium sparks assays at 25 μM, and no complications with precipitation were observed. Additionally, *ent*-verticilide maintains activity *in vivo*,[162] indicating some level of aqueous solubility. This increase in lipophilicity could, however, still be a factor contributing to the loss of activity. If the target binding surface includes numerous hydrogen bonding sites, the pharmacophore could have surpassed a non-polar threshold in the larger macrocycles. Furthermore, increases in lipophilicity could reduce the target specificity,

[184] Alog P values were calculated using the Virtual Computational Chemistry Laboratory ALOGPS 2.1 program. AlogP values have been shown to have better accuracy than ClogP for molecules with more than 45 atoms; Ghose, A. K.; Viswanadhan, V. N.; Wendoloski, J. J. *J. Phys. Chem. A* **1998**, *102*, 3762
[185] Topical polar surface area was calculated by Dr. Corey Hopkins using QikProp in Schrodinger software suite.
[186] Ertl, P.; Rohde, B.; Selzer, P. *J. Med. Chem.* **2000**, *43*, 3714

resulting in a loss of activity through off-target binding.[187] The smaller ring sizes (6- and 12-membered rings) may suffer from increased rigidity, an effect noted in studies of a decapeptide analogue of cyclosporine.[188]

Table 6. Comparison of CODs by ring-size, molecular weight, calculated AlogP values, and calculated topical polar surface area (TPSA).

Ring Size	molecular weight (g/mol)	calculated AlogP[a]	calculated TPSA (Å^2)[b]
6 (**55**)	213.27	0.95-1.60	66.76
12 (**56**)	426.55	3.11 -3.97	100.71
18 (**57**)	669.83	4.59-5.19	151.69
24 (**33**)	853.11	5.05-5.63	207.06
30 (**58**)	1066.39	5.41-5.83	248.17
36 (**59**)	1335.77	5.67-5.98	303.29

[a]AlogP values were calculated using the Virtual Computational Chemistry Laboratory ALOGPS 2.1 program.
[b]TPSA values were calculated using QikProp in the Schrödinger software suite.

Remarkably, from this study we discovered another potent ring size variant – the 18-membered COD. This finding indicates that the full structure of *ent*-verticilide, a 24-membered cyclic oligomeric depsipeptide, is not critical to its activity. These data support an intriguing hypothesis where a region, rather than total volume of the molecule is responsible for its activity. It also indicates that conformation plays an essential role, as the 12-membered ring and the 12-membered linear precursor, exactly "half" variants of *ent*-verticilide, display no activity, and the consistent finding to-date that no acyclic versions of these exhibit activity.

2.4.3 N-Methylation Patterns

Methylation of nitrogen atoms is a common and vital chemical modification made in nature to regulate biological function, including *N*-methylation of histones and DNA methylation.[9] Furthermore, there are countless examples of diverse, naturally occurring *N*-methylated linear and cyclic peptides. Synthetic chemists have begun to leverage this modification to alter biological activity and improve pharmacokinetic and pharmacodynamic properties of cyclic peptides and

[187] Leeson, P. D.; Springthorpe, B. *Nat. Rev. Drug Discovery* **2007**, *6*, 881
[188] Price, D. A.; Eng, H.; Farley, K. A.; Goetz, G. H.; Huang, Y.; Jiao, Z.; Kalgutkar, A. S.; Kablaoui, N. M.; Khunte, B.; Liras, S.; Limberakis, C.; Mathiowetz, A. M.; Ruggeri, R. B.; Quan, J.-M.; Yang, Z. *Org. Biomol. Chem.* **2017**, *15*, 2501

depsipeptides. *N*-Methylation significantly alters the conformation of cyclic peptides by disrupting their intramolecular hydrogen bonding capabilities.

We were interested in exploring this parameter in *ent*-verticilide, in which all four amides are *N*-methylated. We hypothesized that this functionality was necessary for *ent*-verticilide's biological activity. To test this hypothesis, we prepared the *N*-H precursor of *ent*-verticilide (**64**)[162],

Figure 60. Activity summary of *N*-methylation analogues.

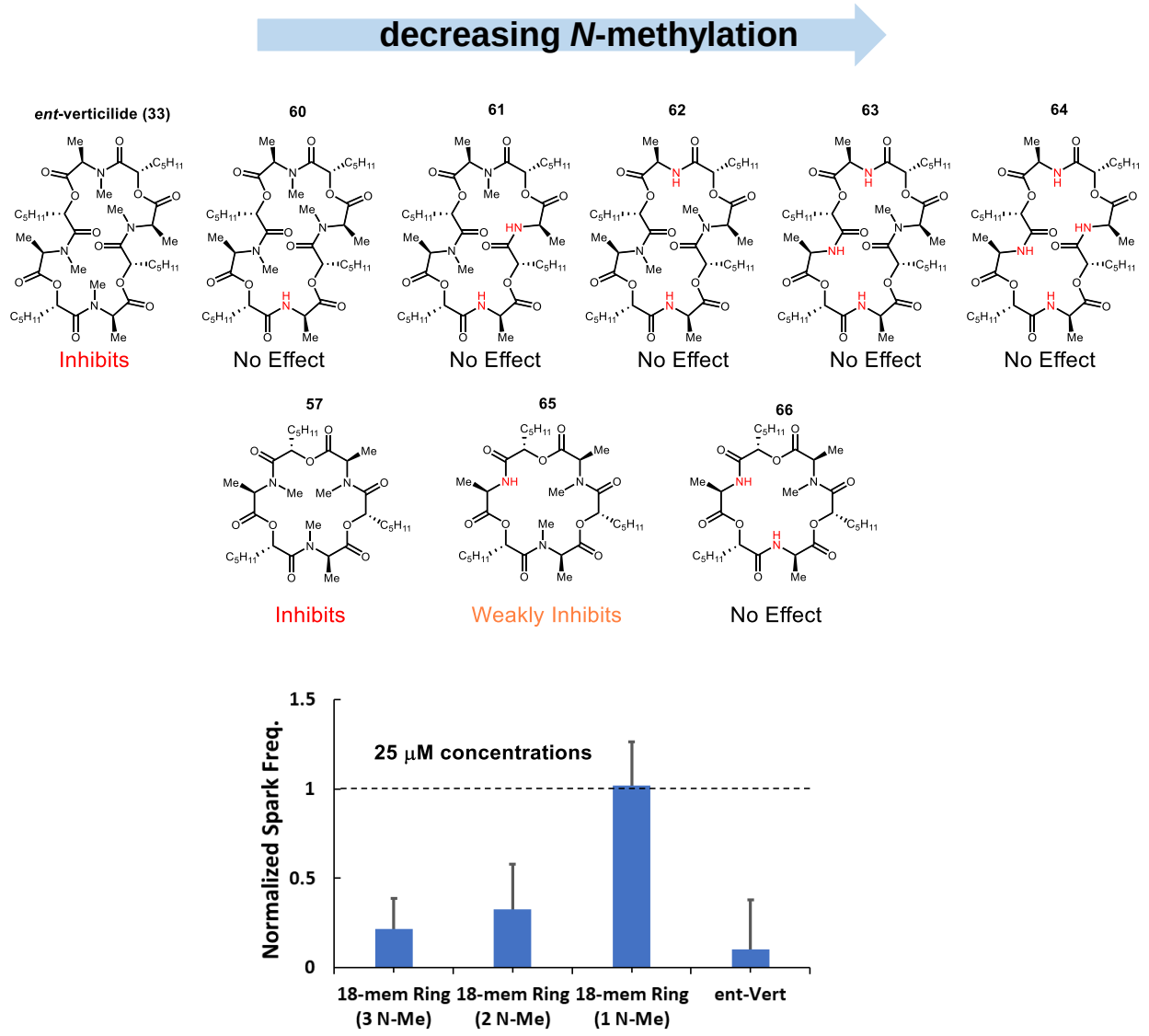

the one *N*-Me analogue (**63**),[189] the half-methylated (2 *N*-Me groups on adjacent residues (**61**)[189] and 2 *N*-Me groups on alternating residues (**62**)) analogues, and the three *N*-Me analogue (**60**),[189]

[189] This analogue was synthesized and characterized by Paige Thorpe

all of which were inactive in our RyR2 calcium sparks assay (Figure 60). We additionally explored variation of *N*-methylation in the 18-membered ring analogue that had previously showed activity in our assay. The results indicate a linear decrease in activity as the number of *N*-Me groups decreases. When the compound is fully methylated, it shows strong activity. One of the partially methylated analogues (**65**) still had activity, albeit a decrease in potency, while the other partially methylated analogue (**66**) lost activity. This decrease in activity in both series may be due to conformational changes in the molecules while generally preserving the pharmacophore. When an *N*-Me group is removed, a new hydrogen bond donor is added. It is well known that *N*-H cyclic peptides tend to form tight, intermolecular hydrogen bonding networks,[190,191] and this could significantly change the orientation of the aliphatic side chains. We have seen evidence of this type of internal hydrogen bonding in solid state structures we have obtained for both the *N*-H 24- and 18-membered rings (Figure 61). In the 24-memered ring, two of the four *N*-H amides are buried inside the macrocycle, forming intramolecular hydrogen bonds with ester carbonyls. This intramolecular bonding orients the four lipophilic pentyl side chains to the same face of the macrocycle. We hypothesize that this arrangement could 1) provide a nonpolar face for *ent*-verticilide to interact with the lipophilic membrane, 2) enable binding to RyR2 through either an all-nonpolar face or an all-polar face, 3) or provide polar and nonpolar faces to different molecules of RyR2 to promote the formation of the multimeric protein assembly This same behavior is seen with the 18-membered *N*-H cyclodepsipeptide, in which two of the three *N*-H amides are buried in intramolecular hydrogen bonds. While most of the *N*-methyl analogues have yet to succumb to crystallization, we have obtained some structural data for the *N*-Me 18-membered ring (Figure 61). In this crystal structure data, the 18-membered ring is bound to either a Na^+ or Mg^{2+} ion and displays a significantly different conformation. The lipophilic side chains are now no longer oriented on a single face. This change in the structure is hypothesized to be influenced by 1) *N*-methylation reducing the conformational space and hydrophilicity,[9] or 2) being bound to an ion. Given the similarity between the two *N*-H analogs, it is possible that this crystal structure is more analogous to *ent*-verticilide than its *N*-H precursor. This preliminary data has led to an overarching

[190] Patel, D. J.; Tonelli, A. E. *Biochemistry* **1973**, *12*, 486
[191] Grochulski, P.; Smith, G. D.; Langs, D. A.; Duax, W. L.; Pletnev, V. Z.; Ivanov, V. T. *Biopolymers* **1992**, *32*, 757

SAR hypothesis that both the degree of *N*-methylation and macrocycle ring size can have strong effects on activity.

Figure 61. Crystal structures of *N*-H 18- and 24-membered CODs and *N*-Me 18-membered COD.

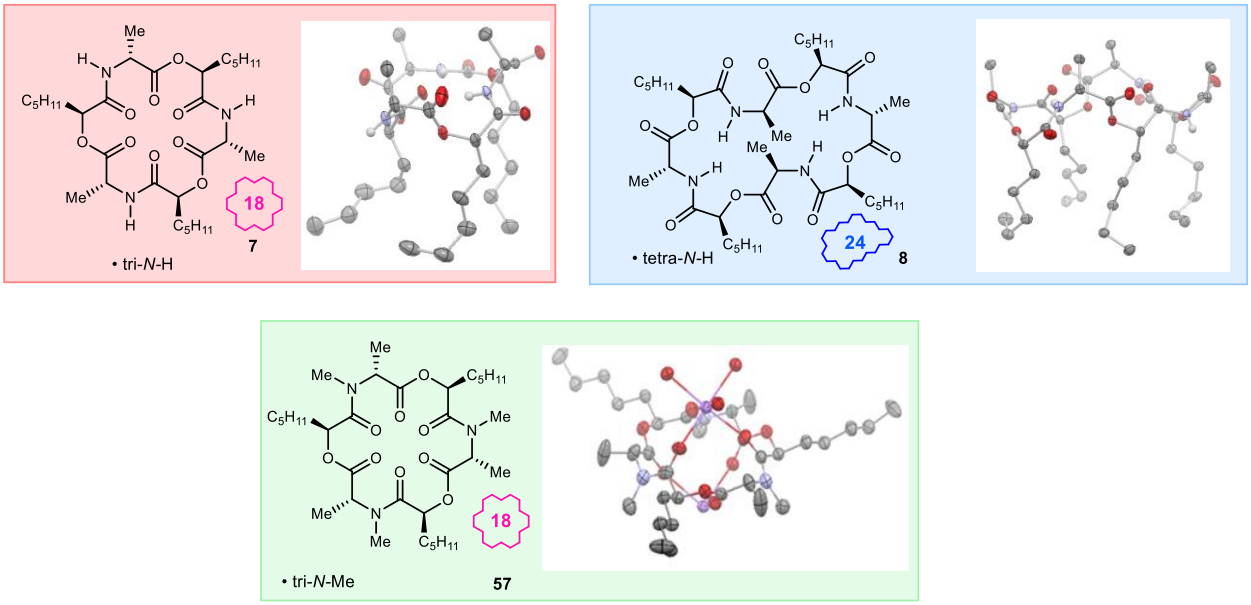

2.4.4 Stereochemical Variation

One of the initial intriguing aspects of the *ent*-verticilide discovery, was the complete lack of activity in the natural product, *nat*-verticilide, in the RyR2-based assays. Chiral natural products are most often produced biosynthetically as a single enantiomer. In rare cases, they can be produced as racemic mixtures, or the enantiomer could be produced by a different species.[192] However, most often, the unnatural enantiomer must be accessed by chemical synthesis. The value of exploring the non-natural enantiomer has been demonstrated with examples like roseophilin[193] and deguelin[194] where the non-natural enantiomer was found to be significantly more potent. However, more often than not, the natural product enantiomers are not accessed for comparison to their natural counterpart due to significant synthetic barriers. To the best of our knowledge, *ent*-

[192] Finefield, J. M.; Sherman, D. H.; Kreitman, M.; Williams, R. M. *Angew. Chem. Int. Ed.* **2012**, *51*, 4802
[193] Boger, D. L.; Hong, J. *J. Am. Chem. Soc.* **2001**, *123*, 8515
[194] Farmer, R. L.; Scheidt, K. A. *Chem. Sci.* **2013**, *4*, 3304

Figure 62. Activity summary of analogues in the natural (D,L) series.

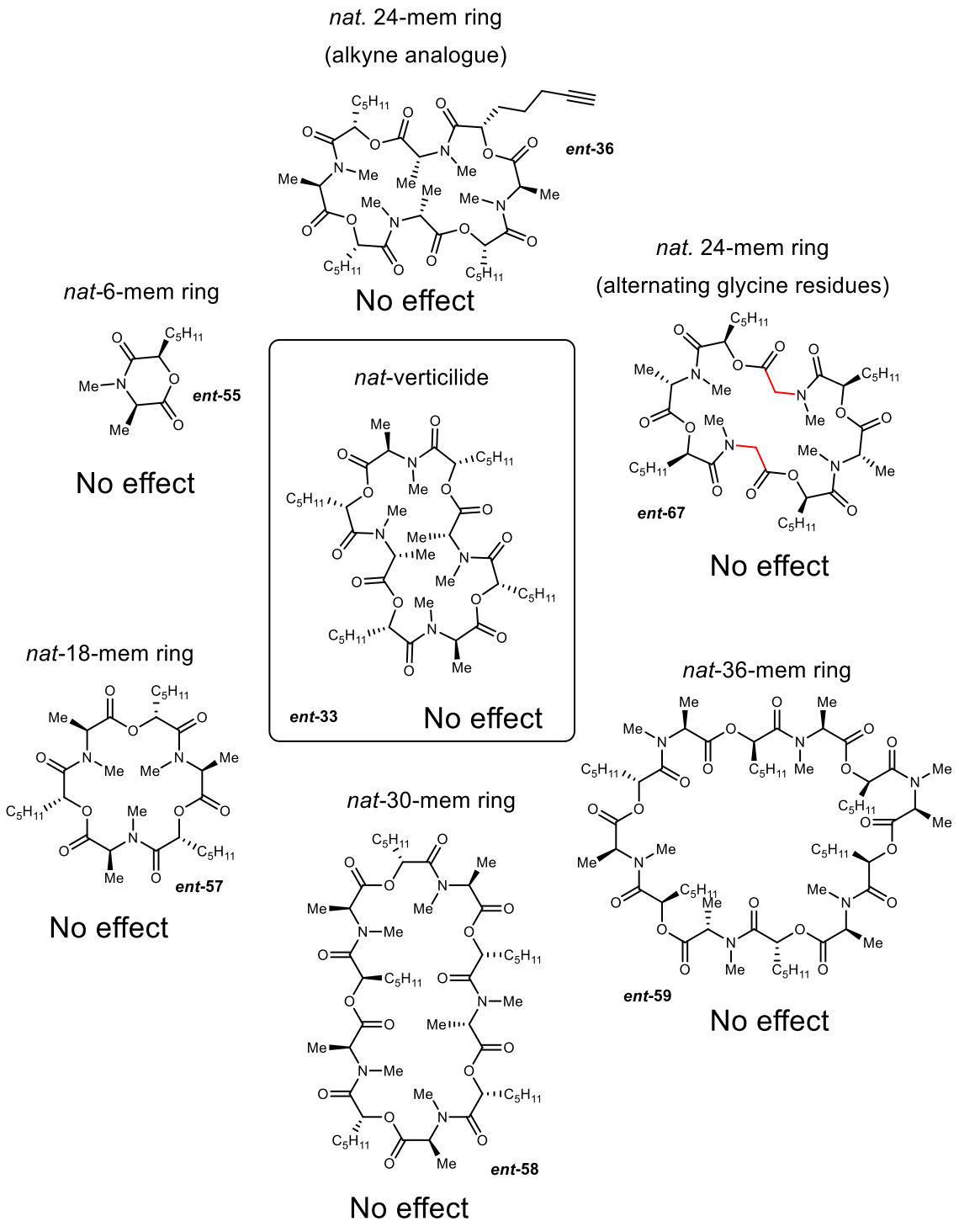

verticilide is the first example of a non-natural enantiomer with potent activity while the natural product displayed no activity at all against the same target.

We have continued to monitor this finding in our SAR studies, synthesizing a variety of complementary analogues in the natural series (D, L) (Figure 62). Specifically, when another hit compound in the *ent*-series is discovered, the "natural" variant is synthesized as a comparison. To date, all *nat*-compounds have been inactive, confirming the suspicion that enantiomeric specific activity holds true in a wide series of analogues. It is however, important to note, that in one case, at high concentrations (25 µM) we saw inhibition of calcium sparks with the natural alternating glycine analogue (***ent*-64**). However, when tested at a lower concentration (3 µM), a reduction in calcium sparks was no longer observed. The hypothesis is that this compound can become cytotoxic at higher concentrations, promoting cell death, and as a result, calcium sparks are not possible. This analogue was therefore considered a "false positive" at higher concentrations. This concentration dependence is monitored in all SAR studies. We have also begun studies to examine the relative stereochemistry of *ent*-verticilide. Having eight chiral centers, a total of 256 diastereomers would be possible to synthesize. Such a comprehensive study was considered, but a more focused hypothesis-driven prioritization was judged to be more prudent. This reflects a deep respect for both rigor, graduate student time and talent, and limited access to automation. Thus far, the two homochiral diastereomers (**68**) and (**69**) shown in Figure 63 have been synthesized.[195]

Figure 63. Homochiral stereochemical analogues.

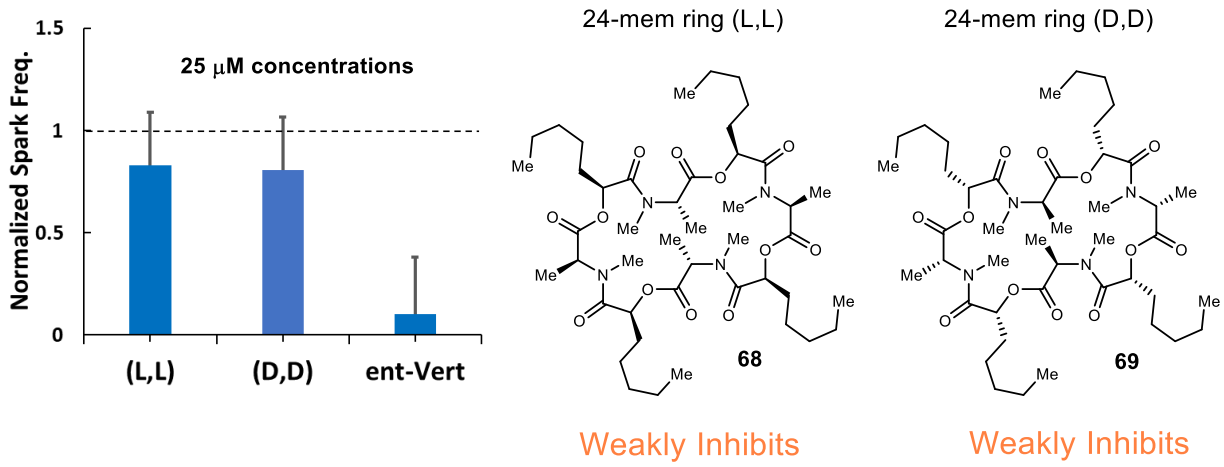

[195] These two compounds were designed by Abby Smith and synthesized and characterized by Paige Thorpe

As anticipated, both of these analogues had little activity against RyR2 calcium sparks. A series in which a selection of other diastereomers are synthesized and examined is forthcoming.

The final stereochemical aspect to mention is the synthesis of several analogues in which stereocenters have been removed (Figure 64; see discussion in section 2.4.5-amino acid variation). This parameter was examined first on the amino acid substituents, by incorporating glycine in place of alanine. While removing all four of the amino acid stereocenters results in a loss of activity, alternating alanine residues can be substituted for glycine with only slight loss of activity. It appears however, if only one alanine residue is substituted for glycine, the molecule becomes cytotoxic at 25 μM concentrations. When lower the concentration to 3 μM, compound **71** becomes inactive. Overall, this indicates there is specificity in which chiral centers can be removed. It is

Figure 64. *ent*-Verticilide glycine substitution analogues.

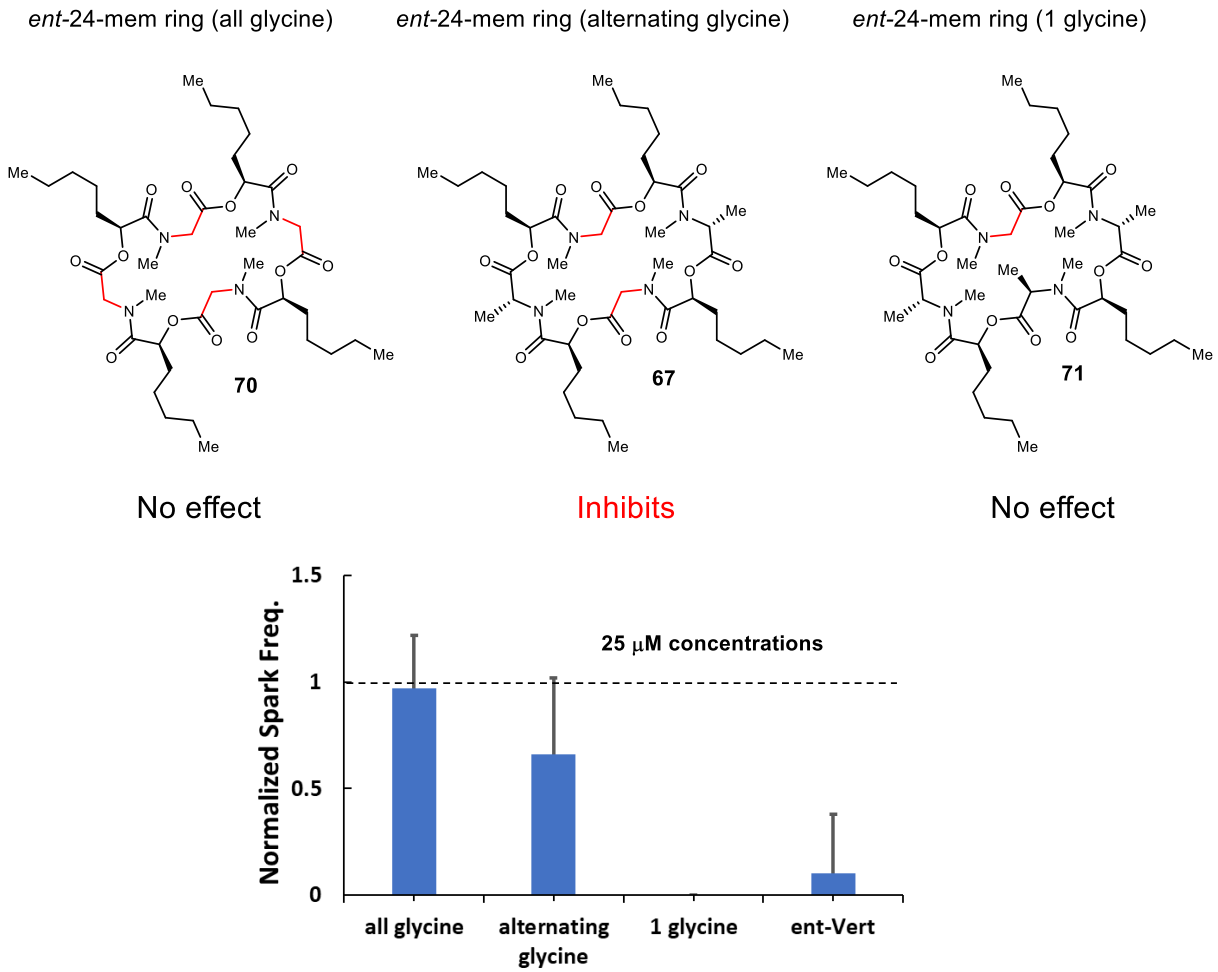

possible that a symmetrical pattern is necessary to maintain an active conformation. Future studies to further investigate this hypothesis are warranted.

2.4.5 Amino Acid Variation

One of the challenges associated with the incorporation of *N*-methyl amino acids is the low commercial availability of them, especially D-amino acids. However, many groups have developed procedures to access these N-methylated amino acids,[196] and several have become adopted at large by the chemical community.[197,198,199,200] Two different protocols were used to access these *N*-Me amino acids, shown in Figure 65. For any amino acids with easily epimerizable α-stereocenters, the oxazolidinone strategy was used, and for all others, direct methylation was accomplished using sodium hydride and methyl iodide.

To date, we have tested a series of naturally occurring amino acids (in the enantiomeric D series). An interesting parameter first explored, was whether replacement of alanine with glycine resulted in a loss of activity. As mentioned earlier, this analogue with all four glycine units was inactive, likely due to the different conformation this less ridged molecule adopts. However, when only two of the alanine residues are replaced with glycine residues, the molecule maintains similar activity as *ent*-verticilide. This demonstrates that the loss of at least two chiral centers, as well as

Figure 65. Synthesis of *N*-methyl amino acids.

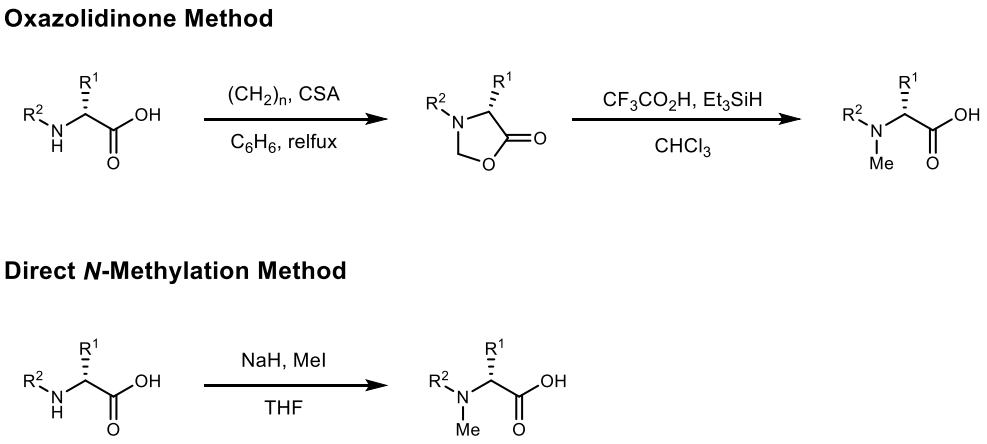

[196] Aurelio, L.; Brownlee, R. T. C.; Hughes, A. B. *Chem. Rev.* **2004**, *104*, 5823
[197] Aurelio, L.; Brownlee, R. T. C.; Hughes, A. B.; Sleebs, B. E. *Aust. J. Chem.* **2000**, *53*, 425
[198] Aurelio, L.; Box, J. S.; Brownlee, R. T. C.; Hughes, A. B.; Sleebs, M. M. *J. Org. Chem.* **2003**, *68*, 2652
[199] Hlavácek, J., et al. *Collect. Czech. Commun.* **1976**, 41, 2079.
[200] Hlavácek, J., et al. *Collect. Czech. Commun.* **1988**, 53, 2473.

some additional conformational flexibilities are tolerated in the SAR parameters. Interestingly, when only one alanine is replaced with glycine, the analogue completely loses activity. This is surprising and indicates that some form of symmetry might be required for activity. An initial hypothesis was that perhaps half of the molecule is responsible for activity, while the other half is only necessary for conformational rigidity. However, the loss of activity with a single glycine unit suggests otherwise. It is possible that somehow, the conformation is drastically different in the single glycine residue analogue, and crystal structure data or computational conformation studies may be helpful in further elucidating the reasoning for the observed behavior.

We have also explored a small series of other amino acids, including leucine, phenyl alanine, and proline. In each of these analogues, all four amino acids were substituted (Figure 66). We hypothesized that while glycine may not be tolerated at all four positions, this could be due to the increase of conformational flexibility rather than the actual functionality. However, except for

Figure 66. Amino acid analogues of *ent*-verticilide.

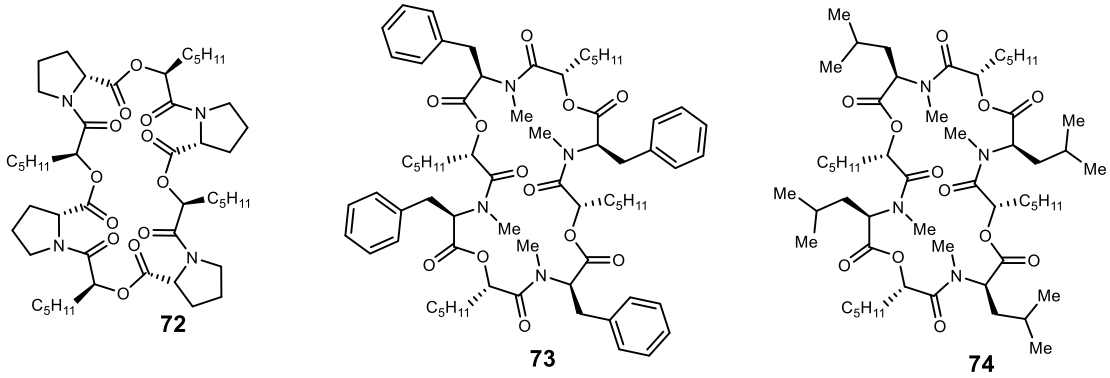

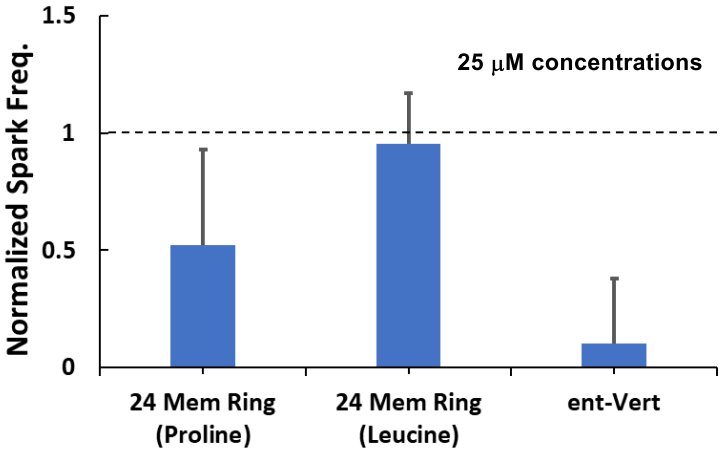

proline (**72**), thus far, no analogue in which all four alanine residues are substituted appears to have activity.[201] Interestingly, the leucine derivative appeared as a single conformer by ^{1}H NMR, strikingly different from other analogues observed thus far. This restricted backbone and change in conformational freedom likely plays a significant role in the loss of activity. Proline maintained a reduction of calcium spark frequency; however, the potency was drastically reduced compared to *ent*-verticilide. This speaks to the necessity of having a tertiary amide, but not necessarily the need for it to be an *N*-methyl amide. Again, computational studies in which the conformational isomers are examined may provide more insight into this finding.

2.4.6 Hydroxy Acid Variation

While our SAR work provided insight into the activity for *ent*-verticilide, our goal early on, was to use the SAR results to help guide the synthesis of the more complex mechanism of action analogues. Towards that end, we recognized the hydroxy acid side chains as a potential residue for alteration in order to synthesize mechanism of action analogues. The rationale behind this decision was two-fold. First, these side chains are the least sterically hindered part of the molecule, making them most likely to be amenable to the conjugation chemistry we were interested in carrying out. Second, we had already developed synthetic methodology to access unnatural α-hydroxy acids and envisioned the ability to make a variety of different analogues without having to drastically adapt the synthetic methodology. These alkyl side chains are an unusual, unique feature to verticilide and *ent*-verticilide, and it is expected that they play a significant role in the activity. However, we hypothesized that we may be able to modify them to some extent. To explore this, two initial analogues were synthesized in which the side chains were changed by a single carbon, increasing to a hexyl side chain in one analogue, and decreasing to a butyl side chain in the other (Figure 67). When these compounds were tested in the calcium sparks assay, both had no inhibition at all. This was disappointing that such a small alteration lost all activity. However, we still had our hypothesis that only part of the molecule was responsible for activity, so we looked at variations of analogues in which only a few of the four side chains were modified. Specifically, we synthesized two analogues in which two adjacent alkyl side chains were either shortened or lengthened by a carbon (Figure 68). Additionally, we synthesized an analogue in which alternating side chains were

[201] Phenylalanine analogue has not been tested yet in calcium sparks assay.

Figure 67. α-Hydroxy acid variation analogues of *ent*-verticilide with A) hexyl alkyl side chains and B) butyl alkyl side chains. C) *ent*-compound effects on calcium spark assay in permeabilized murine cardiomyocytes. All data are normalized to vehicle (DMSO) treatment for the given day. Data presented as mean ± SEM from N > 18 cells per group (1 – 5 independent experiments). Hashed bars are placeholders and were not tested at that concentration. * $p < 0.01$ vs vehicle by Student's t-test. *C was made by Dan Blackwell.

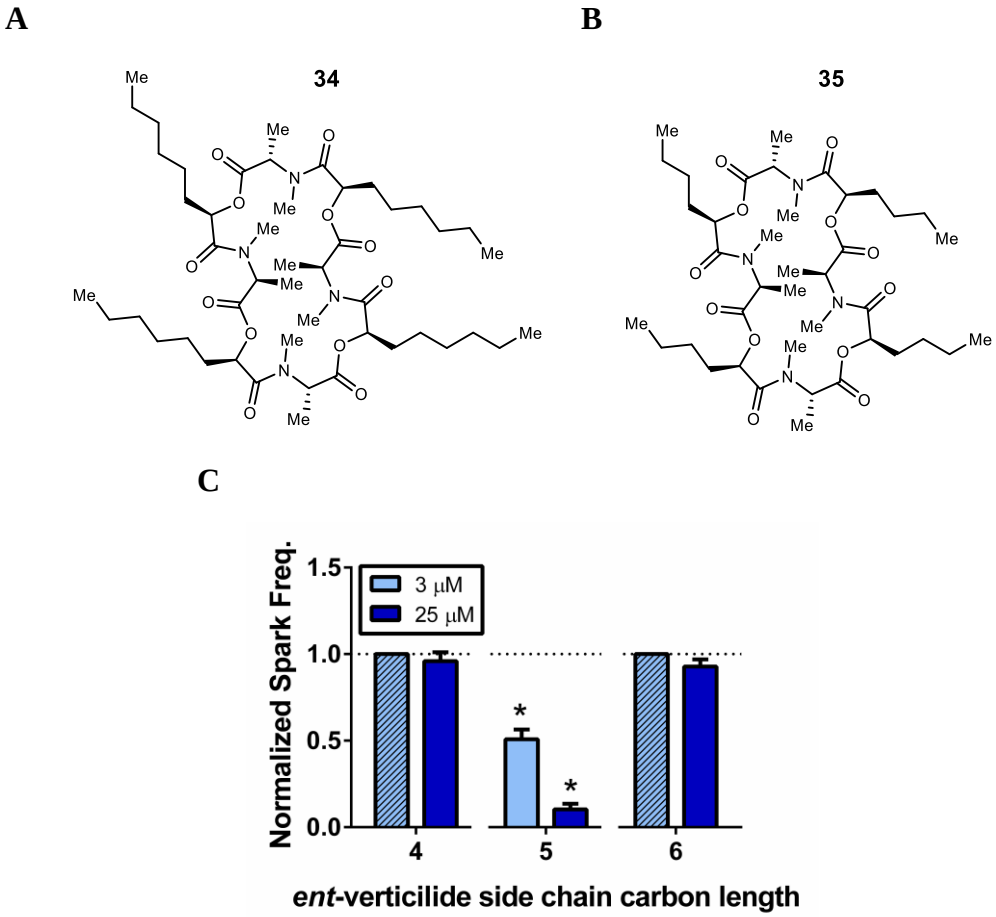

lengthened, to gauge if the symmetry was necessary for activity (Figure 68). When tested in the sparks assay, it was exciting to find that all of these partial altered analogues maintained similar potency to *ent*-verticilide. It is strange however, that no difference in activity is seen between the alternating or adjacent side chain lengthened analogues. We do not anticipate a significant change in conformation between any of these analogues and ent-verticilide, so other factors must be at play here. Additionally, the data from compounds shown in Figure 67 and Figure 68, work against the hypothesis that only half of the molecule is responsible for activity. It would be interesting to further gauge this by synthesizing a variant in which three of the four alkyl side chains are either shortened or lengthened.

Figure 68. α-Hydroxy acid variation analogues of *ent*-verticilide.

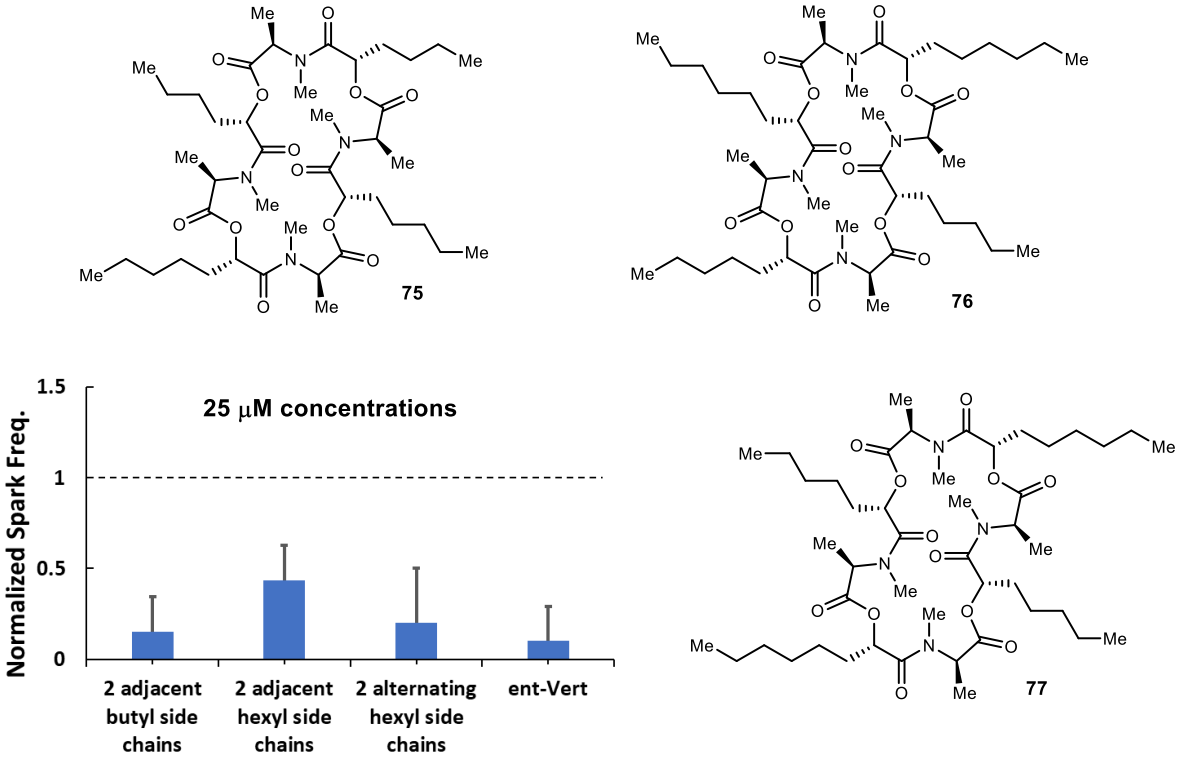

To determine whether the alkyl side chain was important due to structure or just lipophilicity, an analogue in which the five carbon alkyl side chains were contained into a cyclic structure was synthesized (Figure 69). Amazingly, this analogue maintained activity, albeit at a weaker potency than *ent*-verticilide. This suggests that perhaps having the correct balance of lipophilicity plays a more significant role than anticipated. We do, however, know that permeability is not an issue, as these compounds are all tested in permeabilized cardiomyocytes. Again, compound **78** displayed a significantly favored conformation by ^{1}H NMR, compared to our usual conformationally mobile analogues. This increased rigidity could be partially contributing to the decrease seen in activity.

Finally, we looked at a series of analogues in which only a single side chain had been modified. We first synthesized a variant of *ent*-verticilide that incorporated an alkyne onto a single side chain, in order to determine if we would be able to attempt conjugation chemistry for fluorescent analogues (see section 2.5.1 Fluorescent Probes for more details). After significant optimization of the synthesis of this alkyne side chain (see section 2.4.1 Analogue Design and The Development of a New Synthetic Route for more details), we successfully arrived at the desired analogue and

Figure 69. α-Hydroxy acid variation analogues of *ent*-verticilide.

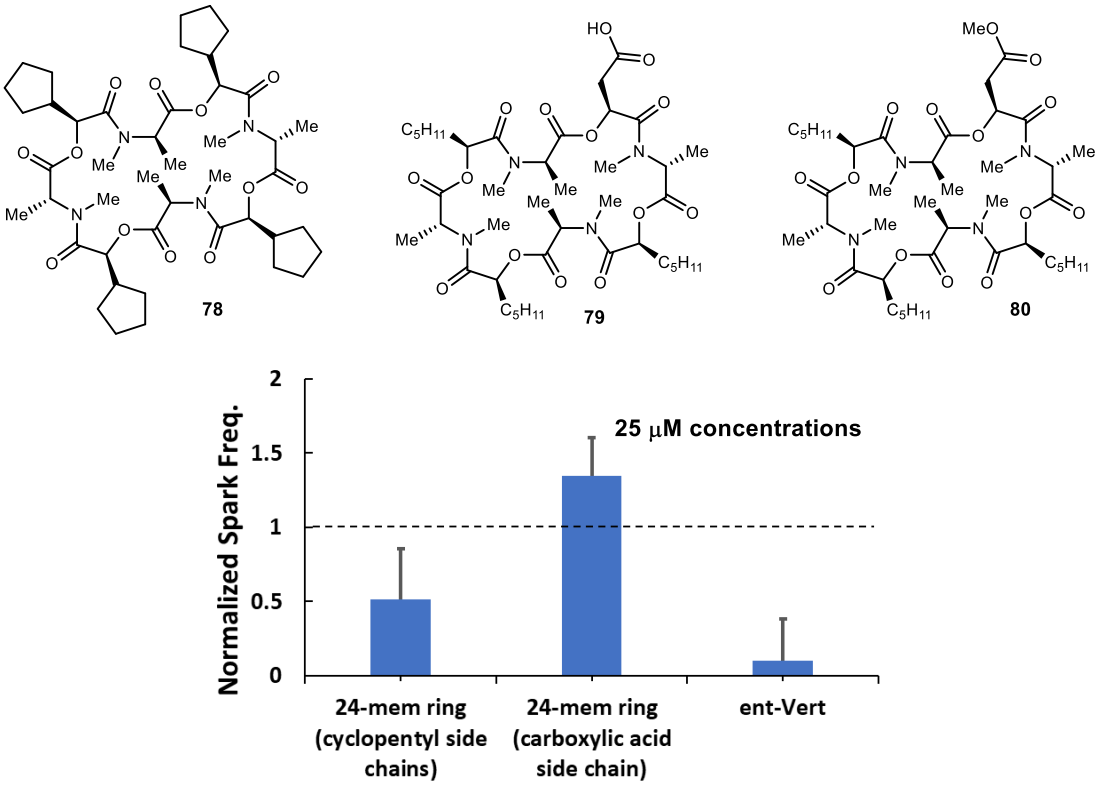

subjected it to the calcium sparks assay. Excitingly, the alkyne analogue maintained the same potency as *ent*-verticilide and prompted us to begin working towards fluorescent derivatives. Another analogue in which a single side chain was modified was in route to a diazirine derivative (see chapter 2.5.4). This analogue incorporated a carboxylic acid into the side chain. Interestingly, analogue **79** displayed an increase in calcium spark frequency. While this is the opposite effect of what we are aiming for, this provides further evidence of *ent*-verticilide interacting with RyR2. Currently, we believe *ent*-verticilide is acting as a negative allosteric modulator. To observe the opposite affect (positive allosteric modulator) with a similar compound, suggests a similar binding pocket. The chance of observing this reversal of behavior if *ent*-verticilide was only affecting RyR2 through an indirect mechanism is highly unlikely. Further work with **79** may greatly assist in mechanism elucidation work. To parallel this analogue, the capped methyl ester variant (**80**) was also synthesized. We have yet to test that activity of this compound in the sparks assay but is sure to be an interesting comparison.

2.4.7 Ester Bond Substitution

Finally, we have been interested in exploring substitutions of the ester bonds in *ent*-verticilide. Ester bonds, being the defining characteristic of depsipeptides, have been demonstrated to be useful as a peptidomimetic. However, the properties of the ester bond in depsipeptides significantly vary from the amide bonds. While the two groups are isosteric and have relatively similar conformational preferences, there is more flexibility around an ester linkage compared to an amide. Ester bonds have shown to play a large role in increasing cell permeability of peptides, yet often can result in decreased stability due to risk of hydrolysis. *ent*-Verticilide contains four ester bonds that could be modified. Starting with ester to amide substitution, we planned out a series of analogues to be synthesized exploring systematic replacement of each ester bond with both N-H and N-Me amides. Each of these analogues would then be tested in the calcium spark assay to assess activity against RyR2 mediated spontaneous calcium release, as well as passive permeability assays (PAMPA), to assess the role that each ester contributes to the passive permeability of these molecules. Finally, microsome stability studies could be conducted on each analogue if desired, to determine how susceptible each ester bond makes *ent*-verticilide to hydrolysis by esterases.

To begin it was necessary to develop a route to synthesize the unnatural amino acid that would be required for these variations (Figure 70). Historically, enantiopure α-amino acids were accessed

Figure 70. Ester to amide substitution in *ent*-verticilide analogues.

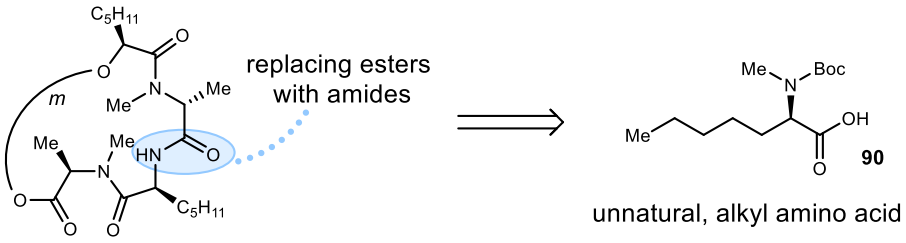

via natural isolation, or chemical/enzymatic resolutions. Over the last 25 years, catalytic, enantioselective methods have come into favor as the preferred method of synthesis.[202] The most employed enantioselective method is the introduction of the α-hydrogen, either through

[202] Nájera, C.; Sansano, J. M. *Chem. Rev.* **2007**, *107*, 4584

hydrogenation of α,β-dehydro-α-amino acids[203,204,205] or less frequently, reductive amination of α-keto esters.[206] Other developed methods include electrophilic amination of ester/amide enolates,[207, 208] Strecker-type reactions,[209,210] Nitro-Mannich reactions, cyclopropanations, cycloadditions, electrophilic alkylations of glycine ester enolates, and nucleophilic alkylations of α-amino esters.[202] Several of these approaches were considered, but ultimately, a methodology paralleling our unnatural hydroxy acid synthesis was leveraged. While many variations of reactions are known to make unnatural α-amino acids, examples with alkyl substrates employing chiral catalysis are not broadly developed. While potentially more step-intensive, we proposed a synthesis of unnatural amino acids that accessed a halo-nitroalkane intermediate, allowing us to utilize this intermediate in either Umpolung Amide Synthesis, or to carry it forward to the carboxylic acid to be used in traditional peptide coupling (Figure 71). The synthesis began with commercially available aldehyde, which was subjected to sulfone formation (Scheme 17). The sulfone was eliminated under basic conditions to afford an alkyl imine **92**, which could be carried forward crude into a BisAmidine catalyzed enantioselective aza-Henry reaction. The conditions used for the aza-Henry reactions were based on prior experiments conducted by former group member Ken Schwieter. Several variants of BisAmidine (BAM) ligands and ligand salts were explored for this substrate (Table 7), with PBAM triflic acid salt providing the best yield and enantioselectivity (70% yield, 91% ee). It should be noted that when a 0% yield was obtained, formation of enamine was observed. The formed halo-nitroalkane **93** can then be carried forward into a debromination reaction, followed by subjection to Mioskowski-Nef reaction conditions to provide carboxylic acid **94**. While it would ultimately be desired to carry out the aza-Henry reaction with nitromethane instead of bromonitromethane to avoid the debromination step, attempts to do so were unfruitful. Each of the ligands shown in Table 7 were also attempted in the aza-Henry reaction employing nitromethane. All attempts however, resulted in tautomerization of the starting imine to the enamine, and no desired product formation. After formation of the carboxylic acid, it can be protected as the benzyl ester. If the *N*-methylated amino acid is desired, a methylation step can be

[203]Knowles, W. S.; Sabacky, M. J. *Chemical Communications (London)* **1968**, 1445
[204] Horner, L.; Siegel, H.; Büthe, H. *Angew. Chem. Int. Ed.* **1968**, *7*, 942
[205] Dang, T. P.; Kagan, H. B. *Journal of the Chemical Society D: Chemical Communications* **1971**, 481
[206] Kadyrov, R.; Riermeier, T. H.; Dingerdissen, U.; Tararov, V.; Börner, A. *J. Org. Chem.* **2003**, *68*, 4067
[207] Morrill, L. C.; Lebl, T.; Slawin, A. M. Z.; Smith, A. D. *Chem. Sci.* **2012**, *3*, 2088
[208] Tokumasu, K.; Yazaki, R.; Ohshima, T. *J. Am. Chem. Soc.* **2016**, *138*, 2664
[209] Spino, C. *Angew. Chem. Int. Ed.* **2004**, *43*, 1764
[210] Ma, J.-A.; Cahard, D. *Angew. Chem. Int. Ed.* **2004**, *43*, 4566

Figure 71. Possible pathways to advance common α-halo nitroalkane intermediate.

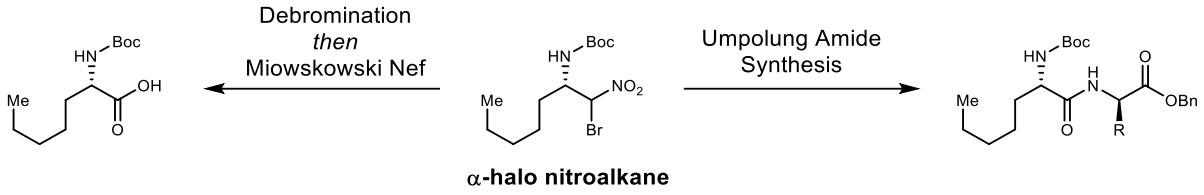

performed using silver oxide and methyl iodide. A final Boc-deprotection with TFA affords amino acid salt **97**, which can be carried forward to synthesize the desired didepsipeptide utilizing traditional peptide coupling reagents. This developed route is easily scalable and has allowed for the synthesis of >20 grams of amino acid. This versatile approach to both α-oxy amides and α-oxy

Scheme 17. Synthesis of nonnatural amino acids.

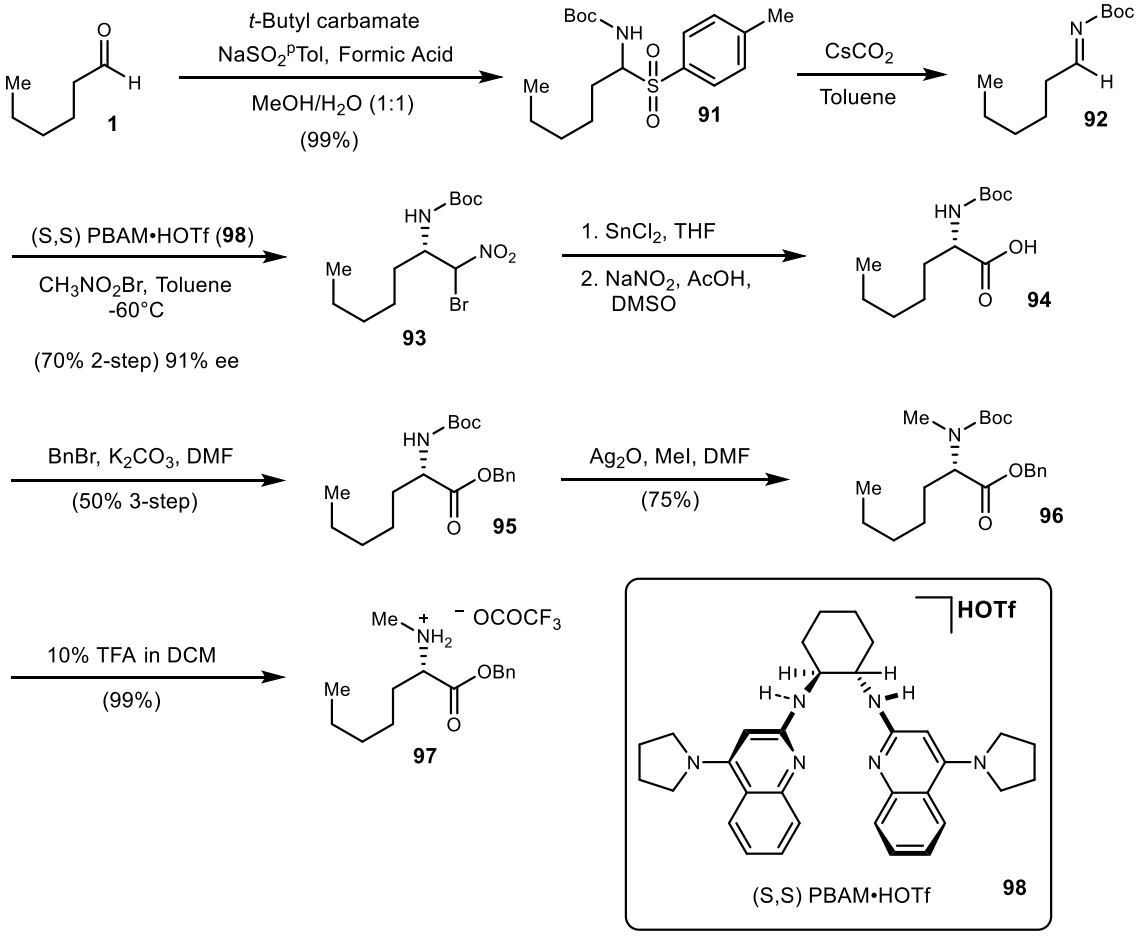

Table 7. Survey of chiral proton catalysts screened.

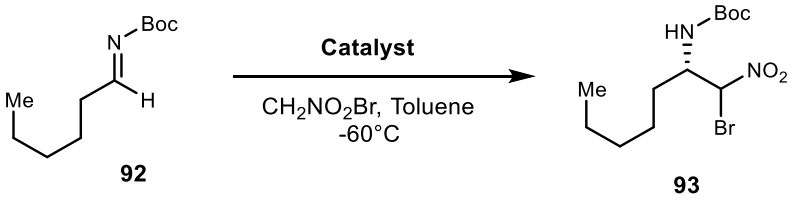

Catalyst	Yield (%)	e.e. (%)	d.r
(*S*,*S*) PBAM	62	86	1:1
(*S*,*S*) PBAM•HOTf	70	91	1:1
(*S*,*S*) StilbBAM	0	-	-
(*S*,*S*) 4MeO-StilbBAM•HOTf	0	-	-
(*S*,*S*) PBAM•$HNTf_2$	30	86	1:1

esters is the key to a current effort to prepare 27 verticilide analogues (Figure 73-Figure 75)[211] that employee these unnatural amino acids.[212] The goal of this work is to take advantage of the symmetry elements of *ent*-verticilide and use them to untangle the roles that each atom plays regarding the activity of the molecule against RyR2, as well as the cell permeability of these molecules. We know from *in vivo* work with *ent*-verticilide, that it can cross a cell membrane, despite the size of the molecule (853 MW) and its violation of Lipinski's rule of five. Using a hypothesis driven approach, these analogues will explore the systematic replacement of each ester and *N*-methylated amide bond to understand which functional groups are responsible for this permeability.

A final ester bond substitution we are interested in exploring is the replacement of each ester with a ketone. While this approach is hypothesized to decrease the flexibility of the molecule, it could also be employed to trouble-shoot hydrolysis problems if necessary. To synthesize this analogue, it was necessary to develop a route to access the ketone variant of the dipeptide (Figure 76). The synthesis began with addition of benzyl malonic acid to *N*-methyl alanine, followed by spontaneous decarboxylation to arrive at the β-keto ester (Scheme 18). A Mitsunobu reaction was then attempted between the formed β-keto ester (**100**) and α-hydroxy ester **101**. The first series of

[211] Figure 73 through Figure 75 show 22 of the 28 analogues. The other 6 analogues are shown in Figure 60 where N-methylation pattern SAR results were discussed.
[212] This work is being carried out now by Paige Thorpe.

Figure 72. Series 2 – all amide *ent*-verticilide that explores varying the *N*-methylation pattern of the alanine α-amino acids.

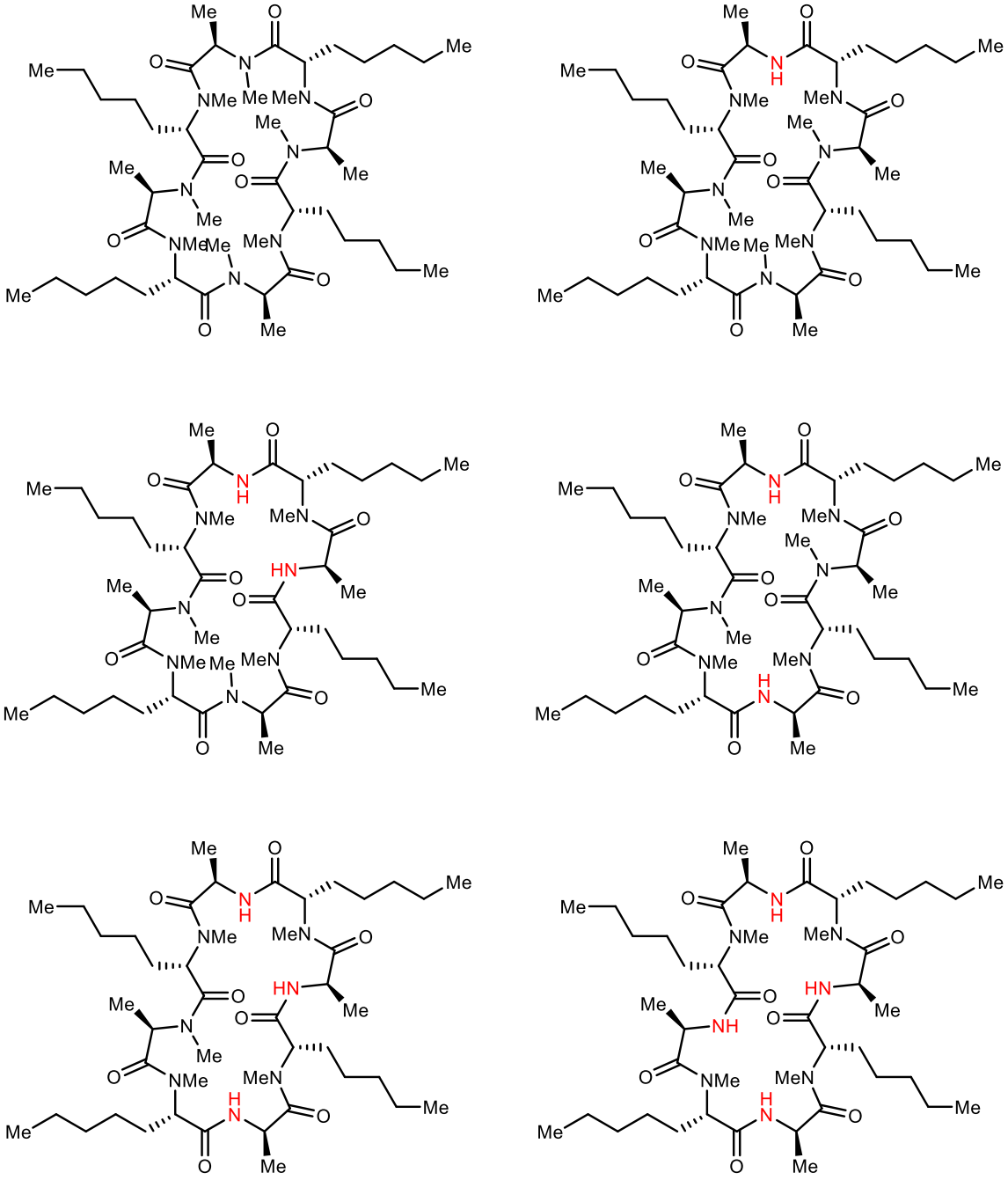

Figure 73. Series 1 – all amide *ent*-verticilide that explores varying the *N*-methylation pattern of the pentyl side chain α-amino acids.

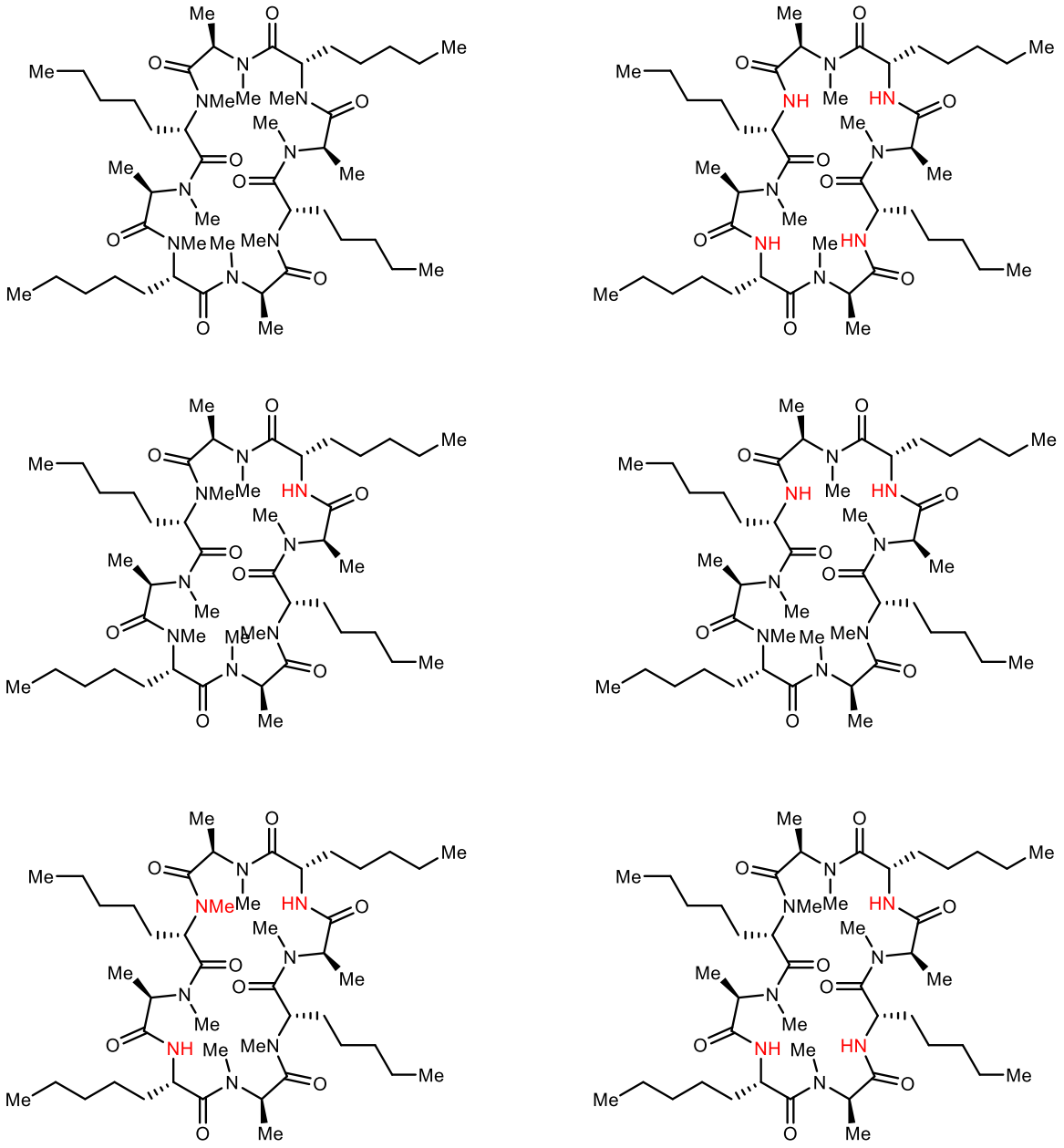

Figure 74. Series 3 – substituting esters for *N*-H amides.

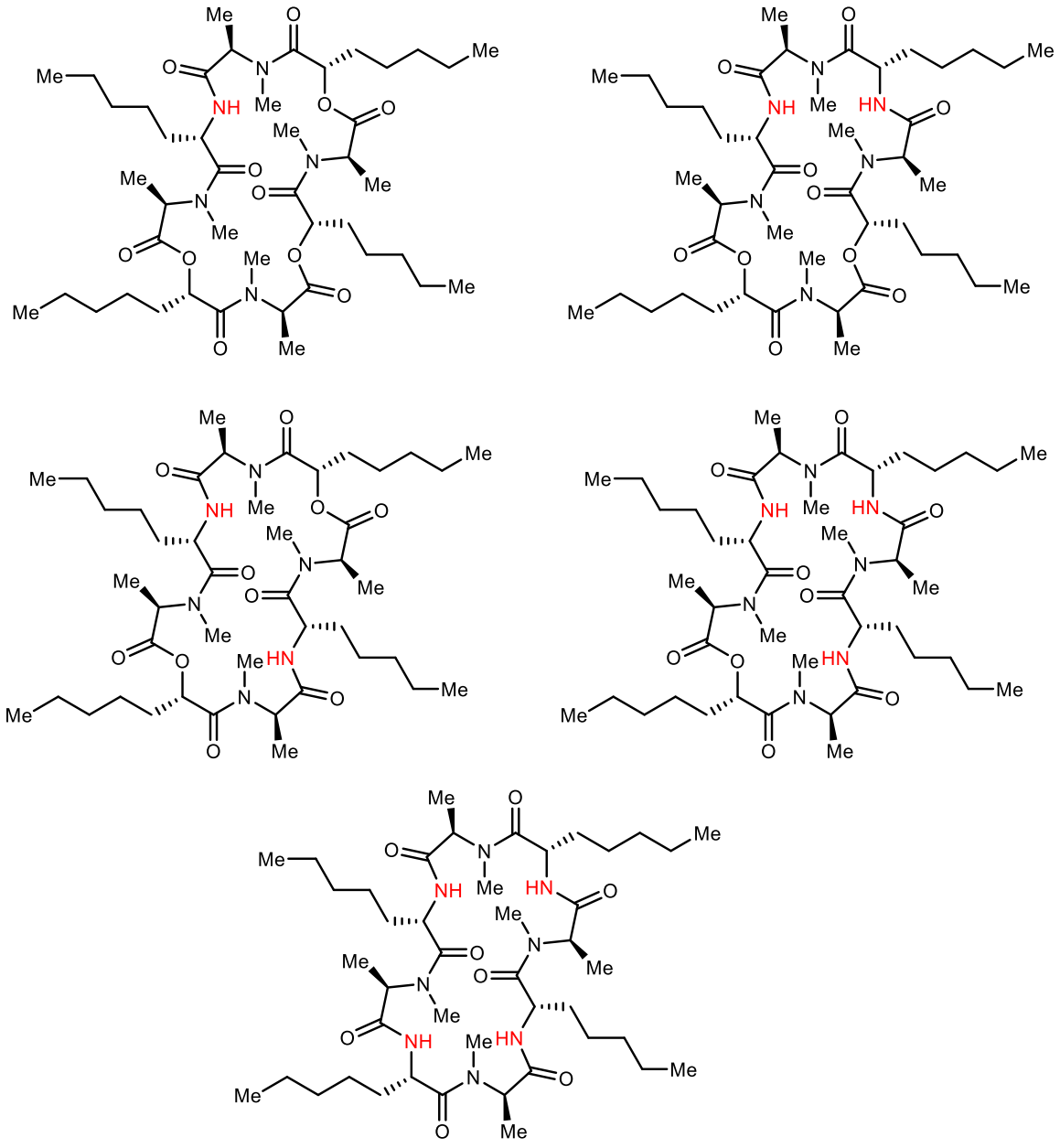

Figure 75. Series 4 – substituting esters for *N*-Me amides.

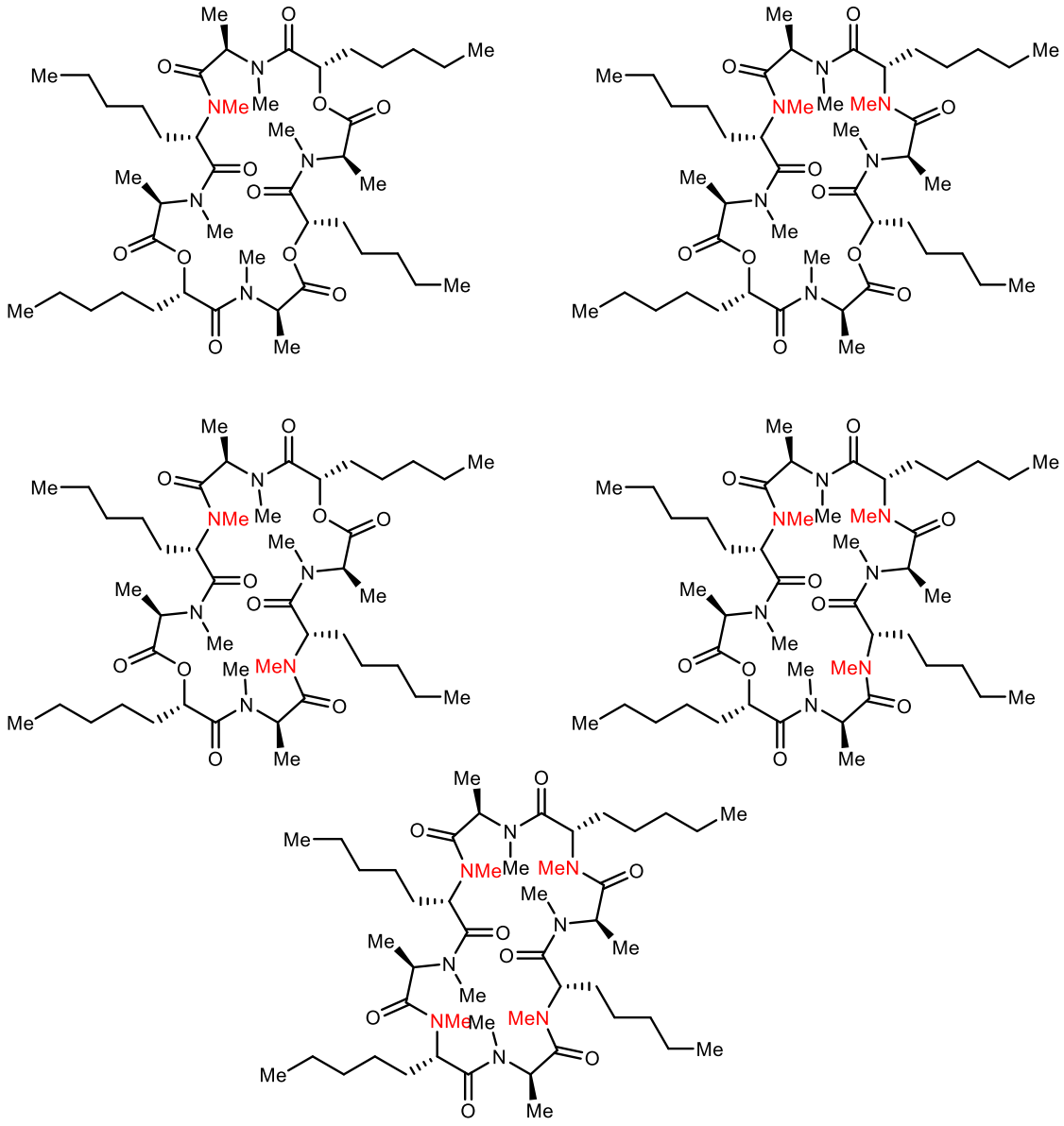

conditions employed were a combination of PPh_3, DIAD, and benzene. However, after several variations, exploring alternative azodicarboxylates, solvents, and concentrations, the highest yielding reaction produced less than 20% of the desired product.[213] Furthermore, it became apparent that the purification of this product away from the hydrazine by-products would not be a trivial task. A series of both normal and reverse-phase purifications were attempted without

[213] 20% NMR yield measured with an internal standard.

Figure 76. Ester to ketone didepsipeptide.

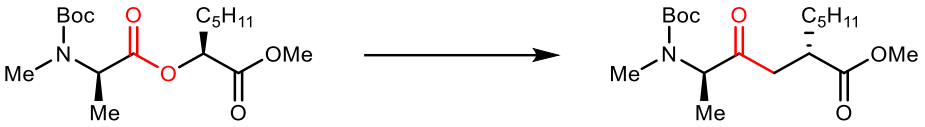

success. Azodicarboxylates that could be removed via a work-up, such as ADDM and DBAD, were tried under the reaction conditions but failed to produce any discernable product. At this point, it was clear that a new synthetic approach would be necessary. A Mitsunobu approach was originally desired for two reasons – the inversion of stereochemistry would allow us to be confident in the assignment of the diastereomer of the dipeptide formed, and we could utilize the already synthesized α-hydroxy heptanoic ester intermediate. When contemplating a new synthetic

Scheme 18. First attempted route towards the ketone dipeptide.

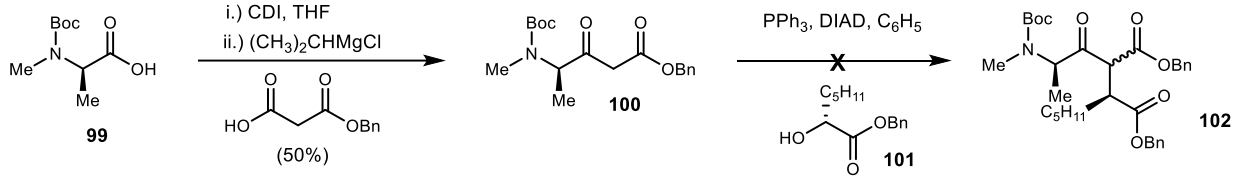

approach, it was noted that these advantages could also be realized using a S_N2-based approach. To this end, the hydroxy ester was converted to the tosyl alcohol, and then subjected to substitution conditions with β-keto ester **100** (Figure 77, eq. 1). Standard substitution reaction conditions, however, again failed to produce the desired product. Different bases, solvent systems, and temperatures were employed with no success (Figure 77, eq. 2-4). Hypothesizing that the nucleophile was not strong enough, Lewis acid was added in an attempt to increase the electrophile strength (Figure 77, eq. 5). However, once again, no desired product was formed. Operating under this same hypothesis, we opted to instead use a methyl ester enolate (**104**) as a stronger nucleophilic species (Figure 77, eq. 6). Yet, once again, this reaction failed to produce any desired product, and instead resulted in the decomposition of the tosyl starting material. Presumably, this decomposition stems from the competitive elimination reaction. In a final effort, both nucleophiles (**100** and **104**) were reacted with the triflate alcohol (**105**), in hopes that a better leaving group would increase the desired substitution pathway (Figure 77, eq. 7-8). However, yet again, no

Figure 77. Second attempted route towards the ketone dipeptide.

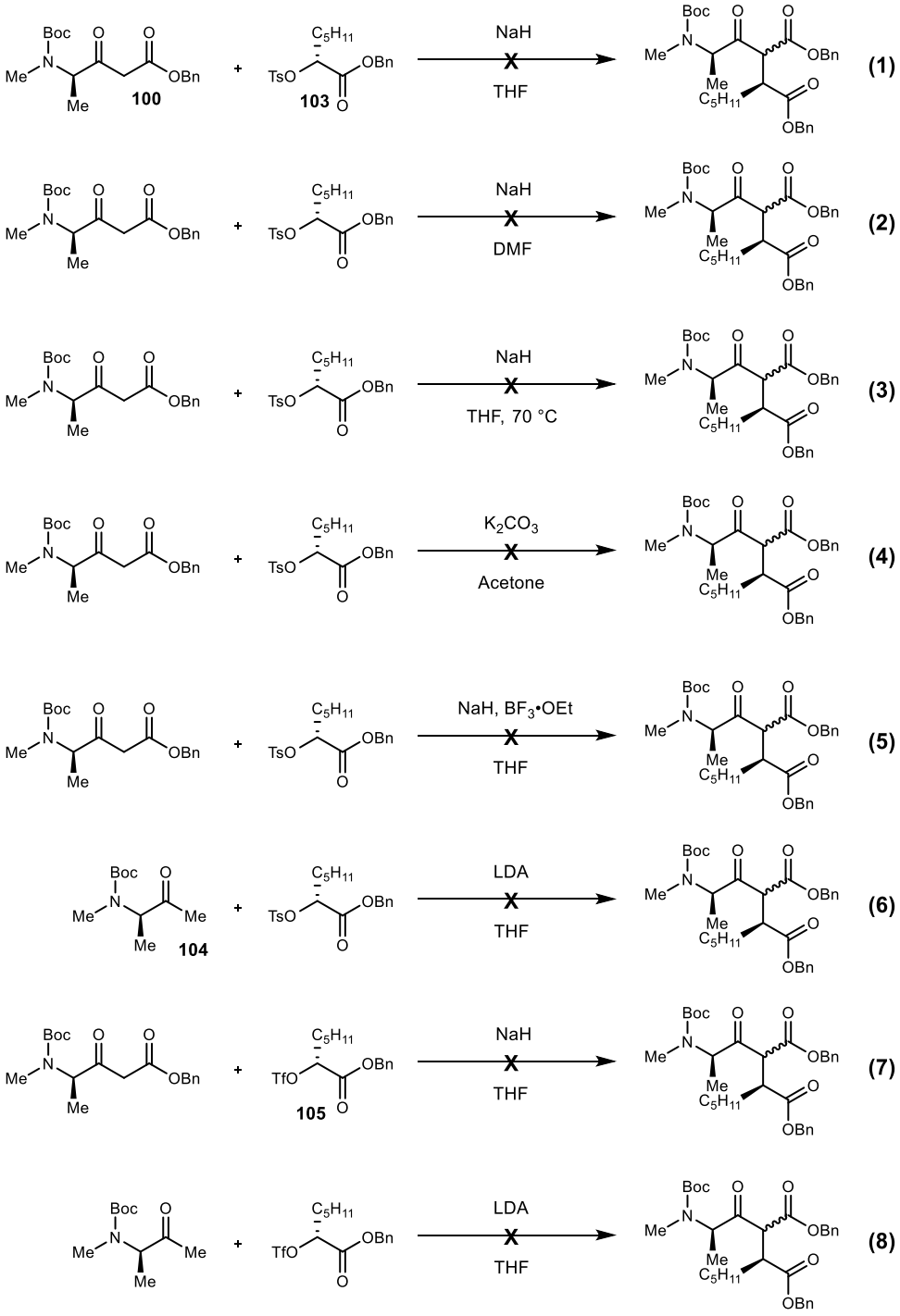

product was observed. While to date, the synthesis of this dipeptide has been unsuccessful, it is still of great interest from an SAR standpoint. Future efforts will focus on the design of an alternative synthetic route to access the desired dipeptide.

2.4.8 Conclusions and Outlook

Thus far, our SAR work has provided insight into the functionality responsible for *ent*-verticilide's activity, but it has also resulted in many more questions. Several important conclusions have been drawn from this body of work:

- we discovered that the 18-membered ring variant is also a potent inhibitor of RyR2-mediated calcium release, generating another hit compound
- other ring sizes synthesized (6,12,30,36) are inactive
- we observe a linear decrease in activity with a decrease in the number of residues *N*-methylated, indicating that full methylation is necessary for potent activity in this series
- all analogues in the natural series (L,D) thus far are inactive
- all homochiral analogues are inactive (D,D) and (L,L)
- the Ala→Gly or Leu analogue is inactive, but Ala→Pro maintains weak activity
- two of the four α-amino ester stereocenters can be removed (Ala→Gly) without loss of activity
- removal of a single α-amino ester stereocenter (Ala→Gly) is detrimental to activity
- we have established that while the alkyl side chains are important for activity, one or two of the four can be altered without significant loss of activity.

Due to the significant amount of effort required to synthesize each SAR analogue of a complex natural product, a focus on mechanism of action work to gain more insight into structural information may yield more fruitful SAR. It might be advantageous to conduct conformational studies of the analogues with the intent to characterize energetically feasible conformations and dynamics. We have initiated studies to do this using contemporary computational methods. This could help to elucidate possible conformational structures of these compounds in solution, which is a closer picture to how they may be interacting with RyR2 than solid state crystal structures for each compound. Further studies that elaborate on the conformational differences between each SAR analogue may provide useful insight into further SAR design. It would also be beneficial to incorporate other in-silico methods, like quantitative structure activity relationship (QSAR) studies. These kinds of studies can be carried out in a variety of different computational programs and in the absence of any structural data. Ultimately, acquisition of structural data via the mechanism of action analogues discussed later, or using cryo-EM methods, would significantly

aid in the SAR studies and development of *ent*-verticilide as an even more potent/selective RyR2 inhibitor, and should be a high priority for future work.

2.5 *ent*-Verticilide Target Engagement and Mechanism of Action Work[214]

The discovery that *ent*-verticilide is the first potent and selective mediator of RyR2-induced calcium flux raises key questions related to its mechanism of action (MOA), selectivity, and complementarity to existing nonspecific small molecule drugs. While SAR studies have aided in the elucidation of the pharmacophore of *ent*-verticilide, we ultimately aimed to uncover more about the mechanism of interaction, as well develop a structure-based approach to advancing this compound. To do so, however, it would be necessary to acquire structural data of *ent*-verticilide interacting with RyR2. Our collaboration with the Knollmann and Cornea labs established *ent*-verticilide's nanomolar activity in [^{3}H]ryanodine binding assays, suggesting a high affinity binding site that could further be explored through monitoring the direct binding of *ent*-verticilide to RyR2. To accomplish this goal, several MOA analogues were proposed, including ent-verticilide fluorescent based probes, and diazirine based probes.

2.5.1 Fluorescent Probes

Our initial interest was in a fluorescent based probe that could be utilized to perform localization studies. It was envisioned that if an analogue of *ent*-verticilide that incorporated an alkyne somewhere in the molecule could be synthesized, we could use a Huisgen cycloaddition reaction to attach a fluorescent label to the molecule. If this analogue maintained activity, it could be used to determine a more specific, subcellular location of *ent*-verticilide in cardiomyocytes. Additionally, it would be possible to employ a fluorescent *ent*-verticilide in fluorescence resonance energy transfer (FRET) experiments with RyR2 regulatory proteins, such as calmodulin or FKBP. The idea behind these experiments would be to employ a fluorescently labeled RyR2 regulatory protein as a donor probe, and a fluorescently labeled *ent*-verticilide as an acceptor probe. Each of these molecules would be incubated in cardiomyocytes, which would then be irradiated with the wavelength of light required to excite the donor probe. If the donor probe and acceptor probe were in close proximity to each other (<10 nm) in the cardiomyocyte, an energy transfer would result in emission of the donor probe. This energy transfer is known as a FRET signal (Figure 78). This

[214] All the biological experiments described in this chapter were carried out by Dr. Dan Blackwell in the Knollmann lab.

would allow us to observe any distance-based energy transfers between *ent*-verticilide and other proteins known to interact with RyR2. If FRET was observed, it would allow us to pinpoint a region of RyR2 in which *ent*-verticilide was interacting with it. This would be more definitive proof that *ent*-verticilide's mechanism of action involves direct interaction with RyR2 and would allow for the determination of a specific segment of the protein to concentrate cryo-EM crystal studies.

Figure 78. FRET experiments in which A is the donor probe (fluorescent RyR2 regulatory protein) and B is the acceptor probe (fluorescent *ent*-verticilide).

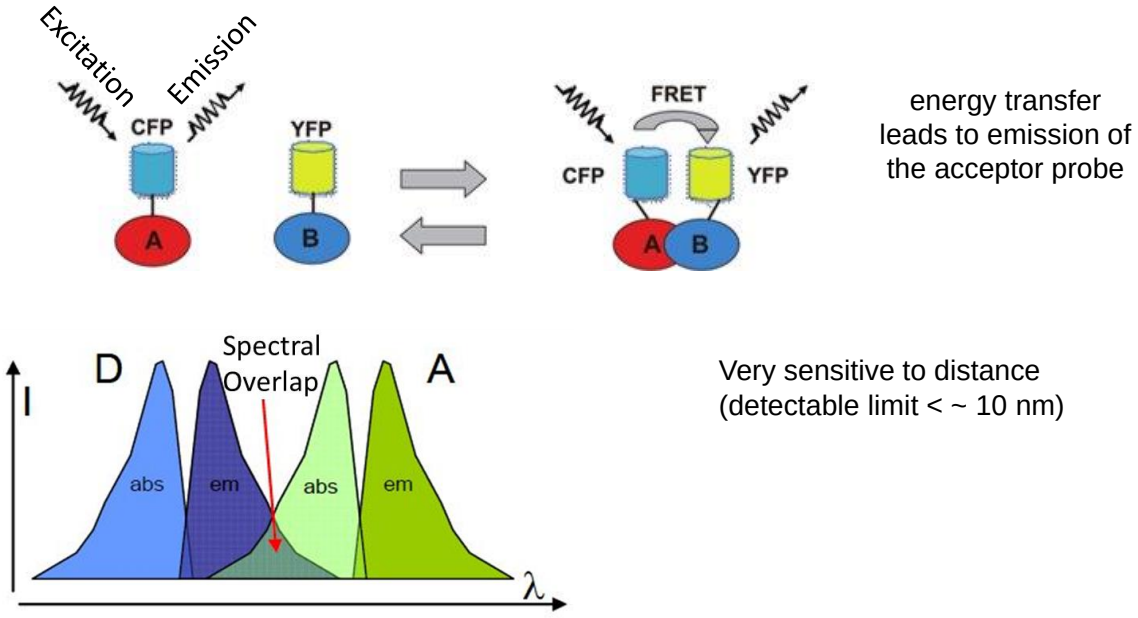

From a synthetic standpoint, it was hypothesized that the hydroxy acid side chains might be a good site for modifications for the MOA analogues. The reasoning here was twofold – first there were four side chains that could be modified, allowing us some flexibility. Second, these side chains were one of the least sterically hindered parts of the molecule, potentially allowing easier access for the conjugation chemistry planned. Using the SAR results as a guide, we synthesized an analogue with a single side chain modified to incorporate an alkyne in 10 steps from hex-5-ynal (see chapter 2.4.1 for synthetic details). Once synthesized, this alkyne analogue was tested in the calcium sparks assay, and it was exciting to find that there was no significant loss in potency. After the *ent*-verticilide alkyne analogue (**36**) was synthesized, the next step was to synthesize the

fluorescent probe. Fluorescein was chosen as the base fluorescent molecule to begin with, as the desired starting material 5-carboxy fluorescein, could be purchased at a reasonable price. The azide

Figure 79. α-Hydroxy acid variation to incorporate an alkyne.

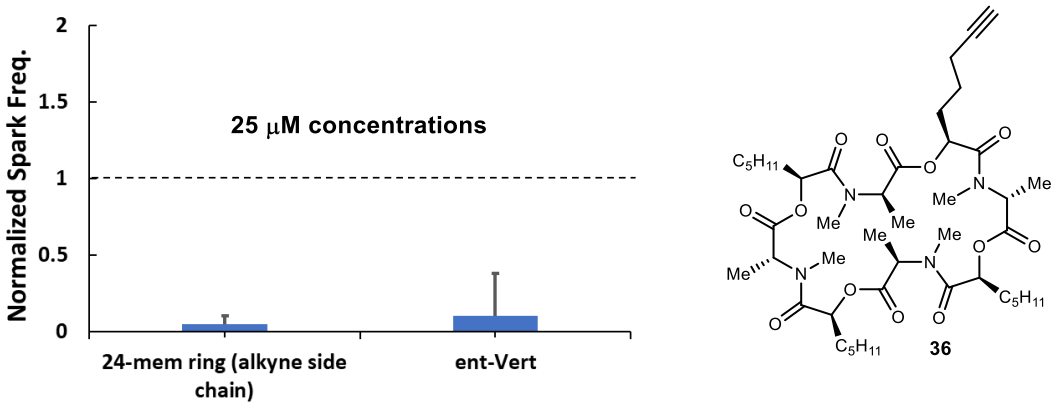

was synthesized in 3 steps from 5-carboxy fluorescein (**106**), beginning with a condensation reaction with 3-chloropropyl amine to afford the amide **107** (Scheme 19).[215] Compound **107** was then subjected to a substitution reaction with sodium azide to provide the desired fluorescein azide derivative (**108**) in a 78% yield. With both precursors in hand, the final Huisgen cycloaddition reaction[216] or "click" reaction was attempted (Scheme 20). Gratifyingly, the desired product formed in the first attempt, in an overall yield of 24%. Optimization of the reaction temperature

Scheme 19. Synthesis of fluorescein azide probe.

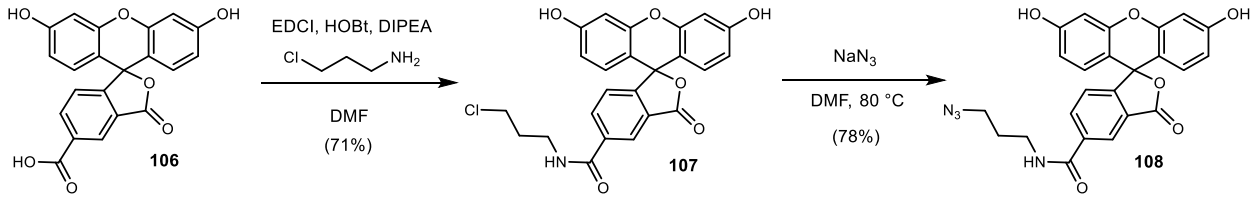

to 50 °C and the time to 4 hours, the overall yield was increased to 90%. We were incredibly excited to find that despite putting a large group on a single side chain, the fluorescein *ent*-verticilide analogue (**109**) was still a potent inhibitor of RyR2 spontaneous calcium release (Figure 80). As a negative control, the fluorescent version of *nat*-verticilide was synthesized as well. As

[215] a) Onizuka, K.; Shibata, A.; Taniguchi, Y.; Sasaki, S. *Chem. Commun.* **2011**, *47*, 5004 b) Aloisi, A.; Franchet, A.; Ferrandon, D.; Bianco, A.; Ménard-Moyon, C. *Bioorg. Med. Chem. Lett.* **2018**, *28*, 2631
[216] Rostovtsev, V. V.; Green, L. G.; Fokin, V. V.; Sharpless, K. B. *Angew. Chem. Int. Ed.* **2002**, *41*, 2596

Scheme 20. Synthesis of fluorescein labeled *ent*-verticilide.

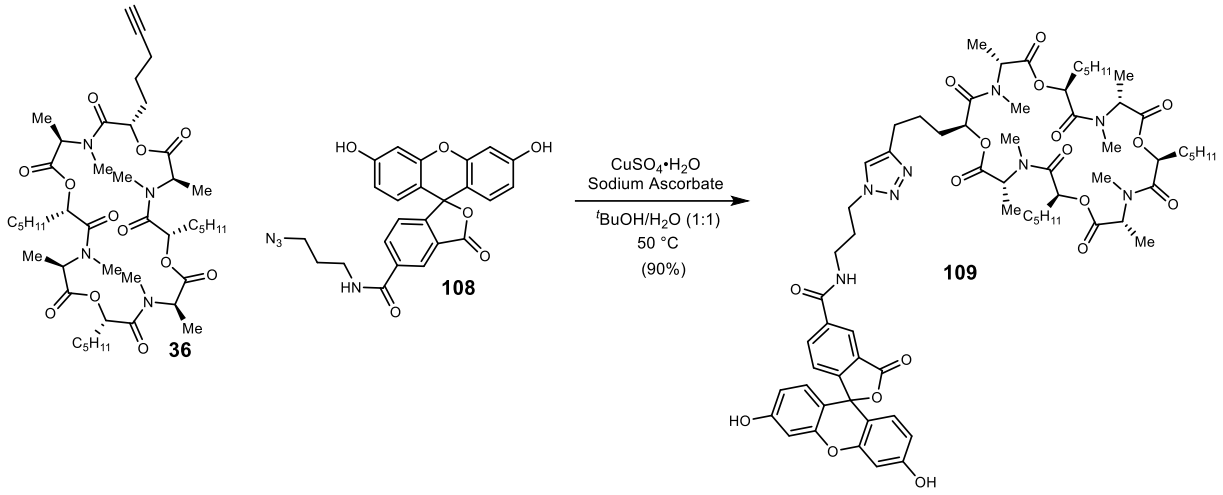

expected, compound ***ent*-109** displayed no reduction in calcium sparks (Figure 80). Once activity of each analogue was confirmed, Dan Blackwell began to perform localization studies. In these initial studies, C57BL/6J murine cardiomyocytes were isolated and incubated for 2 hours with 25 µm 5-carboxy fluorescein (control) or ent-verticilide fluorescein. Fluorescent microscopy pictures,[217] show that neither compound is cell permeable, as after 2 hours of incubation, the cells remained dark (Figure 81). It should be noted that in these images, healthy cardiomyocytes are

Figure 80. *ent*-Verticilide and *nat*-verticilide fluorescein analogues and their calcium sparks data.

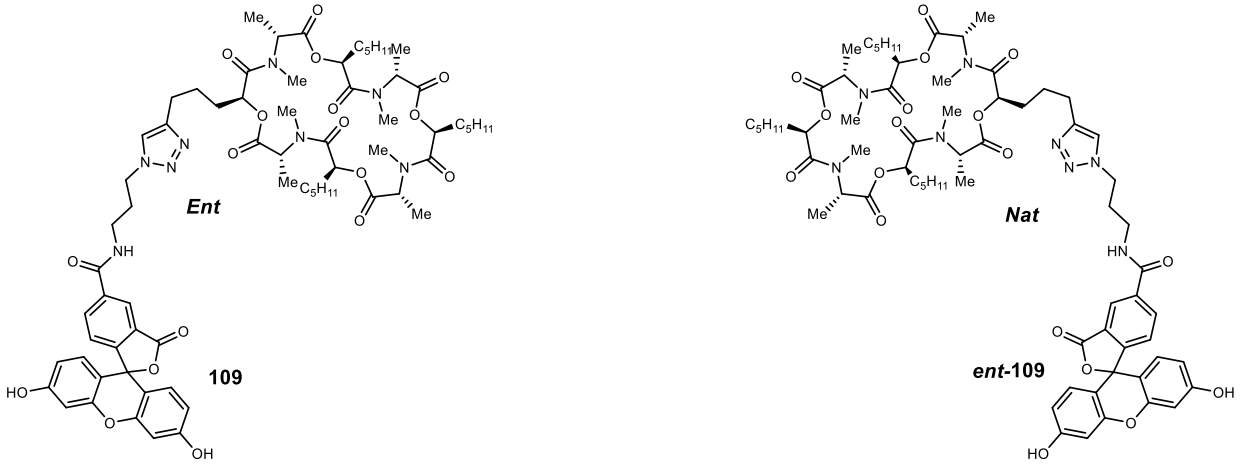

[217] Collected by Dan Blackwell using a Zeiss LSM 880 confocal microscope.

rod-shaped, while the rounded cells are dying. Any measurements made are taken from the healthy cells. Another set of cells were subjected to the saponin protocol used for calcium spark measurements to selectively permeabilize the outer cell membrane, and again incubated with 25 µM of 5-carboxy fluorescein (control) or *ent*-verticilide fluorescein. The *ent*-verticilide fluorescein preferentially localizes in the cell in the permeabilized conditions, as can be seen in Figure 81. This indicates a high affinity binding site within the cell. Currently, it appears that much of the

Figure 81. *ent*-Verticilide and *nat*-verticilide fluorescein analogues and their calcium sparks data.

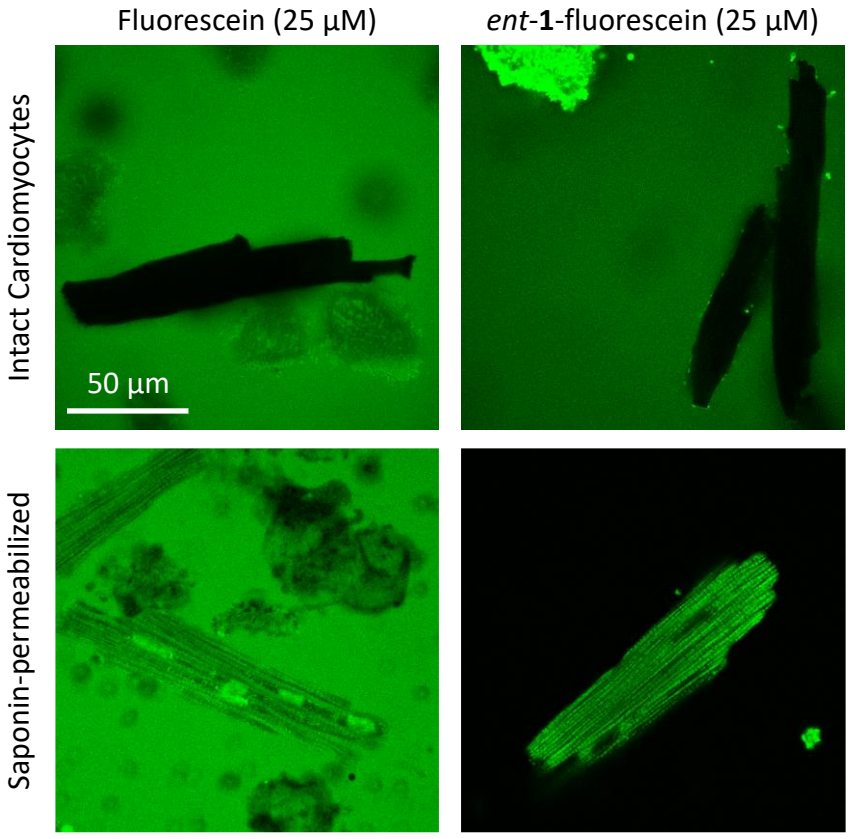

compound is localized at the mitochondria, as the staining pattern looks similar to a mitochondrial stain. However, if binding to the mitochondria is present, it does not appear to disrupt the function, as no effects are observed in mice in the *in vivo* studies.[218] In contrast, the control fluorescein has a diffuse pattern throughout the cell and extracellular membrane. Interestingly, *ent*-verticilide fluorescein does not enter the nucleus, whereas control fluorescein shows bright nuclear

[218] Disruption of mitochondrial function would likely kill the mice.

fluorescence (Figure 81). As an additional comparison, *nat*-verticilide fluorescein was tested. After incubation in permeabilized cardiomyocytes, surprisingly, *nat*-verticilide showed very similar, complete localization inside the cell. These results indicate that the cellular localization visible in these scans is not enantiomeric specific, which likely means there is a significant amount of off-target binding. It is still very plausible that the binding responsible for the activity against RyR mediated spontaneous calcium release is not easily visible with the intense off-target signal. Further studies to lower the concentration, as well as washout experiments could help in elucidating any on-target binding.

Next, we set out to begin FRET work. For these experiments, a new fluorescent analog of *ent*-verticilide was synthesized – Alexa Fluor (AF) 568 labeled. While the fluorescein analogue could be used, Alexa Flour dyes have demonstrated optimal properties for these experiments, specifically in reduced "stickiness" or off-target binding. Furthermore, our collaborator Razvan Cornea, has developed a suite of AF488-labled FKBP and CaM proteins.[219] A requirement of FRET experiments is an overlap in the wavelengths of the donor and acceptor probes. The emission wavelength of the donor probe needs to overlap with the excitation wavelength of the acceptor probe. AF568 labeled ent-verticilide would be the perfect acceptor probe for the already made suite of AF488-labeled FKBP and CaM proteins. The synthesis of this AF568 labeled analogue utilized the same alkyne *ent*-verticilide analogue **36**. This alkyne was subjected to a similar Huisgen cycloaddition reaction, but instead used commercially available AF568 azide as the coupling partner (Scheme 21). While the reaction proceeded smoothly to provide the desired product[220], the workup and purification of this fluorescent analogue proved to be difficult. Upon attempting a similar workup to the fluorescein analogue, it was found that AF568 *ent*-verticilide was water soluble. Fortunately, AF568 *ent*-verticilide was successfully, "salted out" of the water into an organic solvent with the addition of solid sodium chloride. The crude material was then purified via reverse phase preparatory HPLC. The product vials were combined and concentrated to remove any organic solvent, followed by lyophilization. While the proton NMR of the material supported assignment as the desired product, there was not enough material (< 4mg) to obtain a good ^{13}C NMR spectrum. However, 4 mg of product was sufficient for the FRET experiments.

[219] Cornea, R. L.; Nitu, F.; Gruber, S.; Kohler, K.; Satzer, M.; Thomas, D. D.; Fruen, B. R. *Proc. Natl. Acad. Sci. U. S. A.* **2009**, *106*, 6128

[220] Reaction was monitored by MS for both appearance of product mass, and consumption of starting materials.

Due to the expense of the starting AF568 azide ($500 for 5 mg), more material was not synthesized. It is important to note, however, that due to this, a full characterization of this compound (**111**) was not completed. As suspected, when tested in the calcium spark assays, AF568-*ent*-verticilide maintained potent inhibition (Scheme 21).

Scheme 21. Synthesis and calcium spark data for AF568 *ent*-verticilide probe.

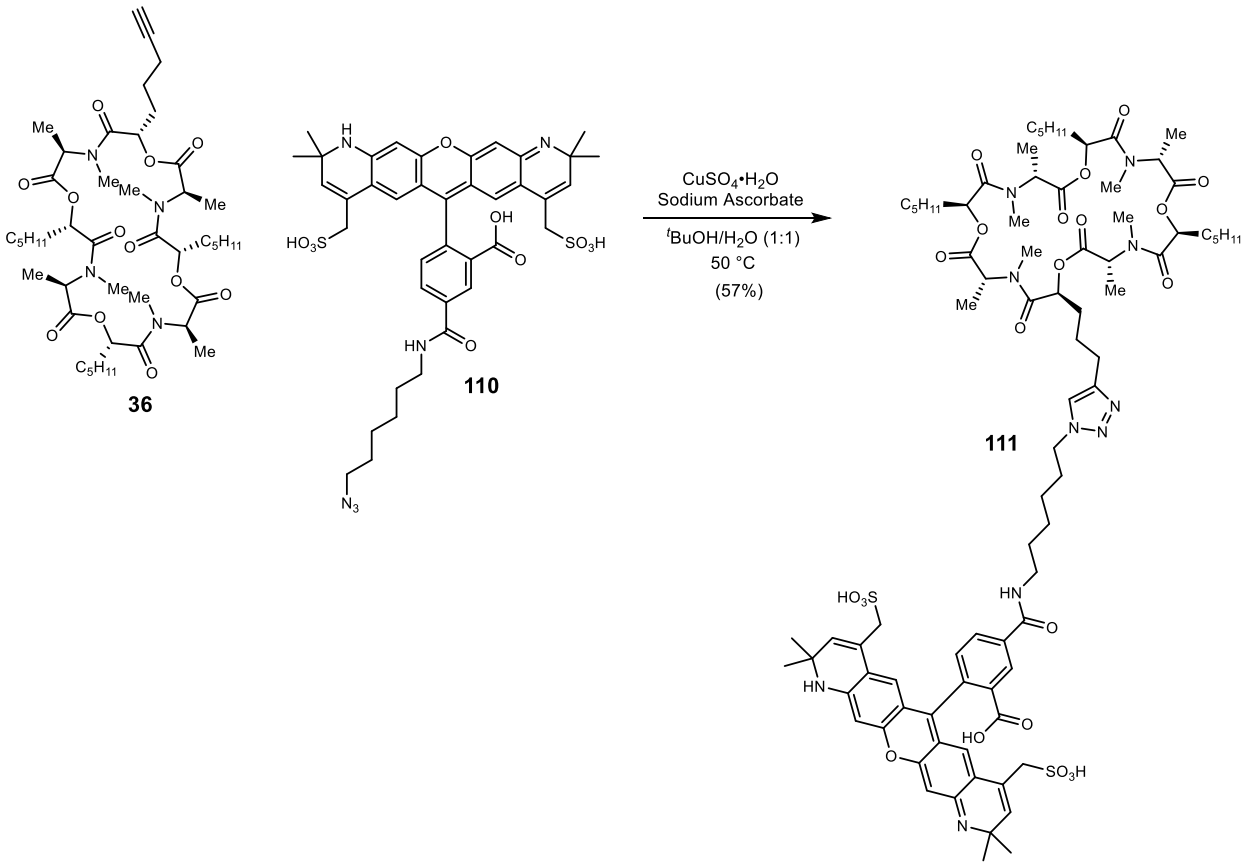

With the desired probe in hand, Dr. Dan Blackwell was able to proceed with the FRET studies.[221] Mouse cardiomyocytes were permeabilized with saponin and incubated with an internal solution designed to facilitate calcium waves.[222] The solution also contained 10 μM of MYK-461[223] to prevent mechanical contractions and movement during imaging, as well as one or two of

[221] All biological experiments and data analysis were carried out by Dr. Dan Blackwell. The following is a summary of the results.
[222] Add it reference here
[223] Myosin ATPase inhibitor.

the probes listed in Table 8.[224] When examined individually, the fluorescently labeled FKBP and CaM probes displayed staining patterns indicative of orientation at the Z-lines (Figure 82 and Table 8, entries 1-3). RyR2 is localized at the Z-lines in cardiomyocytes, so this staining pattern is

Table 8. Initial FRET experiments along with controls of each fluorescent dye.

Entry	Fluorescent Tag # 1	Fluorescent Tag # 2
1	AF488-85C-FKBP12.6	-
2	-	AF568-49-FKBP12.6
3	-	AF568-34-CaM
4	fluorescein e*nt*-verticilide	-
5	-	AF568 e*nt*-verticilide
6	AF488-85C-FKBP12.6	AF568-34-CaM
7	fluorescein-*ent*-verticilide	AF568-49-FKBP12.6
8	AF488-85C-FKBP12.6	AF568-*ent*-verticilide

what would be expected for RyR2 regulatory proteins, or any other molecules interacting with RyR2. Both *ent*-verticilide fluorescent dyes again displayed apparent mitochondrial localization (Table 8, entries 4 and 5). The confocal microscope images of these are shown in Figure 82. A control experiment was conducted in which AF488 FKBP was used as the donor probe and AF568 CaM was used as the acceptor probe (Table 8, entry 6). As expected, FRET was observed between

Figure 82. Confocal microscopy images of fluorescently labeled FKBP 12.6, CaM, and *ent*-verticilide.

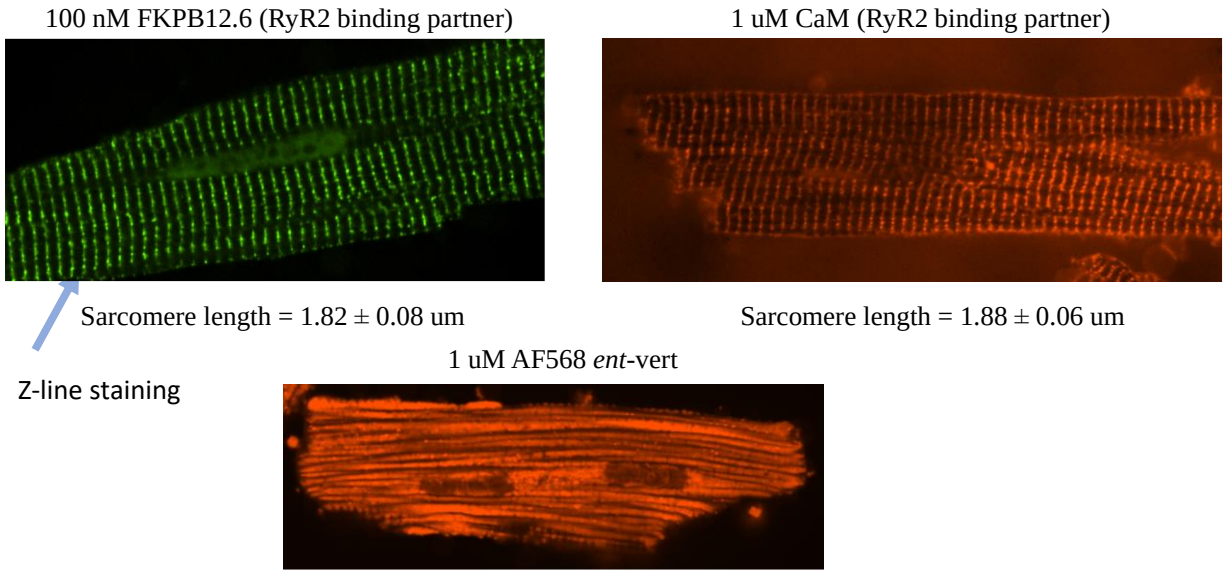

[224] Cells were incubated for 20 minutes before imaging.

Figure 83. Table 8, entry 6; FRET assay between donor AF488-85C-FKBP12.6 and acceptor AF568-34-CaM.

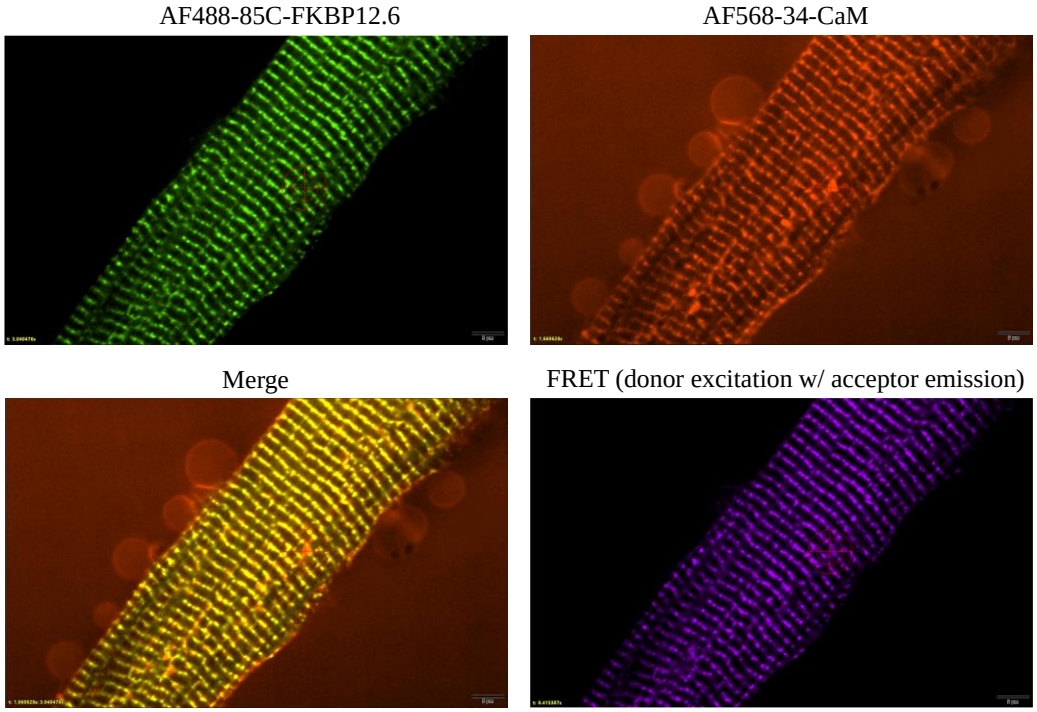

the two (Figure 83). Next, experiments with the fluorescently labeled *ent*-verticilide analogues were conducted (Table 8, entries 7 and 8). First fluorescein-*ent*-verticilide was used as a donor probe with AF568-49-FKBP12.6 as an acceptor probe. Initial results do not appear to show a FRET signal between the two (Figure 84). Alternatively, an experiment was conducted with AF488-85C-FKBP12.6 as a donor probe and AF568-*ent*-verticilide as an acceptor probe. Again, however, FRET was not observed (Figure 85). While disappointing, there was still hope as it was hypothesized that the off-target labeling was significant enough that it was preventing clean visualization of a FRET signal. To circumvent this issue, a series of competition experiments were proposed, with the ultimate goal to "wash out" the off-target bound material. In these experiments, 1 µM AF568 *ent*-verticilide was incubated in permeabilized cardiomyocytes for 10 minutes. Then, 6 µM unlabeled *ent*-verticilide was introduced. The initial data demonstrated that while *ent*-verticilide localization at the mitochondria was still prevalent, striated-like patterns in the background appeared after longer incubation times (Figure 86, 30 minutes after competition). These striated-patterns appear to be more in line with staining at the Z-lines and are promising

Figure 84. Table 8, entry 7; FRET assay between donor fluorescein-*ent*-verticilide and acceptor AF568-49-FKBP12.6.

Fluorescein-ent-verticilide

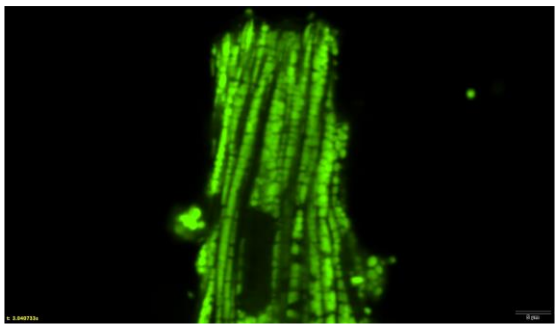

AF568-49-FKBP12.6

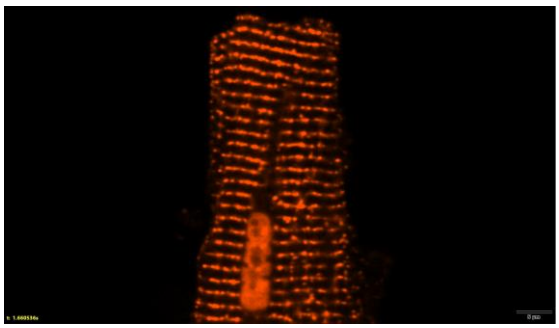

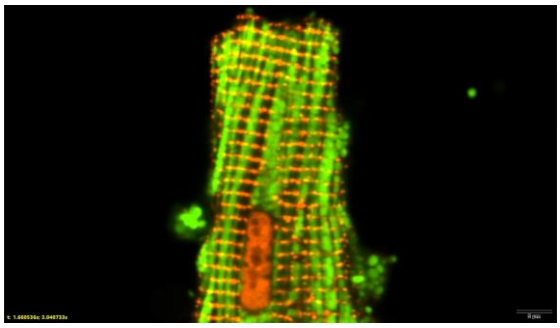

Merge

Figure 85. Table 8, entry 7; FRET assay between donor fluorescein-*ent*-verticilide and acceptor AF568-49-FKBP12.6.

AF488-85C-FKBP12.6

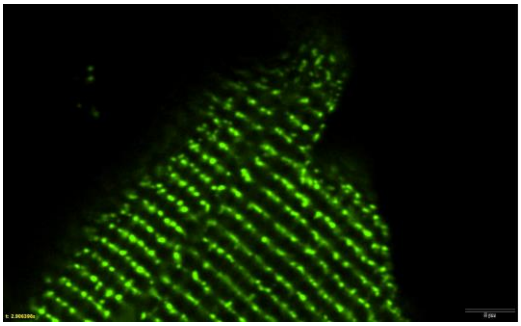

AF568-ent-verticilide

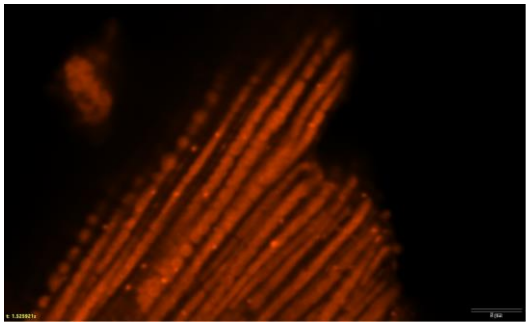

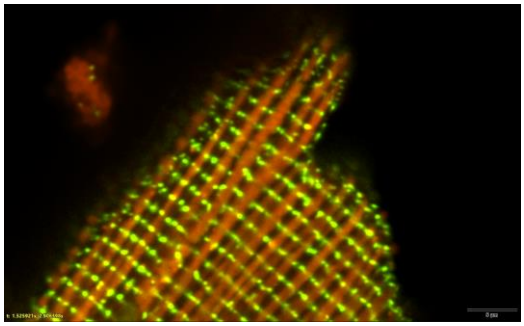

Merge

Figure 86. *In vitro* cardiomyocyte labeling- AF569-*ent*-vert (1 uM) & competition w/ unlabeled ent-vert (6 uM).

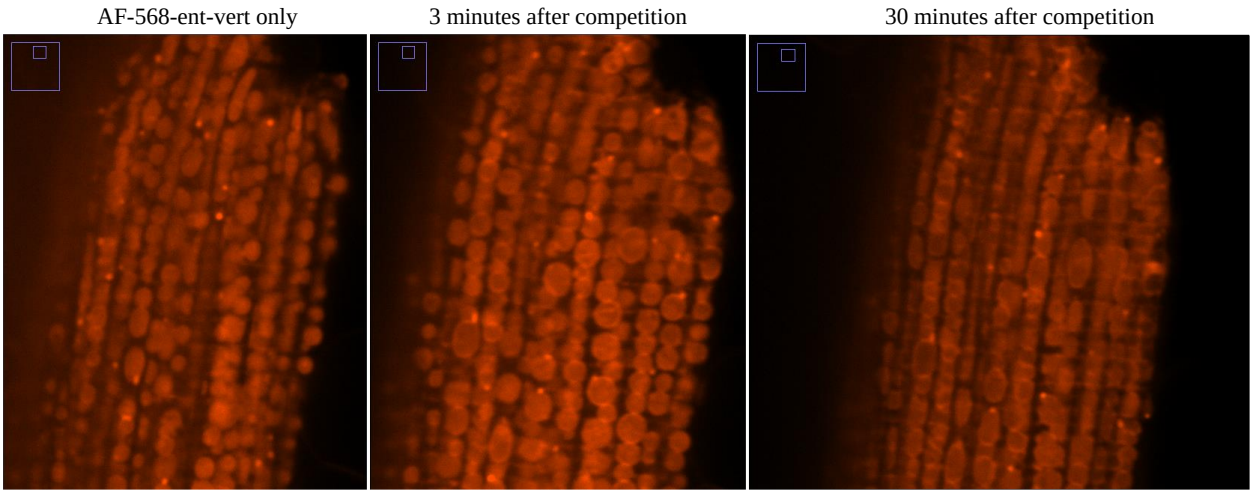

preliminary data. Future effort with these FRET experiments will be focused on additional competition studies to further support these preliminary results, as well as new experiments utilizing other FKBP and CaM acceptor and donor probes. It is estimated that the Cornea group's suite of labeled FKBP and CaM probes covers 97% of RyR residues.[225] Therefore, the quest for potential FRET still holds promise and will continue.

2.5.2 Diazirine Based Probes

The concept of using photoaffinity labeling to study interactions between ligands and macromolecules was first introduced in the early 1960's by Frank Westheimer.[226] Since then, it has become a fundamental tool in understanding pathological processes. The basic conceptual idea involves a ligand that is covalently bound to a photolabile group, which upon irradiation with a specific wavelength of UV light, generates a reactive species. This reactive species will then form a covalent bond with whatever it is near, presumably its target. There are several requirements for a good photolabile group. First and foremost, the addition of a photolabile group must not significantly alter the biological activity or selectivity of the ligand. The best way to address this, is often to use the smallest possible photolabile group. Second, the photolabile group must require

[225] This data is not yet published by the Cornea group, so figures and further elaboration are not included here.
[226] Singh, A.; Thornton, E. R.; Westheimer, F. H. *J. Biol. Chem.* **1962**, *237*, PC3006

only a short period of irradiation. Long irradiation periods present a significant risk of non-specific labeling.[227] Third, the formed reactive species needs to find a balance between reactivity and stability, to avoid intramolecular rearrangements, non-specific labeling, and poor labeling yields. Finally, the wavelength need for irradiation should be compatible with biological molecules.

There are three commonly used photolabile groups: benzophenones, arylazides, and diazirines (Figure 87). While arylazides are perhaps the easiest to prepare, they require a short excitation wavelength, which can often be damaging to biological systems.[228] Furthermore, the excitation step, meant to generate a reactive carbene, often results in a substantial amount of

Figure 87. Common photoaffinity labels.

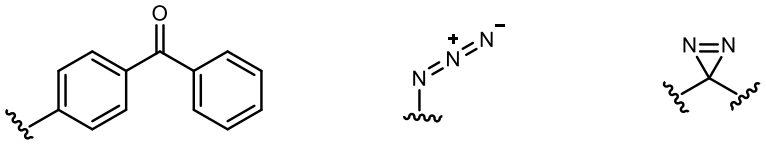

nitrene by-products and therefore, decreased labeling yields.[229] Overall, these limitations have hindered the widespread use of arylazides. Benzophenones on the other hand, are significantly more stable. However, this translates to longer periods of irradiation, and substantial amounts of non-specific labeling.[227] Additionally, their large size often results in a significant change of activity of the molecule. Over the last few decades, diazirine photolabile groups have been gaining an increasing amount of attention, particularly due to their small size. Diazirines are irradiated with UV light to form a reactive carbene that rapidly forms a covalent C-C, C-H, C-O, C-X bond with the nearest target. The formed carbenes are incredibly reactive (existing for only picoseconds),[230] and as such, most will be quenched by water. This generally results in less than 10% labeling yields, but also significantly reduces off-target labeling.[231] Diazirines are stabile at room temperature and under ambient light, as well as to many nucleophiles, acidic, and basic conditions. The required wavelength for irradiation is 350-355 nm, which is compatible with biological systems. Although alkyl diazirines are favored for their small size, trifluoromethylaryl diazirines

[227] Prestwich, G. D.; Dormán, G.; Elliott, J. T.; Marecak, D. M.; Chaudhary, A. *Photochem. Photobiol.* **1997**, *65*, 222
[228] Dubinsky, L.; Krom, B. P.; Meijler, M. M. *Bioorg. Med. Chem.* **2012**, *20*, 554
[229] Platz, M. S. *Acc. Chem. Res.* **1995**, *28*, 487
[230] Hatanaka, Y. *Chem Pharm Bull (Tokyo)* **2015**, *63*, 1
[231] A. Fleming, S. *Tetrahedron* **1995**, *51*, 12479

are often used to overcome potential diazo compound formation, and other undesirable, internal rearrangements.[232]

When deciding what photoaffinity label to incorporate on *ent*-verticilide, we ultimately landed on diazirines for the aforementioned benefits. Specifically, based off the initial SAR studies, it was anticipated that the alkyl side chains of *ent*-verticilide would be amendable to incorporation of a small, alkyl diazirine. While it was noted that these alkyl derivatives could lead to unfavorable rearrangement products, it was hypothesized that an aryl diazirine would be more likely to disrupt the activity of *ent*-verticilide. Furthermore, we aimed to incorporate an alkyne on the molecule as well, to allow for attachment of either a fluorescent probe or to use for affinity enrichment during a purification stage (Figure 88). This type of bifunctional probe would help to eliminate concerns of poor affinity.[233]

Figure 88. Diazirine analogue for receptor labeling.

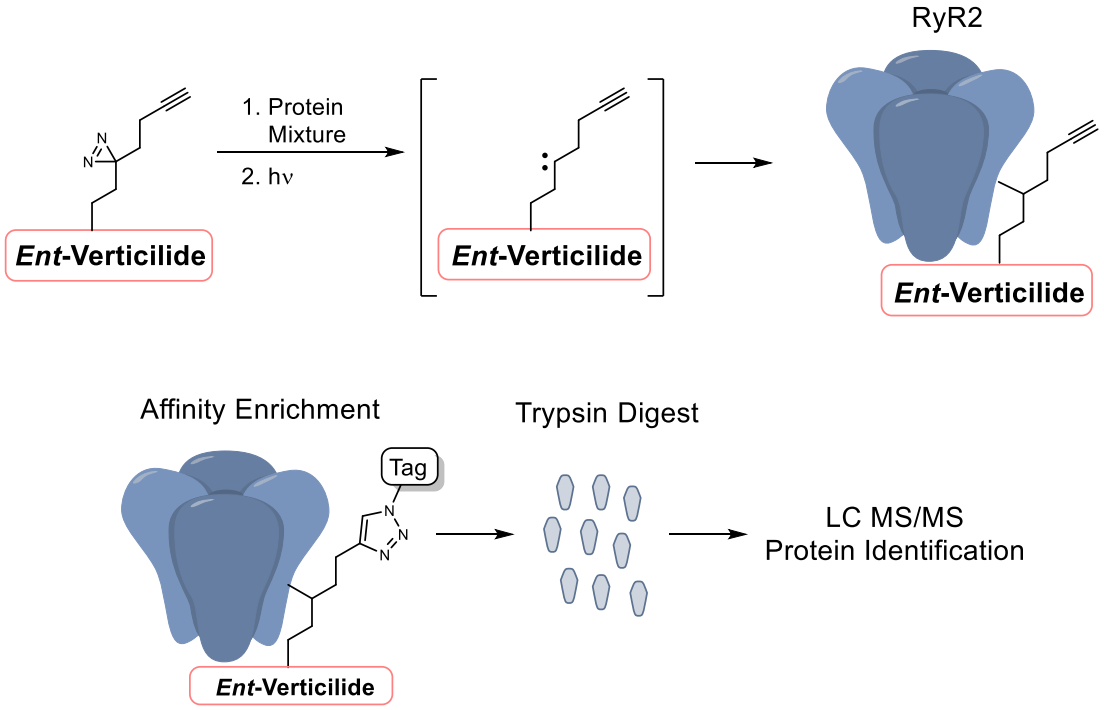

[232] Brunner, J.; Senn, H.; Richards, F. M. *J. Biol. Chem.* **1980**, *255*, 3313
[233] Li, Z.; Hao, P.; Li, L.; Tan, C. Y. J.; Cheng, X.; Chen, G. Y. J.; Sze, S. K.; Shen, H.-M.; Yao, S. Q. *Angew. Chem. Int. Ed.* **2013**, *52*, 8551

2.5.3 Optimization of Diazirine Formation and Generation 1.0 Diazirine Synthesis

After settling on a diazirine photo-affinity label, we designed an *ent*-verticilide diazirine analogue for synthesis. When considering how to attach the diazirine, several important parameters were taken into consideration. First, the conditions required to install the diazirine itself were relatively harsh and involved refluxing in ammonia. Given the previous lability seen with the ester bonds in depsipeptides, it was unlikely that installation on a late stage depsipeptide would be possible. This left two options: install the diazirine early in the synthesis or install the diazirine via a "linker unit" that could be attached at a late stage under mild conditions.

To begin, it was necessary to optimize the formation of the diazirine itself. There are a variety of different procedures reported in the literature for diazirine formation.[234,235] However, the most-employed approach is a three-step route (Scheme 22) in which a ketone is treated with liquid

Scheme 22. General route for diazirine synthesis.

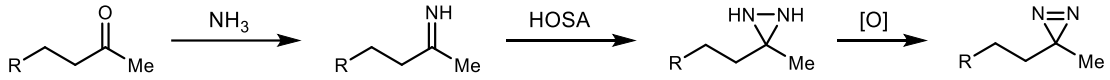

Figure 89. First-proposed diazirine analogue for mapping by cross-linking.

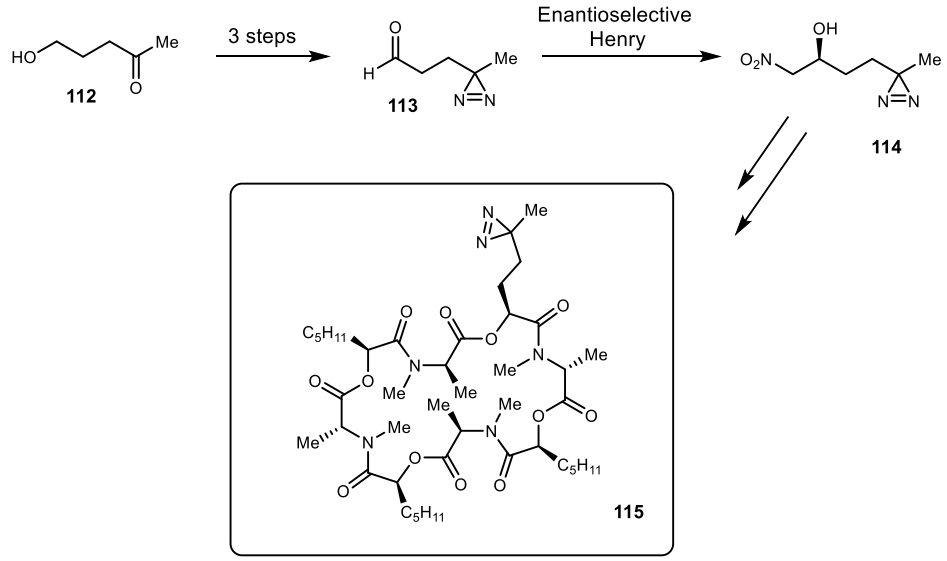

[234] Hill, J. R.; Robertson, A. A. B. *J. Med. Chem.* **2018**, *61*, 6945
[235] Dubinsky, L.; Krom, B. P.; Meijler, M. M. *Bioorg. Med. Chem.* **2012**, *20*, 554

ammonia to form an imine, followed by reaction with hydroxylamine-*O*-sulfonic acid (HOSA) to form the diaziridine intermediate.[236] This diaziridine can then be easily oxidized to the corresponding diazirine with a variety of different reagents.[237] This method was chosen to synthesize the desired diazirine. 4-Hydroxybutan-2-one (**112**) was initially proposed as a starting ketone, in hopes that after diazirine formation, the terminal alcohol could be oxidized to the aldehyde (**113**), and then subjected to enantioselective Henry conditions (Figure 89). If this reaction sequence was successful, it would allow for the incorporation of the diazirine early in the synthesis, as well as the use of chemistry we had already developed. However, our initial attempts to form the diazirine with 4-hydroxybutan-2-one were unsuccessful, despite carefully following the literature procedures.[233] NMR spectra of the crude reaction mixtures displayed no signs of product, and consisted either of starting material, or what appeared to be the oxime (Scheme 23, **117**). Presumably, this arises from condensation of HOSA onto the ketone instead of ammonia, which upon workup would hydrolyze to generate the observed oxime. To mitigate this, a variety

Scheme 23. Attempted formation of diazirine.

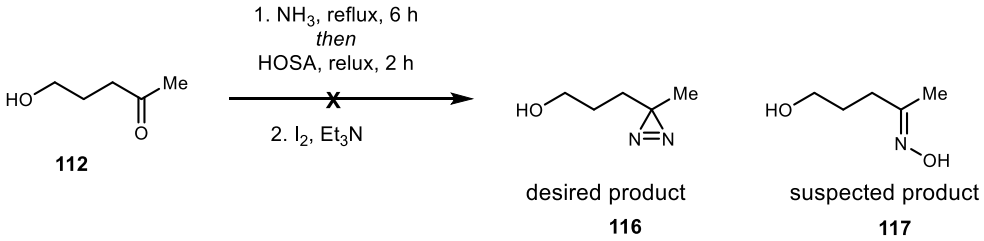

of different conditions were attempted. First, portion-wise addition of solid HOSA over 30 min was explored (Scheme 24, eq 1). However, under these reaction conditions, oxime was still the observed product. Next, HOSA was again added portion-wise over 30 min, but in a solution of MeOH instead (Scheme 24, eq 2). We were incredibly excited to find that under these conditions, while oxime was still formed, the desired diazirine was also formed in about a 20% yield.[238] The use of drying reagents was also explored to help promote the formation of imine with ammonia. While 4 Å MS increased the ratio of desired diazirine to oxime to 1:1 (Scheme 24, eq 3), the

[236] Church, R. F. R.; Kende, A. S.; Weiss, M. J. *J. Am. Chem. Soc.* **1965**, *87*, 2665
[237] Church, R. F. R.; Weiss, M. J. *J. Org. Chem.* **1970**, *35*, 2465
[238] Based on NMR yield calculated using an internal standard, not isolated yield.

addition of sodium sulfate gave only the desired diazirine (Scheme 24, eq 4) in a 50% overall isolated yield. Several repetitions reproducibly succeeded with yields ranging from 45-65%.

Scheme 24. Reaction condition modifications for diazirine formation.

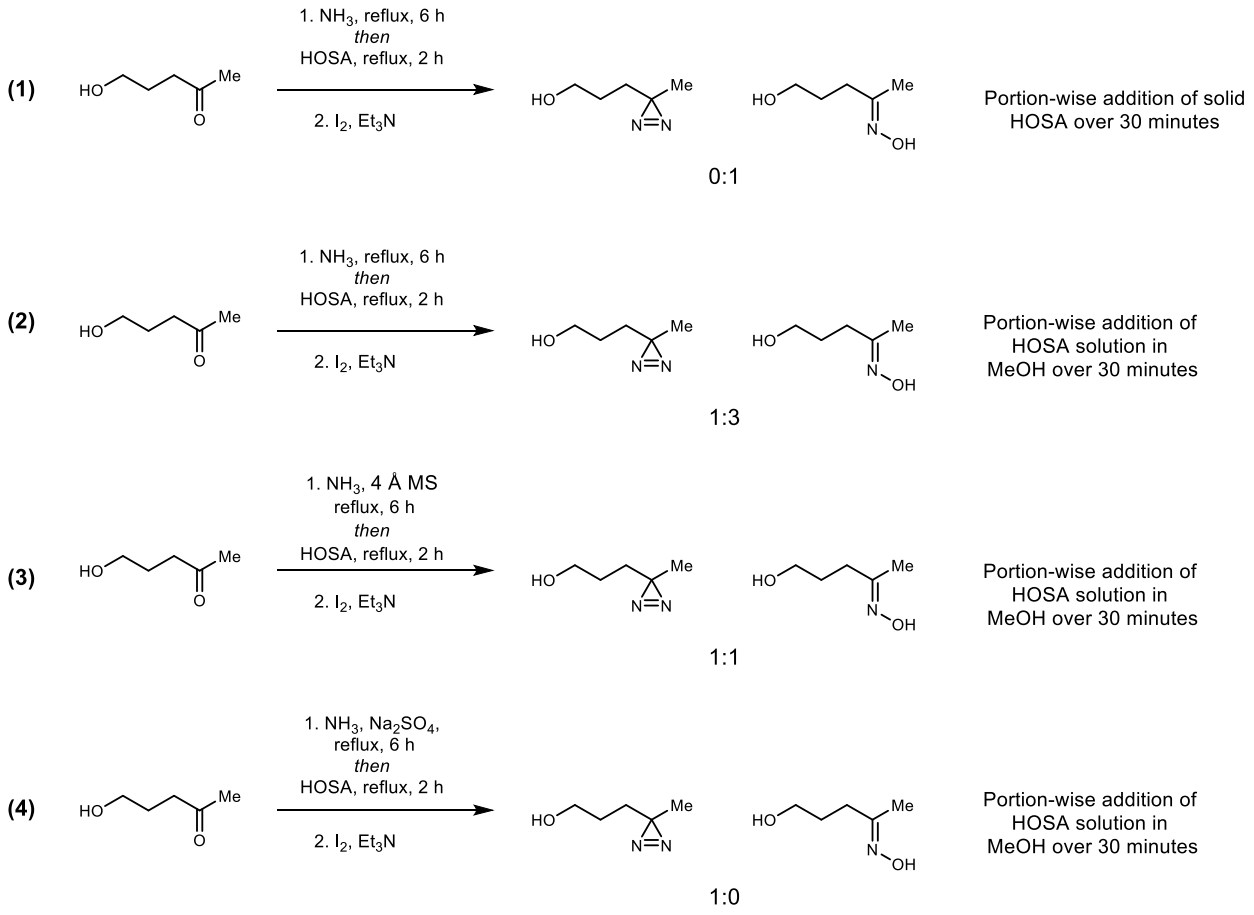

Once the construction of the diazirine was complete, the material was subjected to oxidation with IBX to form the aldehyde. This diazirine aldehyde was then subjected to enantioselective Henry conditions to generate the enantioenriched α-hydroxy nitroalkane (Scheme 25). However, despite several different attempts, no product was formed. This is believed to be due to rapid decomposition of the starting diazirine aldehyde, as later it was found that this compound was unstable upon sitting. Due to the apparent difficulties of this route, the idea of installing a diazirine late stage via a linker unit was reevaluated.

Many mild approaches could be taken to attach the linker and *ent*-verticilide analogue, including amidations, esterifications, substitution-based approaches, or carbon-carbon bond

Scheme 25. Attempted Henry reaction conditions.

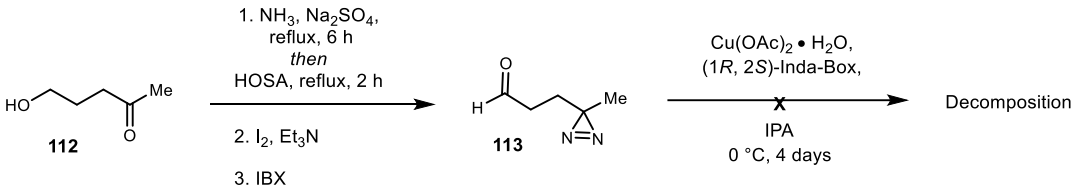

forming reactions (Figure 90). Any conditions in which a nucleophilic species was attached to the macrocycle was avoided, due to concerns of potential intramolecular reactions that may cleave labile ester bonds within the depsipeptide backbone. An approach such as a Grubbs metathesis reaction was also avoided, due to the ultimate desire to incorporate an alkyne in the molecule, as chemoselectivity would likely be an issue. Ultimately, we opted for an esterification approach, in which the electrophilic species, the carboxylic acid, was incorporated onto *ent*-verticilide, and the nucleophilic species would be a 4-hydroxy diazirine.

Figure 90. Potential methods to attach a diazirine linker and diazirine generation 1.0.

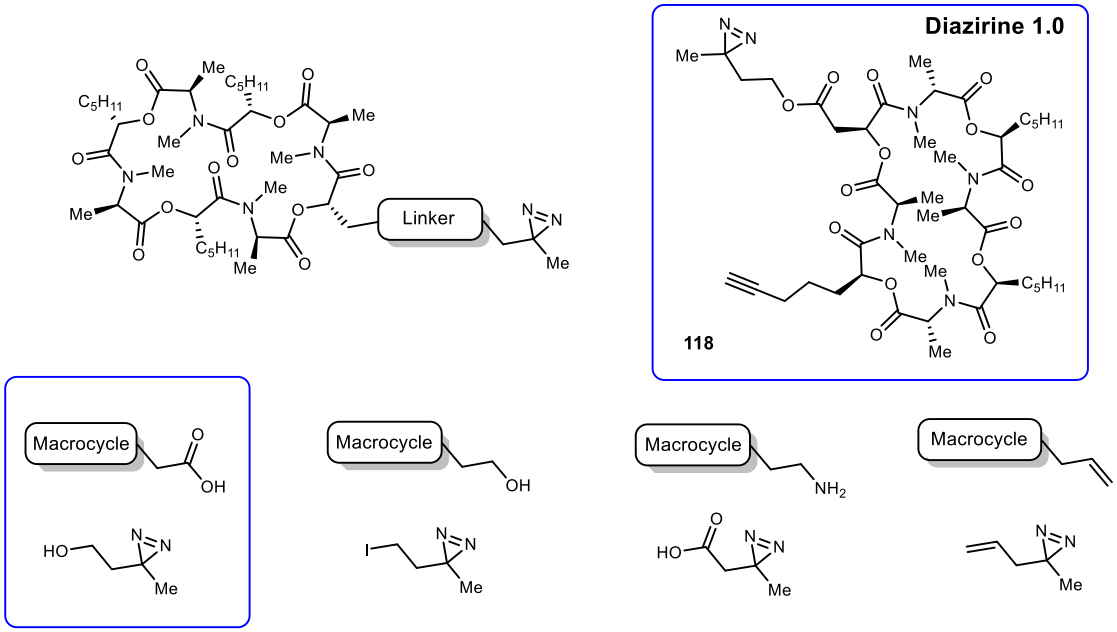

After optimization of the diazirine formation, the next synthetic focus was a carboxylic acid analogue of *ent*-verticilide. From a retrosynthesis standpoint, incorporating a carboxylic acid on the α-hydroxy acid side chain would allow for the use of chiral pool starting material. The synthesis

began with commercially available malic acid, which was protected as mono-PMB ester **120** (Scheme 26). An esterification was then employed to incorporate the diazirine side chain, albeit in a low yield of 31%. While the proposed route would allow for later stage introduction of the diazirine via an esterification, this would require additional steps to add and remove a protecting group from the carboxylic acid. As the remaining reaction conditions were all mild deprotections and peptide coupling reactions, it was anticipated that the diazirine might be stable throughout. Diazirine hydroxy acid **121** was then subjected to another esterification reaction with Boc-*N*-Me-D-Ala to form a didepsipeptide in high yield. After a Boc deprotection, diazirine didepsipeptide **123** coupling with hexadepsipeptide **106** (synthesized via the route discussed in Chapter 2.4.1) was attempted. Using our developed coupling conditions with PyBrop, Hunig's base, and dichloromethane, no product formation was detected. A variety of optimizations were attempted,

Scheme 26. Diazirine generation 1.0 synthesis.

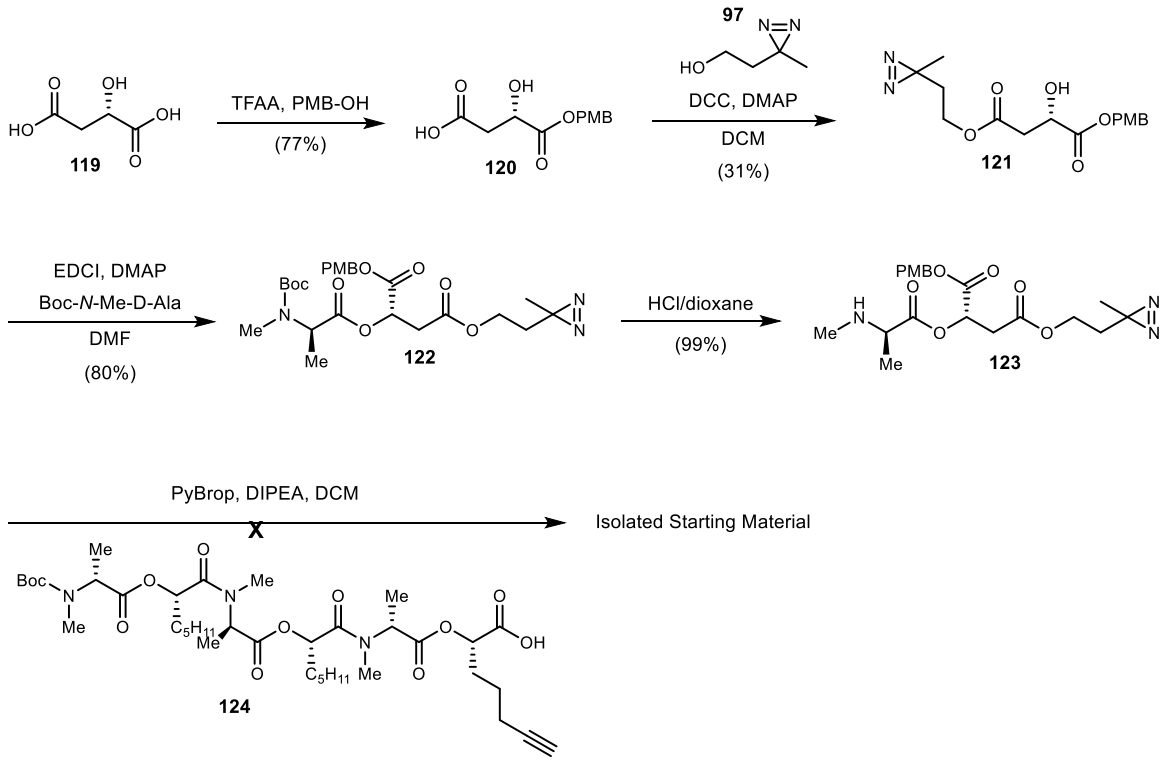

including different solvent systems, coupling reagents, temperatures, and pre-activation of the carboxylic acid (Table 9). However, all reactions returned starting material. It was hypothesized that some sort of hydrogen bonding or steric interaction was occurring with the presence of both a

diazirine and alkyne, preventing the coupling from occurring. To test this hypothesis, the diazirine didepsipeptide was instead subjected to a coupling with a tetradepsipeptide[239] lacking an alkyne (Scheme 27). Without the alkyne present, the coupling proceeded in a 60% yield, under our standard coupling conditions. As a proof of concept, hexadepsipeptide **124** was globally deprotected, and cyclized to afford the 18-membered ring diazirine analogue (**128**) in a 26% yield. Successful incorporation of a diazirine into the side chain of an 18-membered ring analogue left us assured that this would be possible with our 24-membered ring. This indeed proved to be the case, as we were able to use the same route to synthesize the 24-membered ring (**129**). However, the ability to also incorporate an alkyne into the molecule would be important for photoaffinity labeling studies, and still a large interest. To do so, we went back to the drawing board on a synthesis plan.

Table 9. Coupling condition optimization.

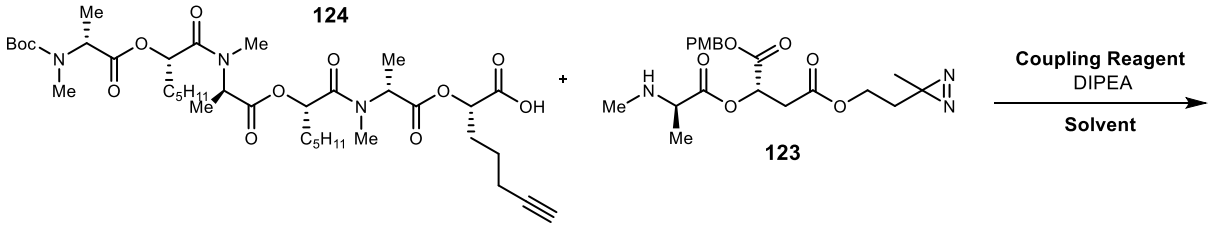

Experiment	Solvent	Coupling Reagent	Temperature	Pre-activated?	Yield
1	DCM	PyBrop	0 °C to RT	No	0 %
2	DMF	PyBOP	0 °C to RT	No	0 %
3	DMF	HATU	0 °C to RT	No	0 %
4	DMF	EDCI	0 °C to RT	No	0 %
5	DMF	DEPBT	0 °C to RT	No	0 %
6	DMF	PyBrop	0 °C to RT	Yes	0 %
7	DMF	HATU	0 °C to RT	Yes	0 %
8	DMF	PyBrop	0 °C to 50 °C	No	0 %
9	DMF	PyBrop	0 °C to 50 °C	Yes	0 %

[239] A tetradepsipeptide was chosen as the coupling partner as this material was already synthesized and available in large quantities.

Scheme 27. Synthesis of 18- and 24-membered rings incorporating a diazirine into the α-hydroxy acid side chain.

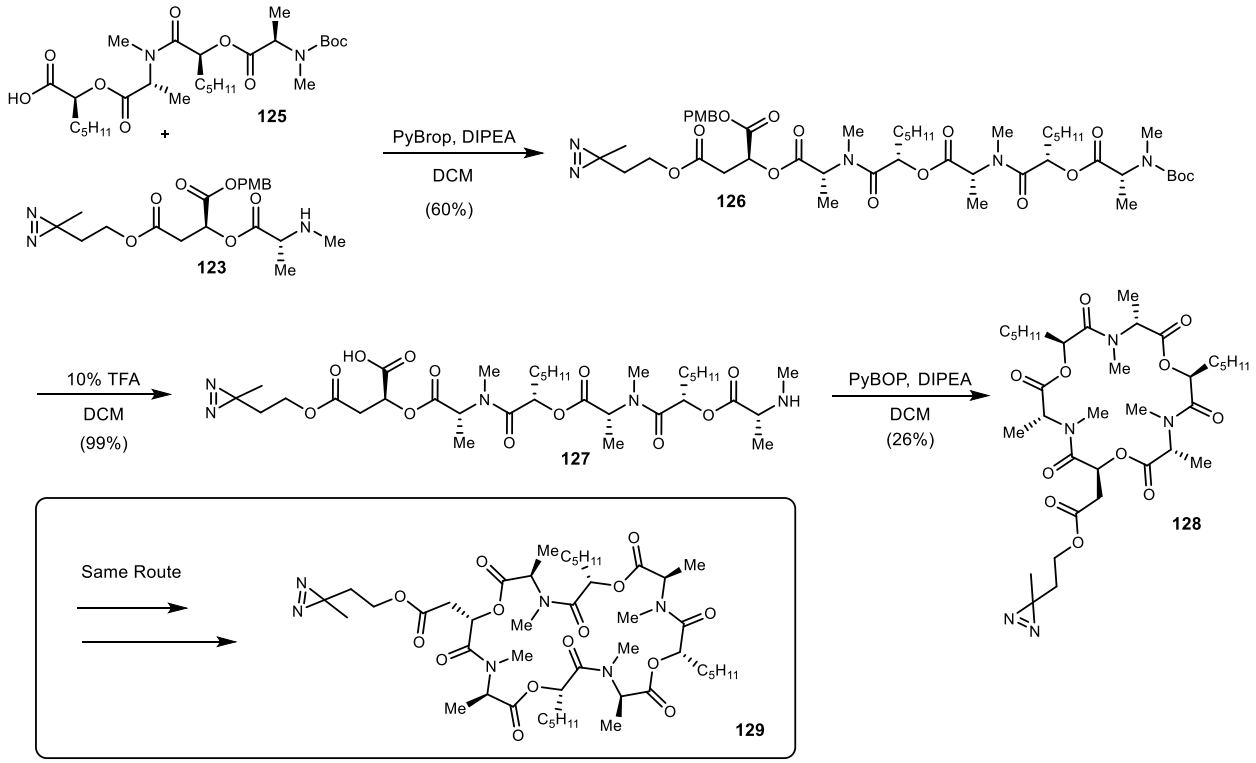

2.5.4 Generation 2.0 Diazirine Synthesis

Since the synthesis of the carboxylic acid variant of *ent*-verticilide had already been carried out and optimized, options to incorporate an alkyne into the diazirine linker unit were explored. Following the work of Li and coworkers,[240] we set out to synthesize a small linker unit containing both a diazirine and alkyne. To begin, ethyl acetoacetate (**130**) was alkylated using LDA and propargyl bromine to incorporate the alkyne (Scheme 28). The ketone was then protected as a ketal to allow for reduction of the ester to the alcohol. Deprotection back to the ketone, followed by our optimized diazirine-forming conditions, afforded linker **135**. It should be noted that several modifications of the reported literature procedure were required. This included the alkylation step, reduction step, and diazirine formation. When first carrying out the alkylation with propargyl bromide, only very low yields were observed. It was discovered that to obtain better conversion,

[240] Li, Z.; Hao, P.; Li, L.; Tan, C. Y. J.; Cheng, X.; Chen, G. Y. J.; Sze, S. K.; Shen, H.-M.; Yao, S. Q. *Angew. Chem. Int. Ed.* **2013**, *52*, 8551

it was necessary to add LiCl[241] and utilize freshly distilled propargyl bromide. When attempting the reduction of the ester with LAH, we were unable to get any conversion. At the time, it was suspected that the lab had several "bad" sources of LAH in which an oxidized coating had formed on the outer layer. However, the successful use of the same batches of LAH in other reactions argued against this hypothesis. For reasons still unknown, we were not able to replicate those results. The reduction, however, proceeded smoothly to **133** using Red-Al, and this protocol was used instead. Finally, the formation of the diazirine proceeded well using our optimized conditions (see chapter 2.5.3 discussion). This robust synthetic route was amenable to scale-up and allowed for the synthesis of over 2 grams of the linker unit.

Scheme 28. Diazirine alkyne linker synthesis.

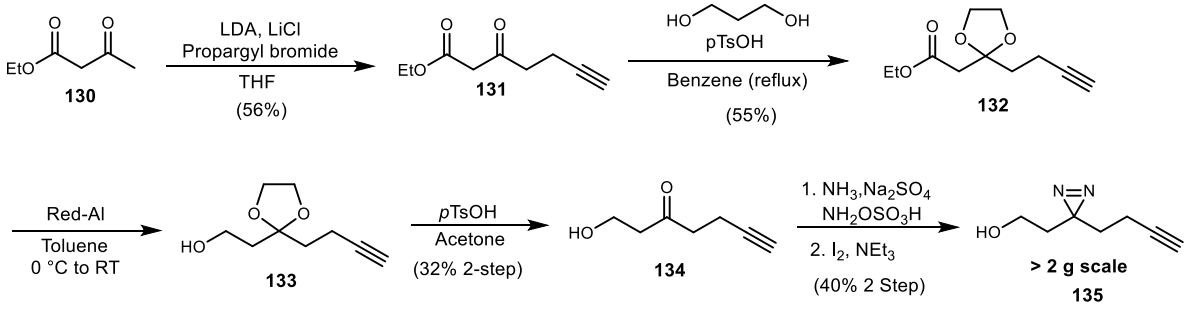

Following the successful synthesis of the linker unit, we planned an esterification route. In this variant of the diazirine, it was opted to attempt the esterification to combine the linker and *ent*-verticilide analogue as the final step, to avoid any further complication with the linker under coupling conditions. This required a slight modification of the *ent*-verticilide portion of the molecule, shown in Scheme 29. Instead of attaching the linker unit in the second step, a benzyl protecting group was added. α-Hydroxy ester **137** was then carried through the same series of couplings, global deprotection, and cyclization. A final hydrogenolysis of the benzyl group provided the free acid side chain (**79**), ready for an esterification reaction. The first esterification conditions attempted were the use of EDCI and DMAP in dichloromethane. However, after

[241]a) Ma, Y.; Hoepker, A. C.; Gupta, L.; Faggin, M. F.; Collum, D. B. *J. Am. Chem. Soc.* **2010**, *132*, 15610 b) Ma, Y.; Stivala, C. E.; Wright, A. M.; Hayton, T.; Liang, J.; Keresztes, I.; Lobkovsky, E.; Collum, D. B.; Zakarian, A. *J. Am. Chem. Soc.* **2013**, *135*, 16853 c) Yu, K.; Lu, P.; Jackson, J. J.; Nguyen, T.-A. D.; Alvarado, J.; Stivala, C. E.; Ma, Y.; Mack, K. A.; Hayton, T. W.; Collum, D. B.; Zakarian, A. *J. Am. Chem. Soc.* **2017**, *139*, 527

Scheme 29. Diazirine generation 2.0 synthesis.

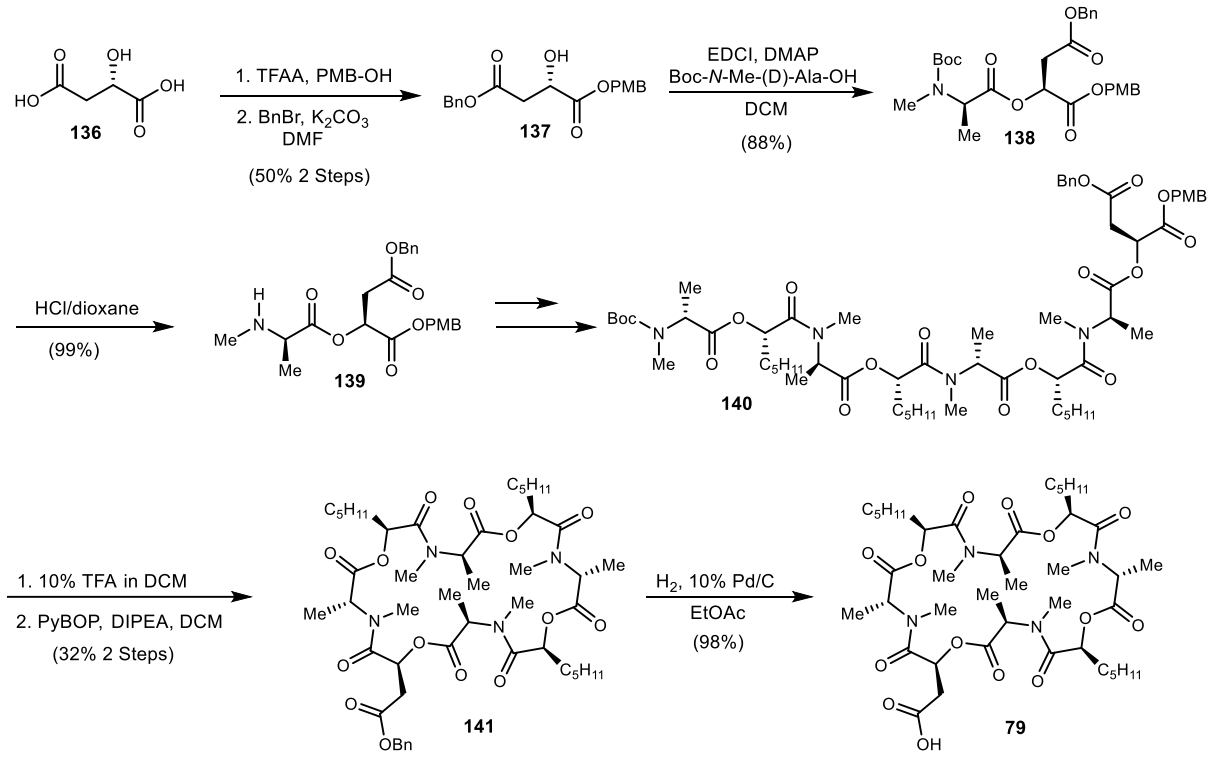

working up the reaction, several different products were observed. While by LRMS, the desired product had formed, it was a minor product. The other two major products were determined to be ring-opened variants of the molecule (Scheme 30). It was hypothesized that these side products were occurring following formation of the active ester. When the carboxylic acid is activated, the α-proton pK_a is significantly lower. If this proton were to be deprotonated under basic conditions, it could lead to an elimination that opens the macrocycle (Scheme 30). From that point, the esterification reaction could take place at the desired carboxylic acid, or the newly formed carboxylic acid via the ring opening. It was hypothesized that this pathway may be circumvented by using less basic conditions. First, the same conditions without the use of DMAP were attempted. However, these conditions produced the same ratio of desired product to ring opened product. Hypothesizing that the tertiary amide on EDCI was acting as a base itself, the esterification was carried out using DCC instead. This unfortunately led to isolation of only starting material. Next, the use of a racemization suppressing agent, HOBt was employed. Excitingly, the use of DCC, HOBt and DIPEA gave a 1:1 ratio of the desired product **142** to the doubly esterified, ring opened

Scheme 30. First esterification attempt in diazirine 2.0 synthesis.

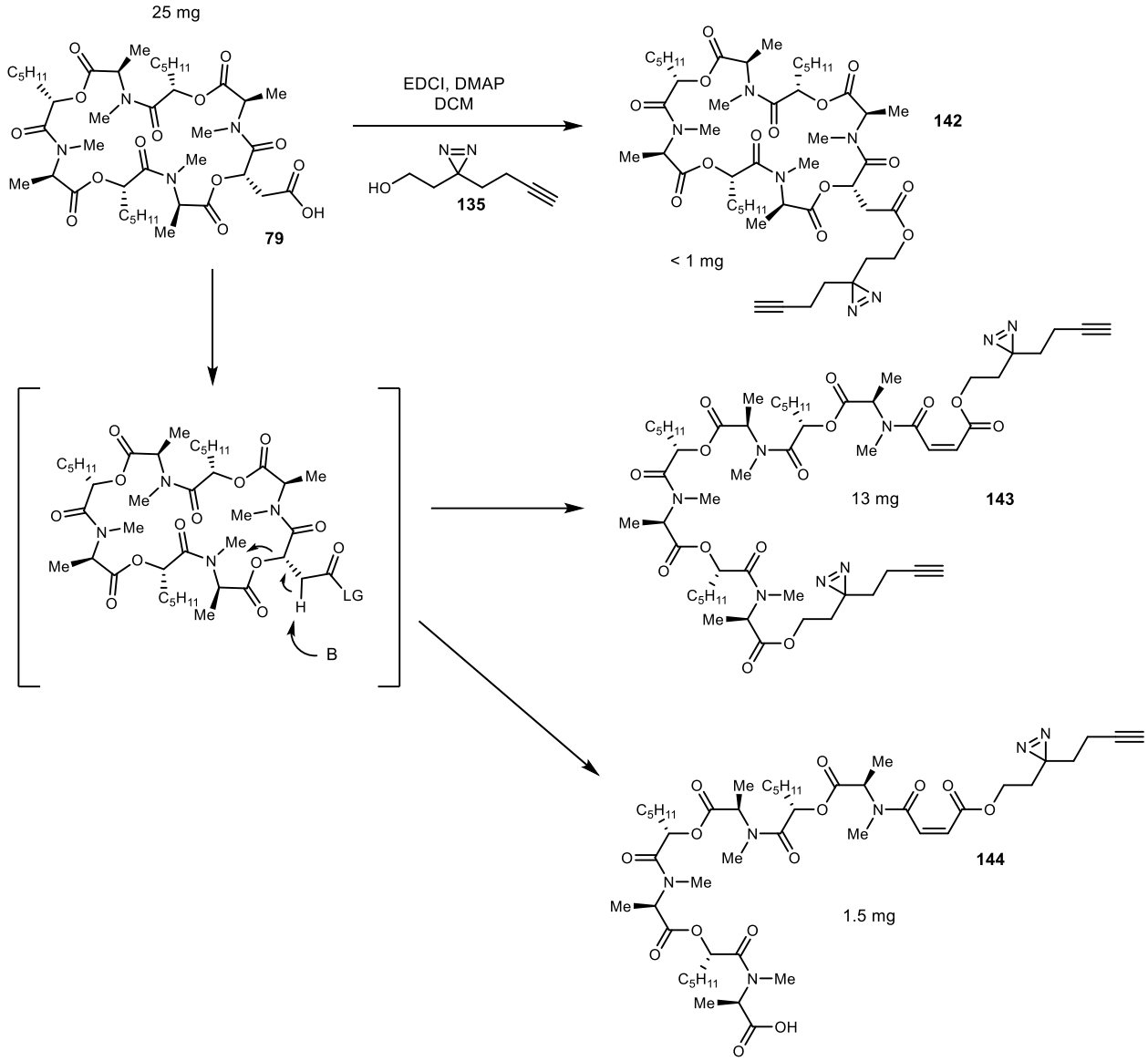

product **144**. These conditions provided ample product to characterize the material and ensure that we had indeed made our desired diazirine probe. As a final optimization, we explored reversing the reactivity of our two reagents in the esterification reaction. By activating the carboxylic acid as a nucleophile, the formation of an activated ester would be avoided, and therefore, so should the ring-opened products. It was gratifying to see that this idea indeed worked, and using Mitsunobu conditions, we were able to form only the desired diazirine product in a 65% yield (Scheme 31).

Scheme 31. Mitsunobu esterification to synthesize diazirine 2.0.

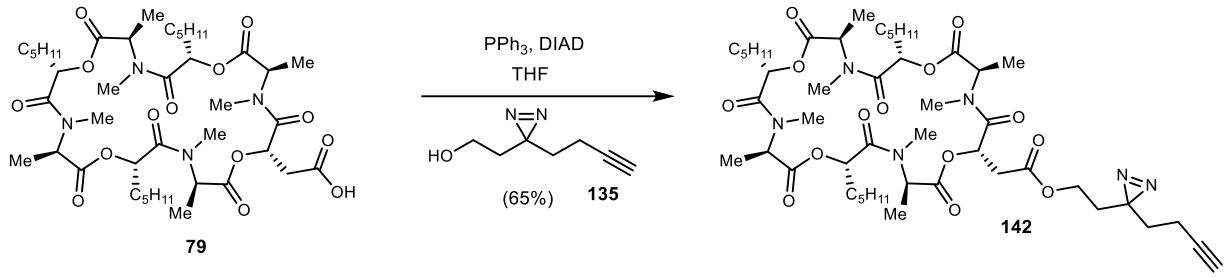

Upon completion of the diazirine analogues, several were given to Dr. Dan Blackwell to test for activity in the calcium spark assay. Alongside the 24-membered ring **142**, one of the ring-opened products (**144**) as well as the 18-membered ring diazirine analogue (**128**) were tested. Not surprisingly, the ring opened product and 18-membered ring had no activity against calcium sparks (Figure 91). While the 24-membered diazirine appeared to inhibit calcium sparks, a reduction in

Figure 91. Diazirine compounds tested for activity and calcium sparks assay data.

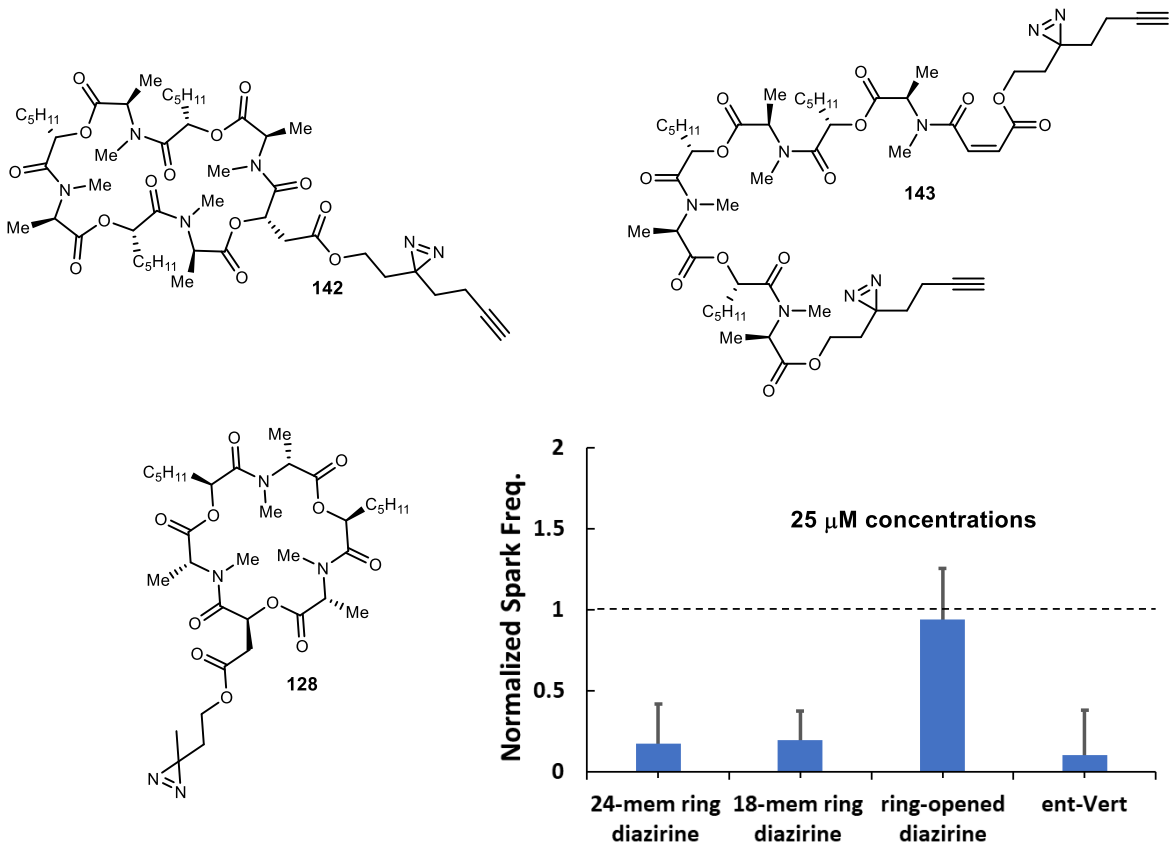

potency compared to *ent*-verticilide was noticed. Unfortunately, this loss in activity would likely be a problem in photo-affinity labeling, as the labeling yields are already expected to be low. The fluorescent version of the molecule was synthesized via a Huisgen cycloaddition reaction to the fluorescein azide (**108**) prepared previously and tested in the sparks assay as well (Figure 92).[242] Interestingly, this compound appeared to inhibit calcium sparks more than its alkyne precursor (**142**). This result calls into question the previous results with the diazirine series. At this time, it's not clear which result is misleading, but further side-by-side examination of each of the compounds in the calcium sparks assay may clarify the data. However, in the meantime, this potential lack of activity led us back to the drawing board with the next generation of diazirine to synthesize.

Figure 92. Diazirine 2.0 with attached fluorescent tag.

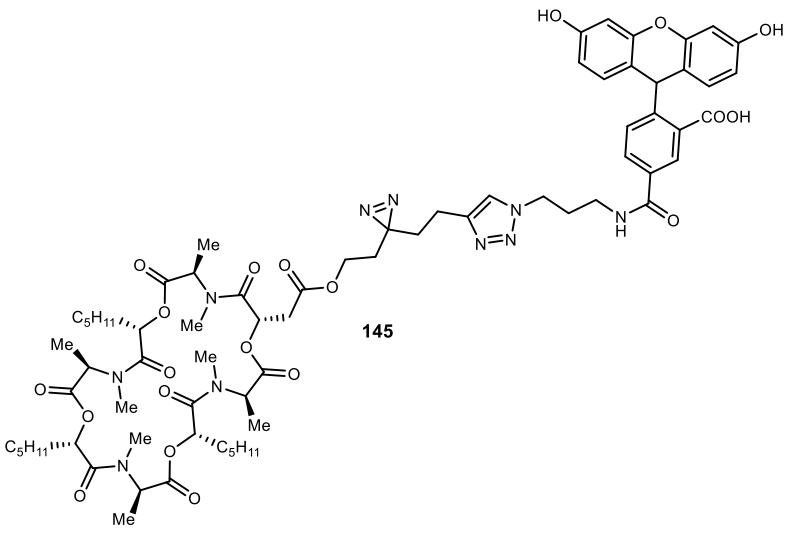

2.5.5 Generation 3.0 Diazirine Synthesis

One of the possible factors causing a loss of activity in diazirine 2.0 was the addition of an ester bond into the side chain. The addition of new hydrogen bond acceptors that close to the peptide backbone could significantly alter its interaction with the target. When moving forward with a third generation diazirine, we once again considered possible routes to incorporate a diazirine directly on the backbone of one of the alkyl side chains. It was evident from our previous

[242] It should be noted that while we are confident product X was formed from ^{1}H NMR and HRMS, < 2 mg was synthesized and was not enough material for a full characterization. If this compound were to be used in photoaffinity labeling, a larger amount would need to be synthesized and characterized.

attempts that we would likely need to plan a new route to access the enantioenriched α-hydroxy acid. An initial idea was to begin with hex-5-en-1-ol (**131**), following our previous route to form the α-hydroxy acid, and then subject the material to a Wacker oxidation to generate a methyl ketone on the sidechain (Scheme 32). However, when subjecting an alkene to Mioskowski-Nef

Scheme 32. Attempted route with alkene precursor.

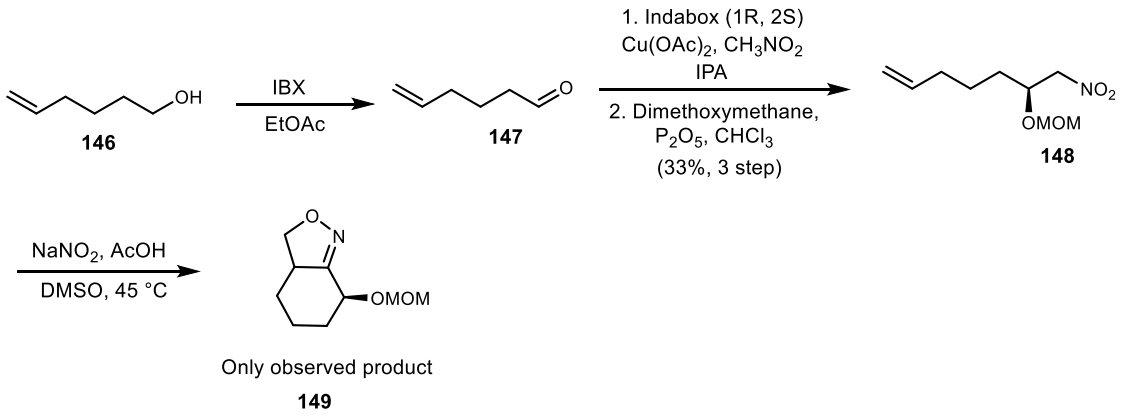

conditions, a cycloaddition product, similar to **46** (see Scheme 14) was formed as the sole product, despite using our already optimized conditions. We then attempted to carry out the Wacker oxidation prior to the Miowskowski Nef reaction. While the oxidation proceeded in high yield, when the ketone was subject to the Nef conditions, Henry-like cyclization products were observed (Scheme 33). At this point, other options were explored, with a particular focus on employing the chiral pool for the α-hydroxy acid synthesis.

To this end, it was envisioned that via diazotization chemistry, α-hydroxy acids could be

Scheme 33. Second attempted route with alkene precursor.

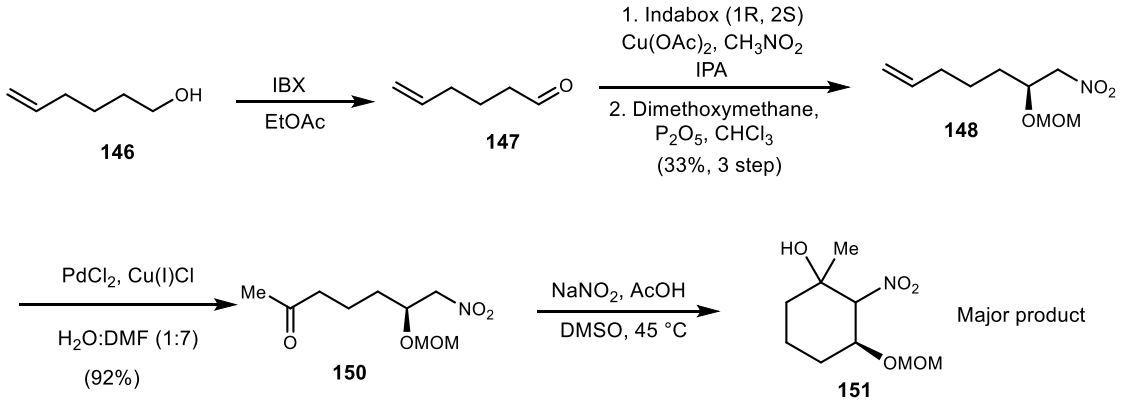

synthesized from their amino acid precursors. Furthermore, because this chemistry occurs with a net retention of stereochemistry, the desired hydroxy acid could be accessed from the natural version (L) of an amino acid. With a plan under way, we began a new synthesis starting with glutamic acid (**152**) (Scheme 34). First, the carboxylic acid side chain was protected as the methyl ester, followed by protection of the amine as the *tert*-butyl carbamate, and protection of the other carboxylic acid as the *tert*-butyl ester. The methyl ester was then deprotected and converted to

Scheme 34. Synthesis of diazirine 3.0 didepsipeptide.

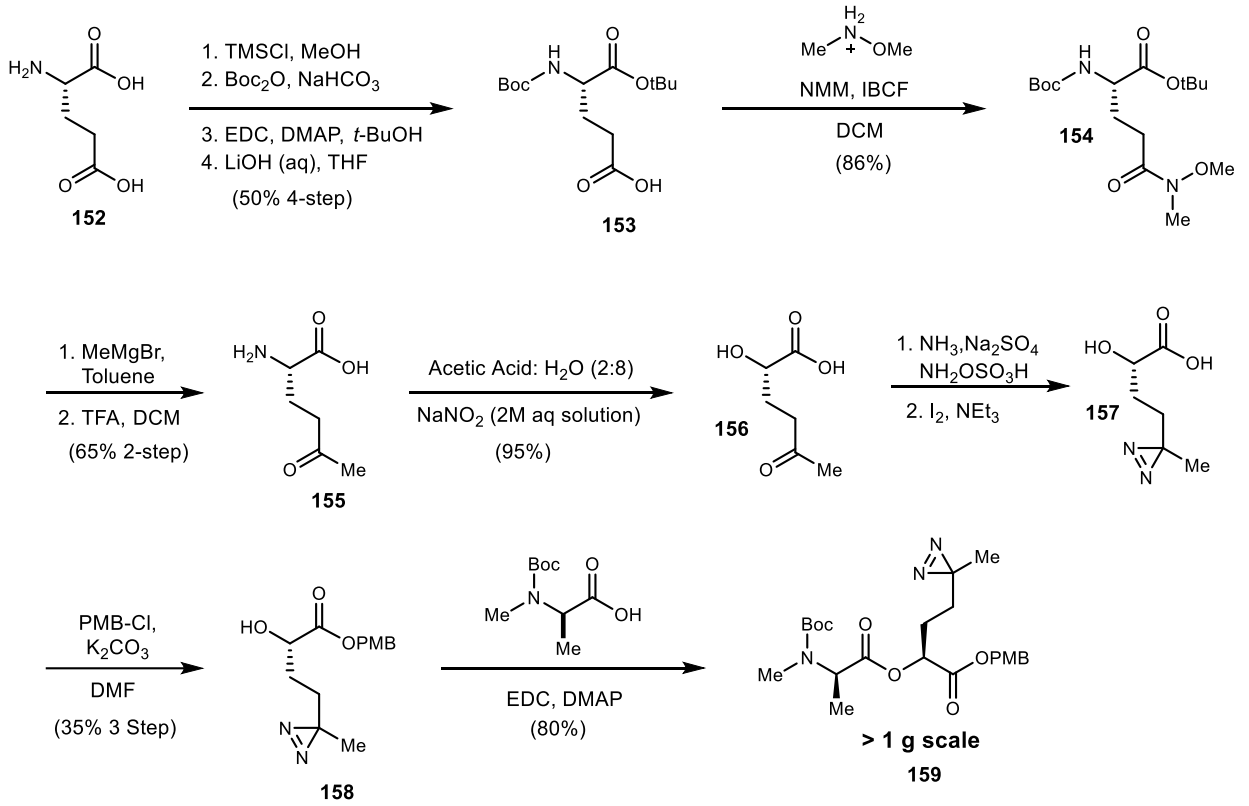

Weinreb amide **154**, which was the subjected to a Grignard reaction to afford the methyl ketone. Upon ketone formation, a global deprotection gave the free amino acid **155**, which could be subjected to diazotization chemistry to form free α-hydroxy acid **156**. The α-hydroxy acid proved difficult to purify, as the compound was water soluble. Taking this into consideration, acetic acid was removed by vacuum, and then the aqueous solution was lyophilized. The resulting mixture could then be dissolved in MeOH, filtered to remove salts, and concentrated to afford fairly clean hydroxy acid. This material was then taken forward into the diazirine-forming reaction conditions.

Due to the difficulty with water solubility in the previous step, it was anticipated that intermediate **157** would also be water soluble. Due to this, the material was carried forward crude into a protection as the PMB ester. The resulting product could easily be purified to afford α-hydroxy ester **158** in 35% yield over 3-steps. A final esterification with *N*-Me-D-Ala afforded didepsipeptide **159**. The developed route worked reliably well on up to a gram scale.[243]

Upon synthesis of the didepsipeptide, coupling was attempted once again with the alkyne hexadepsipeptide **124** (Scheme 35). While difficulties with this step were anticipated due to our

Scheme 35. Synthesis of diazirine 3.0.

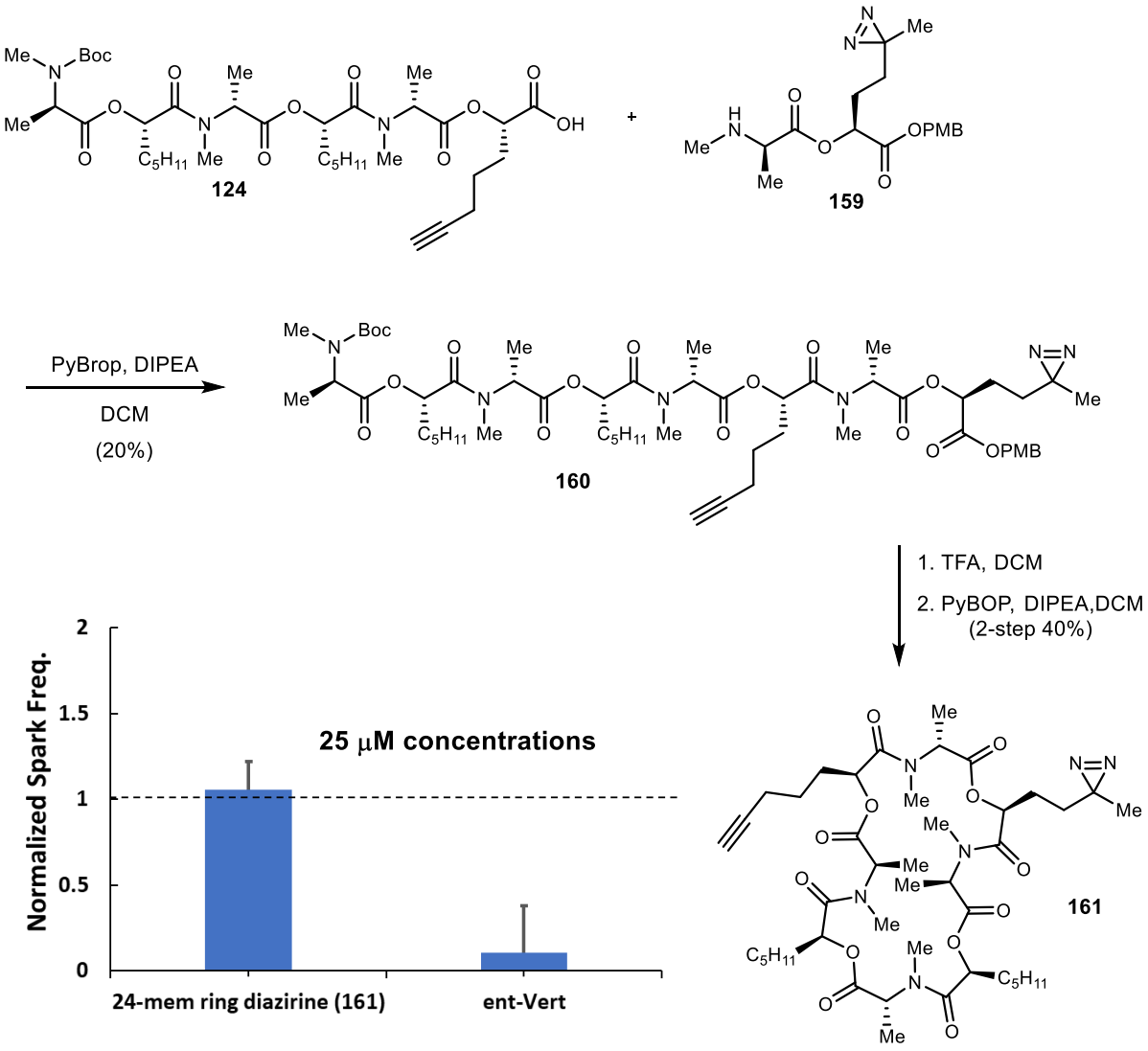

[243] It is anticipated that this procedure would scale even larger but was never tried.

previous experiences, we were pleasantly surprised to see octadepsipeptide product formation with the first attempt. It is possible that although both the diazirine and alkyne are present in these coupling conditions, the decreased steric bulk in didepsipeptide **159** compared to **123** is also responsible for the difference in reactivity. While the yield was low (20%), 12 mg of clean product was isolated to carry forward. A final global deprotection with TFA and cyclization yielded diazirine 3.0 (**161**) in an overall 40% yield. After successful completion of the synthesis, Dr. Dan Blackwell tested the analogue in the calcium sparks assay. Unfortunately, once again preliminary data shows low activity – interestingly, it appears the activity is even lower than diazirine 2.0. However, additional runs still need to be conducted to confirm these results. If this indeed proves to be the case, once again we will need to return to the drawing board. A preliminary hypothesis for this loss of activity is that introducing an alkyne and diazirine on two separate side chains is problematic. If so, a new synthetic route will likely be necessary.

2.6 *ent*-Verticilide Initial Pharmacokinetic Studies

Many peptide/depsipeptide natural products, categorically coined as the "beyond rule of five (bRo5)" class alluding to Lipinski's rule, are well outside the conventional definition of druglikeness. Even though this class of molecules has been making significant headway in drug discovery settings, they are still significantly less likely to be explored as potential therapeutics compared to their small molecule counterparts. Despite blockbuster drugs in this size regime, including octreotide, valinomycin, cyclosporin, oxytocin, vasopressin, and daptomycin, it is estimated that peptide drugs (cyclic and linear) only contribute around 5% of the global pharmaceutical market.[244,245] The success these macrocyclic molecules with traditionally difficult targets, like protein-protein interactions, highlight why they are an incredibly rich well of untapped chemical potential. One of the biggest barriers to circumvent, however, is the relatively small amount of information available to guide the design of these molecules to optimize both binding and pharmacokinetic (PK) properties. Noteworthy contributions have been made by several recent contributors, including Scott Lokey, Andre Yudin, David Craik, David Fairlie, Joshua Kritzer, Dehua Pei, Horst Kessler, and Michael Dunn.

[244] Zorzi, A.; Deyle, K.; Heinis, C. *Curr. Opin. Chem. Biol.* **2017**, *38*, 24
[245] Buckton, L. K.; Rahimi, M. N.; McAlpine, S. R. *Chem. Eur. J.* **2021**, *27*, 1487

To accomplish our ultimate goal of developing *ent*-verticilide as a therapeutic, an important aspect will involve optimization of pharmacokinetic properties. To this end, we have begun preliminary PK studies in collaboration with both the Knollmann lab here at Vanderbilt and Dr. Scott Akers at Lipscomb. While these studies are still a work in progress, preliminary data is summarized here. Ultimately, our goals were to determine the plasma stability of *ent*-verticilide, as well as determine the maximum and minimum dosing requirements for future studies. It is suspected that the dosing used in vivo studies currently is higher than it needs to be. Finding accurate values will allow for conservation of materials, until very large-scale protocols are developed.

Stability studies were carried out in mouse plasma as a preliminary step. First, calibration curves were generated using deuterated *ent*-verticilide (**162**) as an internal standard. This compound was synthesized following the MCO protocol (see Scheme 1) and replacing methyl iodide with CD_3I in the final methylation step (Scheme 36). Following calibration, stability studies

Scheme 36. Synthesis of deuterated *ent*-verticilide.

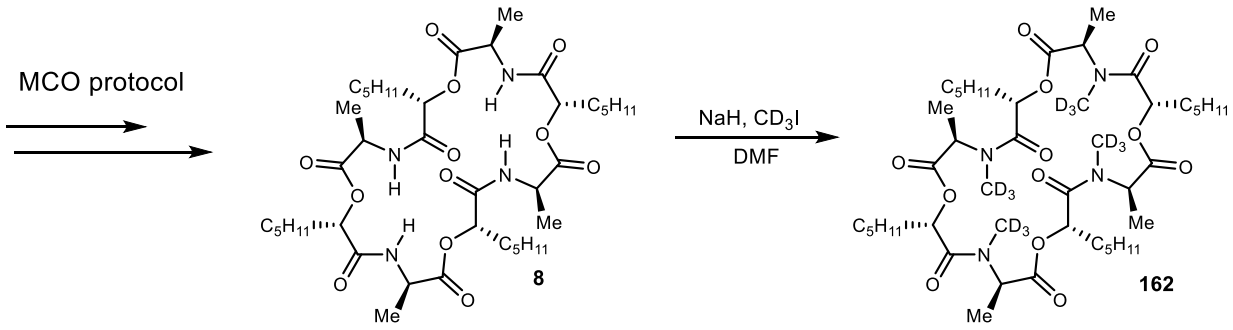

were conducted. The results from this assay indicated that *ent*-verticilide is stable in mouse plasma for 6 hours at 4 °C and 37 °C (Figure 93). The findings here provided support that *ent*-verticilide would be stable in plasma for sample collection, processing, and *in vitro* time and temperature-dependent studies for determining plasma protein binding. *nat*-Verticilide on the other hand, had remarkably decreased plasma stability. It was found to be highly unstable at both 4 °C and 37 °C, degrading in under 1 hour (Figure 93). This striking different in stability between the two enantiomers could shed light on the difference in activity and is ultimately something to consider going forward.

Upon determined that *ent*-verticilide would be stable enough in mouse plasma, further PK studies were conducted by Dr. Dan Blackwell and Dr. Scott Akers. *ent*-Verticilide was administered to mice via I.P. injection in normal saline. They were then subjected to an arrythmia catecholamine challenge[159] and blood was collected at a variety of timepoints, from 5 minutes to

Figure 93. Plasma stability of *ent*-verticilide and *nat*-verticilide.

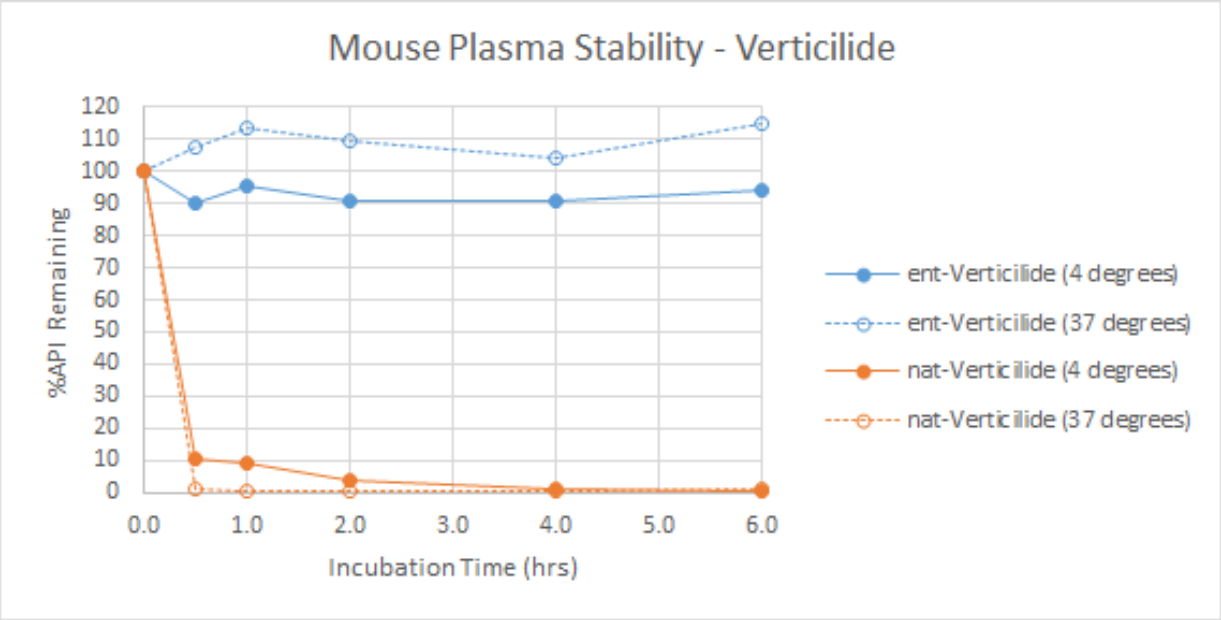

1440 minutes. From these samples, a variety of different PK parameters were determined. Those results are shown in Table 10. A few important parameters worth noting, is a 10-fold increase in the observed C_{max} between the 3.0 mg/kg dose and the 30.0 mg/kg dose. This indicates that high dose *ent*-verticilide may be showing signs of absorption and elimination saturation with an estimated half-life of 523 minutes vs 161 minutes in the 3 mg/kg dose group. It cannot be ruled out at this time, however, that this difference is related to significant experimental variability in the study. Currently, another round of PK studies are under way with a different injection method – continuous diffusion via osmotic mini-pumps implanted into mice – in hopes to resolve potential variability.

Table 10. Initial estimated pharmacokinetic parameters of *ent*-verticilide.

Species	Dose (mg/kg)	Route	Number of samples	Ke (1/min)	Half Life (min)	Tmax (min)
Mouse	3.0	IP	8	0.0043	160.8	5
Mouse	30.0	IP	9	0.0013	523.3	5

Cmax (ng/mL)	AUClast (min*ng/mL)	AUCINF_obs (min*ng/mL)	Vz_F_obs (mL/kg)	Cl_F_obs (mL/min/kg)
1459	45749	49389	14092.79	60.74
14086	540752	590978	38321.46	50.76

2.7 Conclusions and Outlook

Preliminary mechanism of action studies have shown some promising results, but much work remains to be carried out. Several experiments remain to be conducted using the fluorescent probes and FRET. Ultimately, the ability to observes a FRET signal between *ent*-verticilide and an RyR2 regulatory protein would provide definative proof that *ent*-verticilide was localizing within RyR2. Furthermore, this would allow us to pin-point a specific region of RyR2 in which *ent*-verticilide was acting. This could have big implications in cryo-EM experiments currently underway with Philip Van Petegem at UBC, potentially enabling 3D structural data. The acquisition of structural data would also make possible a structure-based design approach with the SAR studies, allowing much more insight to the current proposed hypotheses.

Photo-affinity labeling, while far from a trivial task, still holds significant promise towards uncovering the mechanism of action. Though diazirine analgoues made thus far have been unsuccessful, many synthetic hurdles towards these analogues have been solved. This preliminary work should provide a nice pathway towards new analogues. If the current hypotheses behind diazirine 3.0 are proved correct, a new synthetic pathway is suggested here (Scheme 37). Furthermore, from a synthetic standpoint, while a “medium-scale” protocol for the synthesis of *ent*-verticilide has been developed, there is still room for improvement. While reliable, the peptide coupling reactions use large amounts of solvent, superstoichiometric amounts of reagents, and require extensive purification. While SPPS is traditionally employed in large scale peptide synthesis, this option is still fairly limited for depsipeptide synthesis. Methods to incorporate catalytic amide bond formation into the synthesis could yield drastic improvements. Optimiziation

Scheme 37. Proposed synthesis for diazirine 4.0.

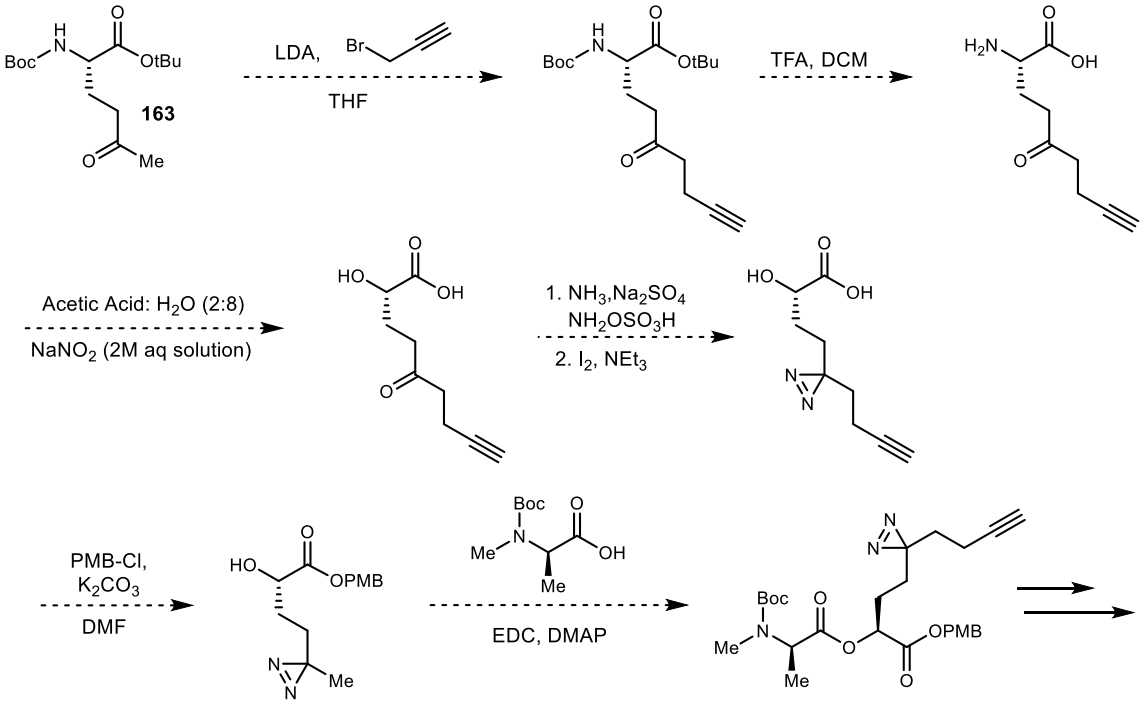

for larger scale is anticipated to be necessary in the coming years, as *ent*-verticilide hopefully continues to move forward into human studies.

Finally, work remains to be done towards improving the PK properties of *ent*-verticilide. Though preliminary studies show remarkable plasma stability, and several promising estimated parameters other factors will also need to be studied, including cell permeability, metabolism, solubility, oral bioavailability, and delivery methods. To date, *ent*-verticilide remains an oil, which is unsuitable for administration as a drug. Paige Thorpe's work in uncovering the features responsible for cell permability with these molecules is likely to provide significant aid in progressing this side of development. As the development of *ent*-verticilide continues, computational studies should be considered and applied where appropriate. Significant advances in the last decade have made computational chemistry an incredible asset in drug discovery that we should not hesistate to use here. Overall, the future for *ent*-verticilide is bright, and I cannot wait to see where the team takes it from here.

Chapter III

III. EXPERIMENTAL SECTION

3.1 General Experimental Information

Glassware was flame-dried under vacuum for all non-aqueous reactions. All reagents and solvents were commercial grade and purified prior to use when necessary. Benzene, dichloromethane (CH_2Cl_2), toluene, tetrahydrofuran (THF), and acetonitrile were dried by passage through a column of activated alumina as described by Grubbs.[246] Flash column chromatography was performed using Sorbent Technologies 230-400 mesh silica gel with solvent systems indicated. Analytical thin layer column chromatography was performed using Sorbent Technologies 250 μm glass backed UV254 silica gel plates and were visualized by fluorescence upon 250 nm radiation and/or the by use of ceric ammonium molybdate (CAM), phosphomolybdic acid (PMA), or potassium permanganate ($KMnO_4$). Solvent removal was affected by rotary evaporation under vacuum (~ 25-40 mm Hg). All extracts were dried with $MgSO_4$ or $NaSO_4$ unless otherwise noted. Preparative HPLC was performed on an Agilent 1260 system (column: Zorbax Eclipse XDB-C18; 21.2 mm x 150 mm, 5 μm, flow rate 8 mL/min) with 210 nm monitoring wavelength and acetonitrile/water (+0.1% TFA) gradient as indicated unless otherwise noted. Nuclear magnetic resonance spectra (NMR) were acquired on a Bruker AV-400 (400 MHz), Bruker DRX500 (500 MHz), or Bruker AV II-600 (600 MHz) instrument. Chemical shifts are measured relative to residual solvent peaks as an internal standard set to δ 7.26 and δ 77.16 ($CDCl_3$), unless otherwise specified. Mass spectra were recorded by use of chemical ionization (CI), electron impact ionization (EI), or electro-spray ionization (ESI) on a high resolution Thermo Electron Corporation MAT 95XP-Trap by the Indiana University Mass Spectrometry Facility or on a TQ-Orbitrap 3 XL Penn or Orbitrap 2 Classic FPG in the Vanderbilt Mass Spectrometry Core Laboratory. IR spectra were recorded on a Nicolet Avatar 360 spectrophotometer or a Nicolet IR 200 spectrophotometer and are reported in wavenumbers (cm^{-1}) as neat films on a NaCl plate (transmission). Melting points were measured using an OptiMelt automated melting point system (Stanford Research Systems) and are not corrected. Chiral HPLC analysis was conducted on an Agilent 1100 series Infinity instrument using the

[246] Pangborn, A. B.; Giardello, M. A.; Grubbs, R. H.; Rosen, R. K.; Timmers, F. J. *Organometallics* **1996**, *15*, 1518

designated ChiralPak column. Optical rotations were measured on either a Jasco P-2000 polarimeter or an AUTOPOL III (Rudolph Research Analytical) polarimeter. ITC measurements were performed using a Microcal PEAQ-ITC instrument (MicroCal Inc. Northampton, MA). All experiments were performed at 25 °C in anhydrous methanol. Optimal settings for consistent results in methanol include reference power set to 5 µcal/mol, stir speed set to 1000 rpm and instrument feedback set to low.

3.2 General Procedures

Methoxymethylene ether (MOM) Deprotection: A flame-dried round-bottom flask was charged with the depsipeptide (1 equiv) dissolved in dry dichloromethane (0.05 M), pentamethyl benzene (3 equiv), and $BF_3 \cdot Et_2O$ (3 equiv). The reaction was allowed to stir for 50 minutes at ambient temperature. The crude reaction mixture was quenched with satd aq $NaHCO_3$, washed with brine, dried, concentrated, and subjected to flash column chromatography to afford the alcohol.

Benzyl Deprotection: A round-bottom flask was charged with the depsipeptide (1 equiv) dissolved in methanol (0.1 M) and treated with 10% Pd/C (10 mol %). The reaction flask was evacuated with a light vacuum (~40 Torr). Hydrogen (balloon) was added and then the flask was cycled through a light vacuum three times. The reaction was stirred for 1.5 h. The crude reaction mixture was filtered through Celite and concentrated to afford the carboxylic acid.

tert-Butyloxycarbonyl (Boc) Deprotection: A round-bottom flask was charged with the depsipeptide (1 equiv) and dissolved in 4 M HCl/dioxane (1 M in depsipeptide). The reaction was allowed to stir for 50 minutes at ambient temperature. The crude reaction mixture was concentrated, toluene was added, and the mixture was then reconcentrated. This procedure was repeated 3 times with toluene and 3 times with diethyl ether.

Didepsipeptide MCO: A flame-dried round-bottomed flask under inert atmosphere was charged with *seco*-acid (1 equiv), PPh_3 (6 equiv), and benzene (0.02 M). DIAD (5 equiv) was then added to the stirred solution in 15 aliquots over 120 minutes. The reaction was allowed to stir at ambient temperature for 24 hours and then concentrated to afford a residue that was subjected to the MCO Purification Protocol.

Tetradepsipeptide MCO: A flame-dried round-bottomed flask under inert atmosphere was charged with *seco*-acid (1 equiv), PPh_3 (3 equiv), and benzene (0.005 M). DIAD (2.5 equiv) was then added to the stirred solution in 5 aliquots over 40 minutes. The reaction was allowed to stir at ambient temperature for 24 hours, and then concentrated to afford a residue that was subjected to the MCO Purification Protocol.

3.3 General MCO Purification Information

The crude residue was filtered through a silica gel plug (2 cm x 9 cm) to remove excess Mitsunobu reagents. A stepwise MeOH/DCM gradient was used, and the mixture was collected into two fractions (Fraction 1: 0.5 – 1 % MeOH in DCM; Fraction 2: 20% MeOH in DCM). After analysis by ^{1}H NMR, fraction 1 was discarded as Mitsunobu byproducts only. Fraction 2 was subjected to HPLC purification. Preparative HPLC was performed on an Agilent 1260 system (column: Zorbax Eclipse XDB-C18; 21.2 mm x 150 mm, 5 μm, 8 mL/min flow rate) with 210, 254, and 198 nm monitoring wavelength. The gradient used is listed in the supporting information. HPLC fractions containing depsipeptides (macrocyclic or linear) were then subjected to extractive workup with ethyl acetate. These compounds are sensitive to cleavage under the high-heat conditions necessary to remove the acidic water-acetonitrile solvent system via rotary evaporation. Additionally, these compounds retain polar solvents & TFA, so the washes (water for acidic depsipeptides, satd aq $NaHCO_3$ for non-acidic depsipeptides) are necessary for complete removal. Preparative HPLC was performed on an Agilent 1260 system (column: Zorbax Eclipse XDB-C18; 21.2 mm x 150 mm, 5 μm, 8 mL/min flow rate) with 210, 254, and 198 nm monitoring wavelength. The gradient used is listed in Table S11.

Table S11. MCO HPLC purification gradient.

Time (min)	MeCN (%)
2.0	5
9.0	40
20.0	87
30.0	87
37.0	95
40.0	5
43.0	5

3.4 General ITC Information

ITC measurements were performed using a Microcal PEAQ-ITC instrument (MicroCal Inc. Northampton, MA). All experiments were performed at 25 °C in anhydrous methanol. Optimal settings for consistent results in methanol include reference power set to 5 µcal/mol, stir speed set to 1000 rpm and instrument feedback set to low. These settings are important for methanol to avoid instrumental overcompensation for measured heats.

3.5 Experimental and Characterization Data for Reported Compounds

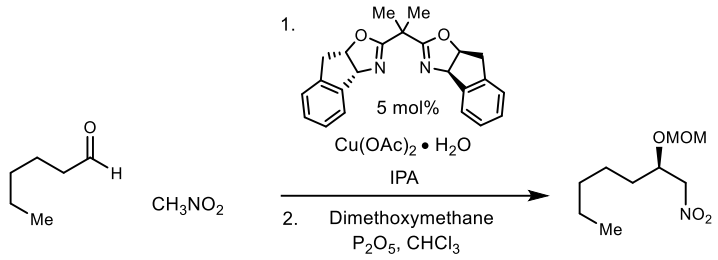

(*R*)-2-(methoxymethoxy)-1-nitroheptane (9). Following the Evans protocol,[1] IndaBOX[2] (321 mg, 897 μmol) and $Cu(OAc)_2 \bullet H_2O$ (162 mg, 813 μmol) were stirred at ambient temperature in isopropanol (32.6 mL) for 1 h. The cerulean blue solution was then cooled to 0 °C, and hexanal (2.00 mL, 16.3 mmol) was added and allowed to stir for 10 m before nitromethane (9.95 mL, 163 mmol) addition. After stirring for 4 days at ambient temperature, the reaction was quenched dropwise at 0 °C with 1 M aq HCl and the aqueous layer was extracted with CH_2Cl_2. Following drying and concentration under reduced pressure, the crude alcohol was dissolved in $CHCl_3$ (81.6 mL), treated with P_2O_5 (23.1 g, 163 mmol) and dimethoxymethane (33.9 mL, 326 mmol), and stirred at ambient temperature overnight. The reaction mixture was diluted with DCM and decanted from the solid. The organic layer was then washed with satd aq $NaHCO_3$ and brine. The organic layers were dried and concentrated to afford an oil that was subjected to flash column chromatography (SiO_2, 3-6% diethyl ether in hexanes) to afford the title compound as a pale-yellow oil (2.54 g, 76%, 2 steps). All spectral data are in agreement with literature values.[3] ANS-2-254.

(*S*)-2-(methoxymethoxy)-1-nitroheptane (*ent*-9). Prepared following an identical procedure as **1**. Flash column chromatography (SiO_2, 3-6% ethyl acetate in hexanes) afforded the hydroxy-nitroalkane with spectroscopic data identical to its enantiomer, except the major/minor peaks were reversed by chiral HPLC analysis. The enantiopurity was determined to be 95% ee by chiral HPLC analysis (Chiralcel OD-H, 2% ^{i}PrOH /hexanes, 0.4 mL/min, $t_r(e_1$, minor) = 16.7 min, $t_r(e_2$, major) = 19.1 min). ANS-2-291.

---

[1] Evans, D. A.; Seidel, D.; Rueping, M.; Lam, H. W.; Shaw, J. T.; Downey, C. W.; *J. Am. Chem. Soc.* **2003,** *125*, 12692.

[2] Kurosu, M.; Porter, J. R.; Foley, M. A. An efficient synthesis of indane-derived bis(oxazoline) and its application to hetero Diels–Alder reactions on polymer support, *Tetrahedron Lett.* **2004**, *45*, 145-148.

[3] Batiste, et al., *Proc. Natl. Acad. Sci.* **2016,** 14893.

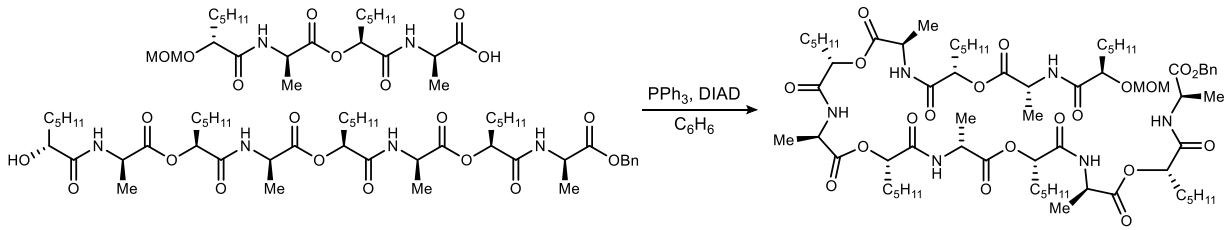

Benzyl ((*S*)-2-((((*S*)-2-((((*S*)-2-((((*S*)-2-((((*S*)-2-((((*R*)-2-(methoxymethoxy)heptanoyl)-D-alanyl)oxy)heptanoyl)-D-alanyl)oxy)heptanoyl)-D-alanyl)oxy)heptanoyl)-D-alanyl)oxy)heptanoyl)-D-alanyl)oxy)heptanoyl)-D-alaninate (16). A flame-dried round-bottom flask was charged with PPh_3 (56.7 mg, 216 μmol), DIAD (43 μL, 216 μmol), and benzene (2.2 mL). The reaction was allowed to stir for 30 m at ambient temperature. The alcohol (98.0 mg, 108 μmol) was added, followed by the acid (54.8 mg, 119 μmol), and the reaction was allowed to stir for 24 h. The crude reaction mixture was concentrated and subjected to flash column chromatography (SiO_2, 20-50% ethyl acetate in hexanes) to afford the didecadepsipeptide (108 mg, 72%) as a colorless oil. $[\alpha]_D^{20}$ -23 (*c* 0.86, $CHCl_3$); R_f = 0.37 (40% EtOAc/hexanes); IR (film) 3311, 2930, 2862, 1752, 1657, 1539, 1456, 1380, 1311, 1195, 1155 cm^{-1}; ^1H NMR (600 MHz, $CDCl_3$) δ 7.75 (d, *J* = 5.3 Hz, 2H), 7.71 (d, *J* = 4.1 Hz, 1H), 7.66 (d, *J* = 6.0 Hz, 1H), 7.39 (d, *J* = 7.4 Hz, 1H), 7.36-7.28 (m, 5H), 7.00 (d, *J* = 5.7 Hz, 1H), 5.21-5.11 (m, 5H), 5.19 (d, *J* = 12.9 Hz, 1H), 5.13 (d, *J* = 12.4 Hz, 1H), 4.70 (dd, *J* = 8.8, 6.7 Hz, 2H), 4.63 (dq, *J* = 7.3, 7.3 Hz, 1H), 4.33-4.17 (m, 5H), 4.04 (dd, *J* =6.3, 4.8 Hz, 1H), 3.42 (s, 3H), 1.96-1.69 (series of m, 12H), 1.50 (d, *J* = 7.4 Hz, 3H), 1.498 (d, *J* = 7.0 Hz, 3H), 1.496 (d, *J* = 7.1 Hz, 3H), 1.491 (d, *J* = 7.4 Hz, 3H), 1.486 (d, *J* = 7.2 Hz, 3H), 1.45 (d, *J* = 7.4 Hz, 3H), 1.41-1.27 (m, 36H), 0.90-0.84 (m, 18H); ^{13}C NMR (150 MHz, $CDCl_3$): Due to extensive overlap of methylene peaks, line listing is not given. Refer to the image of the ^{13}C spectrum; HRMS (EI): Exact mass calcd for $C_{69}H_{115}N_6O_{20}$ $[M+H]^+$ 1347.8161, found 1347.8120. ANS-2-42.

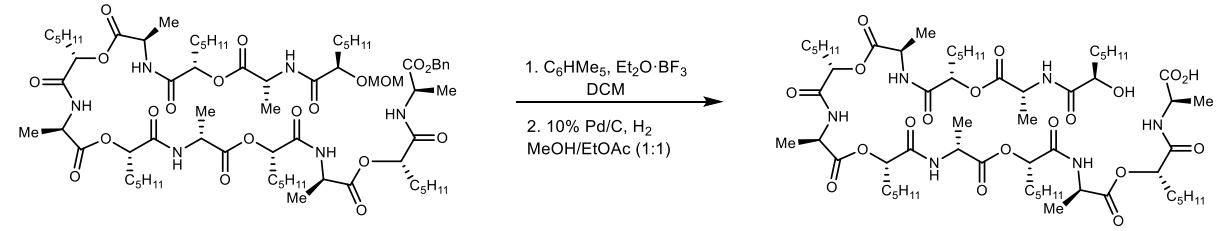

((2*S*)-2-((((2*S*)-2-((((2*S*)-2-(((2-((((*S*)-2-((((*R*)-2-Hydroxyheptanoyl)-D-alanyl)oxy)heptanoyl)-D-alanyl)oxy)heptanoyl)-D-alanyl)oxy)heptanoyl)-D-alanyl)oxy)heptanoyl)-D-alanyl)oxy)heptanoyl)-D-alanine (S1). A flame-dried vial was

charged with *N*-H depsipeptide (48.0 mg, 35.6 μmol), pentamethyl benzene (26.4 mg, 178 μmol) and dry DCM (712 μL). $BF_3{\cdot}Et_2O$ (22 μL, 180 μmol) was then added to the reaction mixture. The reaction was allowed to stir at ambient temperature for 45 m, and it was then quenched by the dropwise addition of satd aq $NaHCO_3$. The aqueous layer was extracted with DCM. The organic layer was dried and concentrated. The crude reaction mixture was concentrated and subjected to flash column chromatography (SiO_2, 40% ethyl acetate in hexanes) to afford the alcohol as a colorless oil (39.4 mg, 30.2 μmol). This material was loaded into a vial and then treated with 10% Pd/C (39.4 mg, l mass equiv.) and dissolved in a 1:1 MeOH/CH_2Cl_2 mixture (302 μL). The reaction vial was evacuated and backfilled with hydrogen (balloon), and this cycle was repeated. The reaction was allowed to stir for 35 minutes. After purging the flask with nitrogen, the crude reaction mixture was filtered through Celite and concentrated. The reaction mixture was then purified by preparative HPLC (45–95% aqueous acetonitrile, 210 nm, flow rate: 20 mL/min, R_t = 9.8 m) to afford the depsipeptide (35 mg, 95%) as a yellow oil. $[\alpha]_D^{20}$ +2.0 (*c* 0.34, $CHCl_3$); R_f = 0.26 (4% MeOH/DCM); IR (film) 3315, 2928, 2861, 1752, 1657, 1541, 1457, 1380, 1196, 1155, 1065 cm^{-1}; ^1H NMR (600 MHz, $CDCl_3$) δ 7.74 (d, *J* = 4.8 Hz, 2H), 7.66 (d, *J* = 5.5 Hz, 1H), 7.64 (d, *J* = 6.2 Hz, 1H), 7.31 (d, *J* = 6.9 Hz, 1H), 7.12 (d, *J* = 5.3 Hz, 1H), 5.23 (dd, *J* = 8.1, 4.3 Hz, 1H), 5.20 (dd, *J* = 5.9, 4.0 Hz, 1H), 5.18 (dd, *J* = 4.9, 3.9 Hz, 1H), 5.16 (dd, *J* = 7.9, 3.8 Hz, 1H), 5.12 (dd, *J* = 8.1, 3.7 Hz, 1H), 4.55 (dq, *J* = 7.2, 7.2 Hz, 1H), 4.45 (dq, *J* = 6.9, 6.9, 1H), 4.38 (dq, *J* = 7.2, 7.2 Hz, 1H), 4.31 (dq, *J* = 7.2, 7.2 Hz, 2H), 4.23 (dq, *J* = 7.1, 7.0 Hz, 1H), 4.12 (dd, *J* = 7.9, 3.8 Hz, 1H), 1.97-1.76 (series of m, 12H), 1.67-1.59 (m, 1H), 1.50 (d, *J* = 7.2 Hz, 6H), 1.49 (d, *J* = 7.0 Hz, 3H), 1.48 (d, *J* = 7.9 Hz, 3H), 1.47 (d, *J* = 7.3 Hz, 3H), 1.46 (d, *J* = 7.2 Hz, 3H), 1.45-1.27 (m, 36H), 0.89 (t, *J*= 7.0 Hz, 3H), 0.88 (t, *J*= 6.9 Hz, 6H), 0.87 (t, *J*= 6.7 Hz, 6H), 0.86 (t, *J*= 6.8 Hz, 3H), [*CO_2H* not observed]; ^{13}C NMR (150 MHz, $CDCl_3$) Due to extensive overlap of methylene peaks, line listing is not given. Refer to image of ^{13}C spectrum; HRMS (EI): Exact mass calcd for $C_{60}H_{105}N_6O_{19}$ $[M+H]^+$ 1213.7429, found 1213.7387. ANS-2-46.

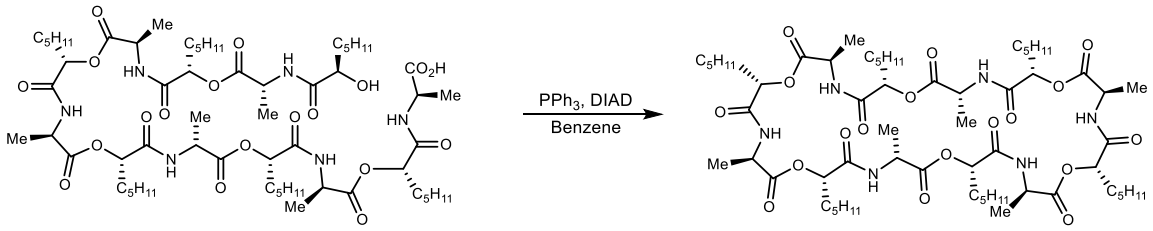

(3*R*,6*S*,9*R*,12*S*,15*R*,18*S*,21*R*,24*S*,27*R*,30*S*,33*R*,36*S*)-3,9,15,21,27,33-Hexamethyl-6,12,18,24,30,36-hexapentyl-1,7,13,19,25,31-hexaoxa-4,10,16,22,28,34-

hexaazacyclohexatriacontane-2,5,8,11,14,17,20,23,26,29,32,35-dodecaone (17). A flame-dried round-bottom flask was charged with the *seco*-acid (10.0 mg, 8.2 μmol) dissolved in dichloromethane (100 μL). The *seco*-acid was diluted with benzene (8.2 mL) and PPh_3 (12.9 mg, 41 μmol) was added. DIAD (8.1 μL, 50 μmol) was added over 40 minutes in 5 aliquots. The reaction was allowed to stir at ambient temperature for 12 h. The crude mixture was concentrated and passed through a silica plug (F1: 0.5% MeOH/DCM, 1% MeOH/DCM; F2: 20% MeOH/DCM). Fraction 2 was purified by preparative HPLC (45–95% aqueous acetonitrile, 210 nm, flow rate: 20 mL/min, R_t = 9.8 m) to afford the 36-membered macrocycle (4.2 mg, 42%) as a colorless oil. $[\alpha]_D^{23}$ -13 (*c* 0.40, $CHCl_3$); R_f = 0.60 (4% MeOH/DCM); IR (film) 3316, 2955, 2926, 2857, 1750, 1657, 1544, 1457, 1379, 1193, 1156, 1064 cm^{-1}; ^1H NMR (400 MHz, $CDCl_3$) δ 7.25 (d, *J* = 7.8 Hz, 1H), 5.16 (dd, *J* = 8.5, 4.1 Hz, 1H), 4.45 (dq, *J* = 7.0, 7.0 Hz, 1H), 1.93-1.70 (series of m, 2H), 1.47 (d, *J* = 7.3 Hz, 3H), 1.40-1.28 (m, 6H), 0.87 (t, *J*= 6.7 Hz, 3H); ^{13}C NMR (150 MHz, $CDCl_3$) ppm 171.6, 170.6, 74.4, 48.7, 31.5, 31.4, 24.7, 22.5, 17.2, 14.1; HRMS (EI): Exact mass calcd for $C_{60}H_{103}N_6O_{18}$ $[M+H]^+$ 1195.7323, found 1195.7355. ANS-2-63.

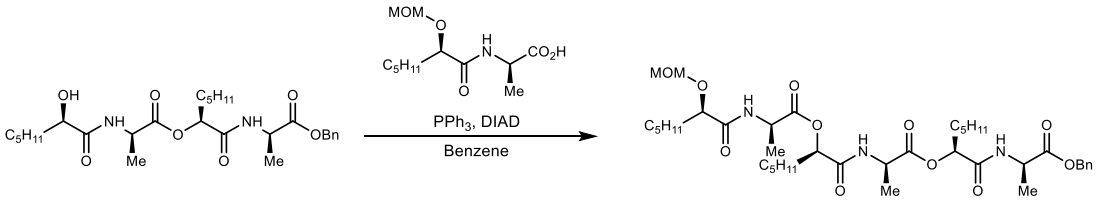

Benzyl ((*S*)-2-((((*R*)-2-((((*R*)-2-(methoxymethoxy)heptanoyl)-D-alanyl)oxy)heptanoyl)-D-alanyl)oxy)heptanoyl)-D-alaninate (18). A flame-dried round-bottom flask was charged with PPh_3 (97.5 mg, 372 μmol), DIAD (73.2 μL, 372 μmol), and benzene (3.7 mL). The reaction was allowed to stir for 30 minutes at ambient temperature. The alcohol (94.0 mg, 186 μmol) was added, followed by the acid (53.3 mg, 204 μmol), and the reaction was allowed to stir for 24 h. The crude reaction mixture was concentrated and subjected to flash column chromatography (SiO_2, 20-30% ethyl acetate in hexanes) to afford the hexadepsipeptide (130 mg, 93%) as a colorless oil. $[\alpha]_D^{20}$ +2.3 (*c* 1.42, $CHCl_3$); R_f = 0.33 (40% EtOAc/hexanes); IR (film) 3295, 2952, 2956, 2857, 1749, 1655, 1541, 1457, 1378, 1155 cm^{-1}; ^1H NMR (600 MHz, $CDCl_3$) δ 7.51 (d, *J* = 4.8 Hz, 1H), 7.36-7.30 (m, 5H), 7.34 (d, *J* = 7.0 Hz, 1H), 6.99 (d, *J* = 5.6 Hz, 1H), 5.20 (d, *J* = 12.4 Hz, 1H), 5.20-5.18 (m, 2H), 5.13 (d, *J* = 12.4 Hz, 1H), 4.70 (d, *J* = 6.7 Hz, 1H), 4.68 (d, *J* = 6.7 Hz, 1H), 4.62 (dq, *J* = 7.3, 7.3 Hz, 1H), 4.32 (dq, *J* = 7.0, 5.6 Hz, 1H), 4.31 (dq, *J* = 7.1, 5.4 Hz, 1H), 4.04 (dd, *J* = 6.4, 4.8 Hz, 1H), 3.42 (s, 3H), 1.97-1.71 (series of m, 6H), 1.48 (d, *J* = 7.2 Hz, 3H), 1.48 (d, *J* =

7.2 Hz, 3H), 1.44 (d, *J* = 7.3 Hz, 3H), 1.40-1.21 (br m, 18H), 0.89-0.85 (m, 9H); ^{13}C NMR (150 MHz, $CDCl_3$) ppm 173.6, 172.6, 172.5, 172.4, 170.5, 169.8, 135.8, 128.6, 128.3, 128.2, 96.5, 77.7, 74.4, 74.3, 67.0, 56.4, 49.4, 49.0, 48.1, 32.7, 31.6, 31.5, 31.39, 31.36, 29.8, 24.7, 24.5, 24.4, 22.6, 22.52, 22.47, 17.5, 16.9, 16.4, 14.12, 14.09, 14.0; HRMS (EI): Exact mass calcd for $C_{39}H_{63}N_3NaO_{11}$ $[M+Na]^+$ 772.4360, found 772.4361. ANS-1-82.

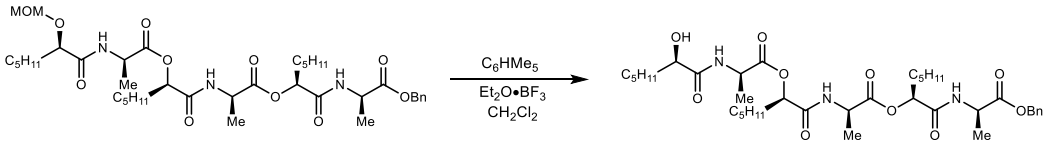

Benzyl ((*S*)-2-((((*R*)-2-((((*R*)-2-hydroxyheptanoyl)-D-alanyl)oxy)heptanoyl)-D-alanyl)oxy)heptanoyl)-D-alaninate (19). A flame-dried round-bottom flask was charged with the hexadepsipeptide (130 mg, 173 μmol) dissolved in dry dichloromethane (0.05 M), pentamethyl benzene (129 mg, 866 μmol), and $BF_3{\cdot}Et_2O$ (107 μL, 867 μmol). The reaction was allowed to stir for 50 minutes at ambient temperature. The crude reaction mixture was quenched with satd aq $NaHCO_3$, brine, and then dried and concentrated, and subjected to flash column chromatography (SiO_2, 20-40% ethyl acetate in hexanes) to afford the alcohol (104.0 mg, 85%) as a colorless oil. $[\alpha]_D^{20}$ -4.1 (*c* 1.27, $CHCl_3$); R_f = 0.20 (40% EtOAc/hexanes); IR (film) 3312, 2955, 2927, 2859, 1749, 1655, 1538, 1457, 1381, 1155 cm^{-1}; ^{1}H NMR (600 MHz, $CDCl_3$) δ 7.54 (d, *J* = 5.1 Hz, 1H), 7.37-7.30 (m, 5H), 7.30 (d, *J* = 7.6 Hz, 1H), 7.04 (d, *J* = 5.6 Hz, 1H), 5.20 (d, *J* = 12.4 Hz, 1H), 5.19-5.16 (m, 2H), 5.13 (d, *J* = 12.4 Hz, 1H), 4.63 (dq, *J* = 7.3, 7.3 Hz, 1H), 4.32 (dq, *J* = 7.0, 5.6 Hz, 1H), 4.31 (dq, *J* = 7.1, 5.4 Hz, 1H), 4.11 (ddd, *J* = 8.2, 8.2, 4.3 Hz, 1H), 2.85 (d, *J* = 4.9 Hz, 1H), 1.97-1.59 (series of m, 6H), 1.47 (d, *J* = 7.2 Hz, 3H), 1.47 (d, *J* = 7.1 Hz, 3H), 1.44 (d, *J* = 7.3 Hz, 3H), 1.40-1.22 (br m, 18H), 0.90-0.85 (m, 9H); ^{13}C NMR (150 MHz, $CDCl_3$) ppm 174.9, 172.7, 172.6, 172.4, 170.5, 169.9, 135.7, 128.7, 128.4, 128.2, 74.42, 74.36, 72.2, 67.0, 49.3, 49.0, 48.1, 34.6, 31.7, 31.6, 31.5, 31.40, 31.37, 24.69, 24.67, 24.5, 22.6, 22.52, 22.48, 17.5, 16.8, 16.5, 14.11, 14.08, 14.0; HRMS (EI): Exact mass calcd for $C_{37}H_{59}N_3NaO_{10}$ $[M+Na]^+$ 728.4098, found 728.4083. ANS-1-83.

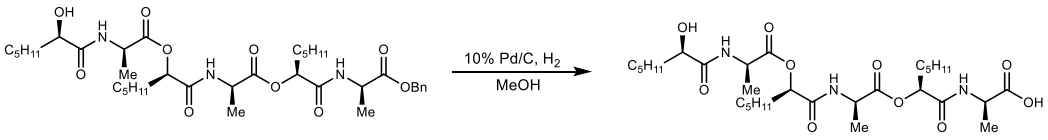

((*S*)-2-((((*R*)-2-((((*R*)-2-Hydroxyheptanoyl)-D-alanyl)oxy)heptanoyl)-D-alanyl)oxy)heptanoyl)-D-alanine (20). A round-bottom flask was charged with the

hexadepsipeptide (140 mg, 198 μmol) dissolved in methanol (0.1 M), and 10% Pd/C (140 mg, 1 mass eq.). The reaction flask was evacuated with light vacuum (50 Torr). Hydrogen (balloon) was added, and the cycle was repeated once more. The reaction was allowed to stir for 25 minutes. The crude reaction mixture was filtered through Celite and concentrated to afford the deprotected hexadepsipeptide (119 mg, 98%) as a colorless oil. $[\alpha]_D^{20}$ -0.7 (*c* 0.98, $CHCl_3$); R_f = 0.17 (80% EtOAc/hexanes); IR (film) 3310, 3073, 2930, 2863, 1749, 1655, 1540, 1457, 1380, 1203, 1155, 1064 cm^{-1}; ^1H NMR (400 MHz, $(CD_3)_2SO$) δ 8.30 (d, *J* = 7.3 Hz, 1H), 8.24 (d, *J* = 7.0 Hz, 1H), 7.93 (d, *J* = 5.6 Hz, 1H), 4.94 (dd, *J* = 7.6, 4.7 Hz, 1H), 4.91 (dd, *J* = 7.5, 4.9 Hz, 1H), 4.35 (dq, *J* = 7.1, 4.5 Hz, 1H), 4.34 (dq, *J* = 7.0, 4.6 Hz, 1H), 4.12 (dq, *J* = 7.0, 7.0 Hz, 1H), 3.88 (dd, *J* = 7.7, 4.0 Hz, 1H), 1.75-1.39 (series of m, 6H), 1.34 (d, *J* = 7.2 Hz, 6H), 1.33-1.16 (br m, 18 H), 1.25 (d, *J* = 7.2 Hz, 3H), 0.87-0.83 (m, 9H), [*OH* and *CO_2H* not observed]; ^{13}C NMR (150 MHz, $(CD_3)_2SO$) ppm 174.6, 173.7, 171.8, 171.5, 169.5, 168.4, 73.6, 73.4, 70.6, 47.8, 47.73, 47.67, 34.1, 31.3 (2C), 31.1, 30.79, 30.77, 24.2, 24.0, 23.8, 22.0, 21.88, 21.86, 17.4, 17.0, 16.7, 13.9, 13.8 (2C); HRMS (EI): Exact mass calcd for $C_{30}H_{53}N_3NaO_{10}$ $[M+Na]^+$ 638.3629, found 638.3624. ANS-1-84.

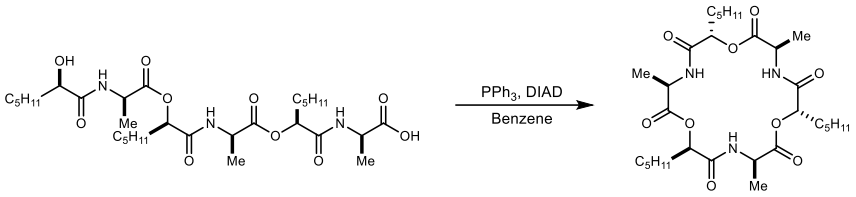

(3*R*,6*S*,9*R*,12*S*,15*R*,18*S*)-3,9,15-Trimethyl-6,12,18-tripentyl-1,7,13-trioxa-4,10,16-triazacyclooctadecane-2,5,8,11,14,17-hexaone (8). A flame-dried round-bottom flask was charged with the fully deprotected hexadepsipeptide (10.0 mg, 16.2 μmol), PPh_3 (12.8 mg, 48.7 μmol), and benzene (1.62 mL). DIAD (8.00 μL, 40.5 μmol) was added in 5 aliquots over 40 minutes. The reaction was allowed to stir at ambient temperature for 24 h. The crude reaction mixture was concentrated and subjected to the general MCO purification to afford the 18-membered macrocycle (6.0 mg, 62%, R_t = 23.8 min) as an amorphous white solid. $[\alpha]_D^{23}$ +25 (*c* 0.95, $CHCl_3$); R_f = 0.30 (6% MeOH/DCM); IR (film) 3208, 3046, 2922, 2852, 1756, 1669, 1556, 1456, 1379, 1260, 1211, 1171, 1105 cm^{-1}; ^1H NMR (400 MHz, $CDCl_3$) δ 6.98 (d, *J* = 7.8 Hz, 1H), 5.13 (dd, *J* = 7.6, 4.7 Hz, 1H), 4.58 (dq, *J* = 7.4, 7.3 Hz, 1H), 1.93-1.74 (m, 2H), 1.47 (d, *J* = 7.1 Hz, 3H), 1.40-1.22 (series of m, 6H), 0.88 (t, *J* = 6.8 Hz, 3H); $^{13}C\{^1H\}$ NMR (100 MHz, $CDCl_3$) ppm 171.6, 169.9, 75.0, 48.7, 31.6, 31.5, 24.7, 22.6, 17.5, 14.1; HRMS (ESI) m/z: $[M+Na]^+$ calcd for $C_{30}H_{51}N_3NaO_9$ 620.3523; Found 620.3518. ANS-1-216.

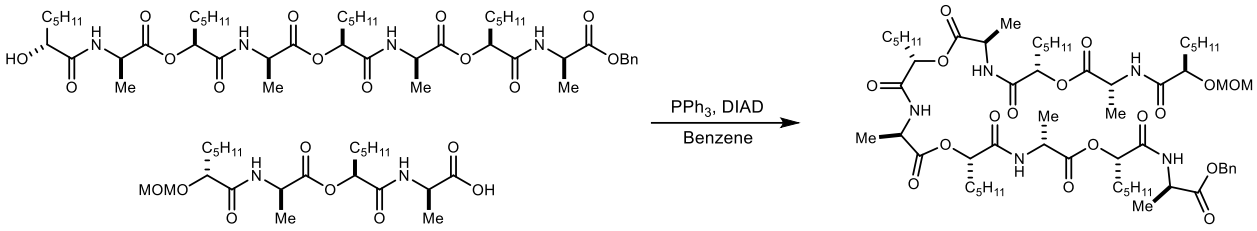

Benzyl ((*S*)-2-((((*S*)-2-((((*S*)-2-((((*S*)-2-((((*R*)-2-(methoxymethoxy)heptanoyl)-D-alanyl)oxy)heptanoyl)-D-alanyl)oxy)heptanoyl)-D-alanyl)oxy)heptanoyl)-D-alanyl)oxy)heptanoyl)-D-alaninate (S2). A flame-dried round-bottom flask was charged with PPh_3 (56.7 mg, 216 μmol), DIAD (43 μL, 216 μmol), and benzene (2.2 mL). The reaction was allowed to stir for 30 m at ambient temperature. The alcohol (98.0 mg, 108 μmol) was added, followed by the acid (54.8 mg, 120 μmol), and the reaction was allowed to stir for 24 h. The crude reaction mixture was concentrated and subjected to flash column chromatography (SiO_2, 20-50% ethyl acetate in hexanes) to afford the decadepsipeptide[4] (27 mg, 20%) as a colorless oil. $[\alpha]_D^{20}$ -7.8 (*c* 0.42, $CHCl_3$); R_f = 0.36 (40% EtOAc/Hexanes); IR (film) 3327, 2924, 2856, 1750, 1655, 1539, 1456, 1377, 1154, 1101, 1061 cm^{-1}; ^1H NMR (600 MHz, $CDCl_3$) δ 7.70 (d, *J* = 4.5 Hz, 1H), 7.69 (d, *J* = 4.1 Hz, 1H), 7.64 (d, *J* = 5.0 Hz, 1H), 7.39 (d, *J* = 7.4 Hz, 1H), 7.36-7.29 (m, 5H), 6.99 (d, *J* = 5.5 Hz, 1H), 5.21-5.16 (m, 4H), 5.19 (d, *J* = 12.4 Hz, 1H), 5.13 (d, *J* = 12.0 Hz, 1H), 4.70 (dd, *J* = 8.8, 6.7 Hz, 2H), 4.63 (dq, *J* = 7.2, 7.2 Hz, 1H), 4.33-4.18 (m, 4H), 4.05 (dd, *J* =6.3, 4.9 Hz, 1H), 3.43 (s, 3H), 1.96-1.73 (series of m, 10H), 1.50 (d, *J* = 6.5 Hz, 3H), 1.50 (d, *J* = 6.5 Hz, 3H), 1.49 (d, *J* = 6.4 Hz, 3H), 1.49 (d, *J* = 6.4 Hz, 3H), 1.44 (d, *J* = 7.4 Hz, 3H), 1.41-1.27 (m, 30H), 0.90-0.81 (m, 15H); ^{13}C NMR (150 MHz, $CDCl_3$): Due to extensive overlap of methylene peaks, line listing is not given. Refer to the image of the ^{13}C spectrum; HRMS (EI): Exact mass calcd for $C_{59}H_{97}N_5NaO_{17}$ $[M+Na]^+$ 1170.6772, found 1170.6797. ANS-2-67.

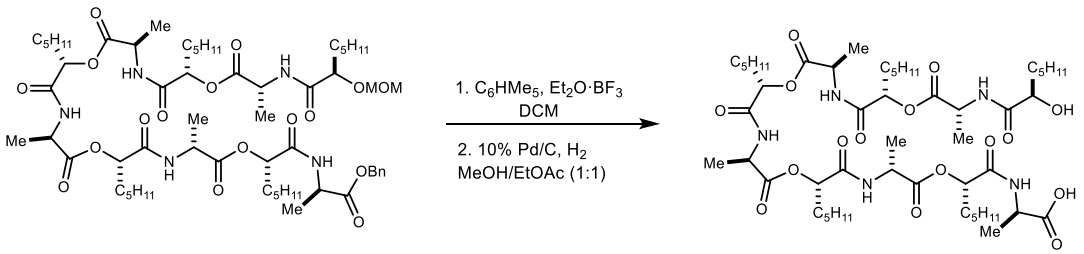

[4] This is the correct product for this reaction. While it is not the expected product, it is a minor side-product isolated in this reaction.

((*S*)-2-((((*S*)-2-((((*S*)-2-((((*S*)-2-((((*R*)-2-Hydroxyheptanoyl)-D-alanyl)oxy)heptanoyl)-D-alanyl)oxy)heptanoyl)-D-alanyl)oxy)heptanoyl)-D-alanyl)oxy)heptanoyl)-D-alanine (S3). A flame-dried vial was charged with *N*-H depsipeptide (30.0 mg, 22.3 μmol), pentamethyl benzene (16.5 mg, 114 μmol) and dry DCM (500 μL). $BF_3{\cdot}Et_2O$ (16 μL, 114 μmol) was then added to the reaction mixture. The reaction was allowed to stir at ambient temperature for 45 m, and it was then quenched by the dropwise addition of satd aq $NaHCO_3$. The aqueous layer was extracted with DCM. The organic layer was dried and concentrated. The crude reaction mixture was concentrated and subjected to flash column chromatography (SiO_2, 40% ethyl acetate in hexanes) to afford the alcohol as a colorless oil (29.0 mg, 22.3 μmol). This material was loaded into a vial and then treated with 10% Pd/C (2.9 mg) and dissolved in a 1:1 methanol to dichloromethane mixture (223 μL). The reaction vial was evacuated and backfilled with hydrogen (balloon), and this cycle was repeated. The reaction was allowed to stir for 35 minutes. After purging the flask with nitrogen, the crude reaction mixture was filtered through Celite and concentrated. The reaction mixture was then purified by preparative HPLC (45–95% aqueous acetonitrile, 210 nm, flow rate: 20 mL/min, R_t = 13.6 m) to afford the depsipeptide (2.7 mg, 10% 2 step) as a colorless oil. $[\alpha]_D^{20}$ 2.0 (*c* 0.34, $CHCl_3$); R_f = 0.16 (4% MeOH/DCM); IR (film) 3308, 2925, 2855, 1750, 1655, 1542, 1458, 1377, 1194, 1154, 1101, 1064 cm^{-1}; ^1H NMR (600 MHz, $CDCl_3$) δ 7.69 (d, *J* = 4.3 Hz, 1H), 7.65 (d, *J* = 6.2 Hz, 1H), 7.63 (d, *J* = 5.3 Hz, 1H), 7.37 (d, *J* = 6.9 Hz, 1H), 7.11 (d, *J* = 5.3 Hz, 1H), 5.21 (dd, *J* = 8.1, 3.8 Hz, 1H), 5.21 (dd, *J* = 8.1, 3.8 Hz, 1H), 5.19 (dd, *J* = 8.6, 3.7 Hz, 1H), 5.14 (dd, *J* = 8.0, 4.2 Hz, 1H), 4.56 (dq, *J* = 7.2, 7.2 Hz, 1H), 4.43 (dq, *J* = 6.5, 6.5 Hz, 1H), 4.40 (dq, *J* = 7.3, 7.3 Hz, 1H), 4.32 (dq, *J* =7.1, 7.0 Hz, 1H), 4.23 (dq, *J* =7.2, 7.1 Hz, 1H), 4.12 (dd, *J* =7.9, 3.9 Hz, 1H), 1.97-1.74 (series of m, 12H), 1.50 (d, *J* = 7.1 Hz, 3H), 1.497 (d, *J* = 7.4 Hz, 3H), 1.492 (d, *J* = 7.1 Hz, 3H), 1.48 (d, *J* = 7.7 Hz, 3H), 1.45 (d, *J* = 7.3 Hz, 3H), 1.39-1.28 (m, 30H), 0.90-0.85 (m, 15H); ^{13}C NMR (150 MHz, $CDCl_3$): Due to extensive overlap of methylene peaks, line listing is not given. Refer to the image of the ^{13}C spectrum. HRMS (EI): Exact mass calcd for $C_{50}H_{88}N_5O_{16}$ $[M+H]^+$ 1012.6075, found 1012.6108. ANS-2-46.

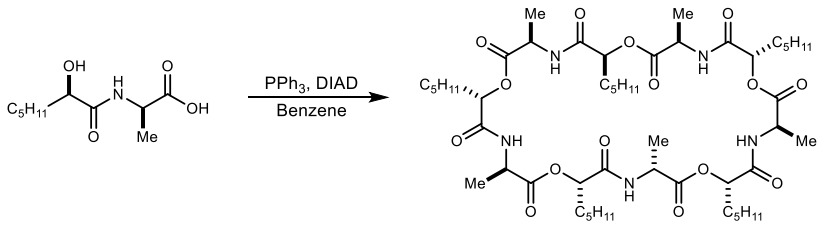

(3*R*,6*S*,9*R*,12*S*,15*R*,18*S*,21*R*,24*S*,27*R*,30*S*)-3,9,15,21,27-Pentamethyl-6,12,18,24,30-pentapentyl-1,7,13,19,25-pentaoxa-4,10,16,22,28-pentaazacyclotriacontane-2,5,8,11,14,17,20,23,26,29-decaone (21). Following the didepsipeptide MCO general procedure, *seco*-acid (55.0 mg, 253 mmol) was stirred for 24 h at ambient temperature to afford a pale-yellow oil. Preparative HPLC following the general MCO purification protocol afforded the 30-membered macrocycle (4.0 mg, 8%, R_t = 35.6 min) as a colorless oil. $[\alpha]_D^{23}$ -15 (*c* 0.65, $CHCl_3$); R_f = 0.35 (4% MeOH/DCM); IR (film) 3315, 2957, 2924, 2853, 1747, 1664, 1547, 1458, 1380, 1260, 1199, 1158, 1064 cm^{-1}; ^1H NMR (400 MHz, $CDCl_3$) δ 7.10 (d, *J* = 6.4 Hz, 1H), 5.10 (dd, *J* = 8.1, 4.0 Hz, 1H), 4.45 (dq, *J* = 6.9, 6.9 Hz, 1H), 1.93-1.83 (m, 1H), 1.83-1.68 (m, 1H), 1.45 (d, *J* = 7.2 Hz, 3H), 1.41-1.20 (m, 6H), 0.88 (t, *J*= 6.6 Hz, 3H); $^{13}C\{^1H\}$ NMR (100 MHz, $CDCl_3$) ppm 172.1, 170.4, 74.4, 48.7, 31.5, 31.4, 24.8, 22.6, 17.1, 14.1; HRMS (ESI) m/z: $[M+Na]^+$ calcd for $C_{50}H_{85}NaN_5O_{15}$ 1018.5934; Found 1018.5936. ANS-1-169.

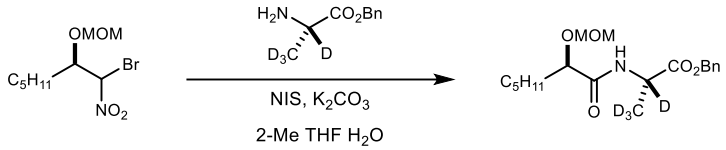

Benzyl ((*R*)-2-(methoxymethoxy)heptanoyl)-L-alaninate-2,3,3,3-d_4 (S4). A round-bottom flask was charged with bromonitroalkane (230 mg, 715 μmol), amine (131 mg, 715 μmol), 2-Me THF (3.6 mL), and H_2O (64 μL) and cooled to 0 °C. The mixture was then treated with NIS (161 mg, 715 μmol), K_2CO_3 (198 mg, 1.43 mmol) and O_2 (balloon). The heterogeneous solution was vigorously stirred for 2 days at 0 °C and then treated with 1 M aq HCl and poured into CH_2Cl_2. The aqueous layer was extracted with CH_2Cl_2, and the combined organic layers were washed with satd aq $Na_2S_2O_3$, dried, and concentrated. The crude residue was subjected to flash column chromatography (SiO_2, 15% ethyl acetate in hexanes) to afford the amide as a light-yellow solid (148 mg, 58%). $[\alpha]_D^{24}$ -49 (*c* 0.72, $CHCl_3$); Mp 52-56 °C; R_f = 0.17 (20% EtOAc/hexanes); IR (film) 3260, 2952, 2892, 1739, 1652, 1527, 1268, 1129, 1059 cm^{-1}; ^1H NMR (600 MHz, $CDCl_3$) δ 7.40-7.27 (m, 5H), 7.09 (s, 1H), 5.16 (d, *J* = 12.2 Hz, 1H), 5.11 (d, *J* = 12.2 Hz, 1H), 4.62 (s, 2H), 4.05 (dd, *J* = 5.2 Hz, 1H), 3.34 (s, 3H), 1.80-1.66 (m, 2H), 1.48-1.12 (series of m, 6H), 0.86 (t, *J* = 6.7 Hz, 3H); ^{13}C NMR (150 MHz, $CDCl_3$) ppm 172.6, 172.1, 135.3, 128.6, 128.4, 128.1, 96.0, 77.3, 67.1, 56.1, 47.1 (t, *J* = 22.0 Hz, 1C), 32.7, 31.5, 24.3, 22.4, 17.5 (sept, *J* = 19.6 Hz, 1C), 13.9; HRMS (EI): Exact mass calcd for $C_{19}D_4H_{25}NNaO_5$ $[M+Na]^+$ 378.2189, found 378.2191. ANS-5-256.

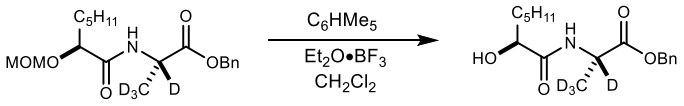

Benzyl ((S)-2-hydroxyheptanoyl)-L-alaninate-2,3,3,3-d$_4$ (S5). A flame-dried round-bottom flask was charged with the didepsipeptide (100 mg, 281 μmol) dissolved in dry dichloromethane (5.6 mL), pentamethyl benzene (125 mg, 844 μmol), and $BF_3{\cdot}Et_2O$ (104 μL, 844 mmol). The reaction was allowed to stir for 50 minutes at ambient temperature. The crude reaction mixture was quenched with satd aq $NaHCO_3$ and the organic layer was washed with brine, dried and concentrated. The residue was subjected to flash column chromatography (SiO_2, 15-40% ethyl acetate in hexanes) to afford the alcohol (83.6 mg, 96%) as a pale-yellow oil. $[\alpha]_D^{23}$ -29 (*c* 0.90, $CHCl_3$); R_f = 0.18 (40% EtOAc/hexanes); IR (film) 3389, 2953, 2925, 2857, 1741, 1650, 1518, 1455, 1377, 1270, 1172, 1127 cm^{-1}; ^{1}H NMR (400 MHz, $CDCl_3$) δ 7.40-7.30 (m, 5H), 7.04 (s, 1H), 5.20 (d, *J* = 12.3 Hz, 1H), 5.15 (d, *J* = 12.3 Hz, 1H), 4.13 (ddd, *J* = 7.5, 3.9, 3.9 Hz, 1H), 3.00 (broad s, 1H), 1.88-1.73 (m, 1H), 1.62 (ddt, *J* = 14.7, 7.5, 7.3 Hz, 1H), 1.46-1.23 (series of m, 6H), 0.88 (t, *J* = 6.5 Hz, 3H); ^{13}C NMR (150 MHz, $CDCl_3$) ppm 174.0, 173.0, 135.4, 128.8, 128.6, 128.2, 72.2, 67.3, 47.5 (t, *J* = 22.0 Hz, 1C), 34.8, 31.7, 24.7, 22.6, 17.5 (sept, *J* = 20.9 Hz, 1C), 14.1; HRMS (EI): Exact mass calcd for $C_{17}D_4H_{21}NNaO_4$ $[M+Na]^+$ 334.1927, found 334.1929. ANS-6-04.

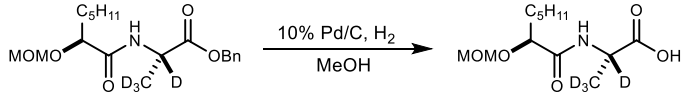

((*S*)-2-(Methoxymethoxy)heptanoyl)-L-alanine-2,3,3,3-d$_4$ (S6). A round-bottom flask was charged with the didepsipeptide (90 mg, 250 μmol) dissolved in methanol (2 mL) and treated with 10% Pd/C (9 mg). The reaction flask was evacuated with a light vacuum (50 Torr). Hydrogen (balloon) was added and then the flask was cycled through a light vacuum once again. The reaction was stirred for 1.5 h. The crude reaction mixture was filtered through Celite and concentrated to afford the deprotected didepsipeptide (67 mg, 99%) as a colorless oil. $[\alpha]_D^{23}$ -46.1 (*c* 1.22, $CHCl_3$); R_f = 0.16 (5% MeOH/DCM); IR (film) 3401, 2953, 2929, 2859, 1731, 1633, 1525, 1466, 1237, 1154, 1033 cm^{-1}; ^{1}H NMR (600 MHz, $CDCl_3$) δ 10.40 (br s, 1H), 7.16 (s, 1H), 4.69 (br s, 2H), 4.10 (dd, *J* = 6.4, 4.5 Hz, 1H), 3.41 (s, 3H), 1.81-1.68 (m, 2H), 1.44-1.22 (series of m, 6H), 0.87 (t, *J* = 6.9 Hz, 3H); ^{13}C NMR (150 MHz, $CDCl_3$) ppm 176.3, 173.2, 96.3, 77.5, 56.4, 47.3 (t, *J* = 21.1 Hz, 1C), 32.8, 31.6, 24.4, 22.6, 17.4 (sept, *J* = 19.4 Hz, 1C), 14.1; HRMS (EI): Exact mass calcd for $C_{12}D_4H_{19}NNaO_5$ $[M+Na]^+$ 288.1720, found 288.1722. ANS-6-13.

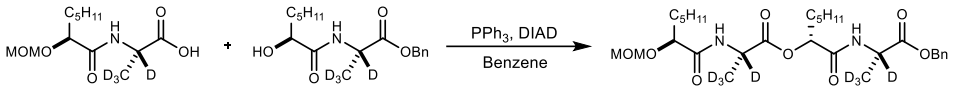

Benzyl ((5*S*,8*S*,11*R*)-8-(methyl-d$_3$)-6,9-dioxo-5,11-dipentyl-2,4,10-trioxa-7-azadodecan-12-oyl-8-d)-L-alaninate-2,3,3,3-d$_4$ (S7). A flame-dried round-bottom flask was charged with PPh_3 (133 mg, 506 μmol), DIAD (100 μL, 506 μmol), and benzene (5.1 mL). The reaction was allowed to stir for 30 minutes at ambient temperature. The alcohol (83.6 mg, 268 μmol) was added, followed by the acid (67.0 mg, 131 μmol), and the reaction was allowed to stir for 24 h. The crude reaction mixture was concentrated and subjected to flash column chromatography (SiO_2, 15-60% ethyl acetate in hexanes) to afford the tetradepsipeptide (121 mg, 86%) as a pale-yellow solid. $[\alpha]_D^{23}$ -20.4 (*c* 1.18, $CHCl_3$); Mp 106-110 °C; R_f = 0.27 (20% EtOAc/hexanes); IR (film) 3294, 2954, 2928, 2859, 1744, 1651, 1524, 1455, 1376, 1260, 1122, 1046 cm^{-1}; ^{1}H NMR (600 MHz, $CDCl_3$) δ 7.38-7.28 (m, 5H), 7.12 (s, 1H), 6.98 (s, 1H), 5.20 (d, *J* = 12.4 Hz, 1H), 5.18 (dd, *J* = 8.4, 4.0 Hz, 1H), 5.12 (d, *J* = 12.4 Hz, 1H), 4.67 (s, 2H), 4.02 (dd, *J* = 6.6, 4.6 Hz, 1H), 3.40 (s, 3H), 1.96-1.66 (series of m, 4H), 1.45-1.20 (series of m, 12H), 0.87 (t, *J* = 7.1 Hz, 3H), 0.86 (t, *J* = 7.1 Hz, 3H); ^{13}C NMR (150 MHz, $CDCl_3$) ppm 173.2, 172.6, 172.3, 169.5, 135.7, 128.6, 128.4, 128.2, 96.4, 77.6, 74.7, 67.0, 56.4, 48.1 (t, *J* = 21.6 Hz, 1C), 47.7 (t, *J* = 21.5 Hz, 1C), 32.8, 31.7, 31.6, 31.4, 24.6, 24.4, 22.6, 22.5, 16.7 (sept, *J* = 21.1 Hz), 16.6 (sept, *J* = 21.1 Hz), 14.1, 14.0; HRMS (EI): Exact mass calcd for $C_{29}D_8H_{38}N_2NaO_8$ $[M+Na]^+$ 581.3649, found 581.3647. ANS-6-29.

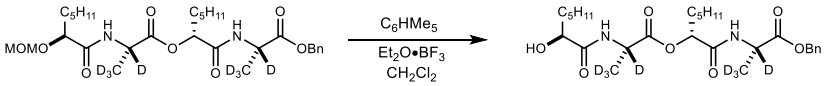

Benzyl ((*R*)-2-((((*S*)-2-hydroxyheptanoyl)-L-alanyl-2,3,3,3-d$_4$)oxy)heptanoyl)-L-alaninate-2,3,3,3-d$_4$ (S8). A flame-dried round-bottom flask was charged with the didepsipeptide (121 mg, 216 μmol) dissolved in dry dichloromethane (4.3 mL), pentamethyl benzene (96.1 mg, 648 μmol), and $BF_3{\cdot}Et_2O$ (80 μL, 650 μmol). The reaction was allowed to stir for 50 minutes at ambient temperature. The crude reaction mixture was quenched with satd aq $NaHCO_3$, washed with brine, dried, and concentrated. The residue was subjected to flash column chromatography (SiO_2, 15-40% ethyl acetate in hexanes) to afford the alcohol (88 mg, 79%) as a colorless oil. $[\alpha]_D^{23}$ -15.6 (*c* 1.13, $CHCl_3$); R_f = 0.26 (40% EtOAc/hexanes); IR (film) 3304, 2954, 2927, 2858, 1745, 1652, 1525, 1455, 1377, 1265, 1173, 1127, 1049 cm^{-1}; ^{1}H NMR (600 MHz, $CDCl_3$) δ 7.38-7.28 (m, 5H), 7.23 (br s, 1H), 7.10 (br s, 1H), 5.20 (d, *J* = 12.4 Hz, 1H), 5.16 (dd, *J* = 8.0, 3.9 Hz, 1H), 5.12 (d,

J = 12.3 Hz, 1H), 4.07 (dd, *J* = 7.7, 3.6 Hz, 1H), 3.34 (broad s, 1H), 1.94-1.74 (series of m, 3H), 1.64-1.55 (m, 1H), 1.44-1.19 (m, 12H), 0.87 (t, *J* = 7.0 Hz, 3H), 0.86 (t, *J* = 7.0 Hz, 3H); ^{13}C NMR (150 MHz, $CDCl_3$) ppm 174.9, 172.7, 172.5, 169.7, 135.6, 128.7, 128.4, 128.2, 74.7, 72.0, 67.1, 48.2 (t, *J* = 21.5 Hz), 47.8 (t, *J* = 21.4 Hz), 34.6, 31.7, 31.6, 31.4, 24.7, 24.6, 22.6, 22.5, 16.7 (sept, *J* = 19.6 Hz), 16.3 (sept, *J* = 19.6 Hz), 14.1, 14.0; HRMS (EI): Exact mass calcd for $C_{27}D_8H_{34}N_2NaO_7$ $[M+Na]^+$ 537.3386, found 537.3385. ANS-6-33.

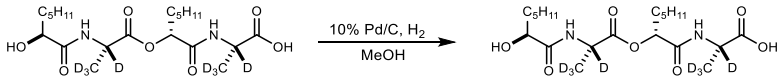

((*R*)-2-((((*S*)-2-hydroxyheptanoyl)-L-alanyl-2,3,3,3-d$_4$)oxy)heptanoyl)-L-alanine-2,3,3,3-d$_4$ (25). A round-bottom flask was charged with the tetradepsipeptide (88.0 mg, 171 μmol) dissolved in methanol (2.5 mL) and treated with 10% Pd/C (10 mg). The reaction flask was evacuated with a light vacuum (50 Torr). Hydrogen was added and the flask was cycled through a light vacuum once more. The reaction was allowed to stir for 1.5 h. The crude reaction mixture was filtered through Celite and concentrated to afford the deprotected tetradepsipeptide (72 mg, 99%) as a colorless oil. $[\alpha]_D^{23}$ -17 (*c* 0.67, $CHCl_3$); R_f = 0.10 (60% EtOAc/hexanes); IR (film) 3306, 2955, 2927, 2860, 1739, 1649, 1531, 1466, 1378, 1257, 1171, 1127, 1049 cm^{-1}; ^{1}H NMR (600 MHz, ($CDCl_3$) δ 7.37 (br s, 1H), 7.29 (br s, 1H), 5.17 (dd, *J* = 7.9, 3.9 Hz, 1H), 4.13 (ddd, *J* = 7.6, 3.7, 3.7 Hz, 1H), 1.96-1.74 (series of m, 3H), 1.65-1.56 (m, 1H), 1.45-1.22 (m, 12H), 0.88 (t, *J* = 6.2, 3H), 0.87 (t, *J* = 6.3, 3H) [OH and CO_2H not observed]; ^{13}C NMR (150 MHz, $CDCl_3$) ppm 175.5, 175.2, 172.6, 170.4, 74.8, 72.1, 48.4-47.5 (m, 2C), 34.5, 31.7, 31.6, 31.4, 24.7, 24.6, 22.6, 22.5, 17.0-16.0 (m, 2C), 14.1, 14.0; HRMS (EI): Exact mass calcd for $C_{20}D_8H_{28}N_2NaO_7$ $[M+Na]^+$ 547.2917, found 547.2918. ANS-6-37.

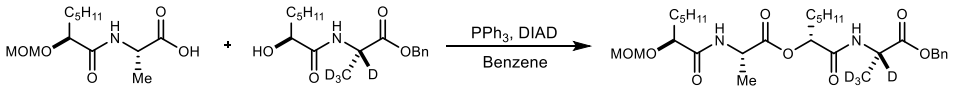

Benzyl ((*R*)-2-((((*S*)-2-(methoxymethoxy)heptanoyl)-L-alanyl)oxy)heptanoyl)-L-alaninate-2,3,3,3-d$_4$ (S9). A flame-dried round-bottom flask was charged with PPh_3 (92.3 mg, 352 μmol), DIAD (69.3 μL, 352 μmol), and benzene (3.5 mL). The reaction was allowed to stir for 30 minutes at ambient temperature. The alcohol (57.2 mg, 176 μmol) was added, followed by the acid (46 mg, 180 μmol), and the reaction was allowed to stir for 24 h. The crude reaction mixture was concentrated, and the residue was subjected to flash column chromatography (SiO_2, 15-60% ethyl acetate in hexanes) to afford the tetradepsipeptide (81.5 mg, 84%) as a white solid. $[\alpha]_D^{23}$ -19 (*c*

0.80, $CHCl_3$); Mp 110-115 °C; R_f = 0.11 (20% EtOAc/hexanes); IR (film) 3304, 2953, 2929, 2859, 1746, 1657, 1531, 1455, 1377, 1262, 1155, 1048 cm^{-1}; ^1H NMR (600 MHz, $CDCl_3$) δ 7.38-7.29 (m, 5H), 7.12 (s, 1H), 7.00 (d, *J* = 6.5 Hz, 1H), 5.20 (d, *J* = 12.3 Hz, 1H), 5.18 (dd, *J* = 8.3, 3.9 Hz, 1H), 5.12 (d, *J* = 12.4 Hz, 1H), 4.68 (s, 2H), 4.45 (dq, *J* = 7.0, 7.0 Hz, 1H), 4.03 (dd, *J* = 6.6, 4.6 Hz, 1H), 3.40 (s, 3H), 1.96-1.66 (series of m, 5H), 1.46 (d, *J* = 7.2 Hz, 3H), 1.42-1.20 (series of m, 15H), 0.87 (t, *J* = 7.1 Hz, 3H), 0.86 (t, *J* = 7.1 Hz, 3H); ^{13}C NMR (150 MHz, $CDCl_3$) ppm 173.2, 172.6, 172.3, 169.5, 135.7, 128.6, 128.4, 128.2, 96.4, 77.6, 74.8, 67.0, 56.4, 48.5, 47.7 (t, *J* = 21.8 Hz, 1C), 32.8, 31.7, 31.6, 31.4, 24.6, 24.4, 22.6, 22.5, 17.4, 16.7 (sept, *J* = 21.9 Hz), 14.11, 14.10; HRMS (EI): Exact mass calcd for $C_{31}D_4H_{46}N_2NaO_8$ $[M+Na]^+$ 577.3397, found 577.3397. ANS-6-172.

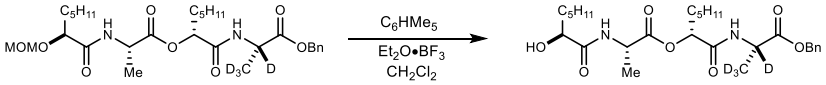

Benzyl ((*R*)-2-((((*S*)-2-hydroxyheptanoyl)-L-alanyl)oxy)heptanoyl)-L-alaninate-2,3,3,3-d_4 (S10). A flame-dried round-bottom flask was charged with the didepsipeptide (81.5 mg, 147 μmol) dissolved in dry dichloromethane (3.0 mL), pentamethyl benzene (65.4 mg, 441 μmol), and $BF_3{\cdot}Et_2O$ (55.0 μL, 441 μmol). The reaction was allowed to stir for 50 minutes at ambient temperature. The crude reaction mixture was quenched with satd aq $NaHCO_3$, washed with brine, dried, concentrated, and subjected to flash column chromatography (SiO_2, 15-40% ethyl acetate in hexanes) to afford the alcohol (68 mg, 91%) as a colorless oil. $[\alpha]_D^{23}$ -9.60 (*c* 1.35, $CHCl_3$); R_f = 0.16 (40% EtOAc/hexanes); IR (film) 3304, 2959, 2928, 2859, 1746, 1651, 1531, 1455, 1378, 1263, 1133, 1050 cm^{-1}; ^1H NMR (600 MHz, $CDCl_3$) δ 7.37-7.29 (m, 5H), 7.21 (br s, 1H), 7.09 (d, *J* = 6.3 Hz, 1H), 5.20 (d, *J* = 12.3 Hz, 1H), 5.17 (dd, *J* = 8.1, 4.0 Hz, 1H), 5.12 (d, *J* = 12.5 Hz, 1H), 4.44 (dq, *J* = 7.0, 6.9 Hz, 1H), 4.08 (dd, *J* = 7.6, 3.5 Hz, 1H), 3.30 (broad s, 1H), 2.00-1.73 (series of m, 3H), 1.64-1.55 (m, 1H), 1.46 (d, *J* = 7.6 Hz, 3H), 1.44-1.20 (m, 12H), 0.87 (t, *J* = 7.2 Hz, 3H), 0.86 (t, *J* = 7.3 Hz, 3H); ^{13}C NMR (150 MHz, $CDCl_3$) ppm 174.8, 172.8, 172.5, 169.7, 135.6, 128.7, 128.4, 128.2, 74.8, 72.1, 67.2, 48.6, 47.8 (t, *J* = 21.8 Hz), 34.6, 31.7, 31.6, 31.4, 24.7, 24.6, 22.6, 22.5, 17.1, 16.7 (sept, *J* = 19.8 Hz), 14.1, 14.0; HRMS (EI): Exact mass calcd for $C_{27}D_4H_{38}N_2NaO_7$ $[M+Na]^+$ 533.3135, found 533.3135. ANS-6-174.

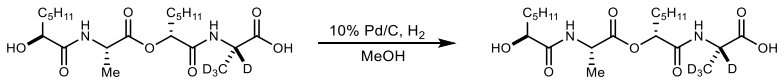

((*R*)-2-((((*S*)-2-hydroxyheptanoyl)-L-alanyl)oxy)heptanoyl)-L-alanine-2,3,3,3-d$_4$ (26). A round-bottom flask was charged with the tetradepsipeptide (68.0 mg, 133 μmol) dissolved in methanol (2.0 mL), and treated with 10% Pd/C (7 mg). The reaction flask was evacuated with a light vacuum (50 Torr). Hydrogen was added and the flask was cycled through a light vacuum once more. The reaction was allowed to stir for 1.5 h. The crude reaction mixture was filtered through Celite and concentrated to afford the deprotected tetradepsipeptide (55 mg, 99%) as a colorless oil. $[\alpha]_D^{23}$ -13.3 (*c* 1.15, $CHCl_3$); R_f = 0.13 (70% EtOAc/hexanes); IR (film) 3320, 2956, 2930, 2860, 1745, 1651, 1537, 1455, 1380, 1259, 1157, 1055 cm^{-1}; ^{1}H NMR (600 MHz, ($CDCl_3$) δ 7.38 (br d, *J* = 8.8 Hz, 1H), 7.34 (br d, *J* = 7.1 Hz, 1H), 5.20-5.14 (broad m, 1H), 4.55 (dq, *J* = 7.2, 7.1 Hz, 1H), 4.15-4.10 (broad m, 1H), 1.96-1.72 (series of m, 3H), 1.65-1.56 (m, 1H), 1.47 (d, *J* = 6.6 Hz, 3H), 1.44-1.22 (m, 12H), 0.873 (t, *J* = 5.9, 3H), 0.867 (t, *J* = 6.0, 3H) [OH and CO_2H not observed]; ^{13}C NMR (150 MHz, $CDCl_3$) ppm 175.5, 175.3, 172.6, 170.4, 74.8, 72.0, 48.5, 48.1-47.5 (m, 1C), 34.5, 31.7, 31.6, 31.4, 24.7, 24.6, 22.6, 22.5, 17.3, 16.9-16.0 (m, 1C), 14.12, 14.06; HRMS (EI): Exact mass calcd for $C_{20}D_4H_{32}N_2NaO_7$ $[M+Na]^+$ 443.2666, found 443.2666. ANS-6-177.

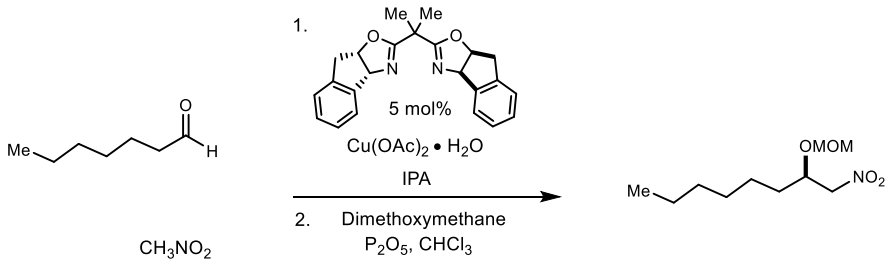

(*R*)-2-(Methoxymethoxy)-1-nitrooctane (S11). Following the Evans enantioselective Henry procedure,[1] IndaBOX[2] (141 mg, 394 μmol) and $Cu(OAc)_2$•H_2O (71.5 mg, 358 μmol) were stirred at ambient temperature in IPA (14 mL) for 1 h. The cerulean blue solution was then cooled to 0 °C and heptanal (1.0 mL, 7.12 mmol) was added and allowed to stir for 10 m before nitromethane (3.85 mL, 71.6 mmol) addition. After stirring for 5 days at ambient temperature, the reaction was quenched dropwise at 0 °C with 1 M aq HCl and the aqueous layer was extracted with CH_2Cl_2. After drying and concentration under reduced pressure, the crude alcohol was dissolved in $CHCl_3$ (35.6 mL), treated with P_2O_5 (10.1 g, 7.13 mmol) and dimethoxymethane (14.8 mL, 143 mmol), and stirred at ambient temperature overnight. The reaction mixture was diluted with DCM and decanted from the solid. The organic layer was then washed with satd aq $NaHCO_3$ and brine. The organic layers were dried and concentrated to afford an oil that was subjected to flash column

chromatography (SiO_2, 3-6% diethyl ether in hexanes) to afford the title compound as a colorless oil (1.09 g, 70%, 2 steps). The enantiopurity was determined to be 94% ee by chiral HPLC analysis (Chiralcel OD-H, 2% ^{i}PrOH /hexanes, 0.4 mL/min, t_r(e_1, major) = 16.2 min, t_r(e_2, minor) = 19.2 min). $[\alpha]_D^{24}$ -9.4 (c 0.44, $CHCl_3$); R_f = 0.17 (10% Et_2O/hexanes); IR (film) 2930, 2859, 1556, 1463, 1382, 1216, 1154, 1105, 1034 cm^{-1}; ^{1}H NMR (400 MHz, $CDCl_3$) δ 4.67 (d, J = 7.1 Hz, 1H), 4.64 (d, J = 7.1 Hz, 1H), 4.49 (dd, J= 12.5, 8.2 Hz, 1H), 4.41 (dd, J = 12.4, 3.9 Hz, 1H), 4.27 (dddd, J = 8.1, 6.1, 6.1, 3.9 Hz, 1H), 3.35 (s, 3H), 1.71-1.51 (m, 2H), 1.40-1.25 (m, 8H), 0.89 (t, J = 6.5 Hz, 3H); ^{13}C NMR (100 MHz, $CDCl_3$) ppm 96.4, 79.2, 75.1, 56.0, 32.5, 31.8, 29.3, 25.0, 22.7, 14.2; HRMS (EI): Exact mass calcd for $C_{10}H_{20}NO_4$ $[M-H]^+$ 218.1471, found 218.1390. ANS-2-253.

(*S*)-2-(Methoxymethoxy)-1-nitrooctane (*ent*-S11). Prepared following an identical procedure as **S11**. Flash column chromatography (SiO_2, 3-6% diether ether in hexanes) afforded the hydroxy-nitroalkane with spectroscopic data identical to its enantiomer, except the major/minor peaks were reversed by chiral HPLC analysis. The enantiopurity was determined to be 94% ee by chiral HPLC analysis (Chiralcel OD-H, 2% ^{i}PrOH /hexanes, 0.4 mL/min, t_r(e_1, minor) = 16.2 min, t_r(e_2, major) = 19.2 min). ANS-3-96.

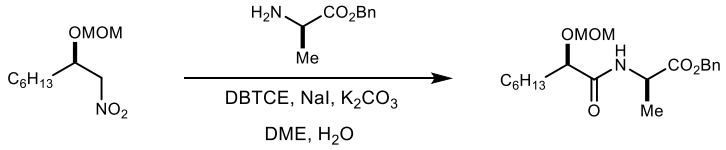

Benzyl ((*R*)-2-(methoxymethoxy)octanoyl)-D-alaninate (S12). A round-bottom flask was charged with nitroalkane (1.09 g, 4.97 mmol), amine (1.78 g, 9.95 mmol), DME (19.9 mL), and H_2O (450 μL, 5 equiv.). The mixture was then treated with DBTCE (1.94 g, 5.96 mmol) followed by NaI (74 mg, 497 μmol), K_2CO_3 (1.40 g, 9.95 mmol) and O_2 (balloon). The heterogeneous solution was vigorously stirred for 2 days at ambient temperature, and then treated at 0 °C with 1 M aq HCl and poured into CH_2Cl_2. The aqueous layer was extracted with CH_2Cl_2, and the combined organic layers were washed with satd aq $Na_2S_2O_3$, dried, and concentrated. The crude residue was subjected to flash column chromatography (SiO_2, 15% ethyl acetate in hexanes) to afford the amide as an orange solid (478 mg, 27%). $[\alpha]_D^{24}$ +46.5 (c 1.31, $CHCl_3$); R_f = 0.18 (20% EtOAc/hexanes); IR (film) 3409, 2930, 2859, 1742, 1666, 1523, 1454, 1209, 1156, 1030 cm^{-1}; ^{1}H NMR (400 MHz, $CDCl_3$) δ 7.40-7.30 (m, 5H), 7.08 (d, J = 7.5 Hz, 1H), 5.20 (d, J = 12.2 Hz, 1H), 5.15 (d, J = 12.2 Hz, 1H), 4.69 (dq, J= 7.5, 7.5 Hz, 1H), 4.66 (d, J = 6.6 Hz, 1H), 4.64 (d, J = 6.7

Hz, 1H), 4.07 (dd, *J* = 5.8, 5.2 Hz, 1H), 3.38 (s, 3H), 1.79-1.69 (m, 2H), 1.43 (d, *J* = 7.1 Hz, 3H) 1.40-1.23 (m, 8H), 0.87 (t, *J* = 6.6 Hz, 3H); ^{13}C NMR (100 MHz, $CDCl_3$) ppm 172.8, 172.2, 135.4, 128.8, 128.6, 128.3, 96.2, 77.6, 67.3, 56.3, 47.7, 32.9, 31.8, 29.2, 24.7, 22.7, 18.7, 14.2; HRMS (EI): Exact mass calcd for $C_{20}H_{32}NO_5$ $[M+H]^+$ 366.2275, found 366.2267. ANS-2-256.

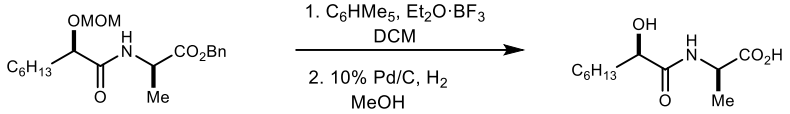

((*R*)-2-Hydroxyoctanoyl)-D-alanine (S13). A flame-dried round-bottom flask was charged with the depsipeptide (478 mg, 1.31 mmol), dry dichloromethane (26 mL), pentamethyl benzene (775 mg, 5.23 mmol), and $BF_3{\cdot}Et_2O$ (650 μL, 15.2 mmol). The reaction was allowed to stir for 50 m at ambient temperature. The crude reaction mixture was quenched with satd aq $NaHCO_3$, washed with brine, dried, concentrated, and subjected to flash column chromatography (SiO_2, 20-40% ethyl acetate in hexanes) to afford the alcohol as a colorless oil. This material was loaded into a round-bottom flask, dissolved in MeOH (8.2 mL), and treated with 10% Pd/C (27 mg). The reaction flask was evacuated with light vacuum (50 Torr). Hydrogen (balloon) was added the flask, and the cycle was repeated once more. The reaction was allowed to stir for 1 h. After purging the flask with nitrogen, the crude reaction mixture was filtered through Celite and concentrated to afford the deprotected depsipeptide (170 mg, 56%, 2 step) as a colorless oil. $[\alpha]_D^{26}$ +30 (*c* 0.99, $CHCl_3$); R_f = 0.12 (20% MeOH/DCM); IR (film) 3382, 2929, 2860, 1729, 1648, 1534, 1457, 1222, 1154 cm^{-1}; ^{1}H NMR (400 MHz, $CDCl_3$) δ 7.18 (br s, 1H), 4.53 (br s, 1H), 4.14 (br s, 1H), 1.83-1.53 (series of m, 3H), 1.48 (d, *J* = 5.7 Hz, 3H), 1.44-1.25 (m, 8H), 0.88 (t, *J* = 6.4 Hz, 3H), [*CO_2H* not observed]; ^{13}C NMR (150 MHz, $CDCl_3$) ppm 176.0, 175.9, 72.3, 48.1, 34.5, 31.8, 29.1, 25.1, 22.7, 17.6, 14.2; HRMS (EI): Exact mass calcd for $C_{11}H_{21}NNaO_4$ $[M+Na]^+$ 254.1363, found 254.1364. ANS-2-274.

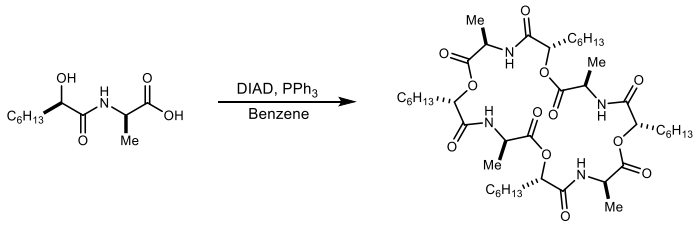

(3*R*,6*S*,9*R*,12*S*,15*R*,18*S*,21*R*,24*S*)-6,12,18,24-Tetrahexyl-3,9,15,21-tetramethyl-1,7,13,19-tetraoxa-4,10,16,22-tetraazacyclotetracosan-2,5,8,11,14,17,20,23-octaone (S14). A flame-dried round-bottom flask under inert atmosphere was charged with the depsipeptide (25.0 mg, 108

μmol), PPh_s (170 mg, 648 μmol), and benzene (5.4 mL). DIAD (106 μL, 540 μmol) was then added to the stirred solution in 15 aliquots over 2 h and 20 m. The reaction was allowed to stir for 24 h at ambient temperature. The crude reaction mixture was concentrated and filtered through a plug of silica gel to remove excess Mitsunobu reagents and to roughly separate macrocyclic products prior to separation using preparatory HPLC. A stepwise methanol in dichloromethane gradient allowed the crude mixture to be separated into two fractions (Fraction 1: 0.5-1.0% MeOH/DCM; Fraction 2: 15% MeOH/DCM). Fraction 2 was purified by preparative HPLC (45–95% aqueous acetonitrile, 210 nm, flow rate: 8 mL/min, R_t = 31.3 m) to afford the 24-membered macrocycle (5.0 mg, 22%) as a white solid. $[\alpha]_D^{26}$ +11 (*c* 0.56, $CHCl_3$); R_f = 0.33 (4% MeOH/DCM); IR (film) 3294, 2926, 2856, 1748, 1657, 1549, 1452, 1206, 1153, 1070 cm^{-1}; ^1H NMR (600 MHz, $CDCl_3$) δ 7.16 (d, *J* = 7.2 Hz, 1H), 5.10 (dd, *J* = 6.8, 5.4 Hz, 1H), 4.22 (dq, *J* = 7.2, 7.2 Hz, 1H), 1.94-1.85 (m, 1H), 1.70-1.59 (m, 1H), 1.46 (d, *J* = 6.9 Hz, 3H), 1.39-1.21 (m, 8H), 0.87 (t, *J* = 6.8 Hz, 3H); ^{13}C NMR (150 MHz, $CDCl_3$) ppm 171.2, 171.1, 74.4, 48.7, 31.8, 31.6, 29.0, 25.1, 22.7, 16.1, 14.2; HRMS (EI): Exact mass calcd for $C_{44}H_{76}N_4NaO_{12}$ $[M+Na]^+$ 875.5352, found 875.5354. ANS-2-276.

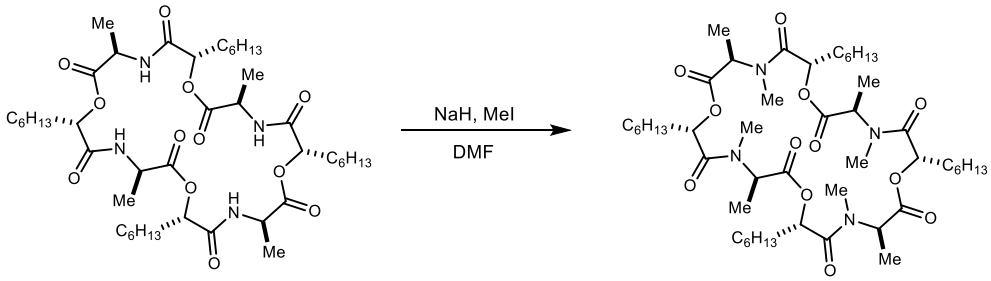

(3*R*,6*S*,9*R*,12*S*,15*R*,18*S*,21*R*,24*S*)-6,12,18,24-Tetrahexyl-3,4,9,10,15,16,21,22-octamethyl-1,7,13,19-tetraoxa-4,10,16,22-tetraazacyclotetracosan-2,5,8,11,14,17,20,23-octaone (34). A flame-dried round-bottom flask was charged with N-H depsipeptide (21.0 mg, 24.6 μmol) and dry DMF (492 μL) at 0 °C. Methyl iodide (61 μL, 980 μmol) was then added to the reaction mixture, and NaH (5.90 mg, 246 μmol in DMF (246 μL)) was added in 3 aliquots of 50 μL over 15 m. The reaction was allowed to stir at 0 °C for 20 m, and it was then quenched by the dropwise addition of satd aq NH_4Cl. The aqueous layer was extracted with EtOAc. The combined organic layers were washed with satd aq $NaHCO_3$, satd aq $Na_2S_2O_3$, water, brine, dried, concentrated, and subjected to flash column chromatography (SiO_2, 1-10% methanol in dichloromethane) to afford the alcohol (11.6 mg, 52%) as a colorless oil. $[\alpha]_D^{26}$ +28 (*c* 0.58, $CHCl_3$); R_f = 0.27 (4% MeOH/DCM); IR (film) 2927, 2857, 1743, 1662, 1461, 1198, 1089 cm^{-1}; ^1H NMR (600 MHz,

$CDCl_3$) This compound exists in multiple conformations, causing significant peak overlap. Refer to image of the ^1H NMR spectrum; ^{13}C NMR (150 MHz, $CDCl_3$) This compound exists in multiple conformations, causing significant peak overlap. Refer to image of the ^{13}C NMR spectrum; HRMS (EI): Exact mass calcd for $C_{48}H_{85}N_4O_{12}$ $[M+H]^+$ 909.6159, found 909.6162. ANS-3-09.

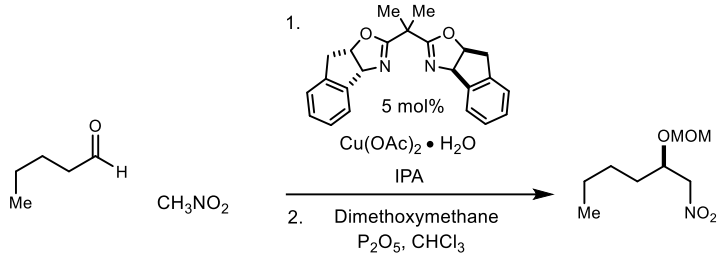

(*R*)-2-(Methoxymethoxy)-1-nitrohexane (S15). Following the Evans protocol,[1] IndaBOX (177 mg, 495 μmol) and $Cu(OAc)_2$•H_2O (89.8 mg, 450 μmol) were stirred at ambient temperature in isopropanol (18 mL) for 1 h. The cerulean blue solution was then cooled to 0 °C, and hexanal (1.0 mL, 9.0 mmol) was added and allowed to stir for 10 m before nitromethane (4.8 mL, 90 mmol) addition. After stirring for 4 days at ambient temperature, the reaction was quenched dropwise at 0 °C with 1 M aq HCl and the aqueous layer was extracted with CH_2Cl_2. Following drying and concentration under reduced pressure, the crude alcohol was dissolved in $CHCl_3$ (45.0 mL), treated with P_2O_5 (12.8 g, 89.9 mmol) and dimethoxymethane (18.7 mL, 179 mmol), and stirred at ambient temperature overnight. The reaction mixture was diluted with DCM and decanted from the solid. The organic layer was then washed with satd aq $NaHCO_3$ and brine. The organic layers were dried and concentrated to afford an oil that was subjected to flash column chromatography (SiO_2, 3-6% diethyl ether in hexanes) to afford the title compound as a pale-yellow oil (1.31 g, 77%, 2 steps). The enantiopurity was determined to be 95% ee by chiral HPLC analysis (Chiralcel OD-H, 2% ^{i}PrOH /hexanes, 0.4 mL/min, t_r(*e1*, major) = 16.2 min, t_r(*e2*, minor) = 18.0 min). $[\alpha]_D^{22}$ -26.0 (*c* 1.47, $CHCl_3$); R_f = 0.40 (10% Et_2O/hexanes); IR (film) 2957, 2871, 1556, 1383, 1038 cm^{-1}; ^1H NMR (600 MHz, $CDCl_3$) δ 4.62 (d, *J* = 7.2 Hz, 1H), 4.64 (d, *J* = 6.9 Hz, 1H), 4.49 (dd, *J*= 12.4, 8.1 Hz, 1H), 4.41 (dd, *J* = 12.6, 3.7 Hz, 1H), 4.27 (dddd, *J* = 8.2, 6.2, 6.2, 4.0 Hz, 1H), 3.35 (s, 3H), 1.70-1.62 (m, 1H), 1.62-1.54 (m, 1H), 1.40-1.30 (m, 4H), 0.92 (t, *J* = 7.0 Hz, 3H); ^{13}C NMR (150 MHz, $CDCl_3$) ppm 96.4, 79.2, 75.0, 56.0, 32.2, 27.2, 22.7, 14.0; HRMS (EI): Exact mass calcd for $C_8H_{16}NO_4$ $[M-H]^-$ 190.1074, found 190.1078. ANS-2-146.

(*S*)-2-(Methoxymethoxy)-1-nitrohexane (*ent*-S15). Prepared following an identical procedure as **S15**. Flash column chromatography (SiO_2, 3-6% diethyl ether in hexanes) afforded the hydroxy-

nitroalkane with spectroscopic data identical to its enantiomer, except the major/minor peaks were reversed by chiral HPLC analysis. The enantiopurity was determined to be 93% ee by chiral HPLC analysis (Chiralcel OD-H, 2% ^{i}PrOH /hexanes, 0.4 mL/min, t_r(e_1, minor) = 16.2 min, t_r(e_2, major) = 18.0 min). ANS-3-97.

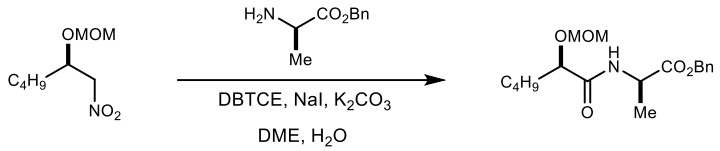

Benzyl ((*R*)-2-(methoxymethoxy)hexanoyl)-D-alaninate (S16). A round-bottom flask was charged with nitroalkane (1.30 g, 6.80 mmol), amine (2.44 g, 13.6 mmol), DME (27.2 mL), and H_2O (612 μL, 5 e.). The mixture was then treated with DBTCE (2.66 g, 8.16 mmol) followed by NaI (102 mg, 680 μmol), K_2CO_3 (1.88 g, 13.6 mmol) and O_2 (balloon). The heterogeneous solution was vigorously stirred for 2 days at ambient temperature, and then treated at 0 °C with 1 M aq HCl and poured into CH_2Cl_2. The aqueous layer was extracted with CH_2Cl_2, and the combined organic layers were washed with satd aq $Na_2S_2O_3$, dried, and concentrated. The crude residue was subjected to flash column chromatography (SiO_2, 15% ethyl acetate in hexanes) to afford the amide as an orange solid (529 mg, 23%). $[\alpha]_D^{24}$ +41 (*c* 0.94, $CHCl_3$); Mp 63-67 °C; R_f = 0.14 (20% EtOAc/hexanes); IR (film) 3409, 3033, 2955, 1740, 1664, 1526, 1455, 1381, 1213, 1156, 1032 cm^{-1}; ^{1}H NMR (600 MHz, $CDCl_3$) δ 7.40-7.32 (m, 5H), 7.09 (d, *J* = 7.7 Hz, 1H), 5.20 (d, *J* = 12.2 Hz, 1H), 5.15 (d, *J* = 12.2 Hz, 1H), 4.69 (dq, *J*= 7.4, 7.4 Hz, 1H), 4.66 (d, *J* = 6.7 Hz, 1H), 4.65 (d, *J* = 6.5 Hz, 1H), 4.07 (dd, *J* = 6.3, 4.7 Hz, 1H), 3.38 (s, 3H), 1.83-1.69 (m, 2H), 1.43 (d, *J* = 6.9 Hz, 3H), 1.40-1.29 (m, 4H), 0.89 (t, *J* = 7.1 Hz, 3H); ^{13}C NMR (150 MHz, $CDCl_3$) ppm 172.8, 172.2, 135.4, 128.8, 128.6, 128.3, 96.2, 77.5, 67.3, 56.3, 47.7, 32.6, 26.9, 22.6, 18.7, 14.1; HRMS (EI): Exact mass calcd for $C_{18}H_{28}NO_5$ $[M+H]^+$ 338.1962, found 338.1990. ANS-2-152.

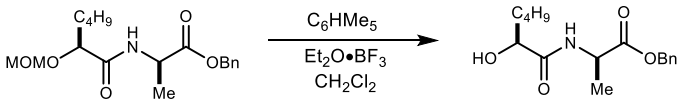

Benzyl ((*S*)-2-hydroxyhexanoyl)-D-alaninate (S17). A flame-dried round-bottom flask was charged with the didepsipeptide (600 mg, 1.78 mmol) dissolved in dry dichloromethane (0.05 M), pentamethyl benzene (1.05 g, 7.22 mmol), and $BF_3{\cdot}Et_2O$ (880 μL, 7.22 mmol). The reaction was allowed to stir for 50 minutes at ambient temperature. The crude reaction mixture was quenched with satd aq $NaHCO_3$, washed with brine, dried, concentrated, and subjected to flash column chromatography (SiO_2, 15-40% ethyl acetate in hexanes) to afford the alcohol (397.0 mg, 77%) as

a pale-yellow oil. $[\alpha]_D^{20}$ +38 (*c* 0.58, $CHCl_3$); R_f = 0.12 (20% EtOAc/hexanes); IR (film) 3392, 2965, 2869, 1742, 1655, 1526, 1455, 1385, 1206, 1156 cm^{-1}; ^1H NMR (600 MHz, $CDCl_3$) δ 7.39-7.31 (m, 5H), 6.98 (d, *J* = 7.5 Hz, 1H), 5.20 (d, *J* = 12.4 Hz, 1H), 5.16 (d, *J* = 12.2 Hz, 1H), 4.65 (ddd, *J* = 7.4, 7.4, 7.4 Hz, 1H), 4.12 (dq, *J* = 4.6, 4.0 Hz, 1H), 2.66 (d, *J* = 5.0 Hz, 1H), 1.87-1.78 (m, 1H), 1.67-1.60 (m, 1H), 1.44 (d, *J* = 7.4 Hz, 3H), 1.42-1.28 (m, 4H), 0.90 (t, *J* = 7.2 Hz, 3H); ^{13}C NMR (150 MHz, $CDCl_3$) ppm 173.6, 172.9, 135.4, 128.8, 128.6, 128.3, 72.2, 67.4, 47.9, 34.6, 27.2, 22.6, 18.6, 14.1; HRMS (EI): Exact mass calcd for $C_{16}H_{24}NO_4$ $[M+H]^+$ 294.1700, found 294.1706. ANS-2-200.

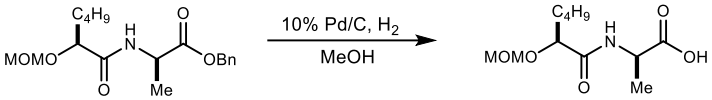

((*S*)-2-(Methoxymethoxy)hexanoyl)-D-alanine (S18). A round-bottom flask was charged with the didepsipeptide (504 mg, 1.49 mmol) dissolved in methanol (0.1 M), and treated with 10% Pd/C (50 mg). The reaction flask was evacuated with a light vacuum (50 Torr). Hydrogen (balloon) was added and then the flask was cycled through a light vacuum once again. The reaction was stirred for 1.5 h. The crude reaction mixture was filtered through Celite and concentrated to afford the deprotected didepsipeptide (331 mg, 90%) as a pale-yellow oil. $[\alpha]_D^{20}$ +57.8 (*c* 1.09, $CHCl_3$); R_f = 0.20 (4% MeOH/DCM); IR (film) 3401, 3316, 2956, 1737, 1642, 1533, 1457, 1215, 1156, 1037cm^{-1}; ^1H NMR (600 MHz, $CDCl_3$) δ 10.85 (br s, 1H), 7.18 (d, *J* = 7.0 Hz, 1H), 4.69 (br s, 2H), 4.62 (ddd, *J* = 7.2, 7.2, 7.2 Hz, 1H), 4.14-4.07 (m, 1H), 3.41 (s, 3H), 1.85-1.69 (m, 2H), 1.46 (d, *J* = 6.9 Hz, 3H), 1.43-1.27 (m, 4H), 0.88 (t, *J* = 7.1 Hz, 3H); ^{13}C NMR (150 MHz, $CDCl_3$) ppm 176.3, 173.2, 96.3, 77.5, 56.4, 47.8, 32.6, 26.8, 22.6, 18.3, 14.0; HRMS (EI): Exact mass calcd for $C_{11}H_{20}NO_5$ $[M-H]^-$ 246.1347, found 246.1342. ANS-2-201.

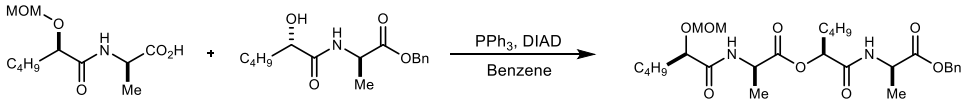

Benzyl ((*S*)-2-((((*R*)-2-(methoxymethoxy)hexanoyl)-D-alanyl)oxy)hexanoyl)-D-alaninate (S19). A flame-dried round-bottom flask was charged with PPh_3 (626 mg, 2.38 mmol), DIAD (468 μL, 2.38 mmol), and benzene (23.8 mL). The reaction was allowed to stir for 30 minutes at ambient temperature. The alcohol (350 mg, 1.19 mmol) was added, followed by the acid (325 mg, 1.31 mmol), and the reaction was allowed to stir for 24 h. The crude reaction mixture was concentrated and subjected to flash column chromatography (SiO_2, 15-60% ethyl acetate in hexanes) to afford the tetradepsipeptide (614 mg, 98%) as a pale yellow solid. $[\alpha]_D^{20}$ +28 (*c* 0.20, $CHCl_3$); Mp 90-93

°C; R_f = 0.24 (40% EtOAc/hexanes); IR (film) 3304, 2924, 2854, 1747, 1659, 1534, 1457, 1378, 1202, 1155, 1006 cm^{-1}; ^1H NMR (600 MHz, $CDCl_3$) δ 7.39-7.30 (m, 5H), 7.11 (d, *J* = 7.2 Hz, 1H), 6.99 (d, *J* = 6.5 Hz, 1H), 5.21 (d, *J* = 12.4 Hz, 1H), 5.19 (dd, *J* = 8.3, 4.1 Hz, 1H), 5.13 (d, *J* = 12.4 Hz, 1H), 4.68 (s, 2H), 4.60 (dq, *J* = 7.3, 7.3 Hz, 1H), 4.45 (dq, *J* = 7.0, 7.0 Hz, 1H), 4.04 (dd, *J* = 6.6, 4.4 Hz, 1H), 3.41 (s, 3H), 2.0-1.89 (m, 1H), 1.88-1.68 (series of m, 3H), 1.48 (d, *J* = 7.2 Hz, 3H), 1.44 (d, *J* = 7.2 Hz, 3H), 1.39-1.28 (br m, 8H), 0.89 (t, *J* = 7.2 Hz, 3H), 0.88 (t, *J* = 7.2 Hz, 3H); ^{13}C NMR (150 MHz, $CDCl_3$) ppm 173.2, 172.6, 172.3, 169.5, 135.7, 128.7, 128.4, 128.2, 96.5, 77.7, 74.8, 67.1, 56.4, 48.6, 48.2, 32.5, 31.5, 27.1, 26.9, 22.6, 22.4, 17.6, 17.4, 14.1, 14.0; HRMS (EI): Exact mass calcd for $C_{27}H_{42}N_2NaO_8$ $[M+Na]^+$ 545.2833, found 545.2835. ANS-2-203.

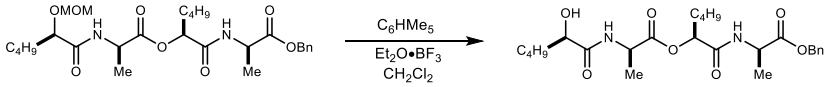

Benzyl ((*S*)-2-((((*R*)-2-hydroxyhexanoyl)-D-alanyl)oxy)hexanoyl)-D-alaninate (S20). A flame-dried round-bottom flask was charged with the didepsipeptide (614 mg, 1.17 mmol) dissolved in dry dichloromethane (0.05 M), pentamethyl benzene (697 mg, 4.70 mmol), and $BF_3{\cdot}Et_2O$ (580 μL, 4.70 mmol). The reaction was allowed to stir for 50 minutes at ambient temperature. The crude reaction mixture was quenched with satd aq $NaHCO_3$, washed with brine, dried, concentrated, and subjected to flash column chromatography (SiO_2, 15-40% ethyl acetate in hexanes) to afford the alcohol (528 mg, 93%) as a pale-yellow oil. $[\alpha]_D^{26}$ +20 (*c* 0.96, $CHCl_3$); R_f = 0.20 (40% EtOAc/hexanes); IR (film) 3313, 2956, 2868, 1747, 1654, 1534, 1455, 1380, 1201, 1155 cm^{-1}; ^1H NMR (600 MHz, $CDCl_3$) δ 7.38-7.30 (m, 5H), 7.18 (br s, 1H), 7.00 (br s, 1H), 5.21 (d, *J* = 12.2 Hz, 1H), 5.19 (dd, *J* = 8.0, 4.0 Hz, 2H), 5.13 (d, *J* = 12.4 Hz, 1H), 4.59 (dq, *J* = 7.2, 7.2 Hz, 1H), 4.49-4.42 (m, 1H), 4.10 (ddd, *J* = 7.8, 7.8, 3.9 Hz, 1H), 3.00-2.79 (br m, 1H), 1.96-1.88 (m, 1H), 1.87-1.76 (m, 2H), 1.66-1.57 (m, 1H), 1.47 (d, *J* = 7.4 Hz, 3H), 1.43 (d, *J* = 7.6 Hz, 3H), 1.41-1.27 (series of m, 8H), 0.90 (t, *J* = 7.9 Hz, 3H), 0.87 (t, *J* = 7.3 Hz, 3H); ^{13}C NMR (150 MHz, $CDCl_3$) ppm 174.6, 172.8, 172.3, 169.5, 135.6, 128.7, 128.5, 128.2, 74.8, 72.1, 67.2, 48.6, 48.2, 34.4, 31.5, 27.1, 27.0, 22.5, 22.4, 17.7, 17.2, 14.1, 14.0; HRMS (EI): Exact mass calcd for $C_{25}H_{38}N_2NaO_7$ $[M+Na]^+$ 501.2571, found 501.2579. ANS-2-206.

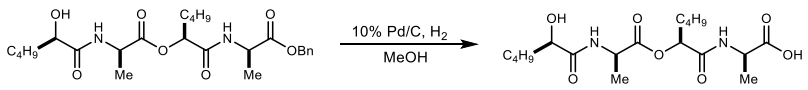

((*S*)-2-((((*R*)-2-Hydroxyhexanoyl)-D-alanyl)oxy)hexanoyl)-D-alanine (S21). A round-bottom flask was charged with the tetradepsipeptide (520 mg, 1.08 mmol) dissolved in methanol (0.1 M), and treated with 10% Pd/C (50 mg). The reaction flask was evacuated with a light vacuum (50 Torr). Hydrogen was added and the flask was cycled through a light vacuum once more. The reaction was allowed to stir for 1.5 h. The crude reaction mixture was filtered through Celite and concentrated to afford the deprotected tetradepsipeptide (360 mg, 86%) as a pale-yellow oil. $[\alpha]_D^{26}$ +17 (*c* 0.21, $CHCl_3$); R_f = 0.40 (10% MeOH/DCM); IR (film) 3317, 2957, 2870, 1745, 1652, 1536, 1457, 1380, 1208, 1155, 1058 cm^{-1}; ^1H NMR (600 MHz, ($CDCl_3$) δ 7.42 (br d, *J* = 5.1 Hz, 1H), 7.18 (br s, 1H), 5.17 (dd, *J* = 7.9, 4.1 Hz, 1H), 4.58-4.46 (br m, 2H), 4.15 (br s, 1H), 1.99-1.77 (series of m, 3H), 1.68-1.58 (m, 1H), 1.49 (d, *J* = 7.2 Hz, 3H), 1.45 (d, *J* = 7.2 Hz, 3H), 1.42-1.29 (m, 8H), 0.91 (t, *J* = 7.1, 3H), 0.90 (t, *J* = 6.6, 3H) [OH and CO_2H not observed]; ^{13}C NMR (150 MHz, $CDCl_3$) ppm 175.2, 174.9, 172.5, 170.7, 77.3, 74.8, 72.1, 48.5, 34.3, 31.4, 27.14, 27.10, 22.5, 22.4, 17.2 (2C), 14.1, 14.0; HRMS (EI): Exact mass calcd for $C_{18}H_{33}N_2O_7$ $[M+H]^+$ 389.2282, found 389.2285. ANS-2-208.

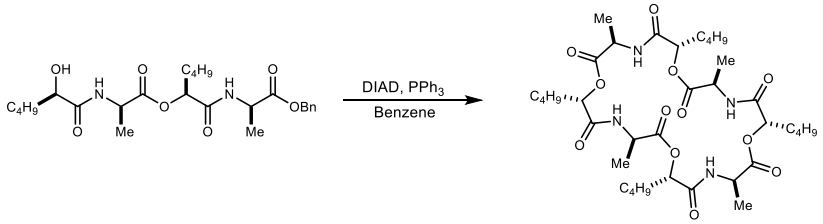

(3*R*,6*S*,9*R*,12*S*,15*R*,18*S*,21*R*,24*S*)-6,12,18,24-Tetrabutyl-3,9,15,21-tetramethyl-1,7,13,19-tetraoxa-4,10,16,22-tetraazacyclotetracosan-2,5,8,11,14,17,20,23-octaone (S22). A flame-dried round-bottom flask under inert atmosphere was charged with the tetradepsipeptide (25.0 mg, 64.4 μmol), PPh_s (50.6 mg, 193 μmol), and benzene (12.9 mL). DIAD (31.7 μL, 161 μmol) was then added to the stirred solution in 5 aliquots over 40 m. The reaction was allowed to stir for 24 h at ambient temperature. The crude reaction mixture was concentrated and filtered through a plug of silica gel to remove excess Mitsunobu reagents and to roughly separate macrocyclic products prior to separation using preparatory HPLC. A stepwise methanol in dichloromethane gradient allowed the crude mixture to be separated into two fractions (Fraction 1: 0.5-1.0% MeOH/DCM; Fraction 2: 15% MeOH/DCM). Fraction 2 was purified by preparative HPLC (45–95% aqueous acetonitrile, 210 nm, flow rate: 8 mL/min, R_t = 21.3 m) to afford the 24-membered macrocycle (9.7 mg, 41%) as a white solid. $[\alpha]_D^{26}$ +17 (*c* 0.97, $CHCl_3$); R_f = 0.27 (4% MeOH/DCM); IR (film) 3302, 2931, 2863, 1747, 1658, 1548, 1453, 1208, 1156 cm^{-1}; ^1H NMR (600 MHz, $CDCl_3$) δ 7.16

(d, *J* = 7.2 Hz, 1H), 5.10 (dd, *J* = 7.2, 5.3 Hz, 1H), 4.22 (dq, *J* = 7.1, 7.1 Hz, 1H), 1.96-1.85 (m, 1H), 1.71-1.61 (m, 1H), 1.47 (d, *J* = 6.9 Hz, 3H), 1.38-1.25 (m, 4H), 0.87 (t, *J* = 6.8 Hz, 3H); ^{13}C NMR (150 MHz, $CDCl_3$) ppm 171.2, 171.1, 74.4, 48.7, 31.4, 27.3, 22.5, 16.1, 14.0; HRMS (EI): Exact mass calcd for $C_{36}H_{60}N_4NaO_{12}$ $[M+Na]^+$ 763.4100, found 763.4101. ANS-2-209.

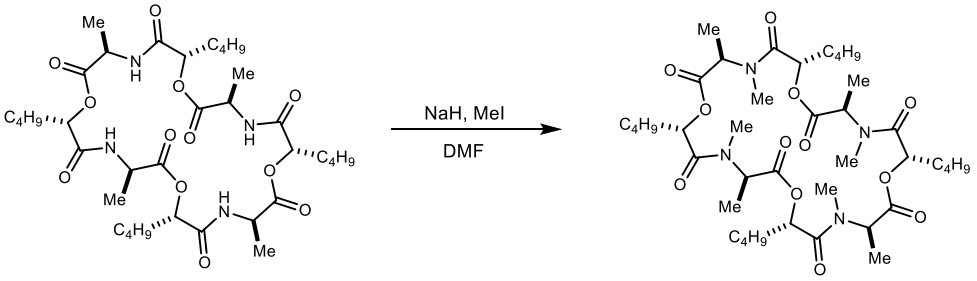

(3*R*,6*S*,9*R*,12*S*,15*R*,18*S*,21*R*,24*S*)-6,12,18,24-Tetrabutyl-3,4,9,10,15,16,21,22-octamethyl-1,7,13,19-tetraoxa-4,10,16,22-tetraazacyclotetracosan-2,5,8,11,14,17,20,23-octaone (35). A flame-dried round-bottom flask was charged with N-H depsipeptide (24.1 mg, 32.5 μmol) and dry DMF (650 μL) at 0 °C. Methyl iodide (80 μL, 1.30 mmol) was then added to the reaction mixture, and NaH (7.8 mg, 325 μmol in DMF (325 μL)) was added in 3 aliquots of 65 μL over 15 m. The reaction was allowed to stir at 0 °C for 20 m, and it was then quenched by the dropwise addition of satd aq NH_4Cl. The aqueous layer was extracted with EtOAc. The combined organic layers were washed with satd aq $NaHCO_3$, satd aq $Na_2S_2O_3$, water, brine, dried, concentrated, and subjected to flash column chromatography (SiO_2, 1-10% methanol in dichloromethane) to afford the alcohol (9.4 mg, 36%) as a colorless oil. $[\alpha]_D^{26}$ +34 (*c* 0.73, $CHCl_3$); R_f = 0.46 (4% MeOH/DCM); IR (film) 2930, 2855, 1742, 1662, 1461, 1412, 1196, 1086 cm^{-1}; ^{1}H NMR (600 MHz, $CDCl_3$) This compound exists in multiple conformations, causing significant peak overlap. Refer to image of the ^{1}H NMR spectrum; ^{13}C NMR (150 MHz, $CDCl_3$) This compound exists in multiple conformations, causing significant peak overlap. Refer to image of the ^{13}C NMR spectrum; HRMS (EI): Exact mass calcd for $C_{40}H_{68}N_4NaO_{12}$ $[M+Na]^+$ 819.4726, found 819.4748. ANS-2-235.

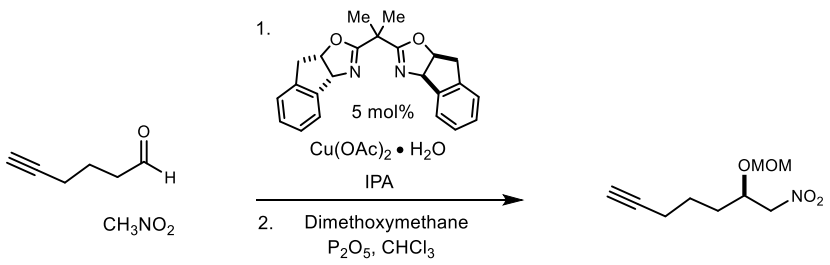

(*R*)-6-(Methoxymethoxy)-7-nitrohept-1-yne (39). Following the Evans enantioselective Henry procedure,[1] IndaBOX[2] (82.0 mg, 230 μmol) and $Cu(OAc)_2 \bullet H_2O$ (41.5 mg, 210 μmol) were stirred at ambient temperature in isopropanol (8.3 mL) for 1 h. The cerulean blue solution was then cooled to 0 °C and heptanal (400 mg, 4.16 mmol) was added and allowed to stir for 10 m before nitromethane (2.20 mL, 41.6 mmol) addition. After stirring for 5 days at ambient temperature, the reaction was quenched dropwise at 0 °C with 1 M aq HCl and the aqueous layer was extracted with CH_2Cl_2. Following drying and concentration under reduced pressure, the crude alcohol was dissolved in $CHCl_3$ (20.8 mL), treated with P_2O_5 (5.90 g, 41.6 mmol) and dimethoxymethane (8.6 mL, 83.2 mmol), and stirred at ambient temperature overnight. The reaction mixture was diluted with DCM and decanted from the solid. The organic layer was then washed with satd aq $NaHCO_3$ and brine. The organic layers were dried and concentrated to afford an oil that was subjected to flash column chromatography (SiO_2, 3-6% diethyl ether in hexanes) to afford the title compound as a colorless oil (238 mg, 30%, 2 steps). The enantiopurity was determined to be 93% ee by chiral HPLC analysis (Chiralcel OD-H, 20% ^{i}PrOH /hexanes, 0.4 mL/min, t_r(*e1*, major) = 15.6 min, t_r(*e2*, minor) = 17.6 min). $[\alpha]_D^{24}$ -14 (*c* 0.69, $CHCl_3$); R_f = 0.19 (15% Et_2O/hexanes); IR (film) 3293, 2946, 1556, 1433, 1383, 1234, 1151, 1105, 1031 cm^{-1}; ^{1}H NMR (400 MHz, $CDCl_3$) δ 4.68 (d, *J* = 7.2 Hz, 1H), 4.66 (d, *J* = 7.2 Hz, 1H), 4.52 (dd, *J*= 12.4, 8.0 Hz, 1H), 4.42 (dd, *J* = 12.4, 3.9 Hz, 1H), 4.34-4.27 (m, 1H), 3.36 (s, 3H), 2.25 (td, *J* = 6.8, 2.6 Hz, 2H), 1.98 (t, *J* = 2.7 Hz, 1H), 1.80-1.70 (m, 2H), 1.70-1.56 (m, 2H); ^{13}C NMR (100 MHz, $CDCl_3$) ppm 96.5, 83.5, 79.1, 74.6, 69.3, 56.1, 31.5, 23.9, 18.4; HRMS (EI): Exact mass calcd for $C_9H_{14}NO_4$ $[M-H]^+$ 200.0917, found 200.0917. ANS-2-259.

(*S*)-6-(Methoxymethoxy)-7-nitrohept-1-yne (*ent*-39). Prepared following an identical procedure as **39**. Flash column chromatography (SiO_2, 3-6% diethyl ether in hexanes) afforded the hydroxy-nitroalkane with spectroscopic data identical to its enantiomer, except the major/minor peaks were reversed by chiral HPLC analysis. The enantiopurity was determined to be 92% ee by chiral HPLC analysis (Chiralcel OD-H, 20% ^{i}PrOH /hexanes, 0.4 mL/min, t_r(*e1*, minor) = 15.6 min, t_r(*e2*, major) = 17.5 min). ANS-3-189.

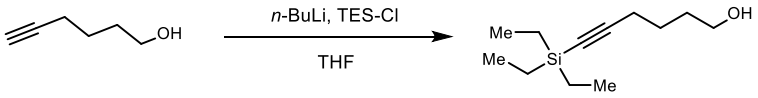

6-(Triethylsilyl)hex-5-yn-1-ol (S23). A flame-dried round-bottom flask was charged with 5-hexyn-1-ol (1.0 mL, 10.2 mmol), and THF (31 mL). The mixture was cooled to -78 °C and then

n-BuLi (10.8 mL, 2 M in hexanes, 23.4 mmol) was added. The reaction was allowed to stir for 1 h under an argon atmosphere at -78 °C. TES-Cl (6.2 mL, 37 mmol) was added and the reaction was allowed to warm to ambient temperature and stir for an additional 4 h. The reaction was treated with 1 M aq HCl and poured into EtOAc. The aqueous layer was extracted with EtOAC, and the combined organic layers were washed with water and, brine, dried, and concentrated. The crude residue was subjected to flash column chromatography (SiO_2, 20% ethyl acetate in hexanes) to afford the product as a pale-yellow oil (1.85 g, 85%). R_f = 0.22 (20% EtOAc/hexanes); IR (film) 3346, 2953, 2875, 2171, 1458, 1045, 1016, 726 cm^{-1}; ^1H NMR (600 MHz, $CDCl_3$) δ 3.69 (ddd, *J* = 8.4, 8.4, 6.4 Hz, 2H), 2.29 (t, *J* = 6.9 Hz, 2H), 1.72-1.65 (m, 2H), 1.62-1.59 (m, 2H), 1.28 (br s, 1H), 0.98 (t, *J* = 8.0 Hz, 9H), 0.57 (q, *J* = 8.0 Hz, 6H); ^{13}C NMR (150 MHz, $CDCl_3$) ppm 108.4, 82.1, 62.6, 31.9, 25.2, 19.8, 7.6, 4.7; HRMS (EI): Exact mass calcd for $C_{12}H_{25}OSi$ $[M+H]^+$ 213.1669, found 213.1669. ANS-3-169.

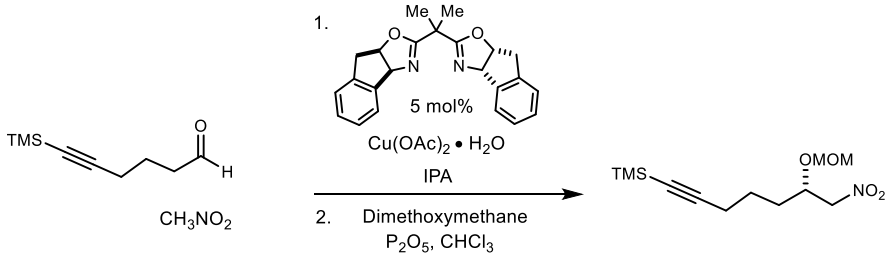

(*S*)-(6-(Methoxymethoxy)-7-nitrohept-1-yn-1-yl)trimethylsilane (47). Following the Evans enantioselective Henry procedure,[1] IndaBOX[2] (87.4 mg, 244 μmol), and $Cu(OAc)_2$•H_2O (44.2 mg, 222 μmol) were stirred at ambient temperature in IPA (8.6 mL) for 1 h. The cerulean blue solution was then cooled to 0 °C and the aldehyde (746 mg, 4.43 mmol) was added and allowed to stir for 10 m before nitromethane (2.34 mL, 44.3 mmol) addition. After stirring for 5 days at ambient temperature, the reaction was quenched dropwise at 0 °C with 1 M aq HCl and the aqueous layer was extracted with CH_2Cl_2. After drying and concentration under reduced pressure, the crude alcohol was dissolved in $CHCl_3$ (22.2 mL), treated with P_2O_5 (6.3 g, 44.4 mmol) and dimethoxymethane (9.3 mL, 89 mmol), and stirred at ambient temperature overnight. The reaction mixture was diluted with DCM and decanted from the solid. The organic layer was then washed with satd aq $NaHCO_3$ and brine. The organic layers were dried and concentrated to afford an oil that was subjected to flash column chromatography (SiO_2, 5-10% Et_2O/hexanes) to afford the title compound as a colorless oil (376 mg, 31%, 2 steps). $[\alpha]_D^{24}$ +15.5 (*c* 1.20, CHCl3); R_f = 0.30 (10% Et_2O/hexanes); IR (film) 2957, 2174, 1557, 1249, 1151, 1034, 844 cm^{-1}; ^1H NMR (400 MHz,

$CDCl_3$) δ 4.66 (d, *J* = 7.2 Hz, 1H), 4.63 (d, *J* = 7.2 Hz, 1H), 4.5 (dd, *J*= 12.4, 8.1 Hz, 1H), 4.41 (dd, *J* = 12.6, 4.0 Hz, 1H), 4.34-4.27 (m, 1H), 3.34 (s, 3H), 2.25 (apparent t, *J* = 6.8 Hz, 2H), 1.78-1.54 (series of m, 4H), 0.13 (s, 9H); ^{13}C NMR (100 MHz, $CDCl_3$) ppm 106.2, 96.4, 85.3, 79.0, 74.5, 56.0, 31.4, 23.9, 19.8, 0.2; HRMS (EI): Exact mass calcd for $C_{12}H_{23}NNaO_4Si$ $[M+Na]^+$ 296.1289, found 296.1280. ANS-3-118.[5]

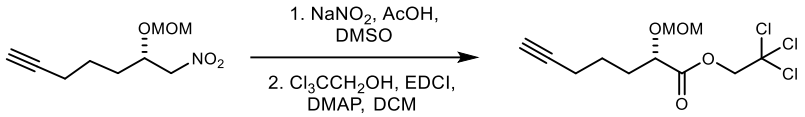

2,2,2-Trichloroethyl (*S*)-2-(methoxymethoxy)hept-6-ynoate (50). A round-bottom flask was charged with nitroalkane (823 mg, 4.09 mmol), $NaNO_2$ (847 mg, 12.3 mmol), AcOH (3.2 mL, 61.4 mmol), and DMSO (32 mL). The mixture was stirred at 60 °C for 18 h under an argon atmosphere. The reaction was then allowed to cool to ambient temperature, treated with 1 N HCl, and poured into CH_2Cl_2. The aqueous layer was extracted with CH_2Cl_2, and the combined organic layers were washed with water and brine, dried, and concentrated. The crude mixture was then added to a round-bottom flask and charged with trichloroethanol (376 μL, 3.90 mmol). The reaction was cooled to 0 °C and then treated with EDCI (855 mg, 4.46 mmol) and DMAP (13.6 mg, 112 μmol). The reaction was allowed to stir at 0 °C for 30 min, then warmed to ambient temperature and stirred for an additional 1.5 h. The reaction was poured into H_2O and extracted with EtOAc. The organic layer was washed with water and brine, dried and concentrated. The crude residue was subjected to flash column chromatography (SiO_2, 10% ethyl acetate in hexanes) to afford the product as a pale-yellow oil (257 mg, 36%, 2 steps). $[\alpha]_D^{24}$ -52 (*c* 0.43, CHCl3); R_f = 0.42 (20% Et_2O/hexanes); IR (film) 3301, 2953, 2898, 1765, 1443, 1150, 1114, 1032 cm^{-1}; ^{1}H NMR (600 MHz, $CDCl_3$) δ 4.89 (d, *J* = 12.0 Hz, 1H), 4.74 (d, *J* = 7.1 Hz, 1H), 4.72 (d, *J* = 11.9 Hz, 1H), 4.70 (d, *J* = 7.0 Hz, 1H), 4.30 (dd, *J* = 7.9, 4.8 Hz, 1H), 3.41 (s, 3H), 2.26 (td, *J* = 7.0, 2.6 Hz, 2H), 2.05-1.91 (m, 2H), 1.96 (t, *J* = 2.6 Hz, 1H) 1.78-1.67 (m, 2H); ^{13}C NMR (125 MHz, $CDCl_3$) ppm 171.1, 96.4, 94.8, 83.6, 74.8, 74.2, 69.1, 56.4, 31.8, 24.2, 18.2; HRMS (EI): Exact mass calcd for $C_{11}H_{16}Cl_3O_4$ $[M+H]^+$ 317.0109, found 307.0109. ANS-3-242.

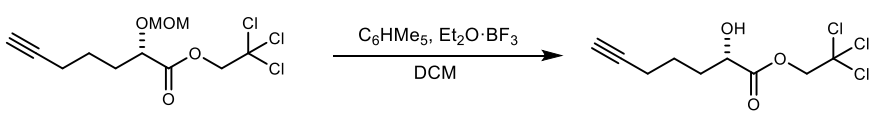

[5] The enantioenrichment was never determined – this analogue was not carried forward due to difficulties with the TMS group in the next stage. Will need to be determined later if used.

2,2,2-Trichloroethyl (*S*)-2-hydroxyhept-6-ynoate (51). A flame-dried round-bottom flask was charged with the protected alcohol (72.0 mg, 22.7 μmol) dissolved in dry dichloromethane (4.5 mL), pentamethyl benzene (67.3 mg, 45.4 μmol), and $BF_3{\cdot}Et_2O$ (56 μL, 45 μmol). The reaction was allowed to stir for 1 h and 20 min at ambient temperature. The crude reaction mixture was quenched with satd aq $NaHCO_3$, washed with brine, dried, concentrated, and subjected to flash column chromatography (SiO_2, 20% ethyl acetate in hexanes) to afford the alcohol (23.4 mg, 38%) as a pale-yellow oil. $[\alpha]_D^{23}$ -9.15 (*c* 1.05, $CHCl_3$); R_f = 0.17 (20% EtOAc/hexanes); IR (film) 3507, 3303, 2954, 1756, 1582, 1439, 1269, 1167, 1109 cm^{-1}; ^1H NMR (400 MHz, $CDCl_3$) δ 4.93 (d, *J* = 11.8 Hz, 1H), 4.73 (d, *J* = 11.8 Hz, 1H), 4.38 (ddd, *J* = 7.4, 5.7, 4.4 Hz, 1H), 2.65 (d, *J* = 6.0 Hz, 1H), 2.27 (td, *J* = 6.9, 2.6 Hz, 2H), 2.10-1.99 (m, 1H), 1.96 (t, *J* = 2.6 Hz, 1H) 1.91-1.64 (series of m, 3H); ^{13}C NMR (125 MHz, $CDCl_3$) ppm 173.7, 94.5, 83.7, 74.6, 70.2, 69.1, 33.3, 23.9, 18.2; HRMS (EI): Exact mass calcd for $C_9H_{12}Cl_3O_3$ $[M+H]^+$ 272.9847, found 272.9847. ANS-3-234.

2,2,2-Trichloroethyl (*R*)-2-hydroxyhept-6-ynoate (*ent*-51). Prepared following an identical procedure as **51**. Flash column chromatography (SiO_2, 20% ethyl acetate in hexanes) afforded the alcohol with spectroscopic data identical to its enantiomer, except $[\alpha]_D^{23}$ +9.4 (*c* 0.65, $CHCl_3$). ANS-4-83.

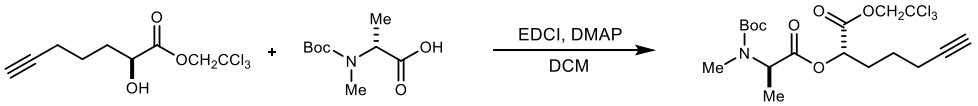

2,2,2-Trichloroethyl (*S*)-2-((*N*-(*tert*-butoxycarbonyl)-*N*-methyl-D-alanyl)oxy)hept-6-ynoate (52). A round-bottom flask was charged with the amine (20 mg, 98 μmol), alcohol (23.4 mg, 85.6 μmol), and DCM (1.0 mL). The mixture was cooled to 0 °C and then EDCI (19.7 mg, 103 μmol) and DMAP (1.0 mg, 4.3 μmol) were added. The reaction was stirred at 0 °C for 30 min, then allowed to warm to ambient temperature and stir for an additional 1.5 h. The reaction mixture was poured into water and extracted with DCM. The combined organic layers were washed with satd aq $NaHCO_3$ and brine, dried, and concentrated to afford the product as a colorless oil (34.9 mg, 88%). $[\alpha]_D^{24}$ +5.0 (*c* 0.87, $CHCl_3$); R_f = 0.39 (20% EtOAc/hexanes); IR (film) 2973, 1750, 1695, 1452, 1390, 1156, 1089 cm^{-1}; ^1H NMR (600 MHz, $CDCl_3$) This compound exists as a 1.4:1 ratio of rotamers causing significant peak broadening and overlap. Refer to the image of the ^1H NMR spectrum. ^{13}C NMR (150 MHz, $CDCl_3$) This compound is a 1.4:1 ratio of rotamers causing significant peak broadening and overlap. Refer to the image of the ^{13}C NMR spectrum; HRMS (EI): Exact mass calcd for $C_{18}H_{26}Cl_3NO_6Na$ $[M+Na]^+$ 480.0718, found 480.0731. ANS-3-243.

2,2,2-Trichloroethyl (*R*)-2-((*N*-(*tert*-butoxycarbonyl)-*N*-methyl-L-alanyl)oxy)hept-6-ynoate (*ent*-52). Prepared following an identical procedure as **52**. Concentration of organic layers afforded the didepsipeptide with spectroscopic data identical to its enantiomer, except $[\alpha]_D^{23}$ -5.7 (*c* 0.53, $CHCl_3$). ANS-4-86.

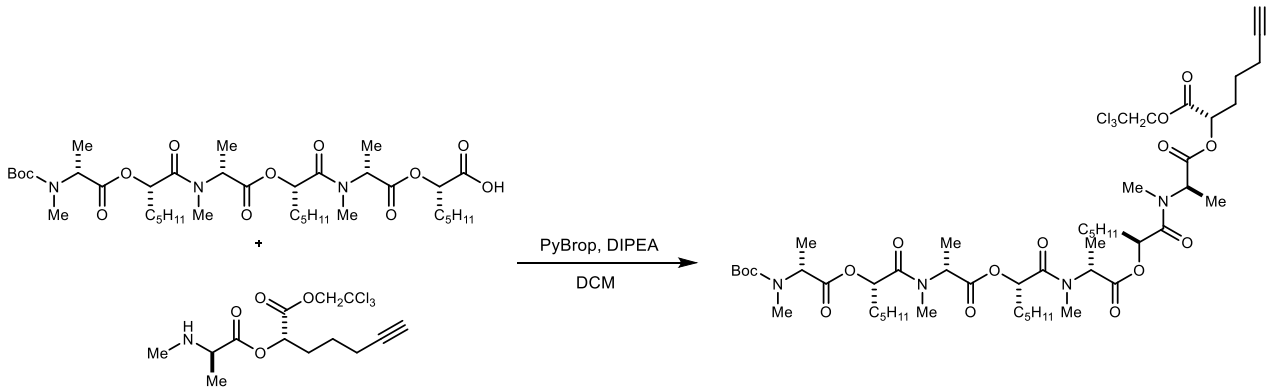

2,2,2-Trichloroethyl (*S*)-2-(((6*R*,9*S*,12*R*,15*S*,18*R*,21*S*,24*R*)-2,2,5,6,11,12,17,18,23,24-decamethyl-4,7,10,13,16,19,22-heptaoxo-9,15,21-tripentyl-3,8,14,20-tetraoxa-5,11,17,23-tetraazapentacosan-25-oyl)oxy)hept-6-ynoate (54). A round-bottom flask was charged with the amine (14.8 mg, 41.5 μmol), acid (33.9 mg, 44.8 μmol), and DCM (450 μL). The mixture was cooled to 0 °C and then DIPEA (23.0 μL, 134 μmol) and PyBrop (31.3 mg, 67.2 μmol) were added. The reaction was stirred at 0 °C for 30 min, then allowed to warm to ambient temperature and stir for an additional 1.5 h. The reaction mixture was poured into cold 10% aq citric acid and extracted with DCM. The combined organic layers were washed with satd aq $NaHCO_3$ and brine, dried, and concentrated. The crude residue was subjected to flash column chromatography (SiO_2, 30-50% ethyl acetate in hexanes) to afford the product as a colorless oil (33.2 mg, 67%). $[\alpha]_D^{24}$ +38 (*c* 0.48, $CHCl_3$); R_f = 0.21 (40% EtOAc/hexanes); IR (film) 2930, 2864, 1742, 1663, 1457, 1384, 1216, 1159, 1085 cm^{-1}; ^1H NMR (600 MHz, $CDCl_3$) This compound exists as a mixture of rotamers causing significant peak broadening and overlap. Refer to the image of the ^1H NMR spectrum; ^{13}C NMR (150 MHz, $CDCl_3$) This compound is a mixture of rotamers causing significant peak broadening and overlap. Refer to the image of the ^{13}C NMR spectrum; HRMS (EI): Exact mass calcd for $C_{51}H_{83}Cl_3N_4NaO_{15}$ $[M+Na]^+$ 1119.4813, found 1119.4836. ANS-3-263.

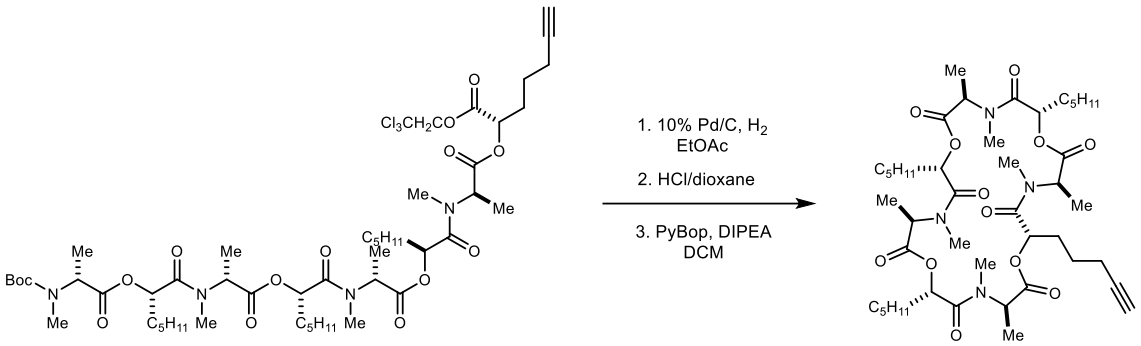

(3*R*,6*S*,9*R*,12*S*,15*R*,18*S*,21*R*,24*S*)-3,4,9,10,15,16,21,22-Octamethyl-6-(pent-4-yn-1-yl)-12,18,24-tripentyl-1,7,13,19-tetraoxa-4,10,16,22-tetraazacyclotetracosan-2,5,8,11,14,17,20,23-octaone (36). A round-bottom flask was charged with the depsipeptide (26.0 mg, 23.7 μmol), dissolved in THF (1.47 mL) and 1 M NH_4OAc (260 μL), and treated with zinc dust (77 mg). The reaction was allowed to stir for 2 h and then the crude reaction mixture was filtered through Celite. To the crude material was added 4 M HCl in dioxane (400 μL) and the reaction mixture was allowed to stir for 30 min. The reaction mixture was concentrated and added to a flame-dried round-bottom flask. DCM (5.1 mL) was added and the reaction was cooled to 0 °C. Once at 0 °C, DIPEA (9.6 μL, 56 μmol) and PyBrop (13.9 mg, 26.8 μmol) were added. The reaction was stirred at 0 °C for 1 h, then allowed to warm to ambient temperature and stir for an additional 1 h. The reaction mixture was poured into cold 10% aq citric acid and extracted with DCM. The combined organic layers were washed with satd aq $NaHCO_3$ and brine, and then dried and concentrated. Preparative HPLC (5 – 95% aqueous acetonitrile, 210 nm, flow rate: 8 mL/min, R_t = 21 m) afforded the 24-membered macrocycle (8.1 mg, 38%) as a colorless oil. $[\alpha]_D^{24}$ +34 (*c* 0.51, $CHCl_3$); R_f = 0.18 (4% MeOH/DCM); IR (film) 3284, 2931, 2862, 1742, 1661, 1461, 1414, 1317, 1199, 1085 cm^{-1}; ^1H NMR (600 MHz, $CDCl_3$) This compound exists in multiple conformations, causing significant peak overlap. Refer to the image of the ^1H NMR spectrum; ^{13}C NMR (150 MHz, $CDCl_3$) This compound exists in multiple conformations, causing significant peak overlap. Refer to the image of the ^{13}C NMR spectrum; HRMS (EI): Exact mass calcd for $C_{44}H_{72}N_4NaO_{12}$ $[M+Na]^+$ 871.5039, found 871.5051. ANS-3-270.

(3*S*,6*R*,9*S*,12*R*,15*S*,18*R*,21*S*,24*R*)-3,4,9,10,15,16,21,22-Octamethyl-6-(pent-4-yn-1-yl)-12,18,24-tripentyl-1,7,13,19-tetraoxa-4,10,16,22-tetraazacyclotetracosan-2,5,8,11,14,17,20,23-octaone (*ent*-36). Prepared following an identical procedure as **36**. Preparative HPLC (5 – 95% aqueous acetonitrile, 210 nm, flow rate: 8 mL/min, R_t = 21 m)

afforded the 24-membered macrocycle with spectroscopic data identical to its enantiomer, except $[\alpha]_D^{24}$ -33 (*c* 0.52, $CHCl_3$). ANS-4-104.

Benzyl (*S*)-2-(methoxymethoxy)heptanoate (S24). A round-bottom flask was charged with nitroalkane (1.36 g, 6.63 mmol), $NaNO_2$ (1.37 g, 19.9 mmol), AcOH (5.7 mL, 99.5 mmol), and DMSO (51.0 mL). The mixture was stirred at 45 °C for 18 h under an argon atmosphere. The reaction was then allowed to cool to ambient temperature, treated with 1 N HCl, and poured into CH_2Cl_2. The aqueous layer was extracted with CH_2Cl_2, and the combined organic layers were washed with water, brine, dried, and concentrated. The crude mixture was then added to a round-bottom flask with K_2CO_3 (2.75 g, 19.9 mmol) and DMF (13.2 mL). The mixture was then treated with BnBr (950 μL, 7.95 mmol) and the reaction was allowed to stir overnight at ambient temperature under an argon atmosphere (balloon). The reaction was quenched with 1 M aq HCl and extracted with Et_2O. The organic layer was washed with 1 M HCl, water, brine, dried and concentrated. The crude residue was subjected to flash column chromatography (SiO_2, 5% diethyl ether in hexanes) to afford the product as a pale-yellow oil (1.30 g, 70%, 2 steps). $[\alpha]_D^{20}$ -52.2 (*c* 1.04, $CHCl_3$); R_f = 0.22 (15% Et_2O/hexanes); IR (film) 2953, 2863, 1749, 1457, 1262, 1156, 1126, 1037 cm^{-1}; ^1H NMR (400 MHz, $CDCl_3$) δ 7.40-7.26 (m, 5H), 5.19 (d, *J* = 12.4 Hz, 1H), 5.15 (d, *J*= 12.3 Hz, 1H), 4.68 (d, *J* = 6.9 Hz, 1H), 4.65 (d, *J* = 6.9 Hz, 1H), 4.14 (dd, *J* = 6.3, 6.3 Hz, 1H), 3.34 (s, 3H), 1.75 (dddd, *J* = 7.3, 7.3, 7.3, 7.3 Hz, 2H), 1.45-1.20 (m, 6H), 0.86 (t, *J* = 6.6 Hz, 3H); ^{13}C NMR (100 MHz, $CDCl_3$) ppm 172.7, 135.7, 128.6, 128.4, 128.3, 96.3, 75.7, 66.5, 56.0, 32.9, 31.5, 24.9, 22.5, 14.0; HRMS (EI): Exact mass calcd for $C_{16}H_{24}O_4Na$ $[M+Na]^+$ 303.1567, found 303.1569. ANS-2-273.

Benzyl (*R*)-2-((*N*-(*tert*-butoxycarbonyl)-*N*-methyl-L-alanyl)oxy)heptanoate (S25). A round-bottom flask was charged with the amine (1.19 g, 5.84 mmol), alcohol (1.20 g, 5.08 mmol), and DCM (51 mL). The mixture was cooled to 0 °C and then EDCI (1.17 g, 6.09 mmol) and DMAP (31.0 mg, 254 μmol) were added. The reaction was stirred at 0 °C for 30 min, then allowed to warm to ambient temperature and stir for an additional 1.5 h. The reaction mixture was poured

into water and extracted with DCM. The combined organic layers were washed with satd aq $NaHCO_3$ and brine, and then dried and concentrated. The crude residue was subjected to flash column chromatography (SiO_2, 5% ethyl acetate in hexanes) to afford the product as a colorless oil (1.88 g, 88%). All spectral data are in agreement with literature values.[6] ANS-3-08.

Benzyl (*S*)-2-((*N*-(*tert*-butoxycarbonyl)-*N*-methyl-D-alanyl)oxy)heptanoate (*ent*-S25). Prepared following an identical procedure as **S25**. Flash column chromatography (SiO_2, 5% ethyl acetate in hexanes) afforded the depsipeptide with spectroscopic data identical to its enantiomer, except $[\alpha]_D^{26}$ +12 (*c* 0.94, $CHCl_3$). ANS-2-282.

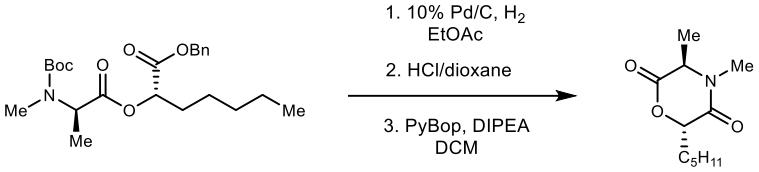

(3*R*,6*S*)-3,4-Dimethyl-6-pentylmorpholine-2,5-dione (55). A round-bottom flask was charged with the depsipeptide (24.0 mg, 56.9 μmol), dissolved in EtOAc (2.0 mL), and treated with 10% Pd/C (3.0 mg). The reaction flask was evacuated with light vacuum (50 Torr). A hydrogen (balloon) was added, and the cycle was repeated once more. The reaction mixture was stirred for 1 h. After purging the flask with nitrogen, the crude reaction mixture was filtered through Celite. To the crude material was added 4 M HCl in dioxane (5 mL), and the reaction mixture was allowed to stir for 30 min. The reaction mixture was concentrated and transferred to a flame-dried round bottom flask. DMF (11.3 mL) was added and the reaction was cooled to 0 °C. DIPEA (21.4 μL, 125 μmol) and PyBop (32.4 mg, 62.4 μmol) were added. The reaction was stirred at 0 °C for 30 min, then allowed to warm to ambient temperature and stir for an additional 2 h. The reaction mixture was poured into cold 10% aq citric acid and extracted with DCM. The combined organic layers were washed with satd aq $NaHCO_3$ and brine, and then dried and concentrated. Preparative HPLC (5 – 95% aqueous acetonitrile, 210 nm, flow rate: 8 mL/min, R_t = 15.6 m) afforded the 6-membered ring (11.3 mg, 94%) as a colorless oil. $[\alpha]_D^{25}$ -110 (*c* 0.48, $CHCl_3$); R_f = 0.33 (4% MeOH/DCM); IR (film) 2927, 2860, 1754, 1671, 1491, 1451, 1378, 1315, 1258, 1061 cm^{-1}; ^1H NMR (600 MHz, $CDCl_3$) δ 4.78 (dd, *J* = 7.4, 3.8 Hz, 1H), 4.13 (q, *J* = 7.3 Hz, 1H), 2.98 (s, 3H), 2.10 (dddd, *J* = 14.5, 10.8, 5.7, 3.8 Hz, 1H), 1.92 (dddd, *J* = 14.5, 10.6, 7.5, 4.7 Hz, 1H), 1.56 (d, *J* = 7.3 Hz, 3H), 1.53-1.40 (series of m, 2H), 1.37-1.28 (m, 4H), 0.89 (t, *J* = 7.1 Hz, 3H); ^{13}C NMR

[6] Monma, et al., *Org. Lett.* **2006,** 5601.

(150 MHz, $CDCl_3$) ppm 168.1, 165.7, 77.7, 56.9, 32.0, 31.5, 31.3, 24.3, 22.6, 16.8, 14.1; HRMS (EI): Exact mass calcd for $C_{11}H_{19}NO_3$ $[M]^+$ 213.1365, found 213.1361. ANS-6-75.

(3*S*,6*R*)-3,4-Dimethyl-6-pentylmorpholine-2,5-dione (*ent*-55). Prepared following an identical procedure as **55**. Preparative HPLC (5 – 95% aqueous acetonitrile, 210 nm, flow rate: 8 mL/min, R_t = 15.6 m) afforded the 6-membered ring with spectroscopic data identical to its enantiomer, except $[\alpha]_D^{23}$ +109 (*c* 0.57, $CHCl_3$). ANS-3-113.

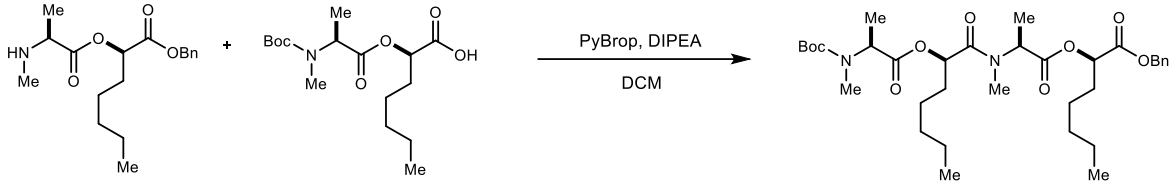

Benzyl (*R*)-2-(((6*S*,9*R*,12*S*)-2,2,5,6,11,12-hexamethyl-4,7,10-trioxo-9-pentyl-3,8-dioxa-5,11-diazatridecan-13-oyl)oxy)heptanoate (S26). A round-bottom flask was charged with the amine (231 mg, 717 μmol), acid (236 mg, 717 μmol), and DCM (4.0 mL). The mixture was cooled to 0 °C and then DIPEA (370 μL, 2.15 mmol) and PyBrop (502 mg, 1.08 mmol) were added. The reaction was stirred at 0 °C for 1 h. The reaction mixture was poured into cold 10% citric acid and extracted with DCM. The combined organic layers were washed with satd aq $NaHCO_3$ and brine, and then dried and concentrated. The crude residue was subjected to flash column chromatography (SiO_2, 10-40% ethyl acetate in hexanes) to afford the product as a colorless oil (330 mg, 73%). All spectral data are in agreement with literature values.[6] ANS-3-19.

Benzyl (*S*)-2-(((6*R*,9*S*,12*R*)-2,2,5,6,11,12-hexamethyl-4,7,10-trioxo-9-pentyl-3,8-dioxa-5,11-diazatridecan-13-oyl)oxy)heptanoate (*ent*-S26). Prepared following an identical procedure as S**26**. Flash column chromatography (SiO_2, 10-40% ethyl acetate in hexanes) afforded the depsipeptide with spectroscopic data identical to its enantiomer, except $[\alpha]_D^{26}$ +28.0 (*c* 1.00, $CHCl_3$). ANS-2-288.

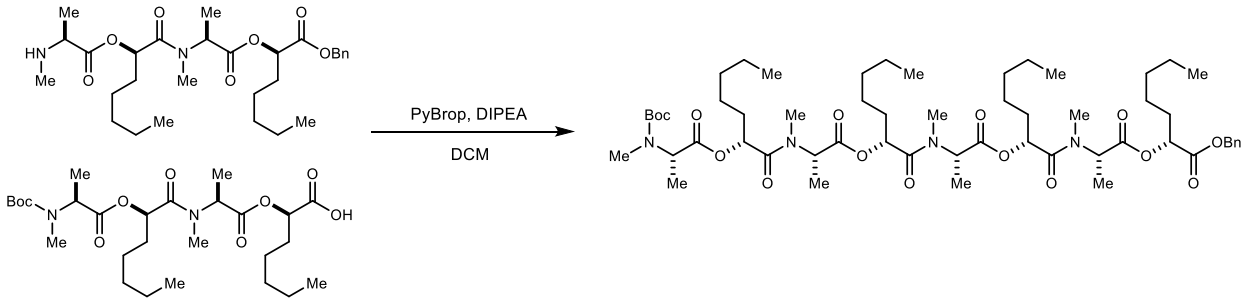

Benzyl (*R*)-2-(((6*S*,9*R*,12*S*,15*R*,18*S*,21*R*,24*S*)-2,2,5,6,11,12,17,18,23,24-decamethyl-4,7,10,13,16,19,22-heptaoxo-9,15,21-tripentyl-3,8,14,20-tetraoxa-5,11,17,23-tetraazapentacosan-25-oyl)oxy)heptanoate (S27). A round-bottom flask was charged with the amine (195 mg, 365 μmol), acid (199 mg, 365 μmol), and DCM (3.7 mL). The mixture was cooled to 0 °C and then DIPEA (187 μL, 1.09 mmol) and PyBrop (255 mg, 547 μmol) were added. The reaction was stirred at 0 °C for 30 min, then allowed to warm to ambient temperature and stir for an additional 1.5 h. The reaction mixture was poured into cold 10% citric acid and extracted with DCM. The combined organic layers were washed with satd aq $NaHCO_3$ and brine, and then dried and concentrated. The crude residue was subjected to flash column chromatography (SiO_2, 10-50% ethyl acetate in hexanes) to afford the product as a colorless oil (320 mg, 83%). All spectral data are in agreement with literature values.[6] ANS-3-72.

Benzyl (*S*)-2-(((6*R*,9*S*,12*R*,15*S*,18*R*,21*S*,24*R*)-2,2,5,6,11,12,17,18,23,24-decamethyl-4,7,10,13,16,19,22-heptaoxo-9,15,21-tripentyl-3,8,14,20-tetraoxa-5,11,17,23-tetraazapentacosan-25-oyl)oxy)heptanoate (*ent*-S27). Prepared following an identical procedure as **S27**. Flash column chromatography (SiO_2, 10-50% ethyl acetate in hexanes) afforded the depsipeptide with spectroscopic data identical to its enantiomer, except $[\alpha]_D^{26}$ +42 (*c* 0.94, $CHCl_3$). ANS-2-292.

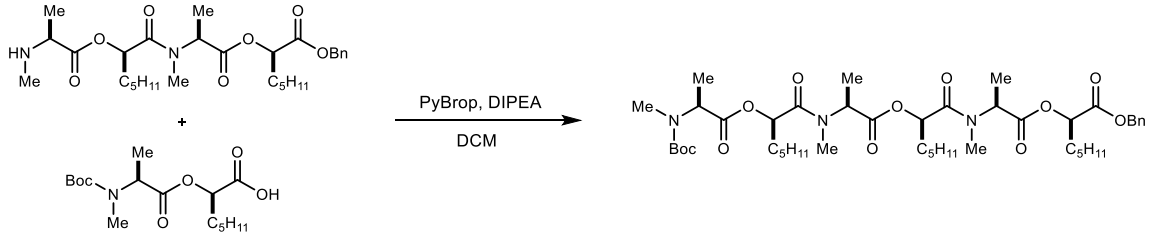

Benzyl (*R*)-2-(((6*S*,9*R*,12*S*,15*R*,18*S*)-2,2,5,6,11,12,17,18-octamethyl-4,7,10,13,16-pentaoxo-9,15-dipentyl-3,8,14-trioxa-5,11,17-triazanonadecan-19-oyl)oxy)heptanoate (S28). A round-bottom flask was charged with the amine (21.1 mg, 39.5 μmol), acid (13.1 mg, 39.5 μmol), and DCM (0.4 mL). The mixture was cooled to 0 °C and then DIPEA (20.3 μL, 119 μmol) and PyBrop (28.0 mg, 59.3 μmol) were added. The reaction was stirred at 0 °C for 30 min, then allowed to warm to ambient temperature and stir for an additional 1.5 h. The reaction mixture was poured into cold 10% citric acid and extracted with DCM. The combined organic layers were washed with satd aq $NaHCO_3$ and brine, and then dried and concentrated. The crude residue was subjected to flash column chromatography (SiO_2, 10-50% ethyl acetate in hexanes) to afford the product as a

colorless oil (32 mg, 96%). $[\alpha]_D^{25}$ – 34 (*c* 0.95, $CHCl_3$); R_f = 0.14 (20% EtOAc/hexanes); IR (film) 2932, 2865, 1743, 1666, 1458, 1316, 1187, 1086 cm^{-1}; ^1H NMR (600 MHz, $CDCl_3$) This compound exists as a mixture of rotamers causing significant peak broadening and overlap. Refer to image of the ^1H NMR spectrum; ^{13}C NMR (150 MHz, $CDCl_3$) This compound is a mixture of rotamers causing significant peak broadening and overlap. Refer to the image of the ^{13}C NMR spectrum; HRMS (EI): Exact mass calcd for $C_{45}H_{73}N_3NaO_{12}$ $[M+Na]^+$ 870.5092, found 870.5071. ANS-3-31.

Benzyl (*S*)-2-(((6*R*,9*S*,12*R*,15*S*,18*R*)-2,2,5,6,11,12,17,18-octamethyl-4,7,10,13,16-pentaoxo-9,15-dipentyl-3,8,14-trioxa-5,11,17-triazanonadecan-19-oyl)oxy)heptanoate (*ent*-S28). Prepared following an identical procedure as **S28**. Flash column chromatography (SiO_2, 10-50% ethyl acetate in hexanes) afforded the protected depsipeptide with spectroscopic data identical to its enantiomer, except $[\alpha]_D^{20}$ +33 (*c* 0.90, $CHCl_3$). ANS-3-150.

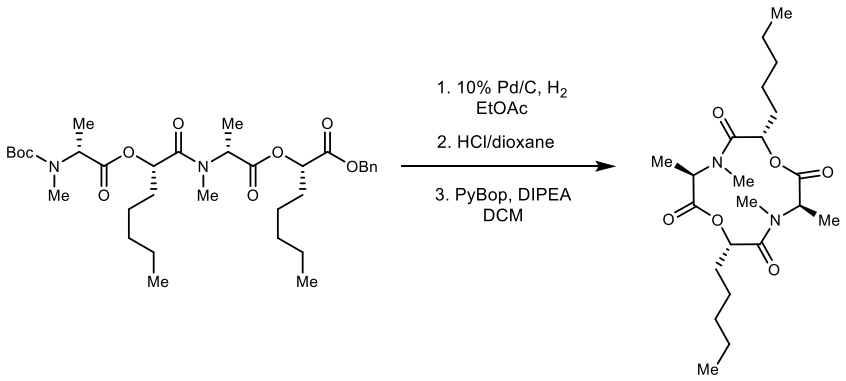

(3*S*,6*R*,9*S*,12*R*)-3,4,9,10-Tetramethyl-6,12-dipentyl-1,7-dioxa-4,10-diazacyclododecane-2,5,8,11-tetraone (56). A round-bottom flask was charged with the depsipeptide (62.2 mg, 98.0 μmol) in EtOAc (5.0 mL), and treated with 10% Pd/C (7 mg). The flask was evacuated with light vacuum (50 Torr). Hydrogen (balloon) was added, and the cycle was repeated once more. The mixture was stirred for 1 h. After purging the flask with nitrogen, the crude mixture was filtered through Celite. To the crude material was added 4 M HCl in dioxane (5 mL) and the mixture was allowed to stir for 30 min. The mixture was concentrated and transferred to a flame-dried round bottom flask. DMF (20.6 mL) was added and the reaction was cooled to 0 °C. DIPEA (38.8 μL, 22.7 μmol) and PyBop (58.8 mg, 113 μmol) were added. The reaction was stirred at 0 °C for 30 min, then allowed to warm to ambient temperature and stir for an additional 2 h. The reaction mixture was poured into cold 10% aq citric acid and extracted with DCM. The combined organic layers were washed with satd aq $NaHCO_3$ and brine, and then dried and concentrated. Preparative

HPLC (5 – 95% aqueous acetonitrile, 210 nm, flow rate: 8 mL/min, R_t = 19.1 m) afforded the 12-membered ring (9.0 mg, 21%) as a colorless oil. $[\alpha]_D^{25}$ + 21 (*c* 0.50, $CHCl_3$); R_f = 0.37 (4% MeOH/DCM); IR (film) 2954, 2929, 2859, 1749, 1649, 1488, 1456, 1434, 1379, 1314, 1260, 1149, 1086 cm^{-1}; ^1H NMR (600 MHz, $CDCl_3$) This compound exists in multiple conformations. There is a clear major conformation (see spectra) and the line listing for that conformation is: δ 5.17 (dd, *J* = 9.1, 5.7 Hz, 2H), 4.88 (q, *J* = 7.2 Hz, 2H), 2.99 (s, 6H), 1.93-1.77 (m, 4H), 1.48 (d, *J* = 7.2 Hz, 6H), 1.61-1.28 (series of m, 12H), 0.90 (t, *J* = 7.1 Hz, 6H); ^{13}C NMR (150 MHz, $CDCl_3$) ppm 170.6, 169.3, 78.4, 53.6, 32.0, 31.3, 29.7, 25.5, 22.5, 16.1, 14.1; HRMS (EI): Exact mass calcd for $C_{22}H_{38}N_2NaO_6$ $[M+Na]^+$ 449.2622, found 449.2623. ANS-6-119.

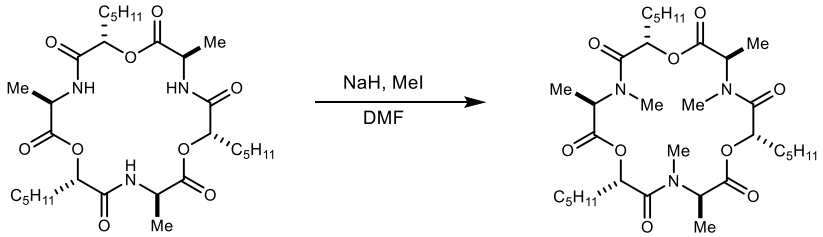

(3*R*,6*S*,9*R*,12*S*,15*R*,18*S*)-3,9,15-Trimethyl-6,12,18-tripentyl-1,7,13-trioxa-4,10,16-triazacyclooctadecane-2,5,8,11,14,17-hexaone (57). A flame-dried round-bottom flask was charged with N-H depsipeptide (16.7 mg, 27.9 μmol) and dry DMF (558 μL) at 0 °C. Methyl iodide (70 μL, 1.12 mmol) was then added to the reaction mixture, and NaH (6.7 mg, 279 μmol in DMF (279 μL)) was added slowly to the reaction mixture in 56 μL aliquots over 15 minutes. The reaction was allowed to stir at 0 °C for 25 m, and it was then quenched by the dropwise addition of satd aq NH_4Cl. The aqueous layer was extracted with EtOAc, and the combined organic layers were washed with satd aq $NaHCO_3$, satd aq $Na_2S_2O_3$, water and brine. The organic layer was then dried and concentrated to afford a colorless oil. Preparative HPLC (55 – 95% aqueous acetonitrile, 210 nm, flow rate: 8 mL/min, R_t = 28.7 m) afforded the 18-membered macrocycle (7.5 mg, 42%). $[\alpha]_D^{20}$ +7.5 (*c* 0.40, $CHCl_3$); R_f = 0.67 (10% MeOH/DCM); IR (film) 2924, 2855, 1746, 1665, 1462, 1199, 1100 cm^{-1}; ^1H NMR (600 MHz, CD_3OD) δ 5.35 (dd, *J* = 8.8, 4.6 Hz, 1H), 5.00 (q, *J* = 7.5 Hz, 1H), 3.09 (s, 3H), 1.84 –1.76 (m, 2H), 1.45 (d, *J* = 7.6 Hz, 3H), 1.39-1.29 (m, 6H), 0.93 (t, *J*= 6.8 Hz, 3H); ^{13}C NMR (150 MHz, CD_3OD) ppm 172.9, 172.4, 72.8, 53.7, 32.5, 31.9, 31.3, 26.2, 23.6, 14.5, 14.3; HRMS (EI): Exact mass calcd for $C_{33}H_{57}N_3NaO_9$ $[M+Na]^+$ 662.3987, found 662.4021. ANS-1-52.

(3*S*,6*R*,9*S*,12*R*,15*S*,18*R*)-3,9,15-Trimethyl-6,12,18-tripentyl-1,7,13-trioxa-4,10,16-triazacyclooctadecane-2,5,8,11,14,17-hexaone (*ent*-57). Prepared following an identical procedure as **57**. Preparative HPLC (55 – 95% aqueous acetonitrile, 210 nm, flow rate: 8 mL/min, R_t = 28.7 m) afforded the 18-membered macrocycle with spectroscopic data identical to its enantiomer, except $[\alpha]_D^{25}$ -7.2 (*c* 0.59, $CHCl_3$).

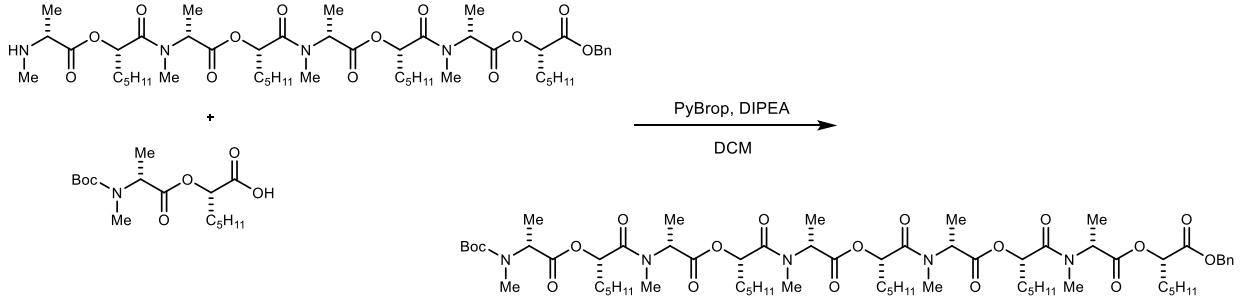

Benzyl (*S*)-2-(((6*R*,9*S*,12*R*,15*S*,18*R*,21*S*,24*R*,27*S*,30*R*)-2,2,5,6,11,12,17,18,23,24,29,30-dodecamethyl-4,7,10,13,16,19,22,25,28-nonaoxo-9,15,21,27-tetrapentyl-3,8,14,20,26-pentaoxa-5,11,17,23,29-pentaazahentriacontan-31-oyl)oxy)heptanoate (S29). A round-bottom flask was charged with the amine (45.0 mg, 47.1 μmol), acid (16.0 mg, 47.1 μmol), and DCM (0.5 mL). The mixture was cooled to 0 °C and then DIPEA (24 μL, 71 μmol) and PyBrop (33.0 mg, 70.7 μmol) were added. The reaction was stirred at 0 °C for 30 min, then allowed to warm to ambient temperature and stir for an additional 1.5 h. The reaction mixture was poured into cold 10% citric acid and extracted with DCM. The combined organic layers were washed with satd aq $NaHCO_3$ and brine, and then dried and concentrated. The crude residue was subjected to flash column chromatography (SiO_2, 10-60% ethyl acetate in hexanes) to afford the product as a colorless oil (50 mg, 83%). $[\alpha]_D^{25}$ +47.4 (*c* 1.00, $CHCl_3$); R_f = 0.21 (40% EtOAc/hexanes); IR (film) 2933, 2865, 1742, 1664, 1459, 1315, 1213, 1085 cm^{-1}; ^1H NMR (600 MHz, $CDCl_3$) This compound exists as a mixture of rotamers causing significant peak broadening and overlap. Refer to image of the ^1H NMR spectrum; ^{13}C NMR (150 MHz, $CDCl_3$) This compound is a mixture of rotamers causing significant peak broadening and overlap. Refer to the image of the ^{13}C NMR spectrum; HRMS (EI): Exact mass calcd for $C_{67}H_{115}N_6O_{18}$ $[M+NH_4]^+$ 1291.8262, found 1291.8259. ANS-2-298.

Benzyl (*R*)-2-(((6*S*,9*R*,12*S*,15*R*,18*S*,21*R*,24*S*,27*R*,30*S*)-2,2,5,6,11,12,17,18,23,24,29,30-dodecamethyl-4,7,10,13,16,19,22,25,28-nonaoxo-9,15,21,27-tetrapentyl-3,8,14,20,26-pentaoxa-5,11,17,23,29-pentaazahentriacontan-31-oyl)oxy)heptanoate (*ent*-S29). Prepared

following an identical procedure as **S29**. Flash column chromatography (SiO_2, 10-60% ethyl acetate in hexanes) afforded the protected depsipeptide with spectroscopic data identical to its enantiomer, except $[\alpha]_D^{22}$ -30 (*c* 0.16, $CHCl_3$). ANS-3-40.

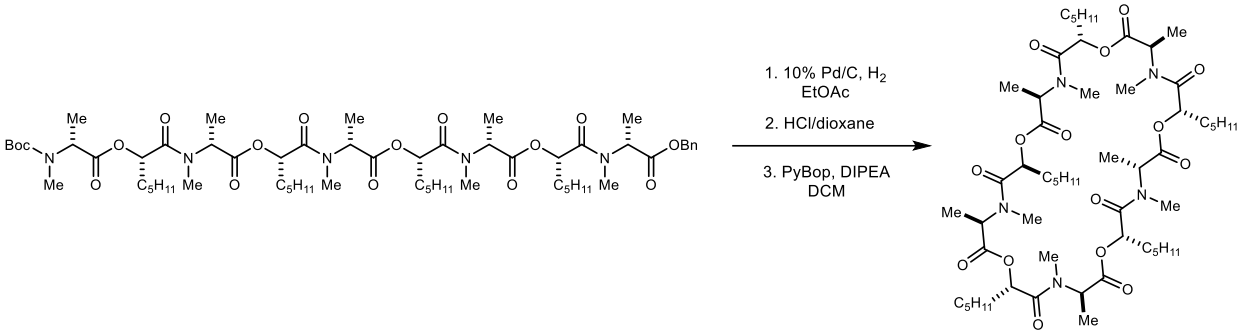

(3*R*,6*S*,9*R*,12*S*,15*R*,18*S*,21*R*,24*S*,27*R*,30*S*)-3,4,9,10,15,16,21,22,27,28-Decamethyl-6,12,18,24,30-pentapentyl-1,7,13,19,25-pentaoxa-4,10,16,22,28-pentaazacyclotriacontane 2,5,8,11,14,17,20,23,26,29-decaone (59). A round-bottom flask was charged with the depsipeptide (50.0 mg, 39.3 μmol), dissolved in EtOAc (0.3 mL), and treated with 10% Pd/C (1.0 mg). The reaction flask was evacuated with light vacuum (50 Torr). Hydrogen (balloon) was added, and the cycle was repeated once more. The reaction was stirred for 1 h. After purging the flask with nitrogen, the crude reaction mixture was filtered through Celite. To the crude material was added 4 M HCl in dioxane (0.4 mL) and the reaction mixture was allowed to stir for 30 min. The reaction mixture was concentrated and added to a flame-dried round bottom flask. DCM (7.84 mL) was added and the reaction was cooled to 0 °C. DIPEA (15 μL, 86 μmol) and PyBrop (21.4 mg, 86.2 μmol) were added. The reaction was stirred at 0 °C for 30 min, then allowed to warm to ambient temperature and stir for an additional 1.5 h. The reaction mixture was poured into cold 10% citric acid and extracted with DCM. The combined organic layers were washed with satd aq $NaHCO_3$ and brine, and then dried and concentrated. Preparative HPLC (5 – 95% aqueous acetonitrile, 210 nm, flow rate: 8 mL/min, R_t = 25-28 m) afforded the 30-membered macrocycle (12.3 mg, 30%) as a colorless oil. $[\alpha]_D^{20}$ +40 (*c* 0.62, $CHCl_3$); R_f = 0.34 (4% MeOH/DCM); IR (film) 2930, 2861, 1743, 1653, 1462, 1204, 1093 cm^{-1}; ^1H NMR (600 MHz, $CDCl_3$) This compound exists in multiple conformations, causing significant peak overlap. Refer to image of the ^1H NMR spectrum; ^{13}C NMR (150 MHz, $CDCl_3$) This compound exists in multiple conformations, causing significant peak overlap. Refer to image of the ^{13}C NMR spectrum; HRMS (EI): Exact mass calcd for $C_{55}H_{96}N_5O_{15}$ $[M+H]^+$ 1066.6897, found 1066.6889. ANS-3-05.

(3*S*,6*R*,9*S*,12*R*,15*S*,18*R*,21*S*,24*R*,27*S*,30*R*)-3,4,9,10,15,16,21,22,27,28-Decamethyl-6,12,18,24,30-pentapentyl-1,7,13,19,25-pentaoxa-4,10,16,22,28-pentaazacyclotriacontane 2,5,8,11,14,17,20,23,26,29-decaone (*ent*-59). Prepared following an identical procedure as **59**. Preparative HPLC (5 – 95% aqueous acetonitrile, 210 nm, flow rate: 8 mL/min, R_t = 25-28 m) afforded the 30-membered macrocycle with spectroscopic data identical to its enantiomer, except $[\alpha]_D^{20}$ -33 (*c* 0.68, $CHCl_3$). ANS-3-50.

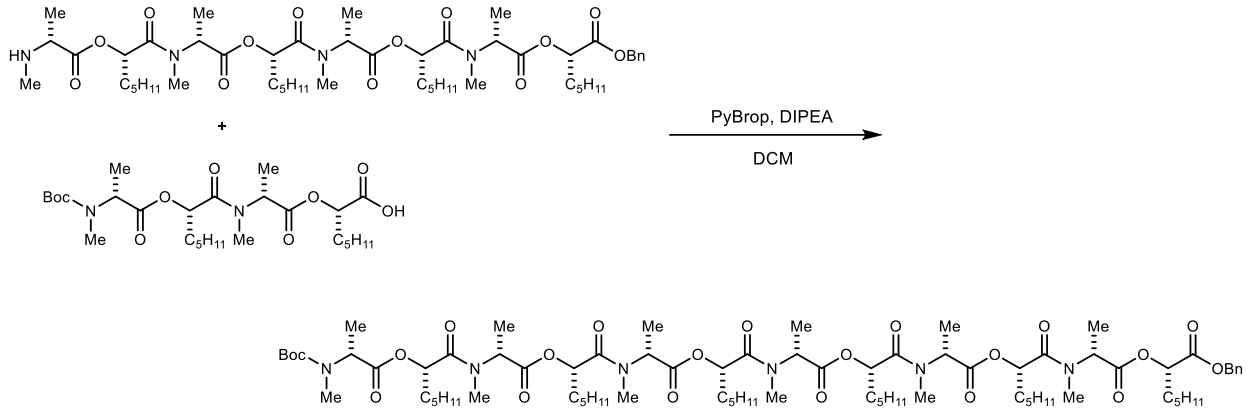

Benzyl (*S*)-2-(((6*R*,9*S*,12*R*,15*S*,18*R*,21*S*,24*R*,27*S*,30*R*,33*S*,36*R*)-2,2,5,6,11,12,17,18,23,24,29,30,35,36-tetradecamethyl-4,7,10,13,16,19,22,25,28,31,34-undecaoxo-9,15,21,27,33-pentapentyl-3,8,14,20,26,32-hexaoxa-5,11,17,23,29,35-hexaazaheptatriacontan-37-oyl)oxy)heptanoate (S30). A round-bottom flask was charged with the amine (45.0 mg, 47.1 μmol), acid (25.7 mg, 47.1 μmol), and DCM (0.5 mL). The mixture was cooled to 0 °C and then DIPEA (24 μL, 71 μmol) and PyBrop (33.0 mg, 70.7 μmol) were added. The reaction mixture was stirred at 0 °C for 30 min, then allowed to warm to ambient temperature and stir for an additional 1.5 h. The reaction mixture was poured into cold 10% citric acid and extracted with DCM. The combined organic layers were washed with satd aq $NaHCO_3$ and brine, and then dried and concentrated. The crude residue was subjected to flash column chromatography (SiO_2, 10-60% ethyl acetate in hexanes) to afford the product as a colorless oil (70 mg, 99%). $[\alpha]_D^{20}$ +53 (*c* 0.95, $CHCl_3$); R_f = 0.15 (50% EtOAc/hexanes); IR (film) 2932, 2864, 1743, 1664, 1458, 1315, 1215, 1085 cm^{-1}; ^1H NMR (600 MHz, $CDCl_3$) This compound exists as a mixture of rotamers causing significant peak broadening and overlap. Refer to image of the ^1H NMR spectrum; ^{13}C NMR (150 MHz, $CDCl_3$) This compound is a mixture of rotamers causing significant peak broadening and overlap. Refer to the image of the ^{13}C NMR spectrum; HRMS (EI): Exact mass calcd for $C_{78}H_{134}N_7O_{21}$ $[M+NH_4]^+$ 1504.9627, found 1504.9620. ANS-2-300.

Benzyl (*R*)-2-(((6*S*,9*R*,12*S*,15*R*,18*S*,21*R*,24*S*,27*R*,30*S*,33*R*,36*S*)-2,2,5,6,11,12,17,18,23,24,29,30,35,36-tetradecamethyl-4,7,10,13,16,19,22,25,28,31,34-undecaoxo-9,15,21,27,33-pentapentyl-3,8,14,20,26,32-hexaoxa-5,11,17,23,29,35-hexaazaheptatriacontan-37-oyl)oxy)heptanoate (*ent*-S30). Prepared following an identical procedure as **S30**. Flash column chromatography (SiO_2, 10-60% ethyl acetate in hexanes) afforded the depsipeptide with spectroscopic data identical to its enantiomer, except $[\alpha]_D^{20}$ -42 (*c* 0.15, $CHCl_3$). ANS-3-39.

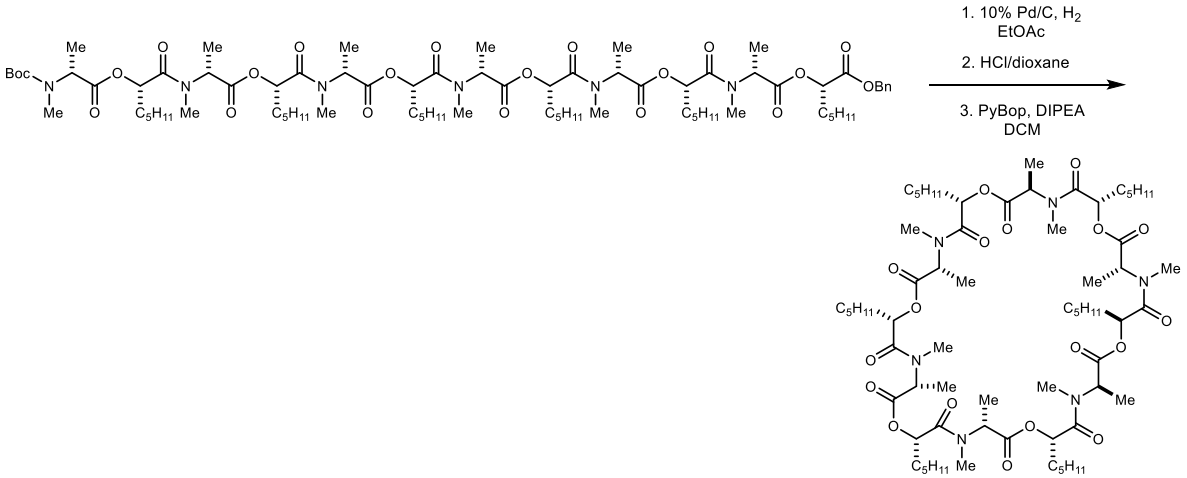

(3*R*,6*S*,9*R*,12*S*,15*R*,18*S*,21*R*,24*S*,27*R*,30*S*,33*R*,36*S*)-3,4,9,10,15,16,21,22,27,28,33,34-Dodecamethyl-6,12,18,24,30,36-hexapentyl-1,7,13,19,25,31-hexaoxa-4,10,16,22,28,34-hexaazacyclohexatriacontane-2,5,8,11,14,17,20,23,26,29,32,35-dodecaone (58). A round-bottom flask was charged with the depsipeptide (70 mg, 47 μmol), dissolved in EtOAc (0.3 mL), and treated with 10% Pd/C (1.0 mg). The reaction flask was evacuated with light vacuum (50 Torr). Hydrogen (balloon) was added, and the cycle was repeated once more. The reaction was stirred for 1 h. After purging the flask with nitrogen, the crude reaction mixture was filtered through Celite. To the crude material was added 4 M HCl in dioxane (0.3 mL) and the reaction mixture was allowed to stir for 30 min. The reaction mixture was concentrated and added to a flame-dried round bottom flask. DCM (7.8 mL) was added and the reaction was cooled to 0 °C. DIPEA (24 μL, 71 μmol) and PyBrop (33.0 mg, 70.7 μmol) were added. The reaction was stirred at 0 °C for 30 min, then allowed to warm to ambient temperature and stir for an additional 1.5 h. The reaction mixture was poured into cold 10% citric acid and extracted with DCM. The combined organic layers were washed with satd aq $NaHCO_3$ and brine, and then dried and concentrated. Preparative HPLC (5 – 95% aqueous acetonitrile, 210 nm, flow rate: 8 mL/min, R_t = 30-32 m)

afforded the 36-membered macrocycle (30 mg, 55%) as a colorless oil. $[\alpha]_D^{25}$ +33 (*c* 0.46, $CHCl_3$); R_f = 0.22 (4% MeOH/DCM); IR (film) 2932, 2864, 1743, 1660, 1461, 1212, 1102 cm^{-1}; ^1H NMR (400 MHz, $CDCl_3$) This compound exists in multiple conformations, causing significant peak overlap. Refer to image of the ^1H NMR spectrum; ^{13}C NMR (150 MHz, $CDCl_3$) This compound exists in multiple conformations, causing significant peak overlap. Refer to image of the ^{13}C NMR spectrum; HRMS (EI): Exact mass calcd for $C_{66}H_{115}N_6O_{18}$ $[M+H]^+$ 1279.8262, found 1279.8259. ANS-3-06.

(3*S*,6*R*,9*S*,12*R*,15*S*,18*R*,21*S*,24*R*,27*S*,30*R*,33*S*,36*R*)-3,4,9,10,15,16,21,22,27,28,33,34-Dodecamethyl-6,12,18,24,30,36-hexapentyl-1,7,13,19,25,31-hexaoxa-4,10,16,22,28,34-hexaazacyclohexatriacontane-2,5,8,11,14,17,20,23,26,29,32,35-dodecaone (*ent*-58). Prepared following an identical procedure as **58**. Preparative HPLC (5 – 95% aqueous acetonitrile, 210 nm, flow rate: 8 mL/min, R_t = 30-32 m) afforded the 36-membered macrocycle with spectroscopic data identical to its enantiomer, except $[\alpha]_D^{20}$ -36 (*c* 0.51, $CHCl_3$). ANS-3-49.

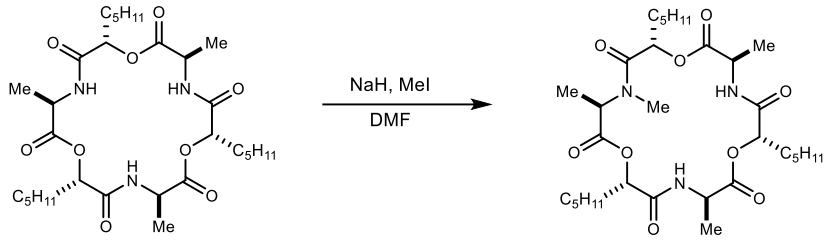

(3*R*,6*S*,9*R*,12*S*,15*R*,18S)-3,4,9,15-Tetramethyl-6,12,18-tripentyl-1,7,13-trioxa-4,10,16-triazacyclooctadecane-2,5,8,11,14,17-hexaone (66). A flame-dried round-bottom flask was charged with N-H depsipeptide (14.3 mg, 23.9 μmol) and dry DMF (478 μL) at 0 °C. Methyl iodide (60 μL, 960 μmol) was then added to the reaction mixture, and NaH (5.7 mg, 240 μmol in DMF (239 μL)) was added in 3 aliquots of 48 μL over 15 m. The reaction was allowed to stir at 0 °C for 3 m, and it was then quenched by the dropwise addition of satd aq NH_4Cl. The aqueous layer was extracted with EtOAc, and the combined organic layers were washed with satd aq $NaHCO_3$, satd aq $Na_2S_2O_3$, water, and brine. The organic layer was dried and concentrated to afford a colorless oil. Preparative HPLC (55 – 95% aqueous acetonitrile, 210 nm, flow rate: 8 mL/min, R_t = 26.8 m) afforded the 18-membered macrocycle (5 mg, 34%) as a colorless oil. $[\alpha]_D^{20}$ +46 (*c* 0.53, $CHCl_3$); R_f = 0.34 (4% MeOH/DCM); IR (film) 3317, 2925, 2857, 1748, 1681, 1635, 1243, 1454, 1376, 1209, 1063 cm^{-1}; ^1H NMR (600 MHz, $CDCl_3$) δ 7.39 (d, *J* = 8.8 Hz, 2H), 5.40 (dd, *J* = 5.4, 5.4 Hz, 1H), 5.28 (dd, *J* = 8.3, 4.5 Hz, 1H), 5.01 (dq, *J* = 8.0, 7.1 Hz, 1H), 4.84 (dd, *J*

= 8.6, 4.1 Hz, 1H), 4.79 (dq, *J* = 7.0, 7.0, 1H), 3.94 (q, *J* = 7.0 Hz, 1H), 3.16 (s, 3H), 1.93-1.63 (series of m, 6H), 1.55 (d, *J* = 7.1 Hz, 3H), 1.40 (d, *J* = 7.2 Hz, 3H), 1.35 (d, *J* = 7.1 Hz, 3H), 1.33-1.27 (m, 18H), 0.91 (t, *J*= 6.9 Hz, 3H), 0.88 (t, *J*= 7.6 Hz, 3H), 0.86 (t, *J*= 7.8 Hz, 3H); ^{13}C NMR (150 MHz, $CDCl_3$) ppm 173.4, 171.0, 170.8, 169.8, 169.5, 169.2, 77.4, 74.1, 72.7, 59.3, 47.81, 47.76, 36.6, 31.9, 31.55, 31.47, 31.2, 30.5, 29.8, 25.6, 25.2, 23.9, 22.62, 22.60, 22.57, 19.1, 17.0 (2C), 14.3, 14.13, 14.10; HRMS (EI): Exact mass calcd for $C_{31}H_{53}N_3NaO_9$ $[M+Na]^+$ 634.3674, found 634.3708. ANS-1-293B.

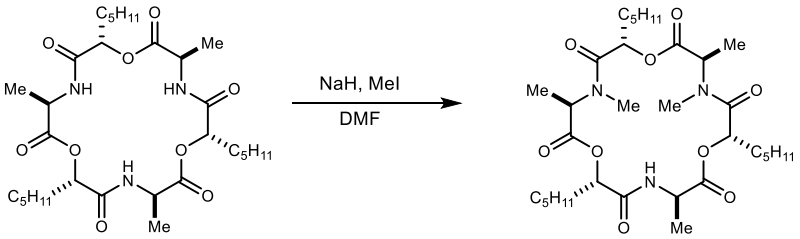

(3*R*,6*S*,9*R*,12*S*,15*R*,18*S*)-3,4,9,10,15-Pentamethyl-6,12,18-tripentyl-1,7,13-trioxa-4,10,16-triazacyclooctadecane-2,5,8,11,14,17-hexaone (65). A flame-dried round-bottom flask was charged with N-H depsipeptide (14.3 mg, 23.9 μmol) and dry DMF (478 μL) at 0 °C. Methyl iodide (60 μL, 960 μmol) was then added to the reaction mixture, and NaH (5.7 mg, 240 μmol in DMF (240 μL)) was added in 3 aliquots of 48 μL over 15 m. The reaction was allowed to stir at 0 °C for 3 m, and it was then quenched by the dropwise addition of satd aq NH_4Cl. The aqueous layer was extracted with EtOAc, and the combined organic layers were washed with satd aq $NaHCO_3$, satd aq $Na_2S_2O_3$, water, and brine. The organic layer was dried and concentrated to afford a colorless oil. Preparative HPLC (55 – 95% aqueous acetonitrile, 210 nm, flow rate: 8 mL/min, R_t = 27.6 m) afforded the 18-membered macrocycle (3.3 mg, 22%) as a colorless oil. $[\alpha]_D^{20}$ +19 (*c* 0.30, $CHCl_3$); R_f = 0.40 (4% MeOH/DCM); IR (film) 3309, 2924, 2855, 1742, 1664, 1549, 1458, 1376, 1342, 1210, 1098 cm^{-1}; ^{1}H NMR (400 MHz, $CDCl_3$) δ 7.37 (d, *J* = 9.4 Hz, 1H), 5.58 (q, *J* = 7.3 Hz, 1H), 5.47 (dd, *J* = 6.5, 6.5 Hz, 1H), 5.24 (dd, *J* = 9.4, 3.5 Hz, 1H), 4.95 (dq, *J* = 7.3, 7.3 Hz, 1H), 4.88 (dd, *J* = 9.1, 4.1 Hz, 1H), 4.01 (q, *J* = 7.1 Hz, 1H), 3.12 (s, 3H), 2.85 (s, 3H), 2.05-1.66 (series of m, 6H), 1.50 (d, *J* = 6.8 Hz, 3H), 1.42 (d, *J* = 7.1 Hz, 3H), 1.38 (d, *J* = 7.2 Hz, 3H), 1.33-1.28 (m, 18H), 0.92-0.86 (m, 9H); ^{13}C NMR (150 MHz, $CDCl_3$) ppm 171.5, 171.0, 170.4, 170.14, 170.12, 170.10, 76.7, 71.9, 70.9, 58.2, 50.9, 48.0, 35.7, 31.73, 31.70, 31.5, 31.4, 31.0, 30.6, 30.0, 25.3, 25.2, 24.9, 22.61, 22.57 (2C), 19.1, 14.29, 14.26, 14.12, 14.10, 13.2;

HRMS (EI): Exact mass calcd for $C_{32}H_{55}N_3NaO_9$ $[M+Na]^+$ 648.3831, found 648.3866. ANS-1-293A.

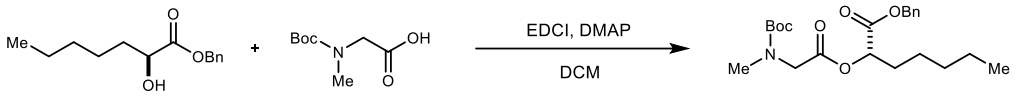

Benzyl (*S*)-2-((*N*-(*tert*-butoxycarbonyl)-*N*-methylglycyl)oxy)heptanoate (S31). A round-bottom flask was charged with the amine (92.1 mg, 487 μmol), alcohol (100 mg, 423 μmol), and DCM (4.2 mL). The mixture was cooled to 0 °C and then EDCI (97.4 mg, 508 μmol) and DMAP (2.6 mg, 21 μmol) were added. The reaction was stirred at 0 °C for 30 min, then allowed to warm to ambient temperature and stir for an additional 1.5 h. The reaction mixture was poured into water and extracted with DCM. The combined organic layers were washed with satd aq $NaHCO_3$ and brine, and then dried and concentrated to afford the product as a colorless oil (171 mg, 99%). $[\alpha]_D^{24}$ -24 (*c* 0.63, $CHCl_3$); R_f = 0.38 (20% EtOAc/hexanes); IR (film) 3399, 2958, 2867, 2362, 1752, 1703, 1455, 1389, 1244, 1180, 1149 cm^{-1}; ^1H NMR (600 MHz, $CDCl_3$) This compound exists as a mixture of 1.4:1 rotamers causing significant peak overlap. Refer to the image of the ^1H NMR spectrum.^{13}C NMR (150 MHz, $CDCl_3$) This compound is a mixture of 1:1 rotamers causing peak broadening and overlap. Refer to the image of the ^{13}C NMR spectrum; HRMS (EI): Exact mass calcd for $C_{22}H_{33}NNaO_6$ $[M+Na]^+$ **Benzyl (*R*)-2-((*N*-(*tert*-butoxycarbonyl)-*N*-methylglycyl)oxy)heptanoate (*ent*-S31).** Prepared following an identical procedure as **S31**, with spectroscopic data identical to its enantiomer, except $[\alpha]_D^{23}$ +22 (*c* 0.69, $CHCl_3$). ANS-6-16.

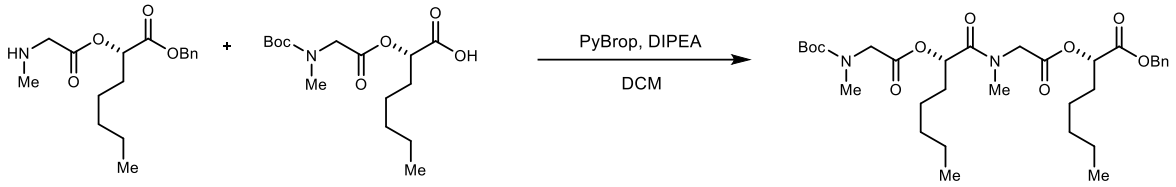

Benzyl (*S*)-2-(((*S*)-2,2,5,11-tetramethyl-4,7,10-trioxo-9-pentyl-3,8-dioxa-5,11-diazatridecan-13-oyl)oxy)heptanoate (S32). A round-bottom flask was charged with the amine (42.7 mg, 139 μmol), acid (44.1 mg, 139 μmol), and DCM (700 μL). The mixture was cooled to 0 °C and then DIPEA (71 μL, 420 μmol) and PyBrop (97.2 mg, 209 μmol) were added. The reaction was stirred at 0 °C for 1 h. The reaction mixture was poured into cold 10% aq citric acid and extracted with DCM. The combined organic layers were washed with satd aq $NaHCO_3$ and brine, and then dried and concentrated. The crude residue was subjected to flash column chromatography (SiO_2, 30% ethyl acetate in hexanes) to afford the product as a colorless oil (65 mg, 77%). $[\alpha]_D^{24}$ -32 (*c* 0.82,

$CHCl_3$); R_f = 0.10 (20% EtOAc/hexanes); IR (film) 2931, 2864, 1751, 1701, 1671, 1456, 1389, 1245, 1181, 1150 cm^{-1}; ^1H NMR (600 MHz, $CDCl_3$) This compound exists as a mixture of rotamers causing significant peak broadening and overlap. Refer to the image of the ^1H NMR spectrum.^{13}C NMR (150 MHz, $CDCl_3$) This compound is a mixture of rotamers causing peak doubling, broadening, and overlap. Refer to the image of the ^{13}C NMR spectrum; HRMS (EI): Exact mass calcd for $C_{32}H_{50}N_2NaO_9$ $[M+Na]^+$ 629.3409, found 629.3416. ANS-3-284.

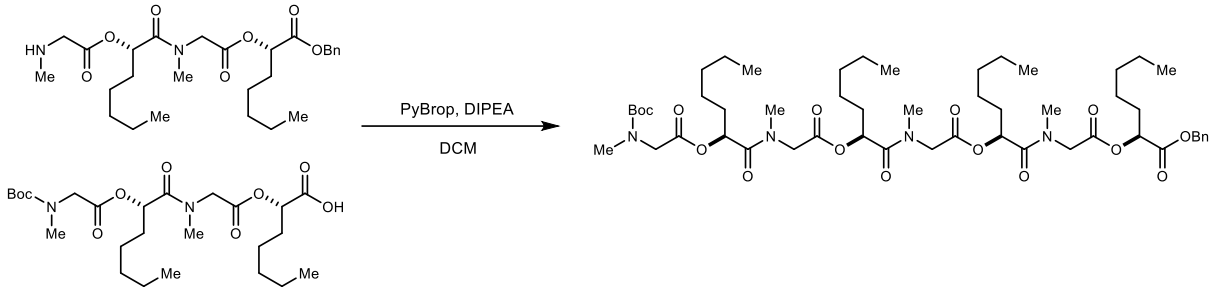

Benzyl (*S*)-2-(((9*S*,15*S*,21*S*)-2,2,5,11,17,23-hexamethyl-4,7,10,13,16,19,22-heptaoxo-9,15,21-tripentyl-3,8,14,20-tetraoxa-5,11,17,23-tetraazapentacosan-25-oyl)oxy)heptanoate (S33). A round-bottom flask was charged with the amine (27.1 mg, 53.5 μmol), acid (27.6 mg, 53.5 μmol), and DCM (0.55 mL). The mixture was cooled to 0 °C and then DIPEA (27.5 μL, 161 μmol) and PyBrop (37.4 mg, 80.3 μmol) were added. The reaction was stirred at 0 °C for 30 min, then allowed to warm to ambient temperature and stir for an additional 1.5 h. The reaction mixture was poured into cold 10% aq citric acid and extracted with DCM. The combined organic layers were washed with satd aq $NaHCO_3$ and brine, and then dried and concentrated. The crude residue was subjected to flash column chromatography (SiO_2, 60% ethyl acetate in hexanes) to afford the product as a colorless oil (37.8 mg, 70%). $[\alpha]_D^{24}$ -42 (*c* 1.02, MeOH); R_f = 0.10 (60% EtOAc/hexanes); IR (film) 2955, 2934, 2863, 1750, 1665, 1460, 1392, 1189, 1152, 1112 cm^{-1}; ^1H NMR (600 MHz, $CDCl_3$) This compound exists as a mixture of rotamers causing significant peak overlap. Refer to the image of the ^1H NMR spectrum.^{13}C NMR (150 MHz, $CDCl_3$) This compound is a mixture of rotamers causing peak broadening and overlap. Refer to the image of the ^{13}C NMR spectrum; HRMS (EI): Exact mass calcd for $C_{52}H_{84}N_4NaO_{15}$ $[M+Na]^+$ 1027.5825, found 1027.5843. ANS-3-296.

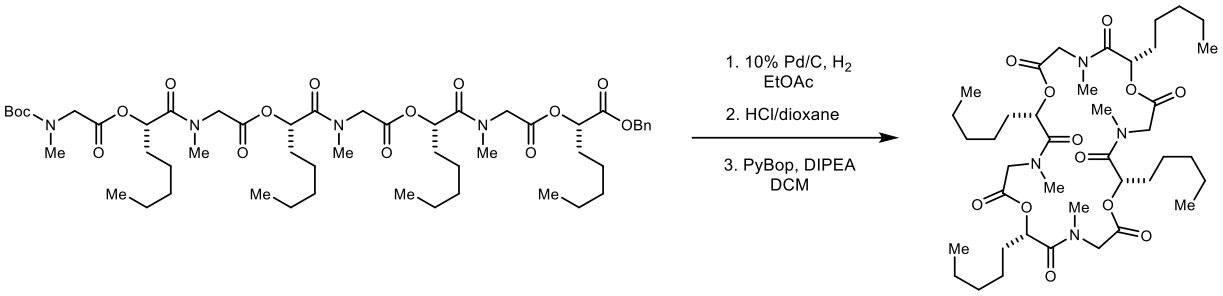

(6*S*,12*S*,18*S*,24*S*)-4,10,16,22-tetramethyl-6,12,18,24-tetrapentyl-1,7,13,19-tetraoxa-4,10,16,22-tetraazacyclotetracosan-2,5,8,11,14,17,20,23-octaone (70). A round-bottom flask was charged with the depsipeptide (37.8 mg, 37.6 μmol), dissolved in EtOAc (750 μL), and treated with 10% Pd/C (4.0 mg). The reaction flask was evacuated with light vacuum (50 Torr). Hydrogen (balloon) was added, and the flask was cycled once more. The reaction was allowed to stir for 2 h. After purging the flask with nitrogen, the crude reaction mixture was filtered through Celite. To the crude material was added 4 M HCl in dioxane (400 μL) and the reaction mixture was allowed to stir for 30 min. The reaction mixture was concentrated and added to a flame-dried round-bottom flask. DCM (7.5 mL) was added and the reaction was cooled to 0 °C. Once at 0 °C, DIPEA (14.2 μL, 82.7 μmol) and PyBrop (22.0 mg,41.4 μmol) were added. The reaction was stirred at 0 °C for 1.5 h, then allowed to warm to ambient temperature and stir for an additional 1 h. The reaction mixture was poured into cold 10% aq citric acid and extracted with DCM. The combined organic layers were washed with satd aq $NaHCO_3$ and brine, and then dried and concentrated. Preparative HPLC (5 – 95% aqueous acetonitrile, 210 nm, flow rate: 8 mL/min, R_t = 20.6 m) afforded the 24-membered macrocycle (16.4 mg, 55%) as a colorless oil. $[\alpha]_D^{24}$ – 8.2 (*c* 0.61, $CHCl_3$); R_f = 0.46 (10% MeOH/DCM); IR (film) 2932, 2863, 1751, 1663, 1489, 1464, 1406, 1253, 1190 cm^{-1}; ^1H NMR (600 MHz, $CDCl_3$) This compound exists in multiple conformations, causing significant peak overlap. Refer to the image of the ^1H NMR spectrum; ^{13}C NMR (150 MHz, $CDCl_3$) This compound exists in multiple conformations, causing significant peak overlap. Refer to the image of the ^{13}C NMR spectrum; HRMS (EI): Exact mass calcd for $C_{40}H_{68}N_4NaO_{12}$ $[M+Na]^+$ 819.4726, found 819.4727. ANS-4-03.

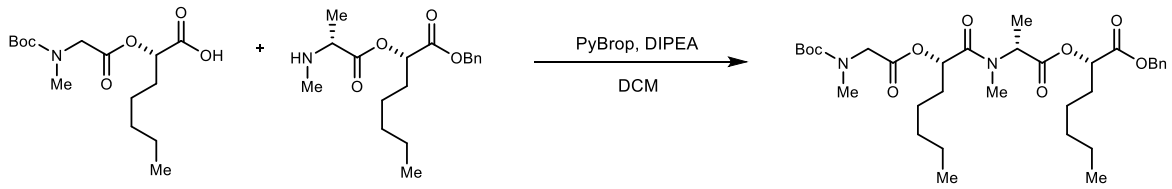

Benzyl (*S*)-2-(((9*S*,12*R*)-2,2,5,11,12-pentamethyl-4,7,10-trioxo-9-pentyl-3,8-dioxa-5,11-diazatridecan-13-oyl)oxy)heptanoate (S34). A round-bottom flask was charged with the amine (37.9 mg, 118 μmol), acid (37.4 mg, 118 μmol), and DCM (1.2 mL). The mixture was cooled to 0 °C and then DIPEA (61 μL, 350 μmol) and PyBrop (82.5 mg, 177 μmol) were added. The reaction was stirred at 0 °C for 30 min, then allowed to warm to ambient temperature and stir for an additional 1.5 h. The reaction mixture was poured into cold 10% aq citric acid and extracted with DCM. The combined organic layers were washed with satd aq $NaHCO_3$ and brine, and then dried and concentrated. The crude residue was subjected to flash column chromatography (SiO_2, 30% ethyl acetate in hexanes) to afford the product as a colorless oil (36.1 mg, 49%). $[\alpha]_D^{23}$ +7.7 (*c* 0.96, $CHCl_3$); R_f = 0.16 (20% EtOAc/hexanes); IR (film) 2953, 2926, 2857, 1745, 1701, 1665, 1458, 1387, 1243, 1185, 1149 cm^{-1}; ^1H NMR (600 MHz, $CDCl_3$) This compound exists as a mixture of rotamers causing peak broadening and overlap. Refer to the image of the ^1H NMR spectrum.^{13}C NMR (150 MHz, $CDCl_3$) This compound is a mixture of rotamers causing peak doubling, broadening, and overlap. Refer to the image of the ^{13}C NMR spectrum; HRMS (EI): Exact mass calcd for $C_{33}H_{56}N_3O_9$ $[M+NH_4]^+$ 638.4011, found 638.4014. ANS-4-285.

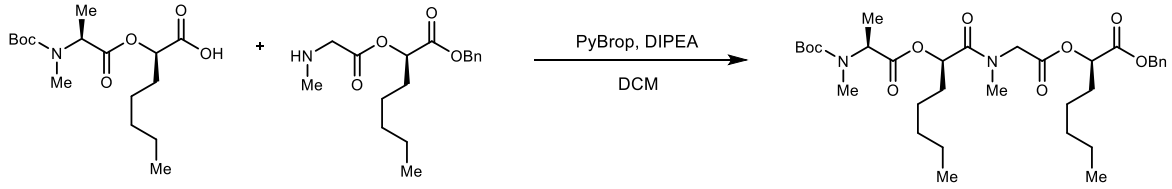

Benzyl (*R*)-2-(((6*S*,9*R*)-2,2,5,6,11-pentamethyl-4,7,10-trioxo-9-pentyl-3,8-dioxa-5,11-diazatridecan-13-oyl)oxy)heptanoate (S35). A round-bottom flask was charged with the amine (48.0 mg, 156 μmol), acid (51.7 mg, 156 μmol), and DCM (1.6 mL). The mixture was cooled to 0 °C and then DIPEA (80.0 μL, 468 μmol) and PyBrop (109 mg, 234 μmol) were added. The reaction was stirred at 0 °C for 30 min, then allowed to warm to ambient temperature and stir for an additional 1.5 h. The reaction mixture was poured into cold 10% aq citric acid and extracted with DCM. The combined organic layers were washed with $NaHCO_3$ and brine, and then dried and concentrated. The crude residue was subjected to flash column chromatography (SiO_2, 30% ethyl acetate in hexanes) to afford the product as a colorless oil (79.6 mg, 82%). $[\alpha]_D^{23}$ +6.5 (*c* 0.53, $CHCl_3$); R_f = 0.10 (20% EtOAc/hexanes); IR (film) 2955, 2929, 2860, 1743, 1692, 1671, 1455, 1389, 1336, 1314, 1177, 1152, 1106, 1080 cm^{-1}; ^1H NMR (600 MHz, $CDCl_3$) This compound exists as a mixture of rotamers causing peak broadening and overlap. Refer to the image of the ^1H

NMR spectrum.[13]C NMR (150 MHz, $CDCl_3$) This compound is a mixture of rotamers causing peak doubling, broadening, and overlap. Refer to the image of the [13]C NMR spectrum; HRMS (EI): Exact mass calcd for $C_{33}H_{52}N_2NaO_9$ $[M+Na]^+$ 643.3565, found 643.3567. ANS-6-28.

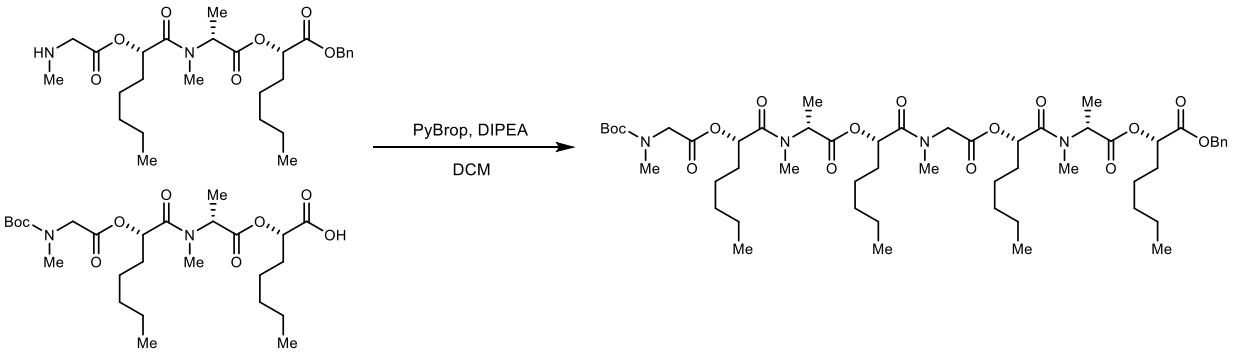

Benzyl (*S*)-2-(((9*S*,12*R*,15*S*,21*S*,24*R*)-2,2,5,11,12,17,23,24-octamethyl-4,7,10,13,16,19,22-heptaoxo-9,15,21-tripentyl-3,8,14,20-tetraoxa-5,11,17,23-tetraazapentacosan-25-oyl)oxy)heptanoate (S36). A round-bottom flask was charged with the amine (15.2 mg, 29.1 μmol), acid (15.4 mg, 29.1 μmol), and DCM (300 μL). The reaction mixture was cooled to 0 °C and then DIPEA (15 μL, 87 μmol) and PyBrop (20.4 mg, 43.7 μmol) were added. The solution was stirred at 0 °C for 30 min, then allowed to warm to ambient temperature and stir for an additional 1.5 h. The reaction mixture was poured into cold 10% aq citric acid and extracted with DCM. The combined organic layers were washed with satd aq $NaHCO_3$ and brine, and then dried and concentrated. The crude residue was subjected to flash column chromatography (SiO_2, 30% ethyl acetate in hexanes) to afford the product as a colorless oil (18.2 mg, 60%). $[\alpha]_D^{23}$ +5.0 (*c* 0.72, $CHCl_3$); R_f = 0.10 (40% EtOAc/hexanes); IR (film) 2956, 2929, 2859, 1746, 1699, 1661, 1456, 1392, 1259, 1190, 1149 cm^{-1}; [1]H NMR (600 MHz, $CDCl_3$) This compound exists as a mixture of rotamers causing peak broadening and overlap. Refer to the image of the [1]H NMR spectrum.[13]C NMR (150 MHz, $CDCl_3$) This compound is a mixture of rotamers causing peak doubling, broadening, and overlap. Refer to the image of the [13]C NMR spectrum; HRMS (EI): Exact mass calcd for $C_{54}H_{92}N_5O_{15}$ $[M+NH_4]^+$ 1050.6584, found 1050.6588. ANS-4-292.

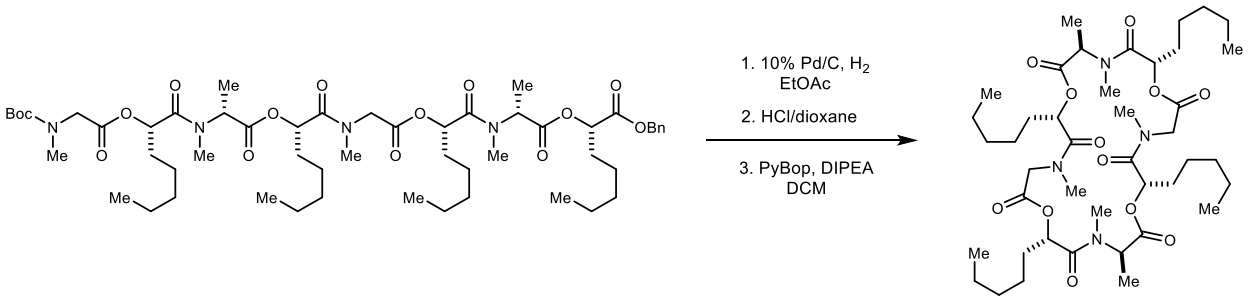

(3*R*,6*S*,12*S*,15*R*,18*S*,24*S*)-3,4,10,15,16,22-hexamethyl-6,12,18,24-tetrapentyl-1,7,13,19-tetraoxa-4,10,16,22-tetraazacyclotetracosan-2,5,8,11,14,17,20,23-octaone (67). A round-bottom flask was charged with the depsipeptide (18.2 mg, 17.6 μmol), dissolved in EtOAc (2.0 mL), and treated with 10% Pd/C (2.0 mg). The reaction flask was evacuated with light vacuum (50 Torr). Hydrogen (balloon) was added, and the process was cycled once more. The reaction was allowed to stir for 2 h. After purging the flask with nitrogen, the crude reaction mixture was filtered through Celite. To the crude material was added 4 M HCl in dioxane (1.5 mL) and the reaction mixture was allowed to stir for 30 min. The reaction mixture was concentrated and added to a flame-dried round-bottom flask. DCM (3.5 mL) was added and the reaction was cooled to 0 °C. Once at 0 °C, DIPEA (6.6 μL, 39 μmol) and PyBrop (10.1 mg, 19.4 μmol) were added. The reaction mixture was stirred at 0 °C for 1.5 h, then allowed to warm to ambient temperature and stir for an additional 1 h. The reaction mixture was poured into cold 10% aq citric acid and extracted with DCM. The combined organic layers were washed with satd aq $NaHCO_3$ and brine, and then dried and concentrated. Preparative HPLC (5 – 95% aqueous acetonitrile, 210 nm, flow rate: 8 mL/min, R_t = 22.0 m) afforded the 24-membered macrocycle (8.4 mg, 58%) as a colorless oil. $[\alpha]_D^{23}$ +7.5 (*c* 0.56, $CHCl_3$); R_f = 0.33 (5% MeOH/DCM); IR (film) 2929, 2858, 1745, 1665, 1462, 1410, 1377, 1191, 1110 cm^{-1}; ^1H NMR (600 MHz, $CDCl_3$) This compound exists in multiple conformations, causing significant peak overlap. Refer to the image of the ^1H NMR spectrum; ^{13}C NMR (150 MHz, $CDCl_3$) This compound exists in multiple conformations, causing significant peak overlap. Refer to the image of the ^{13}C NMR spectrum; HRMS (EI): Exact mass calcd for $C_{42}H_{72}N_4NaO_{12}$ $[M+Na]^+$ 847.5039, found 847.5041. ANS-4-297.

(3*S*,6*R*,12*R*,15*S*,18*R*,24*R*)-3,4,10,15,16,22-hexamethyl-6,12,18,24-tetrapentyl-1,7,13,19-tetraoxa-4,10,16,22-tetraazacyclotetracosan-2,5,8,11,14,17,20,23-octaone (*ent*-67). Prepared following an identical procedure as **67**. Preparative HPLC (30 – 95% aqueous acetonitrile, 210

nm, flow rate: 8 mL/min, R_t = 22.0 m) afforded the 24-membered macrocycle with spectroscopic data identical to its enantiomer, except $[\alpha]_D^{23}$ -7.2 (*c* 0.64, $CHCl_3$). ANS-6-67.

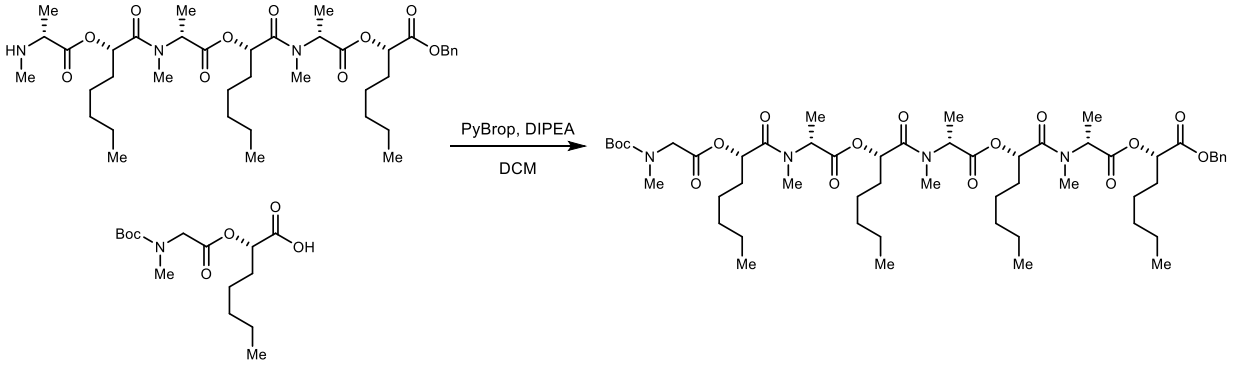

Benzyl (*S*)-2-(((9*S*,12*R*,15*S*,18*R*,21*S*,24*R*)-2,2,5,11,12,17,18,23,24-nonamethyl-4,7,10,13,16,19,22-heptaoxo-9,15,21-tripentyl-3,8,14,20-tetraoxa-5,11,17,23-tetraazapentacosan-25-oyl)oxy)heptanoate (S37). A round-bottom flask was charged with the amine (22 mg, 29 μmol), acid (9.2 mg, 29 μmol), and DCM (300 μL). The mixture was cooled to 0 °C and then DIPEA (15 μL, 87 μmol) and PyBrop (20.3 mg, 44.1 μmol) were added. The reaction was stirred at 0 °C for 30 min, then allowed to warm to ambient temperature and stir for an additional 1.5 h. The reaction mixture was poured into cold 10% aq citric acid and extracted with DCM. The combined organic layers were washed with satd aq $NaHCO_3$ and brine, and then dried and concentrated. The crude residue was subjected to flash column chromatography (SiO_2, 50% ethyl acetate in hexanes) to afford the product as a colorless oil (17 mg, 56%). $[\alpha]_D^{23}$ +26 (*c* 0.68, $CHCl_3$); R_f = 0.20 (40% EtOAc/hexanes); IR (film) 2955, 2930, 2907, 2870, 1742, 1704, 1698, 1666, 1456, 1386, 1260, 1190, 1149 cm^{-1}; ^1H NMR (600 MHz, $CDCl_3$) This compound exists as a mixture of rotamers causing peak broadening and overlap. Refer to the image of the ^1H NMR spectrum.^{13}C NMR (150 MHz, $CDCl_3$) This compound is a mixture of rotamers causing peak doubling, broadening, and overlap. Refer to the image of the ^{13}C NMR spectrum; HRMS (EI): Exact mass calcd for $C_{55}H_{90}N_4NaO_{15}$ $[M+Na]^+$ 1069.6295, found 1069.6291. ANS-6-68.

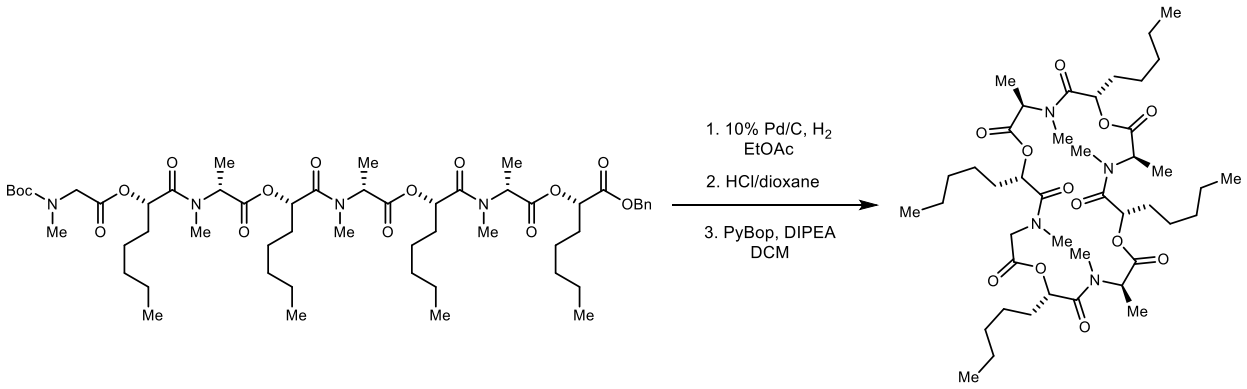

(3*R*,6*S*,9*R*,12*S*,15*R*,18*S*,24*S*)-3,4,9,10,15,16,22-Heptamethyl-6,12,18,24-tetrapentyl-1,7,13,19-tetraoxa-4,10,16,22-tetraazacyclotetracosan-2,5,8,11,14,17,20,23-octaone (71). A round-bottom flask was charged with the depsipeptide (17.0 mg, 16.2 μmol), dissolved in EtOAc (2.0 mL), and treated with 10% Pd/C (2.0 mg). The reaction flask was evacuated with light vacuum (50 Torr). Hydrogen (balloon) was added, and the flask was cycled once more. The reaction was allowed to stir for 2 h. After purging the flask with nitrogen, the crude reaction mixture was filtered through Celite. To the crude material was added HCl/EtOAc (5.0 mL) and the reaction mixture was allowed to stir for 1 h. The reaction mixture was concentrated and added to a flame-dried round-bottom flask. DCM (3.2 mL) was added and the mixture was cooled to 0 °C. Once at 0 °C, the solution was treated with DIPEA (6.1 μL, 36 μmol) and PyBrop (9.3 mg, 18 μmol). The reaction was stirred at 0 °C for 1.5 h, then allowed to warm to ambient temperature and stir for an additional 1 h. The reaction mixture was poured into cold 10% aq citric acid and extracted with DCM. The combined organic layers were washed with satd aq $NaHCO_3$ and brine, and then dried and concentrated. Preparative HPLC (5 – 95% aqueous acetonitrile, 210 nm, flow rate: 8 mL/min, R_t = 23.1 m) afforded the 24-membered macrocycle (6.6 mg, 49%) as a colorless oil. $[\alpha]_D^{23}$ +22 (*c* 0.55, $CHCl_3$); R_f = 0.14 (4% MeOH/DCM); IR (film) 3054, 2929, 2858, 1743, 1661, 1462, 1417, 1378, 1264, 1191, 1082 cm^{-1}; ^1H NMR (600 MHz, $CDCl_3$) This compound exists in multiple conformations, causing significant peak overlap. The peaks that could be distinguished are listed. See ^1H NMR for the rest of peaks; ^{13}C NMR (150 MHz, $CDCl_3$) This compound exists in multiple conformations, causing significant peak overlap. Refer to the image of the ^{13}C NMR spectrum; HRMS (EI): Exact mass calcd for $C_{43}H_{74}N_4NaO_{12}$ $[M+Na]^+$ 861.5195, found 861.5194. ANS-6-74.

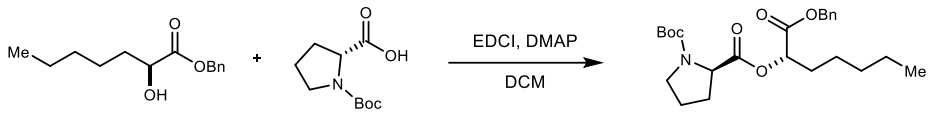

2-((*S*)-1-(Benzyloxy)-1-oxoheptan-2-yl) 1-(*tert*-butyl) (*R*)-pyrrolidine-1,2-dicarboxylateheptanoate (S38). A round-bottom flask was charged with the amine (206 mg, 959 μmol), alcohol (189 mg, 799 μmol), and DCM (8.0 mL). The mixture was cooled to 0 °C and then EDCI (184 mg, 959 μmol) and DMAP (4.9 mg, 40 μmol) were added. The reaction was stirred at 0 °C for 30 min, then allowed to warm to ambient temperature and stir for an additional 1.5 h. The reaction mixture was poured into water and extracted with DCM. The combined organic layers were washed with satd aq $NaHCO_3$ and brine, and then dried and concentrated to afford the product as a colorless oil (210 mg, 61%). $[\alpha]_D^{23}$ +24 (*c* 0.61, $CHCl_3$); R_f = 0.29 (20% EtOAc/hexanes); IR (film) 2957, 2931, 2871, 1747, 1702, 1478, 1396, 1366, 1258, 1172, 1120 cm^{-1}; ^1H NMR (400 MHz, $CDCl_3$) Several peaks show a clear doubling for the *cis* and *trans* amide products. Other peaks are overlapping and appear only once. Those that are doubled have both values listed. δ 7.40-7.25 (m, 5H), 5.20 (d, *J* = 12.4 Hz, 1H), 5.13 (d, *J* = 11.8 Hz, 1H), 5.10/5.03 (dd, *J* = 6.2, 6.2 Hz, 1H), 4.35/4.30 (dd, *J* = 8.6, 3.6 Hz, 1H), 3.57-3.31 (m, 2H), 2.31-1.72 (series of m, 6H), 1.45/1.40 (s, 9H), 1.37-1.20 (m, 6H), 0.85 (t, *J* = 6.8 Hz, 3H); ^{13}C NMR (100 MHz, $CDCl_3$) The line listing for both *cis* and *trans* amide isomers is given, as a clear doubling of many peaks is evident. Whenever the isomer peaks overlap, it is stated that the particular peak is representing 2 or more carbons. ppm 172.7, 172.5, 170.2, 170.0, 154.3, 153.9, 135.42, 135.36, 128.69(2C), 128.66(2C) 128.57, 128.5, 128.5(4C), 80.1, 79.7, 72.7, 72.5, 67.1(2C), 59.4, 59.3, 46.6, 46.4, 31.4, 31.3(2C), 31.2(2C), 30.9, 28.5(3C), 28.4(3C), 24.8, 24.6, 24.3, 23.5, 22.4(2C), 14.04, 14.00; HRMS (EI): Exact mass calcd for $C_{24}H_{36}NO_6$ $[M+H]^+$ 434.2537, found 434.2543. ANS-5-16.

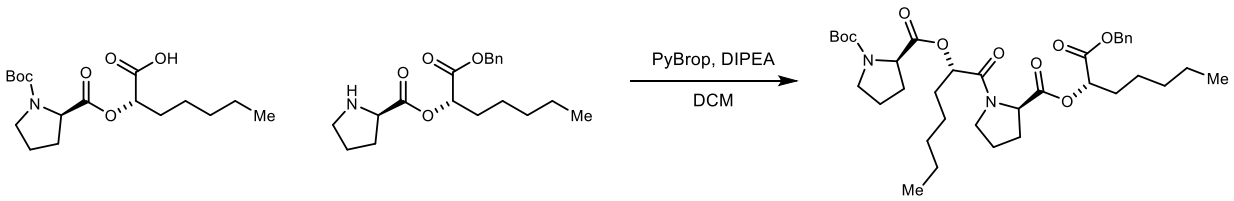

2-((*S*)-1-((*R*)-2-((((*S*)-1-(Benzyloxy)-1-oxoheptan-2-yl)oxy)carbonyl)pyrrolidin-1-yl)-1-oxoheptan-2-yl) 1-(*tert*-butyl) (*R*)-pyrrolidine-1,2-dicarboxylate (S39). A round-bottom flask was charged with the amine (80.7 mg, 242 μmol), acid (83.2 mg, 242 μmol), and DCM (2.4 mL). The mixture was cooled to 0 °C and then DIPEA (124 μL, 726 μmol) and PyBrop (169 mg, 363

μmol) were added. The reaction was stirred at 0 °C for 30 min, then allowed to warm to ambient temperature and stir for an additional 1.5 h. The reaction mixture was poured into cold 10% aq citric acid and extracted with DCM. The combined organic layers were washed with satd aq $NaHCO_3$ and brine, and then dried and concentrated. The crude residue was subjected to flash column chromatography (SiO_2, 30% ethyl acetate in hexanes) to afford the product as a pale-yellow oil (116 mg, 73%). $[\alpha]_D^{23}$ +35.3 (*c* 1.47, $CHCl_3$); R_f = 0.2 (30% EtOAc/hexanes); IR (film) 2956, 2930, 2872, 1745, 1698, 1665, 1439, 1397, 1365, 1259, 1162 cm^{-1}; ^1H NMR (600 MHz, $CDCl_3$) This compound exists as a mixture of rotamers causing peak broadening and overlap. Refer to the image of the ^1H NMR spectrum.^{13}C NMR (150 MHz, $CDCl_3$) This compound is a mixture of rotamers causing peak doubling, broadening, and overlap. Refer to the image of the ^{13}C NMR spectrum; HRMS (EI): Exact mass calcd for $C_{36}H_{55}N_2O_9$ $[M+H]^+$ 659.3902, found 659.3915. ANS-5-21.

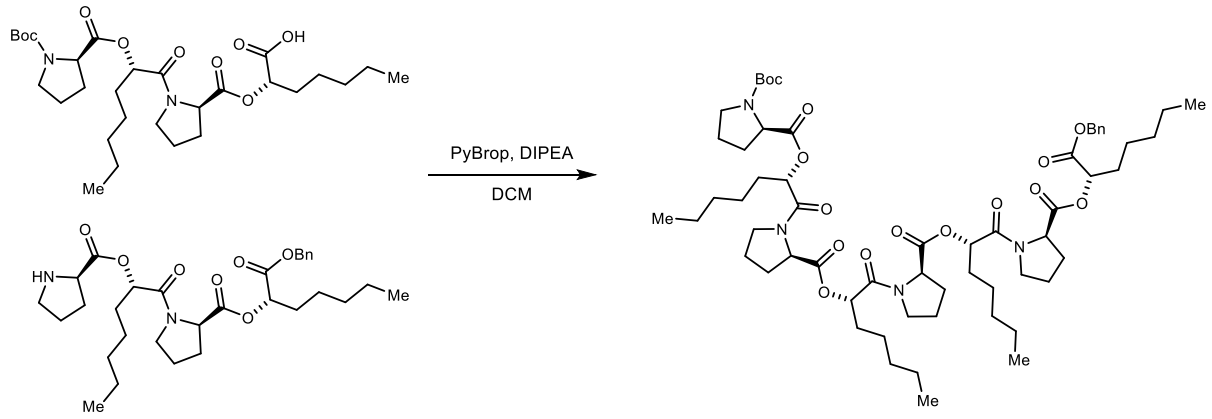

2-((*S*)-1-((*R*)-2-((((*S*)-1-((*R*)-2-((((*S*)-1-((*R*)-2-((((*S*)-1-(Benzyloxy)-1-oxoheptan-2-yl)oxy)carbonyl)pyrrolidin-1-yl)-1-oxoheptan-2-yl)oxy)carbonyl)pyrrolidin-1-yl)-1-oxoheptan-2-yl)oxy)carbonyl)pyrrolidin-1-yl)-1-oxoheptan-2-yl) 1-(*tert*-butyl) (*R*)-pyrrolidine-1,2-dicarboxylate (S40). A round-bottom flask was charged with the amine (49.1 mg, 88.0 μmol), acid (50.0 mg, 88.0 μmol), and DCM (880 μL). The mixture was cooled to 0 °C and then DIPEA (45 μL, 260 μmol) and PyBrop (61.5 mg, 132 μmol) were added. The reaction was stirred at 0 °C for 30 min, then allowed to warm to ambient temperature and stir for an additional 1.5 h. The reaction mixture was poured into cold 10% aq citric acid and extracted with DCM. The combined organic layers were washed with satd aq $NaHCO_3$ and brine, and then dried and concentrated. The crude residue was subjected to flash column chromatography (SiO_2, 40% ethyl acetate in hexanes) to afford the product as a pale-yellow oil (73 mg, 75%). $[\alpha]_D^{23}$ +28.7 (*c*

1.34, $CHCl_3$); R_f = 0.17 (50% EtOAc/hexanes); IR (film) 2956, 2930, 2871, 1745, 1697, 1661, 1448, 1397, 1278, 1163, 1118 cm^{-1}; ^1H NMR (600 MHz, $CDCl_3$) This compound exists as a mixture of rotamers causing peak broadening and overlap. Refer to the image of the ^1H NMR spectrum.^{13}C NMR (150 MHz, $CDCl_3$) This compound is a mixture of rotamers causing peak doubling, broadening, and overlap. Refer to the image of the ^{13}C NMR spectrum; HRMS (EI): Exact mass calcd for $C_{60}H_{96}N_5O_{15}$ $[M+NH_4]^+$ 1126.6897, found 1126.6918. ANS-5-26.

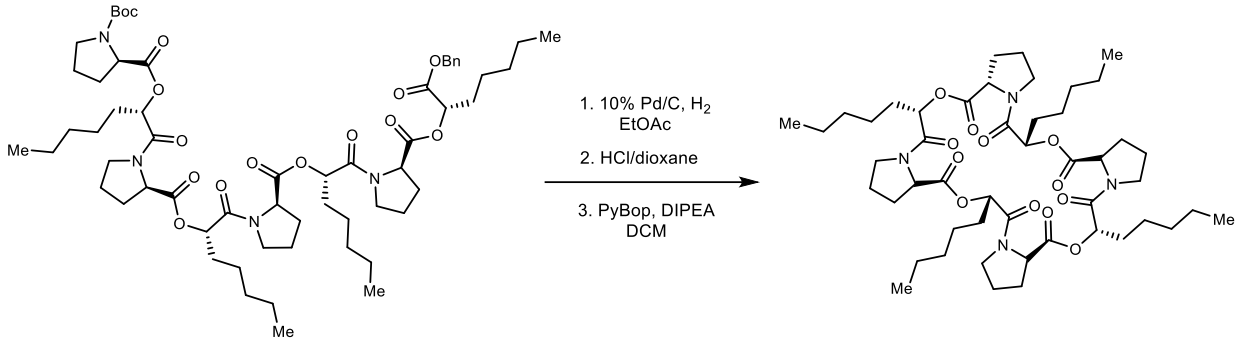

(6*S*,8a*R*,14*S*,16a*R*,22*S*,24a*R*,30*S*,32a*S*)-6,14,22,30-Tetrapentylhexadecahydro-8H,16H,24H,32H-tetrapyrrolo[2,1-c:2',1'-i:2'',1''-o:2''',1'''-u][1,7,13,19]tetraoxa[4,10,16,22]tetraazacyclotetracosin-5,8,13,16,21,24,29,32(6H,14H,22H,30H)-octaone (72). A round-bottom flask was charged with the depsipeptide (73 mg, 55.3 μmol), dissolved in EtOAc (2.5 mL), and treated with 10% Pd/C (8.0 mg). The reaction flask was evacuated with light vacuum (50 Torr). Hydrogen (balloon) was added, and the flask was cycled once more. The reaction was allowed to stir for 2 h. After purging the flask with nitrogen, the crude reaction mixture was filtered through Celite. To the crude material was added 4 M HCl in dioxane (2.0 mL) and the reaction mixture was allowed to stir for 30 min. The reaction mixture was concentrated and added to a flame-dried round-bottom flask. DCM (13.2 mL) was added and the reaction was cooled to 0 °C. Once at 0 °C, DIPEA (25.0 μL, 145 μmol) and PyBrop (36.0 mg, 69.1 μmol) were added. The reaction was stirred at 0 °C for 1.5 h, then allowed to warm to ambient temperature and stir for an additional 1 h. The reaction mixture was poured into cold 10% aq citric acid and extracted with DCM. The combined organic layers were washed with satd aq $NaHCO_3$ and brine, and then dried and concentrated. Preparative HPLC (5 – 95% aqueous acetonitrile, 210 nm, flow rate: 8 mL/min, R_t = 23.4 m) afforded the 24-membered macrocycle (21.6 mg, 36%) as a colorless oil. $[\alpha]_D^{23}$ +21 (*c* 0.69, $CHCl_3$); R_f = 0.23 (5% MeOH/DCM); IR (film) 2955, 2929, 2871, 1742, 1659, 1444, 1341, 1274, 1174, 1092 cm^{-1}; ^1H

NMR (600 MHz, $CDCl_3$) This compound exists in multiple conformations, causing significant peak overlap. Refer to the image of the ^{1}H NMR spectrum; ^{13}C NMR (150 MHz, $CDCl_3$) This compound exists in multiple conformations, causing significant peak overlap. Refer to the image of the ^{13}C NMR spectrum; HRMS (EI): Exact mass calcd for $C_{48}H_{80}N_5O_{12}$ $[M+NH_4]^+$ 918.5798, found 918.5784. ANS-5-31.

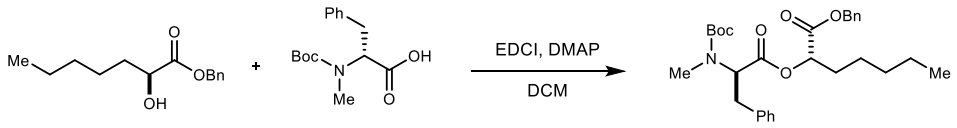

Benzyl (*S*)-2-((*N*-(*tert*-butoxycarbonyl)-*N*-methyl-D-phenylalanyl)oxy)heptanoate (S41). A round-bottom flask was charged with the amine (260 mg, 930 μmol), alcohol (200 mg, 846 μmol), and DCM (8.5 mL). The mixture was cooled to 0 °C and then EDCI (195 mg, 1.02 mmol) and DMAP (5.2 mg, 42 μmol) were added. The reaction was stirred at 0 °C for 30 min, then allowed to warm to ambient temperature to stir for an additional 1.5 h. The reaction mixture was poured into water and extracted with DCM. The combined organic layers were washed with satd aq $NaHCO_3$ and brine, and then dried and concentrated to afford the product as a pale-yellow oil (362 mg, 86%). $[\alpha]_D^{23}$ +22 (*c* 0.86, $CHCl_3$); R_f = 0.56 (5% EtOAc/hexanes); IR (film) 2955, 2929, 2860, 1743, 1697, 1454, 1390, 1365, 1314, 1170, 1139 cm^{-1}; ^{1}H NMR (400 MHz, $CDCl_3$) Several peaks show a clear doubling for the *cis* and *trans* amide products. Other peaks are overlapping and appear only once. Those that are doubled have both values listed. δ 7.41-7.11 (m, 10H), 5.23 (d, *J* = 12.2 Hz, 1H), 5.19/4.94 (dd, *J* = 11.2, 4.5 Hz, 1H), 5.14 (d, *J* = 12.2 Hz, 1H), 5.07 (dd, *J* = 6.2, 6.2 Hz, 1H), 3.34/3.30 (dd, *J* = 15.3, 4.9 Hz, 1H), 3.03-3.23 (m, 1H), 2.78/2.71 (s, 3H), 1.90-1.78 (m, 2H), 1.36/1.30 (s, 9H), 1.42-1.20 (m, 6H), 0.86 (t, *J* = 6.7 Hz, 3H); ^{13}C NMR (100 MHz, $CDCl_3$) The line listing for both *cis* and *trans* amide isomers is given, as a clear doubling of many peaks is evident. Whenever the isomer peaks overlap, it is stated that the particular peak is representing 2 or more carbons. ppm 171.3, 171.0, 169.9, 169.8, 156.0, 155.2, 137.5, 137.3, 135.4, 135.3, 129.0(4C), 128.7(4C), 128.6(4C), 128.4(4C), 126.8(2C), 126.6(2C), 80.2, 79.9, 73.2, 73.0, 67.2, 67.1, 60.4, 58.8, 35.1, 34.9, 31.3(2C), 31.0(2C), 30.9(2C), 28.3(3C), 28.2(3C), 24.8, 24.6, 22.4(2C), 14.0(2C); HRMS (EI): Exact mass calcd for $C_{29}H_{39}NaNO_6$ $[M+Na]^+$ 520.2670, found 520.2670. ANS-6-06.

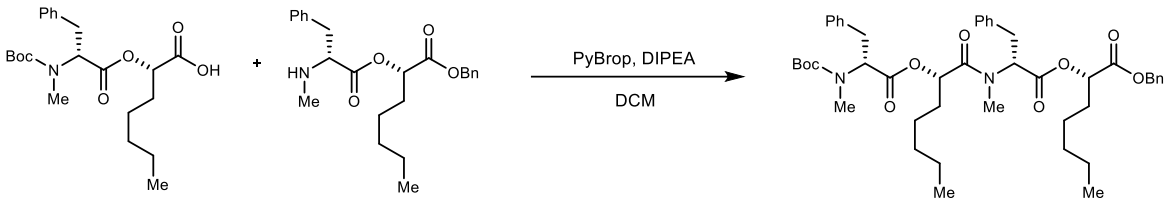

Benzyl (*S*)-2-(((6*R*,9*S*,12*R*)-6,12-dibenzyl-2,2,5,11-tetramethyl-4,7,10-trioxo-9-pentyl-3,8-dioxa-5,11-diazatridecan-13-oyl)oxy)heptanoate (S42). A round-bottom flask was charged with the amine (31.4 mg, 79.2 μmol), acid (32.3 mg, 79.2 μmol), and DCM (800 μL). The mixture was cooled to 0 °C and then DIPEA (40.7 μL, 238 μmol) and PyBrop (55.4 mg, 119 μmol) were added. The reaction was stirred at 0 °C for 30 min, then allowed to warm to ambient temperature and stir for an additional 1.5 h. The reaction mixture was poured into cold 10% aq citric acid and extracted with DCM. The combined organic layers were washed with satd aq $NaHCO_3$ and brine, and then dried and concentrated. The crude residue was subjected to flash column chromatography (SiO_2, 30% ethyl acetate in hexanes) to afford the product as a white solid (44.2 mg, 71%). $[\alpha]_D^{23}$ +30 (*c* 0.94, $CHCl_3$); Mp 85-90 °C; R_f = 0.28 (20% EtOAc/hexanes); IR (film) 3054, 2956, 2930, 2861, 1739, 1689, 1667, 1455, 1418, 1391, 1366, 1264 cm^{-1}; ^1H NMR (400 MHz, $CDCl_3$) This compound exists as a mixture of rotamers causing peak broadening and overlap. Refer to the image of the ^1H NMR spectrum.^{13}C NMR (100 MHz, $CDCl_3$) This compound is a mixture of rotamers causing peak doubling, broadening, and overlap. Refer to the image of the ^{13}C NMR spectrum; HRMS (EI): Exact mass calcd for $C_{46}H_{62}N_2NaO_9$ $[M+Na]^+$ 809.4348, found 809.4352. ANS-6-159.

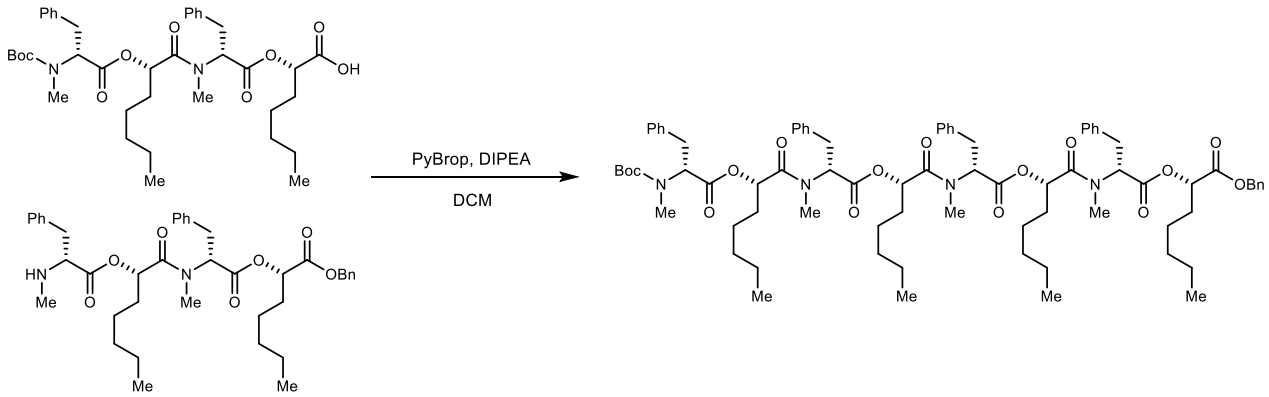

Benzyl (*S*)-2-(((6*R*,9*S*,12*R*,15*S*,18*R*,21*S*,24*R*)-6,12,18,24-tetrabenzyl-2,2,5,11,17,23-hexamethyl-4,7,10,13,16,19,22-heptaoxo-9,15,21-tripentyl-3,8,14,20-tetraoxa-5,11,17,23-tetraazapentacosan-25-oyl)oxy)heptanoate (S43). A round-bottom flask was charged with the

amine (61.9 mg, 90.2 μmol), acid (62.8 mg, 90.2 μmol), and DCM (1.0 mL). The mixture was cooled to 0 °C and then DIPEA (46.3 μL, 271 μmol) and PyBrop (63.1 mg, 135 μmol) were added. The reaction was stirred at 0 °C for 30 min, then allowed to warm to ambient temperature and stir for an additional 1.5 h. The reaction mixture was poured into cold 10% aq citric acid and extracted with DCM. The combined organic layers were washed with satd aq $NaHCO_3$ and brine, and then dried and concentrated. The crude residue was subjected to reverse phase column chromatography (C18, 10-100% linear gradient; acetonitrile in H_2O (0.1% TFA buffer)) to afford the product as a colorless foam (27.3 mg, 22%). $[\alpha]_D^{23}$ +38 (*c* 0.64, $CHCl_3$); R_f = 0.13 (20% EtOAc/hexanes); IR (film) 2954, 2928, 2857, 1738, 1694, 1665, 1455, 1260, 1170, 1063 cm^{-1}; ^1H NMR (600 MHz, $CDCl_3$) This compound exists as a mixture of rotamers causing peak broadening and overlap. Refer to the image of the ^1H NMR spectrum.^{13}C NMR (150 MHz, $CDCl_3$) This compound is a mixture of rotamers causing peak doubling, broadening, and overlap. Refer to the image of the ^{13}C NMR spectrum; HRMS (ESI): Exact mass calcd for $C_{80}H_{112}N_5O_{15}$ $[M+NH_4]^+$ 1382.8149, found 1382.8149 ANS-6-235.

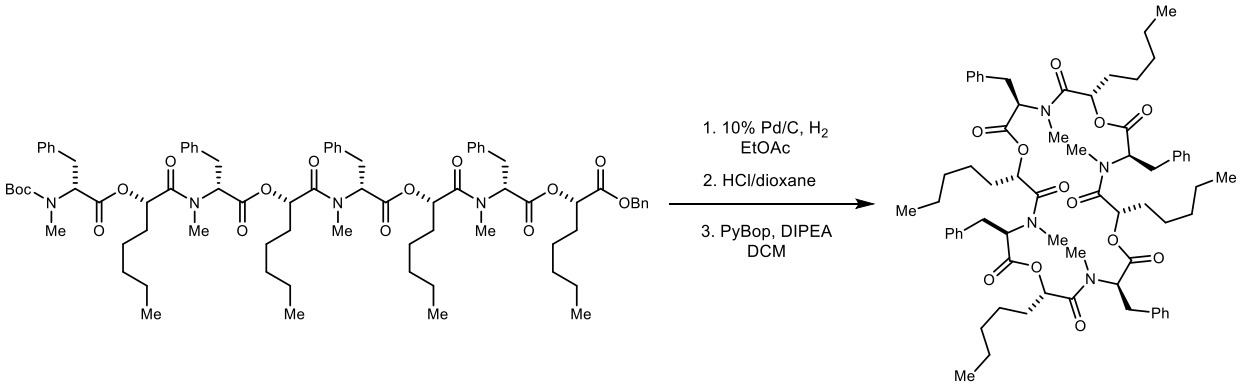

(3*R*,6*S*,9*R*,12*S*,15*R*,18*S*,21*R*,24*S*)-3,9,15,21-Tetrabenzyl-4,10,16,22-tetramethyl-6,12,18,24-tetrapentyl-1,7,13,19-tetraoxa-4,10,16,22-tetraazacyclotetracosan-2,5,8,11,14,17,20,23-octaone (73). A round-bottom flask was charged with the depsipeptide (27.3 mg, 19.9 μmol), dissolved in EtOAc (2.0 mL), and treated with 10% Pd/C (3.0 mg). The reaction flask was evacuated with light vacuum (50 Torr). Hydrogen (balloon) was added, and the flask was cycled once more. The reaction was allowed to stir for 2 h. After purging the flask with nitrogen, the crude reaction mixture was filtered through Celite. To the crude material was added 4 M HCl in dioxane (2.0 mL) and the reaction mixture was allowed to stir for 1 h. The reaction mixture was concentrated and added to a flame-dried round-bottom flask. DCM (4.0 mL) was added and the reaction was cooled to 0 °C. Once at 0 °C, DIPEA (10.2 μL, 59.7 μmol) and PyBrop (15.5 mg,

29.8 μmol) were added. The reaction was stirred at 0 °C for 1.5 h, then allowed to warm to ambient temperature and stir for an additional 1 h. The reaction mixture was poured into cold 10% aq citric acid and extracted with DCM. The combined organic layers were washed with satd aq $NaHCO_3$ and brine, and then dried and concentrated. Reverse phase column chromatography (5 – 95% aqueous acetonitrile, linear gradient) afforded the 24-membered macrocycle (7.6 mg, 33%) as a light-yellow oil. $[\alpha]_D^{23}$ +23 (*c* 0.54, $CHCl_3$); R_f = 0.37 (10% MeOH/DCM); IR (film) 2953, 2928, 2858, 1740, 1666, 1455, 1258, 1193 cm^{-1}; ^1H NMR (600 MHz, $CDCl_3$) This compound exists in multiple conformations, causing significant peak overlap. Refer to the image of the ^1H NMR spectrum; ^{13}C NMR (150 MHz, $CDCl_3$) This compound exists in multiple conformations, causing significant peak overlap. Refer to the image of the ^{13}C NMR spectrum; HRMS (EI): Exact mass calcd for $C_{68}H_{94}N_5O_{12}$ $[M+NH_4]^+$ 1174.7050, found 1174.7051. ANS-6-250.

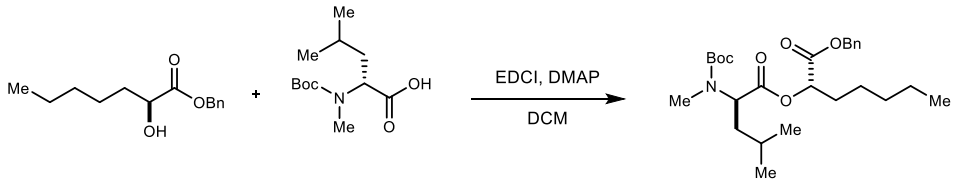

Benzyl (*S*)-2-((*N*-(*tert*-butoxycarbonyl)-*N*-methyl-D-leucyl)oxy)heptanoate (S44). A round-bottom flask was charged with the amine (235 mg, 959 μmol), alcohol (189 mg, 799 μmol), and DCM (8.0 mL). The mixture was cooled to 0 °C and then EDCI (184 mg, 959 μmol) and DMAP (4.9 mg, 40 μmol) were added. The reaction was stirred at 0 °C for 30 min, then allowed to warm to ambient temperature to stir for an additional 1.5 h. The reaction mixture was poured into water and extracted with DCM. The combined organic layers were washed with satd aq $NaHCO_3$ and brine, and then dried and concentrated to afford the product as a colorless oil (272 mg, 74%). $[\alpha]_D^{23}$ +18 (*c* 0.67, $CHCl_3$); R_f = 0.31 (5% EtOAc/hexanes); IR (film) 2957, 2871, 1744, 1697, 1455, 1390, 1366, 1184, 1150 cm^{-1}; ^1H NMR (400 MHz, $CDCl_3$) Several peaks show a clear doubling for the *cis* and *trans* amide products. Other peaks are overlapping and appear only once. Those that are doubled have both values listed. δ 7.40-7.30 (m, 5H), 5.20 (d, *J* = 12.2 Hz, 1H), 5.11 (d, *J* = 12.2 Hz, 1H), 5.03 (dd, *J* = 6.2, 6.2 Hz, 1H), 4.99/4.76 (dd, *J* = 11.0, 4.8 Hz, 1H), 2.76/2.73 (s, 3H), 1.90-1.50 (series of m, 5H), 1.46/1.45 (s, 9H), 1.41-1.20 (m, 6H), 0.94 (d, *J* = 7.1 Hz, 3H), 0.92 (d, *J* = 6.7 Hz, 3H), 0.86 (t, *J* = 6.8 Hz, 3H); ^{13}C NMR (100 MHz, $CDCl_3$) The line listing for both *cis* and *trans* amide isomers is given, as a clear doubling of many peaks is evident. Whenever the isomer peaks overlap, it is stated that the particular peak is representing 2 or more carbons.

ppm 172.3, 172.2, 170.1, 169.9, 156.4, 155.7, 135.43, 135.39, 128.7(4C), 128.61, 128.57, 128.5(4C), 80.3, 79.9, 72.9, 72.8, 67.2, 67.1, 56.8(2C), 55.8(2C), 37.7, 37.3, 31.4, 31.3(2C), 30.3, 29.9, 28.5(6C), 24.9, 24.8, 24.6, 23.4, 23.3, 22.5(2C), 21.5, 21.2, 14.0(2C); HRMS (EI): Exact mass calcd for $C_{26}H_{42}NO_6$ $[M+H]^+$ 464.3007, found 464.3010. ANS-5-06.

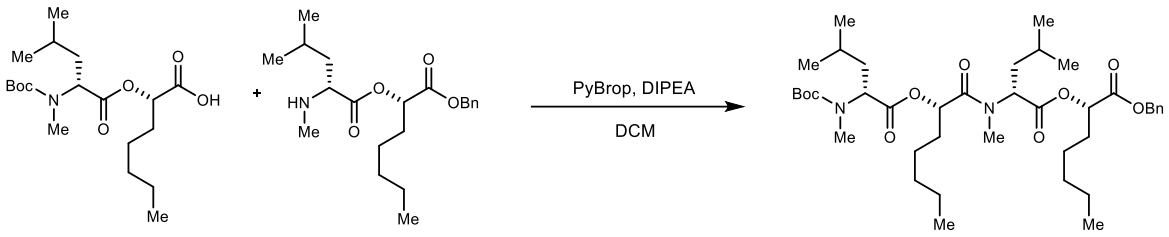

Benzyl (*S*)-2-(((6*R*,9*S*,12*R*)-6,12-diisobutyl-2,2,5,11-tetramethyl-4,7,10-trioxo-9-pentyl-3,8-dioxa-5,11-diazatridecan-13-oyl)oxy)heptanoate (S45). A round-bottom flask was charged with the amine (78.1 mg, 215 μmol), acid (80.6 mg, 215 μmol), and DCM (2.2 mL). The mixture was cooled to 0 °C and then DIPEA (110 μL, 645 μmol) and PyBrop (151 mg, 323 μmol) were added. The reaction was stirred at 0 °C for 30 min, then allowed to warm to ambient temperature and stir for an additional 1.5 h. The reaction mixture was poured into cold 10% aq citric acid and extracted with DCM. The combined organic layers were washed with satd aq $NaHCO_3$ and brine, and then dried and concentrated. The crude residue was subjected to flash column chromatography (SiO_2, 30% ethyl acetate in hexanes) to afford the product as a colorless oil (113 mg, 73%). $[\alpha]_D^{23}$ +31 (*c* 1.37, $CHCl_3$); R_f = 0.19 (10% EtOAc/hexanes); IR (film) 2956, 2870, 1741, 1696, 1669, 1456, 1390, 1366, 1185, 1150 cm^{-1}; ^1H NMR (600 MHz, $CDCl_3$) This compound exists as a mixture of rotamers causing peak broadening and overlap. Refer to the image of the ^1H NMR spectrum.^{13}C NMR (150 MHz, $CDCl_3$) This compound is a mixture of rotamers causing peak doubling, broadening, and overlap. Refer to the image of the ^{13}C NMR spectrum; HRMS (EI): Exact mass calcd for $C_{40}H_{67}N_2O_9$ $[M+H]^+$ 719.4841, found 719.4847. ANS-5-10.

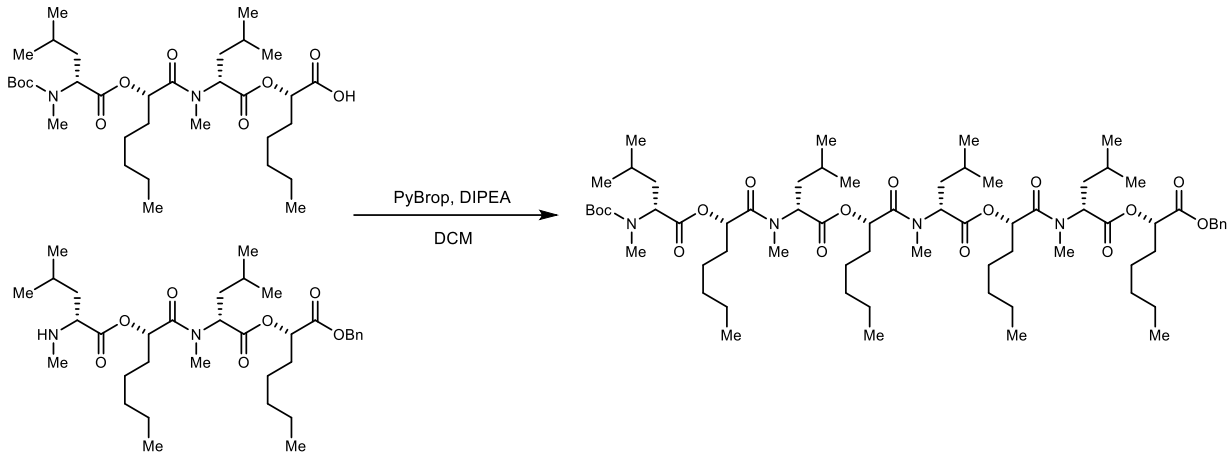

Benzyl (*S*)-2-(((6*R*,9*S*,12*R*,15*S*,18*R*,21*S*,24*R*)-6,12,18,24-tetraisobutyl-2,2,5,11,17,23-hexamethyl-4,7,10,13,16,19,22-heptaoxo-9,15,21-tripentyl-3,8,14,20-tetraoxa-5,11,17,23-tetraazapentacosan-25-oyl)oxy)heptanoate (S46). A round-bottom flask was charged with the amine (48.2 mg, 77.9 μmol), acid (48.9 mg, 77.9 μmol), and DCM (800 μL). The mixture was cooled to 0 °C and then DIPEA (40 μL, 230 μmol) and PyBrop (54.4 mg, 117 μmol) were added. The reaction was stirred at 0 °C for 30 min, then allowed to warm to ambient temperature and stir for an additional 1.5 h. The reaction mixture was poured into cold 10% aq citric acid and extracted with DCM. The combined organic layers were washed with satd aq $NaHCO_3$ and brine, and then dried and concentrated. The crude residue was subjected to flash column chromatography (SiO_2, 30% ethyl acetate in hexanes) to afford the product as an amorphous white foam (68 mg, 71%). $[\alpha]_D^{23}$ +40.3 (*c* 1.08, $CHCl_3$); R_f = 0.12 (20% EtOAc/hexanes); IR (film) 2956, 2870, 1739, 1694, 1666, 1468, 1389, 1367, 1263, 1126 cm^{-1}; ^1H NMR (600 MHz, $CDCl_3$) This compound exists as a mixture of rotamers causing peak broadening and overlap. Refer to the image of the ^1H NMR spectrum.^{13}C NMR (150 MHz, $CDCl_3$) This compound is a mixture of rotamers causing peak doubling, broadening, and overlap. Refer to the image of the ^{13}C NMR spectrum; HRMS (EI): Exact mass calcd for $C_{68}H_{120}N_5O_{15}$ $[M+NH_4]^+$ 1246.8774, found 1246.8782. ANS-5-15.

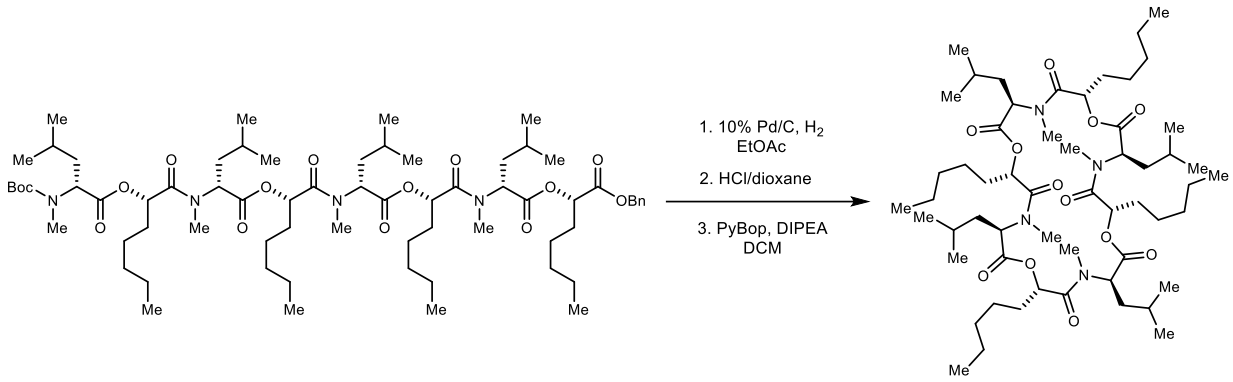

(3*R*,6*S*,9*R*,12*S*,15*R*,18*S*,21*R*,24*S*)-3,9,15,21-tetraisobutyl-4,10,16,22-tetramethyl-6,12,18,24-tetrapentyl-1,7,13,19-tetraoxa-4,10,16,22-tetraazacyclotetracosan-2,5,8,11,14,17,20,23-octaone (74). A round-bottom flask was charged with the depsipeptide (68 mg, 55 μmol), dissolved in EtOAc (2.0 mL), and treated with 10% Pd/C (7.0 mg). The reaction flask was evacuated with light vacuum (50 Torr). Hydrogen (balloon) was added, and the flask was cycled once more. The reaction was allowed to stir for 2 h. After purging the flask with nitrogen, the crude reaction mixture was filtered through Celite. To the crude material was added 4 M HCl in dioxane (2.0 mL) and the reaction mixture was allowed to stir for 30 min. The reaction mixture was concentrated and added to a flame-dried round-bottom flask. DCM (11.0 mL) was added and the reaction was cooled to 0 °C. Once at 0 °C, DIPEA (20.8 μL, 122 μmol) and PyBrop (30.2 mg, 58.0 μmol) were added. The reaction was stirred at 0 °C for 1.5 h, then allowed to warm to ambient temperature and stir for an additional 1 h. The reaction mixture was poured into cold 10% aq citric acid and extracted with DCM. The combined organic layers were washed with satd aq $NaHCO_3$ and brine, and then dried and concentrated. Preparative HPLC (5 – 95% aqueous acetonitrile, 210 nm, flow rate: 8 mL/min, R_t = 33.2 m) afforded the 24-membered macrocycle (9.0 mg, 16%) as a colorless oil. $[\alpha]_D^{23}$ +8.7 (*c* 0.58, $CHCl_3$); R_f = 0.17 (4% MeOH/DCM); IR (film) 2954, 2931, 2870, 1742, 1666, 1456, 1456, 1416, 1386, 1261, 1190, 1126, 1099, 1061 cm^{-1}; ^1H NMR (600 MHz, $CDCl_3$) This compound exists in multiple conformations, causing significant peak broadening. Refer to the image of the ^1H NMR spectrum; ^{13}C NMR (150 MHz, $CDCl_3$) This compound exists in multiple conformations, causing significant peak overlap. Refer to the image of the ^{13}C NMR spectrum; HRMS (EI): Exact mass calcd for $C_{56}H_{100}N_4NaO_{12}$ $[M+Na]^+$ 1043.7230, found 1043.7232. ANS-5-22.

Benzyl (*S*)-2-(methoxymethoxy)hexanoate (S47). A round-bottom flask was charged with nitroalkane (496 mg, 2.56 mml), $NaNO_2$ (530 mg, 7.68 mmol), AcOH (2.2 mL, 38.4 mmol), and DMSO (17 mL). The mixture was stirred at 45 °C for 18 h under an argon atmosphere. The reaction mixture was then allowed to cool to ambient temperature, treated with 1 N HCl, and poured into CH_2Cl_2. The aqueous layer was extracted with CH_2Cl_2, and the combined organic layers were washed with water, brine, dried, and concentrated. The crude mixture was then added to a round-bottom flask with K_2CO_3 (1.06 g, 7.68 mmol) and DMF (5.2 mL). The mixture was then treated with BnBr (365 μL, 3.07 mmol) under argon (balloon). The reaction was stirred overnight at ambient temperature. The reaction was quenched with 1 M aq HCl and extracted with Et_2O. The organic layer was washed with 1 M HCl, water, brine, dried and concentrated. The crude residue was subjected to flash column chromatography (SiO_2, 5% diethyl ether in hexanes) to afford the product as a pale-yellow oil (327 mg, 48%, 2 steps). $[\alpha]_D^{20}$ -56 (*c* 0.63, $CHCl_3$); R_f = 0.28 (20% Et_2O/hexanes); IR (film) 2955, 2858, 1749, 1457, 1264, 1155, 1124, 1031 cm^{-1}; ^1H NMR (400 MHz, $CDCl_3$) δ 7.38-7.28 (m, 5H), 5.18 (d, *J* = 12.4 Hz, 1H), 5.15 (d, *J*= 12.4 Hz, 1H), 4.68 (d, *J* = 7.0 Hz, 1H), 4.64 (d, *J* = 6.9 Hz, 1H), 4.14 (dd, *J* = 6.4, 6.4 Hz, 1H), 3.33 (s, 3H), 1.76 (dddd, *J* = 8.3, 6.5, 6.5, 6.5 Hz, 2H), 1.44-1.20 (series of m, 4H), 0.87 (t, *J* = 6.9 Hz, 3H); ^{13}C NMR (100 MHz, $CDCl_3$) ppm 172.6, 135.7, 128.6, 128.31, 128.30, 96.3, 75.7, 66.5, 56.0, 32.6, 27.3, 22.3, 13.9; HRMS (EI): Exact mass calcd for $C_{15}H_{23}O_4$ $[M+H]^+$ 267.1589, found 267.1591. ANS-3-101.

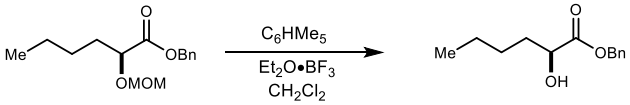

Benzyl (*S*)-2-hydroxyhexanoate (S48). A flame-dried round-bottom flask was charged with the protected alcohol (326 mg, 1.23 mmol) dissolved in dry dichloromethane (0.05 M), pentamethyl benzene (547 mg, 3.69 mmol), and $BF_3{\cdot}Et_2O$ (455 μL, 3.69 mmol). The reaction was allowed to stir for 50 minutes at ambient temperature. The crude reaction mixture was quenched with satd aq $NaHCO_3$, washed with brine, and then dried concentrated, and subjected to flash column chromatography (SiO_2, 10-40% ethyl acetate in hexanes) to afford the alcohol (177 mg, 65%) as a pale-yellow oil. $[\alpha]_D^{25}$ -12 (*c* 0.42, $CHCl_3$); R_f = 0.36 (20% EtOAc/hexanes); IR (film) 3464, 2955, 2867, 1734, 1456, 1261, 1196, 1132 cm^{-1}; ^1H NMR (400 MHz, $CDCl_3$) δ 7.42-7.30 (m, 5H), 5.23

(d, *J* = 12.3 Hz, 1H), 5.19 (d, *J* = 12.3 Hz, 1H), 4.26-4.20 (m, 1H), 2.94 (br s, 1H), 1.87-1.57 (series of m, 2H), 1.50-1.20 (m, 4H), 0.88 (t, *J* = 7.1 Hz, 3H); ^{13}C NMR (125 MHz, $CDCl_3$) ppm 175.3, 135.4, 128.7, 128.6, 128.4, 70.6, 67.2, 34.1, 26.9, 22.4, 13.9; HRMS (EI): Exact mass calcd for $C_{13}H_{18}NaO_3$ $[M+Na]^+$ 245.1148, found 245.1150. ANS-3-108.

Benzyl (*S*)-2-((*N*-(*tert*-butoxycarbonyl)-N-methyl-D-alanyl)oxy)hexanoate (S49). A round-bottom flask was charged with the amine (186 mg, 916 μmol), alcohol (177 mg, 796 μmol), and DCM (8.0 mL). The mixture was cooled to 0 °C and the EDCI (183 mg, 955 μmol) and DMAP (4.8 mg, 40 μmol) were added. The reaction was stirred at 0 °C for 30 min, then allowed to warm to ambient temperature and stir for an additional 1.5 h. The reaction mixture was poured into water and extracted with DCM. The combined organic layers were washed with satd aq $NaHCO_3$ and brine, and then dried and concentrated. The crude residue was subjected to flash column chromatography (SiO_2, 5-20% ethyl acetate in hexanes) to afford the product as a colorless oil (223 mg, 69%). $[\alpha]_D^{20}$ +11.0 (*c* 1.01, $CHCl_3$); R_f = 0.52 (20% EtOAc/hexanes); IR (film) 2956, 2870, 1743, 1697, 1456, 1387, 1315, 1184, 1151, 1084 cm^{-1}; ^{1}H NMR (600 MHz, $CDCl_3$) This compound exists as a mixture of 1:1.2 rotamers causing significant peak broadening and overlap. Refer to image of the ^{1}H NMR spectrum. ^{13}C NMR (150 MHz, $CDCl_3$) This compound is a mixture of 1:1.2 rotamers causing significant peak broadening and overlap. Refer to the image of the ^{13}C NMR spectrum; HRMS (EI): Exact mass calcd for $C_{22}H_{34}NO_6$ $[M+H]^+$ 408.2381, found 408.2390. ANS-3-112.

Benzyl (*S*)-2-(((6*R*,9*S*,12*R*)-9-butyl-2,2,5,6,11,12-hexamethyl-4,7,10-trioxo-3,8-dioxa-5,11-diazatridecan-13-oyl)oxy)hexanoate (S50). A round-bottom flask was charged with the amine (37.7 mg, 123 μmol), acid (38.9 mg, 123 μmol), and DCM (1.3 mL). The mixture was cooled to 0 °C and then DIPEA (63 μL, 370 μmol) and PyBrop (85.8 mg, 184 μmol) were added. The reaction was stirred at 0 °C for 1 h. The reaction mixture was poured into cold 10% citric acid and extracted with DCM. The combined organic layers were washed with satd aq $NaHCO_3$ and brine, and then

dried and concentrated. The crude residue was subjected to flash column chromatography (SiO_2, 20% ethyl acetate in hexanes) to afford the product as a colorless oil (57 mg, 77%). $[\alpha]_D^{25}$ +24 (*c* 0.75, $CHCl_3$); R_f = 0.13 (20% EtOAc/hexanes); IR (film) 2959, 2870, 1743, 1694, 1668, 1457, 1316, 1188, 1133, 1084 cm^{-1}; ^1H NMR (600 MHz, $CDCl_3$) This compound exists as a mixture of rotamers causing significant peak broadening and overlap. Refer to image of the ^1H NMR spectrum; ^{13}C NMR (150 MHz, $CDCl_3$) This compound is a mixture of rotamers causing significant peak broadening and overlap. Refer to the image of the ^{13}C NMR spectrum; HRMS (EI): Exact mass calcd for $C_{32}H_{50}N_2NaO_9$ $[M+Na]^+$ 629.3409, found 629.3426. ANS-3-142.

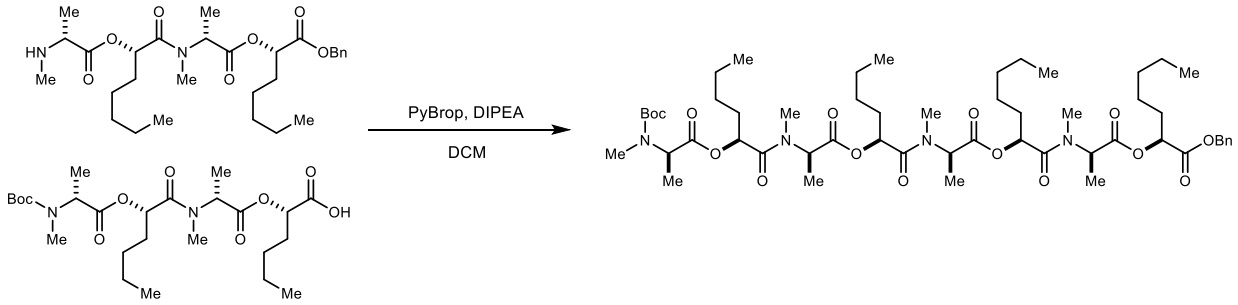

Benzyl (*S*)-2-(((6*R*,9*S*,12*R*,15*S*,18*R*,21*S*,24*R*)-9,15-dibutyl-2,2,5,6,11,12,17,18,23,24-decamethyl-4,7,10,13,16,19,22-heptaoxo-21-pentyl-3,8,14,20-tetraoxa-5,11,17,23-tetraazapentacosan-25-oyl)oxy)heptanoate (S51). A round-bottom flask was charged with the amine (24.6 mg, 46.0 μmol), acid (23.7 mg, 46.0 μmol), and DCM (500 μL). The mixture was cooled to 0 °C and then DIPEA (23.6 μL, 138 μmol) and PyBrop (32.2 mg, 69.0 μmol) were added. The reaction was stirred at 0 °C for 30 min, then allowed to warm to ambient temperature and stir for an additional 1.5 h. The reaction mixture was poured into cold 10% citric acid and extracted with DCM. The combined organic layers were washed with satd aq $NaHCO_3$ and brine, and then dried and concentrated. The crude residue was subjected to flash column chromatography (SiO_2, 10-50% ethyl acetate in hexanes) to afford the product as a colorless oil (24 mg, 50%). $[\alpha]_D^{25}$ +42.7 (*c* 1.00, $CHCl_3$); R_f = 0.21 (40% EtOAc/Hexanes); IR (film) 2932, 2866, 1742, 1664, 1458, 1385, 1212, 1085 cm^{-1}; ^1H NMR (600 MHz, $CDCl_3$) This compound exists as a mixture of rotamers causing significant peak broadening and overlap. Refer to image of the ^1H NMR spectrum; ^{13}C NMR (150 MHz, $CDCl_3$) This compound is a mixture of rotamers causing significant peak broadening and overlap. Refer to the image of the ^{13}C NMR spectrum; HRMS (EI): Exact mass calcd for $C_{54}H_{88}N_4NaO_{15}$ $[M+Na]^+$ 1055.6138, found 1055.6171. ANS-3-149.

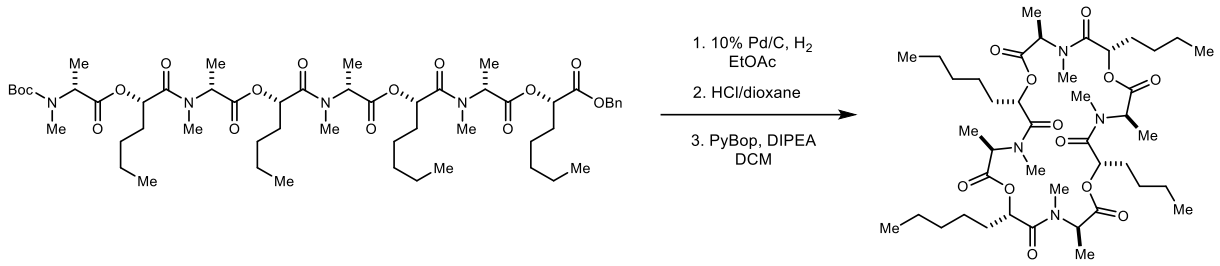

(3*R*,6*S*,9*R*,12*S*,15*R*,18*S*,21*R*,24*S*)-6,12-Dibutyl-3,4,9,10,15,16,21,22-octamethyl-18,24-dipentyl-1,7,13,19-tetraoxa-4,10,16,22-tetraazacyclotetracosan-2,5,8,11,14,17,20,23-octaone (75). A round-bottom flask was charged with the depsipeptide (24.0 mg, 23.2 μmol), dissolved in EtOAc (0.5 mL), and treated with 10% Pd/C (2.4 mg). The reaction flask was evacuated with light vacuum (50 Torr). Hydrogen (balloon) was added and the cycle was repeated once more. The reaction was stirred for 2 h. After purging the flask with nitrogen, the crude reaction mixture was filtered through Celite. To the crude material was added 4 M HCl in dioxane (0.5 mL) and the reaction mixture was allowed to stir for 30 min. The reaction mixture was concentrated and added to a flame-dried round bottom flask. DCM (4.7 mL) was added and the reaction was cooled to 0 °C. At 0 °C, DIPEA (8.7 μL, 51 μmol) and PyBrop (12.7 mg, 24.4 μmol) were added. The reaction was stirred at 0 °C for 1.5 h, then allowed to warm to ambient temperature and stir for an additional 1 h. The reaction mixture was poured into cold 10% citric acid and extracted with DCM. The combined organic layers were washed with satd aq $NaHCO_3$ and brine, and then dried and concentrated. Preparative HPLC (5 – 95% aqueous acetonitrile, 210 nm, flow rate: 8 mL/min, R_t = 21.7 m) afforded the 24-membered macrocycle (6.0 mg, 31%) as a colorless oil. $[\alpha]_D^{25}$ +40 (*c* 0.50, $CHCl_3$); R_f = 0.15 (4% MeOH/DCM); IR (film) 2932, 2865, 1742, 1662, 1461, 1196, 1085 cm^{-1}; ^1H NMR (600 MHz, $CDCl_3$) This compound exists in multiple conformations, causing significant peak overlap. Refer to image of the ^1H NMR spectrum; ^{13}C NMR (150 MHz, $CDCl_3$) This compound exists in multiple conformations, causing significant peak overlap. Refer to image of the ^{13}C NMR spectrum; HRMS (EI): Exact mass calcd for $C_{42}H_{73}N_4O_{12}$ $[M+H]^+$ 825.5220, found 825.5247. ANS-3-156.

Benzyl (*S*)-2-(methoxymethoxy)octanoate (S52). A round-bottom flask was charged with nitroalkane (457 mg, 2.09 mml), $NaNO_2$ (432 mg, 6.30 mmol), AcOH (1.8 mL, 31.3 mmol), and

DMSO (16 mL). The mixture was stirred at 45 °C for 18 h under an argon atmosphere. The reaction was then allowed to cool to ambient temperature, treated with 1 N HCl, and poured into CH_2Cl_2. The aqueous layer was extracted with CH_2Cl_2, and the combined organic layers were washed with water, brine, dried, and concentrated. The crude mixture was then added to a round-bottom flask with K_2CO_3 (865 mg, 6.25 mmol) and DMF (4.7 mL). The mixture was then treated with BnBr (300 μL, 2.5 mmol) under argon (balloon). The reaction was allowed to stir overnight at ambient temperature. The reaction was quenched with 1 M aq HCl and extracted with Et_2O. The organic layer was washed with 1 M HCl, water, brine, dried and concentrated. The crude residue was subjected to flash column chromatography (SiO_2, 5% diethyl ether in hexanes) to afford the product as a pale-yellow oil (373 mg, 61%, 2 steps). $[\alpha]_D^{20}$ -46 (*c* 0.62, $CHCl_3$); R_f = 0.31 (20% Et_2O/hexanes); IR (film) 2929, 2858, 1749, 1457, 1261, 1155, 1108, 1033 cm^{-1}; ^1H NMR (400 MHz, $CDCl_3$) δ 7.37-7.27 (m, 5H), 5.19 (d, *J* = 12.4 Hz, 1H), 5.15 (d, *J*= 12.2 Hz, 1H), 4.68 (d, *J* = 6.9 Hz, 1H), 4.64 (d, *J* = 6.9 Hz, 1H), 4.41 (dd, *J* = 6.5, 6.5 Hz, 1H), 3.33 (s, 3H), 1.76 (dddd, *J* = 6.8, 6.8, 6.8, 6.8 Hz, 1H), 1.76 (dddd, *J* = 6.8, 6.8, 6.8, 6.8 Hz, 1H), 1.44-1.20 (series of m, 8H), 0.87 (t, *J* = 6.8 Hz, 3H); ^{13}C NMR (100 MHz, $CDCl_3$) ppm 172.7, 135.7, 128.6, 128.4, 128.3, 96.3, 75.7, 66.5, 56.0, 32.9, 31.7, 28.9, 25.1, 22.6, 14.0; HRMS (EI): Exact mass calcd for $C_{17}H_{27}O_4$ $[M+H]^+$ 295.1901, found 295.1904. ANS-3-100.

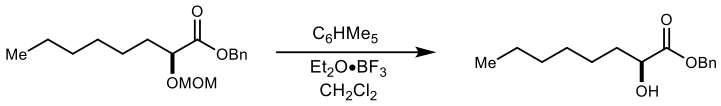

Benzyl (*S*)-2-hydroxyoctanoate (S53). A flame-dried round-bottom flask was charged with the protected alcohol (373 mg, 1.27 mmol) dissolved in dry dichloromethane (0.05 M), pentamethyl benzene (563 mg, 3.80 mmol), and $BF_3{\cdot}Et_2O$ (469 μL, 3.80 mmol). The reaction was allowed to stir for 50 minutes at ambient temperature. The crude reaction mixture was quenched with satd aq $NaHCO_3$ and brine, and then dried and concentrated. The crude mixture was subjected to flash column chromatography (SiO_2, 10-30% ethyl acetate in hexanes) to afford the alcohol (188 mg, 59%) as a pale-yellow oil. $[\alpha]_D^{25}$ -15 (*c* 0.77, $CHCl_3$); R_f = 0.37 (20% EtOAc/hexanes); IR (film) 3475, 2953, 2927, 2858, 1736, 1655, 1457, 1261, 1211, 1133 cm^{-1}; ^1H NMR (400 MHz, $CDCl_3$) δ 7.42-7.30 (m, 5H), 5.24 (d, *J* = 12.2 Hz, 1H), 5.20 (d, *J* = 12.2 Hz, 1H), 4.23 (ddd, *J* = 7.6, 4.9, 4.9 Hz, 1H), 2.85 (d, *J* = 5.6 Hz, 1H), 1.85-1.75 (m, 1H), 1.71-1.60 (m, 1H), 1.48-1.20 (m, 8H), 0.88 (t, *J* = 6.7 Hz, 3H); ^{13}C NMR (125 MHz, $CDCl_3$) ppm 175.4, 135.4, 128.7, 128.6, 128.4, 70.6,

67.3, 34.5, 31.7, 29.0, 24.7, 22.6, 14.1; HRMS (EI): Exact mass calcd for $C_{15}H_{22}NaO_3$ $[M+Na]^+$ 273.146, found 273.1463. ANS-3-107.

Benzyl (*S*)-2-((*N*-(*tert*-butoxycarbonyl)-*N*-methyl-D-alanyl)oxy)octanoate (S54). A round-bottom flask was charged with the amine (175 mg, 862 μmol), alcohol (188 mg, 749 μmol), and DCM (7.5 mL). The mixture was cooled to 0 °C and the EDCI (173 mg, 899 μmol) and DMAP (4.6 mg, 38 μmol) were added. The reaction was stirred at 0 °C for 30 min, then allowed to warm to ambient temperature and stir for an additional 1.5 h. The reaction mixture was poured into water and extracted with DCM. The combined organic layers were washed with satd aq $NaHCO_3$ and brine, and then dried and concentrated. The crude residue was subjected to flash column chromatography (SiO_2, 5-20% ethyl acetate in hexanes) to afford the product as a colorless oil (288 mg, 88%). $[\alpha]_D^{20}$ +11.0 (*c* 1.01, $CHCl_3$); R_f = 0.24 (10% EtOAc/hexanes); IR (film) 2930, 2860, 1745, 1697, 1455, 1388, 1316, 1152, 1086 cm^{-1}; ^1H NMR (400 MHz, $CDCl_3$) Several peaks show a clear doubling for the *cis* and *trans* amide products. Other peaks are overlapping and appear only once. Those that are doubled have both values listed. δ 7.40-7.26 (m, 5H), 5.19 (d, *J* = 12.4 Hz, 2H), 5.11 (d, *J* = 12.2 Hz, 1H), 5.03 (dd, *J* = 6.2, 6.2 Hz, 1H), 5.00/4.70 (q, *J* = 6.8 Hz, 1H), 2.81/2.76 (s, 3H), 1.89-1.76 (m, 2H), 1.46/1.44 (s, 9H), 1.50-1.16 (m, 11H), 0.86 (t, *J* = 6.9 Hz, 3H); ^{13}C NMR (100 MHz, $CDCl_3$) The line listing for both *cis* and *trans* amide isomers is given, as a clear doubling of many peaks is evident. Whenever the isomer peaks overlap, it is stated that the particular peak is representing 2 carbons. ppm 172.2(2C), 169.9(2C), 156.0, 155.4, 135.4(2C), 128.7(4C), 128.5(2C), 128.4(4C), 80.3, 80.0, 72.9(2C), 67.1(2C), 54.4, 53.2, 31.6(2C), 31.4(2C), 30.2, 30.1, 28.8(2C), 28.4(6C), 25.0, 24.9, 22.6(2C), 15.3, 14.7, 14.1(2C); HRMS (EI): Exact mass calcd for $C_{24}H_{37}NNaO_6$ $[M+Na]^+$ 458.2513, found 458.2499. ANS-3-111.

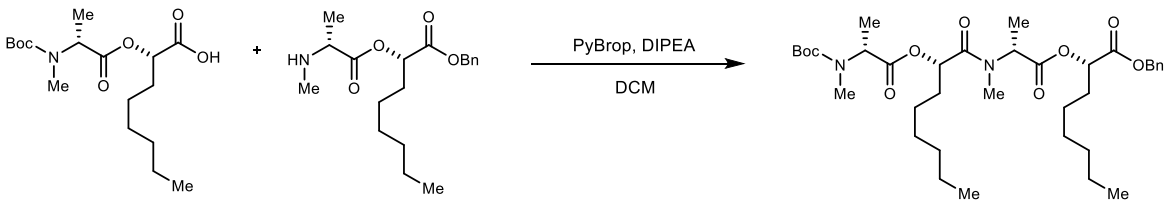

Benzyl (*S*)-2-(((6*R*,9*S*,12*R*)-9-hexyl-2,2,5,6,11,12-hexamethyl-4,7,10-trioxo-3,8-dioxa-5,11-diazatridecan-13-oyl)oxy)octanoate (S55). A round-bottom flask was charged with the amine (42.6 mg, 126 μmol), acid (43.5 mg, 126 μmol), and DCM (1.3 mL). The mixture was cooled to 0

°C and then DIPEA (63.0 μL, 379 μmol) and PyBrop (88.1 mg, 189 μmol) were added. The reaction was stirred at 0 °C for 30 min, then allowed to warm to ambient temperature and stir for an additional 1.5 h. The reaction mixture was poured into cold 10% aq citric acid and extracted with DCM. The combined organic layers were washed with satd aq $NaHCO_3$ and brine, and then dried and concentrated. The crude residue was subjected to flash column chromatography (SiO_2, 30% ethyl acetate in hexanes) to afford the product as a colorless oil (27.9 mg, 33%). $[\alpha]_D^{23}$ +23 (*c* 0.93, $CHCl_3$); R_f = 0.30 (20% EtOAc/hexanes); IR (film) 2954, 2928, 2857, 1742, 1694, 1668, 1455, 1390, 1366, 1315, 1181, 1085, 1080 cm^{-1}; ^1H NMR (600 MHz, $CDCl_3$) This compound exists as a mixture of rotamers causing peak broadening and overlap. Refer to the image of the ^1H NMR spectrum.^{13}C NMR (150 MHz, $CDCl_3$) This compound is a mixture of rotamers causing peak doubling, broadening, and overlap. Refer to the image of the ^{13}C NMR spectrum; HRMS (EI): Exact mass calcd for $C_{36}H_{58}N_2NaO_9$ $[M+Na]^+$ 685.4035, found 685.4038. ANS-6-15.

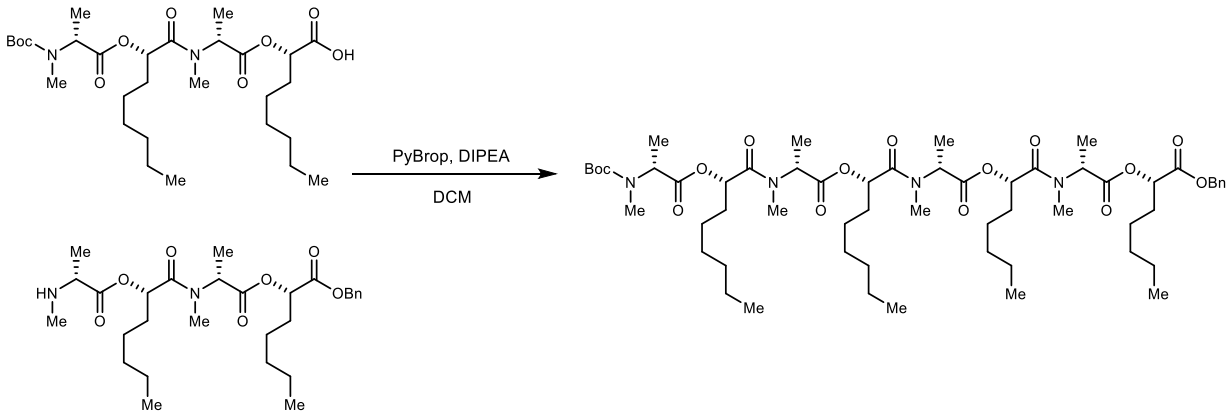

Benzyl (*S*)-2-(((6*R*,9*S*,12*R*,15*S*,18*R*,21*S*,24*R*)-9,15-dihexyl-2,2,5,6,11,12,17,18,23,24-decamethyl-4,7,10,13,16,19,22-heptaoxo-21-pentyl-3,8,14,20-tetraoxa-5,11,17,23-tetraazapentacosan-25-oyl)oxy)heptanoate (S56). A round-bottom flask was charged with the amine (22.5 mg, 42.1 μmol), acid (24 mg, 42.1 μmol), and DCM (500 μL). The mixture was cooled to 0 °C and then DIPEA (22.0 μL, 126 μmol) and PyBrop (29.4 mg, 63.2 μmol) were added. The reaction was stirred at 0 °C for 30 min, then allowed to warm to ambient temperature and stir for an additional 1.5 h. The reaction mixture was poured into cold 10% aq citric acid and extracted with DCM. The combined organic layers were washed with satd aq $NaHCO_3$ and brine, and then dried and concentrated. The crude residue was subjected to flash column chromatography (SiO_2, 50% ethyl acetate in hexanes) to afford the product as a colorless oil (23.9 mg, 52%). $[\alpha]_D^{23}$ +27 (*c* 0.90, $CHCl_3$); R_f = 0.33 (40% EtOAc/hexanes); IR (film) 2954, 2930, 2907, 2858, 1742, 1698,

1666, 1455, 1378, 1366, 1212, 1152, 1084 cm^{-1}; ^1H NMR (600 MHz, $CDCl_3$) This compound exists as a mixture of rotamers causing peak broadening and overlap. Refer to the image of the ^1H NMR spectrum.^{13}C NMR (150 MHz, $CDCl_3$) This compound is a mixture of rotamers causing peak doubling, broadening, and overlap. Refer to the image of the ^{13}C NMR spectrum; HRMS (EI): Exact mass calcd for $C_{58}H_{96}N_4NaO_{15}$ $[M+Na]^+$ 1111.6764, found 1111.6770. ANS-6-40.

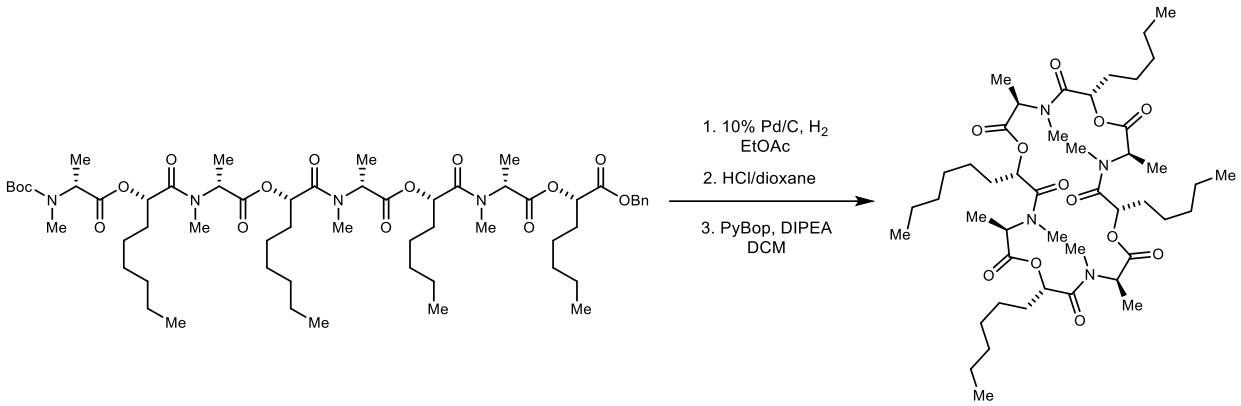

(3*R*,6*S*,9*R*,12*S*,15*R*,18*S*,21*R*,24*S*)-6,12-dihexyl-3,4,9,10,15,16,21,22-octamethyl-18,24-dipentyl-1,7,13,19-tetraoxa-4,10,16,22-tetraazacyclotetracosan-2,5,8,11,14,17,20,23-octaone (76). A round-bottom flask was charged with the depsipeptide (23.9 mg, 21.9 μmol), dissolved in EtOAc (2.5 mL), and treated with 10% Pd/C (3.0 mg). The reaction flask was evacuated with light vacuum (50 Torr). Hydrogen (balloon) was added, and the flask was cycled once more. The reaction was allowed to stir for 2 h. After purging the flask with nitrogen, the crude reaction mixture was filtered through Celite. To the crude material was added 4 M HCl in dioxane (3.0 mL) and the reaction mixture was allowed to stir for 30 min. The reaction mixture was concentrated and added to a flame-dried round-bottom flask. DCM (4.4 mL) was added and the reaction was cooled to 0 °C. Once at 0 °C, DIPEA (8.2 μL, 48 μmol) and PyBrop (13 mg, 24 μmol) were added. The reaction was stirred at 0 °C for 1.5 h, then allowed to warm to ambient temperature and stir for an additional 1 h. The reaction mixture was poured into cold 10% aq citric acid and extracted with DCM. The combined organic layers were washed with satd aq $NaHCO_3$ and brine, and then dried and concentrated. Preparative HPLC (5 – 95% aqueous acetonitrile, 210 nm, flow rate: 8 mL/min, R_t = 24.6 m) afforded the 24-membered macrocycle (6.2 mg, 32% (3 steps)) as a colorless oil. $[\alpha]_D^{23}$ +21 (*c* 0.41, $CHCl_3$); R_f = 0.28 (4% MeOH/DCM); IR (film) 2952, 2930, 2858, 1743, 1663, 1485, 1456, 1415, 1377, 1200, 1085 cm^{-1}; ^1H NMR (600 MHz, $CDCl_3$) This compound exists in multiple conformations, causing significant peak overlap. The peaks that could be

distinguished are listed. See ^{1}H NMR for the rest of peaks; ^{13}C NMR (150 MHz, $CDCl_3$) This compound exists in multiple conformations, causing significant peak overlap. Refer to the image of the ^{13}C NMR spectrum; HRMS (EI): Exact mass calcd for $C_{46}H_{80}N_4NaO_{12}$ $[M+Na]^+$ 903.5665, found 903.5665. ANS-6-58.

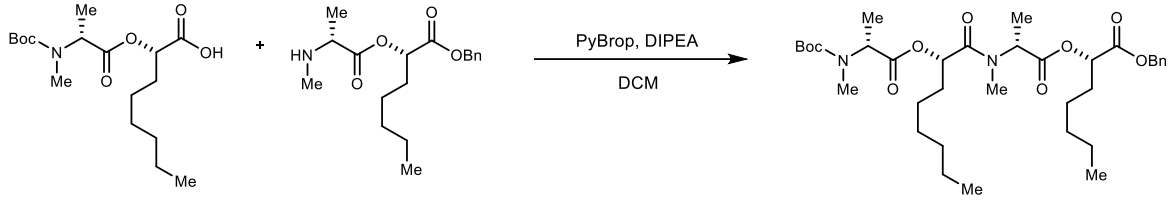

Benzyl (*S*)-2-(((6*R*,9*S*,12*R*)-9-hexyl-2,2,5,6,11,12-hexamethyl-4,7,10-trioxo-3,8-dioxa-5,11-diazatridecan-13-oyl)oxy)heptanoate (S57). A round-bottom flask was charged with the amine (46.6 mg, 145 μmol), acid (50.0 mg, 145 μmol), and DCM (1.5 mL). The mixture was cooled to 0 °C and then DIPEA (74.4 μL, 435 μmol) and PyBrop (101 mg, 218 μmol) were added. The reaction was stirred at 0 °C for 30 min, then allowed to warm to ambient temperature and stir for an additional 1.5 h. The reaction mixture was poured into cold 10% aq citric acid and extracted with DCM. The combined organic layers were washed with satd aq $NaHCO_3$ and brine, and then dried and concentrated. The crude residue was subjected to flash column chromatography (SiO_2, 30% ethyl acetate in hexanes) to afford the product as a colorless oil (52.6 mg, 56%). $[\alpha]_D^{23}$ +26 (*c* 1.31, $CHCl_3$); R_f = 0.17 (20% EtOAc/hexanes); IR (film) 2954, 2929, 2858, 1742, 1694, 1668, 1455, 1365, 1315, 1211, 1184, 1153, 1084 cm^{-1}; ^{1}H NMR (600 MHz, $CDCl_3$) This compound exists as a mixture of rotamers causing peak broadening and overlap. Refer to the image of the ^{1}H NMR spectrum.^{13}C NMR (150 MHz, $CDCl_3$) This compound is a mixture of rotamers causing peak doubling, broadening, and overlap. Refer to the image of the ^{13}C NMR spectrum; HRMS (EI): Exact mass calcd for $C_{35}H_{56}N_2NaO_9$ $[M+Na]^+$ 671.3878, found 671.3880. ANS-6-21.

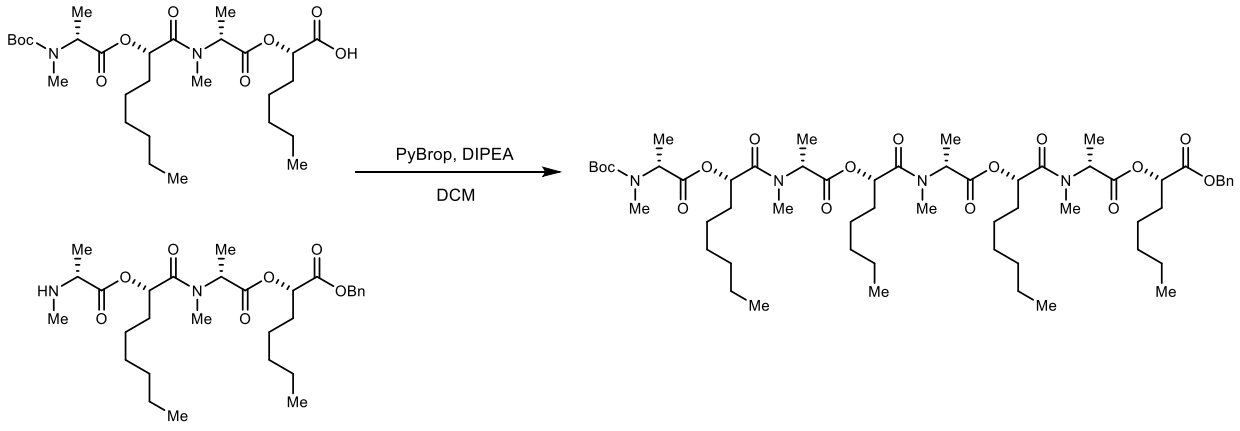

Benzyl (*S*)-2-(((6*R*,9*S*,12*R*,15*S*,18*R*,21*S*,24*R*)-9,21-dihexyl-2,2,5,6,11,12,17,18,23,24-decamethyl-4,7,10,13,16,19,22-heptaoxo-15-pentyl-3,8,14,20-tetraoxa-5,11,17,23-tetraazapentacosan-25-oyl)oxy)heptanoate (S58). A round-bottom flask was charged with the amine (22.6 mg, 40.5 μmol), acid (22.2 mg, 40.5 μmol), and DCM (410 μL). The mixture was cooled to 0 °C and then DIPEA (20.8 μL, 122 μmol) and PyBrop (28.3 mg, 60.8 μmol) were added. The reaction was stirred at 0 °C for 30 min, then allowed to warm to ambient temperature and stir for an additional 1.5 h. The reaction mixture was poured into cold 10% aq citric acid and extracted with DCM. The combined organic layers were washed with satd aq $NaHCO_3$ and brine, and then dried and concentrated. The crude residue was subjected to flash column chromatography (SiO_2, 50% ethyl acetate in hexanes) to afford the product as a colorless oil (37.8 mg, 86%). $[\alpha]_D^{23}$ +34 (*c* 0.97, $CHCl_3$); R_f = 0.28 (40% EtOAc/hexanes); IR (film) 2954, 2931, 2859, 1743, 1667, 1435, 1393, 1363, 1212, 1152, 1084 cm^{-1}; ^1H NMR (600 MHz, $CDCl_3$) This compound exists as a mixture of rotamers causing peak broadening and overlap. Refer to the image of the ^1H NMR spectrum.^{13}C NMR (150 MHz, $CDCl_3$) This compound is a mixture of rotamers causing peak doubling, broadening, and overlap. Refer to the image of the ^{13}C NMR spectrum; HRMS (EI): Exact mass calcd for $C_{58}H_{96}N_4NaO_{15}$ $[M+Na]^+$ 1111.6764, found 1111.6768. ANS-6-43.

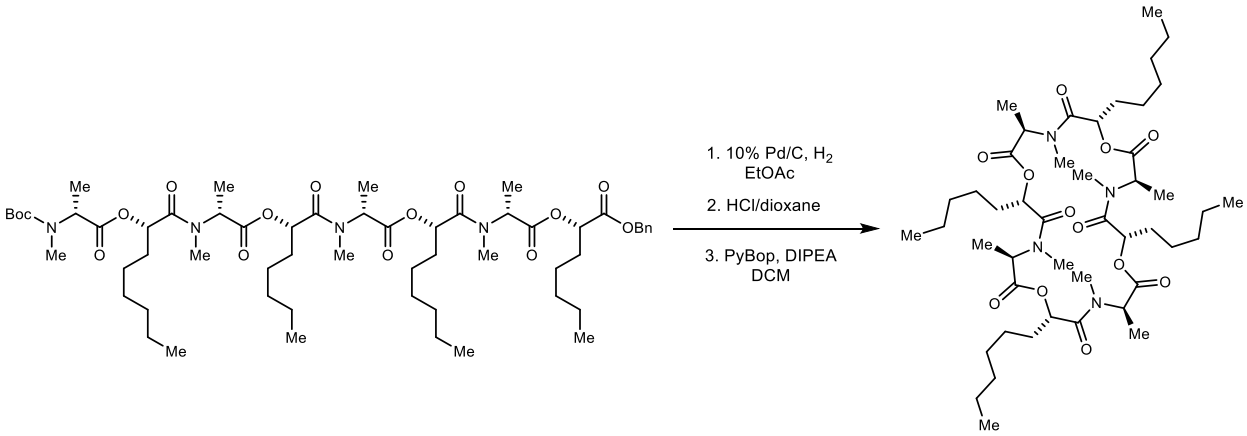

(3*R*,6*S*,9*R*,12*S*,15*R*,18*S*,21*R*,24*S*)-6,18-dihexyl-3,4,9,10,15,16,21,22-octamethyl-12,24-dipentyl-1,7,13,19-tetraoxa-4,10,16,22-tetraazacyclotetracosan-2,5,8,11,14,17,20,23-octaone (77). A round-bottom flask was charged with the depsipeptide (37.8 mg, 34.7 μmol), dissolved in EtOAc (2.5 mL), and treated with 10% Pd/C (4.0 mg). The reaction flask was evacuated with light vacuum (50 Torr). Hydrogen (balloon) was added, and the flask was cycled once more. The reaction was allowed to stir for 2 h. After purging the flask with nitrogen, the crude reaction mixture was filtered through Celite. To the crude material was added 4 M HCl in dioxane (3.0 mL)

and the reaction mixture was allowed to stir for 30 min. The reaction mixture was concentrated and added to a flame-dried round-bottom flask. DCM (6.94 mL) was added and the reaction was cooled to 0 °C. Once at 0 °C, DIPEA (13.1 μL, 76.3 μmol) and PyBrop (19.9 mg, 38.2 μmol) were added. The reaction was stirred at 0 °C for 1.5 h, then allowed to warm to ambient temperature and stir for an additional 1 h. The reaction mixture was poured into cold 10% aq citric acid and extracted with DCM. The combined organic layers were washed with satd aq $NaHCO_3$ and brine, and then dried and concentrated. Preparative HPLC (5 – 95% aqueous acetonitrile, 210 nm, flow rate: 8 mL/min, R_t = 24.3 m) afforded the 24-membered macrocycle (7.7 mg, 25% (3 steps)) as a colorless oil. $[\alpha]_D^{23}$ +30 (*c* 0.51, $CHCl_3$); R_f = 0.3 (4% MeOH/DCM); IR (film) 2953, 2928, 2857, 1742, 1663, 1462, 1415, 1377, 1200, 1084 cm^{-1}; ^1H NMR (600 MHz, $CDCl_3$) This compound exists in multiple conformations, causing significant peak overlap. The peaks that could be distinguished are listed. See ^1H NMR for the rest of peaks; ^{13}C NMR (150 MHz, $CDCl_3$) This compound exists in multiple conformations, causing significant peak overlap. Refer to the image of the ^{13}C NMR spectrum; HRMS (EI): Exact mass calcd for $C_{46}H_{80}N_4NaO_{12}$ $[M+Na]^+$ 903.5665, found 903.5667. ANS-6-59.

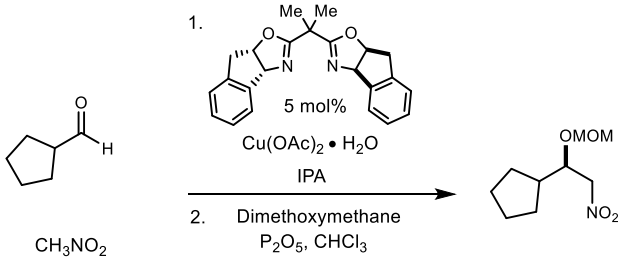

(*R*)-(1-(Methoxymethoxy)-2-nitroethyl)cyclopentane (S59). Following the Evans enantioselective Henry procedure[1], IndaBOX[2] (185 mg, 515 μmol) and $Cu(OAc)_2$•H_2O (93.4 mg, 468 μmol) were stirred at ambient temperature in IPA (19 mL) for 1 h. The cerulean blue solution was then cooled to 0 °C and hexanal (1.0 mL, 9.36 mmol) was added and allowed to stir for 10 m before nitromethane (5.7 mL, 93.6 mmol) addition. After stirring for 5 days at ambient temperature, the reaction was quenched dropwise at 0 °C with 1 M aq HCl and the aqueous layer was extracted with CH_2Cl_2. Following drying and concentration under reduced pressure, the crude alcohol was dissolved in $CHCl_3$ (45.0 mL), treated with P_2O_5 (12.8 g, 90.3 mmol) and dimethoxymethane (19.4 mL, 186 mmol), and stirred at ambient temperature overnight. The reaction mixture was diluted with DCM and decanted from the solid. The organic layer was then washed with satd aq $NaHCO_3$ and brine. The organic layers were dried and concentrated to afford

an oil that was subjected to flash column chromatography (SiO_2, 3-6% diethyl ether in hexanes) to afford the title compound as a colorless oil (1.42 g, 79%, 2 steps). The enantiopurity was determined to be 92% ee by chiral HPLC analysis (Chiralcel OD-H, 3% ^{i}PrOH /hexanes, 0.4 mL/min, t_r(*e*$_1$, major) = 17.8 min, t_r(*e*$_2$, minor) = 20.1 min). $[\alpha]_D^{24}$ -15.0 (*c* 1.19, $CHCl_3$); R_f = 0.13 (5% Et_2O/hexanes); IR (film) 2953, 2871, 1554, 1449, 1423, 1381, 1223, 1148, 1101, 1035 cm^{-1}; ^{1}H NMR (400 MHz, $CDCl_3$) δ 4.68 (d, *J* = 7.2 Hz, 1H), 4.65 (d, *J* = 7.0 Hz, 1H), 4.52 (dd, *J*= 12.3, 7.3 Hz, 1H), 4.47 (dd, *J* = 12.4, 3.9 Hz, 1H), 4.12 (ddd, *J* = 7.2, 7.2, 3.9 Hz, 1H), 3.36 (s, 3H), 2.09 (dtt, *J* = 9.0, 8.3, 7.6, 1H), 1.88-1.54 (series of m, 6H), 1.46-1.23 (series of m, 2H); ^{13}C NMR (100 MHz, $CDCl_3$) ppm 97.0, 79.2, 78.8, 56.0, 42.5, 28.6 (2C), 25.4, 25.3; HRMS (EI): Exact mass calcd for $C_9H_{16}NO_4$ $[M-H]^-$ 202.1074, found 202.1073. ANS-2-162.

(*S*)-(1-(Methoxymethoxy)-2-nitroethyl)cyclopentane (*ent*-S59). Prepared following an identical procedure as **S59**. Flash column chromatography (SiO_2, 3-6% diethyl ether in hexanes) afforded the hydroxy-nitroalkane with spectroscopic data identical to its enantiomer, except the major/minor peaks were reversed by chiral HPLC analysis. The enantiopurity was determined to be 92% ee by chiral HPLC analysis (Chiralcel OD-H, 3% ^{i}PrOH /hexanes, 0.4 mL/min, t_r(*e*$_1$, minor) = 17.8 min, t_r(*e*$_2$, major) = 20.1 min). ANS-3-96.

Benzyl (*S*)-2-cyclopentyl-2-(methoxymethoxy)acetate (S60). A round-bottom flask was charged with nitroalkane (1.46 g, 7.18 mmol), $NaNO_2$ (1.49 g, 21.5 mmol), AcOH (6.2 mL, 107 mmol), and DMSO (55 mL). The mixture was stirred at 45 °C for 18 h under an argon atmosphere. The reaction was then allowed to cool to ambient temperature, treated with 1 N HCl, and poured into CH_2Cl_2. The aqueous layer was extracted with CH_2Cl_2, and the combined organic layers were washed with water, brine, dried, and concentrated. The crude mixture was then added to a round-bottom flask with K_2CO_3 (2.97 g, 21.5 mmol) and DMF (14.3 mL). The mixture was then treated with BnBr (1.0 mL, 8.6 mmol) and an argon balloon. The reaction was allowed to stir overnight at ambient temperature. The reaction was quenched with 1 M aq HCl and extracted with Et_2O. The organic layer was washed with 1 M HCl, water, brine, dried and concentrated. The crude residue was subjected to flash column chromatography (SiO_2, 5% diethyl ether in hexanes) to afford the product as a pale-yellow oil (1.12 g, 56%, 2 steps). $[\alpha]_D^{20}$ -66 (*c* 0.28, $CHCl_3$); R_f = 0.31 (10%

Et_2O/hexanes); IR (film) 2952, 2863, 1746, 1453, 1260, 1152, 1109, 1040 cm^{-1}; ^1H NMR (400 MHz, $CDCl_3$) δ 7.40-7.26 (m, 5H), 5.17 (br s, 2H), 4.67 (d, *J*= 6.8 Hz, 1H), 4.65 (d, *J* = 7.2 Hz, 1H), 3.97 (d, *J* = 7.0 Hz, 1H), 3.34 (s, 3H), 2.29 (dp, *J* = 8.8, 8.8 Hz, 1H), 1.78-1.34 (series of m, 8H); ^{13}C NMR (100 MHz, $CDCl_3$) ppm 172.6, 135.8, 128.7, 128.5, 128.4, 96.7, 79.6, 66.6, 56.2, 42.6, 28.7, 28.6, 25.7, 25.5; HRMS (EI): Exact mass calcd for $C_{16}H_{26}NO_4$ $[M+NH_4]^+$ 296.1853, found 296.1856. ANS-3-86.

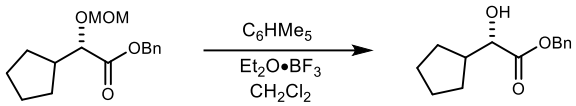

Benzyl (*S*)-2-cyclopentyl-2-hydroxyacetate (S61). A flame-dried round-bottom flask was charged with the protected alcohol (1.12 g, 4.02 mmol) dissolved in dry dichloromethane (0.05 M), pentamethyl benzene (716 mg, 4.83 mmol), and $BF_3 \cdot Et_2O$ (600 μL, 4.83 mmol). The reaction was allowed to stir for 50 minutes at ambient temperature. The crude reaction mixture was quenched with satd aq $NaHCO_3$ and brine, and then dried and concentrated. The crude material was subjected to flash column chromatography (SiO_2, 10-30% ethyl acetate in hexanes) to afford the alcohol (555 mg, 59%) as a yellow oil. $[\alpha]_D^{25}$ -26 (*c* 0.67, $CHCl_3$); R_f = 0.34 (20% EtOAc/hexanes); IR (film) 3468, 2953, 2868, 1732, 1453, 1260, 1210, 1161 cm^{-1}; ^1H NMR (400 MHz, $CDCl_3$) δ 7.44-7.29 (m, 5H), 5.24 (d, *J* = 12.1 Hz, 1H), 5.19 (d, *J* = 12.2 Hz, 1H), 4.17 (dd, *J* = 6.4, 5.1 Hz, 1H), 2.82 (d, *J* = 6.5 Hz, 1H), 2.31-2.18 (m, 1H), 1.76-1.36 (series of m, 8H); ^{13}C NMR (125 MHz, $CDCl_3$) ppm 175.1, 135.4, 128.7, 128.6, 128.4, 72.9, 67.3, 43.5, 28.7, 26.5, 25.8, 25.7; HRMS (EI): Exact mass calcd for $C_{14}H_{18}NaO_3$ $[M+Na]^+$ 257.1148, found 257.1149. ANS-3-93.

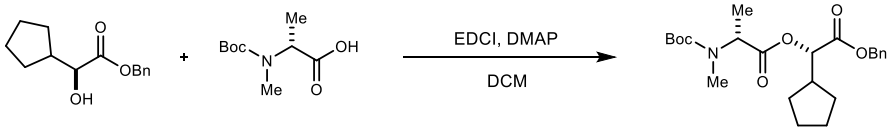

(*S*)-2-(Benzyloxy)-1-cyclopentyl-2-oxoethyl *N*-(*tert*-butoxycarbonyl)-*N*-methyl-D-alaninate (S62). A round-bottom flask was charged with the amine (554 mg, 2.72 mmol), alcohol (555 mg, 2.37 mmol), and DCM (23.7 mL). The mixture was cooled to 0 °C and then EDCI (545 mg, 2.84 mmol) and DMAP (14.5 mg, 118 μmol) were added. The reaction was stirred at 0 °C for 30 min, then allowed to warm to ambient temperature and stir for an additional 1.5 h. The reaction mixture was poured into water and extracted with DCM. The combined organic layers were washed with satd aq $NaHCO_3$ and brine, and then dried and concentrated. The crude residue was subjected to

flash column chromatography (SiO_2, 5-10% ethyl acetate in hexanes) to afford the product as a pale-yellow oil (915 mg, 92%). $[\alpha]_D^{20}$ +1.1 (*c* 0.88, $CHCl_3$); R_f = 0.22 (10% EtOAc in hexanes); IR (film) 2957, 2870, 1744, 1695, 1453, 1388, 1316, 1258, 1152, 1085 cm^{-1}; ^1H NMR (600 MHz, $CDCl_3$) This compound exists as a mixture of 1:1.2 rotamers causing significant peak broadening and overlap. Refer to the image of the ^1H NMR spectrum. ^{13}C NMR (150 MHz, $CDCl_3$) This compound is a mixture of 1:1.2 rotamers causing significant peak broadening and overlap. Refer to the image of the ^{13}C NMR spectrum; HRMS (EI): Exact mass calcd for $C_{23}H_{34}NO_6$ $[M+H]^+$ 420.2381, found 420.2397. ANS-3-94.

(*S*)-2-(((*R*)-1-((*S*)-2-(Benzyloxy)-1-cyclopentyl-2-oxoethoxy)-1-oxopropan-2-yl)(methyl)amino)-1-cyclopentyl-2-oxoethyl *N*-(*tert*-butoxycarbonyl)-*N*-methyl-D-alaninate (S63). A round-bottom flask was charged with the amine (228 mg, 715 μmol), acid (235 mg, 715 μmol), and DCM (3.6 mL). The mixture was cooled to 0 °C and then DIPEA (367 μL, 2.14 mmol) and PyBrop (499 mg, 1.07 mmol) were added. The reaction was stirred at 0 °C for 1 h. The reaction mixture was poured into cold 10% citric acid and extracted with DCM. The combined organic layers were washed with satd aq $NaHCO_3$ and brine, and then dried and concentrated. The crude residue was subjected to flash column chromatography (SiO_2, 10-50% ethyl acetate in hexanes) to afford the product as a colorless oil (332 mg, 74%). $[\alpha]_D^{20}$ +24 (*c* 0.56, $CHCl_3$); R_f = 0.47 (40% EtOAc in hexanes); IR (film) 2956, 2871, 1743, 1694, 1453, 1315, 1211, 1156, 1087 cm^{-1}; ^1H NMR (600 MHz, $CDCl_3$) δ 7.40-7.32 (m, 5H), 5.21 (d, *J* = 12.0 Hz, 1H), 5.12 (d, *J* = 12.2 Hz, 1H), 5.30-4.67 (series of m, 4H), 3.09-2.81 (series of s, 6H), 2.44-2.30 (m, 2H), 1.80-1.30 (series of m, 31H); ^{13}C NMR (150 MHz, $CDCl_3$) This compound is a mixture of 1:1.2 rotamers causing significant peak broadening and overlap. Refer to the image of the ^{13}C NMR spectrum; HRMS (EI): Exact mass calcd for $C_{34}H_{51}N_2O_9$ $[M+H]^+$ 631.3589, found 631.3589. ANS-3-105.

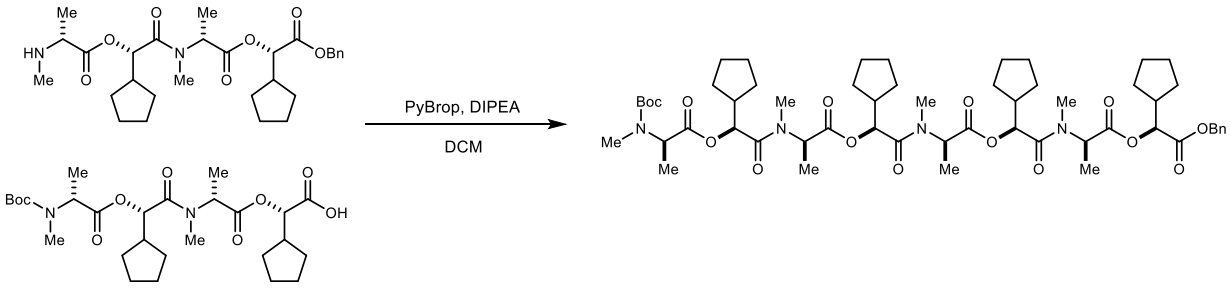

(*S*)-2-(((*R*)-1-((*S*)-2-(Benzyloxy)-1-cyclopentyl-2-oxoethoxy)-1-oxopropan-2-yl)(methyl)amino)-1-cyclopentyl-2-oxoethyl *N*-((6*R*,9*S*,12*R*,15*S*)-9,15-dicyclopentyl-2,2,5,6,11,12-hexamethyl-4,7,10,13-tetraoxo-3,8,14-trioxa-5,11-diazahexadecan-16-oyl)-*N*-methyl-D-alaninate (S64). A round-bottom flask was charged with the amine (84.3 mg, 159 μmol), acid (85.9 mg, 159 μmol), and DCM (1.6 mL). The mixture was cooled to 0 °C and then DIPEA (81.6 μL, 477 μmol) and PyBrop (111 mg, 239 μmol) were added. The reaction was stirred at 0 °C for 30 min, then allowed to warm to ambient temperature and stir for an additional 1.5 h. The reaction mixture was poured into cold 10% citric acid and extracted with DCM. The combined organic layers were washed with satd aq $NaHCO_3$ and brine, and then dried and concentrated. The crude residue was subjected to flash column chromatography (SiO_2, 10-50% ethyl acetate in hexanes) to afford the product as a colorless oil (130 mg, 78%). $[\alpha]_D^{25}$ +39 (*c* 0.72, $CHCl_3$); R_f = 0.13 (40% EtOAc/hexanes); IR (film) 2953, 2870, 1741, 1660, 1453, 1314, 1217, 1156, 1086 cm^{-1}; ^1H NMR (600 MHz, $CDCl_3$) This compound exists as a mixture of rotamers causing significant peak broadening and overlap. Refer to image of the ^1H NMR spectrum; ^{13}C NMR (150 MHz, $CDCl_3$) This compound is a mixture of rotamers causing significant peak broadening and overlap. Refer to the image of the ^{13}C NMR spectrum; HRMS (EI): Exact mass calcd for $C_{56}H_{88}N_5O_{15}$ $[M+NH_4]^+$ 1070.6271, found 1070.6305. ANS-3-123.

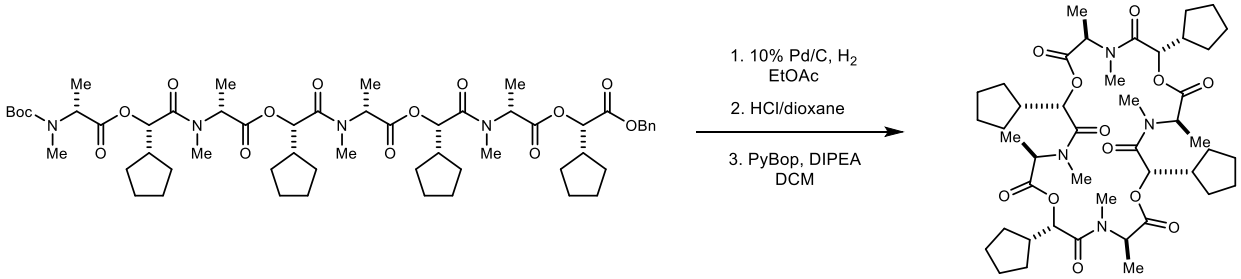

(3*R*,6*S*,9*R*,12*S*,15*R*,18*S*,21*R*,24*S*)-6,12,18,24-Tetracyclopentyl-3,4,9,10,15,16,21,22-octamethyl-1,7,13,19-tetraoxa-4,10,16,22-tetraazacyclotetracosan-2,5,8,11,14,17,20,23-octaone (78). A round-bottom flask was charged with the depsipeptide (50 mg, 48 μmol), dissolved in EtOAc (0.5 mL), and treated with 10% Pd/C (5.0 mg). The reaction flask was evacuated with light vacuum (50 Torr). Hydrogen (balloon) was added, and the flask was cycled once more. The reaction was allowed to stir for 2 h. After purging the flask with nitrogen, the crude reaction mixture was filtered through Celite. To the crude material was added 4 M HCl in dioxane (0.5 mL) and the reaction mixture was allowed to stir for 30 min. The reaction mixture was concentrated and added to a flame-dried round bottom flask. DCM (9.5 mL) was added and the

reaction was cooled to 0 °C. Once at 0 °C, DIPEA (18.0 μL, 104 μmol) and PyBrop (26 mg, 50 μmol) were added. The reaction was stirred at 0 °C for 1.5 h, then allowed to warm to ambient temperature and stir for an additional 1 h. The reaction mixture was poured into cold 10% citric acid and extracted with DCM. The combined organic layers were washed with satd aq $NaHCO_3$ and brine, and then dried and concentrated. Preparative HPLC (5 – 95% aqueous acetonitrile, 210 nm, flow rate: 8 mL/min, R_t = 20.5 m) afforded the 24-membered macrocycle (6.6 mg, 17%) as a colorless oil. $[\alpha]_D^{25}$ +49 (*c* 0.53, $CHCl_3$); R_f = 0.23 (4% MeOH/DCM); IR (film) 2951, 2868, 1741, 1657, 1454, 1201, 1085 cm^{-1}; ^1H NMR (600 MHz, $CDCl_3$) This compound exists in multiple conformations, yet has a clear major, symmetric conformation, which is given in the line listing. Refer to the spectrum for others: δ 5.50 (q, *J* = 7.2 Hz, 1H), 5.31 (d, *J* = 8.8 Hz, 1H), 2.92 (s, 3H), 2.47 (dtt, *J* = 8.3, 8.3, 8.3 Hz, 1H), 1.80-1.17 (series of m, 8H), 1.37 (d, *J* = 7.3 Hz, 3H); ^{13}C NMR (150 MHz, $CDCl_3$) ppm 170.9, 168.2, 74.7, 51.8, 41.2, 30.8, 29.0, 28.6, 25.5, 25.2, 14.4; HRMS (EI): Exact mass calcd for $C_{44}H_{69}N_4O_{12}$ $[M+H]^+$ 845.4907, found 845.4940. ANS-3-130.

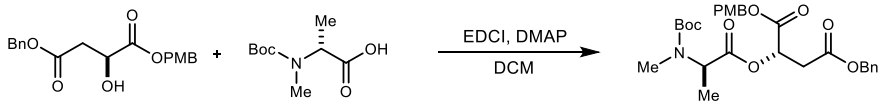

4-Benzyl 1-(4-methoxybenzyl) (*S*)-2-((*N*-(*tert*-butoxycarbonyl)-*N*-methyl-D-alanyl)oxy)succinate (138). A round-bottom flask was charged with the amine (110 mg, 544 μmol), alcohol (156 mg, 453 μmol), and DCM (4.5 mL). The mixture was cooled to 0 °C and then EDCI (104 mg, 544 μmol) and DMAP (5.5 mg, 45 μmol) were added. The reaction was stirred at 0 °C for 30 min, then allowed to warm to ambient temperature and stir for an additional 1.5 h. The reaction mixture was poured into water and extracted with DCM. The combined organic layers were washed with satd aq $NaHCO_3$ and brine, and then dried and concentrated to afford the product as a colorless oil (121 mg, 50%). $[\alpha]_D^{23}$ +7.8 (*c* 0.98, $CHCl_3$); R_f = 0.18 (20% EtOAc/hexanes); IR (film) 2974, 1745, 1695, 1515, 1456, 1389, 1250, 1166, 1091 cm^{-1}; ^1H NMR (600 MHz, $CDCl_3$) Several peaks show a clear doubling for the *cis* and *trans* amide products. Other peaks are overlapping and appear only once. Those that are doubled have both values listed. δ 7.37-7.27 (m, 5H), 7.22 (d, *J* = 8.7 Hz, 2H), 6.87 (d, *J* = 8.6 Hz, 2H), 5.52 (dd, *J* = 6.5, 6.5 Hz, 1H), 5.18-5.02 (m, 4H), 4.96/4.66 (q, *J* = 6.8 Hz, 1H), 3.80 (br s, 3H), 2.92 (d, *J* = 5.9 Hz, 2H), 2.76/2.73 (s, 3H), 1.45/1.42 (s, 9H), 1.32 (d, *J* = 7.3 Hz, 3H); ^{13}C NMR (150 MHz, $CDCl_3$) The line listing for both *cis* and *trans* amide isomers is given, as a clear doubling of many peaks is evident. Whenever the

isomer peaks overlap, it is stated that the particular peak is representing 2 carbons: ppm 171.5(2C), 168.8(2C), 168.4, 168.3, 160.0(2C), 156.0, 155.4, 135.4, 135.0, 130.4(4C), 128.7(4C), 128.5(4C), 127.5, 127.1, 114.1(6C), 80.4, 80.0, 68.85, 68.80, 67.7, 67.5, 67.0, 66.9, 55.4(2C), 54.3, 53.2, 36.3, 36.2, 30.3, 30.0, 28.5(3C), 28.4(3C), 15.2, 14.7; HRMS (EI): Exact mass calcd for $C_{28}H_{35}NNaO_9$ $[M+Na]^+$ 552.2204, found 552.2207. ANS-4-206.

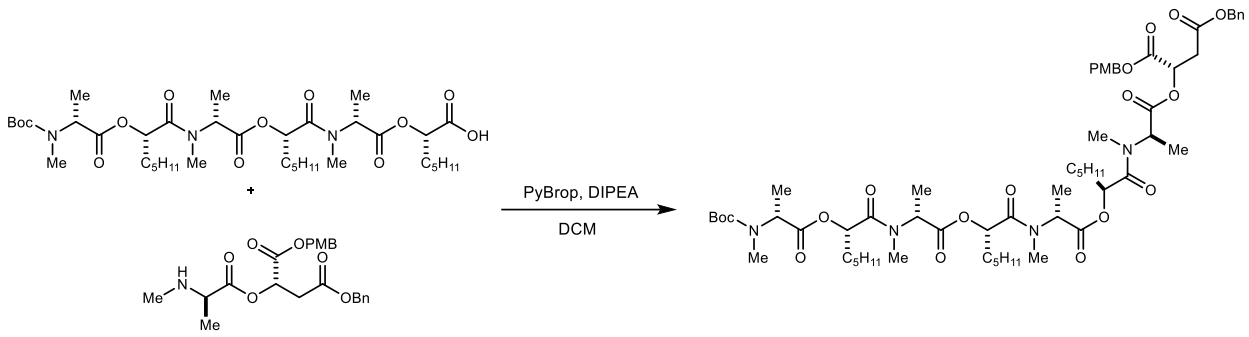

4-Benzyl 1-(4-methoxybenzyl) (*S*)-2-(((6*R*,9*S*,12*R*,15*S*,18*R*,21*S*,24*R*)-2,2,5,6,11,12,17,18,23,24-decamethyl-4,7,10,13,16,19,22-heptaoxo-9,15,21-tripentyl-3,8,14,20-tetraoxa-5,11,17,23-tetraazapentacosan-25-oyl)oxy)succinate (140). A round-bottom flask was charged with the amine (47.7 mg, 111 μmol), acid (83.9 mg, 111 μmol), and DCM (1.2 μL). The mixture was cooled to 0 °C and then DIPEA (57.1 μL, 333 μmol) and PyBrop (77.6 mg, 167 μmol) were added. The reaction was stirred at 0 °C for 30 min, then allowed to warm to ambient temperature and stir for an additional 1.5 h. The reaction mixture was poured into cold 10% aq citric acid and extracted with DCM. The combined organic layers were washed with satd aq $NaHCO_3$ and brine, and then dried and concentrated. The crude residue was subjected to flash column chromatography (SiO_2, 30-50% ethyl acetate in hexanes) to afford the product as a colorless oil (108 mg, 83%). $[\alpha]_D^{24}$ +37 (*c* 0.86, $CHCl_3$); R_f = 0.15 (40% EtOAc/hexanes); IR (film) 2935, 2867, 1742, 1664, 1457, 1387, 1248, 1164, 1106 cm^{-1}; ^1H NMR (600 MHz, $CDCl_3$) This compound exists as a mixture of rotamers causing significant peak broadening and overlap. Refer to the image of the ^1H NMR spectrum; ^{13}C NMR (150 MHz, $CDCl_3$) This compound is a mixture of rotamers causing significant peak broadening and overlap. Refer to the image of the ^{13}C NMR spectrum; HRMS (EI): Exact mass calcd for $C_{61}H_{92}N_4NaO_{18}$ $[M+Na]^+$ 1191.6299, found 1191.6328. ANS-4-232.

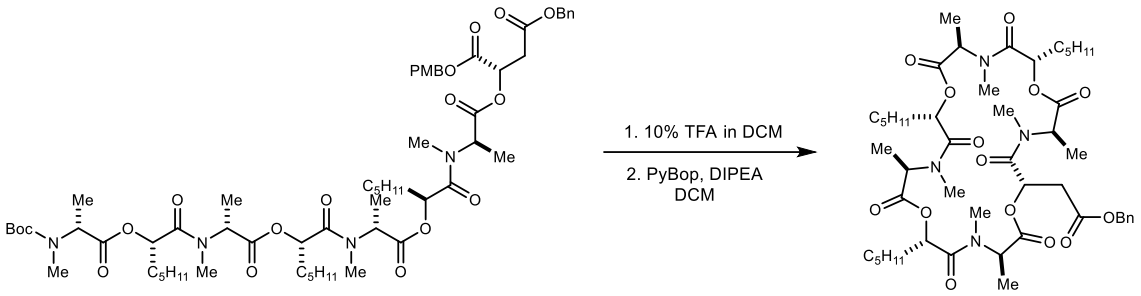

Benzyl 2-((2*S*,5*R*,8*S*,11*R*,14*S*,17*R*,20*S*,23*R*)-4,5,10,11,16,17,22,23-octamethyl-3,6,9,12,15,18,21,24-octaoxo-8,14,20-tripentyl-1,7,13,19-tetraoxa-4,10,16,22-tetraazacyclotetracosan-2-yl)acetate (141). A round-bottom flask was charged with the depsipeptide (108 mg, 92.4 μmol), and dissolved in a mixture of 10% TFA in DCM (0.3 mL TFA, 3.0 mL DCM). The reaction was allowed to stir at ambient temperature for 1 h. The crude reaction mixture was concentrated in vacuo. To the unpurified material in a flame-dried round bottom flask was added DCM (18.5 mL), and the reaction was cooled to 0 °C. At 0 °C, DIPEA (34.8 μL, 203 μmol) and PyBrop (50.5 mg, 97.0 μmol) were added. The reaction was stirred at 0 °C for 30 min, then allowed to warm to ambient temperature and stir for an additional 2 h. The reaction mixture was poured into cold 10% aq citric acid and extracted with DCM. The combined organic layers were washed with satd aq $NaHCO_3$ and brine, and then dried and concentrated. Preparative HPLC (5 – 95% aqueous acetonitrile, 210 nm, flow rate: 8 mL/min, R_t = 26.0 m) afforded the 24-membered macrocycle (27.9 mg, 32%) as a colorless oil. $[\alpha]_D^{24}$ +29 (*c* 0.53, $CHCl_3$); R_f = 0.31 (10% MeOH/DCM); IR (film) 2930, 2860, 1742, 1662, 1459, 1413, 1187, 1110 cm^{-1}; ^1H NMR (600 MHz, $CDCl_3$) This compound exists in multiple conformations, causing significant peak overlap. Refer to the image of the ^1H NMR spectrum; ^{13}C NMR (150 MHz, $CDCl_3$) This compound exists in multiple conformations, causing significant peak overlap. Refer to the image of the ^{13}C NMR spectrum; HRMS (EI): Exact mass calcd for $C_{48}H_{78}N_5O_{14}$ $[M+NH_4]^+$ 948.5540, found 948.5553. ANS-4-236.

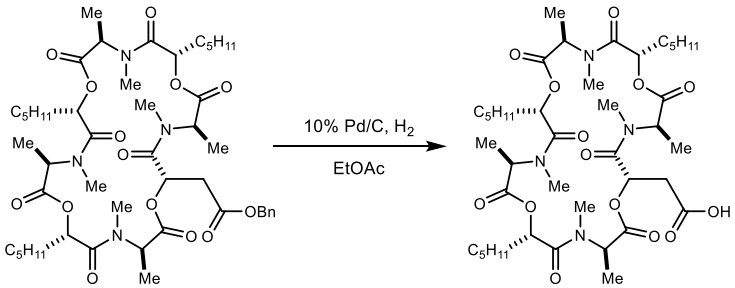

2-((2S,5R,8S,11R,14S,17R,20S,23R)-4,5,10,11,16,17,22,23-Octamethyl-3,6,9,12,15,18,21,24-octaoxo-8,14,20-tripentyl-1,7,13,19-tetraoxa-4,10,16,22-tetraazacyclotetracosan-2-yl)acetic acid (79). A round-bottom flask was charged with the depsipeptide (55 mg, 59 μmol), dissolved in EtOAc (3.0 mL), and treated with 10% Pd/C (6 mg). The reaction flask was evacuated with light vacuum (50 Torr). Hydrogen (balloon) was added, and the flask was cycled once more. The reaction was allowed to stir for 2 h. After purging the flask with nitrogen, the reaction mixture was filtered through Celite to afford the 24-membered macrocycle (40.5 mg, 82%) as a colorless oil. $[\alpha]_D^{23}$ +28 (*c* 0.58, $CHCl_3$); R_f = 0.10 (10% MeOH/DCM); IR (film) 3405, 2954, 2928, 2858, 1745, 1665, 1462, 1190, 1091 cm^{-1}; ^1H NMR (600 MHz, $CDCl_3$) This compound exists in multiple conformations, causing significant peak overlap. Refer to the image of the ^1H NMR spectrum; ^{13}C NMR (150 MHz, $CDCl_3$) This compound exists in multiple conformations, causing significant peak overlap. Refer to the image of the ^{13}C NMR spectrum; HRMS (EI): Exact mass calcd for $C_{41}H_{69}N_4O_{14}$ $[M+H]^+$ 841.4805, found 841.4809. ANS-4-255.

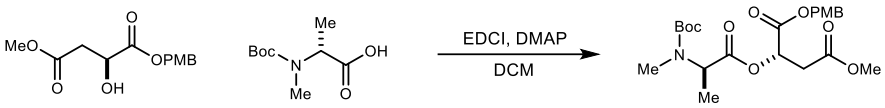

1-(4-Methoxybenzyl) 4-methyl (*S*)-2-((*N*-(*tert*-butoxycarbonyl)-*N*-methyl-D-alanyl)oxy)succinate (S65). A round-bottom flask was charged with the amine (725 mg, 3.57 mmol), alcohol (911 mg, 3.39 mmol), and DCM (34 mL). The mixture was cooled to 0 °C and then EDCI (780 mg, 4.07 mmol) and DMAP (21 mg, 170 μmol) were added. The reaction was stirred at 0 °C for 30 min, then allowed to warm to ambient temperature and stir for an additional 1.5 h. The reaction mixture was poured into water and extracted with DCM. The combined organic layers were washed with satd aq $NaHCO_3$ and brine, and then dried and concentrated. The crude residue was subjected to flash column chromatography (SiO_2, 20% ethyl acetate in hexanes) to afford the product as a colorless oil (1.12 g, 75%). $[\alpha]_D^{23}$ + 9.1 (*c* 0.53, $CHCl_3$); R_f = 0.13 (10% EtOAc/hexanes); IR (film) 2951, 2927, 1744, 1693, 1613, 1515, 1478, 1439, 1390, 1366, 1248, 1167 cm^{-1}; ^1H NMR (600 MHz, $CDCl_3$) Several peaks show a clear doubling for the *cis* and *trans* amide products. Other peaks are overlapping and appear only once. Those that are doubled have both values listed. δ 7.26 (d, *J* = 8.6 Hz, 2H), 6.88 (d, *J* = 8.6 Hz, 2H), 5.48 (dd, *J* = 6.1, 6.1 Hz, 1H), 5.13 (d, *J* = 12.2 Hz, 1H), 5.09 (d, *J* = 12.0 Hz, 1H), 4.98/4.70 (q, *J* = 6.8 Hz, 1H), 3.80 (s, 3H), 3.65 (s, 3H), 2.88 (d, *J* = 5.8 Hz, 2H), 2.78/2.74 (s, 3H), 1.45/1.43 (s, 9H), 1.37 (t, *J* = 7.5 Hz, 3H); ^{13}C NMR (150 MHz, $CDCl_3$) The line listing for both *cis* and *trans* amide isomers is

given, as a clear doubling of many peaks is evident. Whenever the isomer peaks overlap, it is stated that the particular peak is representing 2 carbons: ppm 171.6(2C), 169.5(2C), 168.5, 168.4, 160.0(2C), 156.0, 155.4, 130.4(4C), 127.2 (2C), 114.1 (4C), 80.4, 80.1, 69.0, 68.9, 67.6(2C), 55.4(2C), 54.3, 53.2, 52.2(2C), 36.0(2C), 30.3, 30.0, 28.5(3C), 28.4(3C), 15.3, 14.8; HRMS (EI): Exact mass calcd for $C_{22}H_{32}NO_9$ $[M+H]^+$ 454.2072, found 454.2068. ANS-6-202.

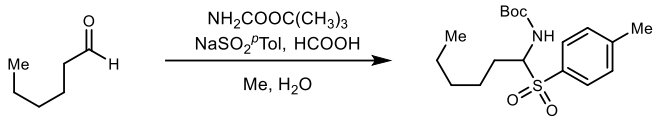

1-Tosylhexan-1-amine (91). A round-bottom flask was charged with hexanal (9.0 mL, 73 mmol), *tert*-butyl carbamate (5.7 g, 49 mmol), and MeOH (73 mL) and stirred until it became a homogenous solution. $NaSO_2{}^pTol$ (17.4 g, 97.6 mmol) was added, along with enough H_2O to dissolve the solids (100 mL). Then formic acid (3.68 mL, 97.6 mmol) was added, and the mixture was allowed to stir at ambient temperature under argon for 4 d. The reaction mixture was filtered and washed with H_2O and hexanes to afford the product as a white solid (15.3 g, 89%). Mp 107-110 °C; R_f = 0.26 (10% EtOAc/hexanes); IR (film) 3334, 2958, 2930, 2861, 1721, 1597, 1518, 1456, 1392, 1316, 1245, 1167, 1142, 1085 cm^{-1}; ^1H NMR (600 MHz, $CDCl_3$) The small doubling of peaks is due to cis and trans amide rotamers. The largely favored isomer is listed here: δ 7.76 (d, *J* = 8.8 Hz, 2H), 7.30 (d, *J* = 7.9 Hz, 2H), 5.10 (d, *J* = 11.0 Hz, 1H), 4.79 (td, *J* = 10.9, 3.4 Hz, 1H), 2.38 (s, 3H), 2.24-2.16 (m, 1H), 1.74-1.65 (m, 1H), 1.55-1.23 (m, 6H), 1.19 (s, 9H) 0.86 (t, *J* = 6.5 Hz, 3H), ; ^{13}C NMR (150 MHz, $CDCl_3$) ppm 154.0, 144.9, 134.0, 129.7, 129.4, 80.6, 31.2, 28.0, 27.7, 26.4, 25.0, 22.4, 21.7, 14.0; HRMS (EI): Exact mass calcd for $C_{18}H_{29}NNaO_4S$ $[M+Na]^+$ 378.1710, found 378.1719. ANS-5-113.

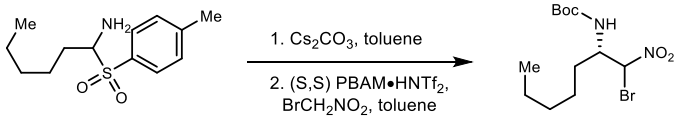

***tert*-Butyl ((2*S*)-1-bromo-1-nitroheptan-2-yl)carbamate (93).** A round-bottom flask was charged with sulfone (6.00 g, 16.8 mmol), Cs_2CO_3 (27.5 g, 84.4 mmol), and toluene (160 mL). The mixture was allowed to stir at ambient temperature under argon for 6 h. The reaction mixture was filtered through a pad of Celite and concentrated. The crude oil was then dissolved in toluene (248 mL) and to it was added (*S*,*S*)-PBAM as its triflimide salt (217.5 mg, 331 μmol). The reaction was cooled to -60 °C and bromonitromethane (1.74 mL, 24.8 mmol) was added. The reaction was allowed to stir for 48 h. The reaction mixture was quenched by running it through a short silica

plug while still cold, with 100% EtOAc. The fractions were combined and concentrated. The crude residue was subjected to flash column chromatography (SiO_2, 5% ethyl acetate in hexanes) to afford the α-bromo nitroalkane (1:1 dr (^{1}H NMR)) as a white solid (3.94 g, 70% 2-step); The diastereomers were determined to be 90% and 89% ee by chiral HPLC analysis (Chiralcel AD-H, 1% ^{i}PrOH /hexanes, 1.0 mL/min, t_r(d_1, major) = 19.6 min, t_r(d_1, minor) = 21.1 min, t_r(d_2, minor) = 25.1 min, t_r(d_2, major) = 29.4 min). $[\alpha]_D^{23}$ -20 (*c* 0.53, $CHCl_3$); Mp 62-66 °C; R_f = 0.60 (10% EtOAc/hexanes); IR (film) 3332, 2958, 2931, 2861, 1706, 1567, 1501, 1458, 1392, 1367, 1248, 1165, 1045 cm^{-1}; ^{1}H NMR (600 MHz, $CDCl_3$, 1:1 mixture of diastereomers) δ 6.19 (d, *J* = 4.4 Hz, 1H), 6.17 (d, *J* = 3.0 Hz, 1H), 4.83 (d, *J* = 8.8 Hz, 1H), 4.73 (d, *J* = 9.1 Hz, 1H), 4.34 (dddd, *J* = 9.2, 9.2, 3.9, 3.9 Hz, 1H), 4.24 (dddd, *J* = 9.2, 9.2, 4.6, 4.6 Hz, 1H), 1.90-1.52 (series of m, 4H), 1.46 (s, 9H), 1.44 (s, 9H), 1.40-1.22 (m, 12H), 0.90 (t, *J* = 7.0 Hz, 3H), 0.88 (t, *J* = 6.9 Hz, 3H); ^{13}C NMR (150 MHz, $CDCl_3$, 1:1 mixture of diastereomers) ppm 155.2, 155.1, 84.5, 83.2, 80.9, 80.8, 55.0, 54.5, 31.32, 31.28, 30.5, 28.5, 28.4, 28.3, 25.6, 25.5, 22.52, 22.51, 14.0(2C); HRMS (EI): Exact mass calcd for $C_{12}H_{23}BrN_2NaO_4$ $[M+Na]^+$ 361.0733, found 361.0737. ANS-5-161.

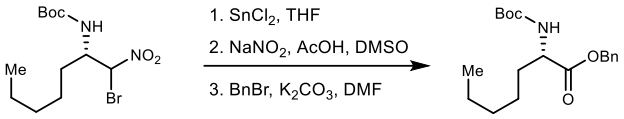

Benzyl (*S*)-2-((*tert*-butoxycarbonyl)amino)heptanoate (95). A flame-dried round-bottom flask was charged with halo-nitro alkane (383 mg, 1.13 mmol), tin chloride (428 mg, 2.26 mmol), and THF (11.3 mL). The mixture was allowed to stir at ambient temperature under argon for 12 h. The reaction mixture was then poured into H_2O, and diethyl ether was added into the separatory funnel. The organic layer was filtered through a pad of Celite, washed with H_2O (three times), dried, and concentrated to afford a pale-yellow oil. The crude oil was then dissolved in DMSO (8.7 mL) and to it was added $NaNO_2$ (234 mg, 3.39 mmol) and AcOH (885 µL, 17.0 mmol). The reaction was heated to 60 °C and allowed to stir for 12 h. The reaction mixture was allowed to cool to ambient temperature, quenched with 1 M aq HCl, poured into a separatory funnel, and extracted with EtOAc. The organic layers were washed with ice water (four times), dried, and concentrated. The crude reaction mixture was dissolved in DMF (2.1 mL), and to it was added K_2CO_3 (427 mg, 3.09 mmol) and BnBr (148 µL, 1.24 mmol). The reaction was allowed to stir at ambient temperature under argon for 12 h. The reaction was quenched with 1 M aq HCl and then extracted with EtOAc. The organic layers were then dried and concentrated. The crude residue was subjected to flash column chromatography (SiO_2, 10% ethyl acetate in hexanes) to afford the product as a colorless

oil (366 mg, 59% (3 steps)); $[\alpha]_D^{23}$ -5.39 (*c* 1.08, $CHCl_3$); R_f = 0.33 (10% EtOAc/hexanes); IR (film) 3365, 2957, 2931, 2861, 1717, 1499, 1456, 1366, 1249, 1161, 1048 cm^{-1}; ^1H NMR (400 MHz, $CDCl_3$) δ 7.40-7.28 (m, 5H), 5.21 (d, *J* = 12.4 Hz, 1H), 5.12 (d, *J* = 12.4 Hz, 1H), 5.02 (d, *J* = 7.8 Hz, 1H), 4.35 (ddd, *J* = 11.7, 6.2, 6.2 Hz, 1H), 1.85-1.70 (m, 1H), 1.68-1.55 (m, 1H), 1.43 (s, 9H), 1.36-1.17 (m, 6H), 0.85 (t, *J* = 6.3 Hz, 3H), ; ^{13}C NMR (100 MHz, $CDCl_3$) ppm 172.9, 156.5, 136.6, 128.7, 128.4, 128.3, 79.8, 66.9, 53.7, 32.7, 31.4, 28.4, 24.9, 22.5, 14.0; HRMS (EI): Exact mass calcd for $C_{19}H_{29}NNaO_4$ $[M+Na]^+$ 358.1989, found 358.1993. ANS-5-130.

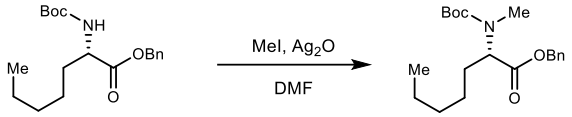

Benzyl (*S*)-2-((*tert*-butoxycarbonyl)(methyl)amino)heptanoate (96). A flame-dried round-bottom flask was charged with the α-amino ester (266 mg, 793 μmol), MeI (789 μg, 12.69 mmol), Ag_2O (735 mg, 3.17 mmol) and DMF (7.9 mL). The reaction vessel was wrapped in aluminum foil, and the mixture was allowed to stir at ambient temperature under argon for 12 h. The reaction mixture was filtered through a pad of Celite and concentrated, and then dissolved in EtOAc, washed with H_2O, dried, and concentrated to afford a pale-yellow oil. The crude residue was subjected to flash column chromatography (SiO_2, 5% ethyl acetate in hexanes) to afford the product as a colorless oil (188 mg, 67%); $[\alpha]_D^{23}$ -20.6 (*c* 1.09, $CHCl_3$); R_f = 0.57 (10% EtOAc/hexanes); IR (film) 3033, 2931, 2860, 1743, 1697, 1455, 1391, 1366, 1327, 1149 cm^{-1}; ^1H NMR (600 MHz, $CDCl_3$) Several peaks show a clear doubling for the *cis* and *trans* amide products. Other peaks are overlapping and appear only once. Those that are doubled have both values listed. δ 7.40-7.28 (m, 5H), 5.15 (broad s, 2H), 4.80/4.47 (dd, *J* = 10.5, 4.8 Hz, 1H), 2.82/2.75 (s, 3H), 1.97-1.86 (m, 1H), 1.79-1.63 (m, 1H), 1.45/1.40 (s, 9H), 1.36-1.23 (m, 6H), 0.88/0.87 (t, *J* = 6.5 Hz, 3H); ^{13}C NMR (150 MHz, $CDCl_3$) ppm) The line listing for both *cis* and *trans* amide isomers is given, as a clear doubling of many peaks is evident. Whenever the isomer peaks overlap, it is stated that the particular peak is representing 2 or more carbons. 172.2, 172.0, 156.5, 155.8, 136.0, 135.8, 128.7, 128.6, 128.4, 128.2, 128.1, 128.0, 80.3, 80.0, 66.7, 66.6, 59.3, 57.9, 31.4(2C), 30.9, 30.5, 29.1, 28.7, 28.5, 28.4, 25.8(2C), 22.6(2C), 14.1, 14.0; HRMS (EI): Exact mass calcd for $C_{20}H_{31}NNaO_4$ $[M+Na]^+$ 372.2145, found 372.2149. ANS-5-143.

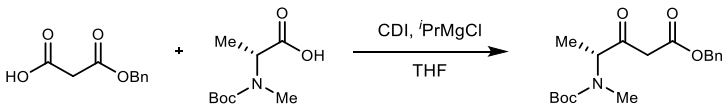

Benzyl (*R*)-4-((*tert*-butoxycarbonyl)(methyl)amino)-3-oxopentanoate (100). A flame-dried round-bottom flask was charged with the amine (200 mg, 984 μmol), CDI (176 mg, 1.08 mmol), and THF (3 mL). Reaction A was stirred at ambient temperature for 2 h. In a separate flame-dried round-bottom flask was added 3-(benzyloxy)-3-oxopropanoic acid (210 mg, 1.08 mmol) and THF (7 mL). Reaction B was cooled to 0 °C, then ^{i}PrMgCl (1.08 mL, 2.16 mmol) was added/ Reaction B was allowed to stir at 0 °C for 30 min, then heated to 50 °C and stirred for an additional 30 min. Reaction B was then cooled to 0 °C, and reaction A was added to reaction B at 0 °C. The reaction mixture was then allowed to warm to ambient temperature and stir for 12 h. The reaction mixture was quenched with 1 M aq HCl and extracted with EtOAc. The combined organic layers were washed with satd aq $NaHCO_3$ and brine, and then dried and concentrated. The crude residue was subjected to flash column chromatography (SiO_2, 10-30% ethyl acetate in hexanes) to afford the product as a colorless oil (100 mg, 30%). $[\alpha]_D^{23}$ +81.5 (*c* 1.33, $CHCl_3$); R_f = 0.14 (10% EtOAc/hexanes); IR (film) 2976, 2934, 1747, 1688, 1479, 1455, 1390, 1367, 1309, 1250, 1153 cm^{-1}; ^{1}H NMR (600 MHz, $CDCl_3$) Several peaks show a clear doubling for the *cis* and *trans* carbamate products. Other peaks are overlapping and appear only once. Those that are doubled have both values listed. δ 7.44-7.27 (m, 5H), 5.16 (broad s, 2H), 4.53/4.11 (q, *J* = 7.0 Hz, 1H), 3.62/3.60 (d, *J* = 15.9 Hz, 1H), 3.49 (d, *J* = 16.1 Hz, 1H), 2.85/2.73 (s, 3H), 1.45/1.40 (s, 9H), 1.35-1.24 (m, 3H); ^{13}C NMR (150 MHz, $CDCl_3$) The line listing for both *cis* and *trans* carbamate isomers is given, as a clear doubling of many peaks is evident. Whenever the isomer peaks overlap, it is stated that the particular peak is representing 2 or more carbons: ppm 201.4, 201.1, 167.3(2C), 158.8, 154.9, 135.5, 135.4, 128.7(4C), 128.5(4C), 81.6, 80.8, 67.3, 67.2, 62.7, 60.7, 45.8, 45.7, 33.4, 31.8, 28.5(2C), 28.4(3C), 28.3(3C), 12.9, 12.3; HRMS (EI): Exact mass calcd for $C_{18}H_{25}NNaO_5$ $[M+Na]^+$ 358.1625, found 358.1627. ANS-6-91.

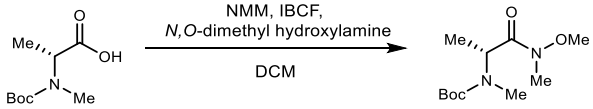

***tert*-Butyl (*R*)-(1-(methoxy(methyl)amino)-1-oxopropan-2-yl)(methyl)carbamate (S66).** A flame-dried round-bottom flask was charged with the acid (500 mg, 2.57 mmol), *N*-methylmorpholine (706 μL, 6.42 mmol), isobutyl chloroformate (433 μL, 3.34 mmol) and DCM (25.7 mL) at 0 °C. The reaction was allowed to stir at 0 °C for 1 h, then was added *N*,*O*-dimethyl hydroxylamine (301 mg, 3.08 mmol). The reaction was allowed to warm to room temperature and stir for 12 h. The reaction mixture was quenched with 1 M aq HCl and extracted with DCM. The

combined organic layers were washed with satd aq $NaHCO_3$ and brine, and then dried and concentrated. The crude residue was subjected to flash column chromatography (SiO_2, 10-30% ethyl acetate in hexanes) to afford the product as a colorless oil (428 mg, 68%). All spectral data are in agreement with literature values.[7] ANS-6-195.

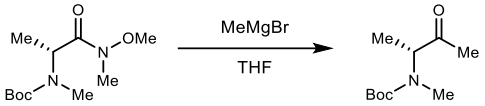

***tert*-Butyl (*R*)-methyl(3-oxobutan-2-yl)carbamate (104).** A flame-dried round-bottom flask was charged with the Weinreb amide (428 mg, 1.74 mmol) and THF (8.7 mL) and cooled to -78 °C. MeMgBr (1.4 mL, 4.0 mmol) was then added dropwise, and the reaction was allowed to stir at -78 °C for 1 hr. The reaction was then allowed to warm to 0 °C and stirred for an additional 1 hr. The reaction mixture was quenched with 1 M aq HCl and extracted with EtOAc. The combined organic layers were washed with satd aq $NaHCO_3$ and brine, and then dried and concentrated to afford the product as a yellow oil (223 mg, 64%). $[\alpha]_D^{23}$ +144 (*c* 0.61, $CHCl_3$); R_f = 0.26 (20% EtOAc/hexanes); IR (film) 2977, 2935, 1732, 1692, 1390, 1153, 1093 cm^{-1}; ^1H NMR (600 MHz, $CDCl_3$) Several peaks show a clear doubling for the *cis* and *trans* carbamate products. Other peaks are overlapping and appear only once. Those that are doubled have both values listed. δ 4.62/4.08 (q, *J* = 6.5 Hz, 1H), 2.85/2.73 (s, 3H), 2.12 (s, 3H), 1.47/1.43 (s, 9H), 1.28/1.25 (d, *J* = 9.7 Hz, 3H); ^{13}C NMR (150 MHz, $CDCl_3$) ppm 207.8, 207.1, 156.0, 155.1, 80.9, 80.4, 62.6, 60.3, 32.4, 30.9, 28.48, 28.45, 26.7, 26.4, 13.3, 12.8; HRMS (EI): Exact mass calcd for $C_{10}H_{20}NO_3$ $[M+H]^+$ 202.1438, found 202.1437. ANS-6-200.

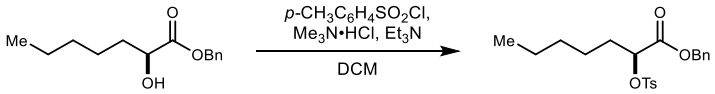

Benzyl (*S*)-2-(tosyloxy)heptanoate (103). A round-bottom flask was charged with *p*-toluenesulfonyl chloride (549 mg, 1.92 mmol), trimethylamine hydrochloric salt (18.3 mg, 192 μmol), and DCM (7.7 mL). The mixture was cooled to 0 °C and then Et_3N (535 μL, 3.84 mmol) was added dropwise, followed by addition of the alcohol (453 mg, 1.92 mmol). The reaction was stirred at 0 °C for 1 h, then quenched by addition of 1 M aq HCl and extracted with DCM. The combined organic layers were washed with brine, dried, and concentrated to afford the product as

[7] Niello, M.; Cintulova, D.; Hellsberg, E.; Jäntsch, K.; Holy, M.; Ayatollahi, L. H.; Cozzi, N. V.; Freissmuth, M.; Sandtner, W.; Ecker, G. F.; Mihovilovic, M. D.; Sitte, H. H. para-Trifluoromethyl-methcathinone is an allosteric modulator of the serotonin transporter, *Neuropharmacology* **2019**, *161*, 107615.

a colorless oil (644 mg, 86%). $[\alpha]_D^{23}$ +6.6 (*c* 0.66, $CHCl_3$); R_f = 0.32 (10% EtOAc/hexanes); IR (film) 3057, 2957, 2930, 2861, 1757, 1597, 1455, 1371, 1264, 1189, 1176 cm^{-1}; ^1H NMR (400 MHz, $CDCl_3$) δ 7.76 (dd, *J* = 8.5, 2.1 Hz, 2H), 7.37-7.22 (m, 7H), 5.06 (broad s, 2H), 4.86 (dd, *J* = 6.4, 6.2 Hz, 1H), 2.38 (s, 3H), 1.85-1.74 (m, 2H), 1.33-1.08 (m, 6H), 0.80 (t, *J* = 6.8 Hz, 3H); ^{13}C NMR (100 MHz, $CDCl_3$) ppm 168.6, 144.9, 134.9, 133.1, 129.7, 128.5, 128.4, 128.2, 127.9, 77.5, 67.1, 32.0, 30.8, 24.0, 22.1, 21.5, 13.7; HRMS (EI): Exact mass calcd for $C_{21}H_{26}NaO_5S$ $[M+Na]^+$ 413.1393, found 413.1395. ANS-6-170.

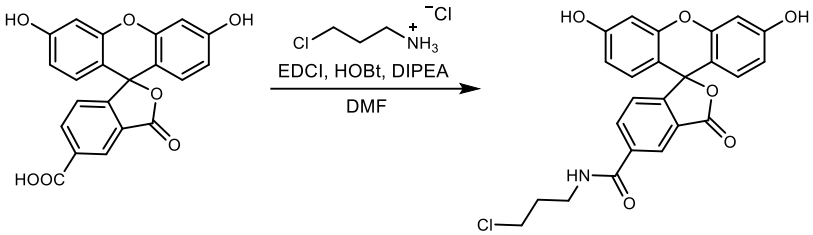

5-(4-Chlorobutanoyl)-3',6'-dihydroxy-3H-spiro[isobenzofuran-1,9'-xanthen]-3-one (107). To a round-bottom flask was added 5-carboxy fluorescein (50 mg, 130 μmol), 3-chloropropyl amine·HCl (25.9 mg, 199 μmol), EDCI (30.6 mg, 159 μmol), and HOBt (22.5 mg, 166 μmol) in DMF (2.66 mL). The reaction mixture was allowed to stir for 15 min, before adding DIPEA (70 μL, 400 μmol). The reaction was stirred for 12 h at ambient temperature, poured into ice cold 10% aq citric acid, and then extracted with ethyl acetate. The organic layer was washed with ice-water and brine, then dried and concentrated. Preparative HPLC (30 – 95% aqueous acetonitrile, 210 nm, flow rate: 20 mL/min, R_t = 8.6 m) afforded an orange solid (42.7 mg, 71%); R_f = 0.15 (50% EtOAc/hexanes); IR (film) 2917, 2850, 1734, 1701, 1578, 1540, 1453, 1241, 1110 cm^{-1}; ^1H NMR (400 MHz, CH_3OD) δ 8.43 (br s, 1H), 8.20 (dd, *J* = 8.1, 1.6 Hz, 1H), 7.30 (d, *J* = 8.0 Hz, 1H), 6.69 (d, *J* = 2.2 Hz, 2H), 6.60 (d, *J* = 8.7 Hz, 2H), 6.53 (dd, *J* = 8.6, 2.3 Hz, 2H), 3.69 (t, *J* = 6.4 Hz, 2H), 3.59 (t, *J* = 6.8 Hz, 2H), 2.13 (p, *J* = 6.6 Hz, 2H) [*OH* and *NH* not observed]; ^{13}C NMR (150 MHz, CH_3OD) ppm 170.6, 168.6, 168.5, 161.4, 154.0, 137.8, 135.5, 130.1, 128.6, 125.7, 124.8, 113.7, 110.8, 103.6, 43.2, 38.9, 38.7, 33.4; HRMS (EI): Exact mass calcd for $C_{24}H_{17}ClNO_6$ $[M-H]^-$ 450.0750, found 450.0742. ANS-4-14.

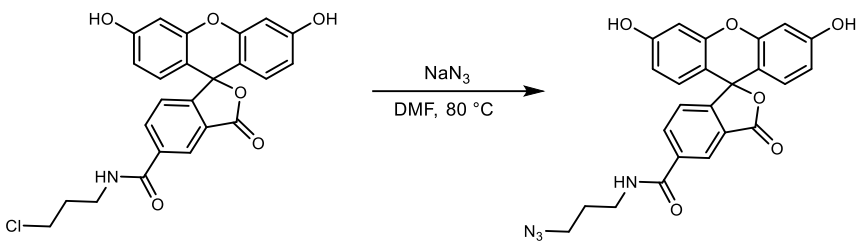

5-(4-Azidobutanoyl)-3',6'-dihydroxy-3H-spiro[isobenzofuran-1,9'-xanthen]-3-one (108). To a microwave vial was added the fluorescein derivative (18.8 mg, 41.5 μmol) and sodium azide (5.4 mg, 83 μmol) in DMF (437 μL). The reaction mixture was heated at 80 °C in an oil bath for 4 hr. The reaction mixture was then allowed to cool to ambient temperature and then poured into ice-water and extracted with ethyl acetate. The organic layer was washed with brine, dried, and concentrated. Preparative HPLC (55 – 95% aqueous acetonitrile, 210 nm, flow rate: 8 mL/min, R_t = 28.7 m) afforded an orange solid (14.9 mg, 78%); All spectral data are in agreement with literature values.[8,9] ANS-4-16.

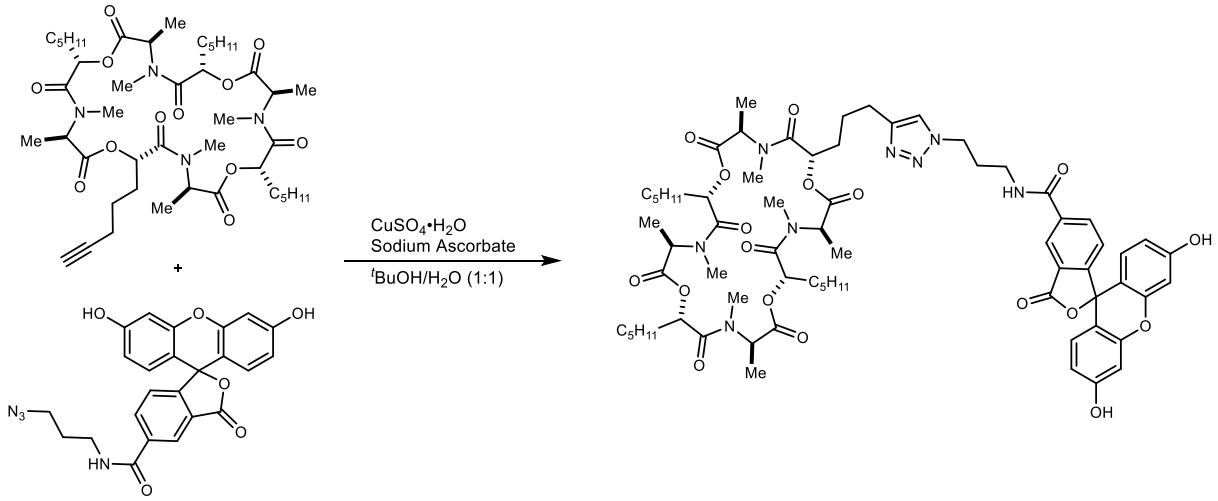

3',6'-Dihydroxy-*N*-(3-(4-(3-((2*S*,5*R*,8*S*,11*R*,14*S*,17*R*,20*S*,23*R*)-4,5,10,11,16,17,22,23-octamethyl-3,6,9,12,15,18,21,24-octaoxo-8,14,20-tripentyl-1,7,13,19-tetraoxa-4,10,16,22-tetraazacyclotetracosan-2-yl)propyl)-1H-1,2,3-triazol-1-yl)propyl)-3-oxo-3H-spiro[isobenzofuran-1,9'-xanthene]-5-carboxamide (109). A microwave vial was charged with the cyclic depsipeptide (5.5 mg, 6.5 μmol), azide (3.0 mg, 6.5 μmol), ^{t}BuOH (170 μL), and H_2O

[8] Onizuka, K.; Shibata, A.; Taniguchi, Y.; Sasaki, S. Pin-point chemical modification of RNA with diverse molecules through the functionality transfer reaction and the copper-catalyzed azide–alkyne cycloaddition reaction, *Chem. Commun.* **2011**, *47*, 5004-5006.

[9] Aloisi, A.; Franchet, A.; Ferrandon, D.; Bianco, A.; Ménard-Moyon, C. Fluorescent-fipronil: Design and synthesis of a stable conjugate, *Bioorg. Med. Chem. Lett.* **2018**, *28*, 2631-2635.

(170 μL). $CuSO_4 \cdot H_2O$ (500 μg, 1.9 μmol) and sodium ascorbate (780 μg, 3.9 μmol) were added, the reaction was sealed with a microwave cap, and then submerged into a 50 °C oil bath. The reaction was allowed to stir at 50 °C for 2.5 h. The crude mixture was then cooled to ambient temperature, poured into H_2O, extracted with ethyl acetate, washed with EDTA·2Na (0.1 N aq) and brine, dried, and concentrated. To the crude material was added 4 M HCl in dioxane (400 μL) and the reaction mixture was allowed to stir for 30 min. Preparative HPLC (30 – 95% aqueous acetonitrile, 210 nm, flow rate: 8 mL/min, R_t = 13.5 m) afforded the tagged 24-membered macrocycle (2.0 mg, 24%) as a bright orange amorphous solid. $[\alpha]_D^{24}$ +25 (*c* 0.20, MeOH); R_f = 0.54 (20% MeOH/DCM); IR (film) 3315, 2921, 2852, 2364, 1746, 1659, 1460, 1377, 1320, 1183, 1096 cm^{-1}; ^1H NMR (600 MHz, CH_3OD) This compound exists in multiple conformations, causing significant peak overlap. The resolved peaks are listed. Refer to the image of the ^1H NMR spectrum for the other peaks: δ 8.41 (br s, 1H), 6.89 (br d, *J* = 8.6, 1H), 7.30 (d, *J* = 8.1 Hz, 1H), 6.70 (br s, 2H), 6.59 (br dd, *J* = 8.6, 2.1 Hz, 2H) 4.51 (t, *J* = 6.9 Hz, 2H); ^{13}C NMR (150 MHz, CH_3OD) This compound exists in multiple conformations, causing significant peak overlap. Refer to the image of the ^{13}C NMR spectrum; HRMS (EI): Exact mass calcd for $C_{68}H_{91}N_8O_{18}$ $[M+H]^+$ 1307.6446, found 1307.6474. ANS-4-18.

3',6'-Dihydroxy-*N*-(3-(4-(3-((2*R*,5*S*,8*R*,11*S*,14*R*,17*S*,20*R*,23*S*)-4,5,10,11,16,17,22,23-octamethyl-3,6,9,12,15,18,21,24-octaoxo-8,14,20-tripentyl-1,7,13,19-tetraoxa-4,10,16,22-tetraazacyclotetracosan-2-yl)propyl)-1H-1,2,3-triazol-1-yl)propyl)-3-oxo-3H-spiro[isobenzofuran-1,9'-xanthene]-5-carboxamide (*ent*-109). Prepared following an identical procedure as **109**. Preparative HPLC (30 – 95% aqueous acetonitrile, 210 nm, flow rate: 8 mL/min, R_t = 13.5 m) afforded the tagged 24-membered macrocycle with spectroscopic data identical to its enantiomer, except $[\alpha]_D^{24}$ -27 (*c* 0.63, MeOH). ANS-4-107.

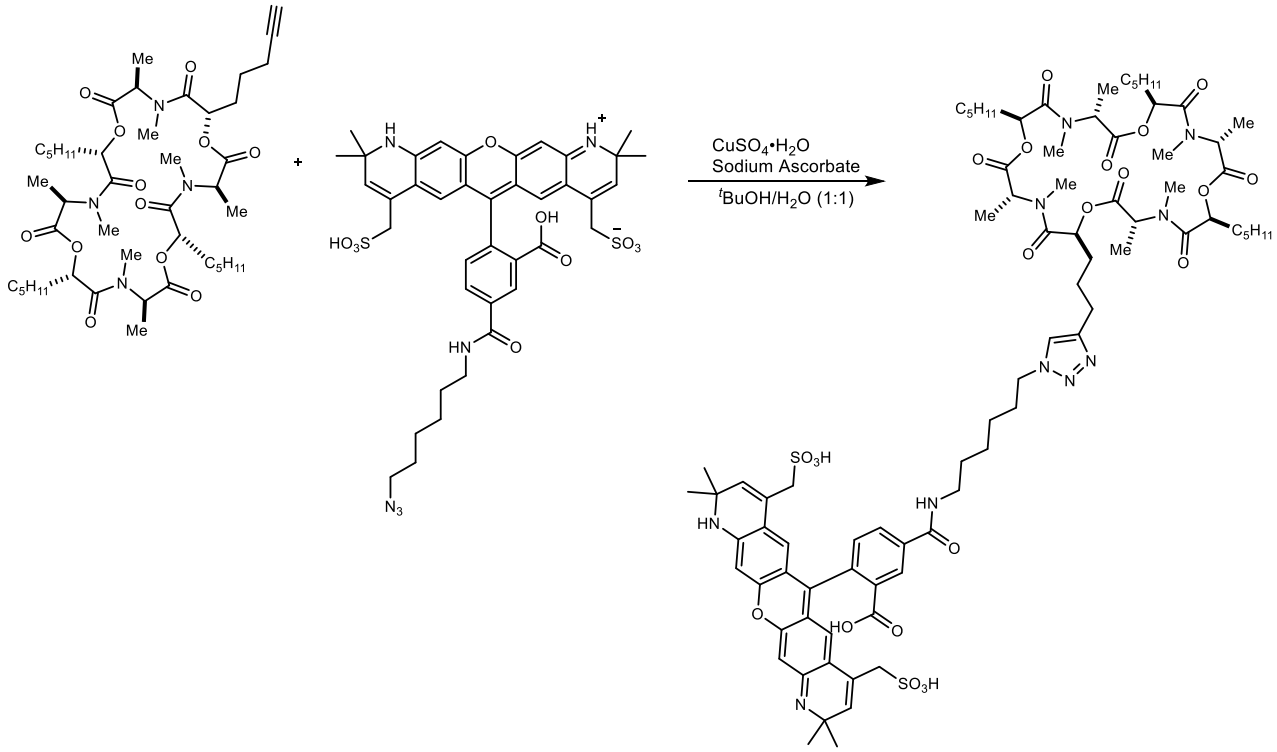

5-((6-(4-(3-((2*S*,5*R*,8*S*,11*R*,14*S*,17*R*,20*S*,23*R*)-4,5,10,11,16,17,22,23-Octamethyl-3,6,9,12,15,18,21,24-octaoxo-8,14,20-tripentyl-1,7,13,19-tetraoxa-4,10,16,22-tetraazacyclotetracosan-2-yl)propyl)-1H-1,2,3-triazol-1-yl)hexyl)carbamoyl)-2-(2,2,10,10-tetramethyl-4,8-bis(sulfomethyl)-1,10-dihydro-2H-pyrano[3,2-g:5,6-g']diquinolin-6-yl)benzoic acid (111). A microwave vial was charged with the cyclic depsipeptide (8.9 mg, 11 μmol), azide (5.0 mg, 6.1 μmol), ^{t}BuOH (500 μL), and H_2O (500 μL). $CuSO_4 \cdot H_2O$ (1 mg, 3.2 μmol) and sodium ascorbate (1.3 mg, 6.3 μmol) were added, the reaction was sealed with a microwave cap, and then submerged into a 50 °C oil bath. The reaction was allowed to stir at 50 °C for 2.5 h. The crude mixture was then cooled to ambient temperature, poured into H_2O, extracted with DCM (seven times). The combined organic layers were washed with 0.1 N aq EDTA·2Na and brine, and then dried and concentrated. Preparative HPLC (30 – 95% aqueous acetonitrile, 210 nm, flow rate: 8 mL/min, R_t = 12.0 m) afforded the tagged 24-membered macrocycle after lyophilization as a bright purple amorphous solid (5.9 mg, 57%). A full characterization was not acquired due to limited material. However, a ^{1}H NMR spectra is provided along with HRMS data; ^{1}H NMR (600 MHz, CH_3OD) This compound exists in multiple conformations, causing significant peak overlap. Refer to the image of the ^{1}H NMR spectrum for

the other peaks: HRMS (EI): Exact mass calcd for $C_{83}H_{113}N_{10}O_{22}S_2$ $[M\text{-}H]^-$ 1665.7478, found 1665.7495. ANS-5-61.

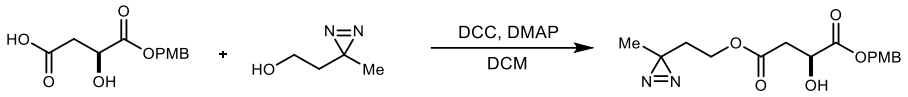

1-(4-Methoxybenzyl) 4-(2-(3-methyl-3H-diazirin-3-yl)ethyl) (*S*)-2-hydroxysuccinateate (121). A round-bottom flask was charged with the acid (100 mg, 393 μmol), alcohol (47.3 mg, 472 μmol), DCC (122 mg, 591 μmol), DMAP (4.8 mg, 39 μmol), and DCM (1.5 mL). The reaction was stirred at ambient temperature overnight. The reaction mixture was poured into water and extracted with DCM. The combined organic layers were washed with 1 M aq HCl, satd aq $NaHCO_3$ and brine, and then dried and concentrated. The crude residue was subjected to flash column chromatography (SiO_2, 20% ethyl acetate in hexanes) to afford the product as a colorless oil (40 mg, 31%). $[\alpha]_D^{24}$ –14.1 (*c* 1.01, $CHCl_3$); R_f = 0.17 (30% EtOAc/hexanes); IR (film) 3486, 3328, 2929, 2846, 1739, 1614, 1584, 1515, 1458, 1249, 1173, 1106, 1033 cm^{-1}; ^1H NMR (600 MHz, $CDCl_3$) δ 7.29 (dd, *J* = 6.3, 2.3 Hz, 2H), 6.89 (dd, *J* = 6.4, 2.1 Hz, 2H), 5.18 (d, *J* = 12.5 Hz, 1H), 5.16 (d, *J* = 12.4 Hz, 1H), 4.52 (ddd, *J* = 5.7, 5.7, 4.7 Hz, 1H), 4.03 (ddd, *J* = 11.3, 6.0, 6.0 Hz, 1H), 4.00 (ddd, *J* = 11.3, 6.0, 6.0 Hz, 1H), 3.81 (s, 3H), 3.24 (br s, 1H), 2.87 (dd, *J* = 16.5, 4.5 Hz, 1H), 2.80 (dd, *J* = 16.5, 6.2 Hz, 1H), 1.61 (t, *J* = 6.5 Hz, 2H), 1.03 (s, 3H); ^{13}C NMR (150 MHz, $CDCl_3$) ppm 173.3, 170.3, 160.1, 130.5, 127.2, 114.2, 67.8, 67.4, 60.1, 55.4, 38.8, 33.7, 24.0, 19.9; HRMS (EI): Exact mass calcd for $C_{16}H_{20}NaO_6$ $[M\text{-}N_2\text{+}Na]^+$ 331.1152, found 331.1153. ANS-4-177.

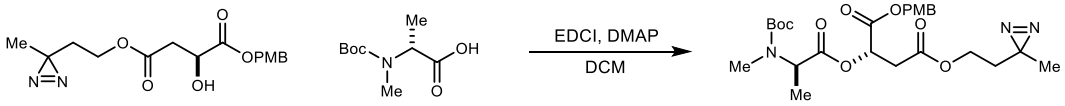

1-(4-Methoxybenzyl) 4-(2-(3-methyl-3H-diazirin-3-yl)ethyl) (*S*)-2-((*N*-(*tert*-butoxycarbonyl)-*N*-methyl-D-alanyl)oxy)succinate (122). A round-bottom flask was charged with the amine (25.8 mg, 127 μmol), alcohol (35.6 mg, 106 μmol), and DCM (1.1 mL). The mixture was cooled to 0 °C and then EDCI (24.3 mg, 127 μmol) and DMAP (1.3 mg, 10 μmol) were added. The reaction was stirred at 0 °C for 30 min, then allowed to warm to ambient temperature and stir for an additional 1.5 h. The reaction mixture was poured into water and extracted with DCM. The combined organic layers were washed with satd aq $NaHCO_3$ and brine, and then dried and concentrated to afford the product as a colorless oil (43.4 mg, 79%). $[\alpha]_D^{24}$ +9.6 (*c* 0.50, $CHCl_3$); R_f = 0.27 (20% EtOAc/hexanes); IR (film) 2969, 1746, 1695, 1613, 1515, 1389, 1251, 1170, 1092 cm^{-11}; ^1H NMR

(600 MHz, $CDCl_3$) Several peaks show a clear doubling for the *cis* and *trans* amide products. Other peaks are overlapping and appear only once. Those that are doubled have both values listed. δ 7.27 (d, *J* = 8.2 Hz, 2H), 6.88 (d, *J* = 8.6 Hz, 2H), 5.51 (dd, *J* = 7.2, 5.3 Hz, 1H), 5.14 (d, *J* = 12.0 Hz, 1H), 5.10 (d, *J* = 12.0 Hz, 1H), 4.98/4.71 (q, *J* = 7.1 Hz, 1H), 4.01 (t, *J* = 6.5 Hz, 2H), 3.81 (s, 3H), 2.92 (dd, *J* = 16.6, 5.1 Hz, 1H), 2.88 (dd, *J* = 16.6, 7.2 Hz, 1H), 2.79/2.75 (s, 3H), 1.65-1.57 (br m, 2H), 1.45/1.43 (s, 9H), 1.37 (t, *J* = 8.3 Hz, 3H), 1.03 (s, 3H); ^{13}C NMR (150 MHz, $CDCl_3$) The line listing for both *cis* and *trans* amide isomers is given, as a clear doubling of many peaks is evident. Whenever the isomer peaks overlap, it is stated that the particular peak is representing 2 carbons: ppm 171.5(2C), 168.8(2C), 168.5, 168.4, 160.0(2C), 156.0, 155.4, 130.4(4C), 127.1(2C), 114.1(4C), 80.4, 80.1, 68.8(2C), 67.6(2C), 60.2(2C), 55.4(2C), 54.3, 53.3, 36.1(2C), 33.7(2C), 30.3, 30.1, 28.5(3C), 28.4(3C), 23.9(2C), 19.9(2C), 15.3, 14.8; HRMS (EI): Exact mass calcd for $C_{25}H_{35}N_3NaO_9$ $[M+Na]^+$ 544.2266, found 544.2267. ANS-4-168.

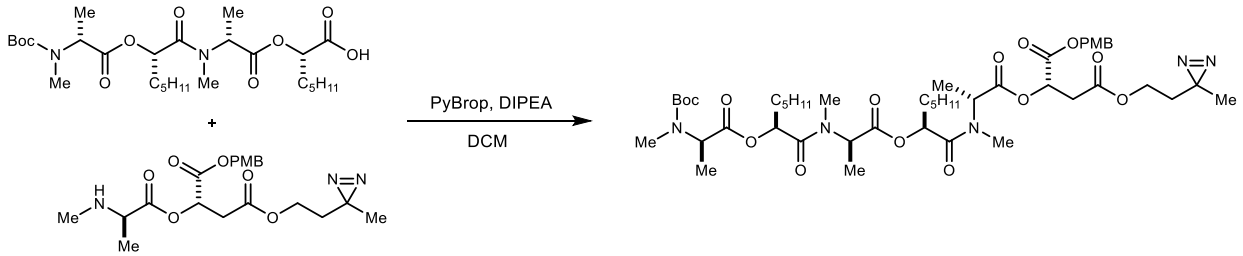

1-(4-Methoxybenzyl) 4-(2-(3-methyl-3H-diazirin-3-yl)ethyl) (*S*)-2-(((6*R*,9*S*,12*R*,15*S*,18*R*)-2,2,5,6,11,12,17,18-octamethyl-4,7,10,13,16-pentaoxo-9,15-dipentyl-3,8,14-trioxa-5,11,17-triazanonadecan-19-oyl)oxy)succinate (126). A round-bottom flask was charged with the amine (19.3 mg, 45.9 μmol), acid (25.0 mg, 45.9 μmol), and DCM (918 μL). The mixture was cooled to 0 °C and then DIPEA (23.6 μL, 138 μmol) and PyBrop (32.1 mg, 68.9 μmol) were added. The reaction was stirred at 0 °C for 30 min, then allowed to warm to ambient temperature and stir for an additional 1.5 h. The reaction mixture was poured into cold 10% aq citric acid and extracted with DCM. The combined organic layers were washed with satd aq $NaHCO_3$ and brine, and then dried and concentrated. The crude residue was subjected to flash column chromatography (SiO_2, 20-40% ethyl acetate in hexanes) to afford the product as a colorless oil (25.6 mg, 59%). $[\alpha]_D^{24}$ +32 (*c* 1.00, $CHCl_3$); R_f = 0.27 (40% EtOAc/hexanes); IR (film) 2931, 2863, 1743, 1664, 1515, 1458, 1249, 1170, 1106 cm^{-1}; ^1H NMR (600 MHz, $CDCl_3$) This compound exists as a mixture of rotamers causing significant peak broadening and overlap. Several key peaks associated with the diazirine portion of the molecule are resolved and are listed. Refer to the image of the ^1H NMR

spectrum for other peaks: δ 3.99 (t, J = 6.4 Hz, 2H), 1.04/1.02 (s, 3H); ^{13}C NMR (150 MHz, $CDCl_3$) This compound is a mixture of rotamers causing significant peak broadening and overlap. Refer to the image of the ^{13}C NMR spectrum; HRMS (EI): Exact mass calcd for $C_{47}H_{77}N_6O_{15}$ $[M+NH_4]^+$ 965.5441, found 965.5446. ANS-4-247.

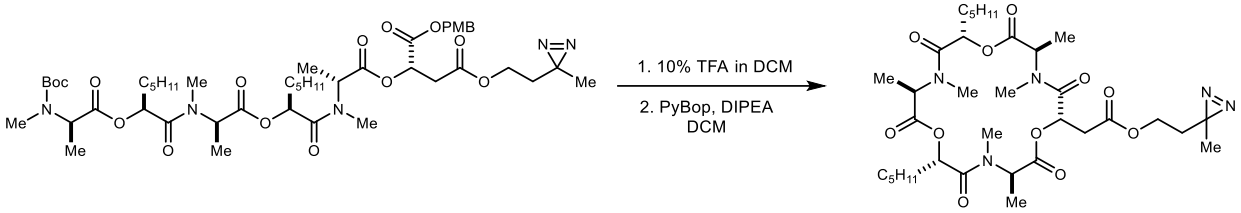

2-(3-Methyl-3H-diazirin-3-yl)ethyl 2-((2*S*,5*R*,8*S*,11*R*,14*S*,17*R*)-4,5,10,11,16,17-hexamethyl-3,6,9,12,15,18-hexaoxo-8,14-dipentyl-1,7,13-trioxa-4,10,16-triazacyclooctadecan-2-yl)acetate (128). A round-bottom flask was charged with the depsipeptide (25.6 mg, 27.0 μmol), and dissolved in a mixture of 10% TFA in DCM (0.15 mL TFA, 1.5 mL DCM). The reaction was allowed to stir at ambient temperature for 45 min. The crude reaction mixture was concentrated in vacuo. The unpurified material was added to a flame-dried round bottom flask, DCM (5.4 mL) was added, and the reaction was cooled to 0 °C. DIPEA (10.2 μL, 59.4 μmol) and PyBrop (14.8 mg, 28.4 μmol) were then added. The reaction was stirred at 0 °C for 30 min, then allowed to warm to ambient temperature and stir for an additional 1.5 h. The reaction mixture was poured into cold 10% aq citric acid and extracted with DCM. The combined organic layers were washed with satd aq $NaHCO_3$ and brine, and then dried and concentrated. Preparative HPLC (5 – 95% aqueous acetonitrile, 210 nm, flow rate: 8 mL/min, R_t = 23.6 m) afforded the 18-membered macrocycle (5.0 mg, 26%) as a colorless oil. $[\alpha]_D^{24}$ +19 (c 0.43, $CHCl_3$); R_f = 0.10 (60% EtOAc/hexanes); IR (film) 2927, 2858, 1743, 1665, 1459, 1412, 1191, 1100 cm^{-1}; ^{1}H NMR (600 MHz, $CDCl_3$) This compound exists in multiple conformations, causing significant peak overlap. Several key peaks associated with the diazirine portion of the molecule are resolved and are listed. Refer to the image of the ^{1}H NMR spectrum for other peaks: δ 3.97/3.96 (t, J = 6.4 Hz, 2H), 0.99/0.98 (s, 3H); ^{13}C NMR (150 MHz, $CDCl_3$) This compound exists in multiple conformations, causing significant peak overlap. Refer to the image of the ^{13}C NMR spectrum; HRMS (EI): Exact mass calcd for $C_{34}H_{59}N_6O_{11}$ $[M+NH_4]^+$ 727.4236, found 727.4216. ANS-4-251.

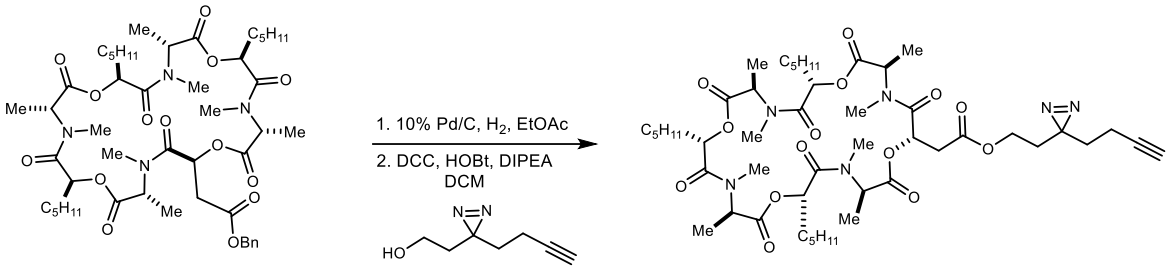

2-(3-(But-3-yn-1-yl)-3H-diazirin-3-yl)ethyl 2-((2*S*,5*R*,8*S*,11*R*,14*S*,17*R*,20*S*,23*R*)-4,5,10,11,16,17,22,23-octamethyl-3,6,9,12,15,18,21,24-octaoxo-8,14,20-tripentyl-1,7,13,19-tetraoxa-4,10,16,22-tetraazacyclotetracosan-2-yl)acetate (142). A round-bottom flask was charged with the cyclic peptide (55 mg, 59 mmol) dissolved in ethyl acetate (3.0 mL) and treated with 10% Pd/C (6 mg). The reaction flask was evacuated with light vacuum (50 Torr). Hydrogen (balloon) was added, and the flask was cycled through vacuum once more. The reaction was allowed to stir for 2 h. The crude reaction mixture was filtered through Celite and concentrated to afford the deprotected cyclic depsipeptide. A flame-dried round-bottom flask was charged with the depsipeptide (10 mg, 11.9 μmol), DCC (2.95 mg, 14.3 μmol), HOBt (2.01 g, 14.9 μmol), and DCM (200 μL). The reaction was cooled to 0 °C and allowed to stir for 10 min. The diazirine (3.3 mg, 23.8 μmol) and DIPEA (2.5 μL, 14.3 μmol) were added and the reaction was allowed to stir at ambient temperature for 1 hour. The reaction mixture was diluted with DCM, filtered through Celite, and concentrated. Preparative HPLC (5 – 95% aqueous acetonitrile, 210 nm, flow rate: 8 mL/min, R_t = 25.7 m) afforded the 24-membered macrocycle (5.5 mg, 48%) as a colorless oil. $[\alpha]_D^{24}$ +23 (*c* 0.46, $CHCl_3$); R_f = 0.24 (100% EtOAc); IR (film) 3308, 2927, 2857, 2360, 1742, 1662, 1556, 1458, 1413, 177, 1318, 1189, 1106 cm^{-1}; ^1H NMR (600 MHz, $CDCl_3$) This compound exists in multiple conformations, causing significant peak broadening and overlap. Refer to the image of the ^1H NMR spectrum; ^{13}C NMR (150 MHz, $CDCl_3$) This compound exists in multiple conformations, causing significant peak broadening and overlap. Refer to the image of the ^{13}C NMR spectrum; HRMS (EI): Exact mass calcd for $C_{48}H_{76}NaN_6O_{14}$ $[M+Na]^+$ 983.5312 found 983.5319. ANS-4-259.

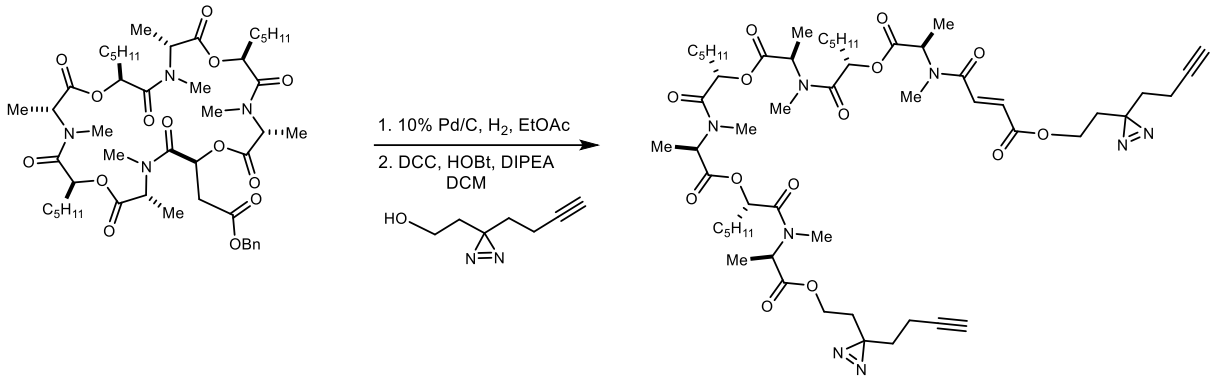

2-(3-(But-3-yn-1-yl)-3H-diazirin-3-yl)ethyl (*E*)-4-(((5*R*,8*S*,11*R*,14*S*,17*R*,20*S*,23*R*)-1-(3-(but-3-yn-1-yl)-3H-diazirin-3-yl)-5,6,11,12,17,18-hexamethyl-4,7,10,13,16,19,22-heptaoxo-8,14,20-tripentyl-3,9,15,21-tetraoxa-6,12,18-triazatetracosan-23-yl)(methyl)amino)-4-oxobut-2-enoate (143). A round-bottom flask was charged with the cyclic peptide (55 mg, 59 mmol) dissolved in ethyl acetate (3.0 mL) and treated with 10% Pd/C (6 mg). The reaction flask was evacuated with light vacuum (50 Torr). Hydrogen (balloon) was added, and the flask was cycled through vacuum once more. The reaction was allowed to stir for 2 h. The crude reaction mixture was filtered through Celite and concentrated to afford the deprotected cyclic depsipeptide. A flame-dried round-bottom flask was charged with the depsipeptide (10 mg, 11.9 μmol), DCC (2.95 mg, 14.3 μmol), HOBt (2.01 g, 14.9 μmol), and DCM (200 μL). The reaction was cooled to 0 °C and allowed to stir for 10 min. The diazirine (3.3 mg, 23.8 μmol) and DIPEA (2.5 μL, 14.3 μmol) were added and the reaction was allowed to stir ambient temperature for 1 hour. The reaction mixture was diluted with DCM, filtered through Celite, and concentrated. Preparative HPLC (5 – 95% aqueous acetonitrile, 210 nm, flow rate: 8 mL/min, R_t = 26.6 m) afforded the ring-opened product (4.4 mg, 34%) as a colorless oil. $[\alpha]_D^{24}$ +38 (*c* 0.65, $CHCl_3$); R_f = 0.42 (60% EtOAc/hexanes); IR (film) 3298, 2930, 2861, 2363, 1739, 1659, 469, 1408, 1299, 1207, 1105 cm^{-1}; ^1H NMR (600 MHz, $CDCl_3$) This compound exists in multiple conformations, causing significant peak broadening and overlap. Several key peaks are resolved and are listed below. Refer to the image of the ^1H NMR spectrum for other peaks: δ 7.45 (d, *J* = 15.3 Hz, 1H), 6.82 (d, *J* = 15.3 Hz, 1H), 4.11 (t, *J* = 6.3 Hz, 2H); ^{13}C NMR (150 MHz, $CDCl_3$) This compound exists in multiple conformations, causing significant peak overlap. Refer to the image of the ^{13}C NMR spectrum; HRMS (EI): Exact mass calcd for $C_{55}H_{88}N_9O_{14}$ $[M+NH_4]^+$ 1098.6445, found 1098.6448. ANS-4-240/259.

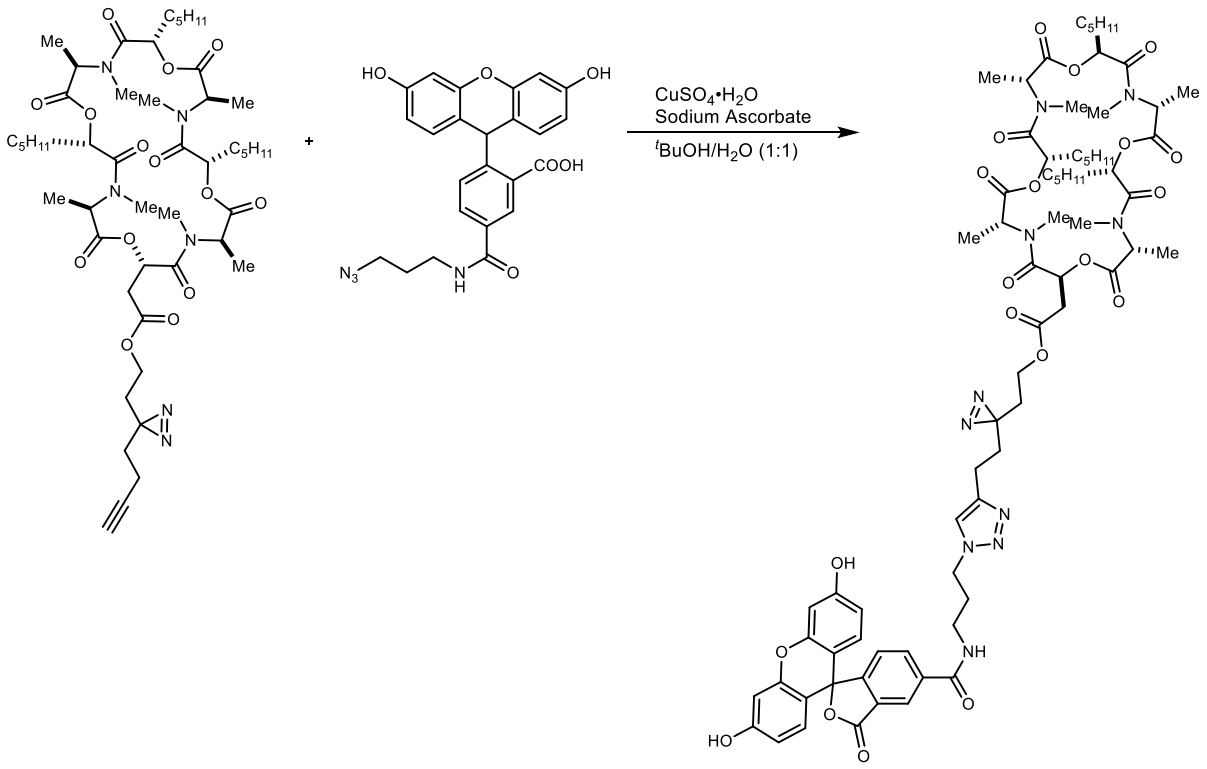

2-(3-(2-(1-(3-(3',6'-Dihydroxy-3-oxo-3H-spiro[isobenzofuran-1,9'-xanthene]-5-carboxamido)propyl)-1H-1,2,3-triazol-4-yl)ethyl)-3H-diazirin-3-yl)ethyl 2-((2*S*,5*R*,8*S*,11*R*,14*S*,17*R*,20*S*,23*R*)-4,5,10,11,16,17,22,23-octamethyl-3,6,9,12,15,18,21,24-octaoxo-8,14,20-tripentyl-1,7,13,19-tetraoxa-4,10,16,22-tetraazacyclotetracosan-2-yl)acetate (145). A microwave vial was charged with the cyclic depsipeptide (8.0 mg, 8.3 μmol), azide (3.9 mg, 8.4 μmol), ^{t}BuOH (250 μL), and H_2O (250 μL). $CuSO_4 \cdot H_2O$ (1 mg, 3 μmol) and sodium ascorbate (1.0 mg, 5.0 μmol) were added, the reaction was sealed with a microwave cap, and then submerged into a 50 °C oil bath. The mixture was allowed to stir at 50 °C for 2.5 h. The crude mixture was then cooled to ambient temperature, poured into H_2O, and extracted with EtOAc (twice). The combined organic layers were washed with 0.1 N aq EDTA·2Na and brine, and then dried and concentrated. The residue was purified by preparative HPLC (30 – 95% aqueous acetonitrile, 210 nm, flow rate: 8 mL/min, R_t = 13.8 m) to afford the tagged 24-membered macrocycle after lyophilization as a bright orange amorphous solid (2.3 mg, 20%). A full characterization was not acquired due to limited material. However, a ^{1}H NMR spectra is provided along with HRMS data; ^{1}H NMR (600 MHz, CH_3OD) This compound exists in multiple conformations, causing significant peak overlap. Refer to the image of the ^{1}H NMR spectrum for

the other peaks: HRMS (ESI): Exact mass calcd for $C_{72}H_{98}N_{10}O_{20}$ $[M+2H]^{2+}$ 710.8435, found 710.8400. ANS-5-50.

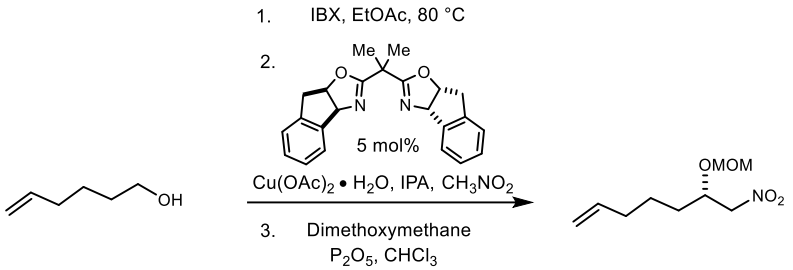

(*S*)-6-(Methoxymethoxy)-7-nitrohept-1-yne (148). A round-bottom flask was charged with the alcohol (2.00 mL, 16.8 mmol), 2-Iodobenzoic acid (5.20 g, 18.7 mmol), and ethyl acetate (120 mL). The reaction was heated to 80 °C and stirred for 3 h. The reaction was then cooled to ambient temperature, filtered, and concentrated. The crude material was carried straight forward into the next reaction. Following the Evans enantioselective Henry procedure,[1] IndaBOX[2] (201 mg, 560 μmol) and $Cu(OAc)_2$•H_2O (101 mg, 509 μmol) were stirred at ambient temperature in isopropanol (20.4 mL) for 1 h. The cerulean blue solution was then cooled to 0 °C and aldehyde (1.0 g, 10.19 mmol) was added and allowed to stir for 10 m before nitromethane (5.50 mL, 102 mmol) addition. After stirring for 4 days at ambient temperature, the reaction was quenched dropwise at 0 °C with 1 M aq HCl and the aqueous layer was extracted with CH_2Cl_2. Following drying and concentration under reduced pressure, the crude alcohol was dissolved in $CHCl_3$ (50.9 mL), treated with P_2O_5 (7.2 g, 51 mmol) and dimethoxymethane (10.6 mL, 102 mmol), and stirred at ambient temperature for 2 h. The reaction mixture was diluted with DCM and decanted from the solid. The organic layer was then washed with satd aq $NaHCO_3$ and brine. The organic layers were dried and concentrated to afford an oil that was subjected to flash column chromatography (SiO_2, 10% ethyl acetate in hexanes) to afford the title compound as a colorless oil (609 mg, 30%, 3 steps). The enantiopurity was determined to be 91% ee by chiral HPLC analysis (Chiralcel OD-H, 10% ^{i}PrOH /hexanes, 0.4 mL/min, t_r(e_1, major) = 14.5 min, t_r(e_2, minor) = 13.2 min). $[\alpha]_D^{24}$ +25 (*c* 0.89, $CHCl_3$); R_f = 0.49 (20% EtOAc/hexanes); IR (film) 2940, 1556, 1384, 1152, 1105, 1032 cm^{-1}; ^{1}H NMR (400 MHz, $CDCl_3$) δ 5.80 (ddt, *J* = 17.0, 10.3, 6.7 Hz, 1H), 5.04-4.94 (m, 2H), 4.65 (d, *J*= 7.2 Hz, 1H), 4.62 (d, *J* = 7.2 Hz, 1H), 4.48 (dd, *J* = 12.4, 8.0 Hz, 1H), 4.40 (dd, *J* = 12.4, 4.0 Hz, 1H), 4.25 (dddd, *J* = 8.0, 6.0, 6.0, 4.0 Hz, 1H), 3.32 (s, 3H), 2.07 (dtt, *J* = 7.1, 7.1, 1.4 Hz, 2H), 1.70 – 1.40 (m, 4H); ^{13}C NMR (100 MHz, $CDCl_3$) ppm 137.9, 115.3, 96.3, 79.1, 74.8, 56.0, 33.5,

31.8, 24.1; HRMS (EI): Exact mass calcd for $C_9H_{17}NO_4$ $[M]^+$ 203.1158, found-not observed due to poor ionization. ANS-3-220.

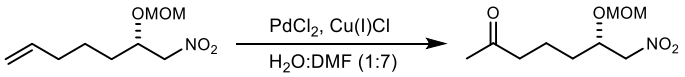

(*S*)-6-(Methoxymethoxy)-7-nitroheptan-2-one (150). To a round-bottom flask was added nitroalkene (250 mg, 1.23 mmol), $PdCl_2$ (21.8 mg, 123 μmol) and CuCl (122 mg, 1.23 mmol) in a H_2O:DMF mixture (10.3 mL, 1:7). The reaction flask was evacuated with house vacuum (50 Torr) three times, followed by addition of an oxygen (balloon). The reaction was allowed to stir for 12 h at ambient temperature. The reaction mixture was poured into 2 M aq HCl and extracted with diethyl ether. The organic layer was then washed with brine, dried, and concentrated to afford an oil that was subjected to flash column chromatography (SiO_2, 35% ethyl acetate in hexanes) to afford the title compound as a colorless oil (249 mg, 92%). $[\alpha]_D^{24}$ +21 (*c* 0.70, $CHCl_3$); R_f = 0.29 (50% EtOAc/hexanes); IR (film) 2947, 2897, 2828, 1711, 1554, 1420, 1366, 1151, 1104, 1031, 918 cm^{-1}; ^1H NMR (600 MHz, $CDCl_3$) δ 4.88 (d, *J* = 11.9 Hz, 1H), 4.74 (d, *J* = 7.0 Hz, 1H), 4.72 (d, *J* = 11.9 Hz, 1H), 4.70 (d, *J* = 7.0 Hz, 1H), 4.30 (dd, *J* = 7.9, 4.8 Hz, 1H), 3.41 (s, 3H), 2.26 (dt, *J* = 6.9, 2.6 Hz, 2H), 2.05-1.92 (m, 2H), 1.96 (t, *J* = 2.5 Hz, 1H), 1.78-1.67 (m, 2H); ^{13}C NMR (150 MHz, $CDCl_3$) ppm 171.1, 96.4, 94.8, 83.6, 74.8, 74.2, 69.1, 56.3, 31.8, 24.2, 18.2; HRMS (EI): Exact mass calcd for $C_{11}H_{16}Cl_3O_4$ $[M+H]^+$ 317.0109, found 317.0109. ANS-3-244.

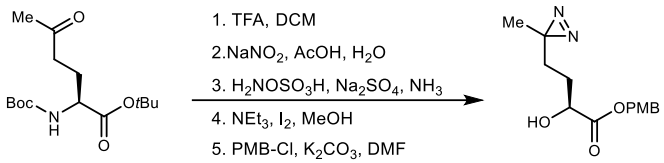

4-Methoxybenzyl (*S*)-2-hydroxy-4-(3-methyl-3H-diazirin-3-yl)butanoate (158). A round-bottom flask was charged with the protected amino acid (524 mg, 1.74 mmol), trifluoroacetic acid (8.6 mL) and DCM (10.8 mL). The reaction mixture was allowed to stir for 2 h, then concentrated and dried under high vacuum overnight. The crude, deprotected material was then dissolved in AcOH (4.1 mL) and deionized. H_2O (16.2 mL) and then cooled to 0 °C. A 2 M aq solution of sodium nitrite was added to the reaction vessel dropwise over 15 min. The reaction mixture was allowed to warm to ambient temperature and stir under argon for 3 h. The crude reaction was concentrated to remove all volatiles, and then placed under high vacuum for 15 h. The material was then solubilized in EtOAc, and the white solid that did not dissolve was filtered off. The organic layer was concentrated to afford the crude α-hydroxy acid. The crude product was then

transferred to a 3-neck round-bottom flask, and Na_2SO_4 (large scoop (~100 mg)) was added. The reaction was cooled to -78°C and ammonia (50 mL) was condensed into the flask. The dry ice/acetone bath was removed, and the reaction was allowed to reflux for 6 h. The reaction was then cooled to -78°C and hydroxylamine *O*-sulfonic acid (109 mg, 961 µL) dissolved in MeOH (2 mL) was added to the reaction in four portions over 30 minutes. The dry ice/acetone bath was removed and the reaction was again allowed to reflux for 2 h. The 3-neck round bottom flask was then opened to atmosphere to allow the ammonia to evaporate overnight. The resulting slurry was solubilized in MeOH and the precipitated white solid was filtered off. The MeOH layer was concentrated to afford a yellow oil. MeOH (30 mL) was added to the crude oil, followed by NEt_3 (112 µL, 801 µmol) and the reaction was allowed to stir for 10 min. I_2 was then added to the light-yellow reaction mixture in small scoops until a deep red color persists (12 small crystals). The reaction was allowed to stir for 2 h at ambient temperature, and then concentrated to afford the crude diazirine to which K_2CO_3 (722 mg, 5.22 mmol) and DMF (18 mL) were added. The reaction was stirred for 10 min, then PMB-Cl (258 µL, 1.91 mmol) was added and the reaction was stirred for 48 h at ambient temperature. The reaction mixture was quenched with 1 M aq HCl and extracted with EtOAc. The combined organic layers were washed with water and brine, and then dried and concentrated. The crude residue was subjected to flash column chromatography (SiO_2, 15% ethyl acetate in hexanes) to afford the product as a colorless oil (66 mg, 15% (5 steps)). $[\alpha]_D^{23}$ -9.8 (*c* 0.76, $CHCl_3$); R_f = 0.17 (20% EtOAc/hexanes); IR (film) 3446, 2917, 2849, 1731, 1611, 1513, 1456, 1301, 1246, 1174, 1032, 817 cm^{-1}; ^1H NMR (600 MHz, $CDCl_3$) δ 7.29 (d, *J* = 8.7 Hz, 2H), 6.90 (d, *J* = 8.7 Hz, 2H), 5.16 (d, *J* = 11.8 Hz, 1H), 5.12 (d, *J* = 11.8 Hz, 1H), 4.15 (ddd, *J* = 7.3, 5.1, 4.0 Hz, 1H), 3.82 (s, 3H), 2.73 (d, *J* = 5.2 Hz, 1H), 1.73-1.64 (m, 1H), 1.54-1.32 (m, 3H), 0.97 (s, 3H); ^{13}C NMR (150 MHz, $CDCl_3$) ppm 174.8, 160.1, 130.5, 127.2, 114.2, 69.6, 67.6, 55.5, 29.8, 28.7, 25.5, 19.8; HRMS (EI): Exact mass calcd for $C_{14}H_{18}N_2NaO_4$ $[M+Na]^+$ 301.1159, found 301.1159. ANS-6-117.

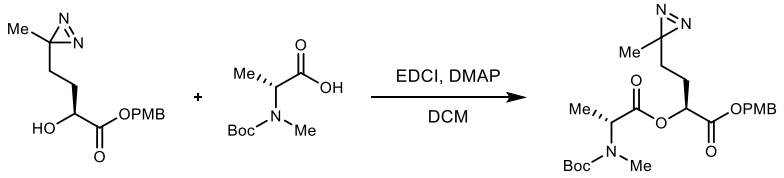

4-Methoxybenzyl (*S*)-2-((*N*-(*tert*-butoxycarbonyl)-*N*-methyl-D-alanyl)oxy)-4-(3-methyl-3H-diazirin-3-yl)butanoate (159). A round-bottom flask was charged with the amine (19.3 mg, 95.0

μmol), alcohol (23 mg, 83 μmol), and DCM (8.0 mL). The mixture was cooled to 0 °C and then EDCI (19.0 mg, 99.1 μmol) and DMAP (1 mg, 8 μmol) were added. The reaction was stirred at 0 °C for 30 min, then allowed to warm to ambient temperature and stir for an additional 1.5 h. The reaction mixture was poured into water and extracted with DCM. The combined organic layers were washed with satd aq $NaHCO_3$ and brine, and then dried and concentrated. The crude residue was subjected to flash column chromatography (SiO_2, 10% ethyl acetate in hexanes) to afford the product as a yellow oil (29.3 mg, 77%). $[\alpha]_D^{23}$ +11 (*c* 0.72, $CHCl_3$); R_f = 0.19 (10% EtOAc/hexanes); IR (film) 2918, 2849, 1743, 1693, 1515, 1455, 1388, 1366, 1316, 1248, 1173, 1149, 1087, 1033 cm^{-1}; ^1H NMR (600 MHz, $CDCl_3$) Several peaks show a clear doubling for the *cis* and *trans* amide products. Other peaks are overlapping and appear only once. Those that are doubled have both values listed. δ 7.26 (d, *J* = 8.6 Hz, 2H), 6.89 (d, *J* = 8.6 Hz, 2H), 5.15/5.13 (d, *J* = 11.8 Hz, 1H), 5.07/5.04 (d, *J* = 12.2 Hz, 1H), 5.02-4.95 (m, 1H), 4.99/4.70 (q, *J* = 6.3 Hz, 1H), 3.81/3.80 (s, 3H), 2.80/2.75 (s, 3H), 1.79-1.64 (m, 2H), 1.47/1.44 (s, 9H), 1.41-1.31 (m, 5H), 0.97/0.96 (s, 3H); ^{13}C NMR (150 MHz, $CDCl_3$) The line listing for both *cis* and *trans* amide isomers is given, as a clear doubling of many peaks is evident. Whenever the isomer peaks overlap, it is stated that the particular peak is representing 2 or more carbons. ppm 172.0, 171.9, 169.4, 169.2, 160.0(2C), 156.1, 155.4, 130.44(4C), 127.3(2C), 114.2(4C), 80.5, 80.2, 71.8(2C), 67.3(2C), 55.4(2C), 54.5, 53.2, 30.3, 30.1, 30.0, 29.8, 28.5(6C), 25.8(2C), 25.1(2C), 19.7(2C), 15.3, 14.7; HRMS (EI): Exact mass calcd for $C_{23}H_{33}N_3NaO_7$ $[M+Na]^+$ 486.2211, found 486.2212. ANS-6-88.

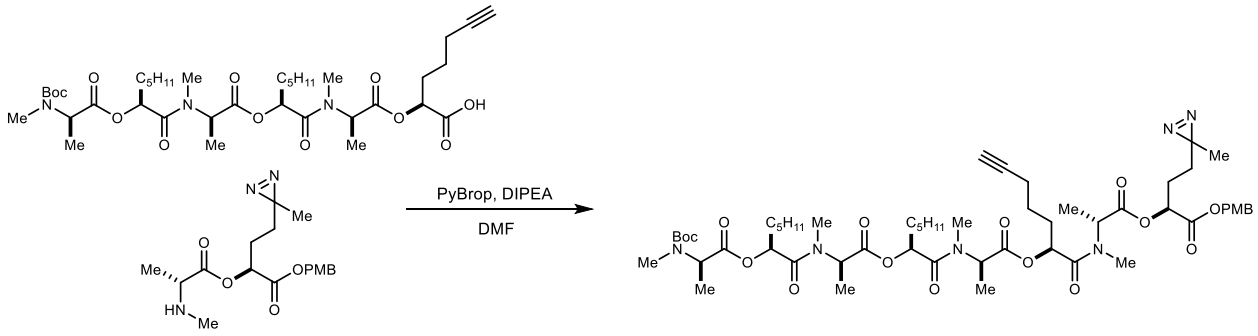

4-Methoxybenzyl (*S*)-2-(((6*R*,9*S*,12*R*,15*S*,18*R*,21*S*,24*R*)-2,2,5,6,11,12,17,18,23,24-decamethyl-4,7,10,13,16,19,22-heptaoxo-21-(pent-4-yn-1-yl)-9,15-dipentyl-3,8,14,20-tetraoxa-5,11,17,23-tetraazapentacosan-25-oyl)oxy)-4-(3-methyl-3H-diazirin-3-yl)butanoate (160). A round-bottom flask was charged with the amine (22.7 mg, 62.6 μmol), acid (42.2 mg, 56.0 μmol), and DCM (1 mL). The mixture was cooled to 0 °C and then DIPEA (29.0 μL, 168

μmol) and PyBrop (39.2 mg, 84.0 μmol) were added. The reaction was stirred at 0 °C for 30 min, then allowed to warm to ambient temperature and stir for an additional 1.5 h. The reaction mixture was poured into cold 10% aq citric acid and extracted with DCM. The combined organic layers were washed with satd aq $NaHCO_3$ and brine, and then dried and concentrated. The crude residue was subjected to reverse-phase flash column chromatography (C_{18} 30 g column, 10-100% MeCN in H_2O over 12 min; 0.1 % TFA buffer, 210 nm, flow rate = 35 mL/min, RT: 6.8-8.5 min) to afford the product as a colorless oil (12.6 mg, 20%). $[\alpha]_D^{23}$ +41 (c 0.63, $CHCl_3$); R_f = 0.16 (40% EtOAc/hexanes); IR (film) 2931, 2859, 1742, 1661, 1515, 1455, 1386, 1317, 1248, 1212, 1174, 1082 cm^{-1}; ^1H NMR (600 MHz, $CDCl_3$) This compound exists as a mixture of rotamers causing peak broadening and overlap. Refer to the image of the ^1H NMR spectrum.^{13}C NMR (150 MHz, $CDCl_3$) This compound is a mixture of rotamers causing peak doubling, broadening, and overlap. Refer to the image of the ^{13}C NMR spectrum; HRMS (EI): Exact mass calcd for $C_{56}H_{86}N_6NaO_{16}$ $[M+Na]^+$ 1121.5993, found 1121.5986. ANS-6-97.

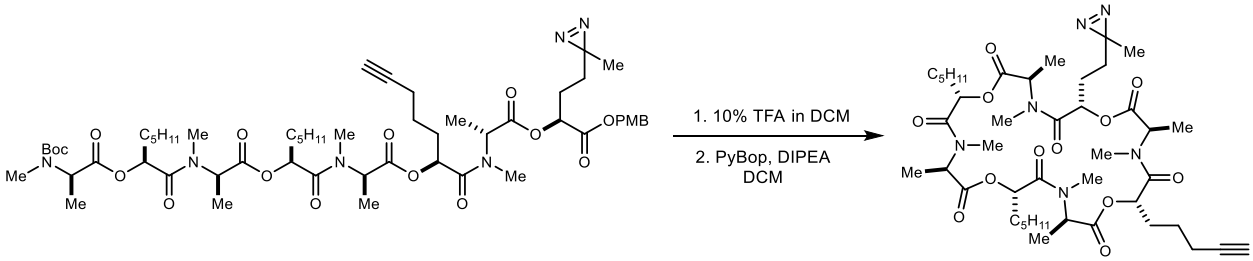

(3*R*,6*S*,9*R*,12*S*,15*R*,18*S*,21*R*,24*S*)-3,4,9,10,15,16,21,22-Octamethyl-6-(2-(3-methyl-3H-diazirin-3-yl)ethyl)-12-(pent-4-yn-1-yl)-18,24-dipentyl-1,7,13,19-tetraoxa-4,10,16,22-tetraazacyclotetracosan-2,5,8,11,14,17,20,23-octaone (161). A round-bottom flask was charged with the depsipeptide (12.6 mg, 11.5 μmol), and dissolved in a mixture of 10% TFA in DCM (0.14 mL TFA, 1.4 mL DCM). The reaction was allowed to stir at ambient temperature for 45 min. The crude reaction mixture was concentrated in vacuo. The unpurified material was added to a flame-dried round bottom flask, DCM (2.3 mL) was added, and the reaction was cooled to 0 °C. DIPEA (5.0 μL, 25 μmol) and PyBrop (6.6 mg, 13 μmol) were then added. The reaction was stirred at 0 °C for 30 min, then allowed to warm to ambient temperature and stir for an additional 1.5 h. The reaction mixture was poured into cold 10% aq citric acid and extracted with DCM. The combined organic layers were washed with satd aq $NaHCO_3$ and brine, and then dried and concentrated. Preparative HPLC (5 – 95% aqueous acetonitrile, 210 nm, flow rate: 8 mL/min, R_t = 19.9 m) afforded the 24-membered macrocycle (1.5 mg, 15%) as a colorless oil. A full characterization

was not acquired due to limited material. However, a ^{1}H NMR spectra is provided; ^{1}H NMR (400 MHz, $CDCl_3$) This compound exists in multiple conformations, causing significant peak overlap. Refer to the image of the ^{1}H NMR spectrum for the other peaks; ANS-6-111.

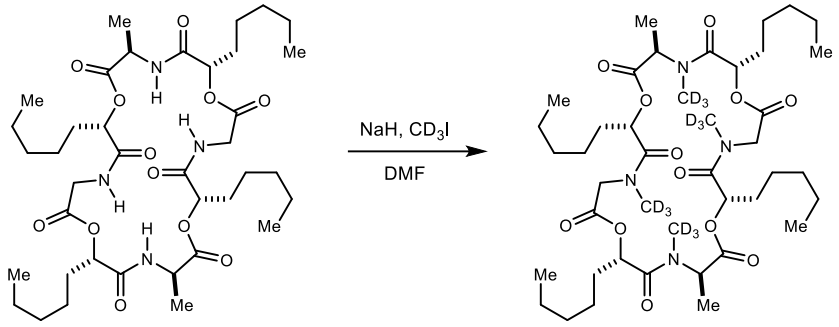

(3*R*,6*S*,12*S*,15*R*,18*S*,24*S*)-3,15-Dimethyl-4,10,16,22-tetrakis(methyl-d3)-6,12,18,24-tetrapentyl-1,7,13,19-tetraoxa-4,10,16,22-tetraazacyclotetracosan-2,5,8,11,14,17,20,23-octaone (162). A flame-dried round-bottom flask was charged with N-H depsipeptide (21.6 mg, 28.1 μmol) and dry DMF (561 μL) at 0 °C. Methyl iodide (68.2 μL, 1.12 mmol) was then added to the reaction mixture, and NaH (6.7 mg, 280 μmol in DMF (281 μL)) was added slowly to the reaction mixture in 3 aliquots over 15 minutes. The mixture was allowed to stir at 0 °C for 25 m, and it was then quenched by the dropwise addition of satd aq NH_4Cl. The aqueous layer was extracted with EtOAc, and the combined organic layers were washed with satd aq $NaHCO_3$, satd aq $Na_2S_2O_3$, water, and brine. The organic layer was then dried and concentrated to afford a colorless oil. Preparative HPLC (55 – 95% aqueous acetonitrile, 210 nm, flow rate: 8 mL/min, R_t = 23.5 m) afforded the 24-membered macrocycle (9.6 mg, 40%). $[\alpha]_D^{23}$ +28 (*c* 0.60, $CHCl_3$); R_f = 0.26 (10% MeOH/DCM); IR (film) 2955, 2930, 2859, 1742, 1661, 1424, 1378, 1193, 1100 cm^{-1}; ^{1}H NMR (600 MHz, $CDCl_3$) This compound exists in multiple conformations, causing significant peak overlap. Refer to the image of the ^{1}H NMR spectrum; ^{13}C NMR (150 MHz, $CDCl_3$) This compound exists in multiple conformations, causing significant peak overlap. Refer to the image of the ^{13}C NMR spectrum; HRMS (EI): Exact mass calcd for $C_{44}H_{64}D_{12}N_4NaO_{12}$ $[M+Na]^+$ 887.6105, found 887.6104. ANS-5-23.

3.6 Experimental Spectra

Figure S1. ^{1}H NMR (600 MHz, $CDCl_3$) of **16**

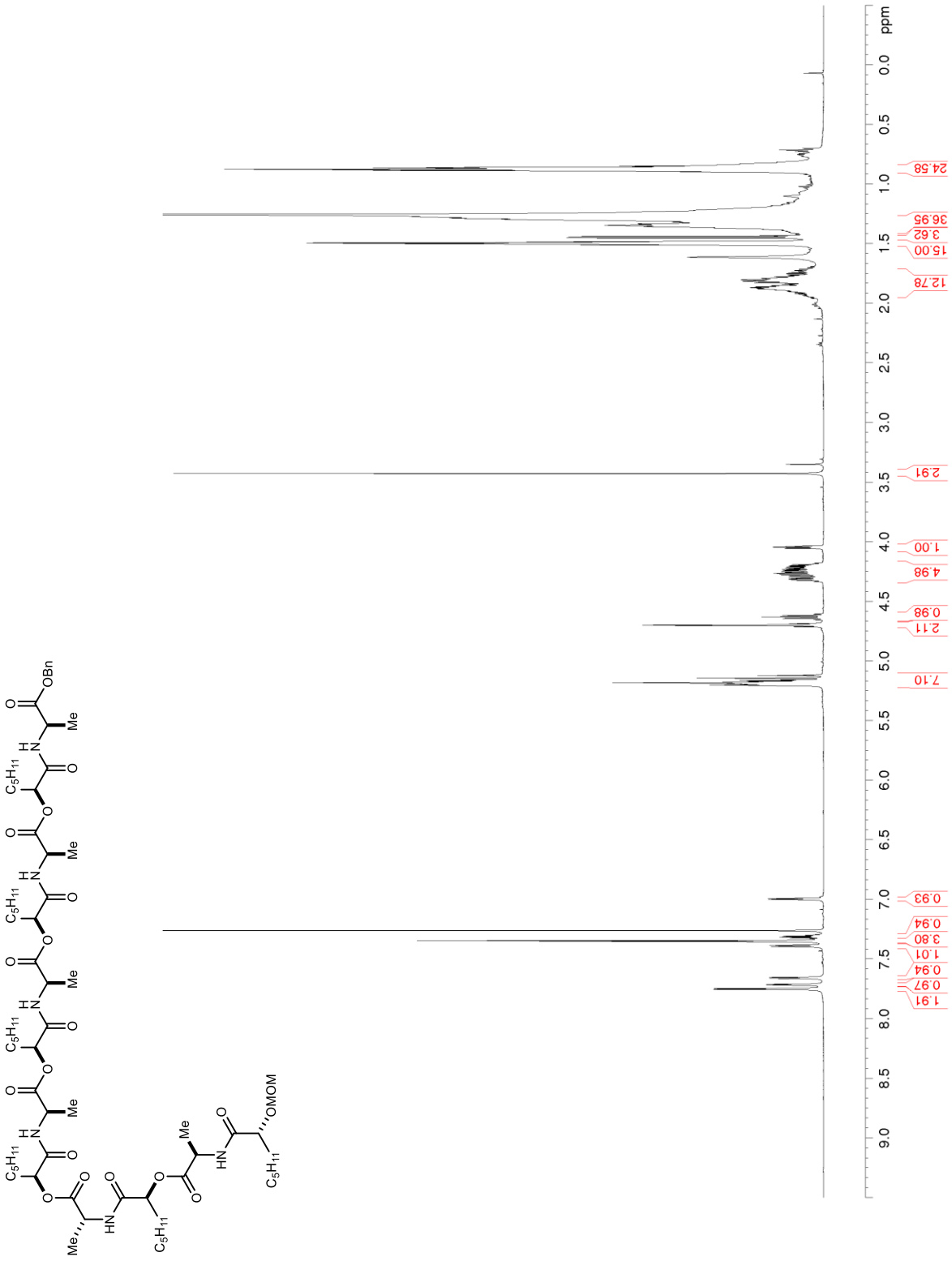

Figure S2. ^{13}C NMR/DEPT (150 MHz, $CDCl_3$) of **16**

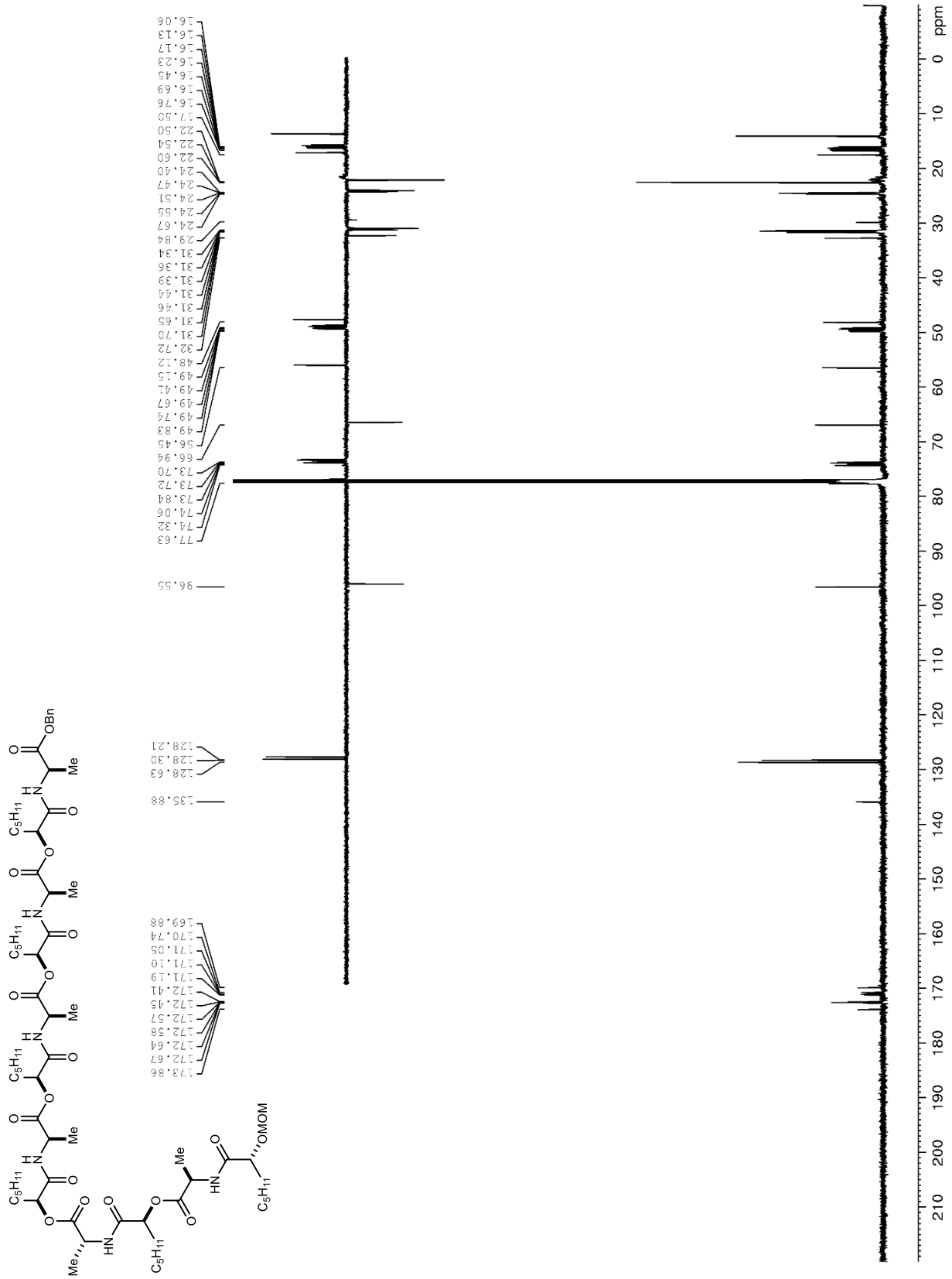

Figure S3. ^{1}H NMR (600 MHz, $CDCl_3$) of **S1**

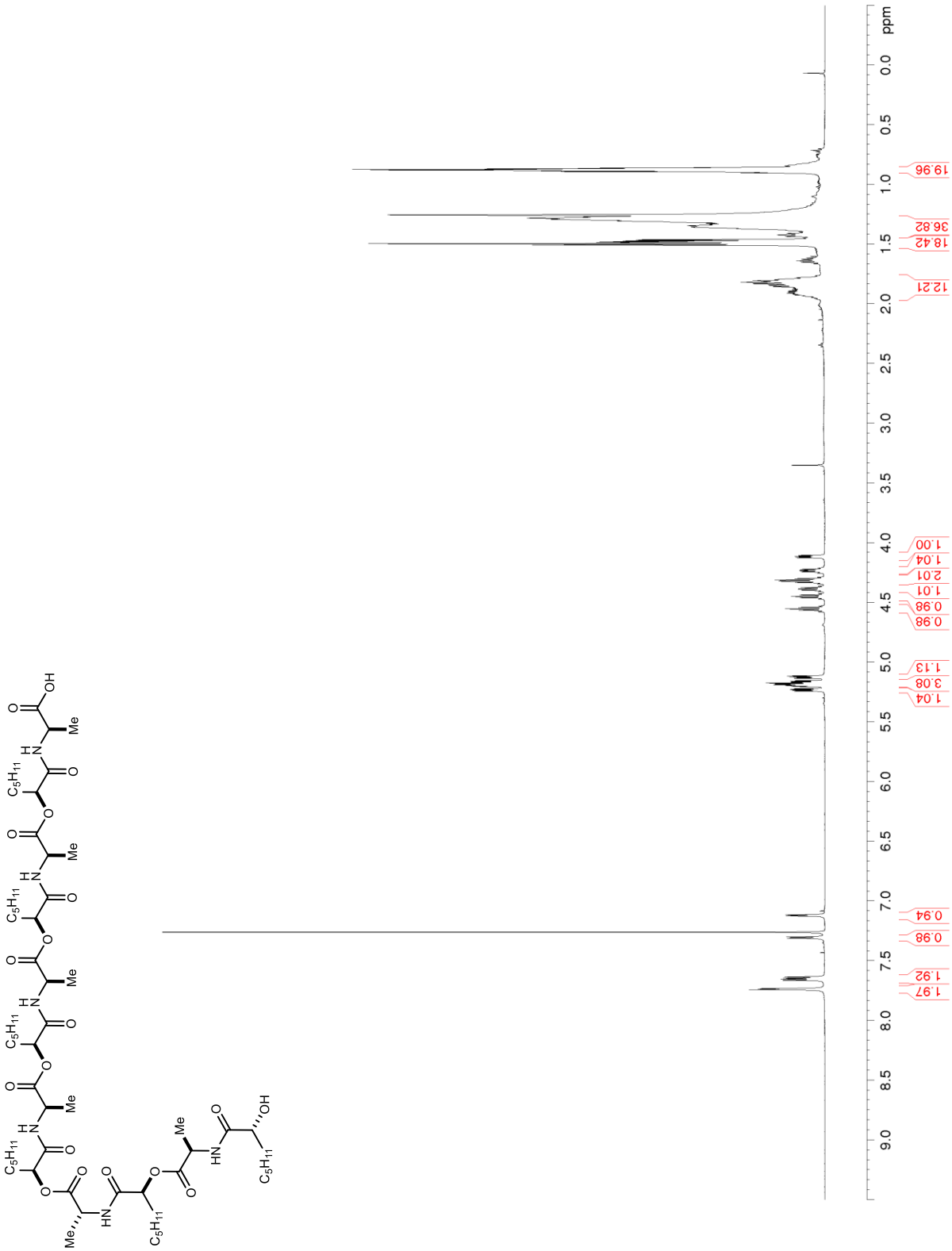

Figure S4. ^{13}C NMR/DEPT (150 MHz, $CDCl_3$) of **S1**

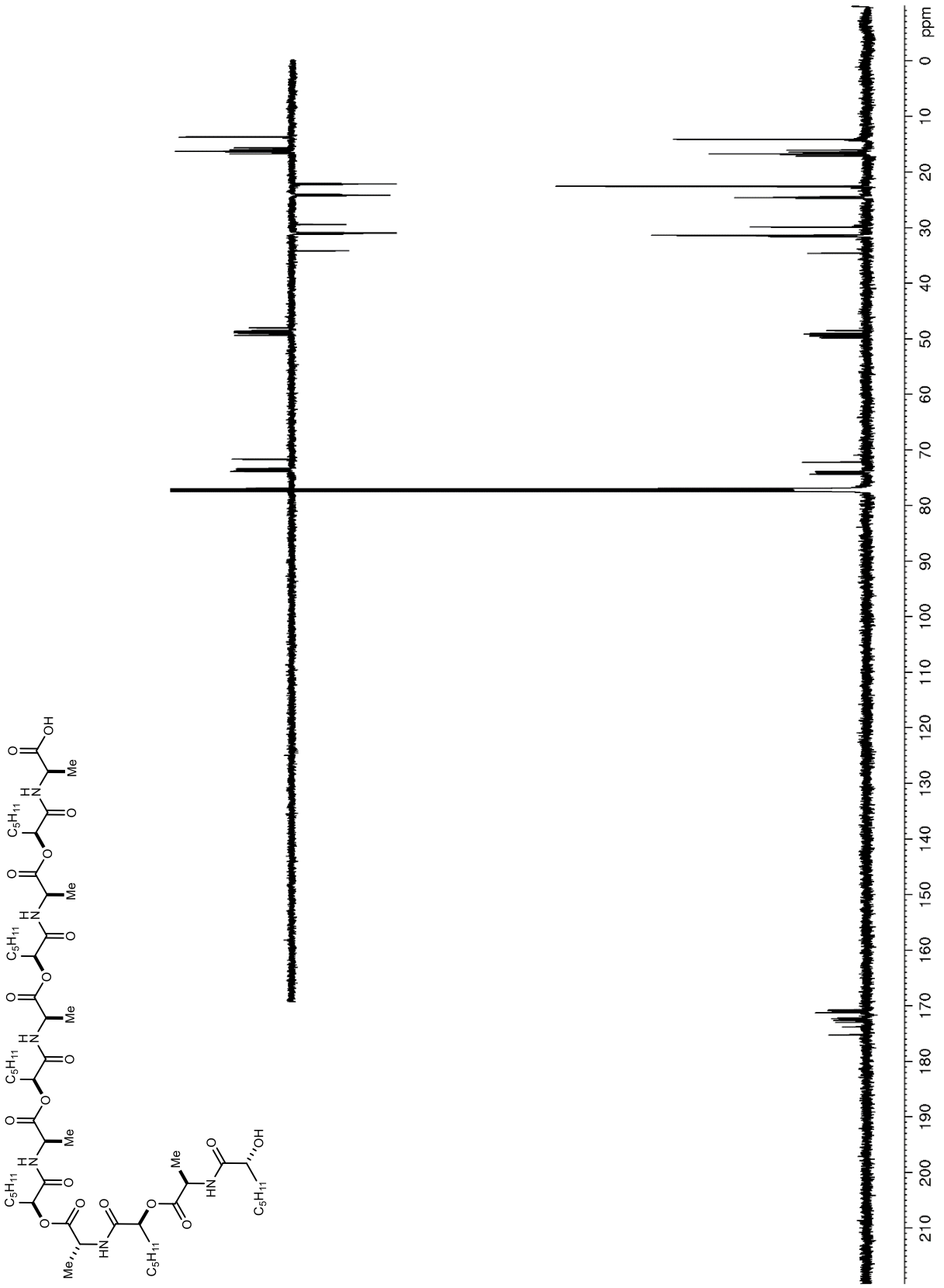

Figure S5. ^{1}H NMR (400 MHz, $CDCl_3$) of **17**

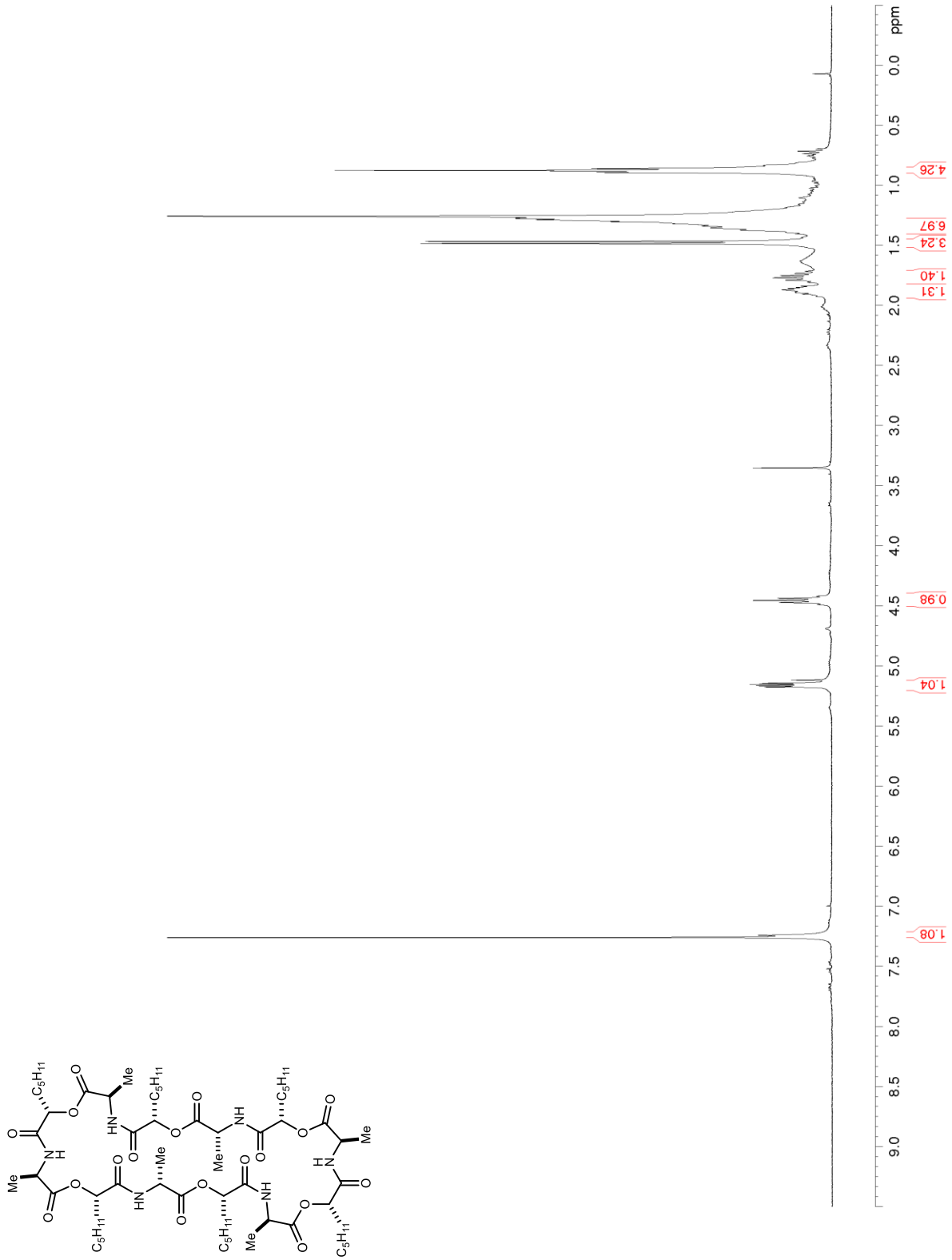

Figure S6. ^{13}C NMR/DEPT (150 MHz, $CDCl_3$) of **17**

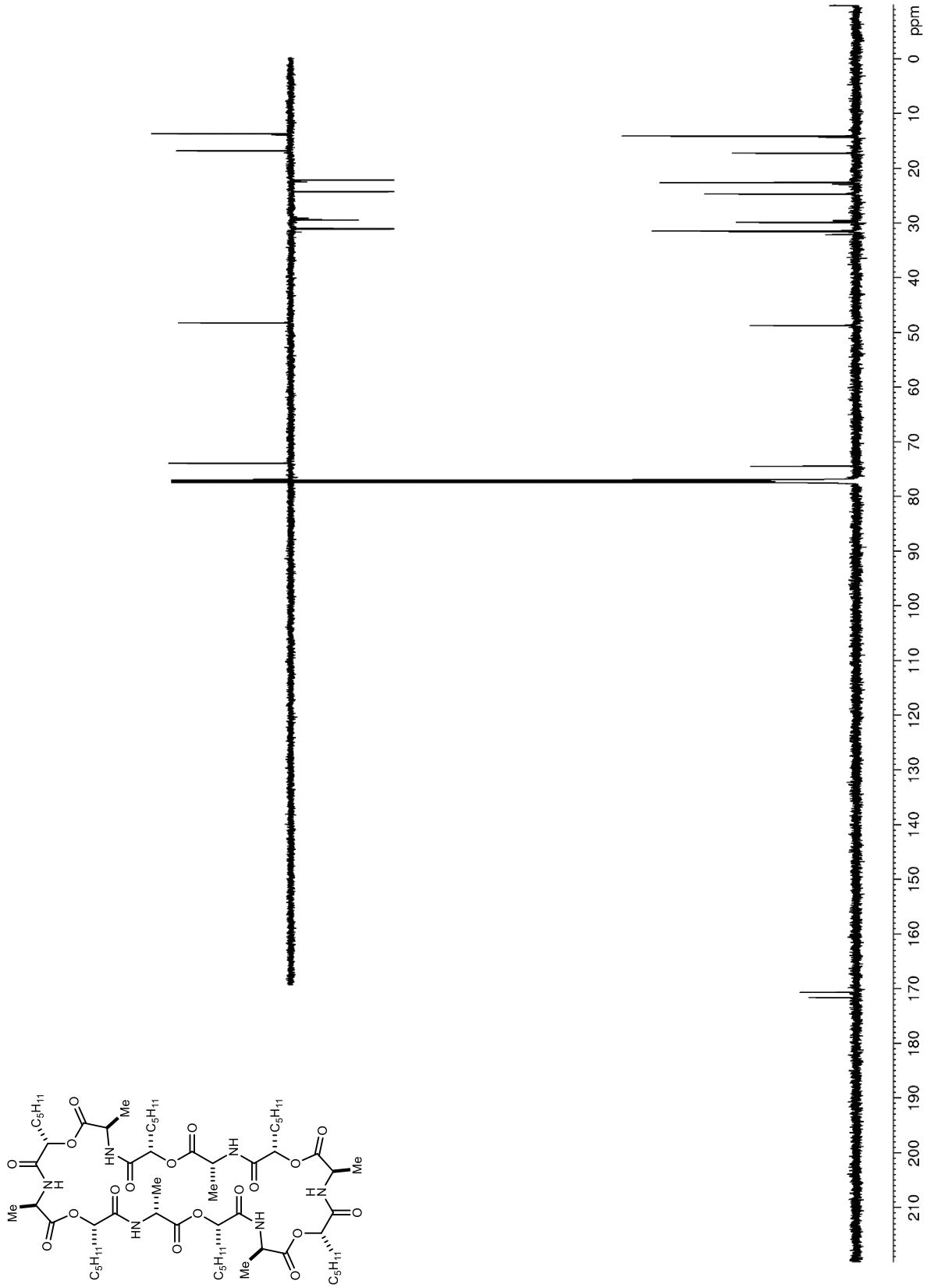

Figure S7. ^{1}H NMR (600 MHz, $CDCl_3$) of **18**

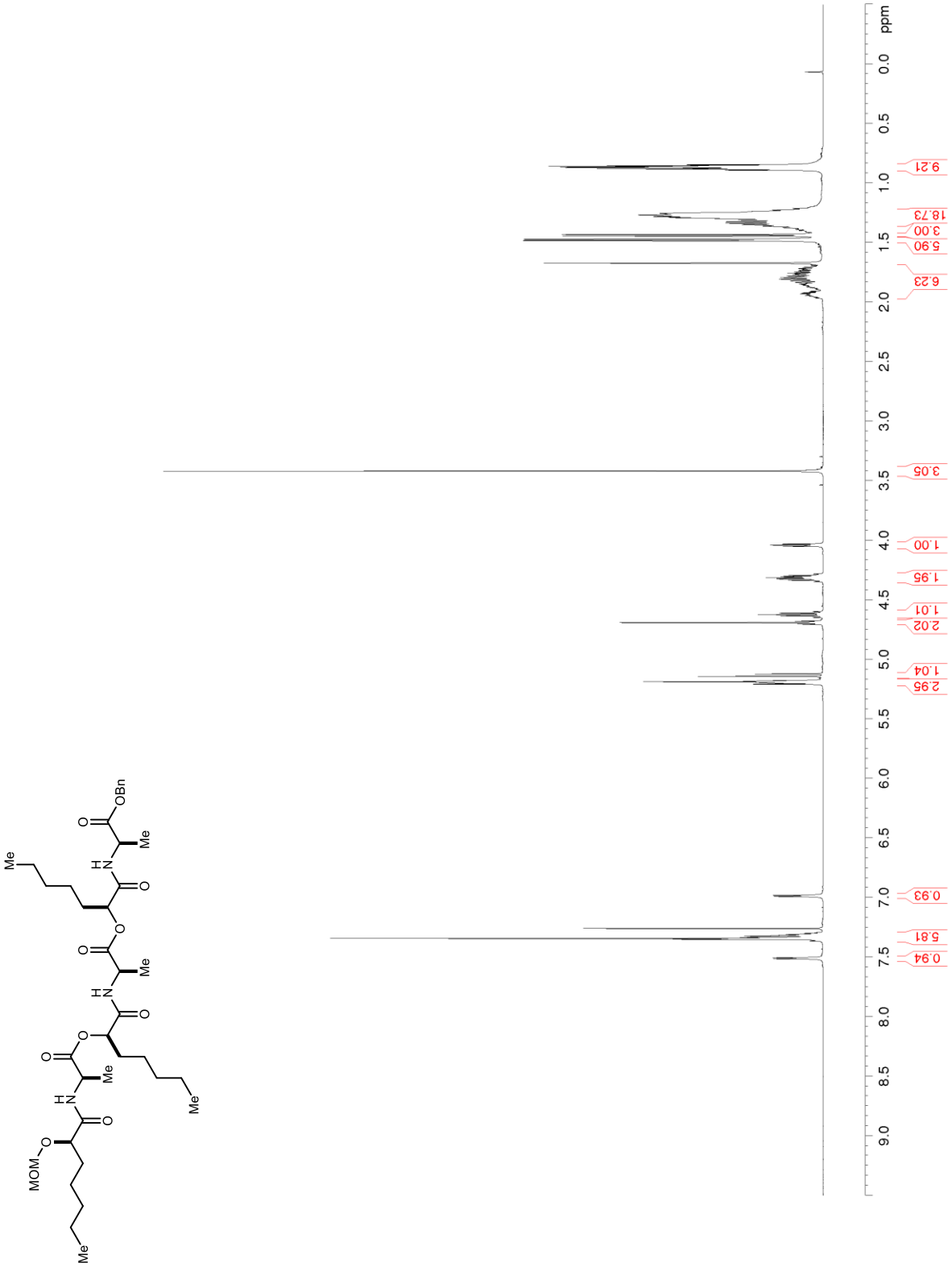

Figure S8. ^{13}C NMR/DEPT (150 MHz, $CDCl_3$) of **18**

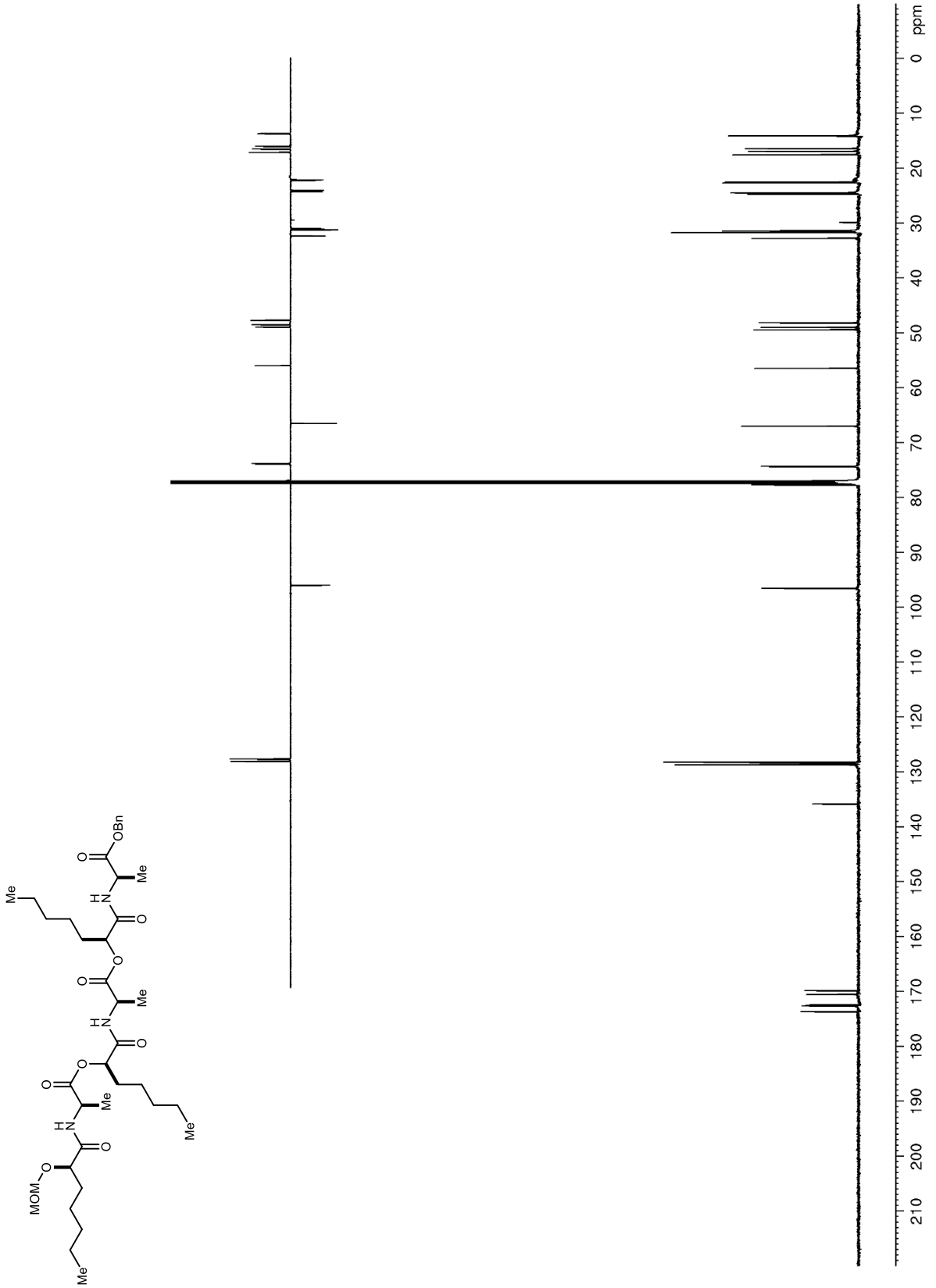

Figure S9. ^{1}H NMR (600 MHz, $CDCl_3$) of **19**

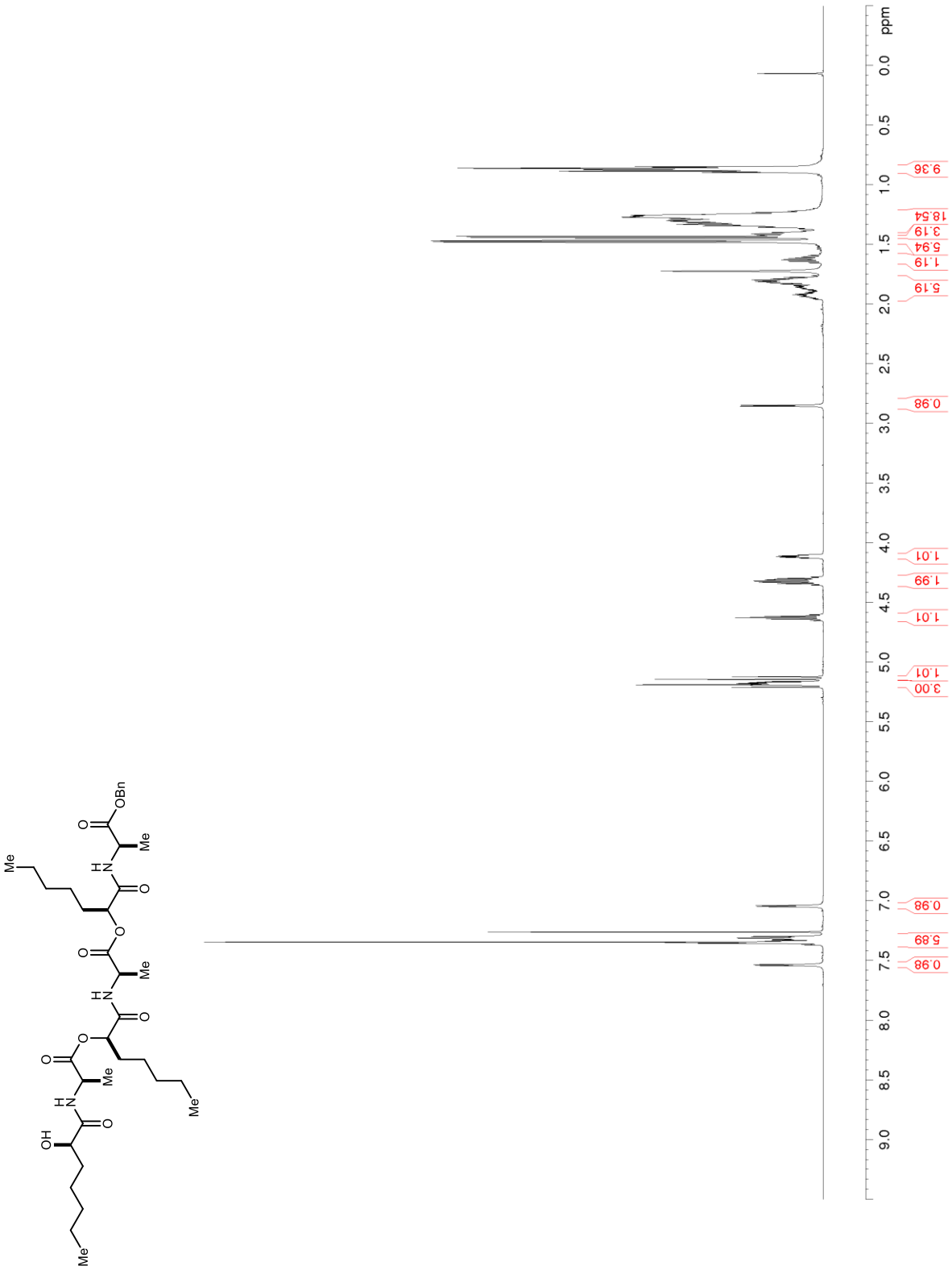

Figure S10. ^{13}C NMR/DEPT (150 MHz, $CDCl_3$) of **19**

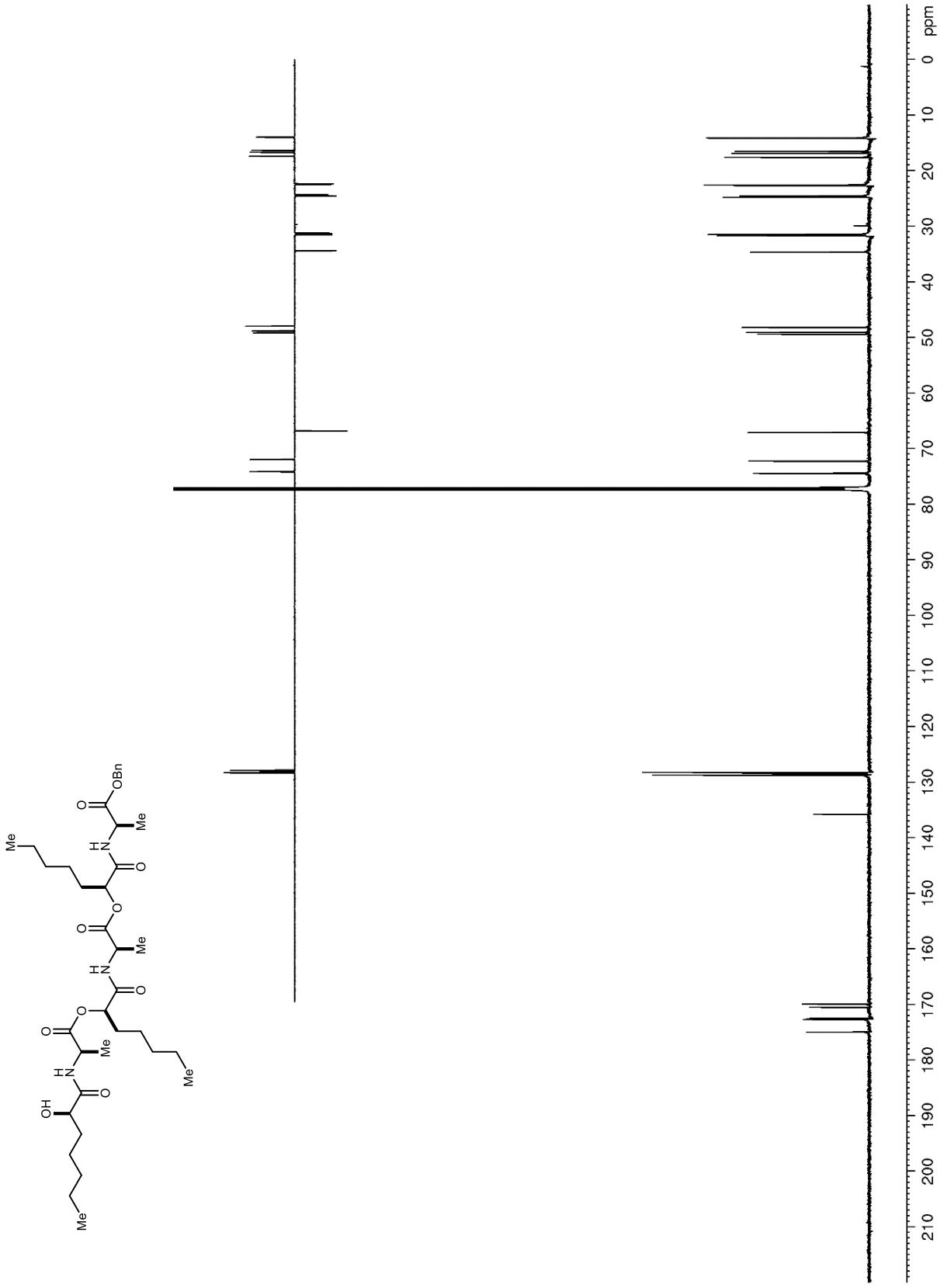

Figure S11. ^{1}H NMR (400 MHz, $(CD_3)_2SO$) of **20**

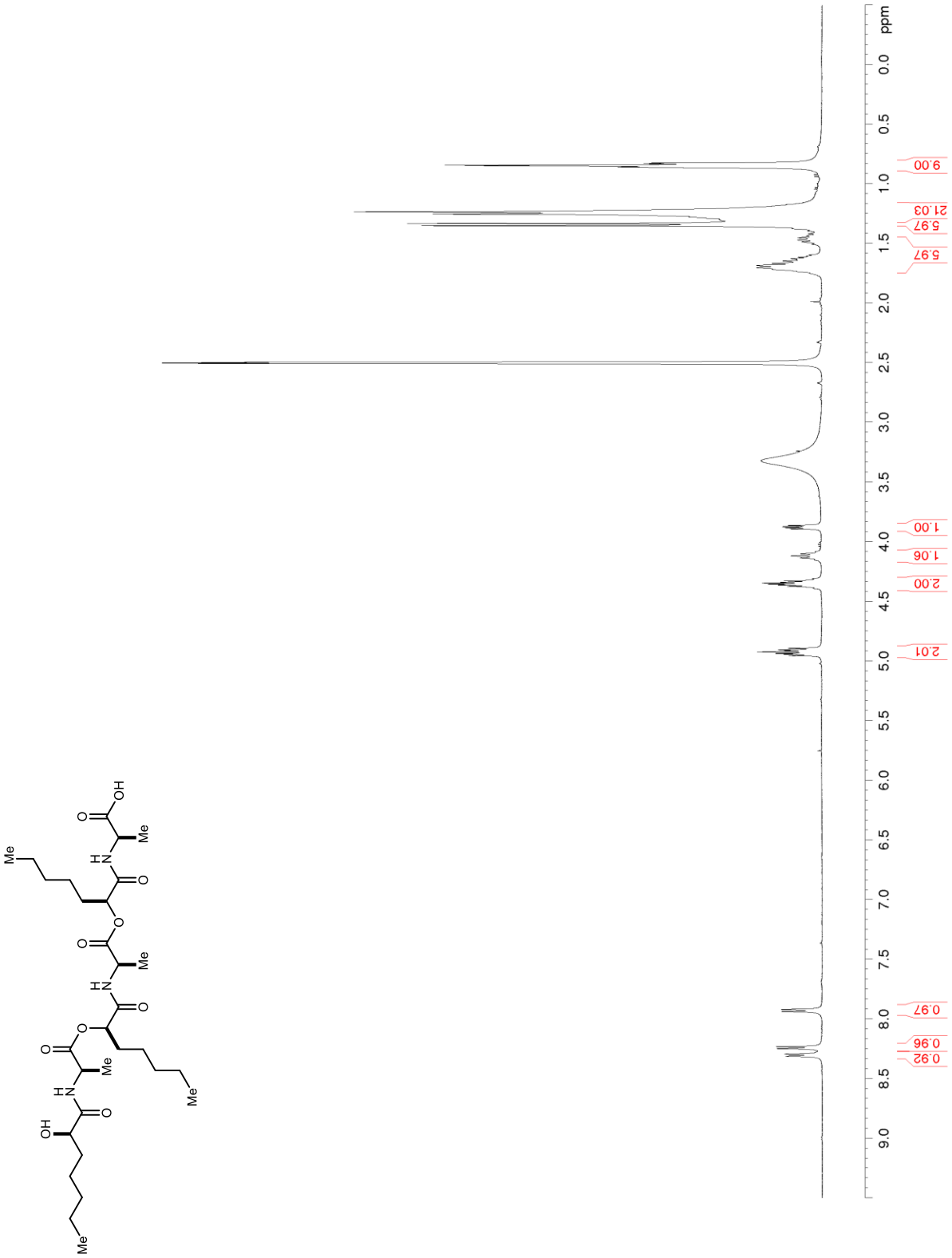

Figure S12. ^{13}C NMR/DEPT (150 MHz, $(CD_3)_2SO$) of **20**

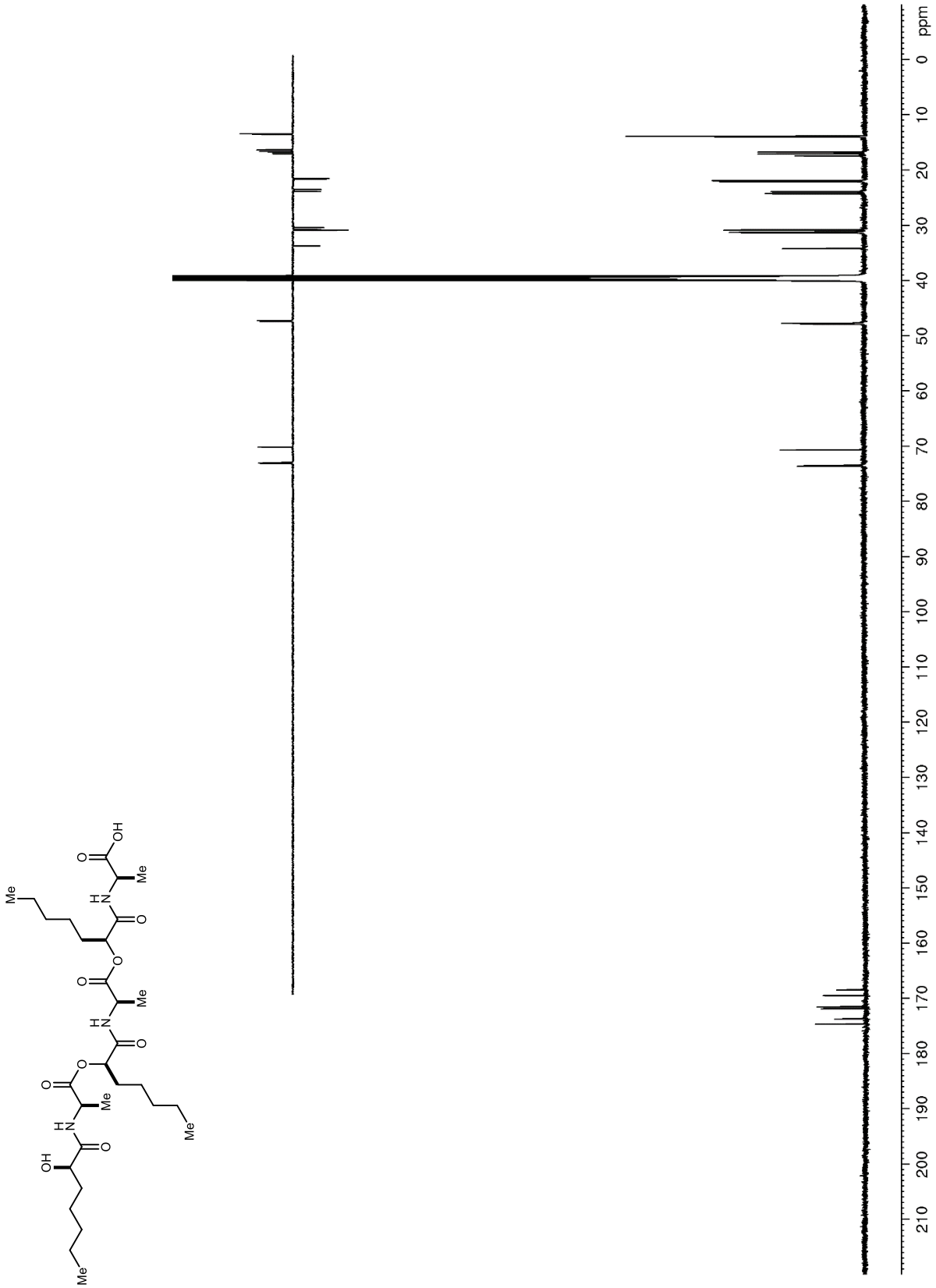

Figure S13. ^{1}H NMR (400 MHz, $CDCl_3$) of **8**

Figure S14. ^{13}C NMR/DEPT (150 MHz, $CDCl_3$) of **8**

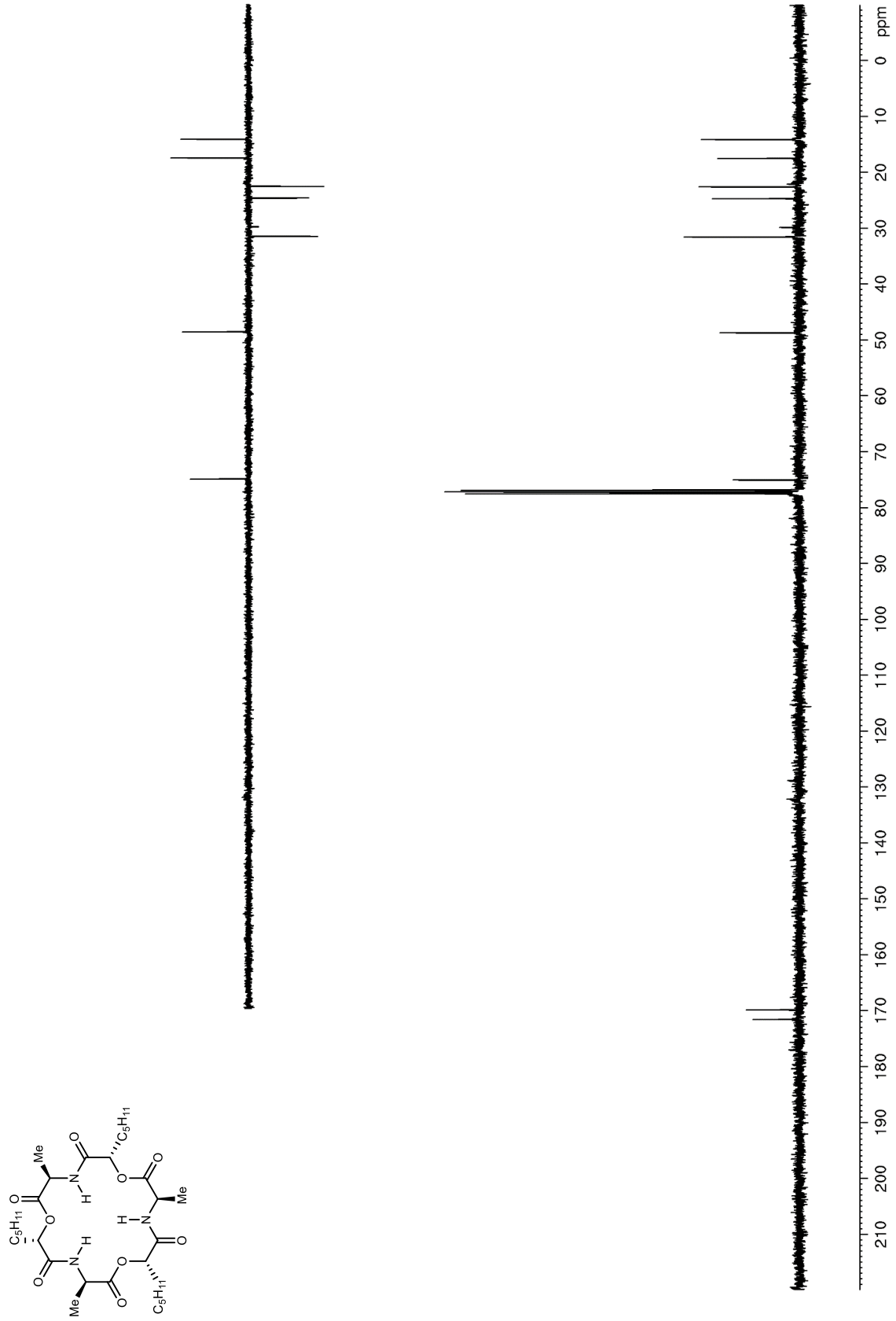

Figure S15. HRMS of **8**

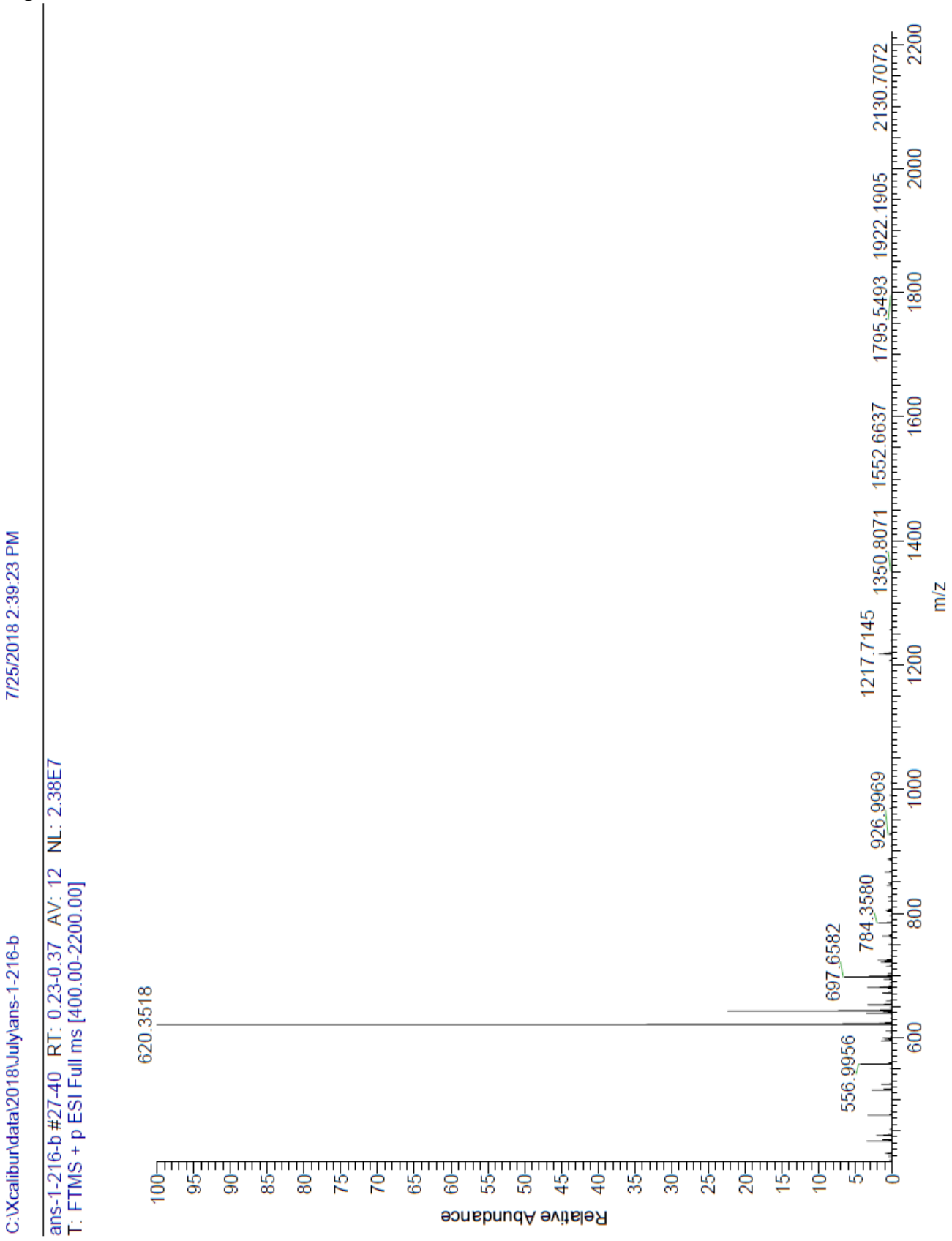

Figure S16. ^{1}H NMR (600 MHz, $CDCl_3$) of **S2**

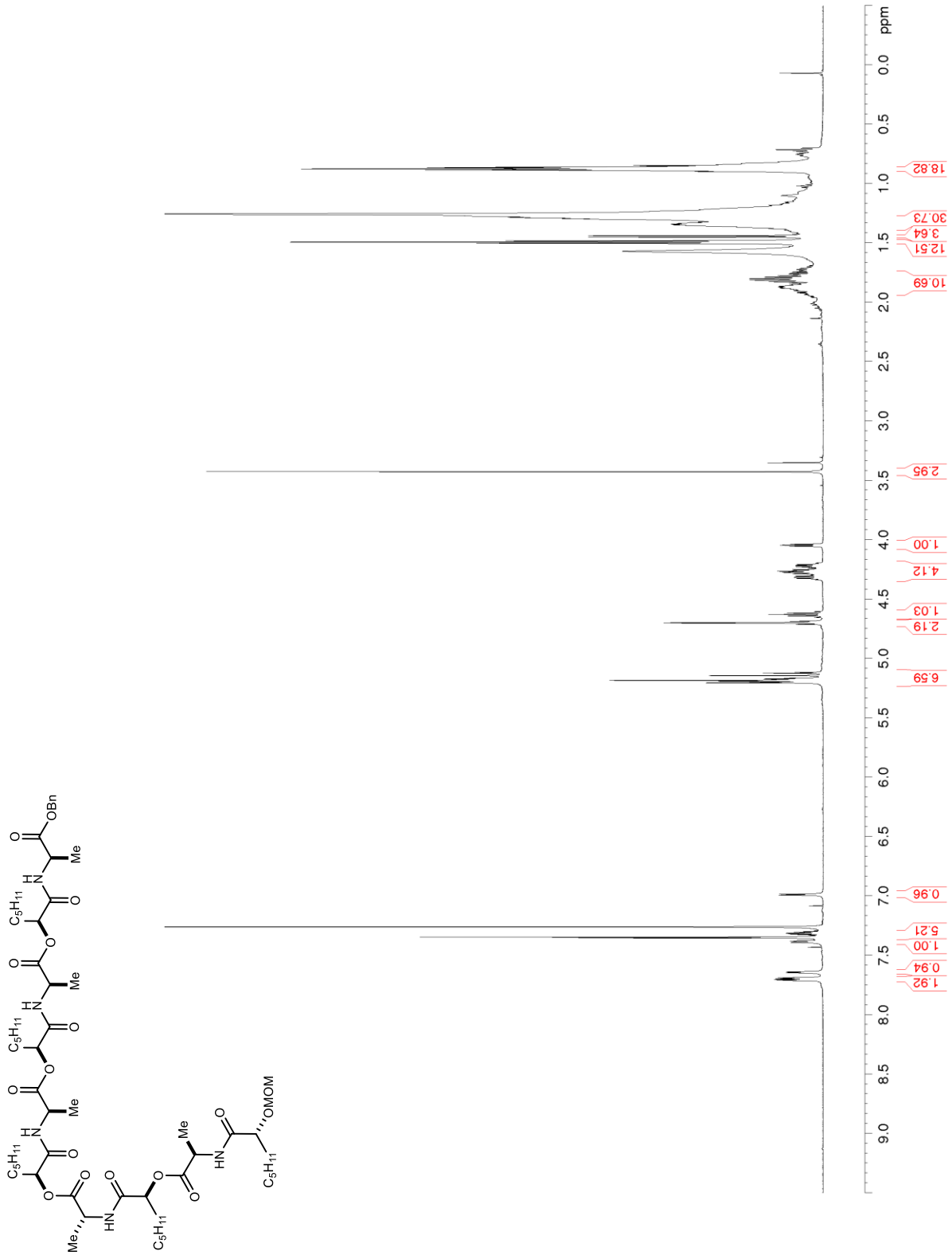

Figure S17. ^{13}C NMR/DEPT (150 MHz, $CDCl_3$) of **S2**

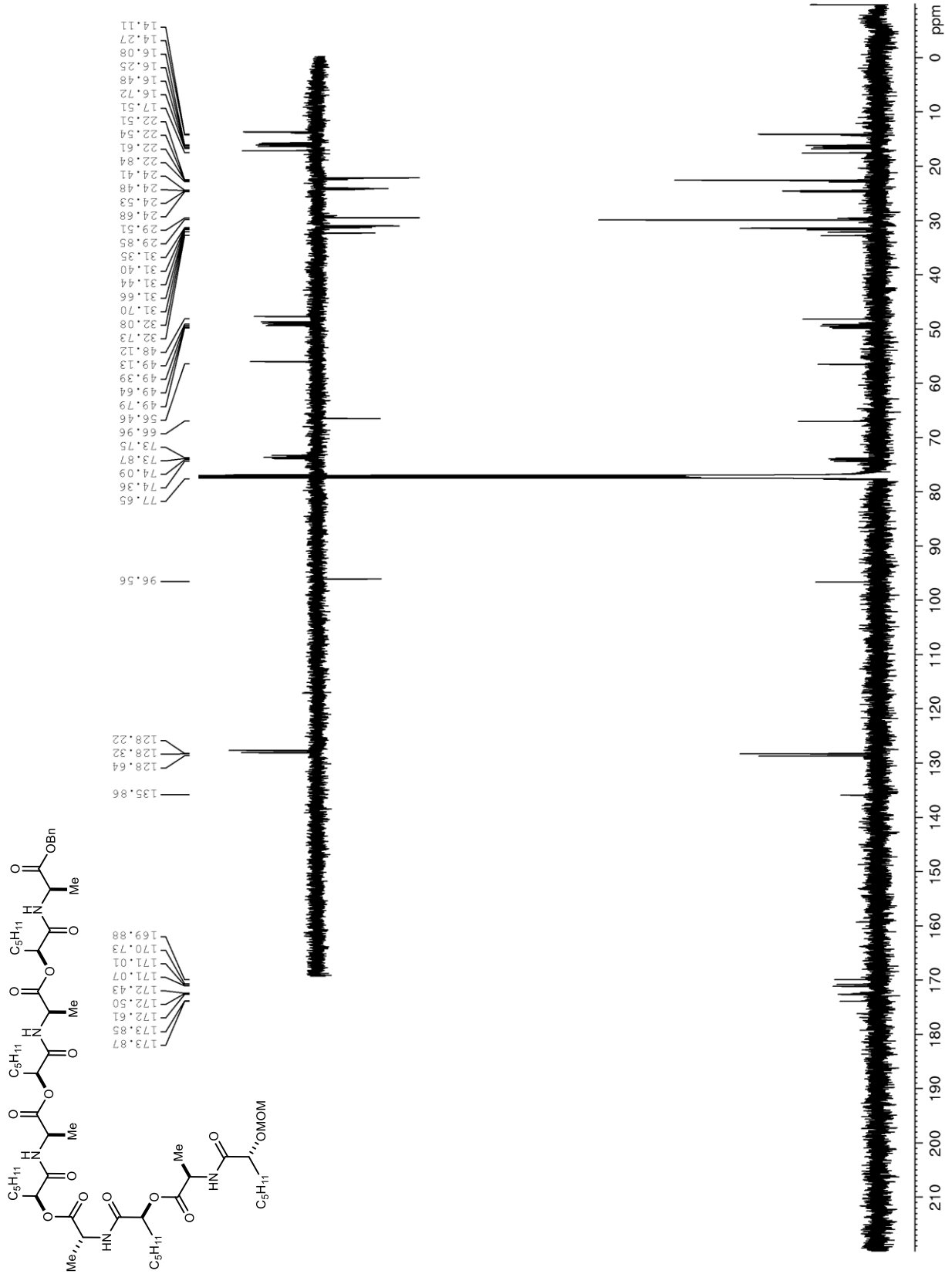

Figure S18. ^{1}H NMR (600 MHz, $CDCl_3$) of **S3**

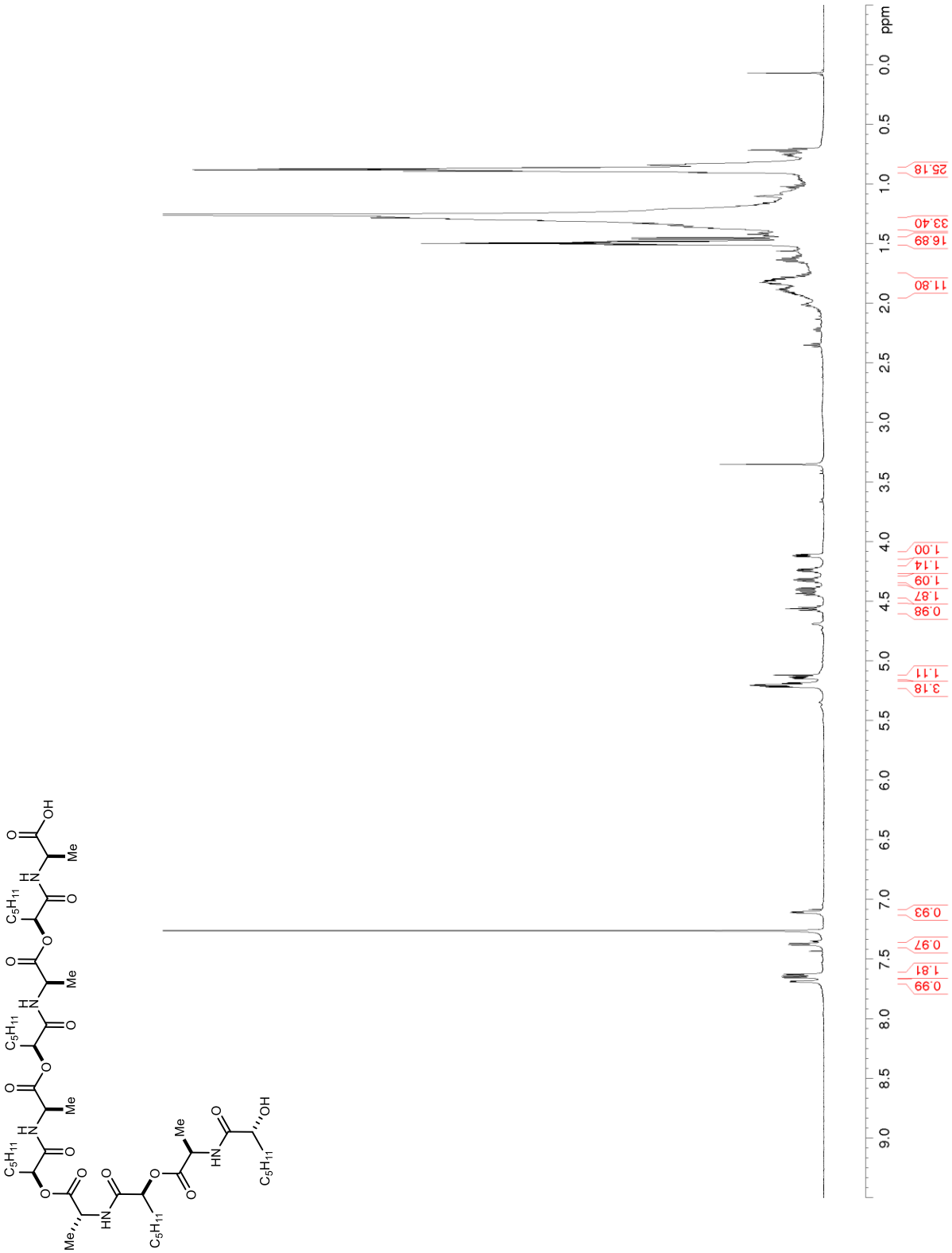

Figure S19. ^{13}C NMR/DEPT (150 MHz, $CDCl_3$) of **S3**

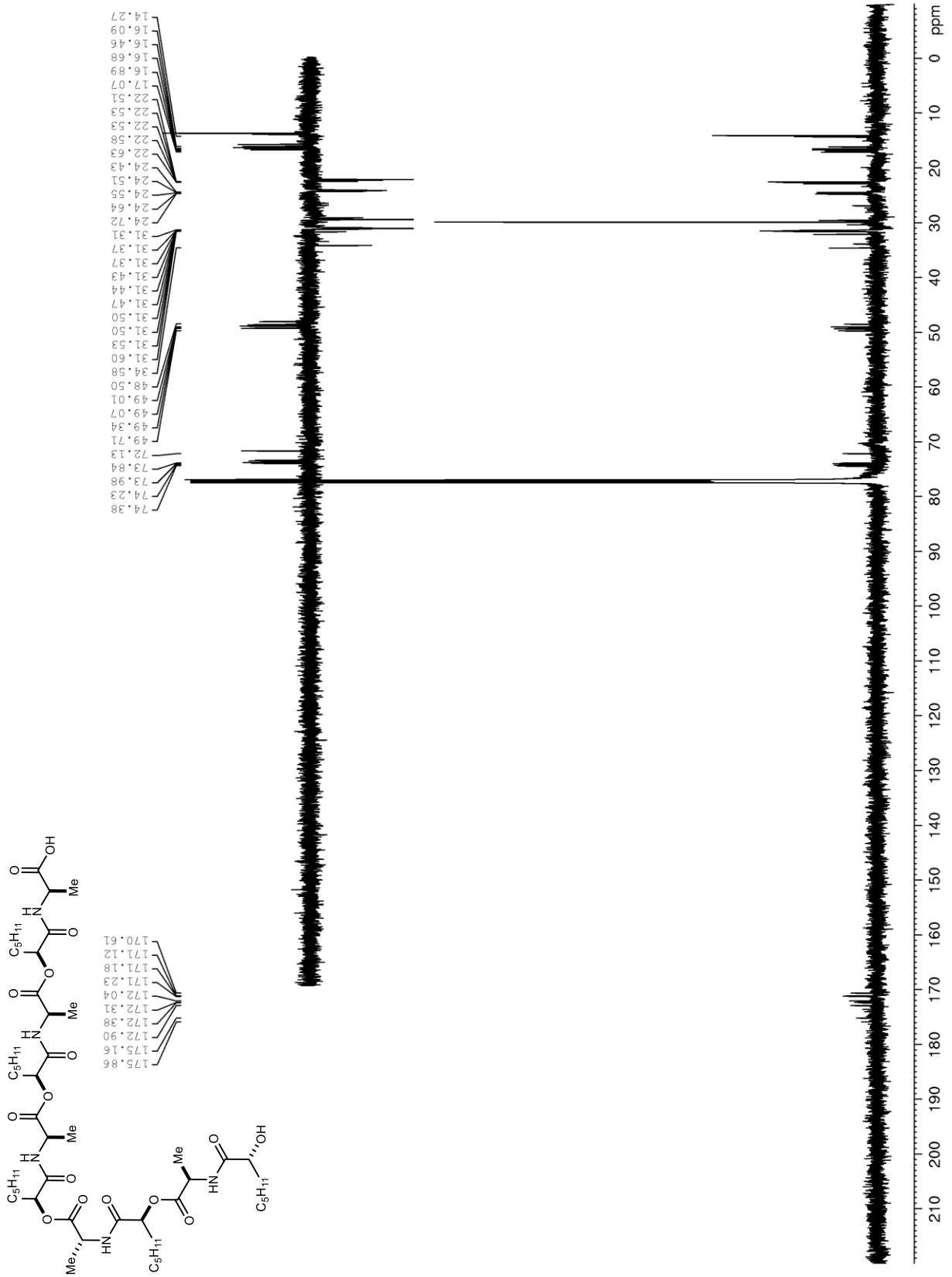

Figure S20. ^{1}H NMR (600 MHz, $CDCl_3$) of **21**

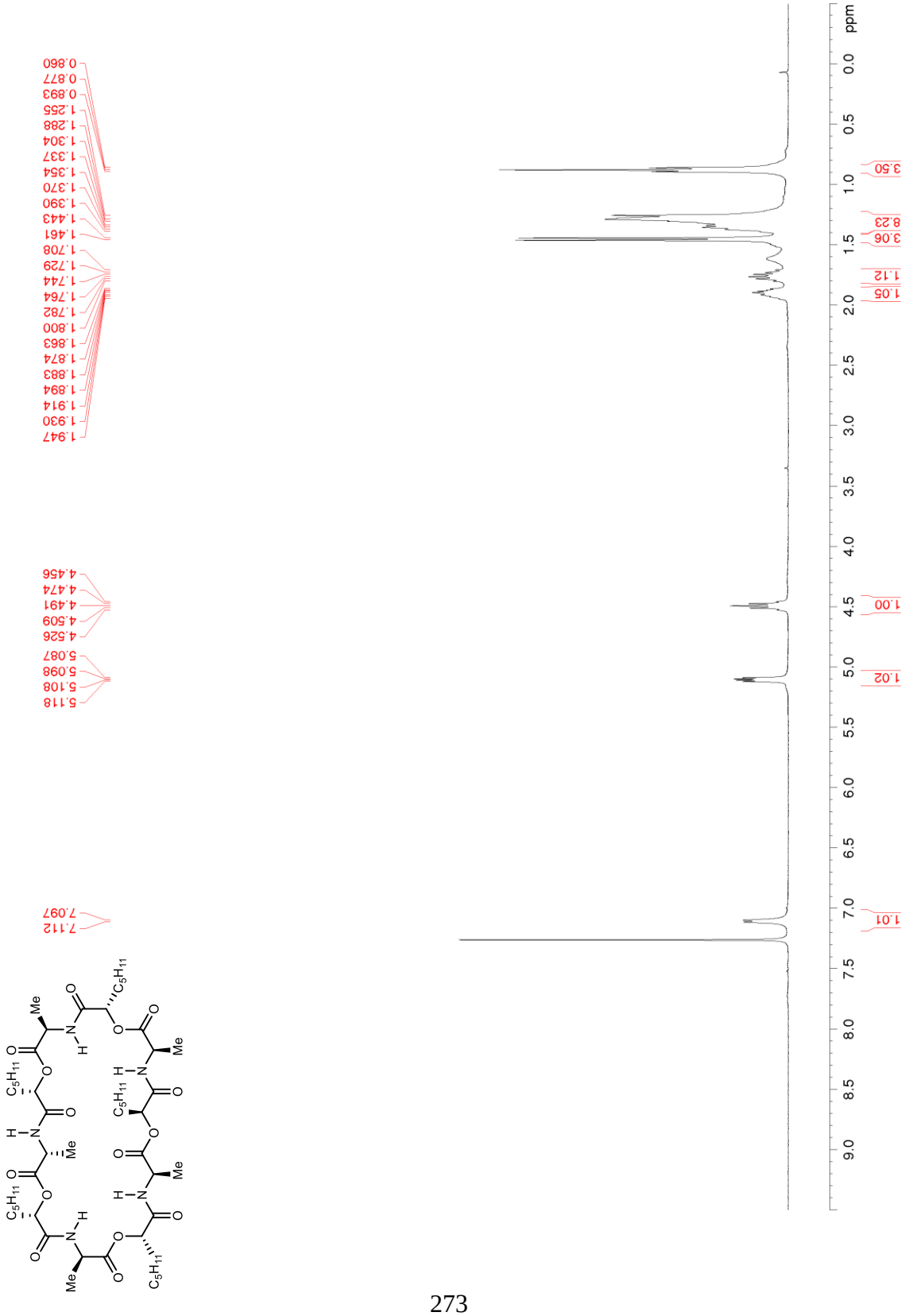

Figure S21. ^{13}C NMR/DEPT (150 MHz, $CDCl_3$) of **S3**

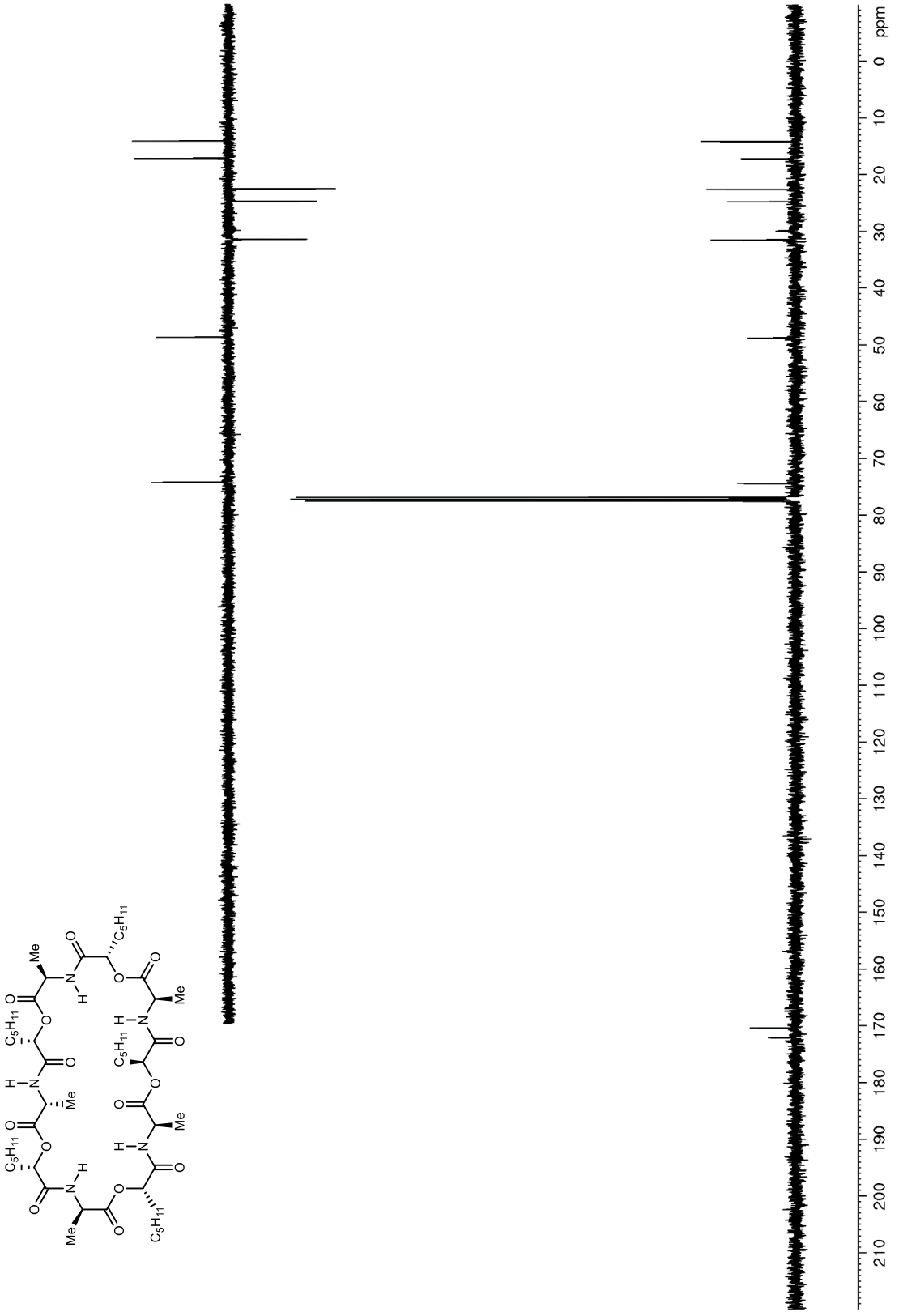

Figure S22. ^{1}H NMR (600 MHz, $CDCl_3$) of **S4**

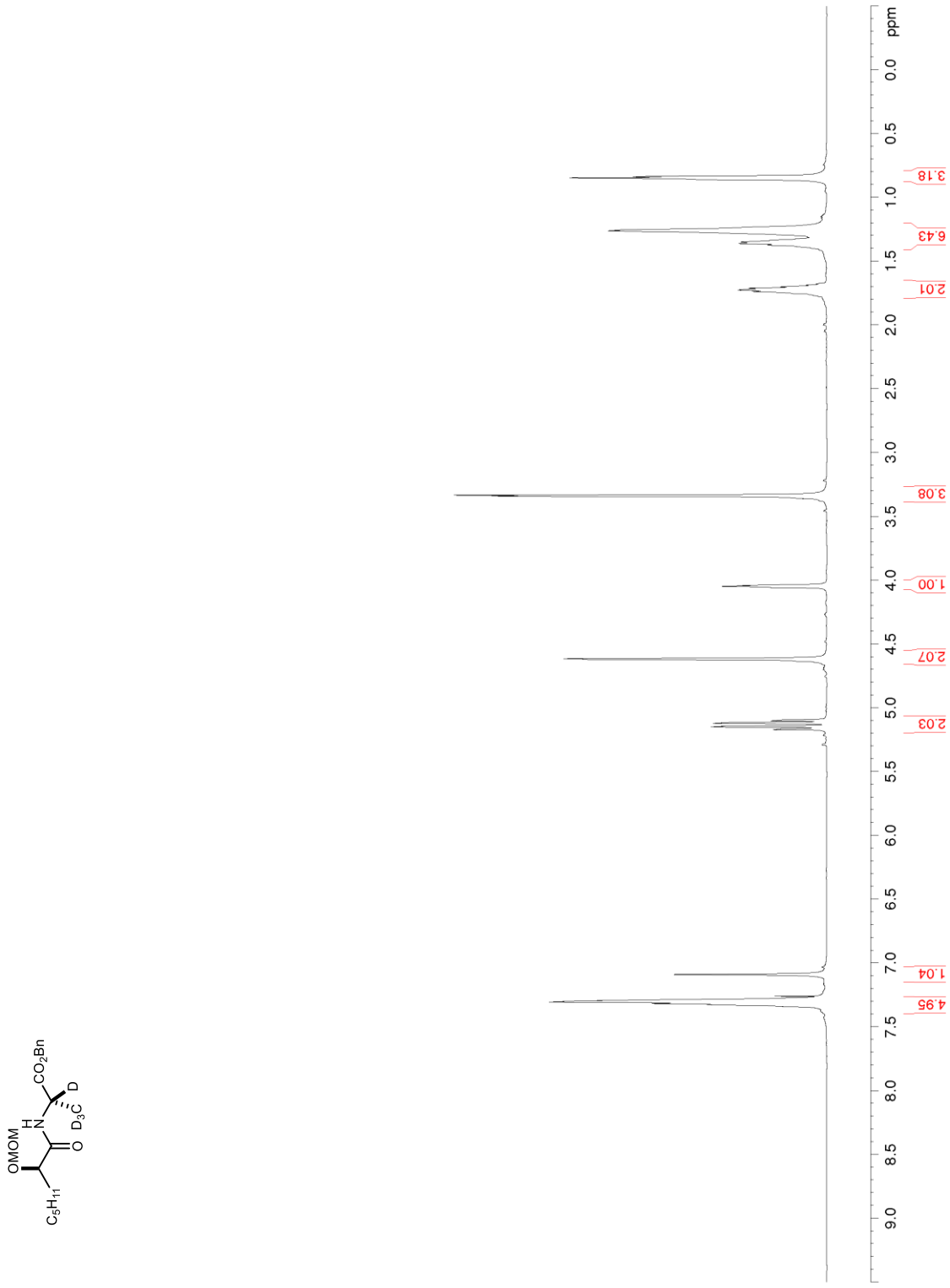

Figure S23. ^{13}C NMR/DEPT (150 MHz, $CDCl_3$) of **S4**

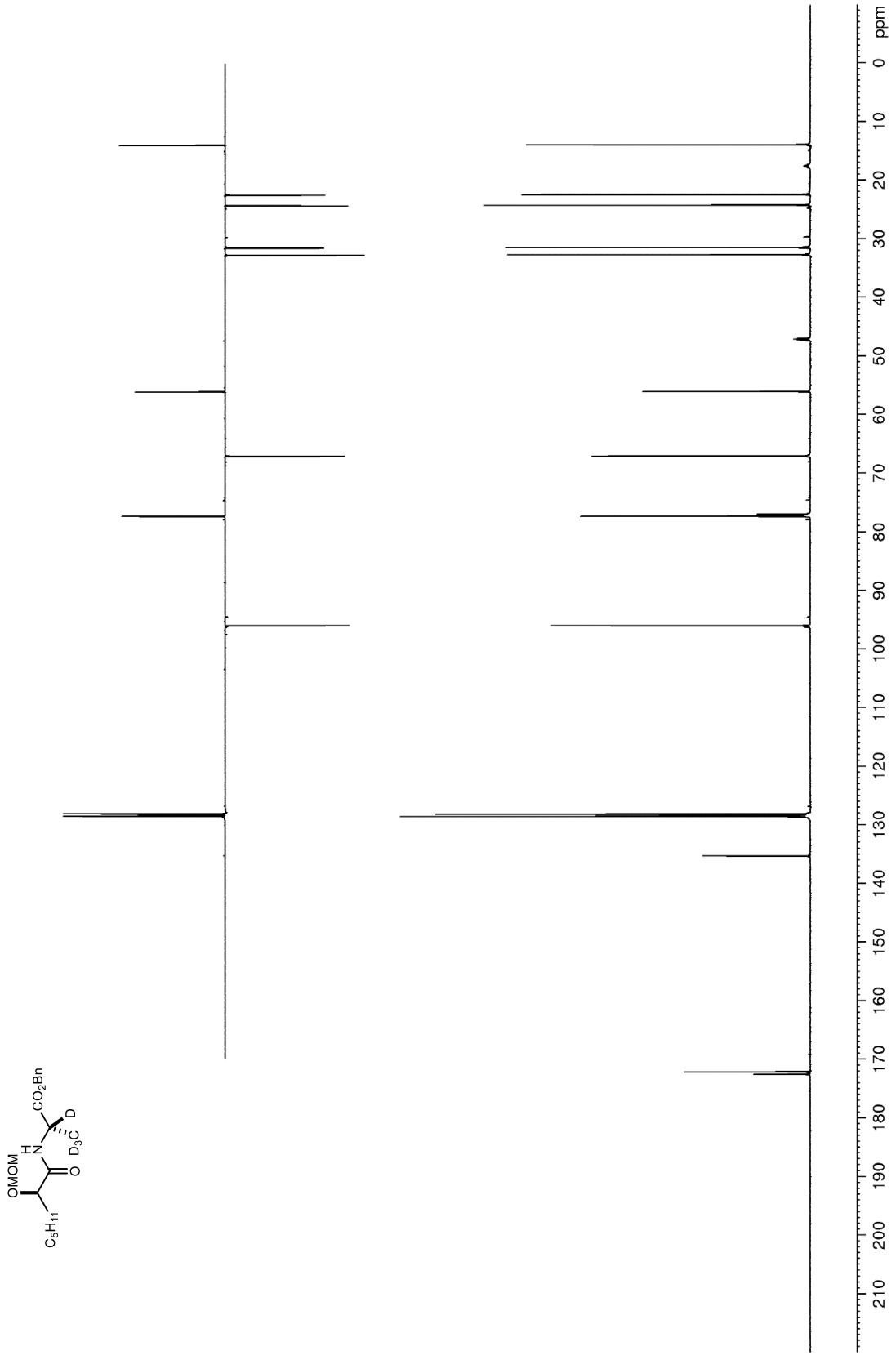

Figure S24. ^{1}H NMR (600 MHz, $CDCl_3$) of **S5**

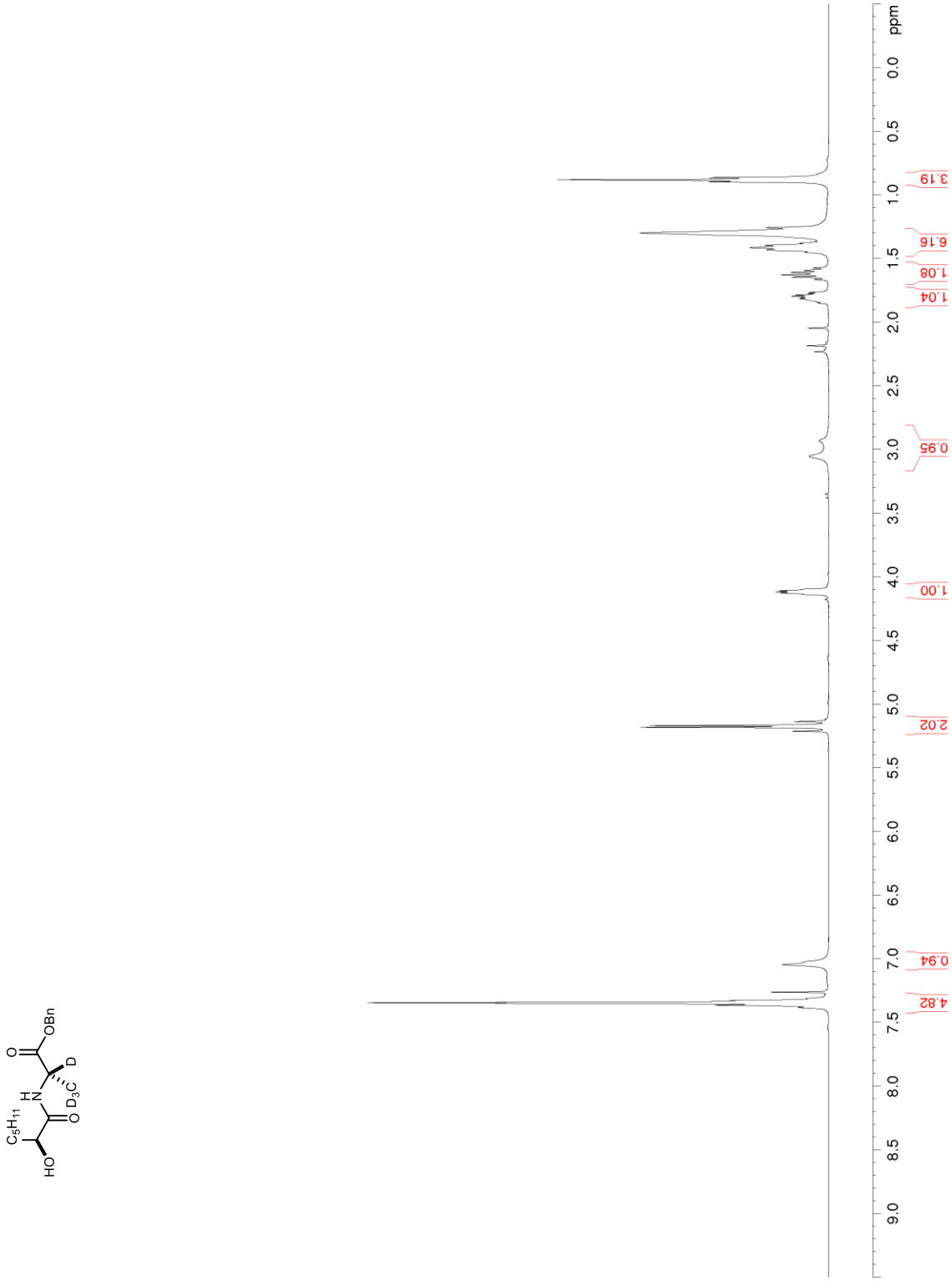

Figure S25. ^{13}C NMR/DEPT (150 MHz, $CDCl_3$) of **S5**

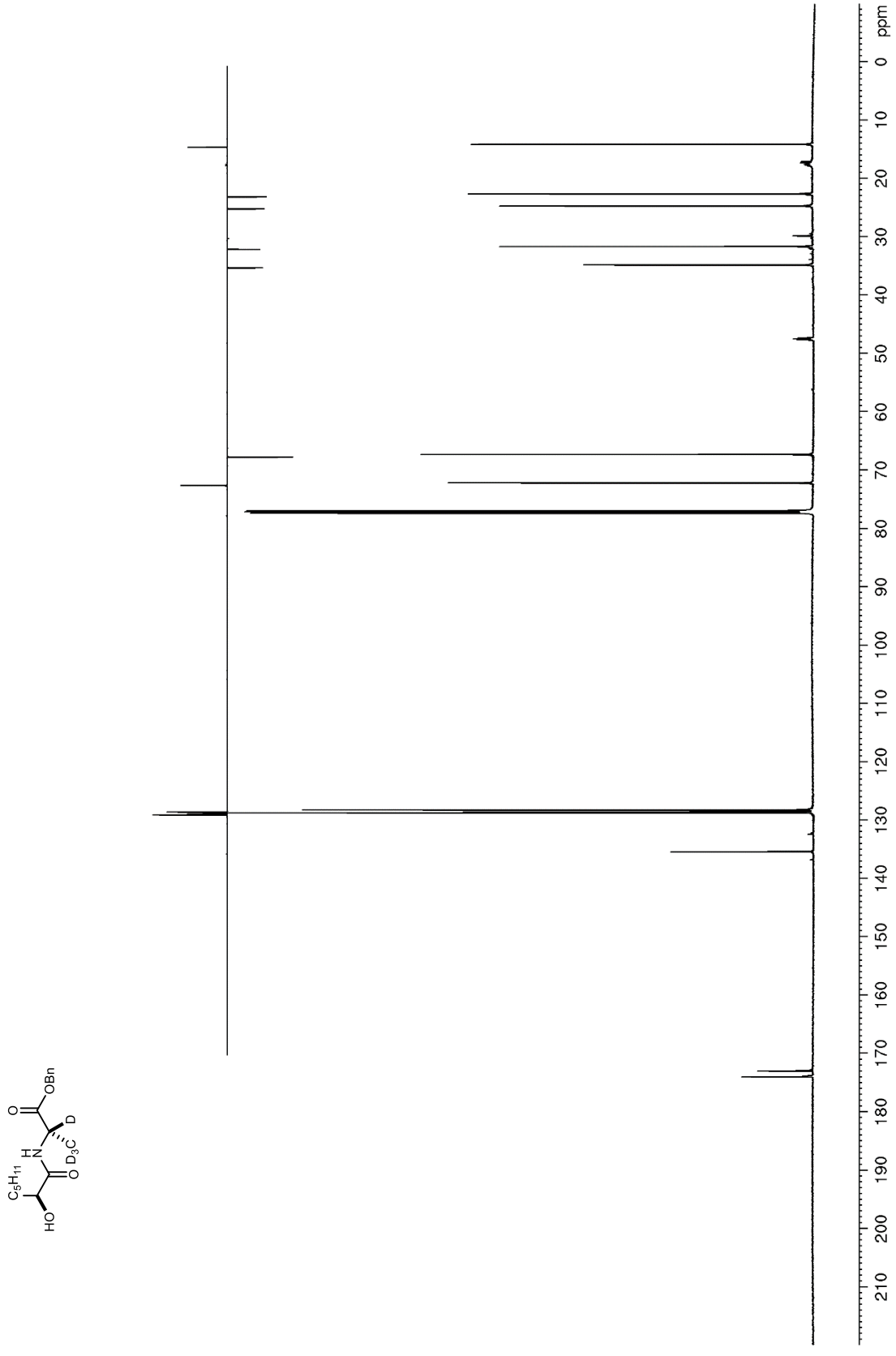

Figure S26. ^{1}H NMR (600 MHz, $CDCl_3$) of **S6**

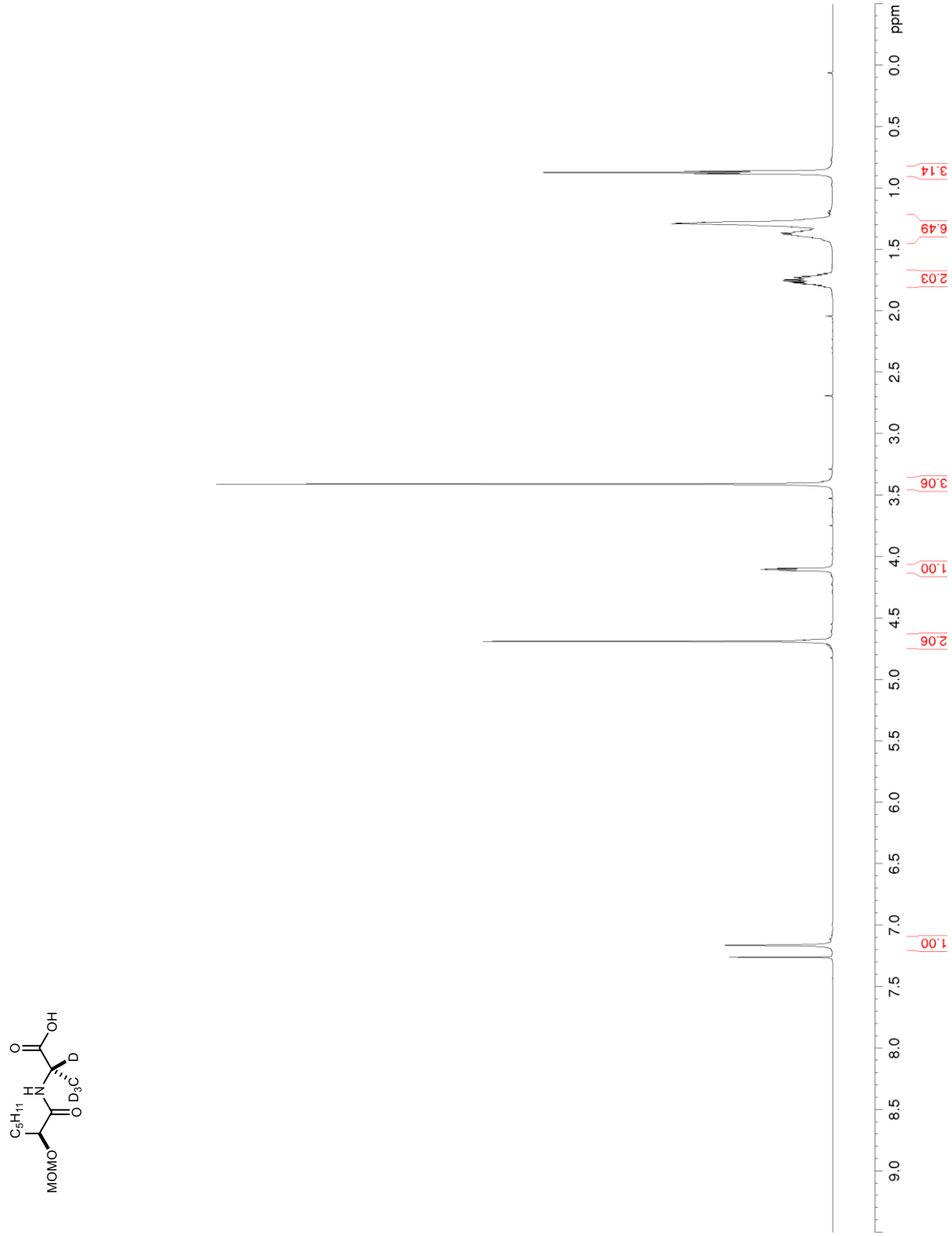

Figure S27. ^{13}C NMR/DEPT (150 MHz, $CDCl_3$) of **S6**

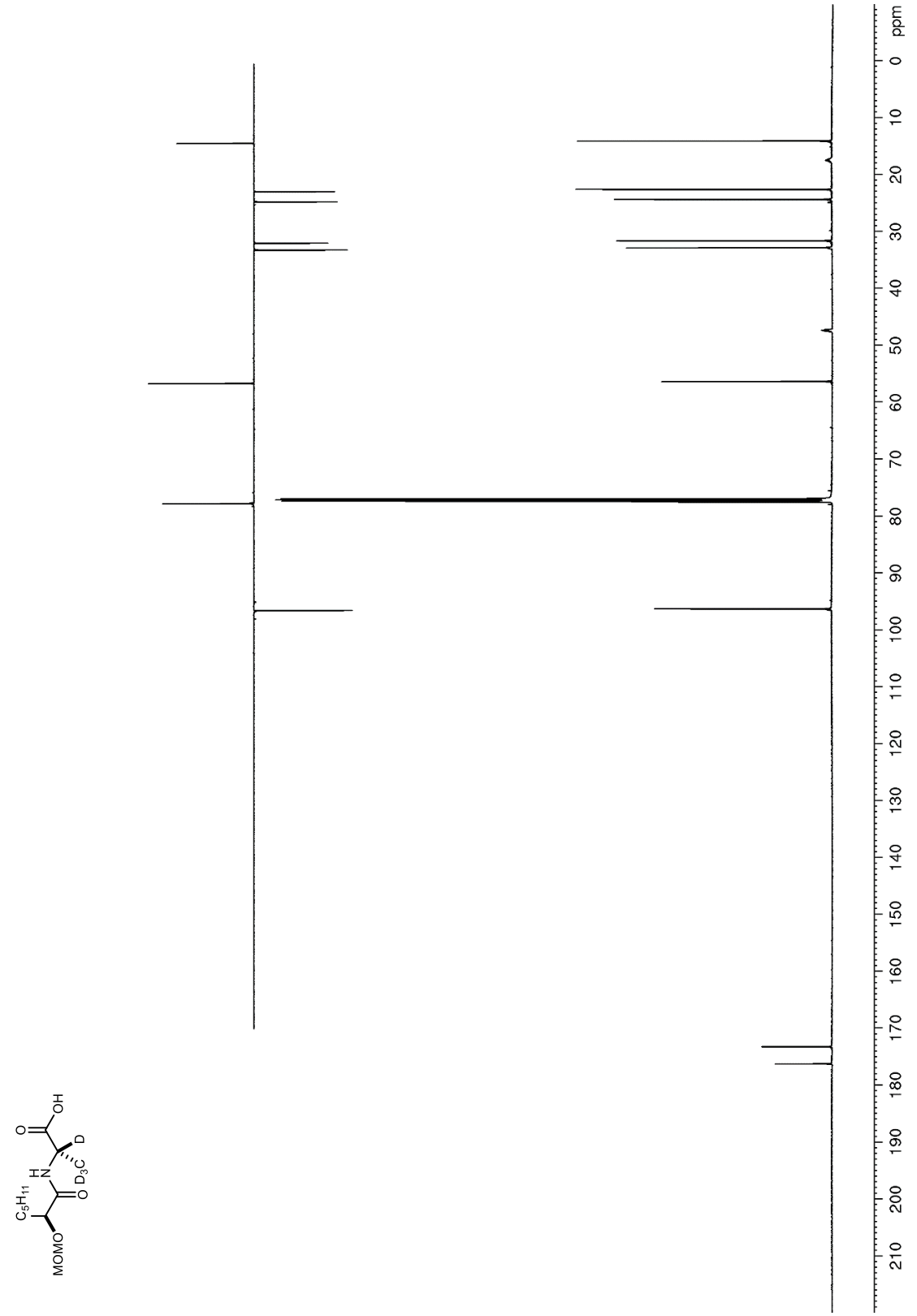

Figure S28. ^{1}H NMR (600 MHz, $CDCl_3$) of **S7**

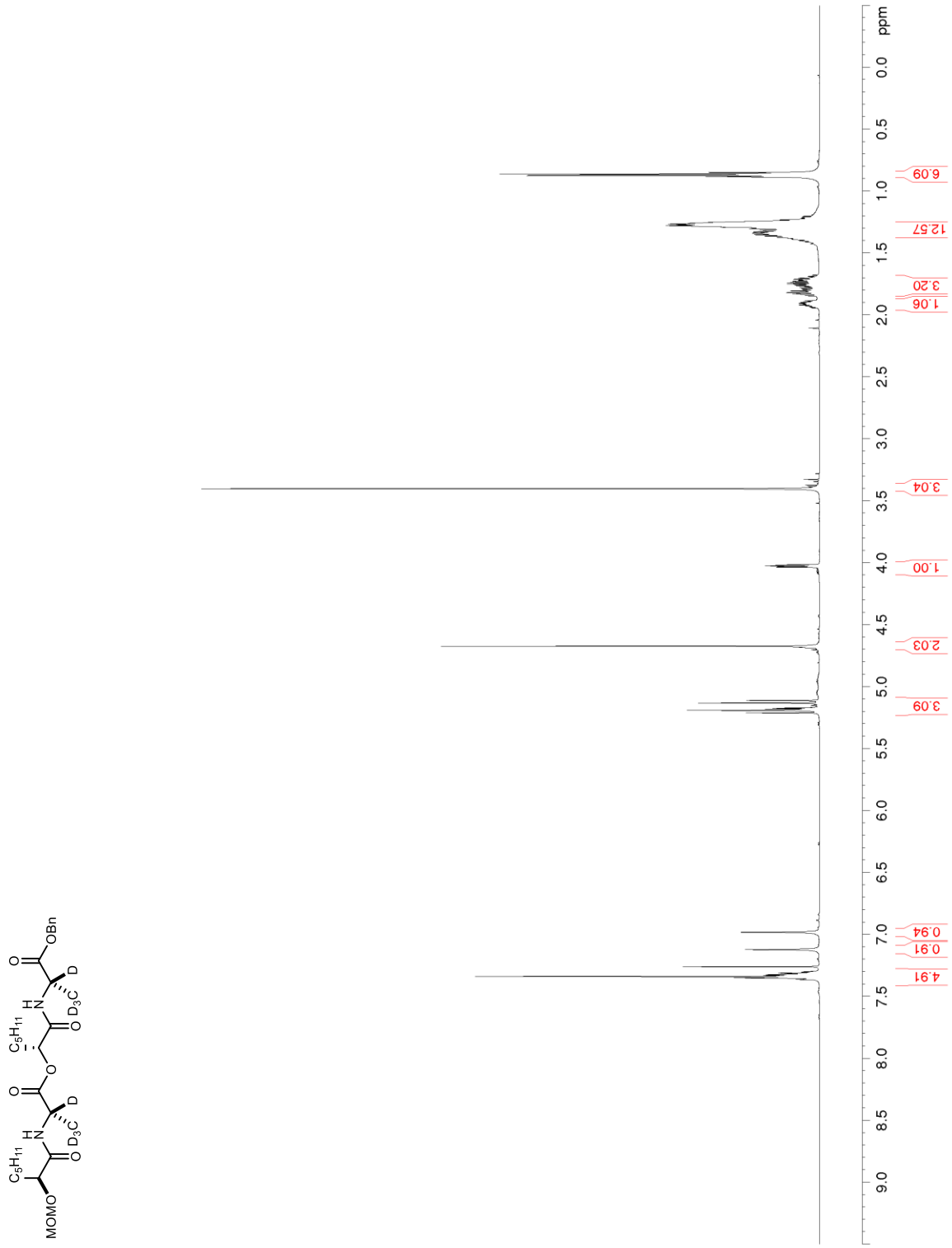

Figure S29. ^{13}C NMR/DEPT (150 MHz, $CDCl_3$) of **S7**

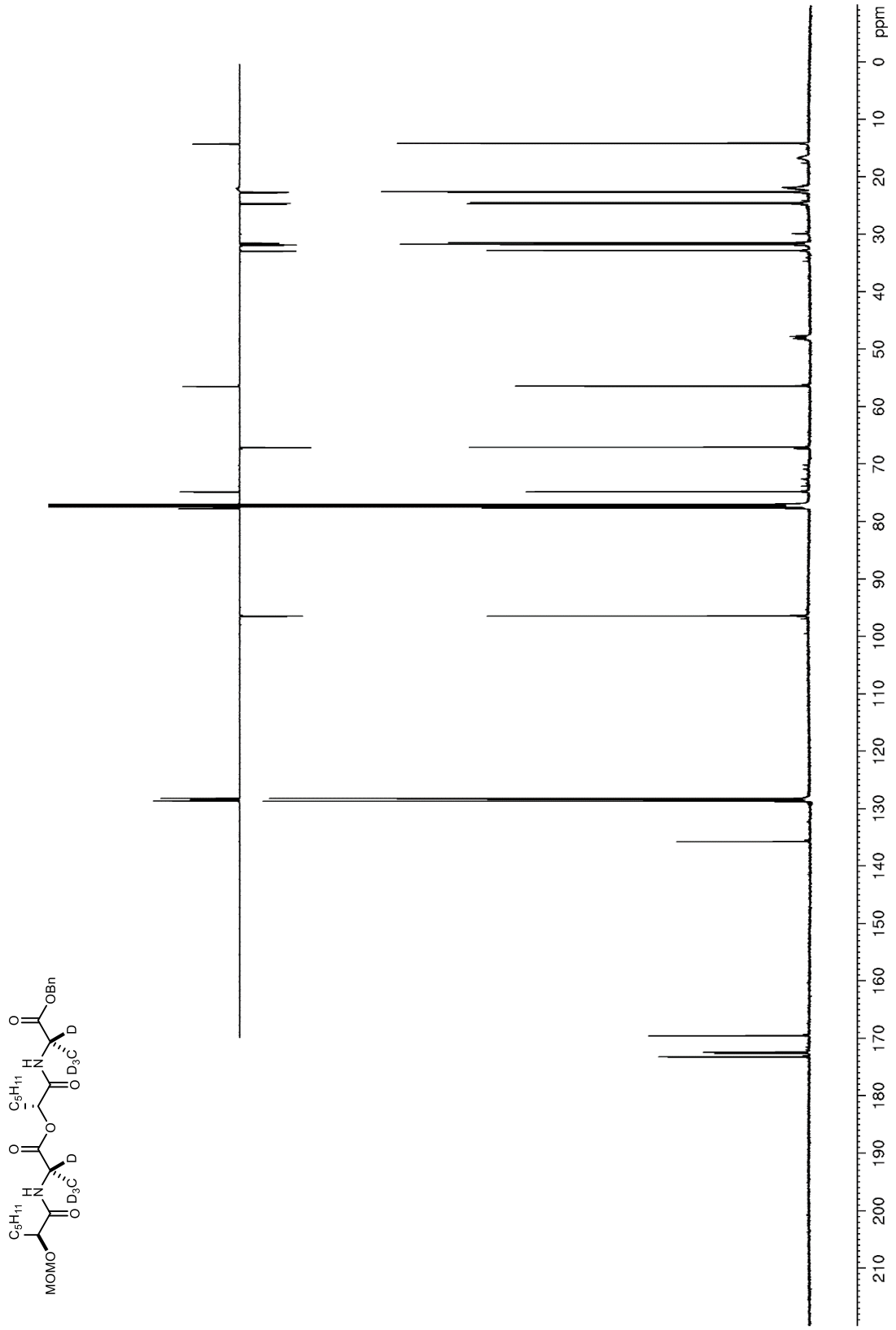

Figure S30. ^{1}H NMR (600 MHz, $CDCl_3$) of **S8**

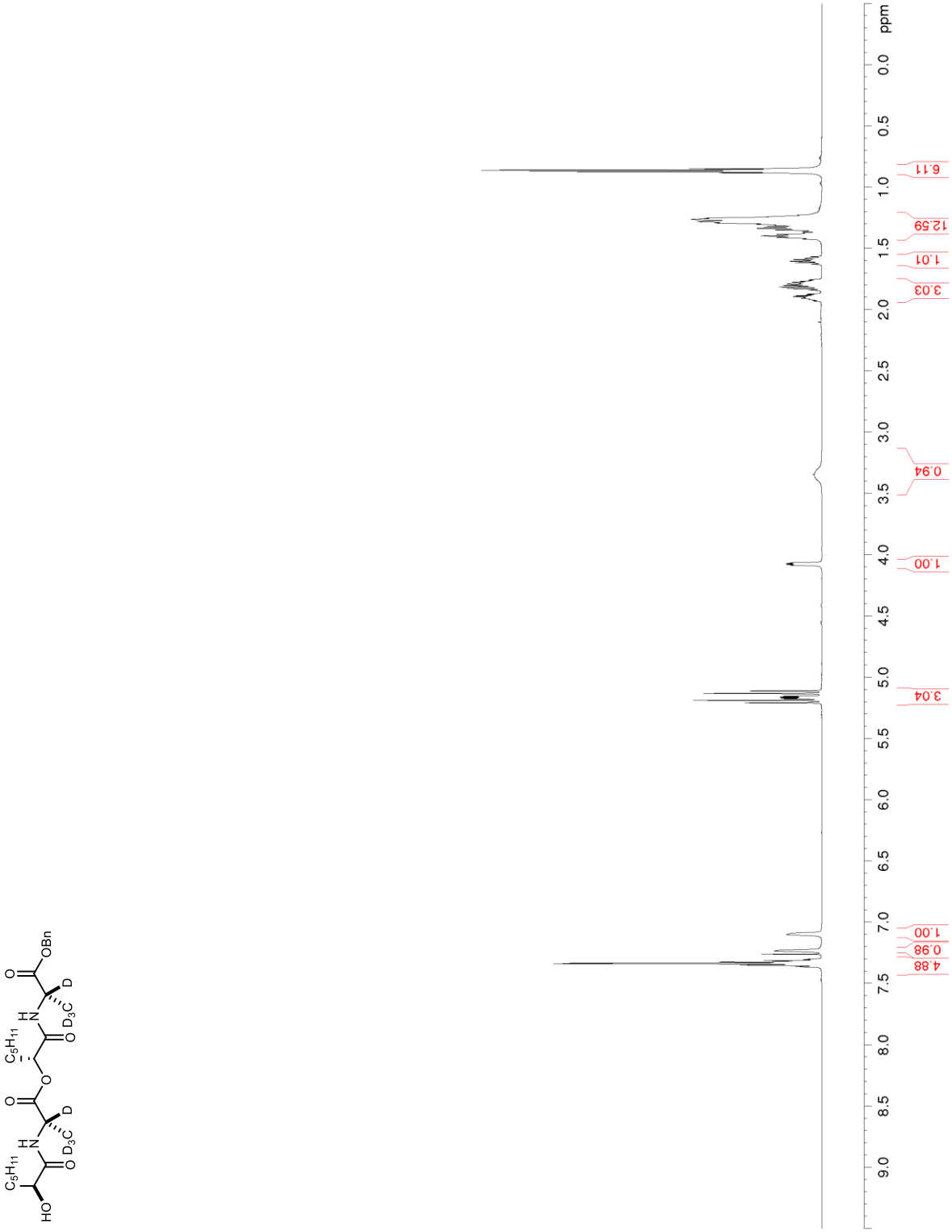

Figure S31. ^{13}C NMR/DEPT (150 MHz, $CDCl_3$) of **S8**

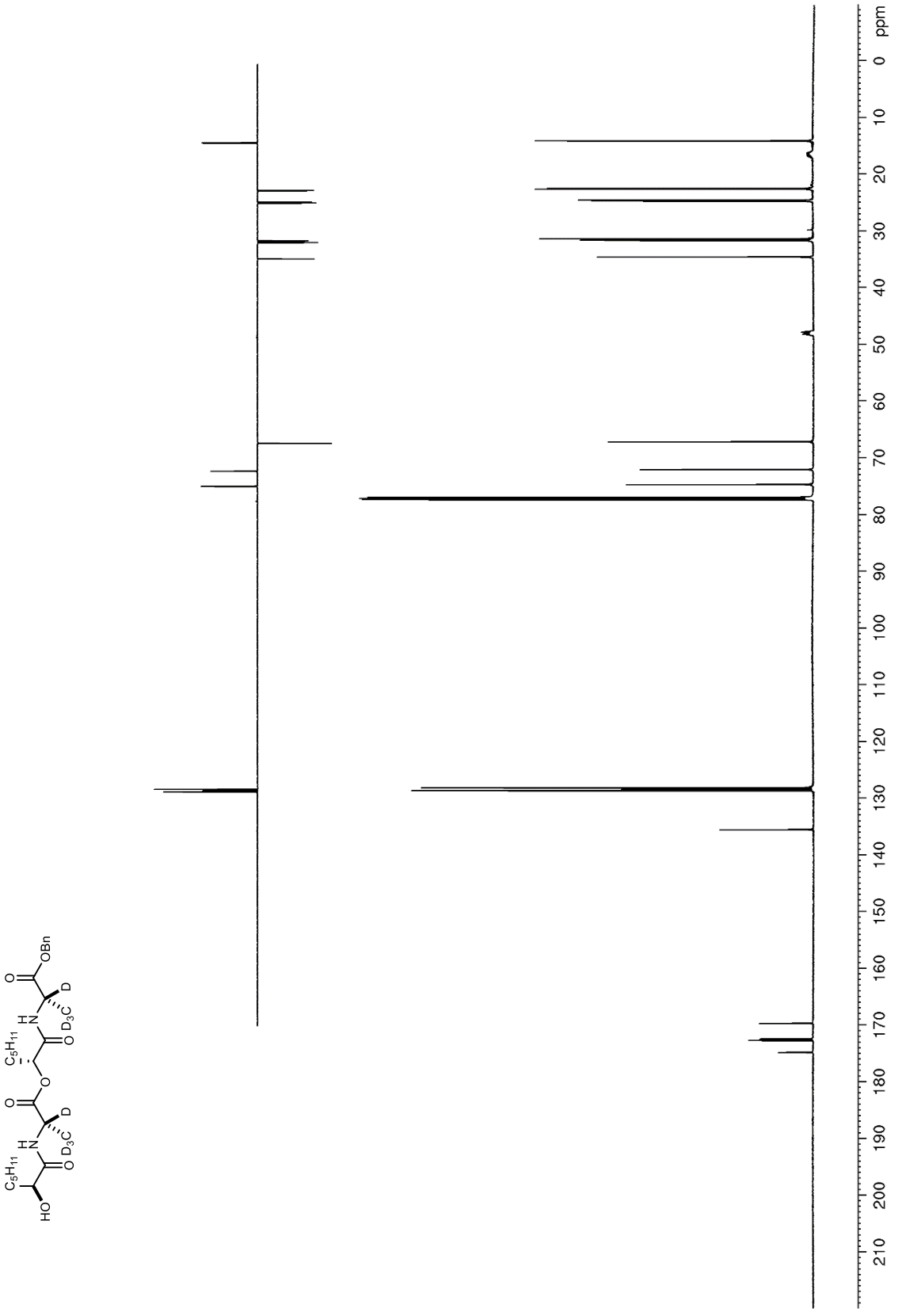

Figure S32. ^{1}H NMR (600 MHz, $CDCl_3$) of **25**

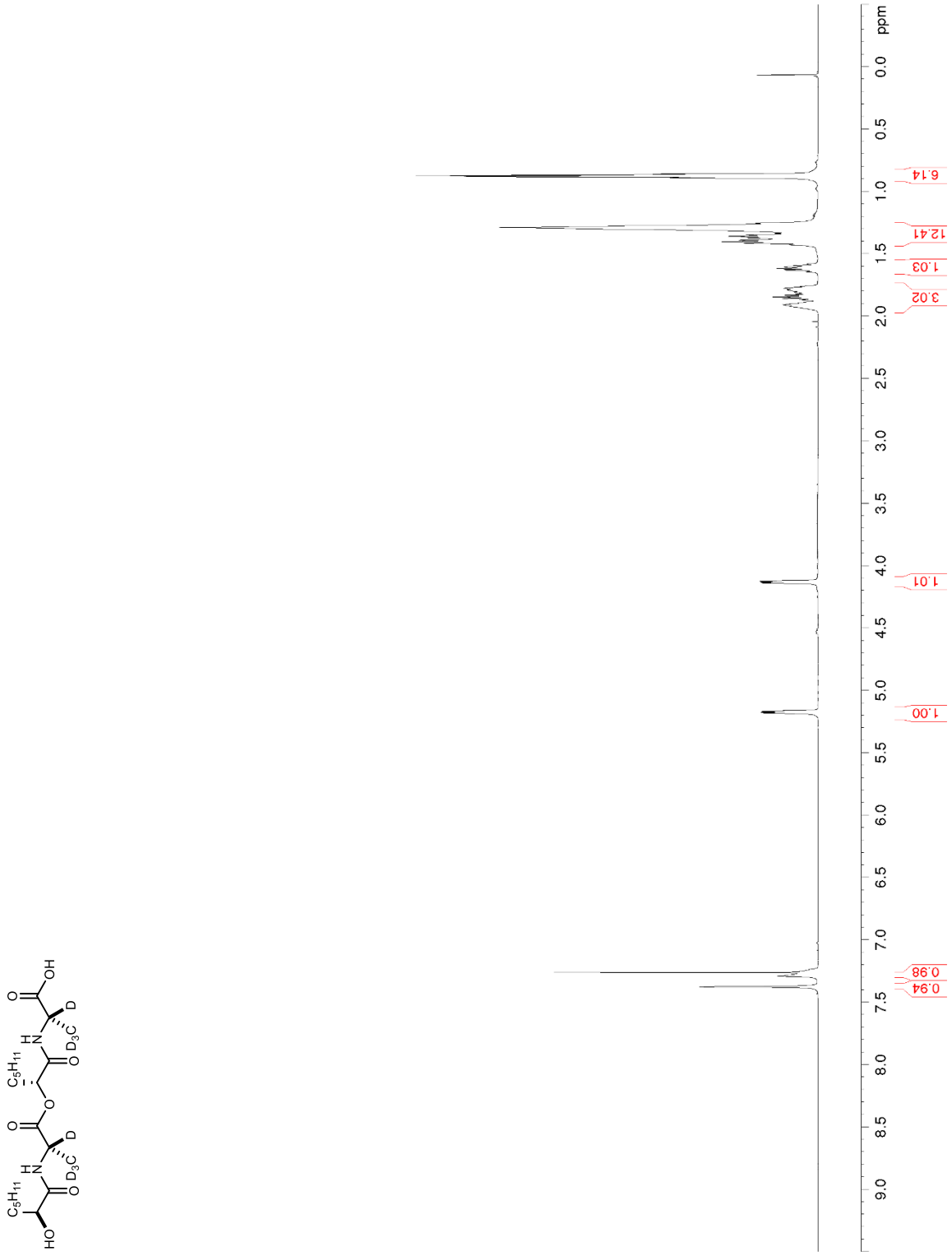

Figure S33. ^{13}C NMR/DEPT (150 MHz, $CDCl_3$) of **25**

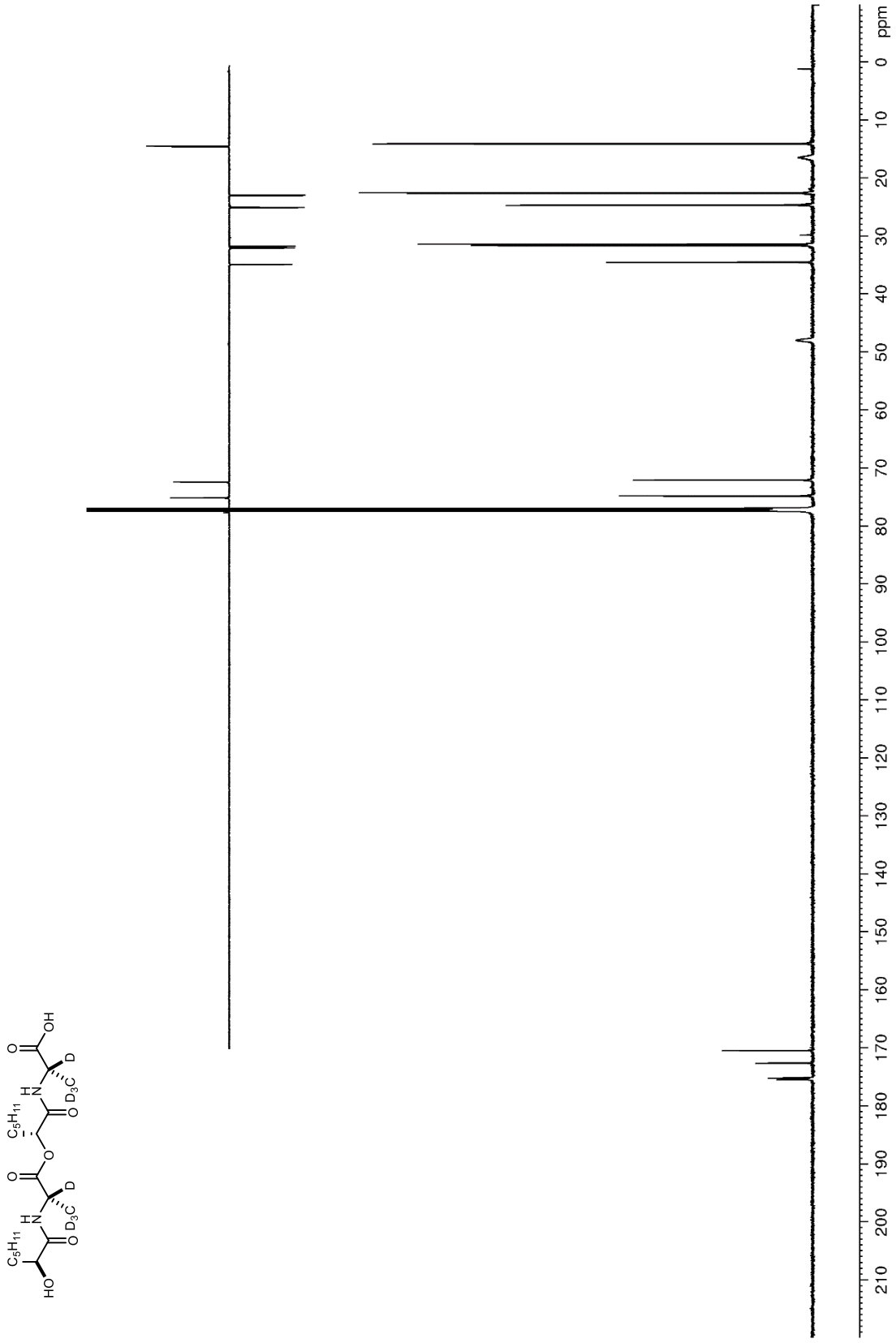

Figure S34. ^{1}H NMR (600 MHz, $CDCl_3$) of **S9**

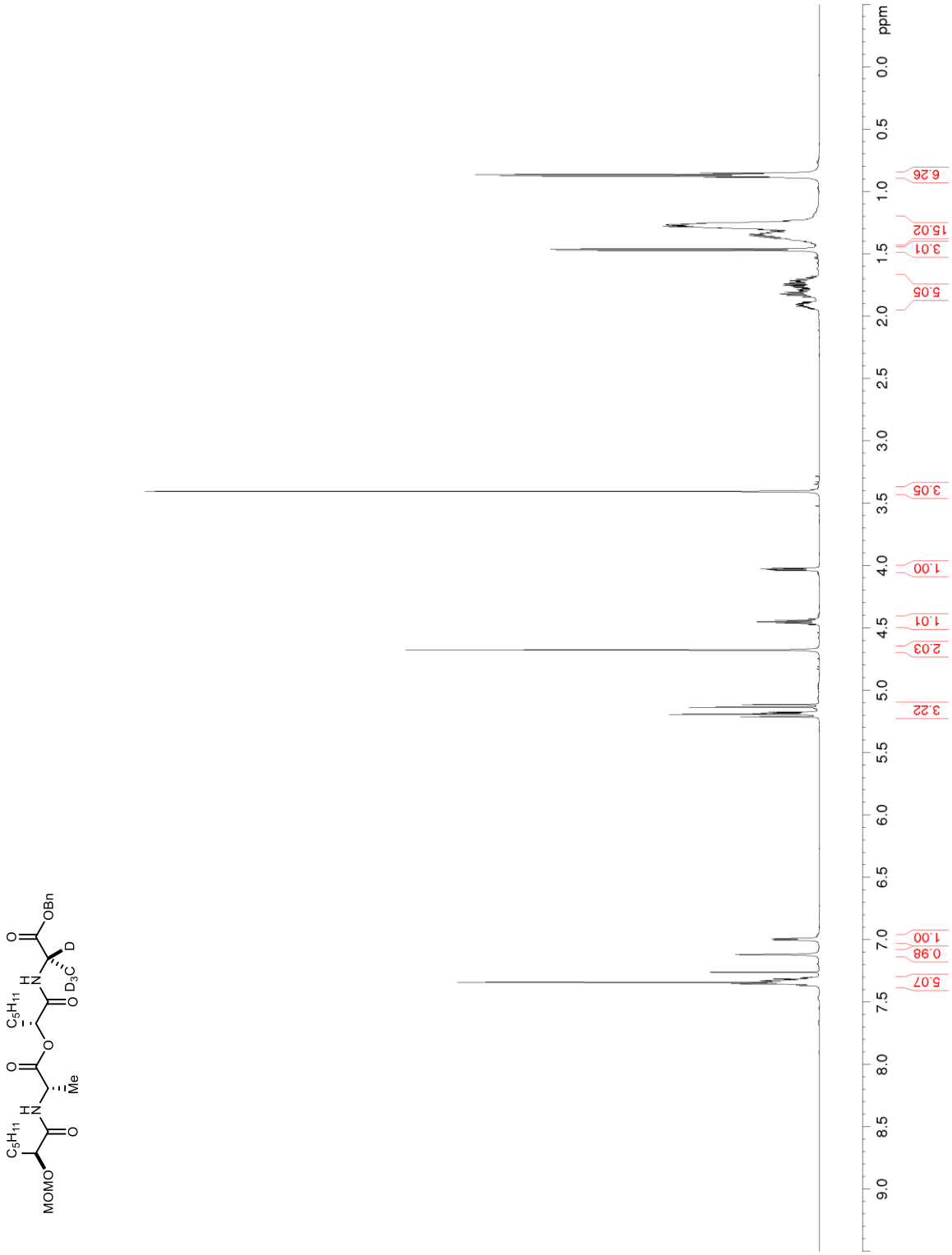

Figure S35. ^{13}C NMR/DEPT (150 MHz, $CDCl_3$) of **S9**

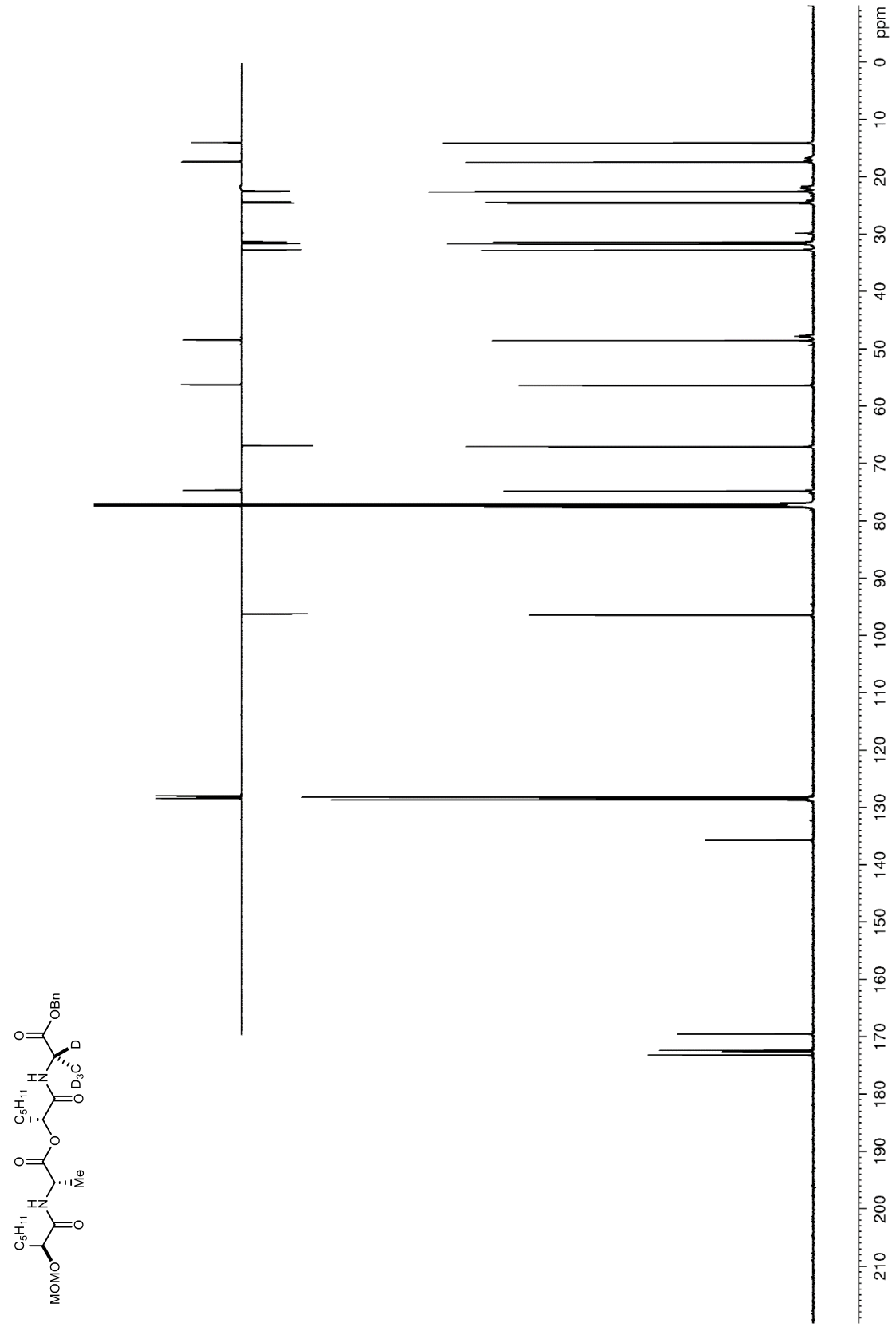

Figure S36. ^{1}H NMR (600 MHz, $CDCl_3$) of **S10**

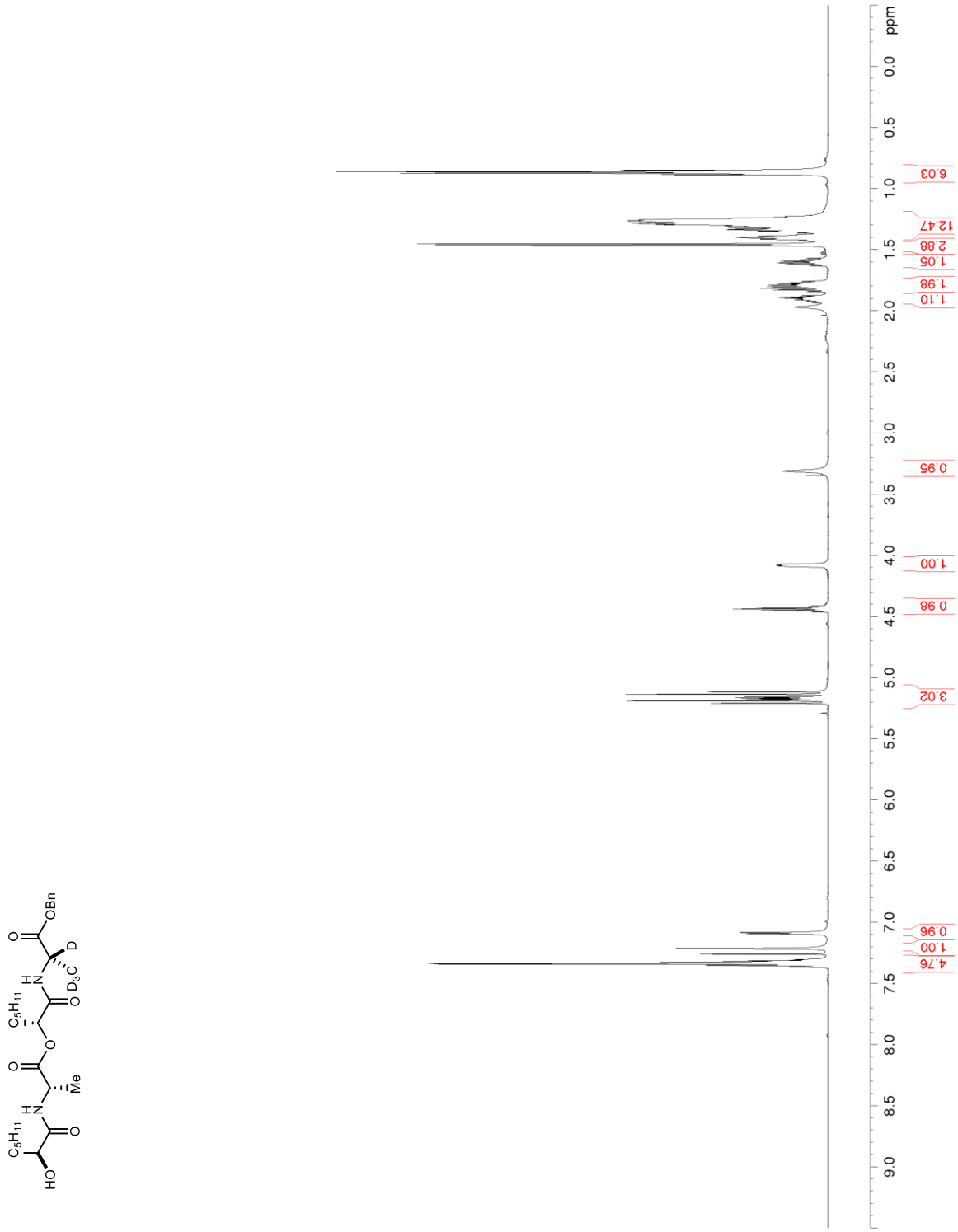

Figure S37. ^{13}C NMR/DEPT (150 MHz, $CDCl_3$) of **S10**

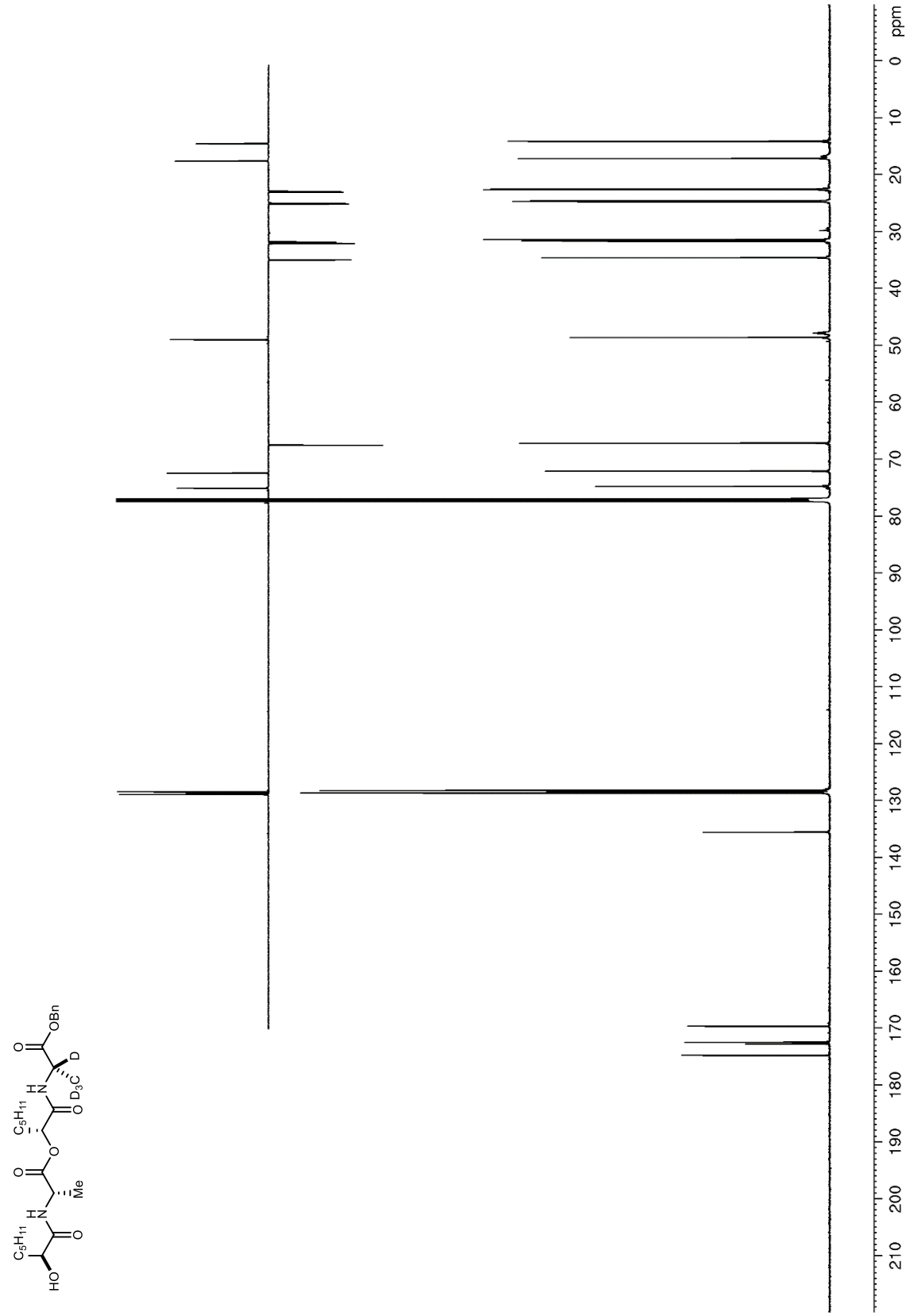

Figure S38. ^{1}H NMR (600 MHz, $CDCl_3$) of **26**

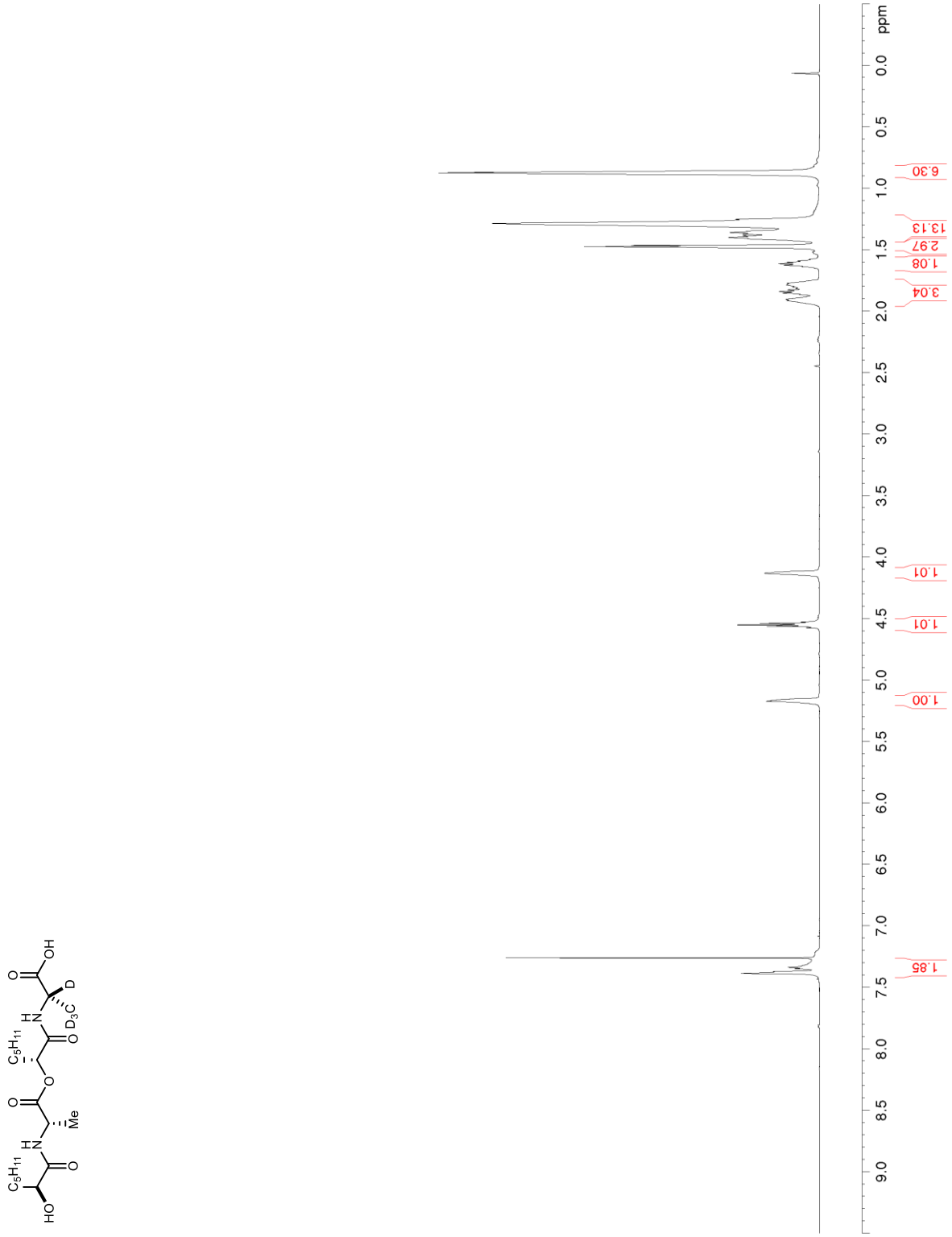

Figure S39. ^{13}C NMR/DEPT (150 MHz, $CDCl_3$) of **26**

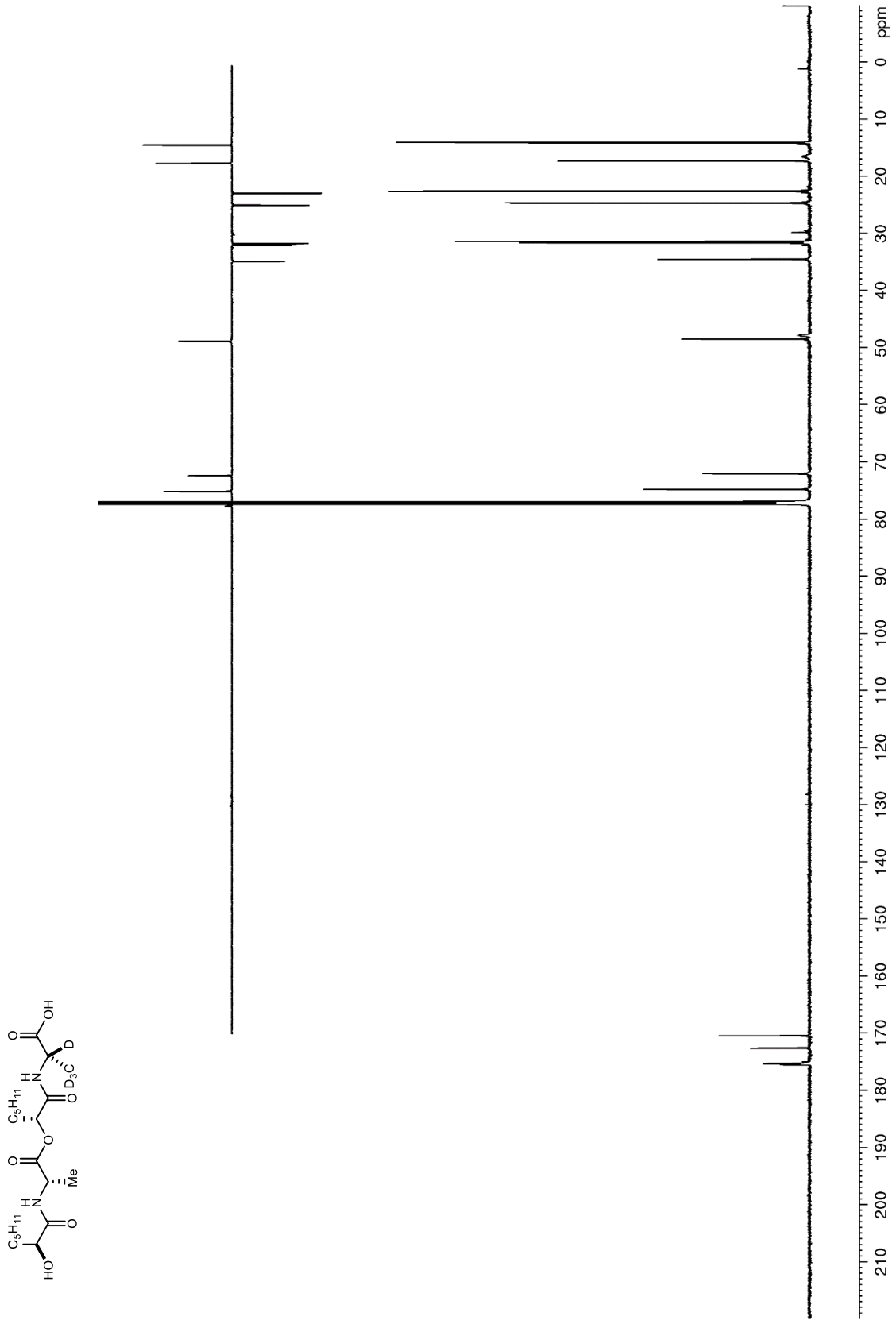

Figure S40. ^{1}H NMR (400 MHz, $CDCl_3$) of **S11**

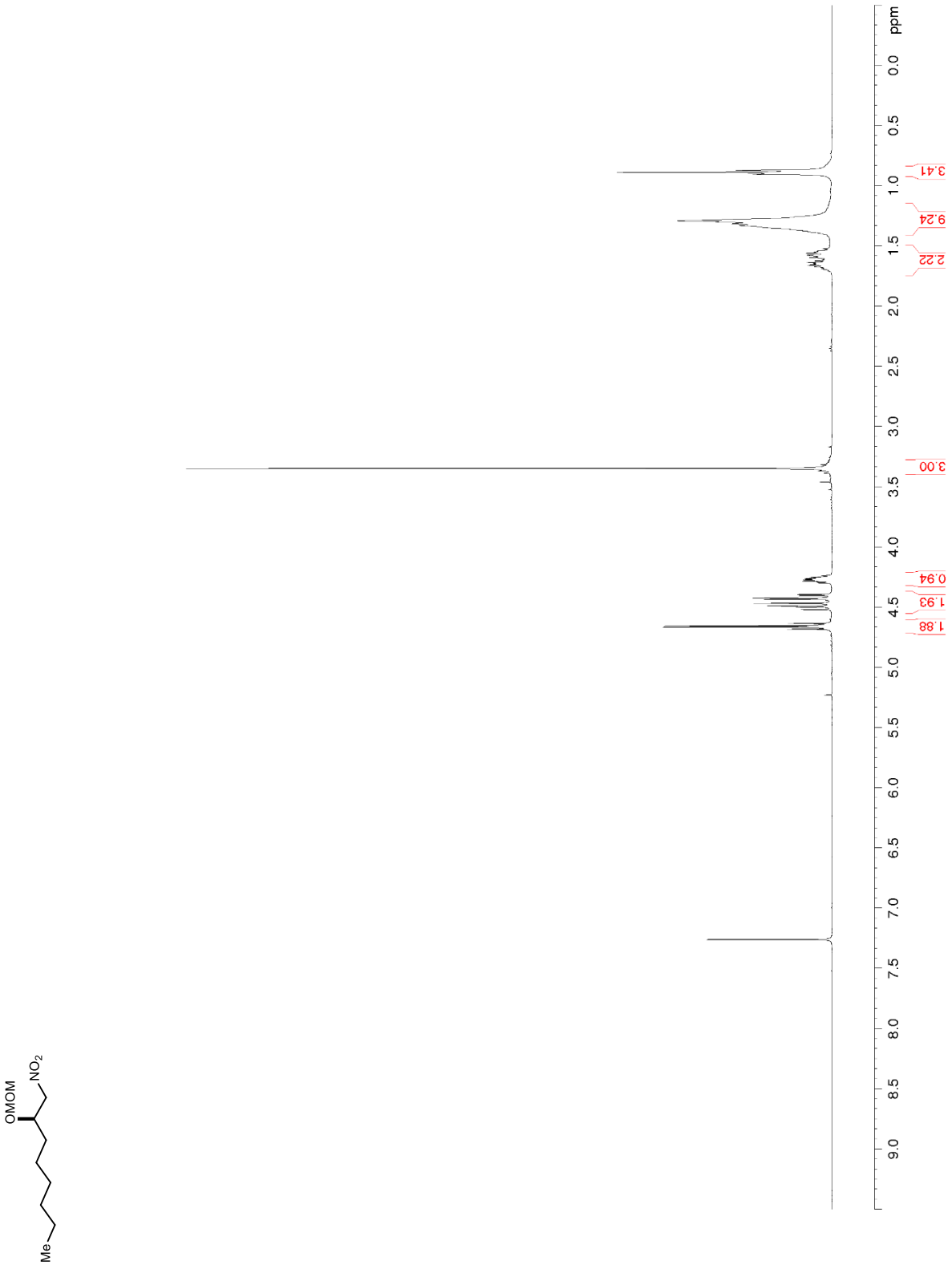

Figure S41. ^{13}C NMR/DEPT (100 MHz, $CDCl_3$) of **S11**

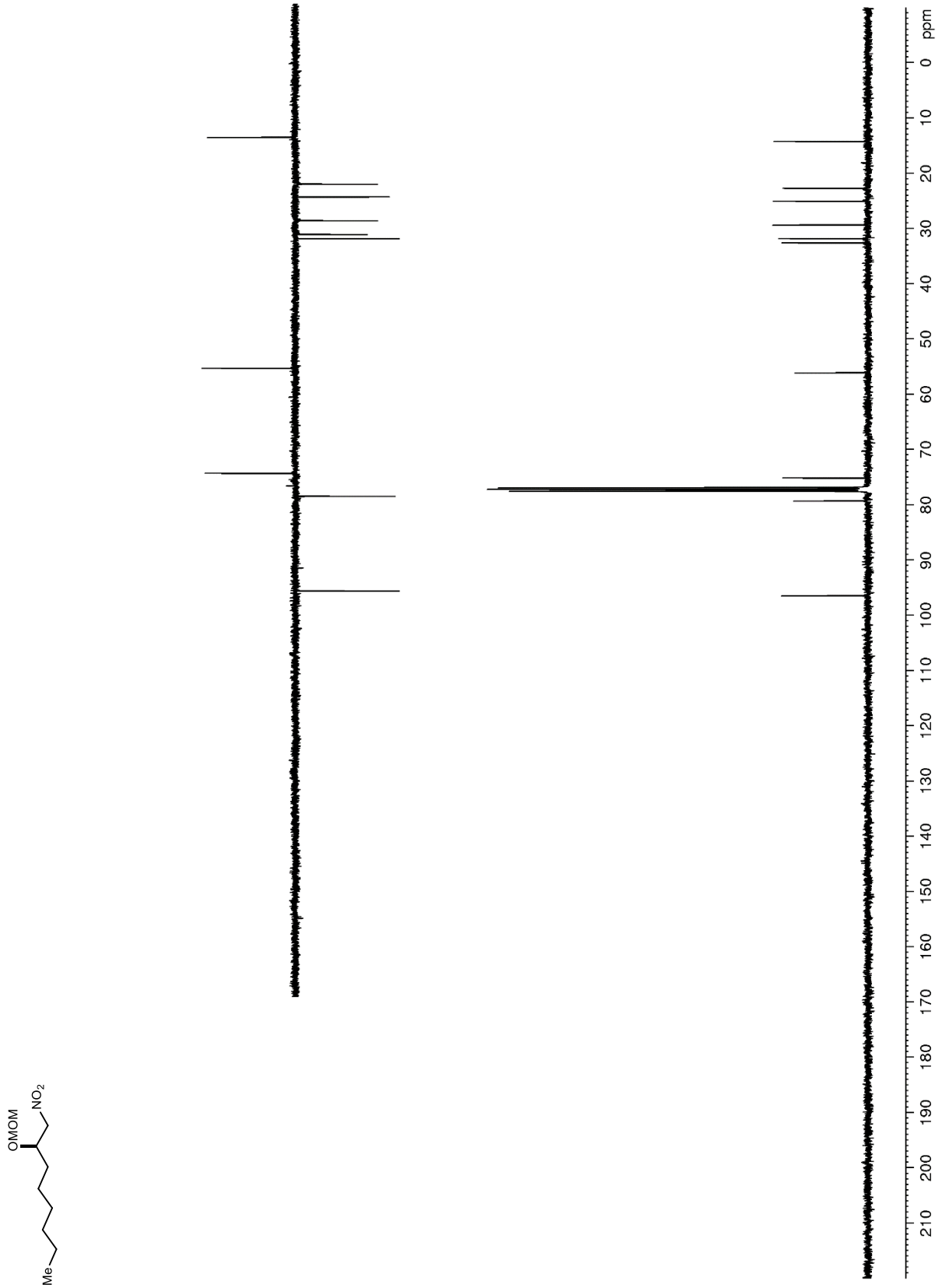

Figure S42. ^{1}H NMR (400 MHz, $CDCl_3$) of **S12**

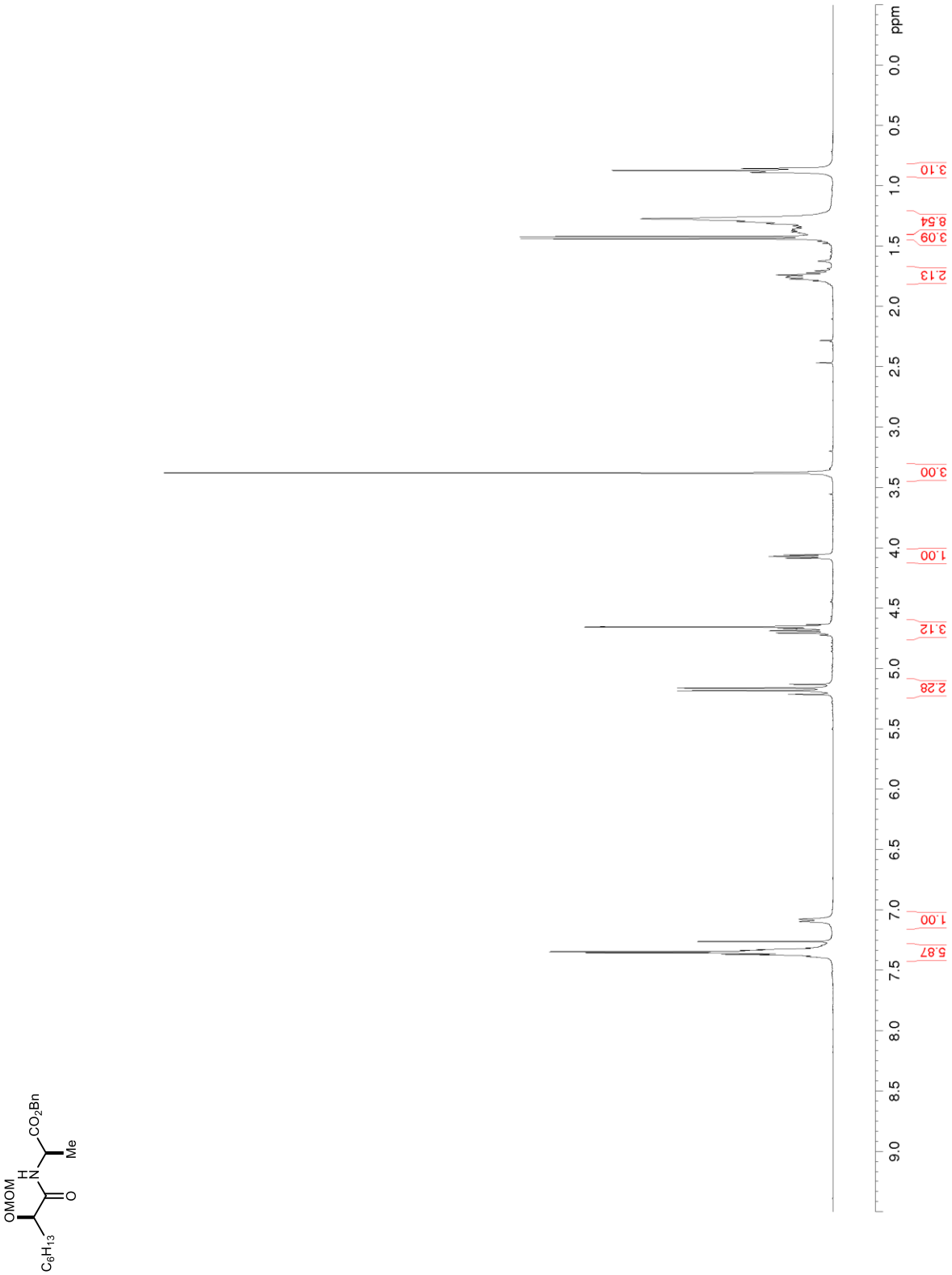

Figure S43. ^{13}C NMR/DEPT (100 MHz, $CDCl_3$) of **S12**

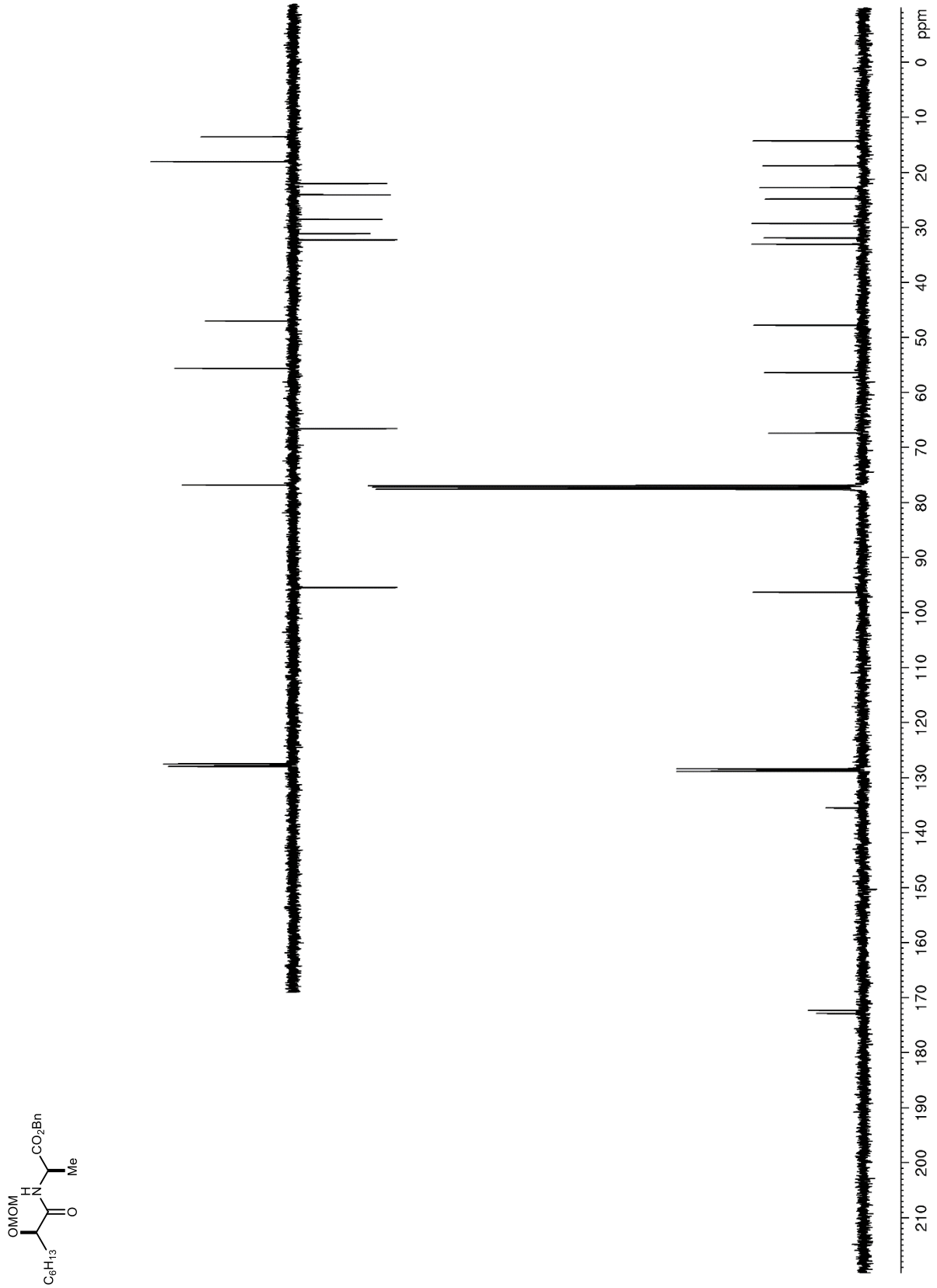

Figure S44. ^{1}H NMR (400 MHz, $CDCl_3$) of **S13**

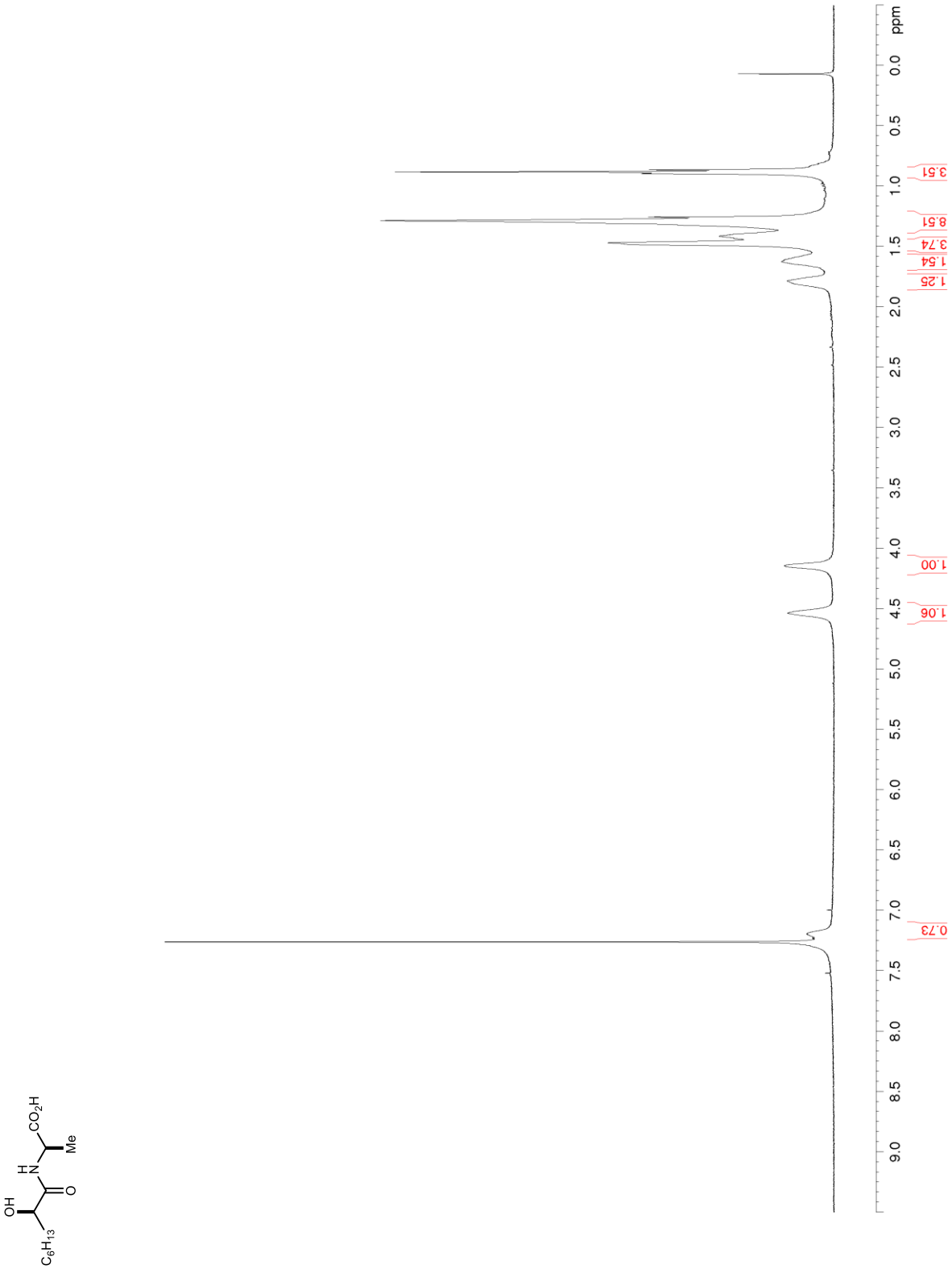

Figure S45. ^{13}C NMR/DEPT (100 MHz, $CDCl_3$) of **S13**

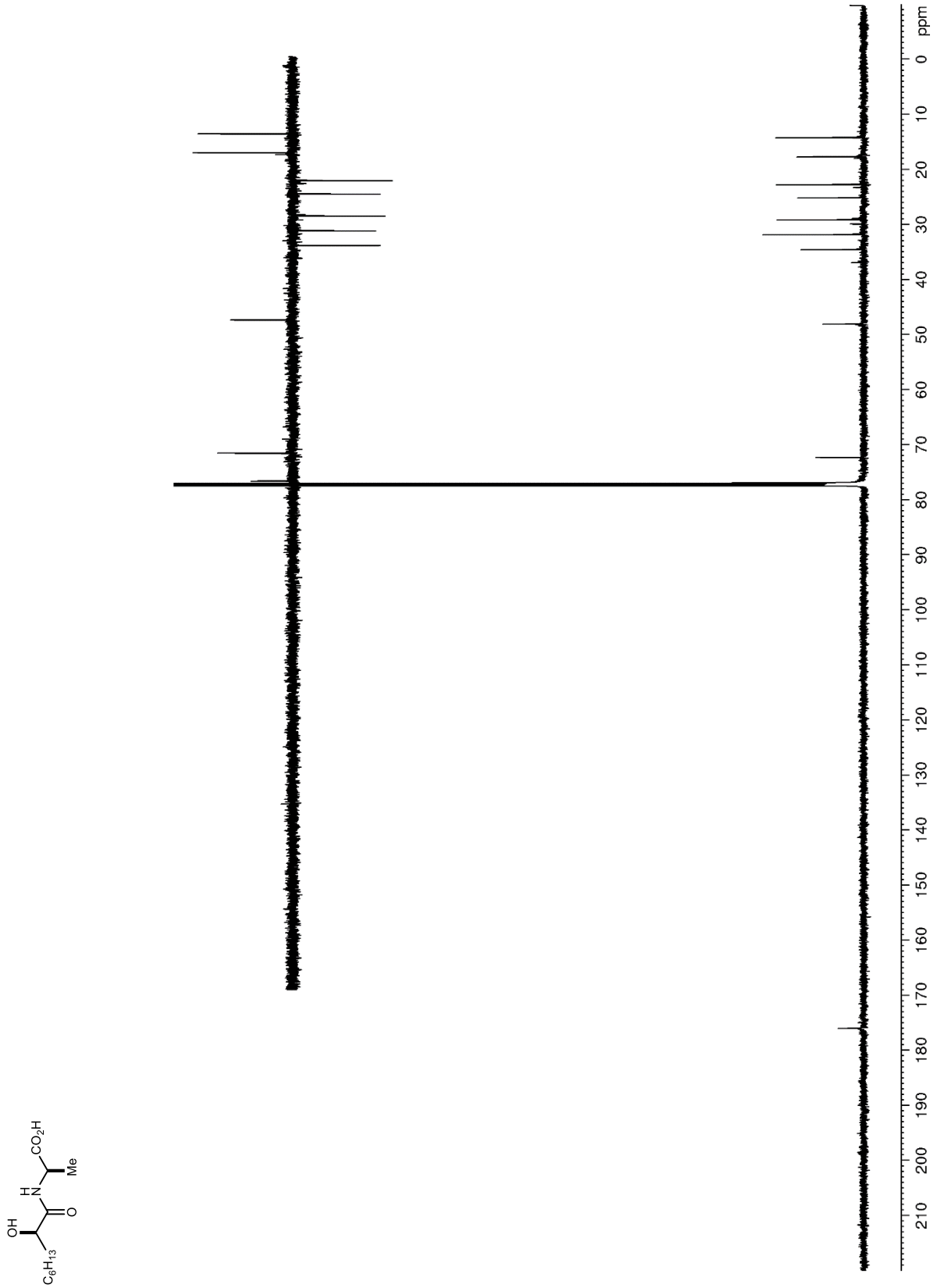

Figure S46. ^{1}H NMR (600 MHz, $CDCl_3$) of **S14**

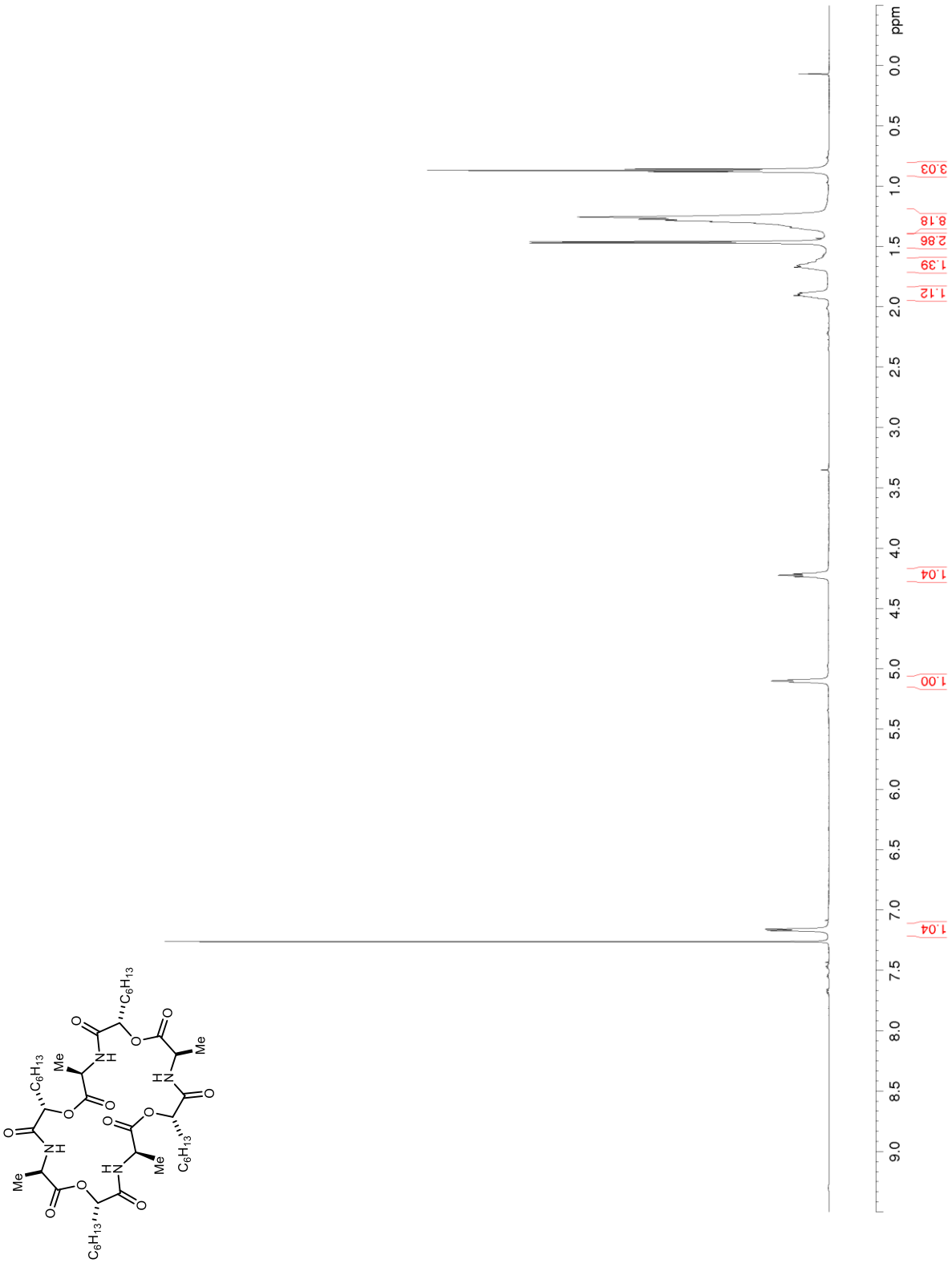

Figure S47. ^{13}C NMR/DEPT (150 MHz, $CDCl_3$) of **S14**

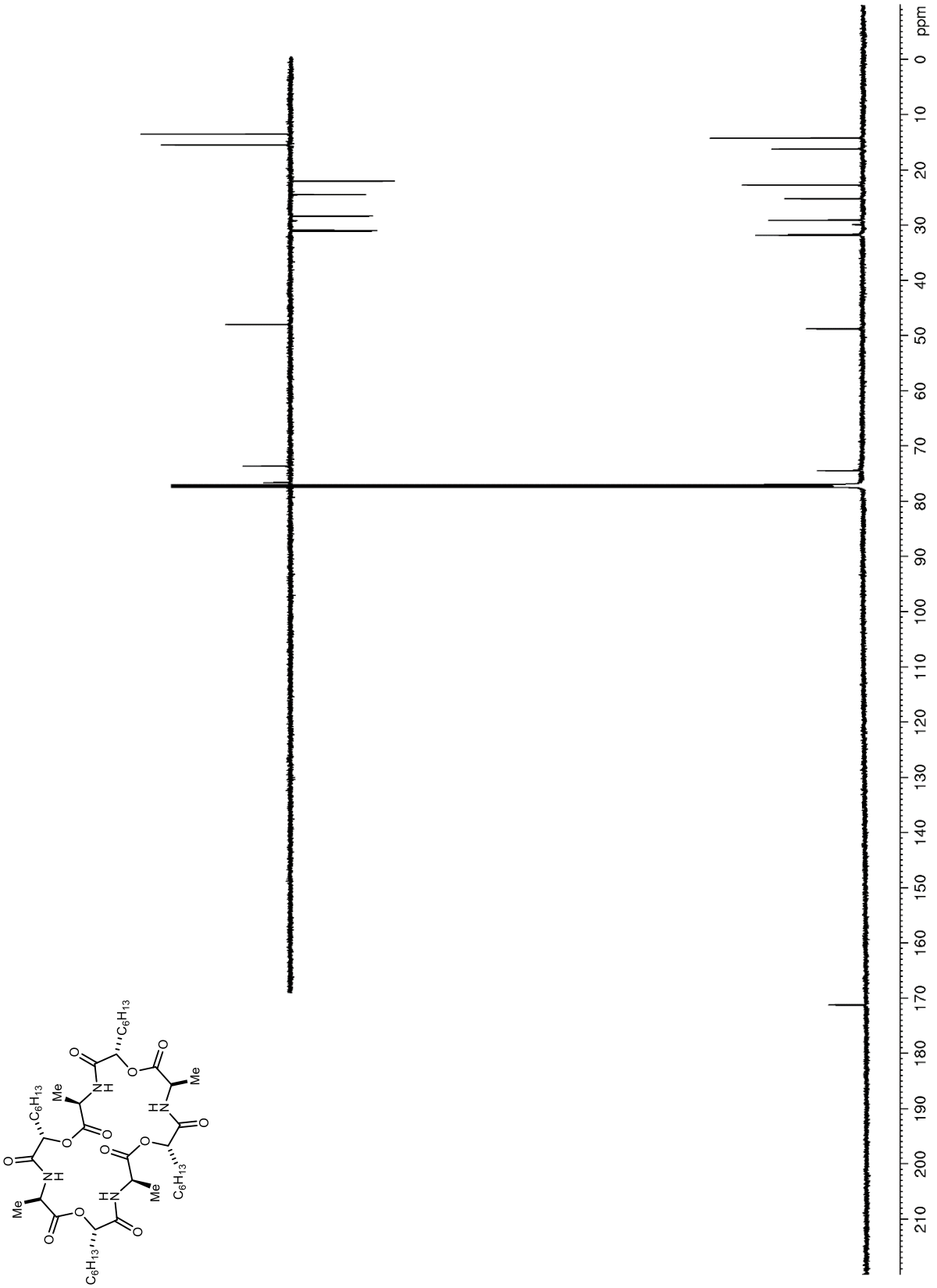

Figure S48. ^{1}H NMR (600 MHz, $CDCl_3$) of **34**

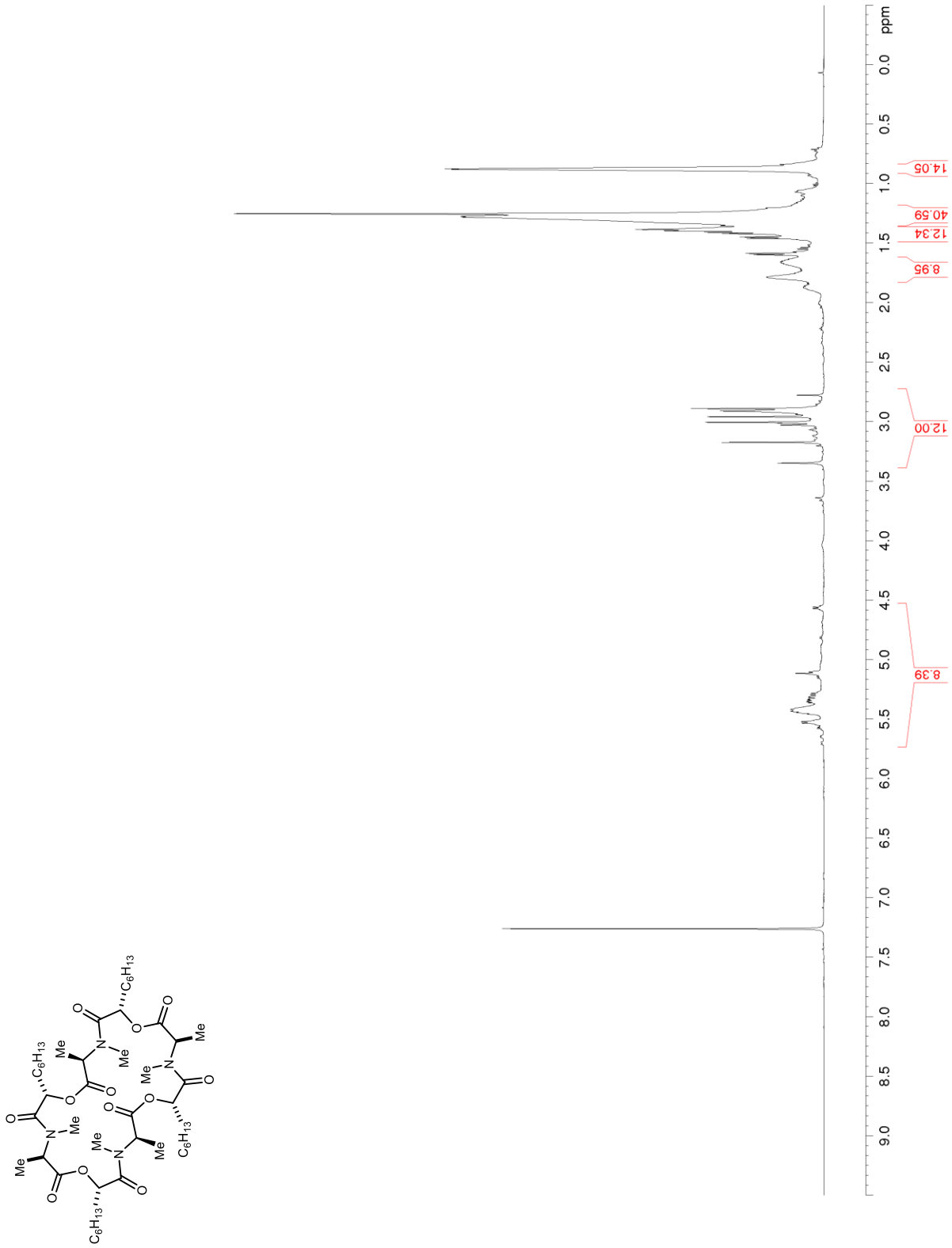

Figure S49. 13C NMR/DEPT (150 MHz, CDCl3) of **34**

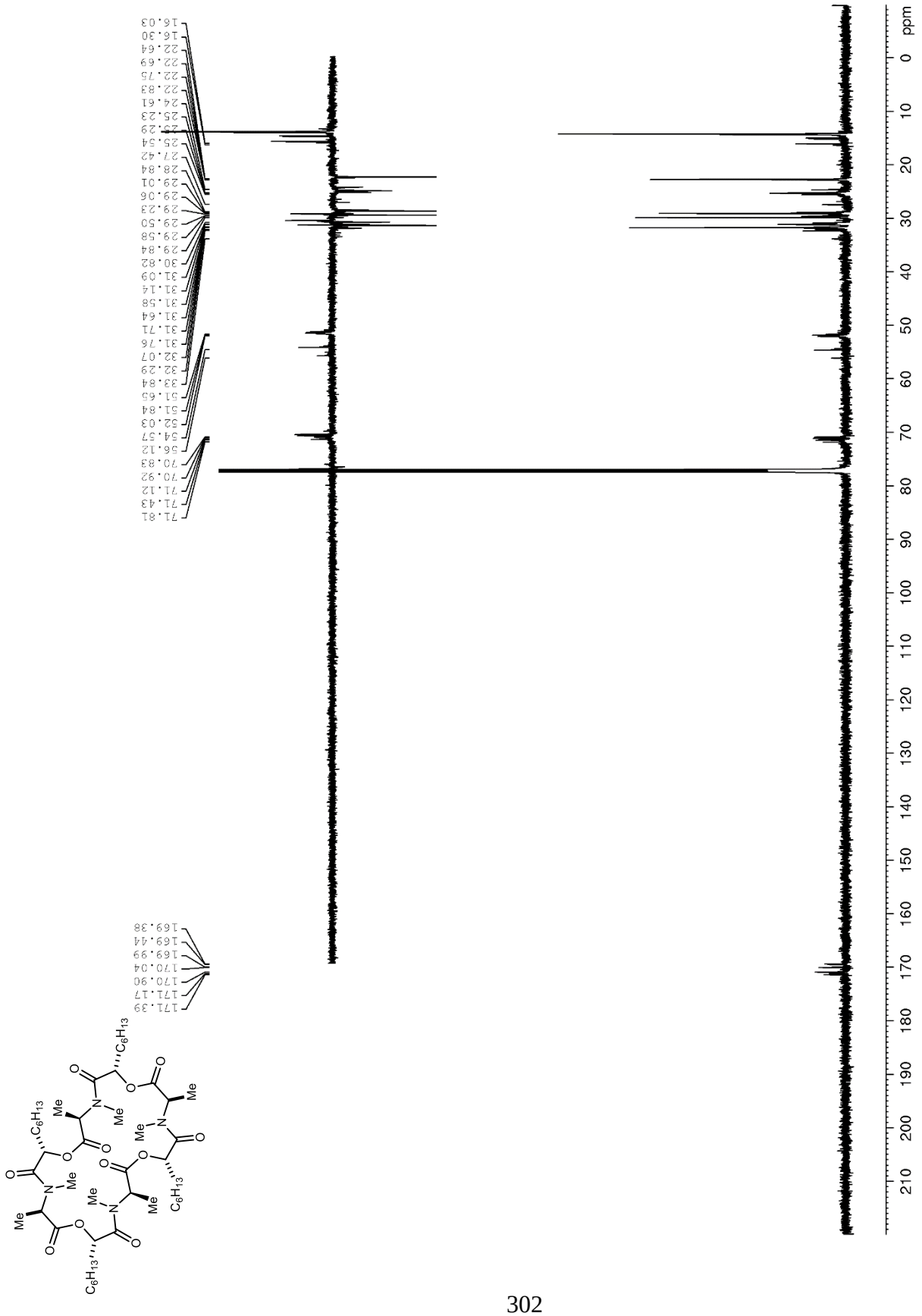

Figure S50. ^{1}H NMR (600 MHz, $CDCl_3$) of **S15**

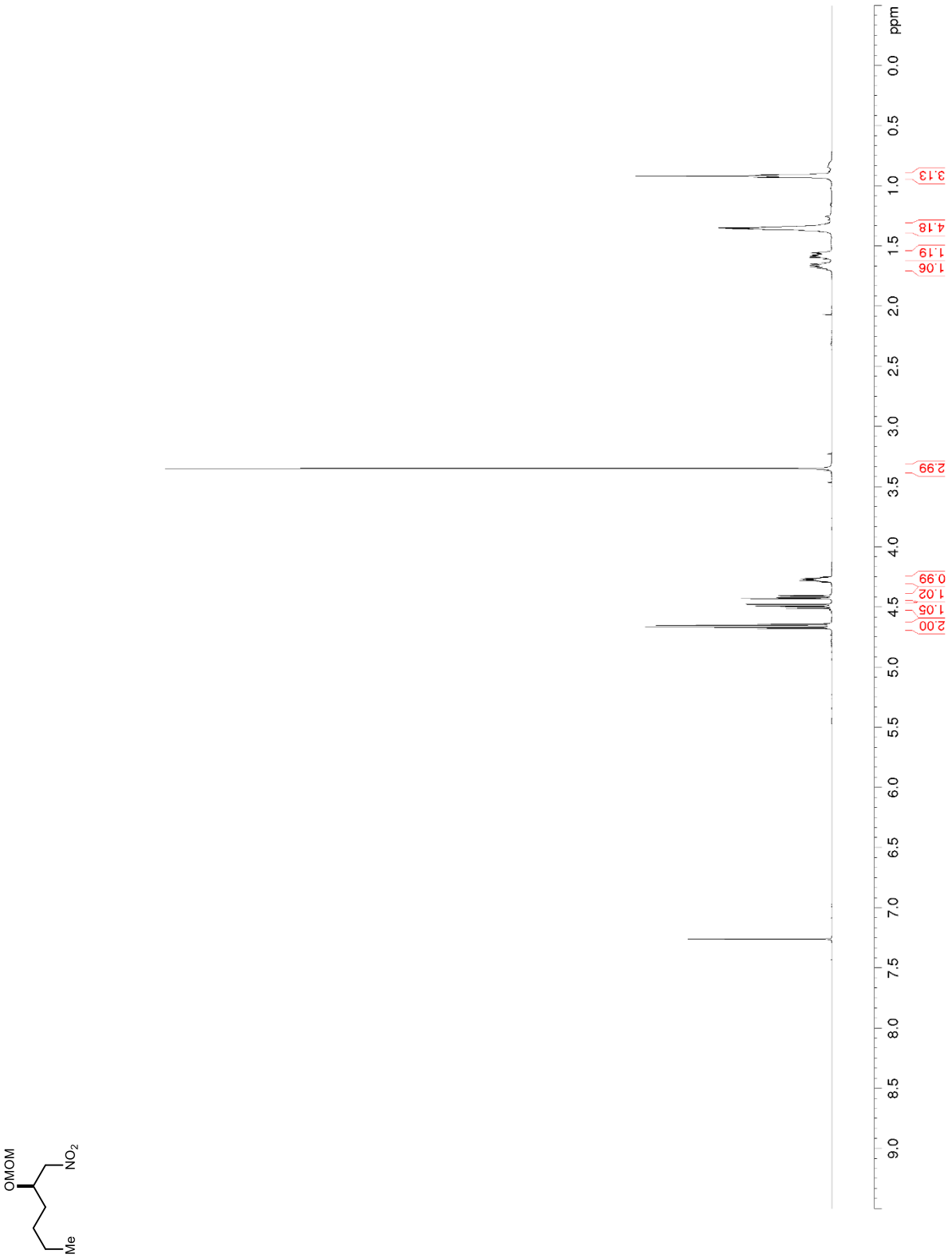

Figure S51. ^{13}C NMR/DEPT (150 MHz, $CDCl_3$) of **S15**

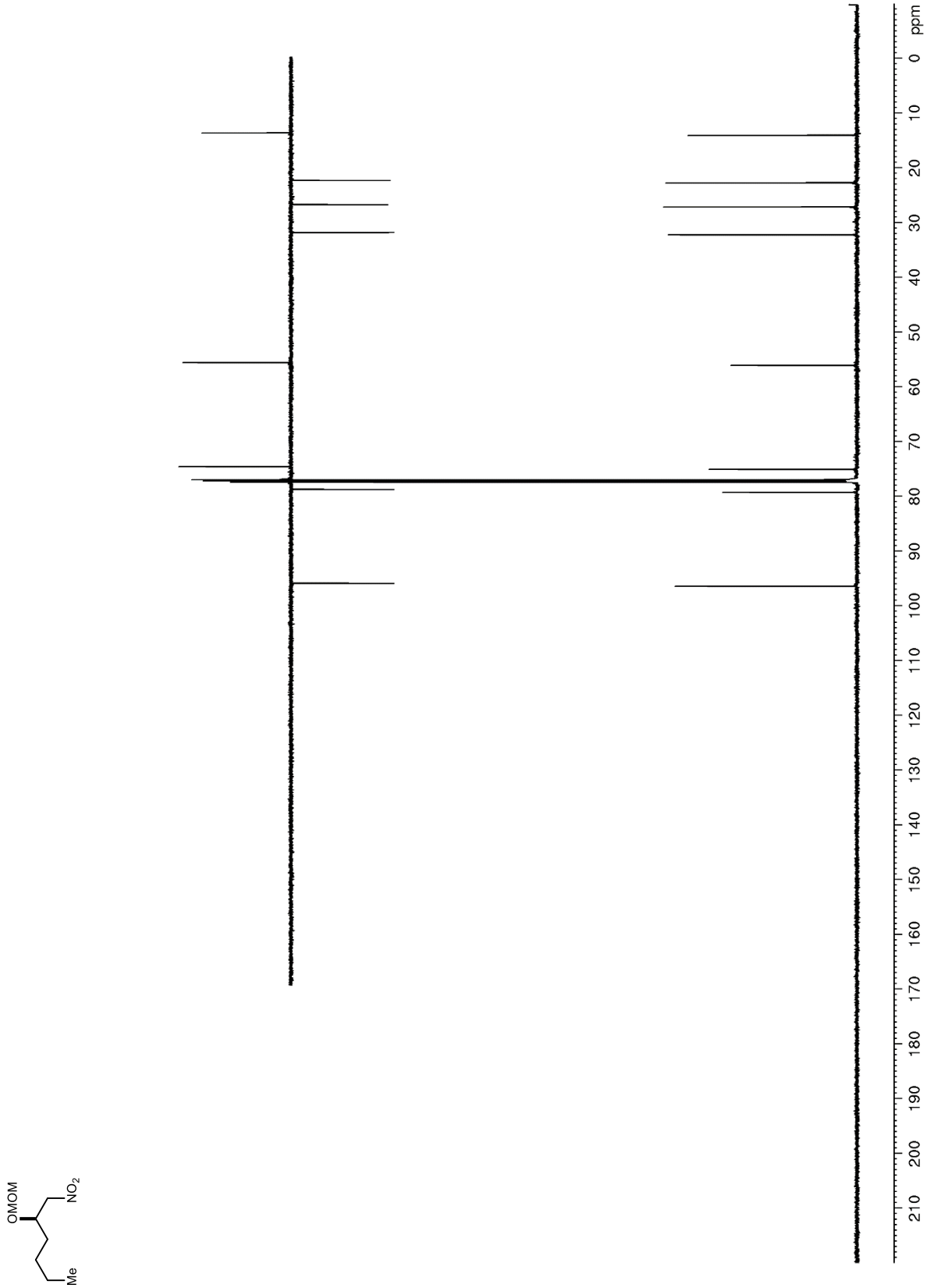

Figure S52. ^{1}H NMR (600 MHz, $CDCl_3$) of **S16**

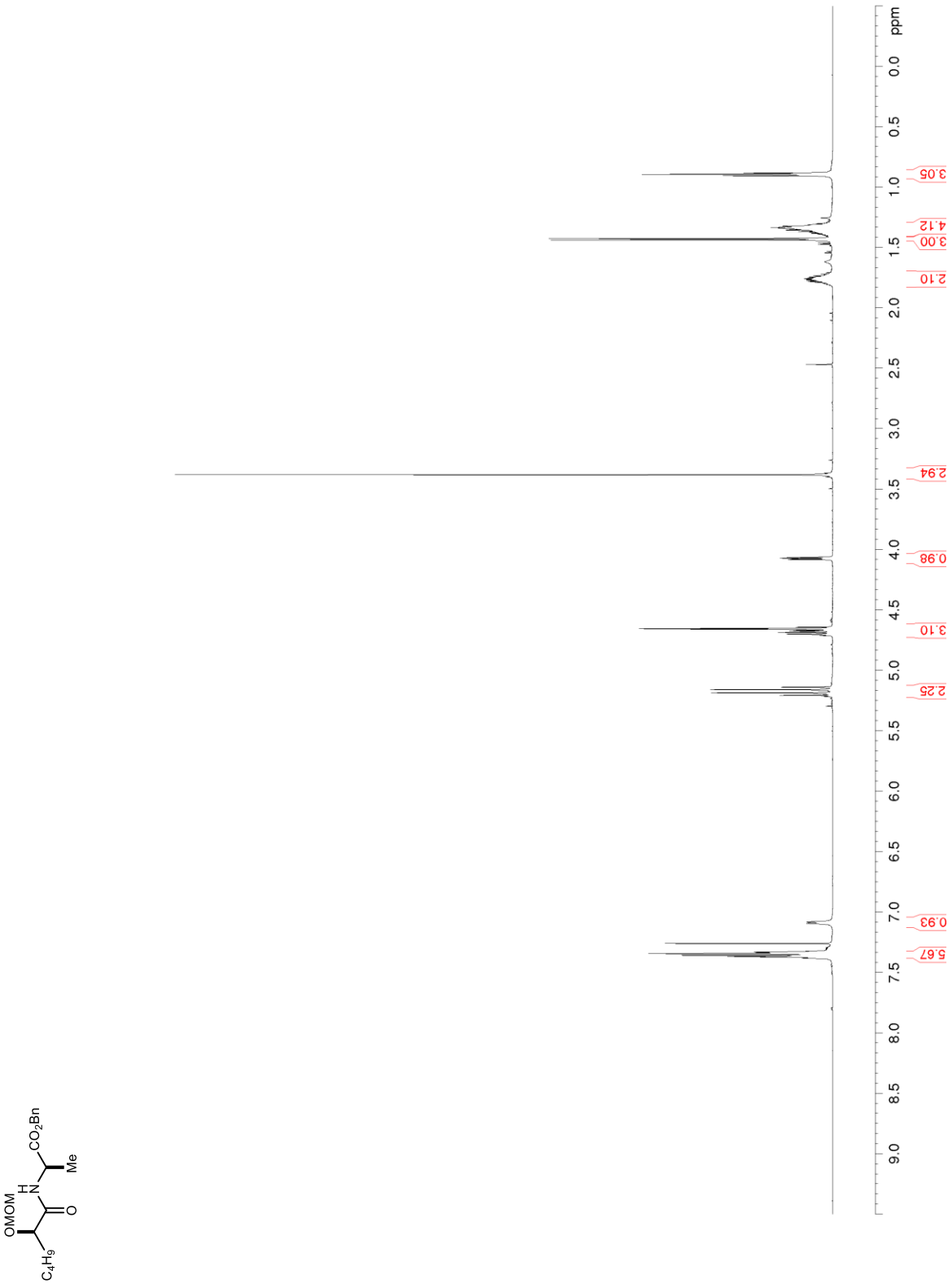

Figure S53. ^{13}C NMR/DEPT (150 MHz, $CDCl_3$) of **S16**

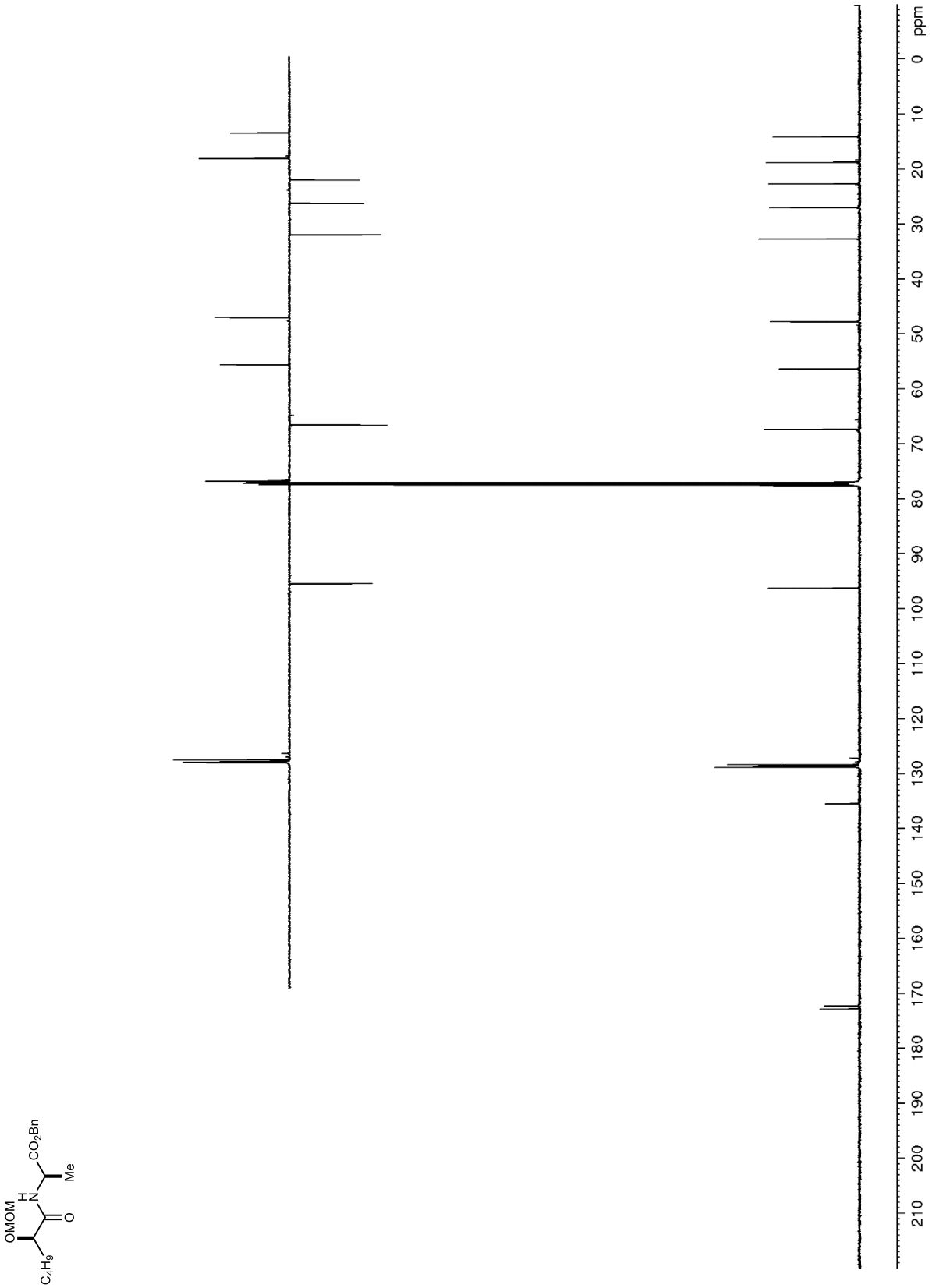

Figure S54. ^{1}H NMR (600 MHz, $CDCl_3$) of **S17**

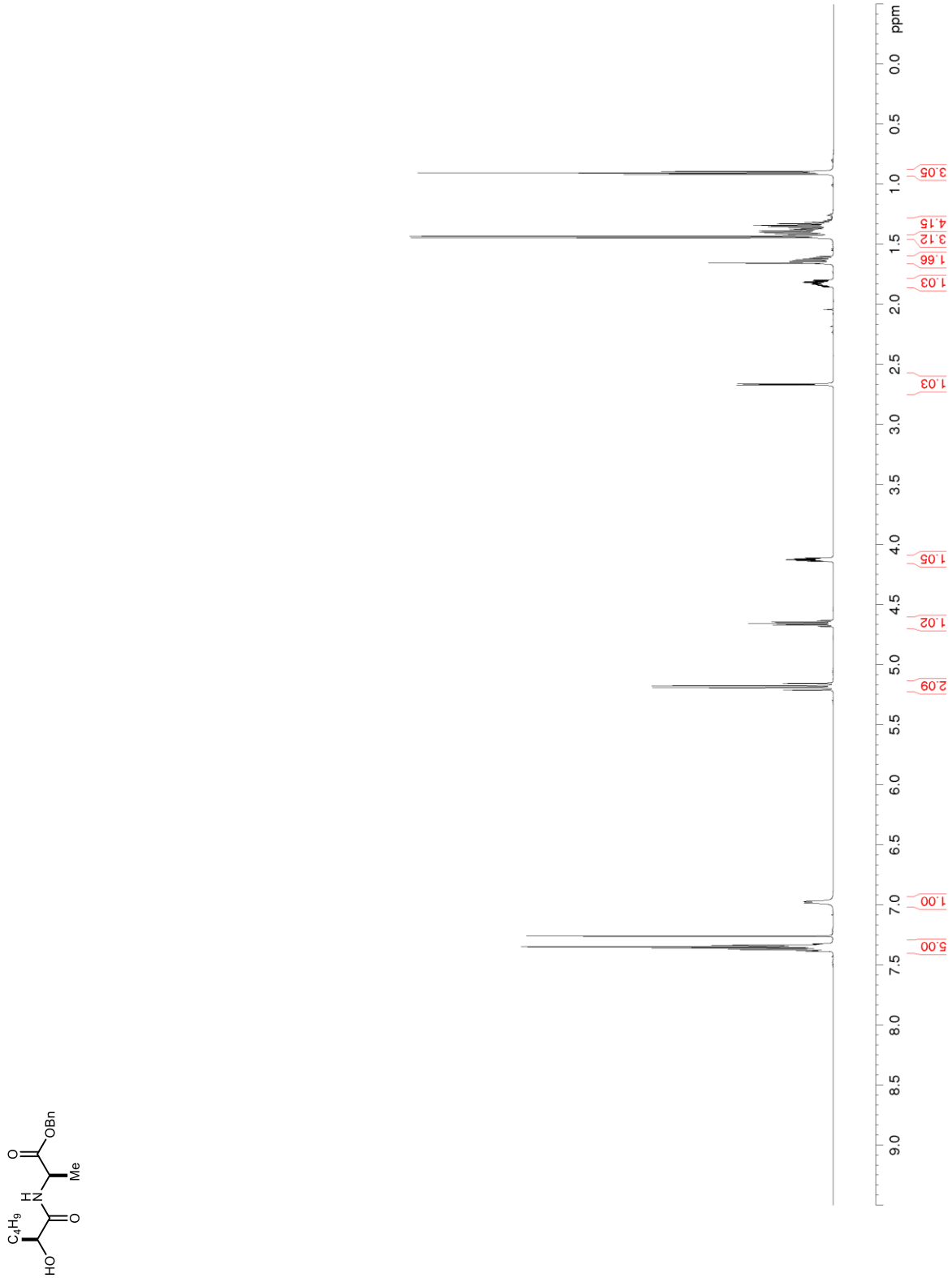

Figure S55. ^{13}C NMR/DEPT (150 MHz, $CDCl_3$) of **S17**

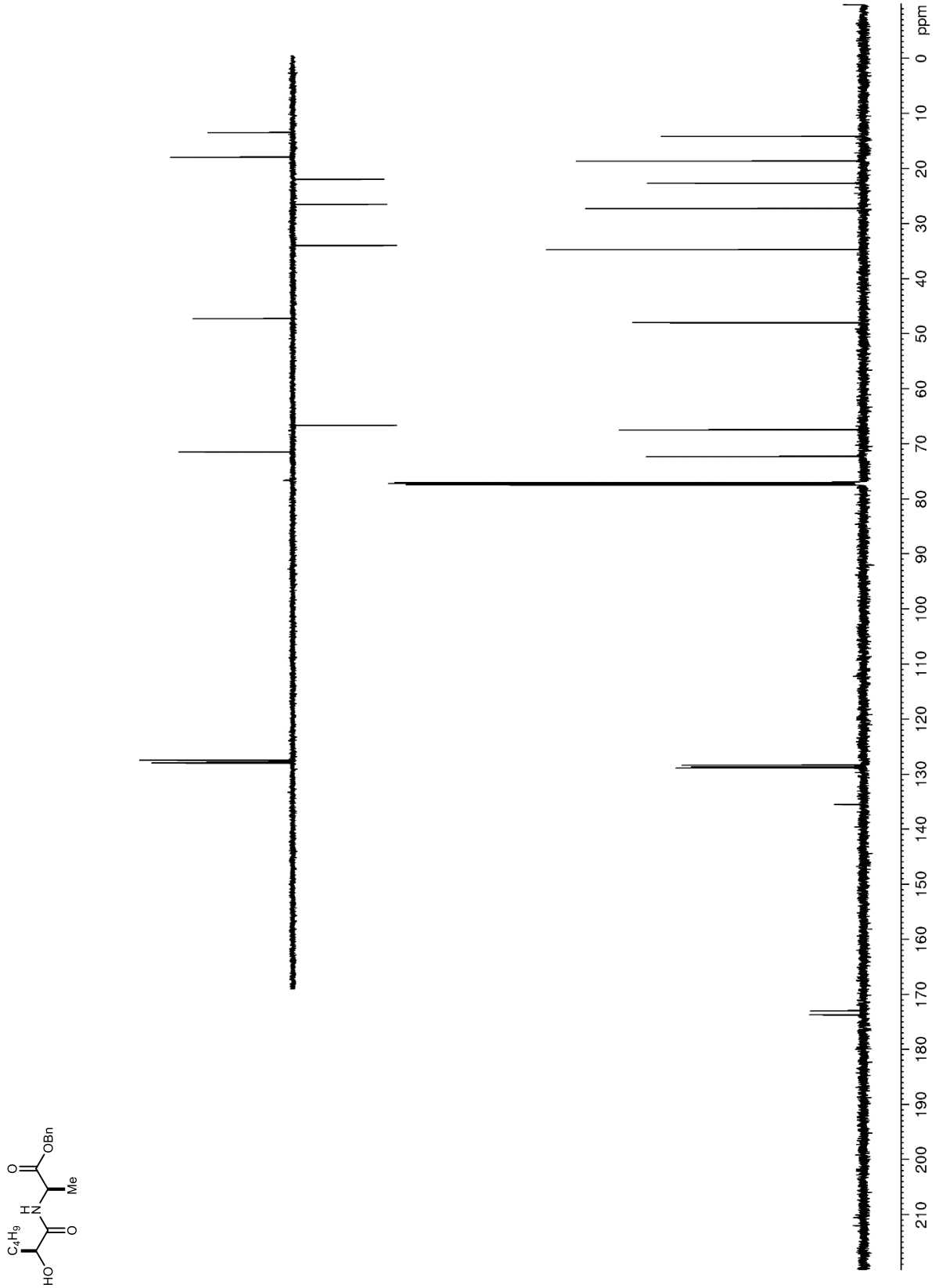

Figure S56. ^{1}H NMR (600 MHz, $CDCl_3$) of **S18**

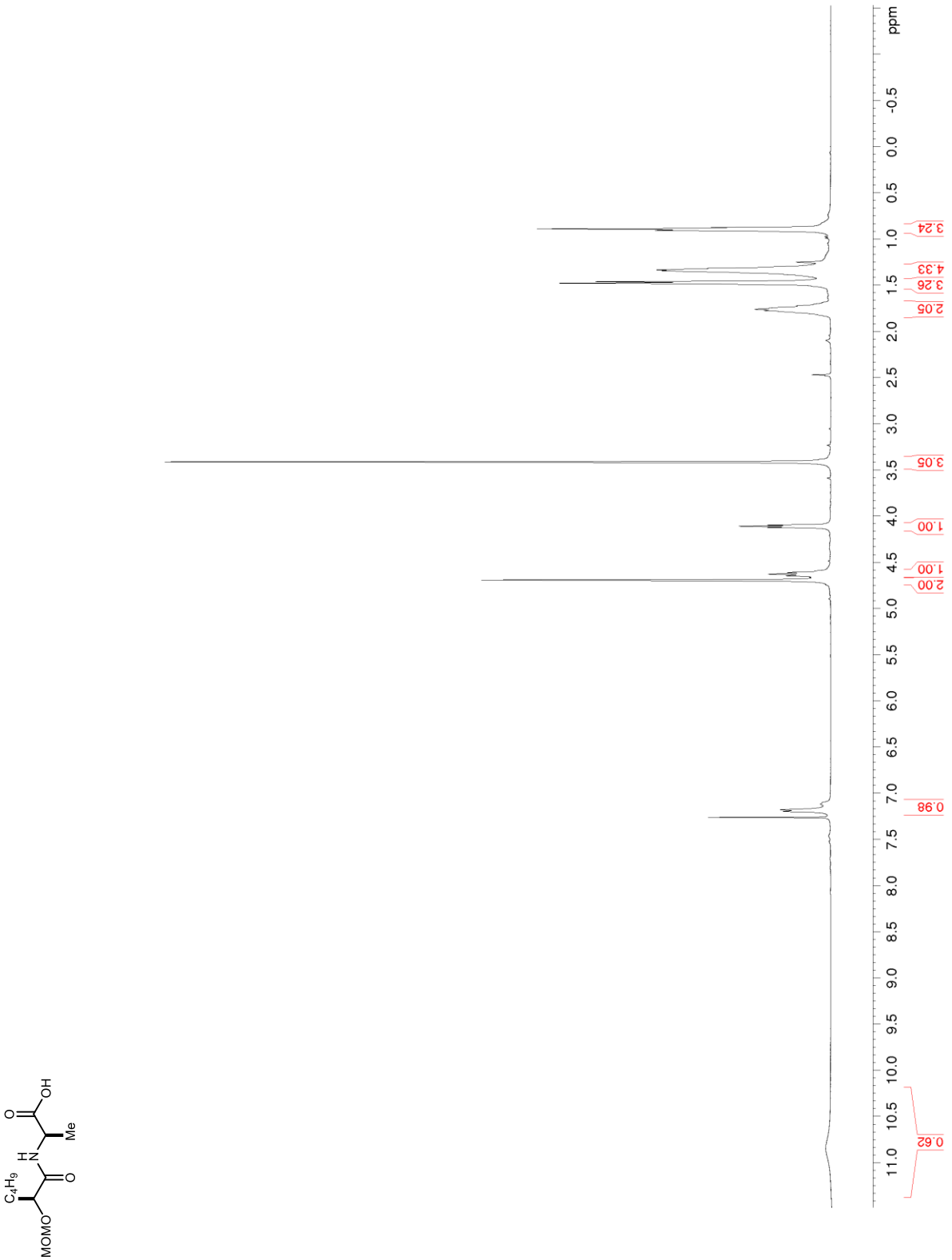

Figure S57. ^{13}C NMR/DEPT (150 MHz, $CDCl_3$) of **S18**

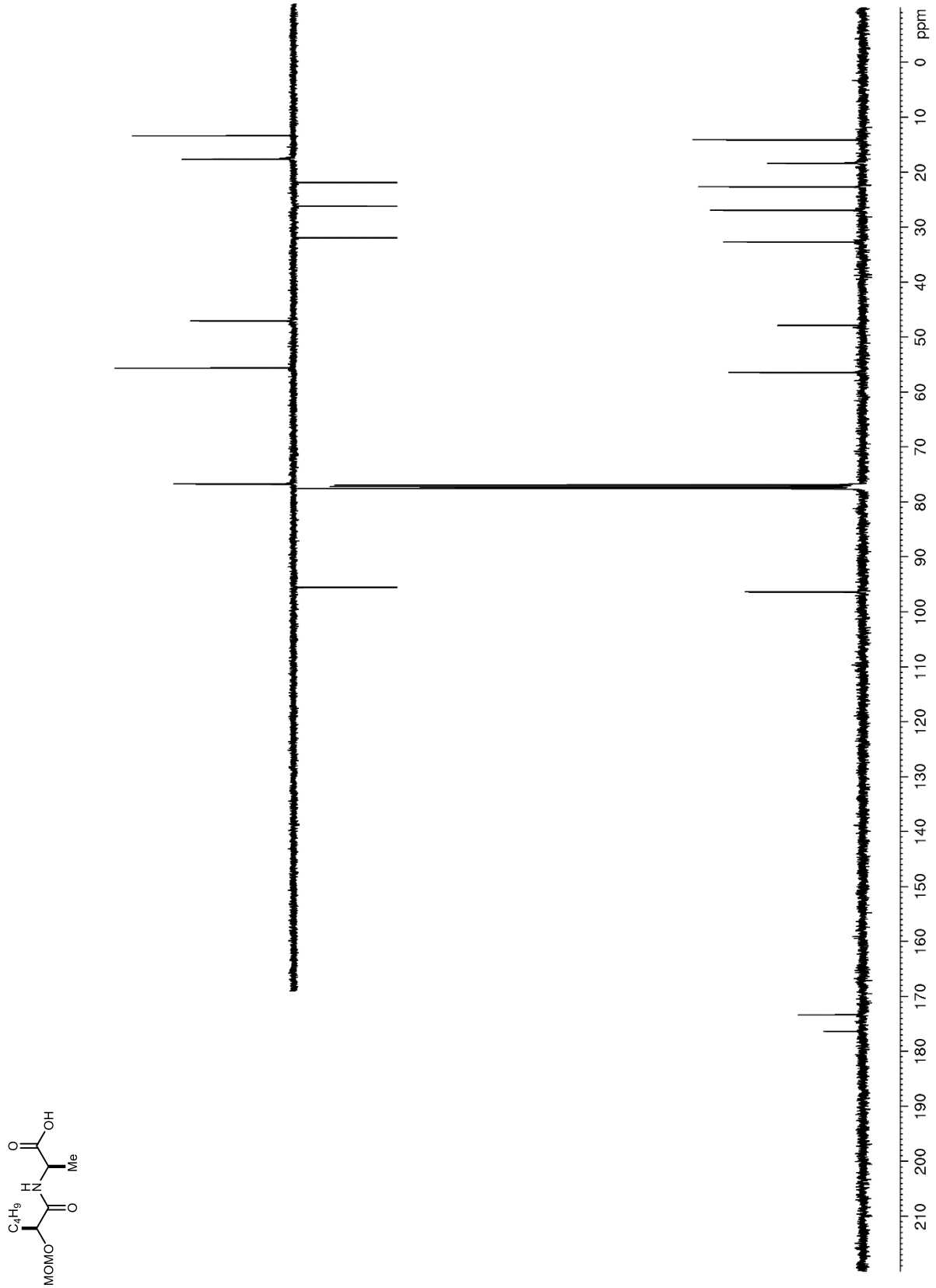

Figure S58. ^{1}H NMR (600 MHz, $CDCl_3$) of **S19**

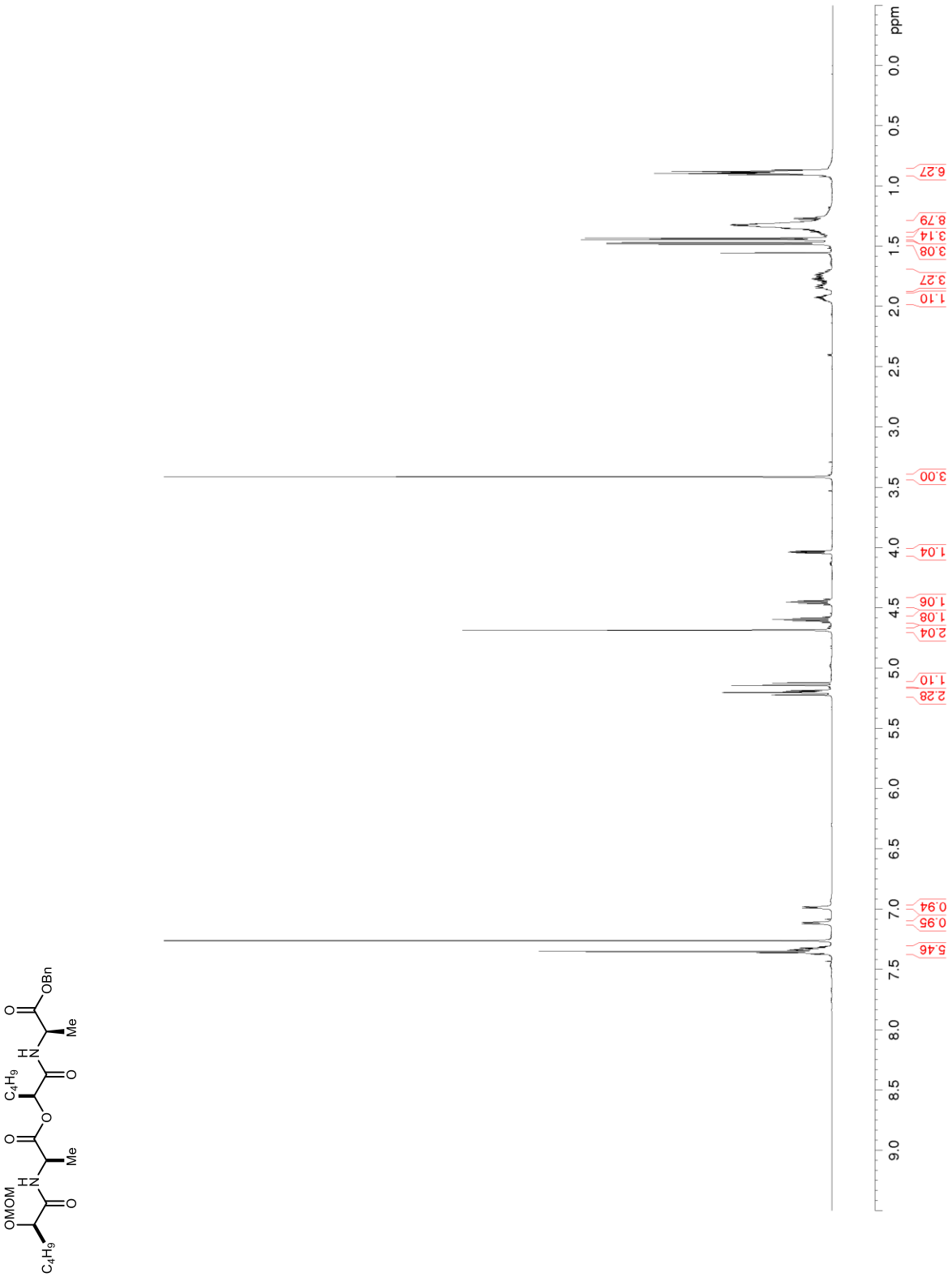

Figure S59. ^{13}C NMR/DEPT (150 MHz, $CDCl_3$) of **S19**

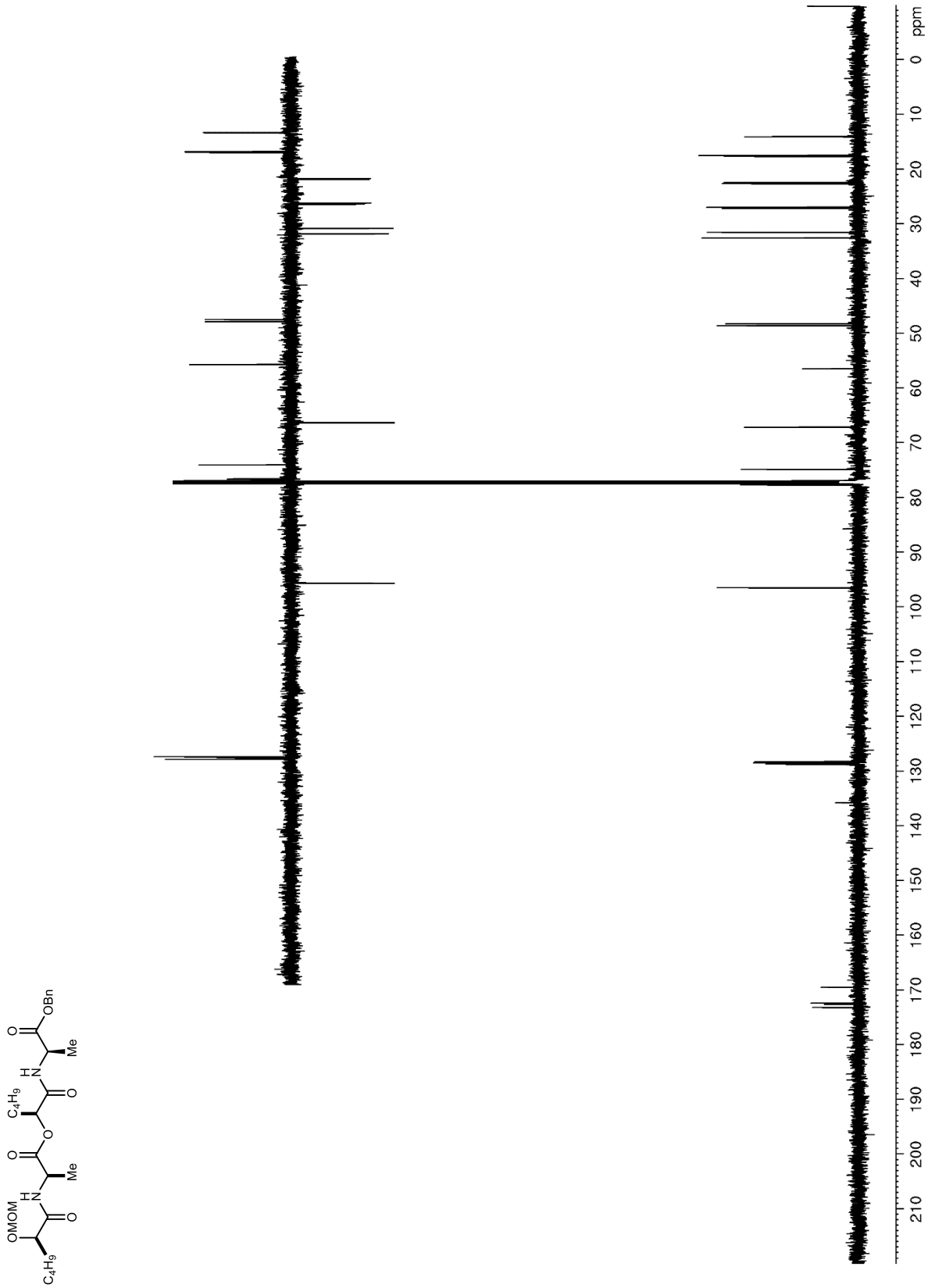

Figure S60. ^{1}H NMR (600 MHz, $CDCl_3$) of **S20**

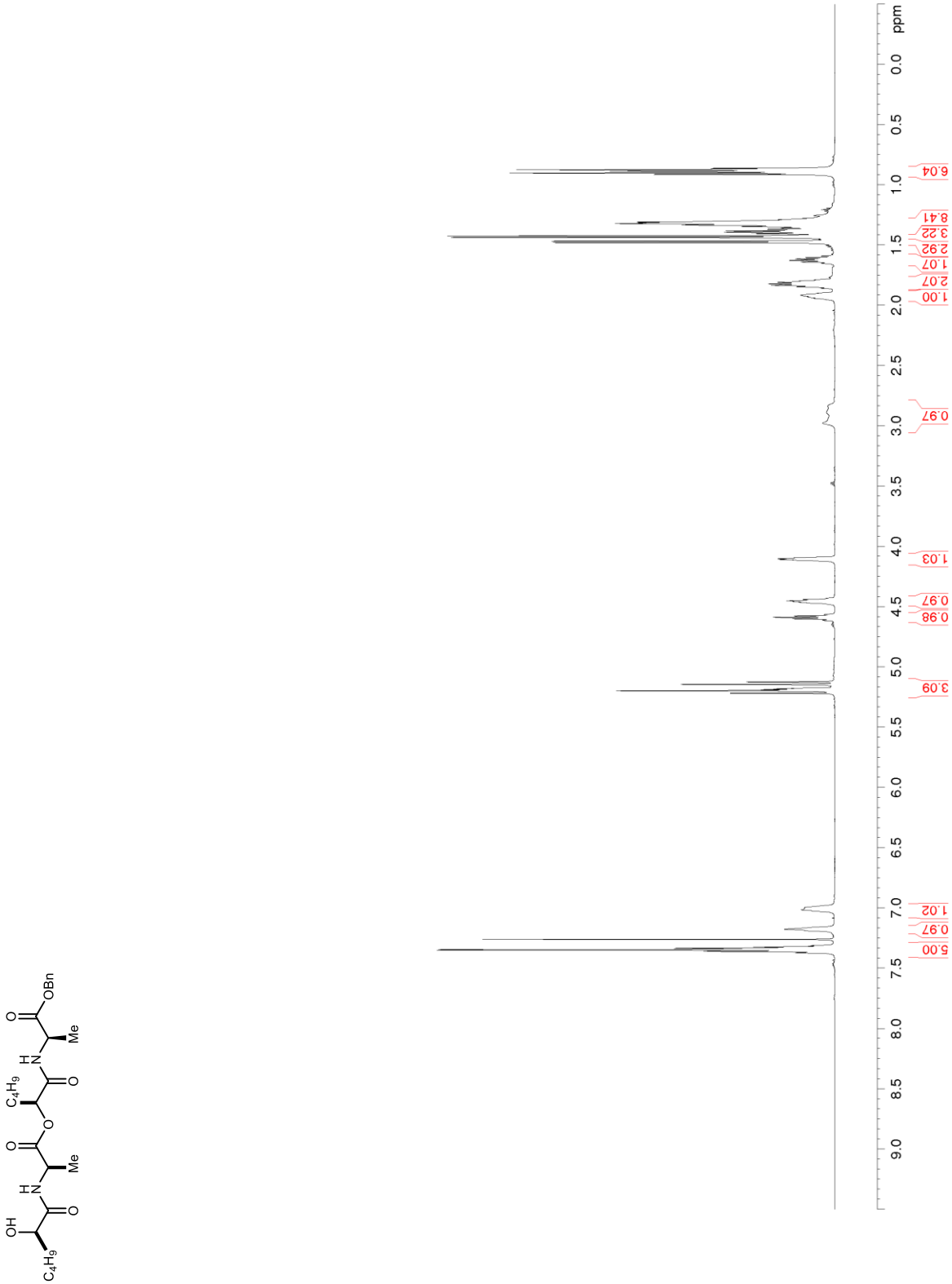

Figure S61. ^{13}C NMR/DEPT (150 MHz, $CDCl_3$) of **S20**

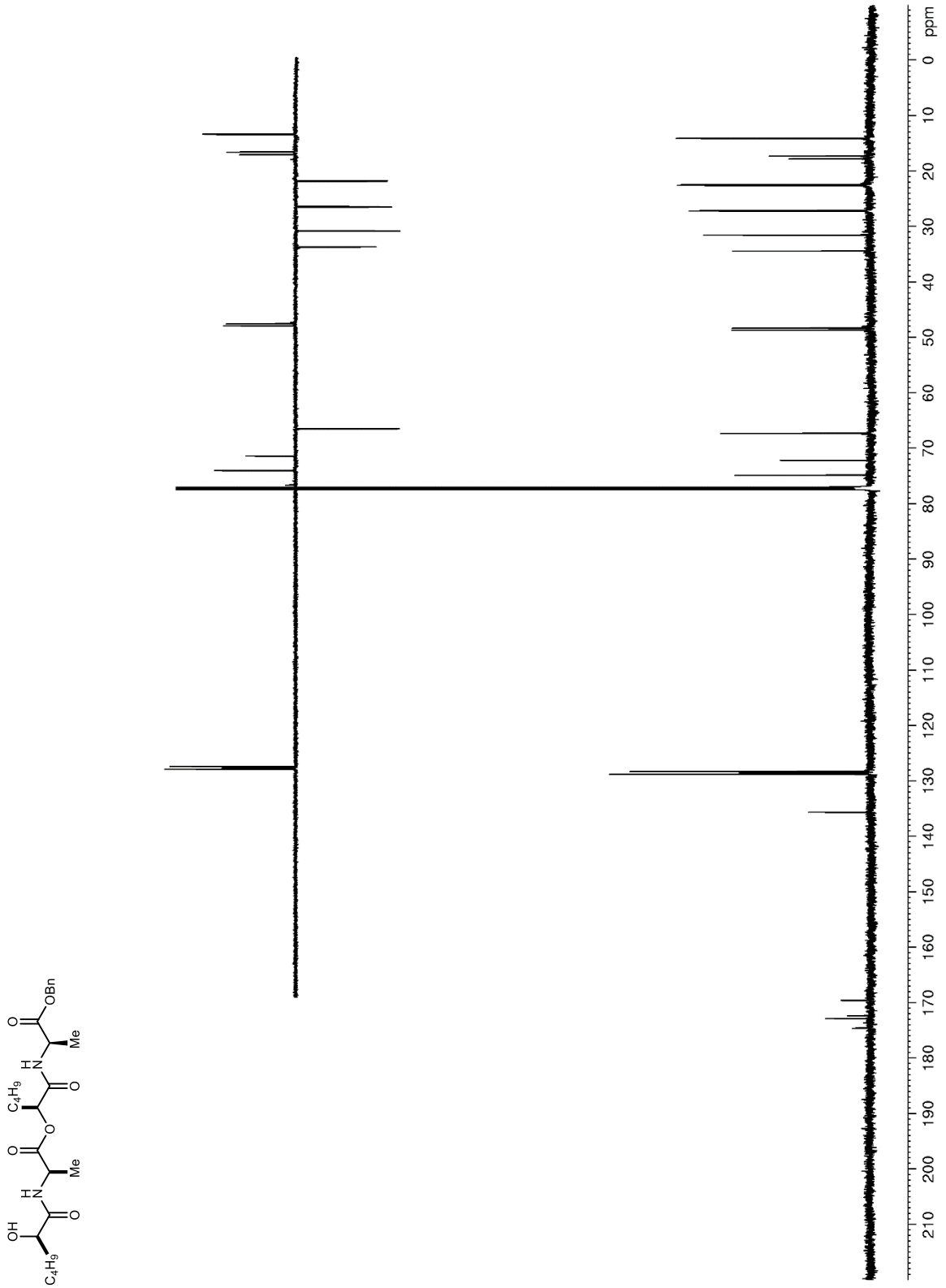

Figure S62. ^{1}H NMR (600 MHz, $CDCl_3$) of **S21**

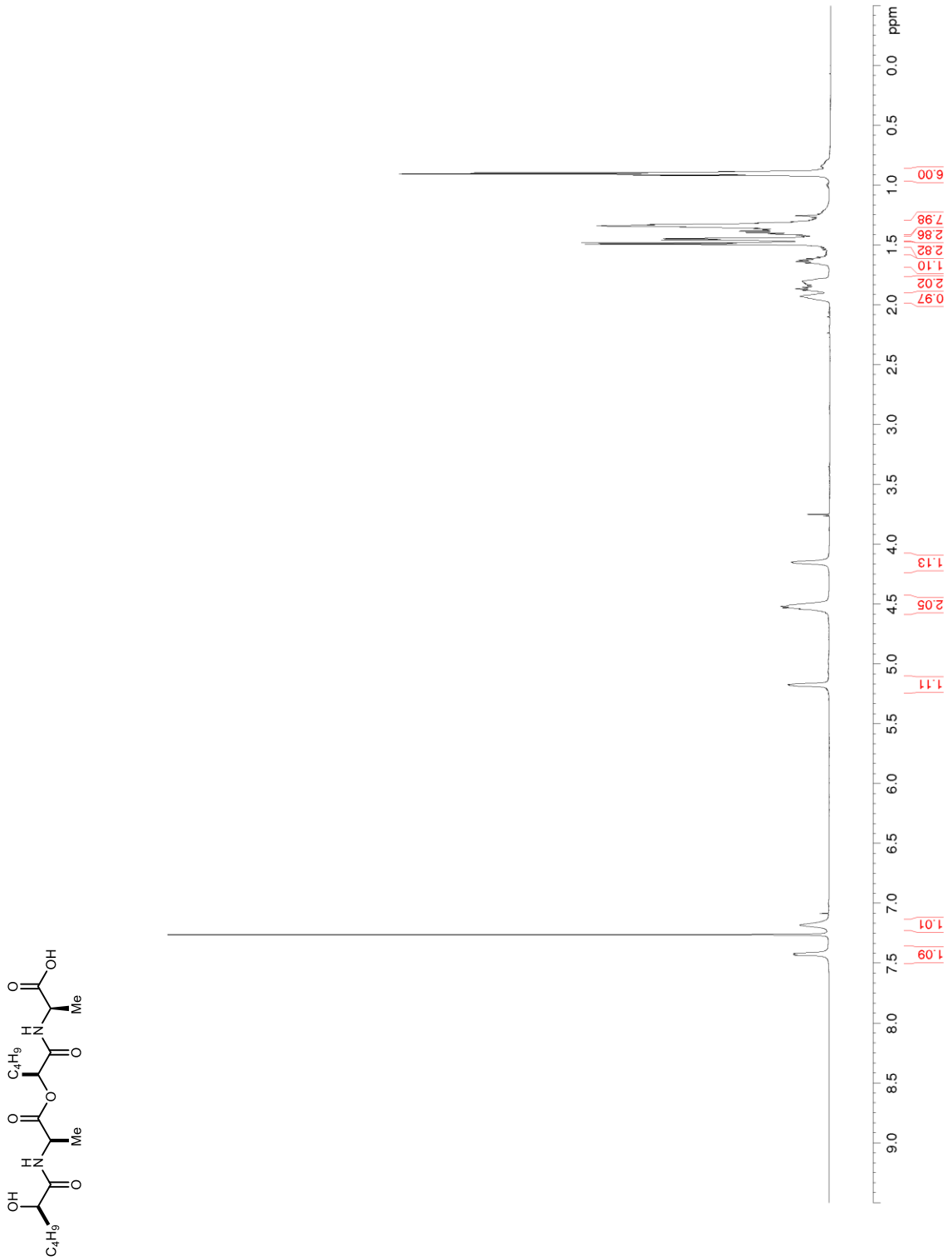

Figure S63. ^{13}C NMR/DEPT (150 MHz, $CDCl_3$) of **S21**

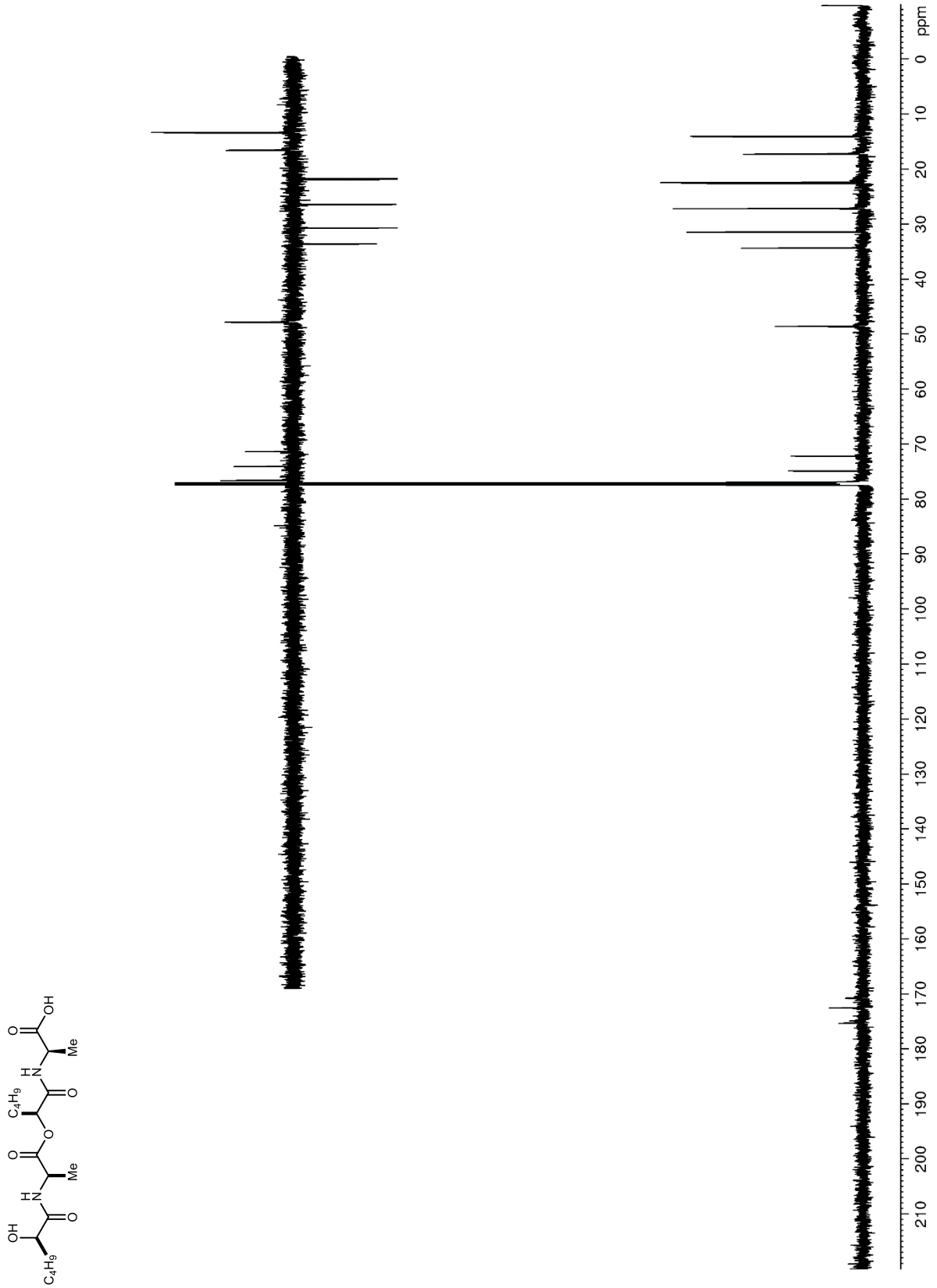

Figure S64. ^{1}H NMR (600 MHz, $CDCl_3$) of **S22**

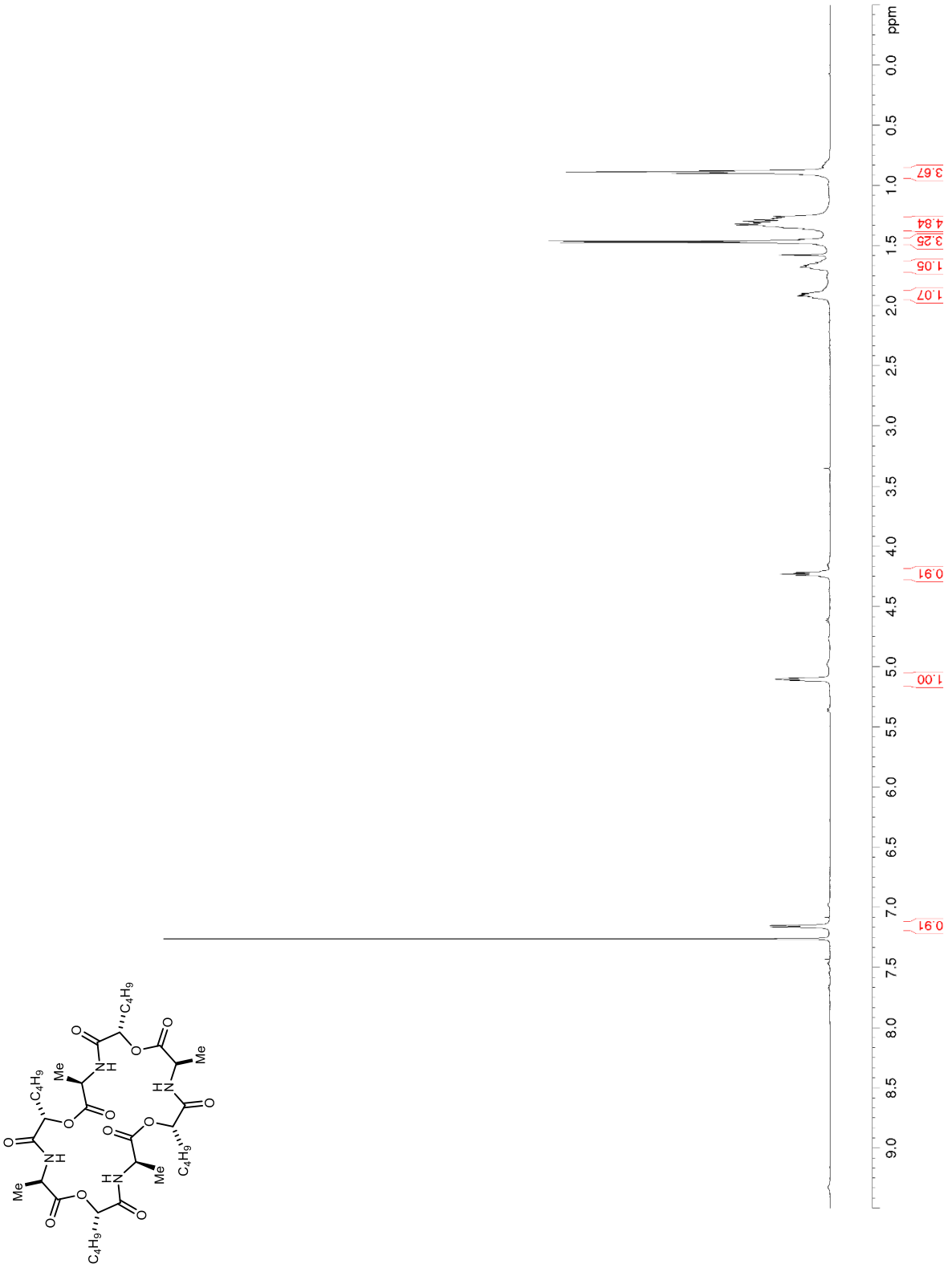

Figure S65. ^{13}C NMR/DEPT (150 MHz, $CDCl_3$) of **S22**

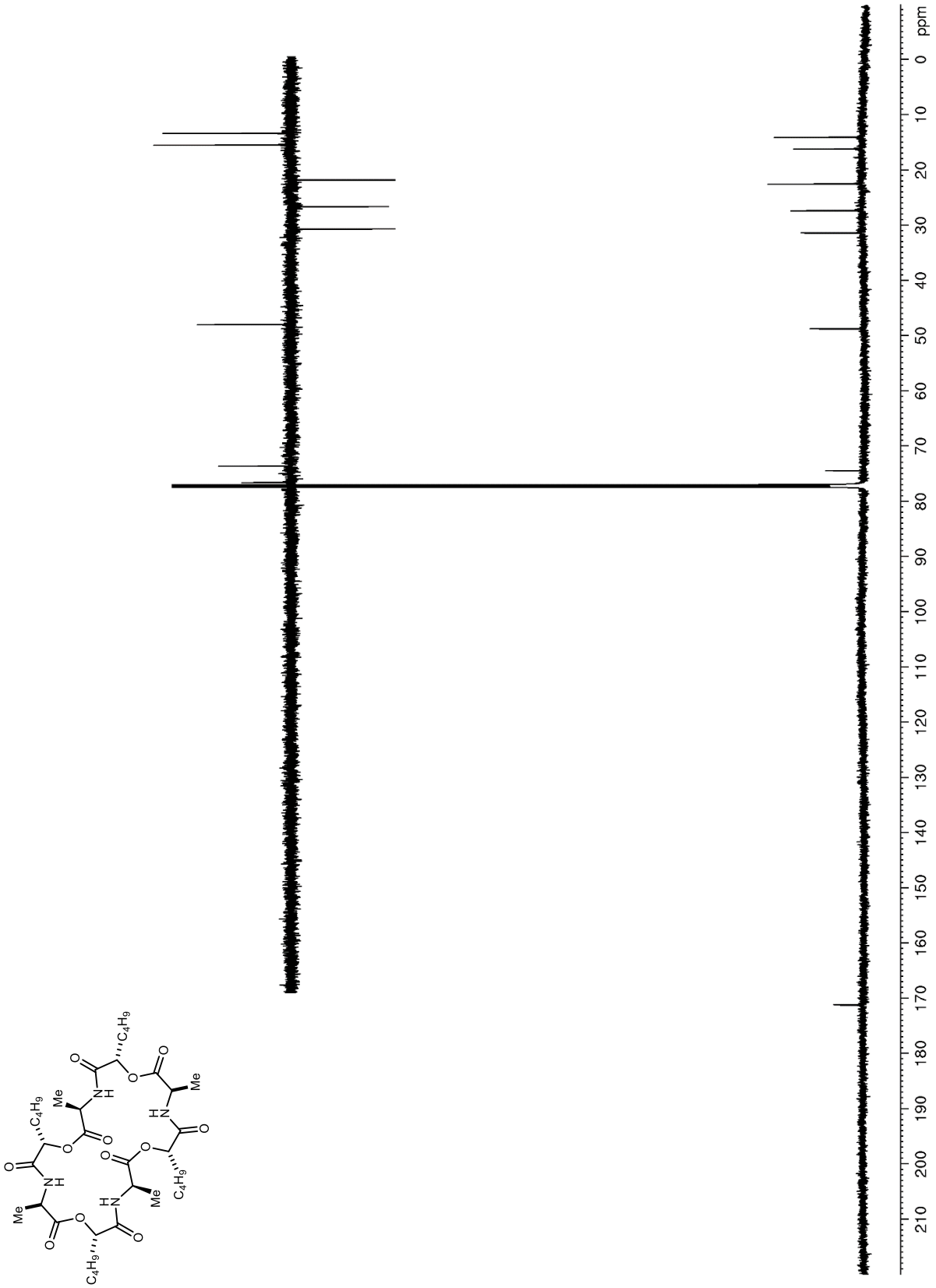

Figure S66. ^{1}H NMR (600 MHz, $CDCl_3$) of **35**

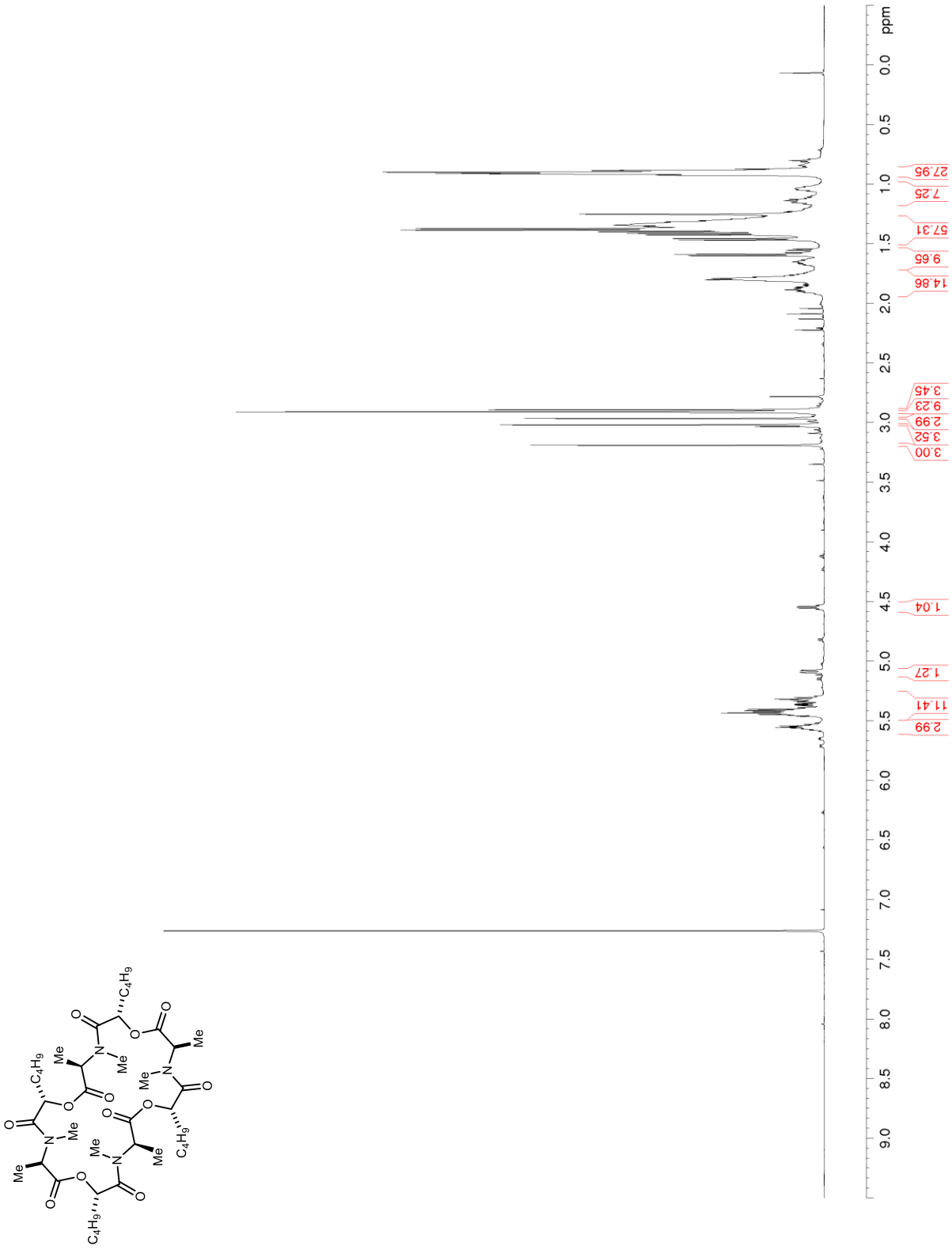

Figure S67. ^{13}C NMR/DEPT (150 MHz, CDCl3) of **35**

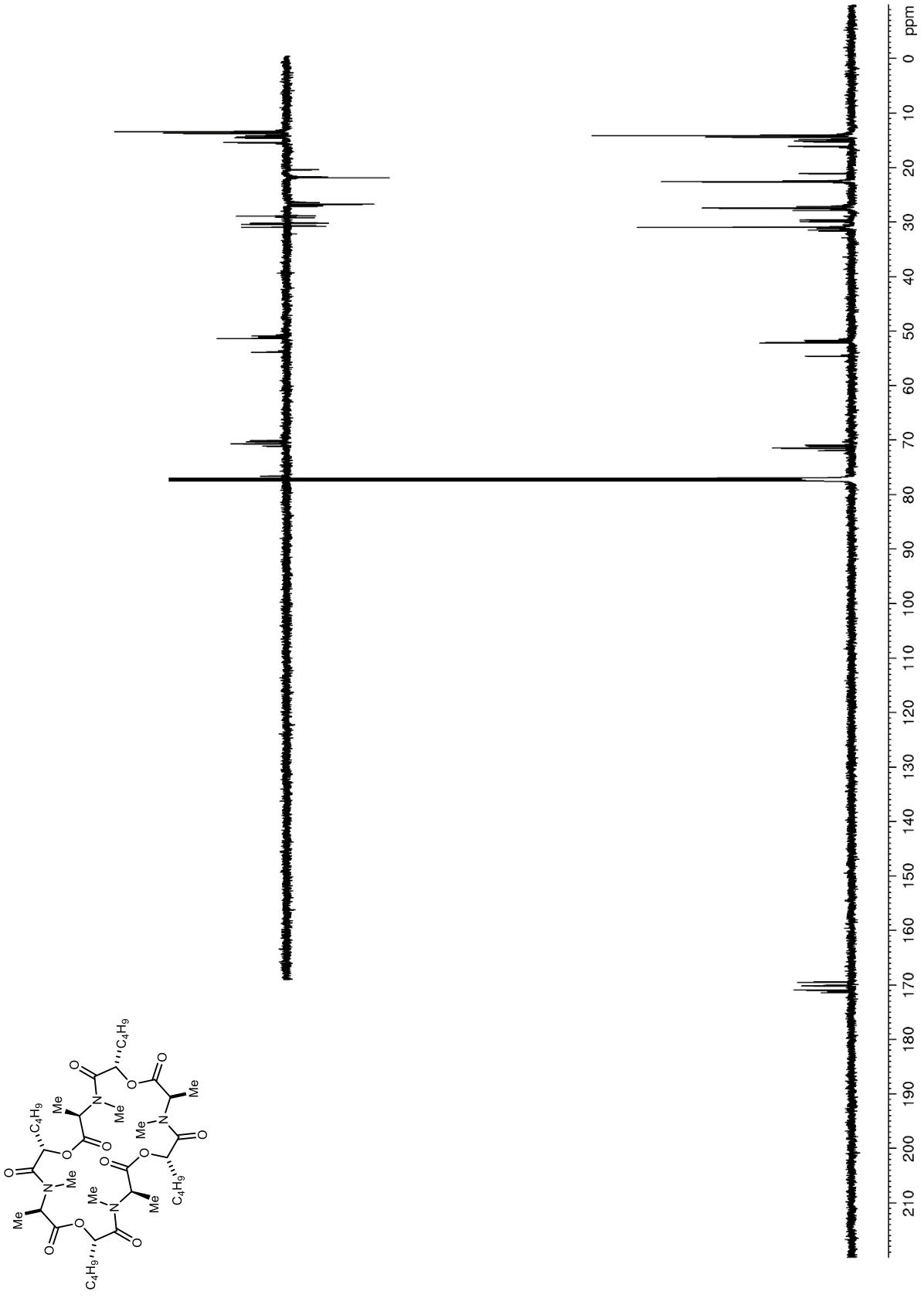

Figure S68. ^{1}H NMR (400 MHz, $CDCl_3$) of **39**

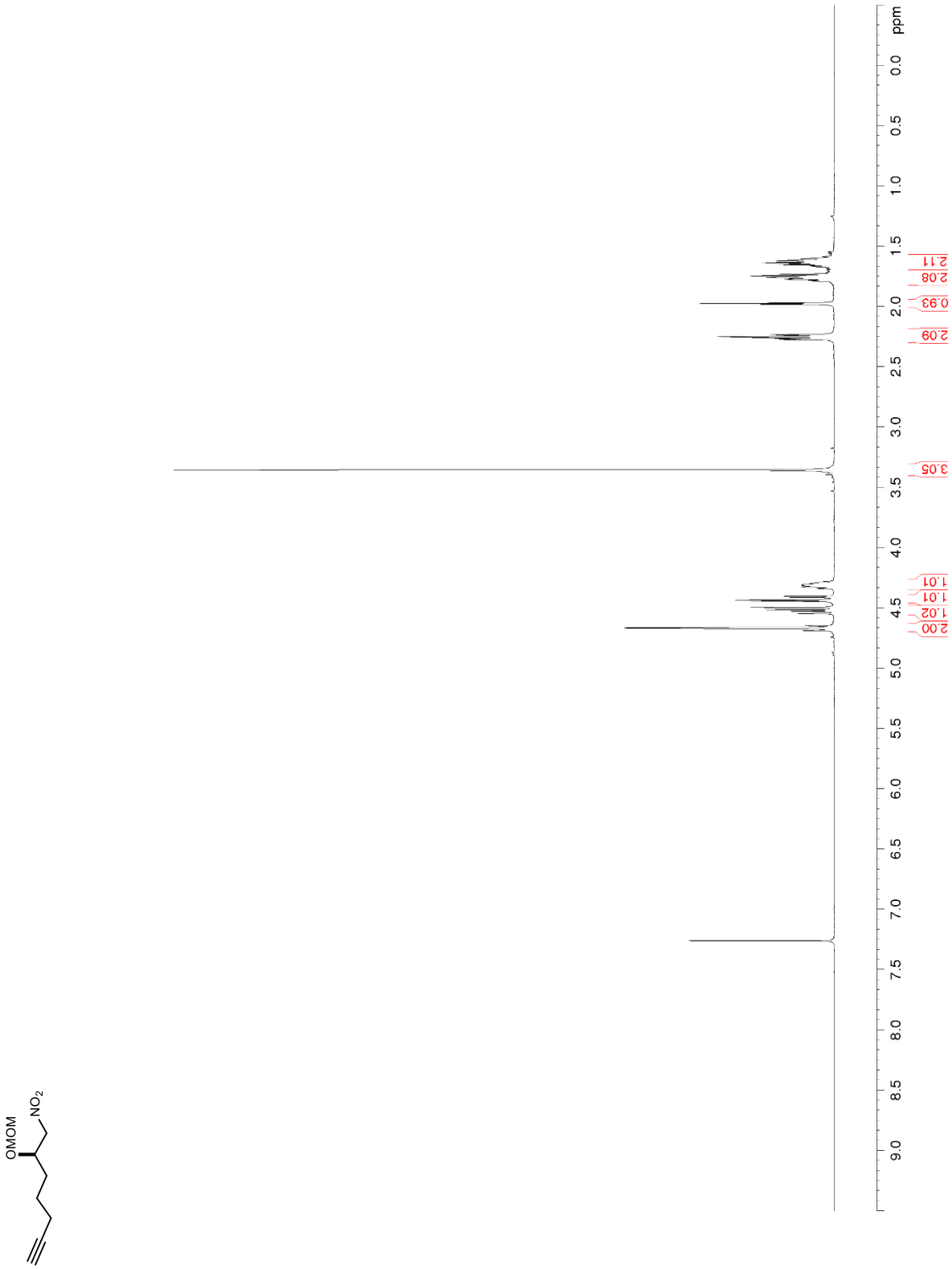

Figure S69. ^{13}C NMR/DEPT (100 MHz, $CDCl_3$) of **39**

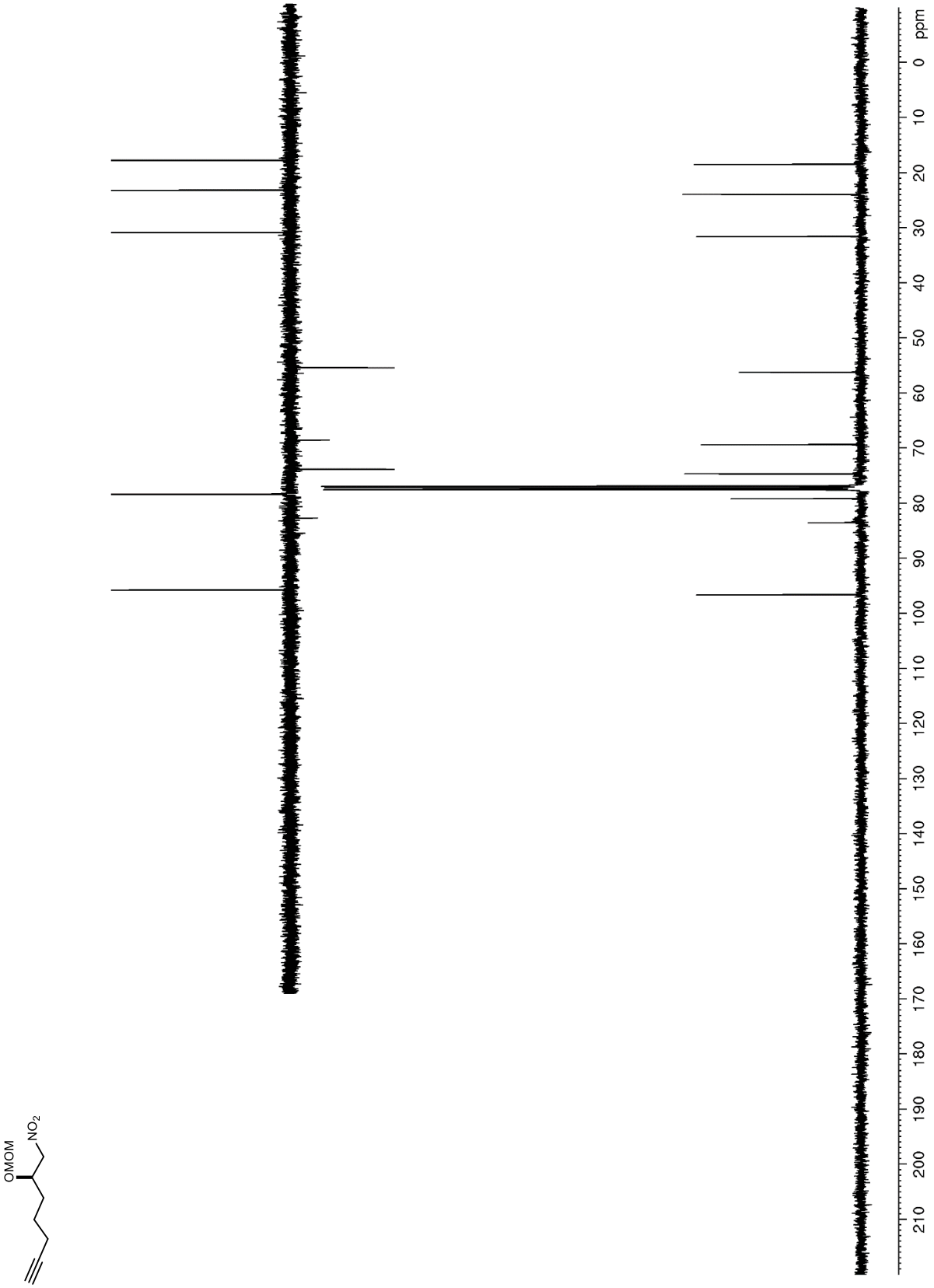

Figure S70. ^{1}H NMR (600 MHz, $CDCl_3$) of **S23**

Figure S71. ^{13}C NMR/DEPT (150 MHz, $CDCl_3$) of **S23**

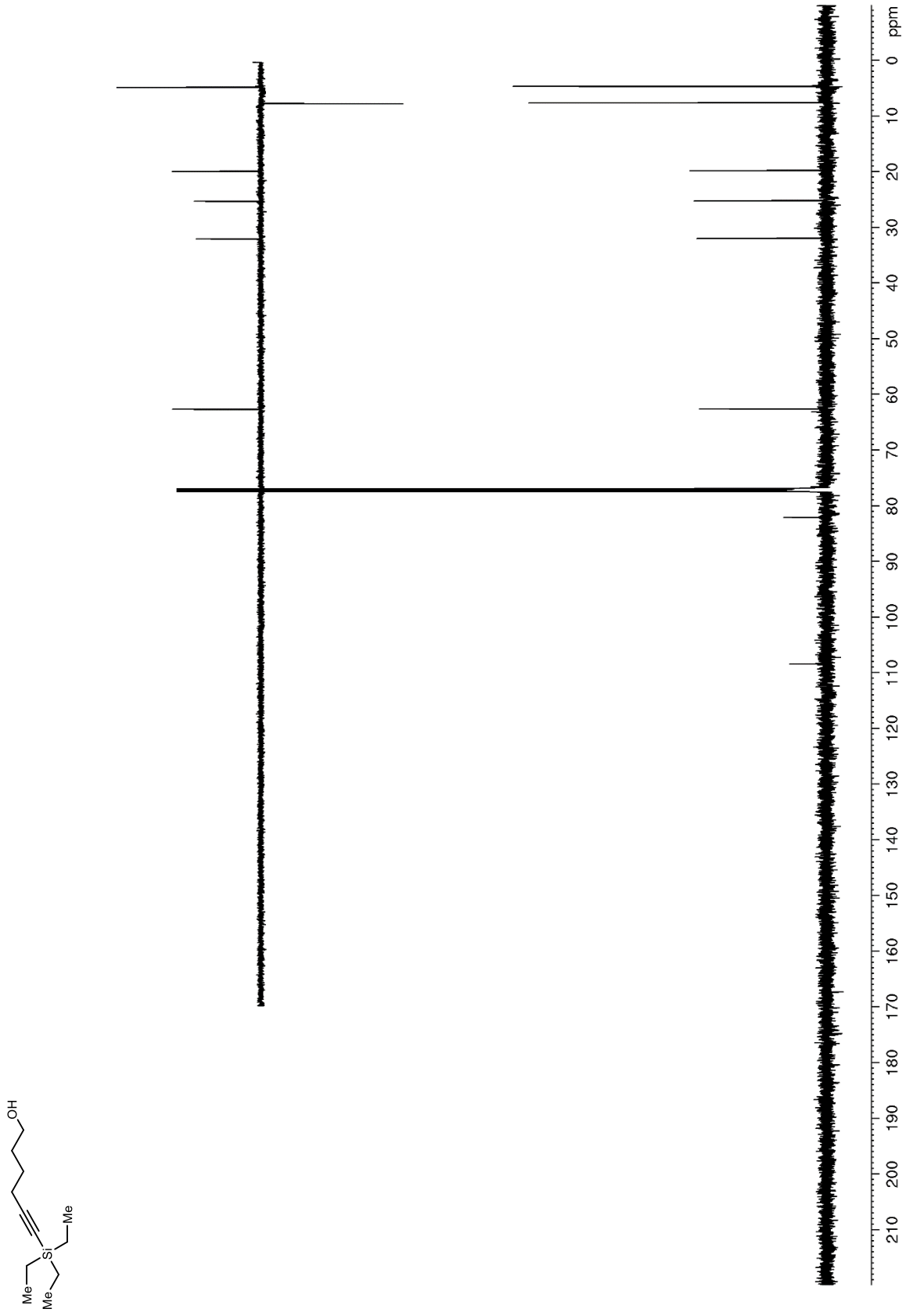

Figure S72. ^{1}H NMR (400 MHz, $CDCl_3$) of **47**

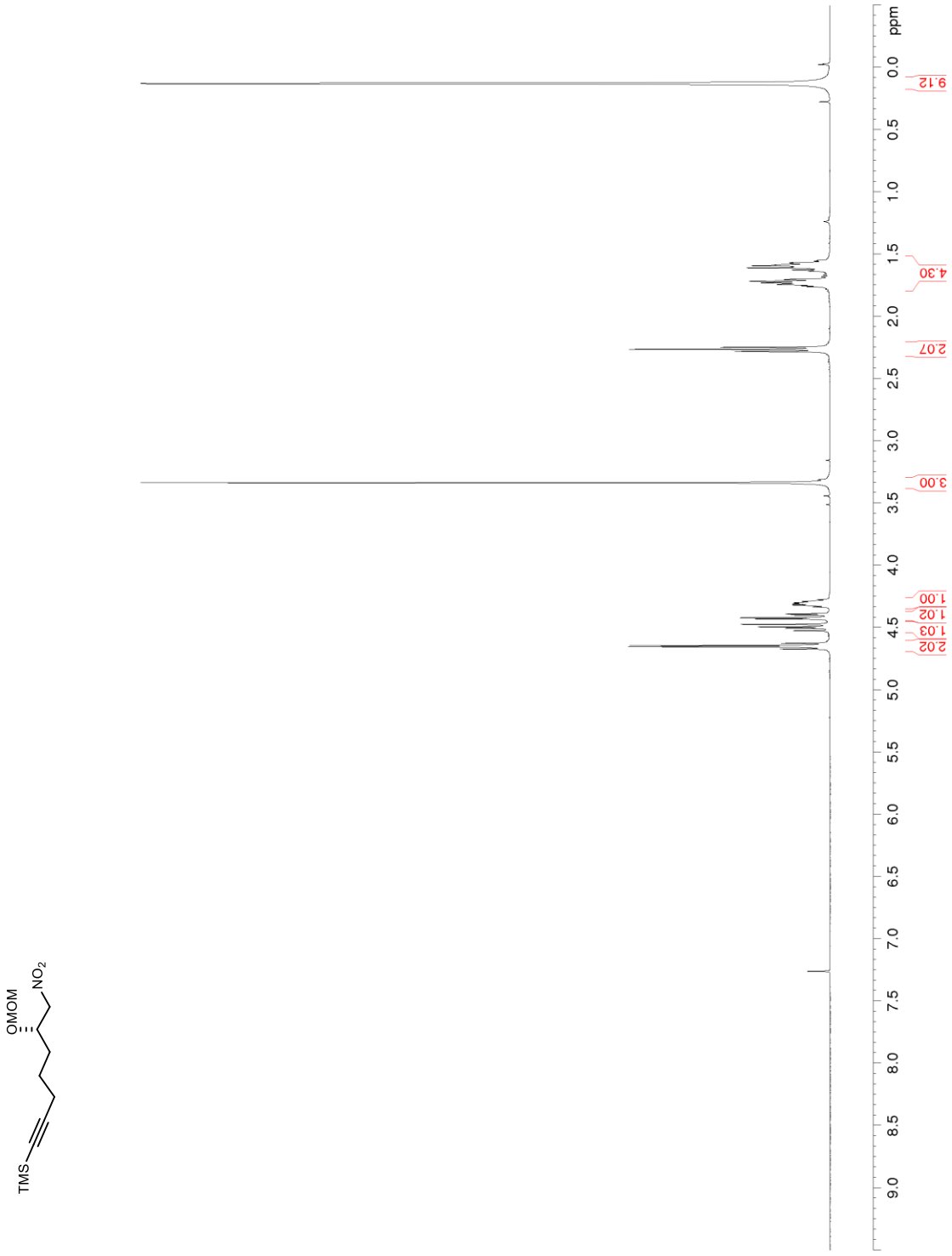

Figure S73. ^{13}C NMR/DEPT (100 MHz, $CDCl_3$) of **47**

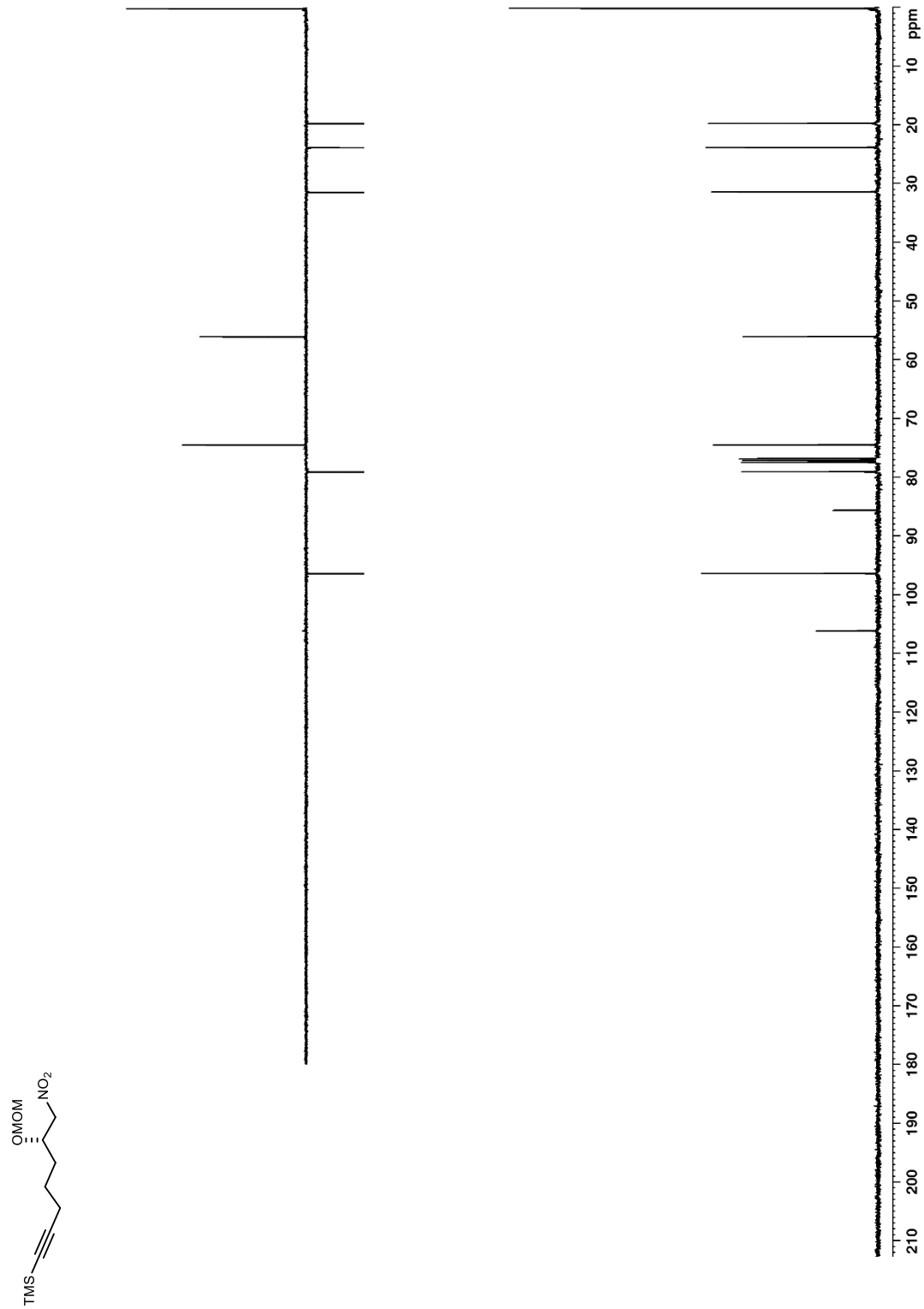

Figure S74. ^{1}H NMR (600 MHz, $CDCl_3$) of **50**

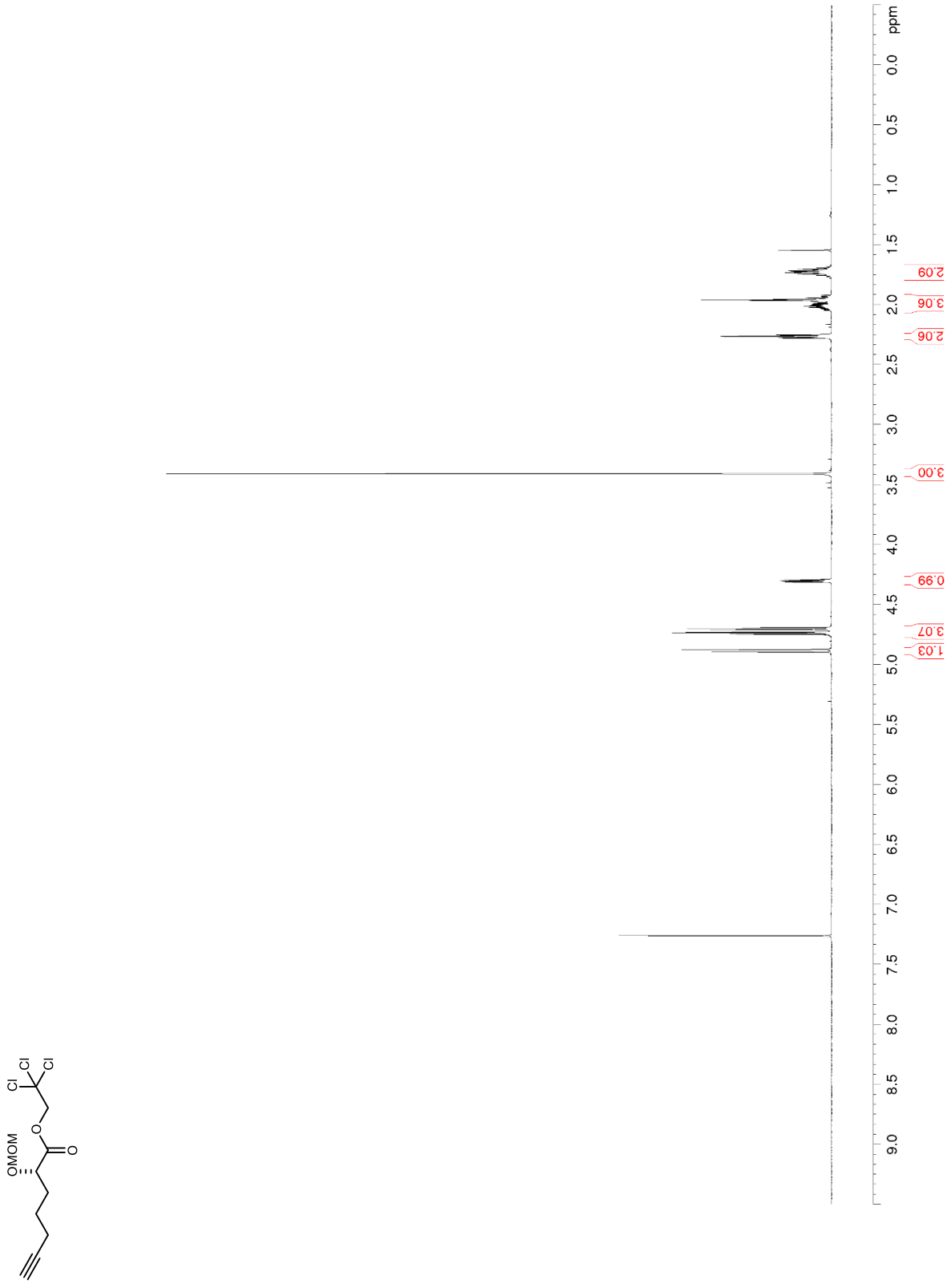

Figure S75. ^{13}C NMR/DEPT (150 MHz, $CDCl_3$) of **650**

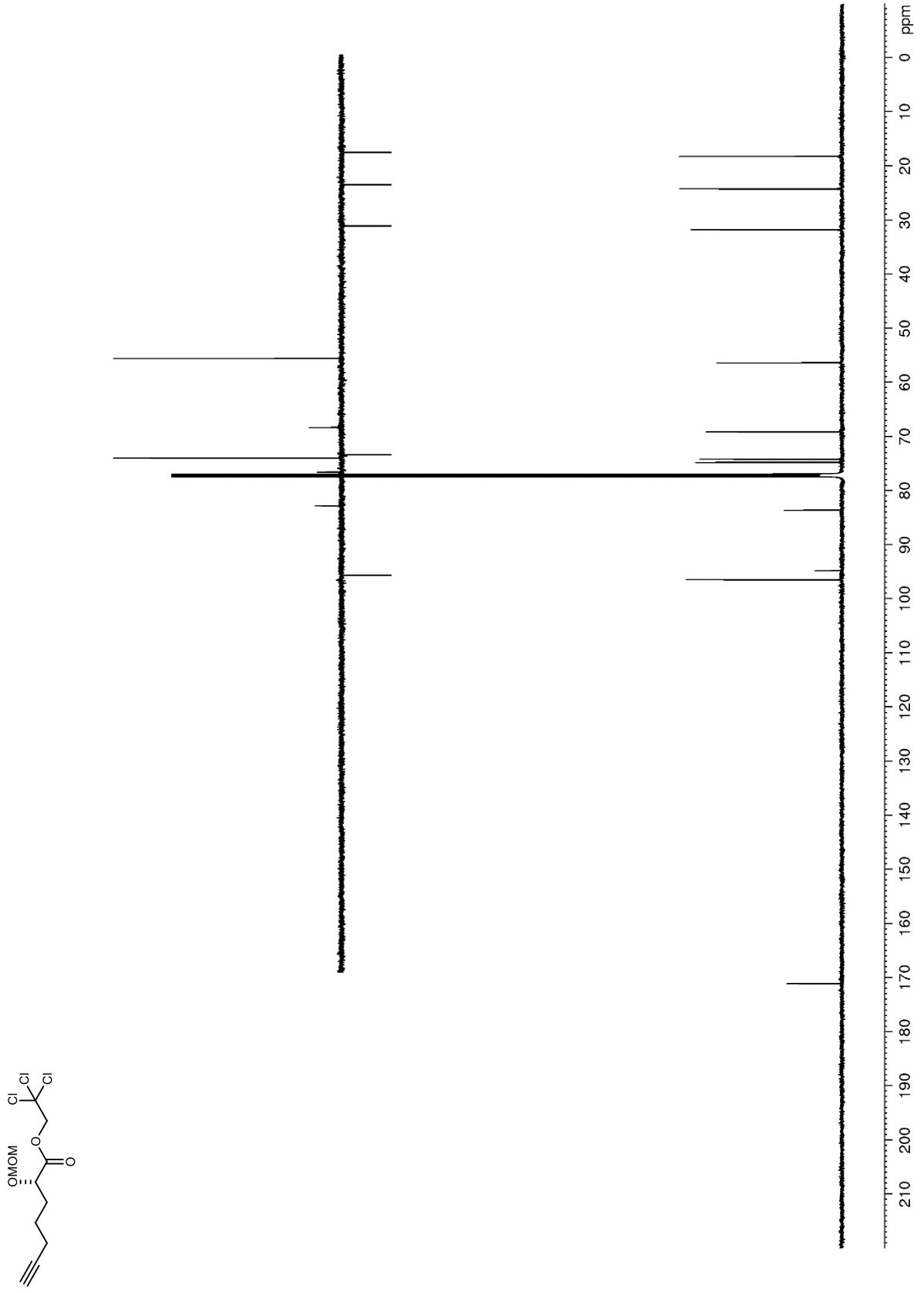

Figure S76. ^{1}H NMR (400 MHz, $CDCl_3$) of **51**

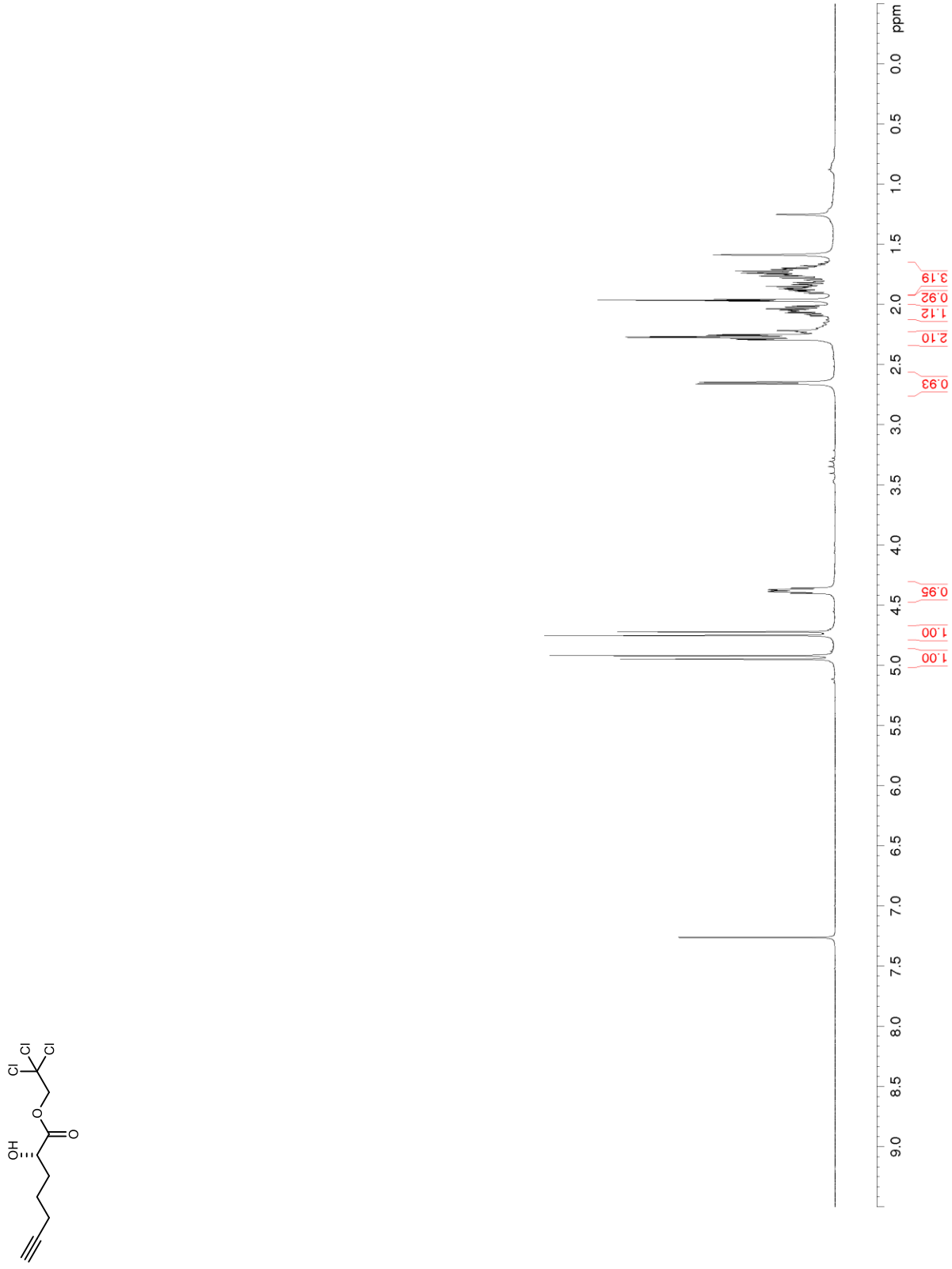

Figure S77. ^{13}C NMR/DEPT (100 MHz, $CDCl_3$) of **51**

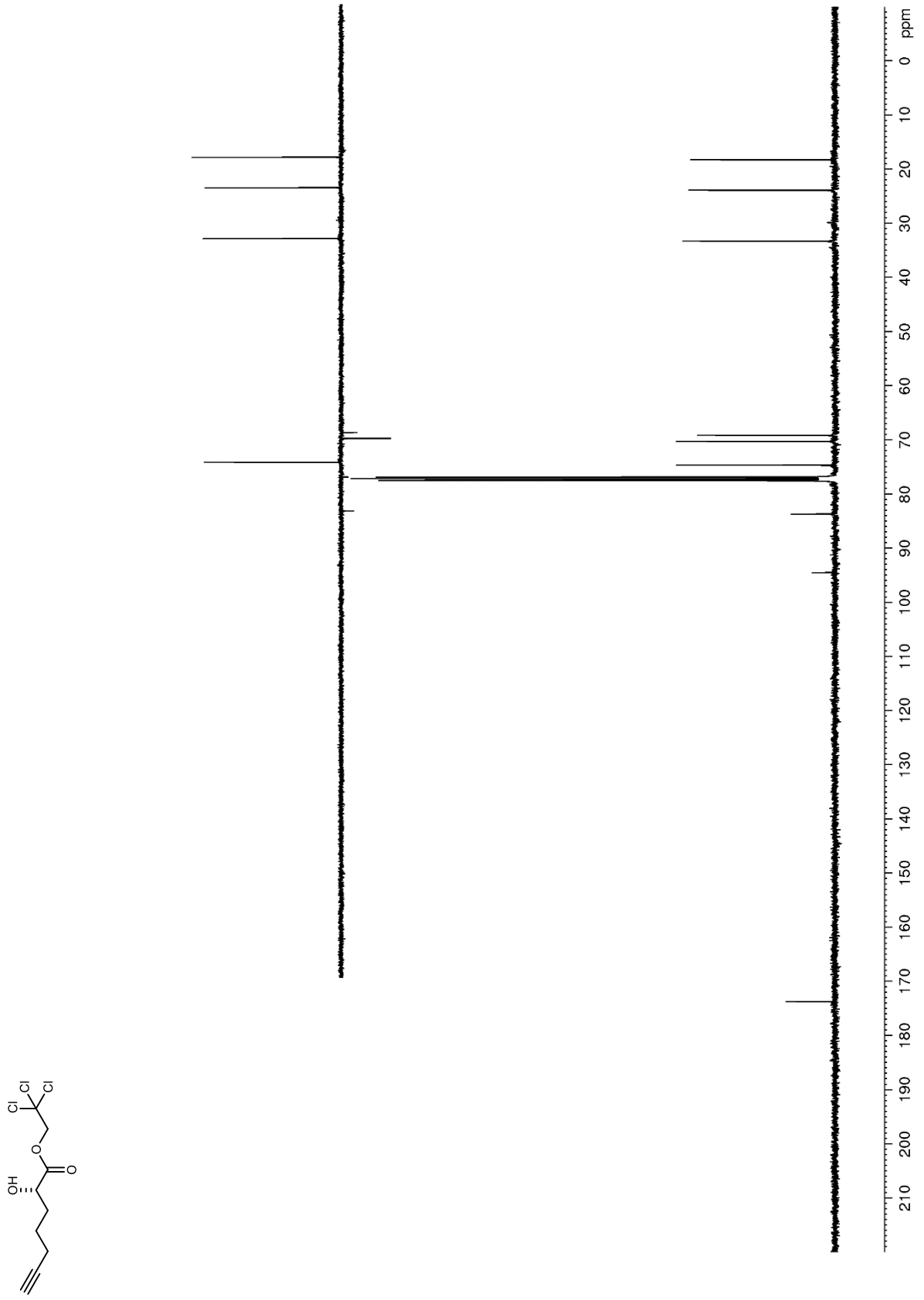

Figure S78. ^{1}H NMR (600 MHz, $CDCl_3$) of **52**

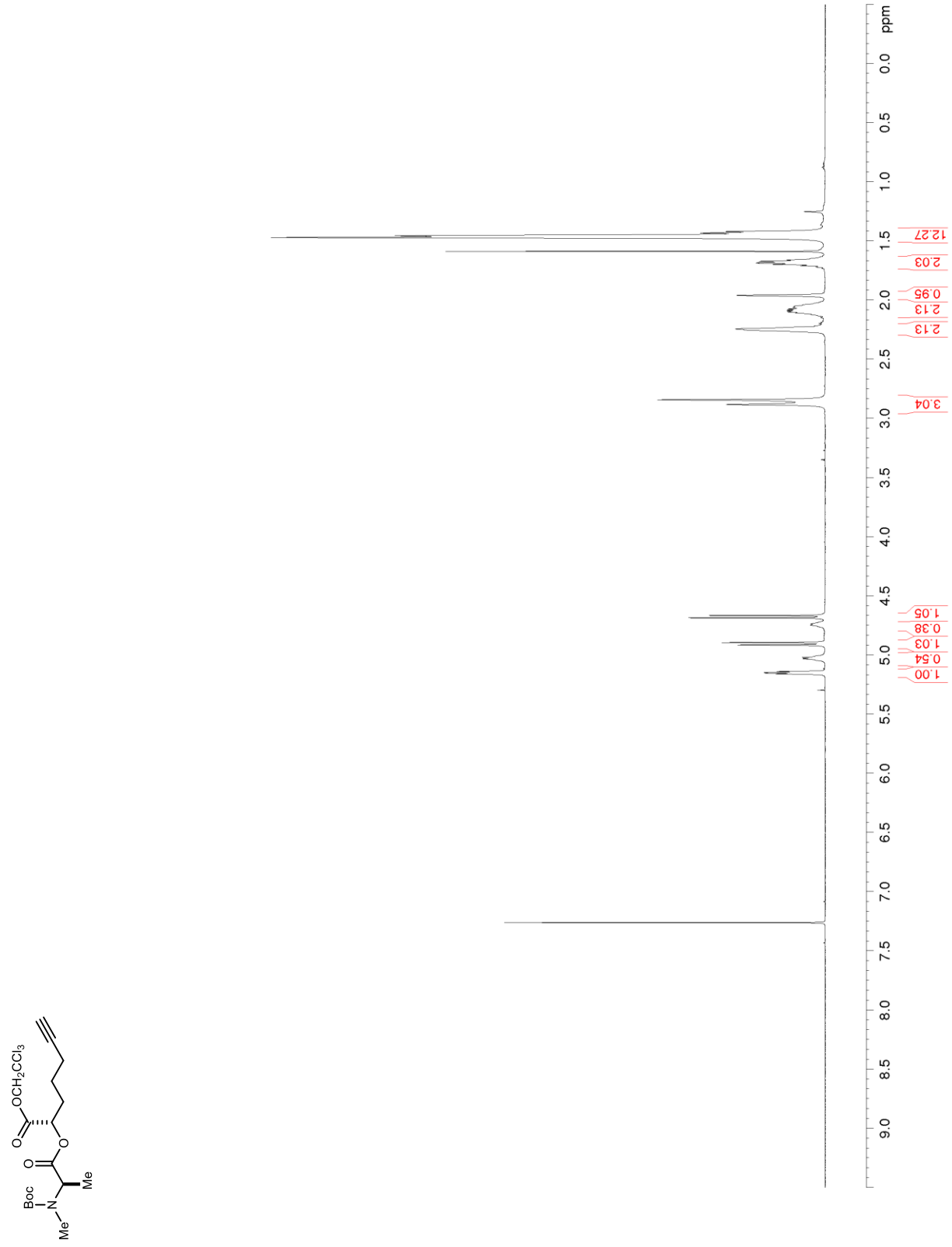

Figure S79. ^{13}C NMR/DEPT (150 MHz, $CDCl_3$) of **52**

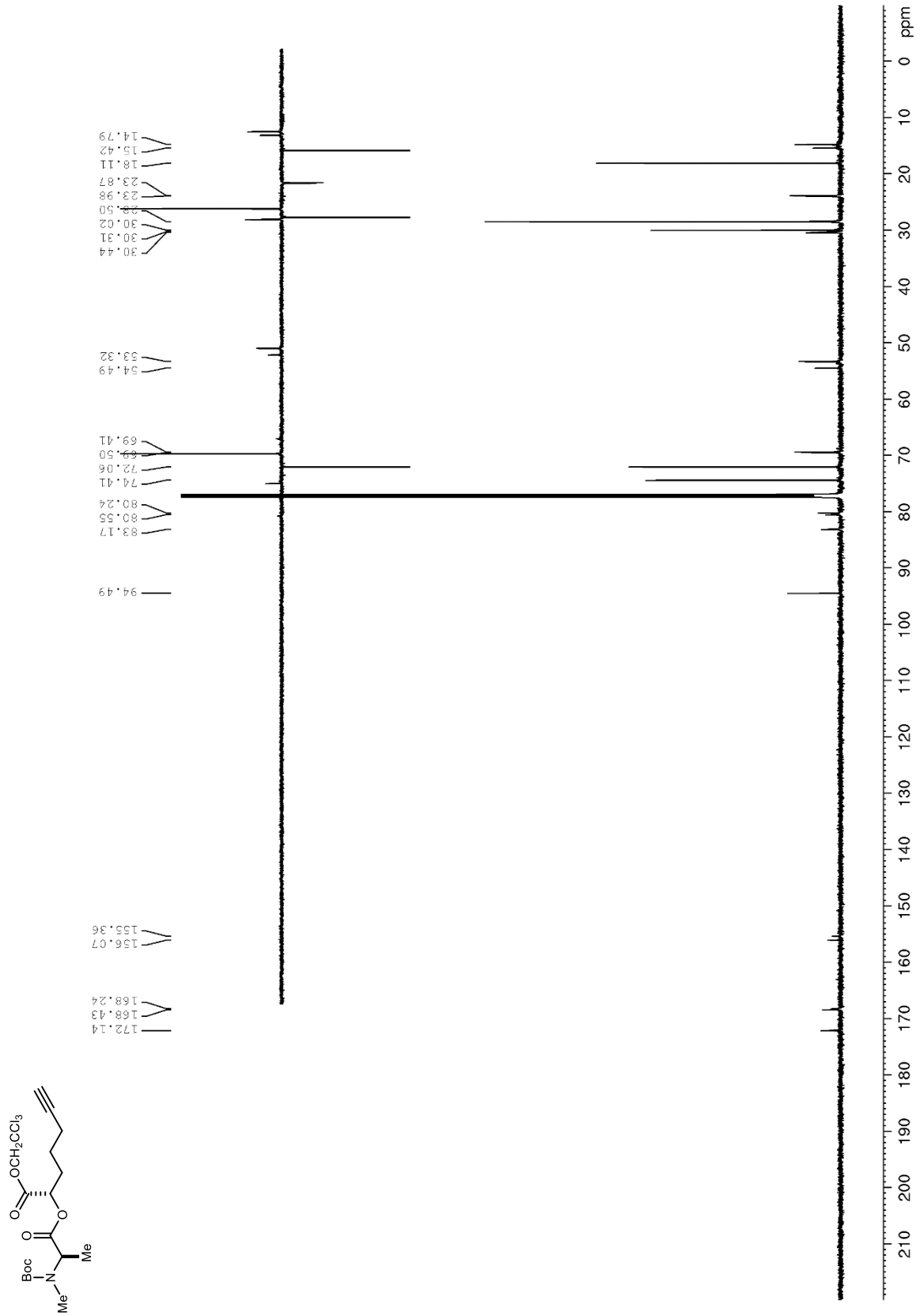

Figure S80. ^{1}H NMR (600 MHz, $CDCl_3$) of **54**

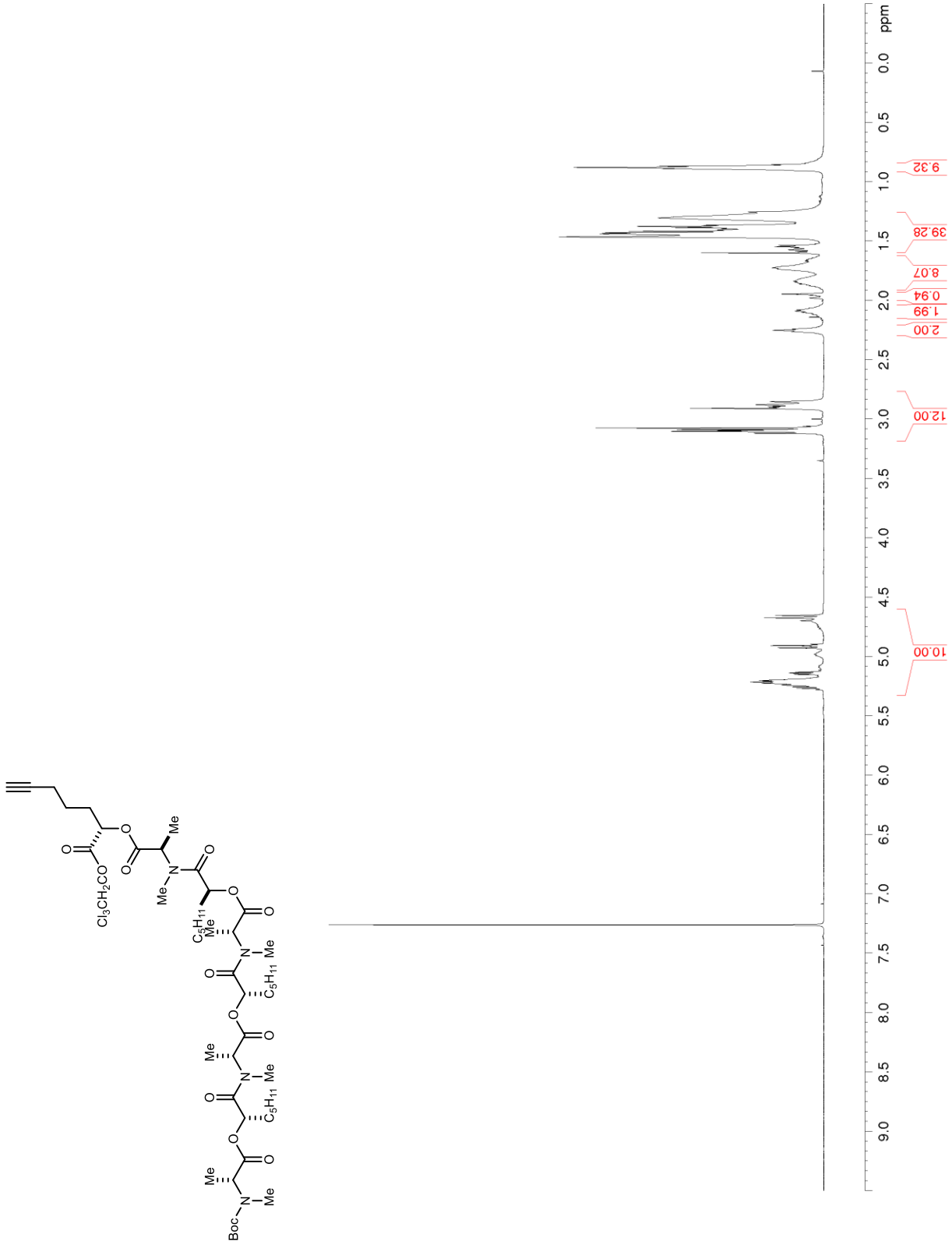

Figure S81. ^{13}C NMR/DEPT (150 MHz, $CDCl_3$) of **54**

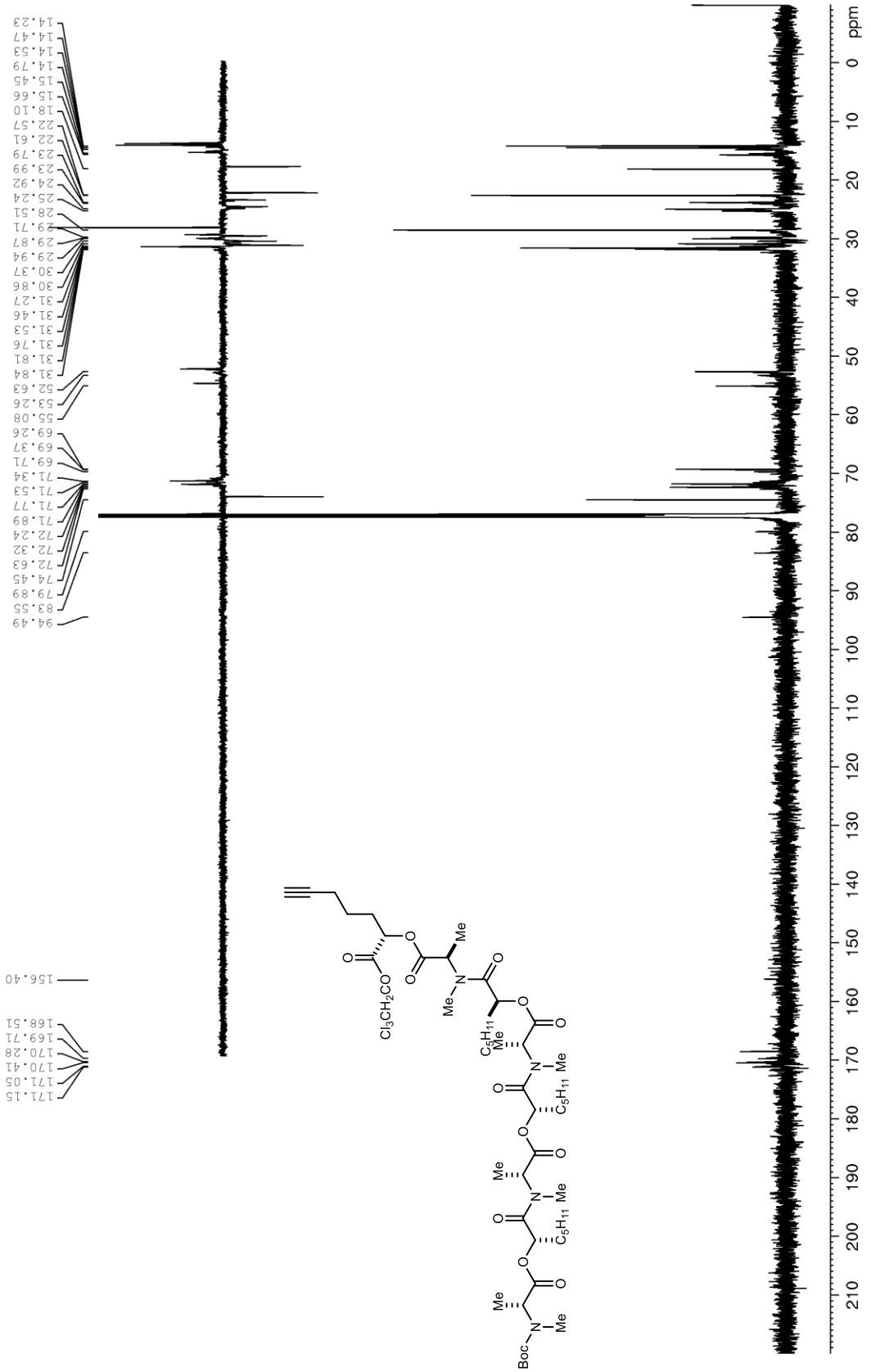

Figure S82. ^{1}H NMR (600 MHz, $CDCl_3$) of **36**

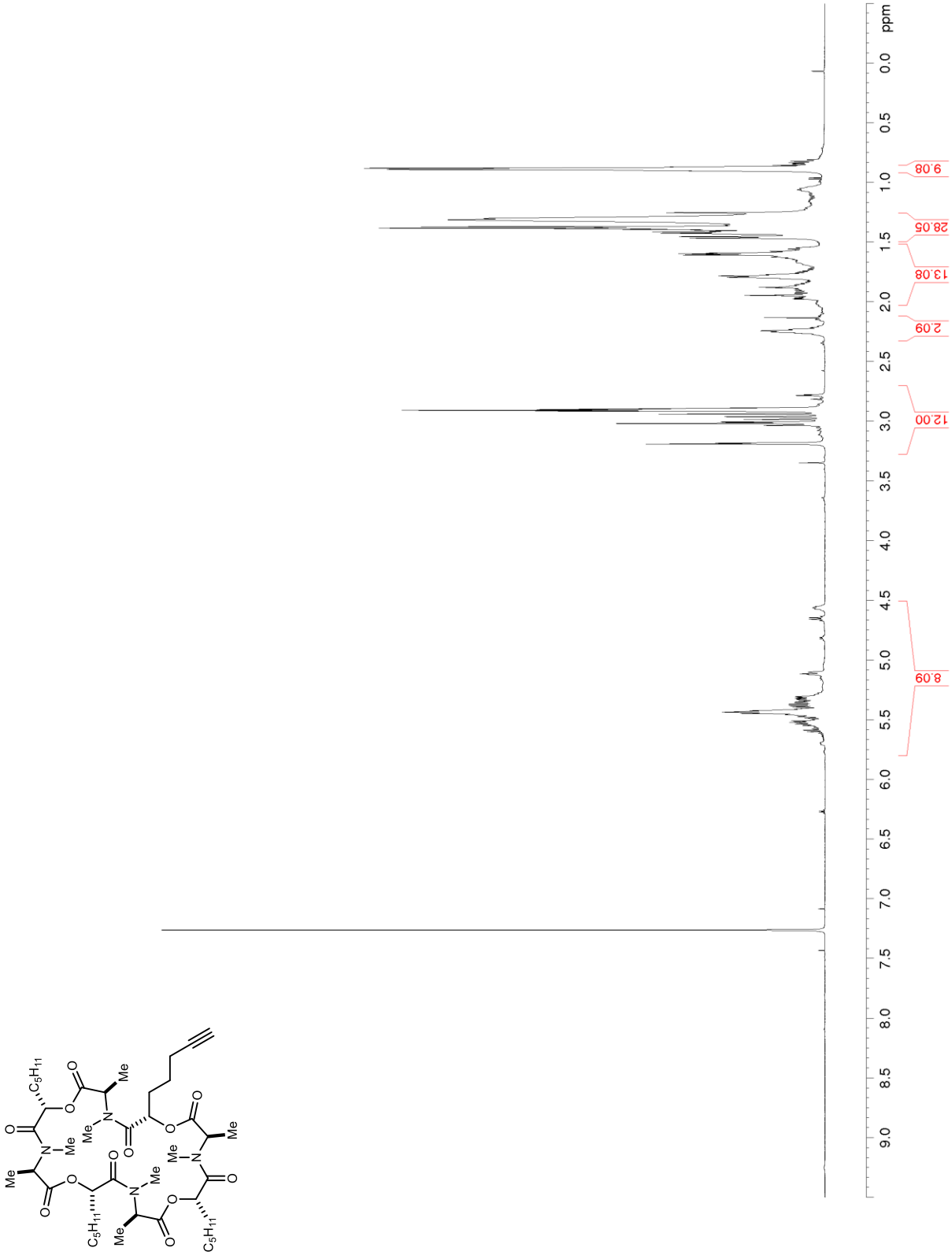

Figure S83. ^{13}C NMR/DEPT (150 MHz, $CDCl_3$) of **36**

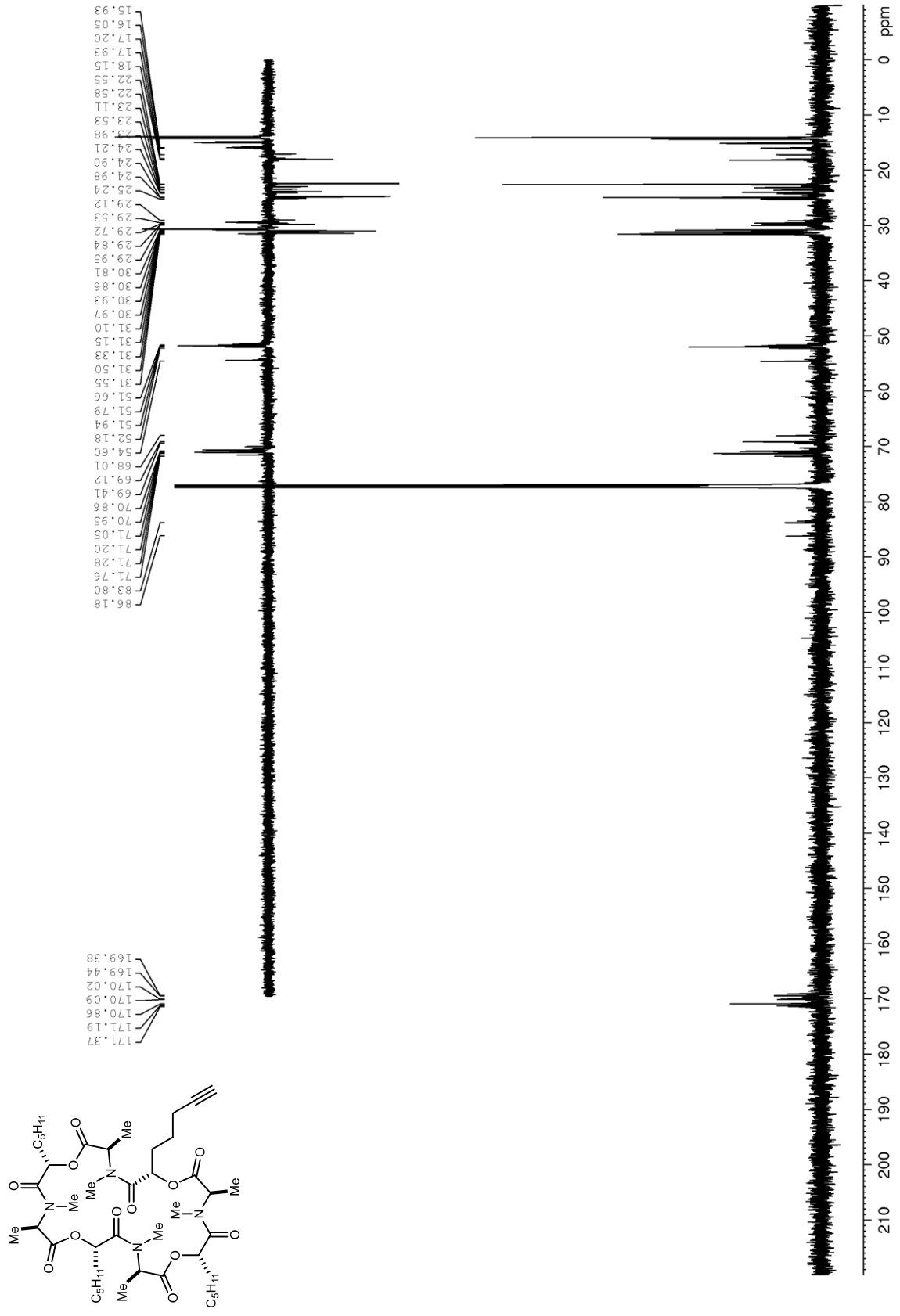

Figure S84. ^{1}H NMR (400 MHz, $CDCl_3$) of **S24**

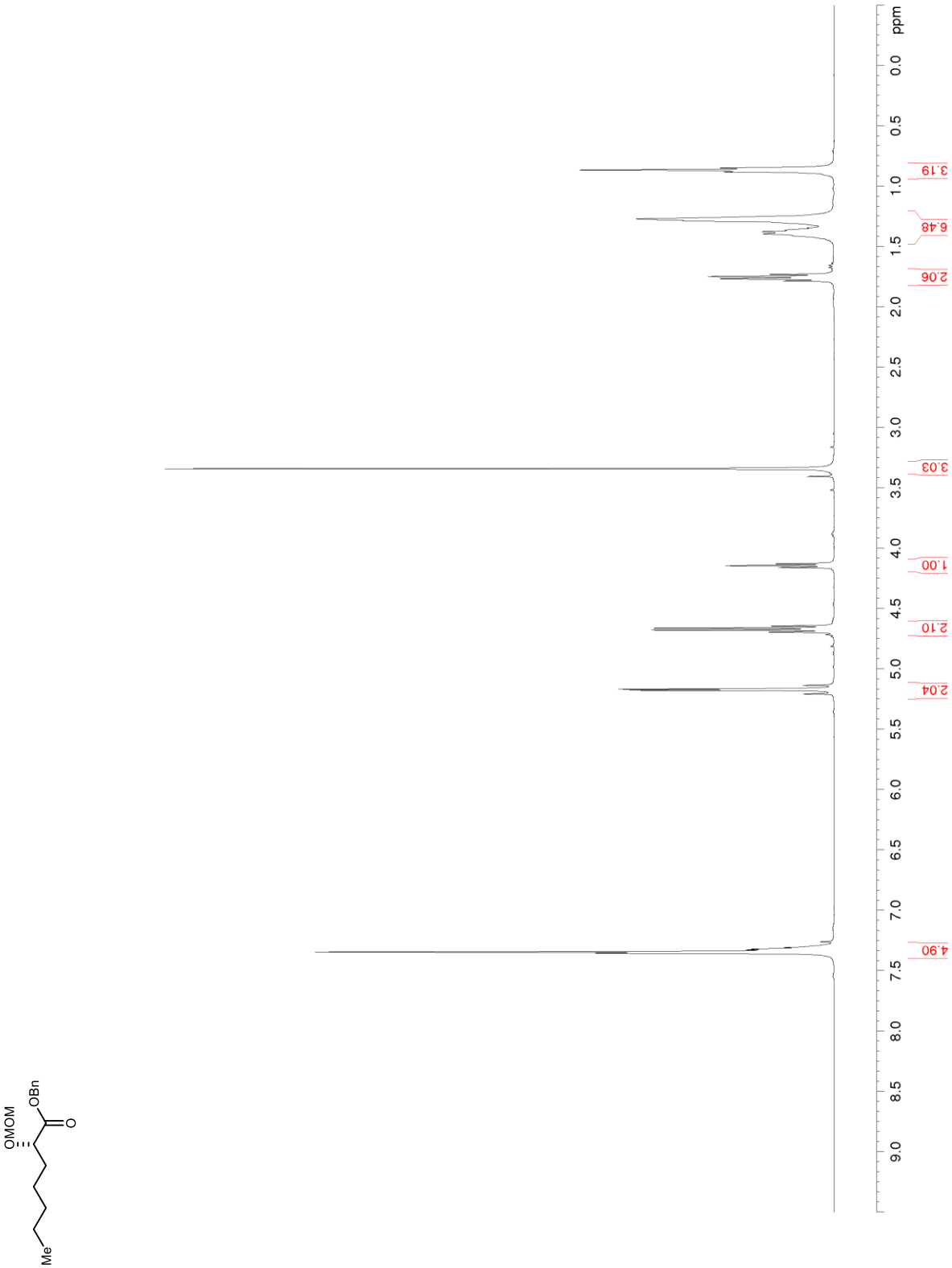

Figure S85. ^{13}C NMR/DEPT (100 MHz, $CDCl_3$) of **S24**

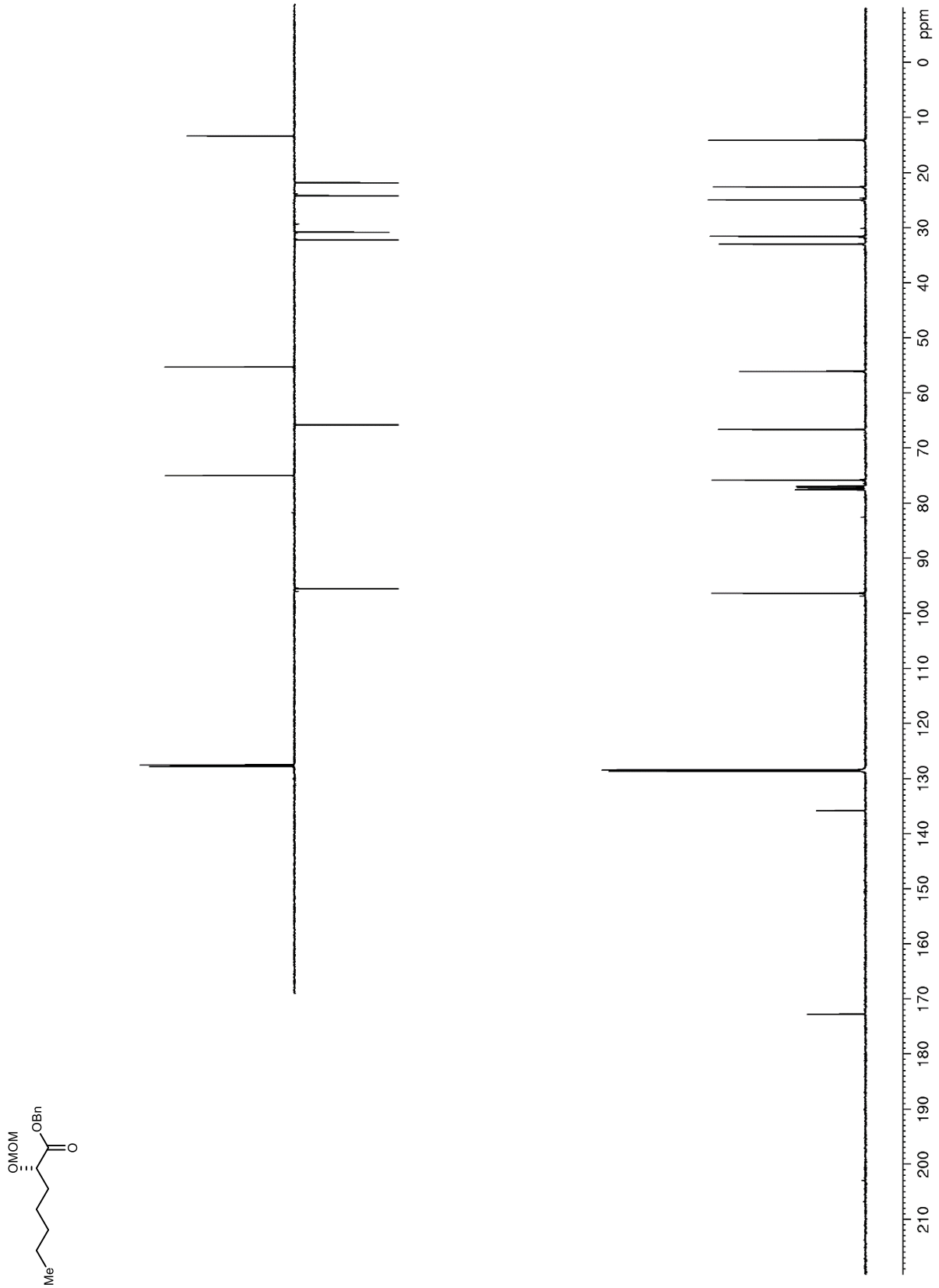

Figure S86. ^{1}H NMR (600 MHz, $CDCl_3$) of **55**

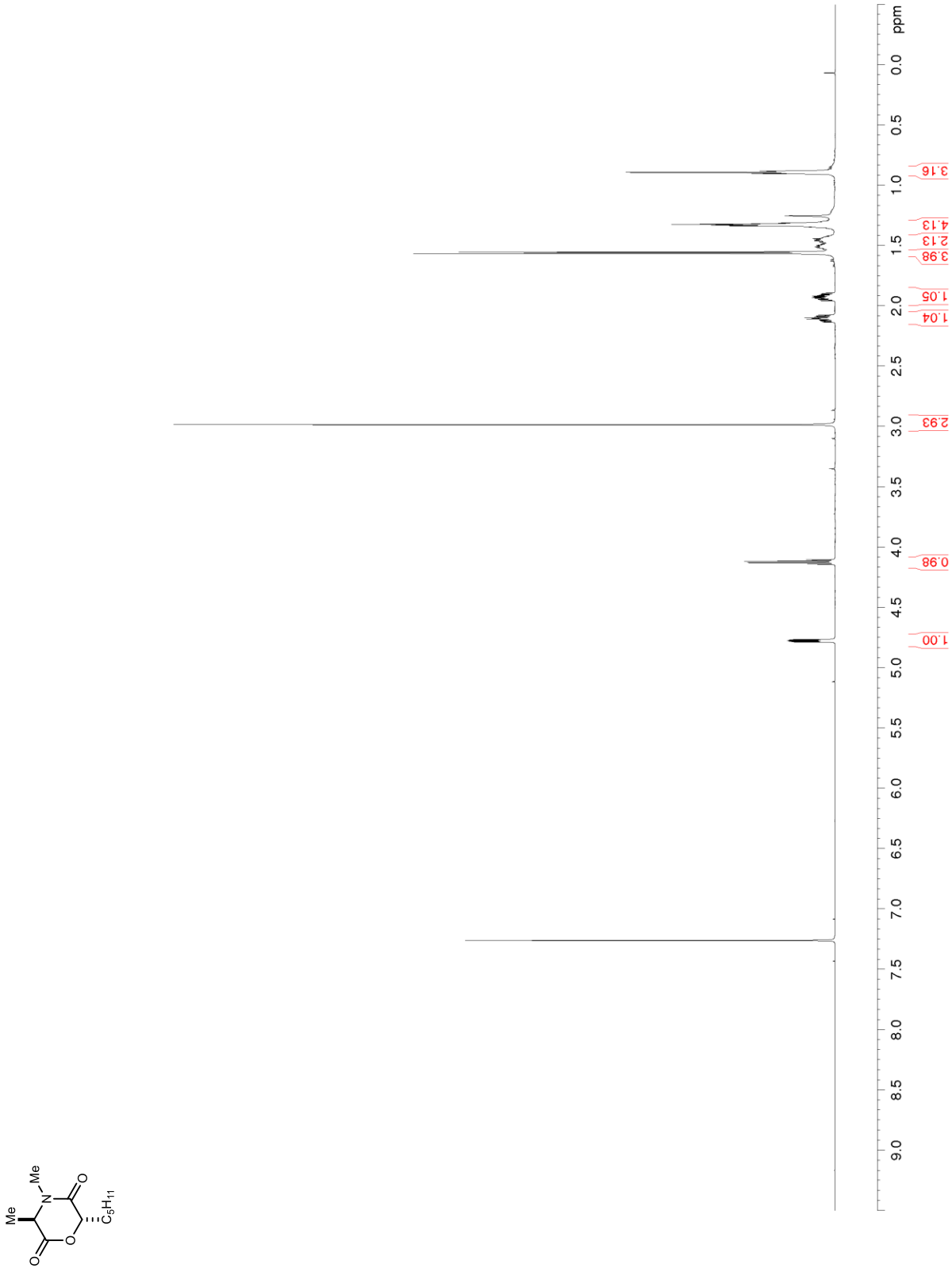

Figure S87. ^{13}C NMR/DEPT (125 MHz, $CDCl_3$) of **55**

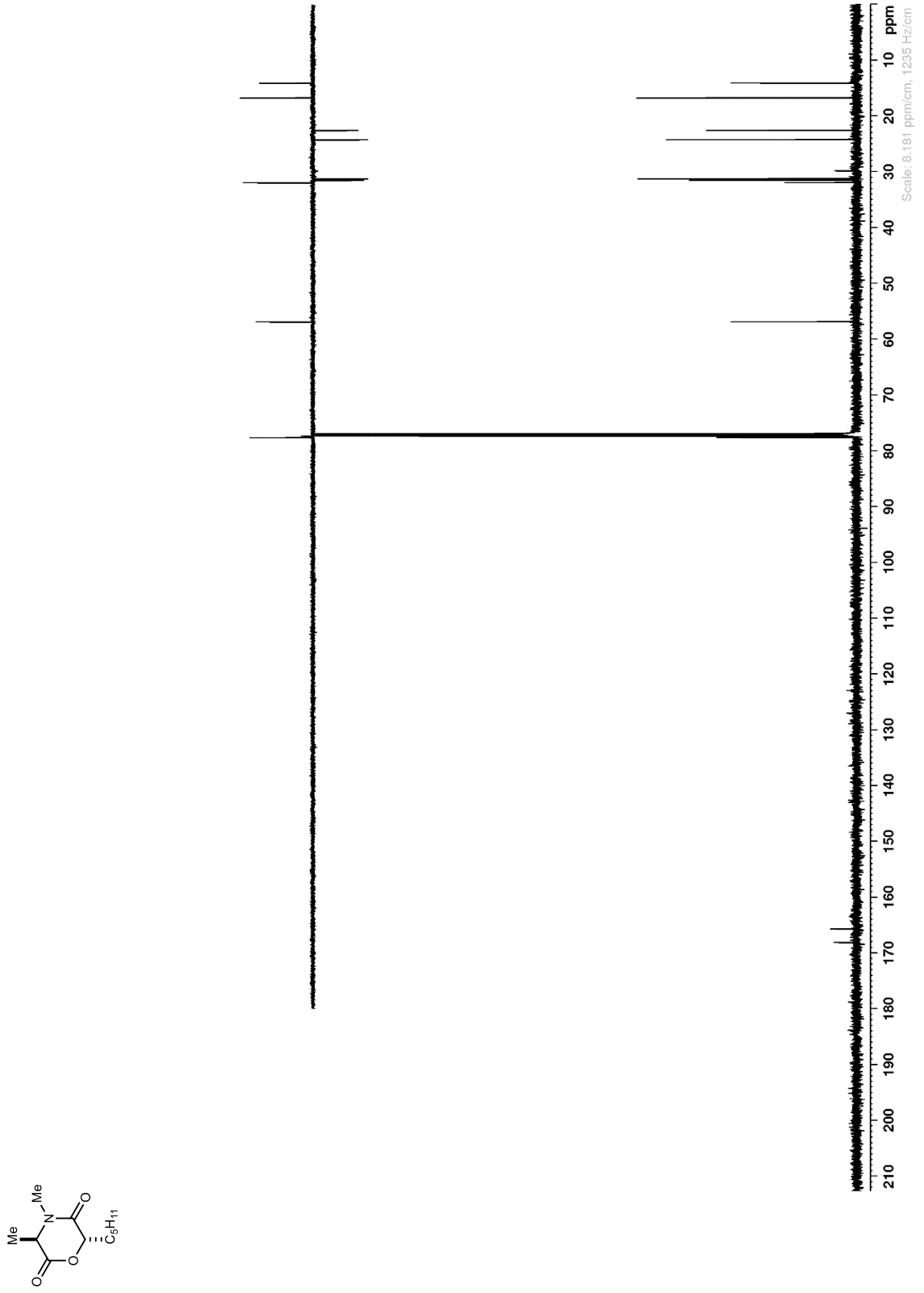

Figure S88. ^{1}H NMR (600 MHz, $CDCl_3$) of **56**

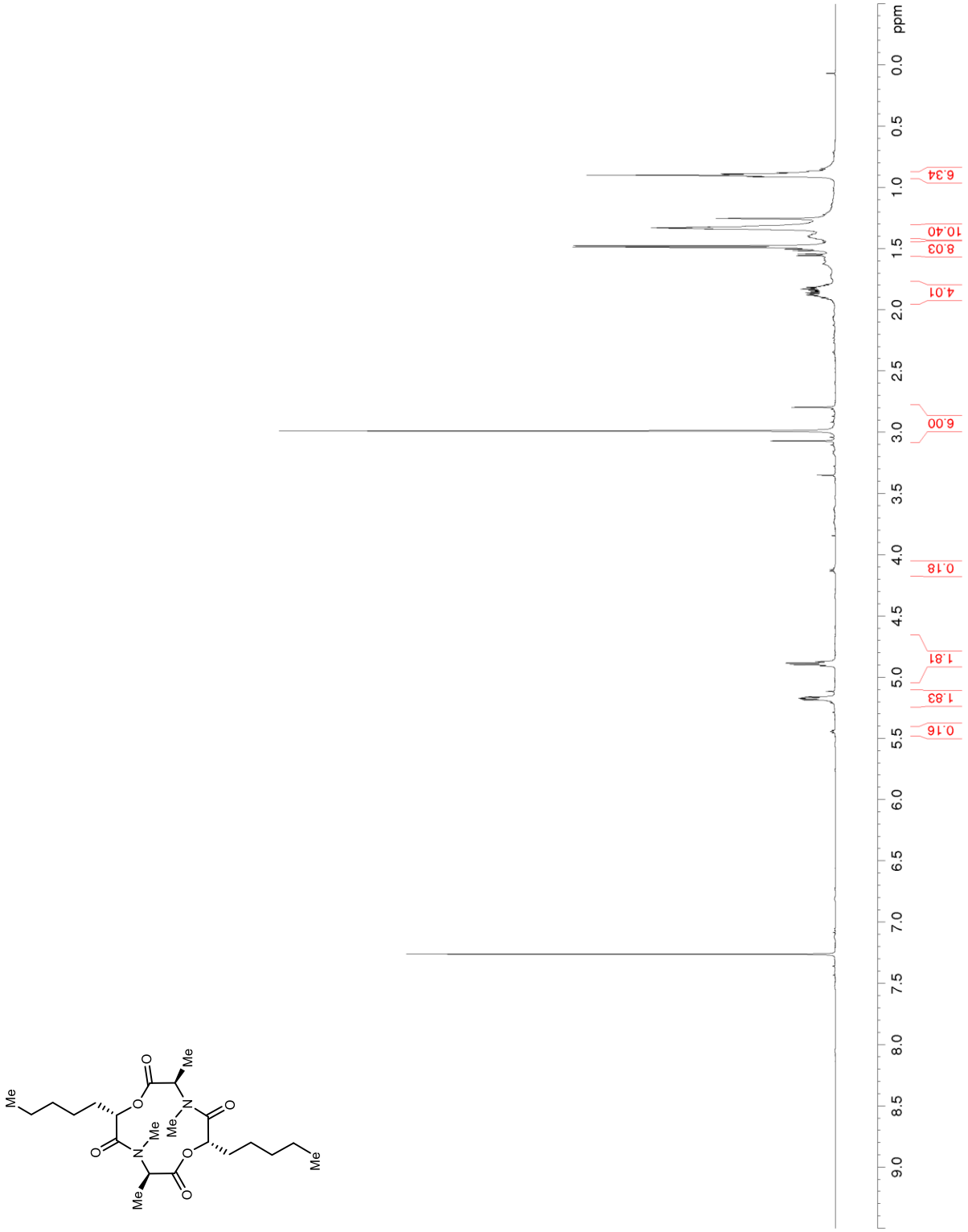

Figure S89. ^{13}C NMR/DEPT (150 MHz, $CDCl_3$) of **56**

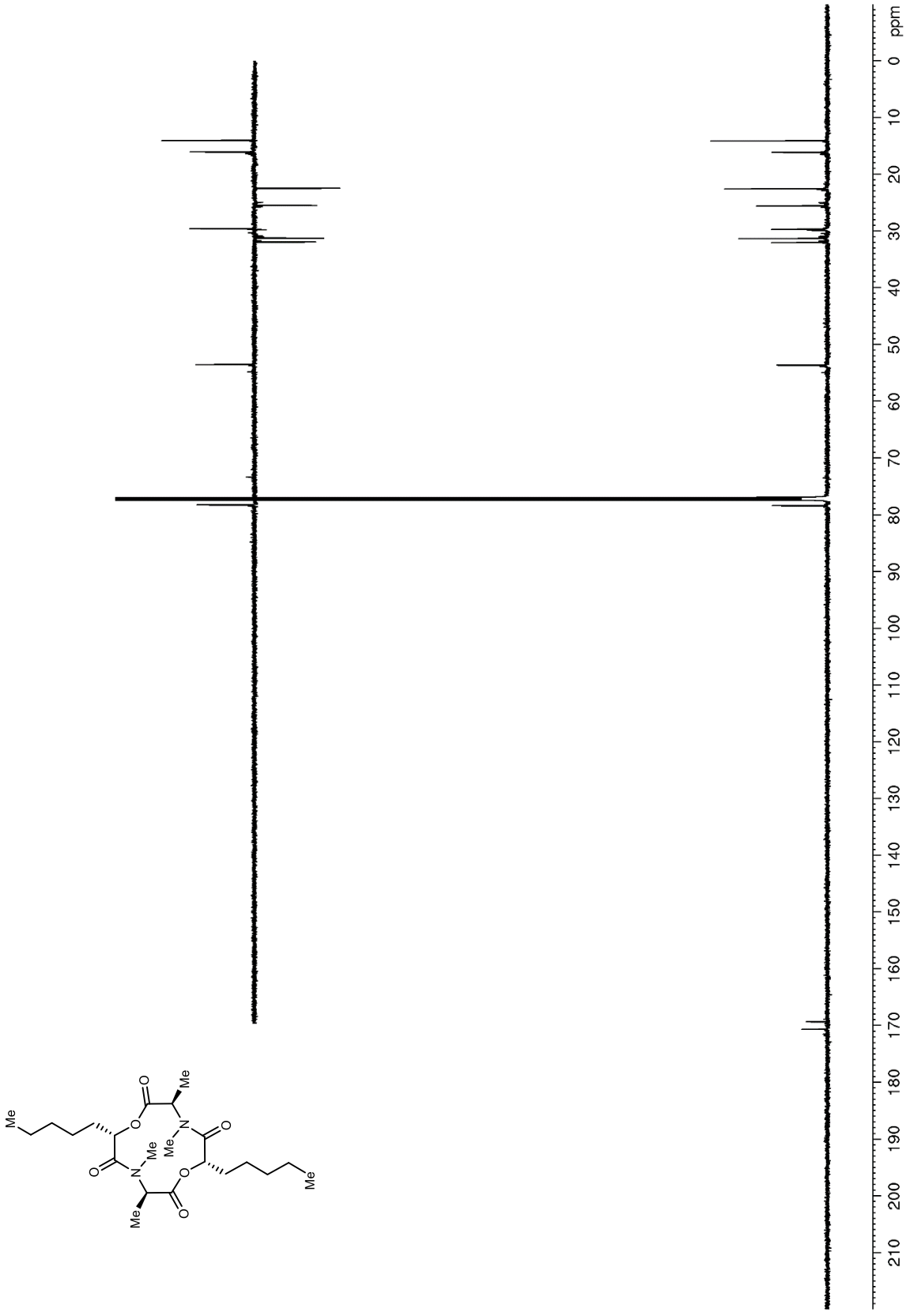

Figure S90. ^{1}H NMR (600 MHz, CD_3OD) of **57**

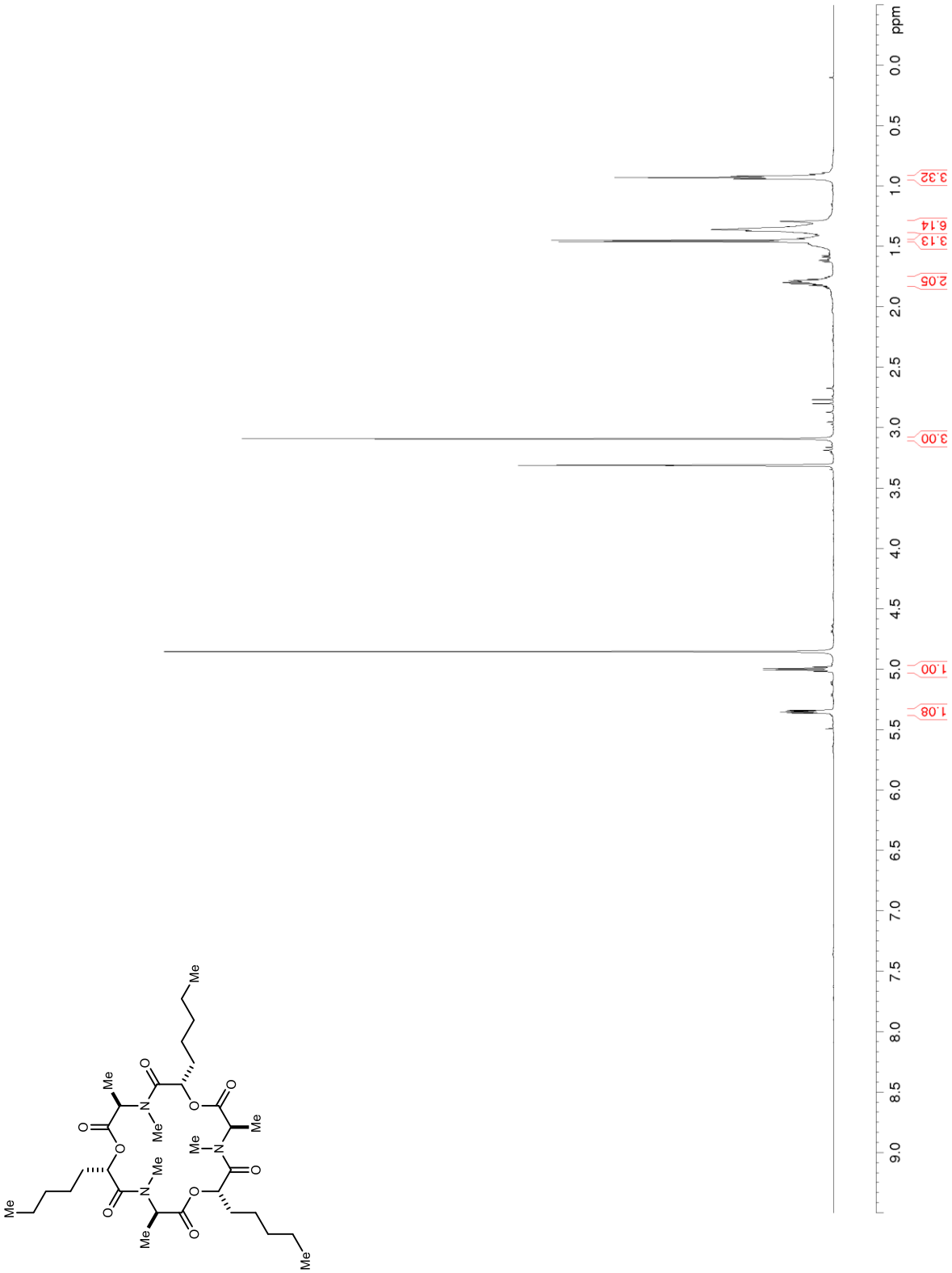

Figure S91. ^{13}C NMR/DEPT (150 MHz, CD_3OD) of **57**

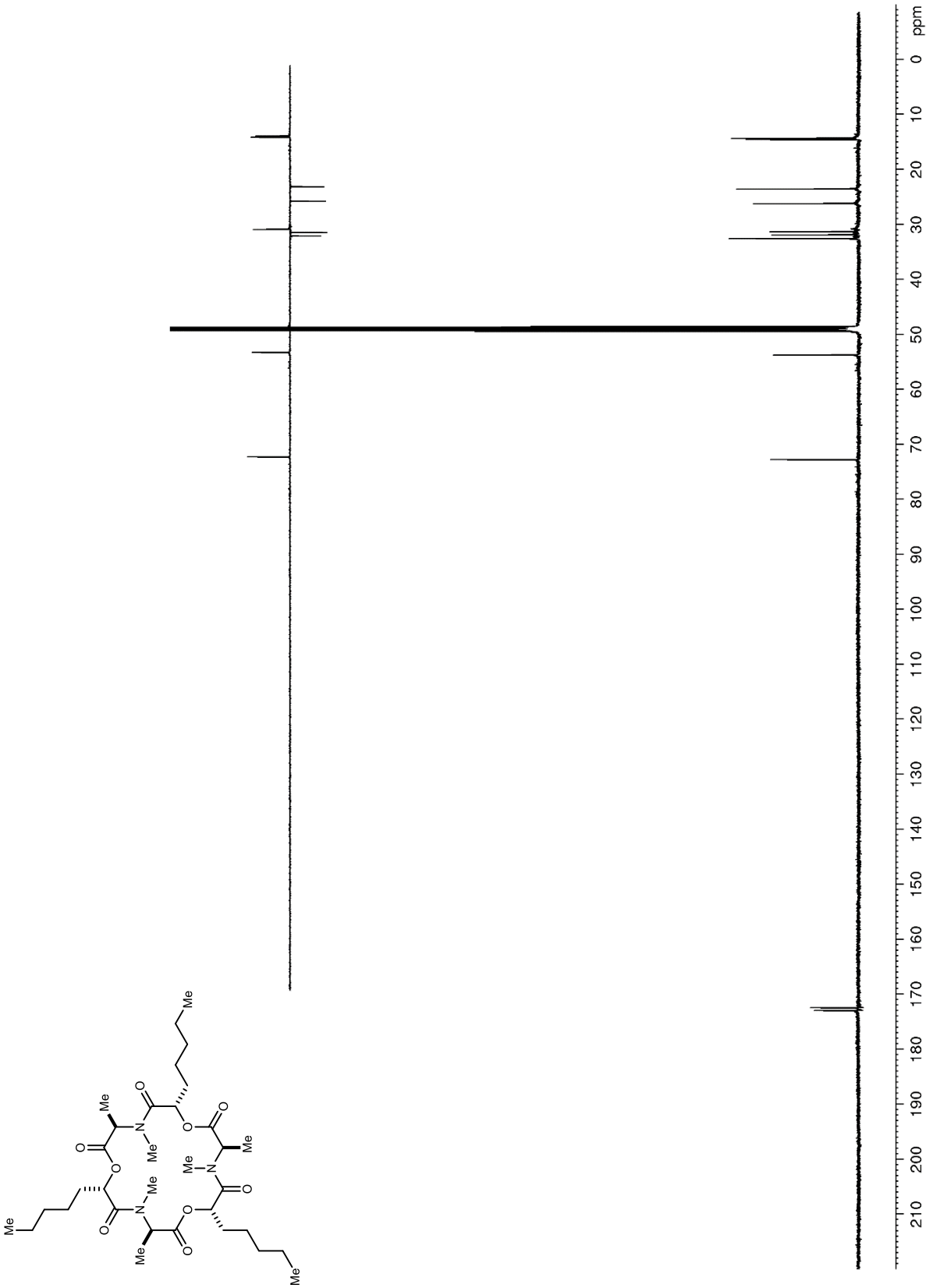

Figure S92. 1H NMR (600 MHz, CDCl3) of **S29**

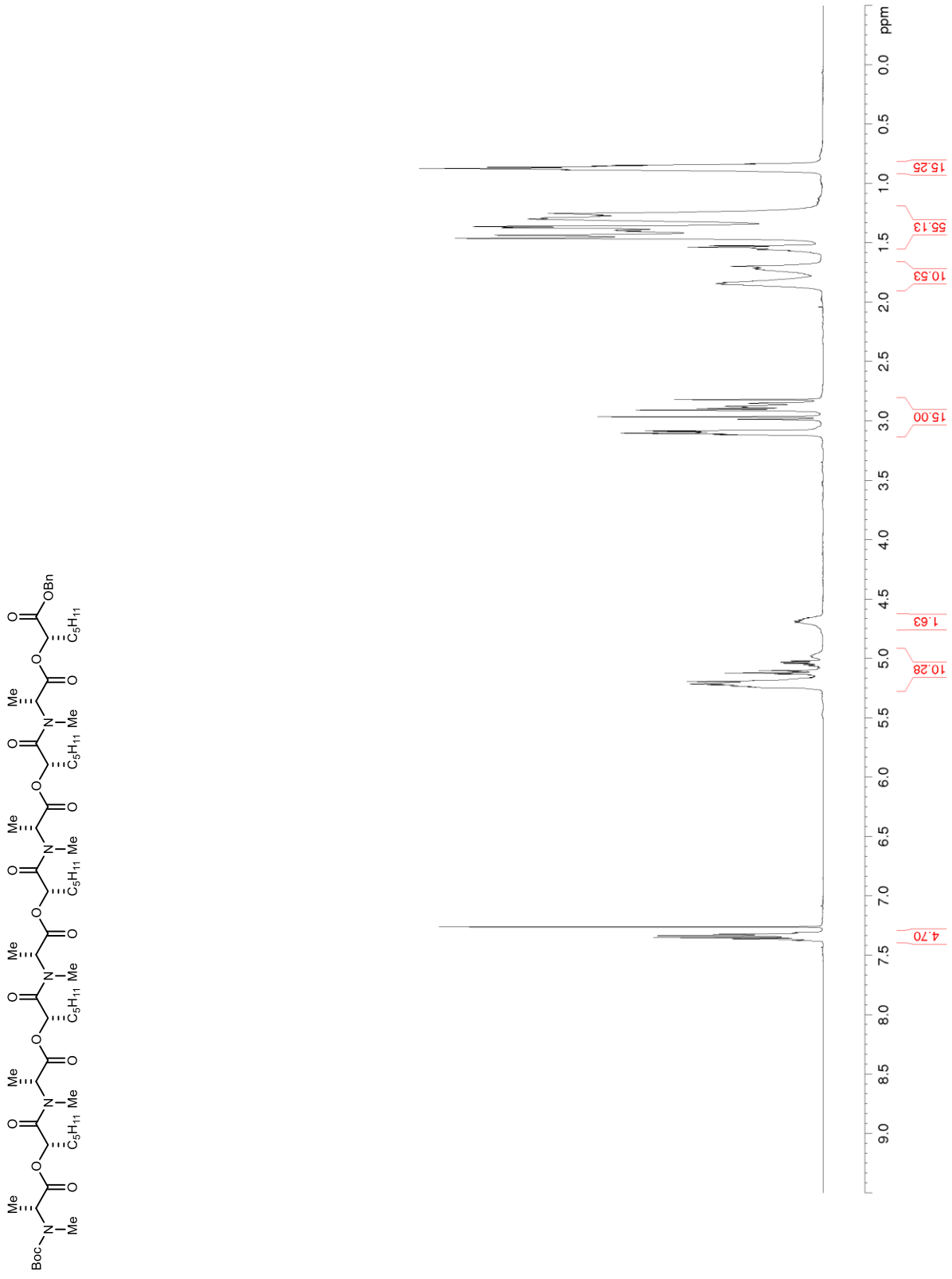

Figure S93. ^{13}C NMR/DEPT (150 MHz, $CDCl_3$) of **S29**

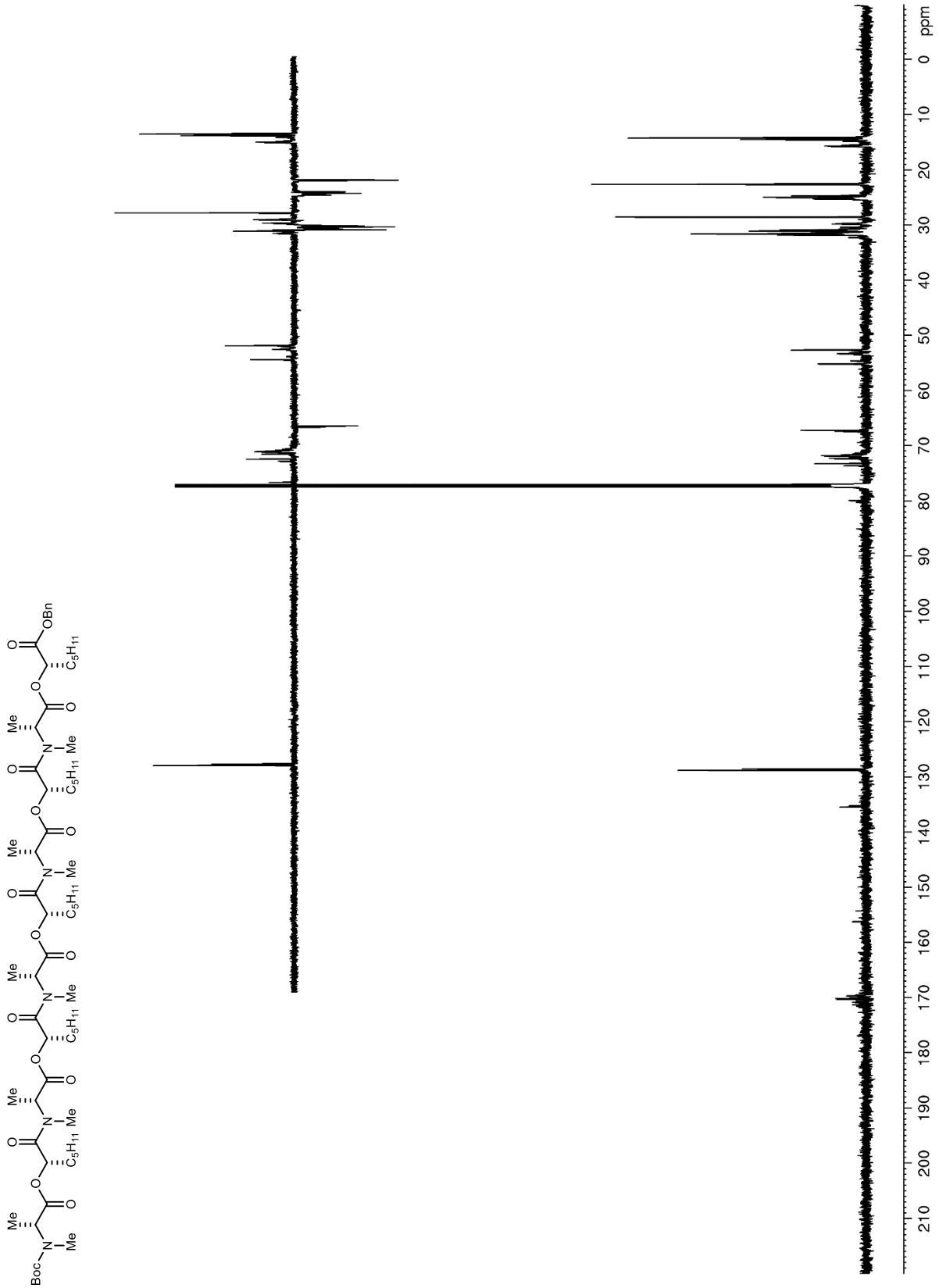

Figure S94. ^{1}H NMR (600 MHz, $CDCl_3$) of **59**

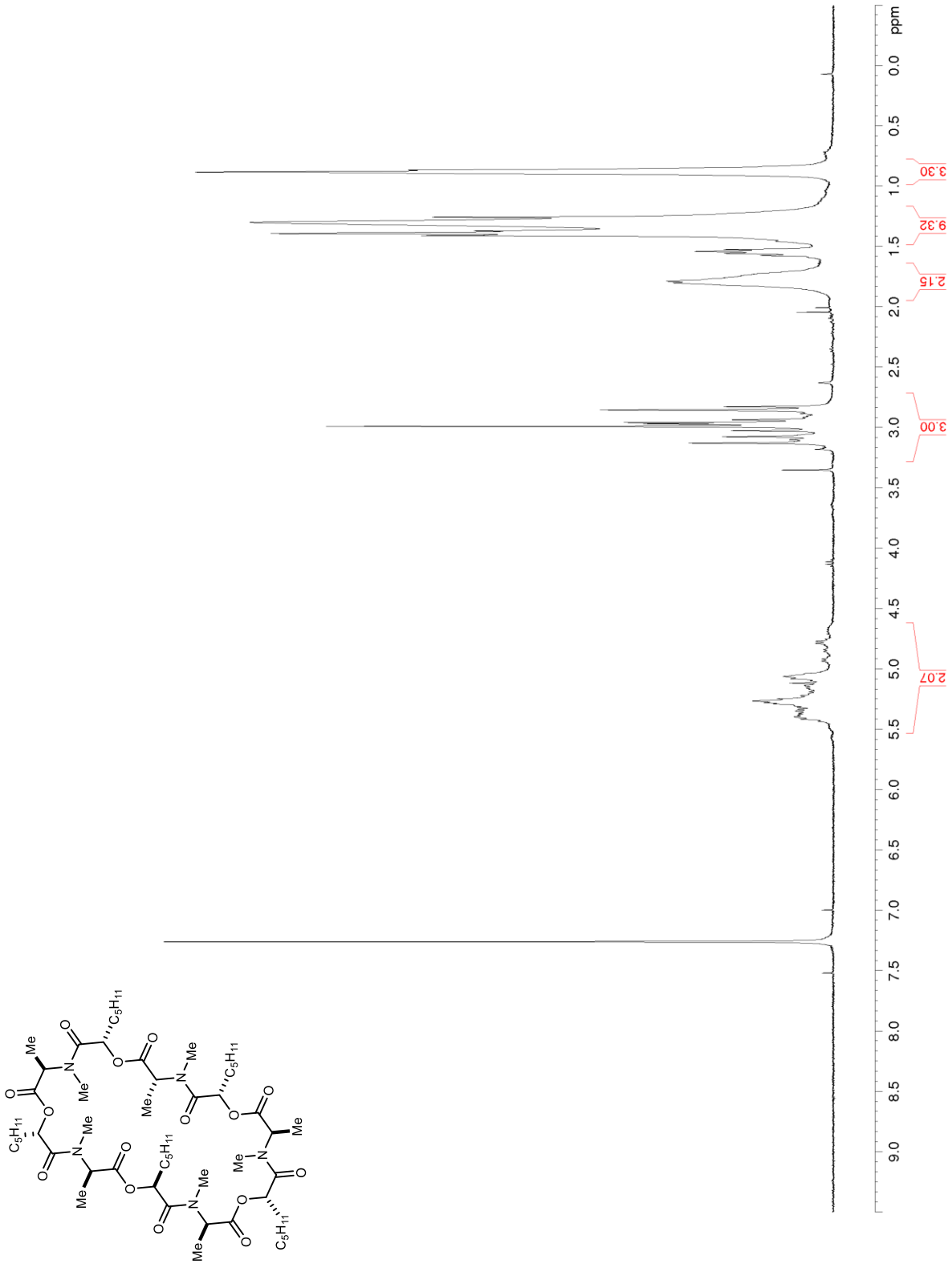

Figure S95. ^{13}C NMR/DEPT (150 MHz, $CDCl_3$) of **59**

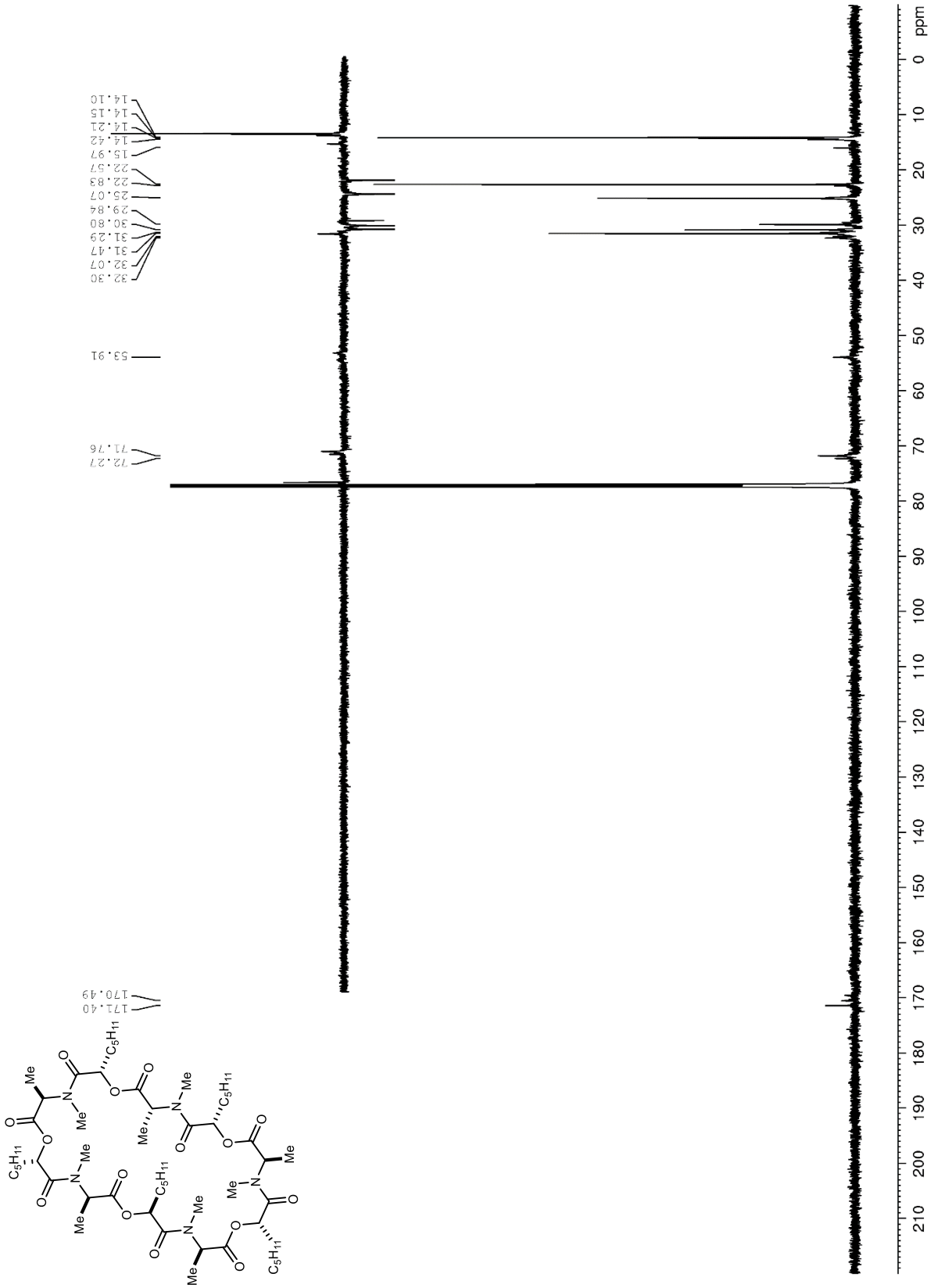

Figure S96. ^{1}H NMR (600 MHz, $CDCl_3$) of **S30**

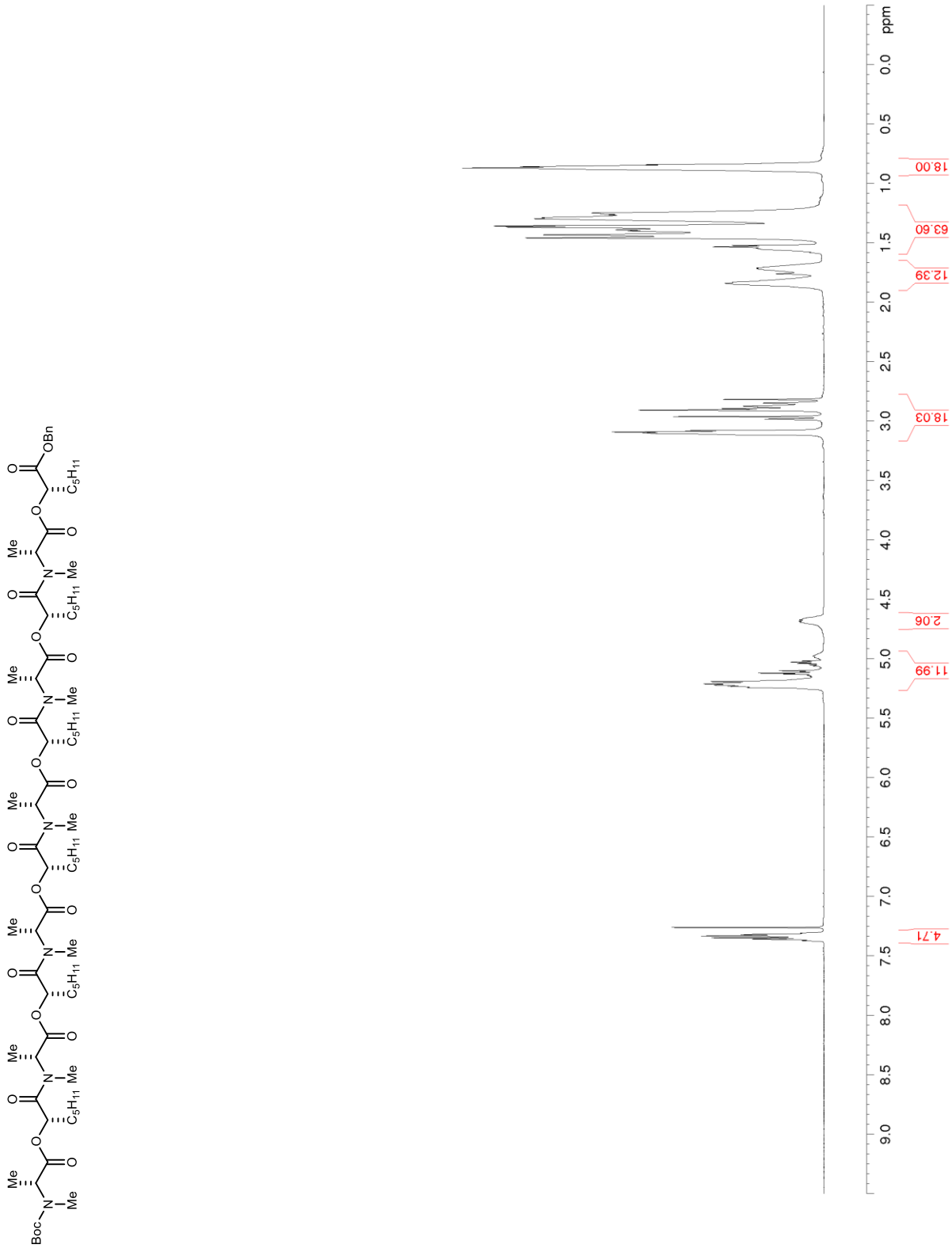

Figure S97. ^{13}C NMR/DEPT (150 MHz, $CDCl_3$) of **S30**

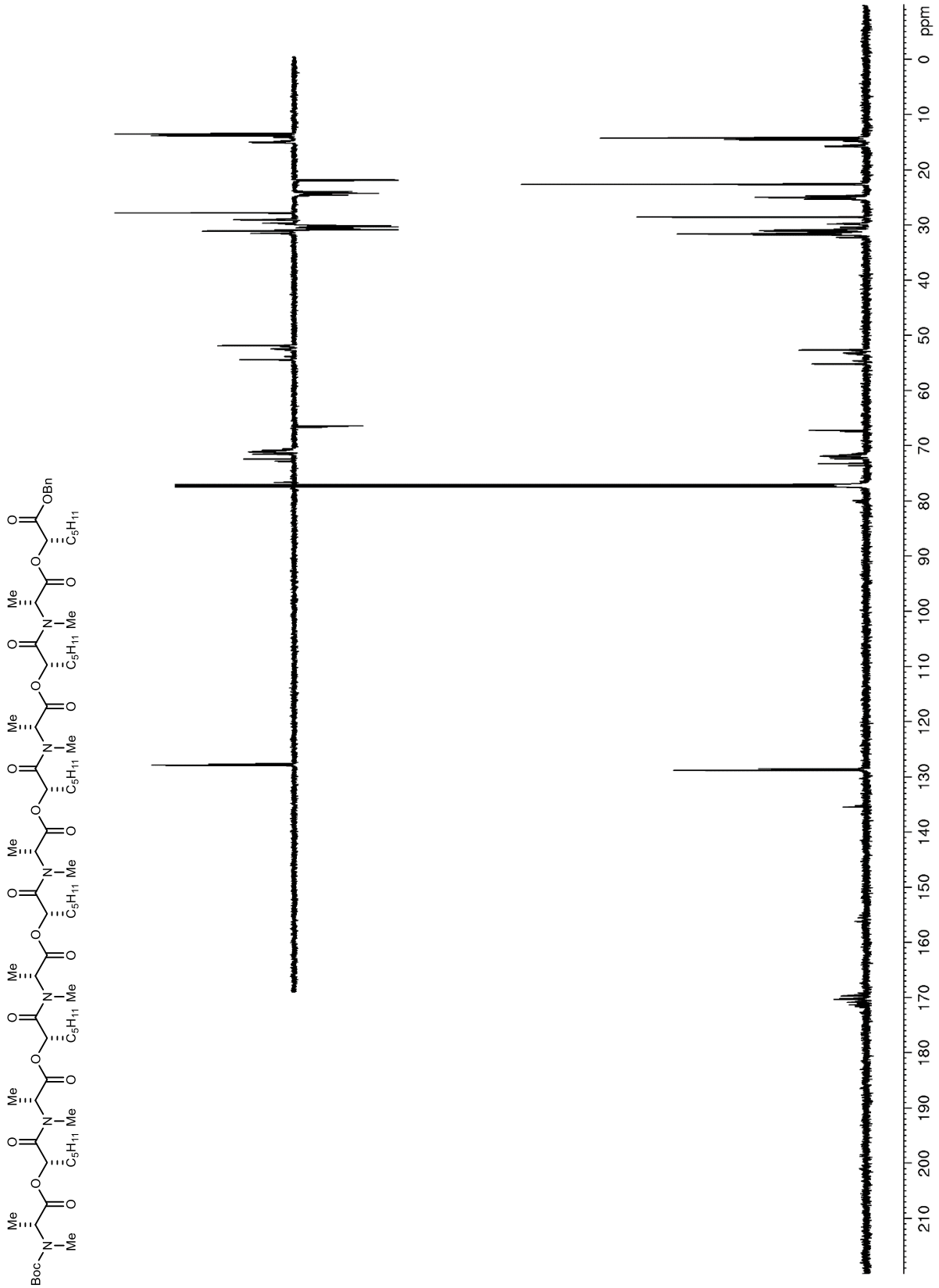

Figure S98. ^{1}H NMR (600 MHz, $CDCl_3$) of **58**

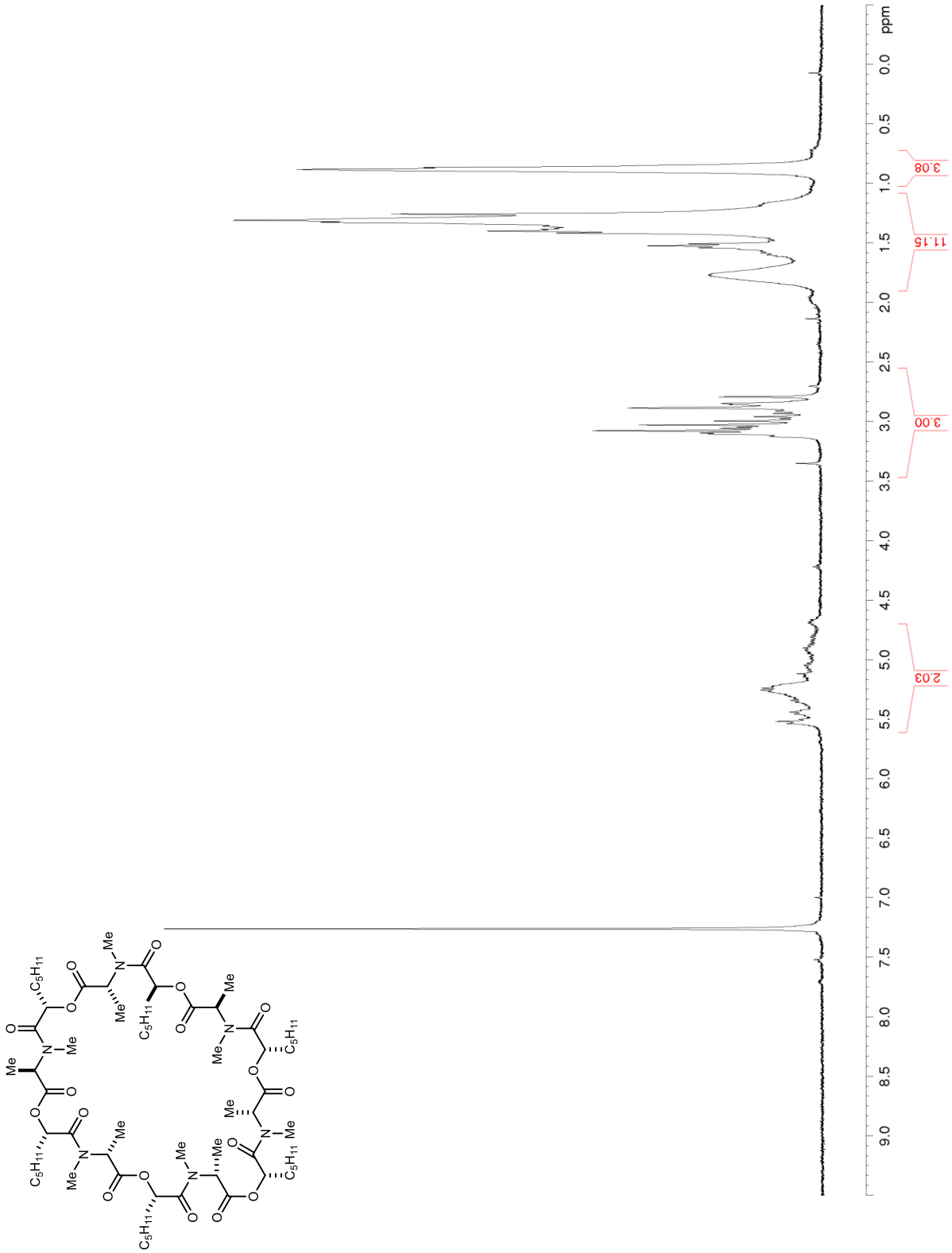

Figure S99. ^{13}C NMR/DEPT (150 MHz, $CDCl_3$) of **58**

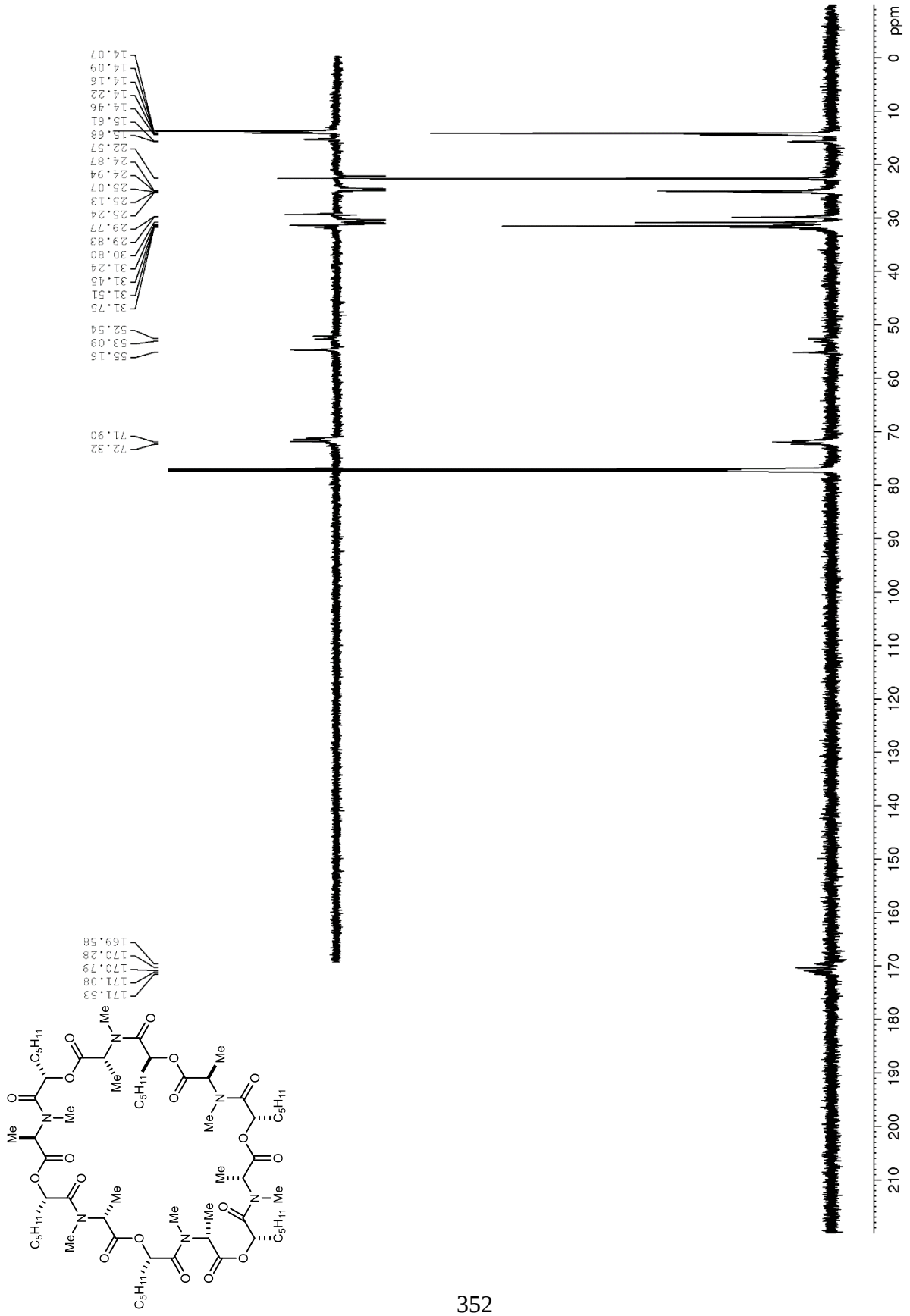

Figure S100. ^{1}H NMR (600 MHz, $CDCl_3$) of **66**

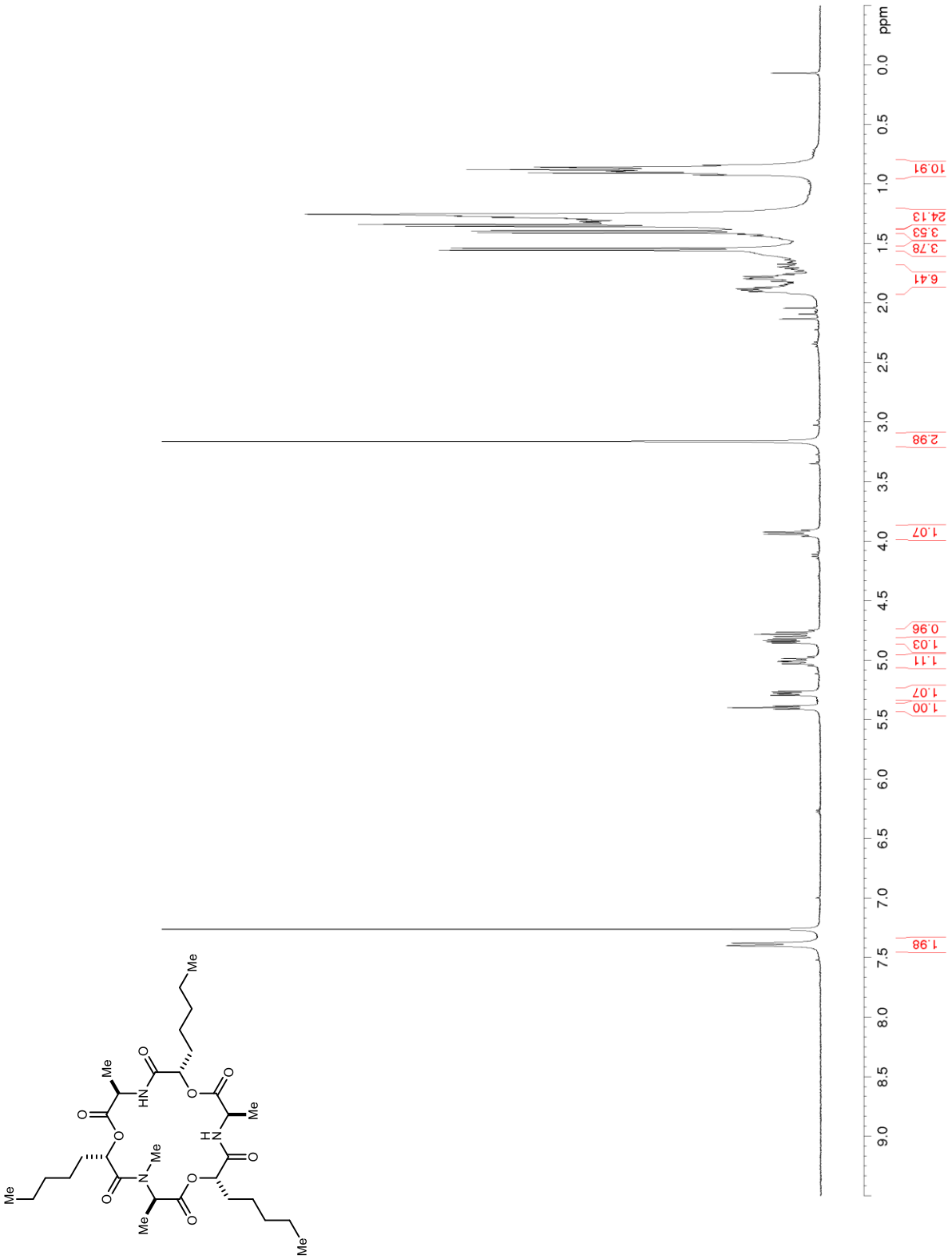

Figure S101. ^{13}C NMR/DEPT (150 MHz, $CDCl_3$) of **66**

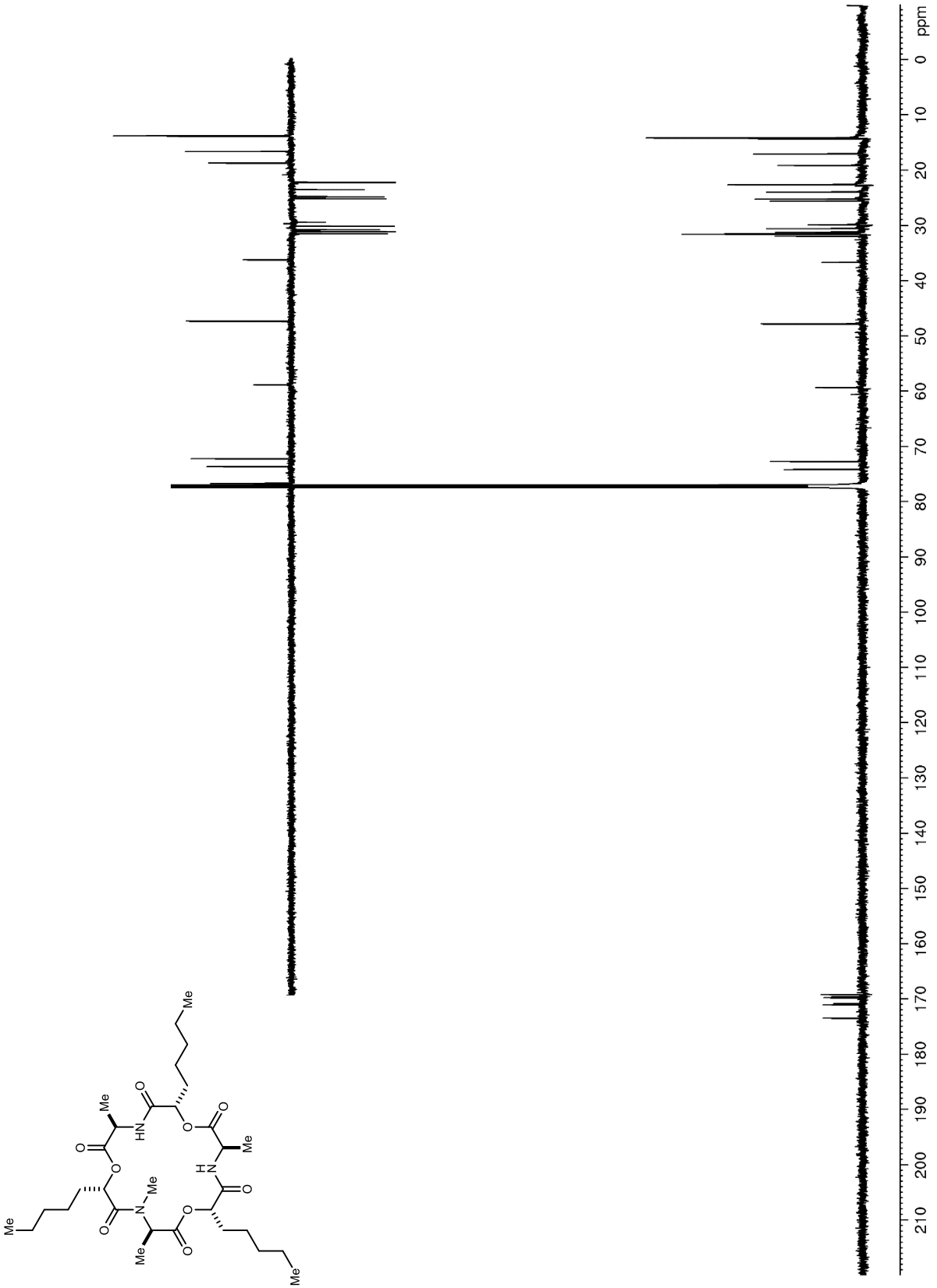

Figure S102. ^{1}H NMR (400 MHz, $CDCl_3$) of **65**

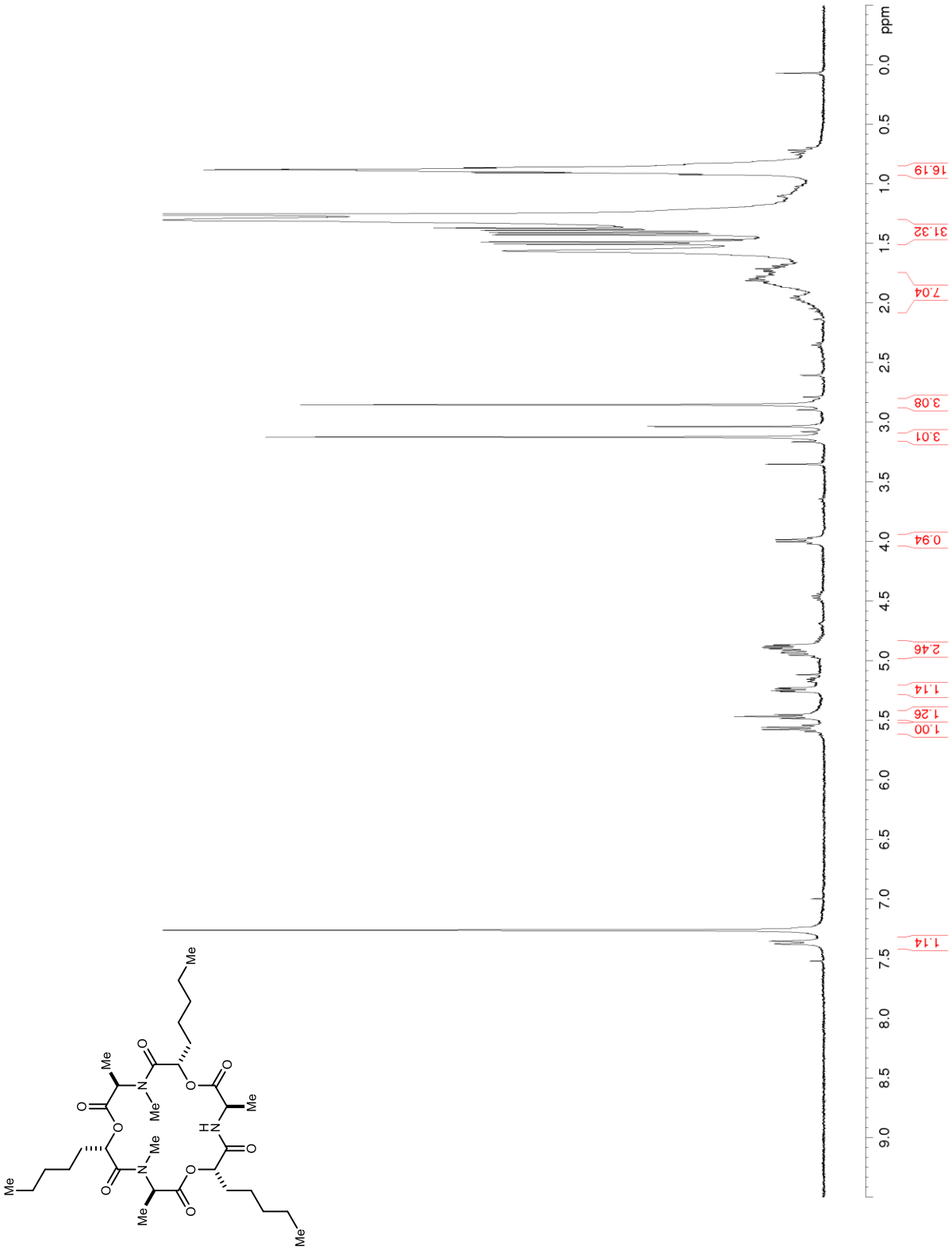

Figure S103. ^{13}C NMR/DEPT (150 MHz, $CDCl_3$) of **65**

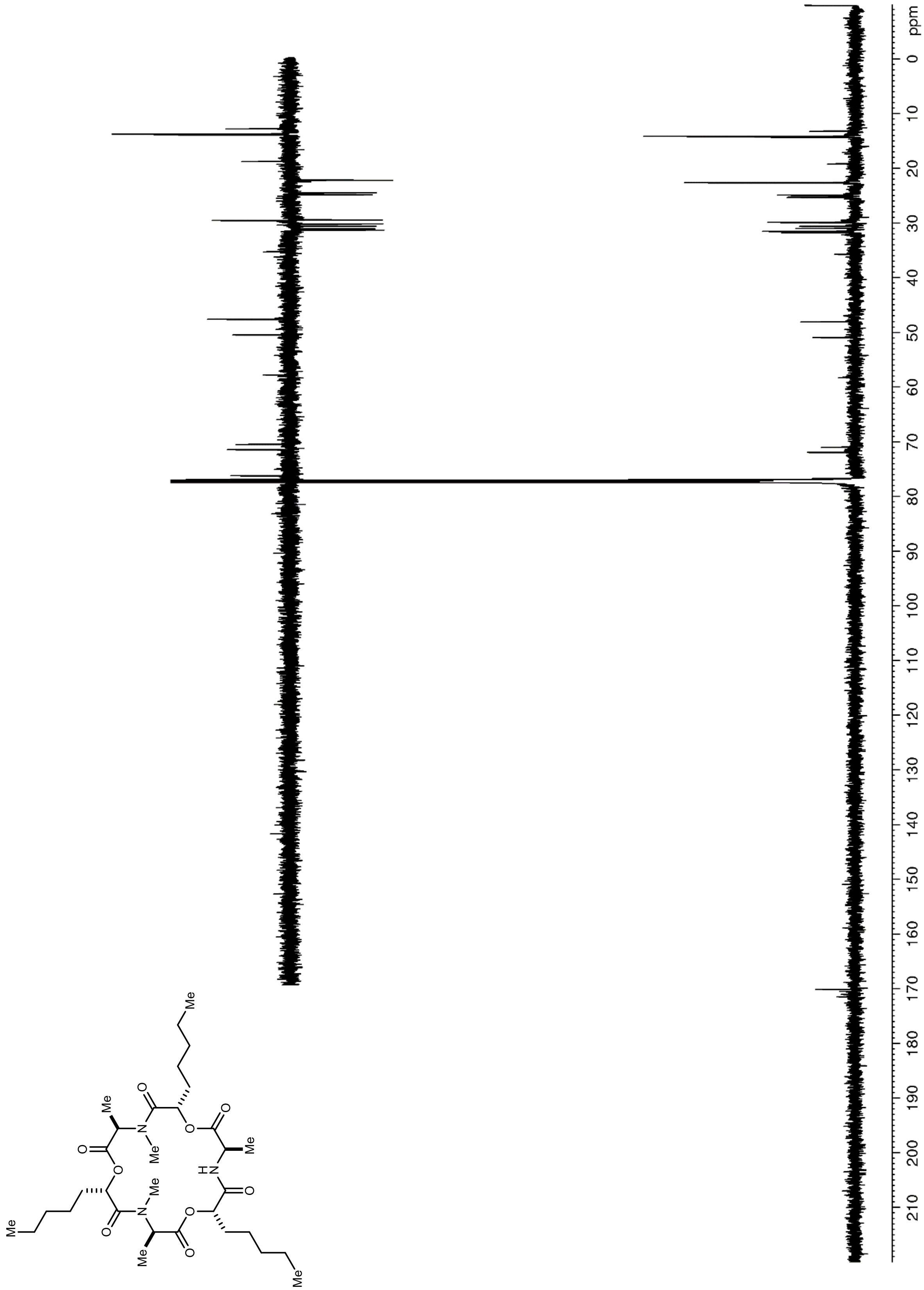

Figure S104. ^{1}H NMR (600 MHz, $CDCl_3$) of **S31**

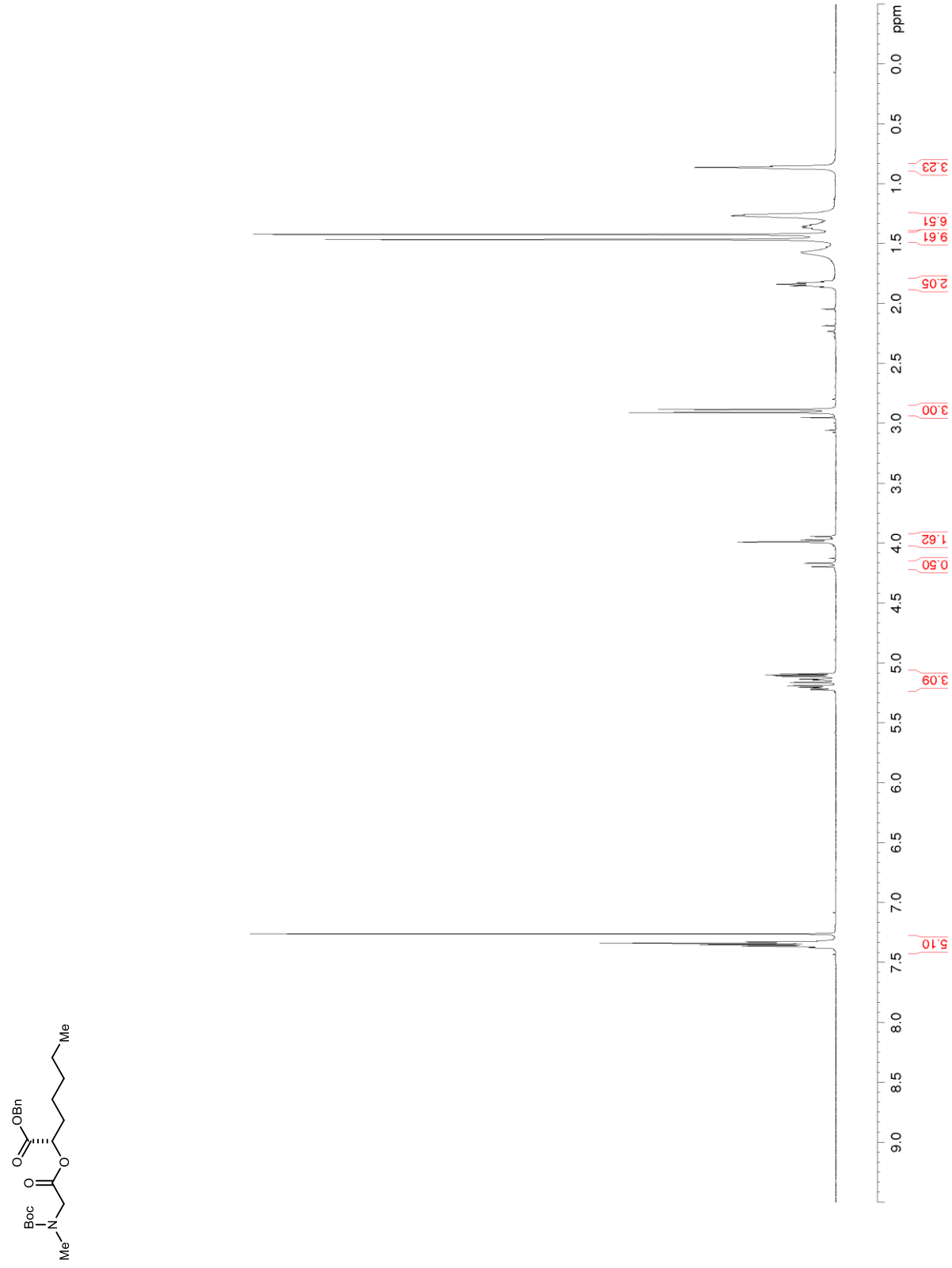

Figure S105. ^{13}C NMR/DEPT (150 MHz, $CDCl_3$) of **S31**

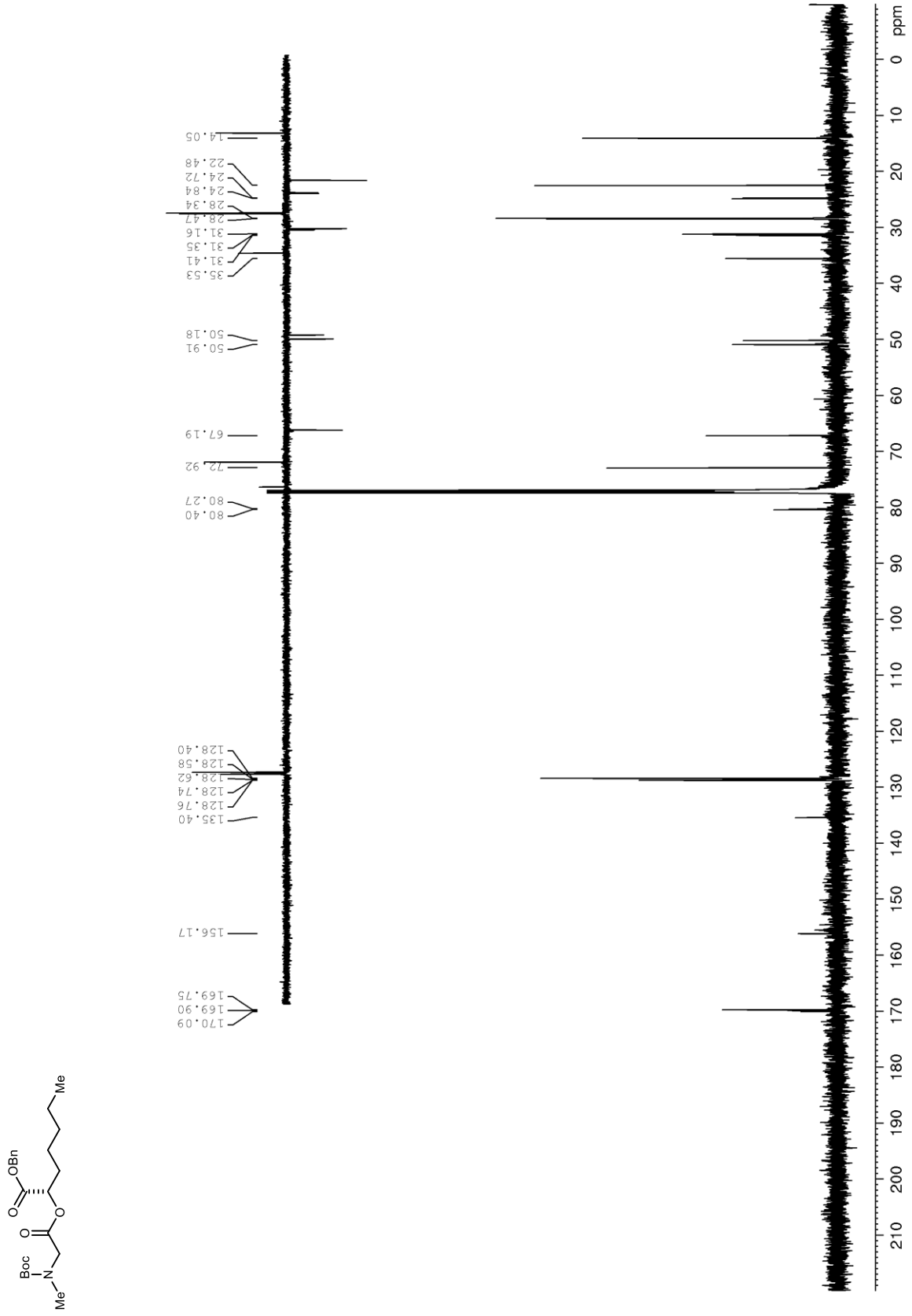

Figure S106. ^{1}H NMR (600 MHz, $CDCl_3$) of **S32**

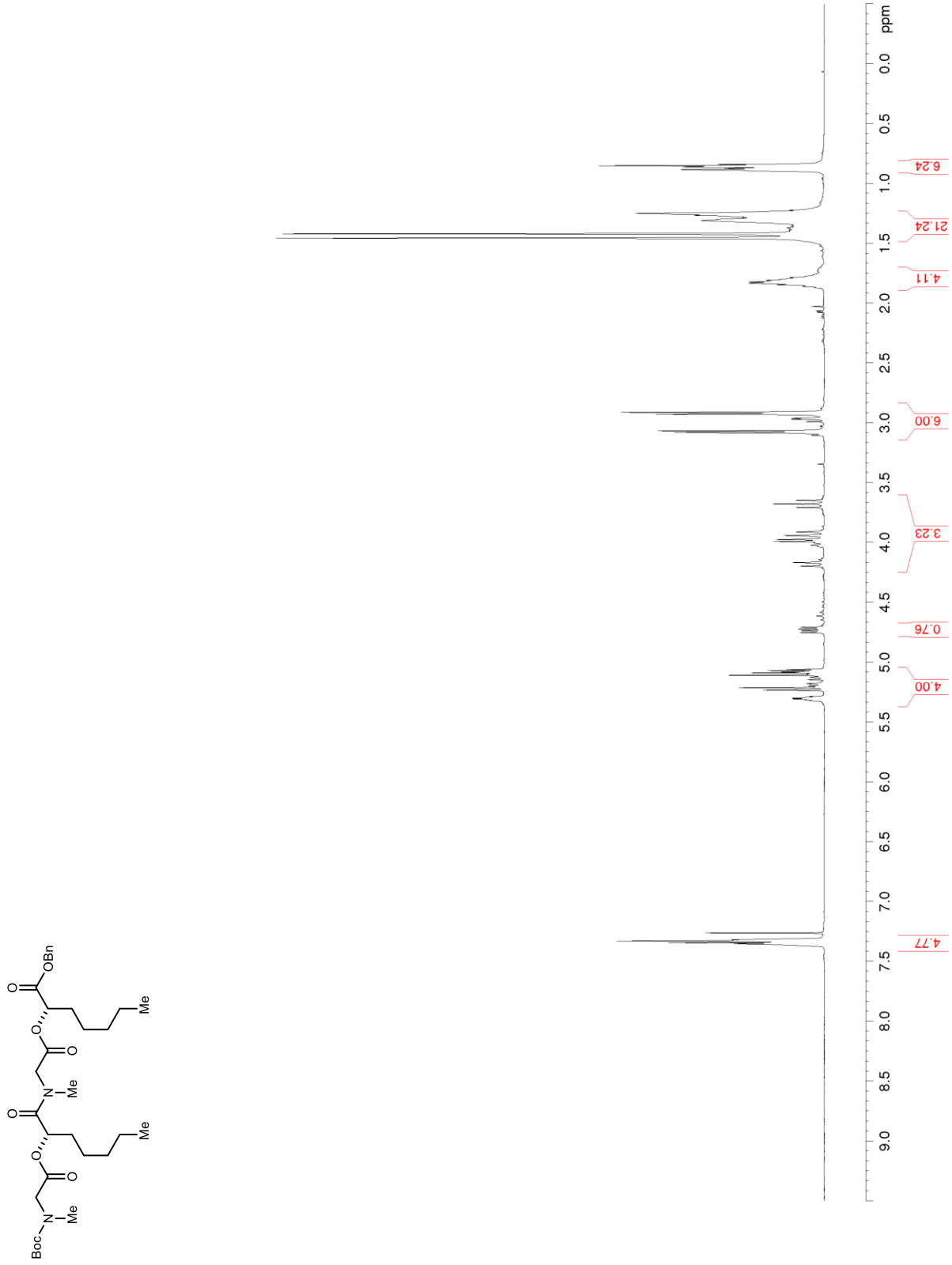

Figure S107. ^{13}C NMR/DEPT (150 MHz, $CDCl_3$) of **S32**

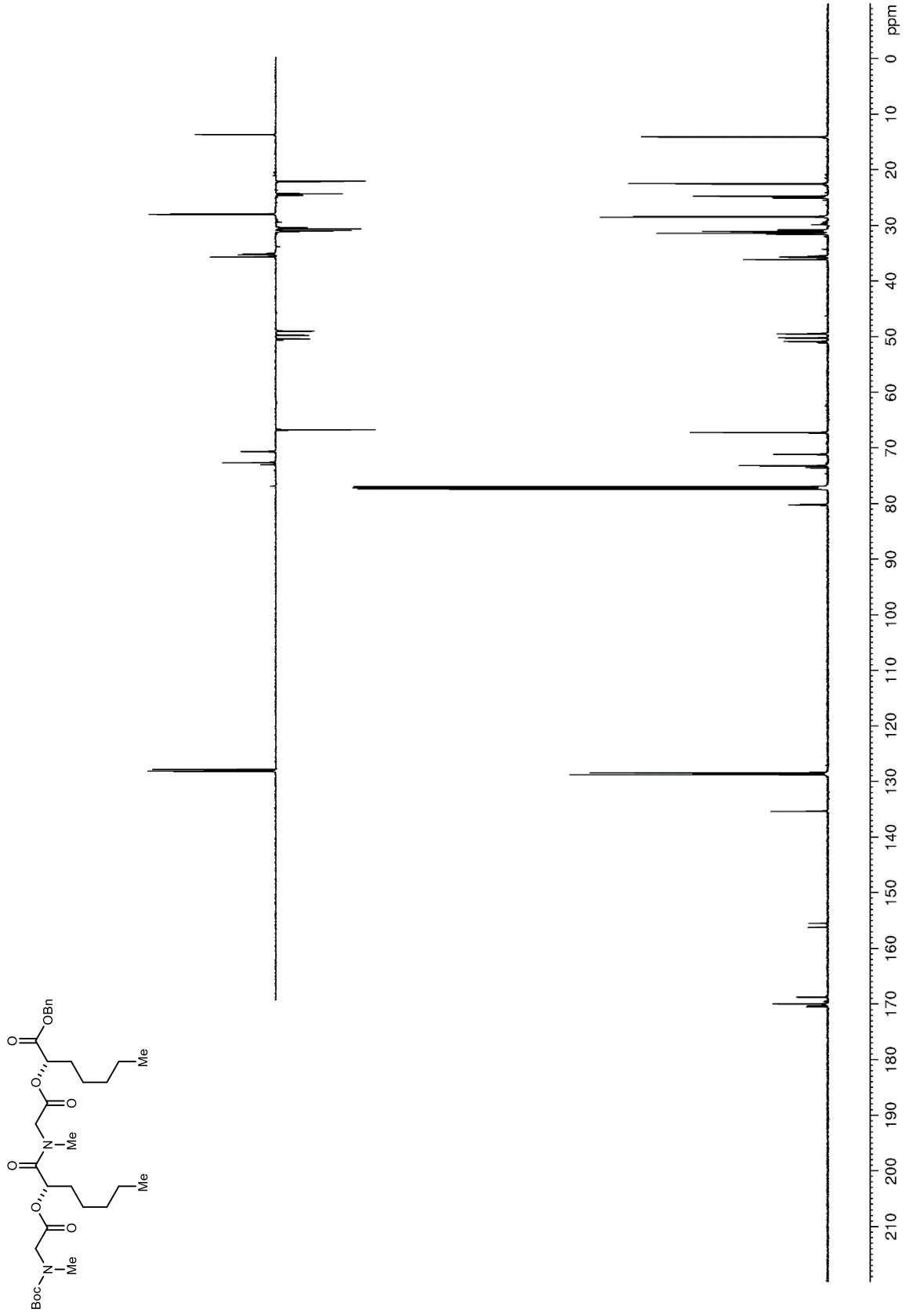

Figure S108. ^{1}H NMR (600 MHz, $CDCl_3$) of **S33**

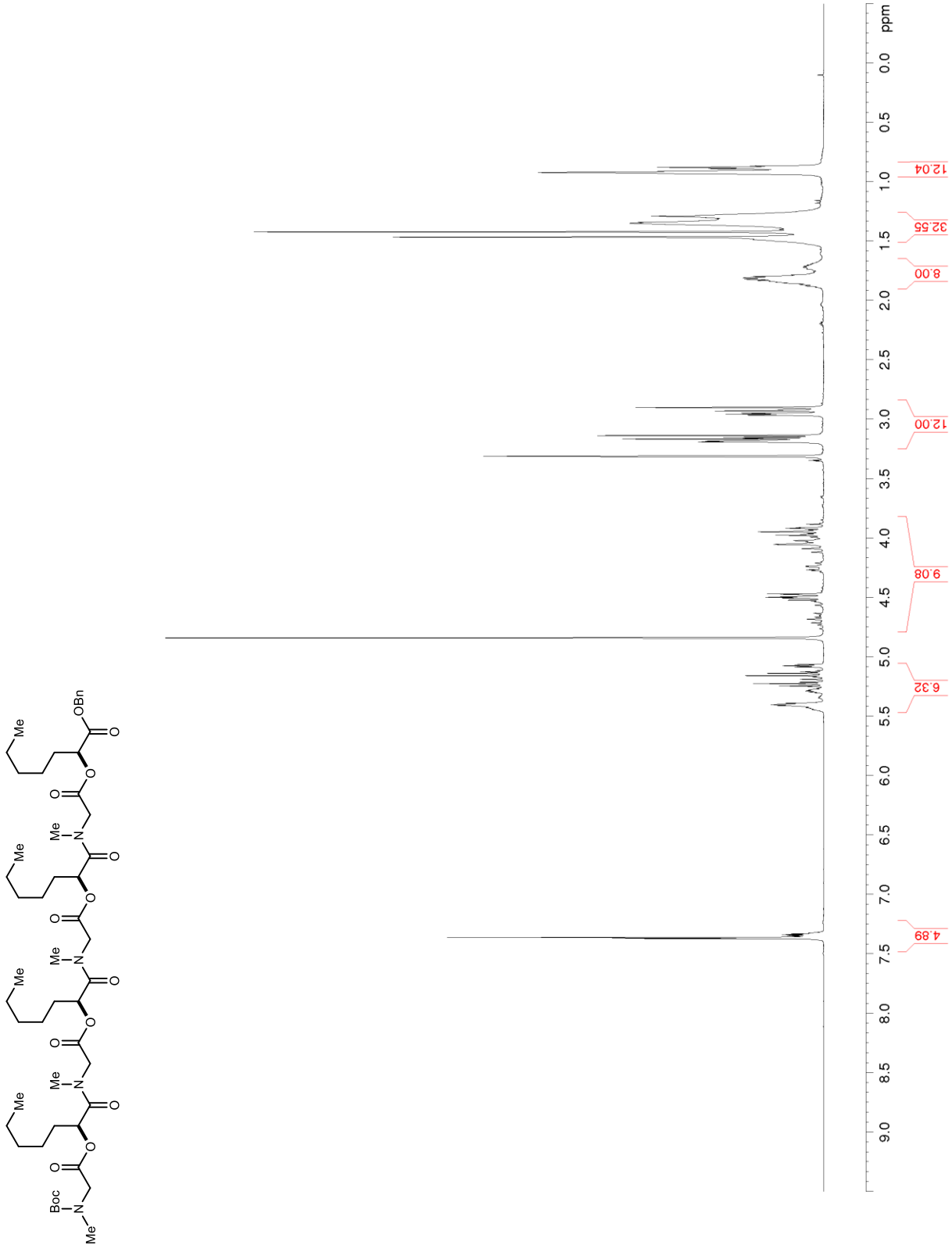

Figure S109. ^{13}C NMR/DEPT (150 MHz, $CDCl_3$) of **S33**

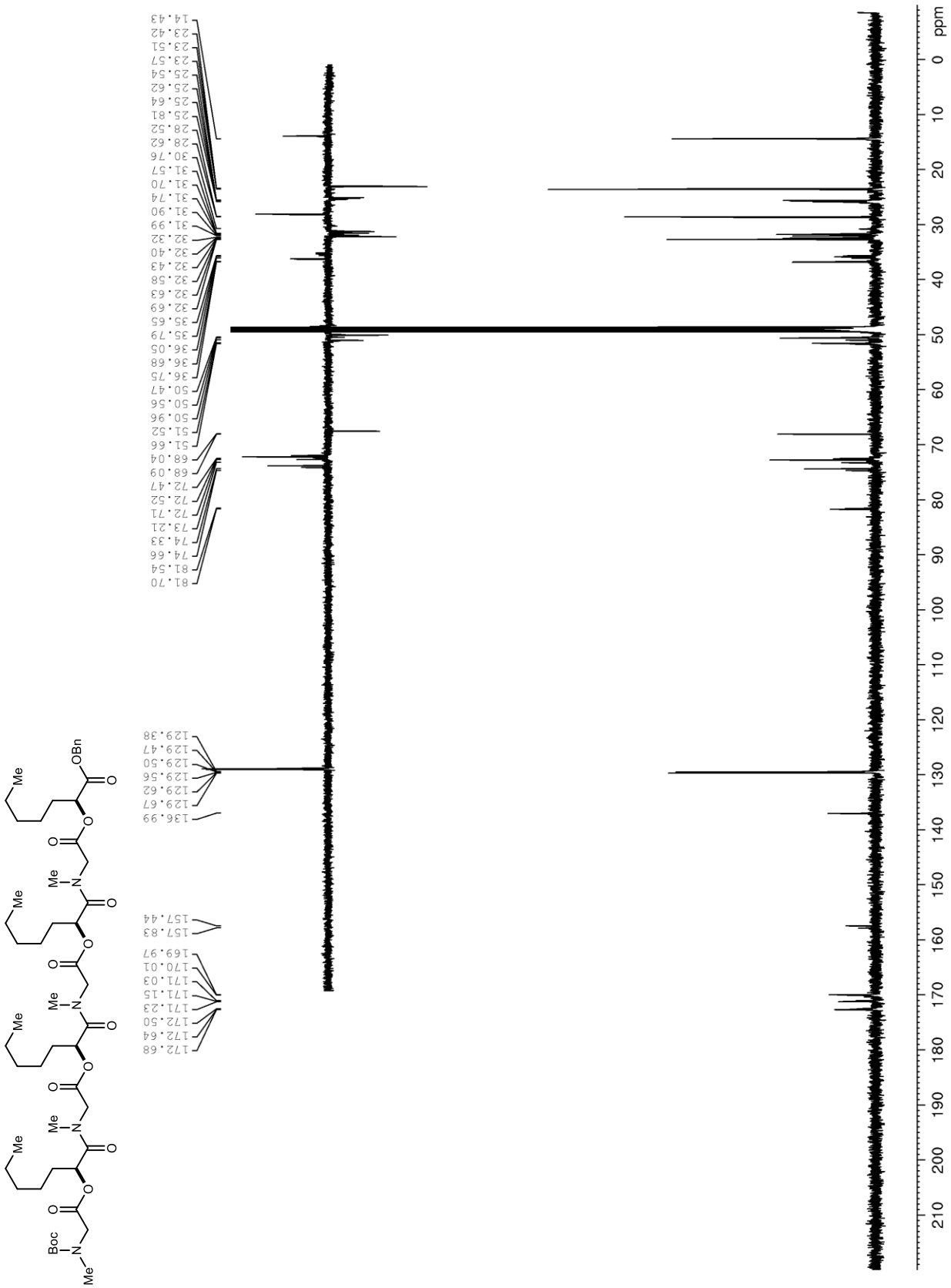

Figure S110. ^{1}H NMR (600 MHz, $CDCl_3$) of **70**

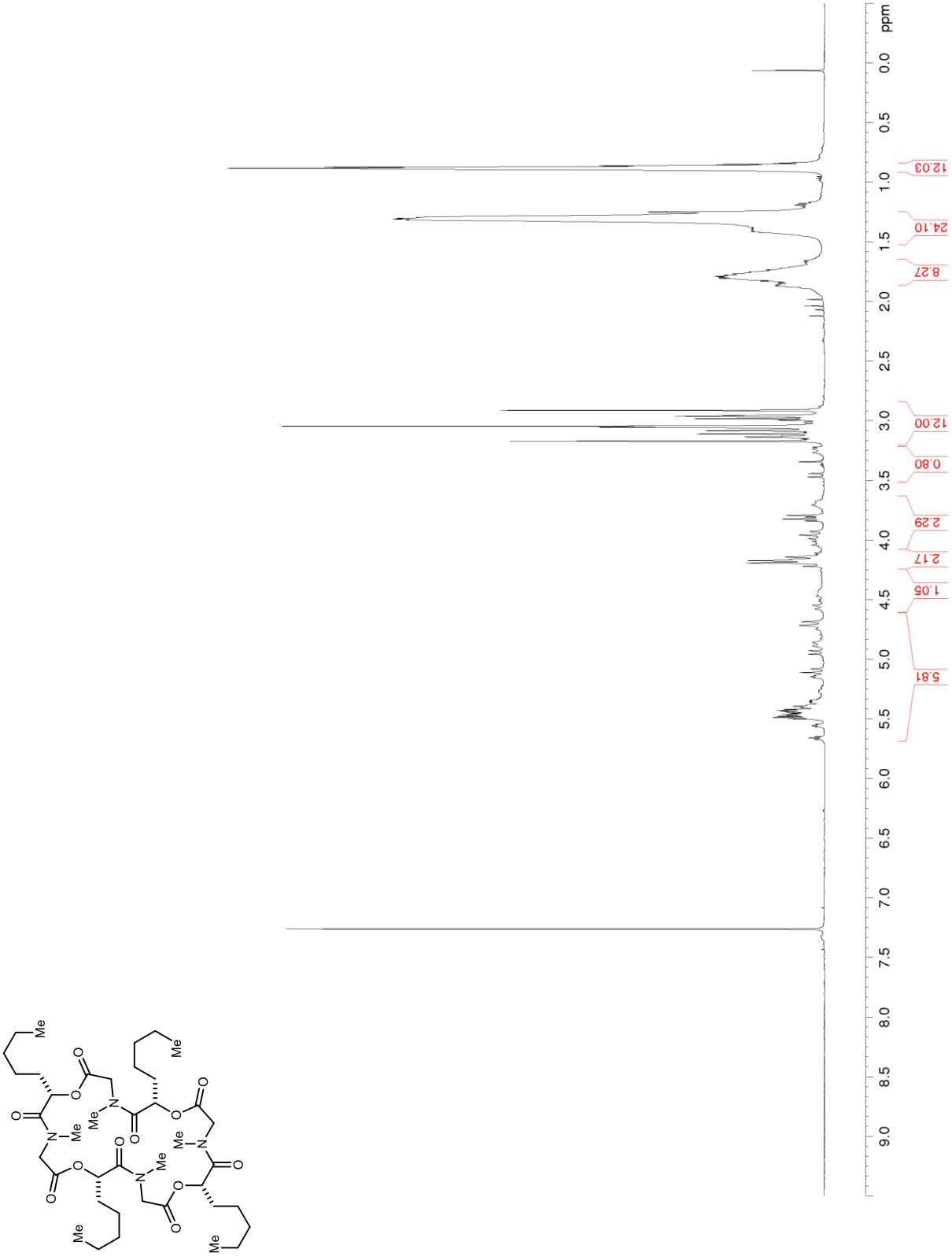

Figure S111. ^{13}C NMR/DEPT (150 MHz, $CDCl_3$) of **70**

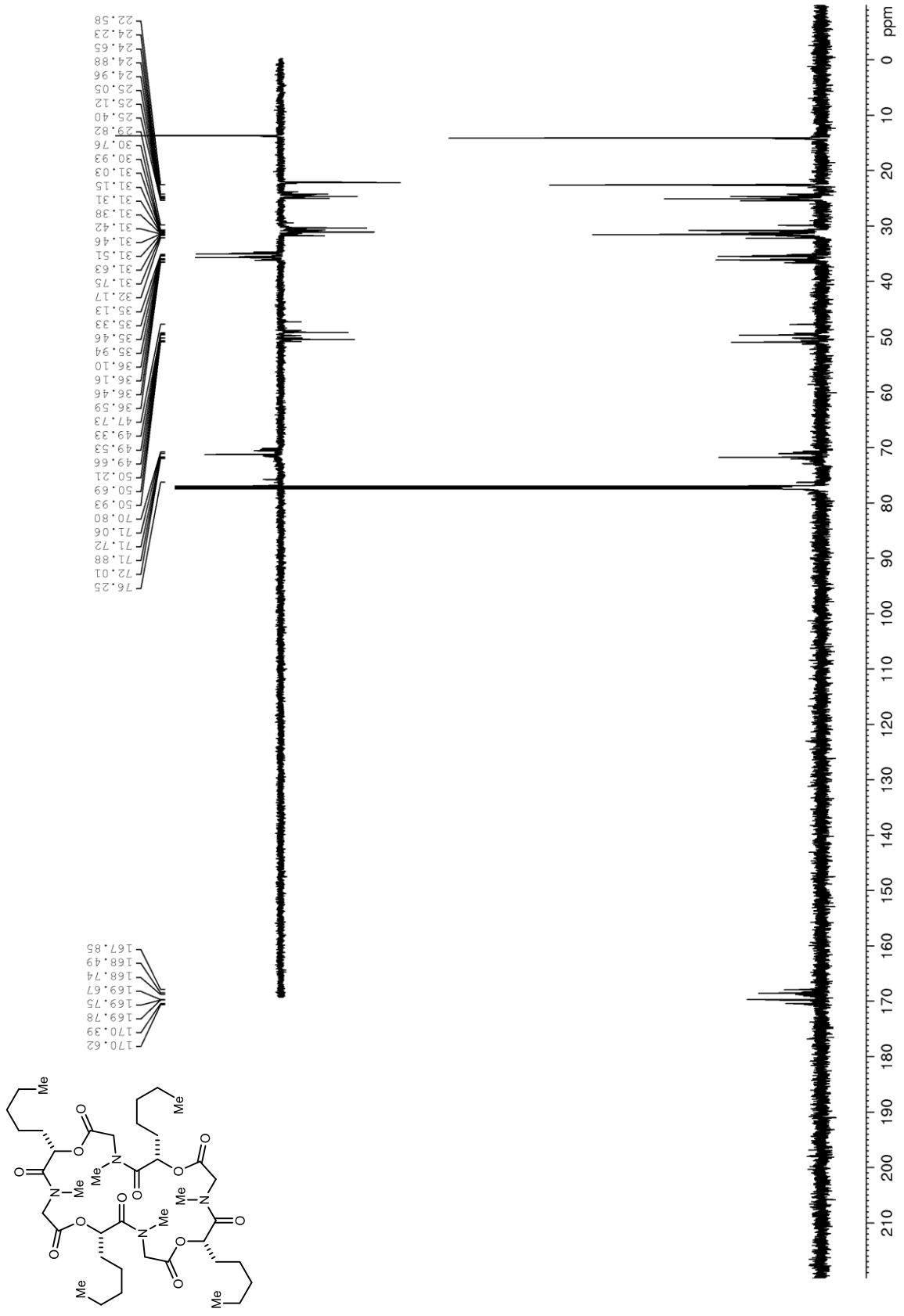

Figure S112. ^{1}H NMR (600 MHz, $CDCl_3$) of **S34**

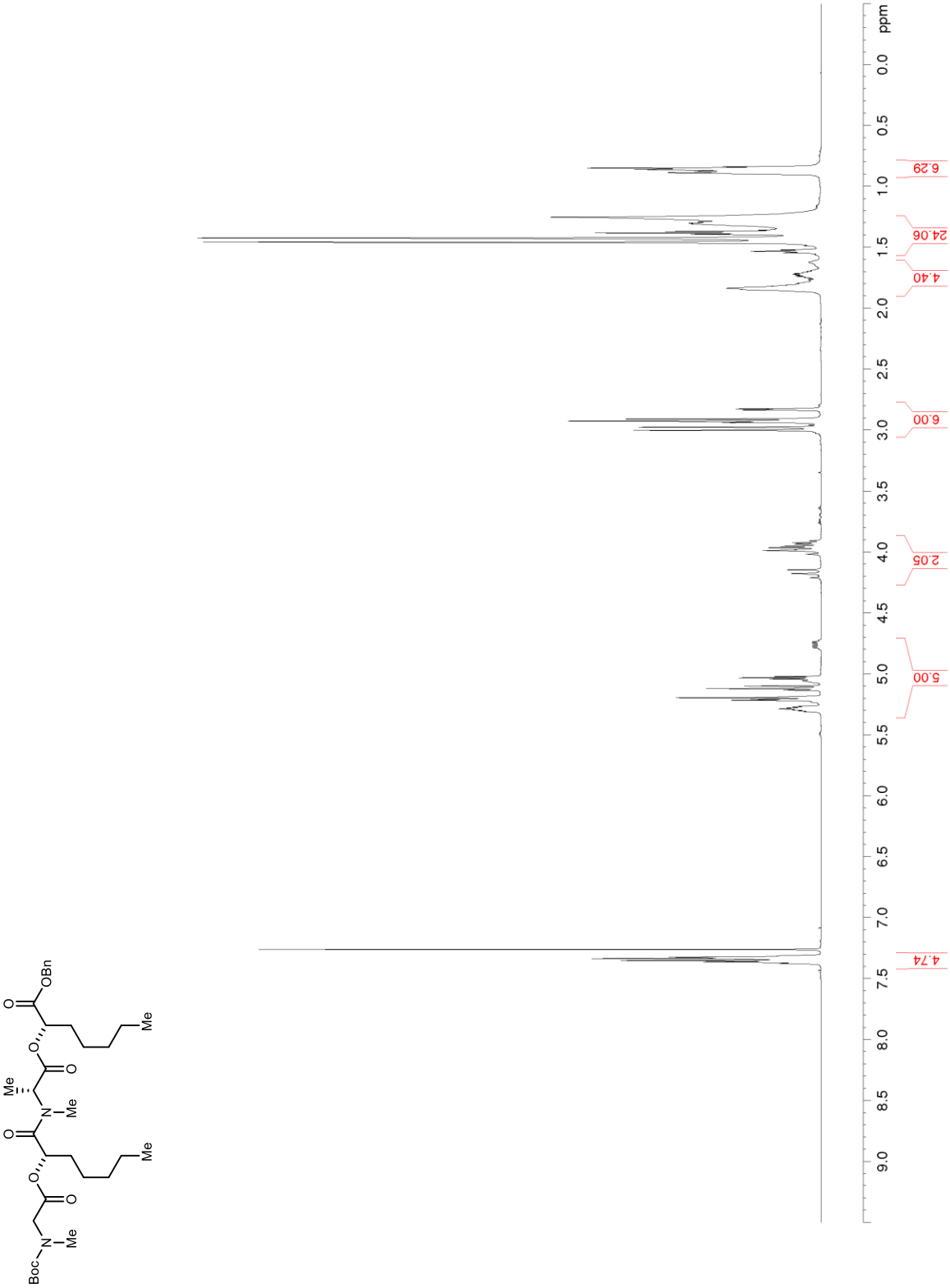

Figure S113. ^{13}C NMR/DEPT (150 MHz, $CDCl_3$) of **S34**

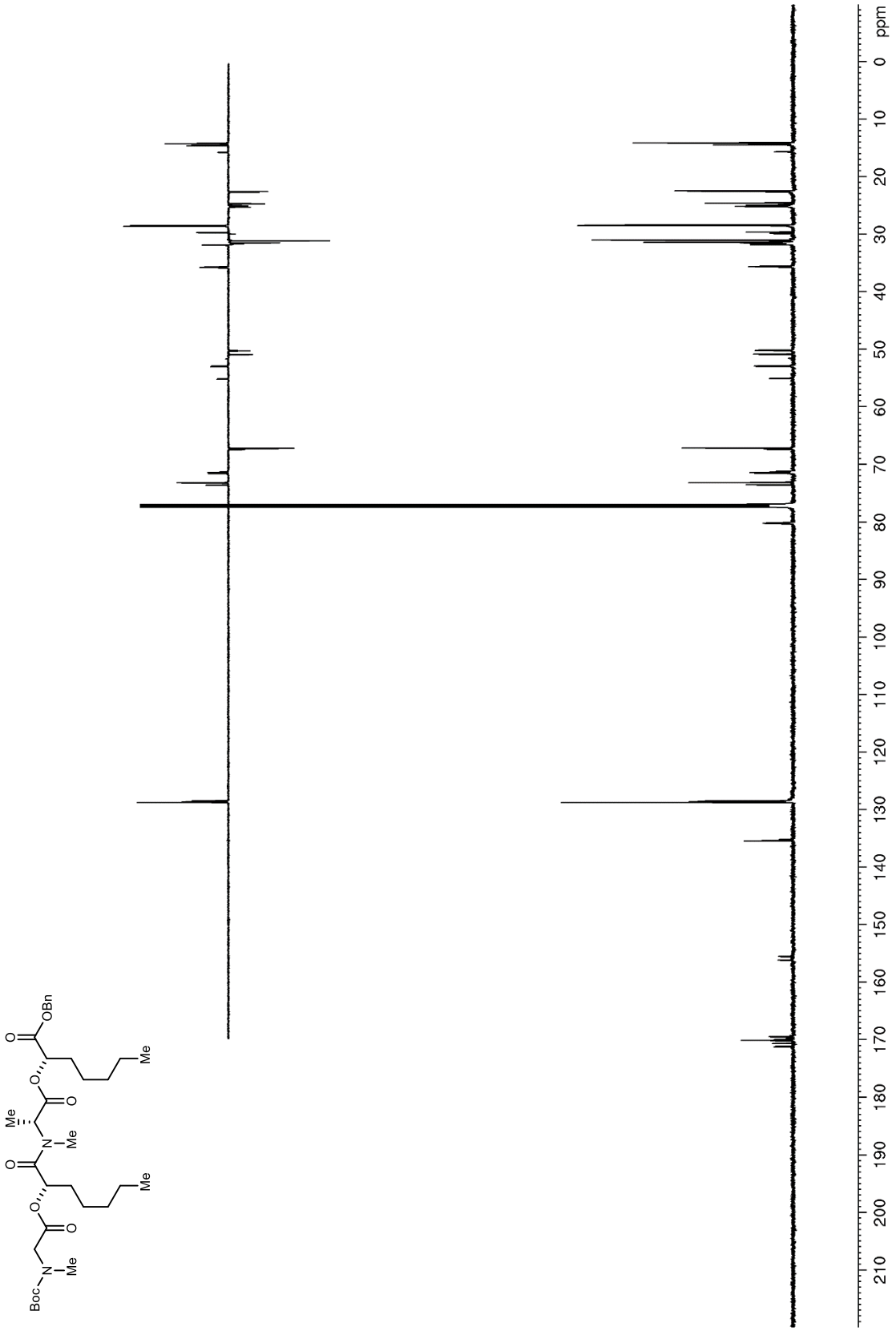

Figure S114. ^{1}H NMR (600 MHz, $CDCl_3$) of **S35**

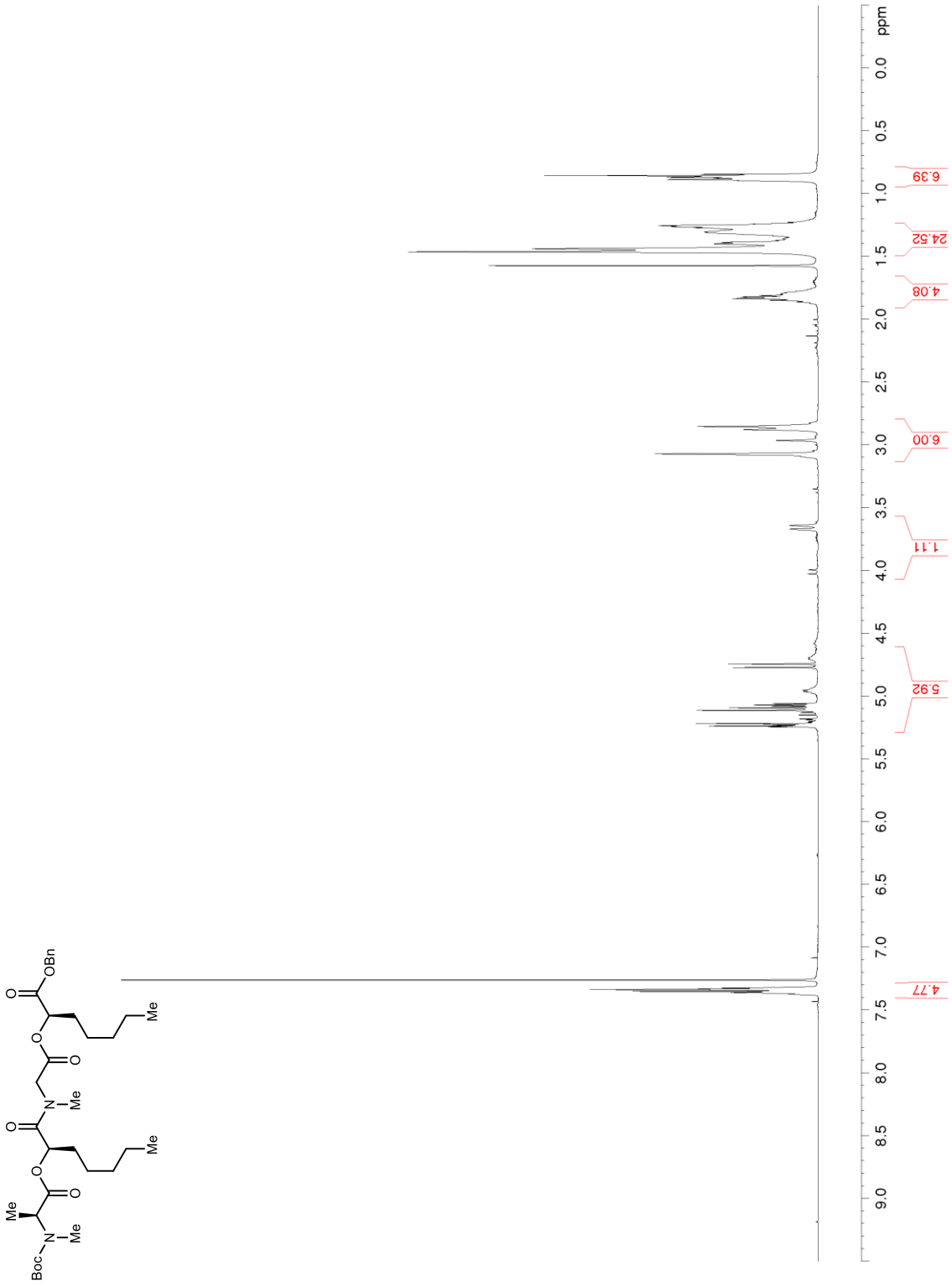

Figure S115. ^{13}C NMR/DEPT (150 MHz, $CDCl_3$) of **S35**

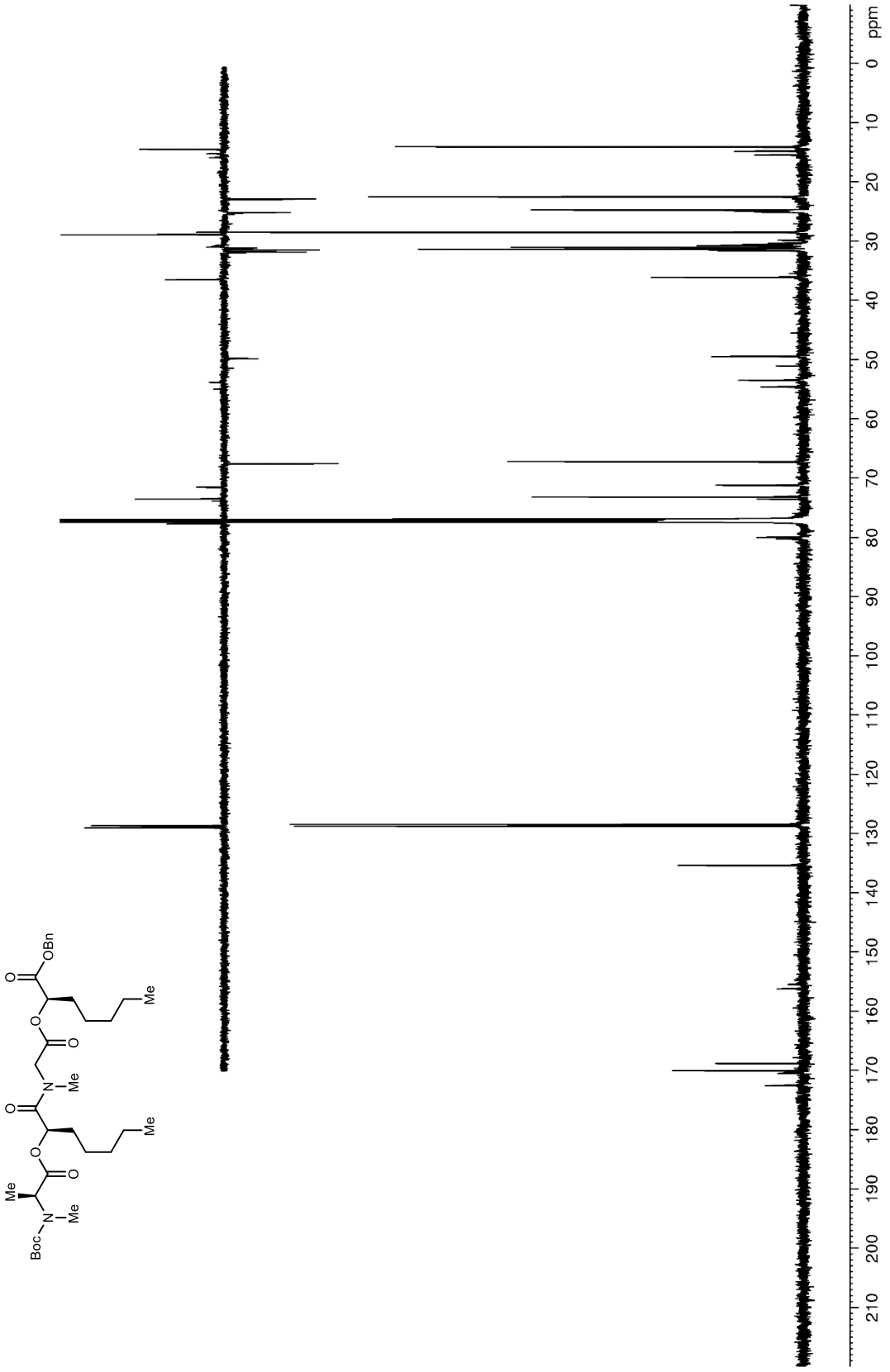

Figure S116. ^{1}H NMR (600 MHz, $CDCl_3$) of **S36**

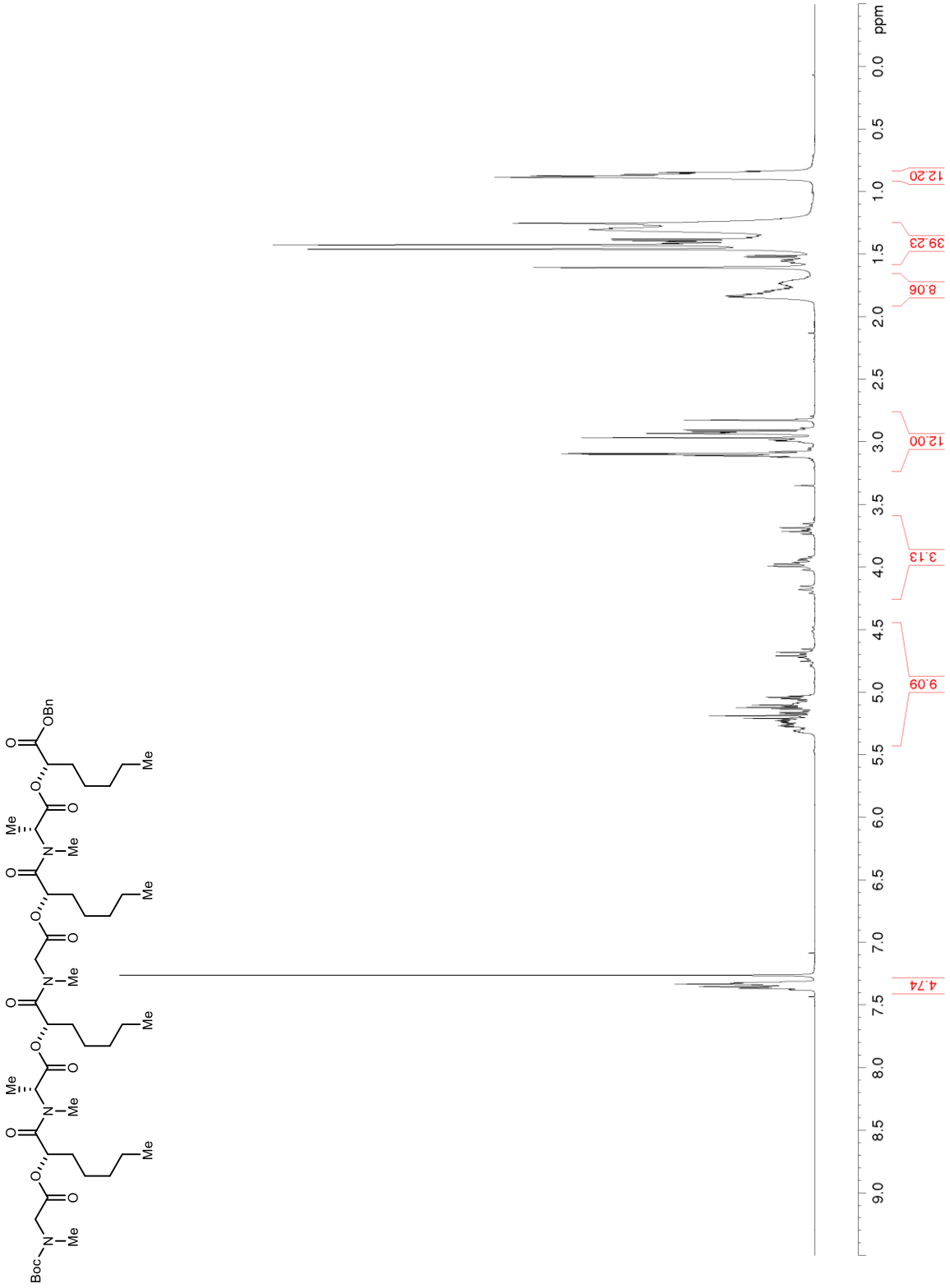

Figure S117. ^{13}C NMR/DEPT (150 MHz, $CDCl_3$) of **S36**

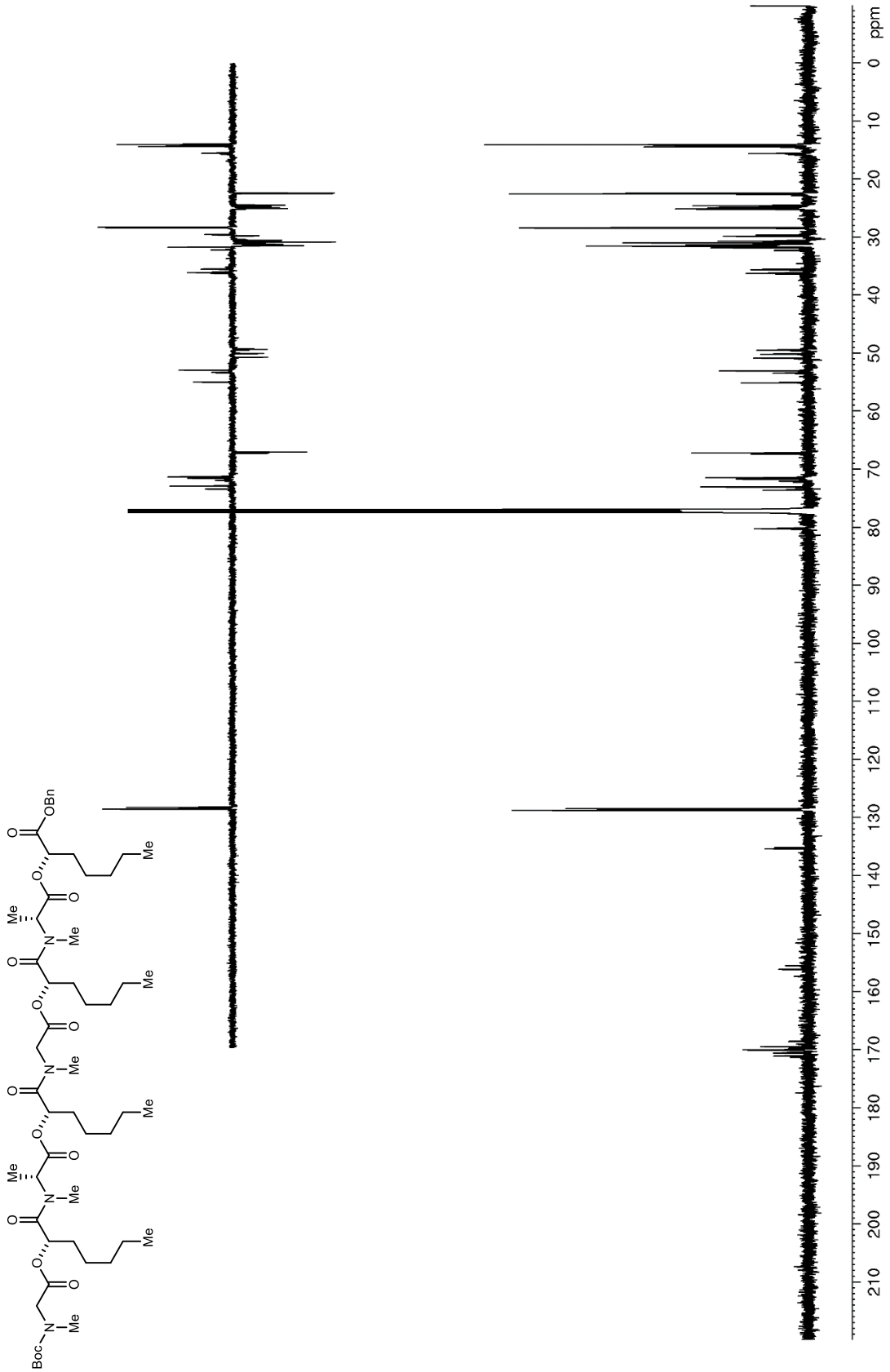

Figure S118. ^{1}H NMR (600 MHz, $CDCl_3$) of **67**

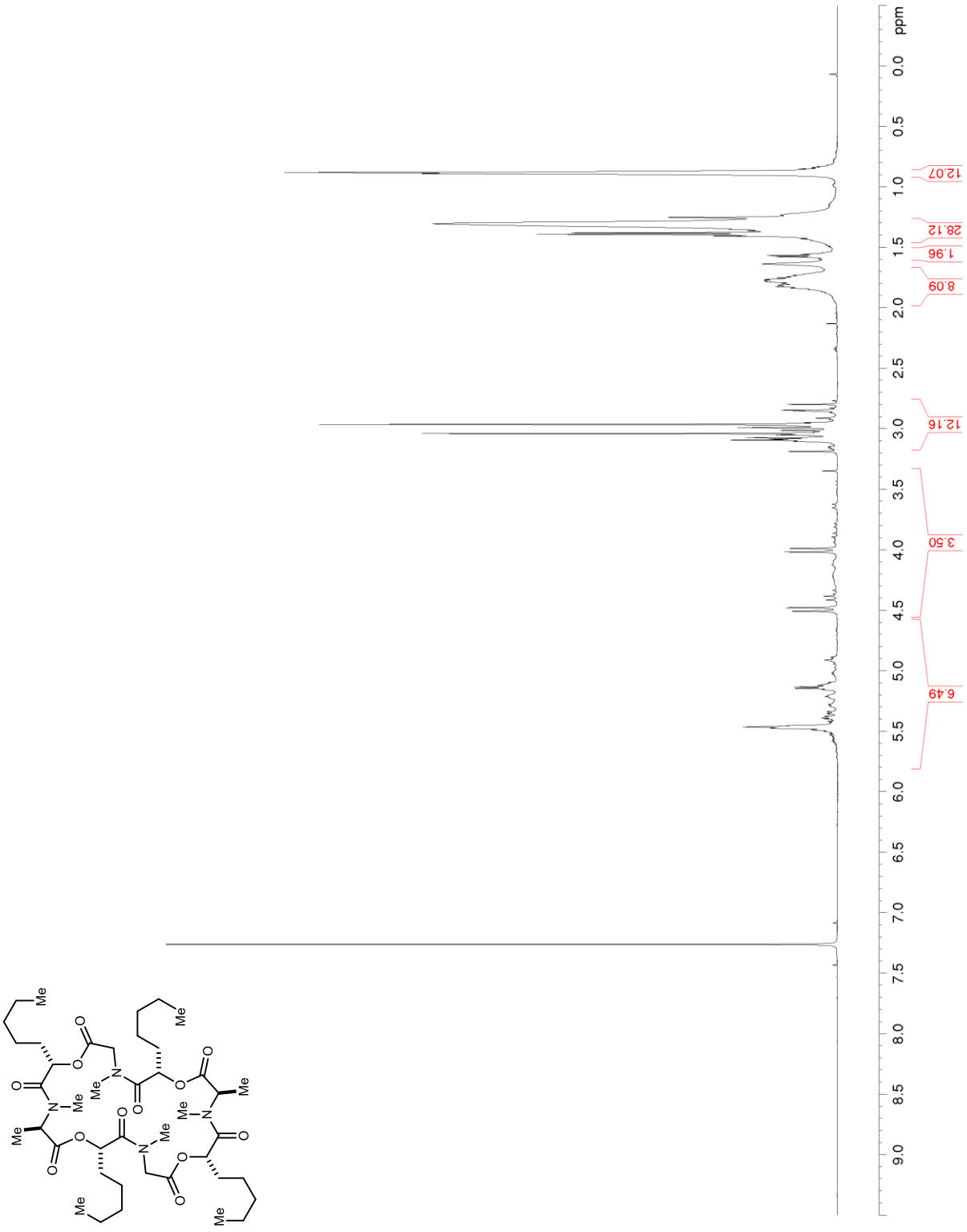

Figure S119. ^{13}C NMR/DEPT (150 MHz, $CDCl_3$) of **67**

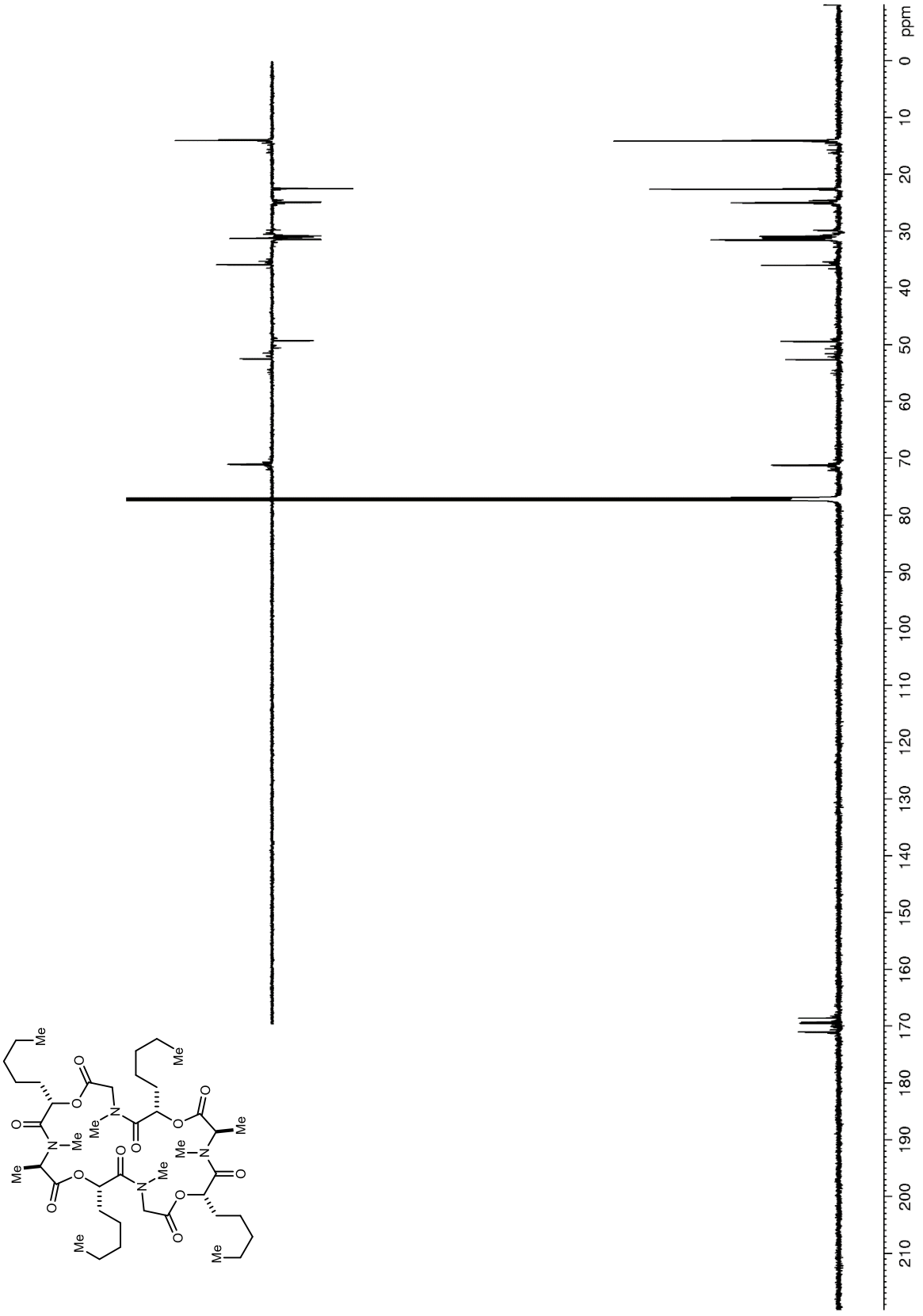

Figure S120. ^{1}H NMR (600 MHz, $CDCl_3$) of **S37**

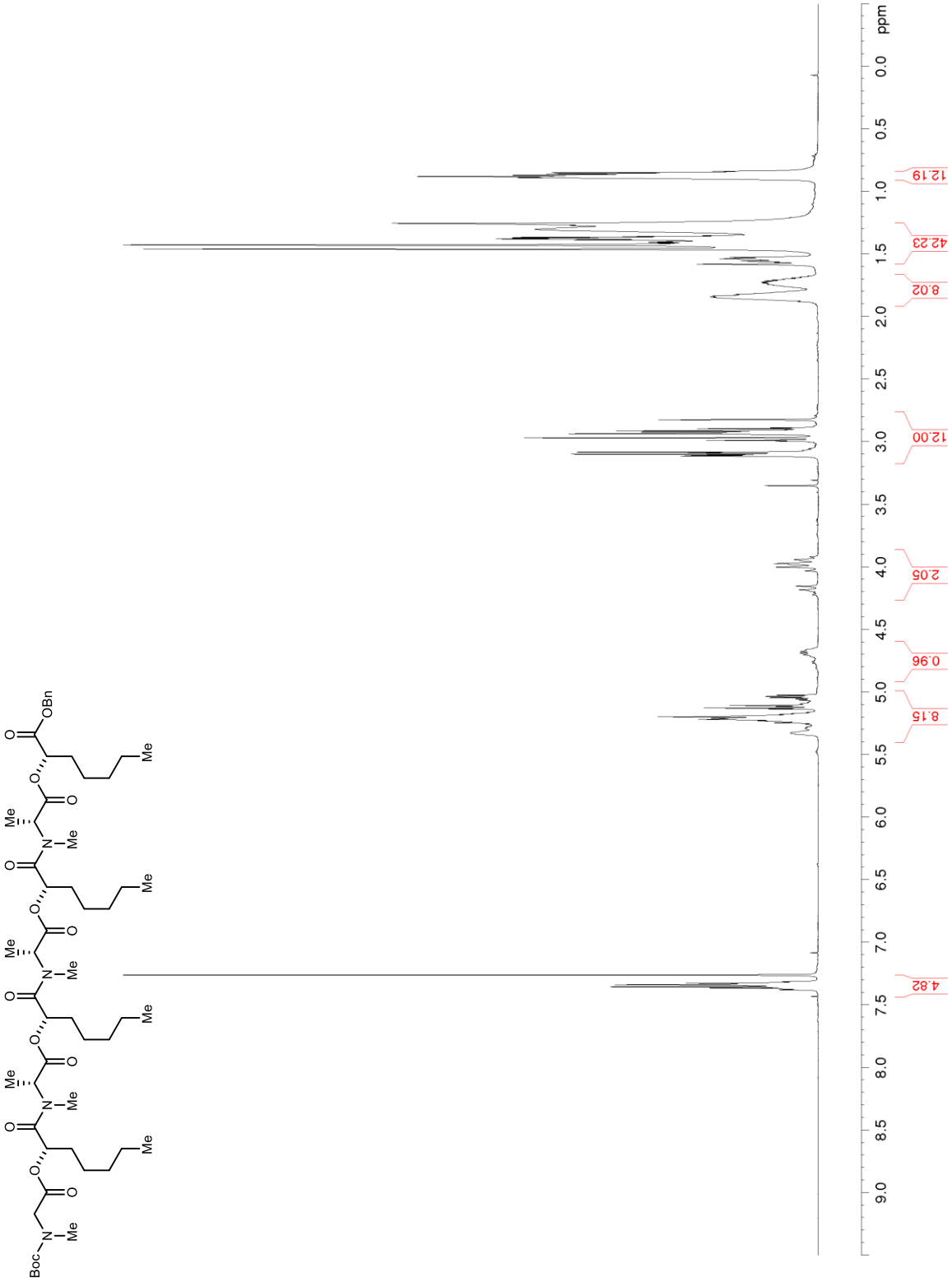

Figure S121. ^{13}C NMR/DEPT (150 MHz, $CDCl_3$) of **S37**

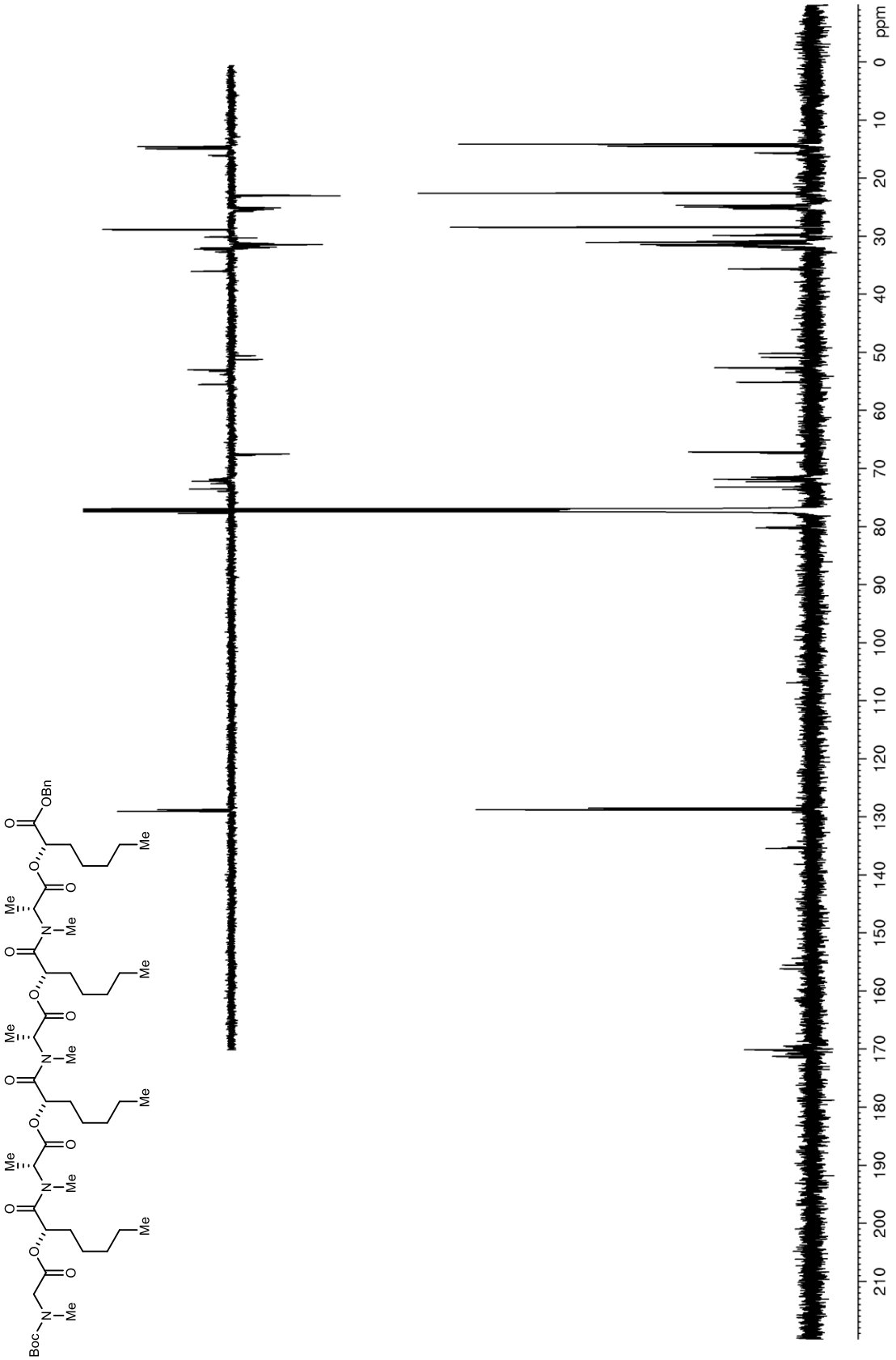

Figure S122. ^{1}H NMR (600 MHz, $CDCl_3$) of **71**

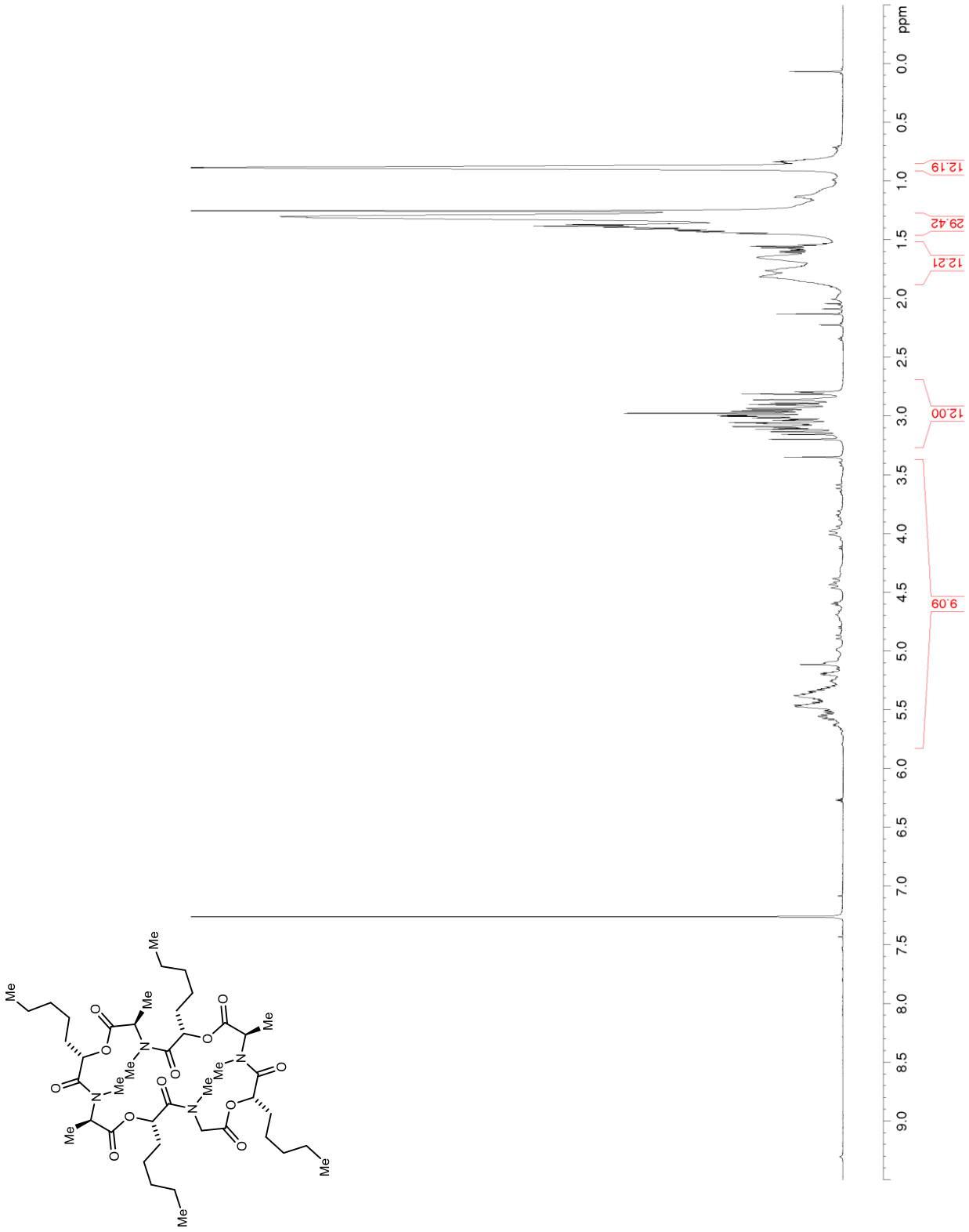

Figure S123. ^{13}C NMR/DEPT (150 MHz, $CDCl_3$) of **71**

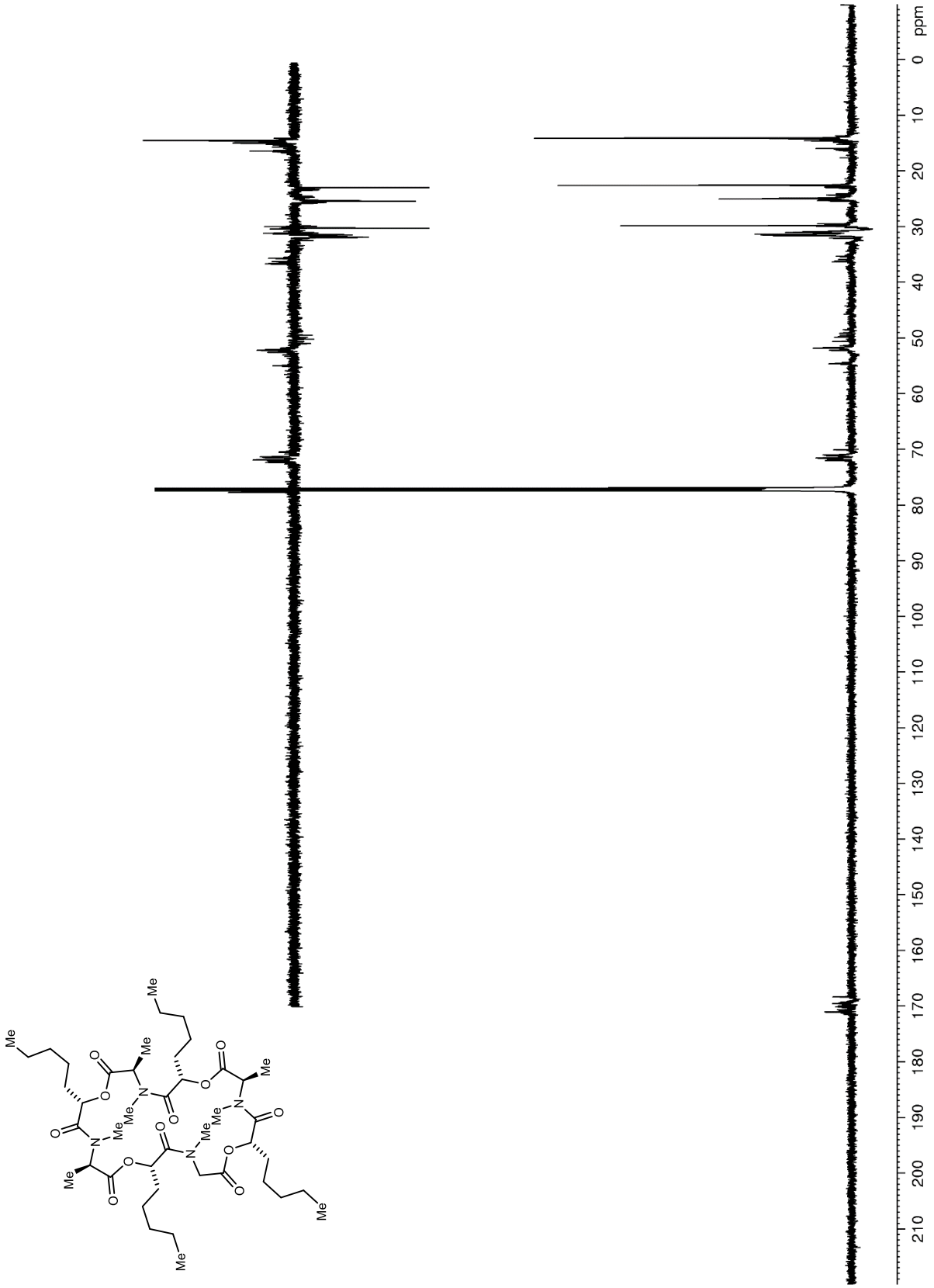

Figure S124. ^{1}H NMR (400 MHz, $CDCl_3$) of **S38**

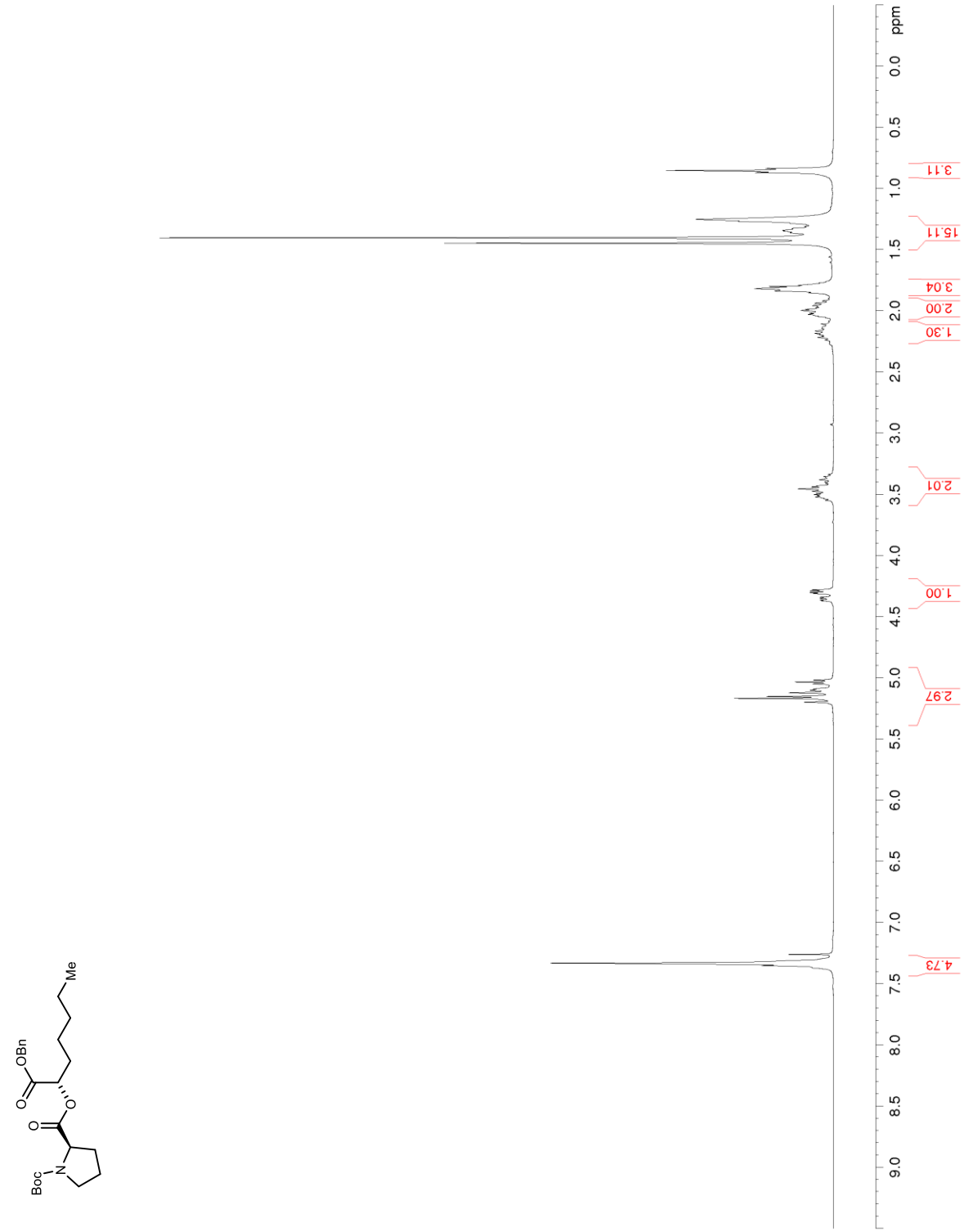

Figure S125. ^{13}C NMR/DEPT (100 MHz, $CDCl_3$) of **S38**

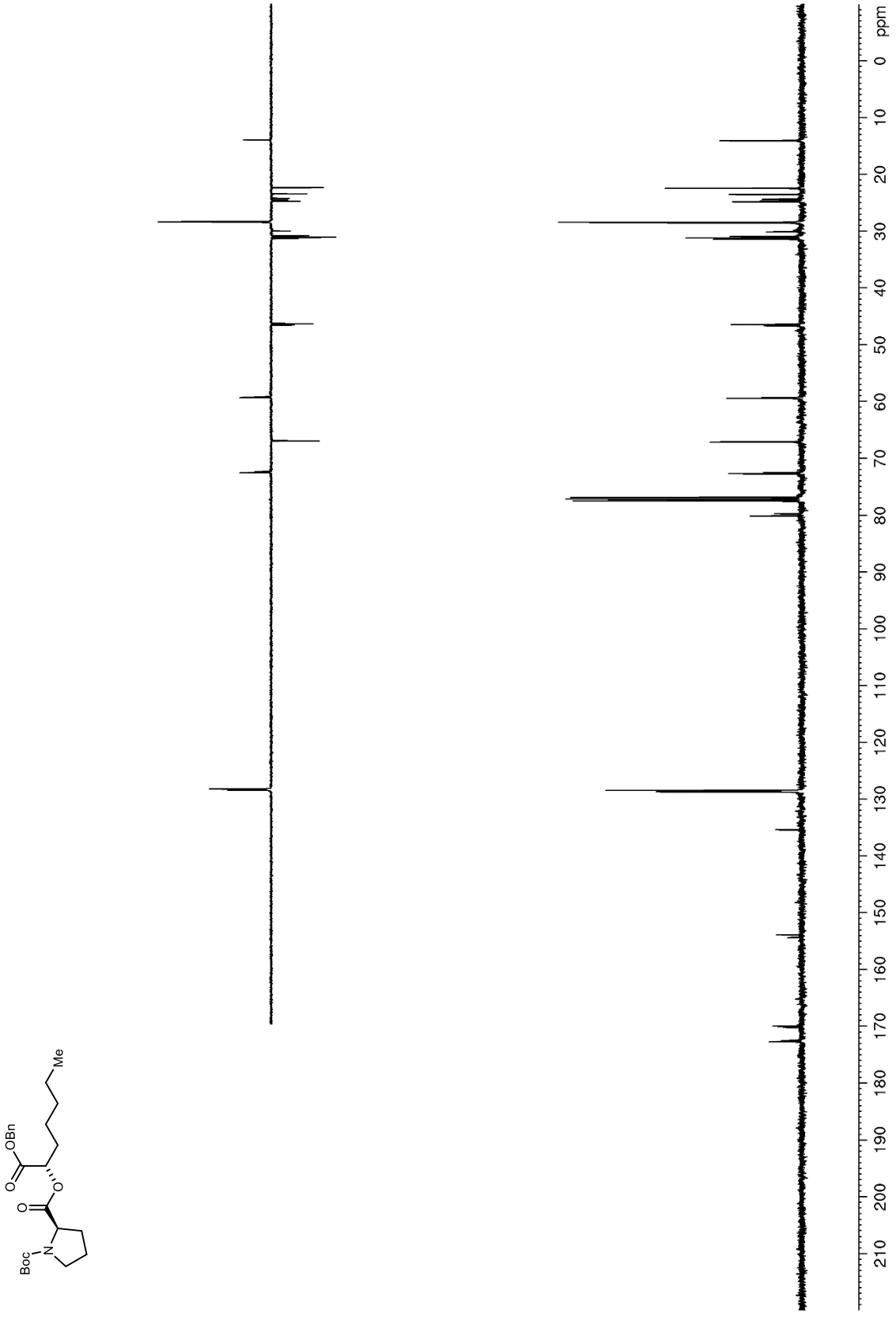

Figure S126. ^{1}H NMR (600 MHz, $CDCl_3$) of **S39**

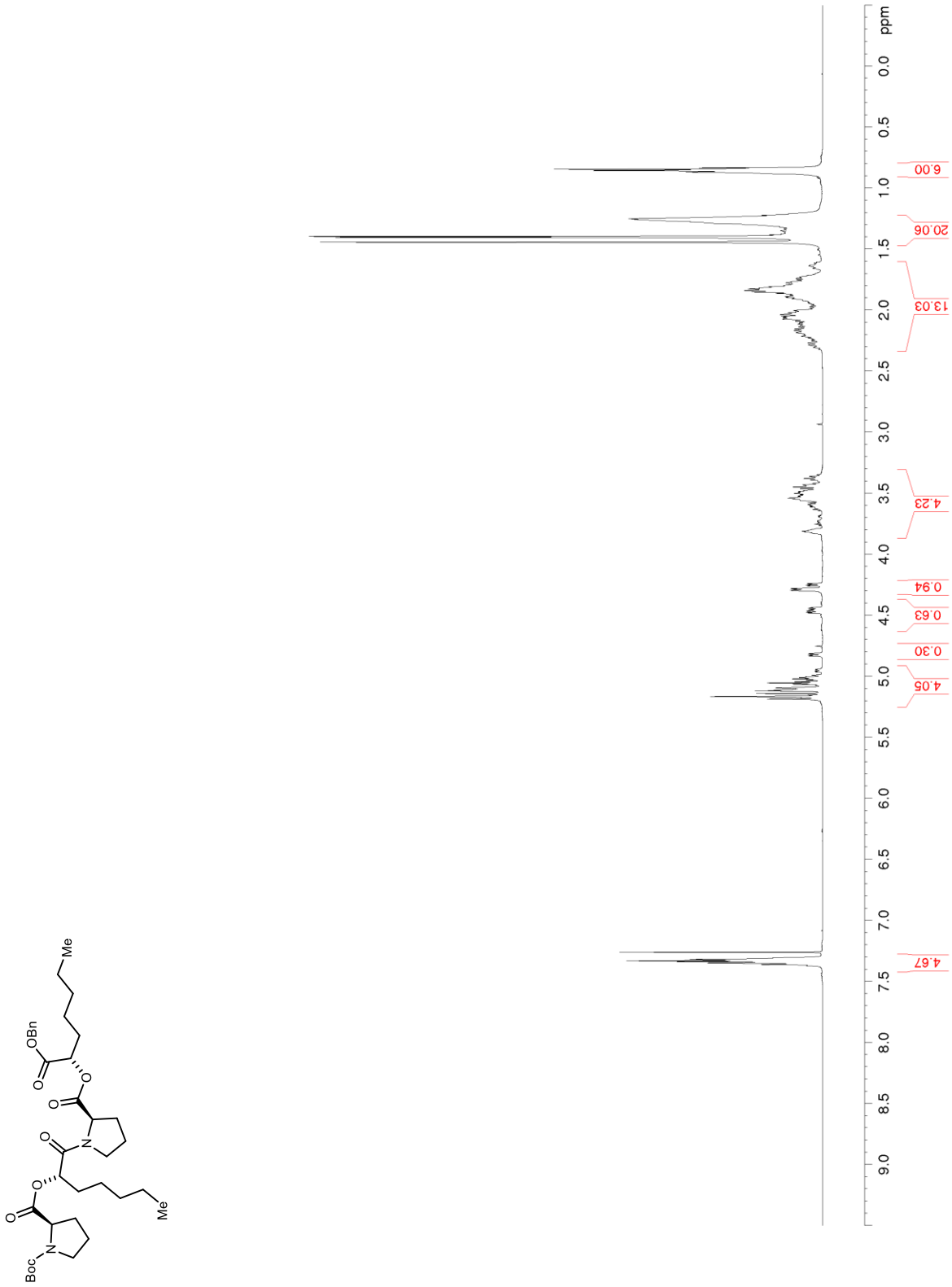

Figure S127. ^{13}C NMR/DEPT (150 MHz, $CDCl_3$) of **S39**

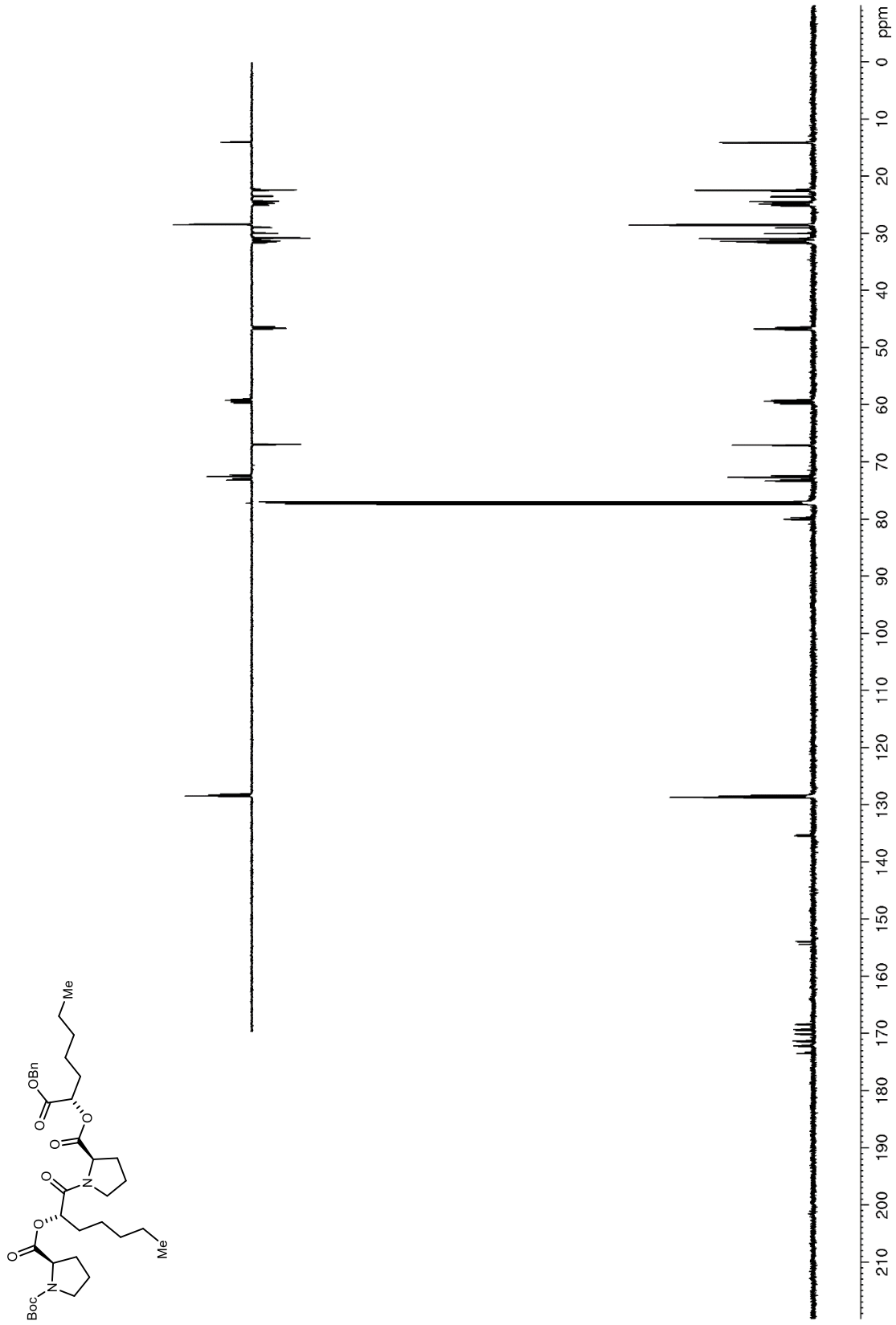

Figure S128. ^{1}H NMR (600 MHz, $CDCl_3$) of **S40**

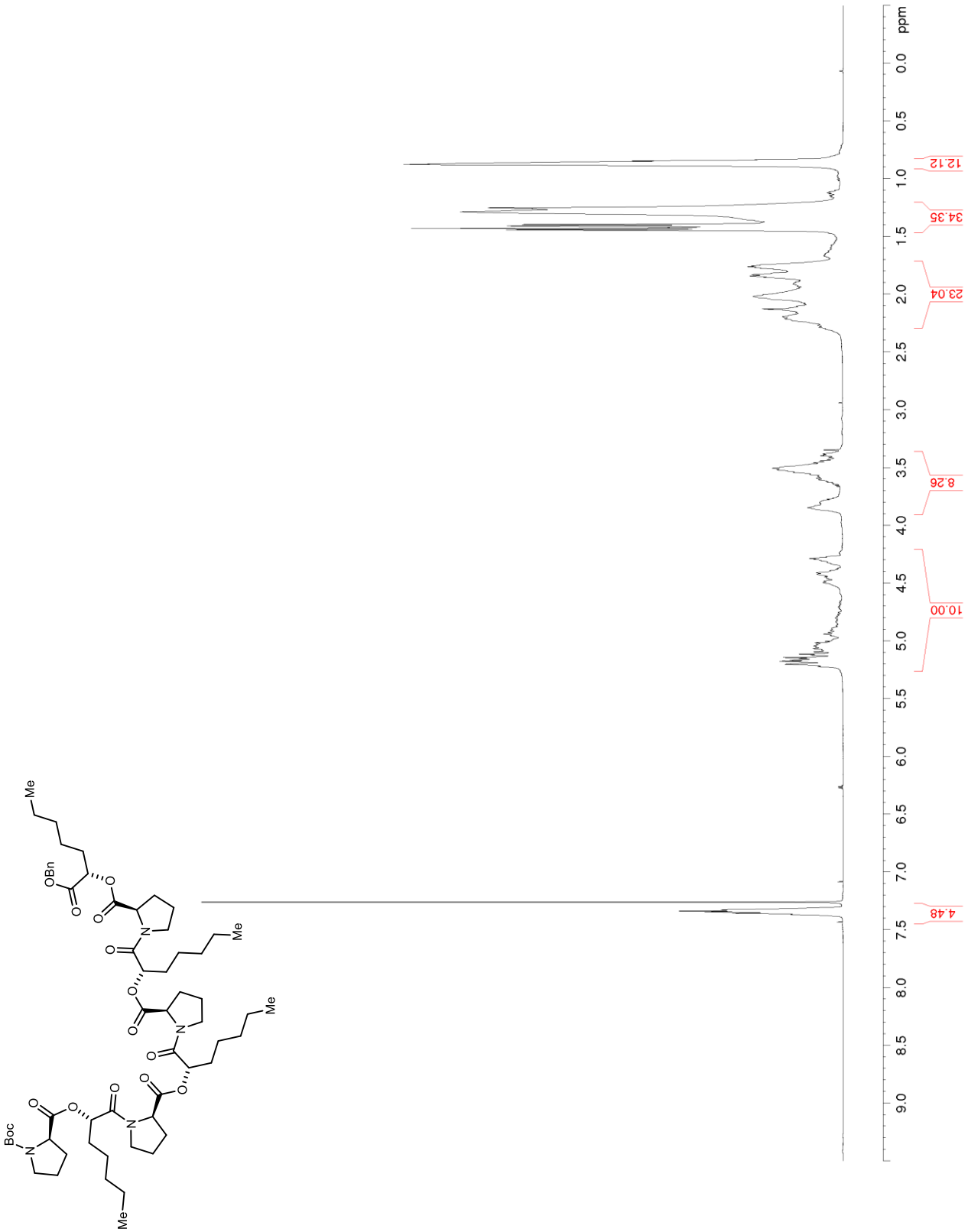

Figure S129. ^{13}C NMR/DEPT (100 MHz, $CDCl_3$) of **S40**

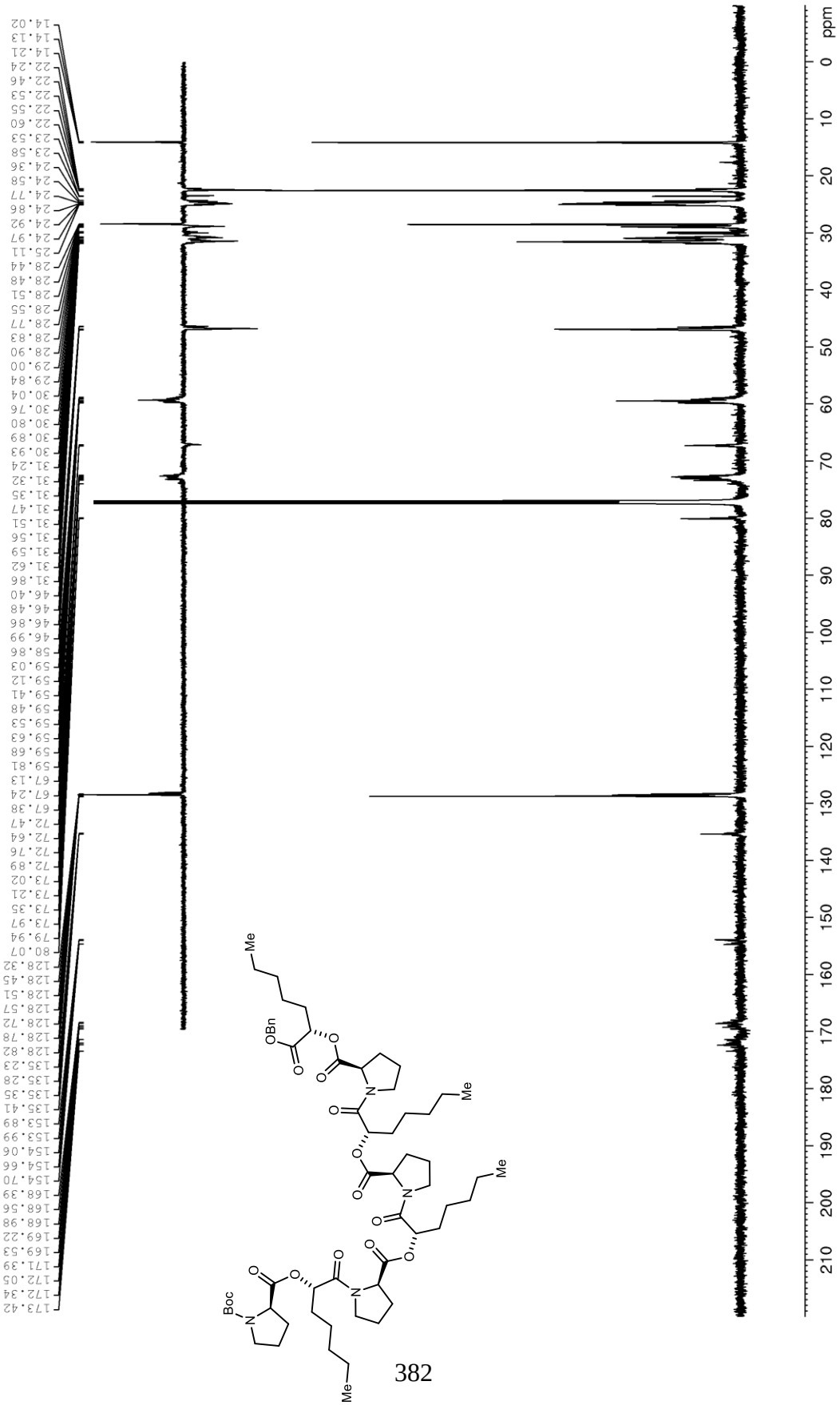

Figure S130. ^{1}H NMR (600 MHz, $CDCl_3$) of **72**

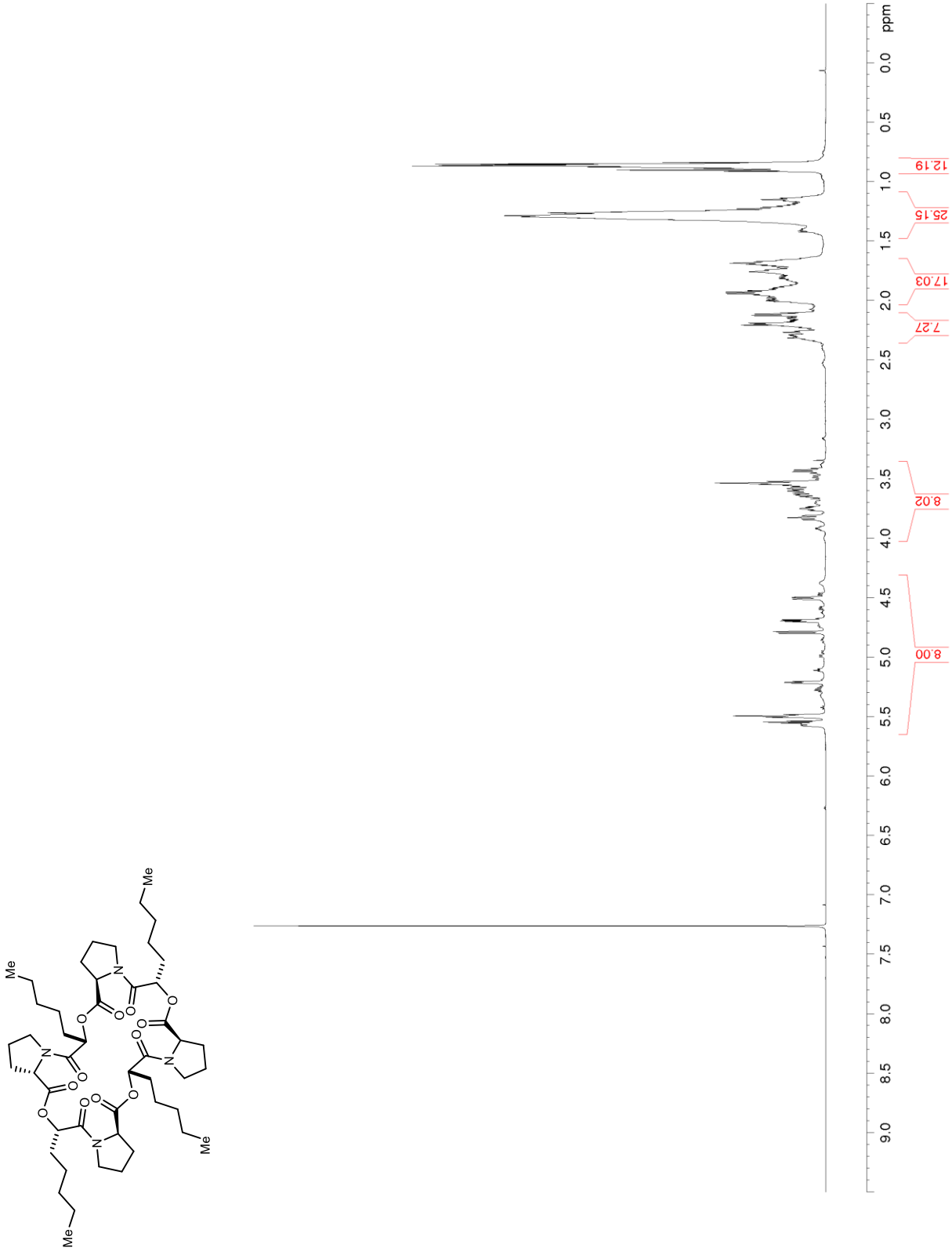

Figure S131. ^{13}C NMR/DEPT (100 MHz, $CDCl_3$) of **72**

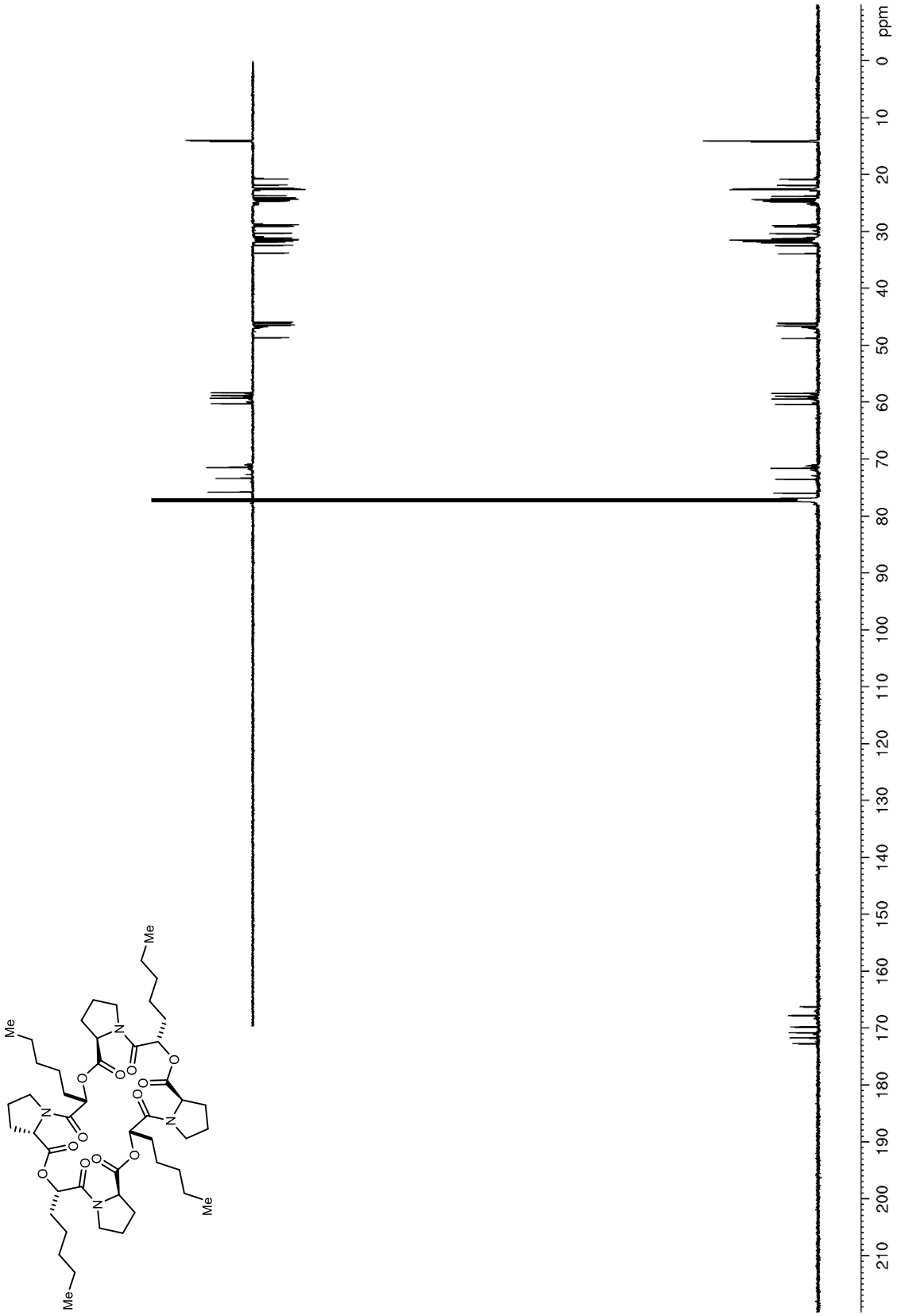

Figure S132. ^{1}H NMR (400 MHz, $CDCl_3$) of **S41**

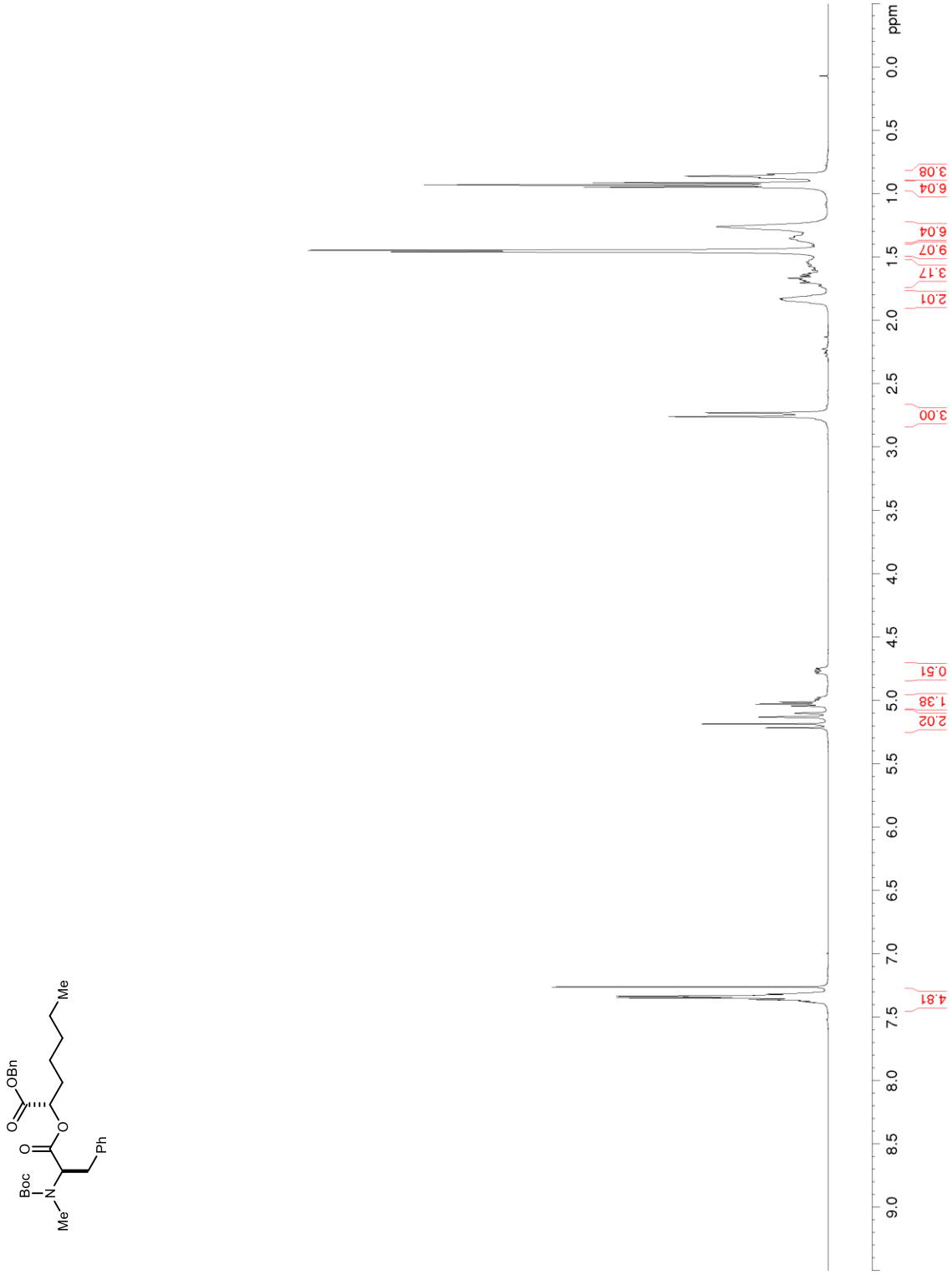

Figure S133. ^{13}C NMR/DEPT (100 MHz, $CDCl_3$) of **S41**

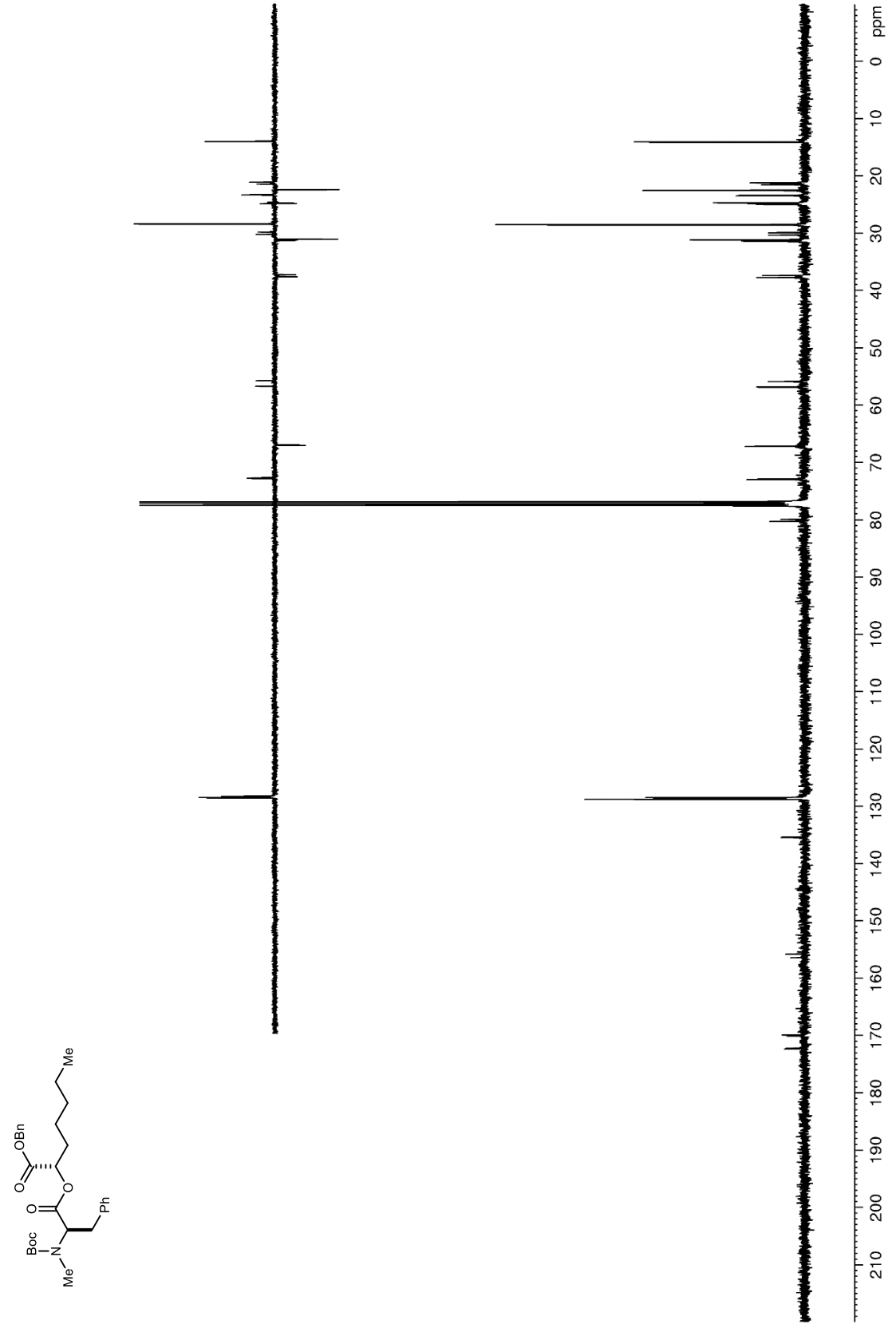

Figure S134. ^{1}H NMR (400 MHz, $CDCl_3$) of **S42**

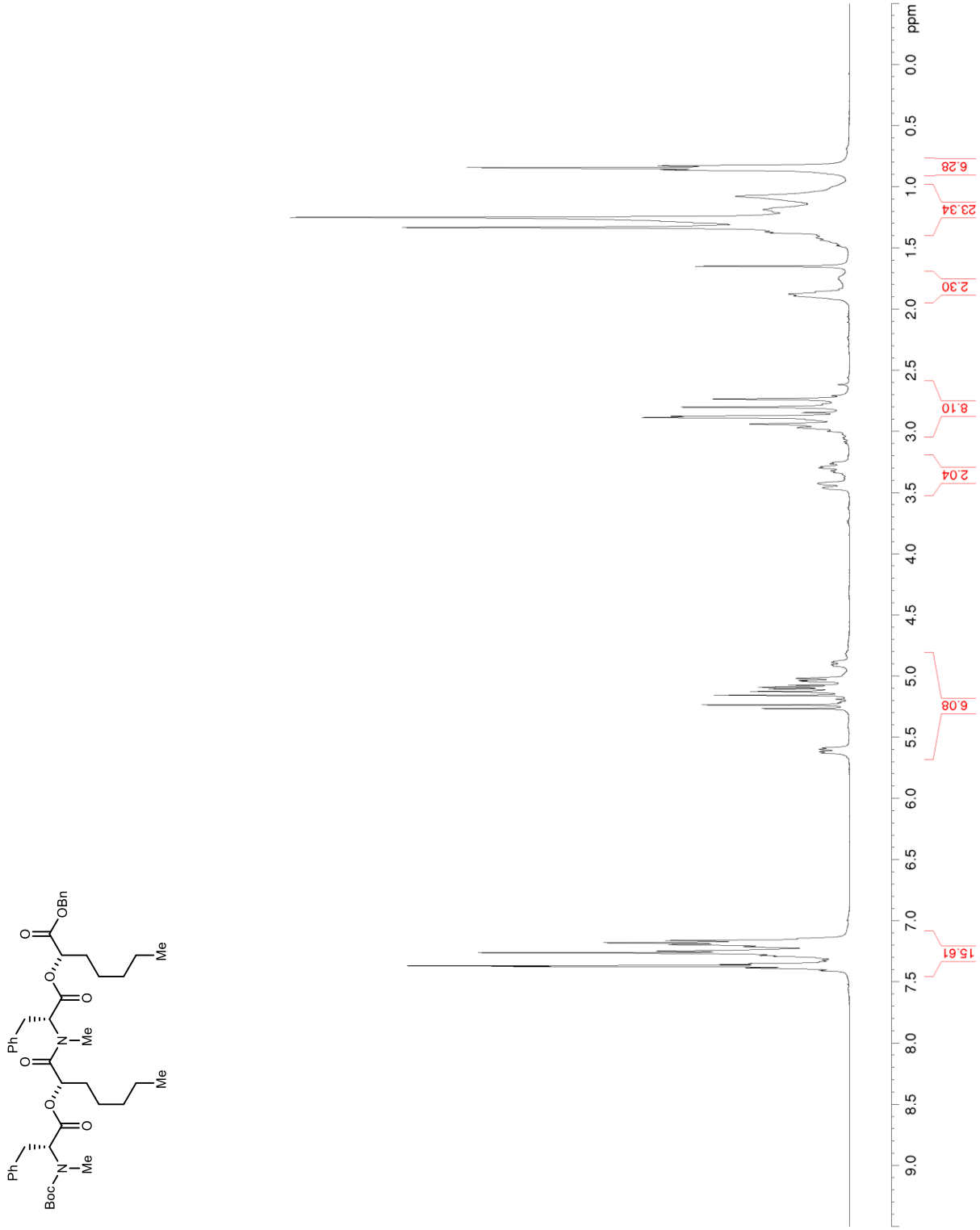

Figure S135. ^{13}C NMR/DEPT (100 MHz, $CDCl_3$) of **S42**

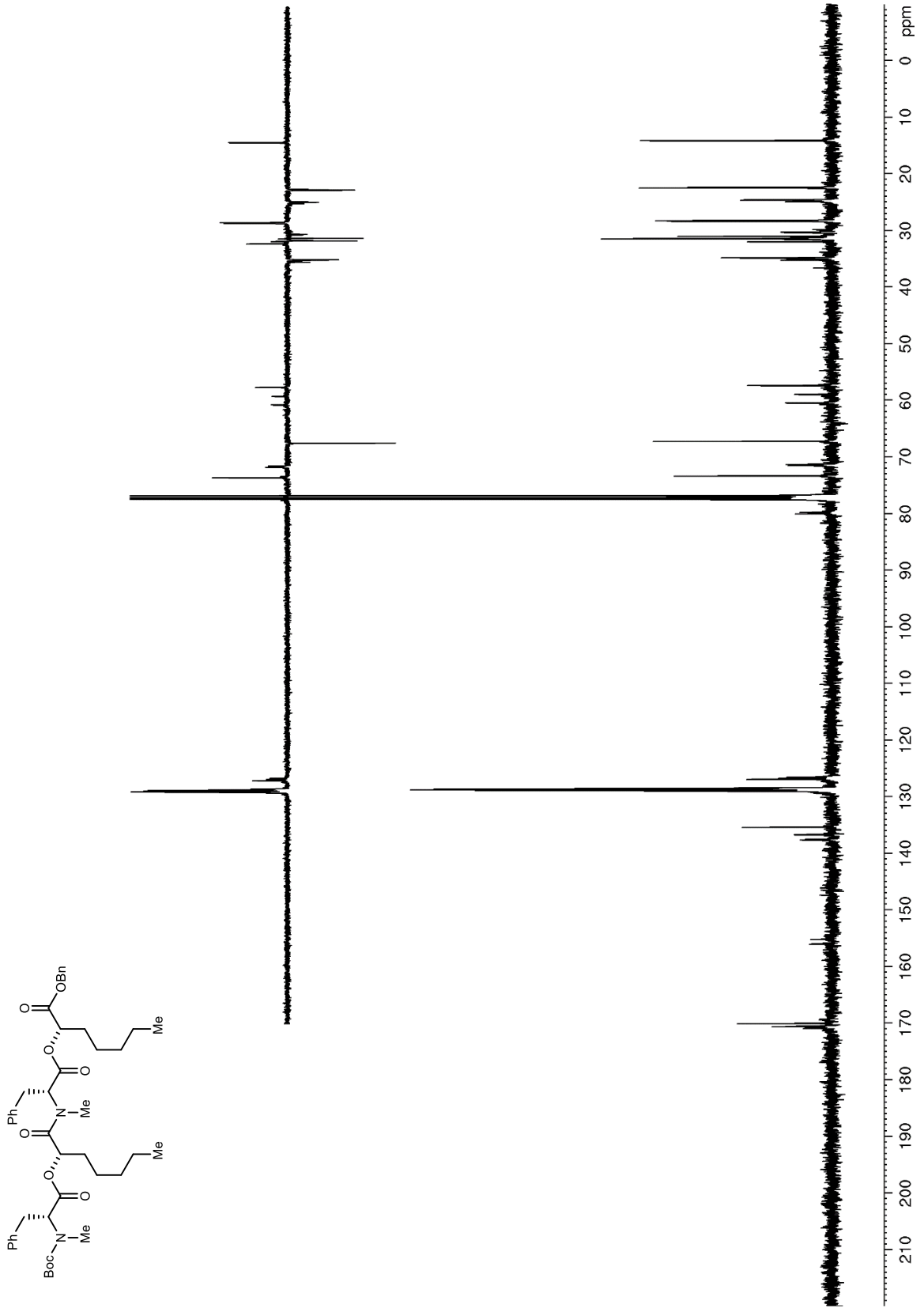

Figure S136. ^{1}H NMR (600 MHz, $CDCl_3$) of **S43**

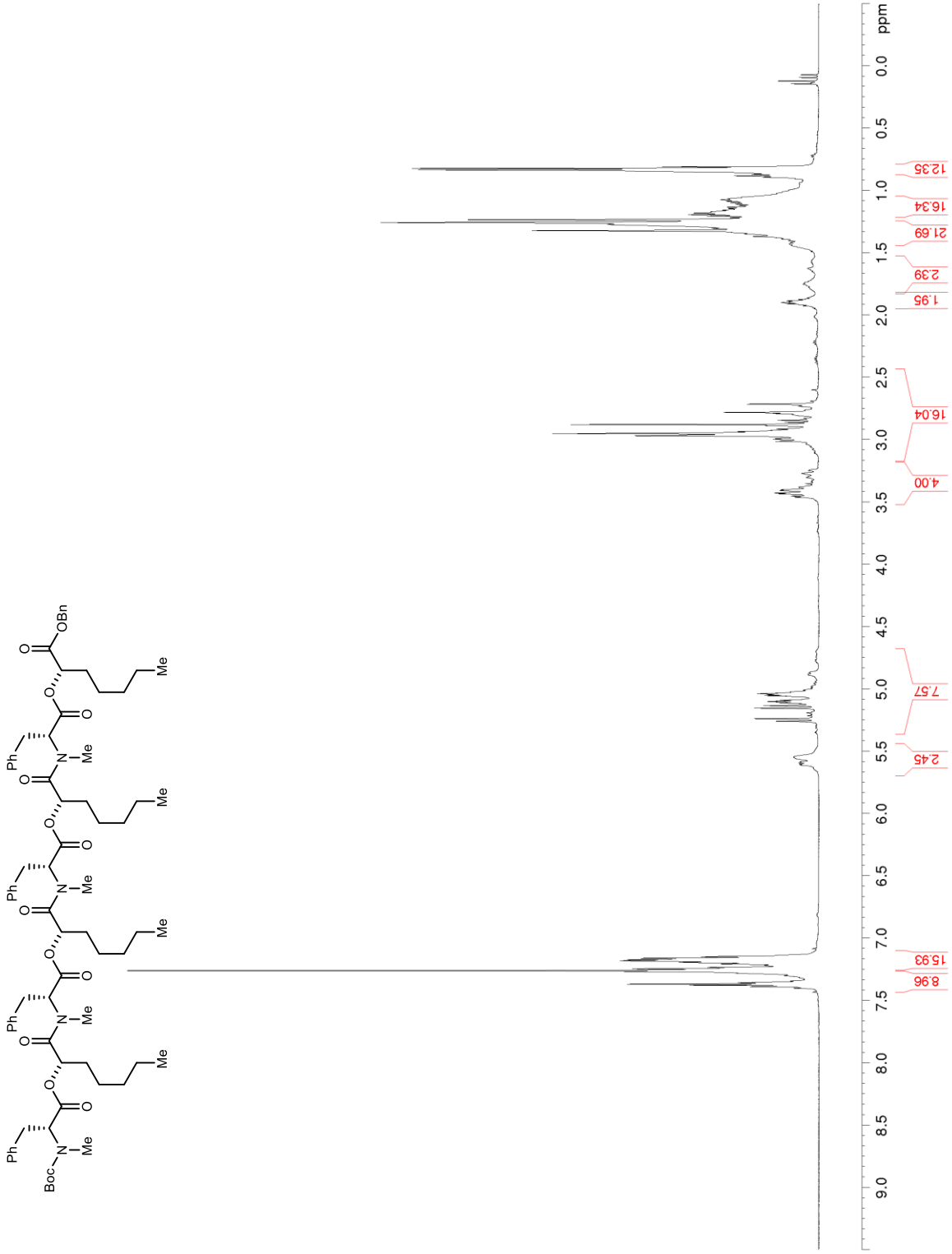

Figure S137. ^{13}C NMR/DEPT (150 MHz, $CDCl_3$) of **S43**

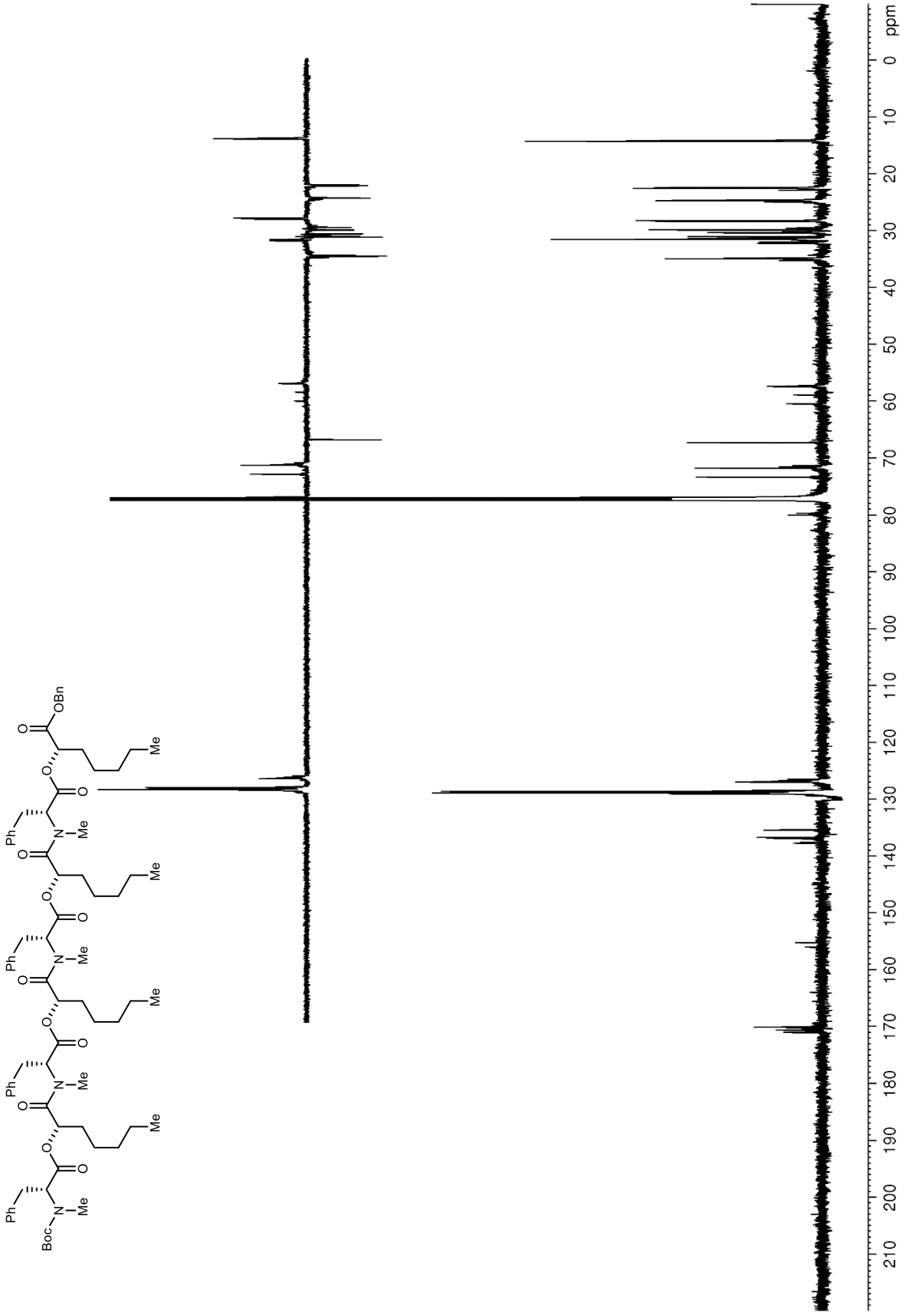

Figure S138. ^{1}H NMR (600 MHz, $CDCl_3$) of **73**

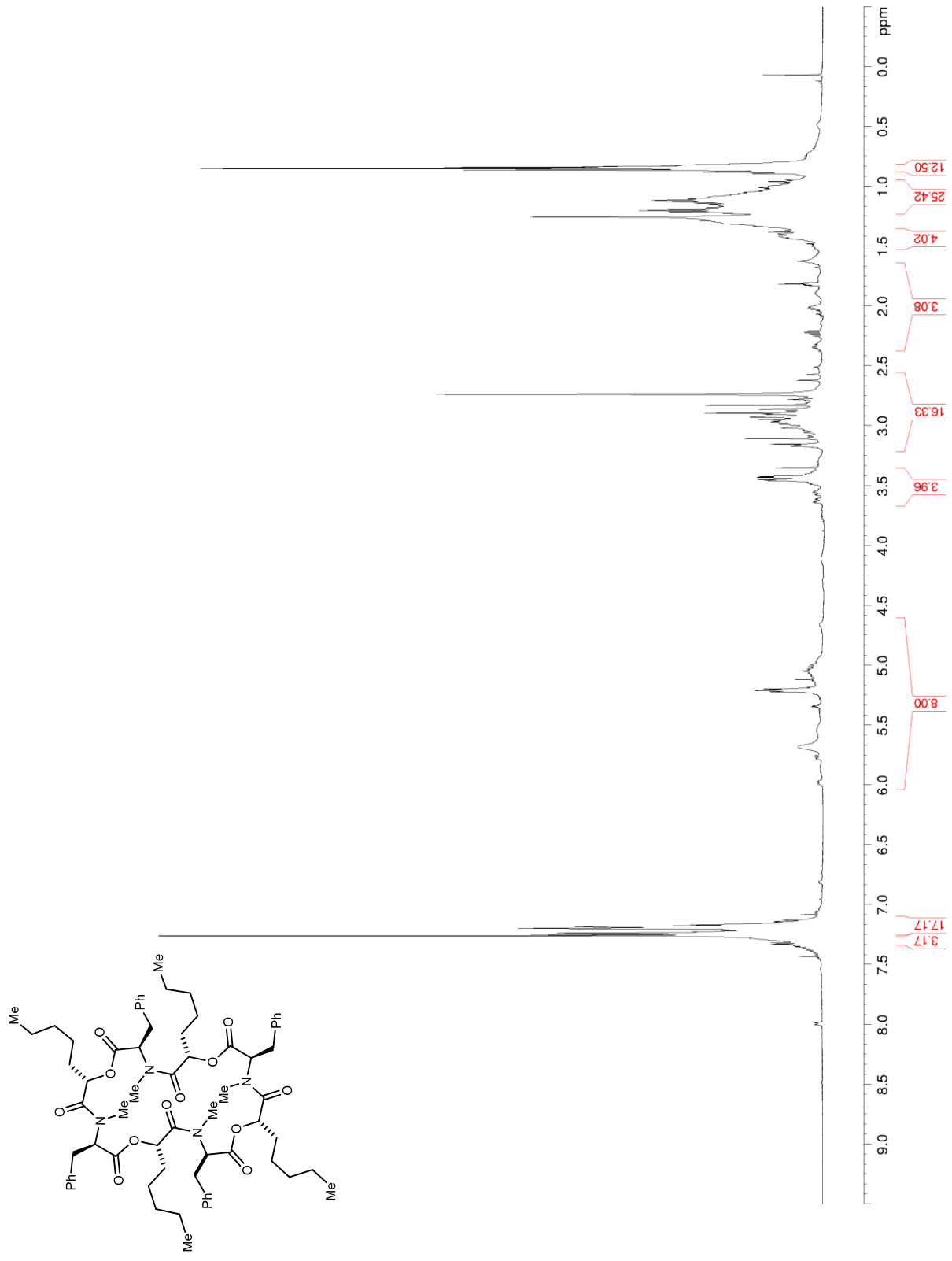

Figure S139. ^{13}C NMR/DEPT (150 MHz, $CDCl_3$) of **73**

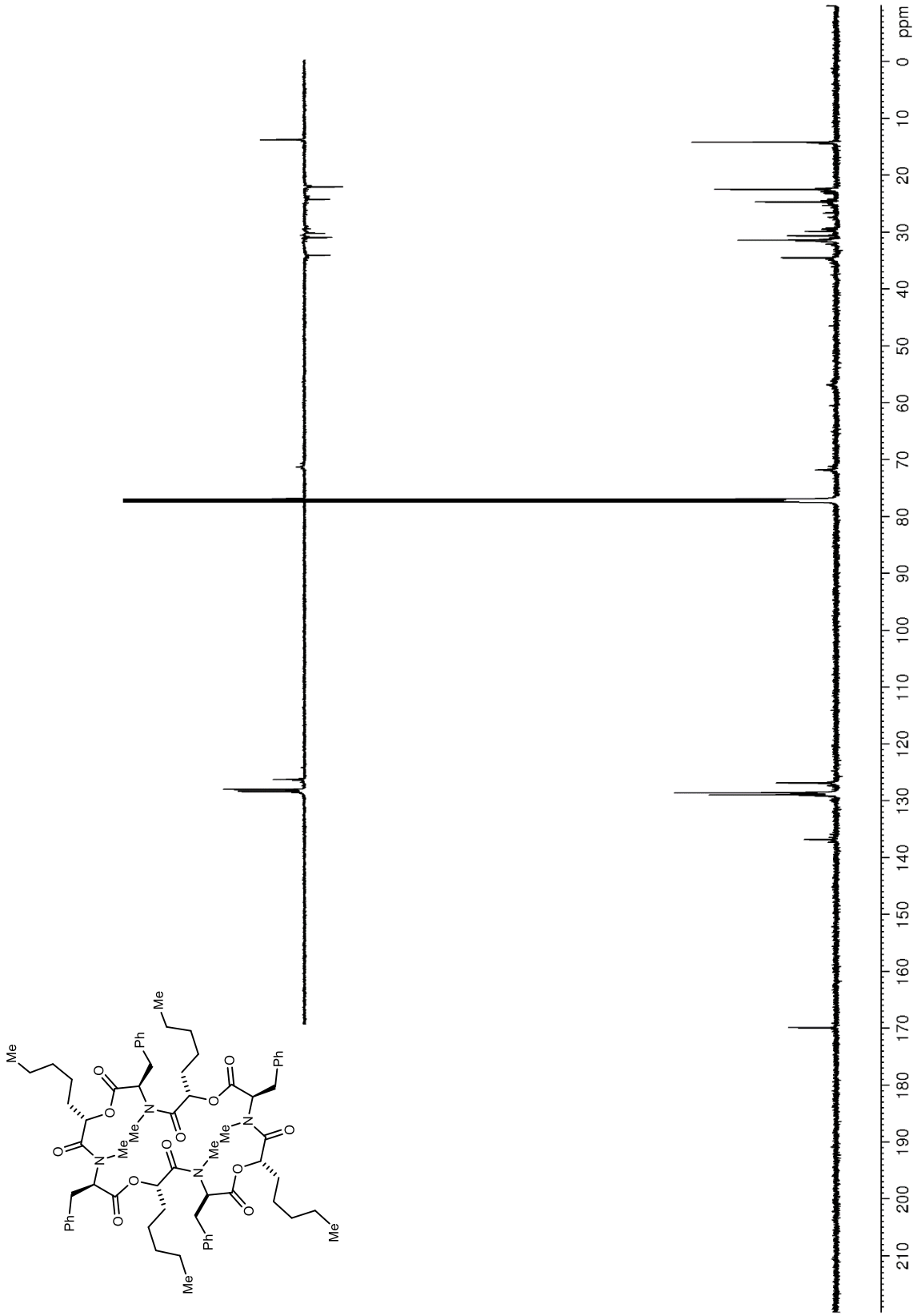

Figure S140. ^{1}H NMR (400 MHz, $CDCl_3$) of **S44**

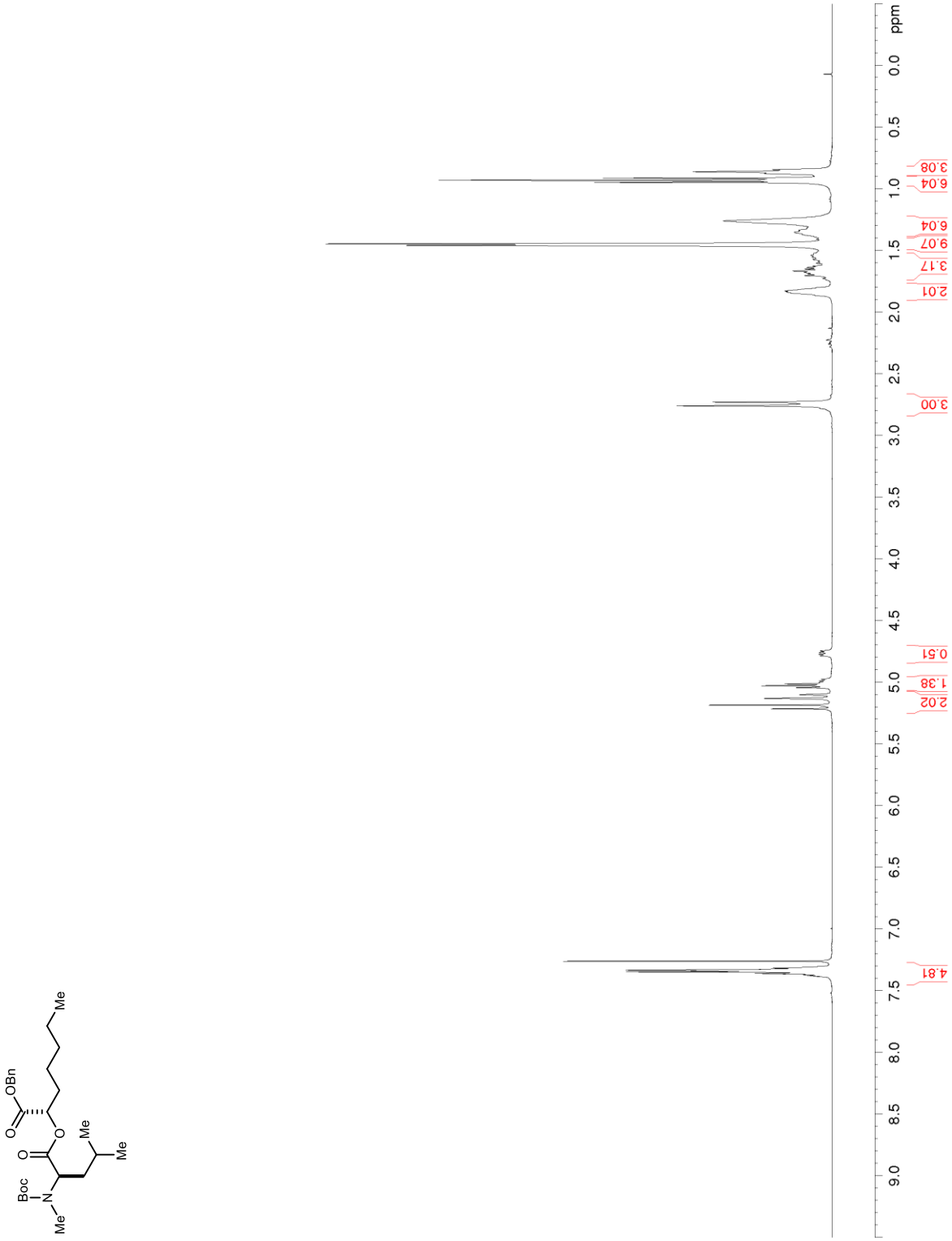

Figure S141. ^{13}C NMR/DEPT (100 MHz, $CDCl_3$) of **S44**

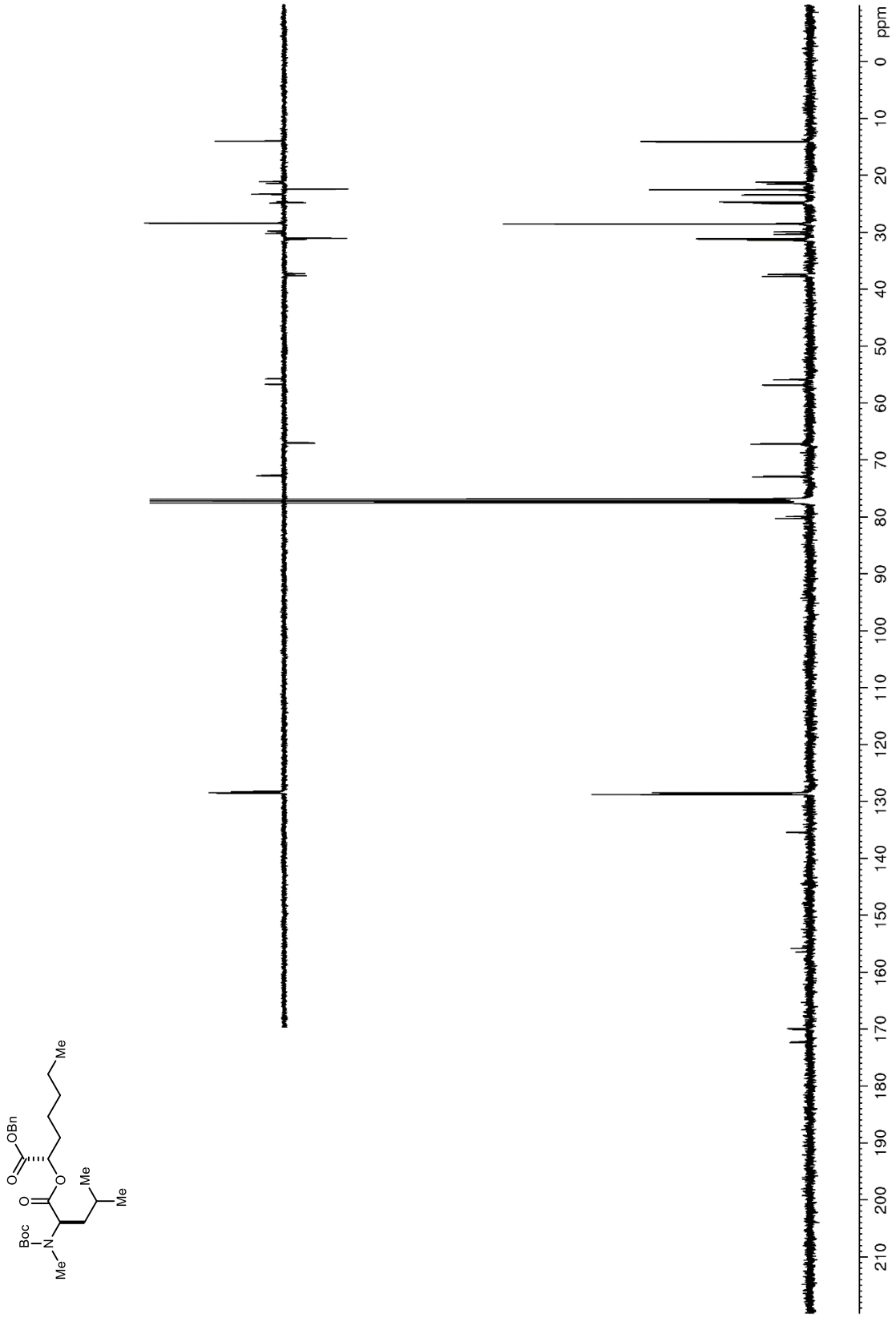

Figure S142. ^{1}H NMR (600 MHz, $CDCl_3$) of **S45**

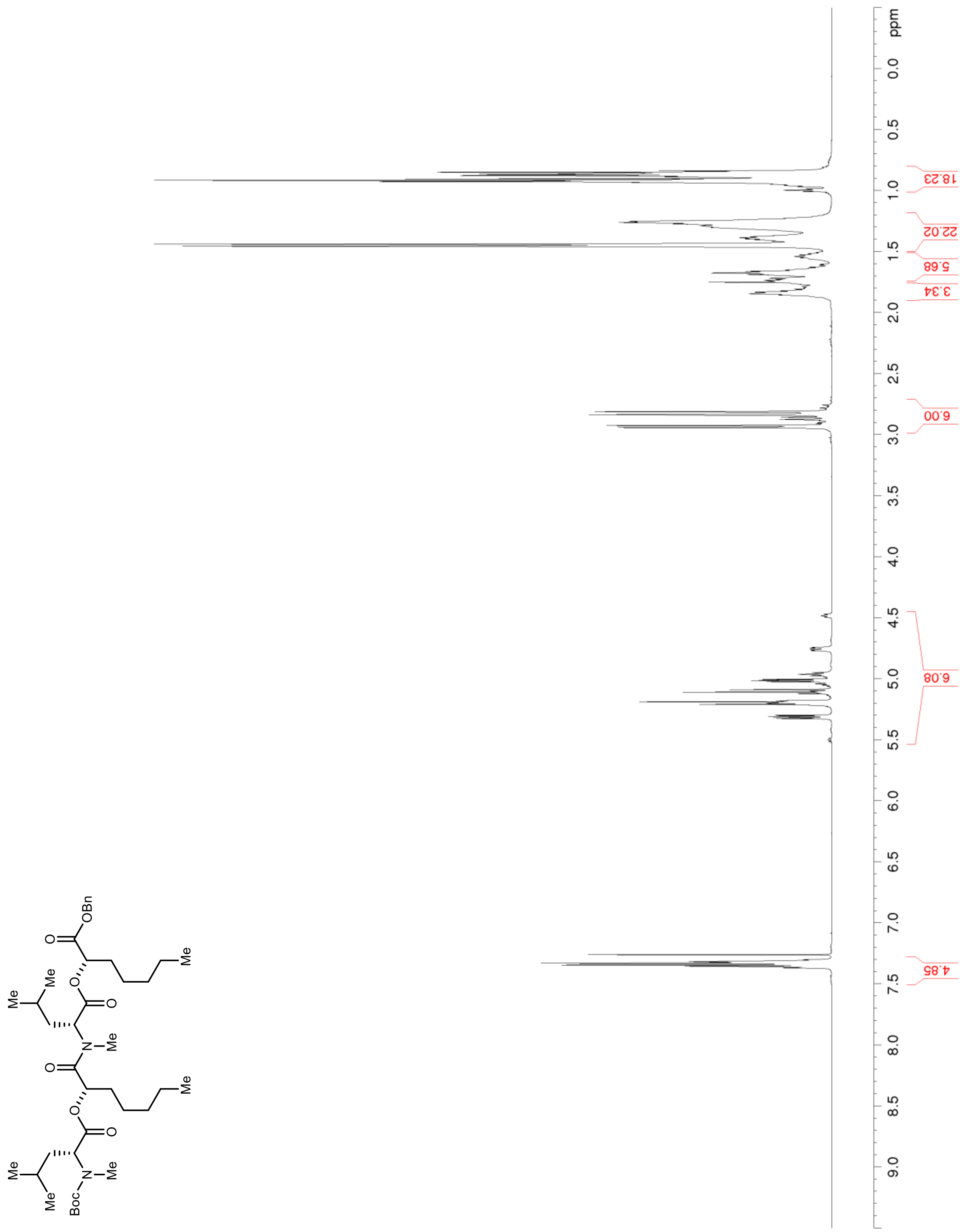

Figure S143. ^{13}C NMR/DEPT (150 MHz, $CDCl_3$) of **S45**

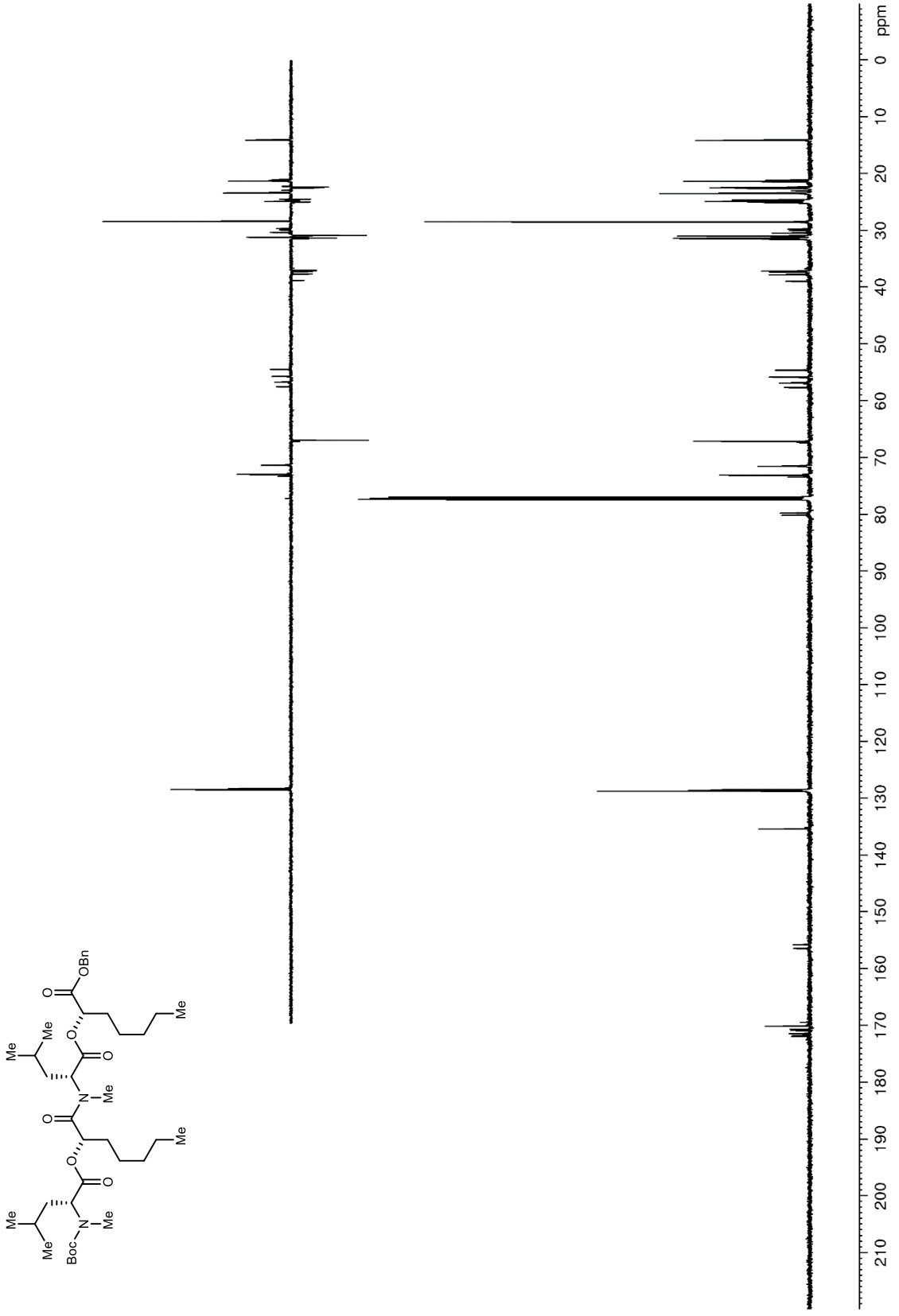

Figure S144. ^{1}H NMR (600 MHz, $CDCl_3$) of **S46**

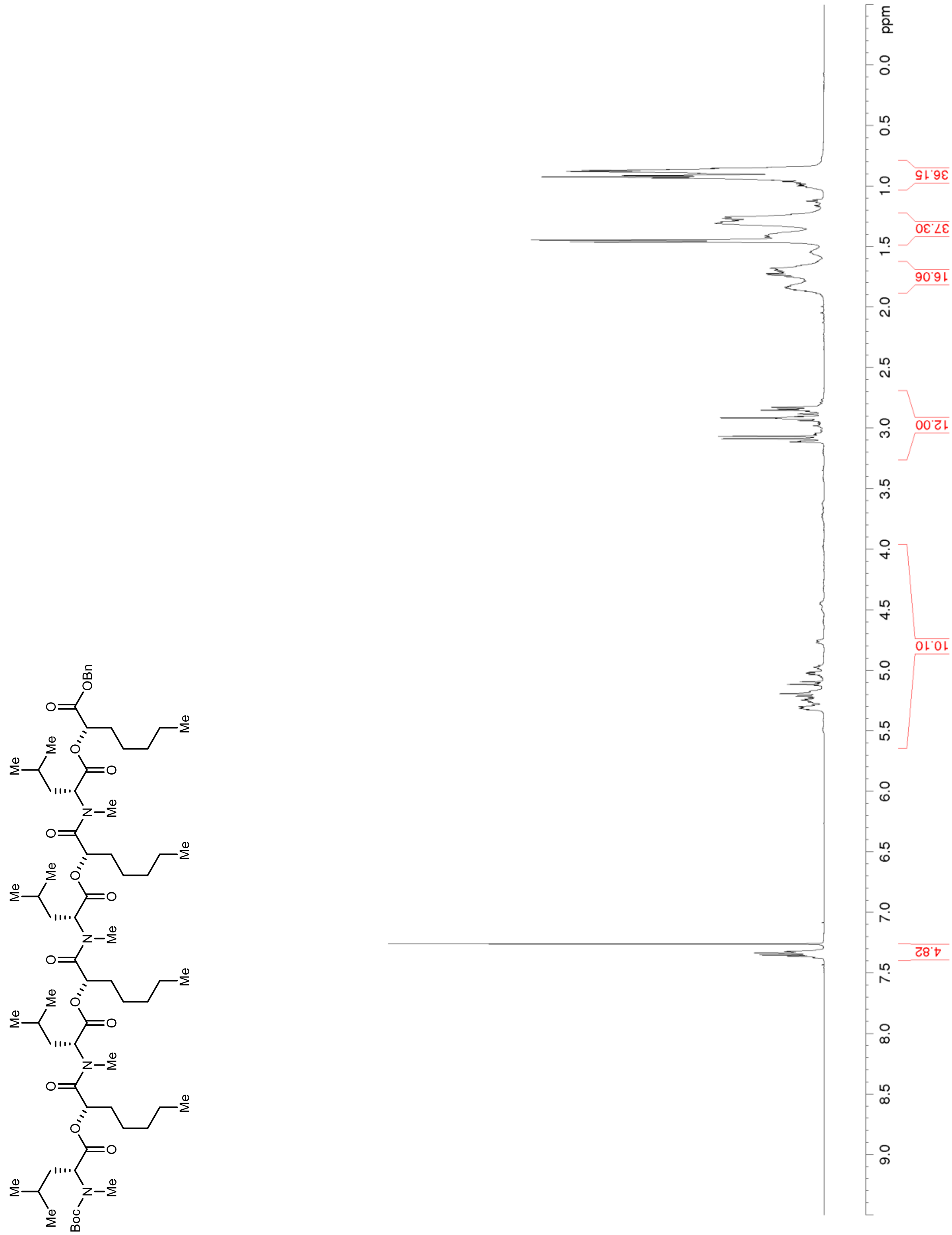

Figure S145. ^{13}C NMR/DEPT (150 MHz, $CDCl_3$) of **S46**

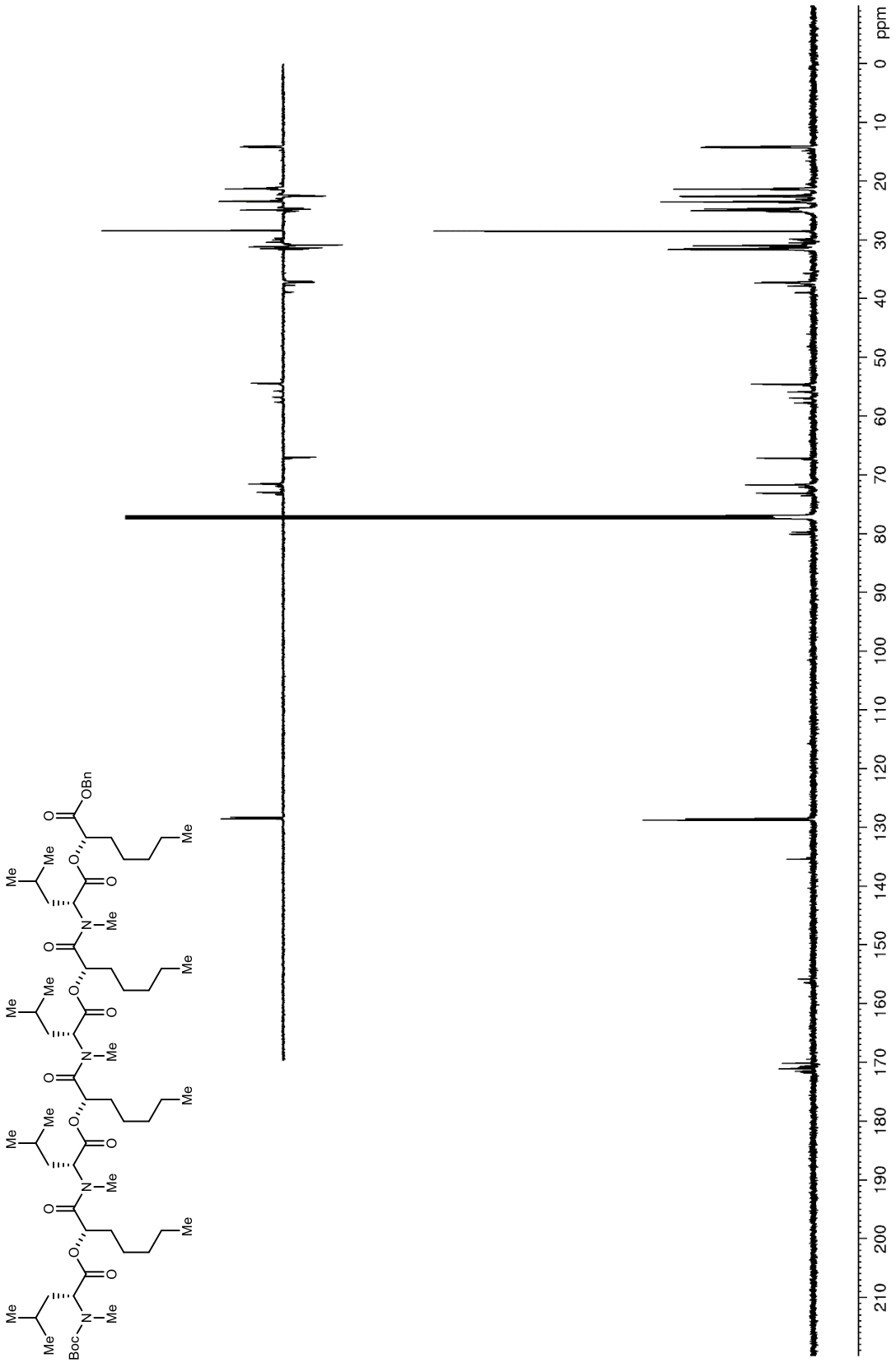

Figure S146. ^{1}H NMR (600 MHz, $CDCl_3$) of **74**

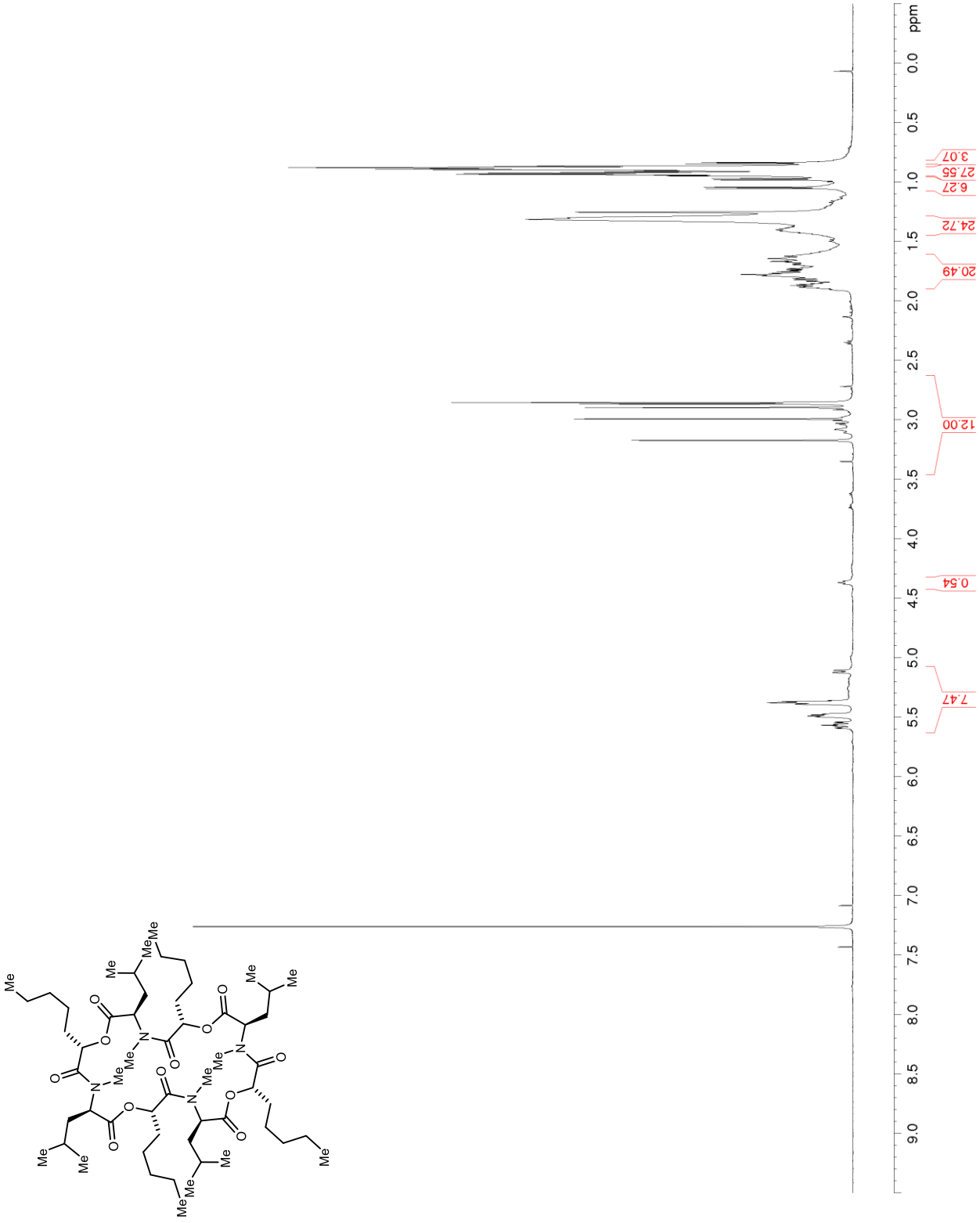

Figure S147. ^{13}C NMR/DEPT (150 MHz, $CDCl_3$) of **74**

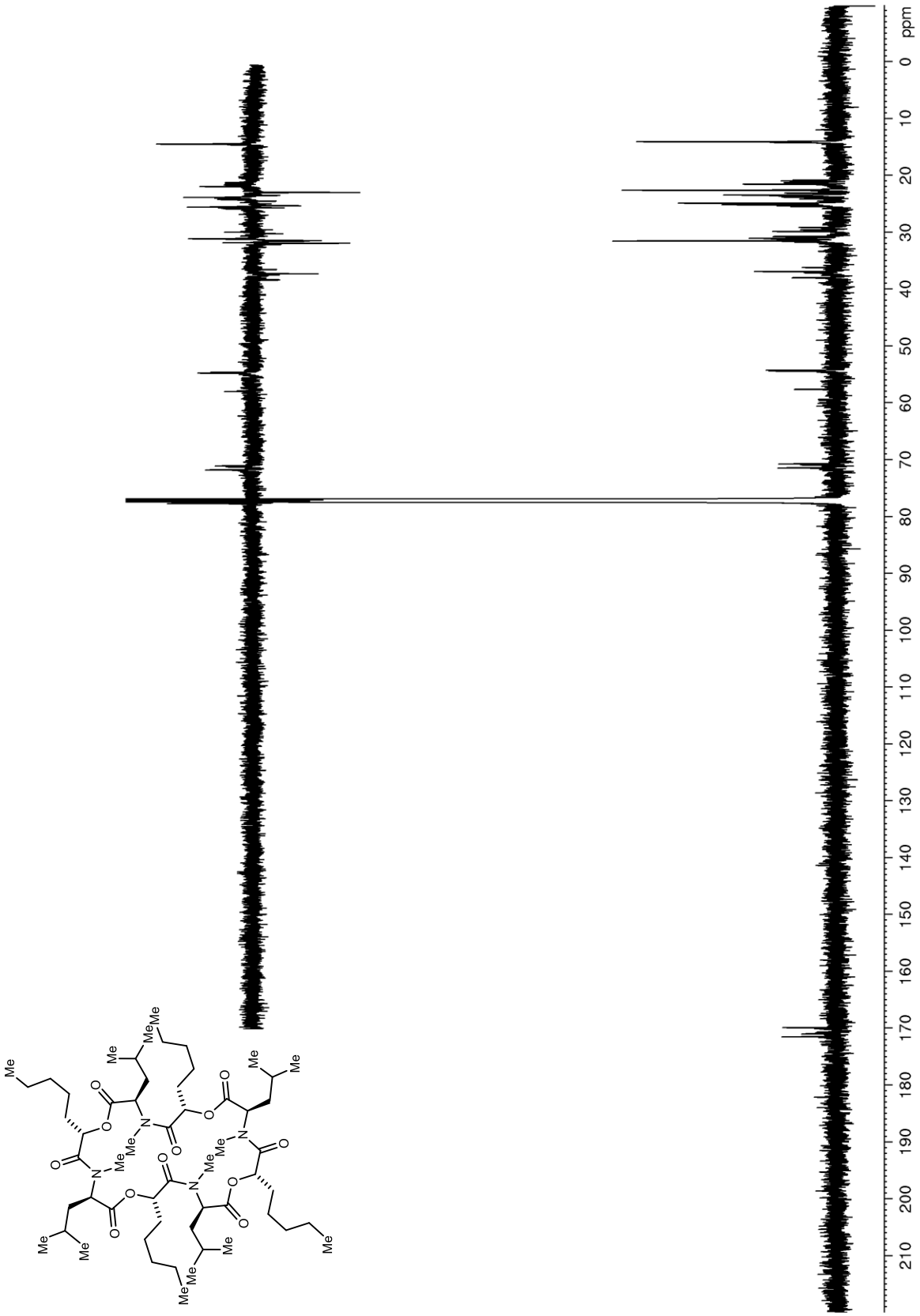

Figure S148. ^{1}H NMR (400 MHz, $CDCl_3$) of **S47**

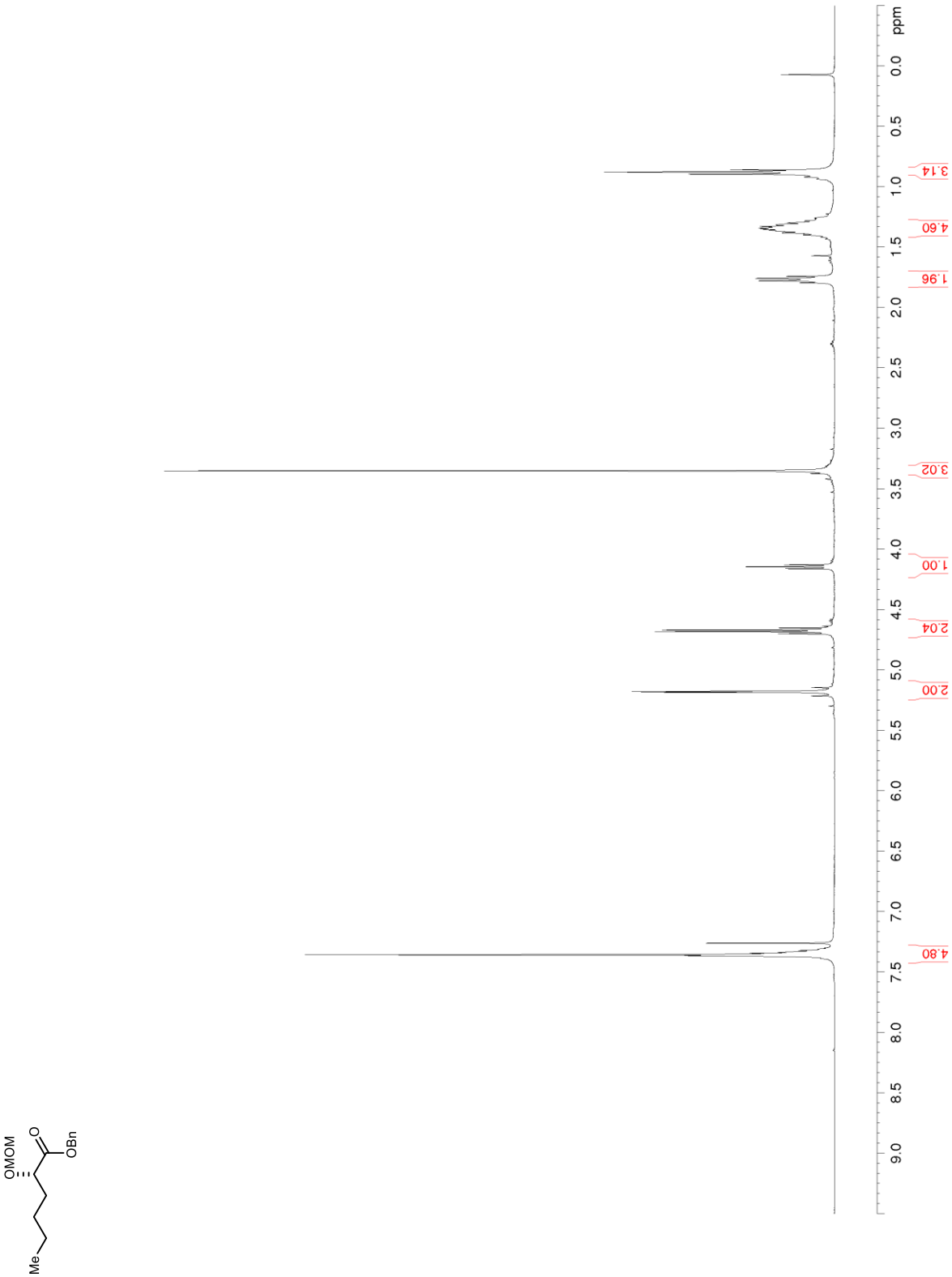

Figure S149. ^{13}C NMR/DEPT (100 MHz, $CDCl_3$) of **S47**

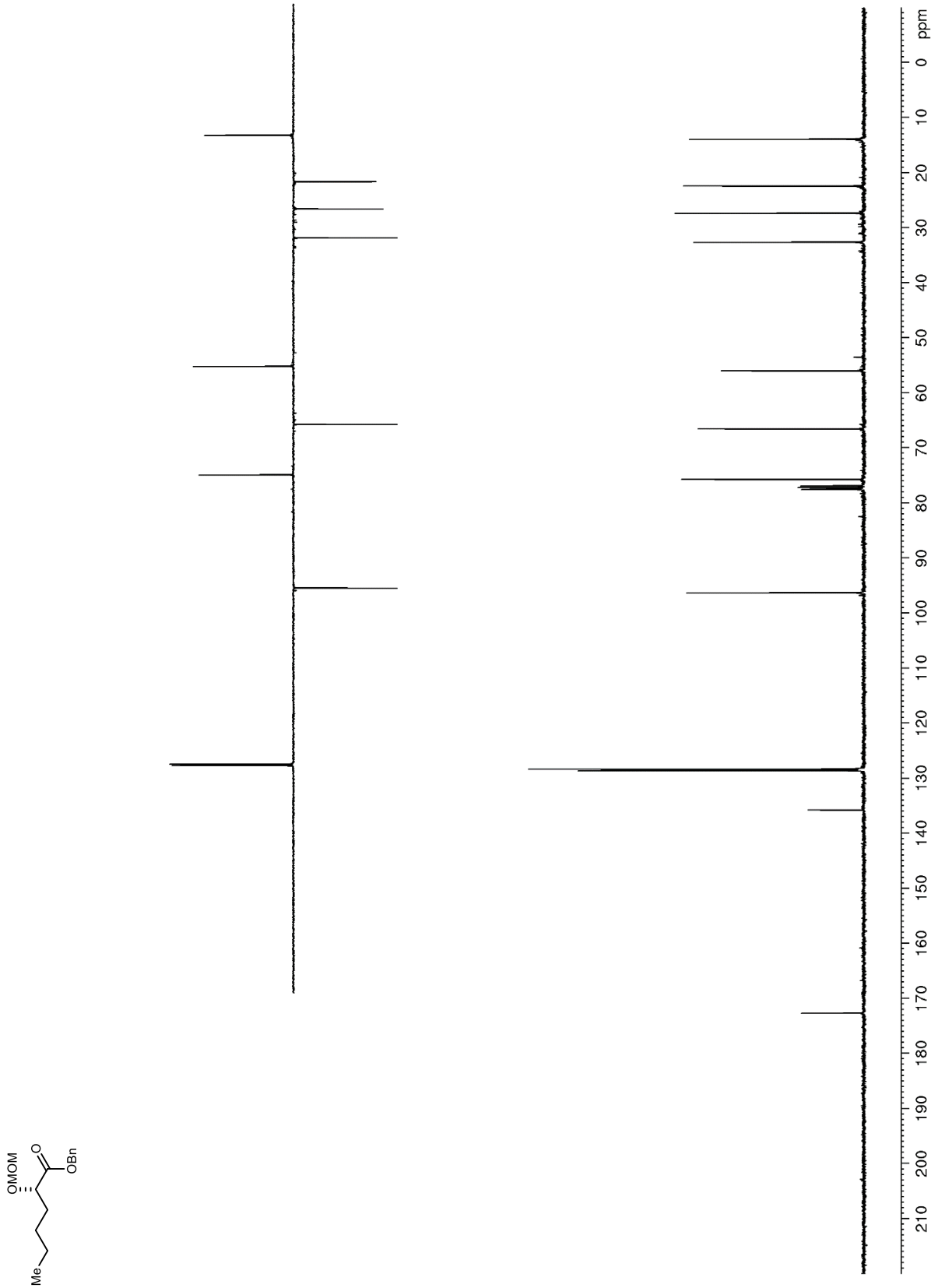

Figure S150. ^{1}H NMR (400 MHz, $CDCl_3$) of **S48**

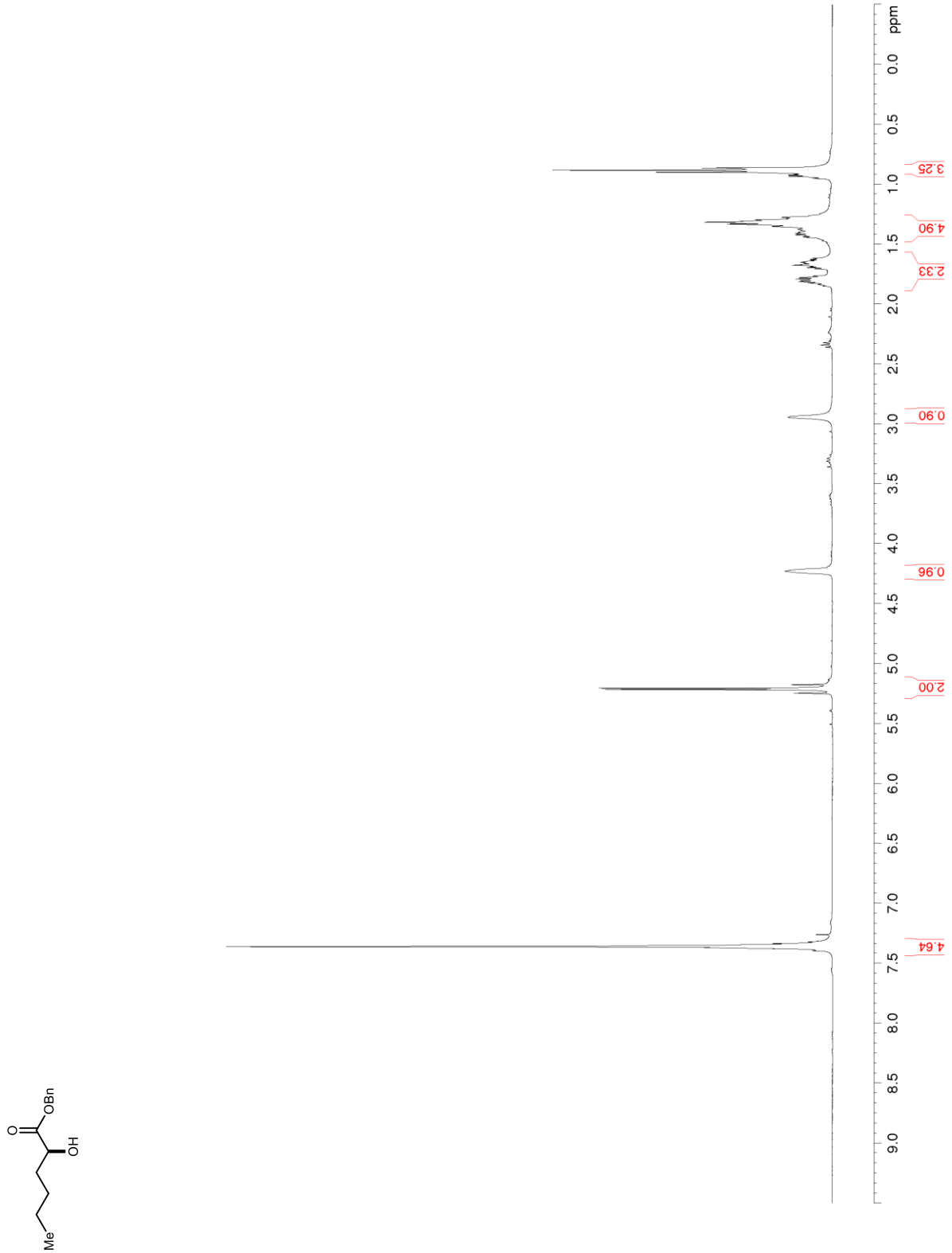

Figure S151. ^{13}C NMR/DEPT (100 MHz, $CDCl_3$) of **S48**

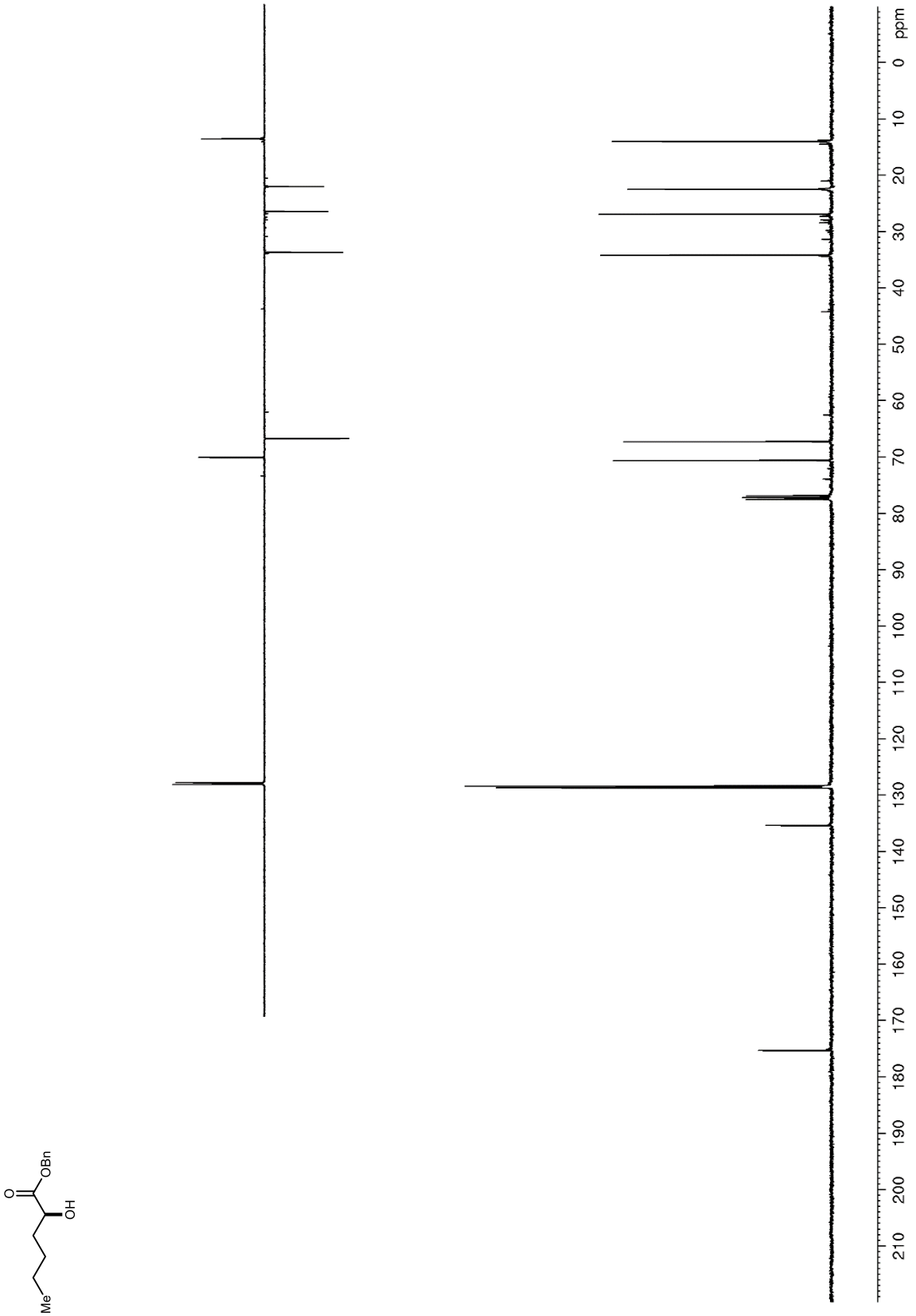

Figure S152. ^{1}H NMR (600 MHz, $CDCl_3$) of **S49**

Figure S153. ^{13}C NMR/DEPT (150 MHz, $CDCl_3$) of **S49**

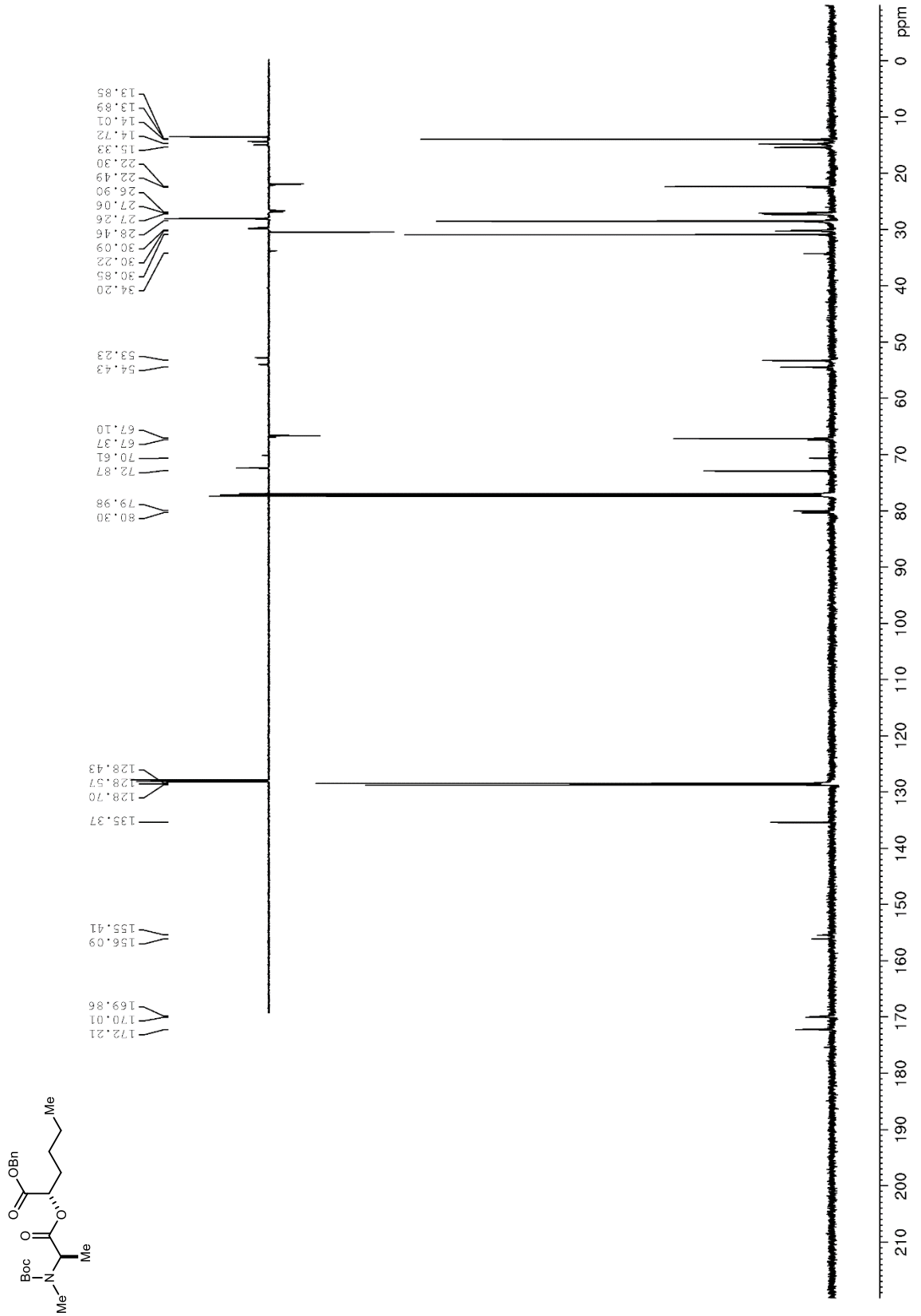

Figure S154. ^{1}H NMR (600 MHz, $CDCl_3$) of **S50**

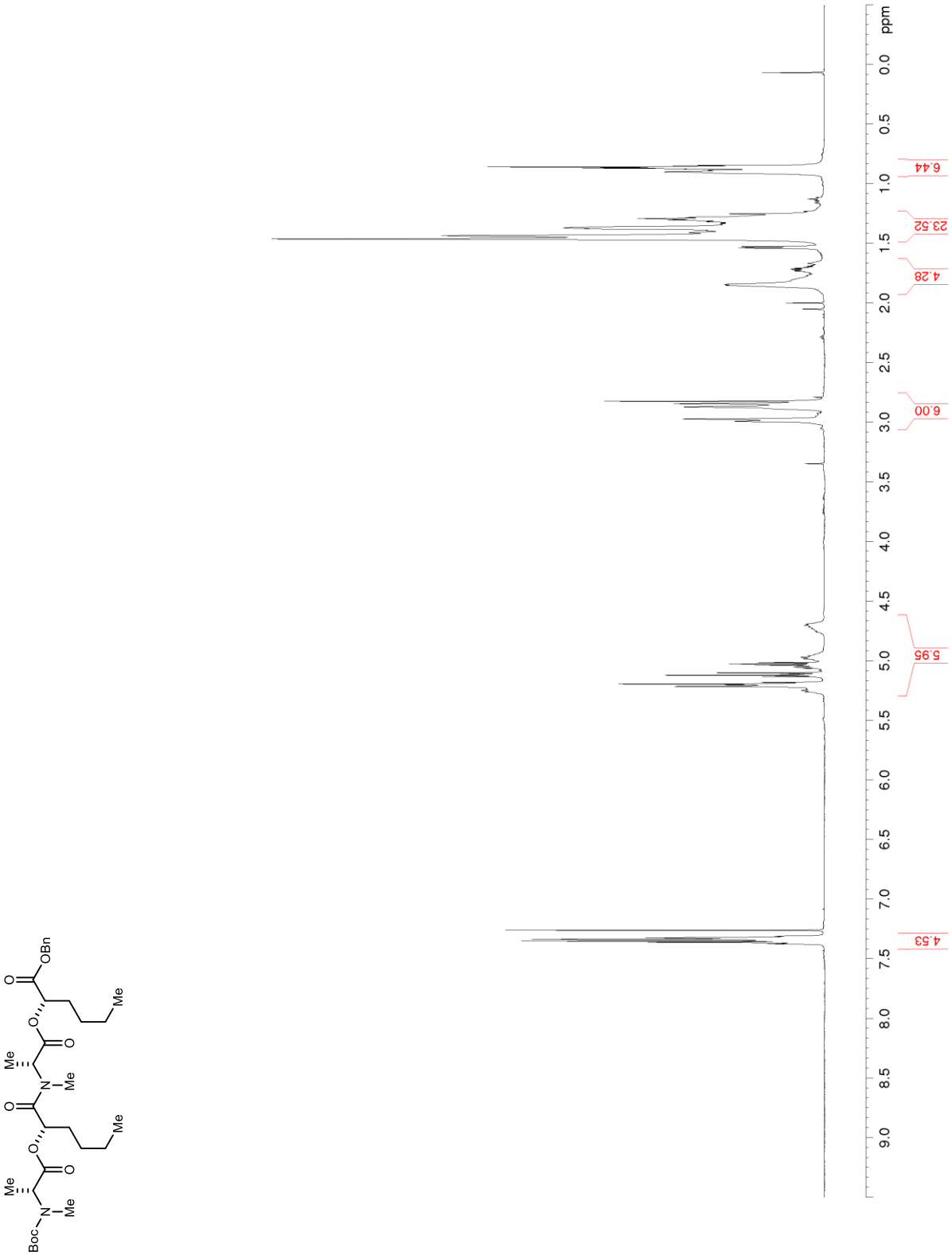

Figure S155. ^{13}C NMR/DEPT (150 MHz, $CDCl_3$) of **S50**

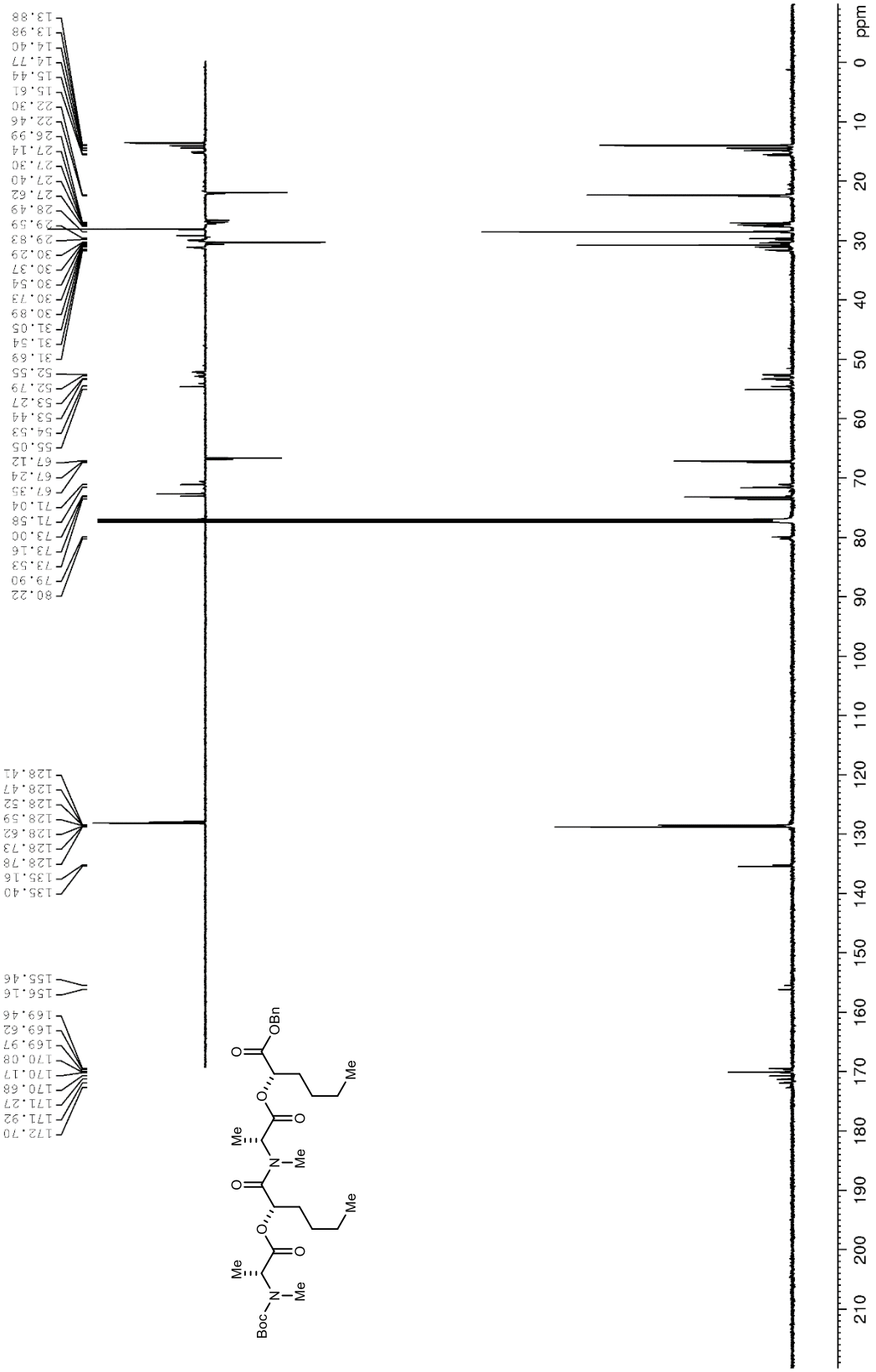

Figure S156. ^{1}H NMR (600 MHz, $CDCl_3$) of **S51**

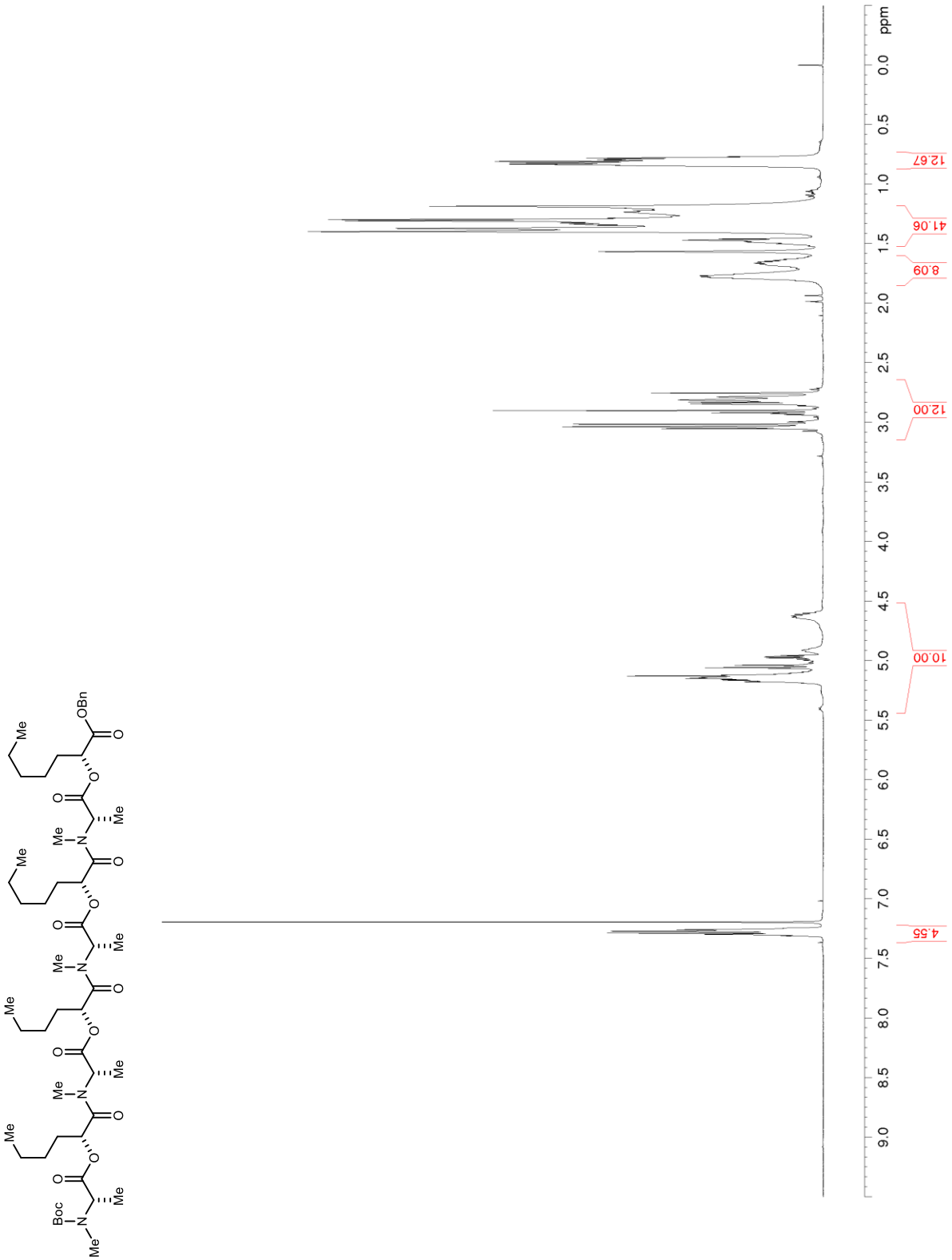

Figure S157. ^{13}C NMR/DEPT (150 MHz, $CDCl_3$) of **S51**

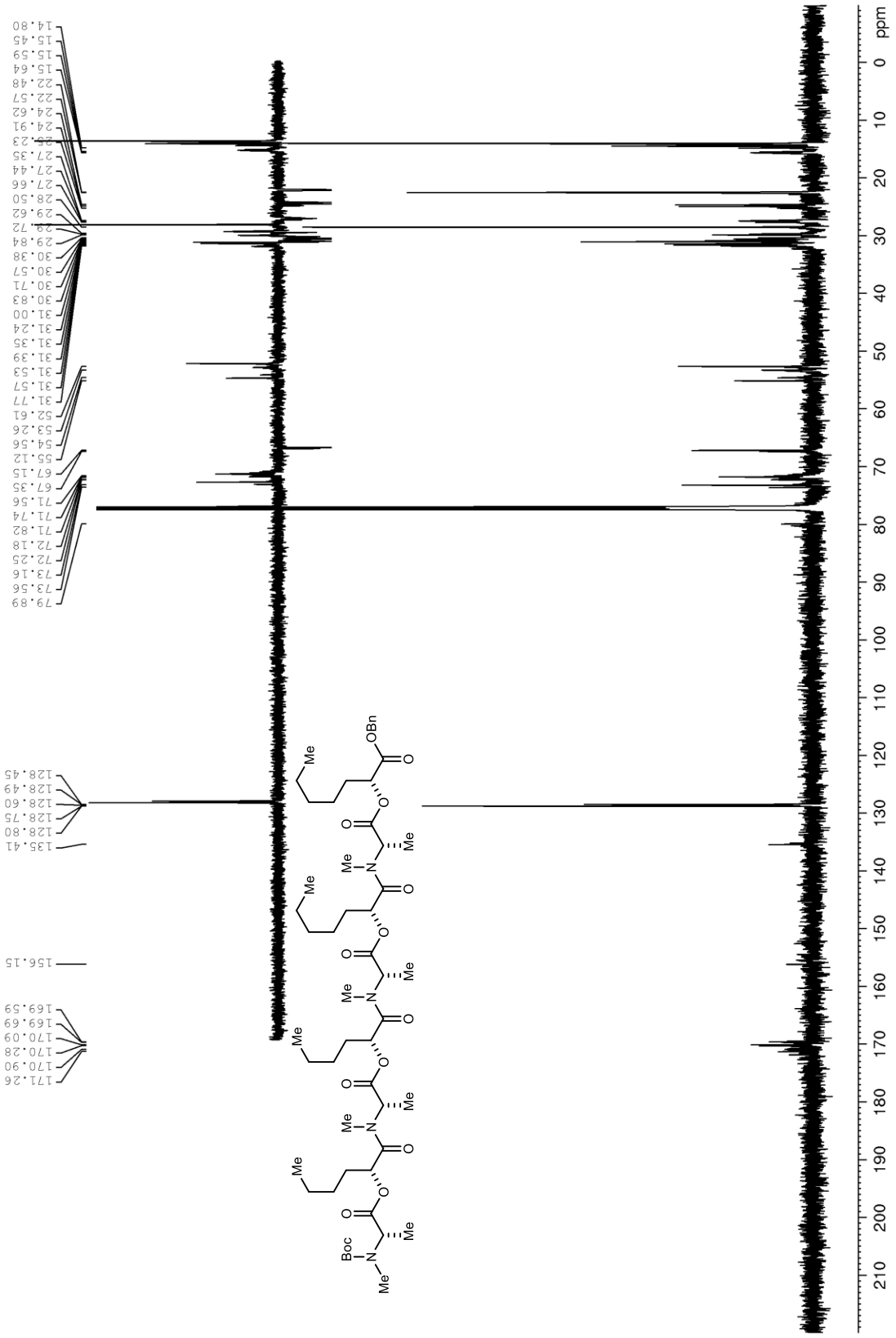

Figure S158. ^{1}H NMR (600 MHz, $CDCl_3$) of **75**

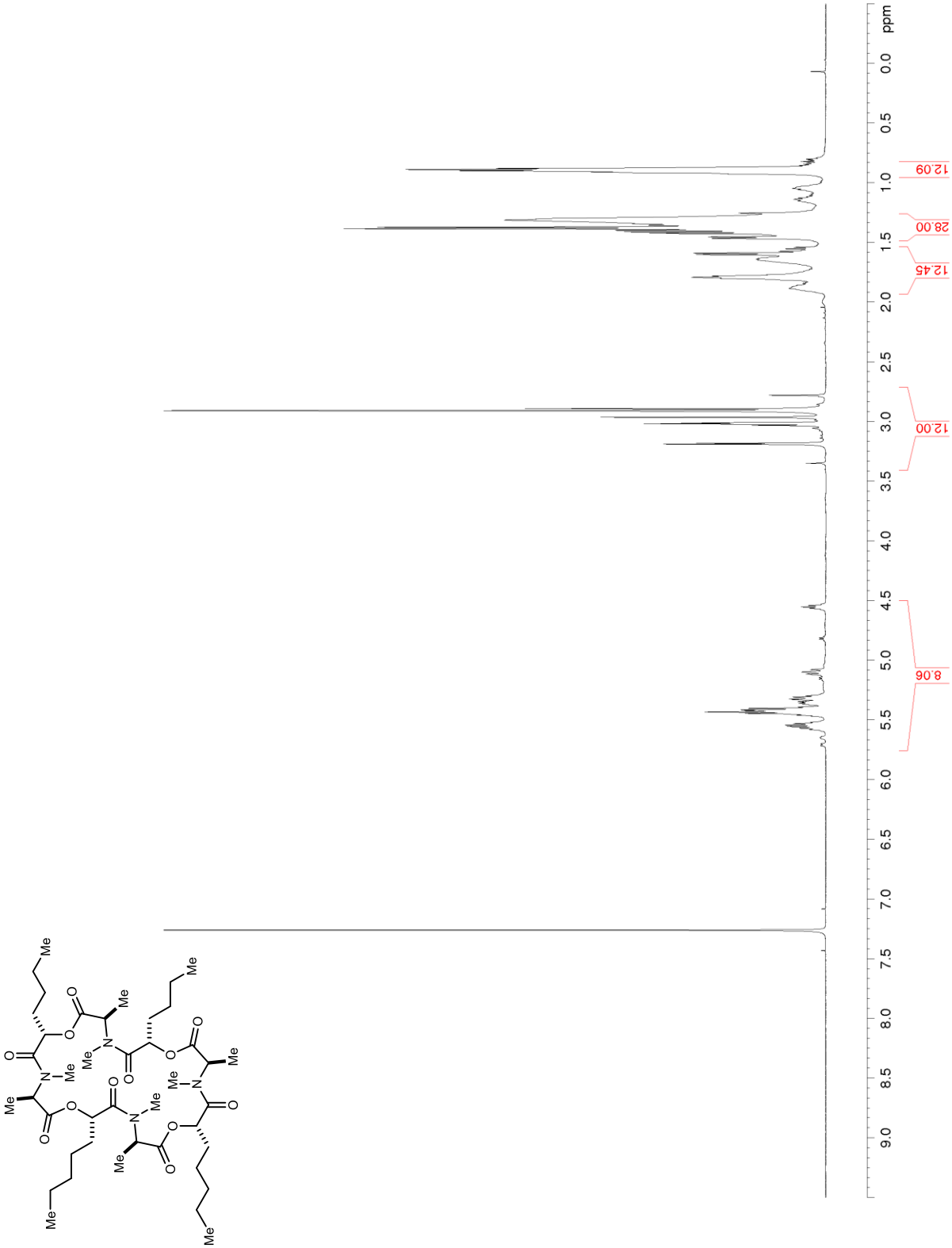

Figure S159. ^{13}C NMR/DEPT (150 MHz, $CDCl_3$) of **75**

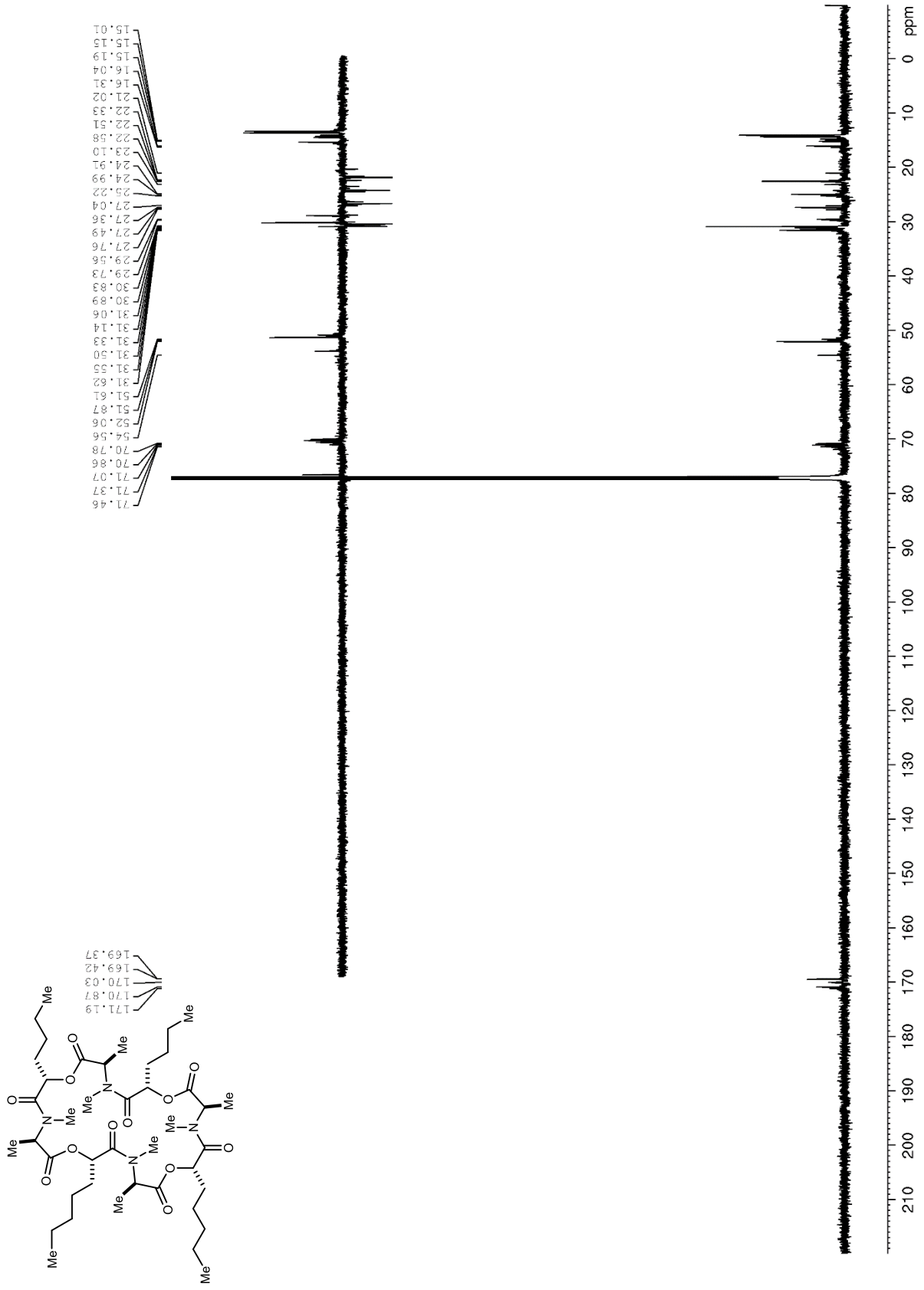

Figure S160. ^{1}H NMR (400 MHz, $CDCl_3$) of **S52**

Figure S161. ^{13}C NMR/DEPT (100 MHz, $CDCl_3$) of **S52**

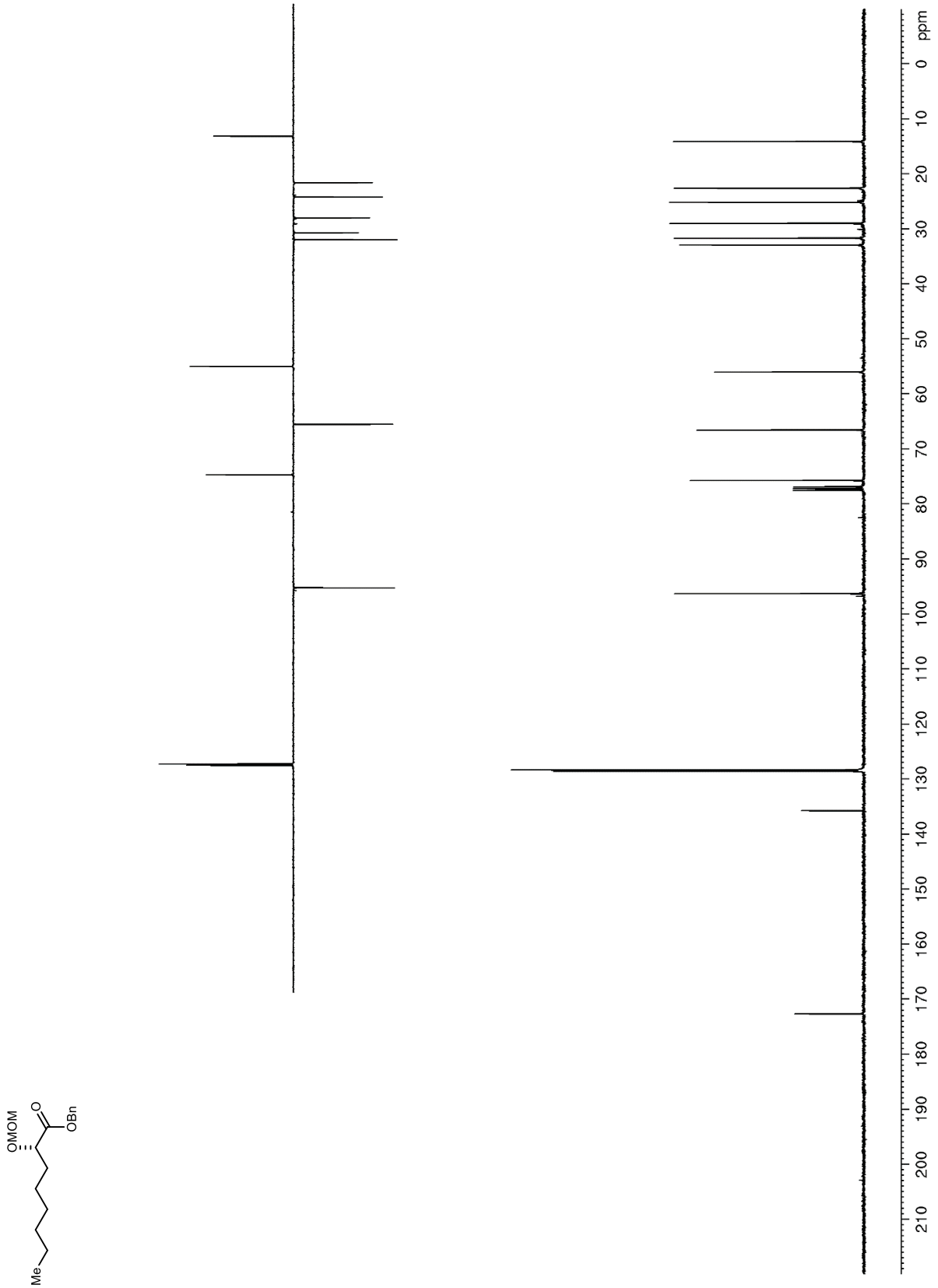

Figure S162. ^{1}H NMR (400 MHz, $CDCl_3$) of **S53**

Figure S163. ^{13}C NMR/DEPT (100 MHz, $CDCl_3$) of **S53**

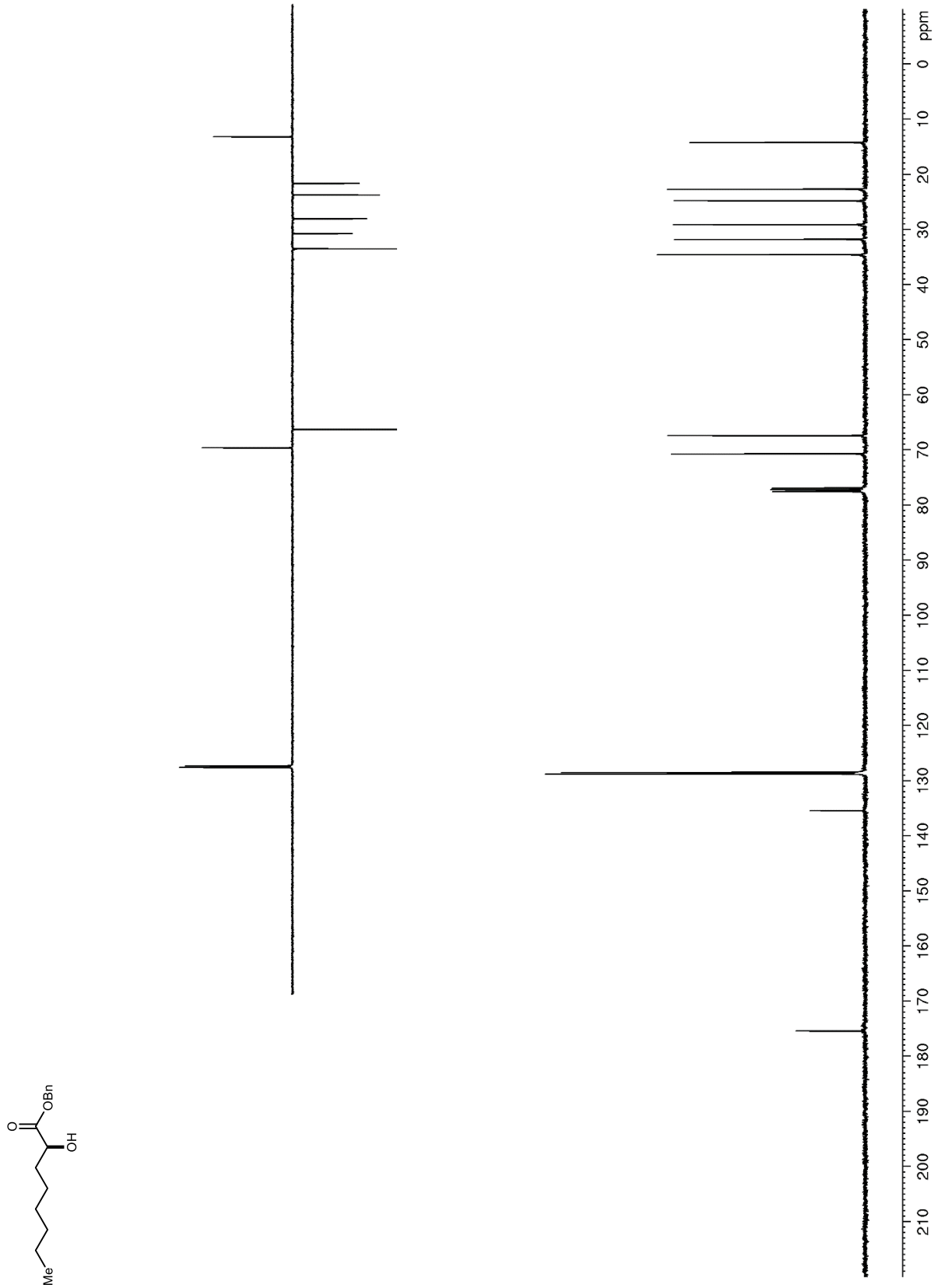

Figure S164. ^{1}H NMR (400 MHz, $CDCl_3$) of **S54**

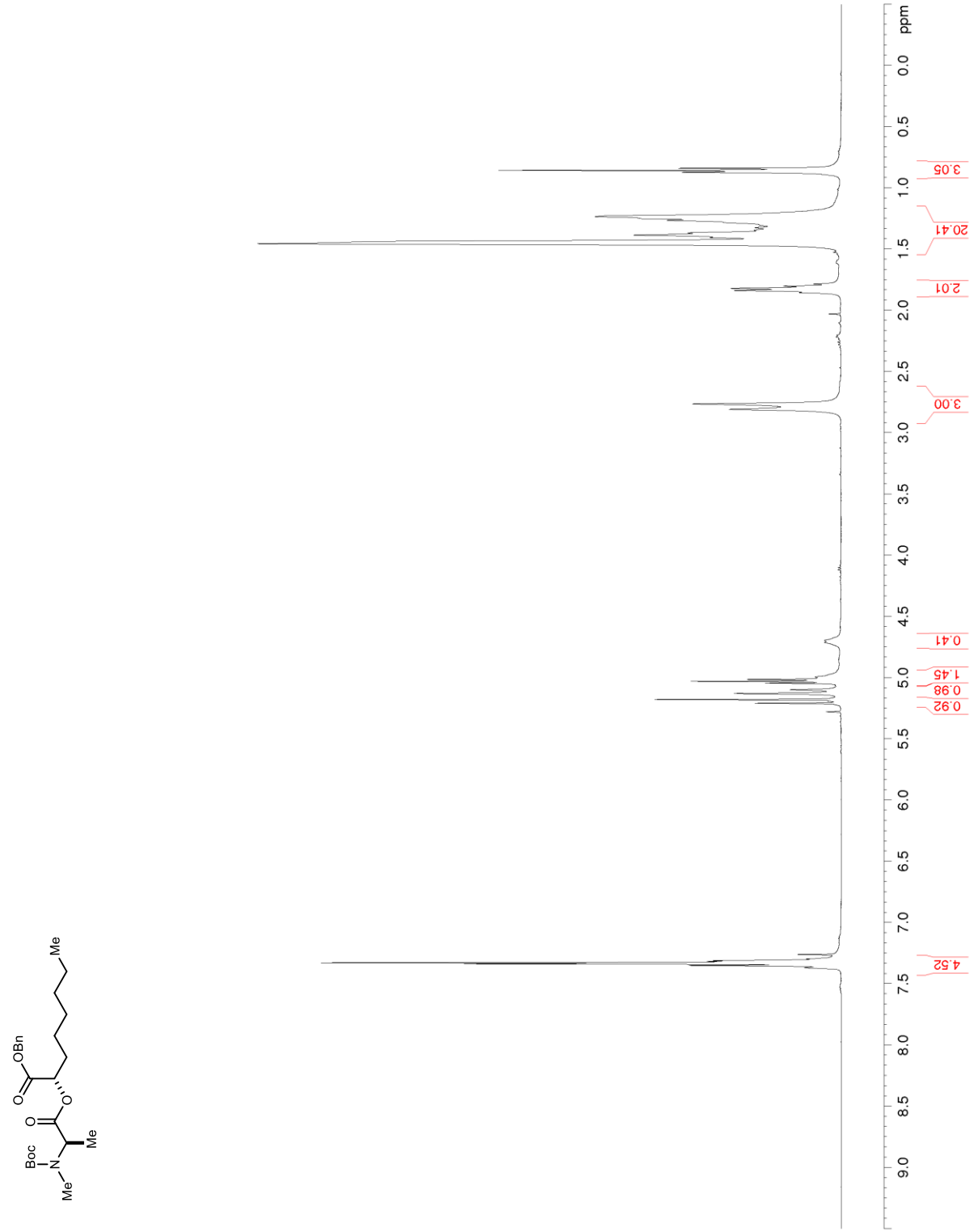

Figure S165. ^{13}C NMR/DEPT (100 MHz, $CDCl_3$) of **S54**

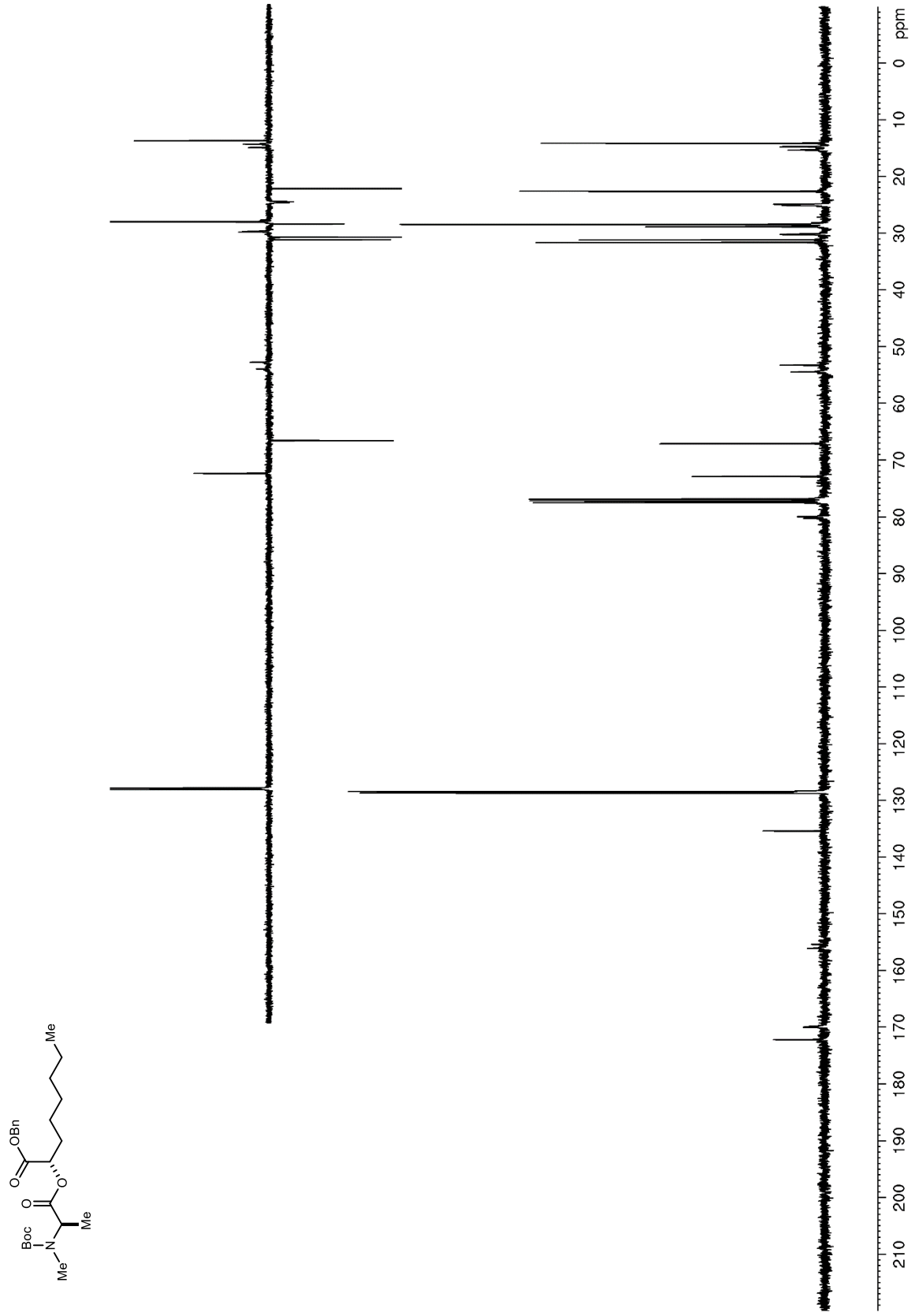

Figure S166. ^{1}H NMR (600 MHz, $CDCl_3$) of **S55**

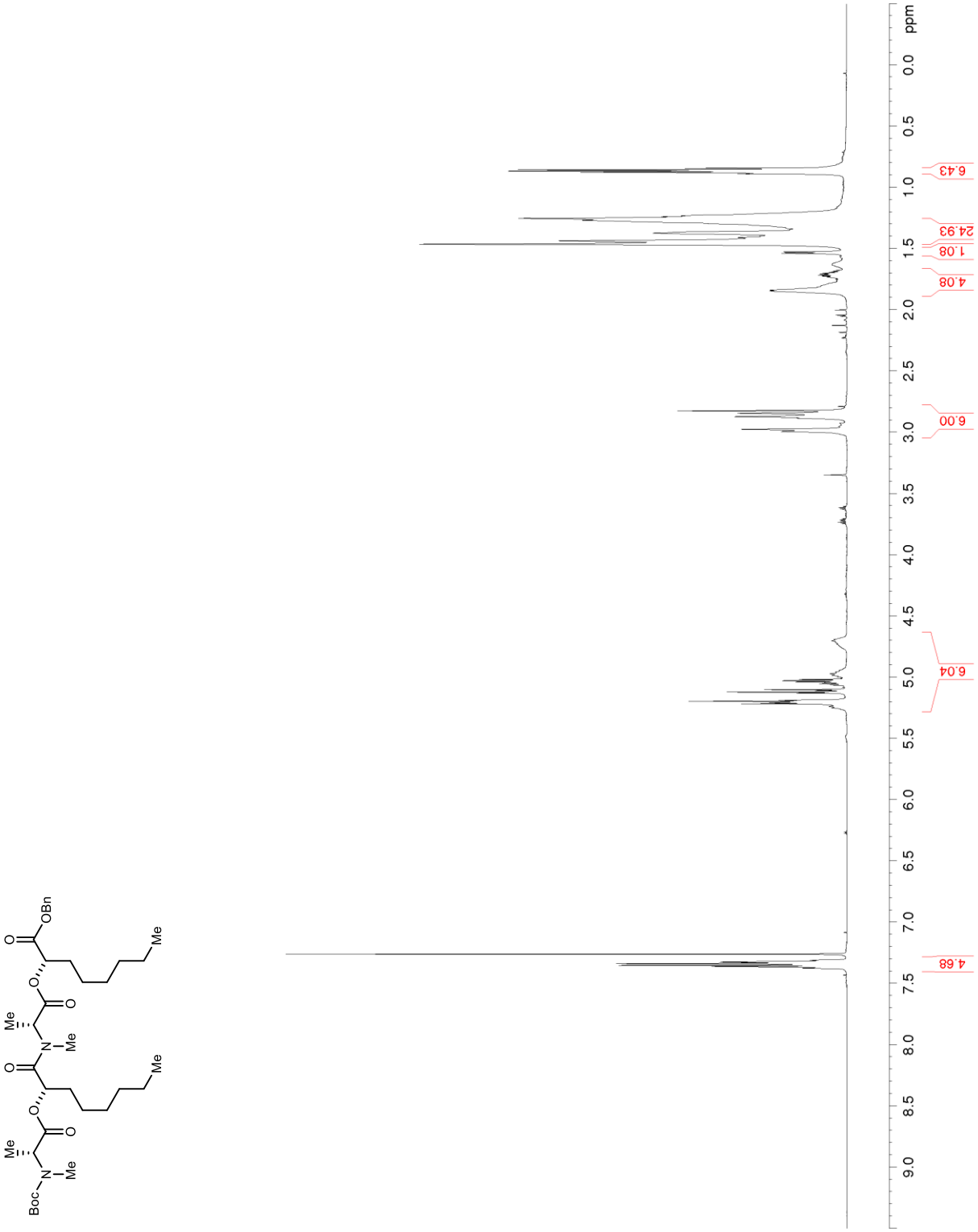

Figure S167. ^{13}C NMR/DEPT (150 MHz, $CDCl_3$) of **S55**

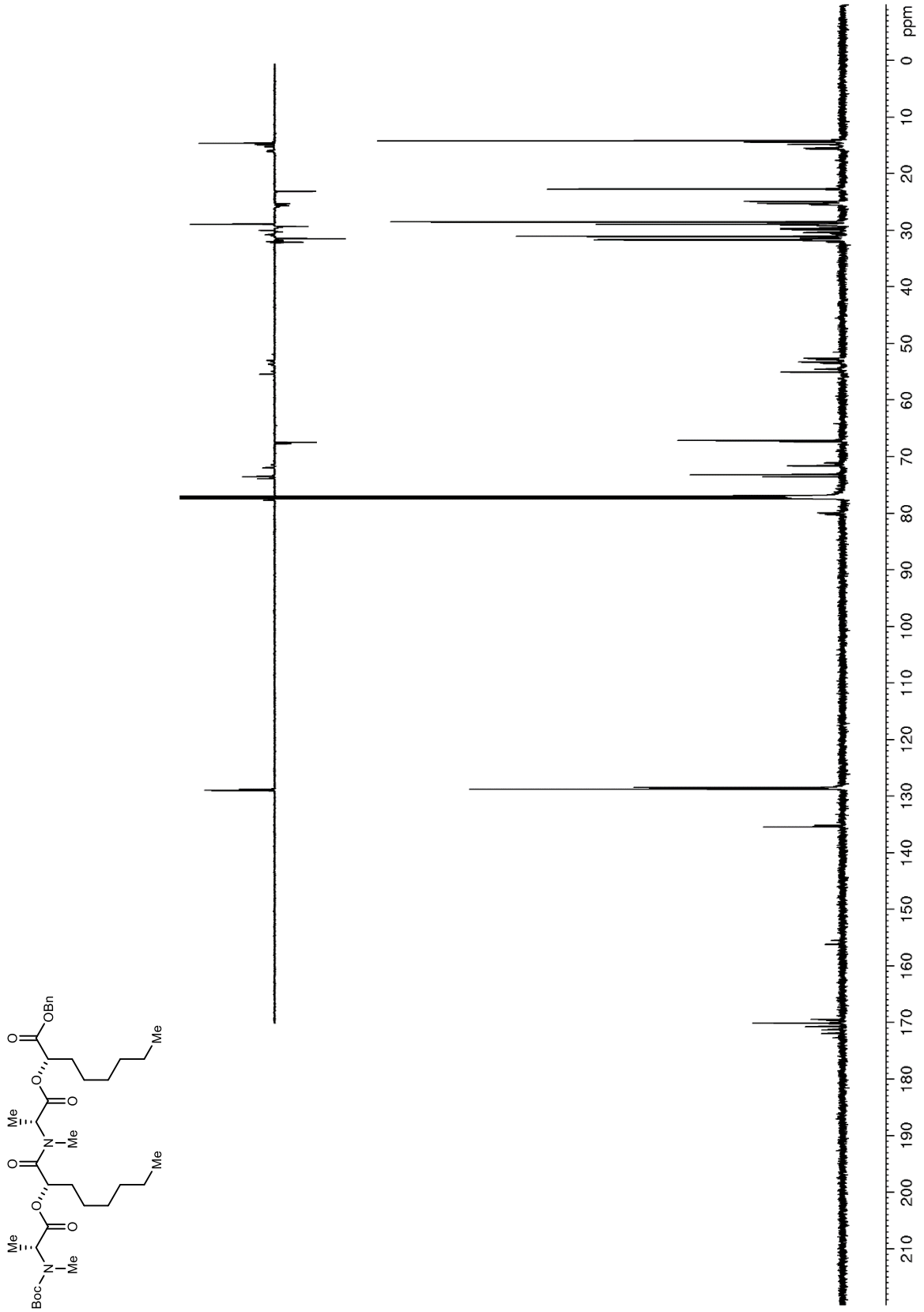

Figure S168. ^{1}H NMR (600 MHz, $CDCl_3$) of **S56**

Figure S169. ^{13}C NMR/DEPT (150 MHz, $CDCl_3$) of **S56**

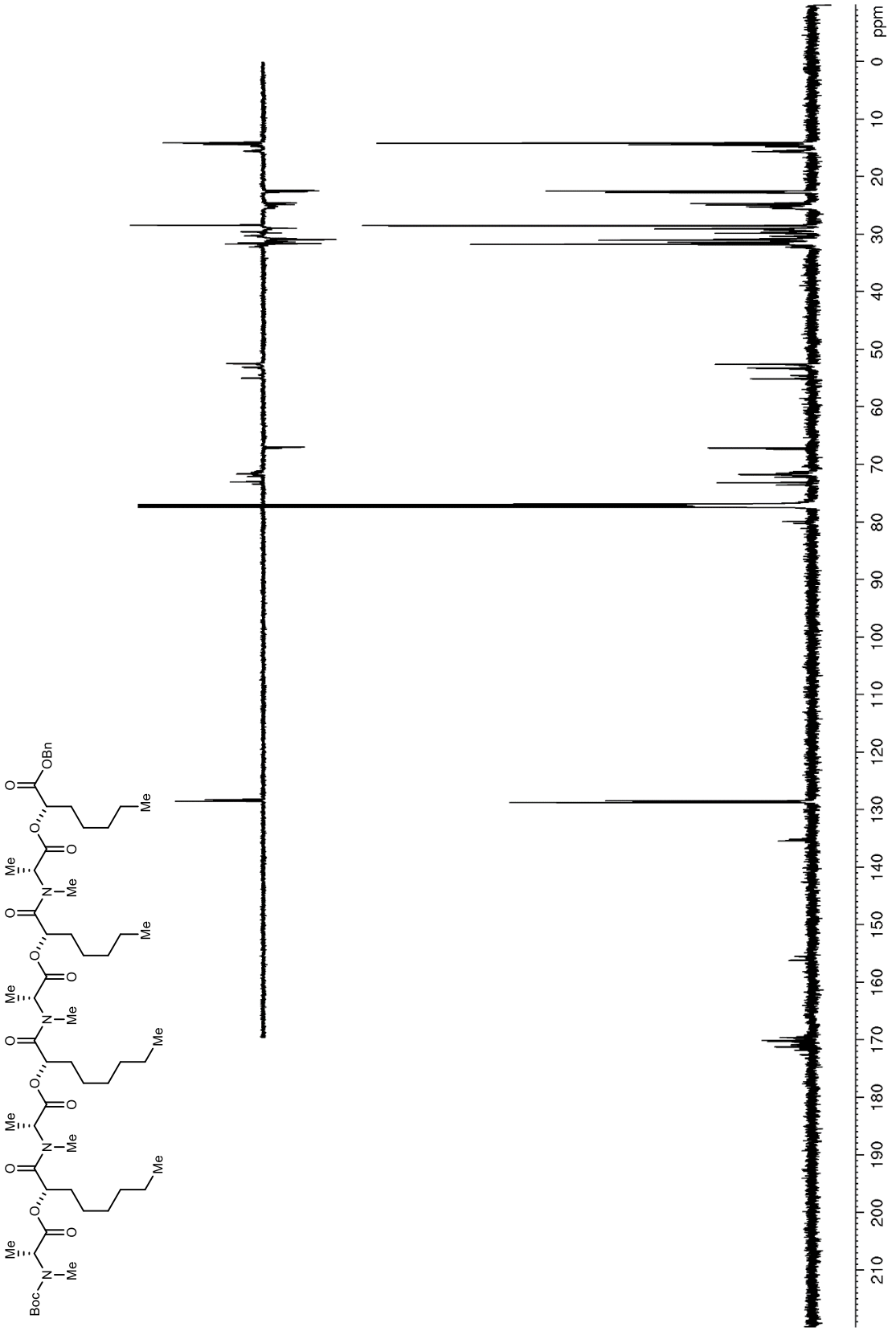

Figure S170. ^{1}H NMR (600 MHz, $CDCl_3$) of **76**

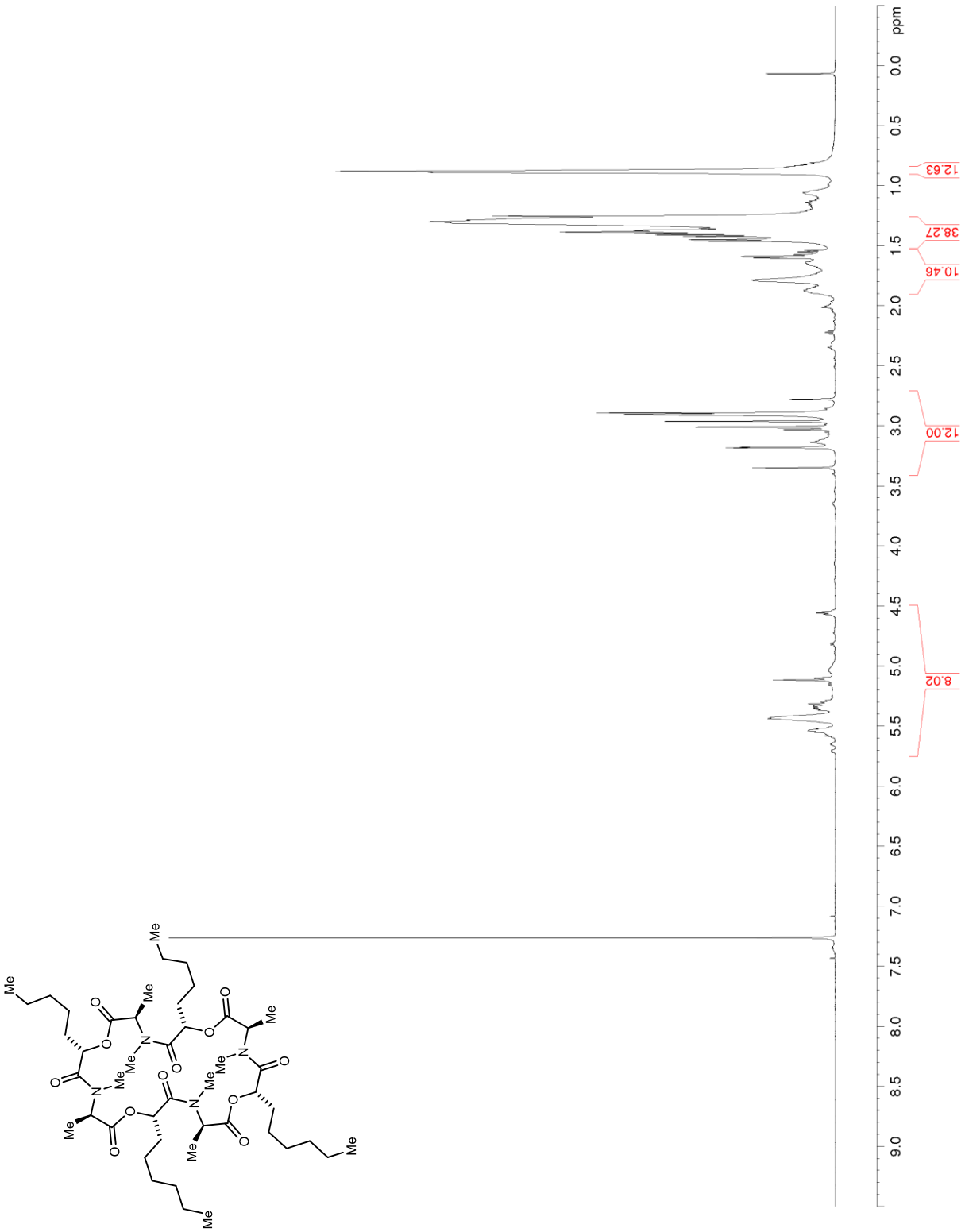

Figure S171. ^{13}C NMR/DEPT (150 MHz, $CDCl_3$) of **76**

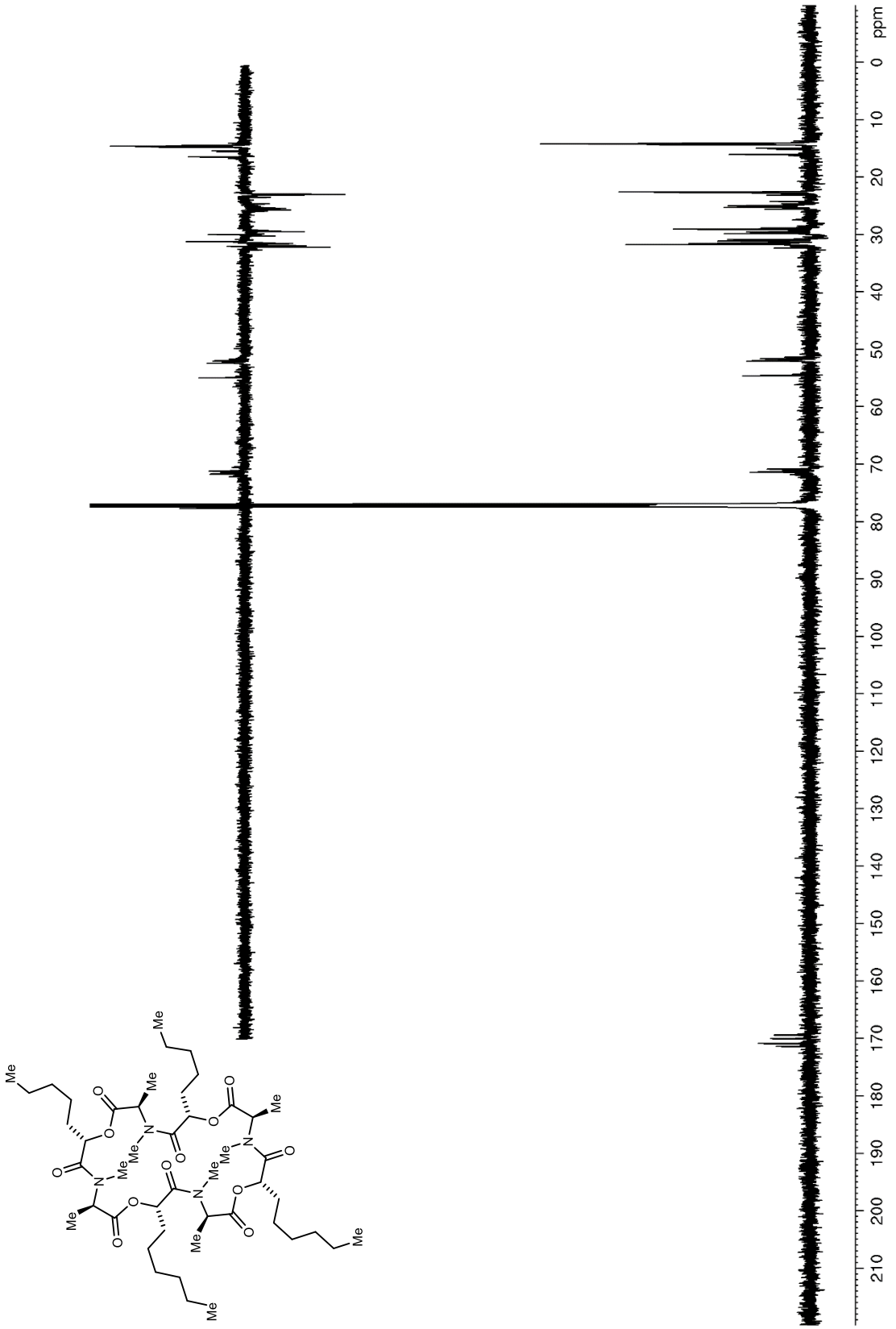

Figure S172. ^{1}H NMR (600 MHz, $CDCl_3$) of **S57**

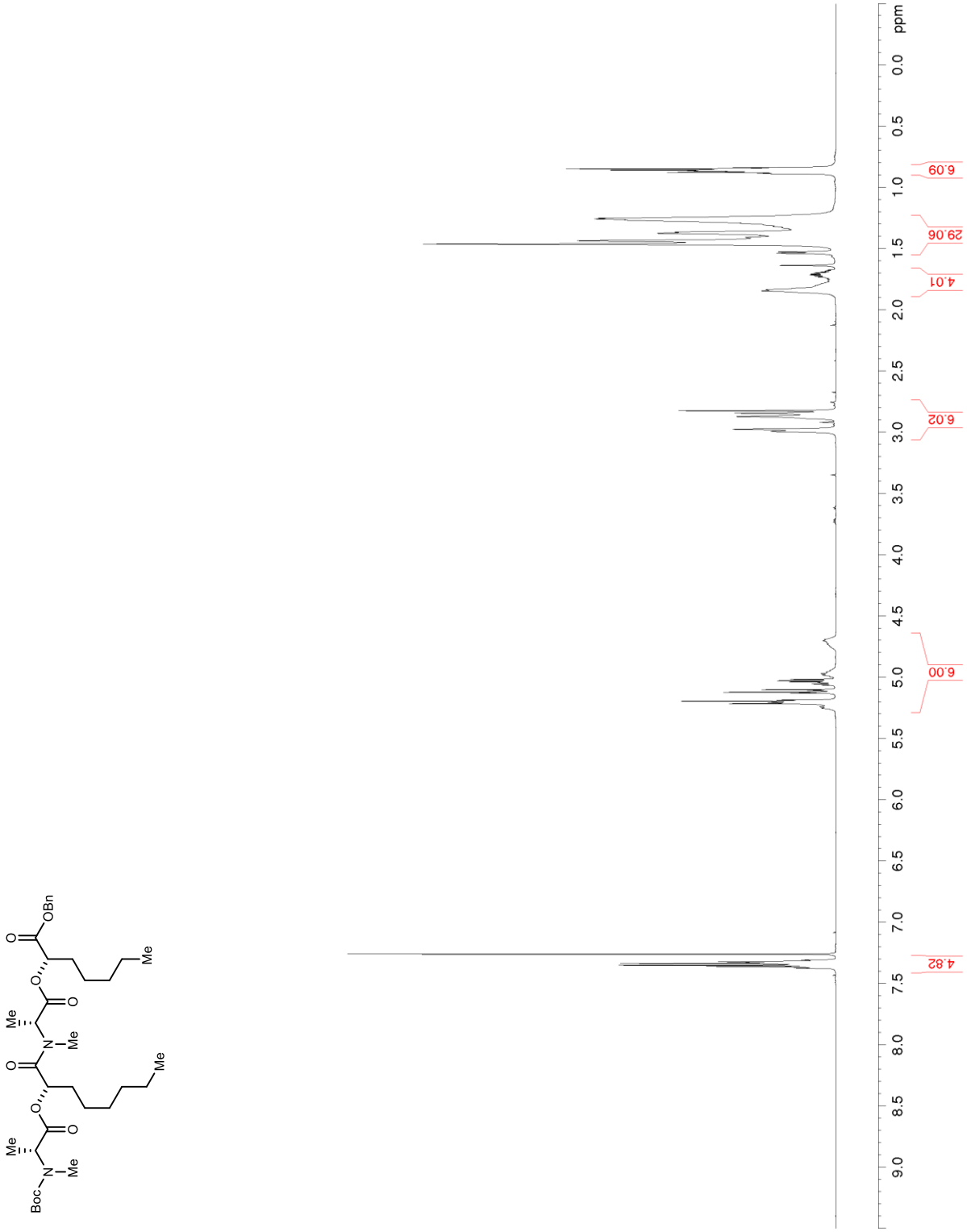

Figure S173. ^{13}C NMR/DEPT (150 MHz, $CDCl_3$) of **S57**

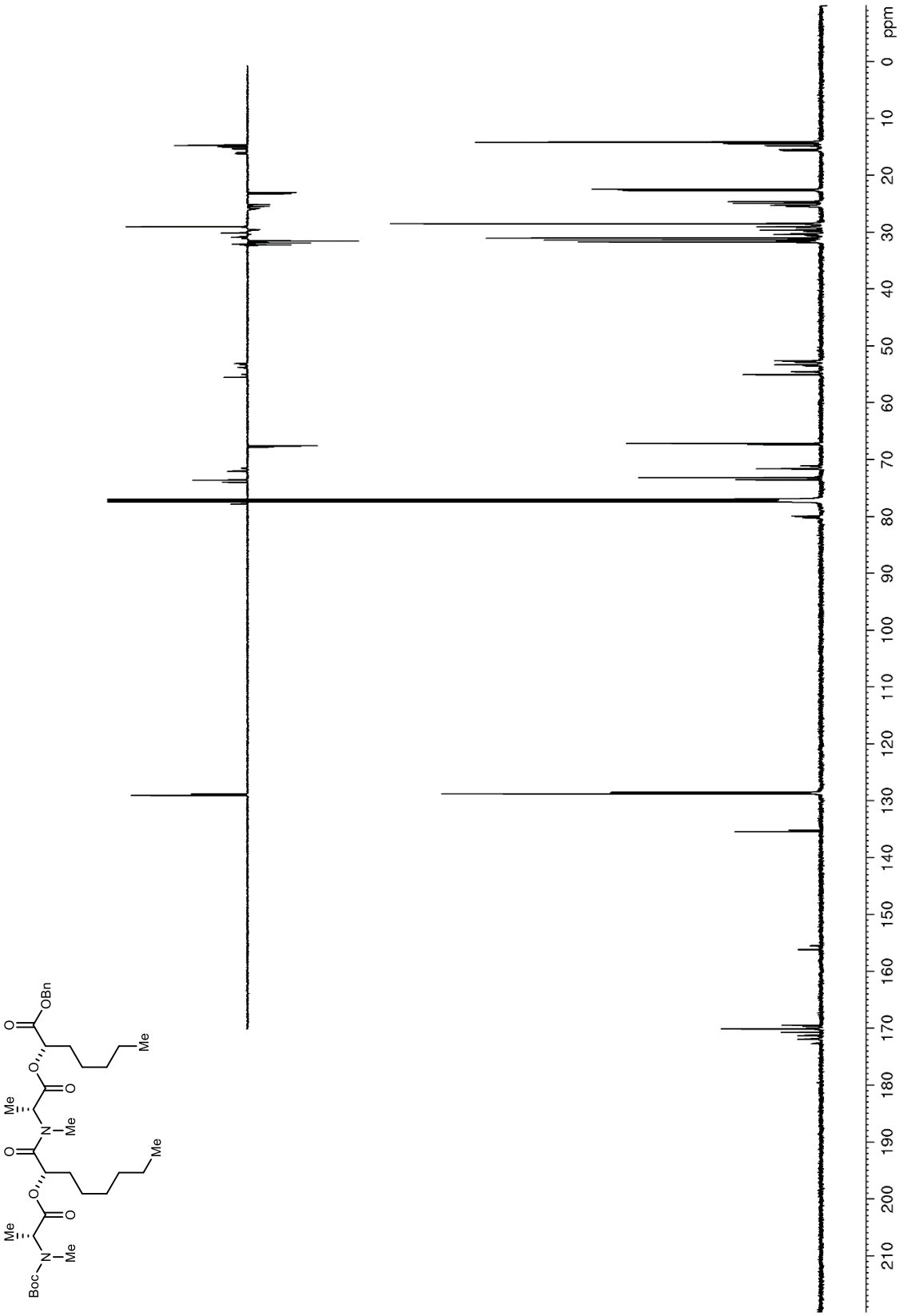

Figure S174. ^{1}H NMR (600 MHz, $CDCl_3$) of **S58**

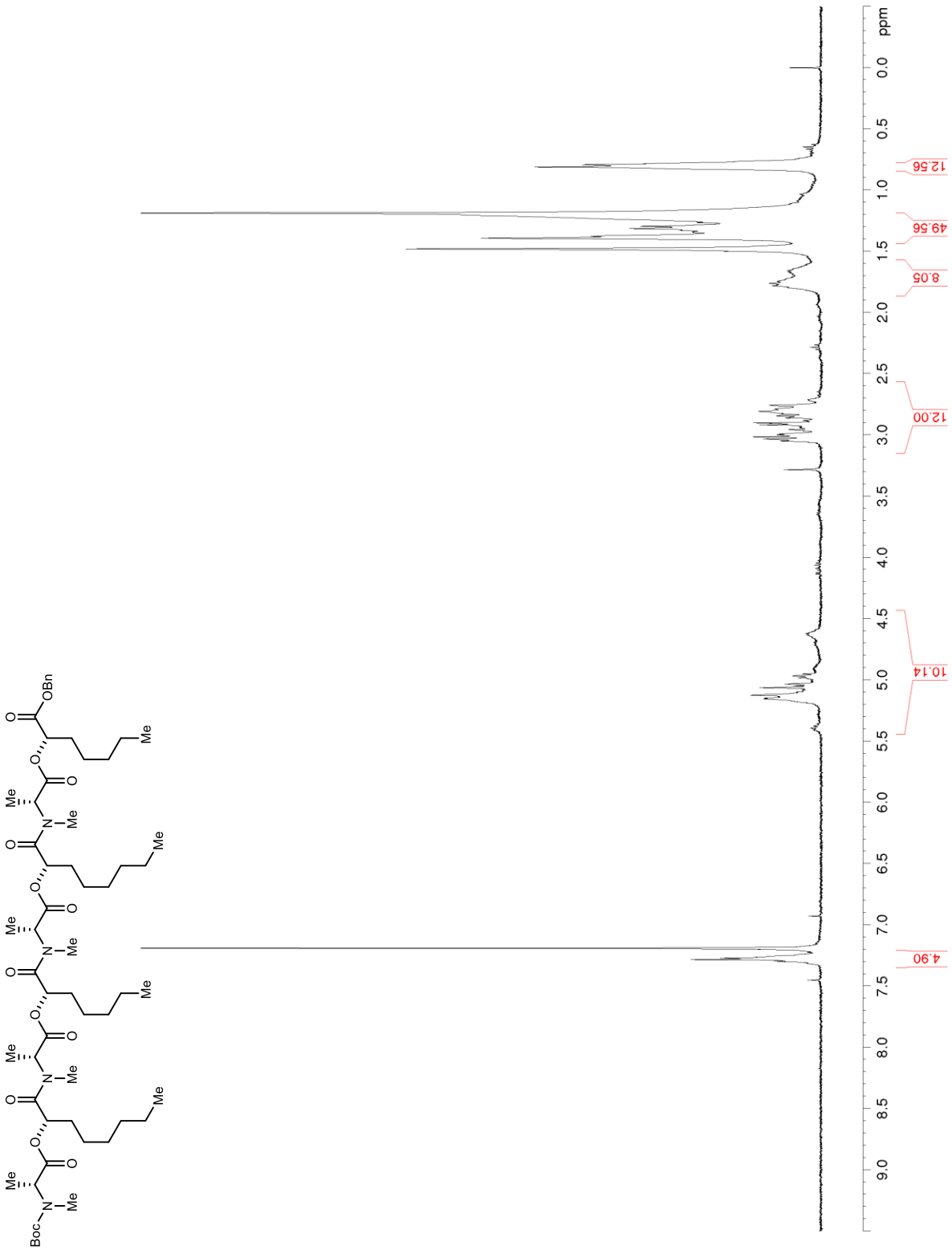

Figure S175. ^{13}C NMR/DEPT (150 MHz, $CDCl_3$) of **S58**

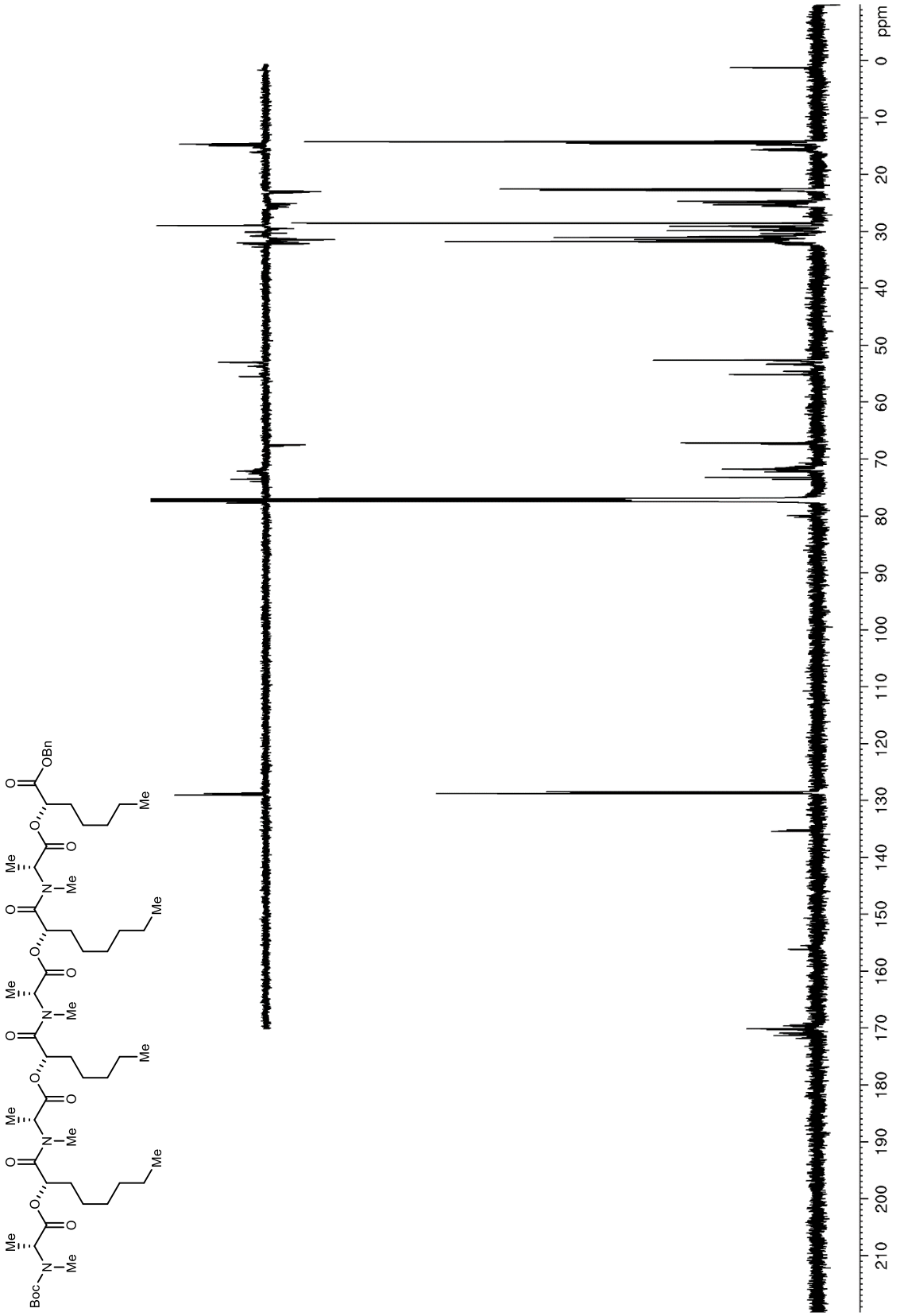

Figure S176. ^{1}H NMR (600 MHz, $CDCl_3$) of **77**

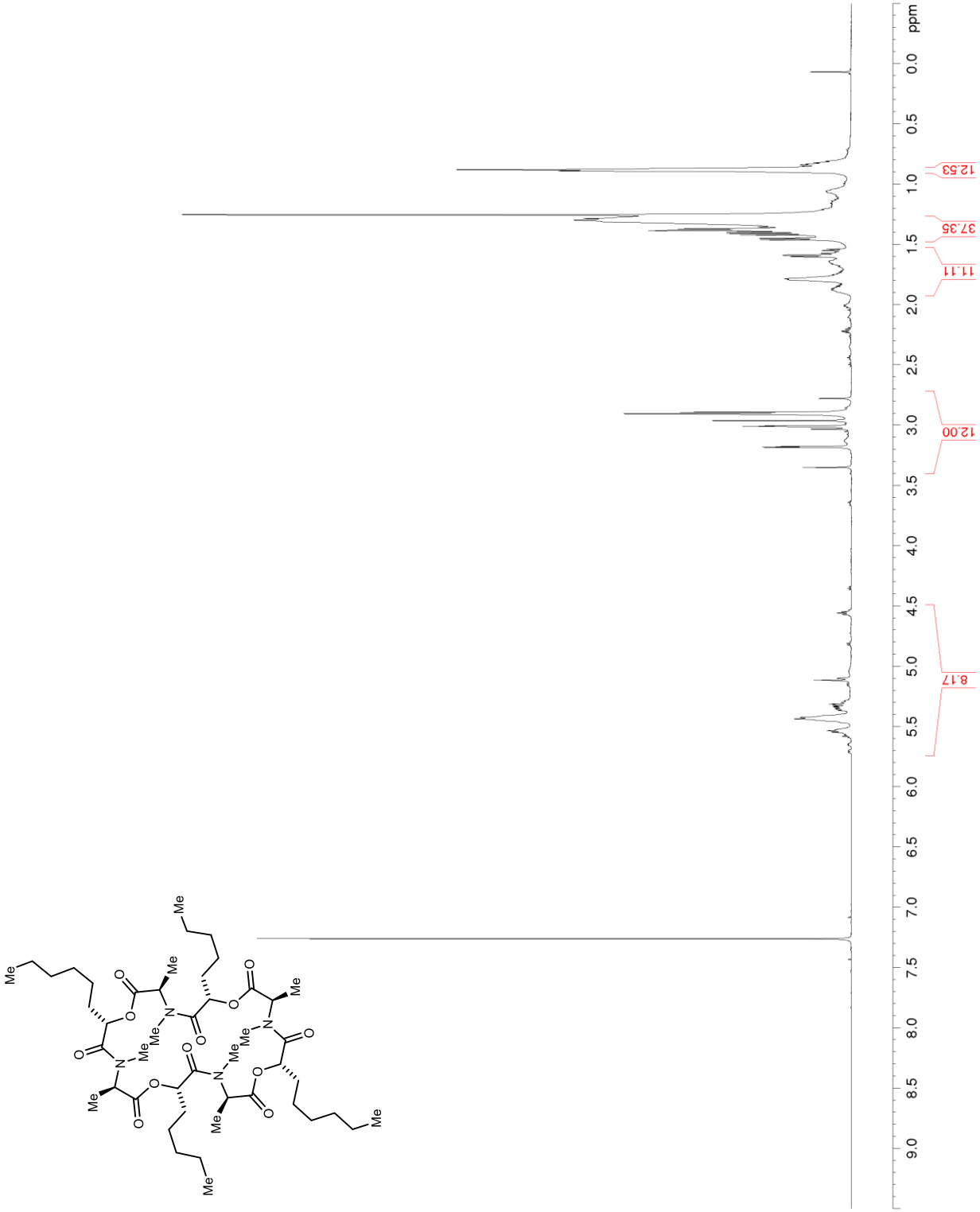

Figure S177. ^{13}C NMR/DEPT (150 MHz, $CDCl_3$) of **77**

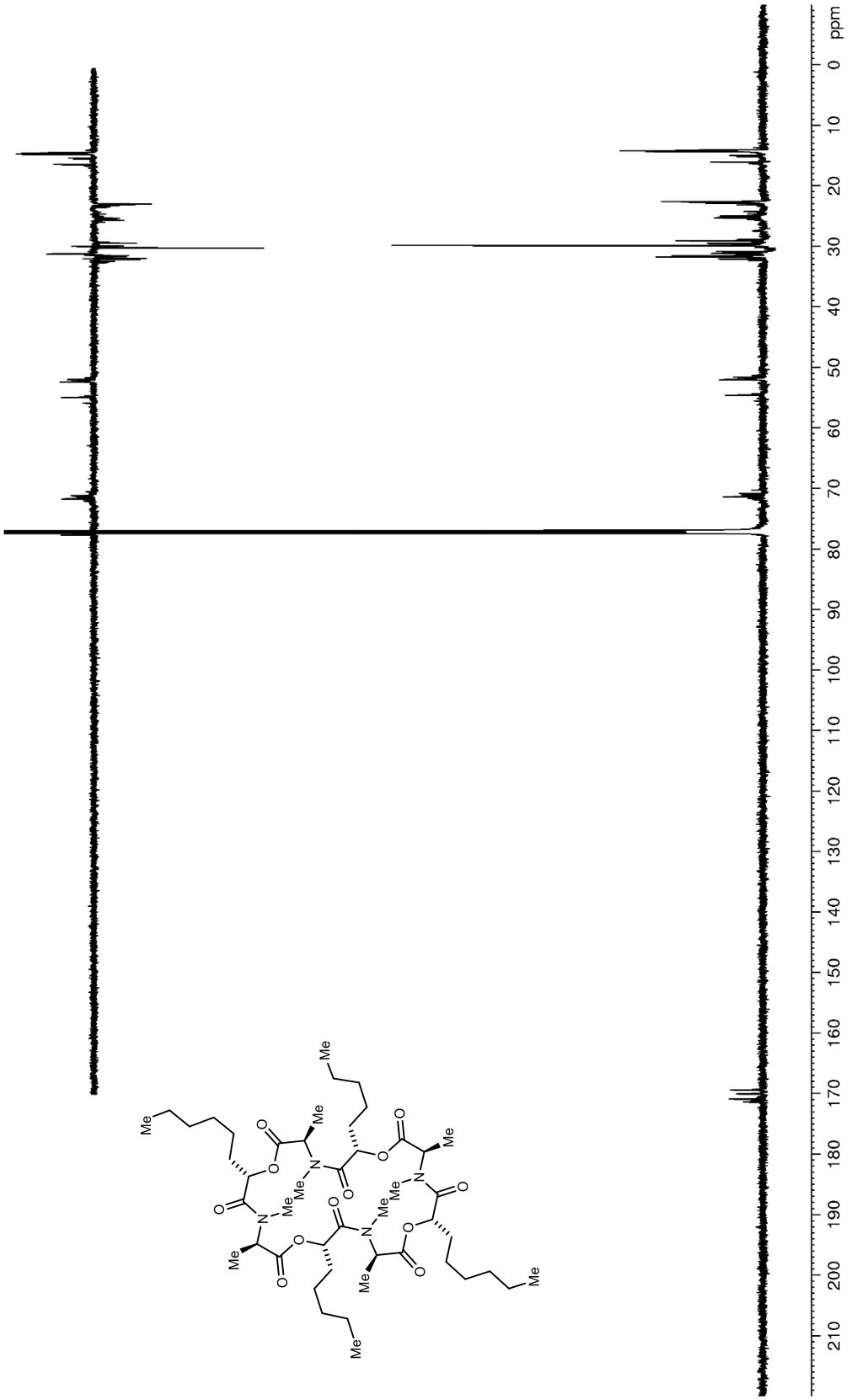

Figure S178. ^{1}H NMR (400 MHz, $CDCl_3$) of **S59**

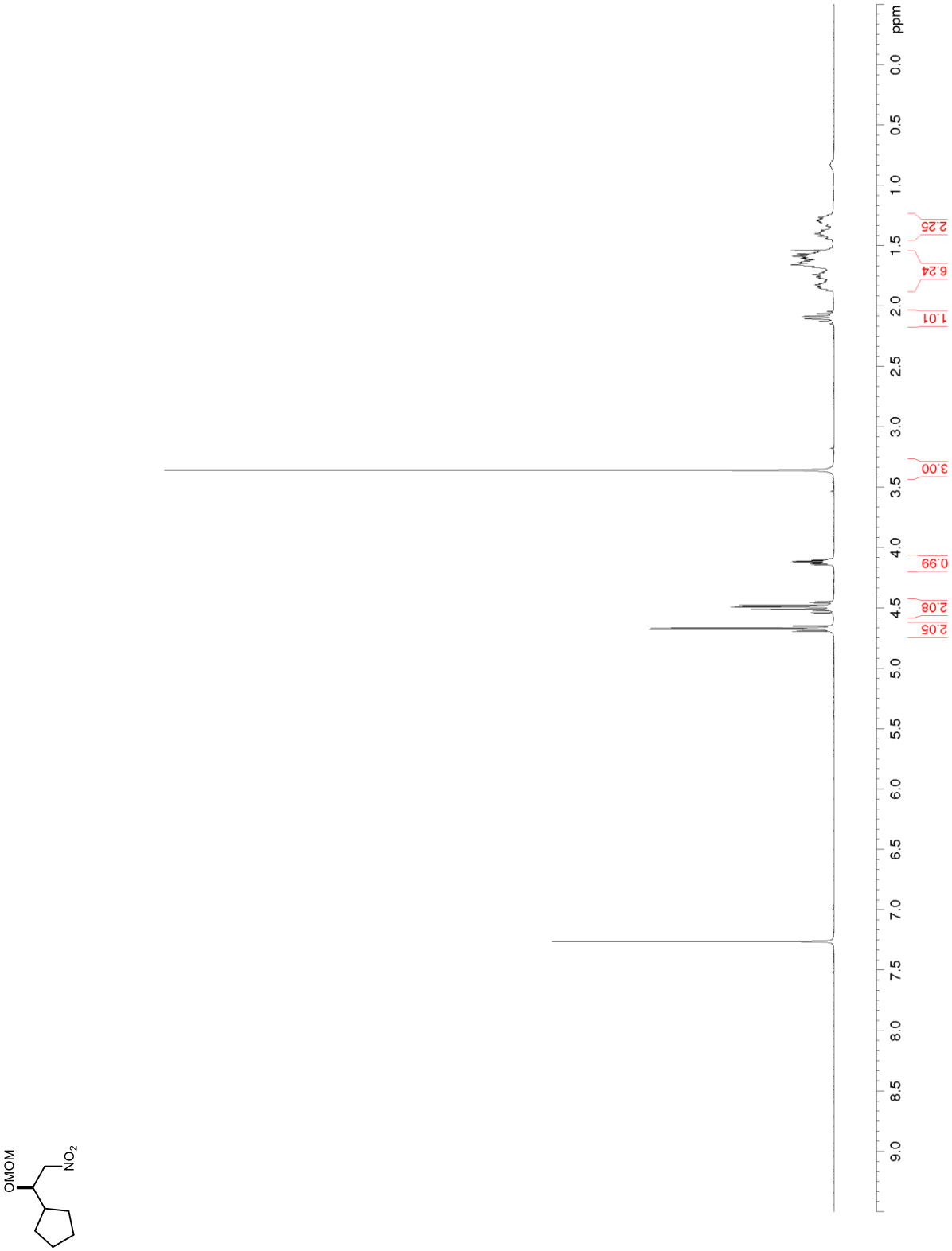

Figure S179. ^{13}C NMR/DEPT (100 MHz, $CDCl_3$) of **S59**

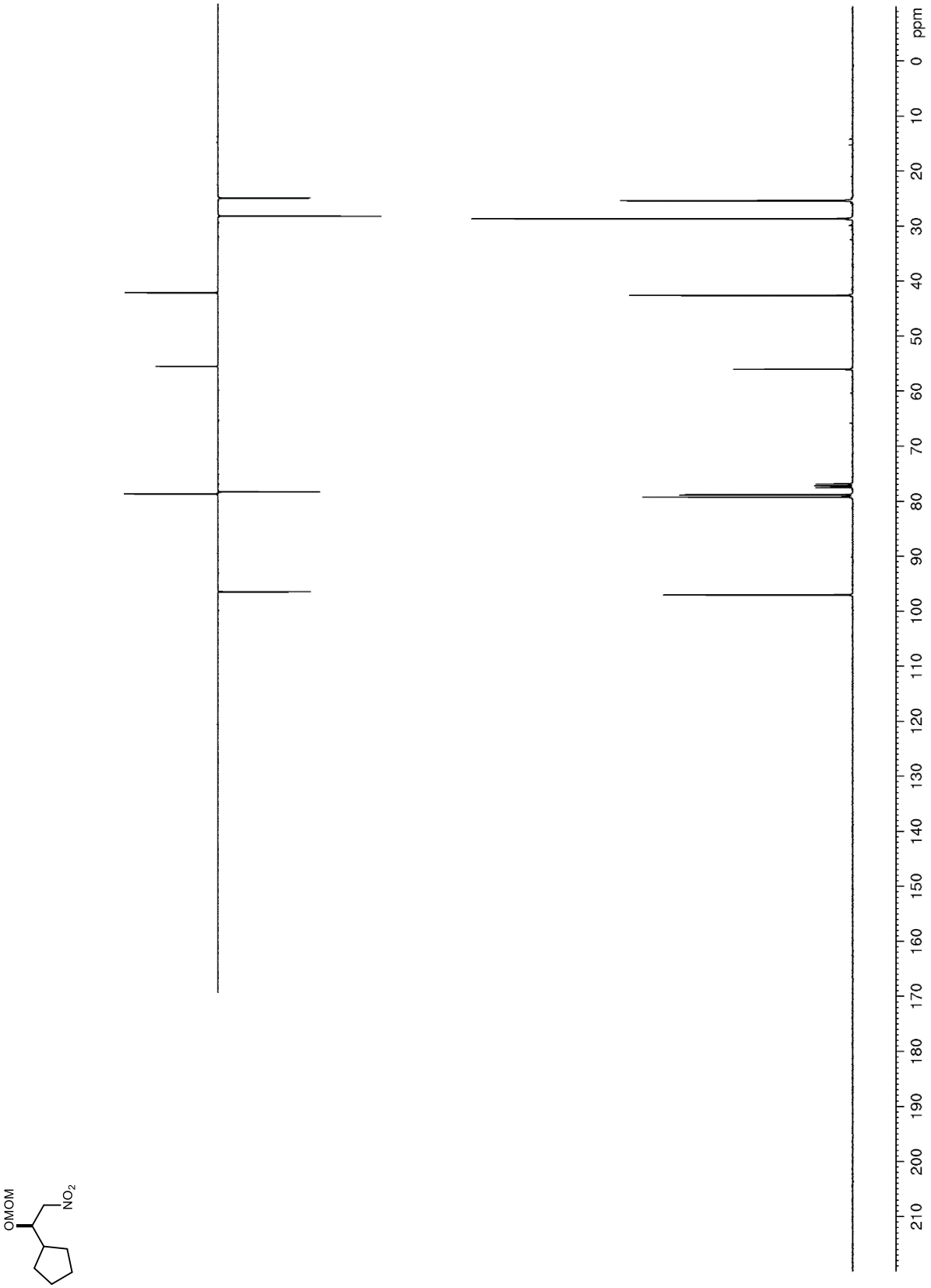

Figure S180. ^{1}H NMR (400 MHz, $CDCl_3$) of **S60**

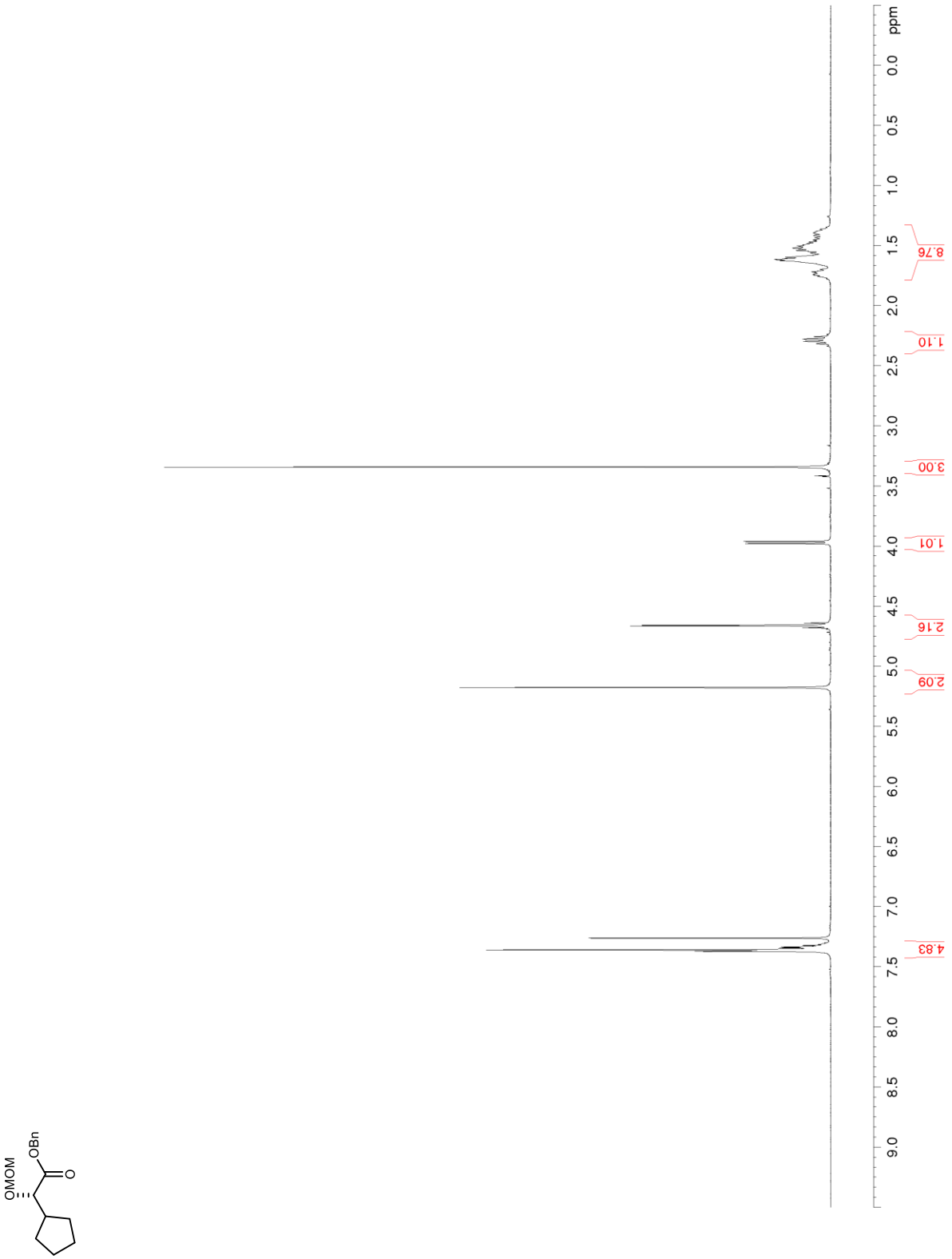

Figure S181. ^{13}C NMR/DEPT (100 MHz, $CDCl_3$) of **S60**

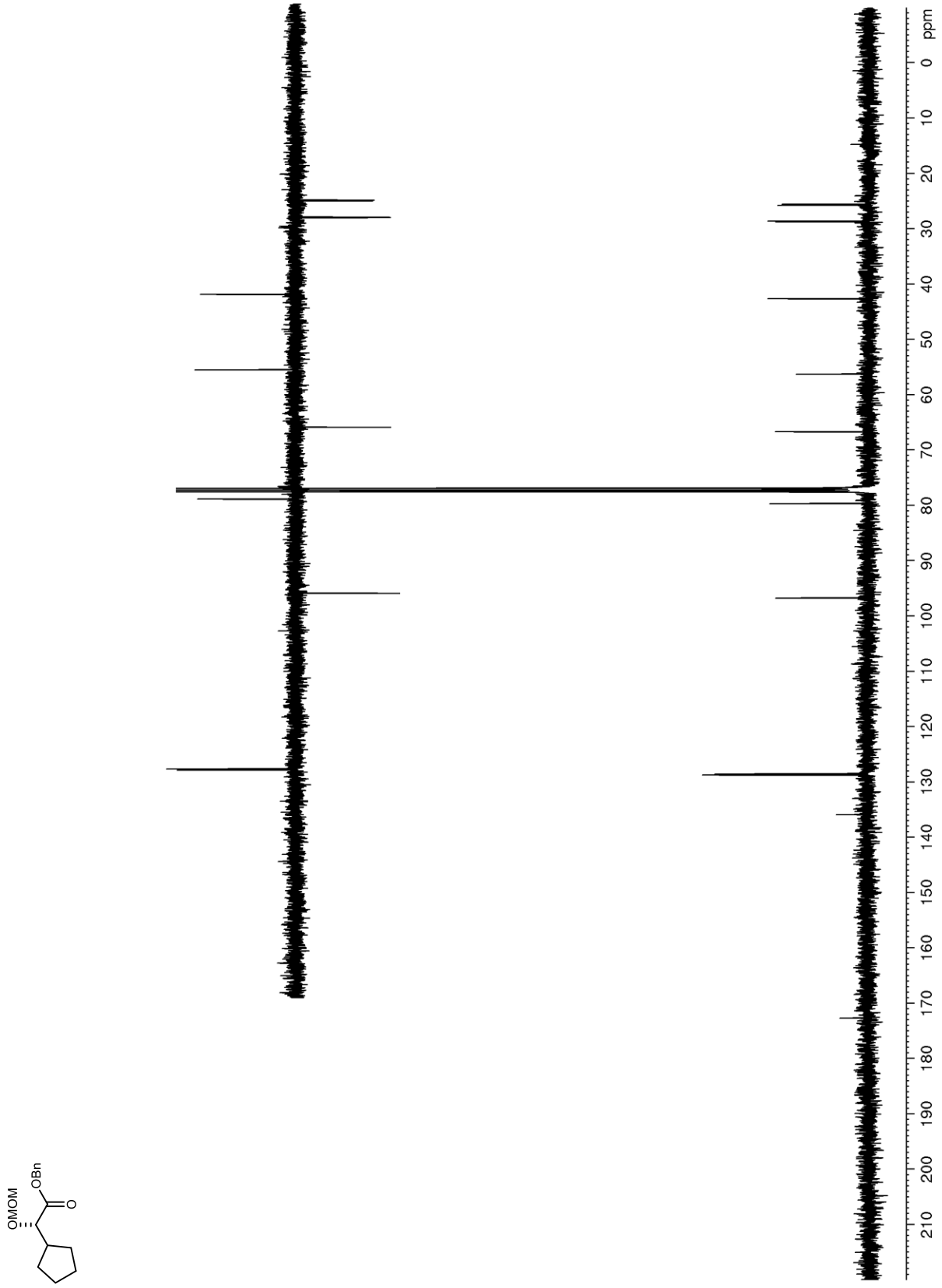

Figure S182. ^{1}H NMR (400 MHz, $CDCl_3$) of **S61**

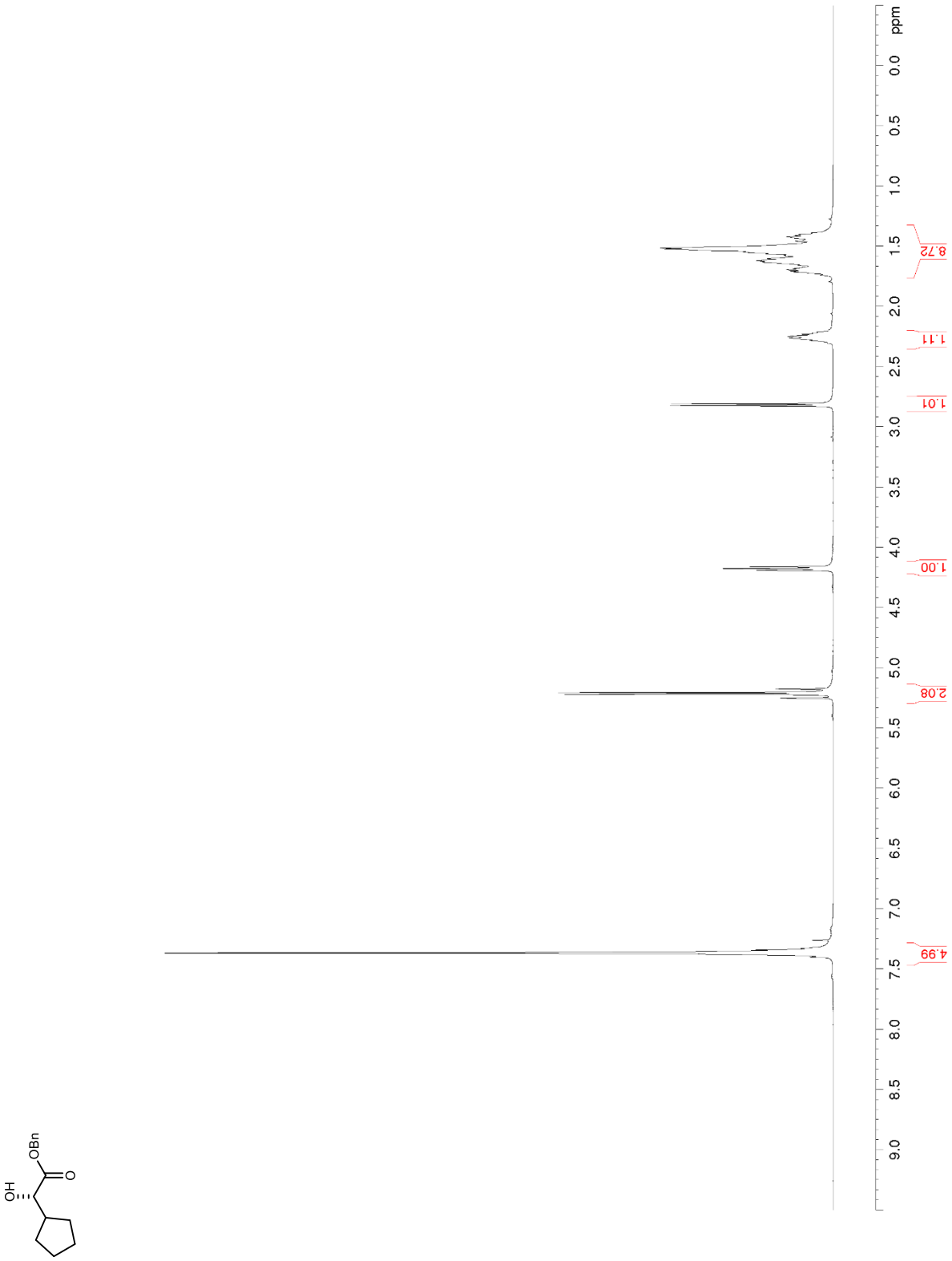

Figure S183. ^{13}C NMR/DEPT (100 MHz, $CDCl_3$) of **S61**

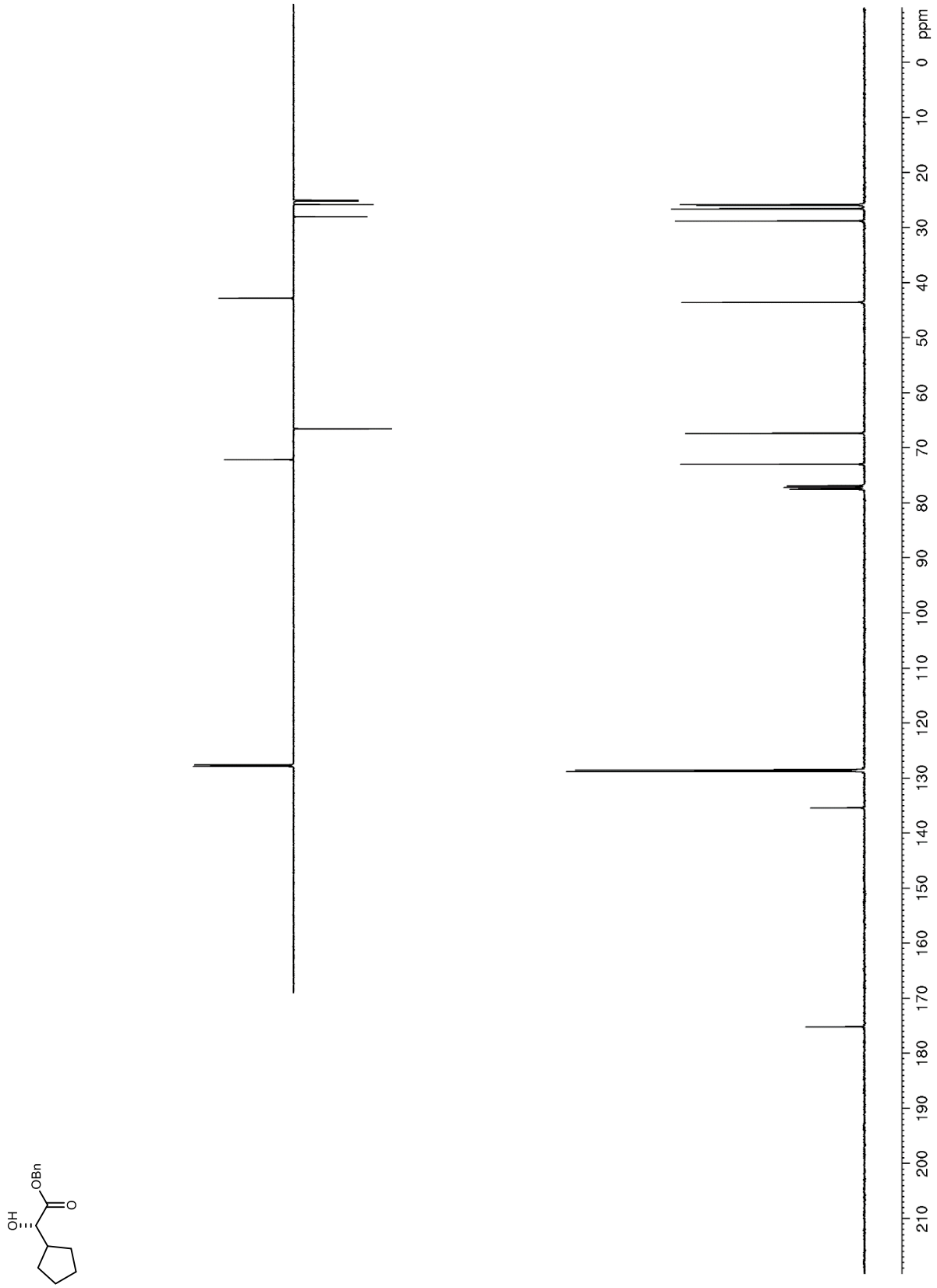

Figure S184. ^{1}H NMR (600 MHz, $CDCl_3$) of **S62**

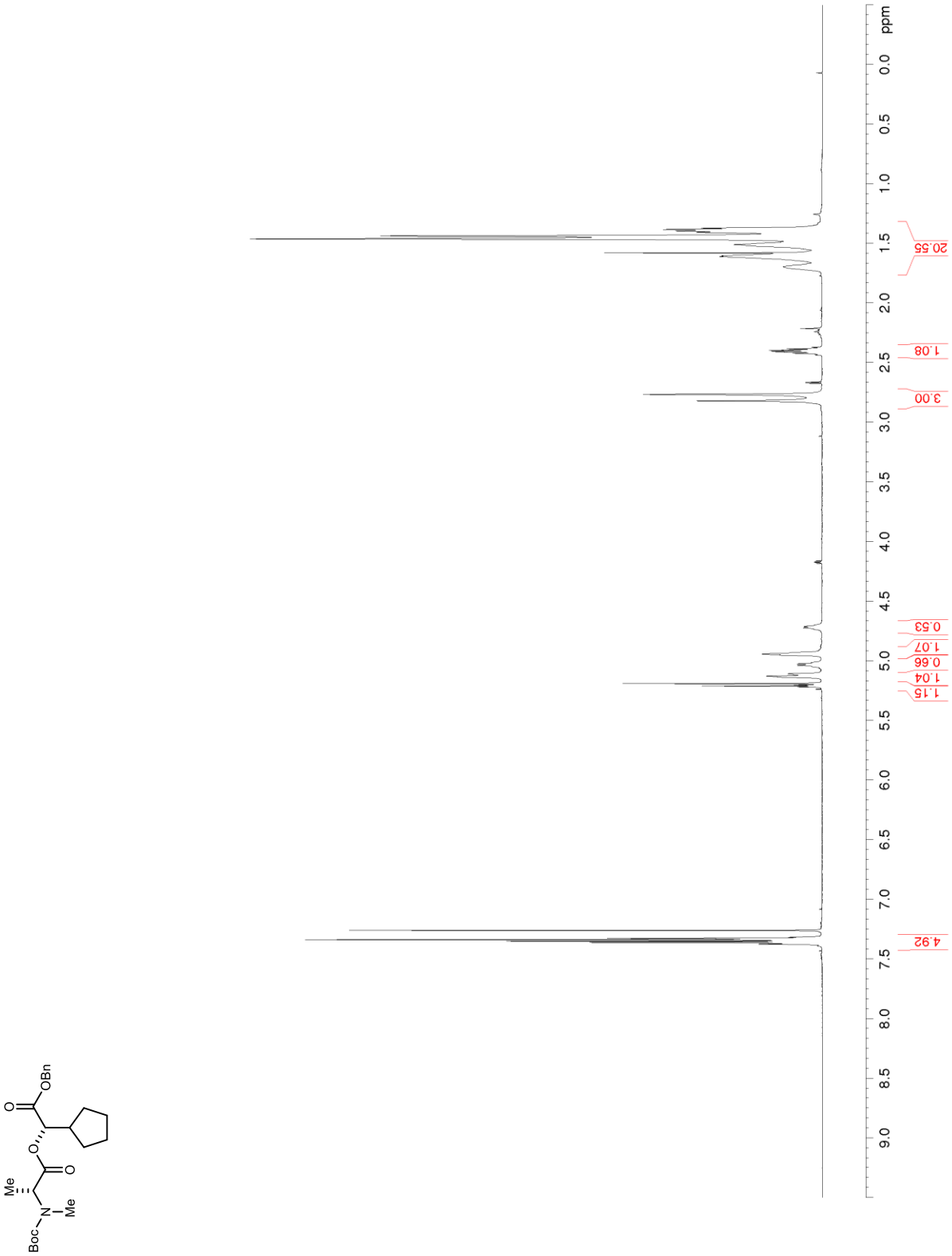

Figure S185. ^{13}C NMR/DEPT (150 MHz, $CDCl_3$) of **S62**

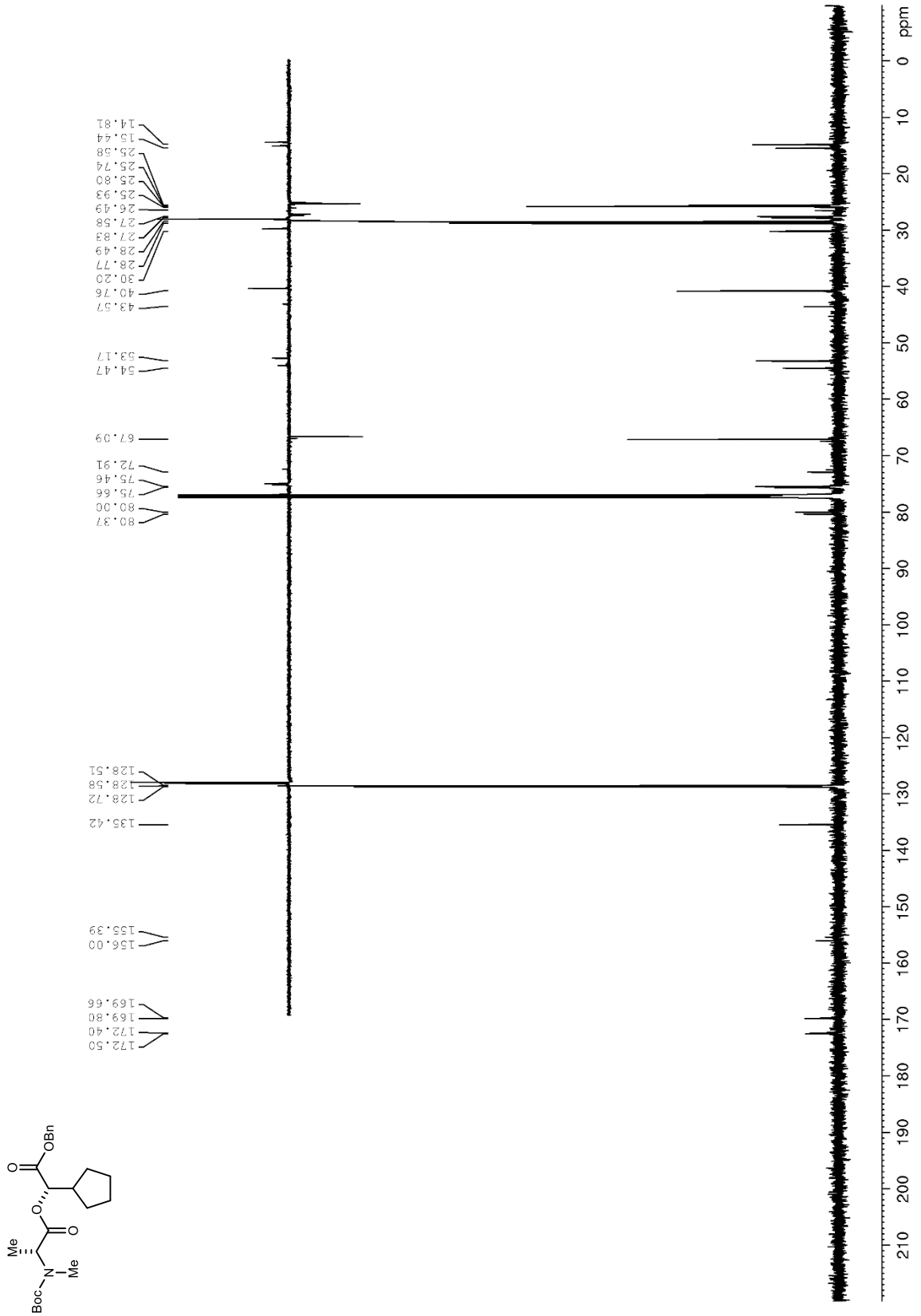

Figure S186. ^{1}H NMR (600 MHz, $CDCl_3$) of **S63**

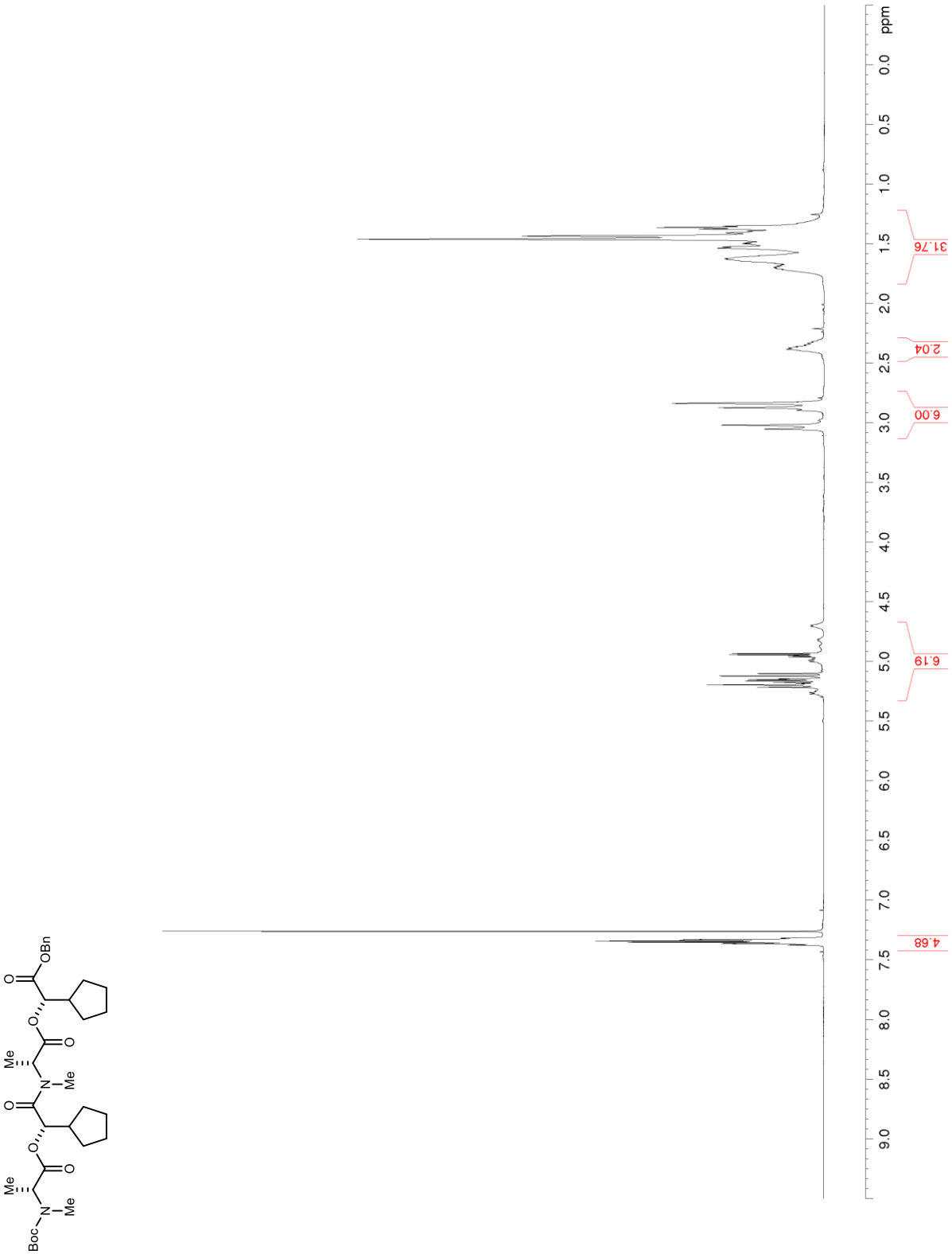

Figure S187. ^{13}C NMR/DEPT (150 MHz, $CDCl_3$) of **S63**

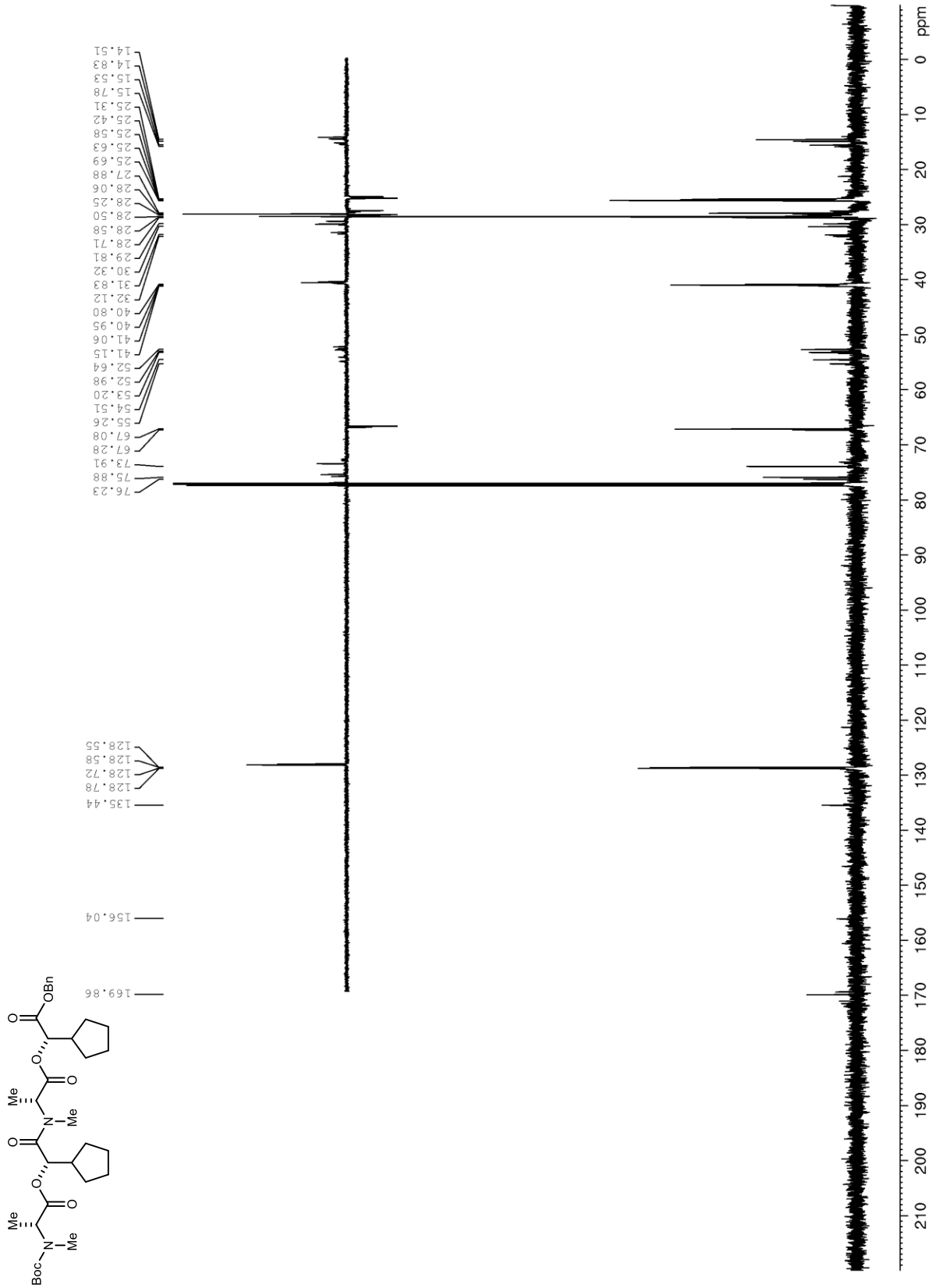

Figure S188. ^{1}H NMR (600 MHz, $CDCl_3$) of **S64**

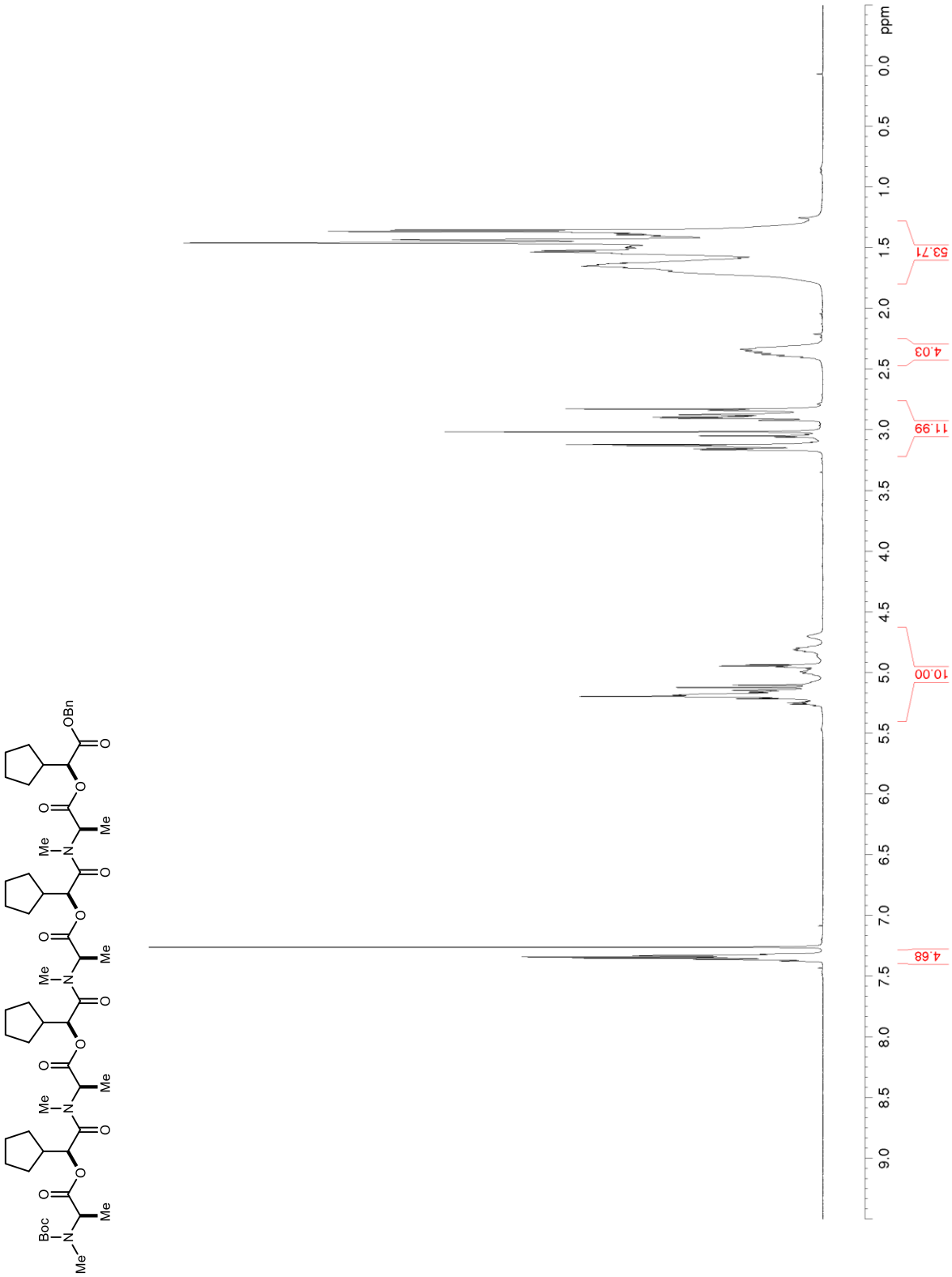

Figure S189. ^{13}C NMR/DEPT (150 MHz, $CDCl_3$) of **S64**

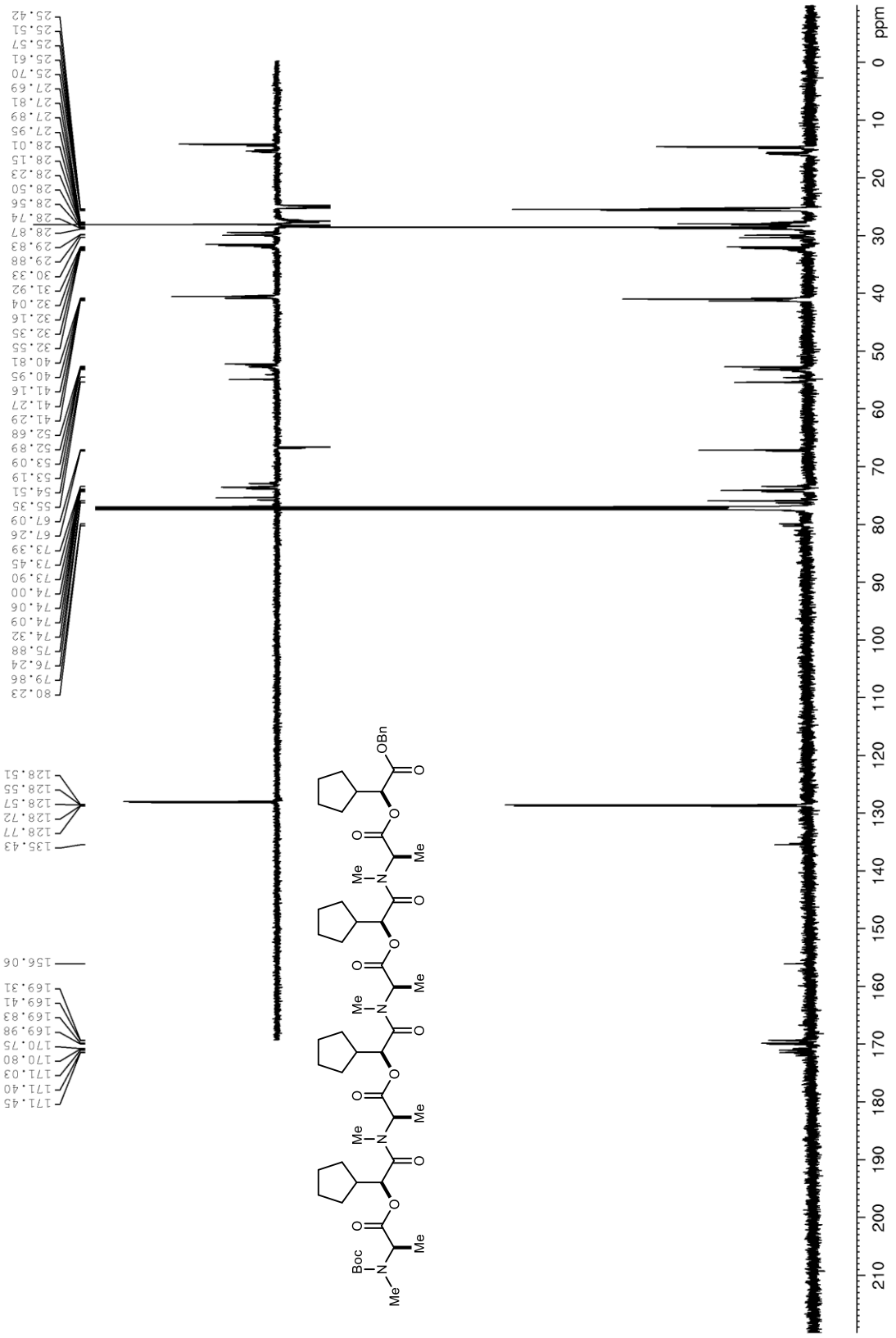

Figure S190. ^{1}H NMR (600 MHz, $CDCl_3$) of **78**

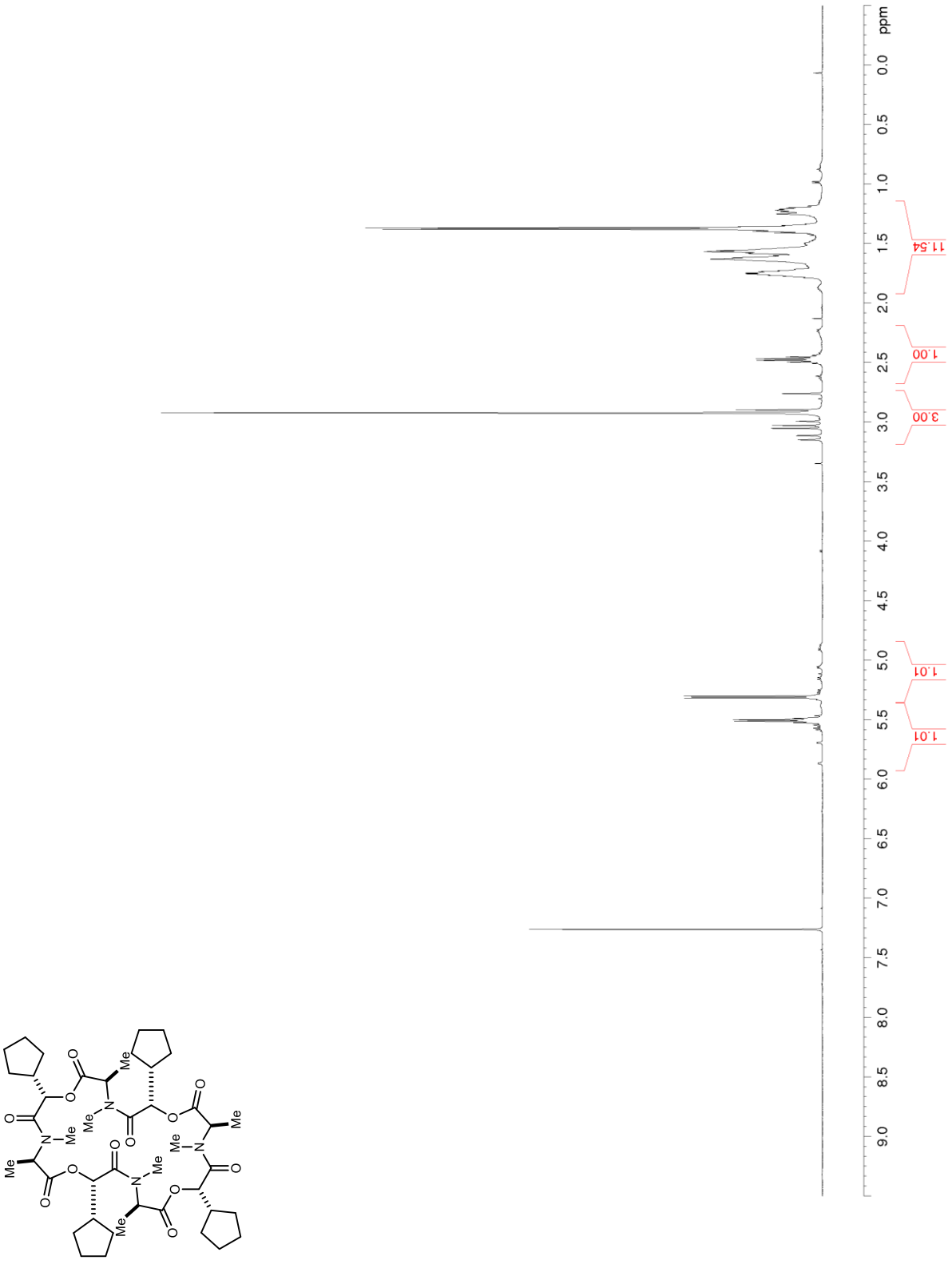

Figure S191. ^{13}C NMR/DEPT (150 MHz, $CDCl_3$) of **78**

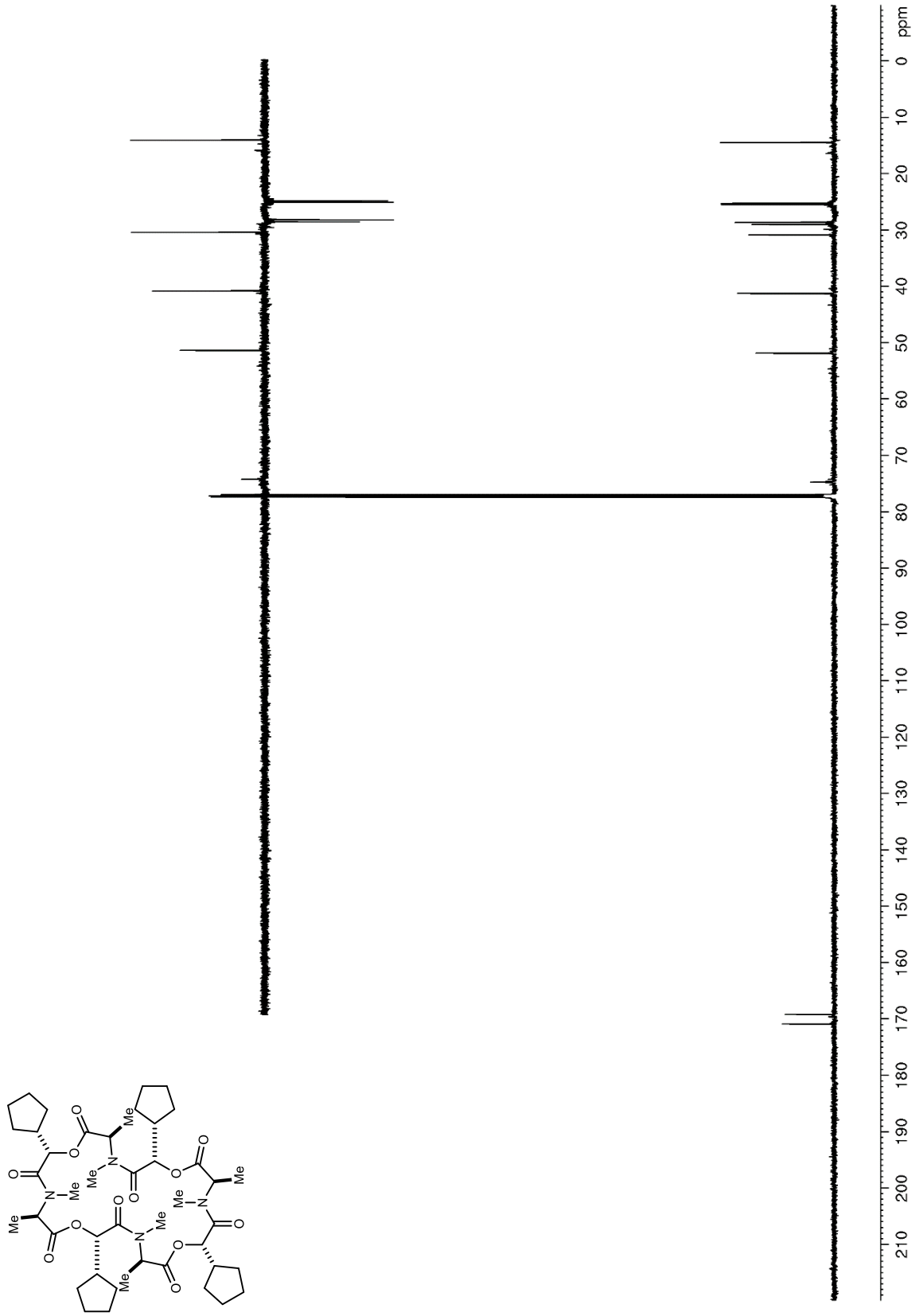

Figure S192. ^{1}H NMR (600 MHz, $CDCl_3$) of **138**

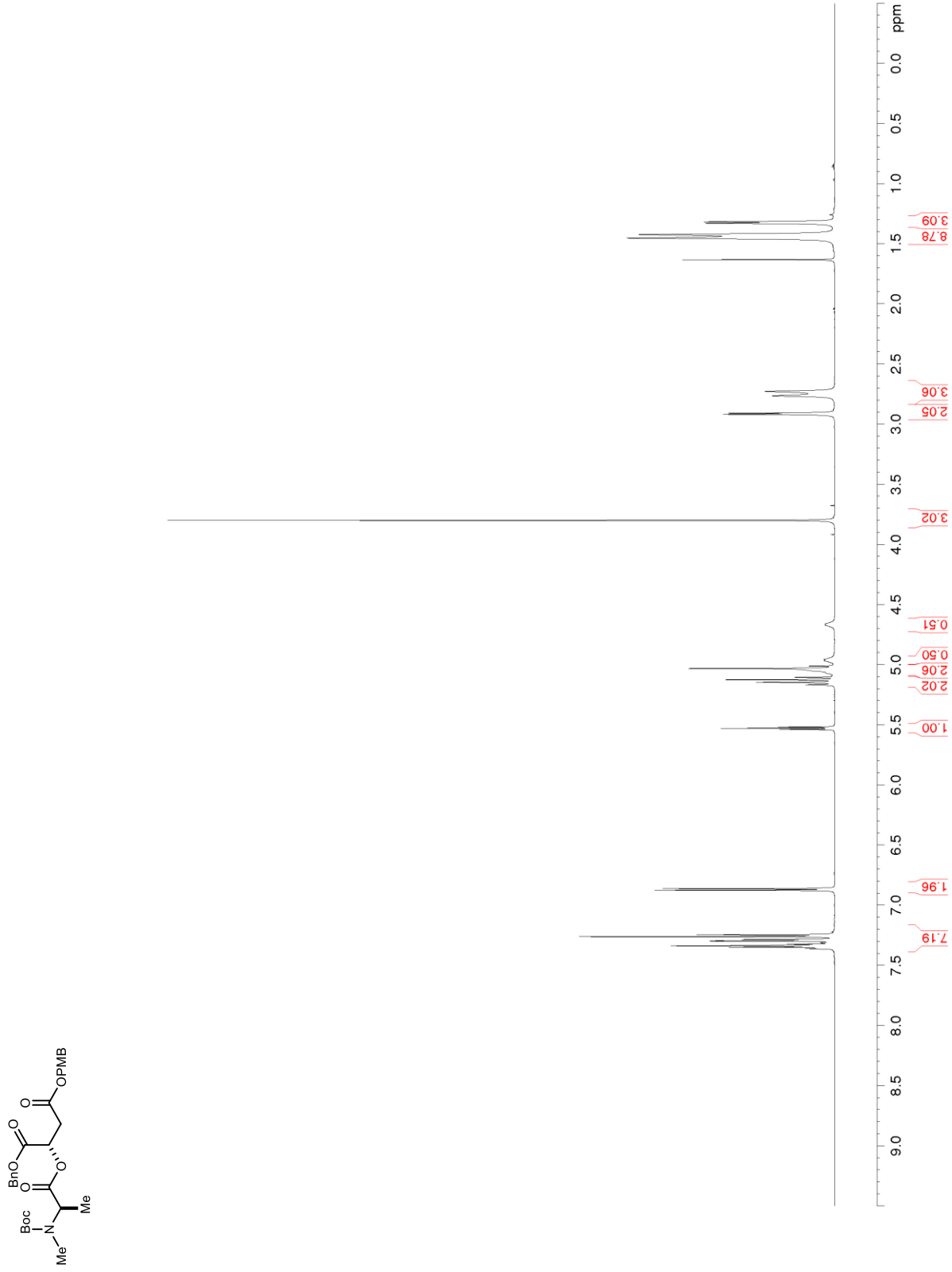

Figure S193. ^{13}C NMR/DEPT (125 MHz, $CDCl_3$) of **138**

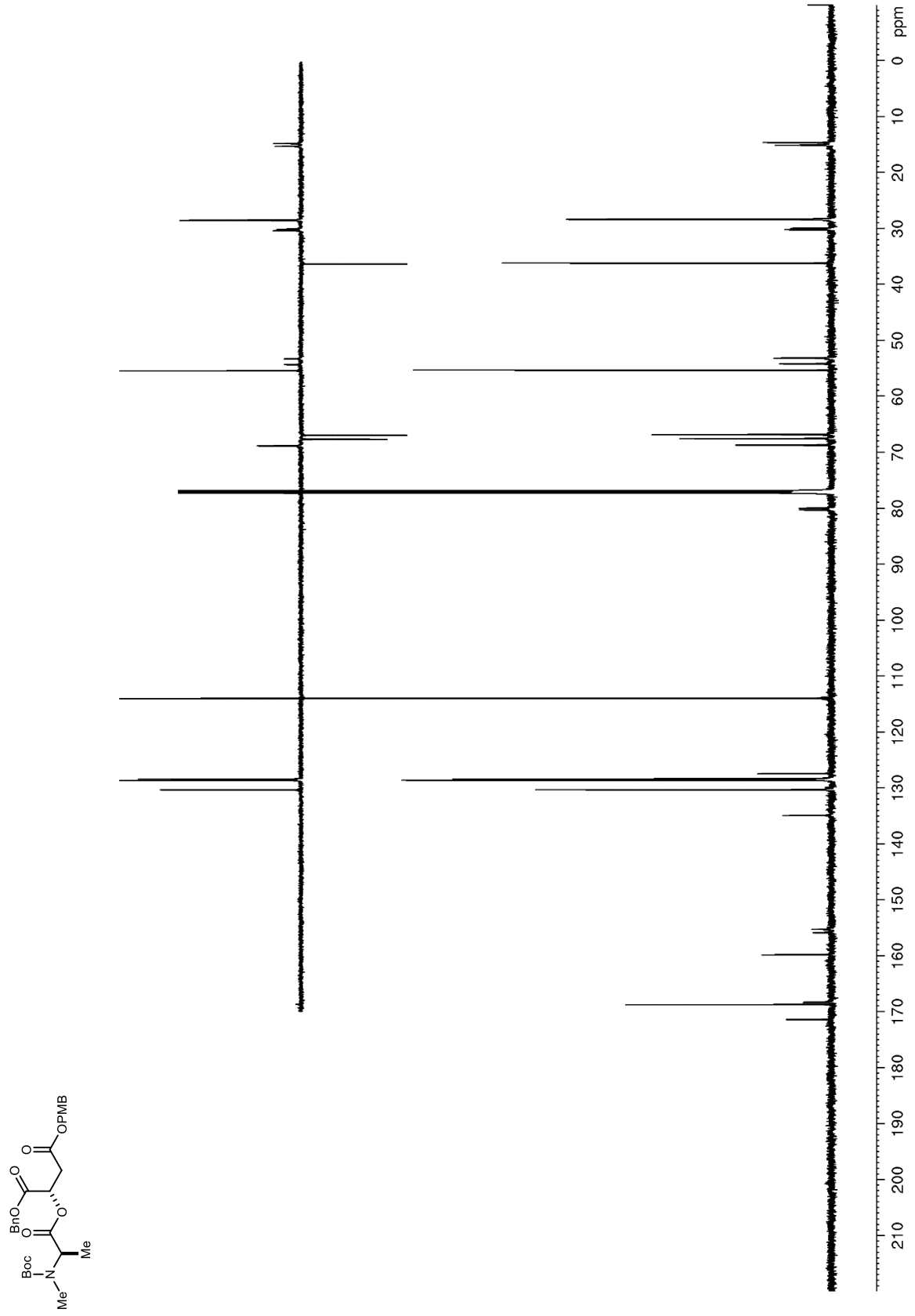

Figure S194. ^{1}H NMR (600 MHz, $CDCl_3$) of **140**

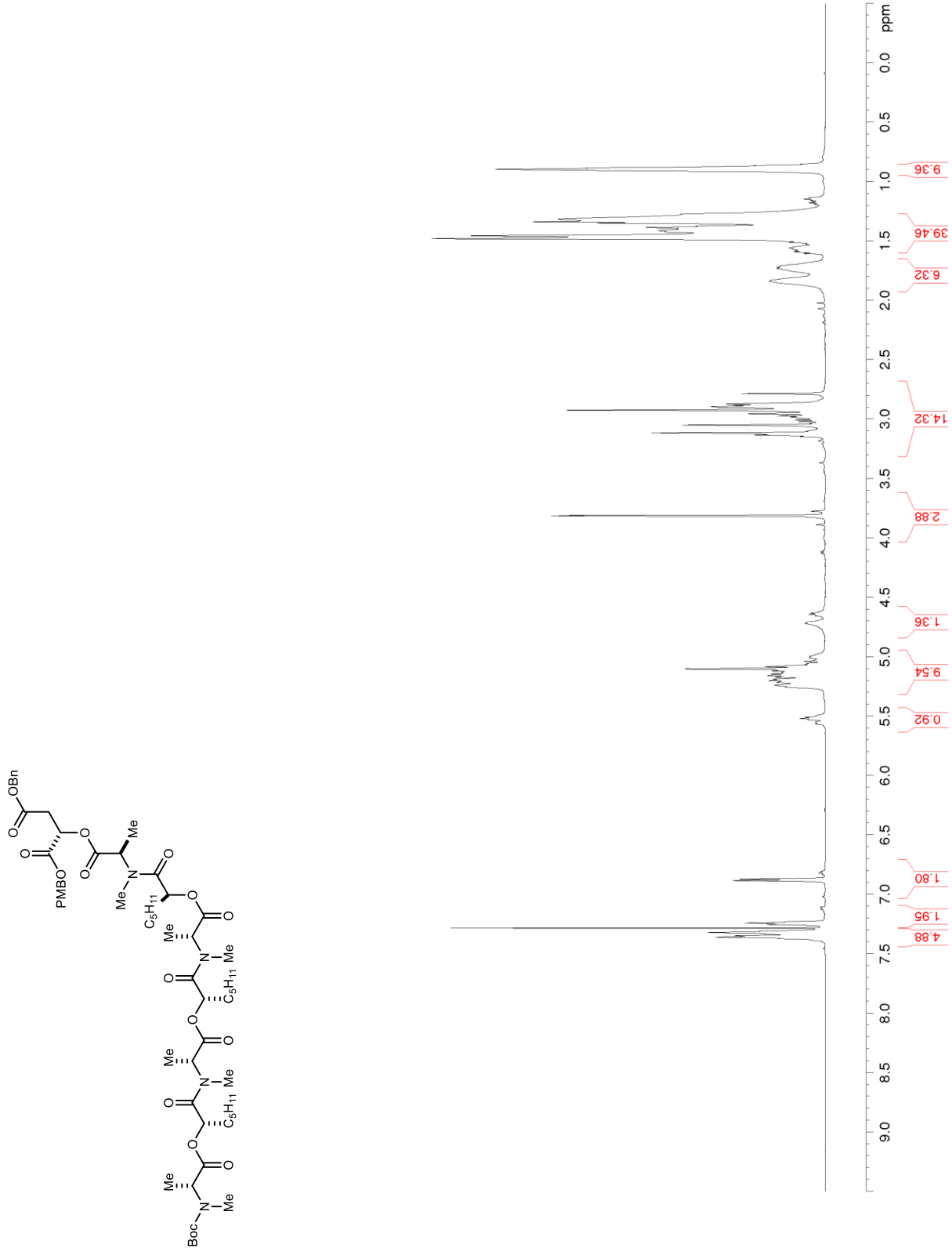

Figure S195. ^{13}C NMR/DEPT (150 MHz, $CDCl_3$) of **140**

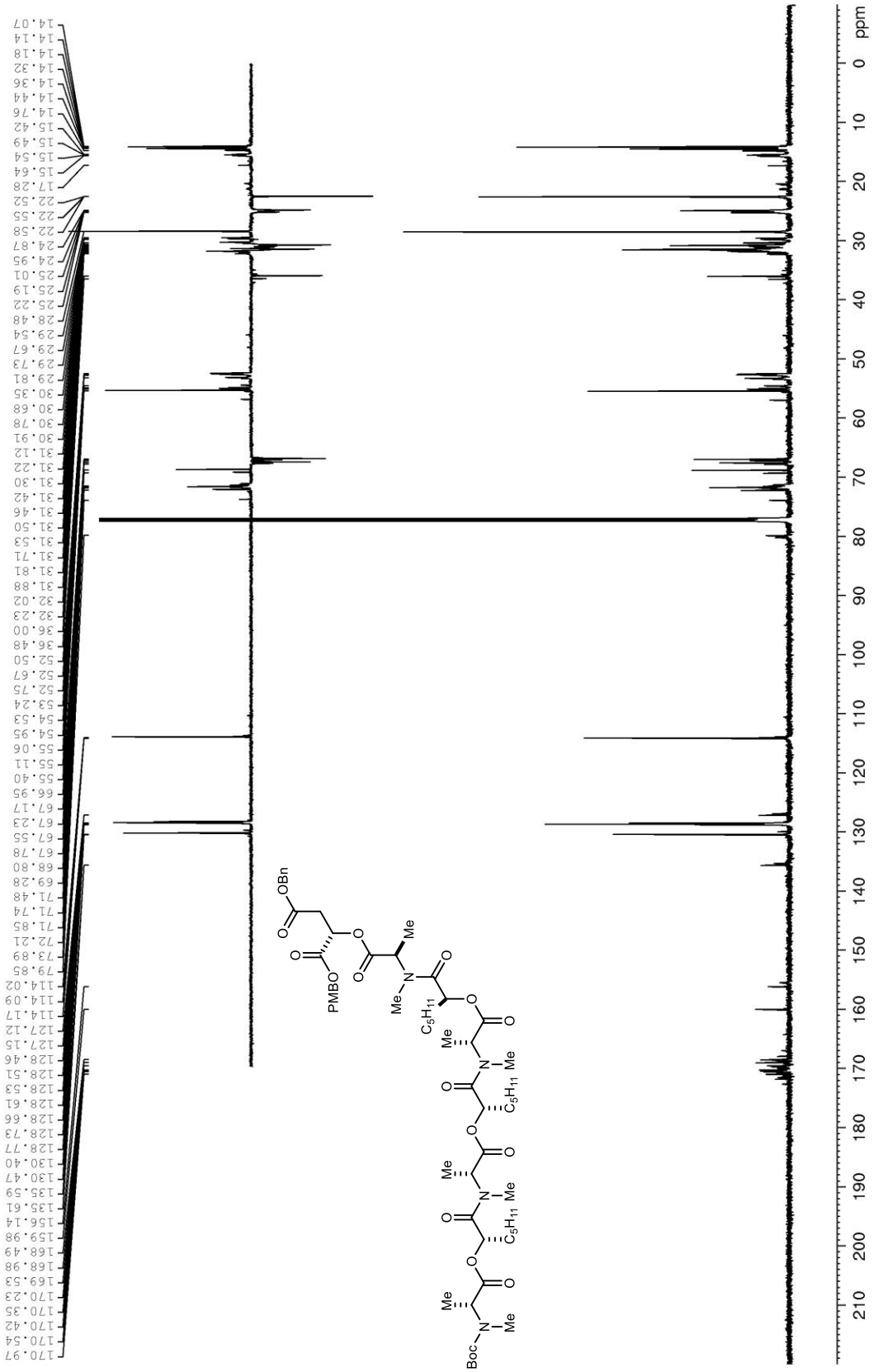

Figure S196. ^{1}H NMR (600 MHz, $CDCl_3$) of 1**41**

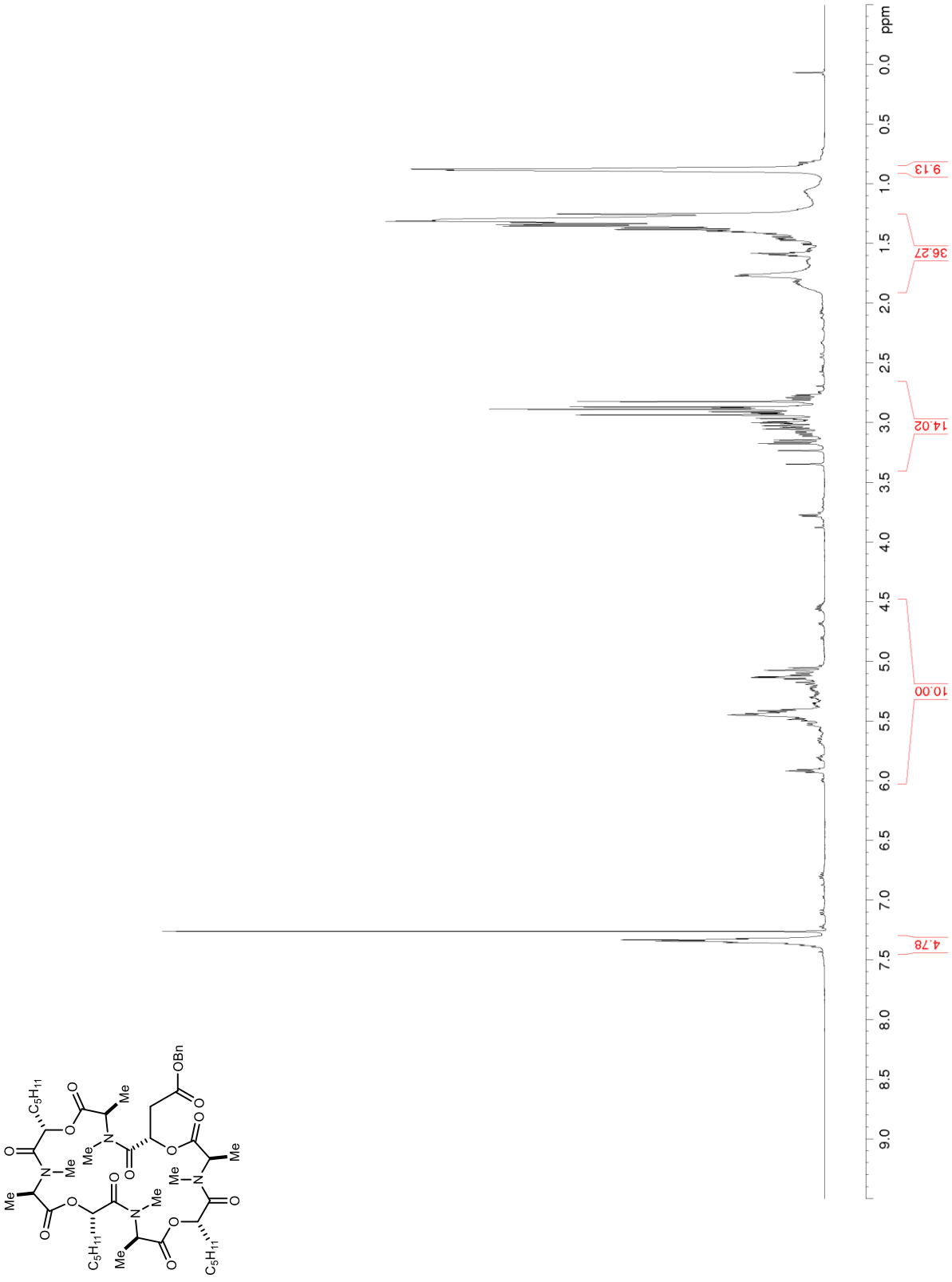

Figure S197. ^{13}C NMR/DEPT (150 MHz, $CDCl_3$) of **141**

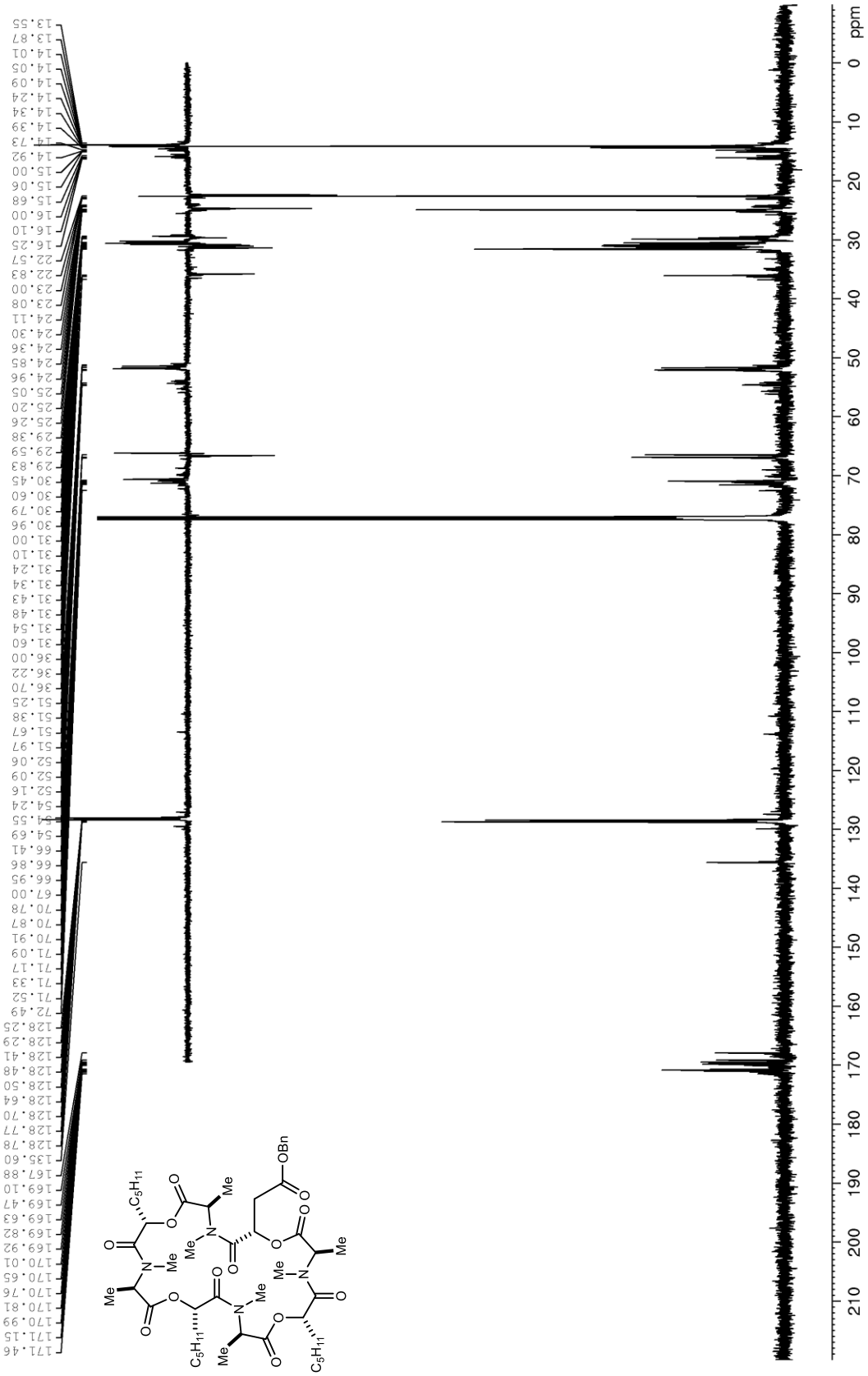

Figure S198. ^{1}H NMR (600 MHz, $CDCl_3$) of **79**

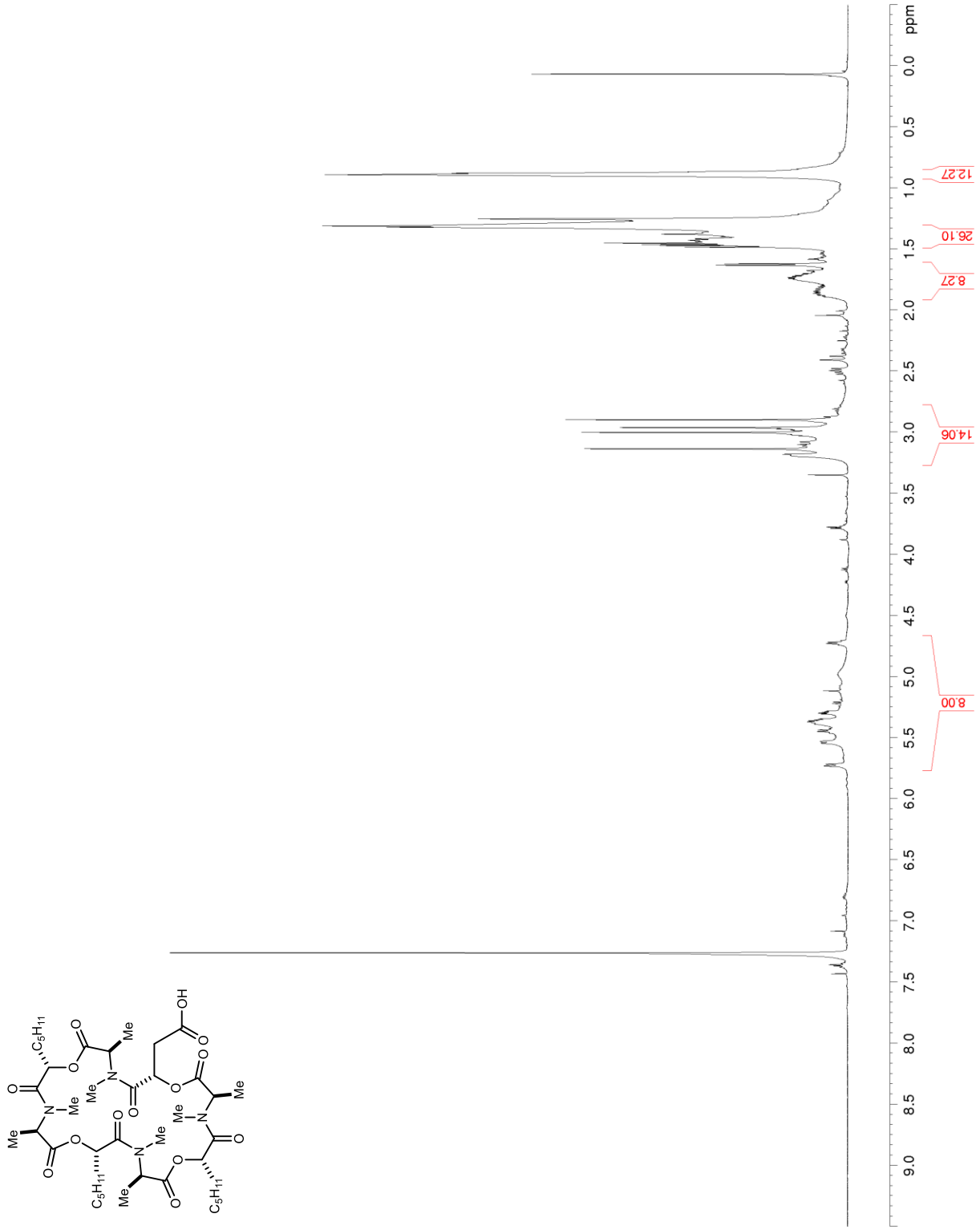

Figure S199. ^{13}C NMR/DEPT (150 MHz, $CDCl_3$) of **79**

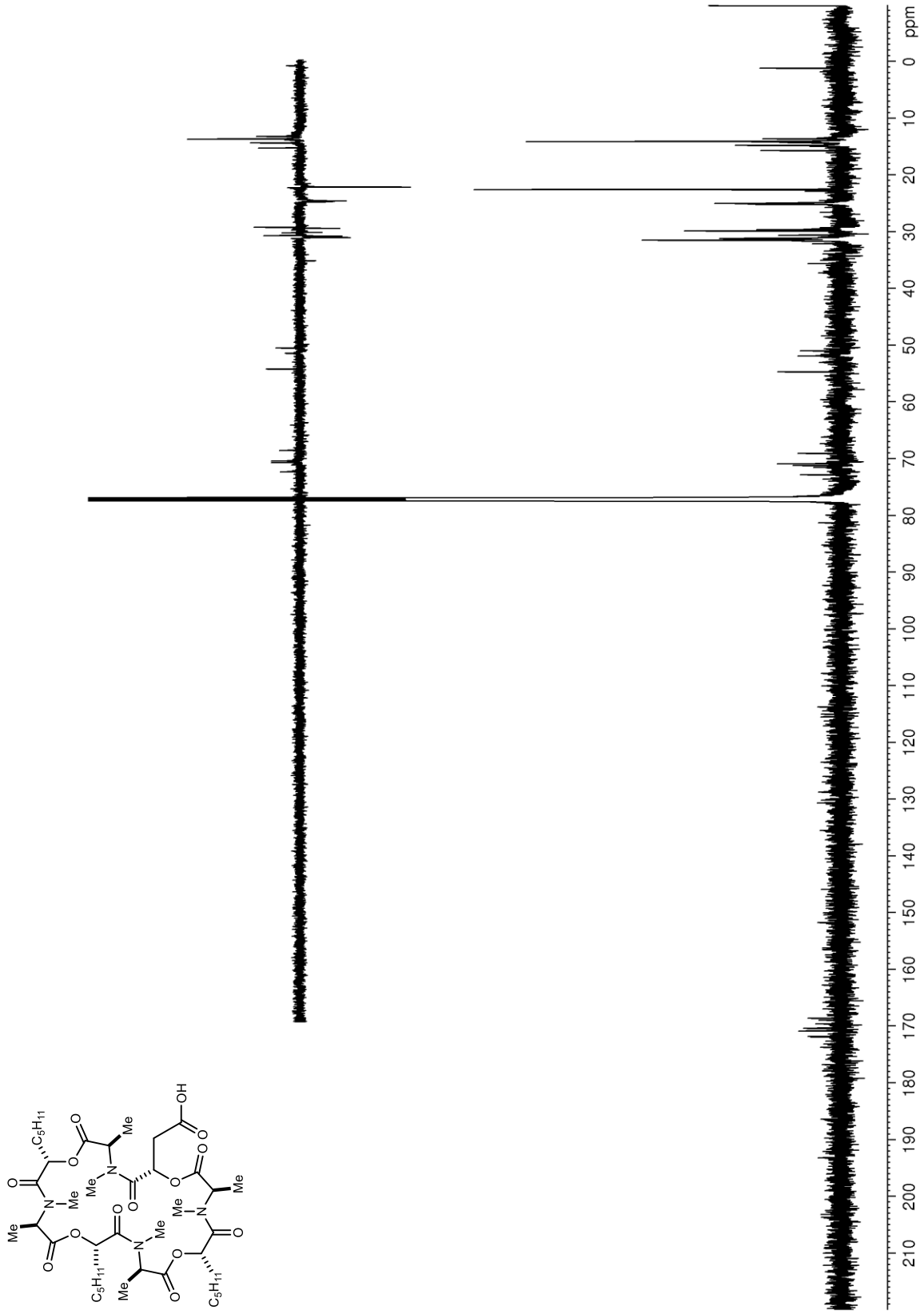

Figure S200. ^{1}H NMR (600 MHz, $CDCl_3$) of **S65**

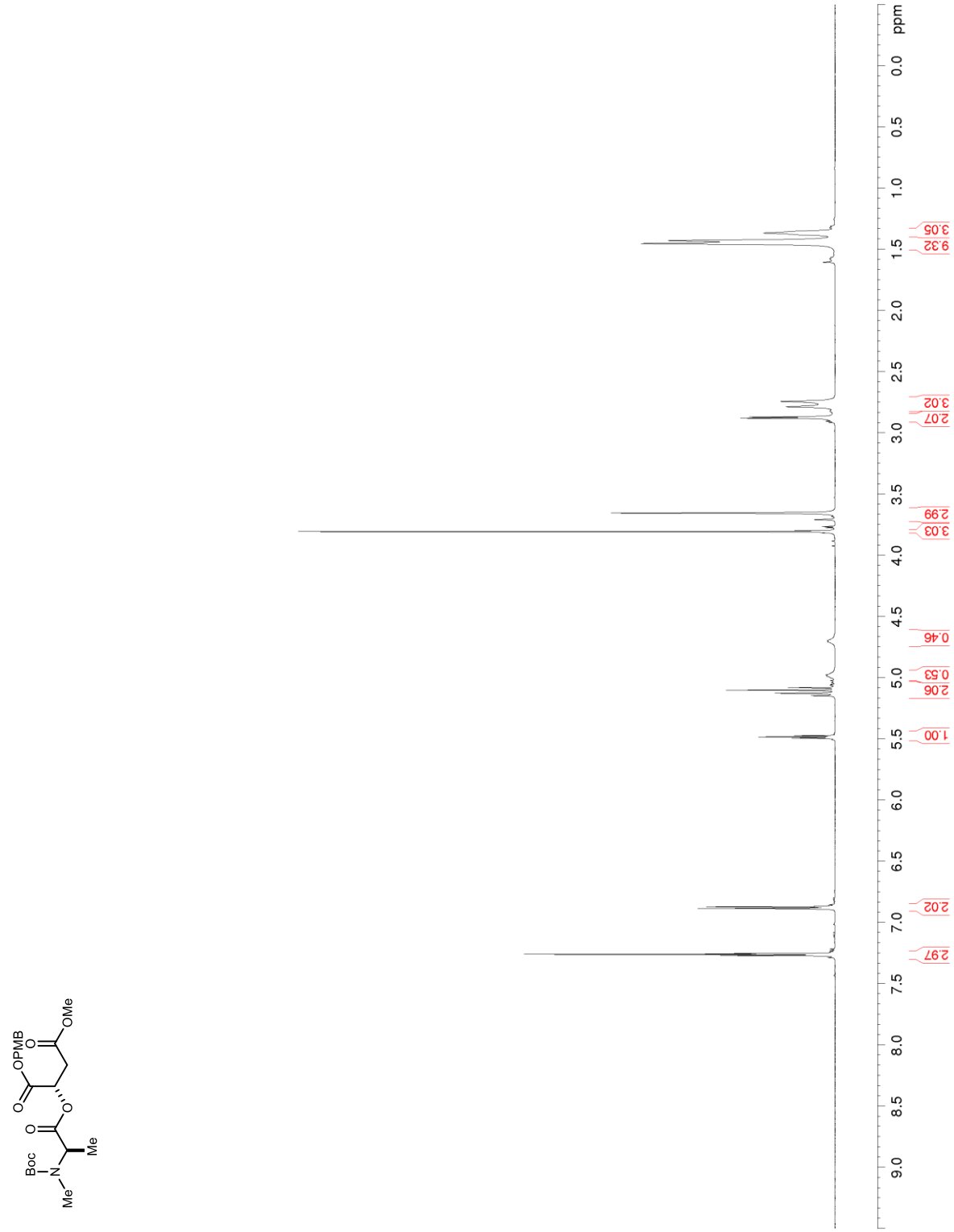

Figure S201. ^{13}C NMR/DEPT (150 MHz, $CDCl_3$) of **S65**

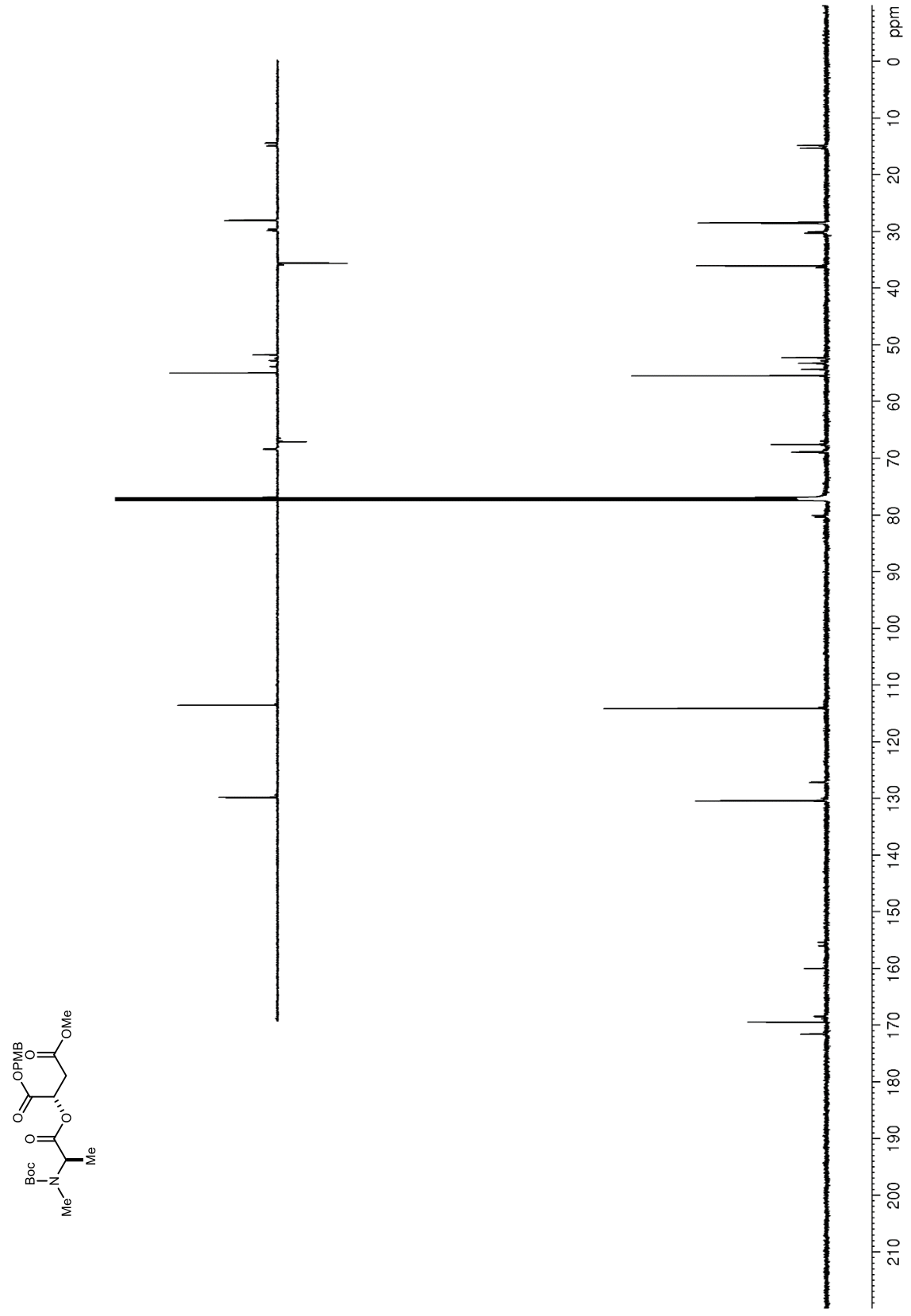

Figure S202. ^{1}H NMR (600 MHz, $CDCl_3$) of **91**

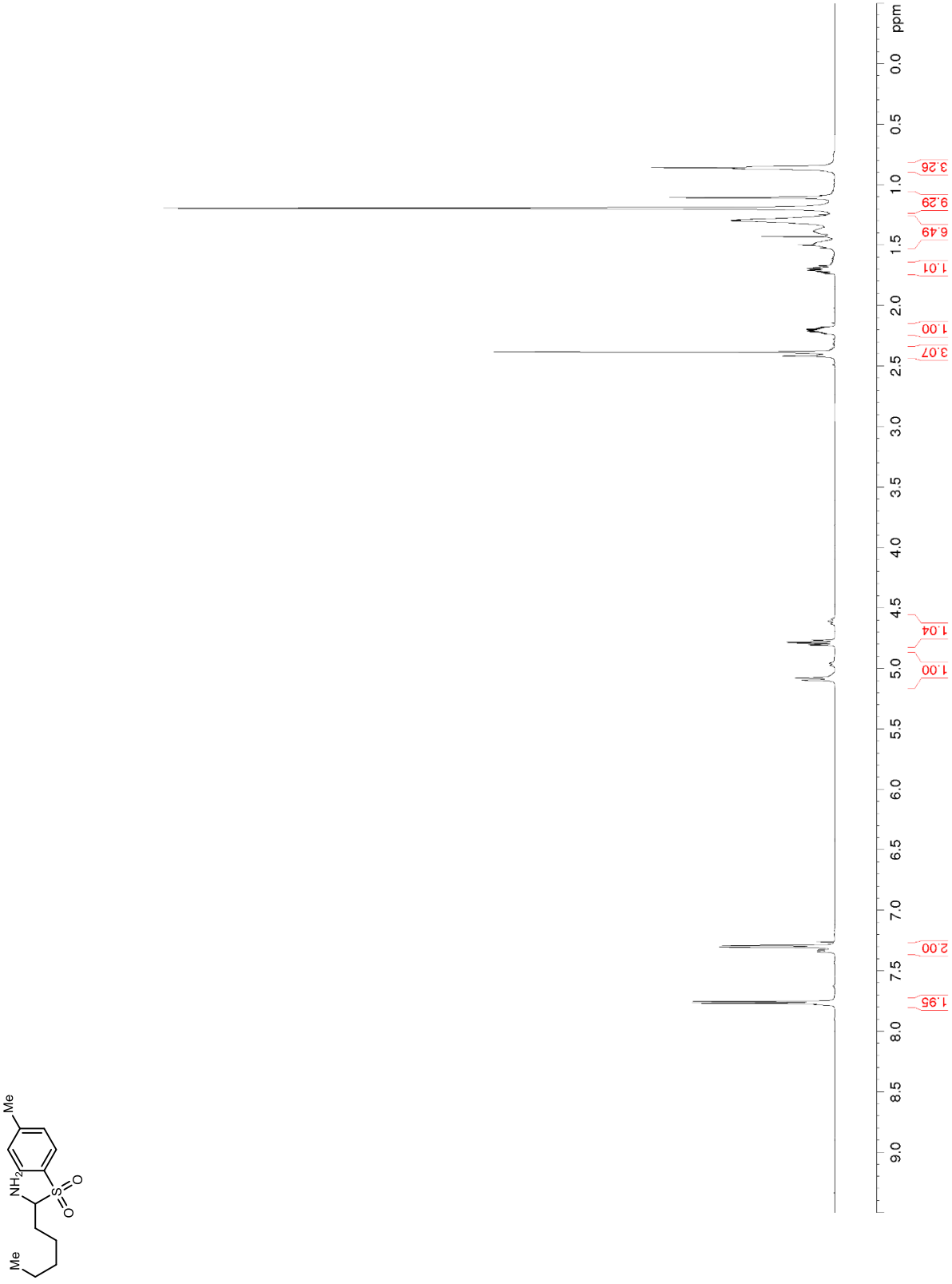

Figure S203. ^{13}C NMR/DEPT (150 MHz, $CDCl_3$) of **91**

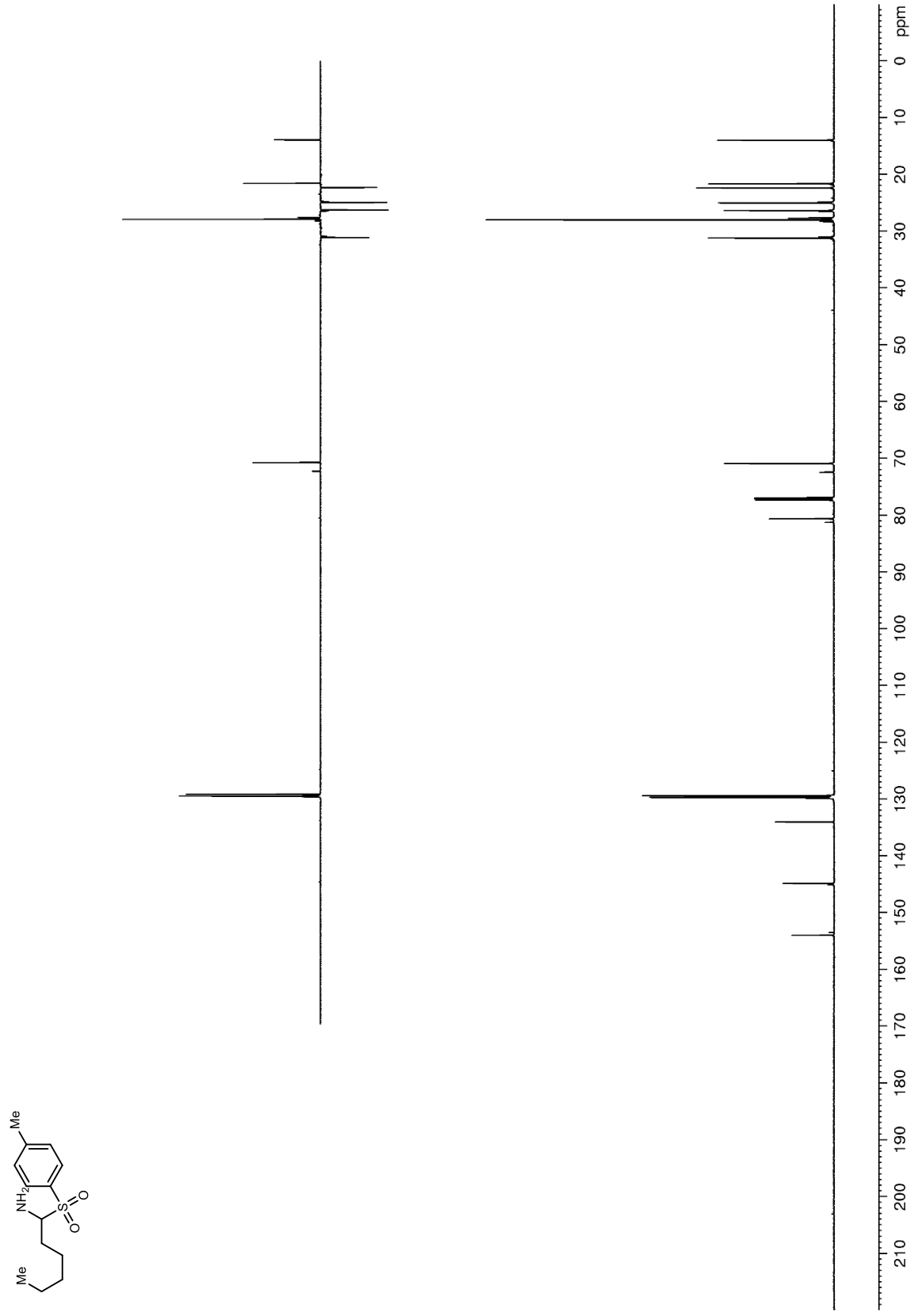

Figure S204. ^{1}H NMR (600 MHz, $CDCl_3$) of **93**

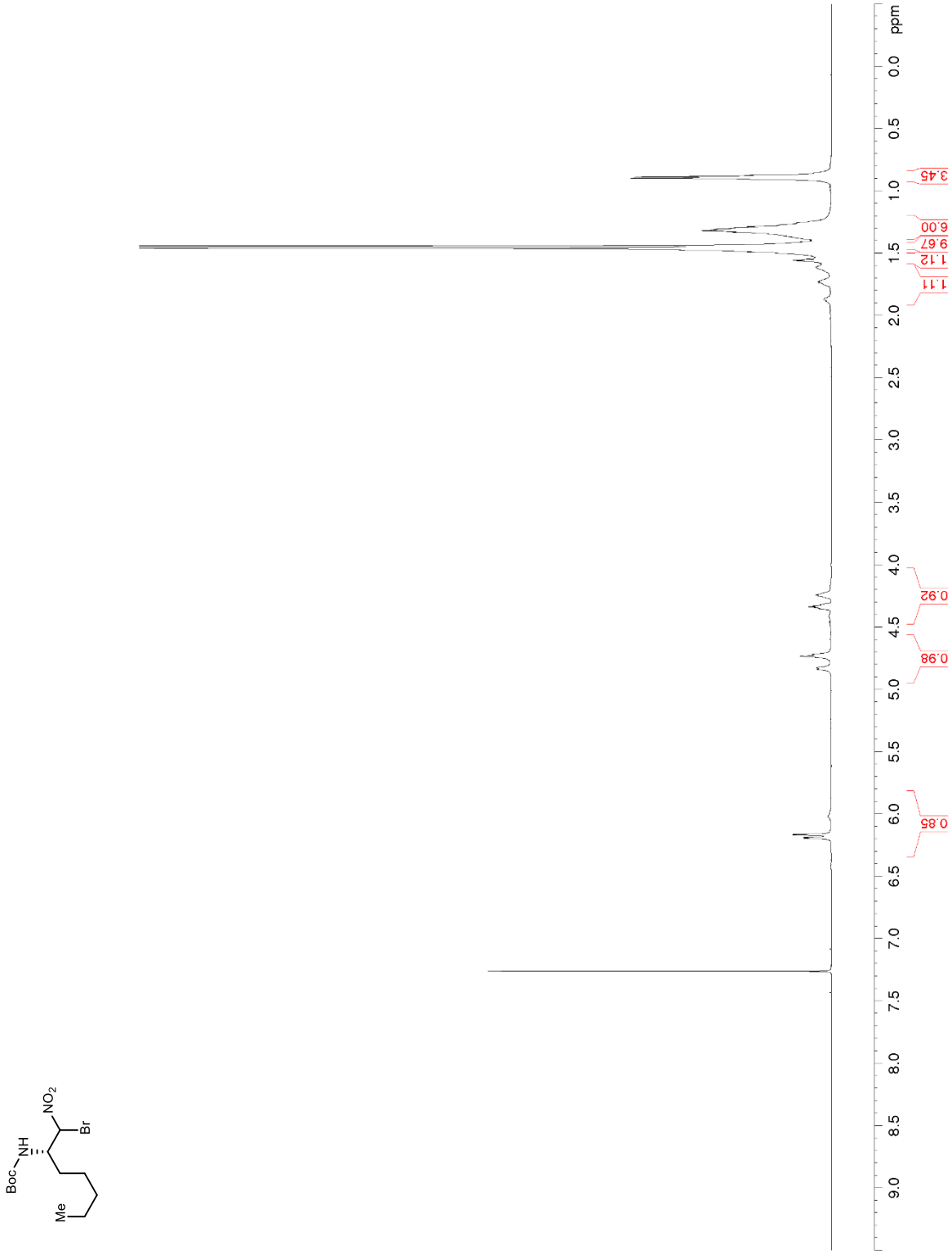

Figure S205. ^{13}C NMR/DEPT (150 MHz, $CDCl_3$) of **93**

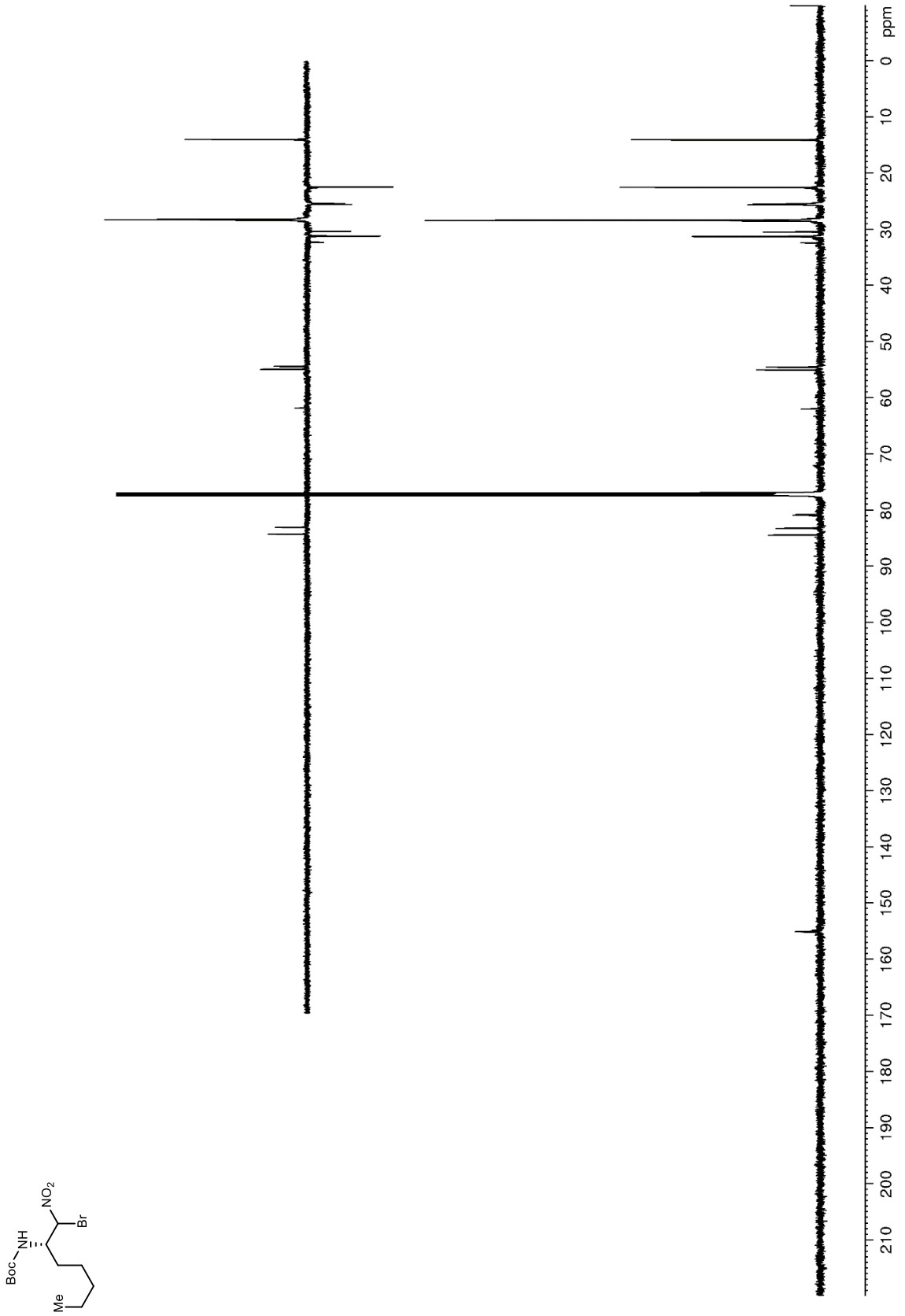

Figure S206. ^{1}H NMR (400 MHz, $CDCl_3$) of **95**

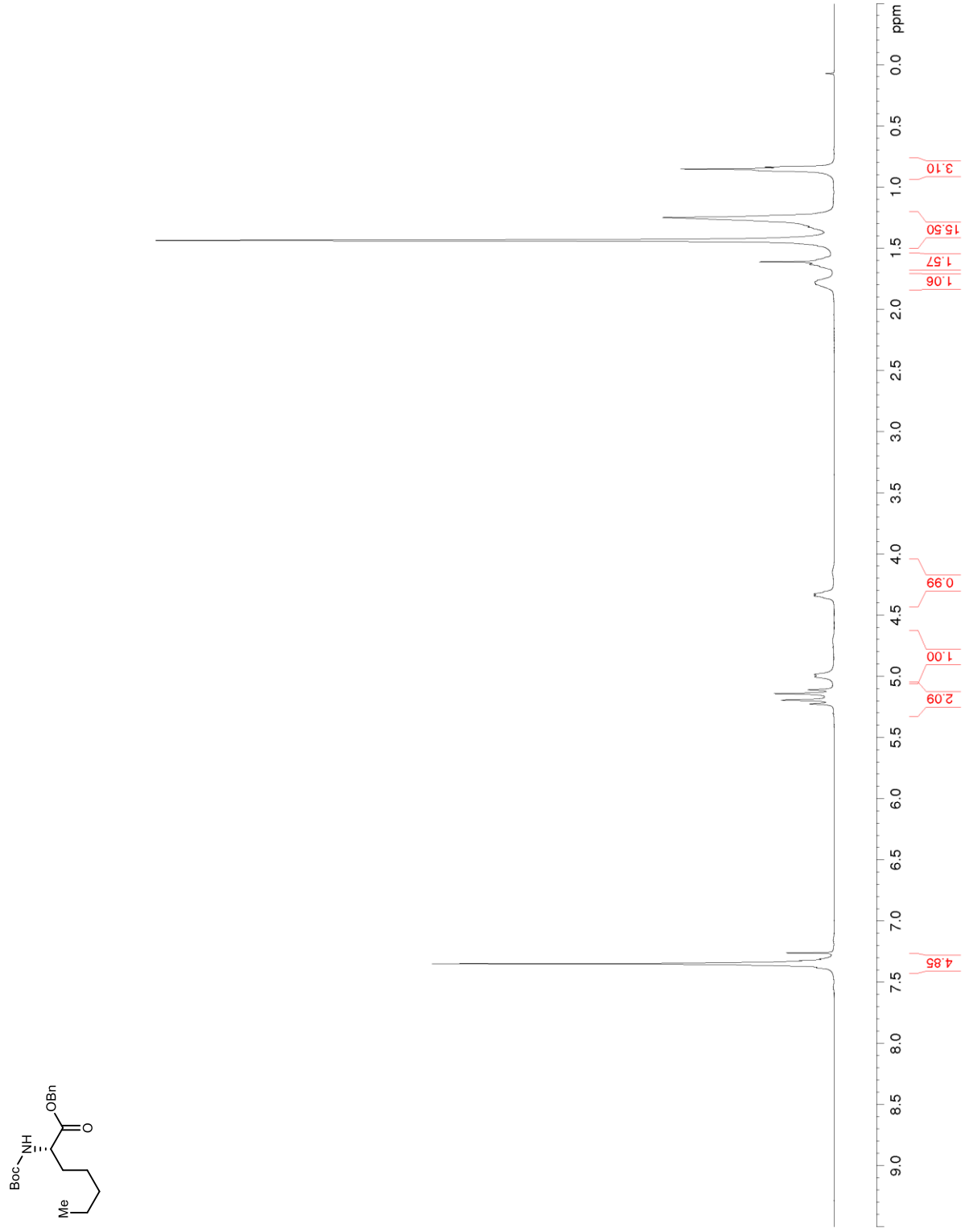

Figure S207. ^{13}C NMR/DEPT (100 MHz, $CDCl_3$) of **95**

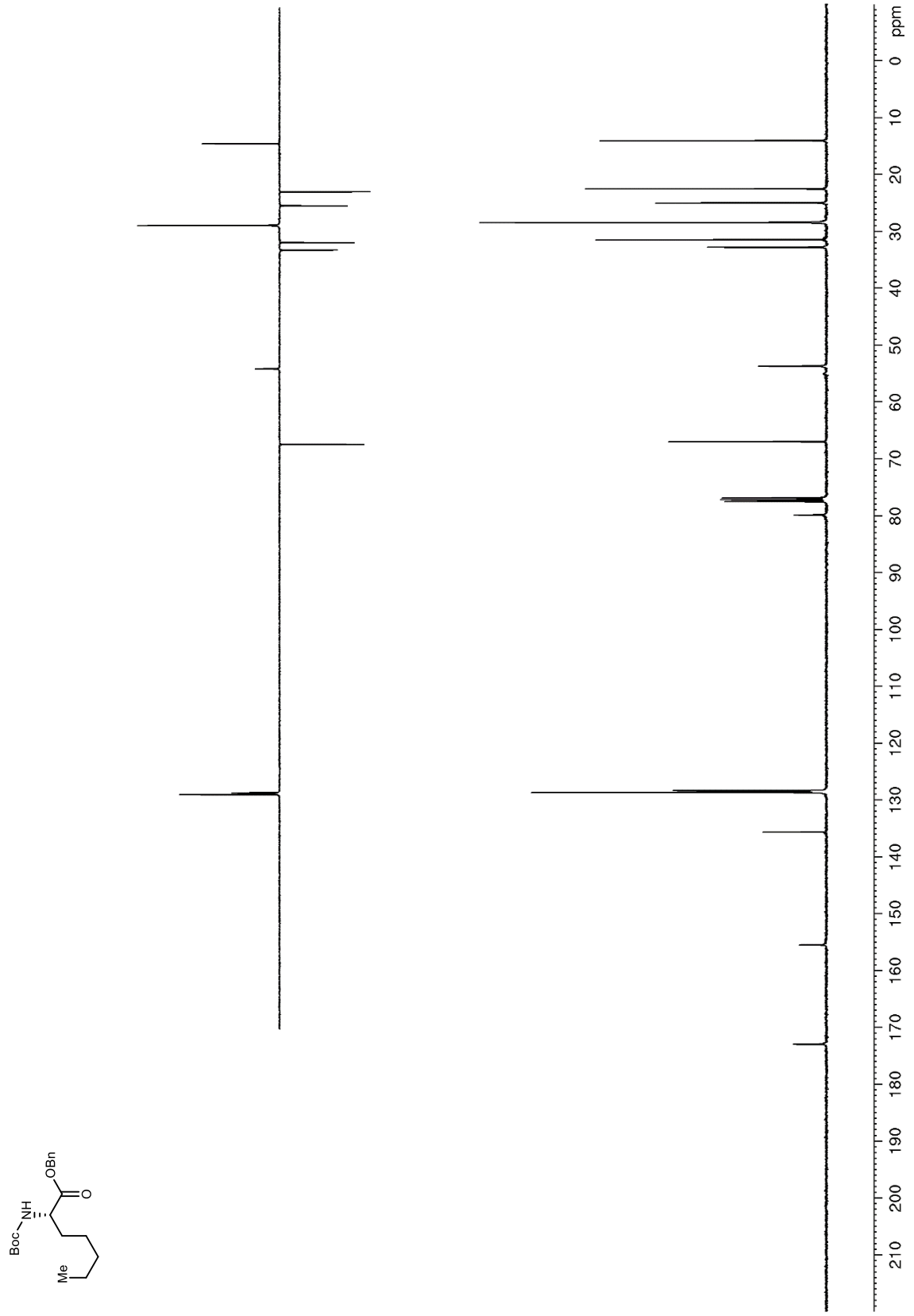

Figure S208. ^{1}H NMR (600 MHz, $CDCl_3$) of **96**

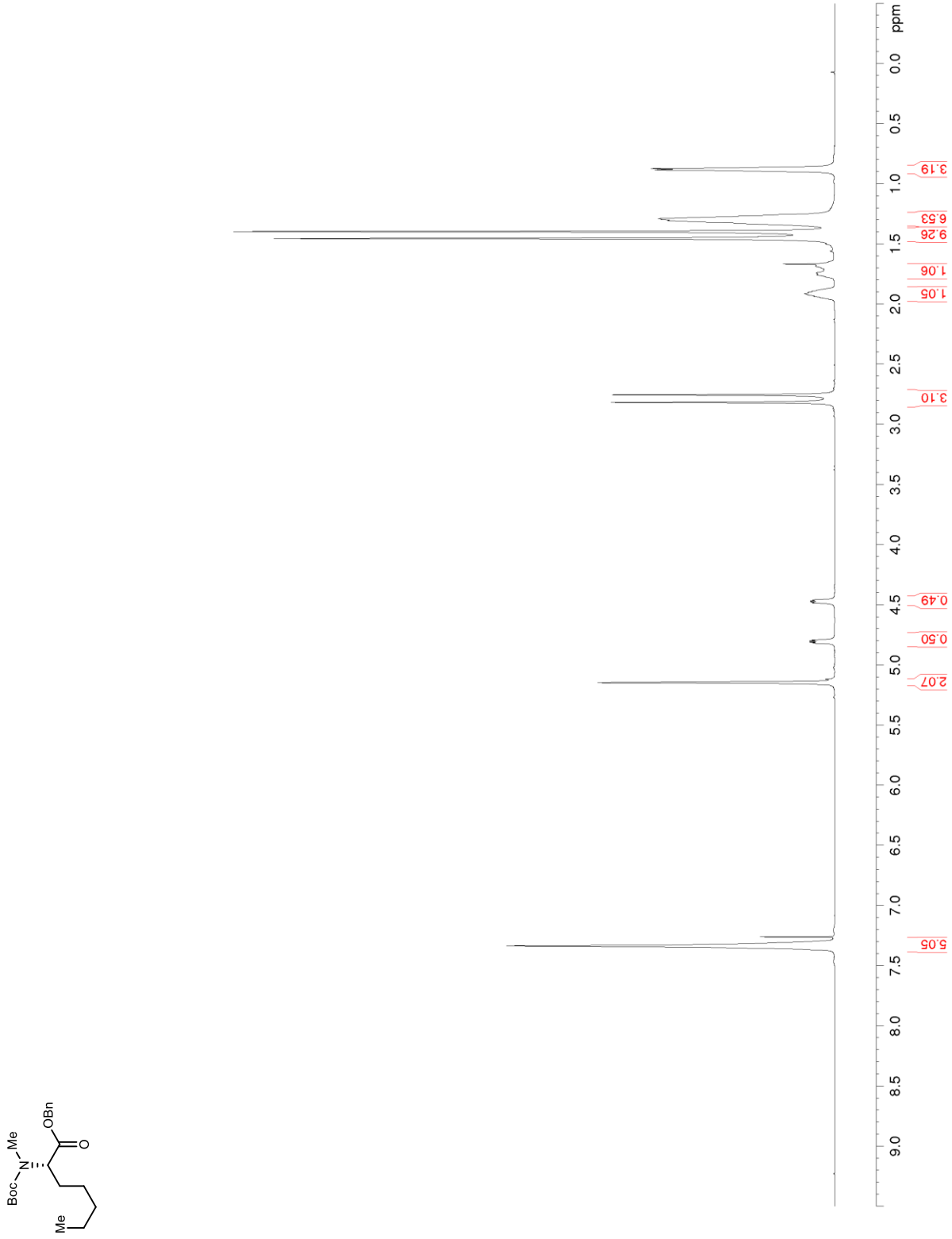

Figure S209. ^{13}C NMR/DEPT (150 MHz, $CDCl_3$) of **96**

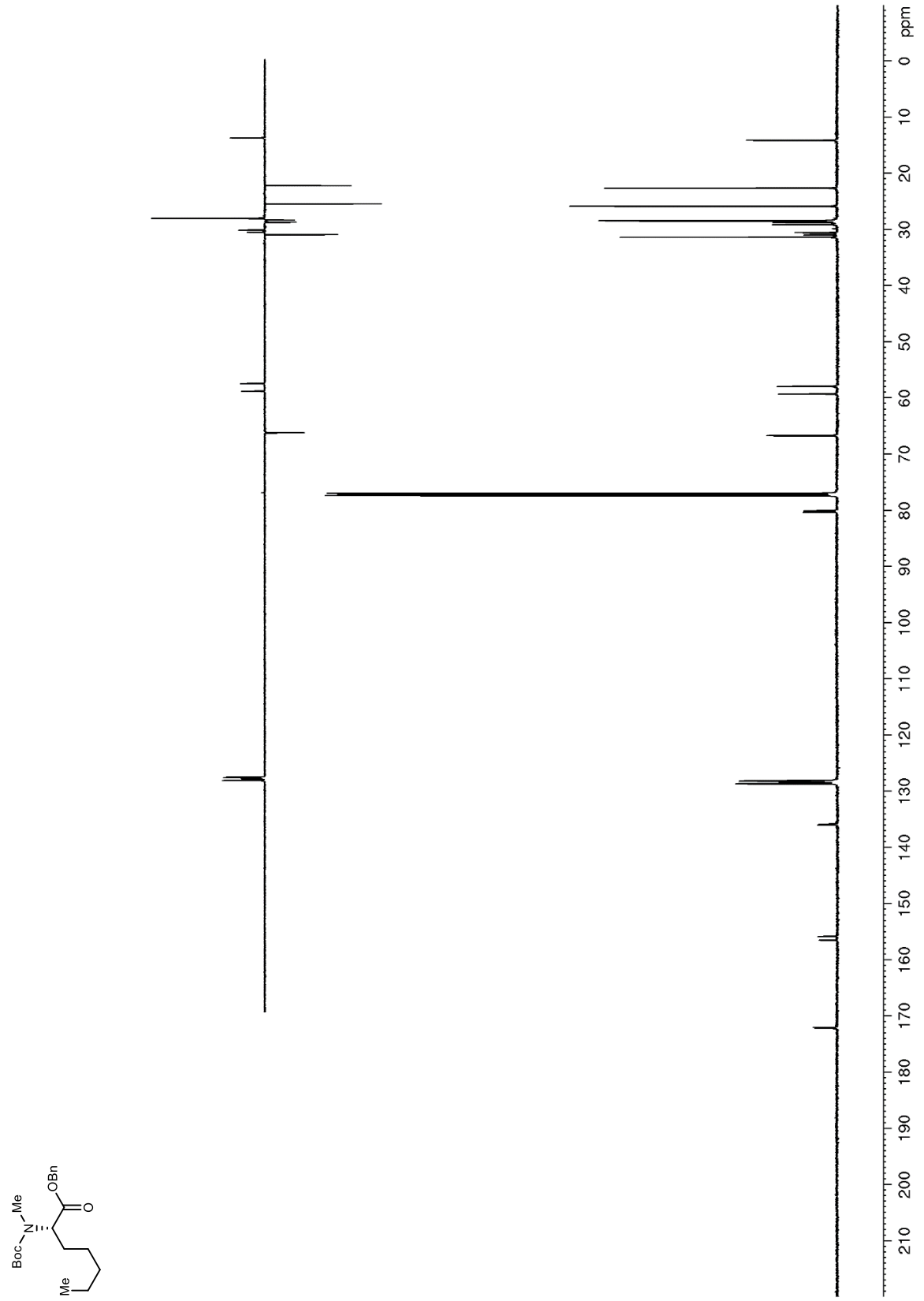

Figure S210. ^{1}H NMR (600 MHz, $CDCl_3$) of **100**

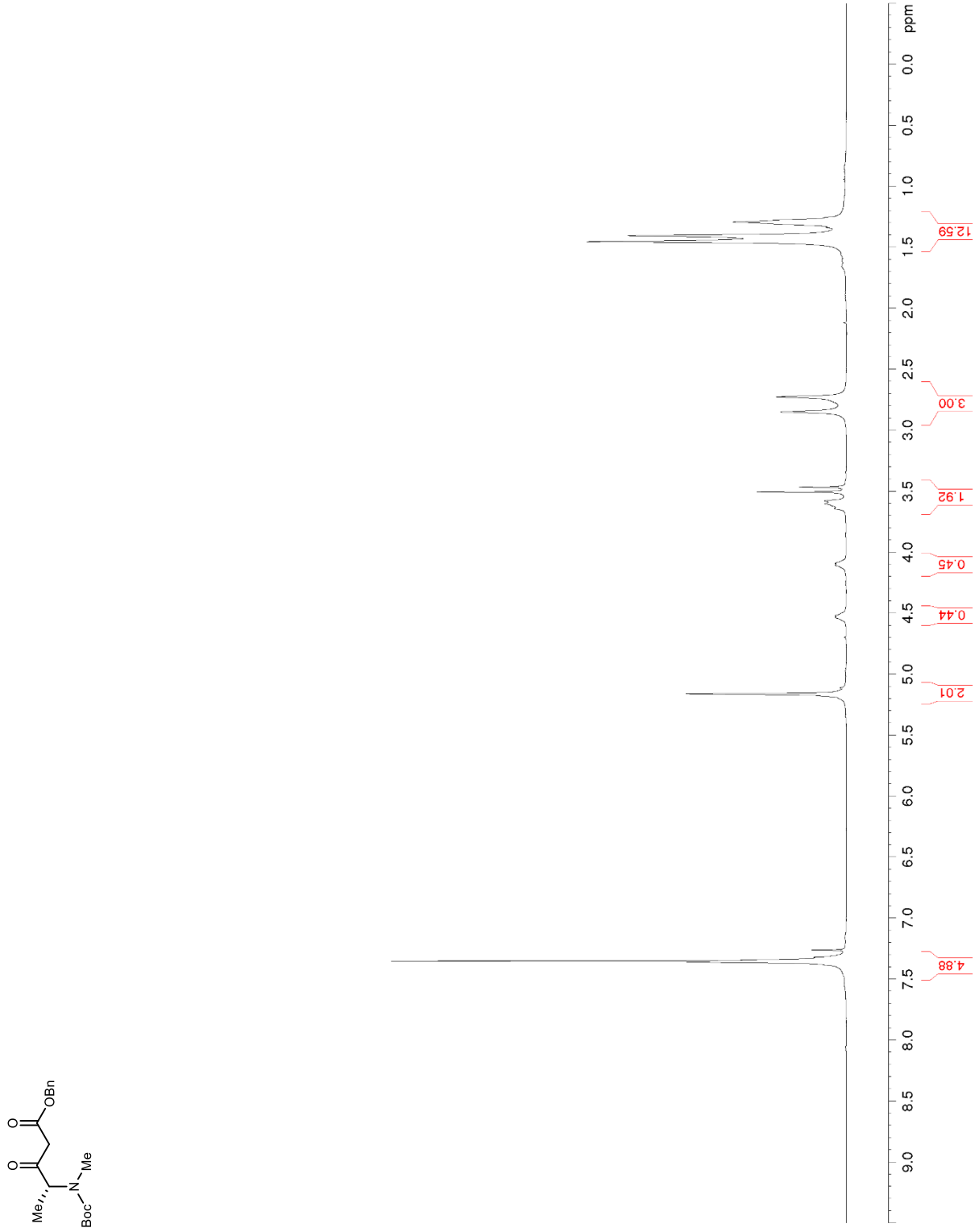

Figure S211. ^{13}C NMR/DEPT (150 MHz, $CDCl_3$) of **100**

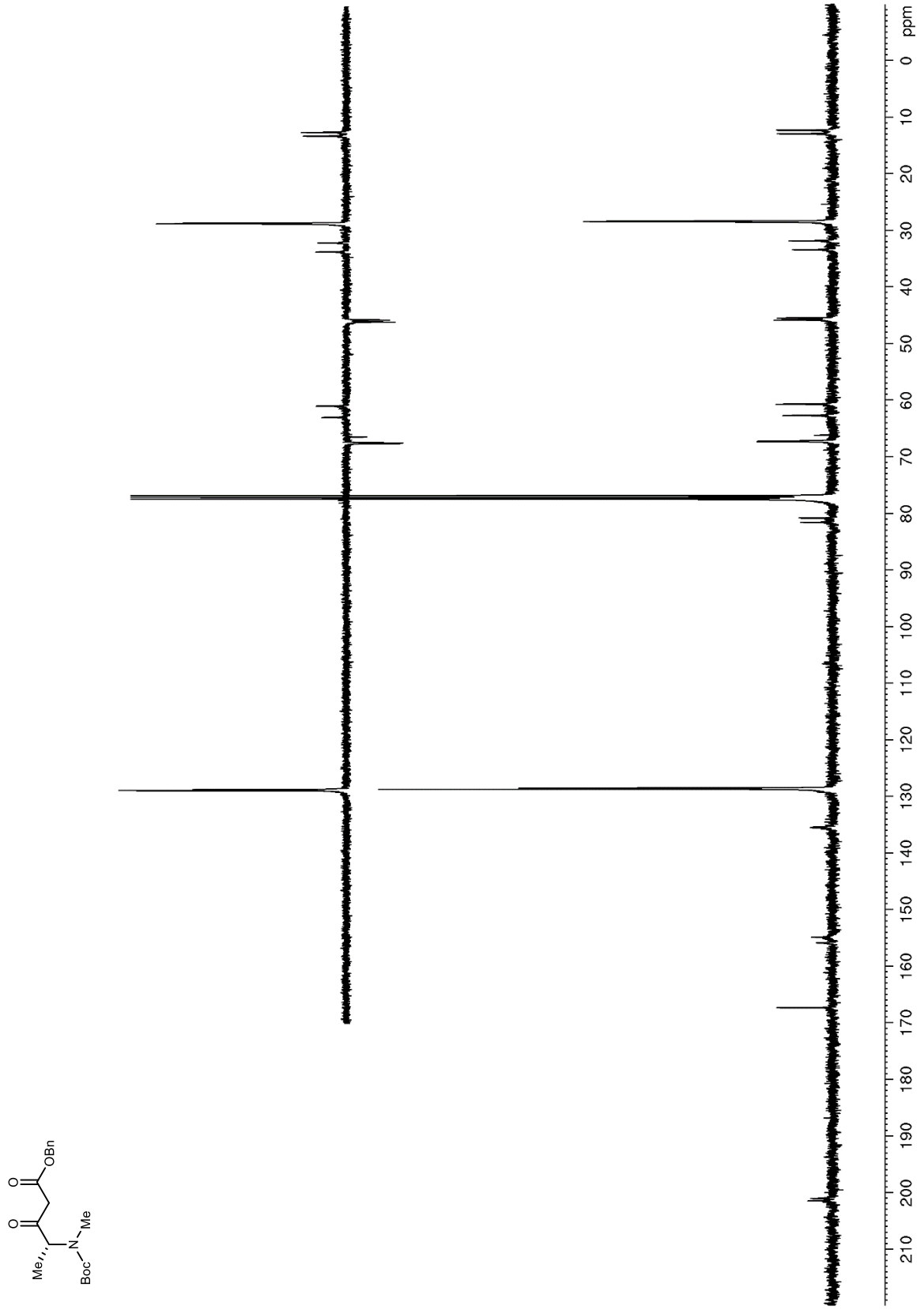

Figure S212. ^{1}H NMR (600 MHz, $CDCl_3$) of **104**

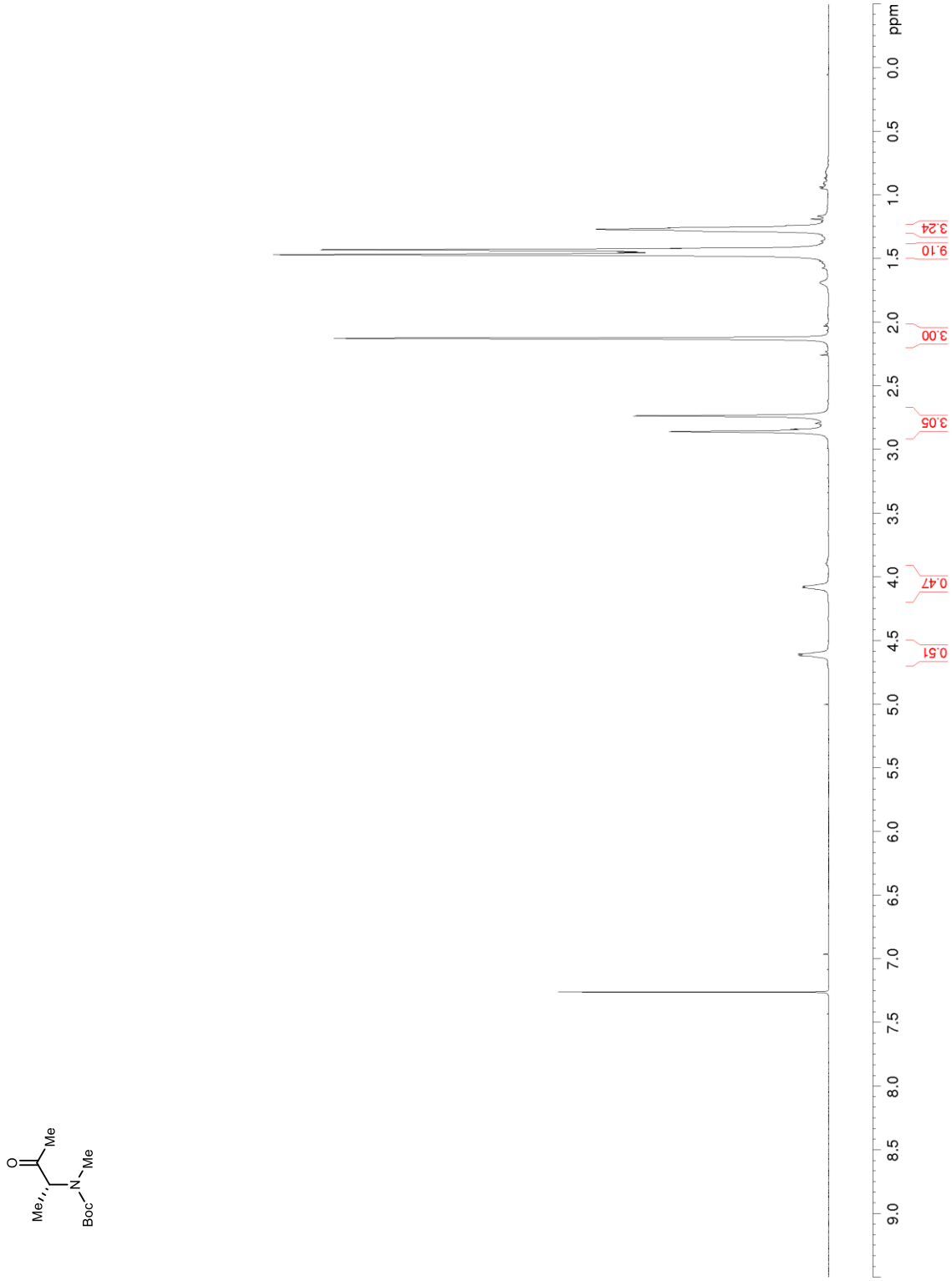

Figure S213. ^{13}C NMR/DEPT (150 MHz, $CDCl_3$) of **104**

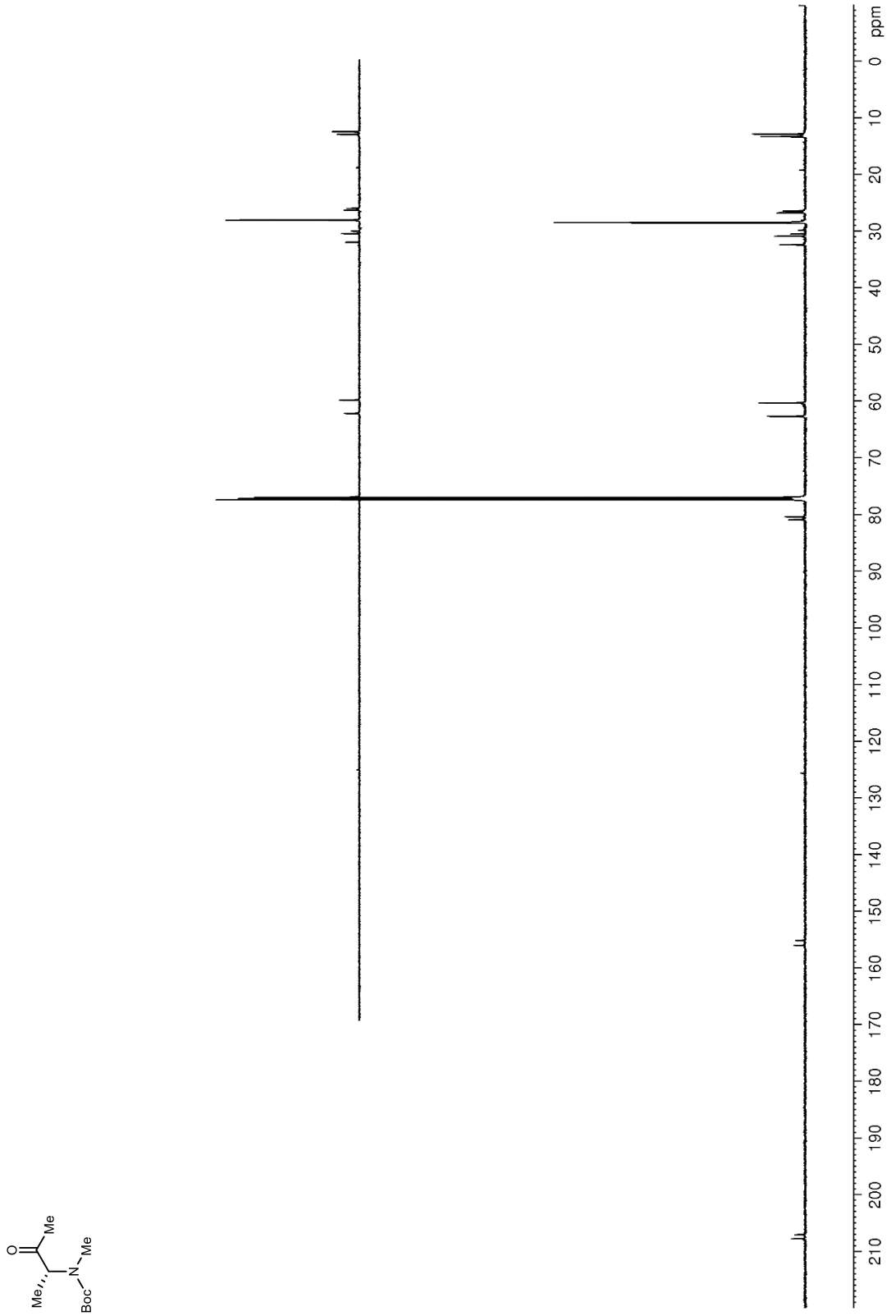

Figure S214. ^{1}H NMR (400 MHz, $CDCl_3$) of **103**

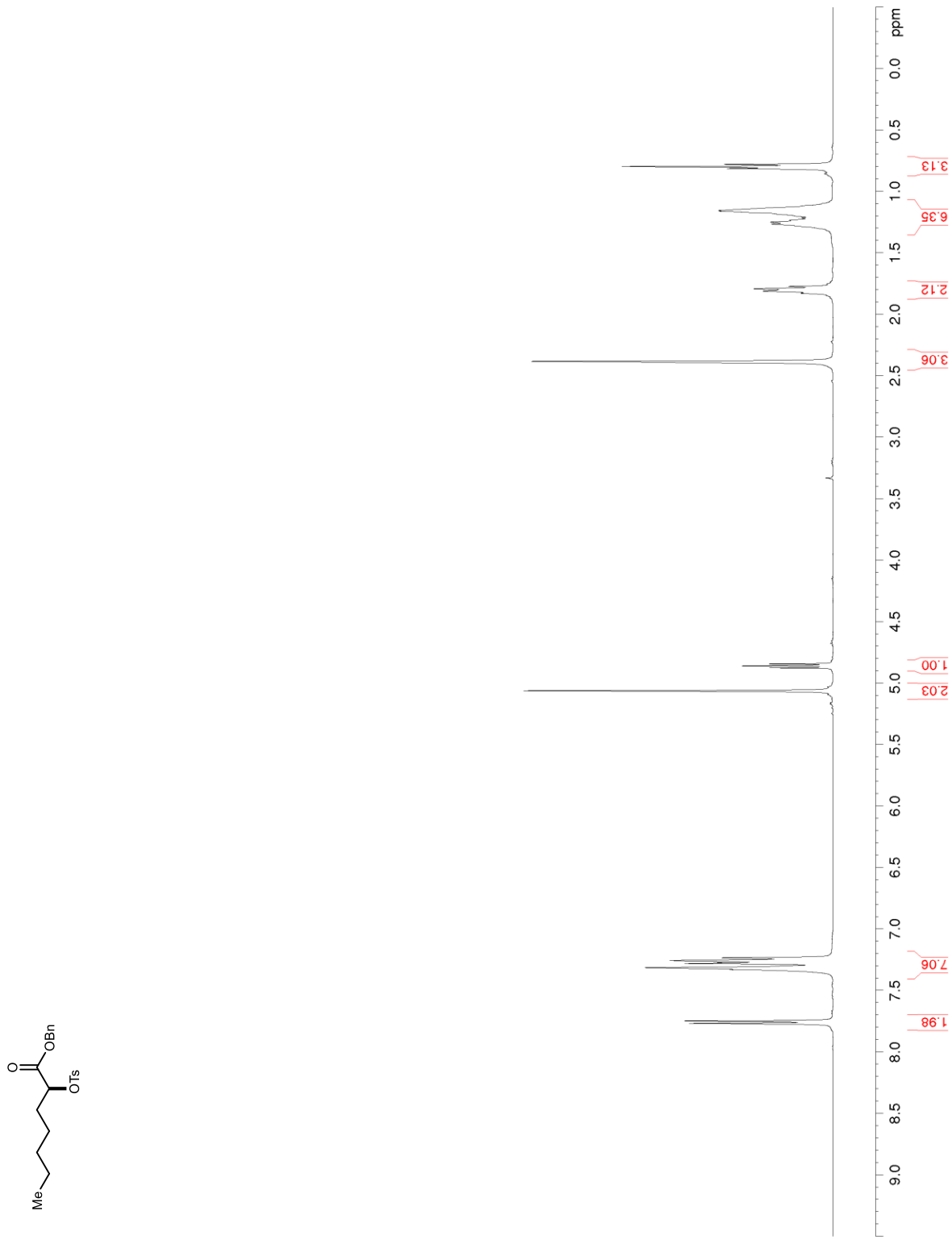

Figure S215. ^{13}C NMR/DEPT (100 MHz, $CDCl_3$) of **103**

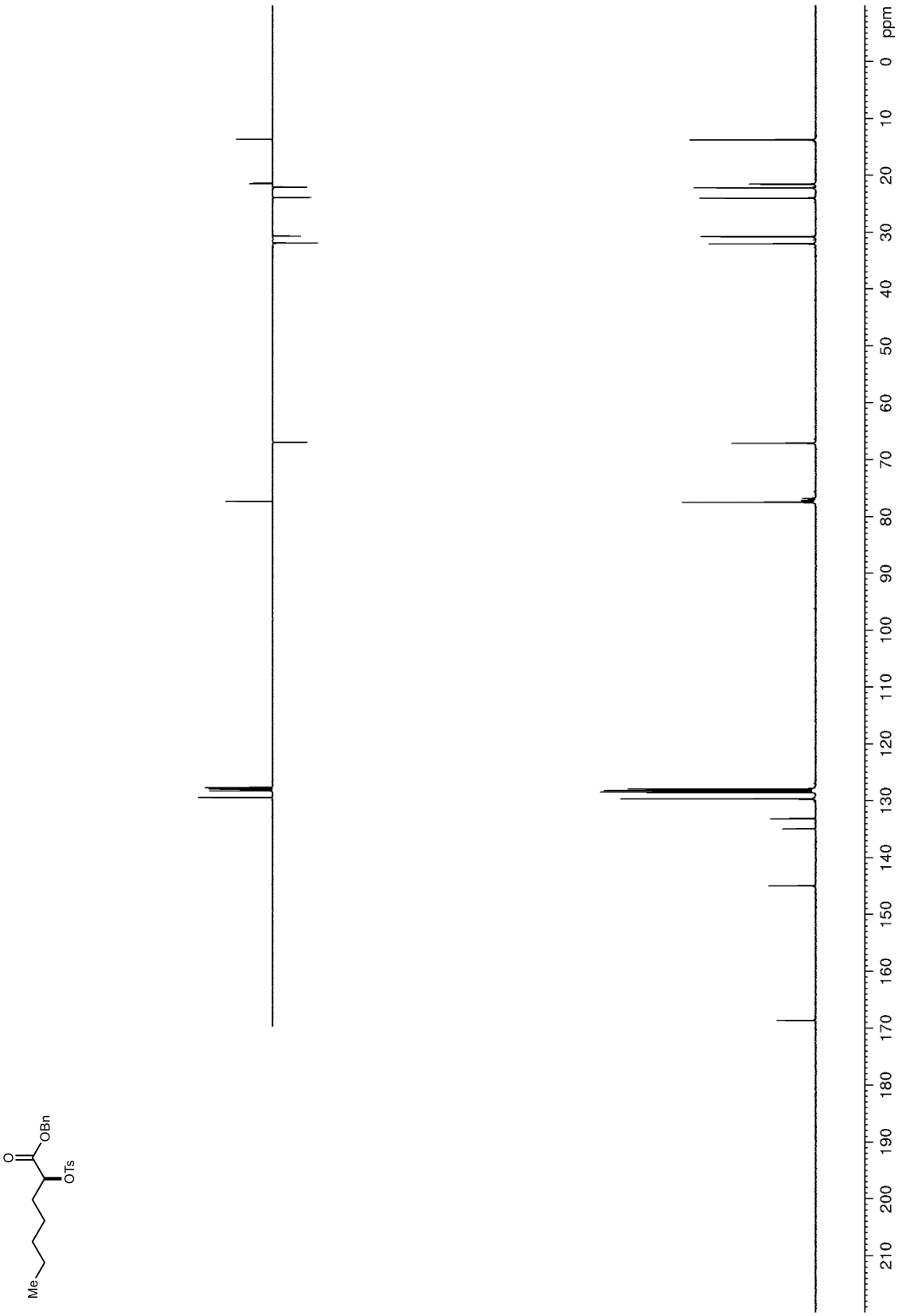

Figure S216. ^{1}H NMR (400 MHz, $CDCl_3$) of **107**

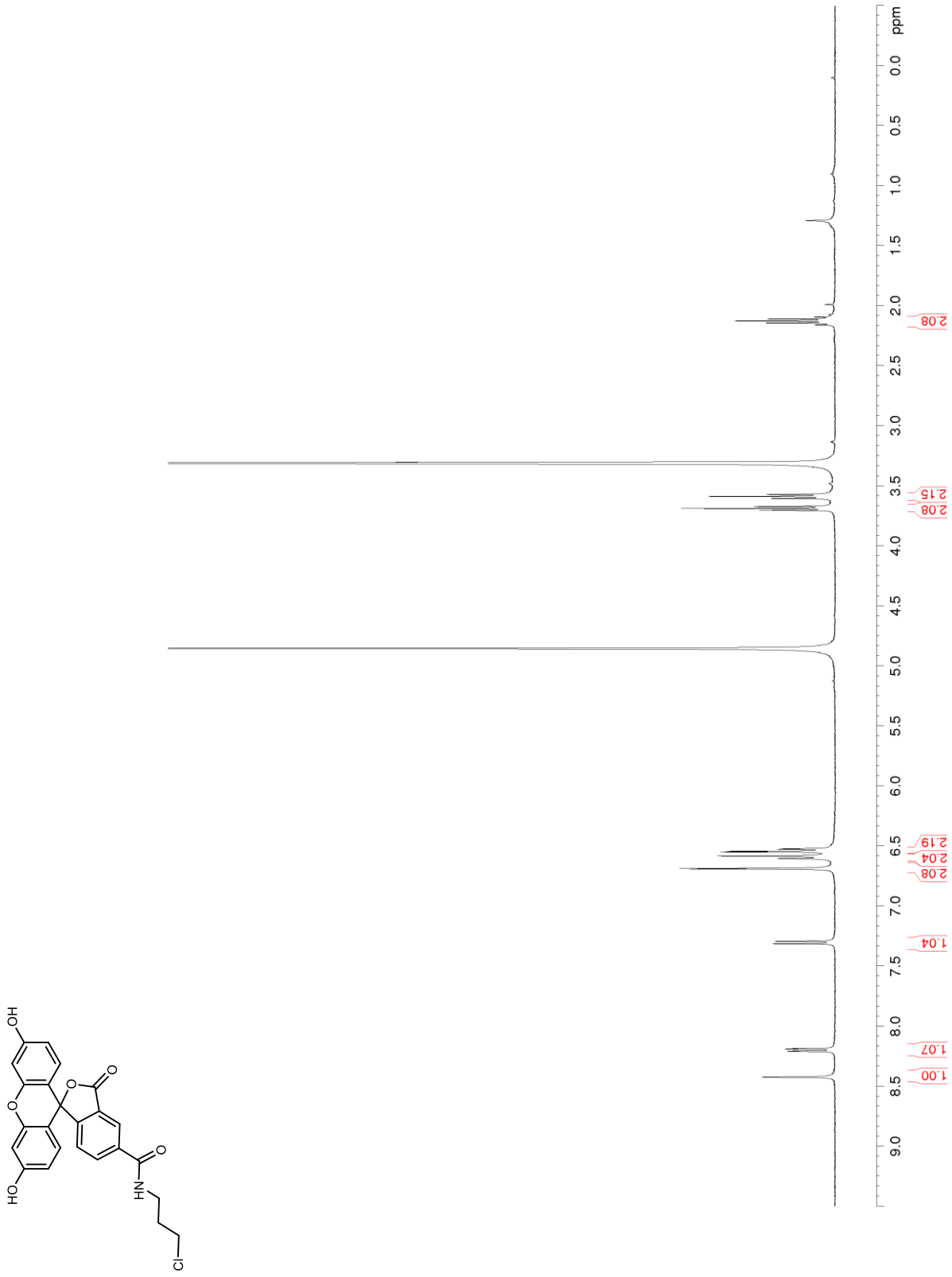

Figure S217. ^{13}C NMR/DEPT (100 MHz, $CDCl_3$) of **107**

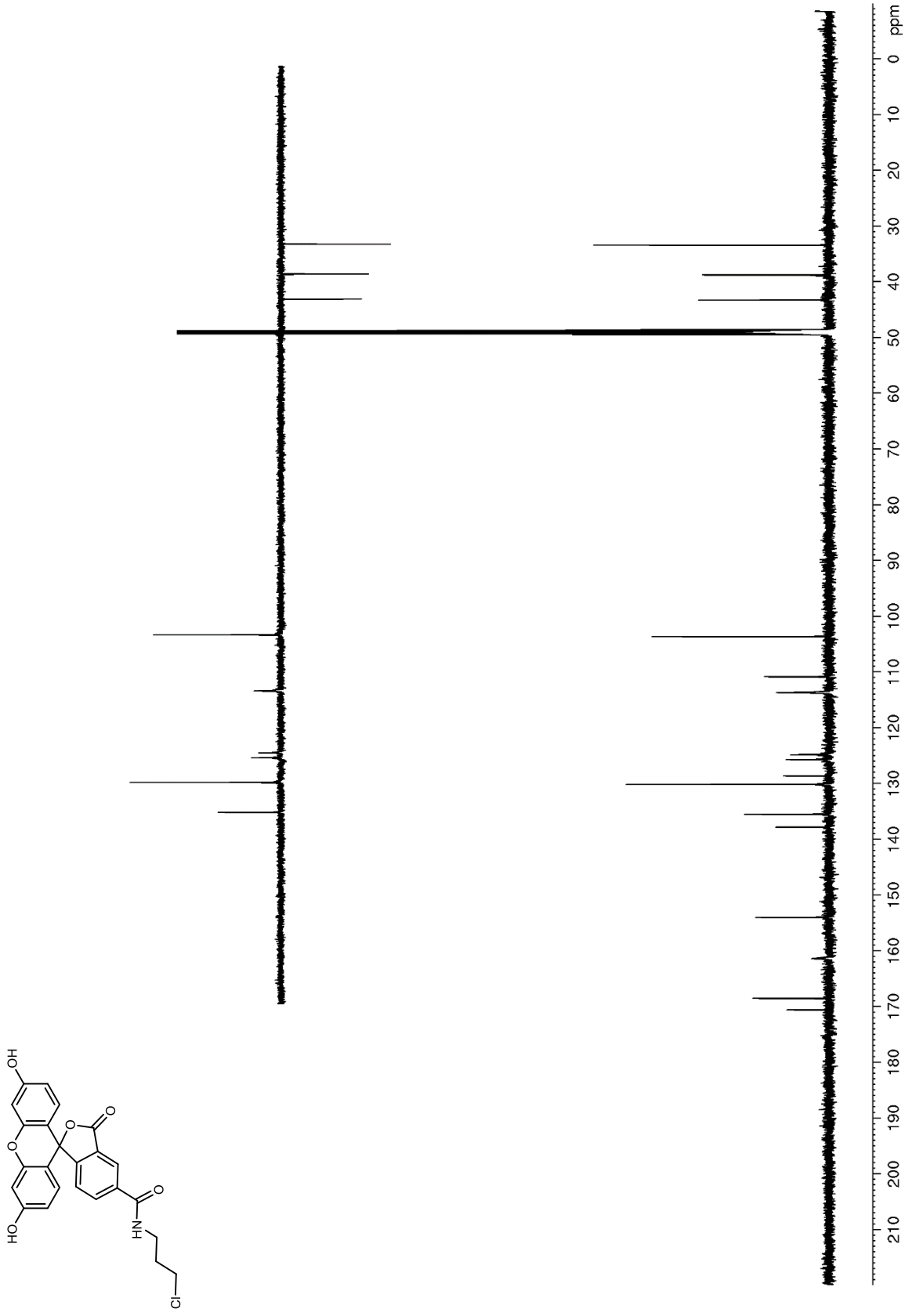

Figure S218. ^{1}H NMR (600 MHz, $CDCl_3$) of **109**

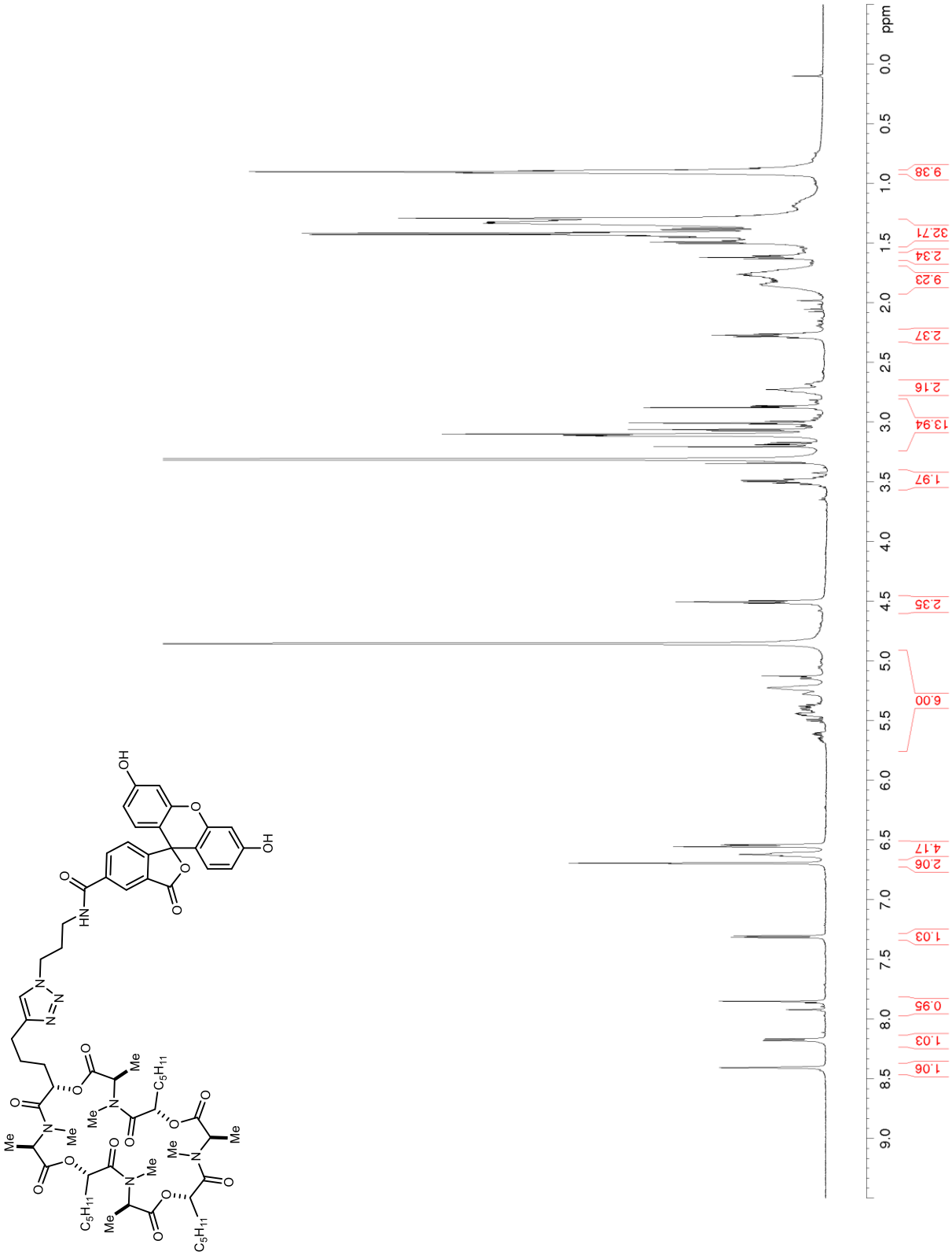

Figure S219. ^{13}C NMR/DEPT (150 MHz, $CDCl_3$) of **109**

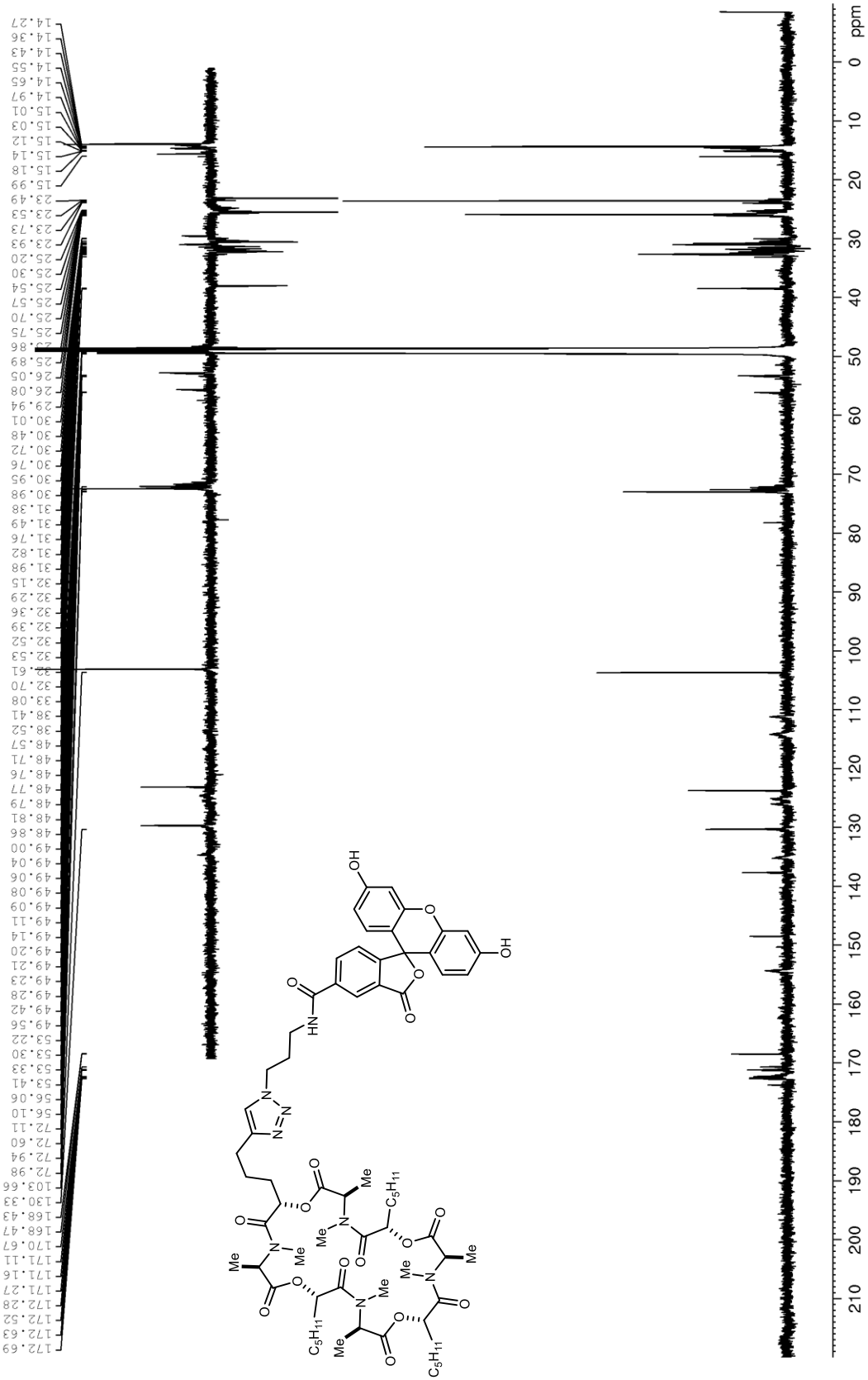

Figure S220. ^{1}H NMR (600 MHz, $CDCl_3$) of **111**

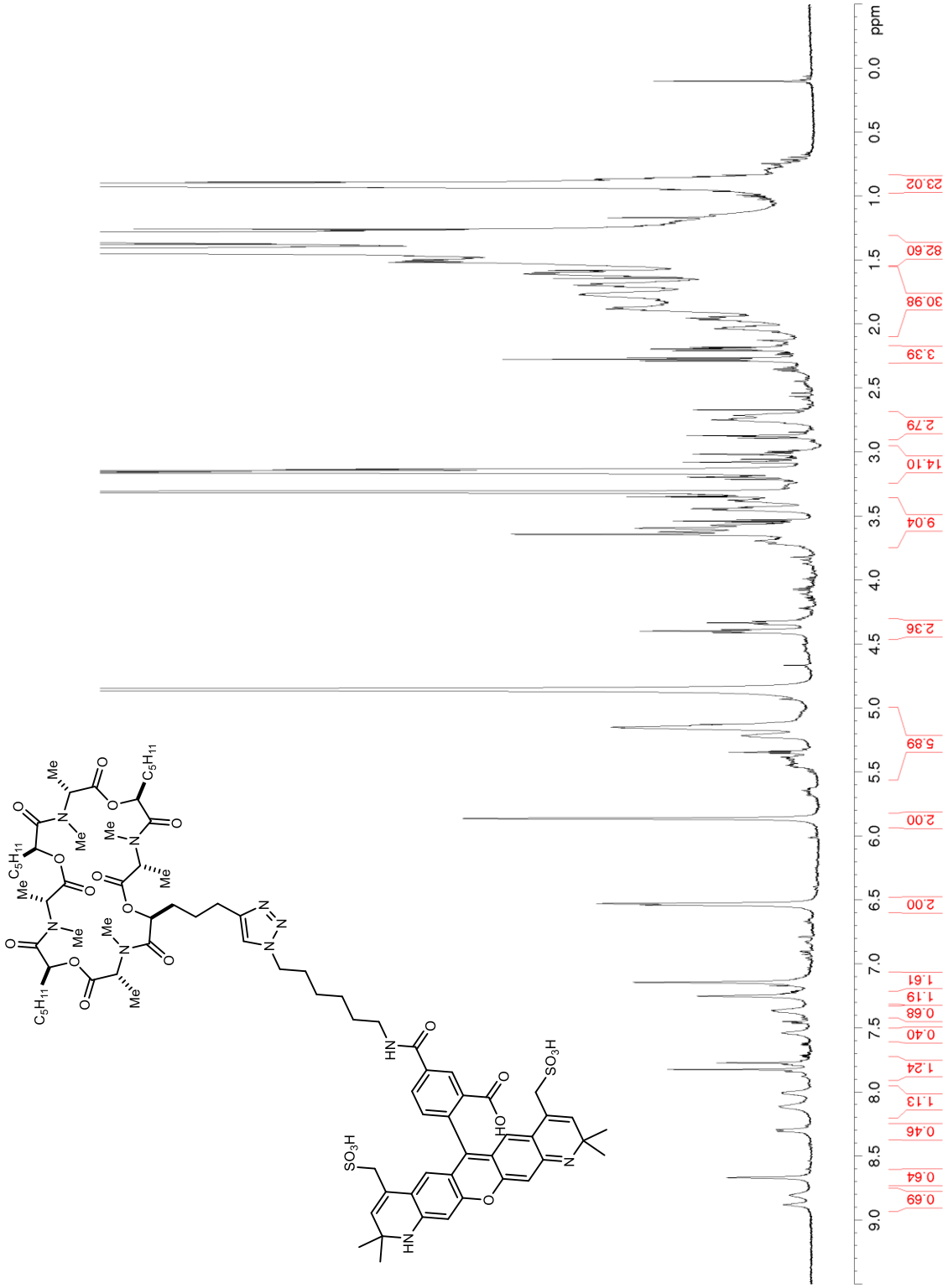

Figure S221. ^{1}H NMR (600 MHz, $CDCl_3$) of **121**

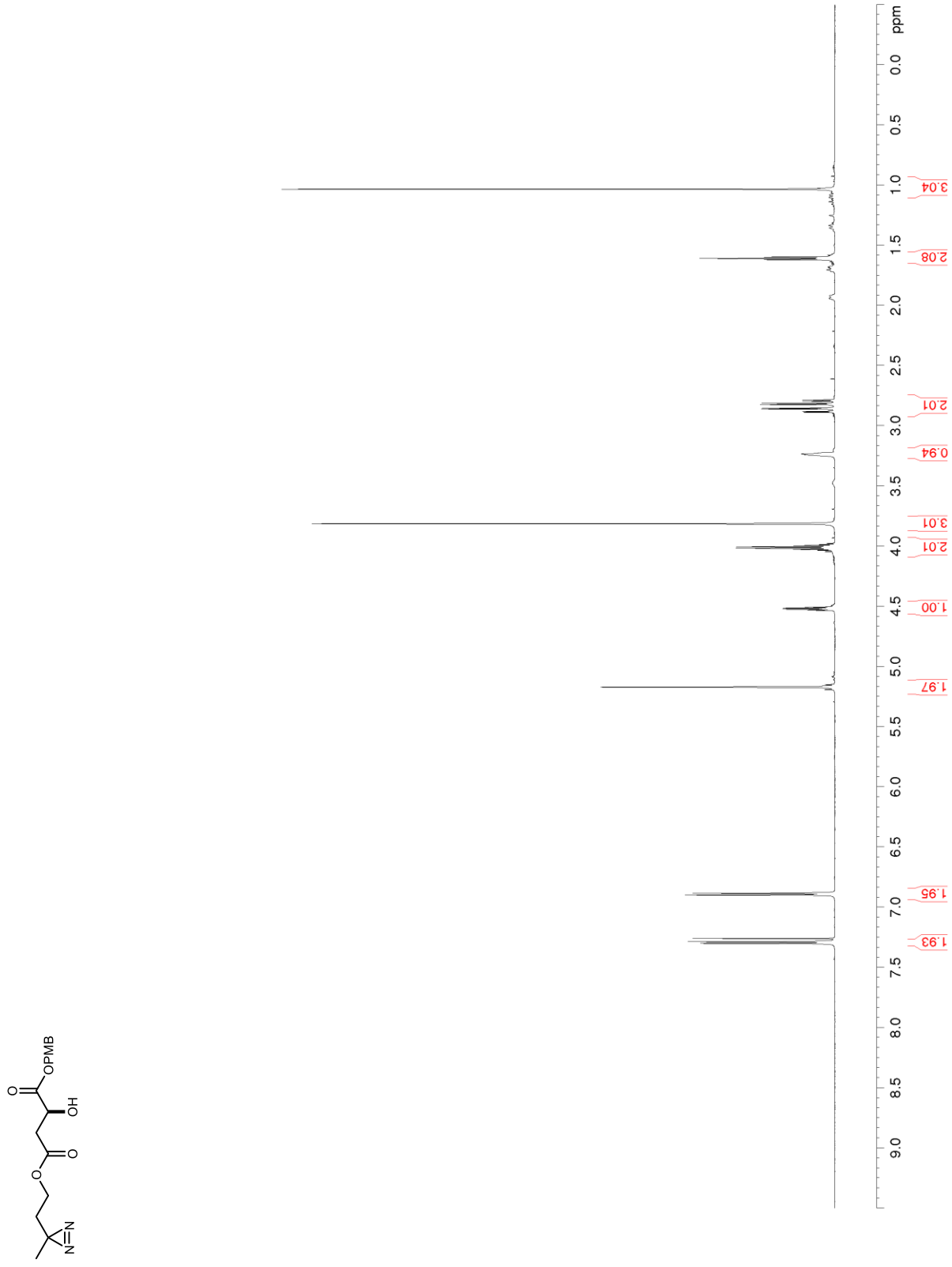

Figure S222. ^{13}C NMR/DEPT (150 MHz, $CDCl_3$) of **121**

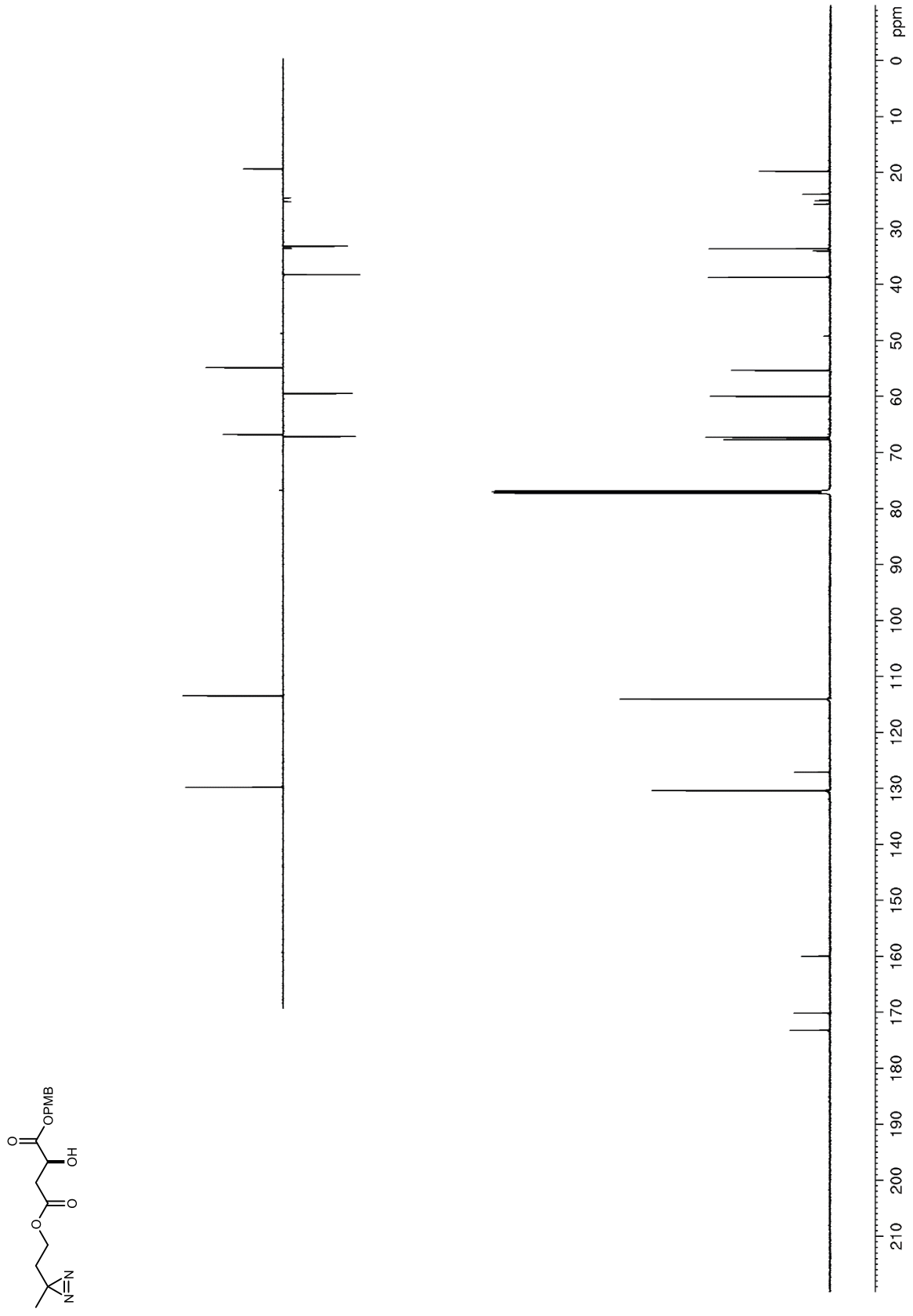

Figure S223. ^{1}H NMR (600 MHz, $CDCl_3$) of **122**

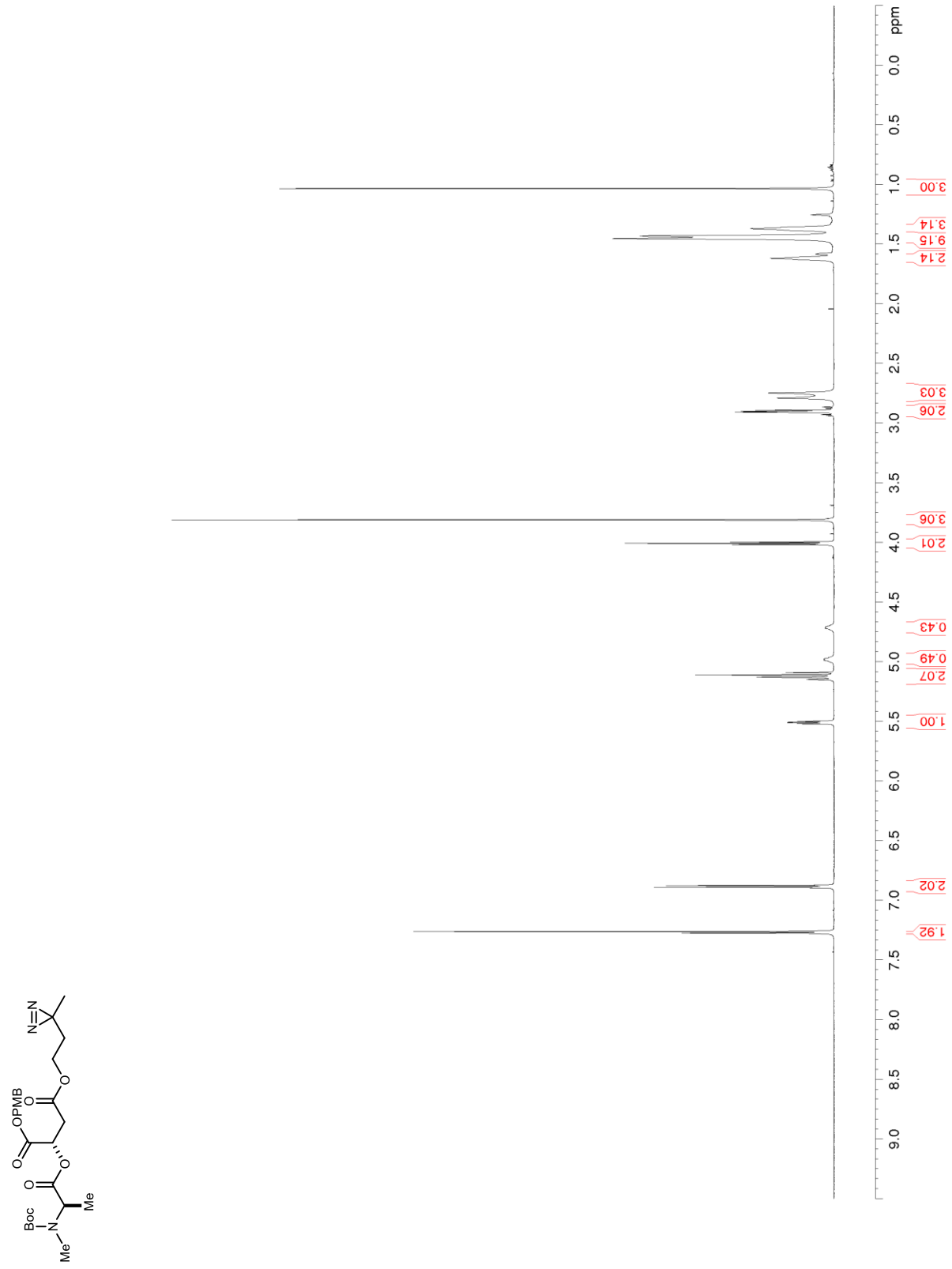

Figure S224. ^{13}C NMR/DEPT (125 MHz, $CDCl_3$) of **122**

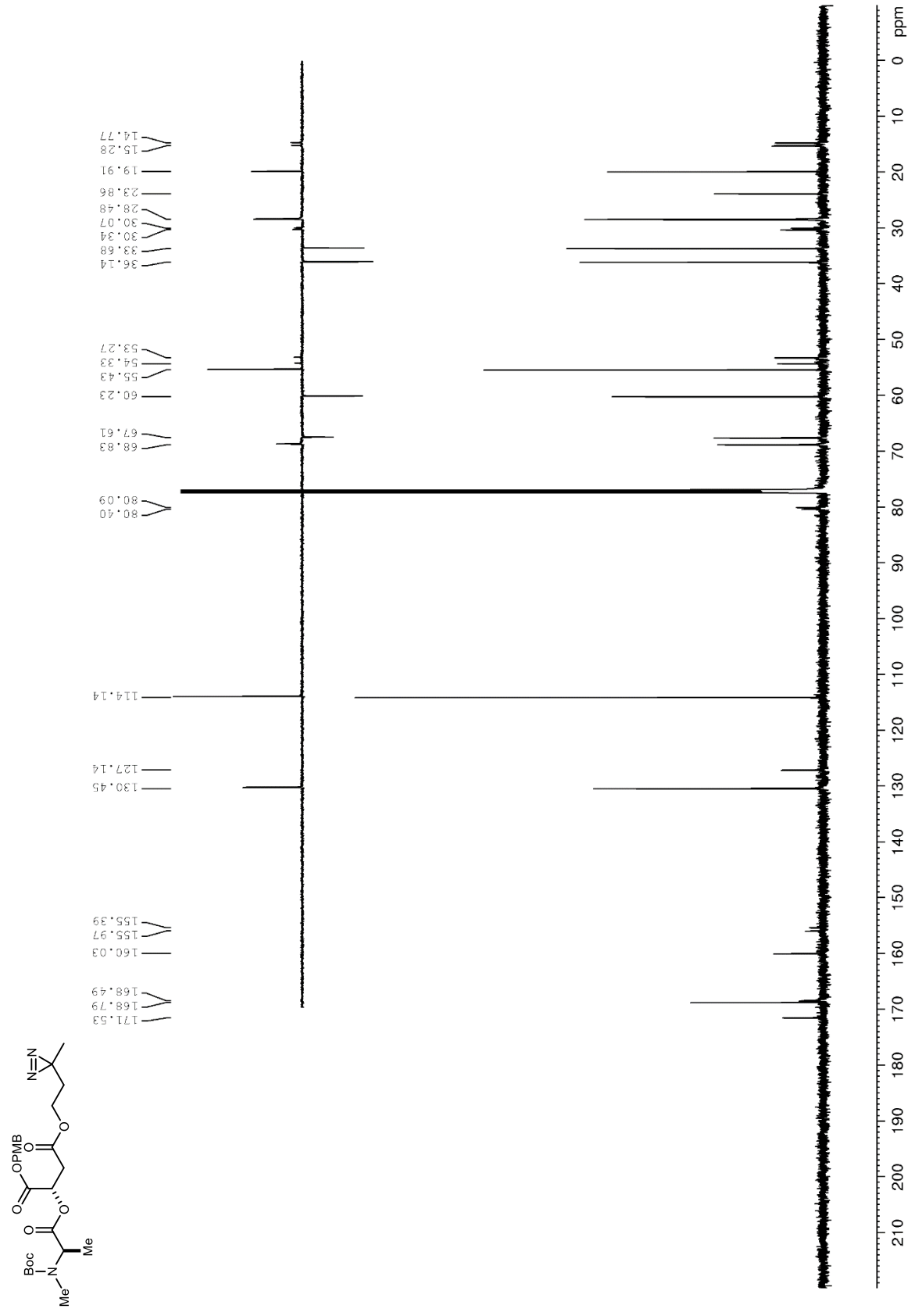

Figure S225. ^{1}H NMR (600 MHz, $CDCl_3$) of **126**

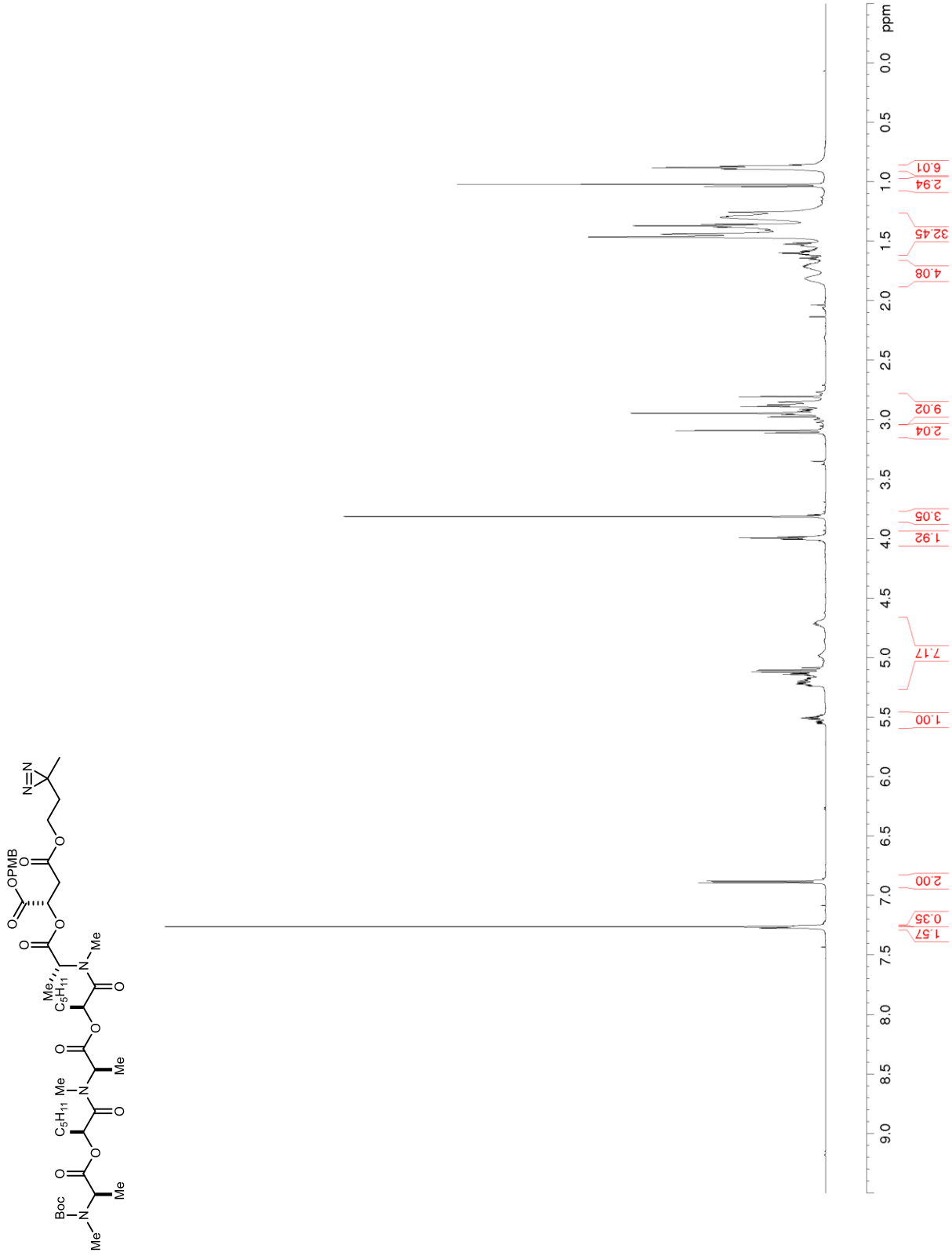

Figure S226. ^{13}C NMR/DEPT (150 MHz, $CDCl_3$) of **126**

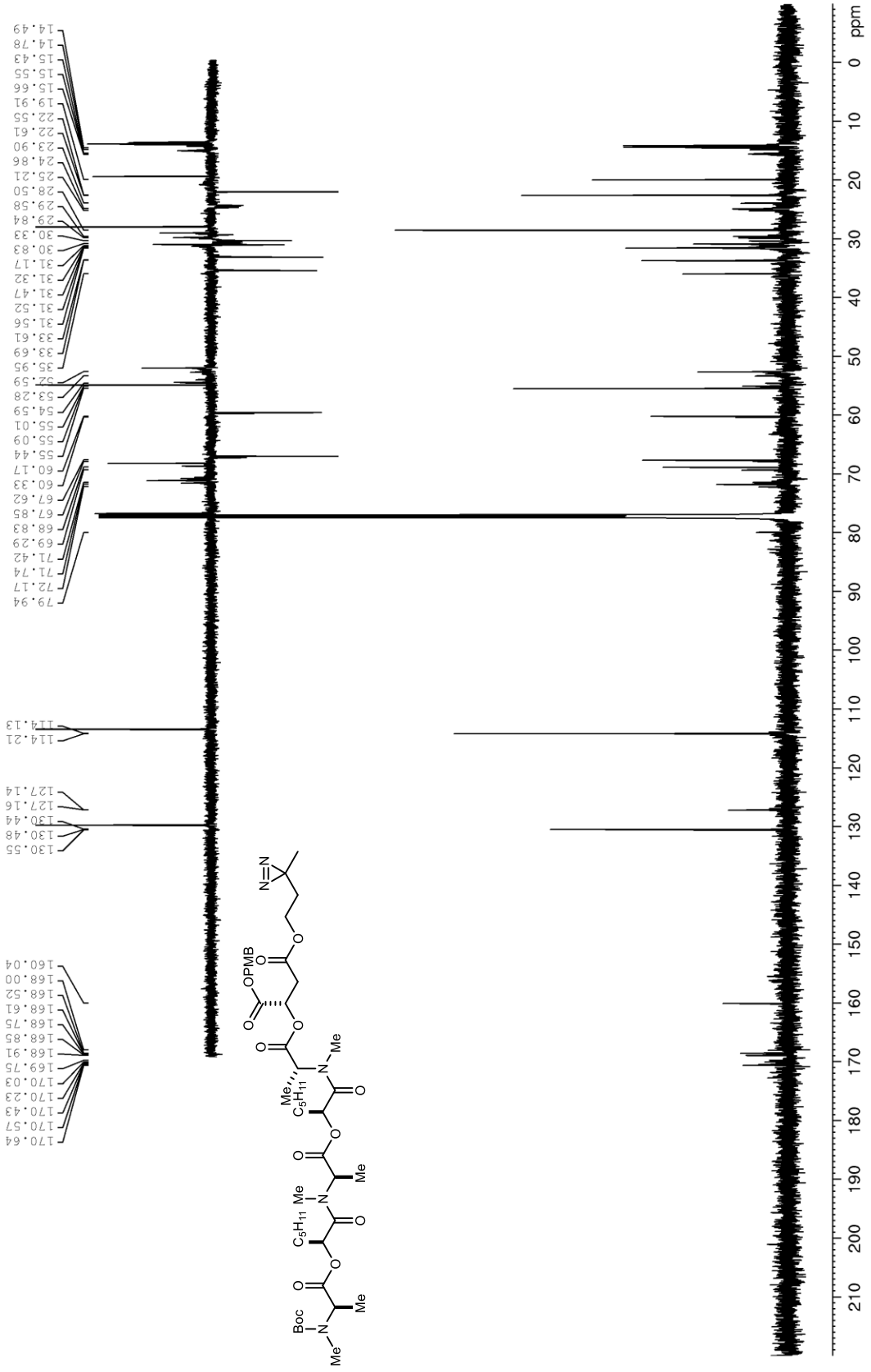

Figure S227. ^{1}H NMR (600 MHz, $CDCl_3$) of **128**

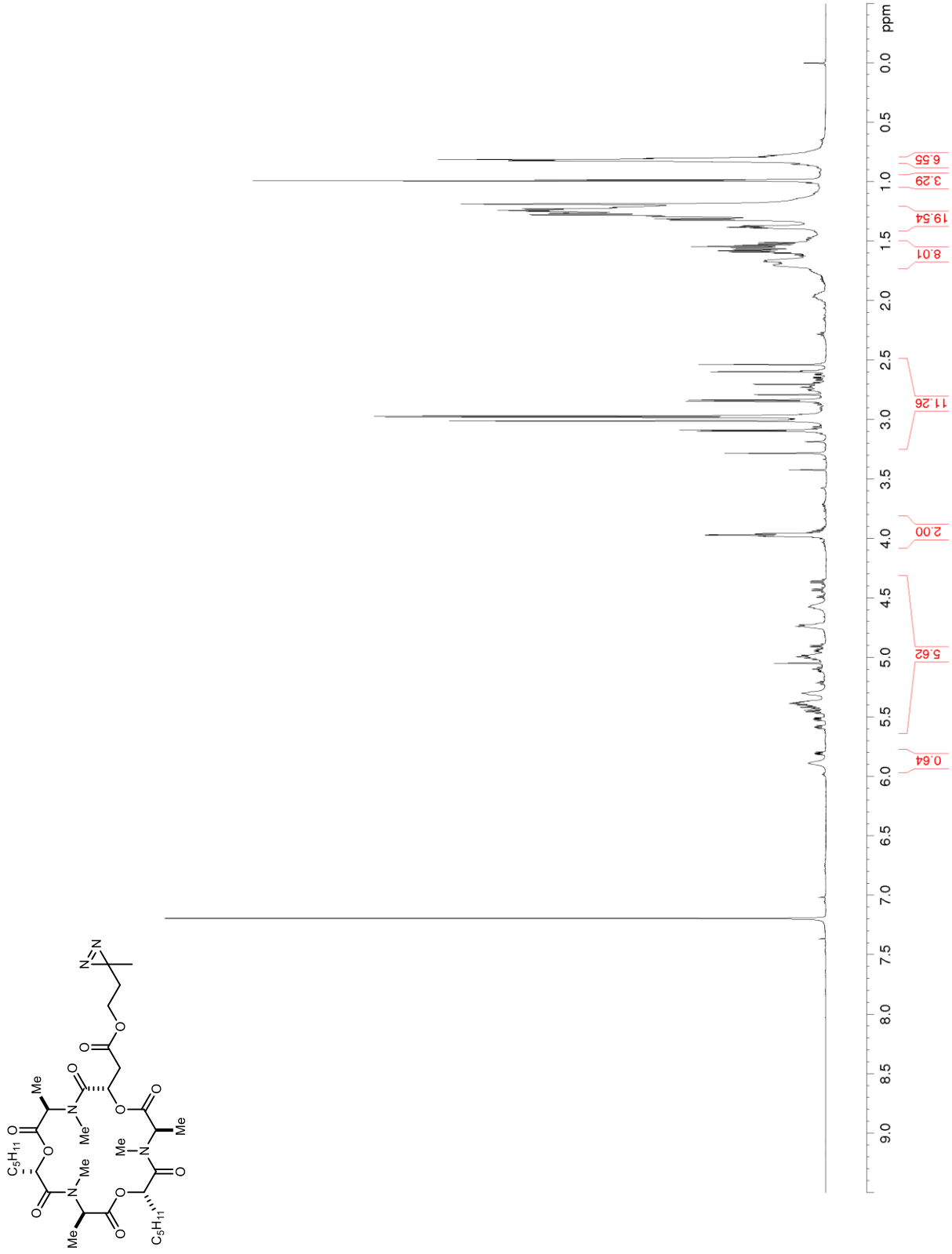

Figure S228. ^{13}C NMR/DEPT (150 MHz, $CDCl_3$) of **128**

Figure S229. ^{1}H NMR (600 MHz, $CDCl_3$) of **142**

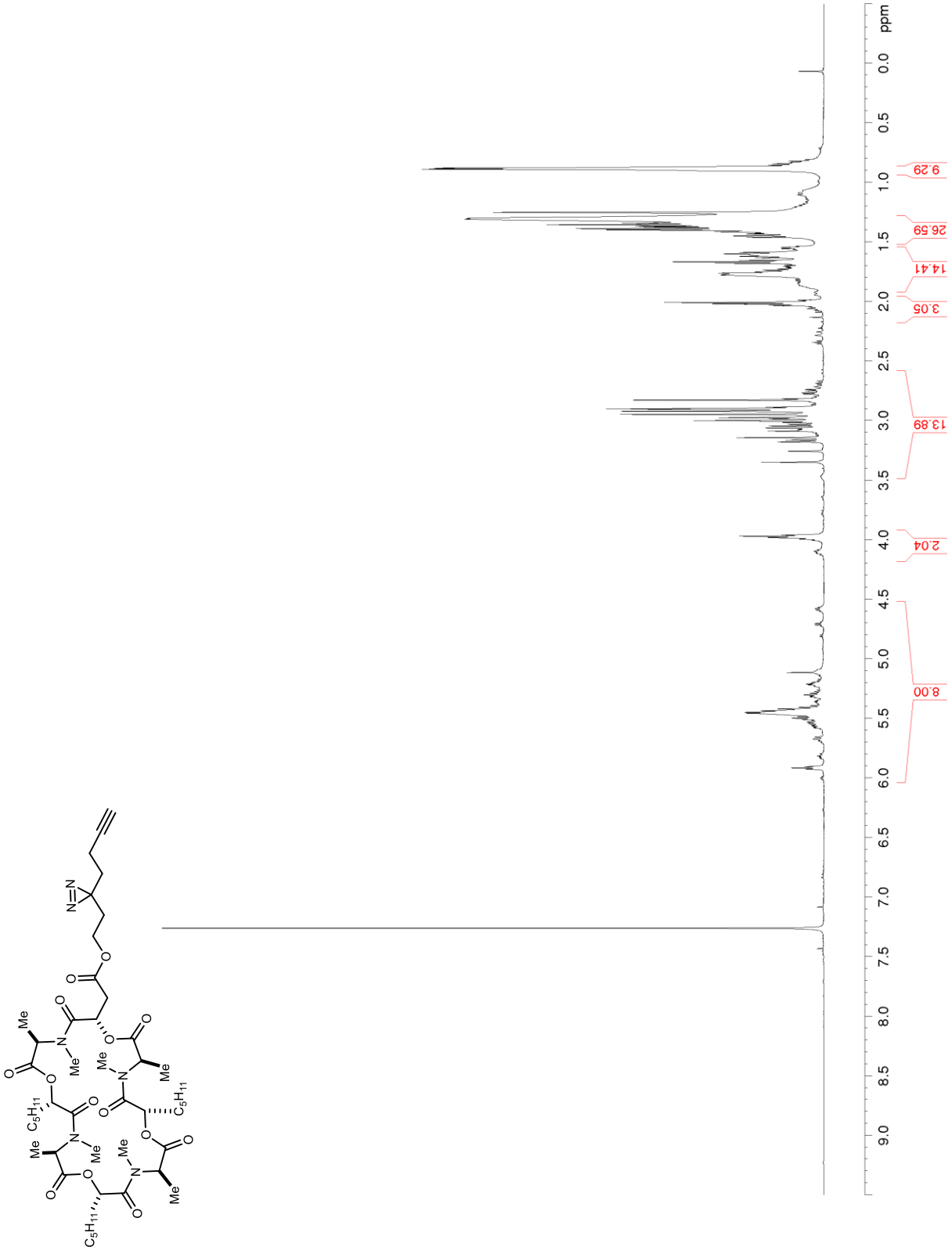

Figure S230. ^{13}C NMR/DEPT (150 MHz, $CDCl_3$) of **142**

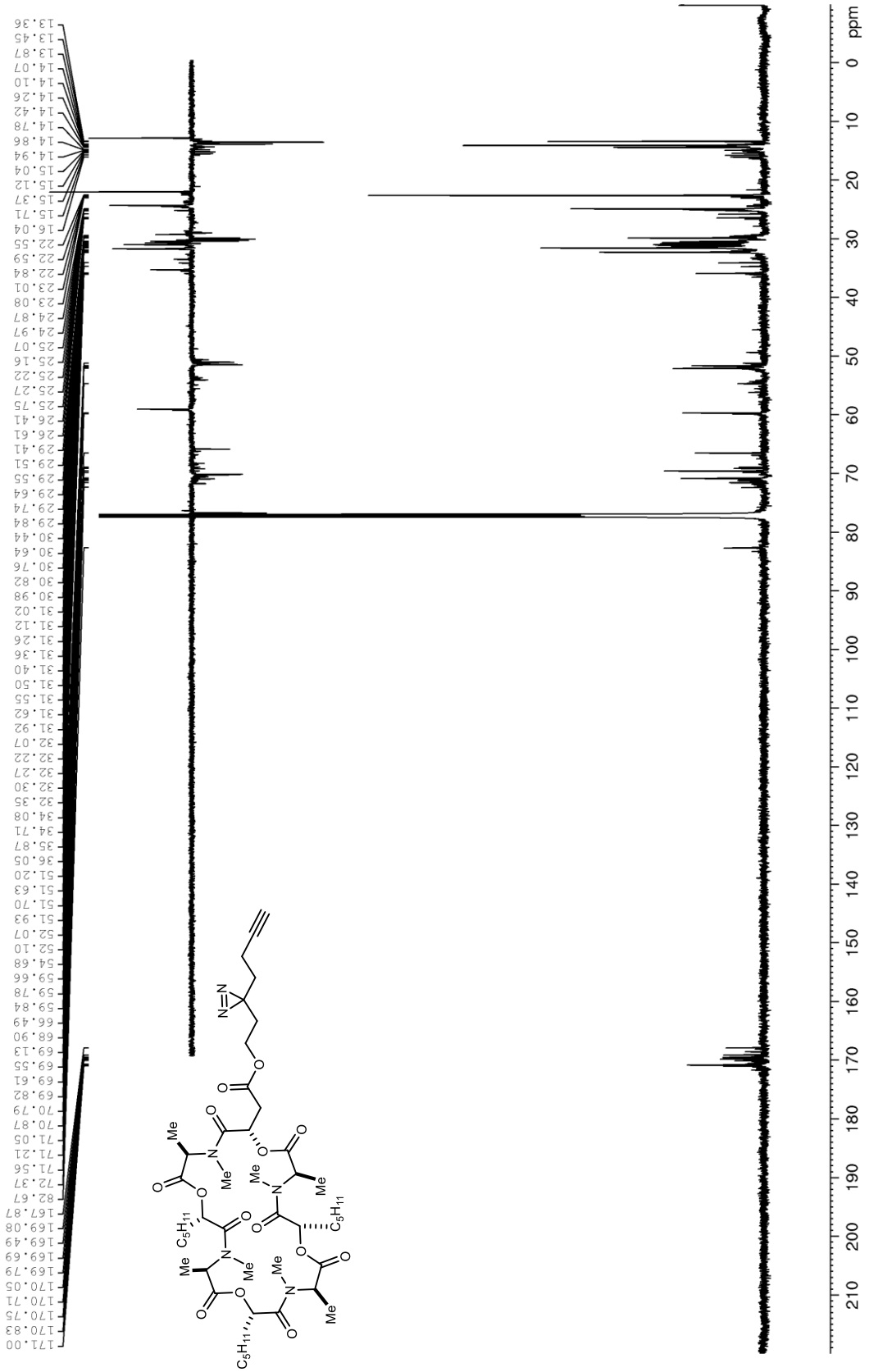

Figure S231. ^{1}H NMR (600 MHz, $CDCl_3$) of **143**

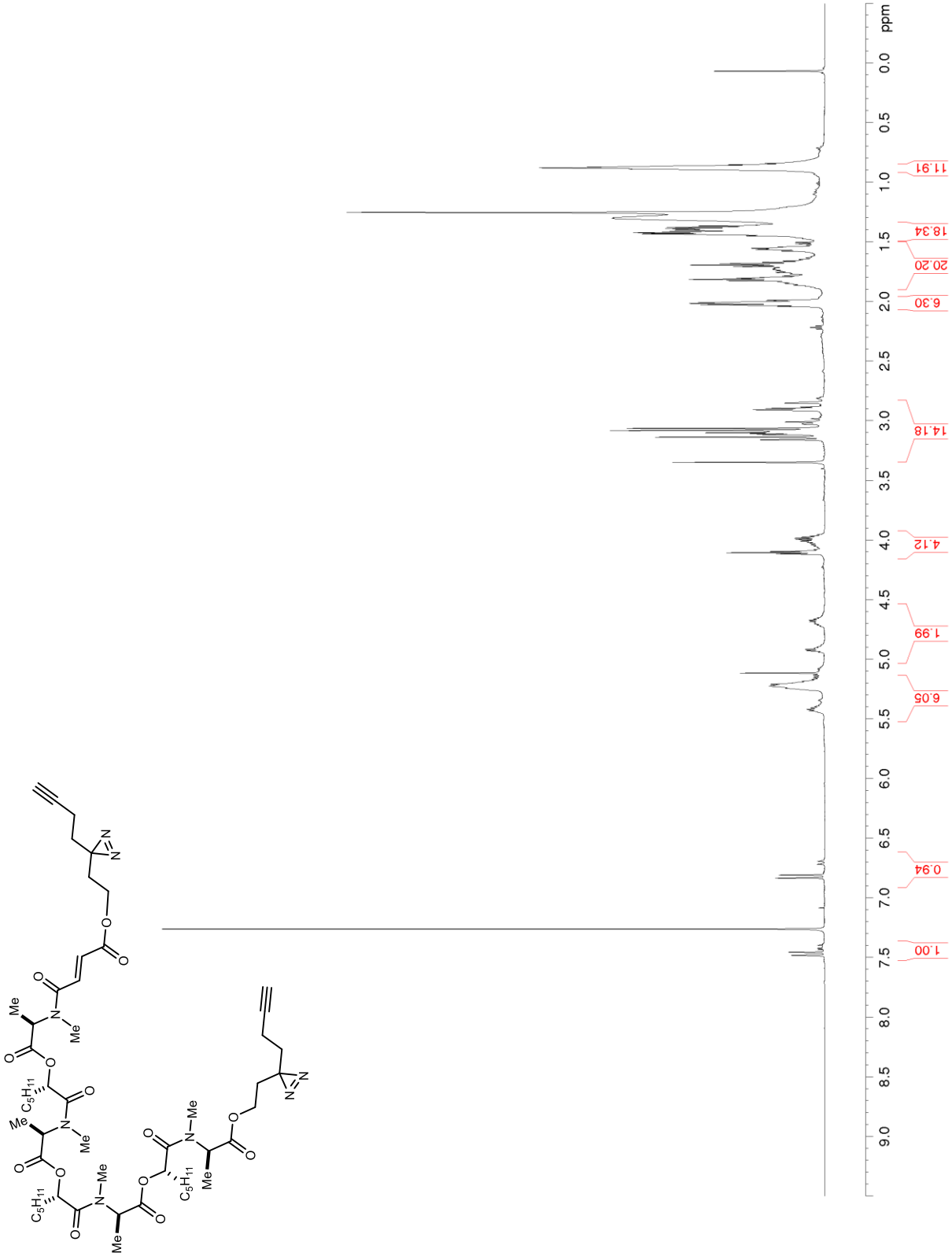

Figure S232. ^{13}C NMR/DEPT (150 MHz, $CDCl_3$) of **143**

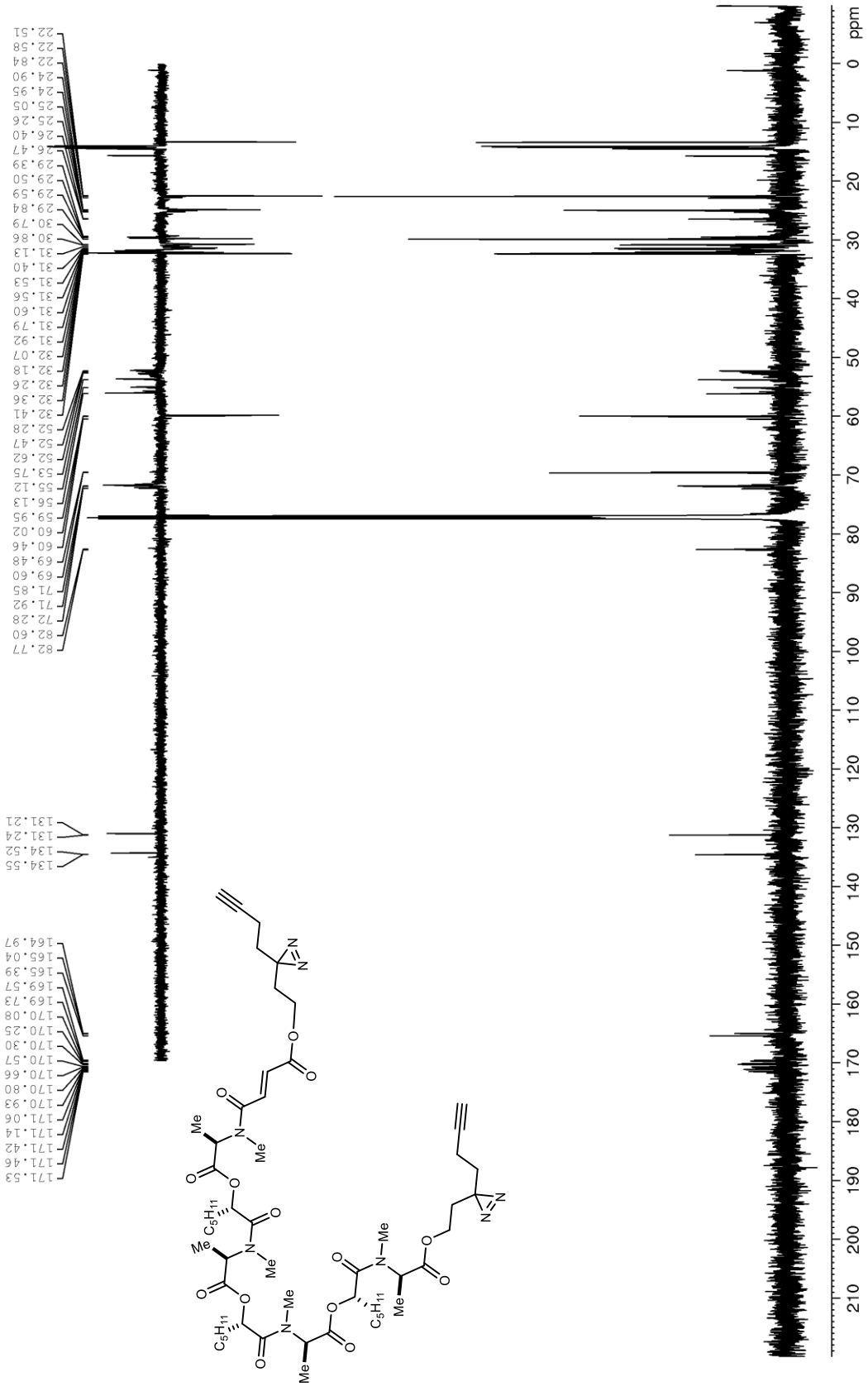

Figure S233. ^{1}H NMR (600 MHz, $CDCl_3$) of **145**

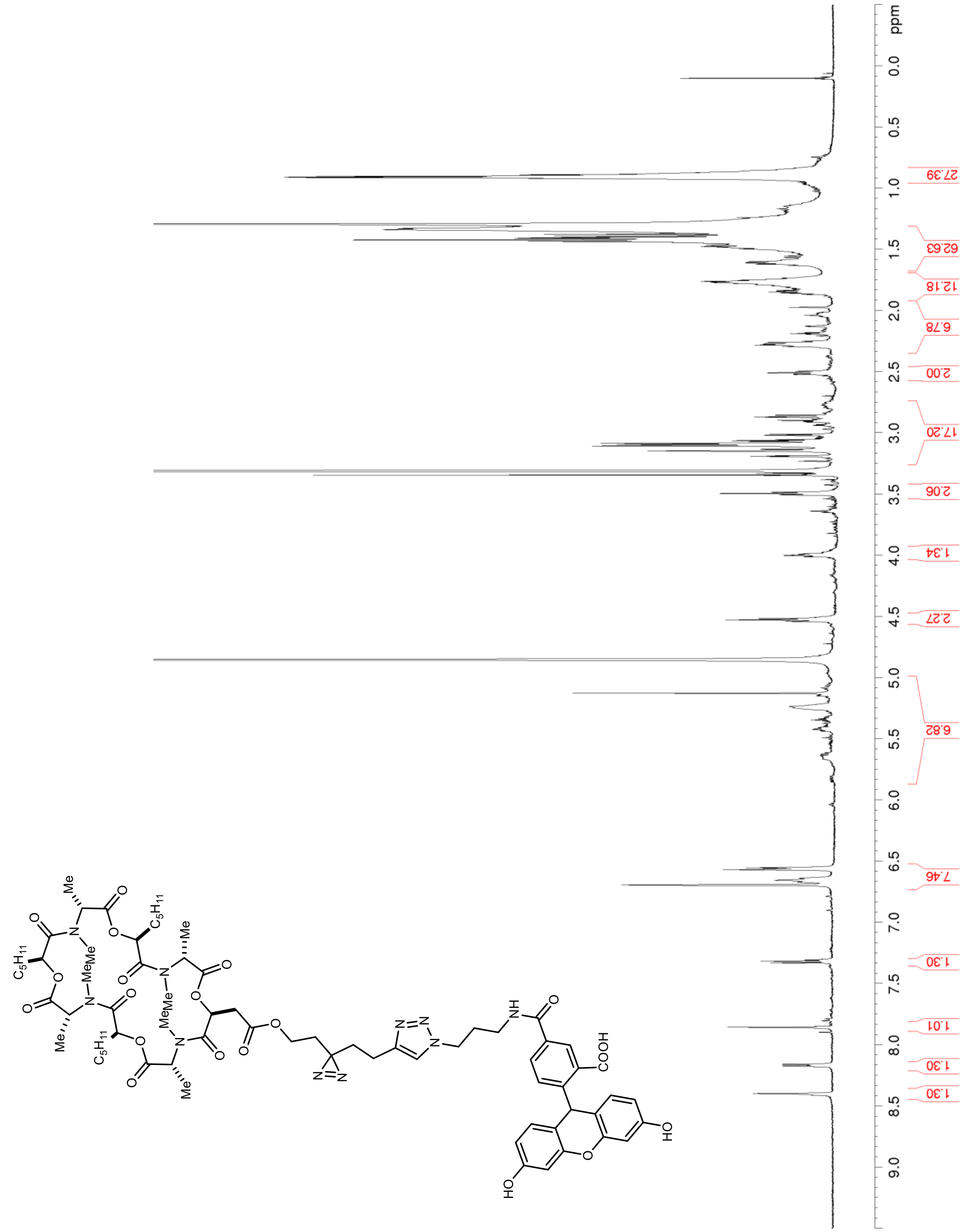

Figure S234. ^{1}H NMR (400 MHz, $CDCl_3$) of **148**

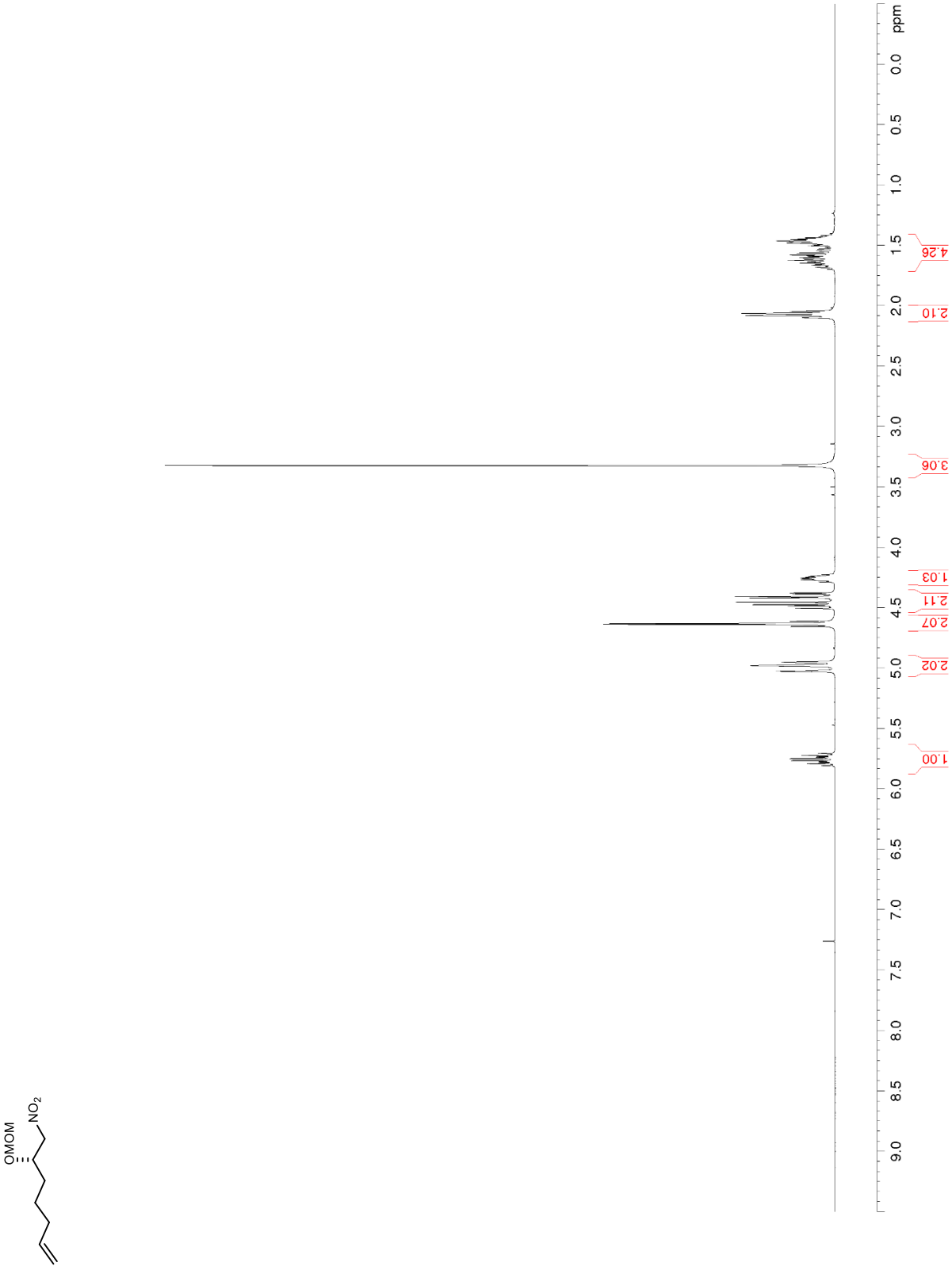

Figure S235. ^{13}C NMR/DEPT (100 MHz, $CDCl_3$) of **148**

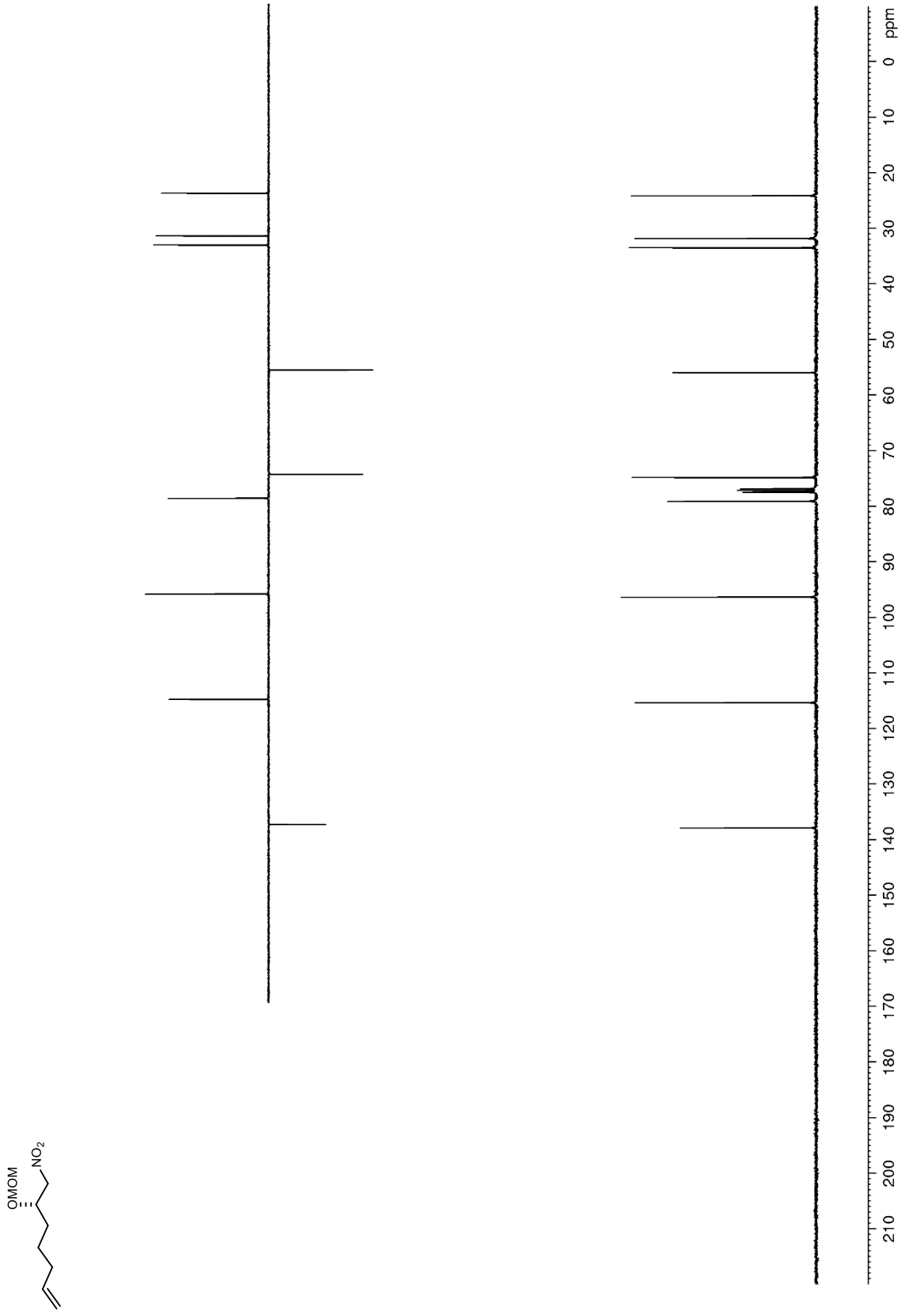

Figure S236. ^{1}H NMR (600 MHz, $CDCl_3$) of **150**

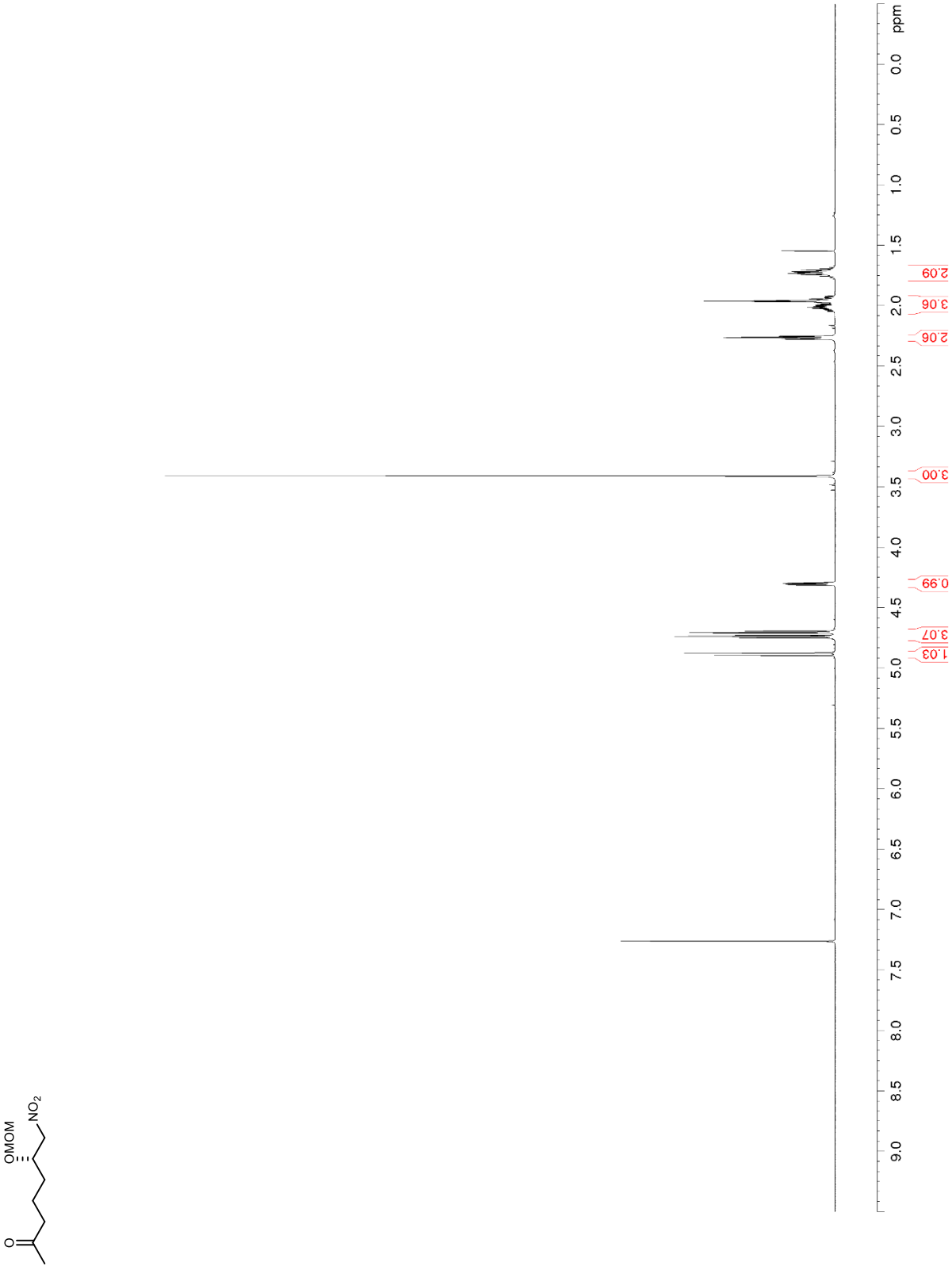

Figure S237. ^{13}C NMR/DEPT (150 MHz, $CDCl_3$) of **150**

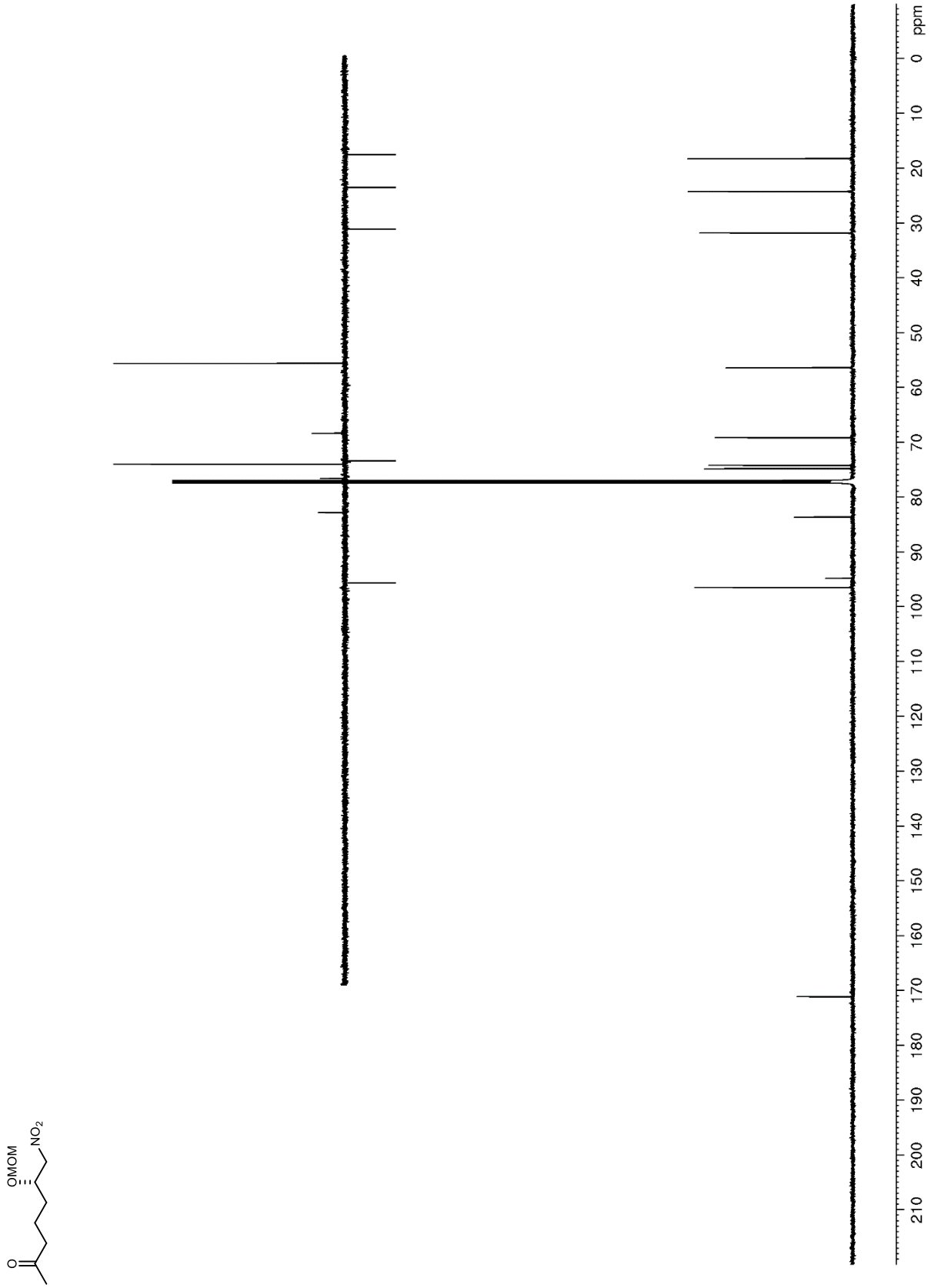

Figure S238. ^{1}H NMR (600 MHz, $CDCl_3$) of **158**

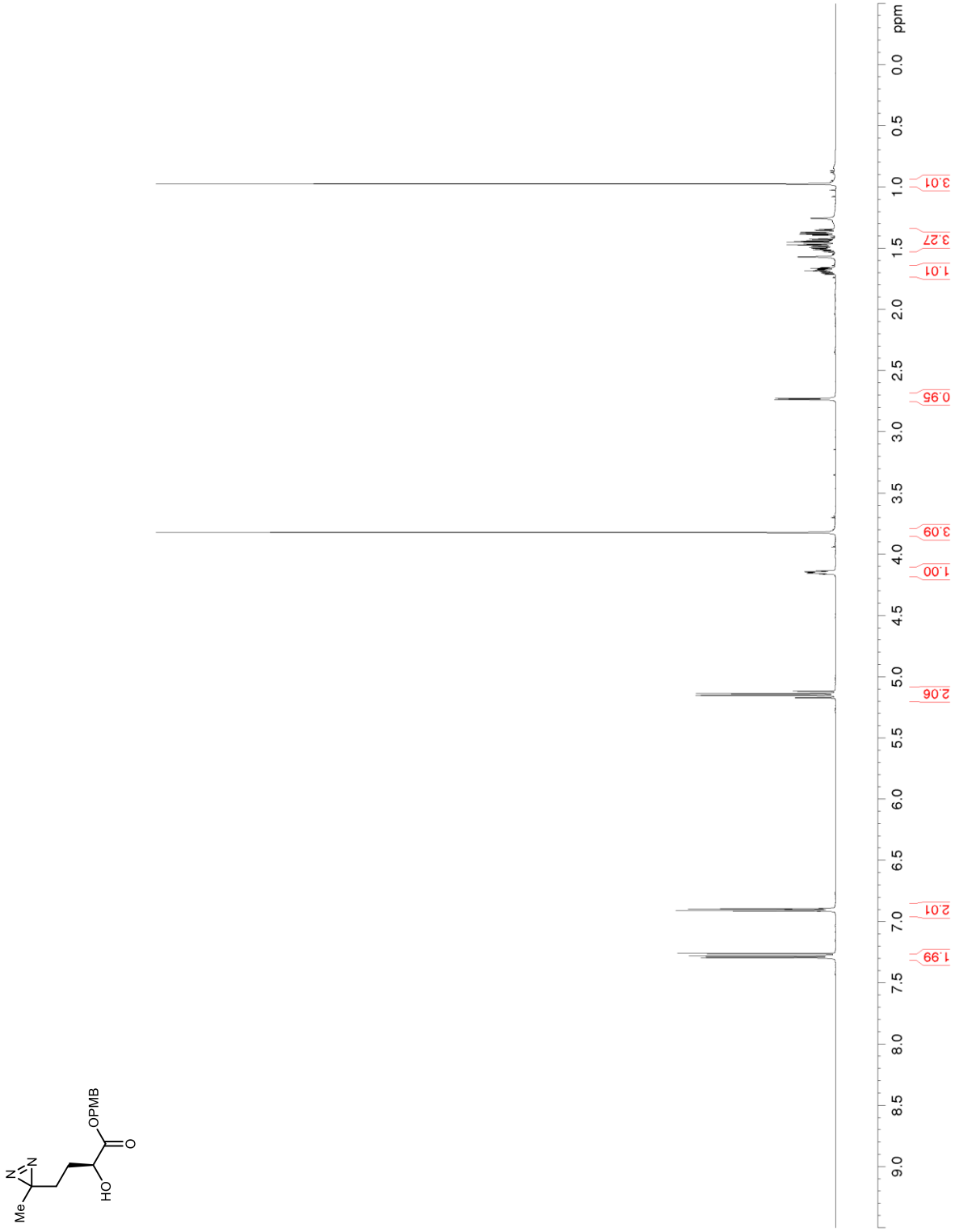

Figure S239. ^{13}C NMR/DEPT (150 MHz, $CDCl_3$) of **158**

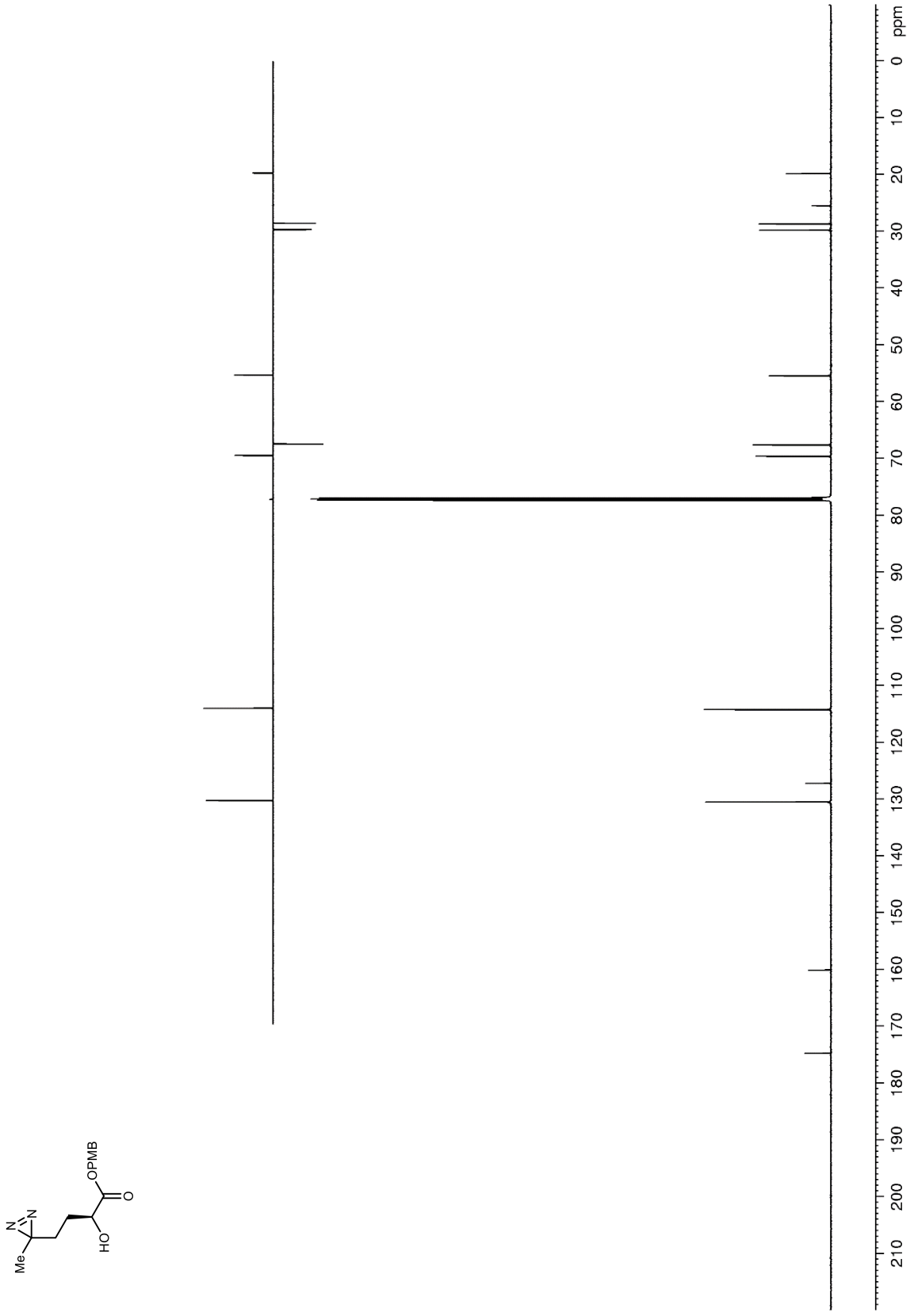

Figure S240. ^{1}H NMR (600 MHz, $CDCl_3$) of **159**

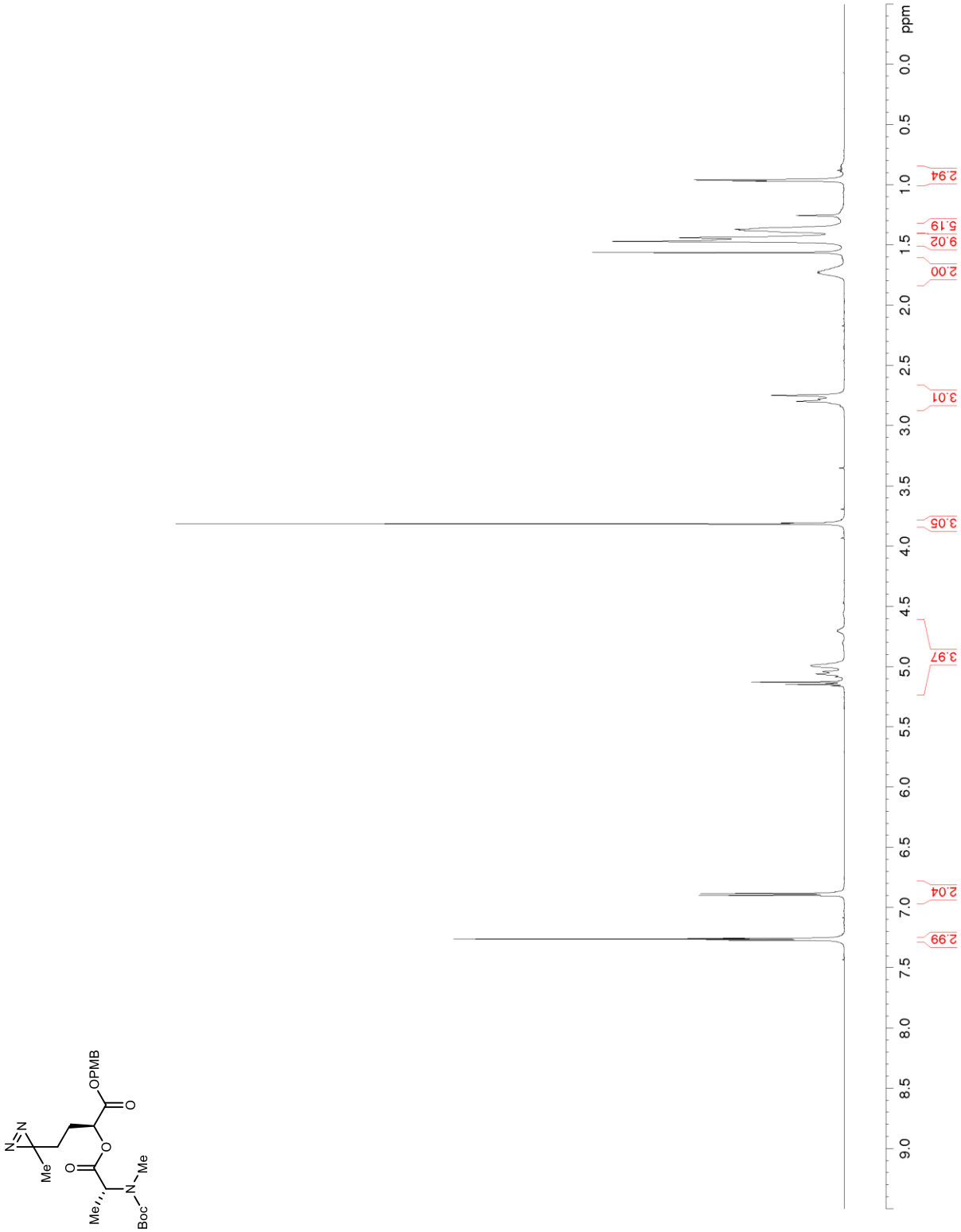

Figure S241. ^{13}C NMR/DEPT (150 MHz, $CDCl_3$) of **159**

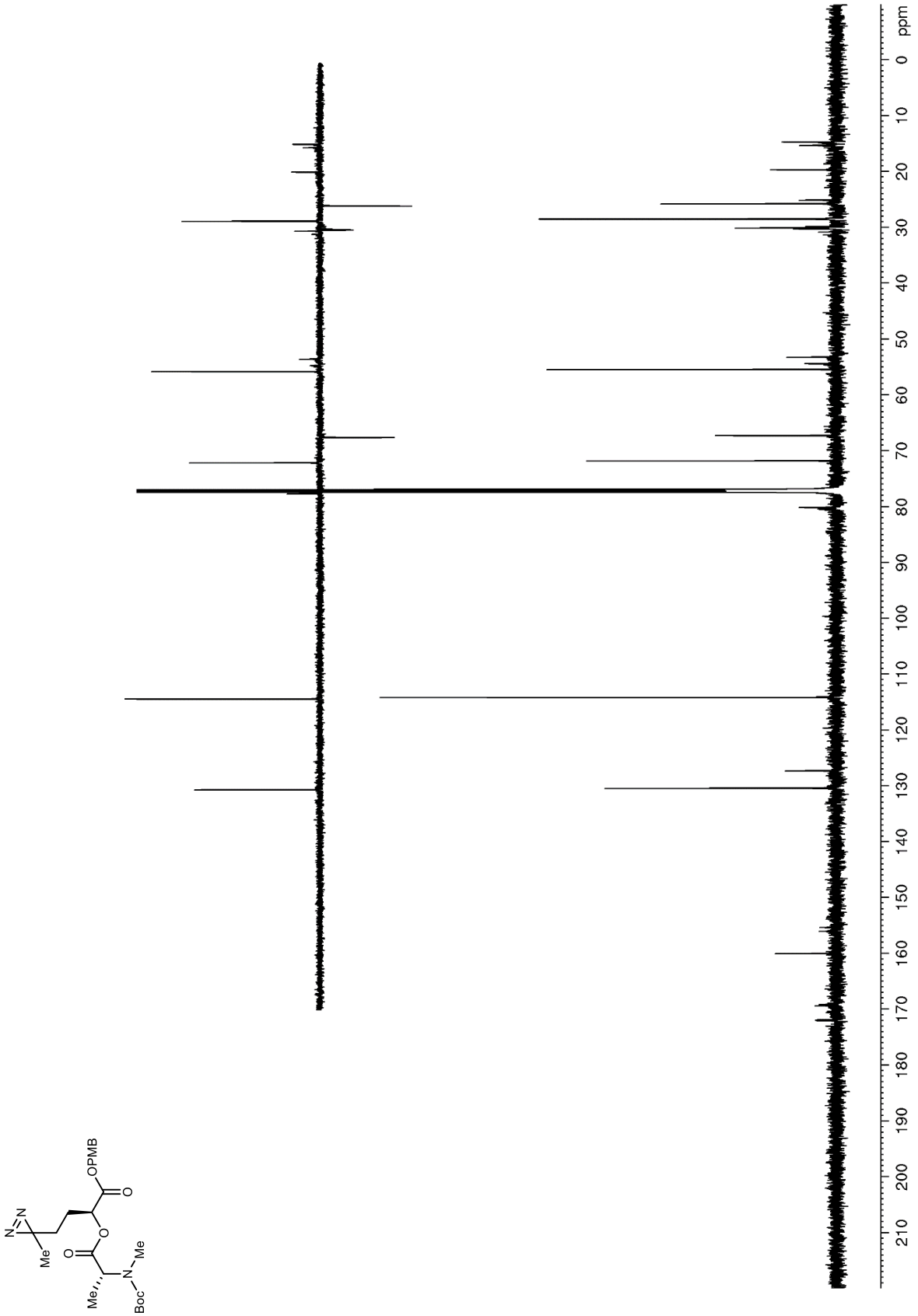

Figure S242. ^{1}H NMR (600 MHz, $CDCl_3$) of **160**

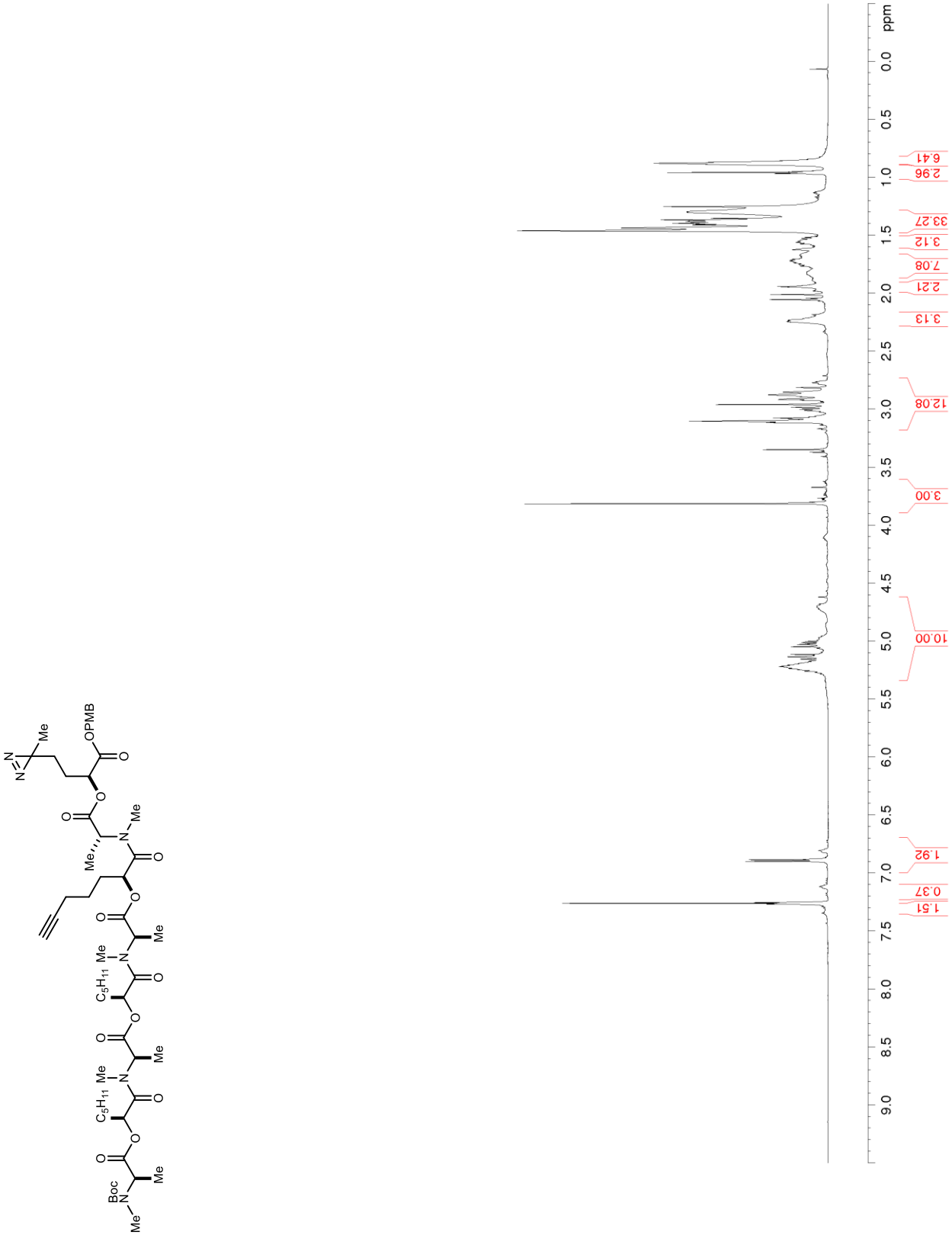

Figure S243. ^{13}C NMR/DEPT (150 MHz, CDCl$_3$) of **160**

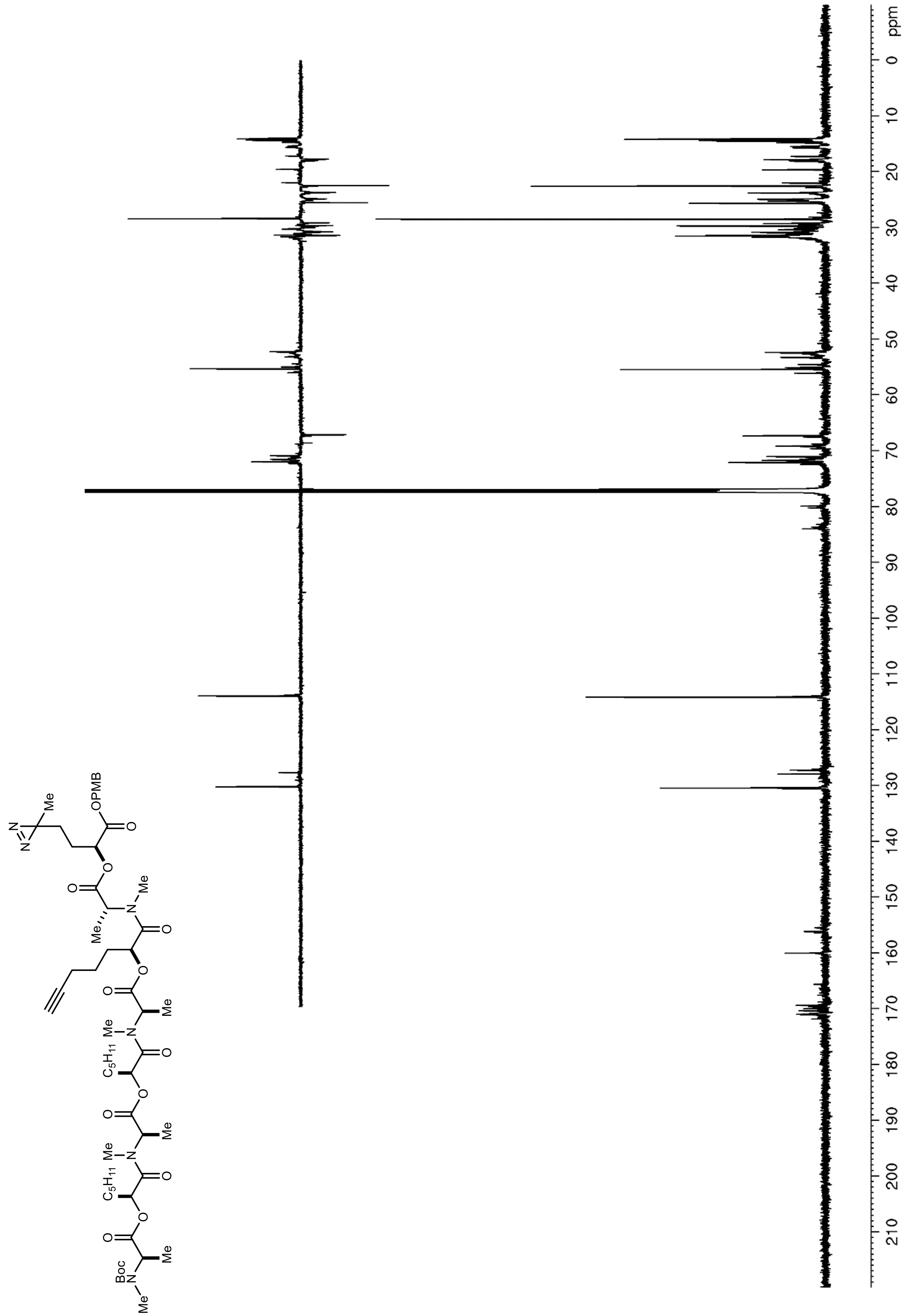

Figure S244. ^{1}H NMR (400 MHz, $CDCl_3$) of **161**

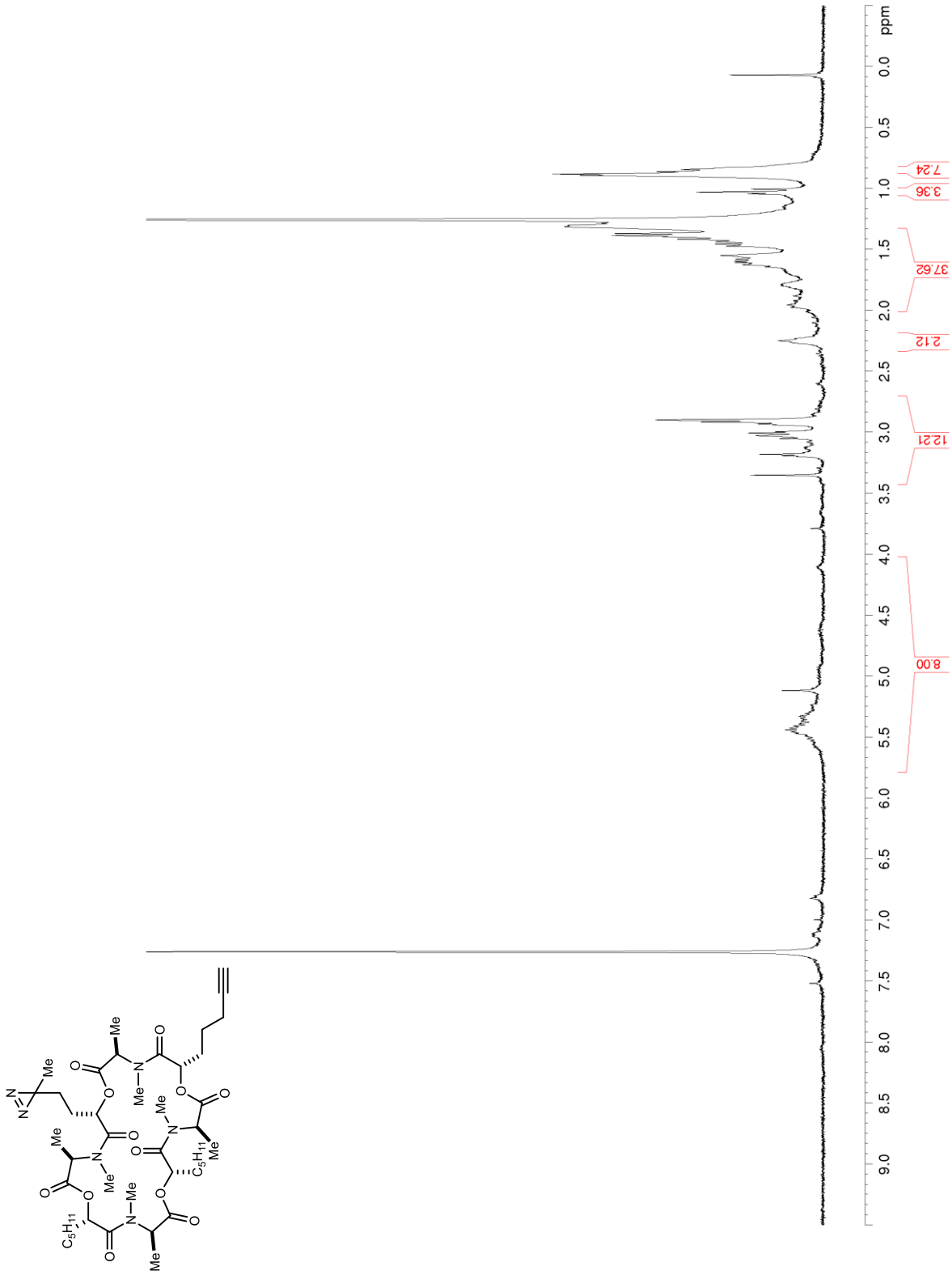

Figure S245. ^{1}H NMR (600 MHz, $CDCl_3$) of **162**

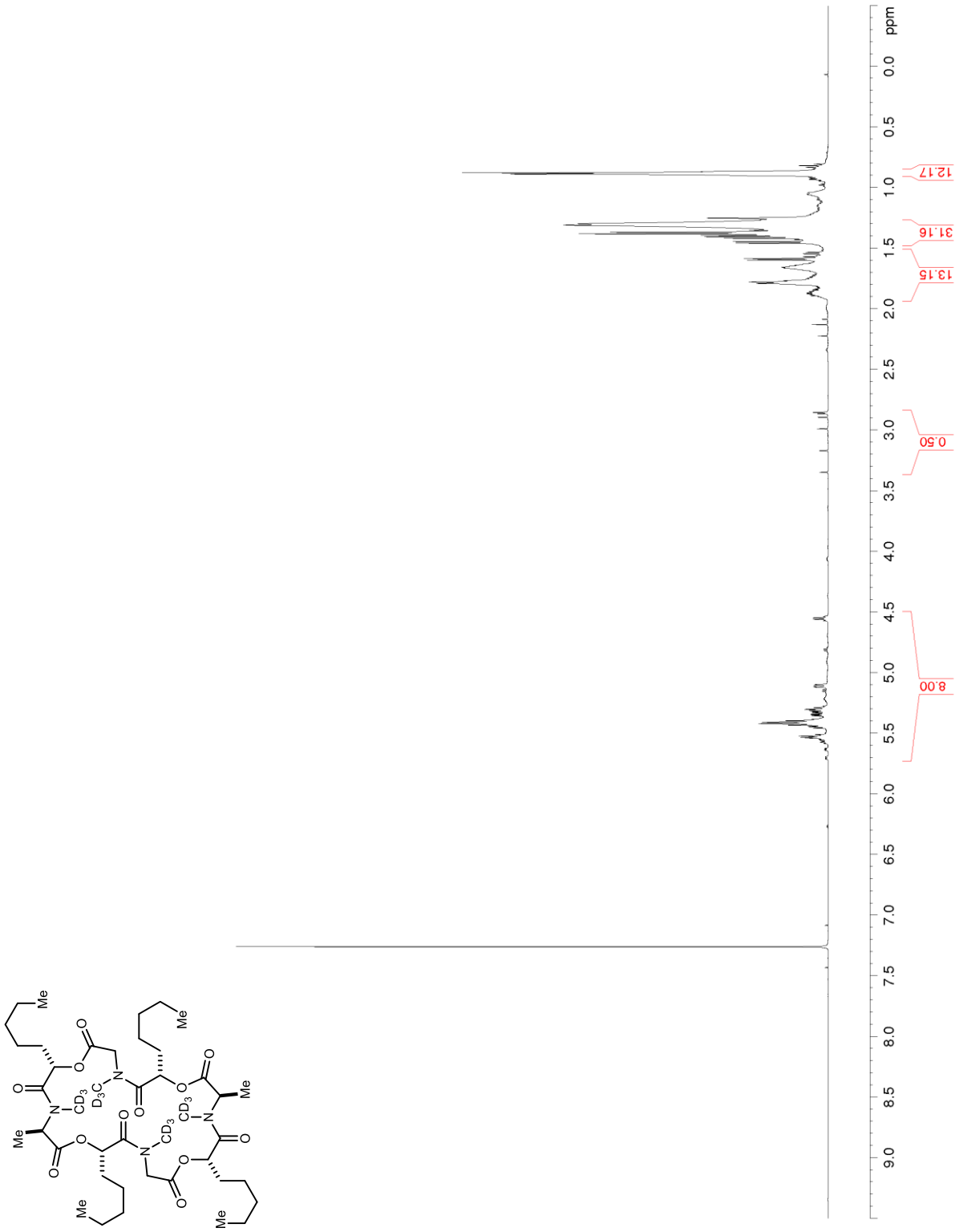

Figure S246. ^{13}C NMR/DEPT (150 MHz, $CDCl_3$) of **162**

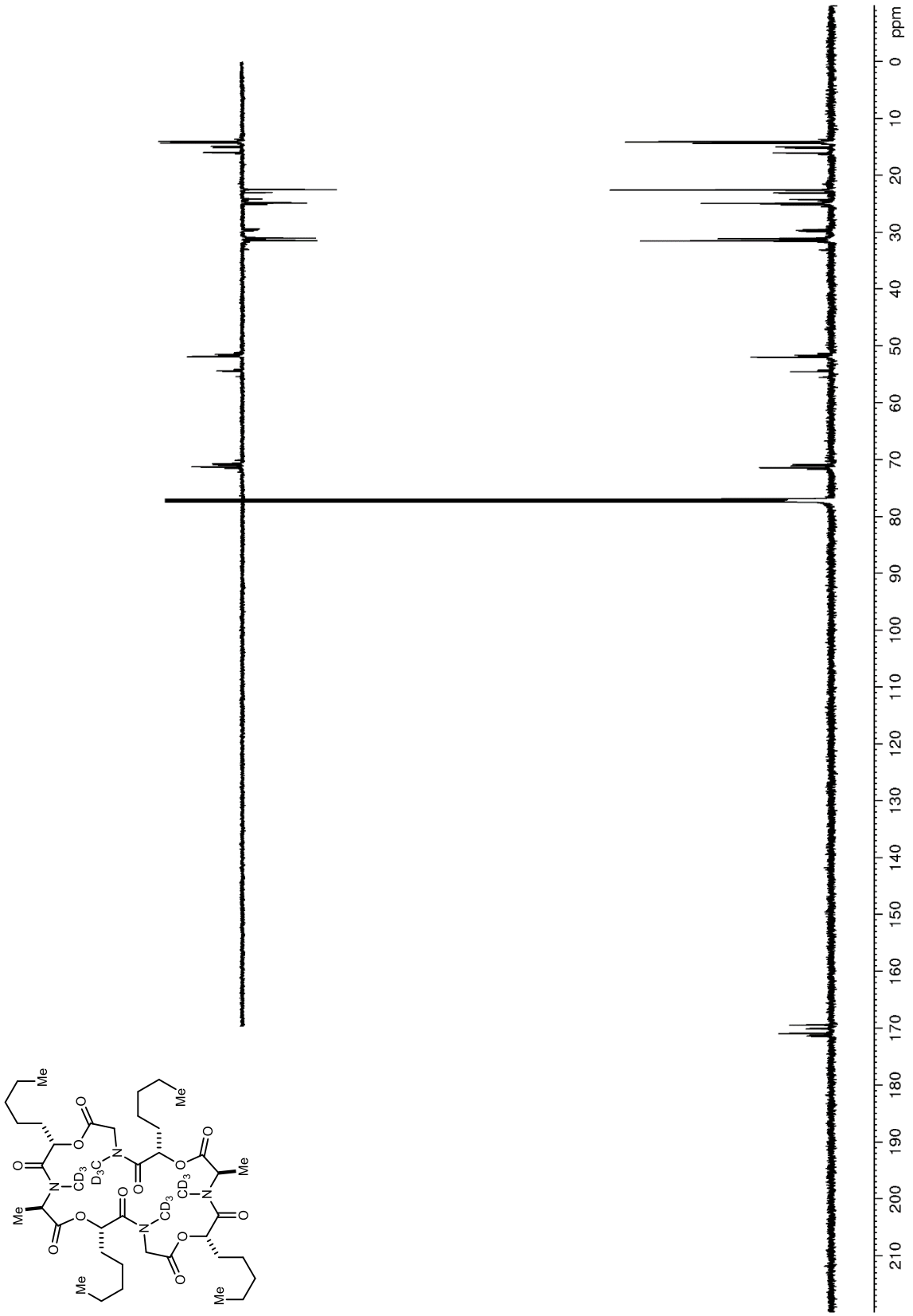

3.7 Crystallography Data

checkCIF/PLATON report

Structure factors have been supplied for datablock(s) ans-1-195

THIS REPORT IS FOR GUIDANCE ONLY. IF USED AS PART OF A REVIEW PROCEDURE FOR PUBLICATION, IT SHOULD NOT REPLACE THE EXPERTISE OF AN EXPERIENCED CRYSTALLOGRAPHIC REFEREE.

No syntax errors found. CIF dictionary Interpreting this report

Datablock: ans-1-195

```
Bond precision:  C-C = 0.0028 A          Wavelength=1.54184

Cell:           a=10.63583(6)    b=13.50231(10)      c=16.01257(9)
                alpha=90         beta=101.7495(5)    gamma=90
Temperature:    100 K

                 Calculated                Reported
Volume           2251.36(2)                2251.36(2)
Space group      P 21                      P 1 21 1
Hall group       P 2yb                     P 2yb
Moiety formula   C40 H68 N4 O12            C40 H68 N4 O12
Sum formula      C40 H68 N4 O12            C40 H68 N4 O12
Mr               796.98                    796.98
Dx,g cm-3        1.176                     1.176
Z                2                         2
Mu (mm-1)        0.709                     0.709
F000             864.0                     864.0
F000'            866.75
h,k,lmax         13,16,19                  13,16,19
Nref             8893[ 4646]               7796
Tmin,Tmax        0.797,0.869               0.503,1.000
Tmin'            0.758

Correction method= # Reported T Limits: Tmin=0.503 Tmax=1.000
AbsCorr = GAUSSIAN

Data completeness= 1.68/0.88       Theta(max)= 72.245

R(reflections)= 0.0274( 7720)      wR2(reflections)= 0.0727( 7796)

S = 1.036                  Npar= 513
```

The following ALERTS were generated. Each ALERT has the format
test-name_ALERT_alert-type_alert-level.
Click on the hyperlinks for more details of the test.

Alert level C

```
PLAT915_ALERT_3_C No Flack x Check Done: Low Friedel Pair Coverage        75 %
```

Alert level G

```
PLAT007_ALERT_5_G Number of Unrefined Donor-H Atoms ..............          4 Report
PLAT142_ALERT_4_G s.u. on b - Axis Small or Missing ..............    0.00010 Ang.
PLAT143_ALERT_4_G s.u. on c - Axis Small or Missing ..............    0.00009 Ang.
PLAT791_ALERT_4_G Model has Chirality at C2          (Chiral SPGR)          S Verify
PLAT791_ALERT_4_G Model has Chirality at C9          (Chiral SPGR)          R Verify
PLAT791_ALERT_4_G Model has Chirality at C12         (Chiral SPGR)          S Verify
PLAT791_ALERT_4_G Model has Chirality at C19         (Chiral SPGR)          R Verify
PLAT791_ALERT_4_G Model has Chirality at C22         (Chiral SPGR)          S Verify
PLAT791_ALERT_4_G Model has Chirality at C29         (Chiral SPGR)          R Verify
PLAT791_ALERT_4_G Model has Chirality at C32         (Chiral SPGR)          S Verify
PLAT791_ALERT_4_G Model has Chirality at C39         (Chiral SPGR)          R Verify
PLAT912_ALERT_4_G Missing # of FCF Reflections Above STh/L=  0.600         31 Note
PLAT978_ALERT_2_G Number C-C Bonds with Positive Residual Density.         16 Info
```

```
   0 ALERT level A = Most likely a serious problem - resolve or explain
   0 ALERT level B = A potentially serious problem, consider carefully
   1 ALERT level C = Check. Ensure it is not caused by an omission or oversight
  13 ALERT level G = General information/check it is not something unexpected

   0 ALERT type 1 CIF construction/syntax error, inconsistent or missing data
   1 ALERT type 2 Indicator that the structure model may be wrong or deficient
   1 ALERT type 3 Indicator that the structure quality may be low
  11 ALERT type 4 Improvement, methodology, query or suggestion
   1 ALERT type 5 Informative message, check
```

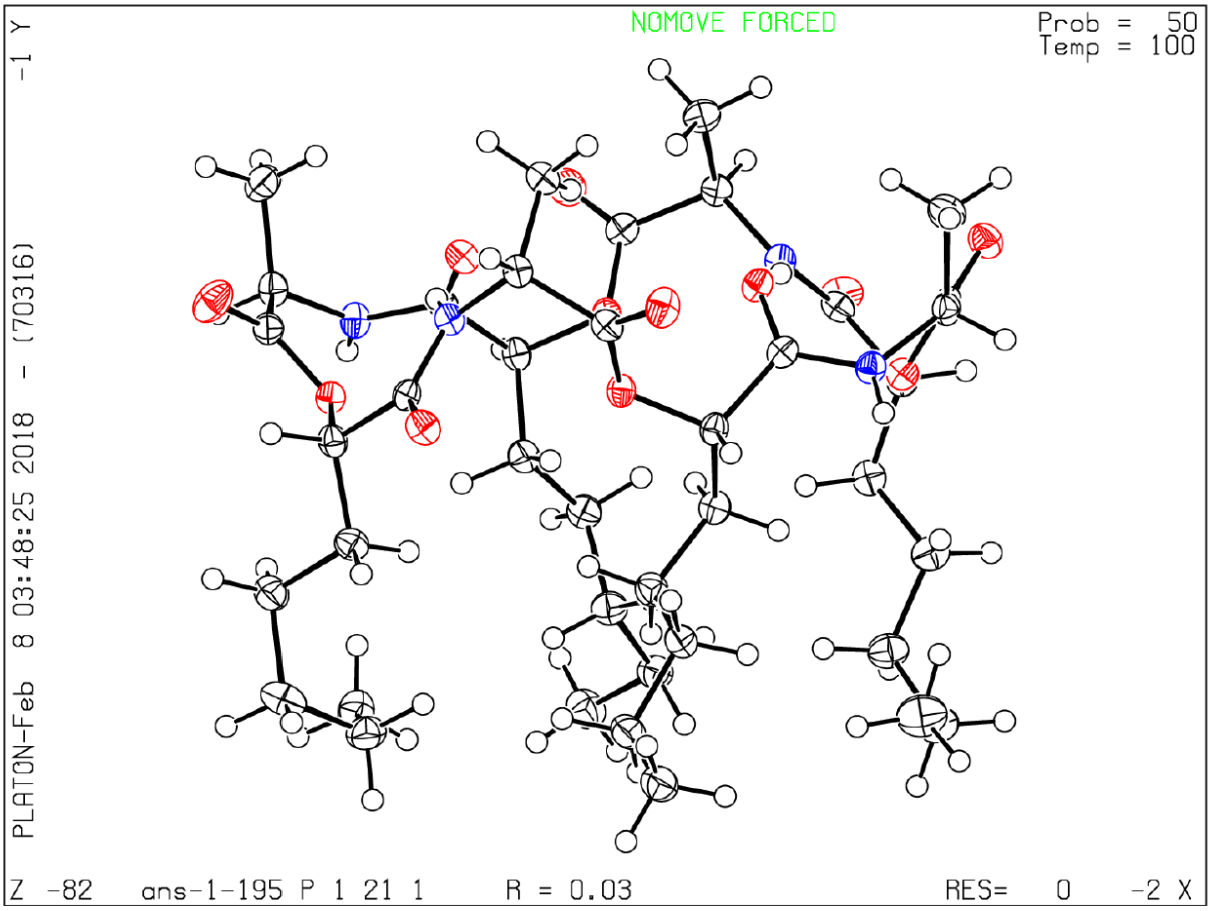
NOMOVE FORCED
Prob = 50
Temp = 100
PLATON-Feb 8 03:48:25 2018 - (70316)
-1 Y
Z -82
ans-1-195 P 1 21 1
R = 0.03
RES= 0
-2 X

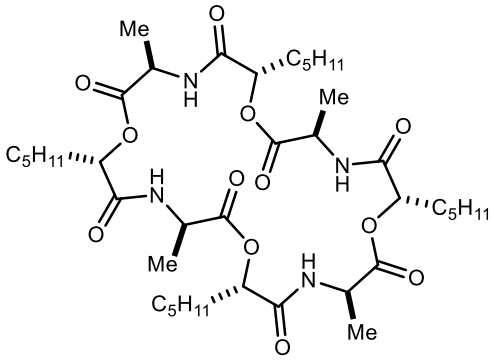
Me
O
N
H
C5H11
Me
O
O
C5H11
O
O
N
H
C5H11
H
N
O
O
O
Me
O
H
N
C5H11
O
Me

checkCIF/PLATON report

Structure factors have been supplied for datablock(s) ans-1-216

THIS REPORT IS FOR GUIDANCE ONLY. IF USED AS PART OF A REVIEW PROCEDURE FOR PUBLICATION, IT SHOULD NOT REPLACE THE EXPERTISE OF AN EXPERIENCED CRYSTALLOGRAPHIC REFEREE.

No syntax errors found. CIF dictionary Interpreting this report

Datablock: ans-1-216

```
Bond precision:  C-C = 0.0070 A          Wavelength=1.54184

Cell:         a=10.56861(18)     b=14.8902(2)      c=23.8406(3)
              alpha=74.4468(12)  beta=83.2958(12)  gamma=70.2128(14)
Temperature:  100 K

                 Calculated                Reported
Volume           3399.58(9)                3399.58(9)
Space group      P 1                       P 1
Hall group       P 1                       P 1
Moiety formula   C30 H51 N3 O9             C30 H51 N3 O9
Sum formula      C30 H51 N3 O9             C30 H51 N3 O9
Mr               597.74                    597.73
Dx,g cm-3        1.168                     1.168
Z                4                         4
Mu (mm-1)        0.704                     0.704
F000             1296.0                    1296.0
F000'            1300.13
h,k,lmax         13,18,29                  13,18,29
Nref             26938[ 13469]             23829
Tmin,Tmax        0.924,0.945               0.585,1.000
Tmin'            0.781

Correction method= # Reported T Limits: Tmin=0.585 Tmax=1.000
AbsCorr = GAUSSIAN

Data completeness= 1.77/0.88       Theta(max)= 72.495

R(reflections)= 0.0588( 22695)     wR2(reflections)= 0.1615( 23829)

S = 1.026                  Npar= 1577
```

The following ALERTS were generated. Each ALERT has the format
test-name_ALERT_alert-type_alert-level.
Click on the hyperlinks for more details of the test.

Alert level B

```
PLAT097_ALERT_2_B Large Reported Max.  (Positive) Residual Density       1.52 eA-3
PLAT230_ALERT_2_B Hirshfeld Test Diff for   C5       --C6        .        7.3 s.u.
PLAT230_ALERT_2_B Hirshfeld Test Diff for   C6       --C7        .        9.2 s.u.
PLAT360_ALERT_2_B Short  C(sp3)-C(sp3) Bond  C6       - C7       .       1.31 Ang.
```

Alert level C

```
DIFMX02_ALERT_1_C  The maximum difference density is > 0.1*ZMAX*0.75
           The relevant atom site should be identified.
PLAT094_ALERT_2_C Ratio of Maximum / Minimum Residual Density ....       3.11 Report
PLAT213_ALERT_2_C Atom C7              has ADP max/min Ratio .....        3.2 prolat
PLAT220_ALERT_2_C Non-Solvent  Resd 2  C   Ueq(max)/Ueq(min) Range        4.8 Ratio
PLAT220_ALERT_2_C Non-Solvent  Resd 3  C   Ueq(max)/Ueq(min) Range        4.3 Ratio
PLAT220_ALERT_2_C Non-Solvent  Resd 4  C   Ueq(max)/Ueq(min) Range        3.2 Ratio
PLAT222_ALERT_3_C Non-Solv.  Resd 2  H   Uiso(max)/Uiso(min) Range        5.7 Ratio
PLAT222_ALERT_3_C Non-Solv.  Resd 3  H   Uiso(max)/Uiso(min) Range        5.1 Ratio
PLAT230_ALERT_2_C Hirshfeld Test Diff for   C24D     --C25D      .        5.3 s.u.
PLAT234_ALERT_4_C Large Hirshfeld Difference C16D     --C17D            0.20 Ang.
PLAT241_ALERT_2_C High   'MainMol' Ueq as Compared to Neighbors of       C14B Check
PLAT241_ALERT_2_C High   'MainMol' Ueq as Compared to Neighbors of       C16D Check
PLAT241_ALERT_2_C High   'MainMol' Ueq as Compared to Neighbors of       C25D Check
PLAT242_ALERT_2_C Low    'MainMol' Ueq as Compared to Neighbors of         C6 Check
PLAT340_ALERT_3_C Low Bond Precision on  C-C Bonds ...............    0.00704 Ang.
PLAT601_ALERT_2_C Structure Contains Solvent Accessible VOIDS of .        54 Ang**3
PLAT790_ALERT_4_C Centre of Gravity not Within Unit Cell: Resd.  #         1 Note
            C30 H51 N3 O9
PLAT911_ALERT_3_C Missing FCF Refl Between Thmin & STh/L=    0.600         4 Report
PLAT915_ALERT_3_C No Flack x Check Done: Low Friedel Pair Coverage        78 %
```

Alert level G

```
PLAT002_ALERT_2_G Number of Distance or Angle Restraints on AtSite        13 Note
PLAT003_ALERT_2_G Number of Uiso or Uij Restrained non-H Atoms ...        10 Report
PLAT007_ALERT_5_G Number of Unrefined Donor-H Atoms ..............        12 Report
PLAT176_ALERT_4_G The CIF-Embedded .res File Contains SADI Records         5 Report
PLAT177_ALERT_4_G The CIF-Embedded .res File Contains DELU Records         1 Report
PLAT178_ALERT_4_G The CIF-Embedded .res File Contains SIMU Records         3 Report
PLAT230_ALERT_2_G Hirshfeld Test Diff for   C14B     --C15B      .        7.7 s.u.
PLAT301_ALERT_3_G Main Residue  Disorder ..............(Resd  1  )        7% Note
PLAT301_ALERT_3_G Main Residue  Disorder ..............(Resd  2  )        2% Note
PLAT432_ALERT_2_G Short Inter X...Y Contact  O6B      ..C28B           2.83 Ang.
PLAT432_ALERT_2_G Short Inter X...Y Contact  O6B      ..C30B           3.00 Ang.
PLAT432_ALERT_2_G Short Inter X...Y Contact  O6C      ..C28C           2.98 Ang.
PLAT432_ALERT_2_G Short Inter X...Y Contact  O6C      ..C30C           3.01 Ang.
PLAT432_ALERT_2_G Short Inter X...Y Contact  O7B      ..C30            2.81 Ang.
PLAT432_ALERT_2_G Short Inter X...Y Contact  O7C      ..C30D           2.84 Ang.
PLAT432_ALERT_2_G Short Inter X...Y Contact  O9       ..C10            2.89 Ang.
PLAT432_ALERT_2_G Short Inter X...Y Contact  O9D      ..C10D           2.97 Ang.
PLAT720_ALERT_4_G Number of Unusual/Non-Standard Labels ..........        56 Note
PLAT790_ALERT_4_G Centre of Gravity not Within Unit Cell: Resd.  #         2 Note
            C30 H51 N3 O9
PLAT791_ALERT_4_G Model has Chirality at C1          (Chiral SPGR)         S Verify
PLAT791_ALERT_4_G Model has Chirality at C1B         (Chiral SPGR)         S Verify
PLAT791_ALERT_4_G Model has Chirality at C1C         (Chiral SPGR)         S Verify
PLAT791_ALERT_4_G Model has Chirality at C1D         (Chiral SPGR)         S Verify
PLAT791_ALERT_4_G Model has Chirality at C8          (Chiral SPGR)         R Verify
PLAT791_ALERT_4_G Model has Chirality at C8B         (Chiral SPGR)         R Verify
PLAT791_ALERT_4_G Model has Chirality at C8C         (Chiral SPGR)         R Verify
PLAT791_ALERT_4_G Model has Chirality at C8D         (Chiral SPGR)         R Verify
PLAT791_ALERT_4_G Model has Chirality at C11         (Chiral SPGR)         S Verify
```

```
PLAT791_ALERT_4_G Model has Chirality at C11B        (Chiral SPGR)          S Verify
PLAT791_ALERT_4_G Model has Chirality at C11C        (Chiral SPGR)          S Verify
PLAT791_ALERT_4_G Model has Chirality at C11D        (Chiral SPGR)          S Verify
PLAT791_ALERT_4_G Model has Chirality at C18         (Chiral SPGR)          R Verify
PLAT791_ALERT_4_G Model has Chirality at C18B        (Chiral SPGR)          R Verify
PLAT791_ALERT_4_G Model has Chirality at C18C        (Chiral SPGR)          R Verify
PLAT791_ALERT_4_G Model has Chirality at C18D        (Chiral SPGR)          R Verify
PLAT791_ALERT_4_G Model has Chirality at C21         (Chiral SPGR)          S Verify
PLAT791_ALERT_4_G Model has Chirality at C21B        (Chiral SPGR)          S Verify
PLAT791_ALERT_4_G Model has Chirality at C21C        (Chiral SPGR)          S Verify
PLAT791_ALERT_4_G Model has Chirality at C21D        (Chiral SPGR)          S Verify
PLAT791_ALERT_4_G Model has Chirality at C28         (Chiral SPGR)          R Verify
PLAT791_ALERT_4_G Model has Chirality at C28B        (Chiral SPGR)          R Verify
PLAT791_ALERT_4_G Model has Chirality at C28C        (Chiral SPGR)          R Verify
PLAT791_ALERT_4_G Model has Chirality at C28D        (Chiral SPGR)          R Verify
PLAT860_ALERT_3_G Number of Least-Squares Restraints .............      105 Note
PLAT910_ALERT_3_G Missing # of FCF Reflection(s) Below Theta(Min).        1 Note
PLAT912_ALERT_4_G Missing # of FCF Reflections Above STh/L=  0.600      184 Note
PLAT933_ALERT_2_G Number of OMIT Records in Embedded .res File ...        1 Note
PLAT978_ALERT_2_G Number C-C Bonds with Positive Residual Density.        1 Info
```

```
  0 ALERT level A = Most likely a serious problem - resolve or explain
  4 ALERT level B = A potentially serious problem, consider carefully
 19 ALERT level C = Check. Ensure it is not caused by an omission or oversight
 48 ALERT level G = General information/check it is not something unexpected

  1 ALERT type 1 CIF construction/syntax error, inconsistent or missing data
 28 ALERT type 2 Indicator that the structure model may be wrong or deficient
  9 ALERT type 3 Indicator that the structure quality may be low
 32 ALERT type 4 Improvement, methodology, query or suggestion
  1 ALERT type 5 Informative message, check
```

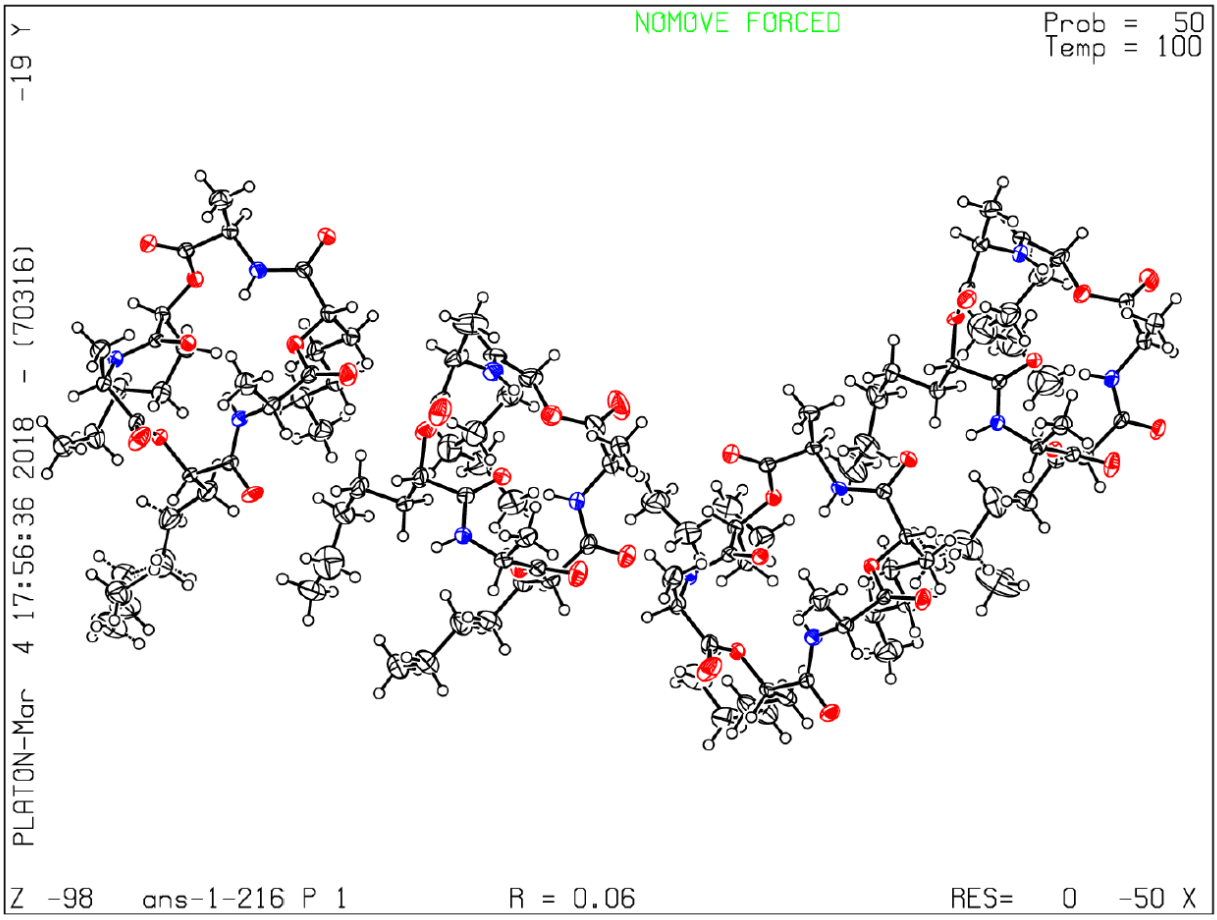
NOMOVE FORCED
Prob = 50
Temp = 100
PLATON-Mar 4 17:56:36 2018 - (70316)
-19 Y
Z -98
ans-1-216 P 1
R = 0.06
RES= 0 -50 X

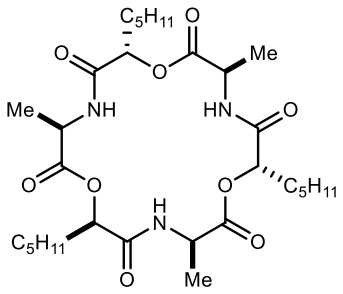
C5H11
O
Me
NH
HN
C5H11
H
N
Me

checkCIF/PLATON report

Structure factors have been supplied for datablock(s) ans-3-043

THIS REPORT IS FOR GUIDANCE ONLY. IF USED AS PART OF A REVIEW PROCEDURE FOR PUBLICATION, IT SHOULD NOT REPLACE THE EXPERTISE OF AN EXPERIENCED CRYSTALLOGRAPHIC REFEREE.

No syntax errors found. CIF dictionary Interpreting this report

Datablock: ans-3-043

```
Bond precision:  C-C = 0.0156 A          Wavelength=1.54184

Cell:          a=9.7566(6)       b=15.4416(7)     c=16.6133(7)
               alpha=68.891(4)   beta=76.736(4)   gamma=72.163(5)
Temperature:   100 K
```

	Calculated	Reported
Volume	2202.6(2)	2202.7(2)
Space group	P 1	P 1
Hall group	P 1	P 1
Moiety formula	C66 H114 N6 Na2 O18, 2(F6 P), 2(C3 H6 O)	1(F6 P), 0.5(C66 H114 N6 Na2 O18), C3 H6 O
Sum formula	C72 H126 F12 N6 Na2 O20 P2	C36 H63 F6 N3 Na O10 P
Mr	1731.71	865.85
Dx,g cm-3	1.306	1.305
Z	1	2
Mu (mm-1)	1.348	1.348
F000	920.0	920.0
F000'	924.08	
h,k,lmax	12,19,20	12,19,20
Nref	17362[8681]	14128
Tmin,Tmax	0.939,0.981	0.696,1.000
Tmin'	0.700	

```
Correction method= # Reported T Limits: Tmin=0.696 Tmax=1.000
AbsCorr = GAUSSIAN

Data completeness= 1.63/0.81      Theta(max)= 72.214

R(reflections)= 0.0777( 9629)     wR2(reflections)= 0.2191( 14128)

S = 1.035                 Npar= 1132
```

The following ALERTS were generated. Each ALERT has the format
test-name_ALERT_alert-type_alert-level.
Click on the hyperlinks for more details of the test.

Alert level B

PLAT340_ALERT_3_B Low Bond Precision on C-C Bonds ..... 0.01559 Ang.

Alert level C

PLAT029_ALERT_3_C _diffrn_measured_fraction_theta_full value Low . 0.978 Why?
PLAT220_ALERT_2_C Non-Solvent Resd 1 C Ueq(max)/Ueq(min) Range 4.6 Ratio
PLAT222_ALERT_3_C Non-Solv. Resd 1 H Uiso(max)/Uiso(min) Range 5.3 Ratio
PLAT241_ALERT_2_C High 'MainMol' Ueq as Compared to Neighbors of C15B Check
PLAT241_ALERT_2_C High 'MainMol' Ueq as Compared to Neighbors of C25A Check
PLAT242_ALERT_2_C Low 'MainMol' Ueq as Compared to Neighbors of C14B Check
PLAT242_ALERT_2_C Low 'MainMol' Ueq as Compared to Neighbors of C26A Check
PLAT244_ALERT_4_C Low 'Solvent' Ueq as Compared to Neighbors of C35 Check
PLAT244_ALERT_4_C Low 'Solvent' Ueq as Compared to Neighbors of C35B Check
PLAT250_ALERT_2_C Large U3/U1 Ratio for Average U(i,j) Tensor .... 2.9 Note
PLAT250_ALERT_2_C Large U3/U1 Ratio for Average U(i,j) Tensor .... 2.1 Note
PLAT260_ALERT_2_C Large Average Ueq of Residue Including P1B 0.113 Check
PLAT360_ALERT_2_C Short C(sp3)-C(sp3) Bond C15B - C16B . 1.43 Ang.

Alert level G

PLAT003_ALERT_2_G Number of Uiso or Uij Restrained non-H Atoms ... 20 Report
PLAT004_ALERT_5_G Polymeric Structure Found with Maximum Dimension 1 Info
PLAT042_ALERT_1_G Calc. and Reported MoietyFormula Strings Differ Please Check
PLAT045_ALERT_1_G Calculated and Reported Z Differ by a Factor ... 0.50 Check
PLAT072_ALERT_2_G SHELXL First Parameter in WGHT Unusually Large 0.11 Report
PLAT187_ALERT_4_G The CIF-Embedded .res File Contains RIGU Records 2 Report
PLAT244_ALERT_4_G Low 'Solvent' Ueq as Compared to Neighbors of P1A Check
PLAT301_ALERT_3_G Main Residue Disorder .....(Resd 1) 2% Note
PLAT302_ALERT_4_G Anion/Solvent/Minor-Residue Disorder (Resd 3) 100% Note
PLAT302_ALERT_4_G Anion/Solvent/Minor-Residue Disorder (Resd 4) 100% Note
PLAT432_ALERT_2_G Short Inter X...Y Contact F4A ..C8B 2.95 Ang.
x,-1+y,z = 1_545 Check
PLAT432_ALERT_2_G Short Inter X...Y Contact O10B ..C19B 2.96 Ang.
x,y,z = 1_555 Check
PLAT720_ALERT_4_G Number of Unusual/Non-Standard Labels ..... 28 Note
PLAT860_ALERT_3_G Number of Least-Squares Restraints ..... 147 Note

---

0 **ALERT level A** = Most likely a serious problem - resolve or explain
1 **ALERT level B** = A potentially serious problem, consider carefully
13 **ALERT level C** = Check. Ensure it is not caused by an omission or oversight
14 **ALERT level G** = General information/check it is not something unexpected

2 ALERT type 1 CIF construction/syntax error, inconsistent or missing data
13 ALERT type 2 Indicator that the structure model may be wrong or deficient
5 ALERT type 3 Indicator that the structure quality may be low
7 ALERT type 4 Improvement, methodology, query or suggestion
1 ALERT type 5 Informative message, check

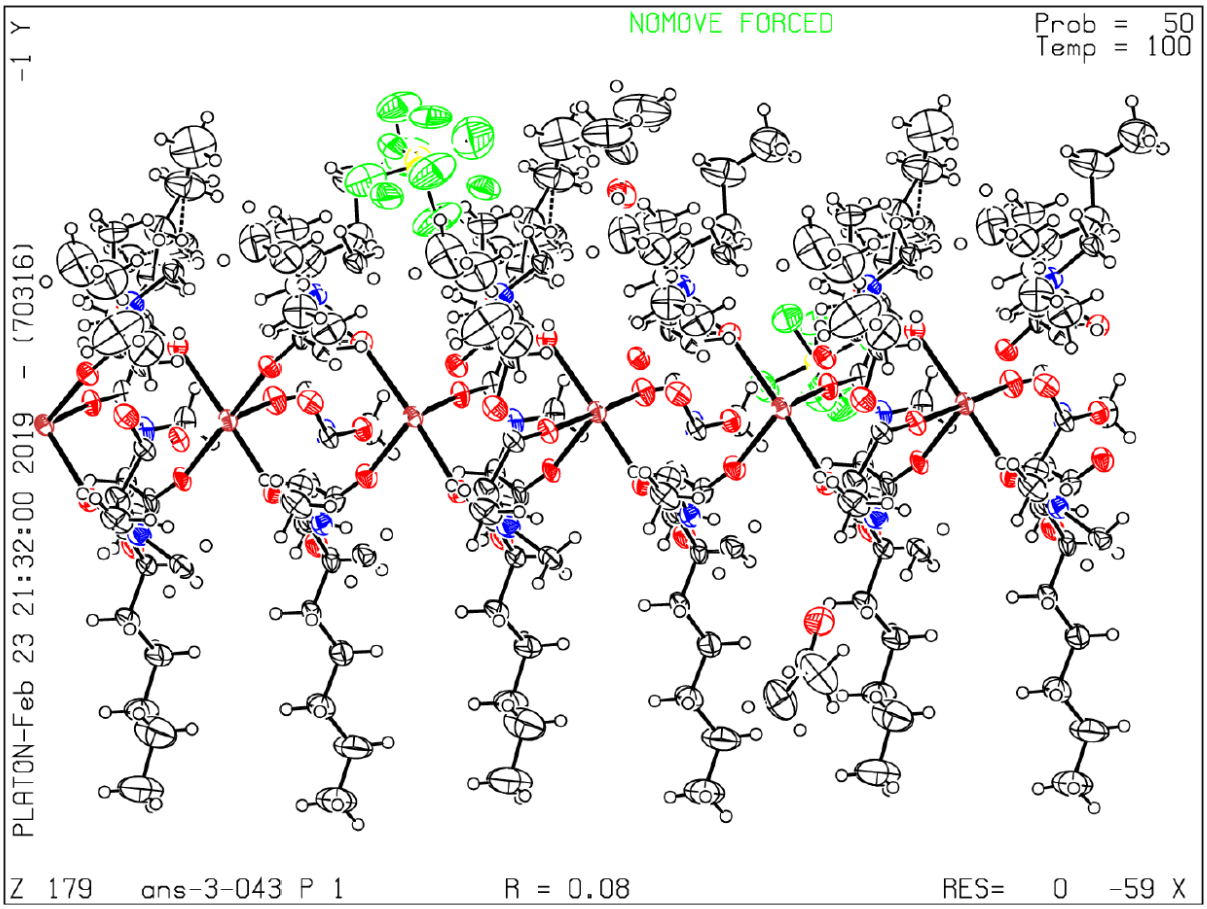
NOMOVE FORCED
Prob = 50
Temp = 100
-1 Y
PLATON-Feb 23 21:32:00 2019 - (70316)
Z 179 ans-3-043 P 1
R = 0.08
RES= 0 -59 X

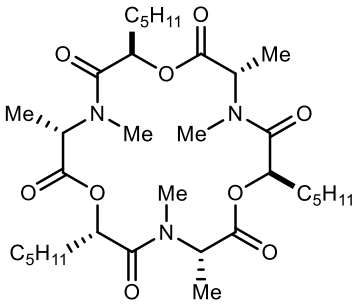
C5H11
O
Me
N
Me
C5H11

ANS-1-85

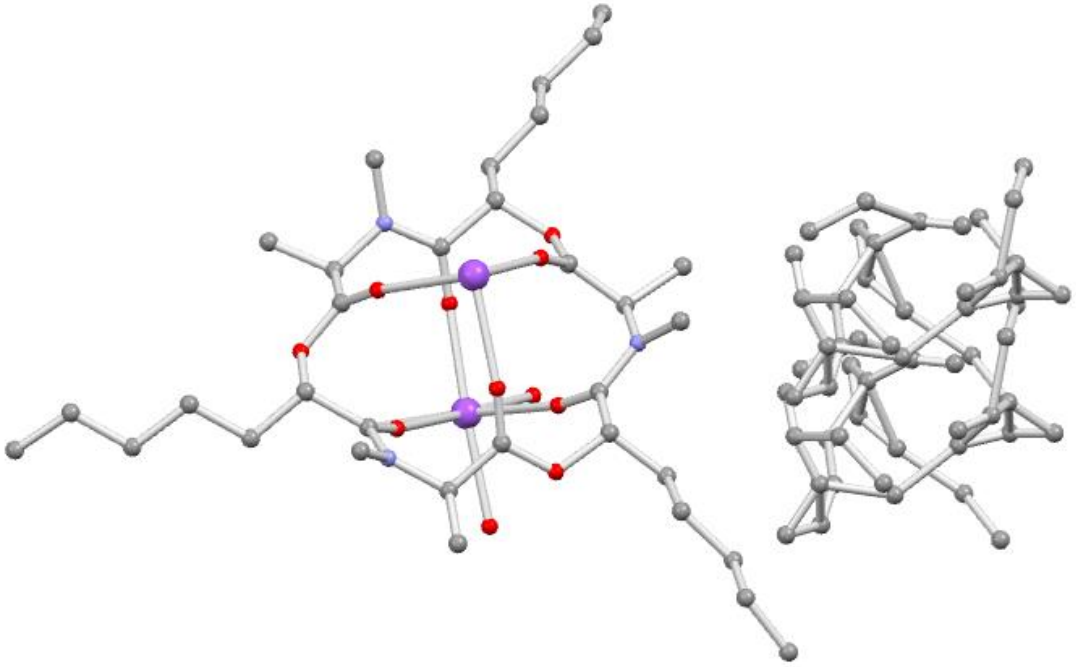

It is clear from this X-ray of ANS-1-85 that it is an 18-mem methylated ring. It is bound to either Na or Mg. However, the disordered solvent and counterion are not able to be matched from these crystals, therefore the cation cannot be positively determined. We therefore do not have publishable data from this crystal structure.

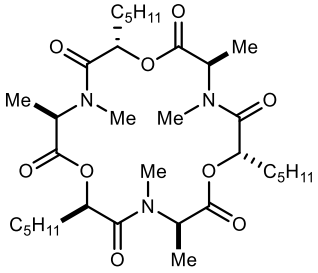

checkCIF/PLATON report

Structure factors have been supplied for datablock(s) ans-3-119

THIS REPORT IS FOR GUIDANCE ONLY. IF USED AS PART OF A REVIEW PROCEDURE FOR PUBLICATION, IT SHOULD NOT REPLACE THE EXPERTISE OF AN EXPERIENCED CRYSTALLOGRAPHIC REFEREE.

No syntax errors found. CIF dictionary Interpreting this report

Datablock: ans-3-119

```
Bond precision:  C-C = 0.0030 A          Wavelength=1.54184

Cell:            a=6.48010(13)     b=9.4692(2)     c=19.5716(5)
                 alpha=90          beta=90         gamma=90
Temperature:     100 K
```

	Calculated	Reported
Volume	1200.94(5)	1200.94(5)
Space group	P 21 21 21	P 21 21 21
Hall group	P 2ac 2ab	P 2ac 2ab
Moiety formula	C11 H19 N O3	C11 H19 N O3
Sum formula	C11 H19 N O3	C11 H19 N O3
Mr	213.27	213.27
Dx,g cm-3	1.180	1.180
Z	4	4
Mu (mm-1)	0.695	0.695
F000	464.0	464.0
F000'	465.44	
h,k,lmax	8,11,24	8,11,24
Nref	2358[1389]	2325
Tmin,Tmax	0.930,0.977	0.744,1.000
Tmin'	0.862	

```
Correction method= # Reported T Limits: Tmin=0.744 Tmax=1.000
AbsCorr = GAUSSIAN

Data completeness= 1.67/0.99      Theta(max)= 72.200

R(reflections)= 0.0297( 2245)     wR2(reflections)= 0.0756( 2325)

S = 1.050                  Npar= 139
```

The following ALERTS were generated. Each ALERT has the format
test-name_ALERT_alert-type_alert-level.
Click on the hyperlinks for more details of the test.

Alert level G

```
PLAT791_ALERT_4_G Model has Chirality at C2          (Chiral SPGR)          R Verify
PLAT791_ALERT_4_G Model has Chirality at C5          (Chiral SPGR)          S Verify
PLAT912_ALERT_4_G Missing # of FCF Reflections Above STh/L=  0.600          5 Note
PLAT978_ALERT_2_G Number C-C Bonds with Positive Residual Density.          3 Info
```

```
   0 ALERT level A = Most likely a serious problem - resolve or explain
   0 ALERT level B = A potentially serious problem, consider carefully
   0 ALERT level C = Check. Ensure it is not caused by an omission or oversight
   4 ALERT level G = General information/check it is not something unexpected

   0 ALERT type 1 CIF construction/syntax error, inconsistent or missing data
   1 ALERT type 2 Indicator that the structure model may be wrong or deficient
   0 ALERT type 3 Indicator that the structure quality may be low
   3 ALERT type 4 Improvement, methodology, query or suggestion
   0 ALERT type 5 Informative message, check
```